Fabiano Montiani-Ferreira
Bret A. Moore
Gil Ben-Shlomo *Editors*

TEXTBOOK

Wild and Exotic Animal Ophthalmology

Volume 2
Mammals

Springer

Wild and Exotic Animal Ophthalmology

Fabiano Montiani-Ferreira • Bret A. Moore •
Gil Ben-Shlomo
Editors

Wild and Exotic Animal Ophthalmology

Volume 2: Mammals

Springer

Editors
Fabiano Montiani-Ferreira
Veterinary Medicine Department
Federal University of Paraná
Curitiba, Brazil

Bret A. Moore
College of Veterinary Medicine
University of Florida
Gainesville, Florida, USA

Gil Ben-Shlomo
College of Veterinary Medicine
Iowa State University
Ames, Iowa, USA

ISBN 978-3-030-81272-0 ISBN 978-3-030-81273-7 (eBook)
https://doi.org/10.1007/978-3-030-81273-7

This Springer imprint is published by the registered company Springer Nature Switzerland AG.
The registered company address is: Gewerbestrasse 11, 6330 Cham, Switzerland

In remembrance of our friend.

Say not in grief 'he is no more' but in thankfulness that he was—*Hebrew proverb*

There is so much to be grateful for when it comes to Gil Ben-Shlomo, whether you knew him well or simply met this gentle giant *at a conference somewhere around the world. Gil's bright smile, keen intellect, hearty laugh, and charisma would always light up a room and bring joy to people around him.*

Our beloved Gil was taken from this world far too soon. He passed away unexpectedly at the age of 50, leaving behind his wife of 20 years, Anna, his two daughters Roni and Noam, his extended family, and two Boxer dogs. Undoubtedly, Gil's family was his greatest accomplishment, a daily source of pride, and the foundation for him to achieve so much in life.

Gil Ben-Shlomo (DACVO 2012) earned his DVM and PhD in Neurobiology from the Koret School of Veterinary Medicine at the Hebrew University of Jerusalem, Israel. He completed his comparative ophthalmology residency at the University of Florida (2007–2010) and joined the faculty at Iowa State University as Assistant Professor in 2010, progressing to Associate Professor with tenure in 2016. As a teacher, Gil served as a role model for students and residents through his professionalism and ethical standards. His passion for veterinary ophthalmology fueled his approach and success in teaching the next generation of veterinarians and veterinary ophthalmologists. His innovative research in retinal neurodegeneration had a significant impact on both the veterinary and human realms, providing a bridge from the bench top to the patient. In the clinic, Gil was always known for the generous number of treats he would give his patients, his warm and welcoming demeanor, his outstanding clinical and surgical skills, and his wonderful smile. In 2019, Gil left Iowa State for an Associate Professor position at Cornell University, where he quickly became an integral member of the Ophthalmology service. Gil was also active on the international scene, serving as the president of the International Society of Veterinary Ophthalmology, as an editorial board member for the journal Veterinary Ophthalmology*, and as a member on committees for various organizations. Most recently, Gil's passion and dedication to the profession led him to serve as an associate editor for two authoritative textbooks,* Veterinary Ophthalmology (6th edition) *and* Exotic and Wild Animal Ophthalmology.

Gil was a doting father, devoted husband, loving brother and son, and a dear friend to many. Gil's impact on my life was a true blessing that I cherish every day; he made me a better ophthalmologist, researcher, teacher, and, more importantly, a better person. Reading the many messages of condolence and the outpouring of love for Gil, it comforts me to know that he had the same positive impact on countless other people around the world.

May our fond memories of Gil, and our gratitude for his exceptional legacy, inspire us to live each day to its fullest, be kind to one another, hold our loved ones very close, and pursue our passion for veterinary ophthalmology with enthusiasm and countless smiles.

Eternal thanks to Gil for his ingenuity and insight in coediting the incredible textbook before you.

With love,

Lionel Sebbag, DVM, PhD, DACVO
Koret School of Veterinary Medicine
Hebrew University of Jerusalem, Israel

Foreword

This work addresses a need that has been long-standing in comparative ophthalmology. Namely, the creation of a single reservoir of information, focused on wild and exotic animal species, from which both comparative vision scientists and clinical veterinarians (from comprehensive practitioners to wildlife and exotic specialists to comparative ophthalmologists) can drink. There are expansive works on comparative vision and ocular structure (Walls 1942, Rochon Duvigneaud 1943, Polyak 1958, Gregory and Cronly-Dillon 1991, Schwab 2012, and Warrant and Nilsson 2006, among others), but these typically lack specific critical details most helpful to a clinician contemplating the wild or exotic patient in front of them with an ocular disorder. Similarly, in the comparative clinical literature, there are numerous mini-reviews available on specific groups of animals (often focused on a vertebrate class or order within a class), and there are a limited number of excellent overviews provided in textbooks of veterinary ophthalmology, but there has, to date, not existed a *comprehensive* resource that summarizes the available literature while providing practitioner insights on evolution, environmental niche, relevant aspects of captive management (in the context of ocular disorders), ocular functional morphology, and known ocular diseases and surgical procedures across the spectrum of wild and exotic patients seen by comparative ophthalmologists. This work goes a long way toward filling that void.

The editors have selected a diverse cast of experts to assemble the encyclopedic information presented in this text. Notably, and appropriately, not all authors are veterinary ophthalmologists, enabling the presentation of the best pertinent information available. All chapters strive to provide a balance of the comparative basic functional morphology and visual ecology with the known clinical entities and reported therapeutic strategies. The text is complemented by a library of high-quality photographic images and informative illustrations. Importantly, knowledge gaps are identified which will hopefully stimulate investigations by current and future comparative ophthalmologists.

The editors are to be applauded for bringing this daunting project to fruition. The tragic loss of one of the editors, Dr. Gil Ben-Shlomo, is felt throughout the profession, but I feel Gil would be truly pleased in seeing the quality of the product his hard work was central to completing.

I note that this is the first edition of what I feel is likely to become a cornerstone reference for comparative ophthalmology. I am very much looking forward to its continued evolution through subsequent editions.

Christopher J. Murphy

Department of Ophthalmology and Vision Science,
Department of Veterinary Surgical and Radiological Sciences,
Schools of Medicine and Veterinary Medicine,
University of California
Davis, CA, USA

Preface

No matter how small or large, the differences between one animal and the next display all the splendor and exulting power of nature. Biologist David Barash once said that it is an innate behavior of us humans to be fascinated with animals, often viewing them as either straight or distorted reflections of ourselves. Our captivation of the animal kingdom has included a curiosity of how animals see, a topic that also has largely been impacted by our personal experiences with the visual perception of our shared world. In fact, for nearly 300 years, the vertebrate eye has been a structure of scientific fascination. Early work provided both insight and foresight into the questions needing to be asked, and those answered have shaped our current understanding of the vertebrate eye. Gordon L. Walls himself said, as he introduced *The Vertebrate Eye and Its Adaptive Radiations* in 1942, that,

> If the comparative ophthalmologists of the world should ever hold a convention, the first resolution they would pass would say: 'Everything in the vertebrate eye means something.' Except for the brain, there is no other organ in the body of which that can be said. . .Man can make optical instruments only from such materials as brass and glass. Nature has succeeded with only such things as leather and water and jelly; but the resulting instrument is so delicately balanced that it will tolerate no tampering.

How right he was, as we continue to learn that we still know relatively very little. This statement was made just a few short decades from the official conception of our college, the American College of Veterinary Ophthalmology, which as of November 2019 celebrated its 50th Anniversary in beautiful Maui, Hawaii, and paid tribute to those who initiated its development (Samuel Vainisi, Roy Bellhorn, Seth Koch, Charles Martin, Milt Wyman, Stephen Bistner, William Magrane, Kirk Gelatt, Craig Fischer, Gustavo Aguirre, and Lionel Rubin). Similarly, our Brazilian (Est. 1987) and European (Est. 1991) Colleges of Veterinary Ophthalmology followed years later.

Over the past 50 years, we have advanced the field of comparative ophthalmology at a near exponential rate. Establishment of a mainstay text for canine and feline ophthalmology was introduced in 1981 by Kirk N. Gelatt, a book that is currently in its sixth edition. A mainstay text of equine ophthalmology has been developed and is now in its third edition thanks to Brian Gilger's dedication, completing the triad of our most commonly treated companion animals. However, as major advances are made with a particular focus on the treatment and prevention of ophthalmic disease in our animal companions, the wonder and beauty of the enormous diversity that is the vertebrate eye can be lost. In many regards, a major gap not yet embodied within our progression as a college is the true comparative nature of our profession. Even in the face of much scientific progress, much of the knowledge to date in wild and exotic animal ophthalmology has depended upon extrapolation from domestic animal ophthalmology. The ocular anatomy, physiology, and most common ophthalmic diseases in many wild and exotic animal species are still largely unknown to veterinarians.

Despite our utmost desire to improve care for the eyes of our domestic animal companions, we are truly privileged to be able to work with all the species of the Earth, from the smallest insect to the largest whale. In honor of the beauty of the vertebrate eye and perhaps its most remarkable attribute—its unimaginable and inspiring diversity—it is with excitement and enthusiasm that we are able to present to you this book, *Wild and Exotic Animal*

Ophthalmology. Our goals have been twofold: (1) to provide a comprehensive yet clinically focused text to guide ophthalmologists and exotic animal and zoological practitioners and (2) to establish a collection of the achievements we have made thus far and, more importantly, a perspective on what achievements we have yet to make in the field of exotic animal ophthalmology.

To accomplish our first goal, a major hurdle of such a text is to organize both clinical and taxonomic aspects in harmony. Before getting into details about vision, eye diseases, and treatment, we introduce each taxonomic class, offering general information on biology, physiology, husbandry, nutrition, and sometimes even common systemic diseases. Because animals are typically grouped by phylogenetic relatedness, understanding taxonomy will assist veterinary ophthalmologists to better categorize our patients, facilitating possible extrapolations of knowledge already constructed in domestic animals or in more familiar exotic species.

This two-volume book begins with an introduction to the origins of photoreception (Chap. 1) and its beginnings in the invertebrates (Chap. 2) and the fishes (Chaps. 3, 4, 5) in Part I. Here, we are introduced to the vertebrate eye, of which the cyclostomata, the jawless fish, provides a view of what perhaps is the earliest of the vertebrate visual systems. The complexity and ophthalmic diversity rapidly grows as we move onto land and discuss ophthalmology of the Amphibia in Part II (Chaps. 6 and 7) and Reptilia in Part III (Chaps. 8, 9, 10, 11, 12, 13, 14, and 15). The Avians (Chaps. 16, 17, 18, 19, 20, 21, 22, 23, 24, and 25) are represented strongly by our clinically prominent groups, the psittacines (Chap. 17), the raptors (Chap. 20), and the Galloanserae (Chap. 24). In addition to Chap. 16: Introduction to Avian Ophthalmology, these three chapters provide a framework for practicing ophthalmology in birds, and specific differences among other avian groups are highlighted within their respective chapters. Approaching the Mammalia (Volume 2) in a similar way would be foolish, as the diversity from a clinical perspective far exceeds that of the Avians (at least to our current understanding). From the vestigial subterranean eyes of moles, to the reptilian-like eye of the echidna, to the 4-kilogram eye of a blue whale, introducing the features of the mammalian eye is best accomplished within each chapter. We end with several Appendices for easy reference.

With our second goal of this book being to arouse memories of old when working with different species, and to stimulate foresight on what could be, we have spent time reflecting on the progression and meaning of our profession. “Let there be light” is an English translation of the Hebrew יְהִי אוֹר (yehi ‘or), found in Genesis 1:3 of the Torah. Light has been the subject of wonder since the dawn of humankind. The word *enlightened* comes from the Latin prefix *en* meaning “in, into” and the word *lux* meaning “light.” Combined, “into the light” describes the entire basis of our field of veterinary ophthalmology. Light notably possesses two characteristics: it is wave-like, interfering in the same way that water ripples cross each other, but it is also particle-like, carrying its energy in discrete bundles known as photons (or quanta). Light stimulus has an intensity, a direction, a spectrum (color), and sometimes a plane of polarization. All of these physical properties are detectable, in varying degrees, by the eyes of 90% of all animal species. Ocular light detection depends on the conversion of light energy (a form of electromagnetic radiation) into an electrical signal, a chemical process called phototransduction, which involves light-absorbing photopigments found in retinal photoreceptors. Moreover, the production and emission of light by a living organism (bioluminescence) also occurs widely among animals, especially in the open sea, including fish, jellyfish, comb jellies, crustaceans, and mollusks, and in numerous insects. We believe that for most veterinary ophthalmologists, light is the closest thing to magic. Inquisitively, we use the light of our instruments to examine and diagnose the very organ that transforms light into vision. Currently, we even use light, in the form of lasers or UV light, to treat several conditions, such as glaucoma, retinal diseases, and corneal conditions. According to the Canadian poet Leonard Cohen: “There is a crack in everything. That’s how the light gets in.” Scientific discoveries made in the eyes of wild animals open the veterinary ophthalmology crack just a little wider, and through it we get a better view not only of animal vision, but also

how the human eye works. For us ophthalmologists, light is all that is, was, or ever will be.

Without sounding too pretentious, we sincerely hope that this book will bring some enlightenment, at least about this specific subject. We hope that this book brings our college together to recapitulate those infrequent experiences over the past 50 years of our field, enabling us to fill the gaps left where limited or no experience was thought to have been obtained. As a result, we hope that this book compels future growth in our field as we continue our fascination, care, and service for the animals of which we share our world.

We must thank all those who have helped us in the production of this book. We have received an enormous amount of help from a very diverse group of authors and coauthors, coming from several different countries, possessing different mother tongues, education backgrounds, religions, and even political views, but all with two very important commonalities: (1) a fascination for the wild and exotic animal eye and (2) a devotion to veterinary ophthalmology. We may sound biased saying this, but the result has been exceptional. We first would like to thank our fellow chapter authors for their tireless work. We also thank our dear former and current mentors, colleagues, and friends who have contributed their vast experiences, shared cases, and images, and have given advice.

Fabiano would like to thank the other editors, especially Bret A. Moore, for having believed in him and embarked on this journey. Without Bret and Gil´s professionalism, dedication, enthusiasm, and expertise the result would certainly be inferior. This book has consumed a considerable amount of time in its creation (4 years)—long hours of organizational meetings, web meetings, countless phone calls, hundreds of e-mails exchanged, literature research and writing, lots of writing. All of these meant time away from our families. During this time Fabiano had a son (Giuseppe), one of our editors (Gil Ben-Shlomo) passed away, and we all went through a difficult period in the COVID-19 pandemic. We faced the most serious socioeconomic and health crisis of recent times. While we all had our struggles, the sense of global community that emerged here, particularly among scientists, will certainly remain a memory to treasure. Therefore, Fabiano would like to dedicate his work on this book to his family, especially Gabrielle Fornazari and Giuseppe Montiani. “There are darknesses in life and there are lights, and you are one of the lights, the light of all lights.”—Bram Stoker.

Bret would like to give his utmost thanks to his Father, “from whom I have been given the freedom, resources, and intellectual ability to professionally explore His design through science, whereby my every attempt to further understand its beauty continually unveils with joyful reverence the wonder of His creation, and that the existence of every living creature is nothing less than a gracious gift to His children, a most perfect design. It is with honor I can present this work to Him and the public in hopes that it displays to His people even a touch of the true splendor of His craftsmanship and brings Him, and only Him, glory.” He also would like to specifically thank his mentors for their guidance and support while enabling him the freedom to pursue such a project, as well as his twin Kelly Knickelbein for enduring his preoccupation and entertaining his constant talking about random animals’ eyes. Additionally, his wonderful parents and sister, Mike, Tina, and Audrey Moore, deserve special attention for their love and support throughout both his childhood and adulthood that got him to where he is today. Finally, Tara M. Czepiel, who every day provides more and more wisdom, support, and an encouraging presence that ultimately made the completion of this book possible.

Finally, we express our deepest condolences on the recent death of Gil Ben-Shlomo. He will always be remembered as a great professional and an even greater friend. His extraordinary scientific knowledge as well as passion for veterinary ophthalmology was only surpassed by his incredible positive influence and zest for life, especially when he was in the company of friends and family.

Curitiba, Brazil — Fabiano Montiani-Ferreira
Gainesville, Florida, USA — Bret A. Moore
Ames, Iowa, USA — Gil Ben-Shlomo

Contents

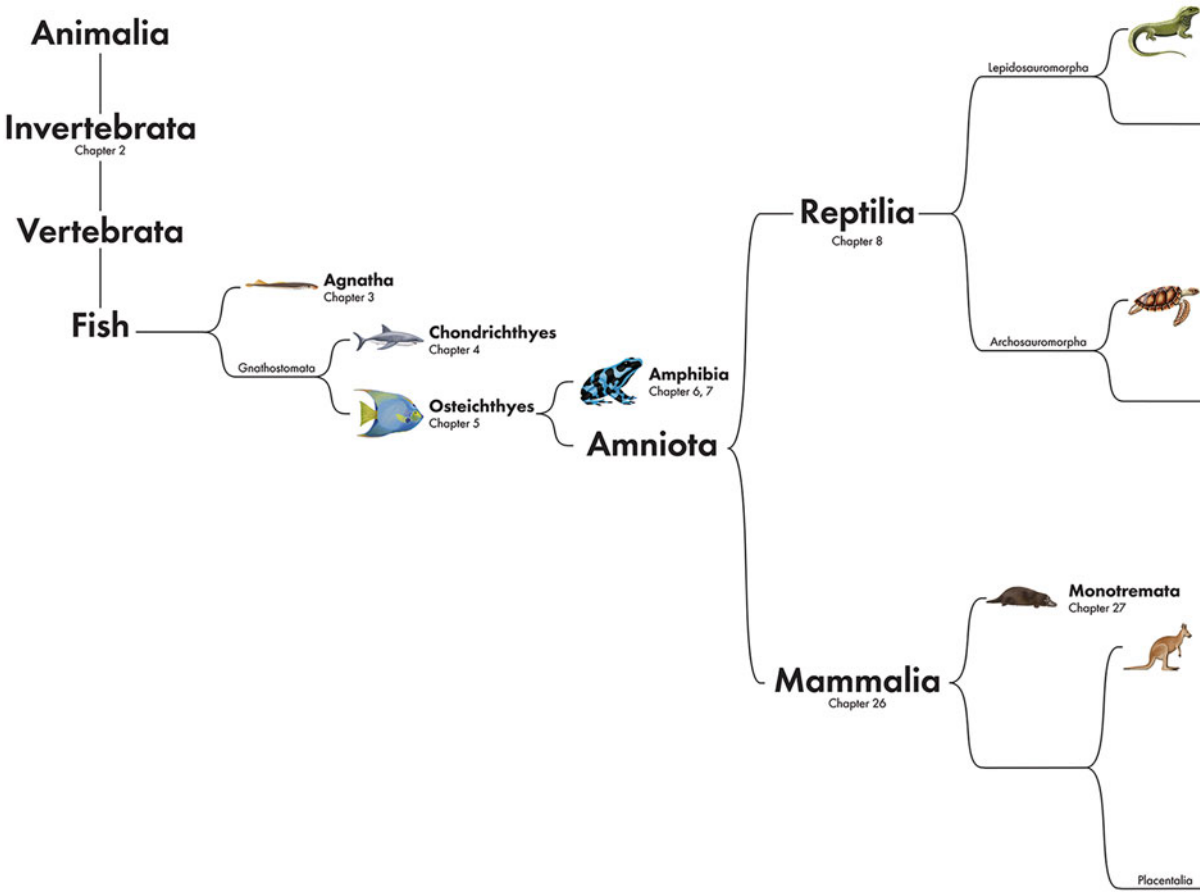
Animalia
Invertebrata
Chapter 2
Vertebrata
Fish
Agnatha
Chapter 3
Gnathostomata
Chondrichthyes
Chapter 4
Osteichthyes
Chapter 5
Amphibia
Chapter 6, 7
Amniota
Reptilia
Chapter 8
Lepidosauromorpha
Archosauromorpha
Mammalia
Chapter 26
Monotremata
Chapter 27
Placentalia

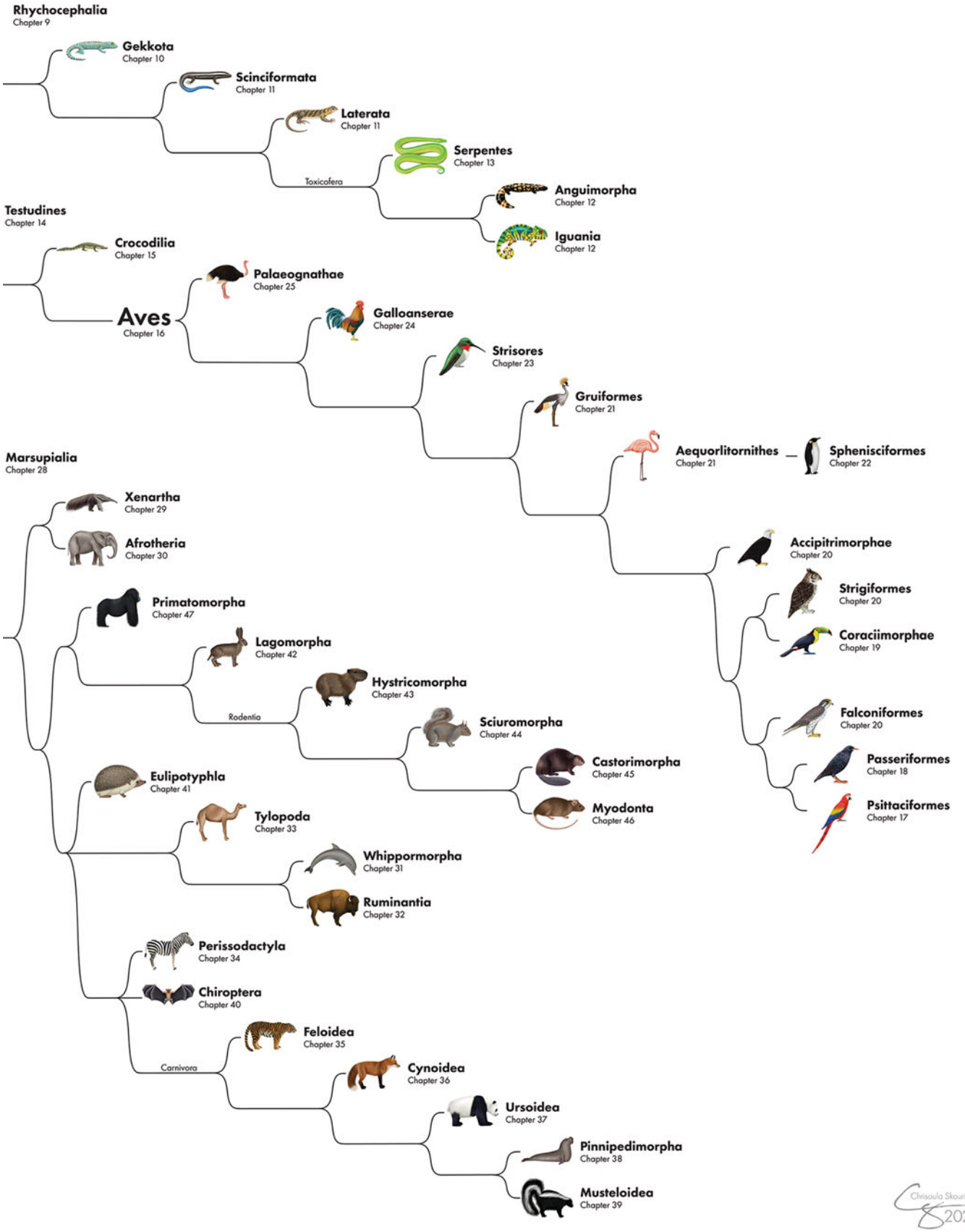

About the Editors

Fabiano Montiani-Ferreira is currently a Full Professor of Comparative Ophthalmology at the Federal University of Paraná, Brazil (UFPR), where he teaches veterinary and graduate students and trains veterinary ophthalmology residents, since 1997. He completed the Senior Veterinary Student Program at the Animal Medical Center, New York, USA. He then obtained his Bachelor of Veterinary Medicine (BVetMed) and a Master of Science (MSc) degree in Veterinary Sciences from the same university (UFPR). In the early 2000s, he obtained a Doctor of Philosophy (PhD) degree from Michigan State University (MSU). Dr. Montiani-Ferreira currently holds an official position and grant as a certified veterinary researcher (PQ2) at the Brazilian National Council for Scientific and Technological Development (CNPQ) and is a Diplomate of the Brazilian College of Veterinary Ophthalmologists (DBCVO). His research activities focus on (1) ocular morphology, physiology, clinical tests, and vision in wild and exotic animals; (2) investigations on animals carrying spontaneous mutations in small animals as models for the study of inherited retinal diseases in humans; and (3) nature and practice of science in addition to medical biostatistics. His clinical interests include (1) inherited retinal diseases in domestic and non-domestic animals; (2) adapting established ophthalmic procedures for wild and exotic animals; (3) and general ophthalmic surgery.

Bret A. Moore is currently Assistant Professor of Comparative Ophthalmology at the University of Florida. He holds a Bachelor of Science in Neurobiology and Physiology (BS), Doctor of Veterinary Medicine (DVM), and Doctor of Philosophy (PhD) from Purdue University, and completed his postdoctoral training/residency in comparative veterinary ophthalmology at the University of California, Davis. His research occupies a unique niche that combines vision, visual ecology, and clinical ophthalmology. From an ecological perspective, his research asks questions that explore unknown or unexplained morphological and physiological adaptations in vision, and seeks to understand the role of multiple visual parameters simultaneously in order to better understand a given species' "visual space," importantly how visual systems align with behavior and enable success in respective ecological niches. Clinically, his research interests are focused on understand-

ing disease processes as well as diagnostic and surgical methodology in exotic animal species. By taking this multifaceted approach to vision and clinical ophthalmology, and evaluating their interactions together, questions can be answered that not only bridge the gap across disciplines, but also become translatable to other disciplines such as conservation biology and the development of new biotechnologies.

Gil Ben-Shlomo (1970–2020) held DVM and PhD degrees from the Hebrew University of Jerusalem, Israel. Following a comparative ophthalmology residency at the University of Florida, he obtained board certification and Diplomate status in the American and European Colleges of Veterinary Ophthalmologists. His latest service was as faculty at the College of Veterinary Medicine, Cornell University, where he taught veterinary and graduate students and trained residents in the field of veterinary ophthalmology. He had been invited to speak at numerous local, national, and international conferences. Prof. Ben-Shlomo was also an associate editor and author of Gelatt's *Veterinary Ophthalmology* (sixth edition), was an editorial board member of the *journal Veterinary Ophthalmology*, and was the most recent President of the International Society of Veterinary Ophthalmology.

General Introduction: Mammalia

26

Carlos E. Rodriguez

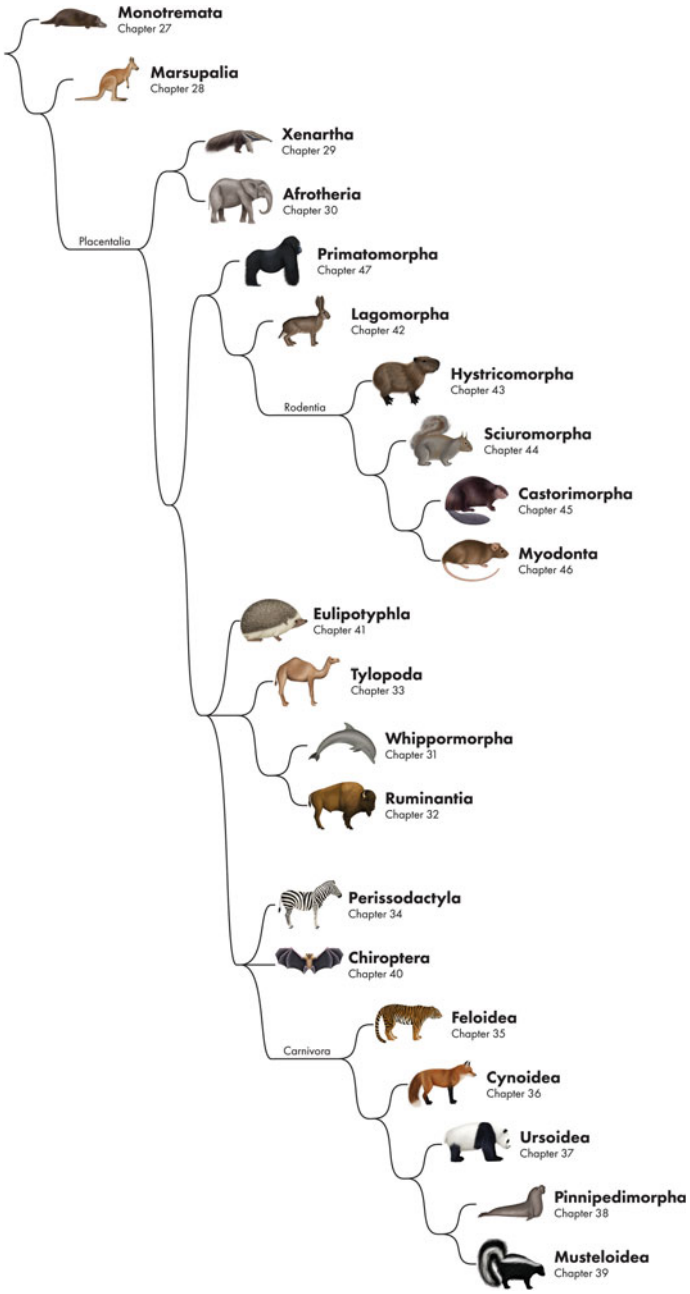

C. E. Rodriguez (✉)
Walt Disney Parks and Resorts, Lake Buena Vista, FL, USA
e-mail: Carlos.e.rodriguez@disney.com

F. Montiani-Ferreira et al. (eds.), *Wild and Exotic Animal Ophthalmology*, https://doi.org/10.1007/978-3-030-81273-7_1

Mammals are a unique and diverse group within the animal kingdom. It is comprised of over 5,000 species and includes as distinct and dissimilar animals as the egg-laying Monotremes, the Marsupials, and the ocean dwelling Cetaceans (McDonald 1984; Wilson and Reeder 2005). This group of animals are believed to have evolved from a primitive reptilian ancestor sometime during the Carboniferous period, the members of the Synapsida family. These primitive reptiles remained a minor player in the world until the sudden disappearance of the dinosaurs in the late Cretaceous period. Several unique skeletal features evolved over time, including modifications of the skull and zygomatic arch to expand the attachment sites for the jaw musculature, and primary development of the dentary bone to become the mandible with its unique articulation to the skull and supporting specialized heterodont teeth. The remaining bones of the complex reptilian jaw are thought to have given rise to the small bones of the inner ear, another mammalian feature (McDonald 1984; Wilson and Reeder 2005). Soft tissue changes also likely followed, such as the development of a novel cutaneous structures, including hair and folliculoadnexal glandular structures; however, these soft tissues are not well preserved in the fossil records. Other characteristically mammalian skeletal changes occurred over time, such as confinement of the ribs to the thoracic cavity, development of a complete diaphragm, modification of the coxofemoral joint for ventral, rather than lateral support of the pelvis as in reptiles, and development of the hard and soft palate. In particular, the development of a complete, imperforate hard and soft palates allowed for the separation of the upper alimentary and respiratory systems. Coupled with the development of another typically mammalian features, the mammary glands, it allows for nutritional support of the mammalian infants (McDonald 1984; Wilson and Reeder 2005). Although not all mammal species retain homeothermy, all are endotherms and generate their own internal body heat. The development of hair allowed for the colonization of cooler habitats and nighttime ecological niches that are generally closed to reptiles. The development of sweat glands, along with other behavioral and physiologic strategies for dissipating excess heat, conferred the ability to adapt to more extreme climatic changes.

The eyes were not exempt from change, and the diversity of the mammalian group is well-exemplified in the great diversity of ocular adaptations. As tetrapods prepared for life on land as amphibians, reptiles, and birds, anatomical changes to the eye became necessary to enable success out of water. Eyelids and a lacrimal system became necessary to prevent desiccation once no longer bathed in water, extraocular muscles provided ocular movement and protection, and improved optics, focusing mechanisms, and increased retinal complexity enabled greater visual acuity. As mammalia began to diversify, first with a group of mammals that defies many of the basic characteristics of this class. The egg-laying Monotremes, including the echidnas and the platypus, have no teeth as adults and the males develop a bony spur that is connected to a modified venom gland (Higgins et al. 2018). Their eyes retain many aspects of the reptilian eye and defy many traditional mammalian characteristics, including the presence of scleral cartilage, a lens annular pad, and an avascular retina with double and single cones containing oil droplets. Marsupials, primarily are endemic to Australia, but can also be found in Africa and in the Americas, began to add vasculature to the retina to accommodate increased thickness and the development of higher visual resolution, such as the North American opossum.

The second most numerous mammalian order is the Chiroptera, or bats, the only mammals capable of true, sustained flight (Buckles 2015; Wilson and Reeder 2005). Approximately 70% of the species of bats are insectivorous while some species are frugivorous. Only a small number of species are hematophagous, making them the only known mammal to be an obligate parasite (Buckles 2015). Bats play an essential role in the ecosystem, not only as insect population control but also playing critical roles as pollinators. Bats are generally divided into two main groups, the Megachiroptera, which include the flying fruit foxes, are generally larger in size, have good eyesight, and feed largely on fruits, nectars, and pollen. The Microchiroptera include smaller bat species adapted to a variety of carnivorous, insectivorous, hematophagous, fruits, and nectar. These tend to have poor eyesight and rely more heavily on echolocation to navigate their environment and find prey (Buckles 2015). With some bats, many of the Megachiroptera, relying heavily on vision for foraging and flight, others developed echolocation and subsequently a decline in vision as evident for much of the Microchiroptera (Schwab 2012). Despite a thick retina in the visually-oriented fruit bats, the retina remains avascular but has choroidal papillations that ensures no portion of the retina is beyond the oxygen diffusion maximum (Schwab 2012).

Further radiations of mammals led to further diversification of the eye. The largest and most diverse mammalian group is the Rodentia, representing approximately half of all placental mammal species (McDonald 1984; Wilson and Reeder 2005; Yarto-Jaramillo 2015). Members of this order are generally characterized by small, compact bodies and short legs. Their weight varies from less than 10 g to over 66 kg and although lifespan is generally short, naked mole-rats can live into their 30s (Wilson and Reeder 2005; Yarto-Jaramillo 2015). Rodents are hosts to a number of important zoonotic diseases. The order Insectivora groups a large assortment of species, typically of small stature with cylindrical bodies and long, narrow snouts that includes the moles, shrews, hedgehogs, tenrecs, and soledons. As most of these

species are fossorial, eyes are small and eyesight is poor. To compensate, these animals have an excellent sense of smell and a variety of tactile appendages along the snout, from vibrissae to Eimer's organ in talpids (D'Agostino 2015). Within the order Carnivora are some of the most recognizable and iconic species of mammals, including canids and felids, the ursids, viverrids, mustelids, hyenids, and pinnipeds. The common and uniting feature of these diverse animals is the presence of carnassial teeth (McDonald 1984). Perissodactylids, Artyodactylids, and the Proboscideans group together the hoofed mammals, from the diminutive mouse deer to the African elephant, the largest terrestrial mammal on the planet. Members of this diverse group of animals have colonized every continent and play a keystone role in many ecosystems (McDonald 1984). The primate order groups together a diverse conglomerate of species that includes the Prosimians, New World and Old World monkeys, and the Great Apes, to which humans belong. Two common evolutionary trends in this relatively recent evolutionary phenomenon are the refinement of the hands and feet for grasping and fine motor control, as well as the shortening of the snout, flattening of the face with less reliance on smell and increased importance on stereoscopic and acute vision (McDonald 1984). Finally, Cetaceans, along with pinnipeds and sirenians, conform a highly specialized group of mammals that have adapted to either an exclusively aquatic or semiaquatic environment. These are thought to have evolved from a terrestrial common ancestor and count amongst its members the largest living creature on the planet, the blue whale (Dold 2015; McDonald 1984). Upon their return to the sea, Cetaceans lost corneal refraction underwater, and became colorblind, a fitting adaptation to an essentially monochromatic environment (Schwab 2012).

Increasing threats from habitat fragmentation and loss, climate change and increasing anthropogenic pressures have resulted in listing of approximately 25% of all mammalian species as threatened by the IUNC (IUCN Red List of Threatened Species). The care and welfare of those under managed care as well as in the wild is as important as ever, and ophthalmic care is no exception. In the subsequent 21 chapters, a discussion of the remarkable diversity of vision, ocular anatomy, and ophthalmology of all 29 mammalian orders is provided.

References

Buckles EL (2015) Chiroptera (Bats). In: Miller RE, Fowler ME (eds) Fowler's zoo and wildlife medicine, vol 8. Elsevier, St. Louis, pp 281–290

D'Agostino J (2015) Insectivores (Insectivora, Macroscelidea, Scandentia). In: Miller RE, Fowler ME (eds) Fowler's zoo and wildlife medicine, vol 8. Elsevier, St. Louis, pp 275–281

Dold C (2015) Cetacea (Whales, dolphins, Porpoises). In: Miller RE, Fowler ME (eds) Fowler's zoo and wildlife medicine, vol 8. Elsevier, St. Louis, pp 422–436

Higgins D, Rose K, Spratt D (2018) Monotremes and Marsupials. In: Terio KA, McAloose D, St. Leger J (eds) Pathology of wildlife and zoo animals. Academic Press, Cambridge, pp 455–456

IUCN Red List of Threatened Species. https://www.iucn.org/resources/conservation-tools/iucn-red-list-threatened-species. Accessed 1 Oct 2019

McDonald D (ed) (1984) The encyclopedia of mammals. Equinox

Schwab IR (2012) Evolution's witness: how eyes evolved. Oxford University Press, Oxford, pp 216–239

Wilson DE, Reeder DM (eds) (2005) Mammal species of the world. A taxonomic and geographic reference, 3rd edn. Johns Hopkins University Press

Yarto-Jaramillo E (2015) Rodentia. In: Miller RE, Fowler ME (eds) Fowler's zoo and wildlife medicine, vol 8. Elsevier, St. Louis, pp 384–422

Ophthalmology of Monotremes: Platypus and Echidnas

27

Benjamin D. Reynolds, Cameron J. Whittaker, Kelly A. Caruso, and Jeffrey Smith

Monotremes are members of the order "Monotremata" and represent the most primitive order of mammals, characterized by certain reptilian features, such as hatching young from eggs and having a single opening for digestive, urinary, and reproductive organs, all while rearing their young from milk like other placental mammals. They are the closest extant relatives to the early synapsid line from which all mammals have derived, and as such, are considered a pivotal group of mammals within evolutionary biology. Order Monotremata includes only five extant species; the platypus (*Ornithorhynchus anatinus*) and four echidna species native to Australia (genus *Tachyglossus*) and Papua New Guinea (genus *Zaglossus*). The ophthalmic anatomy of these monotreme species is unique, having many features that are disparate to the eyes of marsupials and other placental mammals while sharing similarities to the reptilian eye (Newell 1953; O'Day 1938; Schwab 2012). Overall, ophthalmic information in monotremes is extremely limited, with what is known being known discussed below.

Monotreme development occurs primarily within the egg that is laid by the female. By mid-gestation, the embryo's eye is open with early eyelid primordia present, including a partially pigmented retina. By the subterminal pre-hatching stage, the eyelids remain undeveloped, and the retina remains incompletely pigmented. The platypus is born with fused eyelids, which open at a currently unknown period after hatching to form functional lids (Fig. 27.1) (Hughes and Hall 1998).

Ophthalmic examination in monotremes can be challenging for several reasons. Augee et al. (2006) described the echidna as "a remarkably strong animal for its size" due to its musculoskeletal structure. Gates (1973) elucidated the difficulty in restraining echidnas due to their "immense muscular power and body flexibility." Adult male platypuses have spurs on their hindlimbs that secrete venom during the breeding season that can cause severe and long-lasting pain. Echidnas have large spines that surround much of their body and head and can make examination challenging, especially when they curl up (Fig. 27.2a,b). In addition, both platypus and echidna's adult globes are small which makes for a difficult examination, measuring 5.5 mm in axial diameter for the platypus (Newell 1953), and 8–9 mm in axial diameter for short-beaked echidna (Hughes 1977; Augee et al. 2006).

Monotreme eyes are directed forward to some degree, and there is an important overlap of the visual fields and some degree of binocular vision (Augee et al. 2006; Prince 1956). They possess the six extraocular muscles common to all mammals, with most also possessing a retractor bulbi muscle. Monotremes have unique superior oblique musculature. The platypus superior oblique muscle is slightly chondroid in composition, whereas the short-billed echidna has a "slip of muscle" traversing to the nasal aspect of the globe for a wide insertion (Newell 1953; Gates 1973). The platypus has a large and lobulated lacrimal gland in the inferotemporal

B. D. Reynolds · C. J. Whittaker (✉) · K. A. Caruso · J. Smith
Eye Clinic for Animals, Artarmon, NSW, Australia

F. Montiani-Ferreira et al. (eds.), *Wild and Exotic Animal Ophthalmology*, https://doi.org/10.1007/978-3-030-81273-7_2

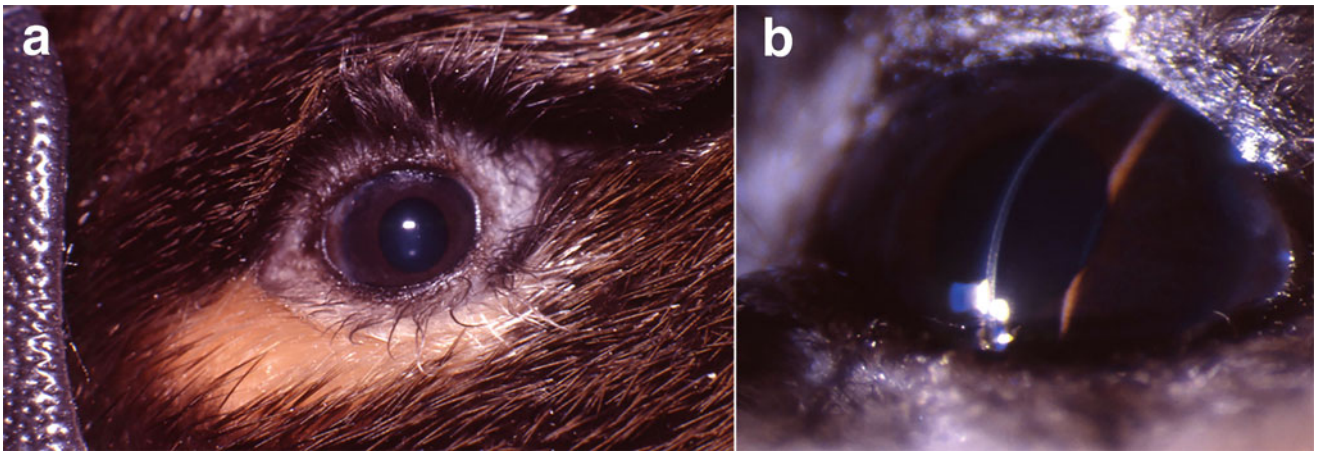

Fig. 27.1 The normal eyes of a platypus (*Ornithorhynchus anatinus*). (**a**) An external photograph displaying the small eye size and lack of cilia. (**b**) A slit beam image displaying a thick cornea. Courtesy of Lawrie Hirst

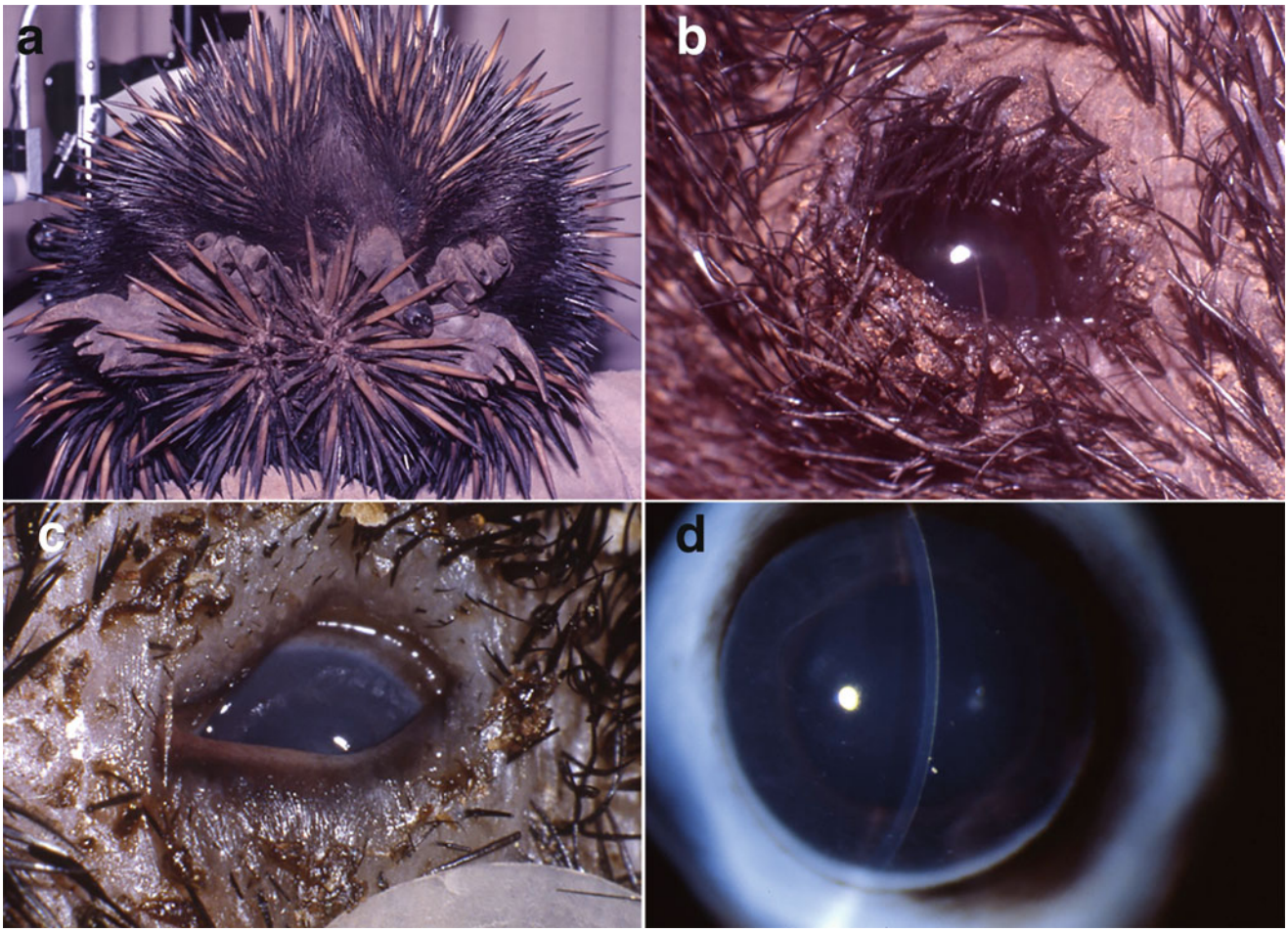

Fig. 27.2 Photographs of clinically normal short-billed echidnas (*Tachyglossus aculeatus*). (**a**) An echidna curling up exposing numerous spines making ophthalmic examination difficult. (**b**,**c**) Normal external photographs of the eyes of echidnas. (**d**) Slit beam photograph of an echidnas showing a thick cornea. *Courtesy of Lawrie Hirst*

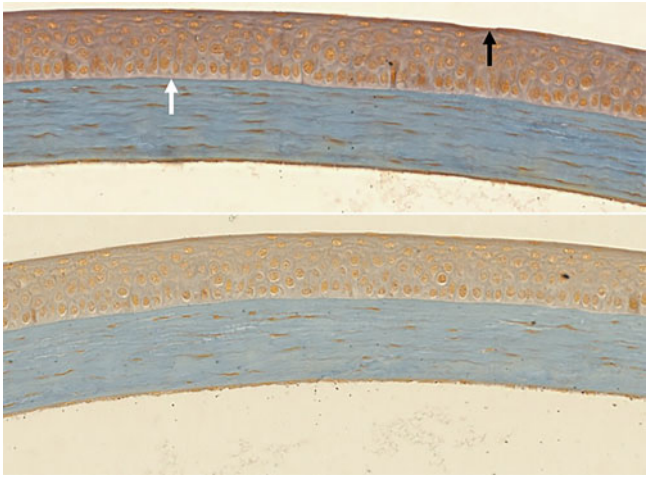

Fig. 27.3 Photomicrographs of the cornea of (**a**) a short-billed echidna (*Tachyglossus anatinus*) and (**b**) a platypus (*Ornithorhynchus anatinus*). Note the thick, stratified squamous corneal epithelial layer (top) relative to the underlying stroma. The echidna cornea (**a**) has a Bowman's membrane (white arrow) and keratinized surface epithelium (black arrow). Trichrome stain, 20× magnification. *Courtesy of the Monash University Kevin O'Day Animal Slides Collection* (https://ilearn.med.monash.edu.au/static/VirtualSlides/ComparativeOccularAnatomy/index.html)

orbit and has a small nictitans gland and a Harderian gland present in the nictitating membrane (Newell 1953; Duke-Elder 1958). Additionally, the orbit of monotremes has the lacrimal bone reduced to nothing more than a simple plate perforated by the nasal canal. The platypus orbit is open, whereas the echidna orbit is closed (Prince 1956).

The platypus possesses a well-developed opaque nictitating membrane that lacks cartilage, whereas the short-billed echidna (*Tachyglossus aculeatus*) lacks a third eyelid entirely (Newell 1953; Gates 1973). Monotremes appear to lack meibomian glands, instead of having densely packed sebaceous glands at the free edge of the eyelid (Newell 1953). The platypus (*Ornithorhynchus anatinus*) lacks all forms of cilia and tarsal plates (Fig. 27.1a), while the short-billed echidna (*Tachyglossus anatinus*) only has an inferior tarsal plate (Fig. 27.2c) (Newell 1953; Gates 1973). The short-billed echidna cornea has a Bowman's membrane and a thick, keratinized stratified squamous corneal epithelium (Fig. 27.3a), similar to that seen in other ant-eating species such as aardvarks and armadillos (Gates 1973). The platypus, on the other hand, lacks a Bowman's layer and has a thick, non-keratinized stratified squamous corneal epithelium (Fig. 27.3b) (Gates 1973). Additionally, the platypus has a deeply pigmented iris that is thin with few vessels on its anterior surface (Newell 1953). All monotremes completely lack a pupillary dilator muscle but have a well-developed pupillary sphincter muscle (Fig. 27.4a) (Gates 1973; Newell 1953). The sclera of monotremes typically can be divided into two portions: the anterior third consisting of collagenous fibers only, and the posterior two thirds containing both collagenous fibers and a cartilaginous cup (Newell 1953) (Fig. 27.4). A hyaline cartilage scleral cup is a feature often observed in avian and piscine eyes but never within mammals beyond the monotremes (Newell 1953). This cartilage in monotremes extends to the level of the ciliary processes (*Ornithorhynchus anatinus),* to the ora ciliaris retinae (*Zaglossus spp*), or immediately posterior to the ora ciliaris retinae (*Tachyglossus spp*). All rectus muscles insert into the posterior cartilaginous region of the sclera due to the apparent lack of rigidity of the scleral collagen, which would otherwise enact accommodation on extraocular muscle contracture (Newell 1953). The cartilaginous cup is perforated to allow for the optic nerve, vasculature, and other nerves to pass. From there, the optic nerve does not enter an optic foramen but rather a large pseudo-optic foramen into the skull (Duke-Elder 1958; Newell 1953).

The lenses of the monotremes are unique regarding their shape, with a flatness index of 2.75 for the short-billed echidna and 1.38–1.50 for the platypus. The flatness of the short-billed echidna's lens is particularly unique, with this value approximating that of higher primates (humans are approximately 2.7) and without accommodation causes hyperopic vision. The lens of monotremes is suspended by zonules to a unique anatomic feature known as the ciliary web (Walls 1942; Gates 1973; Newell 1953). The ciliary web is an interconnection of the ends of ciliary processes forming an annular ring, positioned posteriorly and parallel to the iris (Walls 1942). There is also an apparent lack of ciliary body musculature in the monotreme species (Fig. 27.4); however, retinoscopy in the short-billed echidna demonstrated accommodation (Gates 1973; Newell 1953). Gates (1973) concluded that accommodation in monotreme species is either due to extraocular musculature lengthening the globe or that ciliary body musculature is actually present and anatomic re-examination is required. Nevertheless, in contrast to early reports, the echidna seems to be able to change the accommodate to focus on distant and close objects, suggesting its vision is perhaps more complex than the eye anatomy would indicate (Gates 1973). Further, Gates (1973) also observed that when focusing on nearby objects, short-billed echidnas' eyes would protrude in a relative exophthalmos, likely due to the influence of extraocular musculature. Additionally, the visual cortex of the short-billed echidna seems to be substantially larger than that found in the platypus (Krubitzer et al. 1995; Rowe 1990), supporting the theory that vision plays a substantial role in the biology of this animal. However, these topics require further investigation.

The platypus has a retina that is largely rod dominant, with scarce cones forming a weak visual streak. The cones are both single and double in morphology, with pigmented and clear cone oil droplets present throughout the retina functioning as band-pass filters in this prehistorical retinal model

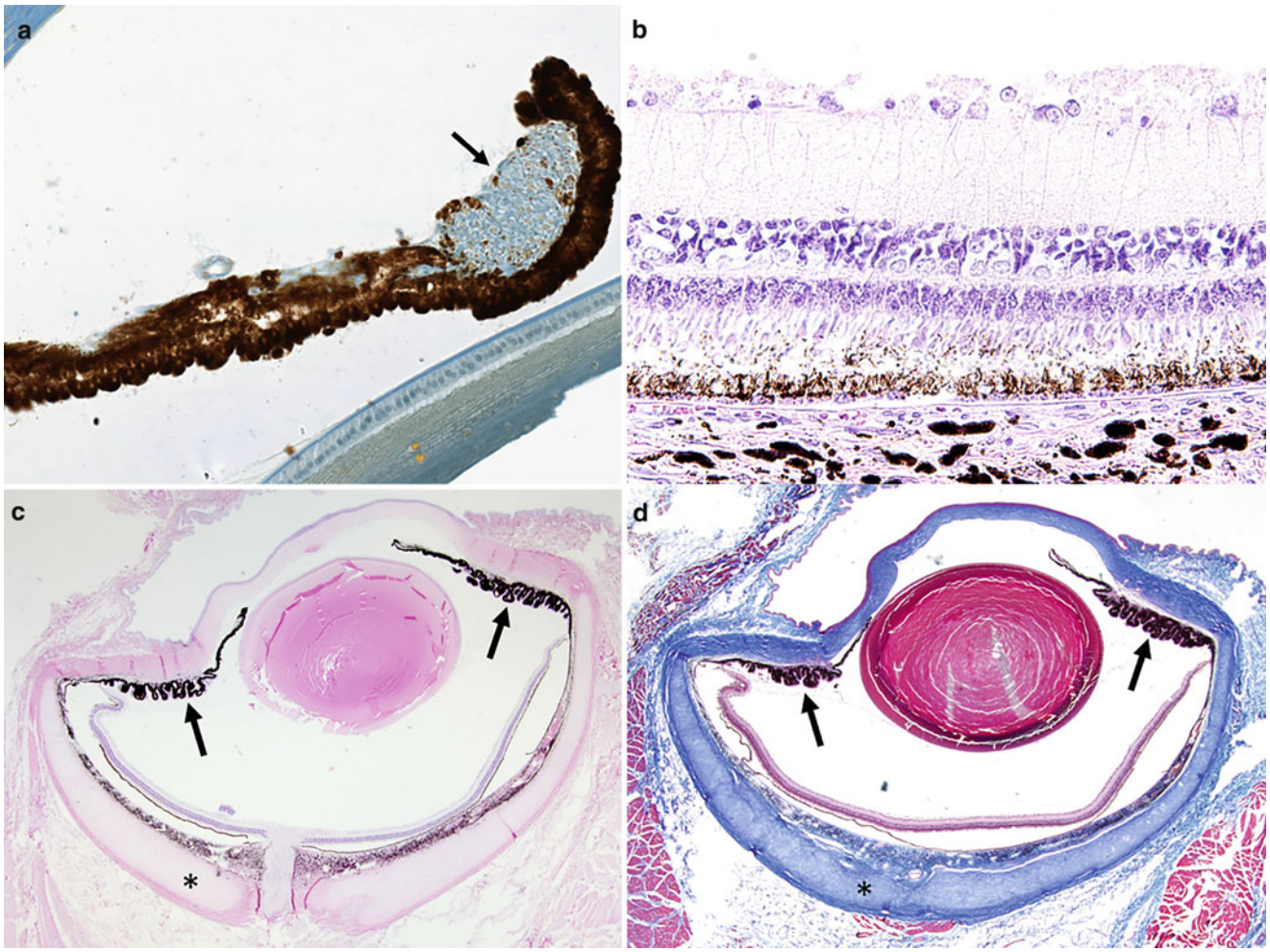

Fig. 27.4 (**a**) Photomicrograph of the iris of a short-billed echidna (*Tachyglossus aculeatus*), displaying the well-developed pupillary sphincter muscle (black arrow) and the absent pupillary dilatory muscle. Trichrome stain, 10× magnification. (**b**,**c**) Histological representation of the eye of the platypus (*Ornithorhynchus anatinus*). (**b**) Retinal cross-section. (**c**, **d**) Subgross parasagittal section of the whole eye showing small vestigial ciliary bodies without apparent ciliary body musculature (black arrows) and scleral cartilage forming the cartilaginous cup (asterisks). Stain B–C: Hematoxylin & Eosin, D: Trichrome. **a**—*Courtesy of the Monash University Kevin O'Day Animal Slides Collection.* (https://ilearn.med.monash.edu.au/static/VirtualSlides/ComparativeOccularAnatomy/index.html). **b**–**d**—*Courtesy of the Comparative Ocular Pathology Laboratory of Wisconsin*

(Zeiss et al. 2011; O'Day 1952). Additionally, the cell bodies of platypus rods and cones contain an equal amount of chromatin, and the inner nuclear layer is thicker than the outer nuclear layer, which are both sauropsidian features and unlike no other group of mammals (Newell 1953). Echidnas do not possess a pure-rod retina as previously thought (O'Day 1952). Cones constitute 10–15% of the photoreceptor population in the short-billed echidna and have all of the typical ultrastructural characteristics of placental mammalian cones. Unlike the cones of the platypus, the cones of the echidna retina do not possess oil droplets (Duke-Elder 1958; Young and Pettigrew 1991; Wakefield et al. 2008). Cone density varies from 9000 cells/mm^2 in the superior periphery to 22,000 cells/mm^2 in the central retina. The cone mosaic in the echidna retina appears to be a result of the presence of single and twin cones in a relatively regular array (Young and Pettigrew 1991). Further, the echidna retinae contain rhodopsin that is dissimilar to mammalian rhodopsins and instead are more similar to other non-mammalian vertebrates such as the chicken or the anole lizard. To compensate for dim-light vision, they may possess further adaptations such as the presence of N83D rhodopsin site mutagenesis, which has been associated with aiding spectral tuning to facilitate dim-light vision (Bickelmann et al. 2012). The echidna and platypus are the only mammalian species that share the long-wave-sensitive-short-wave-sensitive2 pigment gene complex with reptiles, birds, and fishes (Wakefield et al. 2008). Ganglion cell

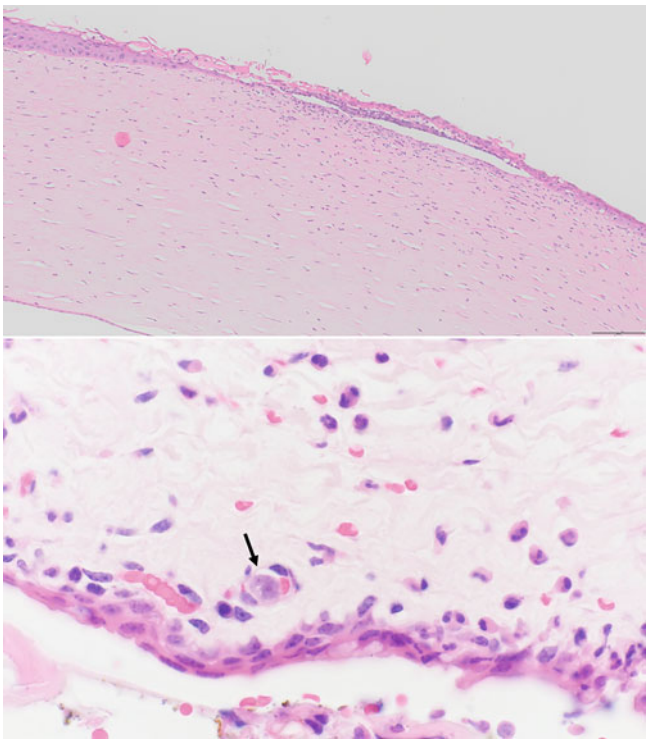

Fig. 27.5 Ophthalmic disease in monotremes. (**a**) A photomicrograph of a corneal ulcer of a short-billed echidna (*Tachyglossus aculeatus*) with severe neutrophilic infiltrate. (**b**) A photomicrograph of the conjunctiva from a short-billed echidna (*Tachyglossus aculeatus*) with severe conjunctivitis. An intravascular schizont is present (black arrow), indicating that the conjunctivitis was likely due to systemic coccidiosis. Stain = Hemotoxylin and eosin stain. *Courtesy of the Australian Registry of Wildlife Health, Taronga Conservation Society Australia*

density is low at only 1800 cells/mm^2 in the short-billed echidna (Arrese et al. 2003). Additionally, platypus' retinas are anangiotic and lack compensatory adaptations such as a pecten, whereas the echidna contains a paurangiotic retina (Newell 1953; Prince 1956).

Ocular disease in monotremes has not been reported. Anecdotal information exists, including corneal ulceration and infectious conjunctivitis (Fig. 27.5). Much greater research is required to understand the role of the eyes in monotreme biology and their propensity for ocular disease.

References

Arrese CA, Rodger J, Beazley LD et al (2003) Topographies of retinal cone photoreceptors in two Australian marsupials. Vis Neurosci 20: 307–311

Augee ML, Gooden BA, Musser AM (2006) Echidna—extraordinary egg-laying mammal. CSIRO Publishing, Collingwood 136 pp

Bickelmann C, Morrow JM, Muller J et al (2012) Functional characterisation of the rod visual pigment of the echidna (*Tachyglossus aculeatus*), a basal mammal. Vis Neurosci 29:211–217

Duke-Elder S (1958) System of ophthalmology: Volume 1- the eye in evolution. Henry Kimpton Publishers, London

Gates GA (1973) Vision in the Monotreme Echidna *Tachyglossus aculeatus*. MSc Thesis, Monash University, Clayton

Hughes A (1977) The topography of vision in mammals of contrasting life style: comparative optics and retinal organisation. In: Crescitelli F (ed) Handbook of sensory physiology, VII/5: the visual system in vertebrates. Springer, Berlin, pp 613–656

Hughes RL, Hall LS (1998) Early development and embryology of the platypus. Philos Trans Royal Soc London B Biol Sci 353:1101–1114

Krubitzer L, Manger P, Pettigrew J, Calford M (1995) The organization of somatosensory cortex in monotremes: in search of the prototypical plan. J Comp Neurol 351:261–306

Newell FW (1953) The eye and ocular adnexa of the monotreme *Ornithorhynchus anatinus*. Trans Am Ophthalmol Soc 51:501–554

O'Day K (1938) The visual cells of the platypus (*Ornithorhynchus*). Br J Ophthalmol 6:321–328

O'Day KJ (1952) Observations on the eye of the monotreme. Trans Ophthalmol Soc Aust 12:95–104

Prince JH (1956) Comparative anatomy of the eye. Springfield, III: Charles C. Thomas; Blackwell Scientific Publications Ltd., Oxford, p 418

Rowe M (1990) Organization of the cerebral cortex in monotremes and marsupials. In: Jones EG, Peters A (eds) Cerebral cortex, vol. 8B: comparative structure and evolution of cerebral cortex, Part II. Plenum Press, New York, pp 263–334

Schwab IR (2012) Mammalia diversifies. Evolution's witness: how eyes evolved. Oxford University Press, New York

Wakefield MJ, Anderson M, Chang E et al (2008) Cone visual pigments of monotremes: filling the phylogenetic gap. Vis Neurosci 25:257–264

Walls GL (1942) The vertebrate eye and its adaptive radiation. Cranbrook Institute of Science Bulletin No. 19. Hills, Cranbrook Press, Michigan

Young HM, Pettigrew JD (1991) Cone photoreceptors lacking oil droplets in the retina of the echidna, Tachyglossus aculeatus (Monotremata). Vis Neurosci 6(5):409–420

Zeiss CJ, Schwab IR, Murphy CJ et al (2011) Comparative retinal morphology of the platypus. J Morphol 272:949–957

Ophthalmology of Marsupials: Opossums, Koalas, Kangaroos, Bandicoots, and Relatives

28

Benjamin D. Reynolds, Kelly A. Caruso, Cameron J. Whittaker, and Jeffrey Smith

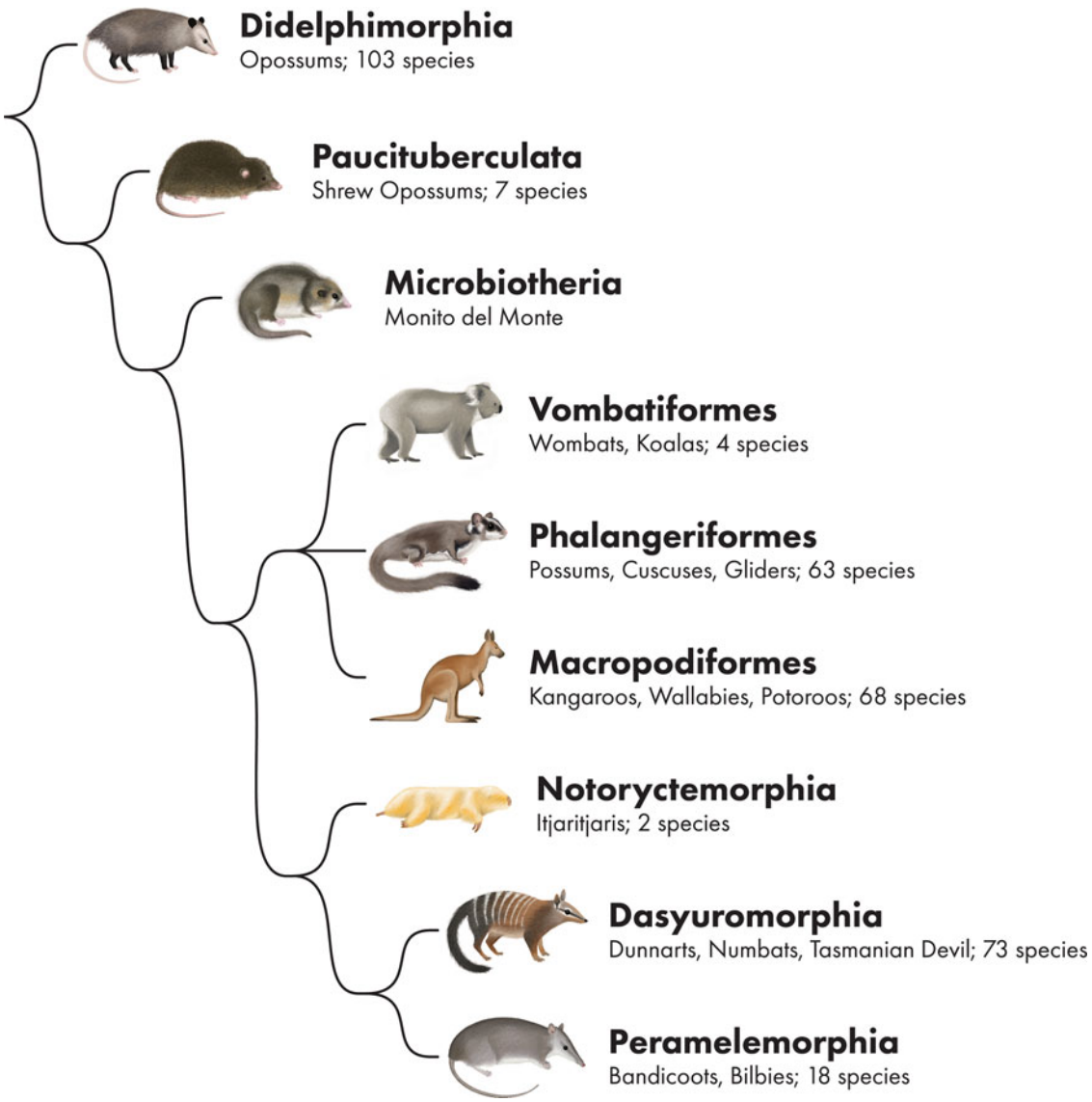

© Chrisoula Skouritakis

B. D. Reynolds · K. A. Caruso · C. J. Whittaker (✉) · J. Smith
Eye Clinic for Animals, Artarmon, NSW, Australia

F. Montiani-Ferreira et al. (eds.), *Wild and Exotic Animal Ophthalmology*, https://doi.org/10.1007/978-3-030-81273-7_3

Introduction

Marsupials are members of the mammalian infraclass "Marsupialia" and are characterized by the presence of a marsupium (or "pouch") on the dam's abdomen, in which their undeveloped young resides after birth. All extant marsupial species are native to the Americas and Australasia, and this group is highly diversified to fill biologic niches within their habitats. Seven marsupial orders are extant, with three being represented in the Americas, and the North American opossum (*Didelphis virginiana*) being the only species present in its title continent. The marsupial group is diverse enough to include domestic cat-sized obligate carnivores such as the tree-dwelling tiger quoll (*Dasyurus maculatus*), while also including the herbivorous tripedal red kangaroo (*Macropus rufus*) whose males can weigh over 90 kg. An example of the anatomic diversity observed in marsupials is such that holangiotic, paurangiotic, and avascular patterns are represented in the retinae of this infraclass (Wislocki 1940; Buttery et al. 1990; Rodger et al. 2001). To add to their uniqueness, some Australian marsupials may be the only non-primate mammals to possess trichromatic vision (Arrese et al. 2002, 2005).

Of the seven marsupial orders (Table 28.1), the Diprotodontia is the largest and perhaps the most diverse, consisting of 155 species in 40 genera. They are the primarily herbivorous marsupials and include kangaroos, wallabies, possums, gliders, wombats, and the koala, among others. They are defined by having a pair of large procumbent incisors on the lower jaw and no lower canines, and syndactyly, or fusion of the second- and third-foot digits up to the claws. Contrarily, the carnivorous marsupials, Dasyuromorphia, consist of over 75 species in 22 genera including the Numbat, Tasmanian devil, quolls, wambengers, and dunnarts. The "omnivorous marsupials," Peramelemorphia, consist of 20 species in 7 genera and include bandicoots and the greater bilby. The greater bilby has very large ears compared to bandicoots and thus may be less visually dependent than bandicoots, and interestingly does not need to drink water (they extract adequate water from food). Notoryctemorphia, the marsupial moles, consists of two species of blind, dwellers of the underground with vestigial eyes. The only member of Microbiotheria is the Mouse opossum, Monito del Monte, and arboreal primarily insectivorous marsupials that look like mice. Finally, Didelphimorphia, the opossums, consists of over 100 species in 19 genera. They are typically omnivorous and are characterized by a prominent sagittal skull crest and long snouts. Interestingly, an involuntary physiologic behavior of "playing dead" may occur when threatened, a reaction that may persist from minutes to even hours. In some ways, one can imagine how ocular examination could be benefited (i.e., by having an immobilized, calm animal) or hindered (with eyelid closure and possible strabismus) by this behavior!

Table 28.1 Orders within the Marsupialia with respective number of genera and species

Marsupial Orders—Scientific Name:	Genera	Species
Didelphimorphia (opossums)	19	103
Paucituberculata (shrew opossums)	1	7
Microbiotheria (mouse opossum)	1	1
Notoryctemorphia (marsupial mole)	1	2
Dasyuromorphia (carnivorous marsupials)	22	75
Peramelemorphia (omnivorous marsupials)	7	20
Diprotodontia (herbivorous marsupials)	40	155

Ocular Development

Marsupials are born drastically under-developed, with the North American opossum (*Didelphis virginiana*) born 13 days after gestation, to resume the majority of their gestational development within the marsupium (Reynolds 1962). Differentiation of the marsupial eye is rapid in the days preceding parturition, as fused eyelids and a vestigial cornea form rapidly in the under-developed neonate to protect the vulnerable eye before refuge is sought within the marsupium (McMenamin and Krause 1993; Hill and Hill 1955; Nelson 1987). To offer an indication of the relative underdevelopment of marsupials at time of birth, the northern quoll (*Dasyurus hallucatus*) is at a gestational stage at birth comparable to where humans (*Homo sapiens)* are 14%, rabbits (*Oryctolagus cuniculus*) are 37% and rats (*Rattus norvegicus*) are 61% through their gestational length (Nelson 1987). The complete neural development of the visual system of marsupials appears to occur during the period of development within the marsupium (Nelson 1987; Kirby et al. 1988; Taylor and Guillery 1994). At postnatal day 9, the North American opossum has an optic nerve of only 2.4% of its adult cross-sectional area, which grows to 30% of adult cross-sectional area by day 75. Simultaneously, the axon populations grow markedly in these developing optic nerves, with approximately 24,000 axons present at postnatal day 5 (approximately 25% of the adult value), before increasing to a maximal count of 267,000 axons at postnatal day 27 (approximately 270% of the adult value). The axons then decrease in number until reaching adult values between postnatal day 50 and 59 (Taylor and Guillery 1994). As seen within other vertebrate species, marsupial intra-ocular pressure decreases with maturity as the relative intra-ocular hypertension observed in young animals may be the driving force of elongation and expansion of the globe (Takle et al. 2010; Whittaker et al. 1995). In the red kangaroo (*Macropus rufus*) the IOP may plateau by 3 years of age, but more work

is needed to document this phenomenon in this species as well as all other marsupial species (Takle et al. 2010).

Ophthalmic Anatomy

The eyes of marsupials display great diversity between species, and so a generalized description of the characteristics of the ophthalmic anatomical regions in this group is impossible to form. Instead, clinically relevant descriptions of specific regions of the eye with information from various studies are provided below.

The orbit of the koala and multiple opossum species lacks a bony roof, and instead possesses an incomplete rim, as the connection between the frontal process of the zygomatic bone and the zygomatic process of the frontal bone is completed by a ligament to allow for greater temporomandibular joint range of motion (Kempster et al. 2002; Wible 2003; Mohamed 2018) (Fig. 28.1). The zygomatic arch of opossums is formed by the temporal process of the zygomatic bone and the zygomatic process of the maxilla and squamosal bones (Mohamed 2018; Wible 2003). The external sagittal crest of the opossum species is prominent, less so in the koala. The larger external sagittal crest is hypothesized to allow for increased chewing strength (Kempster et al. 2002; Wible 2003; Mohamed 2018). The foramina of the skull are similar in opossum species compared to domestic species, except that the maxillopalatine fenestra and the palatal foramen are analogous to the major palatine foramen and the palatine canal, respectively, in domestic animals (Mohamed 2018) (Fig. 28.1b).

Uniquely, in the koala the external carotid artery does not supply the orbital contents but instead enters the orbit by curving around the superficial bones of the skull and

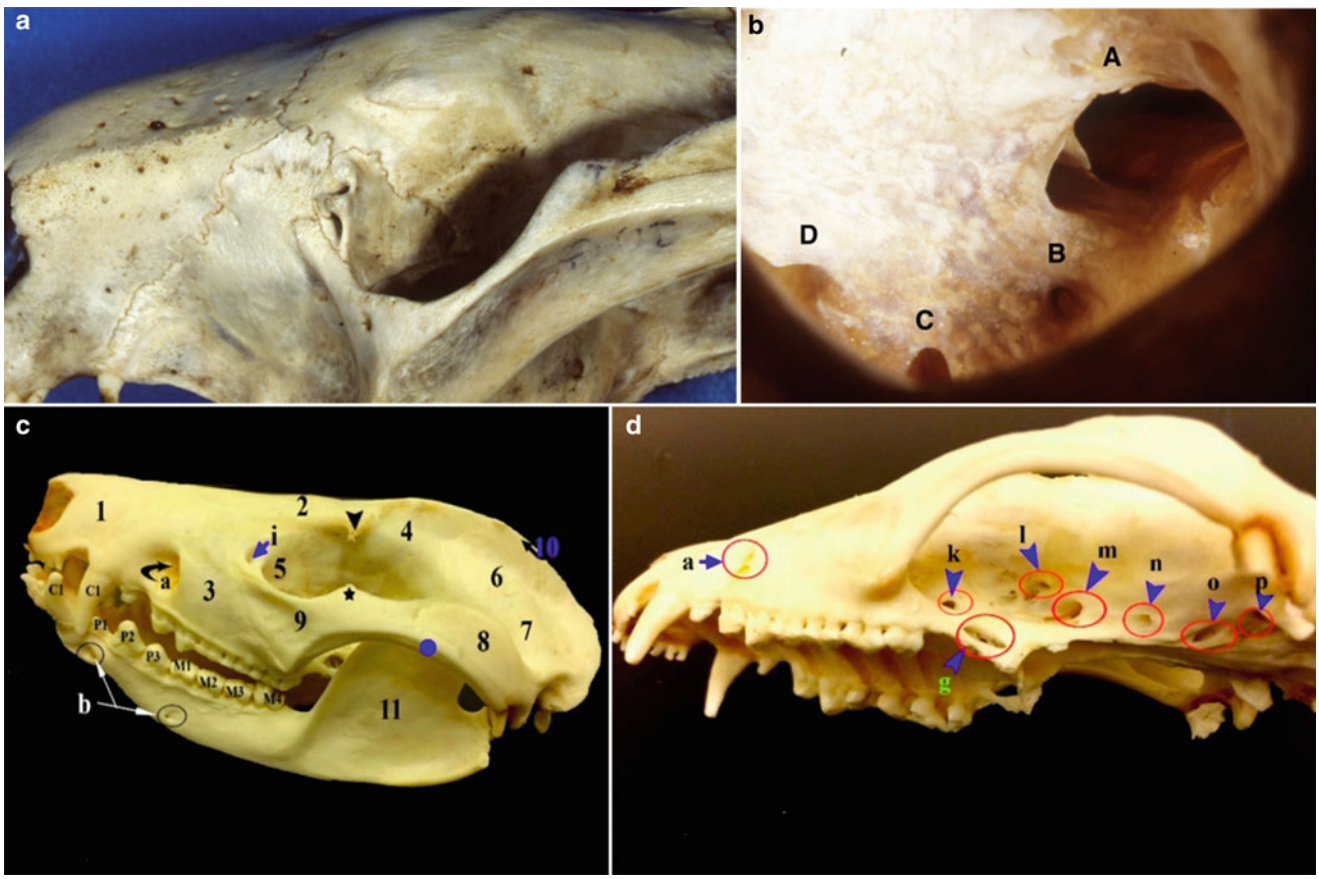

Fig. 28.1 (**a**) The koala (*Phascolarctos cinereus)* has an incomplete orbital rim. (**b**) The orbital foramina of the latero-caudal aspect of the skull of the koala: (A) Common opening of the optic foramen and orbital fissure, (B) rostral alar canal, (C) caudal alar canal, and (D) foramen ovale. (**c**) Photograph displaying the bones of the skull and mandible of the common opossum (*Didelphis marsupialis*): (1) Pre-maxilla, (2) nasal, (3) maxilla, (4) frontal, (5) lacrimal, (6) parietal, (7) squamosal, (8) zygomatic process of squamosal bone, (9) zygomatic, (10) external sagittal crest, (11) mandible, (a) infraorbital foramen, (b) mental foramina, (C1) canine teeth, (P1-3) premolar teeth, and (M1-4) molar teeth. Arrowhead: postorbital process of frontal bone, asterisk: frontal process of zygomatic bone, circle: temporal process of zygomatic bone. (**d**) Photograph showing the foramina in the lateral aspect of the skull of the common opossum (*Didelphis marsupialis*). (A) infraorbital foramen, (G) caudal palatine foramen, (K) sphenopalatine foramen, (L) orbital fissure, (M) foramen rotundum, (N) rostral alar foramen, (O) caudal alar foramen, (P) carotid canal. **a**,**b**—*Courtesy of Lawrie Hirst.* **c**,**d**—*Mohamed R (2018) Anatomical and radiographic study on the skull and mandible of the common opossum (Didelphis marsupialis Linnaeus, 1758) in the Carribbean. Vet Sci 5:44*, used with permission

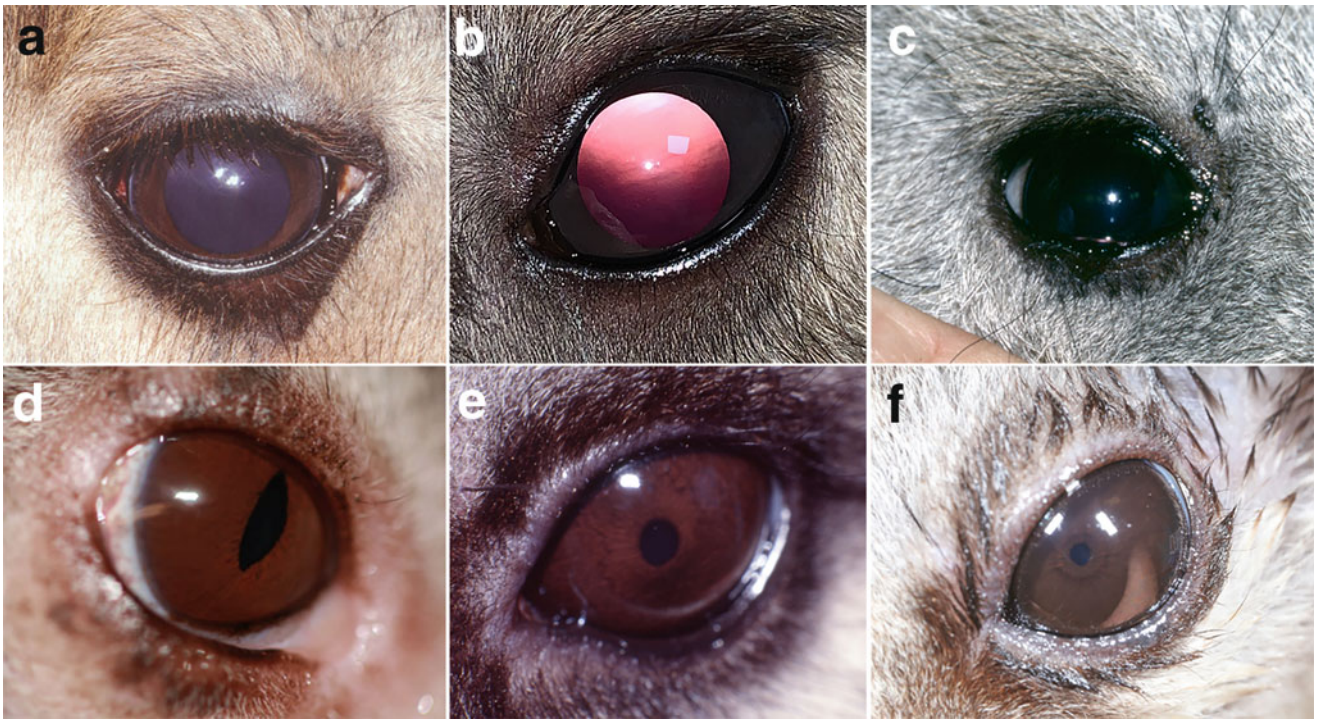

Fig. 28.2 External photographs of normal marsupial eyes. (**a**) Western gray kangaroo (*Macropus fuliginosus*), (**b**) Eastern gray kangaroo (*Macropus giganteus*), (**c**) Wombat *(Vombatus ursinus),* (**d**) Koala (*Phascolarctos cinereus*), (**e**) Common brushtail possum (*Trichosurus vulpecula*), (**f**) Sugar glider (*Petaurus breviceps*). **a**—C*Labelle AL, Low M, Hamor RE, Breaux CB, Langan JN, Zarfoss MK, Zachariah TT (2010) Ophthalmic examination findings in a captive colony of western gray kangaroos (Macropus fuliginosus). J Zoo Wildl Med 41(3):461–467*, used with permission. **b**—*Courtesy of Kelly Caruso.* **c**—*Courtesy of Jeffrey Smith.* **d**—*Liddle VL (2015) Electroretinography in the normal koala (Phascolarctos cinereus). Vet Ophthalmol 18:74–80*, used with permission. **e**—C*ourtesy of Lawrie Hirst.* **f**—Courtesy of *Bret A. Moore*

branching to supply the temporal muscles, eventually becoming the maxillary artery. The arterial supply to the koala orbit is solely derived from one of two internal branches of the internal carotid artery, entering the orbit via the orbital fissure. The other branch turns posteriorly and contributes to the circle of Willis. Further, the koala contains a massive venous sinus located immediately beneath the periorbital membrane, and is responsible for the drainage of orbital venous blood through the orbital fissure to form an intracranial rete (Kempster et al. 2002).

Marsupials possess the six extra-ocular muscles common to all mammals, with most also possessing a retractor bulbi muscle. The koala has a particularly well-developed retractor bulbi muscle, and a unique orientation of the lateral rectus muscle as it contains a double tendinous origin from the roof and floor of the orbital fissure, allowing major nerves including the optic nerve, blood vessels, and the muscle body of the retractor bulbi to enter the rectus cone between this muscle division (Kempster et al. 2002).

Lacrimal glands are located dorso-temporally to the globe, with nictitans glands present and Harderian glands absent. Some variation in the appearance of these glands is observed between species. The koala has a small lacrimal gland, and a very large nicititans gland that extends almost the entire diameter of the globe. Both glands are slightly lobulated in appearance (Kempster et al. 2002). The Sulawesi bear cuscus has a small triangular-shaped lacrimal gland, and a ventromedially positioned nicitans gland. Both glands are pink, flat, and uniform (Kleckowska-Nawrot et al. 2019). Superficial lymphatic drainage of the koala orbit consists of rostral mandibular lymph nodes, mandibular lymph nodes, and superficial parotid lymph nodes draining from the lower palpebral region of the eye (Hanger and Heath 1991).

The eyelid cilia of the Western gray kangaroo (*Macropus fuliginosus*) are thick and black extending from the upper lid, and males can have fine cilia extending from the lower lid, with superior and inferior vibrissae present (Labelle et al. 2010a) (Fig. 28.2a). The Eastern gray kangaroo (*Macropus giganteus*) is similar (Fig. 28.2b). The koala (*Phascolarctos cinereus*) has two rows of darkly pigmented long cilia of the upper eyelid, and scarce cilia of the lower lid and a largely undeveloped tarsal plate (Hirst et al. 1992a) (Fig. 28.2d). The Sulawesi bear cuscus (*Ailurops ursinus*) has short and thin cilia of only the superior eyelid (Kleckowska-Nawrot et al. 2019). Marsupials possess ventro-medially located nictitating membranes, with the koala (*Phascolarctos cinereus*) having a thin membrane extending only 3–5 mm from the medial canthus, whereas the Western gray kangaroo has a thicker and more prominent membrane (Hirst et al. 1992a; Labelle et al. 2010b). A single ventral lacrimal punctum is typical

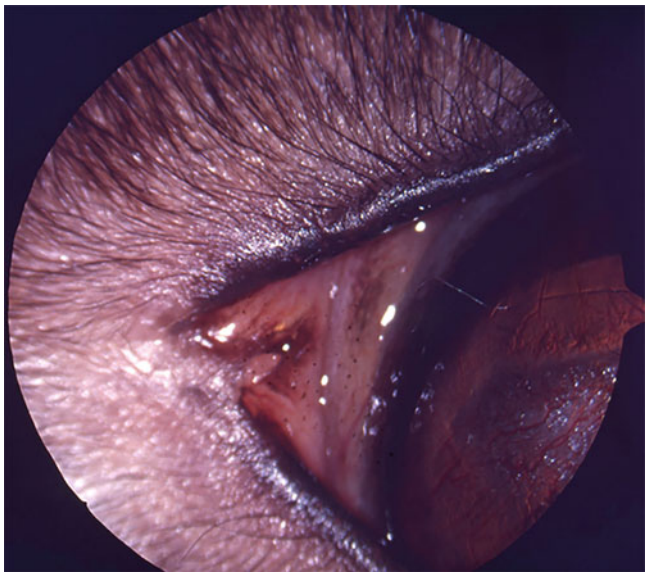

Fig. 28.3 A normal, single lacrimal punctum of a common brushtail possum (*Trichosurus vulpecula*). *Courtesy of Jeffrey Smith*

(Fig. 28.3). Marsupials generally have a cornea that is analogous to other mammalian eyes (Fig. 28.4). Marsupials contain a fibrous sclera without cartilaginous or osseous support. The koala has an axial globe length of 12.6 mm (Hirst et al. 1992a) with a shallow anterior chamber. The pupil is vertically ovoid pupil and the iris is heavily pigmented and contains deep crypts and a vast array of radial vasculature (Hirst et al. 1992a). The Western gray kangaroo and the red kangaroo have a large and circular pupil, with a heavily pigmented dark brown iris (Labelle et al. 2010a; Takle et al. 2010). Some koalas have irides that will not dilate via application of topical tropicamide; however, kangaroo species dilate with ease (Hirst et al. 1992b; Stanley 2002; Labelle et al. 2010a). The ciliary body and ciliary musculature are present and well developed in marsupial species (Duke-Elder 1958). The lenses of Australian diurnal marsupials contain Mu-crystallin, which is a normal component of mammalian retinas (Segovia et al. 1997). This protein is absent from Australian nocturnal marsupials and lenses of any other species, and it is unclear why Australian diurnal marsupials require this adaptation.

The choroid of marsupials is typical of mammals, however a few species including the quoll (*Dasyurus* genus) and the Tasmanian devil (*Sarcophilus harrisii*) have a tapetum fibrosum. Further, the North American opossum has a retinal tapetum, a unique feature not found elsewhere among mammals outside of the fruit-bat genus *Pteropus* (Duke-Elder 1958). The retinal vascularization patterns observed in marsupials vary largely, with the diprotodont group (koala, wombats, possums, macropods, and others) generally being paurangiotic, whereas the polyprotodont group (Tasmanian devil, fat-tailed dunnart, North American opossum, bandicoot, and others) generally possessing a holangiotic retinal vascular supply (Wislocki 1940; Chase 1982; Buttery et al. 1990; Rodger et al. 2001) (Fig. 28.5). Avascular retinae are much thinner than vascular retinae in total, with the inner-plexiform layer being particularly reduced in thickness when avascular (Buttery et al. 1991). Many species have a pronounced vascular tuft sitting over the optic nerve head, possible more common in young (Fig. 28.6). The intraretinal blood vessels of marsupials are very unique, as they display a "paired end artery vascular pattern" where vessels penetrate the retina and branch to form paired capillaries that can extend as far as the outer nuclear layer (Fig. 28.7). These capillary pairs then terminate to form blind-ended hairpin loops. The same paired end artery vascular pattern is displayed throughout the entire central nervous system of mammals (McMenamin 2007; Craigie 1939).

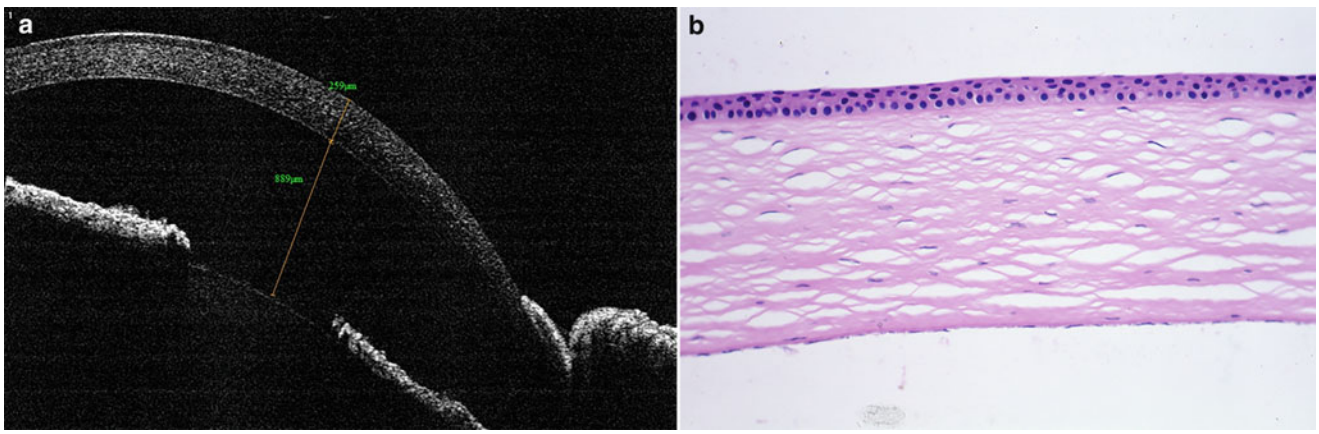

Fig. 28.4 The normal cornea of marsupials. (**a**) Ocular coherence tomography RTVue of the anterior segment of a normal juvenile long-nosed bandicoot (*Perameles nasuta*), with central corneal thickness of 259 μm and an anterior chamber depth of 889 um. (**b**) Photomicrograph demonstrating the normal corneal histology of a common brushtail possum (*Trichosurus vulpecula)*, which is comparable to that of other marsupials. **a**—*Courtesy of Benjamin Reynolds and Eye Clinic for Animals Australia*. **b**—*Courtesy of Jeffrey Smith*

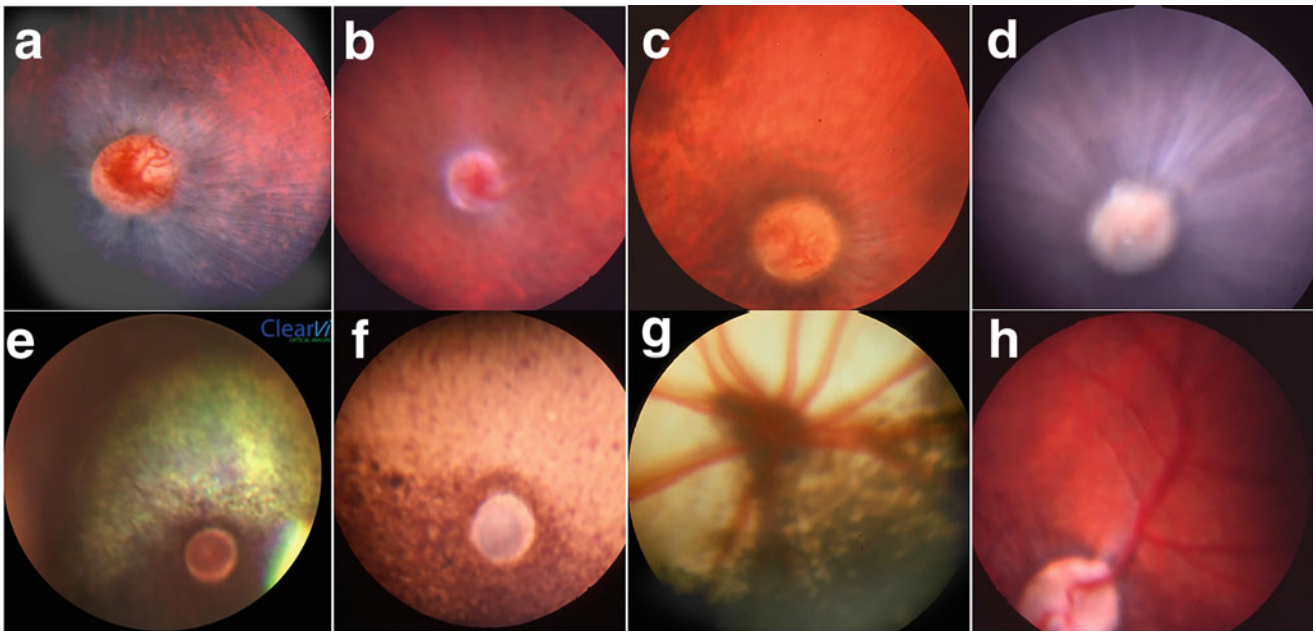

Fig. 28.5 Fundic photographs of normal retinae free of pathology in marsupials. (**a**) Red kangaroo (*Macropus rufus*), (**b**) Common spotted cuscus (*Spilocuscus maculatus*), (**c**) Goodfellow's tree kangaroo (*Dendrolagus goodfellowi*), (**d**) Common wombat (*Vombatus ursinus*), (**e**) Koala (*Phascolarctos cinereus*), (**f**) Common brushtail possum (*Trichosurus vulpecula*), (**g**) North American opossum (*Didelphis virginiana*), (**h**) Tasmanian devil (*Sarcophilus harrisii*). Note the paurangiotic retinae present in the diprotodont group of **a**–**f** whereas the polyprotodont group of **g**–**h** contain holangiotic retinae. **a**, **e**, **g**—*Courtesy of Bret A. Moore and the University of California Davis Comparative Ophthalmology Service.* **b**, **c**, **d**, **f**, **h**—*Courtesy of Jeffrey Smith*

Funduscopically, kangaroos (*Macropus* genus) have an atapetal fundus with retinal vessels extending a short distance circumferentially over the optic disc before tapering away over the orange and non-pigmented fundus (Labelle et al. 2010a; Takle et al. 2010; Reddacliff et al. 1999) (Fig. 28.5a). Myelination of the *Macropus* nerve fiber layer can be seen extending two to three optic disc diameters from the optic disc, particularly in the horizontal plane (Stanley 2002). Koalas have a pigmented ventral non-tapetal fundus, and a green to gray colored tapetum dorsally. Three retinal vessels can occasionally be observed over a pale optic disc ophthalmoscopically, but often are difficult to visualize (Stanley 2002; Hirst et al. 1992b). The gray short-tailed opossum (*Monodelphis domestica*) has radial vasculature that expands the entire retina and a lightly pigmented RPE allowing for some choroidal vasculature to be observed ophthalmoscopically (McMenamin et al. 2017). The optic chiasm of marsupials differs from eutherians, with uncrossed fibers segregating from crossed fibers prechiasmatically in marsupials (Guillery et al. 1999).

Marsupials possess both a visual streak and an area centralis, with a horizontal band of high retinal ganglion

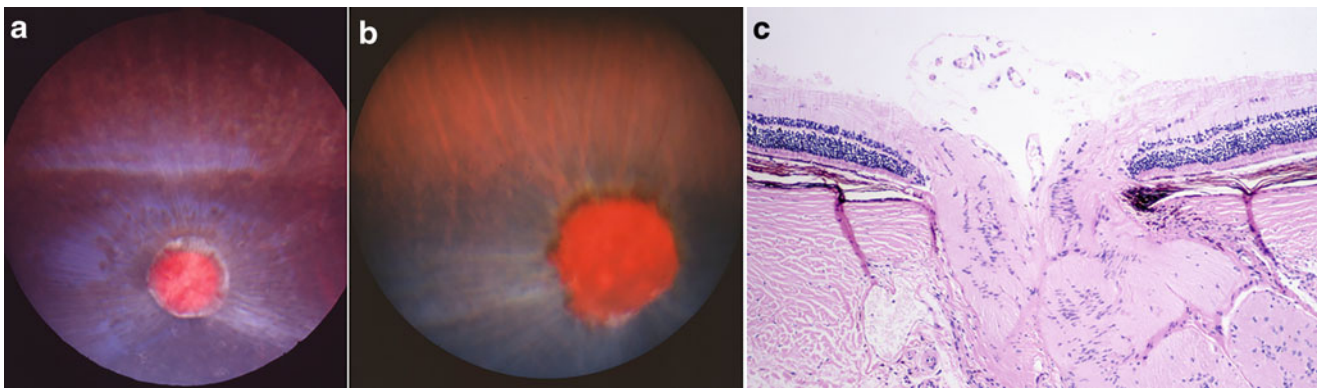

Fig. 28.6 Vasculature overlying the optic disc in marsupials. (**a**) An adult red kangaroo (*Macropus rufus*) with normal pre-optic disc vasculature. (**b**) A normal Bennett's wallaby (*Macropus rufogriseus*) joey with marked but normal pre-optic disc vasculature. (**c**) Histologic section of an adult common brushtail possum (*Trichosurus vulpecula*) showing a vascular tuft overlying the optic nerve head. Stain: hematoxylin and eosin. *Courtesy of Jeffrey Smith*

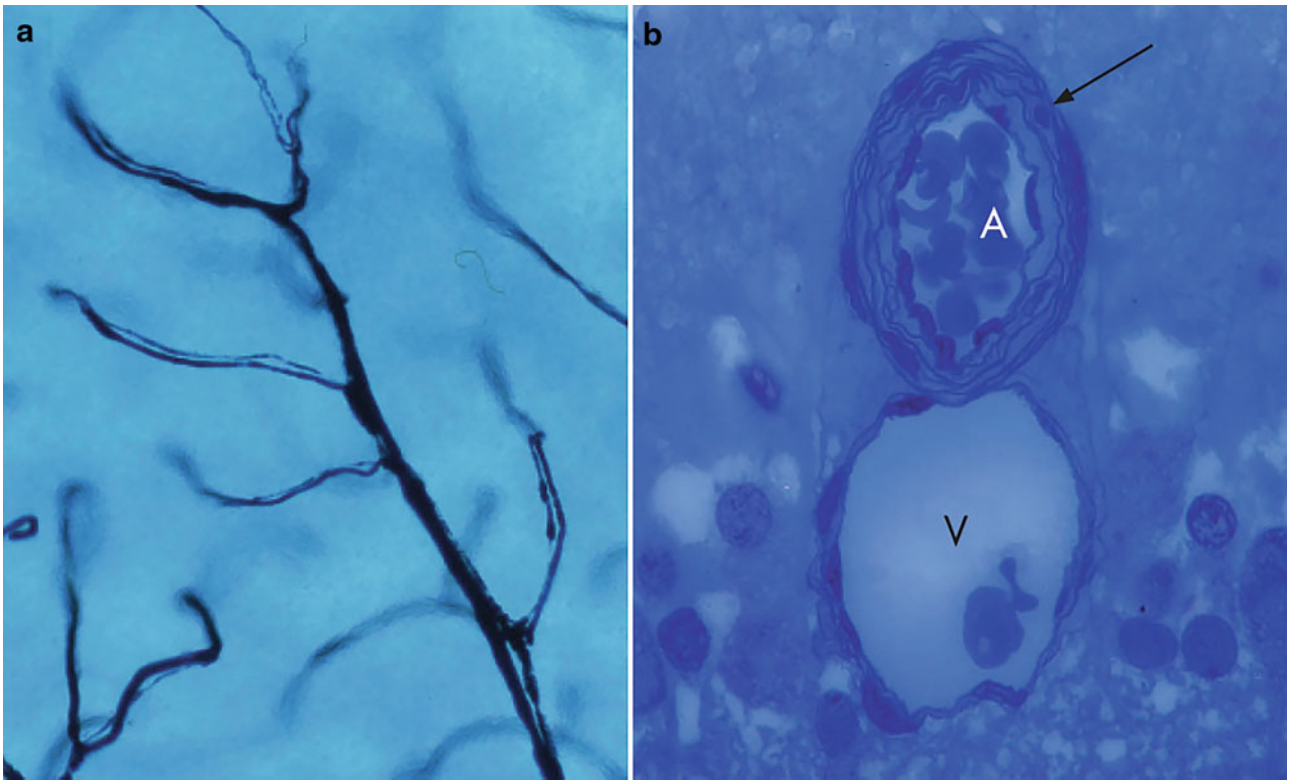

Fig. 28.7 (**a**) The retinal vasculature of the North American opossum (*Didelphis virginiana*) seen in carbon-filled vascular preparations, displaying the paired end artery vascular pattern in a semi-thin section. (**b**) A retinal artery (A) present in the adult numbat (*Myrmecobius fasciatus*) paired with an adjacent vein (V). Note the large number of smooth muscle layers in the artery wall with elastic lamina intervening in a semi-thin section. *Courtesy of Paul McMenamin*

cell and photoreceptor density expanding across the retina with a further increase in concentration at a temporally, respectively. However, the degree of development of these two features varies largely between species (Freeman and Tancred 1978; Tancred 1981; Arrese et al. 2003, 2005; Vlahos et al. 2014). Marsupials are mostly dichromatic, however some Australian marsupials have been found to display trichromacy, which makes them the only non-primate mammal to do so (Arrese et al. 2002, 2005) (Fig. 28.8). Despite dichromacy, some marsupial species likely have a very limited spectrum of useful color vision (Jacobs and Williams 2010).

Retinal ganglion cell density varies greatly between species, which speaks to the vast behavioral differences and evolutionary diversity within the group (Fig. 28.9). The fat-tailed dunnart (*Sminthopsis crassicaudata*) contains a rod dominant retina, with ratios of 40:1 to cones within the area centralis. The presence of a visual streak in the fat-tailed dunnart raises questions surrounding the function of the visual streak in mammals, as it once was believed to be advantageous only in species with a field of view not completely obscured by vegetation, as the fat-tailed dunnart's often is (Arrese et al. 2002) (Fig. 28.9d). To demonstrate the diversity of the retinal projections of other marsupial species, the hairy-nosed wombat (*Lasiorhinus latifrons*) contains a visual streak but lacks an area centralis (Fig. 28.9e), whereas the honey possum (*Tarsipes rostratus*) contains a vestigial visual streak, but a pronounced area centralis (Arrese et al. 2003; Tancred et al. 1981) (Fig. 28.9f). The sugar glider (*Petaurus breviceps breviceps*) contains a largely rod-dominated retina, with functional similarities on ERG testing similar to behaviorally similar species, such as diurnal rat species (Akula et al. 2011) (Table 28.2).

Diagnostic Tests

STT and IOP values have previously been described in few marsupial species to date. Further works should be focused on expanding upon the knowledge of these normative values in other marsupial species. The summary of these previous works can be found in Table 28.3 and Appendix 3.

Normal electroretinogram (ERG) values have been established in numerous marsupial species previously (Fig. 28.10). The koala when tested with a light of 3000 mcd.m/s^2 generated an a-wave peak of 70.5 ± 30.7 uV and a b-wave peak of 122.8 ± 49.3 uV, and when tested with a light of 10,000 mcd.m/s^2 an a-wave

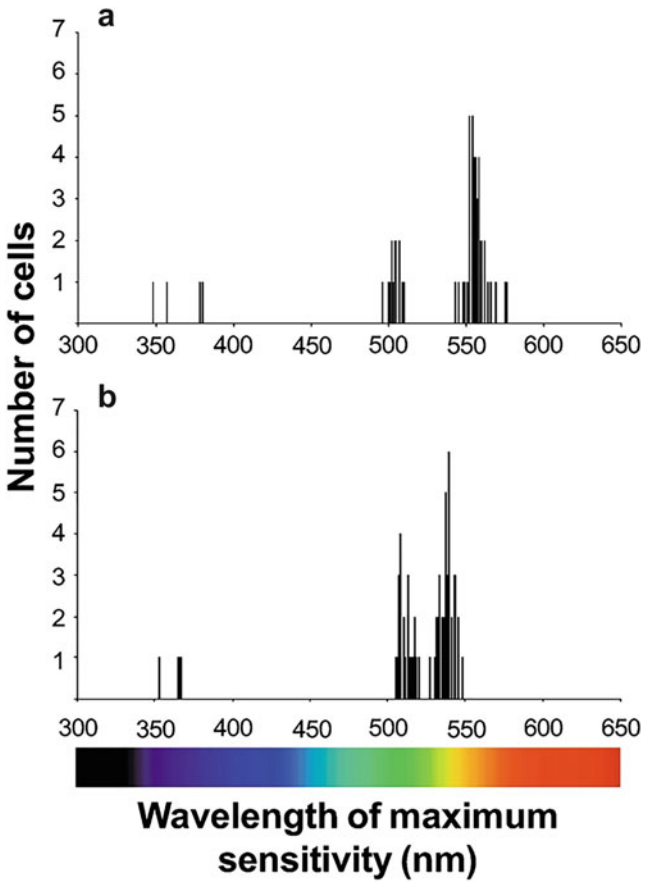

Fig. 28.8 Frequency histograms showing the distribution of the λmax from cones in trichromatic species, (**a**) the honey possum (*Tarsipes rostratus*) and (**b**) the fat-tailed dunnart (*Sminthopsis crassicaudata*) **b**—*Arrese CA, Hart NS, Thomas N et al (2002) Trichromacy in Australian marsupials. Curr Biol 12:657–660*, used with permission

peak of 90.8 ± 37.2 uV and a b-wave peak of 148.3 ± 54.9 uV were created (Liddle 2015) .The western gray kangaroo when tested with a light of 3000 mcd.s/m^2 generates an a-wave peak of 69.9 ± 20.5 uV and a b-wave peak 175.4 ± 35.9 uV, and when tested with a light of 10,000 mcd.s/m^2 an a-wave peak of 89.1 ± 27.1 uV and a b-wave peak of 203.7 ± 41.4 uV are generated (Labelle et al. 2010b). The sugar glider (*Petaurus breviceps breviceps*) had a-wave peaks at −127 ± 22 uV, and b-wave peaks at 87 ± 9 uV when tested with a flash of 7.4 × 10^5 photons um^{-2} saturating the cornea (Akula et al. 2011). Interestingly, a cone a-wave or cone b-wave could not be elicited from the sugar glider, presumed to be due to the small number of cone bipolar cells present. A single Matschie's tree kangaroo (*Dendrolagus matschiei*) has previously been evaluated, with an a-wave amplitude range of 29–51 uV, with implicit times of 19–21 ms and B-wave amplitudes of 62–111 uV (McLean and Zimmerman 2015).

Sedation and Anesthetic Protocols

As there are many marsupial species, there are a plethora of varying sedation and anesthetic protocols that have been previously reported. This summary is by no means comprehensive, but should serve as a guide for appropriate drug dosages within these species. Often within these species, sedation is required at a minimum to perform an ophthalmic examination.

- Eastern gray kangaroo: Author's experience
  - Intramuscular sedation: 0.5–2.0 mg/kg to facilitate intravenous catheterization, and 0.02 mg/kg glycopyrrolate 2–4 min before induction.
  - Anesthesia: Alfaxalone intravenous injection 1–5 mg/kg to effect, intubate with non-cuffed endotracheal tube with xylocaine gel on tube's end. Maintenance via isoflurane on a non-rebreathing circuit.
- Koala (*Phascolarctos cinereus*): Liddle (2015)
  - Intramuscular sedation: 2 mg/kg alfaxalone.

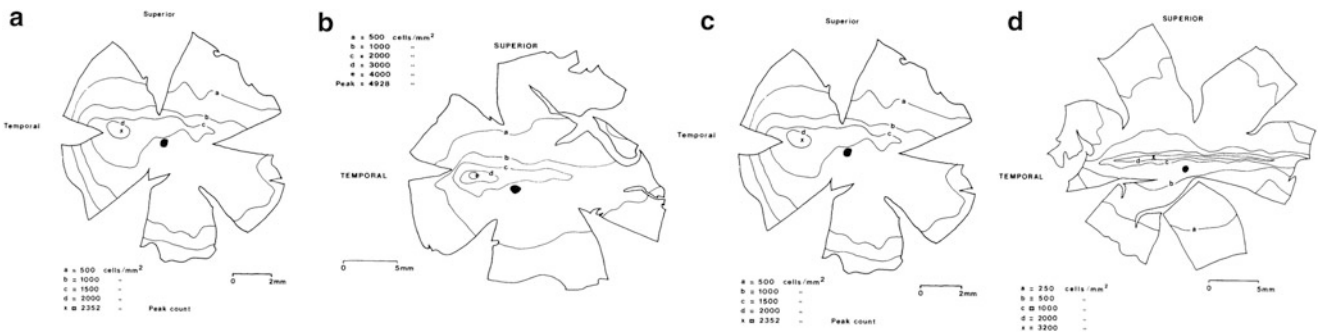

Fig. 28.9 Retinal topographic maps of ganglion cell densities in various marsupial species. Weak visual streaks with a temporal area centralis typical of marsupials exemplified by the (**a**) Tasmanian Devil (*Sarcophilus harrisii*), (**b**) Pademelon wallaby (*Thylogale billiardieri*), (**c**) Brown bandicoot (*Isoodon obesulus*), and the Fat-tailed dunnart (*Sminthopsis crassicaudata*) (not shown). Other species have an elongated visual streak but lack a defined area centralis, such as the (**d**) Hairy-nosed wombat (*Lasiorhinus latifrons*), whereas others have no defined visual streak but a prominent area centralis, such as the honey possum (*Tarsipes rostratus*) (not shown). **a–c**, **d**—*Tancred E. The distribution and sizes of ganglion cells in the retinas of five Australian marsupials. J Comp Neurol. 1981*;196:585–603, used with permission

Table 28.2 Comparison of the types and combinations of retinal specializations formed by ganglion cell density, peak retinal ganglion cell densities (cells/mm^2), visual acuity (cycles/degree), rod:cone ratio, presence of a tapetum, and with of the binocular field (degrees)

Common Name	Scientific name	Retinal specialization	Peak RGC density	Visual acuity	Rod:Cone ratio	Tapetum	Binocular field width
South American opossum	*Didelphis marsupialis aurita*	Area, weak streak	2900	1.25	130:1	Yes	125 degrees
North American opossum	*Didelphis virginiana*	Area, weak streak	2700		50:1	Yes	125
Common Brushtail possum	*Trichosurus Vulpecula*	Area, streak	5000	4.8		Yes	125
Honey possum	*Tarsipes rostratus*	Weak area	9000	0.75		No	90
Tammar wallaby	*Macropus eugenii*	Area, streak	5600			No	60
Quokka	*Setonix brachyurus*	Weak area, streak	5000		20:1	No	80
Fat-tailed dunnart	*Sminthopsis crassicaudata*	Area, streak	8300	2.3	40:1	No	140

Modified from Arrese et al. (1999)

  - Anesthesia: After sedation, administer isoflurane via a face mask to achieve an adequate anesthetic plane to allow intubation and maintenance on isoflurane.
- Sugar glider (*Petaurus breviceps breviceps*): Akula et al. (2011)
  - Anesthesia: animal placed in an induction chamber of 97% oxygen, 3% isoflurane at a flow rate of 0.9 L/min for induction, then a face mask used 2% isolfurane at a flow rate of 0.41 L/min.
- Western gray kangaroo (*Macropus fuliginosus*): Labelle et al. (2010b)
  - Intramuscular sedation: medetomidine 50 ug/kg, ketamine 2 mg/kg.
  - Anesthesia: following the above sedation protocol, isoflurane can be delivered via a facemask for approximately 5 min before intubation and maintenance on isoflurane anesthesia.
- Matschie's tree kangaroo (*Dendrolagus matschiei*): Mclean and Zimmerman (2015)
  - Intramuscular sedation: medetomidine 62 ug/kg, ketamine 3.9 mg/kg, butorphanol 0.13 mg/kg.
  - Anesthesia: following the above sedation protocol, intubation is possible and maintenance on isoflurane anesthesia can be commenced.

Ophthalmic Disease

The non-eutherian mammals possess many unique ophthalmic anatomical features, and fittingly have several conditions related to their unique anatomy. However, there are many conditions that share common similarities with domestic mammals. This section provides an overview of ophthalmic disease within these animals.

Adnexal and Nictitating Membrane Conditions

Poxvirus infections, transmitted by a mosquito vector, cause cutaneous raised wart-like lesions on the eyelids of many macropod species. The Eastern grey kangaroo poxvirus (EKPV) and Western gray kangaroo poxvirus (WKPV)

Table 28.3 Established STT and IOP values for selected marsupial species

Species	STT-1 (mm/min)	IOP (mmHg)
Red kangaroo[a](*Macropus rufus*)	22.6 ± 6.07	17.45 ± 7.23 (*<3 years old)*14.33 ± 3.99 (*>3 years old*)
Koala[b](*Phascolarctos cinereus*)	10.3 ± 3.6 (*conscious)*13.8 ± 3.4 (*anesthetized*)	15.3 ± 5.1 (*conscious*)13.8 ± 3.4 (*anesthetized*)
Western gray kangaroo[c](*Macropus fuliginosus*)	–	8.62 ± 2.12 (*rebound*)13.50 ± 3.50 (*applanation*)
White-eared opossum[d](*Didelphis albiventris*)	0.00 ± 1.63 (*juvenile)*	–
Brazilian common opossum[d](*Didelphis aurita*)	0.00 ± 1.63 (*juvenile*)	–

[a]Takle et al. (2010)
[b]Grundon et al. (2011)
[c]Labelle et al. (2010a)
[d]Oria et al. (2019)

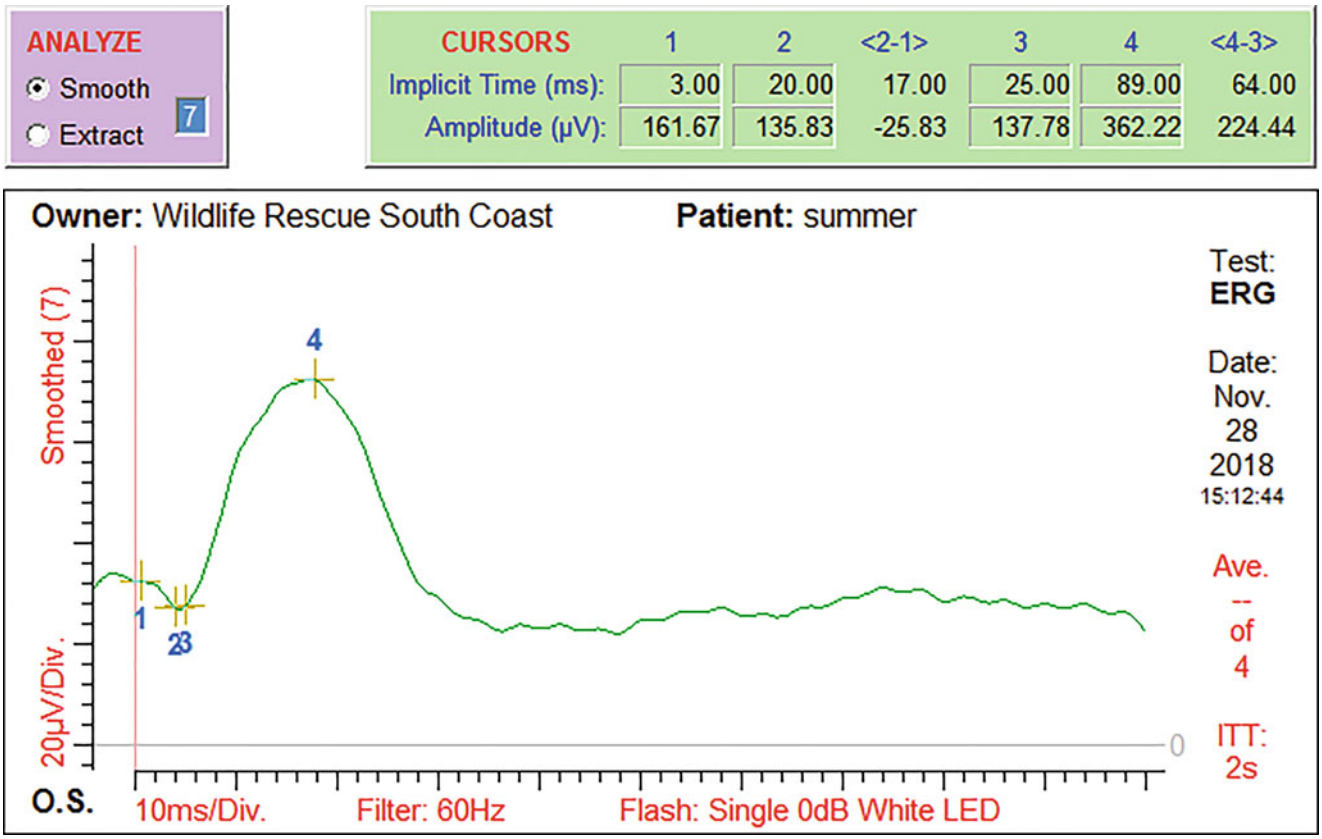

Fig. 28.10 An example of an ERG recorded on an Eastern gray kangaroo (*Macropus giganteus*) joey in the pre-operative assessment prior to surgical lensectomy via phacoemulsification. 1–2 amplitude: a-wave, 3–4 amplitude: b-wave. *Courtesy of Kelly Caruso and Eye Clinic for Animals Australia*

have been genomically characterized, and it is likely that there are many more poxviruses seen within macropod species yet to be classified (Bennett et al. 2017). Poxvirus lesions often affect the eyelids as well as the skin of the face, feet, and tail (McKenzie et al. 1979; Rothwell et al. 1984). This disease is often self-limiting and surgery is only necessitated if the lesions alter eyelid function (Stanley 2002).

Oral necrobacillosis, also known as "lumpy jaw," is characterized by swelling around the face and jaw. This disease is caused from an ascending osteomyelitis infection, starting as periodontitis with saprophytic bacteria invading adjacent mucosa that progresses to osteomyelitis of the mandible or maxilla (Borland et al. 2012; Boever and Leathers 1973) (Fig. 28.11). Though this condition commonly afflicts captive animals, it has been previously reported in high proportions of wild populations of kangaroos under ecological stress due to high food competition (Borland et al. 2012). Ocular manifestations are broad and can range from unilateral blepharospasm with mild ocular discharge to more serious signs such as proptosis of the globe secondary to retrobulbar abscessation (Stanley 2002). The cause of this condition is believed to be multifactorial in captive populations, with fecal contamination of feeding stations, sharp plant awns, and inappropriate soft food diets believed to all be contributory factors. Bacteria species including *Dichelobacter nodosus, Fusobacterium necrophorum, Actinomyces,* and *Corynebacterium* are believed to be implicated in the disease process (Stanley 2002; Boever and Leathers 1973). The development of septicemia can cause death from encephalic and pulmonary infection (Boever and Leathers 1973). Treatment of those with ophthalmic signs should include surgical drainage of retrobulbar abscesses and removal of subsequently infected tissues. Antimicrobial therapy with oral clindamycin at 11 mg/kg twice daily, intramuscular oxytetracycline at 40 mg/kg once every 48 h, long-acting intramuscular amoxicillin at 20 mg/kg every 48 h, long-acting oxytetracycline intramuscularly at 20 mg/kg every 72 h, or the implantation of antibiotic-impregnated polymethyl-methacrylated beads following surgical debridement is recommended (Stanley 2002; Vogelnest and Portas 2008; Hartley and Sanderson 2003). Concurrent use of a sustained release chlorhexidine varnish to the affected teeth may also result in shorter treatment times and prevent recurrence (Bakal-Weiss et al. 2010). However, among captive

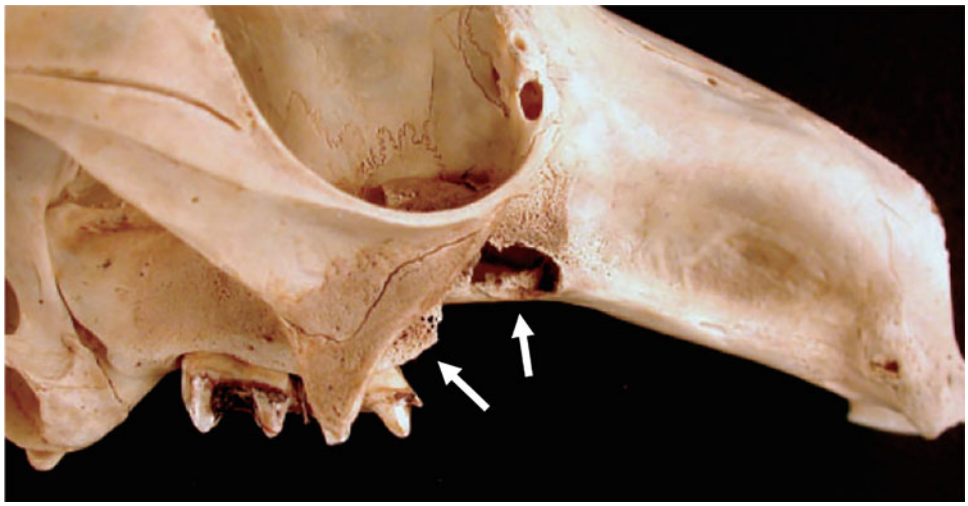

Fig. 28.11 Severe osteolysis of the maxillary dental arcade due to oral necrobacillosis in an eastern gray kangaroo *(Macropus giganteus)*, with tooth loss and osteolysis of the pre-maxilla (arrows). Note the close association with the bony orbit. *Borland D, Coulson G, Beveridge I (2012) Oral necrobacillosis ('lumpy jaw') in a free-ranging population of eastern grey kangaroos (Macropus giganteus) in Victoria. Austr Mammal 24:29–35*, used with permission

animals this is a disease of husbandry failure, prevention by addressing the predisposing factors is the best treatment.

Approximately 5–10% of koalas (*Phascolarctos cinereus*) presenting to Australia Zoo Wildlife Hospital are admitted with ophthalmic lesions. Of these, the most common presentation is eyelid trauma, often caused by a dog or cat attack or motor vehicle accident (Liddle et al. 2014). Koalas are capable of strong globe retraction and extensive third eyelid protection, perhaps explaining why these traumatic incidences rarely involve the globes (Grundon et al. 2011; Liddle et al. 2014). In the experience of the authors, the most common cause of eyelid lesions in kangaroo species are from motor vehicle incidents.

Although the principles of eyelid repair in marsupials are similar to other mammals, a technique that has been utilized by the authors that has proven to be very useful for extensive eyelid defects involves serial (typically two to three) hyaluronic acid filler injections (Restylane©) under sedation over the period of weeks to months, followed by a free-buccal mucosal graft to fill the defect (Fig. 28.12). This technique is useful as the filler expands tissue volume without altering tissue thickness or neuronal sensitivity, and enabling sufficient skin to close both donor and recipient sites (Fang et al. 2013). The injection of fillers applies mechanical forces to the skin, which responds initially by straightening and realignment of collagen fibers. Further elongation, past the skin's natural extensibility results in displacement of water from collagen fibers and micro fragmentation of elastic fibers, a mechanism termed "mechanical creep" (Wilhelmi et al. 1998). The mechanical creep allows for the outward rotation of the eyelid margin defect, with trichiasis and subsequent keratitis being lessened markedly prior to surgery. Additionally, the mechanical creep thickens the region of the eyelid defect and allows for a tarsal-splitting procedure. The free-buccal mucosal graft is then sutured to both portions of the split tarsus to create a new eyelid margin. The donor tissue is best harvested from the muco-cutaneous junction of the patient's mouth. As the donor tissue is expected to contract post-operatively, it is wise to prepare a graft that is approximately 30–50% larger than the size of the defect. Post-operative topical antibiotic ointment and Manuka honey appears to be effective in preserving the graft from infection.

Photosensitization of the eyelids in macropods by steroid saponin plants and *Lantana camara* can cause a necrotizing dermatitis of the adnexa (Steventon et al. 2018; Johnson and Jensen 1998). This syndrome also affected the cornea and sclera and is described in greater detail in the "*corneal and scleral conditions*" section of this chapter. Tetanus, caused by *Clostridium tetani* has been reported in the red kangaroo (*Macropus rufus*) and Eastern gray kangaroo (*Macropus giganteus*). Protrusion of the nictitating membrane is a common ophthalmic sign, with marked tetany of the head, neck, thorax, and limb musculature. Death usually ensues despite treatment following the onset of pulmonary edema (Ramsay 1960). Other eyelid conditions follow similar patterns as in domestic mammalian species (e.g., blepharoconjunctivitis and Meibomian gland dysfunction) (Fig. 28.13).

Conjunctival Conditions

Conjunctivitis is frequently encountered in kangaroos, with foreign bodies being the most common cause (Stanley 2002). The native *Staphylococcus spp* present within red kangaroo (*Macropus rufus*) conjunctiva have been previously reported to display antibiotic resistance to beta-lactam antimicrobials (Labelle et al. 2010b). Herpesvirus is to be suspected as a causative agent if conjunctival blisters are observed in macropods, as macropod herpes virus-1 (MaHV-1) and macropod herpes virus-2 (MaHV-2) are known agents to cause ulcerative conjunctivitis, respiratory signs, neurological signs, pyrexia, and vesicular anogenital lesions (Webber

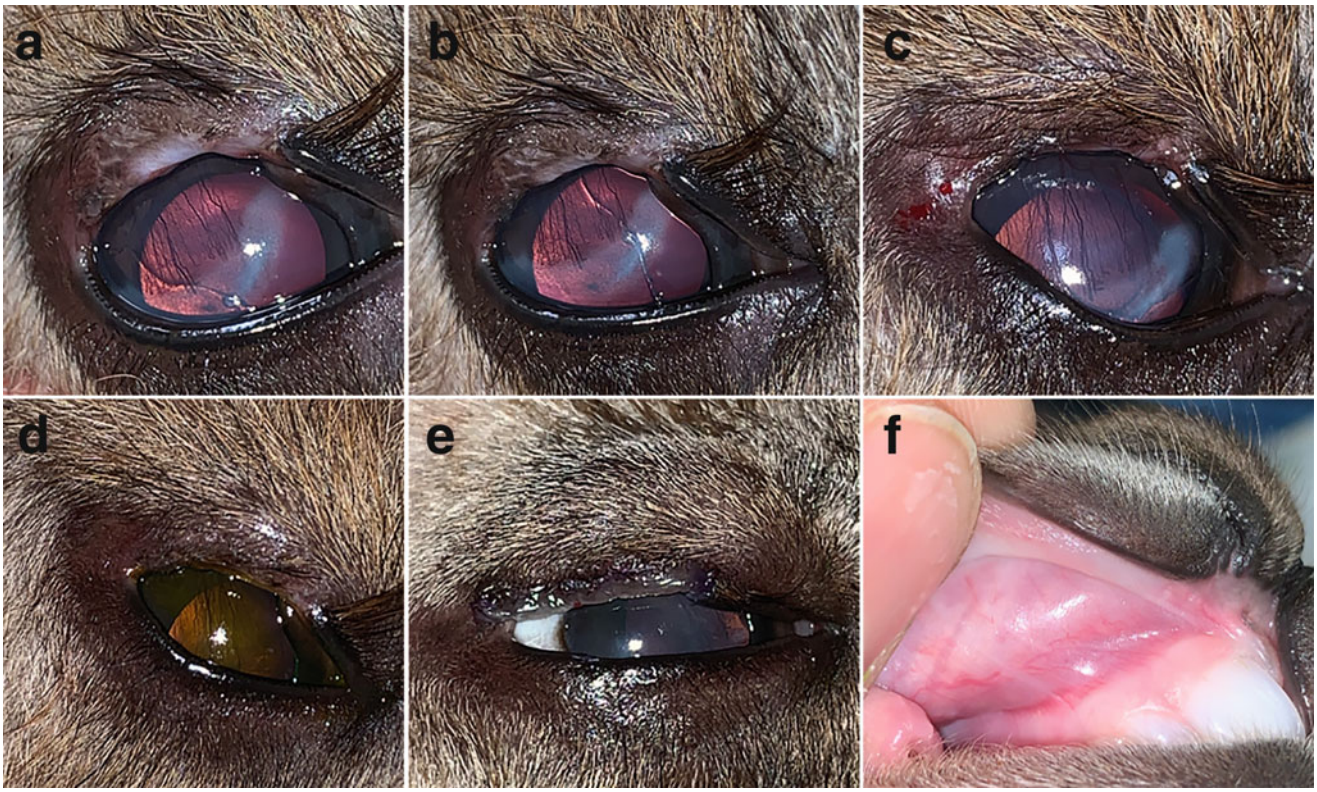

Fig. 28.12 Use of hyaluronic acid filler (Restylane©) injections to prepare an extensive eyelid defect for surgical correction in an Eastern gray kangaroo (*Macropus giganteus*) joey. (**a**) Initial presentation of a severe right superiolateral eyelid defect following a motor vehicle accident had killed its mother while it remained relatively safe in her marsupium. Note the ventral corneal ulcer with superficial vascularization. (**b**) Appearance on presentation immediately after subdermal Restylane© filler was injected into the defect. (**c**) Appearance of the region after a second Restylane© subdermal filler injection, 1 week after initial presentation. (**d**) Appearance of the region 2 months after initial presentation, and after receiving a total of three Restylane© injections. Note how diffusely thickened the region is compared to initial presentation (**a**). (**e**) The region post-operatively 2 months after initial presentation, after the lid was split partial thickness, and a free labial mucocutaneous graft was sutured to both portions of the split lid. (**f**) The site of graft harvesting, on the muco-cutaneous junction of the mouth. *Courtesy of Kelly Caruso*

and Whalley 1978; Wilks et al. 1981). In an experimental setting, MaHV-1 can establish a transient infection of brushtail possums (*Trichosurus vulpecula*), observed clinically as a mild conjunctivitis, however no systemic or latent state was observed (Zheng et al. 2004). Herpes virus was detected in 27.2% of wild Australian marsupial species, with common wombats (*Vombatus ursinus*) having the highest prevalence at 45.4% (Stalder et al. 2015). Bacterial cultures from conjunctival swabs in healthy red kangaroos (*Macropus rufus*) and North American opossums (*Didelphis virginiana*) showed that *Staphylococcus spp.* were most frequently isolated bacterial organism, similar to domestic dogs (Takle et al. 2010; Pinard et al. 2002; Prado et al. 2005). In red kangaroos, *Staphylococcus epidermidis* and *Corynebacterium sp.* were the most common species (Takle et al. 2010). Approximately 65% of the samples grew multiple pathogens, displaying a diverse ocular flora in the conjunctival sac of both species (Takle et al. 2010; Pinard et al. 2002).

The koala (*Phascolarctos cinereus*) is a threatened wildlife species in various parts of Australia, with their long-term viability threatened by a group of obligate intracellular bacteria, *Chlamydia sp.* (Polkinghorne et al. 2013). These infections are clinically associated with ocular manifestations leading to blindness, as well as genital tract issues leading to infertility, chronic severe cystitis with secondary urinary incontinence, and other serious morbidities. *Chlamydia sp.* have been identified in many Australian marsupial species, however are symptomatic only in koalas (Burnard et al. 2017a). Two *Chlamydia* species infect the koala, *C. pecorum* and *C. pneumoniae*, and have been reported in nearly all mainland Australian wild koala populations (Jackson et al. 1999; Devereaux et al. 2003; Cockram and Jackson 1974; Funnell et al. 2013; Patterson et al. 2015; Speight et al. 2016; Nyari et al. 2017). Early records indicate that signs consistent with chlamydiosis, "ophthalmic disease and periostitis of the skull," have been observed since at least the late 1800s (Troughton 1941). *C. pecorum* is always the dominant species present via PCR testing (averaging 57% prevalence), whereas *C. pneumoniae* is less frequently detected (averaging 18% prevalence) (Polkinghorne et al.

Fig. 28.13 Blepharitis and Meibomian gland dysfunction in a common brushtail possum (*Trichosurus vulpecula*). *Courtesy of Jeffrey Smith*

2013). Further, *C. pecorum* produces more severe clinical signs than *C. pneumoniae* (Jackson et al. 1999). Wild koala populations in Australia's northern regions generally have a higher prevalence of chlamydial infections and corresponding clinical disease than koalas of southern Australia (Polkinghorne et al. 2013). There is some evidence to suggest that the immunomodulating koala retrovirus (KoRV) has a role in the pathogenicity of *Chlamydia* in koalas (Tarlinton et al. 2005). To date no studies have been performed to assess the method of transmission of *Chlamydia* in koalas, but clinical observations suggest that it is transmitted sexually, or from mother to joey (Nyari et al. 2017; Polkinghorne et al. 2013). There is evidence to suggest that the microbiota of the mucosal urogenital and ocular mucosal sites may influence the ability of *Chalmydia* infections of koalas to progress to clinical disease, but further work will be required to implicate specific pathogens (Vidgen et al. 2017). To date, no evidence of tick-borne transmission of *Chlamydiaceae* species to native Australian marsupials have been documented, despite the presence of novel *Chlamydia* species detected in native Australian ticks (Burnard et al. 2017b).

Koalas infected with *Chlamydia* have highly variable presentations ranging from obvious clinical disease, inapparent disease only detectable with diagnostic testing, or subclinical carriers with no detectable clinical signs (Loader 2010; Wan et al. 2011; Speight et al. 2016). Genetic variability between the major histocompatability complex gene alleles in koalas impacts which chlamydial antigens are presented to T-cells, thus influencing the immune response generated and ultimately the clinical presentation (Kollipara et al. 2013; Lau et al. 2014). The pathophysiology of chlamydial ocular signs involves the exposure of mucosal surfaces of the eye and conjunctiva to the pathogen. Clinically, this is observed either unilaterally or bilaterally. In early infection the disease manifests as epiphora, blepharospasm, conjunctival hyperemia, and scleral injection (Fig. 28.14a,b) before progressing to mucopurulent ocular discharge, conjunctival hyperplasia, and conjunctival fibrosis and symblepharon that may lead to a micropalpebral fissure (Fig. 28.14c,d). Chronically, residual symblepharon may be noted after chemosis and conjunctival hyperemia have resolved (Fig. 28.14e,f). In severe cases, the cornea can become markedly edematous, develop marked vascularization and fibrosis, and globe rupture may occur following ulceration (Wan et al. 2011). Blindness is often clinically observed, and this may be due to physical obstruction caused by chemosis and conjunctival hyperplasia, symblepharon, corneal opacification, or in severely advanced instances globe rupture and severe ophthalmitis (Polkinghorne et al. 2013). The vascularization pattern of the cornea in these cases is unique, extending from deep to superficial in a peculiar right-angle orientation as the vessels move away from the limbus toward the axial cornea, perhaps due to a unique corneal collagen pattern of these species or some unknown effect of the Chlamydial disease (Hirst LW, personal communication). The other cardinal signs of *Chlamydia* infections in koalas include brown urine staining of the perineum and rump due to urinary incontinence secondary to severe cystitis, and reproductive failure due to pyometra, metritis, vaginitis, or dilatation of the ovarian bursae, oviducts, or uteri (Blanshard and Bodley 2008; Canfield 1989; Patterson et al. 2015; Speight et al. 2016).

Histopathological analysis of acutely inflamed conjunctival biopsies in affected koalas revealed pronounced proprial hyperemia and edema. Marked infiltrate to the conjunctival epithelium was observed, and conjunctival epithelium frequently showed spongiotic and hydropic changes, but was rarely ulcerated (Kempster et al. 1996).

Acute and chronic active cases of keratoconjunctivitis have higher levels of shedding of *Chlamydia* species than chronic cases, and a high individual variation in shedding is observed (Wan et al. 2011). Due to the variable presentation of clinical signs, and varied shedding of the pathogen both within an individual and between individuals, definitive diagnosis of chlamydial keratoconjunctivitis in the koala is generally presumptive and based on clinical signs, often despite the results of antigen detection tests (Polkinghorne et al. 2013). However, swab sampling of the mucosal sites (ocular and genitourinary) for PCR detection of *Chlamydia* organisms has proven to be useful in detecting the pathogen in clinically active cases, and this is the current gold standard diagnostic modality (Wan et al. 2011; Sasche et al. 2009).

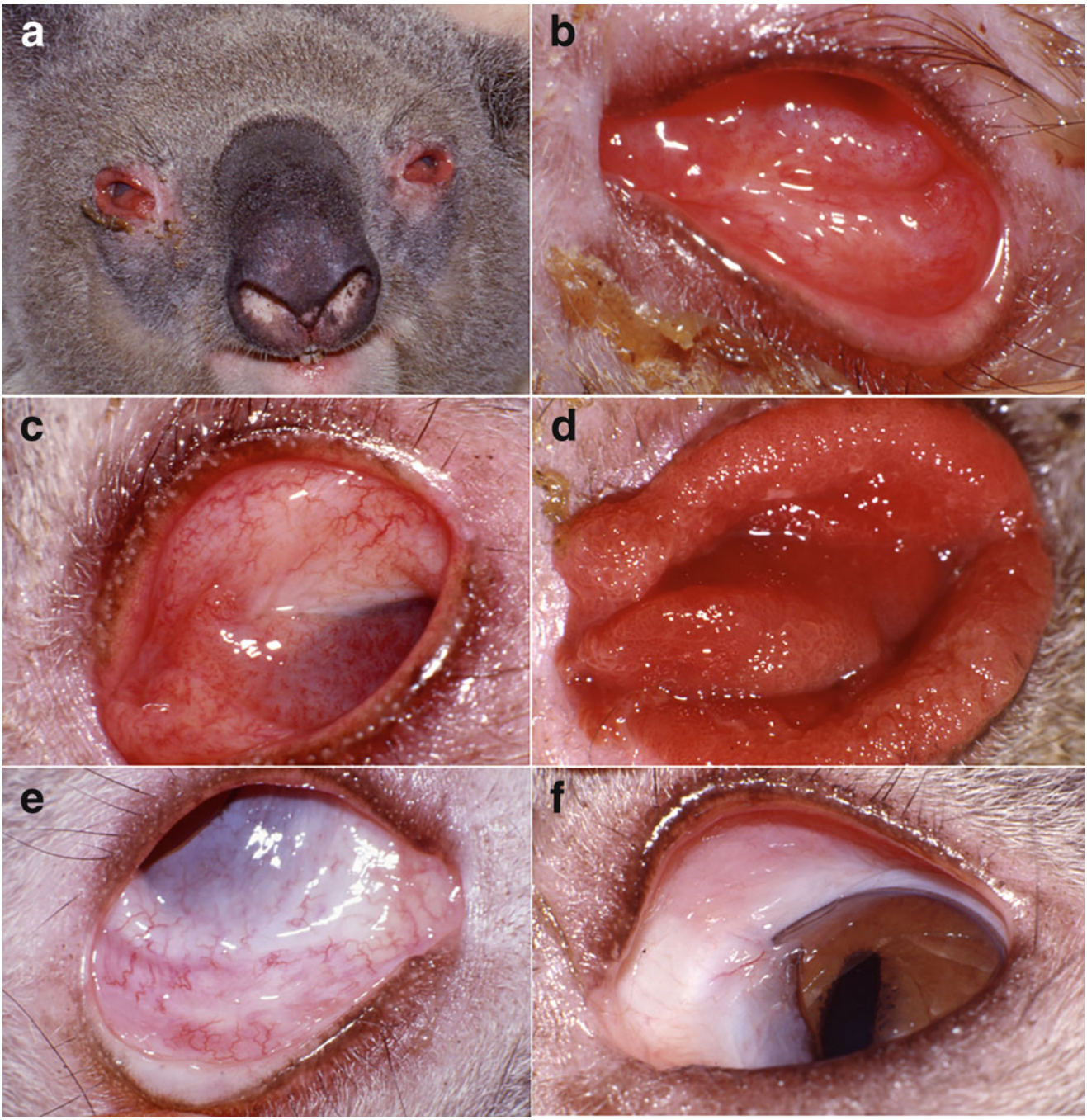

Fig. 28.14 Photographs depicting the classical findings of conjunctivitis caused by *Chlamydia sp*. in the koala (*Phascolarctos cinereus*). (**a**, **b**) Acute, active conjunctivitis characterized by diffuse conjunctival hyperemia and chemosis. (**c**) Chronic active conjunctivitis featuring severe conjunctival hyperemia and the development of symblepharon. (**d**) Chronic active conjunctivitis featuring severe conjunctival hyperemia and conjunctival hyperplasia/proliferation. (**e**, **f**) Chronic inactive Chlamydia conjunctivitis resulting in residual symblepharon with only mild to no conjunctival hyperemia. *Courtesy of Lawrie Hirst*

These PCR methods are often not feasible for point-of-care testing. The "Clearview chlamydia test" is a *Chlamydia* genus specific, qualitative, solid phase direct antigen kit that is sensitive and specific for *C. pecorum* and *C. pneumoniae*, and is also a suitable detection diagnostic modality (Hanger et al. 2013; Wood and Timms 1992).

Treating *Chlamydia* infections in koalas is difficult as koalas are prone to potentially fatal gastrointestinal side effects of drugs within the tetracycline and macrolide classes that are commonly used to treat *Chlamydia* infections in other species, and thus use of these antibiotics is discouraged (Markey et al. 2007; Griffith et al. 2010). Current suggested

treatment regimens by Australian wildlife hospitals for the ocular manifestations of chlamydiosis include a compounded oxytetracycline 1.5% and polymixin B 10,000 units topical ointment twice daily, or a combination of chloramphenicol 60 mg/kg subcutaneously once a day with topical chloramphenicol and prednisolone eyedrops twice daily (Govendir 2018). Previous works have found that chloramphenicol at 60 mg/kg subcutaneously once daily for 45 days results in cessation of *Chlamydia* shedding by 2 weeks post-treatment (as determined by PCR and Clearview Chlamydia assays), and is therefore regarded as the cornerstone of therapy (Markey et al. 2007; Polkinghorne et al. 2013). Conversely, enrofloxacin treatment has been observed to cause rebound *Chlamydia* shedding after cessation of therapy due to incomplete resolution of infection (Griffith et al. 2010). Due to the impact on behavior that vision loss causes in koalas, some clinicians advocate the surgical excision of hyperplastic and fibrosed conjunctiva in chronic cases (Schmid et al. 1991; Stanley 2002). Future therapies will likely involve the use of a recombinant chlamydial major outer membrane protein vaccination, as studies have so far displayed great promise in improving ocular signs in clinically affected animals, regardless of their KoRV infection status (Nyari et al. 2019; Waugh et al. 2016). To date, no studies have assessed if these vaccines are effective in protecting uninfected animals from contracting the disease. Currently, there is no commercially available chlamydial vaccination produced for koalas.

Chlamydial keratoconjunctivitis has also been described in the western barred bandicoot (*Perameles bougainville*) from a wild population in Western Australia. Clinical signs included corneal opacity, conjunctivitis, ocular discharge, and blepharitis. All animals effected responded to 20 mg/kg oxytetracycline intramuscular injection once weekly for 6 weeks, and topical oxytetracycline and neomycin ophthalmic ointment once daily for 4 months (Warren et al. 2005).

Koalas with lymphosarcoma may present with mass lesions seen inside the eye or conjunctiva, and occasional cases presenting with ocular discharge (Stanley 2002; Canfield et al. 1987). This condition is loosely linked to Koala retrovirus B (KoRV-B) infection (Tarlinton et al. 2005; Xu et al. 2013). There is very little information published on treatment guidelines for lymphosarcoma in koalas.

Corneal, Scleral, and Uveal Conditions

The South American gray short-tailed opossum (*Monodelphis domestica*) has proven to be a useful animal model in establishing the etiopathogenesis of ultraviolet-radiation (UVR) induced neoplasia in other mammalian species (Kusewitt et al. 1999). *M. domestica* contains a photolyase that catalyzes the reparation of UVR-induced pyrimidine dimers. However, this process is light dependent. In laboratory studies with low-light exposure to prevent the activation of the photolyase, chronic low-level UVR exposure results in the increased occurrence of corneal fibrosarcoma, hemangiosarcoma, and squamous cell carcinoma (Kusewitt et al. 1999; Sabourin et al. 1993). These tumors are locally invasive, but do not typically metastasize (Kusewitt et al. 1996). *M. domestica* sarcomas possess a mutational spectrum that is very similar to UVR-induced skin tumors of other mammalian species, despite their origin being from mesenchymal rather than epidermal cells (Kusewitt et al. 1999). To date, no naturally occurring corneal neoplasia has been recorded in marsupials.

Toxicity by ingestion of steroidal saponin plants or *Lantana camara* can cause a hepatogenous photosensitization syndrome in kangaroo species that is hallmarked by ocular changes including a mild to severe keratitis and mild to severe corneal edema (Fig. 28.15) (Steventon et al. 2018; Johnson and Jensen 1998). Other clinical signs include blindness, severe photophobia, ocular discharge, marked necrotizing dermatitis of the pinna and eyelids, jaundice, and a severe hepatopathy (Steventon et al. 2018). Due to the profound blindness and associated hepatopathy, this condition is invariably fatal in wild populations (Steventon et al. 2018). The pathophysiology of corneal edema and keratitis within these cases is poorly understood.

Keratitis in marsupials presents similarly to that of other terrestrial mammalian species (Fig. 28.16). Corneal ulcerative keratitis is relatively common in young kangaroos, seemingly as a result of systemic dehydration resulting in a secondary quantitative aqueous tear deficiency. In adult marsupials, foreign body injuries are perhaps the most common cause of corneal ulceration, and they often heal following a marked vascular response (Stanley 2002). Further work to evaluate normal ocular surface microbiota and the pathogens most commonly involved with keratitis is required. Keratitis unrelated to chlamydial infection has been described within koalas (*Phascolarctos cinereus*). In a single study of 70 free-range koalas on an isolated island free of *Chlamydia* infections, 12/70 koalas were found to have chronic bilateral keratitis. All serological analyses for *Chlamydia* were negative, and no cause of keratitis was found (Hirst et al. 1992a). Corneal trauma and lacerations occur less commonly in the koala (*Phascolarctos cinereus*), primarily involving the adnexa as described above (Grundon et al. 2011). Similar to other mammalian species, anterior chamber collapse syndrome has been reported in koalas secondarily to early-life ocular trauma, with clinical signs including massive anterior synechia, a full-thickness corneal scar, and buphthalmia. Histologically, minimal to absent uveal inflammation is present (Liddle et al. 2014) (Fig. 28.17). Anterior chamber collapse syndrome often predisposes individuals to secondary glaucoma, and so enucleation is recommended in

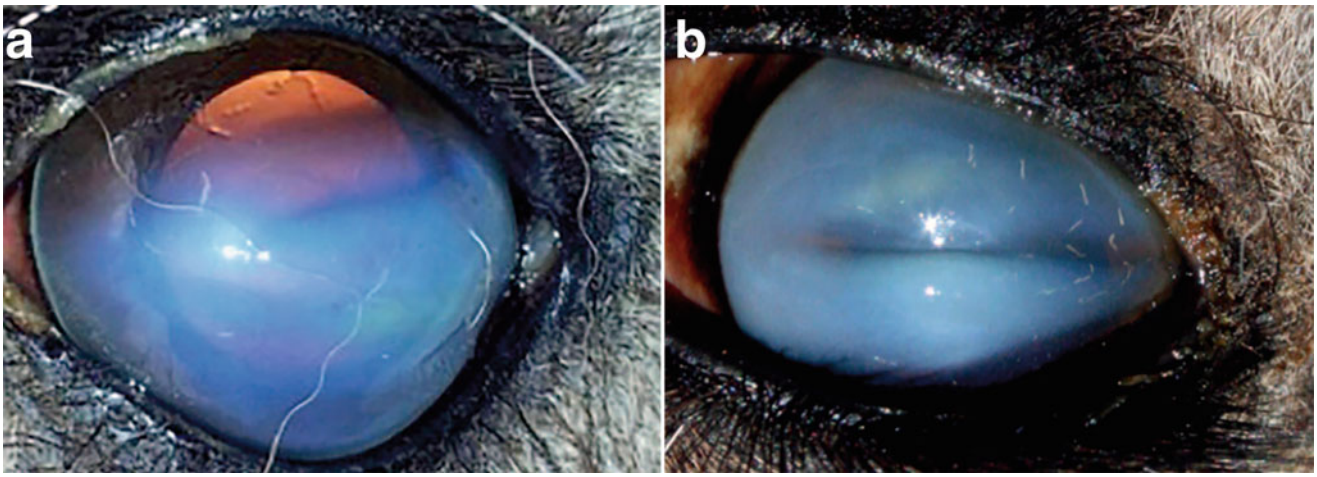

Fig. 28.15 Saponin toxicity induced hepatogenous photosensitization in eastern gray kangaroos (*Macropus giganteus*), displaying corneal edema with keratitis, both mild (**a**) and severe (**b**). *Steventon CA, Raidal SR, Quinn JC et al (2018) Steroidal saponin toxicity in eastern grey kangaroos (Macropus giganteus): a novel clinicopathologic presentation of hepatogenous photosensitisation. J Wildl Dis 54:491–502*, used with permission

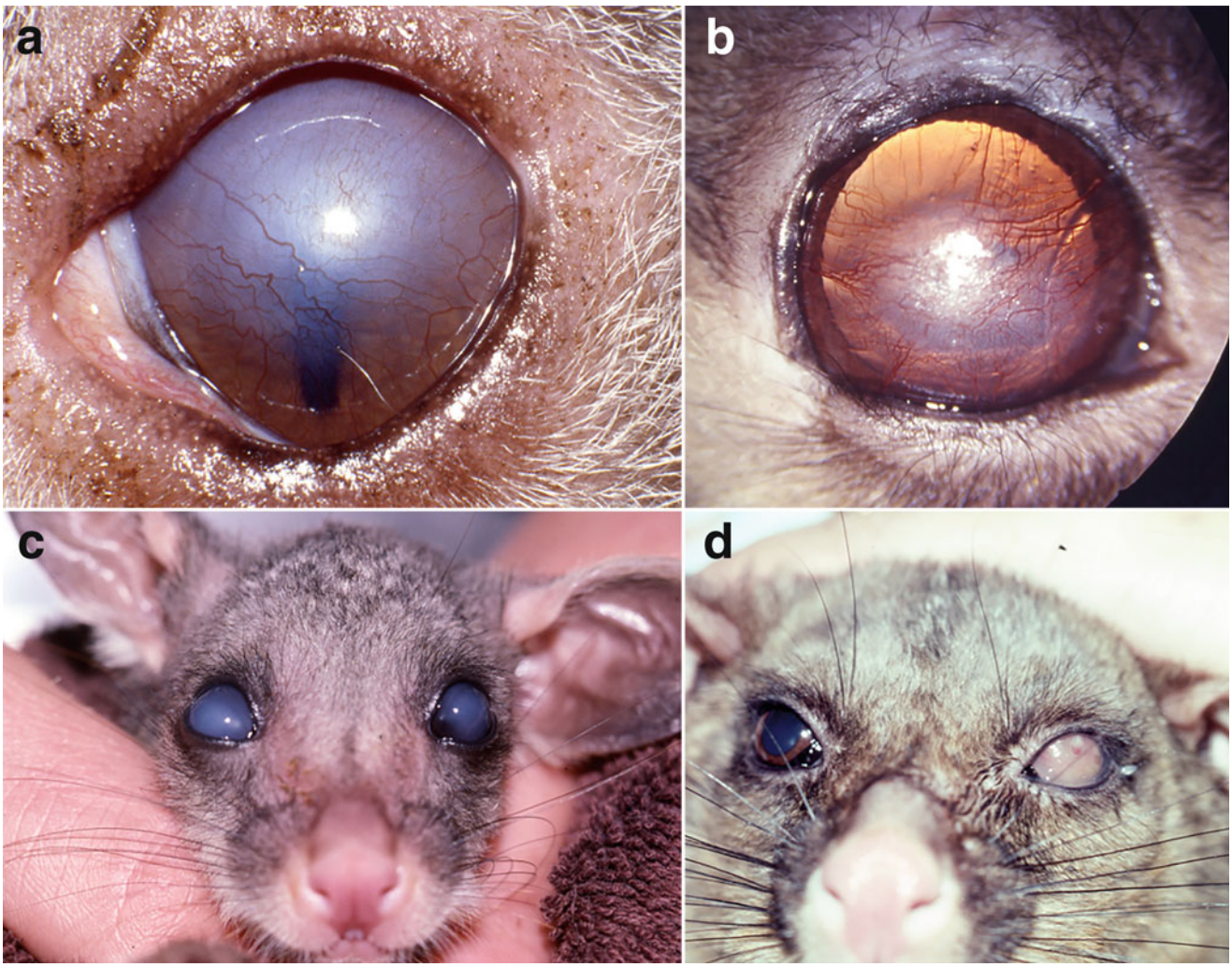

Fig. 28.16 Keratitis in marsupial species. (**a**) Keratitis in a koala (*Phascolarctos cinereus*) believed to be free of chlamydial disease. Note the severe and diffuse superficial corneal vascularization and surrounding corneal edema. (**b**) Corneal fibrosis suspected to be post-traumatic in a common ringtail possum *(Pseudocheirus peregrinus*). (**c**) Diffuse bilateral corneal edema of unknown cause in a common brushtail possum *(Trichosurus vulpecula*). (**d**) Keratitis of unknown cause in a common ringtail possum *(Pseudocheirus peregrinus*). **a**—*Courtesy of Lawrie Hirst.* **b**—*Courtesy of Jeffrey Smith*

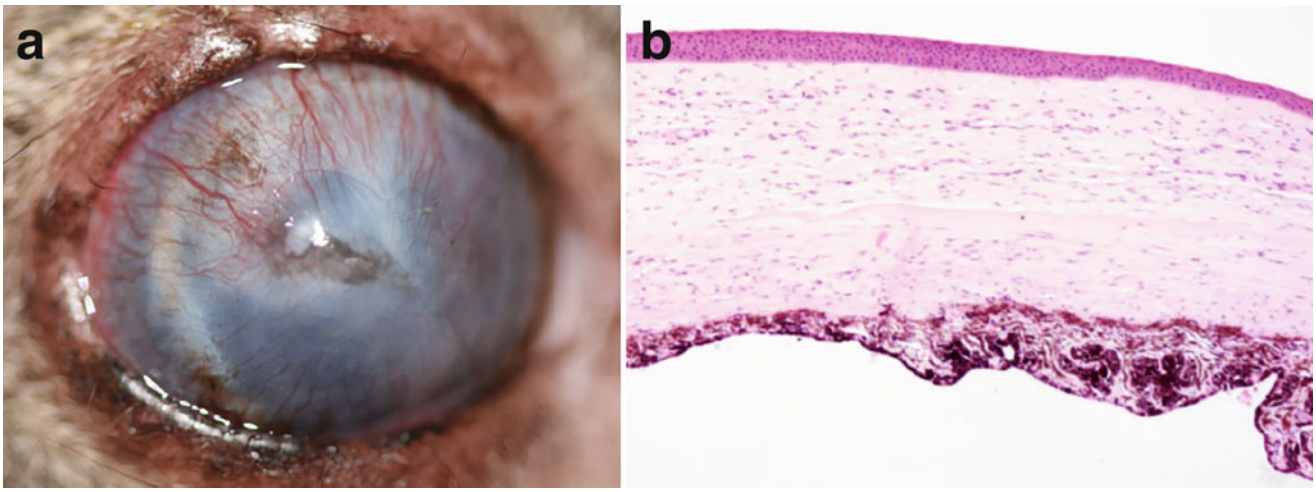

Fig. 28.17 Anterior chamber collapse syndrome in a koala (*Phascolarctos cinereus*). (**a**) Clinical photograph of showing buphthalmos and severe diffuse keratitis with staphyloma. (**b**) Photomicrograph showing iris tissue completely adhered to the posterior aspect of the cornea, obliterating the anterior chamber. Stain: hematoxylin and eosin. *Liddle VL, Naranjo C, Bernays ME (2014) Anterior chamber collapse syndrome in a koala. Aust Vet J 92:179–182*, used with permission

these cases. Other forms of uveitis (infectious, neoplastic, traumatic) present similarly as other mammal species with aqueous flare, anterior chamber cell, and hyphema (Fig. 28.18).

Microphthalmos has been observed in multiple marsupial species bred in captivity (Smith 2019, personal communication) (Fig. 28.19). The cause of this developmental anomaly is thought to mirror those of other mammal species, with no known unique risk factors for marsupial species. Heterochromia iridum has been observed in the koala, although this is thought to be exceedingly rare with only a single report in the literature (Kempster et al. 1994) (Fig. 28.20). The animal was euthanized for unrelated reasons and the eye with a blue iris had an under-developed pupillary sphincter muscle, a thin iridial pupillary zone, and a thickened Descemet's membrane compared to the contralateral eye that was normally pigmented (Kempster et al. 1994).

Fig. 28.18 Anterior uveitis featuring hypopyon in a common brushtail possum *(Trichosurus vulpecula)*. The cause was not determined. *Courtesy of Jeffrey Smith*

Peter's anomaly, a rare ocular developmental dysgenesis, has been reported in a red kangaroo joey (Suedmeyer et al. 2014). Peter's anomaly is typically characterized by a central corneal leukoma due to an initial absence of Descemet's membrane and corneal endothelium, with persistent pupillary membranes also present. Occasionally concurrent cataracts and glaucoma are also present (Harissi-Dagher and Colby 2008). Due to the heritable nature of this condition and the lack of genetic diversity in to the United States' imported captive population of red kangaroos, it is possible that heritable ocular defects may become increasingly more apparent in these animals (Suedmeyer et al. 2014).

Lenticular Conditions

Similar to other species, cataracts in marsupials can be congenital or develop from traumatic, nutritional, inherited, metabolic, and environmental causes (Fig. 28.21). For reasons currently unknown, cataracts appear to occur more frequently in ringtail possum (*Pseudocheirus peregrinus)* populations than other marsupial species in the wild (Smith 2019, personal communication). Galactosemic cataracts are seen frequently in kangaroos, and have also been reported in a cuscus (Slatter et al. 1980; Stephens et al. 1974). Neonatal

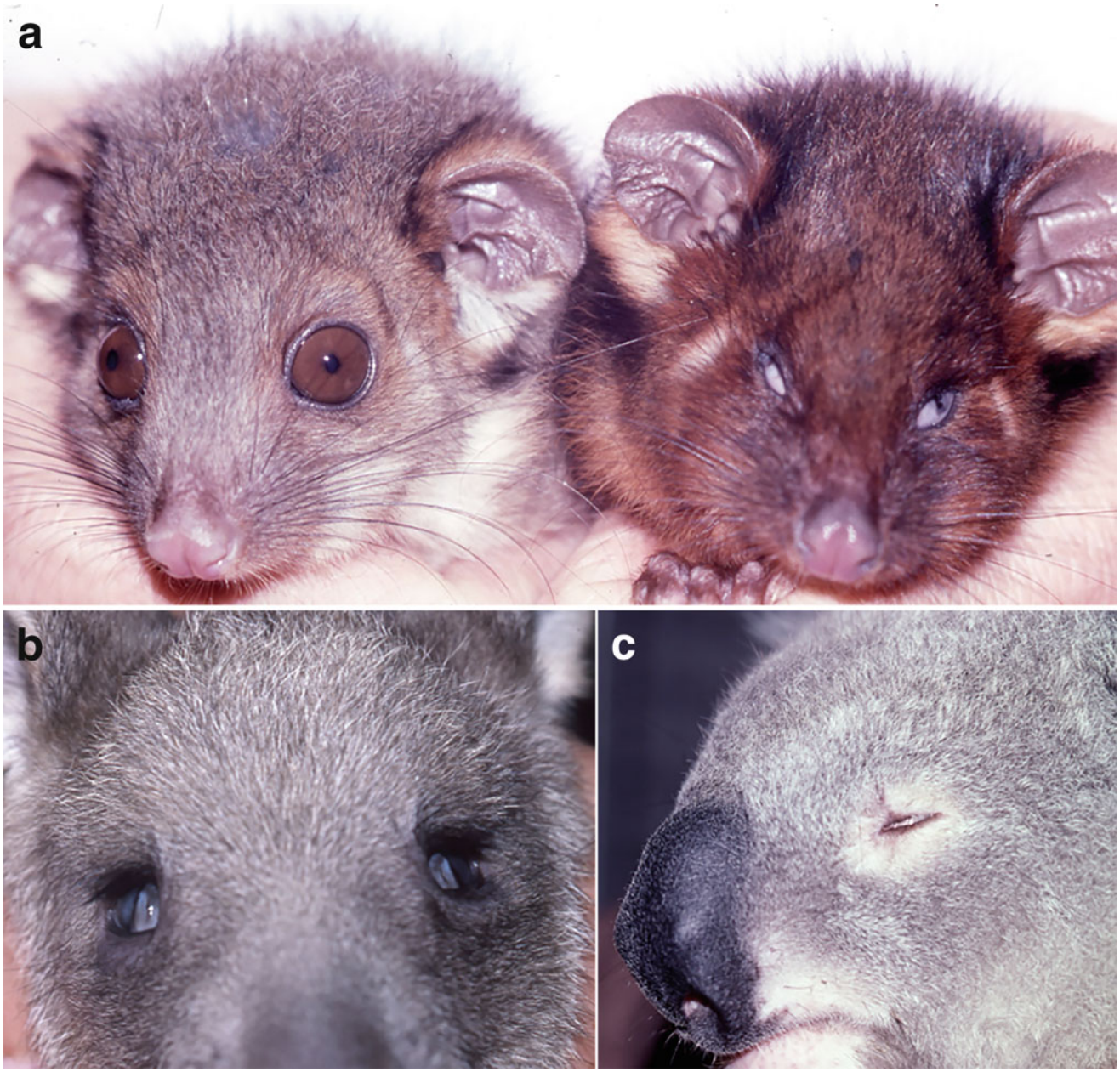

Fig. 28.19 Microphthalmia in marsupials. (**a**) Common ringtail possum (*Pseudocheirus peregrinus*) with unaffected sibling on the left and microphthalmic sibling to the right. (**b**) Eastern gray kangaroo (*Macropus giganteus*) joey. (**c**) Koala (*Phascolarctos cinereus*). *Courtesy of Jeffrey Smith*

marsupials transition from a monogastric phase of gastrointestinal development to a polygastric system, and are often deficient in either galactokinase or galactose-1-phosphate uridyl transferase during the monogastric phase (Stephens et al. 1974). Galactosemic cataracts occur only in pouch-young marsupials, as adults develop ruminal gastrointestinal systems that metabolize galactose into volatile fatty acids within the stomach limiting galactose absorption (Stephens et al. 1975; Wada et al. 1988). Marsupials who develop galactosemic cataracts are typically hand-reared and fed cow's milk (Slatter et al. 1980; Stephens et al. 1974). The lack of these enzymes limits the conversion of the galactose that is omnipresent in cow's milk to lactose, resulting in excess galactose being metabolized by an alternative aldose reductase pathway in the lens to form dulcitol. Dulcitol does not readily diffuse through the lens capsule, and accumulation results in the formation of osmotic cataracts (Kinoshita 1965; Hong-Ming et al. 1990). Subsequent breakdown of the lens capsular barrier and water accumulation disrupt the intracellular Na:K ratio and decrease intracellular

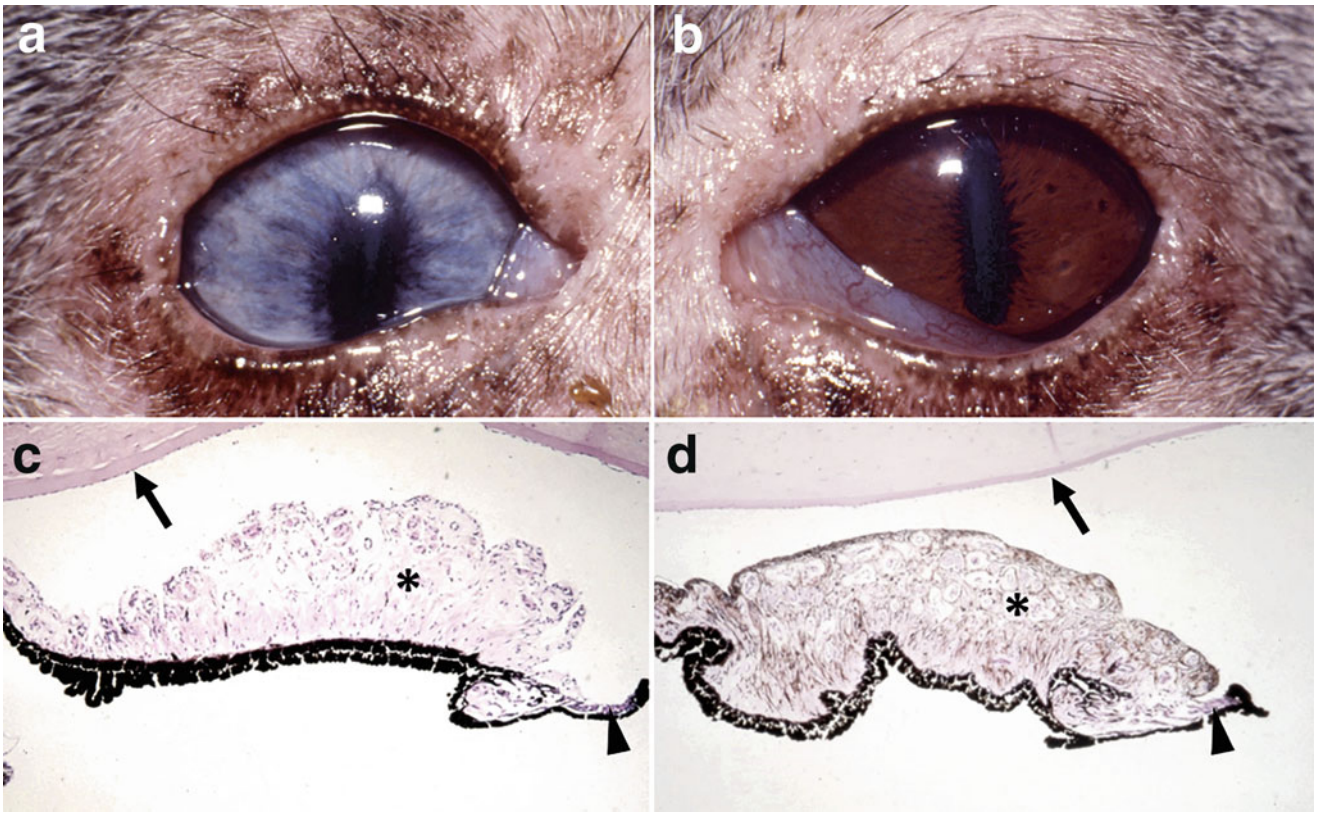

Fig. 28.20 Heterochromia iridum in a koala (*Phascolarctos cinereus*). (**a**) A blue right iris and a (**b**) normally pigmented contralateral eye. Note the iridial vasculature visible in the heterochromic iris. Histologic sections of the blue iris (**c**) and normally pigmented iris (**d**) demonstrating reduced pigment in the iris stroma (asterisk), a hypoplastic pupillary sphincter muscle more notably at the pupillary margin (arrowhead), and a thickened Descemet's membrane (arrow) in the blue iris compared to the iris with normal pigmentation. Stain: hematoxylin & eosin. *Courtesy of Lawrie Hirst*

glutathione, amino acid, and ATP concentrations. This interferes with lens fiber crystalline synthesis resulting in cataract formation (Stambolian 1988; Wada et al. 1988; Hong-Ming et al. 1990). Additionally, high intra-lenticular galactose levels can cause auto-oxidation and exceed the anti-oxidating threshold of the lens and further potentiate cataract formation (Stambolian 1988; Wada et al. 1988). There are commercial diets available for use in various marsupial species, with Wombaroo Adelaide, South Australia (http://www.wombaroo.com.au) providing a specific milk replacer for various marsupial species that will prevent the formation of galactosemic cataracts. Divetelac can be fed as an interim diet until more appropriate milk-replacers can be located.

Ocular ultrasound is recommended prior to surgical intervention for cataracts (Fig. 28.22), as is electroretinogram if feasible (Fig. 28.10). Surgical exposure for phacoemulsification can be obtained without the use of neuromuscular blockade, and in the author's experience, the pupils dilate superbly with topical application of 1% tropicamide. Interestingly, deep vitrectomy is typically required to clear a rather unique, opacification of the vitreous body (Stanley 2002). Historically, surgical lensectomy for galactosemic cataracts in marsupials has been largely unsuccessful due to intraoperative vitreous humor opacification of unknown cause (Stanley 2002; Kern and Colitz 2012). An unpublished biochemical analysis of the opacified vitreous revealed increased galactose levels compared to non-effected kangaroo vitreous samples (Stanley 2002). Additionally, many cataract surgeries in marsupials develop glaucoma 2–12 weeks post-operatively, believed to be due to chronic uveitis (Stanley 2002). The extent of this problem is such that globe evisceration and euthanasia have been reported as sequelae, and as such, some authors do not advocate cataract surgery in these species (Stanley 2002). In the author's experience, phacoemulsification can be rewarding in these species, but the operating technique must be adapted from that performed in canine or feline species given the bizarre phenomenon of vitreous humor opacification.

We will describe the steps of cataract surgery in kangaroos that have provided the greatest success. First, the authors advocate that a side-port incision be made at the start of surgery, with the added benefit enabling post-operative aqueocentesis if indicated by post-operative intra-ocular hypertension. However, this must be performed carefully as

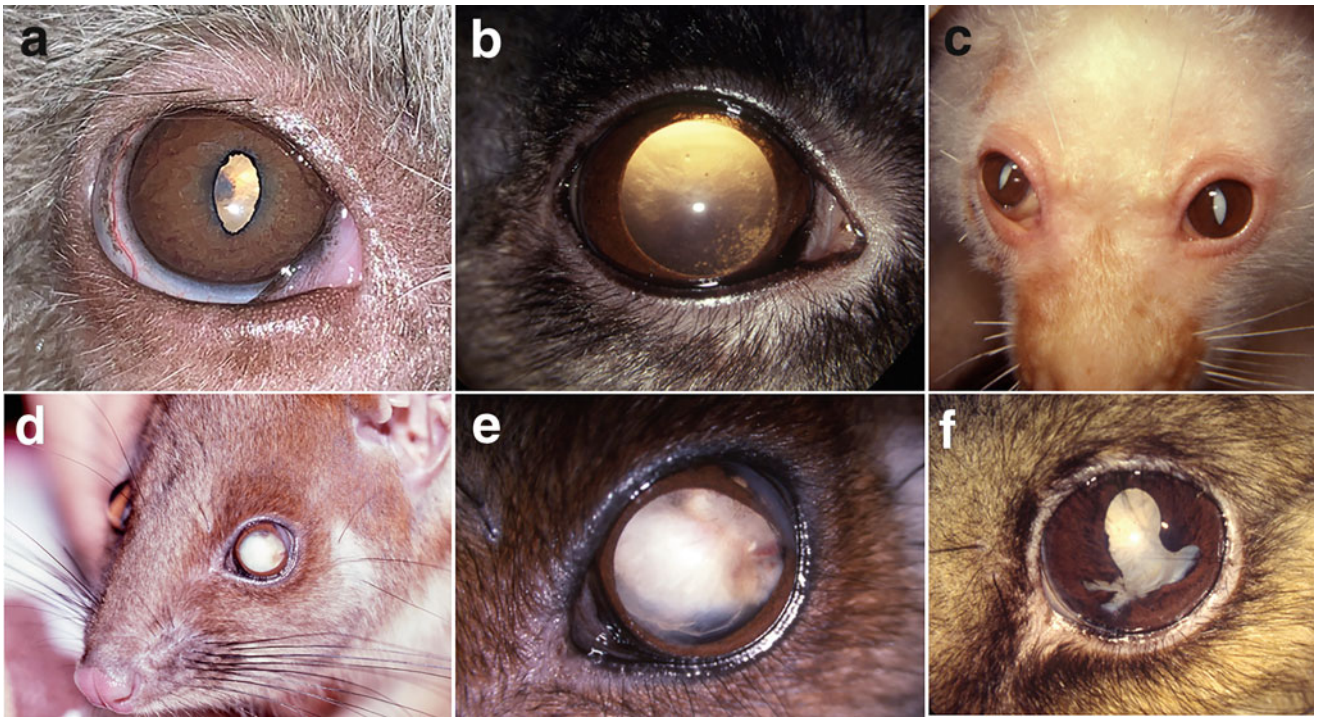

Fig. 28.21 An array of clinical presentations of cataracts in marsupials. (**a**) Incipient cortical cataract in a koala (*Phascolarctos cinereus*). (**b**) Incipient peripheral cortical cataract in a ring-tailed possum (*Pseudocheirus peregrinus*). (**c**) Bilateral, mature cataracts in a common spotted cuscus (*Spilocuscus maculatus*). (**d**, **e**) Hypermature cataract in a ringtail possum showing a vascular membrane advancing over the anterior lens capsule. (**f**) An advanced cataract leading to secondary posterior synechiae and severe dyscoria in a ringtail possum. **a**—*Courtesy of Kelly Caruso.* **b**, **c**, **d**, **e**, **f**—*Courtesy of Jeffrey Smith*

kangaroo species have very shallow anterior chambers and inadvertent iris trauma can occur. Uveal hemorrhage is common intraoperatively, thus administration of dilute epinephrine (1,10,000) is recommended through the side port. The shallow anterior chamber also predisposes marsupials for intraoperative iris prolapse, and visco-occupation of the anterior chamber is recommended to retard this consequence. A 2-step clear corneal incision is made near the 12 o'clock position via a half-thickness corneal groove followed by entry with a 2.75 mm keratome blade. A routine continuous curvilinear capsulorrhexis and phacoemulsification are performed as is routinely done so for other species. Cataracts in kangaroos are typically very soft and can mostly be removed via irrigation and aspiration. It is at this stage when vitreous opacification occurs, and a vitrectomy must be performed to remove the progressive vitreous opacification until a fundic reflection is adequate enough to facilitate the remainder of the phacoemulsification. The posterior lens capsule is subjectively very weak and flimsy in kangaroos, and visco-occupation of the lens capsule is performed to allow for a posterior continuous curvilinear capsulorrhexis to enhance axial vision and allow for a posterior vitrectomy to be performed, removing the opacified vitreous. The vitreous typically expands rapidly through the posterior capsulorrhexis and is easily removed via this method. Triamcinolone is then injected in to the posterior chamber to identify any remaining vitreous for subsequent vitrectomy if required, and also to allow for therapeutic anti-inflammatory effects due to the profound inflammatory response seen in marsupials following intra-ocular surgery.

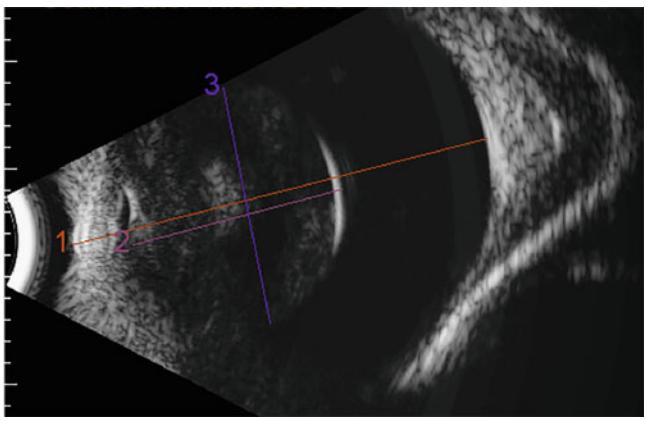

Fig. 28.22 A clinical B-wave ultrasound (12 MHz probe, 60 mm depth, 38 dB gain) in an Eastern gray kangaroo (*Macropus giganteus*) joey. Note the rotund, hyperechoic lens present indicating an intumescent cataract. Line 1 measures—20.47 mm, Line 2–10.35 mm, Line 3–11.5 mm. *Courtesy of Kelly Caruso and Eye Clinic for Animals Australia*

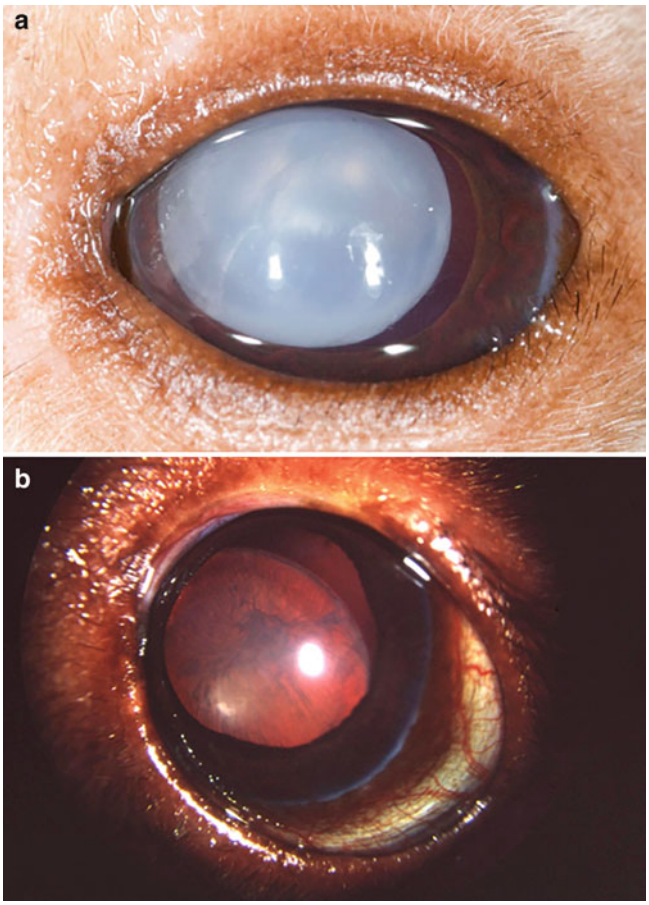

Fig. 28.23 Clinical photographs of lens luxation in marsupials. (**a**) Lens luxation and mature cataract in a Matschie's tree kangaroo (*Dendrolagus matschiei*). Note the temporal aphakic crescent. (**b**) Lens luxation and an incomplete cataract in a Goodfellow's tree kangaroo (*Dendrolagus goodfellowi*). Note the dorsal aphakic crescent. **a**—*McLean NJ, Zimmerman R (2015) Bilateral lens luxation and intracapsular lens extractions in a Matshchie's tree kangaroo. Vet Ophthalmol 18:81–85*, used with permission. **b**—Courtesy of Jeffrey Smith

The clear corneal incision is closed with 9/0 absorbable suture, and the side-port incision is intentionally left patent.

Post-operative care includes strict rest for 2 weeks, and medications of 0.3–0.5 mg/kg meloxicam PO SID for 10 days, 0.03 mg/kg buprenorphine SQ BID for 5 days, topical antibiotic ointment BID for 2 weeks, prednisolone acetate/phenylephrine ophthalmic drops QID initially but reducing in frequency as guided by the degree of post-operative uveitis, and dorzolamide/timolol ophthalmic drops BID for the first month, reduced as guided by intra-ocular pressure measurements. The complication rate in our experience is higher than for our canine and feline patients, but is still much lower than those anecdotally reported by veterinary ophthalmologists. This condition can be successfully managed surgically by phacoemulsification, and we encourage others to pursue this treatment route.

A presumed case of inherited primary lens luxation has previously been reported in a Matschie's tree kangaroo (*Dendrolagus matschiei*) (McLean and Zimmerman 2015). The affected animal had a unilateral lens luxation and a lens subluxation of the contralateral eye in the absence of concurrent ophthalmic disease. Additionally, the animal's mother and sister had both previously suffered anterior lens luxation also without antecedent disease. A potential genetic mutation responsible for the heritability of lens luxation is unknown but would be important information for future breeding programs of the Matschie's tree kangaroo (Farais et al. 2010). An unpublished case of presumed primary lens luxation in a Goodfellow's tree kangaroo (*Dendrolagus goodfellowi*) has been documented, making one consider that some members of the *Dendrolagus* genus may possess genetic predispositions to primary lens luxation (Smith 2019, personal communication).

Surgical intracapsular lensectomy is recommended to remedy lens luxation in *Dendrolagus* species (Fig. 28.23). The clear corneal incision must be made approximately 3 mm anterior to the limbus, as a conventional clear corneal incision closer to the limbus will result in repeated iris prolapse. Unfortunately, the reported case by McLean and Zimmerman (2015) developed a 360-degree rhegmatogenous retinal detachment 6 months post-operatively in one eye. McLean and Zimmerman (2015) recommend the use of subconjunctival injections for post-operative medications as an alternative to topical medications that could not be safely administered. It appears that the post-operative complications encountered in small animal intracapsular lensectomy surgeries may also be seen in marsupial species, though the frequency of which is impossible to determine without further reports.

Conditions of the Retina and Optic Nerve

Kangaroos can be afflicted by "Kangaroo blindness syndrome," which has been observed since at least 1990 in wild populations of Australian kangaroo species (Fig. 28.24). The disease most often affects adult western gray kangaroos (*Macropus fuliginosus*), while red kangaroos (*Macropus rufus*) and eastern gray kangaroos (*Macropus giganteus*) are less commonly affected, and common wallaroos (*Macropus robustus*) rarely so (Durham et al. 1996). This is primarily a disease of adult kangaroos, with no sex predilection. Clinical field reports indicate that up to 30% of animals in an effected mob can exhibit clinical signs including blindness, confusion, high excitability, a high-stepping gait, and frequent stumbling. Affected animals may maintain normal body condition score if sufficient feed is available. On ophthalmic examination, pupillary-light responses may be poor or absent and conjunctivitis is

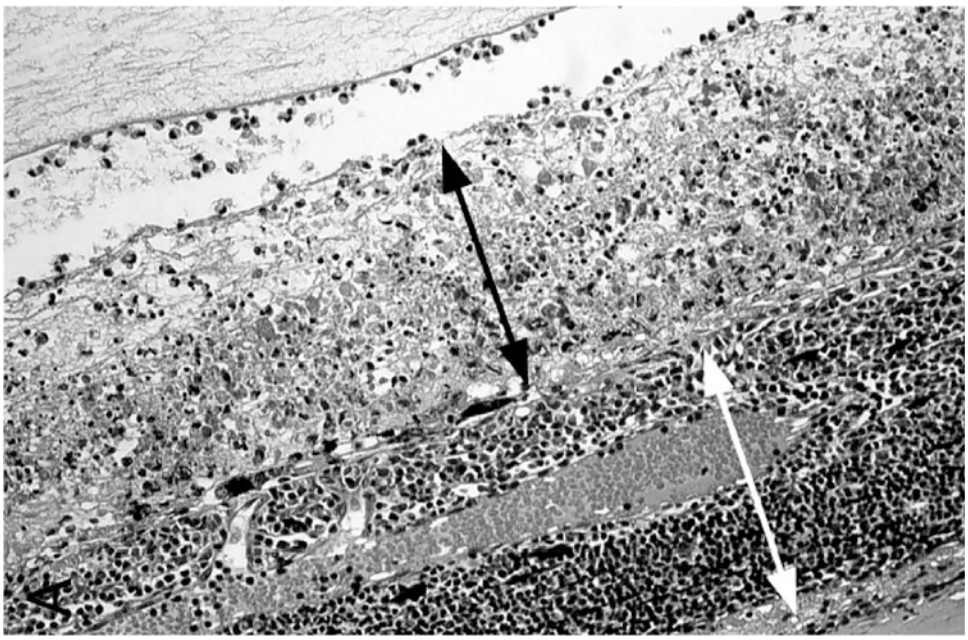

Fig. 28.24 Histologic section of a Western gray kangaroo (*Macropus fuliginosus*) afflicted with kangaroo blindness syndrome by experimental inoculation with Wallal virus. Severe retinal degeneration with mixed inflammatory cell infiltrate is present (black arrow). Proteinaceous exudate is visible in the vitreous overlying, and severe non-suppurative inflammation is present in the underlying choroid (white arrow). Stained with hematoxylin and eosin. *Reddacliff L, Kirkland P, Philbey A et al (1999) Experimental reproduction of viral chorioretinitis in kangaroos. Aust Vet J 77:522–528*, used with permission

variably present (Durham et al. 1996; Reddacliff et al. 1999). Severe bilateral non-suppurative panuveitis with extensive lymphocytic infiltrate, featuring retinitis and retinal degeneration with occasional exudative retinal detachment is commonly observed. Optic neuritis is seen commonly with secondary demyelination of the optic nerve and perivascular lymphocytic cuffing with Wallerian degeneration. Nearly half of the affected cases will also have a concurrent non-suppurative meningoencephalitis hallmarked by mononuclear cellular infiltration (Durham et al. 1996). The orbiviruses, Wallal virus, and Warrego virus were serially isolated from tissues of affected kangaroos, and epidemiologic surveys also implicated these viruses as a likely cause of the syndrome. Further, *Culicoides* mosquitoes that tested positive via PCR for the Wallal and Warrego viruses were found in regions that outbreaks occurred, and are believed to be the culpable vector for outbreaks (Hooper et al. 1999). Healthy kangaroos who were seronegative Wallal virus and Warrego virus were experimentally inoculated with these viruses. Five weeks after inoculation fundic changes were observed that were consistent with the chorioretinitis observed in field cases of kangaroo blindness syndrome. The fundic changes in experimentally affected kangaroos included focal pale regions 1–2 mm in diameter consistent with active retinal and/or choroidal inflammation, and by 10 weeks after inoculation the lesions became pigmented and non-progressive- indicative of retinal pigmented epithelial scar formation. A mild to moderate uveitis was also observed over this period (Reddacliff et al. 1999). It is currently believed that the fundic pathology is as a result of secondary immune-mediated mechanisms as a result of the viral infection (Reddacliff et al. 1999). It is likely that this disease has endemic stability, and outbreaks occur when the vector moves out of its regular micro-habitat to regions where seronegative kangaroos are found (Hooper et al. 1999).

Many other causes of chorioretinal lesions are possible (Fig. 28.25). Toxoplasmosis is a potentially fatal disease that has been documented in various macropod species in both captivity and in the wild (Boorman et al. 1977; Jensen et al. 1985; Miller et al. 1992; Attwood et al. 1975; Johnson et al. 1988; Dubey and Crutchley 2008). Toxoplasmosis is caused by ingestion of sporulated oocysts of the intracellular coccidian parasite, *Toxoplasma gondii,* however transplacental and transmammary transmission is also suspected in macropod species (Parmeswaran et al. 2009). Domestic cats (*Felis catus*) are regarded as the primary source of environmental contamination as oocyst formation is greatest in this species, but in a zoo setting nondomestic felids may be a potential source of infection as well (Canfield et al. 1990). Clinical signs of toxoplasmosis in all marsupial species can include dyspnea, tachypnea, coughing, depression, lymphadenopathy, ataxia, dysphagia, and diarrhea (Dubey and Crutchley 2008; Canfield et al. 1990; Miller et al. 2003; Donahoe et al. 2015). Often, sudden death without prior noted clinical signs occurs (Bermudez et al. 2009; Dubey et al. 1988; Partton et al. 1986). Ocular manifestations include blindness, nystagmus, keratitis, uveitis, chorioretinitis, endophthalmitis, and the development of unilateral or bilateral cataracts (Ladds 2009; Ashton 1979). There is no discernible correlation between the severity of chorioretinitis and the likelihood of developing cataracts (Ashton 1979). The presence of these ocular signs in a macropod should raise concern for toxoplasmosis, however concurrent respiratory, gastrointestinal, or neurological signs

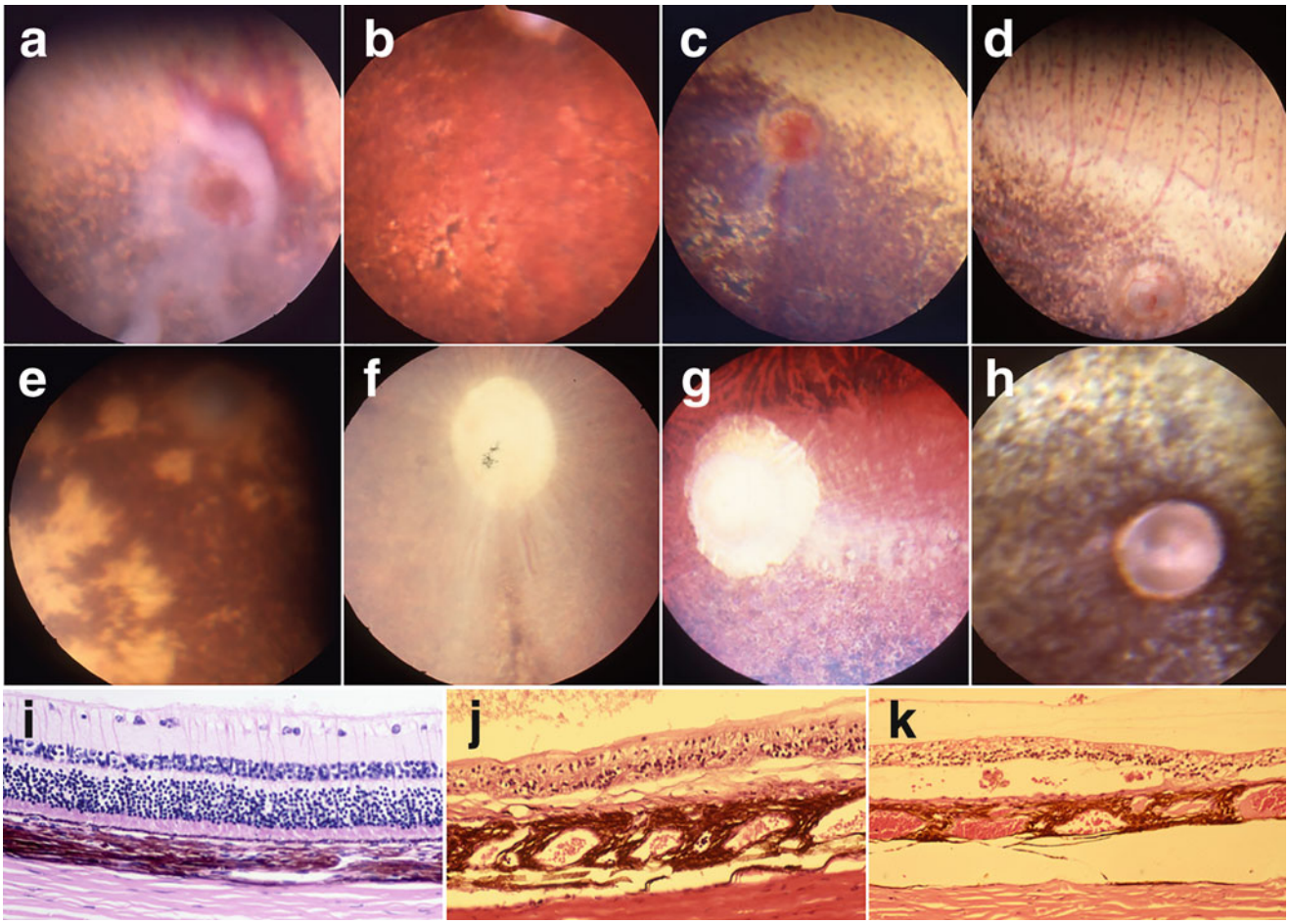

Fig. 28.25 Chorioretinal pathology in marsupials. (**a**) Brushtail possum with optic neuritis, retinal hemorrhage, and retinal edema. (**b**) Brushtail possum with chorioretinal scars (hypo- and hyperpigmentation) of the ventral retina. (**c**) Brushtail possum (*Trichosurus vulpecula*) with ventral retina chorioretinal scars. (**d**) Brushtail possum (*Trichosurus vulpecula*) with retinal atrophy. Note the reduced vasculature overlying the optic nerve head and hypopigmentation. (**e**) Multifocal chorioretinal scars in a ringtail possum (*Pseudocheirus peregrinus*). Chorioretinal scar in a (**f**) red kangaroo (*Macropus rufus*) and a (**g**) western gray kangaroo (*Macropus fuliginosus*). (**h**) Optic nerve coloboma in a koala (*Phascolarctos cinereus*). Histologic cross-sections of the brushtail possum retina *(Trichosurus vulpecula),* showing (**i**) normal retina, (**j**) retinal degeneration, and (**k**) retinal degeneration and detachment with subretinal cellular infiltrate. Stain: hematoxylin & eosin. *Courtesy of Jeffrey Smith*

should further heighten one's index of suspicion (Portas 2010).

An ante-mortem diagnosis in animals with disseminated toxoplasmosis can be made via the examination of leukocytes in peripheral blood smears, however differentiation from other protozoal organisms would not be possible from morphology alone (Portas 2010). Other ante-mortem diagnostics include a modified agglutination test (MAT), which measures *T. gondii* specific immunoglobulin G, although false negatives are common with acute infections. The direct agglutination test (DAT) specific for *T. gondii* antibodies can detect all antibodies, thus if positive is suggestive of an acute *T. gondii* infection if MAT is negative (Johnson et al. 1988). In an unpublished case series of Eastern barred bandicoots (*Perameles gunnii*), ophthalmic lesions including severe conjunctivitis, cataracts, and fundic lesions including chorioretinitis were observed with animals having *Toxoplasma* titers greater than or equal to 1:64 ($P < 0.017$) more likely to have ocular lesions. Additionally, animals with *Toxoplasma* titers greater than 1:256 ($P < 0.007$) were more likely to have cataracts (Stanley 2002). Sadly, diagnosis is often made on post-mortem histopathological analysis in conjunction with immunohistochemistry, with mesenteric lymph nodes and the gastrointestinal tract having the largest numbers of tachyzoites seen, consistent with the sites of *T. gondii* primary replication (Portas. 2010). Polymerase chain reaction can also be performed to confirm *T. gondii* (Parmeswaran et al. 2009).

Treatment has been most successfully documented with the use of atovaquone, a hydroxynapthoquinone with broad spectrum against *T. gondii*, *Babesia* spp., *Plasmodium* spp., and *Pneuomocystis carinii* (Dubey et al. 1988; Johnson-

Delaney 2000). Adverse effects have not yet been reported in macropods, but in humans include maculopapular rash, nausea, diarrhea, elevated liver enzymes, and headache (Portas 2010; Baggish and Hill 2002). Absorption of atovaquone is enhanced when consumed with a fatty meal, and a dose of 100 mg/kg PO SID administered with equal volumes of canola oil or peanut oil has been recommended for a duration of 6–9 months, or until clinical resolution is seen (Dubey and Crutchley 2008; Johnson-Delaney 2000; Portas 2010). Preventative measures to reduce the incidence of toxoplasmosis in macropods include limiting environmental contamination by oocysts from feline feces. This includes limiting access of cats to food preparation areas, barrier nursing between felid enclosures and macropod enclosures, and reducing stressful events to limit the recrudescence of latent infections (Portas 2010).

Koalas are occasionally seen with *Cryptococcus neoformans* var. *gatti* infections, which appears to be associated with the flowering of certain eucalyptus trees (Connolly et al. 1999). Most commonly, cryptococcosis of koalas presents as an isolated nasal cavity lesion (Blanshard and Bodley 2008). However, other clinical signs include pneumonia, upper respiratory tract disease, meningitis, and encephalitis (Krockenberger et al. 2003). Blindness due to optic neuritis or meningitis is occasionally seen (Stanley 2002). Unfortunately, there is limited knowledge on the medical and surgical treatments that may resolve cryptococcosis in koalas (Wynne et al. 2012). A single case study details the confirmed resolution of a *C. neoformans* nasal granuloma via surgical resection and concurrent antifungal therapy with itraconazole at 10 mg/kg orally, twice daily (Wynne et al. 2012). However, it is unclear if this therapy would be of benefit in severely affected patients with visual compromise. A single case has been reported where the only clinical sign of cryptococcosis was exophthalmos due to a nasal granuloma caused by *C neoformans*. Treatment via frontal sinus trephination and incisional biopsy for cytological and microbiological analysis, with adjunctive itraconazole therapy (10 mg/kg orally, twice daily) was unsuccessful and the koala died from progressive neurological disease (Martinez-Nevado et al. 2017).

A single case of bilateral central retinal degeneration in a Goodfellow's tree kangaroo (*Dendrolagus goodfellowi*) has been described. Histologically, total loss of retinal layers external to the inner nuclear layer was observed, and the inner nuclear layer contained loss of nuclei and nuclear disorganization (Schmidt and Toft 1981). No cause was identified.

References

Akula JD, Esdaille TM, Caffe AR et al (2011) The scotopic electroretinogram of the sugar glider related to its histological features of its retina. J Comp Physiol 197:1043–1054

Arrese CA, Dunlop SA, Harman AM et al (1999) Retinal structure and visual acuity in a polyprotodont marsupial, the fat-tailed dunnart (*Sminthopsis crassicaudata*). Brain Behav Evol 53:111–116

Arrese CA, Hart NS, Thomas N et al (2002) Trichromacy in Australian marsupials. Curr Biol 12:657–660

Arrese CA, Rodger J, Beazley LD et al (2003) Topographies of retinal cone photoreceptors in two Australian marsupials. Vis Neurosci 20: 307–311

Arrese CA, Oddy AY, Runham PB et al (2005) Cone topography and spectral sensitivity in two potentially trichromatic marsupials, the quokka (*Setonix brachyurus*) and quenda (*Isoodon obesulus*). Proc Royal Soc B Biol Sci 272:791–796

Ashton N (1979) Ocular toxoplasmosis in wallabies (*Macropus rufigriseus*). Am J Ophthalmol 88:322

Attwood HD, Woolley PA, Rickard MD (1975) Toxoplasmosis in dasyurid marsupials. J Wildl Dis 11:543–551

Baggish AL, Hill DR (2002) Antiparasitic agent atovaquone. Antimicrob Agents Chemother 46:1163–1173

Bakal-Weiss M, Steinberg D, Friedman M et al (2010) Use of a sustained release chlorhexidine varnish as treatment of oral necrobacillosis in Macropus spp. J Zoo Wildl Med 41:371–373

Bennett M, Tu SL, Upton C et al (2017) Complete genomic characterization of two novel poxviruses (WKPV and EKPV) from Western and Eastern grey kangaroos. Virus Res 242:106–121

Bermudez R, Failde LD, Losada AP et al (2009) Toxoplasmosis in Bennett's wallabies (*Macropus rufogriseus*) in Spain. Vet Parasitol 160:155–158

Blanshard W, Bodley K (2008) Koalas. In: Vogelnest L, Woods R (eds) Medicine of Australian mammals. CRISO Publishing, Victoria, Australia, pp 227–327

Boever WJ, Leathers C (1973) Pulmonary and encephalic infection secondary to lumpy jaw in kangaroos. J Zoo Anim Med 4:13–16

Boorman GA, Kollias GV, Taylor RF (1977) An outbreak of toxoplasmosis in wallaroos (*Macropus robustus*) in a Californian zoo. J Wildl Dis 13:64–68

Borland D, Coulson G, Beveridge I (2012) Oral necrobacillosis ('lumpy jaw') in a free-ranging population of eastern grey kangaroos (*Macropus giganteus*) in Victoria. Austr Mammal 24:29–35

Burnard D, Huston WM, Webb JK et al (2017a) Molecular evidence of Chlamydia pecorum and arthropod-associated Chlamydiae in an expanded range of marsupials. Nature 7:12844

Burnard D, Weaver H, Gillett A et al (2017b) Novel Chalamydiales genotypes identified in ticks from Australian wildlife. Parasit Vectors 10:46

Buttery RG, Haight JR, Bell K (1990) Vascular and avascular retinae in mammals. A fundoscopic and fluroscein angiographic study. Brain Behav Evol 35:156–175

Buttery RG, Hinrichson CF, Weller WL et al (1991) How thick should a retina be? A comparative study of mammalian species with and without intraretinal vasculature. Vis Res 31:169–187

Canfield PH, Hartley WJ, Dubey JP (1990) Lesions of toxoplasmosis in Australian marsupials. J Comp Pathol 103:159–167

Canfield PJ (1989) A survey of urinary tract disease in New South Wales koalas. Aust Vet J 66:103–106

Canfield PJ, Brown AS, Kelly WR et al (1987) Spontaneous lymphoid neoplasia in the koala (*Phascolarctos cinereus*). J Comp Pathol 97: 171–178

Chase J (1982) The evolution of retinal vascularisation in mammals: a comparison of vascular and avascular retinae. Ophthalmology 89: 1515–1525

Cockram FA, Jackson ARB (1974) Isolation of a Chlamydia from cases of keratoconjunctivitis in koalas. Aust Vet J 50:82–83

Connolly JH, Krockenberger MB, Malik R et al (1999) Asymptomatic carriage of Cryptococcus neoformans in the nasal cavity of the koala (*Phascolarctos cinereus*). Med Mycol 37:331–338

Craigie EH (1939) The blood vessels in the central nervous system of the kangaroo. Science 88:359–360

Devereaux LN, Polkinghorne A, Meijer A et al (2003) Molecular evidence for novel chlamydial infections in the koala (*Phascolarctos cinereus*). Syst Appl Microbiol 26:245–253

Donahoe SL, Slapeta J, Knowles G et al (2015) Clinical and pathological features of toxoplasmosis in free-ranging common wombats (Vombatus ursinus) with multilocus genotyping of Toxoplasma gondii type II-like strains. Parasitol Int 64:148–153

Dubey JP, Crutchley C (2008) Toxoplasmosis in wallabies (*Macropus rufogriseus* and *Macropus eugenii*): blindness, treatment with atovaquone, and isolation of Toxoplasma gondii. J Parasitol:929–933

Dubey JP, Ott-Joslin J, Torgerson RW et al (1988) Toxoplasmosis in black-faced kangaroos (*Macropus fuliginosus melanops*). Vet Parasitol 30:97–105

Duke-Elder S (1958) System of ophthalmology: Volume 1- the eye in evolution. Henry Kimpton Publishers, London

Durham PJK, Finnie JW, Lawrence DA (1996) Blindness in South Australian kangaroos. *Aust Vet J* 73:111–112

Fang L, Zhou C, Yang M (2013) "Expansion in situ" concept as a new technique for expanding skin and soft tissue. Exp Therap Med 6: 1295–1299

Farais FHG, Johnson GS, Taylor JF et al (2010) An ADAMTS17 splice donor site mutation in dogs with primary lens luxation. Invest Ophthalmol Vis Sci 51:4716–4721

Freeman B, Tancred E (1978) The number and distribution of ganglion cells in the retina of the brush-tailed possum, *Trichosurus vulpecula*. J Comp Neurol 177:557–568

Funnell O, Johnson L, Woolford L et al (2013) Conjunctivitis associated with Chlamydia pecorum in three koalas (*Phascolarctos cinereus*) in the mount lofty ranges, South Australia. J Wildl Dis 49:1066–1069

Govendir M (2018) Review of some pharmacokinetic and pharmacodynamic properties of anti-infective medicines administered to the koala (Phascolarctos cinereus). J Vet Pharmacol Ther 41:1–10

Griffith JE, Higgins DP, Li KM et al (2010) Absorption of enrofloxacin and marbofloxacin after oral and subcutaneous administration in diseased koalas (*Phascolarctos cinereus*). J Vet Pharmacol Ther 33:595–604

Grundon RA, Anderson GA, Lynch M et al (2011) Schirmer tear tests and intraocular pressures in conscious and anesthetised koalas (*Phascolarctos cinereus*). Vet Ophthalmol 14:292–295

Guillery GW, Jeffrey G, Saunders N (1999) Visual abnormalities in albino wallabies: a brief note. J Comp Neurol 403:33–38

Hanger J, Loader J, Wan C et al (2013) Comparison of antigen detection and quantitative PCR in the detection of chlamydial infection in koalas (*Phascolarctos cinereus*). Vet J 195:391–393

Hanger JJ, Heath TJ (1991) Topgraphy of the major superficial lymph nodes and their efferent lymph pathways in the koala (*Phascolarctos cinereus*). J Anat 177:67–73

Harissi-Dagher M, Colby K (2008) Anterior segment dysgenesis: Peters anomaly and sclerocornea. Int Ophthalmol Clin 48:35–42

Hartley MP, Sanderson S (2003) Use of antibiotic impregnanted polymethylmethacrylate beads for the treatment of chronic mandibular osteomyelitis in a Bennett's wallaby (*Macropus rufogriseus rufogriseus*). Aust Vet J 81:742–744

Hill JP, Hill OC (1955) The growth-stages of the pouchyoung of the native cat (*Dasyurus viverrinus*) together with observations on the anatomy of the new-born young. Trans Zool Soc Lond 28:349–453

Hirst LW, Brown AS, Kempster R et al (1992a) Keratitis in free ranging koalas (*Phascolarctos cinereus*) on Magnetic Island, Townsville. J Wildl Dis 28:424–427

Hirst LW, Brown AS, Kempster R et al (1992b) Ophthalmic examination of the normal eye of the koala. J Wildl Dis 28:419–423

Hong-Ming C, Xiong H, Xiong J et al (1990) Metabolic studies of galactosemic cataract. Exp Eye Res 51:345–349

Hooper PT, Lunt RA, Gould AR et al (1999) Epidemic of blindness in kangaroos- evidence of a viral aetiology. Aust Vet J 77:529–536

Jackson M, White N, Giffard P et al (1999) Epizootiology of Chlamydia infections in two free-ranging koala populations. Vet Microbiol 65: 255–264

Jacobs GH, Williams GA (2010) Cone pigments in a North American marsupial, the opossum (*Didelphis virginiana*). J Comp Physiol A 196:379–384

Jensen JM, Patton S, Wright BG et al (1985) Toxoplasmosis in marsupials in a zoological collection. J Zoo Anim Med 16:129–131

Johnson AM, Roberts H, Munday BL (1988) Prevalence of Toxoplasma gondii antibody in wild macropods. Aust Vet J 65:199–201

Johnson JH, Jensen JM (1998) Hepatotoxicity and secondary photosensitisation in a red kangaroo (*Megaleia rufus*) due to ingestion of Lanata camara. J Zoo Wildl Med 29:203–207

Johnson-Delaney CA (2000) Medical problems of pet wallabies. Exotic Pet Pract 5:89–92

Kempster RC, Hirst LW, Powell MW (1994) Heterochromia in a Koala. Vet Comp Ophthalmol 4:125–126

Kempster RC, Hall JS, Hirst LW et al (1996) Ocular response of the koala (*Phascolarctos cinereus*) to infection with *Chlamydia psittaci*. Vet Comp Ophthalmol 6:14–17

Kempster RC, Bancroft BJ, Hirst LW (2002) Intraorbital anatomy of the koala (*Phasolarctos cinereus*). Anat Rec 267:277–287

Kern TJ, Colitz CMH (2012) Exotic animal ophthalmology. Veterinary ophthalmology, 5th edn. Wiley-Blackwell Publishing. Ames, pp 1750–1819

Kinoshita JH (1965) Cataracts in galactosemia. Investig Ophthalmol 4: 786–789

Kirby MA, Wilson PD, Fischer TM (1988) Development of the optic nerve of the opossum (*Didelphis virginiana*). Dev Brain Res 44:37–48

Kleckowska-Nawrot JE, Gozdziewska-Harlajczuk K, Darska M et al (2019) Microstructure of the eye tunics, eyelids and ocular glands of the Sulawesi bear cuscus (Ailurops ursinus Temmick, 1824) (Phalangeridae: Marsupialia) based on anatomical, histological and histochemical studies. Acta Zool 100:182–210

Kollipara A, Polkinghorne A, Wan C (2013) Genetic diversity of Chlamydia pecorum strains in wild koala locations across Australia and the implications for a recombinant C. pecorum major outer membrane protein based vaccine. Vet Microbiol 27:513–522

Krockenberger MB, Canfield PJ, Malik R (2003) Cryptococcus neoformans var. Gatti in the koala (*Phascolarctos cinereus*): a review of 43 cases of cryptococcosis. Med Mycol 41:225–234

Kusewitt DF, Lewis JL, Griffith WC et al (1996) Effect of chronic ultraviolet radiation exposure and photoreactivation on life span and tumour development in the marsupial *Monodelphis domestica*. Rad Res 14:181–191

Kusewitt DF, Sherburn TE, Miska KB et al (1999) The p53 tumour suppressing gene of the marsupial *Monodelphis domestica*: cloning of exons 4-11 and mutations in exons 5-8 in ultraviolet radiation-induced corneal sarcomas. Carcinogenesis 20:963–968

Labelle AL, Law M, Hamor RE et al (2010a) Ophthalmic examination findings in a captive colony of western gray kangaroos (*Macropus fuliginosus*). J Zoo Wildl Med 41:461–467

Labelle AL, Hamor RE, Narfstrom K et al (2010b) Electroretinography in the western grey kangaroo (*Macropus fuliginosus*). Vet Ophthalmol 13:41–46

Ladds P (2009) Pathology of Australian native wildlife. CSIRO Publishing, Collingwood

Lau Q, Griffith JE, Higgins DP (2014) Identification of MHCII variants associated with chlamydial disease in the koala (*Phascolarctos cinereus*). PeerJ 19(2):e443. https://doi.org/10.7717/peerj.443

Liddle VL (2015) Electroretinography in the normal koala (*Phascolarctos cinereus*). Vet Ophthalmol 18:74–80

Liddle VL, Naranjo C, Bernays ME (2014) Anterior chamber collapse syndrome in a koala. Aust Vet J 92:179–182

Loader J (2010) An investigation in to the health of wild koala populations in South-East Queensland. Honours thesis. The University of Queensland. St Lucia, Brisbane, Australia

Markey B, Wan C, Hanger J et al (2007) Use of quantitative real-time PCR to monitor shedding and treatment of chlamydiae in the koala (*Phascolarctos cinereus*). Vet Microbiol 120:334–342

Martinez-Nevado E, Alsonso-Alegre EG, Martinez MAJ et al (2017) Atypical presentation of Cryptococcus neoformans in a koala (*Phascolarctos cinereus*): a magnetic resonance imaging and computed tomography study. J Zoo Wildl Med 48:250–254

McKenzie RA, Fay FR, Prior HC (1979) Poxvirus infection of the skin of an eastern grey kangaroo. Aust Vet J 55:188–190

McLean NJ, Zimmerman R (2015) Bilateral lens luxation and intracapsular lens extractions in a Matshchie's tree kangaroo. Vet Ophthalmol 18:81–85

McMenamin PG (2007) The unique paired retinal vascular pattern in marsupials: structural, functional and evolutionary perspectives based on observations in a range of species. Br J Ophthalmol 91: 1399–1405

McMenamin PG, Krause WJ (1993) Development of the eye in North American opossum (*Didelphis virginiana*). J Anat 183:343–358

McMenamin PG, Golborne CN, Chen X et al (2017) The unique retinal vessels of the gray short-tailed opossum (Monodelphis domestica) and their relationship to astrocytes and microglial cells. Anat Rec 300:1391–1400

Miller DS, Faulkner C, Patton S (2003) Detection of Toxoplasma gondii IgG antibodies in juvenile great grey kangaroos *Macropus giganteus giganteus*. J Zoo Wildl Med 34:189–193

Miller MA, Ehlers K, Dubey JP et al (1992) Outbreak of toxoplasmosis in wallabies on an exotic animal farm. J Vet Diag Invest 4:480–483

Mohamed R (2018) Anatomical and radiographic study on the skull and mandible of the common opossum (*Didelphis marsupialis* Linnaeus, 1758) in the Carribbean. Vet Sci 5:44

Nelson J (1987) The early development of the eye of the pouch young of the marsupial *Dasyurus hallacatus*. Anat Embryol 175:387–398

Nyari S, Waugh CA, Dong J et al (2017) Epidemiology of chlamydial infection and disease in a free-ranging koala (*Phascolarctos cinereus*) population. PLoS One 12:e0190114

Nyari S, Booth R, Quigley BL et al (2019) Therapeutic effect of a Chlamydia pecorum recombinant major outer membrane protein vaccine on ocular disease in koalas (*Phascolarctos cinereus*). PLoS One 14:e0210245

Oria AP, Raposos AC, Araujo LLC et al (2019) Evaluation of tear production in juvenile opossum using three different methods. Br J Vet Res 39:61–65

Parmeswaran N, O'Handley RM, Grigg ME et al (2009) Vertical transmission of *Toxoplasma gondii* in Australian marsupials. Parasitology 136:939–944

Partton S, Johnson SL, Loeffler DG et al (1986) Epizootic of toxoplasmosis in kangaroos, wallabies and potoroos: possible transmission via domestic cats. J Am Vet Med Assoc 189:1166–1169

Patterson JLS, Lynch M, Anderson GA et al (2015) The prevalence and clinical significance of chlamydia infection in island and mainland populations of Victorian koalas (*Phascolarctos cinereus*). J Wildl Dis 51:309–317

Pinard CL, Brightman AH, Yeary TJ et al (2002) Normal conjunctival flora in the North American opossum (*Didelphis virginiana*) and raccoon (*Procyon lotor*). J Wildl Dis 38:851–855

Polkinghorne A, Hanger J, Timms P (2013) Recent advances in understanding the biology, epidemiology and control of chlamydial infections in koalas. Vet Microbiol 16:214–223

Portas TJ (2010) Toxoplasmosis in Macropodids: a review. J Zoo Wildl Med 41:1–6

Prado MR, Rocha MEG, Brito EHS (2005) Survey of bacterial microorganisms in the conjunctival sac of clinically normal dogs and dogs with ulcerative keratitis in Fortaleza, Ceara, Brazil. Vet Ophthalmol 8:33–37

Ramsay WR (1960) Tetanus in the kangaroo. Aust Vet J 10:412

Reddacliff L, Kirkland P, Philbey A et al (1999) Experimental reproduction of viral chorioretinitis in kangaroos. Aust Vet J 77:522–528

Reynolds HC (1962) Studies on reproduction in the opossum (*Didelphis virginiana*). Univ Calif Pub Zool 52:223–275

Rodger J, Dunlop SA, Beaver R et al (2001) The development and mature organization of the end-artery retinal vasculature in a marsupial, the dunnart *Sminthopsis crassicaudata*. Vis Res 41:13–21

Rothwell TLW, Keep JM, Xu FN et al (1984) Poxvirus in marsupial skin lesions. Aust Vet J 61:409–410

Sabourin CLK, Kusewitt DF, Fry RJM et al (1993) Ultraviolet radiation-induced tumors in a South American opossum (*Monodelphis domestica*). J Comp Pathol 108:343–359

Sasche K, Vretou E, Livingstone M et al (2009) Recent developments in laboratory diagnosis of chlamydial infections. Vet Microbiol 135:2–21

Schmid LM, Schmid KL, Brown B (1991) Behavioural determination of visual function in the Koala (*Phascolarctos cinereus*). Wildl Res 18: 367–374

Schmidt RE, Toft JD (1981) Ophthalmic lesions in animals from a zoologic collection. *J Wildl Dis* 17:267–275

Segovia L, Horwitz J, Gasser R et al (1997) Two roles for mu-crystallins: a lens structural protein in diurnal marsupials and a possible enzyme in mammalian retinas. Mol Vis 3:9–12

Slatter DH, Mann IC, Mills JN (1980) Cataracts and depressed galactose-1-phosphate uridyl transferase activity in a cus cus (*Phalanger maculatus*). Aust Vet J 56:141–144

Smith J (2019) Personal communications. Eye Clinic for Animals, Sydney, Australia, p 2064

Speight KN, Polkinghorne A, Penn R et al (2016) Prevalence and pathologic features of Chlamydia pecorum infections in South Australian koalas (*Phascolarctos cinereus*). J Wildl Dis 52:301–306

Stalder K, Vaz PK, Gilkerson JR et al (2015) Prevalence and clinical significance of herpesvirus infection in populations of Australian marsupials. PLoS One 10:e0133807

Stambolian D (1988) Galactose and cataracts. Surv Ophthalmol 3:333–349

Stanley R (2002) Marsupial ophthalmology. Vet Clin Exot Anim Pract 5:371–390

Stephens T, Irvine S, Mutton P et al (1974) Deficiency of two enzymes of galactose metabolism in kangaroos. Nature 248:524–525

Stephens T, Crollini C, Mutton P et al (1975) Galactose metabolism in relation to cataract formation in marsupials. Aust J Exp Biol Med Sci 53:233–239

Steventon CA, Raidal SR, Quinn JC et al (2018) Steroidal saponin toxicity in eastern grey kangaroos (*Macropus giganteus*): a novel clinicopathologic presentation of hepatogenous photosensitisation. J Wildl Dis 54:491–502

Suedmeyer K, Pearce J, Persky M et al (2014) Peters anomaly in a red kangaroo (*Macropus Rufus*). J Zoo Wildl Med 45:715–718

Takle GL, Suedmeyer WK, Hunkeler A (2010) Selected diagnostic ophthalmic tests in the red kangaroo (*Macropus Rufus*). J Zoo Wildl Med 41:224–233

Tancred E (1981) The distribution and sizes of ganglion cells in the retinas of five Australian marsupials. J Comp Neurol 196:585–603

Tarlinton R, Meers J, Hanger J et al (2005) Real-time reverse transcriptase PCR for the endogenous koala retrovirus reveals an association between plasma viral load and neoplastic disease in koalas. J Gen Virol 86:1–5

Taylor JSH, Guillery RW (1994) Early development of the optic chiasm in the gray short-tailed opossum, *Monodelphis domestica*. J Comp Neurol 350:109–121

Troughton ELG (1941) Furred animals of Australia. Angus & Robertson, Sydney

Vidgen ME, Hanger J, Timms P (2017) Microbiota composition of the koala (*Phascolarctos cinereus*) ocular and urogenital sites, and their association with Chlamydia infection and disease. Sci Rep 7:5239

Vlahos LM, Knott B, Valter K et al (2014) Photoreceptor topography and spectral sensitivity in the common Brushtail possum (*Trichosurus vulpecula*). *J Comp Neurol* 522:3423–3436

Vogelnest L, Portas T (2008) Macropods. In: Vogelnest L, Woods R (eds) Medicine of Australian mammals. CSIRO Publishing, Collingwood, pp 133–226

Wada I, Fukushima T, Minato Y (1988) Histopathological observations on galactose-induced cataracts in rats. Jap J Vet Sci 50:659–664

Wan C, Loader J, Hanger J (2011) Using quantitative polymerase chain reaction to correlate Chlamydia pecorum infectious load with ocular, urinary and reproductive tract disease in the koala (*Phascolarctos cinereus*). Aust Vet J 89:409–412

Warren K, Swan R, Bodetti T et al (2005) Ocular chlamydiales infections of western barred bandicoots (*Perameles bougainville*) in Western Australia. J Zoo Wildl Med 36:100–102

Waugh C, Austrin R, Polkinghorne A et al (2016) Treatment of Chlamydia-associated ocular disease via a recombinant protein based vaccine in the koala (*Phascolarctos cinereus*). Biologicals 44:588–590

Webber CE, Whalley JM (1978) Widespread occurrence in Australian marsupials of neutralizing antibodies to a herpesvirus from a Parma wallaby. Aust J Exp Biol Med Sci 56:351–357

Whittaker CJ, Heaton Jones TG, Kubilis PS et al (1995) Intraocular pressure variation associated with body length in young American alligators (Alligator mississippiensis). Am J Vet Res 56:1380–1383

Wible JR (2003) On the cranial osteology of the short-tailed opossum Monodelphis brevicaudata (Didelphidae, Marsupialia). Ann Carnegie Museum 72:137–142

Wilhelmi BJ, Blackwell SJ, Mancoll JS et al (1998) Creep vs. stretch: a review of the viscoelastic properties of skin. Ann Plast Surg 41:215–219

Wilks CR, Kefford B, Callinan RB (1981) Herpesvirus as a cause of fatal disease in Australian wallabies. J Comp Pathol 91:461–465

Wislocki GB (1940) Peculiarities of the cerebral blood vessels of the opossum: diencephalon, area postrema and retina. Anat Rec 78:119–131

Wood MM, Timms P (1992) Comparison of nine antigen detection kits for diagnosis of urogenital infections due to *Chlamydia psittaci* in koalas. J Clin Microbiol 30:3200–3205

Wynne J, Klause S, Stadler C et al (2012) Preshipment testing success: resolution of a nasal sinus granuloma in a captive koala (*Phascolarctos cinereus*) caused by Cryptococcus gattii. J Zoo Wildl Med 43:939–942

Xu W, Stadler CK, Gorman K et al (2013) An exogenous retrovirus isolated from koalas with malignant neoplasias in a US zoo. PNAS 110:11547–11552

Zheng T, Napier AM, O'Keefe JS et al (2004) Experimental infection of possums with macropodid herpesvirus 1. New Zealand Vet J 52:20–25

Ophthalmology of Xenarthra: Armadillos, Anteaters, and Sloths

29

Jessica M. Meekins and Bret A. Moore

© Chrisoula Skouritakis

Xenarthra (from Ancient Greek, meaning xénos, "foreign, alien" +árthron, "joint") is a superorder of placental mammals that originated in South America during the Paleocene era, roughly 59 million years ago. Members of this group are thought to be one of the most ancient groups of mammals and include armadillos, anteaters, and sloths. Although its visual system has historically been understudied, the role of this group as an animal model for several human diseases of rod photoreceptors such as retinitis pigmentosa (Nakamura et al. 2016) and Leber congenital amaurosis (van der Spuy et al. 2005) may prove pivotal: they are considered completely colorblind (rod monochromats), an otherwise non-existent retinal adaptation among vertebrates that are not living underground or deep within the sea (Douglas et al. 1995; Meredith et al. 2013; Emerling and Springer 2014; Mohun et al. 2010). This claim is supported by behavioral (Newman 1913; Mendel et al. 1985; de Sampaio et al. 2016), anatomical (Wislocki 1928; Walls 1942; Watillon and Goffart 1969; Piggins and Muntz 1985), and genomic and phylogenetic (Emerling and Springer 2014) evidence. Despite support for rod monochromacy, many species within *Xenarthra* are diurnal and occupy niches receiving direct or indirect sunlight. Although rod monochromacy does not provide high visual acuity and can even result in total blindness in high luminance conditions, there is debate on how much Xenarthrans rely on vision and whether or not they predominantly use other senses, particularly in photopic conditions (Emerling and Springer 2014). Limited information exists on the visual capabilities, ophthalmic anatomy, and naturally occurring ophthalmic disease processes that affect Xenarthran eyes. In addition, detailed reports of clinical examination findings and comprehensive results of basic ocular diagnostic tests are lacking. Furthering our knowledge of the visual systems and ophthalmic pathologies in this group of animals may aid in conservation efforts (e.g., prevention of vehicular trauma of which Xenarthrans are frequent victims), rehabilitation, or welfare in captivity.

J. M. Meekins (✉)
College of Veterinary Medicine, Kansas State University, Manhattan, KS, USA
e-mail: jslack@vet.k-state.edu

B. A. Moore
College of Veterinary Medicine, University of Florida, Gainesville, FL, USA

F. Montiani-Ferreira et al. (eds.), *Wild and Exotic Animal Ophthalmology*, https://doi.org/10.1007/978-3-030-81273-7_4

Armadillos

The armadillo (from Spanish, meaning "little armored one") is a New World placental mammal, of which 21 extant species have been described. The distinction between species is often associated with the number of armored bands. The various adnexal glandular structures of the armadillo have been described in great detail. Harderian glands have been identified in the medial orbit of the nine-banded armadillo (*Dasypus novemcinctus*) and the South American big hairy armadillo (*Chaetophractus villosus*).(Aldana Marcos and Affanni 2005; Weaker 1981) Histologically, these glands were most recently described as compound-branched tubuloalveolar structures with a single layer of columnar cells surrounded by myoepithelium.(Aldana Marcos and Affanni 2005) Histochemical staining revealed lipids, proteins, and glycoconjugates within secretory vesicles, and the mechanism of secretion was speculated to be either merocrine or apocrine.(Aldana Marcos and Affanni 2005) As with other digging and burrowing species that possess these specialized glands, the presence of a Harderian gland in armadillos is thought to be largely protective, with a production of antibacterial substances and growth factors, as well as lubrication of the ocular surface.

The lacrimal and nictitans glands have also been described in the armadillo (Aldana Marcos et al. 2002). The lacrimal gland is located in the caudal and lateral external portion of the orbit, with dimensions of 0.5 cm in length and 14 mm in width running in a mediolateral direction (Aldana Marcos et al. 2002). The nictitans gland is located in the rostral and lateral external portion of the orbit, with its several lobes wrapped around the nictitating membrane cartilage (Aldana Marcos et al. 2002). The glands were histologically and histochemically identical, composed of mucous cells, seromucous cells, and serous cells (Aldana Marcos et al. 2002). Beyond the reports of structure, content, and proposed function of adnexal glands within this species, no other reports describing ophthalmic anatomy have been published for the armadillo.

Performing a thorough ophthalmic examination in armadillos is challenging without sedation. They are strong and mobile, have large claws for digging, may bite (only the six-banded armadillo, *Euphractus sexcinctus*), and can roll up (*Tolypeutes* spp.). Lateral pressure on the carapace can be used for calming, and *Tolypeutes* spp. will unroll when placed on a firm surface (Aguilar and Superina 2015). Obtaining exposure of the eyes is difficult: they are small and inset and are surrounded by hard, keratinized plates. Additionally, with each blink the eyes retract, and the eyelids roll inward to meet axially (Johnson 1901) preventing adequate globe exposure upon manual opening of the palpebral fissure. The aforementioned globe position and retraction ability, surrounding keratinized plates, plus the presence of thick eyelids with numerous, bristly cilia that emanate from just above and below the dorsal and ventral eyelid margins, respectively, are important mechanisms to protect the eye from dirt and debris as armadillos dig for live insects and other invertebrate prey. Figure 29.1 shows examples of the normal eyes and adnexa of A) the southern three-banded armadillo (*Tolypeutes matacus*) and B–D) the six-banded armadillo (*Euphractus sexcinctus*). The conjunctiva normally has an orange coloration (Fig. 29.1c), but the nictitating membrane is not readily visible. Through thin corneas, a heavily pigmented iris is observed. The pupils are quite small in photopic conditions but dilate markedly with atropine (Johnson 1901). The fundus is homogenously light brown and has a small circular white optic disc with a slight central depression located just dorsotemporal to the optic axis (Fig. 29.1d). Fundic details are difficult to establish due to unequal lenticular refraction (Johnson 1901). No retinal vessels are visible, although a pseudoangiotic to paurangiotic pattern is suspected based on examination of other *Xenathrans*. One report suggested increased sensitivity to light just nasal to the optic disc, possibly indicating the location of a retinal specialization (e.g., rod-based area centralis) (Johnson 1901).

Conjunctivitis is not uncommon in captive armadillos, and has been reported to affect 0.5% of animals in the wild (Dilger-Sanches and Montiani-Ferreira 2018), often related to concurrent respiratory disease. Despite no reports of naturally occurring ocular *Mycobacterium leprae* infections in armadillos, leprosy should be considered in cases of keratoconjunctivitis, as armadillos are the only species other than humans to be considered a natural reservoir for this bacterium. Leprosy is one of the leading causes of human blindness worldwide, with a higher percentage of ocular involvement described in cases of leprosy than any other systemic infection; thus, precautions for zoonotic potential should be taken (Malaty et al. 1990). Early in *M. leprae* infections, armadillos are reported to have skin erosions around the eyes, nose, and footpads (Agnew et al. 2018). *Dasypus sp.* experimentally infected (intracutaneously) with *Mycobacterium leprae* developed frequent ocular infections that were largely corneal (44%) (Malaty and Togni 1988; Malaty et al. 1990). Acid-fast bacilli were detected within keratocytes and macrophages throughout the corneal stromal, causing large granulomas that over time became vascularized (Malaty and Togni 1988). Inflammation was also detected within the eyelids, nictitans, extraocular muscles, and lacrimal and Harderian glands (Brandt et al. 1990a). In mild cases or cases with early signs of infection, intraocular involvement was limited to mild iridocyclitis and macrophage infiltrate within the trabeculae of the iridocorneal angle and limbus. However, severely affected animals showed marked

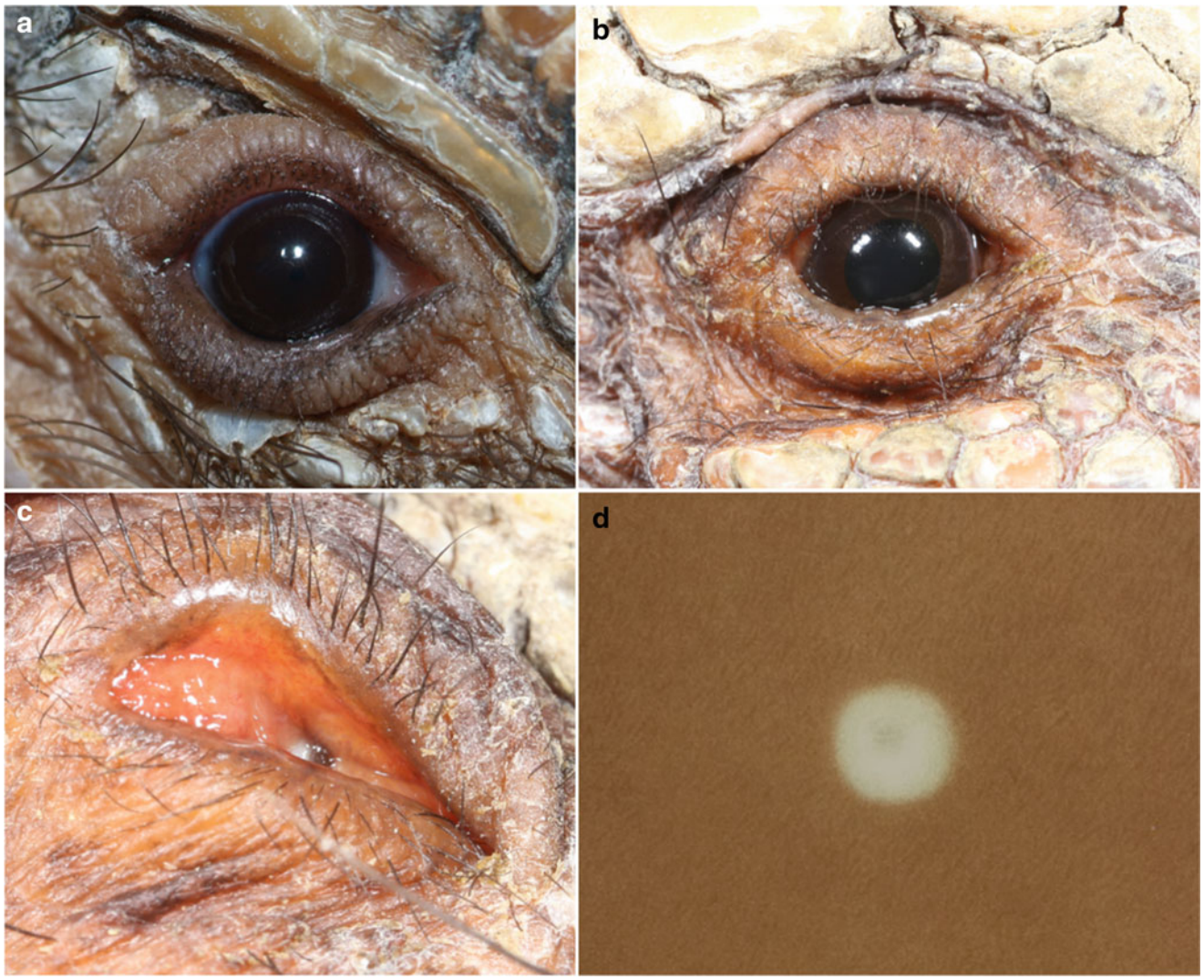

Fig. 29.1 Images showing normal ocular and adnexal structure of armadillos. (**a**) External eye photograph of the southern three-banded armadillo (*Tolypeutes matacus*) and (**b**) the six-banded armadillo (*Euphractus sexcinctus*). (**c**) Normal orange-colored conjunctiva with recessed globe in a six-banded armadillo. (**d**) Fundus drawing of the Hairy Armadillo (*Dasypus villosus*) showing a small, circular, white optic disc and a lack of visible retinal vessels. **d**—Used with permission from Johnson GL. Contributions to the comparative anatomy of the mammalian eye are chiefly based on ophthalmoscopic examination. Philosophical Transactions 1901;194:38. Publisher: Royal Society Publishing

endophthalmitis (predominantly macrophages, but mixed cellular populations were common), as well as granulomas within the cornea, and all tissues contained bacteria (Brandt et al. 1990a, b). Bacteria were found in vascular endothelial cells and peripheral nerve Schwann cells, suggesting either hematogenous or neuronal dissemination to the eye (Brandt et al. 1990a, b; Malaty and Togni 1988). Experimental inoculation of *M. leprae* into the corneal stroma resulted in keratoconjunctivitis, scleritis, and anterior uveitis, and may support the notion that ocular abrasions could serve as a means of transmission in armadillos (Malaty et al. 1990).

Anteaters

The anteater group consists of four extant species in three genera. The giant anteater (*Myrmecophaga tridactyla*) is strictly ground-dwelling, whereas the silky anteater (*Cyclopes didactylus*) and two species of tamandua (*Tamandua tetradactyla* and *T. mexicana*) are strictly and partially arboreal, respectively. The eyes of anteaters, although small, are more accessible than those of armadillos, with a palpebral fissure length of about 16 mm in both giant anteaters and

Fig. 29.2 External eye photograph of the giant anteater (*Myrmecophaga tridactyyla*). Note the marked amount of debris crusted to the skin and hair surrounding the eye and the moderate but normal amount of seromucoid ocular discharge. Additionally, in contrast to armadillos, a third eyelid is visible

Southern tamanduas (*T. tetradactyla)* (Rodarte-Almedia et al. 2016; de Araujo et al. 2017). However, care must be taken to avoid injury by their long, sharp claws which can be covered with gauze and elastic bandages during handling. Giant anteaters have even been reported to kill humans in the wild and in captivity when threatened. Normal ophthalmic findings are similar to that of armadillos, with a few notable differences. A moderate amount of seromucoid ocular discharge is commonly noted in anteaters, and a prominent nictitating membrane is visible in larger species of anteaters (Fig. 29.2). The ocular fundus is less homogenous than in armadillos, with slight pigment mottling, and several tiny capillaries can be seen emanating from a slightly gray optic disc in a pseudoangiotic to paurangiotic pattern. The mean Schirmer tear test 1, endodontic absorbent paper point test, and conjunctival bacterial flora have been evaluated in two species of anteaters (see Table 29.1, Fig. 29.3, and Appendix 3, Rodarte-Almedia et al. 2016; de Araujo et al. 2017). The mean intraocular pressure as measured by rebound tonometry (Table 29.1) was significantly higher in male compared to female *M. tridactyla* (Rodarte-Almeida et al. 2016). Microbiologic assessment of *M. tridactyla* conjunctiva has shown that primarily Gram + bacteria are present, most frequently comprised of Staphylococcus spp. (54%) that are susceptible to neomycin, tobramycin, and gentamicin (Rodarte-Almeida et al. 2016).

There are no known reports of ophthalmic disease in anteaters. Both wild-caught and captive anteaters have been documented with copious white ocular discharge, particularly after introduction to captivity or following changes within their enclosures (Fig. 29.4a). This is thought to be related to stress (Aguilar and Superina 2015), although similar discharge is noted in cases of idiopathic conjunctivitis, which has been successfully treated with neomycin-polymyxin b sulfates-dexamethasone ophthalmic suspension in the Southern tamandua (Fig. 29.4b). Eyelid ecchymotic and petechial hemorrhages can be noted in cases of hypovitaminosis K, which is commonly observed in all species in captivity (Aguilar and Superina 2015). Traumatic injuries are common in adults, both from intraspecific aggression and improper enclosures (Aguilar and Superina 2015), and ulcerative keratitis has been documented as a result (Fig. 29.4c). A unilateral resorbing cataract has been documented in a captive 8-year-old giant anteater without evidence of anterior uveitis (Fig. 29.4d). Several tamanduas with chronic hypervitaminosis D have been reported to develop corneal mineralization (Fig. 29.5) along with widespread systemic mineralization (e.g., arterial vasculature and heart, lungs, kidneys, etc.). The cause is thought to be diet-related. In a single case of a 15-year-old female Southern tamandua, corneal mineralization was limited to the epithelial-subepithelial layer and did not elicit a vascular response, any apparent ocular discomfort, or epithelial defects. Ultimately, the animal died due to complications of widespread systemic mineralization. Taurine deficiency has

Table 29.1 Selected ophthalmic data on the giant anteater (*M. tridactyla*, Rodarte-Almeida et al. 2016) and the Southern tamandua (*T. Tetradactyla*, Cordeiro de Araujo et al. 2017)

	M. tridactyla	*T. tetradactyla*
Axial globe length	1.10 ± 0.11 cm[a]	–
Corneal diameter (horizontal)	0.57 ± 0.07 cm[a]	–
Horizontal palpebral fissure length	8.0 ± 2.0 mm	15.91 ± 2.51 mm
Schirmer tear test 1	8.0 ± 6.20 mm/min	8.5 ± 4.13 mm/min
Endodontic paper point test	–	14.13 ± 3.24 mm/min
Rebound tonometry	10.9 ± 2.4 mmHg	–
% Gram + organisms	–	70.27%
Most common Gram Pos.	Staphylococcus spp., 54%	Staphylococcus spp., 62%
Most common Gram Neg.	–	Pseudomonas spp., 5.4%

[a]Personal data courtesy of Fabiano Montiani-Ferreira

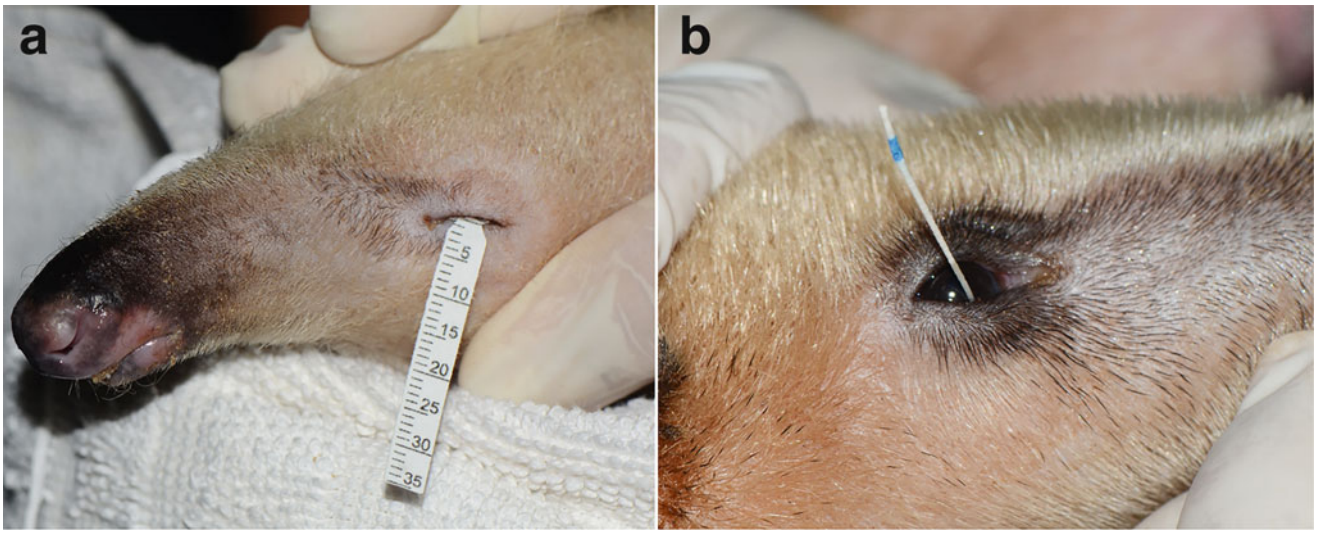

Fig. 29.3 Tear production, as measured by the Schirmer tear test (**a**) and the endodontic absorbent paper point test (**b**), in the Southern tamandua, *Tamandua Tetradactyla*. Courtesy of Arianne Pontes Oria

Fig. 29.4 Ophthalmic conditions in anteaters. Marked mucoid discharge commonly associated with stress (**a**—giant anteater) and conjunctivitis (**b**—Southern tamandua). (**c**) Traumatic corneal injury in a giant anteater caused by intraspecific aggression. (**d**) Unilateral resorbing cataract of unknown cause in the right eye of an 8-year-old giant anteater. **b**, **d**—Courtesy of Fabiano Montiani-Ferriera and Thiago Ferreira, **c**—Courtesy of Danilo Kluyber and Arnaud Desbiez

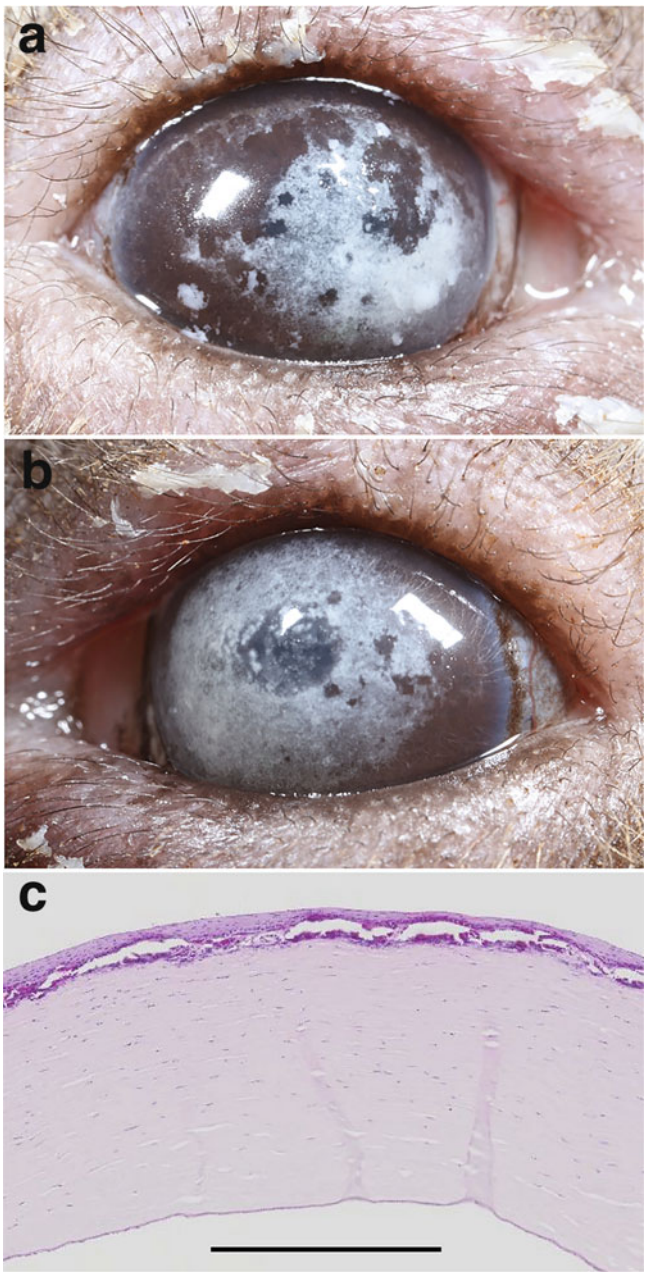

Fig. 29.5 Corneal mineralization in a 15-year-old Southern tamandua (*Tamandua tetradactyla*) with hypervitaminosis D. Although not directly visually tested, the animal appeared sighted during observed interactions with her environment. Dense, widespread mineralization of the epithelial to subepithelial cornea was clinically apparent as multifocal to diffuse coalescing chalky, white deposits in both the right eye (**a**) and left eye (**b**). Histology of the cornea of the left eye (**c**) shows pathology limited to the epithelial-subepithelial region. Scale bar is 0.5 mm. **c**—Photo courtesy of Melissa Roy

been diagnosed in two species of anteaters due to inadequate dietary taurine, although retinopathies as recognized in the Felidae have not been described.

Sloths

Sloths are arboreal mammals that spend most of the time hanging upside down from trees in tropical rainforests. Two families within the sloth group, the two-toed family and the three-toed family, contain six species. Given that sloths are almost strictly arboreal, a trait that is widely considered to require visual acuity as a prerequisite (Clark and Gros 1959), a debate exists regarding their visual capabilities as compared to other Xenarthrans. Early studies showed that the cornea is steeply convex and the crystalline lens is thick (Fig. 29.6a), attributing to retinoscopic values of 3–4 diopters myopic (Watillon and Goffart 1965, 1969). There is no ciliary muscle and thus no ciliary accommodation. A well-developed iris sphincter and a poorly developed iris dilator result in pinhole pupil size even in dim light (Watillon and Goffart 1965, 1969). The globe is relatively small with an overall diameter reported at 10–12.5 mm, the optic nerve is thin, and retinal ganglion cells are sparse (Fig. 29.6b,c) (Watillon and Goffart 1965, 1969). Together, these findings were historically considered suggestive of "poor, short-sighted vision" (Watillon and Goffart 1965, 1969). However, Walls (1942) has suggested that vision in sloths was not necessarily poor; rather, the steep corneal curvature, thick and uniform lens, and a pinhole pupil were ideally suited for both nocturnal and diurnal activities, enabling sharp retinal images without the need for accommodation or a retinal specialization of high acuity. More recently, sloths have been shown to be only slightly myopic (Mendel et al. 1985; Piggins and Muntz 1985), yet behavioral testing suggests that they rely little on vision to conduct normal daily activities (Mendel et al. 1985).

Neuron distribution of the sloth retina, however, speaks otherwise as it seems to be well-aligned to the behavioral ecology of the species. As with all Xenarthrans, the photoreceptor layer of the retina contains only rods; however, the distribution of retinal cells between different sloth species varies. In two-toed sloths (*Choloepus didactylus*), an area centralis lies just temporal to the optic disc and is connected to a horizontal visual streak to provide a maximum visual acuity of 2.38 cycles per degree (Andrade-da-costa et al. 1989), whereas three-toed sloths (*Bradypus variegatus*) have an area centralis in the far ventrotemporal retina that is connected with a vertical visual streak that provides a maximum visual acuity of 2.18 cycles per degree (Costa et al. 1987). Interestingly, the three-toed sloth turns its head to be right-side-up when climbing upside-down on a branch, whereas the two-toed sloth maintains its head in the same upside-down orientation as its body (Mendel 1981). This behavioral difference corresponds well with the organization of each sloth's visual system, as the far ventrally-positioned area centralis and vertical streak in the three-toed sloth would project upward to the branch as it climbs upside-down with

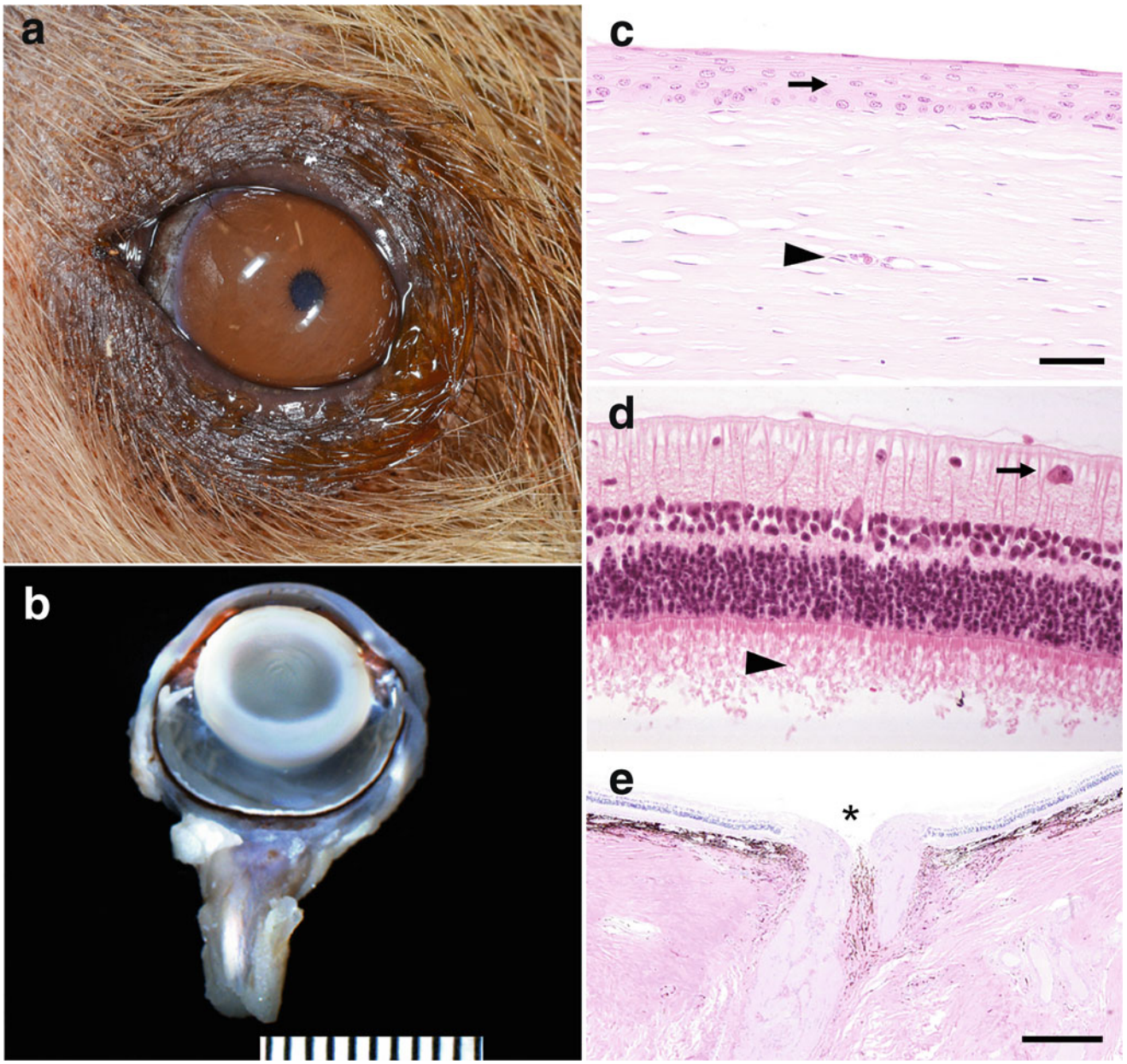

Fig. 29.6 Examples of normal eyes from sloths. (**a**) Color photograph depicting normal external and anterior segment ocular structures of a 7-year-old male two-toed sloth. Note the lack of cilia but occasional trichiasis, and the markedly miotic pupil in photopic conditions. Normal gross (**b**) and histologic (**c**–**e**) examples of the eye of a 13-year-old two-toed sloth. (**b**) Sagittal section showing a large, steeply convex cornea and a thick crystalline lens. (**c**) Photomicrograph of the central cornea, showing mild keratitis (blood vessel denoted by the arrowhead). The stratified squamous non-keratinized epithelium is denoted by the arrow. Scale bar represents 50 μm. (**d**) Histologic section of the retina showing sparse retinal ganglion cells (arrow) and the presence of only rod photoreceptors (arrowhead). (**e**) Histologic section of the posterior pole of the eye showing a thin optic nerve and a deep physiologic optic cup (asterisk; scale bar 500 μm). **a**—Courtesy of Dr. Sabine Chahory, Unit of Ophthalmology, CHUVA, ENVA (France). Sloth from the MNHN-Parc zoologique de Paris (France), **b**–**e**—Courtesy of the Comparative Ocular Pathology Laboratory of Wisconsin

its head rotated right-side-up, whereas the more centrally located area centralis and horizontal streak would align well with upcoming branches as it climbs upside-down (see Fig. 29.7) (Andrade-da-costa et al. 1989). Thus, although perhaps not a requirement, it seems as though vision seems to have a purpose in the life of a sloth.

Despite relatively detailed information on the ophthalmic anatomy of the sloth, there is currently no information on the results of basic ocular diagnostic tests in the species. Anecdotally, ocular examination is very similar to that of armadillos; while the eyes are more accessible for physical examination due to globe position, globe retraction still

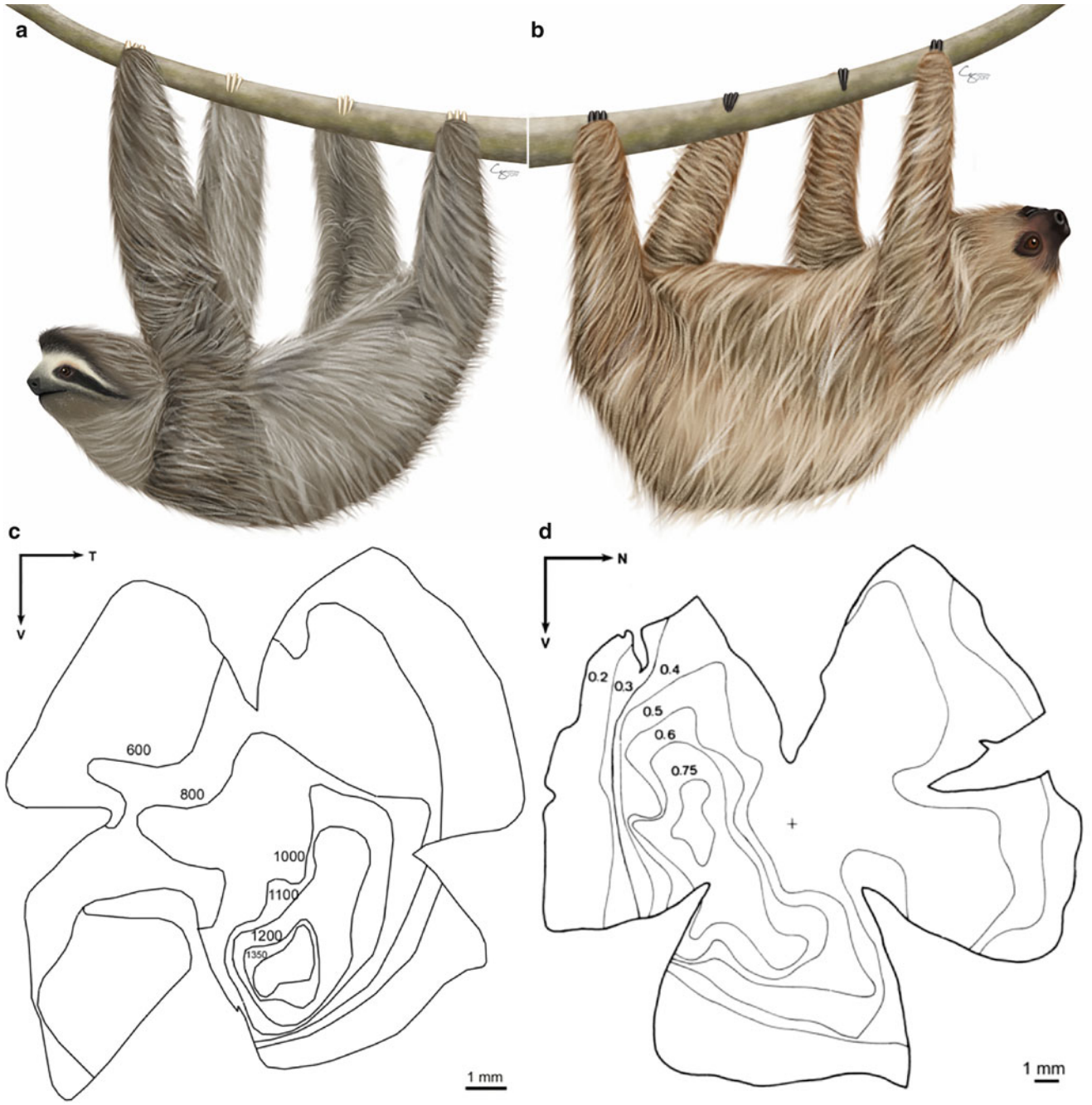

Fig. 29.7 Schematic representation of sloth visual behavior by use of retinal specializations during climbing. The three-toed sloth climbs with its head turned right-side-up (**a**), enabling ventral retinal specialization to be directed upward to the branches as it climbs (**c**—retinal topographic map of ganglion cell density of the left eye). The two-toed sloth climbs with its head upside-down (**b**), enabling positioning of a centrotemporal retinal specialization to the branch in front of it as it climbs (**d**—retinal topographic map of ganglion cell density of the right eye). **a**, **b**—Copyright Chrisoula Skouritakis. **c**—Modified with permission from Figure 2, Costa BL, Pessoa VF, Bousfield JD, Clarke RJ. Unusual distribution of ganglion cells in the retina of the three-toed sloth (*Bradypus variegatus*). *Braz J Med Biol Res*. 1987;20:741–748. **d**—Modified with permission from Figure 1, Andrade-Da-Costa BLS, Pessoa VF, Bousfield JD, Clarke RJ. Ganglion cell size and distribution in the retina of the two-toed sloth (*Choloepus didactylus L.*). *Braz J Med Biol Res*. 1989;22:233–236

occurs. Sloth eyes have been reported to appear more sunken with dehydration and weight loss (Aguilar and Superina 2015). If complete miosis is not present, pupillary light reflexes are slow. A nictitating membrane is not visible, and a pseudoangiotic retinal vascular pattern is present.

While nothing is currently published in the peer-reviewed literature, there are a few anecdotal reports of clinical ophthalmic disease and outcomes in the species. In a case of acute disorientation in a 7-year-old captive sloth, a positive dazzle reflex but no appreciable vision was present, and

electroretinogram showed absent waveforms. The cause of blindness was not determined, but the animal was quickly able to adapt without vision (Personal communication, Sabine Chahory, France). Systemic mineralization with crystalline deposits within the cornea, similar to that described previously in the Southern tamandua, can occur in geriatric sloths. Treatment with tacrolimus (oil-based) is well-tolerated, although mild irritation of the periocular skin can be noted over time. The cause of the systemic mineralization has not been established, but ultimately can lead to death (personal communication, Patricia J. Smith, CA, United States).

As with many exotic animal species, additional research is needed to develop a complete understanding of normal ophthalmic anatomy and the diseases that may impact the eye in the *Xenarthra* group.

References

Agnew D, Nofs S, Delaney MA et al (2018) Xenarthra, Erinacoemorpha, some Afrotheria, and Phloidota. In: Terio KA, McAlosse D, St. Leger J (eds) Pathology of wildlife and zoo animals. Elsevier Inc. London, pp 517–532

Aguilar RF, Superina M (2015) Xenarthra. In: Miller RE, Fowler ME (eds) Fowler's zoo and wild animal medicine. Elsevier, St. Louis, pp 355–369

Aldana Marcos HJ, Affanni JM (2005) Anatomy, histology, histochemistry and fine structure of the Harderian gland in the South American armadillo Chaetophractus villosus (Xenarthra, Mammalia). Anat Embryol (Berl) 209:409–424

Aldana Marcos HJ, Cintia Ferrari C, Cervino C et al (2002) Histology, histochemistry and fine structure of the lacrimal and nictitans gland in the South American armadillo Chaetophractus villosus (Xenarthra, Mammalia). Exp Eye Res 75:731–744

Andrade-da-costa BLS, Pessoa VF, Bousfield JD et al (1989) Ganglion-cell size and distribution in the retina of the 2-toed sloth (*Choloepus-Didactylus L*). Braz J Med Biol Res 22:233–236

Brandt F, Zhou HM, Shi ZR et al (1990a) The pathology of the eye in armadillos experimentally infected with Mycobacterium leprae. Lepr Rev 61:112–131

Brandt F, Zhou HM, Shi ZR et al (1990b) Severity of leprosy eye lesions in armadillos infected with Mycobacterium leprae. Lepr Rev 61: 188–192

Clark WE, Gros LE (1959) The antecedents of man. Edinburgh Univ Press, p 374

Costa BL, Pessoa VF, Bousfield JD et al (1987) Unusual distribution of ganglion cells in the retina of the three-toed sloth (*Bradypus variegatus*). Braz J Med Biol Res 20:741–748

de Araujo NL, Raposo AC, Pinho AC et al (2017) Conjunctival bacterial Flora, Antibiogram, and lacrimal production tests of collared anteater (*tamandua Tetradactyla*). J Zoo Wildl Med 48:7–12

de Sampaio C, Camilo-Alves P, de Miranda Mourao G (2016) Responses of a specialized insectivorous mammal (*Myrmecophaga tridactyla*) to variation in ambient temperature. Biotropica 38:52–56

Dilger-Sanches AW, Montiani-Ferreira F (2018) Gross and histological findings in South American anteater eyes. In: Kluyber D (ed) Proceedings of the 1st Workshop on wild giant anteater health research. Instituto de Conservação de Animais Silvestres. São Paulo, SP, Brazil, p 23

Douglas RJ, Partridge JH, Hope AC (1995) Visual and lenticular pigments in the eyes of demersal deep- sea fishes. J Comp Physiol A 177:111–122

Emerling CA, Springer MS (2014) Eyes underground: regression of visual protein networks in subterranean mammals. Mol Phylogenet Evol 78:260–270

Johnson GL (1901) Contributions to the comparative anatomy of the mammalian eye chiefly based on ophthalmoscopic examination. Philos Trans 194:38

Malaty R, Togni B (1988) Corneal changes in nine-banded armadillos with leprosy. Invest Ophthalmol Vis Sci 29:140–145

Malaty R, Beuerman RW, Pedroza L (1990) Ocular leprosy in nine-banded armadillos following intrastromal inoculation. Int J Lepr Other Mycobact Dis 58:554–559

Mendel FC (1981) Use of hands and feet of two-toed sloths (*Choloepus hoffmanni*) during climbing and terrestrial locomotion. J Mammal 62:413–421

Mendel FC, Piggins D, Fish DR (1985) Vision of 2-toed sloths (Choloepus). J Mammal 66:197–200

Meredith RW, Gatesy J, Emerling CA et al (2013) Rod monochromacy and the coevolution of cetacean retinal opsins. PLoS Genet 9: e1003432

Mohun SM, Davies WL, Bowmaker JK et al (2010) Identification and characterization of visual pigments in caecilians (Amphibia: Gymnophiona), an order of limbless vertebrates with rudimentary eyes. J Exp Biol 213:3586–3592

Nakamura PA, Tang S, Shimchuk AA et al (2016) Potential of small molecule-mediated reprogramming of rod photoreceptors to treat retinitis pigmentosa. Invest Ophthalmol Vis Sci 57:6407–6415

Newman HH (1913) The natural history of the nine-banded armadillo of Texas. Am Nat 47:513–539

Piggins D, Muntz WRA (1985) The eye of the three-toed sloth. In: The evolution and ecology of armadillos, sloths and vermilinguas. Smithsonian Institution Press, Washington, DC, pp 191–197

Rodarte-Almeida ACV, Passos AO, Mergulhao FV et al (2016) The eye of the giant anteater (*Myrmecophaga tridactyla*): biometric findings and reference values for selected ophthalmic diagnostic tests. In: 47th ACVO Annual Proceedings, Monterey, California

Van der Spuy J, Munro PM, Luthert PJ et al (2005) Predominant rod photoreceptor degeneration in Leber congenital amaurosis. Mol Vis 11:542–553

Walls GL (1942) The vertebrate eye and its adaptive radiation. Cranbrook Institute of Science, Bloomfield Hills, p 785

Watillon M, Goffart M (1965) Physiological implications of the structure of the sloth (Choloepus hoffmanni Perers) eye. Arch Int Physiol Biochim 73:163–166

Watillon M, Goffart M (1969) The eye of the sloth (Choloepus hoffmanni Peters). Acta Zool Pathol Antverp 49:107–122

Weaker FJ (1981) Light microscopic and ultrastructural features of the Harderian gland of the nine-banded armadillo. J Anat 133(Pt 1): 49–65

Wislocki GB (1928) Observations on the gross and microscopic anatomy of the sloths (*Bradypus griseus griseus* Gray and *Choloepus hoffmanni* Peters). J Morphol 46:317–397

Ophthalmology of Afrotheria: Aardvarks, Hyraxes, Elephants, Manatees, and Relatives

30

Katie Freeman, Gil Ben-Shlomo, Richard McMullen, and Bret A. Moore

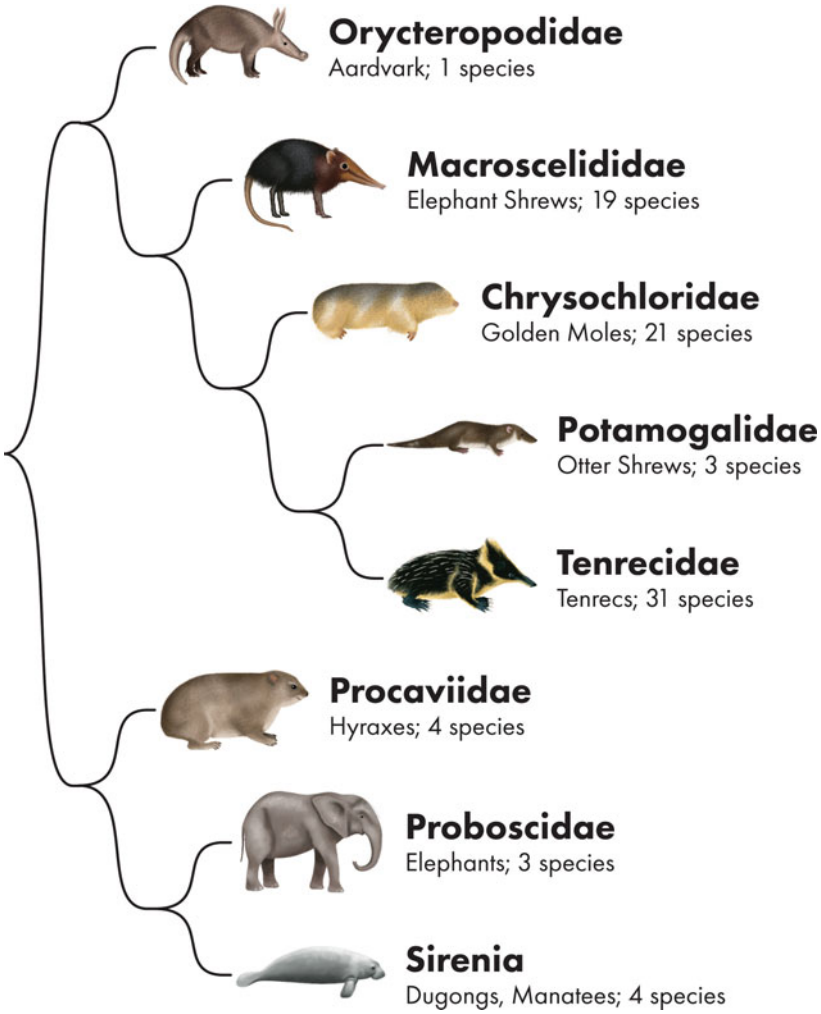

K. Freeman
Veterinary Vision, San Carlos, CA, USA

G. Ben-Shlomo
Cornell University College of Veterinary Medicine, Ithaca, NY, USA
e-mail: gb473@cornell.edu

R. McMullen
Auburn University, College of Veterinary Medicine, Auburn, AL, USA
e-mail: rjm0040@auburn.edu

B. A. Moore (✉)
College of Veterinary Medicine, University of Florida, Gainesville, FL, USA
e-mail: bretthevet@dvm.com

F. Montiani-Ferreira et al. (eds.), *Wild and Exotic Animal Ophthalmology*, https://doi.org/10.1007/978-3-030-81273-7_5

Afrotheria is a unique and highly diverse clade of placental mammals. Their diversity is so great and morphologies so different that only by genomic analysis would one conceive phylogenetic relatedness despite some other clues such as dental eruption and fetal membrane characters (Asher and Lehmann 2008; Murphy et al. 2007; Mess and Carter 2006; Nikolaev et al. 2007; Svartman and Stanyon 2012). Once being a sequestered landmass, Africa diversified and species filled ecological niches through convergent evolution rather than gene flow: insectivores (elephant shrews, golden moles, tenrecs, and aardvarks), rodents (hyraxes), large herbivores (elephants), and aquatic mammals (manatees and dugongs).

Tubulidentata (Aardvarks), Macroscelidea (Elephant Shrews), Tenrecomorpha (Tenrecs), and Hyracoidea (Hyraxes)

Aardvarks (Tubulidentata) consist of a single species, *Orycteropus afer*, further differentiated into 17 poorly defined subspecies (Lehmann 2009). They are nocturnal and feed exclusively on ants and termites that they locate by their impressive sense of smell (Willis et al. 1992). Sedation or anesthesia is recommended to facilitate a safe and less-stressful examination in this species, and oral sedatives (e.g., diazepam) for the first couple days following an anesthetic event is recommended to prevent self-trauma as they tend to become restless and anxious (Matas et al. 2010). Menace response is variable in photopic conditions, potentially due to poor daylight vision (Matas et al. 2010). A complete but thin zygomatic arch is present (Rahm 1990). The superior eyelids have only a couple of vibrissae, whereas the inferior eyelids have two rows of cilia 3–6 mm away from the eyelid margin. A ventromedial third eyelid is present. The cornea has been reported as keratinized, although this has not been evident on examination (O'Day 1952; Griffiths 1968; Stone 1983). A round pupil is centered within a dark-brown iris. Topical tropicamide 1% has a minimal mydriatic effect. Funduscopic evaluation is permitted by a 2.2 panretinal or 28-diopter lens, but a 40-diopter lens is helpful to visualize more of the peripheral retina. The fundus is darkly pigmented, and the retina is anangiotic and without a tapetum. It has been reported that the retina does not contain cone photoreceptors (Rahm 1990), however rod monochromacy has been disproven in related, strongly nocturnal species (see tenrecs below), and further investigation is recommended. The optic nerve head is round and unmyelinated. Intraocular pressures have been reported to be between 14 and17 mmHg (Matas et al. 2010).

Ophthalmic conditions are largely unknown in aardvarks. Chronic conjunctivitis of unknown cause is well recognized, characterized by chemosis and ocular discharge (Stetter 2003; Matas et al. 2010). Lagophthalmos during sleep, and a dusty environment, may contribute, however, conjunctivitis can be self-limiting or may resolve on topical anti-inflammatory or antibiotic medications (Matas et al. 2010). As with many captive animals, longevity increases the occurrence of senile cataracts (Fig. 30.1). A single case report exists on ophthalmic disease in aardvarks (Matas et al. 2010). A 23-year-old male aardvark born in captivity was reported to have a left superior eyelid erosive, papillomatous lesion involving nearly 80% of the margin. Incisional biopsy was performed (wedge resection) and was closed in 2 layers with 5-0 Vicryl (Fig. 30.2). Histopathologic changes were similar to that of papilloma virus in other species, characterized by neutrophilic and lymphoplasmacytic blepharitis and hyperplasia or the mucosa and papillary projections of non-keratinized epithelium. However, following hematoxylin and eosin, Zeihl-Neilson, and periodic acid-Schiff stains, no organisms or koilocytes were found (Matas et al. 2010). Despite good surgical closure and postoperative oral antibiotics and anti-inflammatory therapy, wound dehiscence was noted 3 days later and was suspected to be due to self-trauma, trauma from conspecifics, and environmental contamination (Matas et al. 2010). However, wound dehiscence following cutaneous surgery in aardvarks is not uncommon, largely due to the previously described cause of dehiscence and their propensity to have dry, cracked skin if proper humidity is not maintained (50–70%) (Goldman 1986). Thus, minimally reactive suture with limited skin tension is recommended (Stetter 2003). Repair of the initial surgery was successful by 2-layer closure, consisting of placing 2 large, buried horizontal mattress sutures using 4-0 PDS, and a single buried horizontal mattress at the margin using 6-0 PDS. The same animal (same eye) had a chronically blind eye suspected to have sustained previous trauma. Signs included dorsomedial strabismus (non-restrictive), diffuse corneal edema and scattered fibrosis and melanosis, deep anterior chamber, gray discoloration of the iris and iridodonesis, and no lens visible. Ocular ultrasound revealed no lens and a globe axial length of 18.1 mm. The normal right eye measured 18.6 mm in axial length, and the axial lens diameter measured 6.8 mm.

Elephant shrews (Macroscelidea) are an inconspicuous group of small and mostly diurnal insectivores scattered across Southern Africa. They can be found in some zoological collections. Of the 19 species in 5 genera, no reports of vision, ophthalmic anatomy, or ophthalmic disease exist. Their impressive noses are used to locate insect prey and recognize conspecifics, suggesting that they may not be highly dependent on vision for success (Dengler-Crish et al. 2006). However, their eyes are moderately sized and much larger with respect to their body mass (Fig. 30.3) than their tenrec relatives relative (below). Further work is necessary to understand even the basics of their visual system.

Fig. 30.1 A hypermature cataract in a geriatric captive aardvark *Orycteropus afer*. Not the irregular pupil margin due to posterior synechia secondary to chronic phacolytic uveitis. Used with permission from Christian Colista, Shutterstock.com

Tenrecs (Afrosoricida) are small, mostly insectivo mammals endemic to Madagascar (Fig. 30.4). The 31 species within 8 genera vary in appearance, some resembling hedgehogs, while others like shrews or opossums. The Lesser hedgehog tenrec (*Echinops telfairi*) is common in zoos and has become a part of the pet trade. Most species are highly nocturnal and have poor eyesight, some having markedly reduced eyes, particularly those of the *Microgale* genus (Eisenberg and Gould 1969). However, other senses are strong, primarily relying on audition and olfaction, but sensitive vibrissae exist on the chin, snout, and around the ears and eyes, the longer of which are present in species with more reduced eyes (Gould and Eisenberg 1966; Eisenberg and Gould 1969). The eyelids of tenrecs are closed at birth and open between 7 and 13 days (Gould and Eisenberg 1966). Examining the eye of adult tenrecs can be challenging, not only because of their small eye size but also their temperament. They do not curl completely into a ball like hedgehogs, but they are swift and can bite when threatened or aggravated. Additionally, they can roll their brow forward to cover their eyes and present dorsal spines, further complicating ocular examination (Eisenberg and Gould 1969). In the lesser hedgehog tenrec, spines and hair are reduced approaching the eyelids, where only fine hairs are noted on the superior

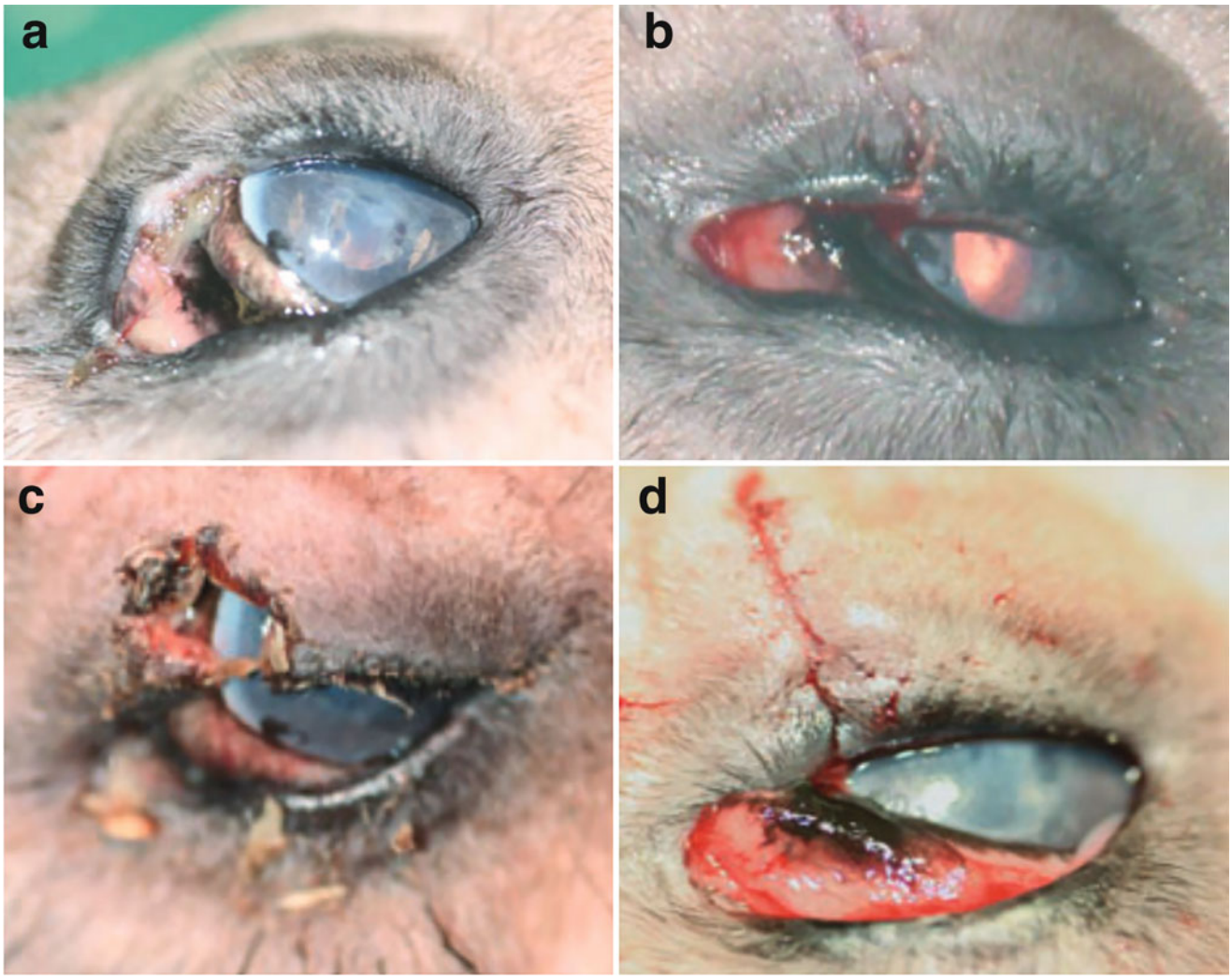

Fig. 30.2 Surgical excision of a superior eyelid erosive, papillomatous lesion in a 23-year-old male aardvark *Orycteropus afer*. (**a**) Note the lesion on the medial aspect of the superior eyelid. (**b**) Incision biopsy via wedge resection was performed and closed in two layers with 5-0 Vicryl. (**c**) Wound dehiscence was evident 3 days later. (**d**) Repair of the dehiscence was successful by placing two large, buried horizontal mattress sutures using 4-0 PDS and a single buried horizontal mattress at the margin using 6-0 PDS. Used with permission from John Wiley and Sons: Matas M, Wise I, Masters NJ, et al. Unilateral eyelid lesion and ophthalmologic findings in an aardvark (*Orycteropus afer*): case report and literature review. Veterinary Ophthalmology 2010; 13: Suppl. 1:116–122

and inferior lids nearly to the eyelid margins, occasionally touching the corneal surface (Fig. 29.2). Secretion of a milky white discharge can be noted around the eyes in males, similar to that of anteaters in captivity (see Chap. 29), but rather than a stress response, it is thought to be related to sexual readiness and mating or a form of chemical communication (Eisenberg and Gould 1969). The optic nerve is located centrally within the retina, of which was previously suggested to contain only rods (Siemen 1976). More recently, a dichromatic organization with both M/L- and S-cones has been described in the lesser hedgehog tenrec, although rods dominate (approximating about 98% of the photoreceptor population) as would be expected for a nocturnal species, reaching densities of 255,000 cells/mm^2 (Peichl et al. 2000). In the same study, the ventral retina was determined to have nearly double the number of cones and an increasing percentage of S-cones such that they even outnumber the M/L-cones, compared to the dorsal retina. This distinction is interesting as it has not been found in other insectivorous species studied to date and considering that the low light activity patterns of such a strongly nocturnal species may negate the quality and utility of color vision (Peichl et al. 2000). Having a high S-cone density may have other implications, such as control of circadian rhythm (Nei et al. 1997), but overall the purpose of such cone distribution in tenrecs is not understood.

Hyraxes (Hyracoidea) are a group of small herbivores similar in appearance to pikas and marmots but are the closest relative to the Tethytheria (elephants and the Sirenia). Five

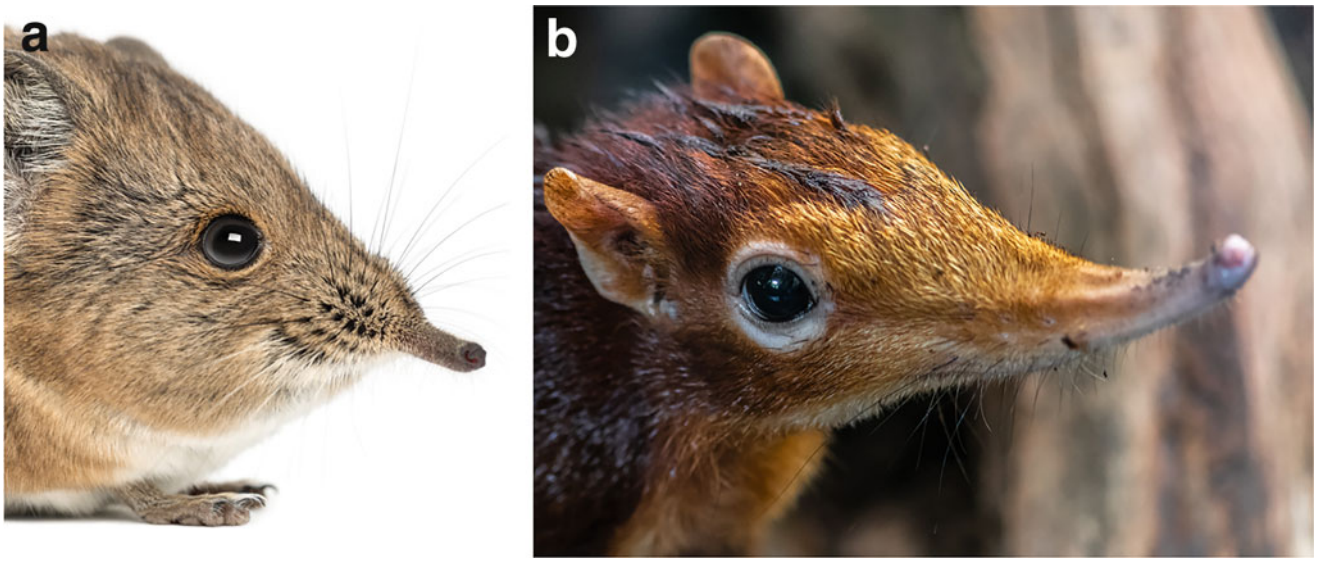

Fig. 30.3 The eyes of an (**a**) round-eared elephant shrew *Macroscelides proboscideus*, and (**b**) black and rufous elephant shrew *Rhynchocyon petersi*. **a**—Used with permission from Eric Isselee, Shutterstock.com. **b**—Used with permission from Hanjo Hellmann, Shutterstock.com

species exist, all but one of which are found exclusively in Africa (the rock hyrax *Procavia capensis* is also found in middle Eastern Asia). They feed close to their den in groups, mainly on broad-leafed plants but will also consume insects (Shoshani 2005). Ocular anatomy in hyraxes is interesting but scantly described. The superior eyelid has long accessory cilia, just dorsal to the eyelid margin, and meibomian glands are absent (Samuelson 2013). A unique, small flap-like prolongation of the superior mesodermal iris, or umbraculum (Fig. 30.5a, Johnson 1901; Millar 1973), protrudes anterioventrally into the anterior chamber and nearly touches the ventral pupillary margin and cornea when fully extended. This structure is highly contractile due to horizontal muscular bands that extend up and into both the medial and temporal areas of insertion, enabling retraction out of the pupillary margin (Johnson 1901). Movement of the umbraculum may be under voluntary control, as its position does not seem to completely align with the degree of solar luminance (Duke Elder 1958). The hyrax is dichromatic, similar to other diurnal herbivores (Ahnelt and Kolb 2000). They have a patchy, pale pigmented paurangiotic fundus that is uniformly colored, and a round, gray optic disc, similar to that of its elephant relative other than color (Fig. 30.5b; Johnson 1901). They were once described ophthalmoscopically to have a tapetum, termed a Tapetrum obscurum, affording a dull, lusterless coloration that is thought to be the forerunner of the fibrous tapetum (Johnson 1901). However, histologically no tapetum is present (personal observation). No reports of ophthalmic disease have been described, although an anterior subcapsular and posterior cortical cataract has been detected histologically in an 8-year-old captive male rock hyrax (personal communication, Richard R. Dubielzig).

Proboscidea (Elephants)

Introduction

There are three different species of elephants, Asian elephants (*Elephas maximus)*, African Savanna elephants (*Loxodonta africana*), and African forest elephants (*Loxodonta cyclotis*). Elephants are the largest living terrestrial animals, and their natural habitats are in Africa and Asia. They are considered to be keystone species and sentinel animals for disruption of their environments. Unfortunately, due in large part to the ivory trade and associated poaching, elephants are listed by the International Union for Conservation of Nature (IUCN) as vulnerable in Africa and endangered in Asia. Similar to dolphins and apes, elephants have been shown to be intelligent and self-aware as they can self-recognize in mirrors. They are also one of only a few different species that have been observed making and using tools.

Overall, elephants rely more heavily on hearing and smelling than on vision. While there are three different species of elephants with differing anatomical features such as ear size and tusk development amongst others, ophthalmologically, they have not been noted to vary significantly. For this reason, all species will be grouped together when discussion elephant ophthalmology. Elephants eat at varying light levels

Fig. 30.4 The normal eyes of tenrecs. (**a**) The lowland streaked tenrec *Hemicentetes semispinosus* is covered in sharp spines all but around the tiny eyes. (**b**) In the Lesser hedgehog tenrec (*Echinops telfairi*), note the reduction of spines and coarse hairs around the eyelids, but (**c**) the presence of fine on the superior and inferior lids nearly to the eyelid margins, occasionally touching the corneal surface. The iris is heavily pigmented, and in photopic conditions the pupil is small, consistent with most nocturnal species. **a**—Used with permission from Ryan M Bolton, Shutterstock.com

ranging from morning to evening and night with a typical rest time of mid-day. This arrhythmic foraging behavior necessitates seeing in different light levels. For this reason, elephants do not have specific mechanisms to regulate light, such as granula iridica. Additionally, while elephants have a tapetum which helps them see better during the evening feedings, unlike true nocturnal species, the tapetum is not very reflective so it is not overwhelming under bright illumination during the day.

Globe and Orbit

Anatomy

In a study using transpalpebral ultrasound on 53 captive Asian elephants, the following globe and orbit measurements were found. Overall, the elephant eye is small compared to its body size and the mean axial length (±SD) was found to be 3.72 ± 0.24 cm for adult males and 3.22 ± 0.18 cm for juvenile males (Bapodra et al. 2010; Suedmeyer 2006). For

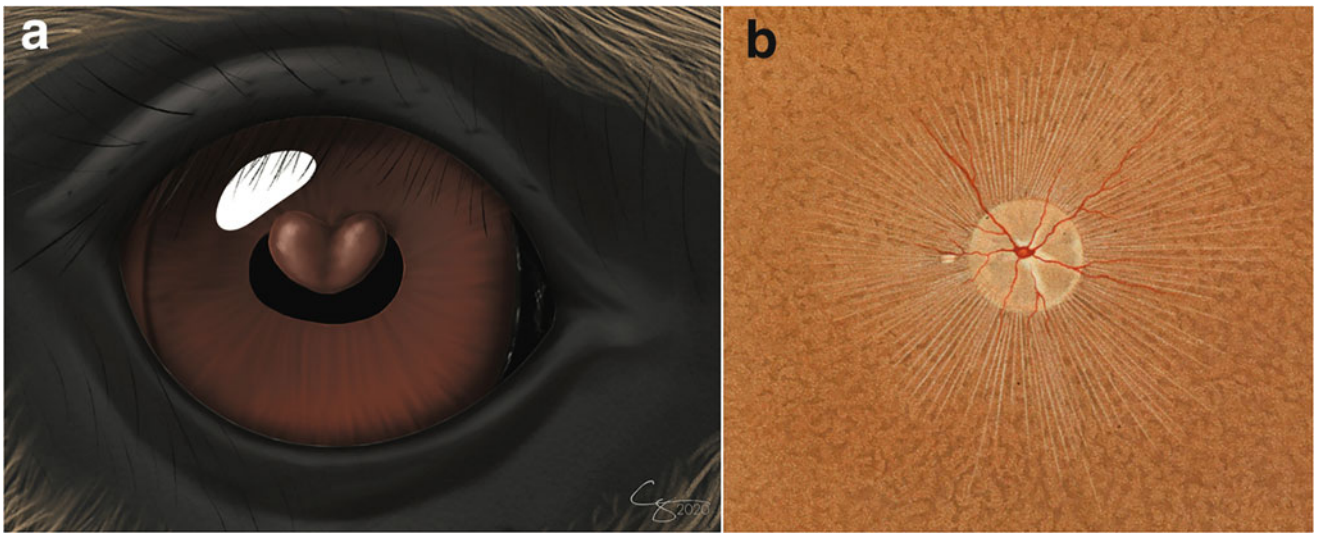

Fig. 30.5 Schematic view of (**a**) the normal adnexal and uveal anatomy and (**b**) normal fundus of the rock hyrax (*Procavia capensis*). (**a**) Note superior ciliar just dorsal to the eyelid margin, as well as the operculum-like umbraculum at the dorsal pupillary margin. (**b**) The fundus is paurangiotic, and has a uniformly patchy, pale pigmented coloration surrounding a round, gray optic disc. **a**—Copyright Chrisoula Skouritakis. **b**—Modified with permission from Johnson GL. Contributions to the comparative anatomy of the mammalian eye are chiefly based on ophthalmoscopic examination. Philosophical Transactions 1901;194:100. Publisher: Royal Society Publishing

adult females, the axial length was 3.48 ± 0.18 cm, and for juvenile females, it was 3.16 ± 0.22 cm. The equatorial diameter was 4.29 ± 0.02 cm for adult males, 3.62 ± 0.08 cm for juvenile males 3.91 ± 0.30 cm for adult females, and 3.59 ± 0.31 cm for juvenile females (Bapodra et al. 2010). A normal African and Asian elephant globe appearance can be seen in Figs. 30.6 and 30.7. Elephant eye positioning, similar to many ruminants and equines, is on the sides of the head, which enables improved peripheral vision and a very small blind spot but provides mostly uniocular vision and a narrow range of binocular vision.

Clinical Cases

Of 300 eyes examined from wild African elephants that died of gunshot, one had phthisis bulbi (McCullagh and Gresham 1969). Phthisis bulbi can occur after multiple diseases and is frequently seen after chronic inflammation. One example of a phthisical eye is seen in an animal at a zoo (Fig. 30.8); this

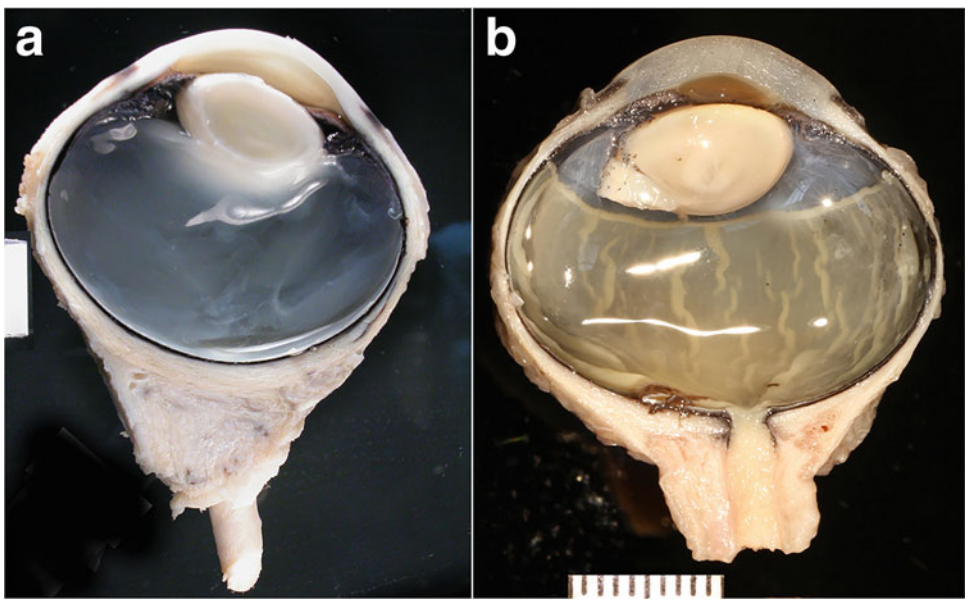

Fig. 30.6 Cross-sectional anatomy of the eye of an (**a**) African savanna elephant *Loxodonta africana*, and (**b**) and Asian elephant *Elephas maximus*. Courtesy of the Comparative Ocular Pathology Laboratory of Wisconsin

Fig. 30.7 Photograph of a normal eye of an African elephant *Loxodonta africana*. Used with permission from Eric Isselee, Shutterstock.com

Fig. 30.8 Phthisis bulbi in an African elephant, *Loxodonta africana.* Note the advanced cataract, conjunctival hyperemia, and appearance of enophthalmos that is really to do having a small eye. Ocular trauma likely caused cataract formation and chronic uvueitis, leading to the development of phthisis

eye likely became phthisical secondary to chronic inflammation from an initial traumatic event.

Eyelids/Musculature/Nasolacrimal

Anatomy

The eyelids of elephants are hairless, but there are long cilia that come from the row of hairs proximal to the upper eyelid that appear as accessory cilia or eyelashes (Fig. 30.9) (Samuelson 2013). These long cilia have been reported to protect the eyes from vegetation, dirt, and debris. The orbital muscles of elephants are similar to other terrestrial mammals, and there are four rectus muscles and two oblique muscles along with a retractor bulbi (Murphy et al. 1992). Elephants have a grove in the skin initiating at the medial canthus that drains tears onto the face. There are no reports on whether a lacrimal punctum exists, and the complete absence of a lacrimal drainage system has been reported (Duke Elder 1958). This claim was later supported by Murphy et al. (1992). Elephants have been reported to have many large glands (secreting both mucous and serous) in the upper and lower eyelids, but they lack meibomian glands (Samuelson 2013).

Clinical Cases

Similar to horses, elephants have very strong orbicularis oculi and extraocular muscles and are able to retract their eye and close the eyelids rather strongly, which makes examining quite difficult (Fig. 30.10). Ring blocks or auriculopalpebral nerve blocks are possible and will aid with the examination.

Cornea/Sclera/Conjunctiva

Anatomy

Similar to cetaceans, the sclera is very thick posteriorly (Soemmering 1818; Walls 1942; Duke Elder 1958). On ultrasound, the mean (±SD) corneal thickness of adult male elephants was found to be 0.18 ± 0.03 cm and 0.16 ± 0.03 cm for juvenile males. For females, it was 0.17 ± 0.02 cm for adults and 0.15 ± 0.01 cm for juveniles (Bapodra et al. 2010). Murphy et al. (1992) found similar values ranging from 1.2 to 1.8 mm for preserved eyes. The cornea was found to be composed of 5 layers based on histology: anterior epithelium with 6–9 cell layers (superficial squamous cells, polygonal wing cells, and cuboidal to columnar basal cells), Bowman's layer, stroma, a thick Descemet's membrane, and posterior endothelium (Hayashi et al. 2002). The mean value for corneal curvature was 21.3 D (Murphy et al. 1992).

Clinical Cases

Corneal disease is one of the most frequently reported ophthalmic conditions in elephants. Conditions that have been reported include corneal ulceration, keratitis, and corneoconjunctival masses, among others. Some of the corneal ulcers have been nonhealing with possible mineral deposits. These nonhealing ulcers may need debridement or keratotomy and contact lens placement (Wolfer and Rich 1992). Other cases that can be frustrating are recurrent, likely autoimmune or viral, keratopathies. Most of these have been reported to be connected with concurrent uveitis. They often present with bilateral corneal edema and vascularization and are stain

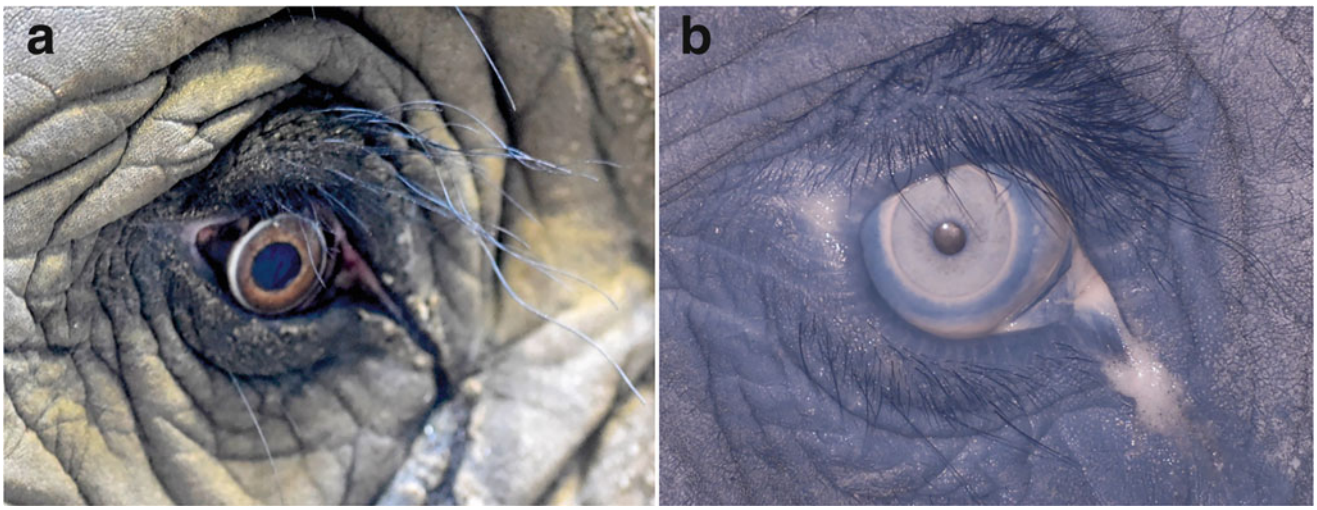

Fig. 30.9 Color (**a**) and infrared (**b**) photographs of elephant eyes demonstrating their long cilia emanating from rows of hair proximal to the upper eyelid. Smaller cilia are noted below the lower eyelid

Fig. 30.10 A gross photograph demonstrating the difficulty of examining the eye of an elephant that does not wish to comply. Contraction of the retractor bulbi muscle causes the globe to retract and the third eyelid to elevate. This, along with strong eyelid closure, can make examination challenging if the elephant chooses to do so

negative. There may be a herpetic viral component to these cases (R. Ofri, personal communication).

In a study with Asian elephants in Sri Lanka, many of the ulcers had both bacterial and fungal infections. In fact, two-thirds of the elephants had a bacterial infection, and over ½ of these were also infected with a fungal disease (Kodikara et al. 1992). A similar study has not been performed in other elephants living in different environments, so it is unknown if this is due to either those specific Asian elephants in Sri Lanka or this is a common concern for elephants worldwide. An ulcerative keratomycosis with a stromal abscess had also been observed in an elderly elephant in a zoological facility in Florida and had been resolved after a prolonged topical medical therapy, as surgical treatment was deemed too risky for the patient (G. Ben-Shlomo, personal communication).

Elephants also get cornea/conjunctival masses. Some of these masses are likely herpetic in origin (Fig. 30.11a). Like other species, elephants have multiple different alpha and gammaherpesviruses. These can cause signs varying from nothing to nodular conjunctivitis and keratitis. Often these elephants will have nodules/masses present elsewhere on their bodies. Treatment has not been reported for these cases, although elephants with herpetic keratouveitis have been reported to respond to oral acyclovir. Other corneal/conjunctival diseases include intraepithelial neoplasia. These are raised, adhered to the conjunctiva, often at the limbus, and have a papilloma-like appearance (Fig. 30.11b,c). Depending on the level of elephant training, any of these masses can be biopsied for confirmation (Fig. 30.12). Surgical excision with adjunctive cryotherapy has been reported to successfully treat the intraepithelial neoplasia cases (Fraunfelder et al. 2006).

Other reported conditions in elephants include keratitis (including vascularization, fibrosis, and pigmentation) from a probable trauma, as well as keratitis from chronic intraocular disease (iridocyclitis and retinitis) (McCullagh and Gresham 1969). Follicular conjunctivitis and keratoconjunctivitis (Fig. 30.13) have also been reported.

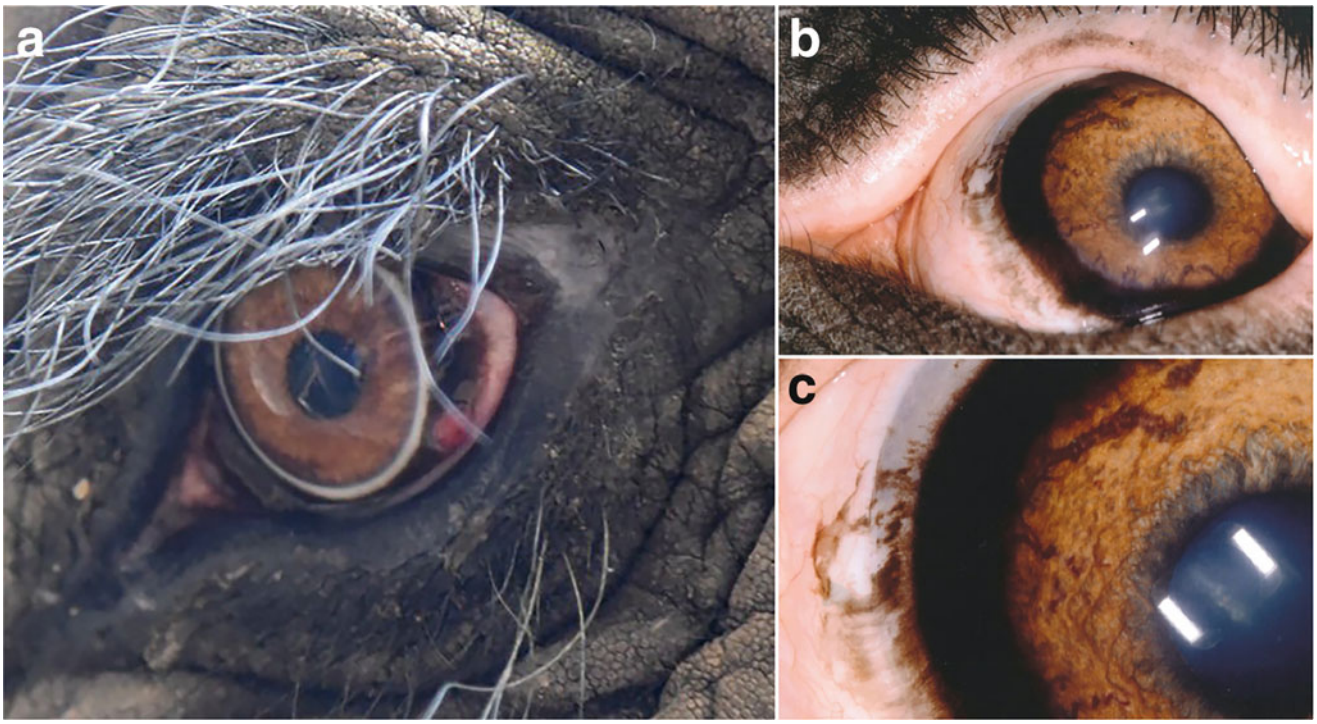

Fig. 30.11 Conjunctival masses in elephants. (**a**) A red, suspected herptic mass in an African elephant *Loxodonta africana*. (**b**, **c**) Epithelial neoplasia of the lateral limbal conjunctiva

Fig. 30.12 A well-trained elephant permitting biopsy of a conjunctival mass

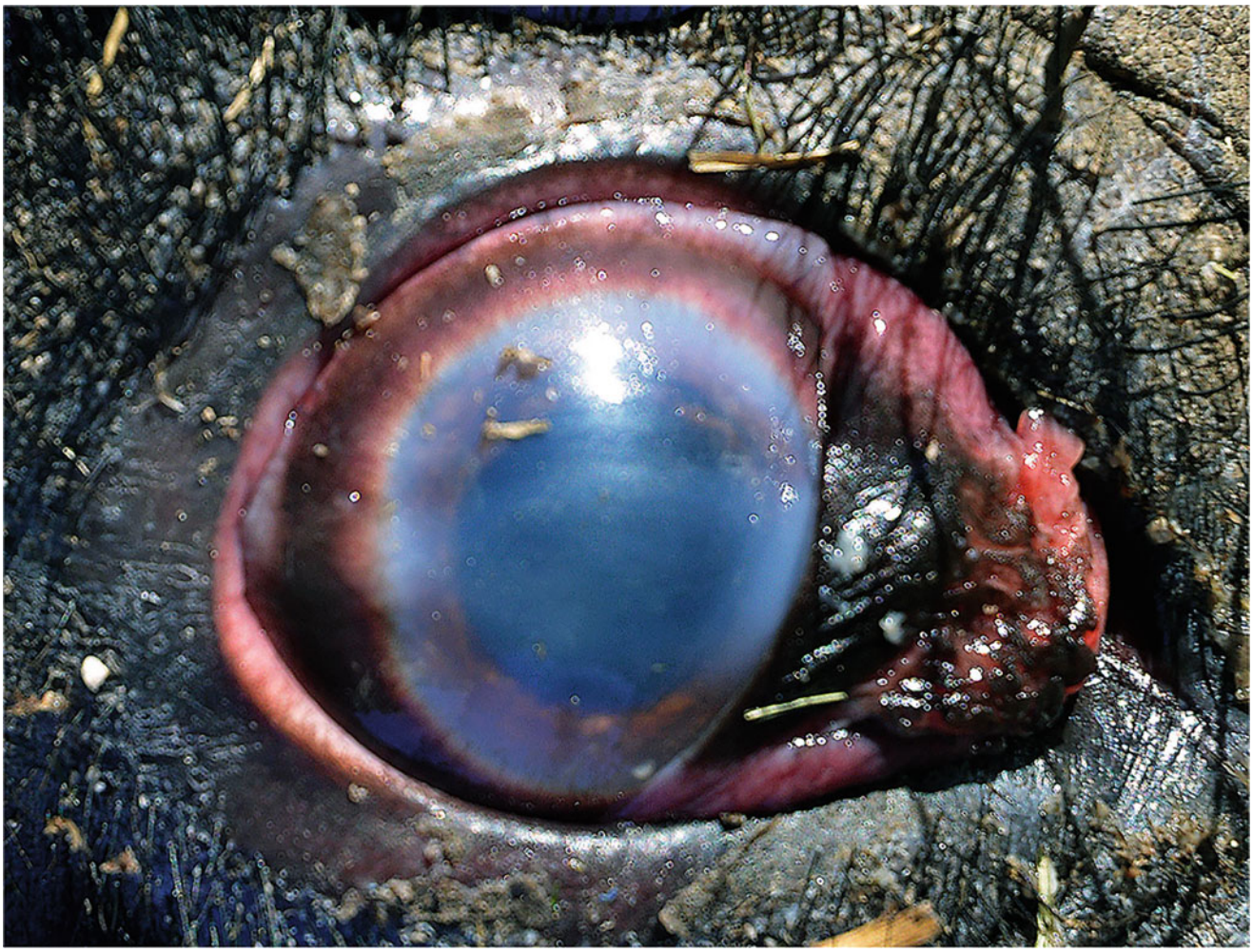

Fig. 30.13 Severe keratoconjunctivitis in an African elephant *Loxodonta africana*

Iridocorneal Angle

Anatomy

Both the uveal and corneoscleral meshwork are well developed (Murphy et al. 1992), but the aqueous outflow of the iridocorneal angle does not appear to have a high-volume capability (Hatfield et al. 2003). Additionally, the conventional aqueous outflow pathway is poorly developed, and there is a lack of evidence supporting the existence of any significant unconventional outflow via the uveoscleral route (Hatfield et al. 2003).

Clinical Cases

Although there is no prospective tonometry study in elephants, both rebound and applanation tonometers were utilized in elephants and most reported intraocular pressures similar to other species ranging from 15 to 25 mmHg (Fig. 30.14). Glaucoma cases have been observed, and the vast majority of them were secondary, often due to chronic cataracts and uveitis. There is, however, at least one reported case of possible primary glaucoma in an elephant (Miller-Michau, personal communication).

Uvea

Anatomy

The anterior segment depth was 0.46 mm for an adult male and a mean (±SD) of 3.4 ± 0.50 mm for juvenile males; for females, it was 4.60 ± 0.60 mm for adults and 3.7 ± 0.80 mm for juveniles (Bapodra et al. 2010). The pupil is round with no granula iridica (Fig. 30.15). The iris has both sphincter and dilator muscles, with the sphincter muscle originating near the pupillary margin and traversing peripherally about 1 mm; the thin dilator extends from the sphincter to the iris base (Murphy et al. 1992). The ciliary body has smooth muscle fibers and is approximately 5.8 mm wide with processes that are about 1.8 mm tall and with a pars plana located

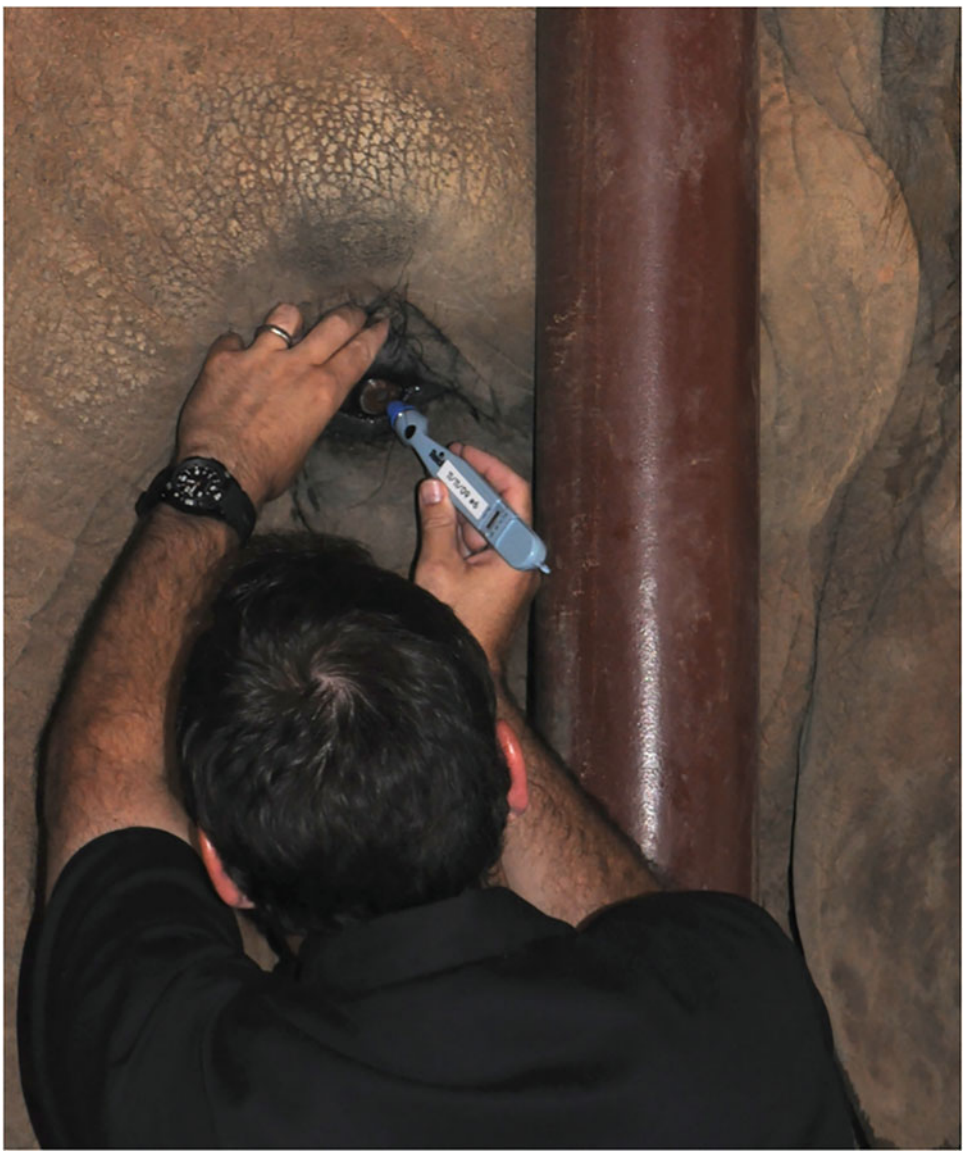

Fig. 30.14 Measurement of intraocular pressure in an elephant using a TonoPen applanation tonometer after administration of a topical anesthetic

at the base of the processes and extending to the ora serrata (Murphy et al. 1992).

Clinical Cases

In the eyes of African elephants that were shot, there was some synechia as well as iritis and cyclitis (McCullagh and Gresham 1969). The veterinary ophthalmology listserve reports multiple cases of recurrent uveitis that often involves keratitis as well. These cases present with a variety of signs ranging from ocular discharge, corneal edema, vascularization, photophobia, miosis, blepharospasm, and flare, sometimes with fibrin or hypopyon. This may be similar to equine recurrent uveitis, although a herpesvirus has also been implicated. Some cases are reported to recur every few months. Treatment has varied, with some cases responding to a typical anti-inflammatory protocol (frequent application of topical 1% prednisolone acetate and systemic non-steroidal anti-inflammatory drugs) and some cases resolving on their own regardless of treatment. Treatments have varied and included antiviral and antibiotic use as well as anti-inflammatory drugs. The most consistently used medication seems topical 1% prednisolone acetate.

Lens-induced uveitis (phacolytic) may present with low-grade signs of anterior uveitis, including epiphora, conjunctival hyperemia, peripheral corneal edema, aqueous flare, rubeosis irides, and a decrease in intraocular pressure (Fig. 30.15). The affected elephant may not display signs of ocular discomfort, and a thorough ophthalmic examination is necessary to make a definitive diagnosis. Treatment with topical non-steroidal anti-inflammatory drugs can be very effective at controlling inflammation and minimizing long-term secondary complications.

Fig. 30.15 The iris of elephants does not contain a dorsal pupillary appendage (e.g., granula iridica, corpora nigra) like many large terrestrial herbivores. Note the circular pupils. Phacolytic uveitis is evident by conjunctival hyperemia, mild rubeosis iridis, and mild peripheral corneal edema

Lens

Anatomy

The lens mean (±SD) diameter was 19.2 ± 0.60 mm for adult males and 17.1 ± 1.20 mm for juvenile males; for females, it was 19.4 ± 1.50 mm for adults and 17.8 ± 2.30 mm for juveniles. The lens depth was 9.7 mm (no mean or SD) for adult males and 10.0 ± 0.80 mm for adult females; it was 9.3 ± 0.90 mm for juvenile male and 9.5 ± 1.10 mm for juvenile female (Bapodra et al. 2010). This is compared to prior reports of lens diameter of 10.5 mm (Murphy et al. 1992), 9.0 mm (Rochon-Duvigneaud 1943) and 7.2 mm (Soemmering 1818). The lens has an anterior capsule which is thick and then thins at the equator and thins further posteriorly from 64 microns to 8 microns at the equator and 2 microns at the posterior aspect (Murphy et al. 1992).

Clinical Cases

Cataracts are frequently reported in elephants and are likely due to multiple causes, including inherited, traumatic, and age and UV-related. Figure 30.16 shows a mature and immature cataract in an African elephant bull. Cataract surgery has successfully been performed in a handful of cases (Cerreta et al. 2019; Manchip et al. 2019; S. Vainisi, personal communications). A complete ophthalmic examination, including ocular ultrasonography (Fig. 30.17) and electroretinography, should be considered, if possible. Ocular ultrasonography provides valuable biometric data (Fig. 30.17) that can be used to assist in surgical planning (e.g., phacoemulsification) and to identify subtle deviations in ocular anatomy that may go undetected during routine ophthalmic examination (e.g., shallow anterior chamber associated with lens instability). Routine placement of a soft water balloon or exam glove filled with tap water prior to performing ocular ultrasound will familiarize the elephant with the pressure associated with the procedure and can dramatically improve compliance. While there are no published reports for performing electroretinography (ERG) in elephants, it is possible to utilize protocols established for horses (Ben-Shlomo et al. 2012). Standard stainless-steel subcutaneous reference and ground electrodes can be easily placed with some placement modification (Fig. 30.18a,b). While the ERG could be performed and a normal waveform could be recognized, more data is required to provide a reference of normal values

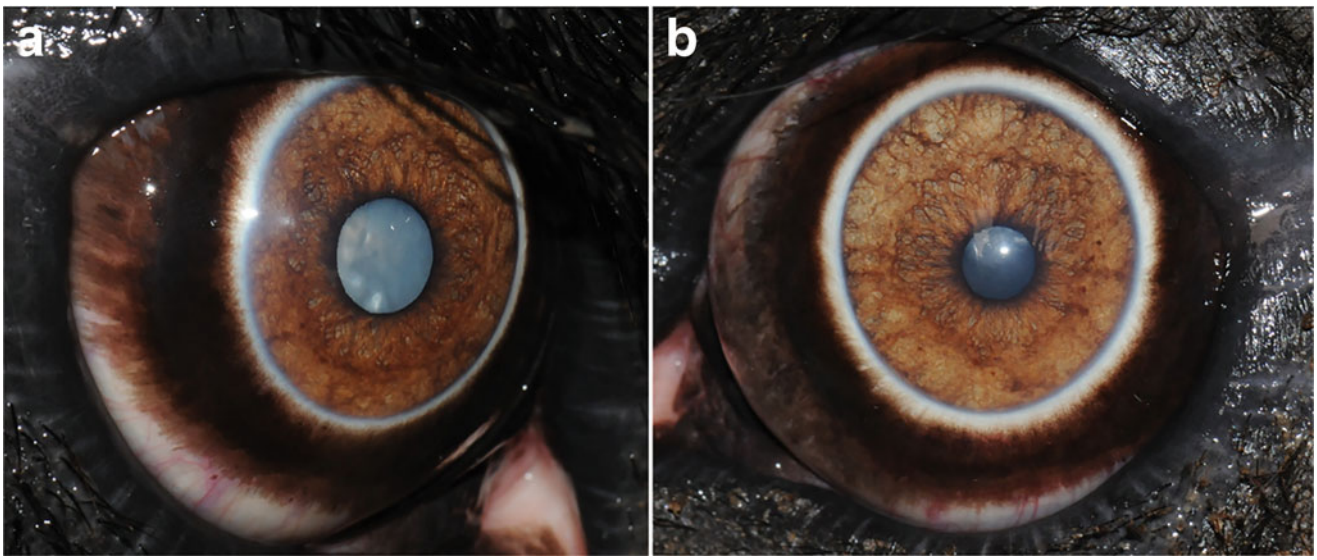

Fig. 30.16 Mature (**a**) and immature (**b**) cataracts in a bull African elephant *Loxodonta africana*

in this species. Extra care should be given to protect the electrodes during ERG testing. After performing the ERG in the right eye of the elephant, the elephant had to be repositioned in order to repeat the process in the left eye. The reference and ground electrodes were easily placed, but several attempts were needed to place the Kojiman electrode (An-Vision, Hennigsdorf, Germany) contact lens electrode (with an integrated light source) onto the cornea as the elephant started to lose patience. After finally placing the corneal electrode and collectively celebrating the small success amongst ourselves, the elephant nonchalantly reached back with his trunk, removed all three leads, and proceeded to eat the reference electrode and the LED light source (Fig. 30.18c).

Following cataract surgery, vision is compromised, and results of streak retinoscopy reveal severe hyperopia of +9.00 to +10.00 D (far-sightedness) if the elephant is left aphakic (no intraocular lens implant (IOL) placed). While IOLs are not commercially available, they can be custom ordered (An-Vision, Hennigsdorf, Germany) based on ocular biometric data described above. Lens instability or posterior lens luxation limits the ability to place an IOL within the capsular bag following phacoemulsification. In these situations, it may be possible to correct postoperative hyperopia by placing corrective contact lenses. Figure 30.19 shows color and an infrared image of a corrective contact lens placed for vision improvement. This corrective contact lens was +9.50 D and measured 32 mm in diameter. Anecdotal observation of the elephant's behavior revealed an instantaneous and obvious change in his interactions with his surroundings. Once the contact was placed, he slowly, and repeatedly, extended his trunk to a specific object, appearing to be processing some new information. He also moved his head away from the restraining bars and turned it back towards his flank, seemingly observing the people standing to his right. The elephant's powerful retractor bulbi muscles and large third eyelid (Fig. 30.10) proved to be a significant obstacle in using the corrective contact lenses, as they were easily dislodged. The contact lens placed in the right eye remained in place for less than 24 h. The use of contact lenses to correct postoperative aphakia shows some promise but must be seen as experimental at this point.

Cataract and lens luxation or dislocation were present in 16/300 elephant eyes in wild African elephants that were shot (McCullagh and Gresham 1969). Additionally, lens subluxation has also been reported in live elephants and is likely associated with chronic uveitis secondary to cataracts. Both lenses were luxated in the elephant that underwent bilateral phacoemulsification in North Carolina (Cerreta et al. 2019).

Retina, Vision, and Optics

Anatomy

The posterior segment mean (±SD) depth was 2.16 ± 0.17 cm for adult males and 1.85 ± 0.17 cm for adult females and 1.75 ± 0.13 cm for juvenile males and 1.70 ± 0.16 cm for juvenile females (Bapodra et al. 2010).

One study of an infant African elephant found that there were two distinct areas of increased ganglion cell density: one in the horizontal visual streak and another in the superior-temporal aspect of the retina (Stone and Halasz 1989).

The elephant retinal vascularization is a paurangiotic vascular pattern, with a yellowish tapetum present and visible stars of Winslow (Fig. 30.20); the retinal pigment epithelium is not pigmented in the tapetal area. The retina is thickest near

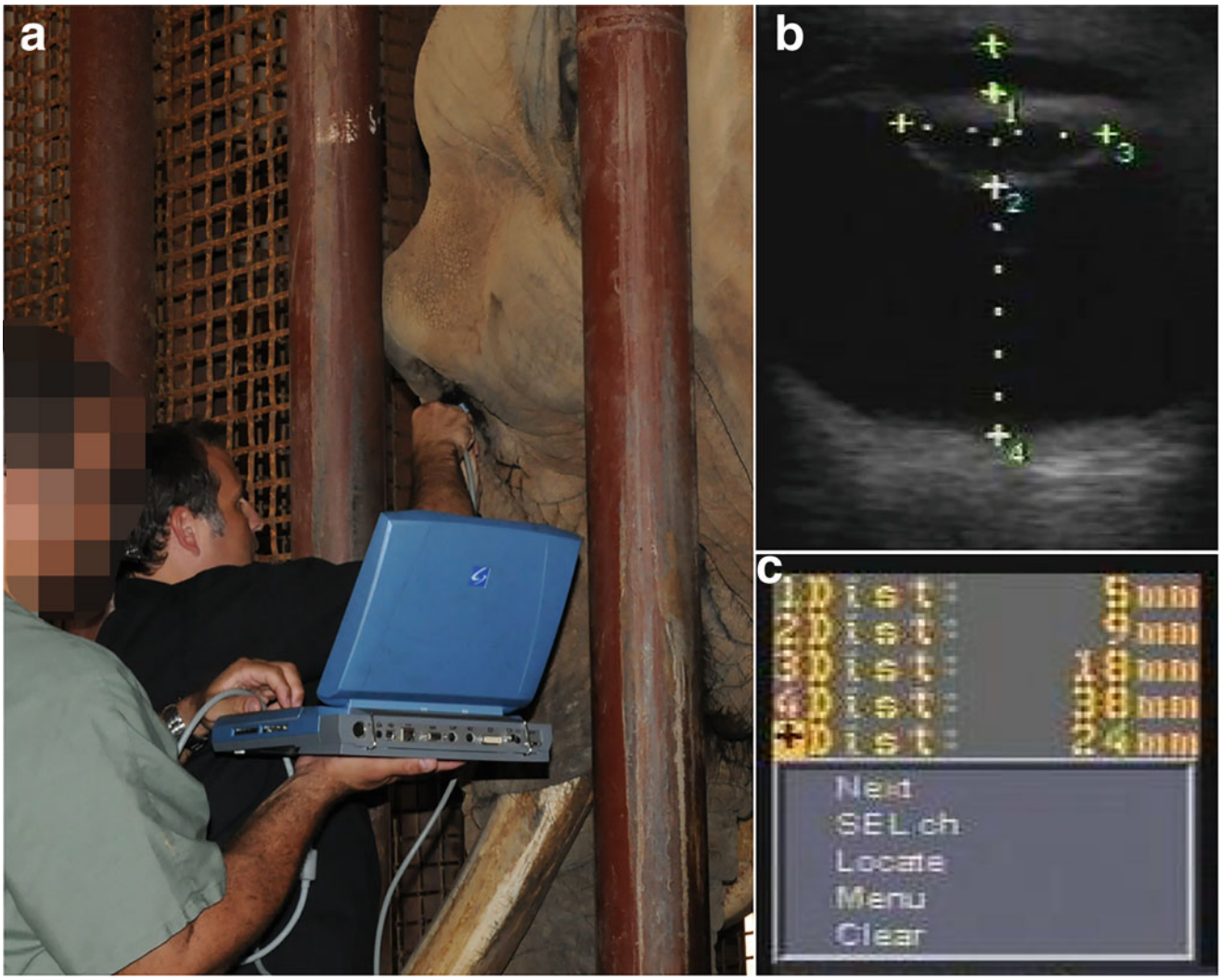

Fig. 30.17 Ocular ultrasonography in an African elephant *Loxodonta africana*. (**a**) A well-trained elephant permits ocular ultrasound after topical anesthetic is administered. (**b**) Ocular ultrasound showing an immature cataract, and (**c**) biometric values of globe dimensions

the optic disc (240 microns) and thins out peripherally and centrally. An analysis of retinal ganglion cells found that there are three regions of ganglion cell density, a temporal area centralis, a horizontal streak, and a nasal area centralis (Pettigrew et al. 2010). A horizontal visual streak is common in grazing mammals (Hughes 1977) and allows for assessing the horizon for either other elephants or predators; in the elephant, this horizontal concentration of ganglion cells is inferior to the optic disc (Samuelson 2013).

In a study (Murphy et al. 1992), the resting refractive state of elephants varied from −4.25 D to 2.74 D. Many of the eyes (9/12) had greater than, or equal to, 0.5 D of astigmatism and the accommodative range was 3.25 D (Murphy et al. 1992). Another study found that elephants have a higher visual acuity than the domestic cat (Cleland et al. 1982), but not as high as humans (Curcio and Allen 1990) and based on retinal whole-mounts, the elephant visual acuity was calculated to be between 13.16 and 14.37 cycles/degrees (Pettigrew et al. 2010).

Elephants have been shown to be dichromatic and have only two cones making them essentially red-green color blind, similar to many other terrestrial animals, including dogs and human deuteranopes (Yokoyama et al. 2005). They have also been shown to have bistratified rod bipolar cells that can aid with their nocturnal vision (Kuhrt et al. 2017).

Clinical Cases

In 300 eyes from deceased African elephants, retinal degeneration was observed in the eyes that also had advanced cataracts or lens subluxation. These changes included cystic or vacuolar degeneration as well as loss of cells in the inner

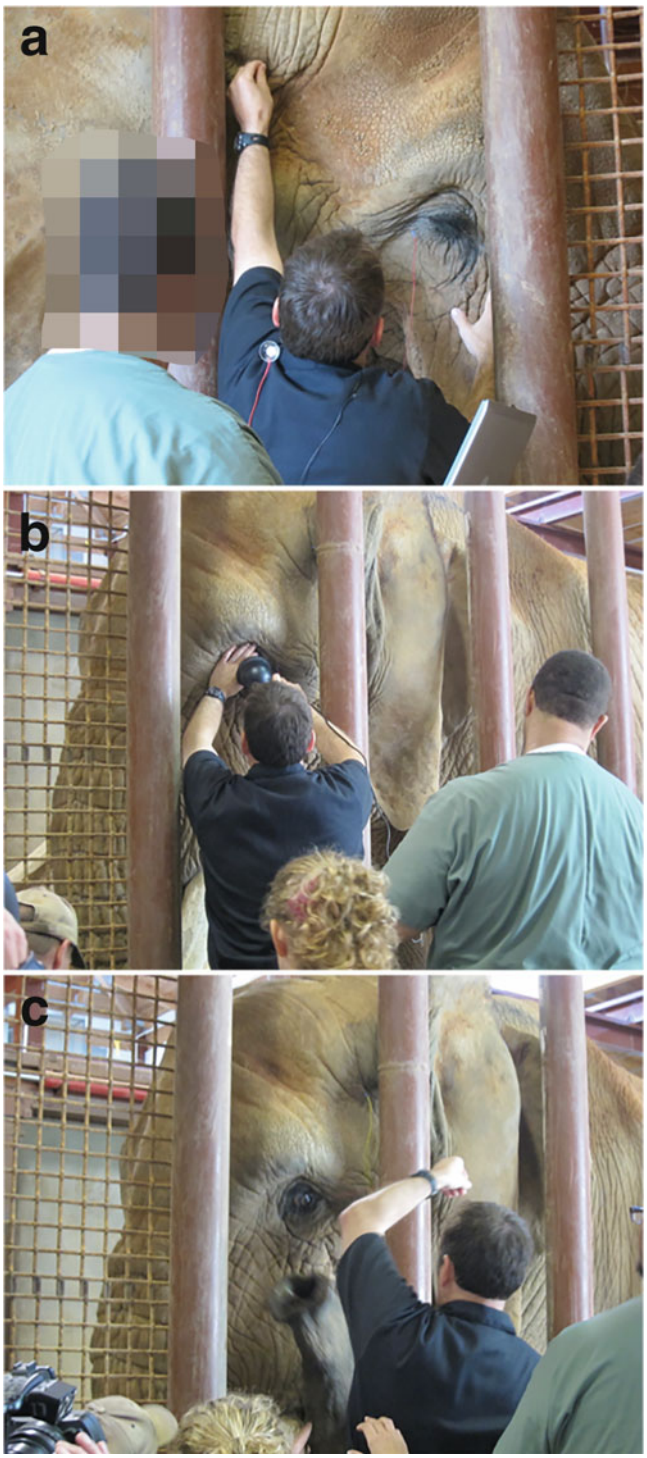

Fig. 30.18 Electroretinography in an African elephant *Loxodonta africana*. (**a**) Standard stainless-steel subcutaneous reference and ground electrodes can be easily placed. (**b**) Performing the electroretinogram. (**c**) An elephant's trunk can remove the electrodes in a matter of seconds

and outer nuclear layers. There was also some thickening and chronic inflammation of the inner plexiform, ganglion cell, and nerve fiber layers as well as some cases of retinal detachment (McCullagh and Gresham 1969).

Sirenia (Manatees and Dugongs)

Introduction

The mammalian order *Sirenia* has two families, the Dugongidae and Trichechidae. The Trichechidae includes three known species of manatee, *Trichechus manatus*, the West Indian Manatee, *Trichechus inunguis,* the Amazon Ox manatee*,* and *Trichechus senegalensis,* the West African manatee. Manatees are most closely related to the terrestrial species elephants and hyraxes, which are all from the phylogenetic group *Paenungulata*. Manatees live in a relatively narrow zone of rivers and the coastal zone of the Southeastern USA, the Caribbean, and parts of Northeastern South America. They forage on sea grasses and, due to a low metabolic rate, can survive for months without eating if needed (Newman and Robinson 2006). The visual acuity of manatees has been a subject of debate and concern for decades as manatees thrive in brackish water, often with reduced visibility, and are frequently victims of boat strike accidents. Can they not see well and therefore are more likely to be hit by a boat propeller? Is this due to the own ocular anatomy or the water quality or both?

Clinical ophthalmology in manatees is difficult. Relative to the rest of the body, the eyes are very small (Fig. 30.21a). They tend to close the eyes when captured or restrained and can retract their globe substantially, making examination challenging (Fig. 30.21b). In captivity and in the wild, manatees most commonly suffer from trauma-induced injuries to the corneas or eyelid skin, although other factors such as environmental stressors can also cause lesions. Treatment is extremely difficult due to the size of the eye and the strength of the orbicularis oculi muscle. Due to the difficulty in assessing lesions and treating, most of this chapter will be more focused on anatomy and less on clinical ophthalmology.

Globe and Orbit

The eye of the manatee is small, about 19 mm in diameter compared to about 24 mm for the human eye and 30 mm for the cow eye. In relation to body size, an adult human averages around 140 pounds, whereas a manatee is about 1000 pounds, and a cow is breed dependent but similar, around 1000–1300 pounds. Thus, compared to body weight, the manatee eye is quite small (Fig. 30.21a).

Eyelids/Adnexal Musculature/Nasolacrimal

Manatees have third eyelids that spread the tear film and help to protect the cornea and function to essentially "blink" like

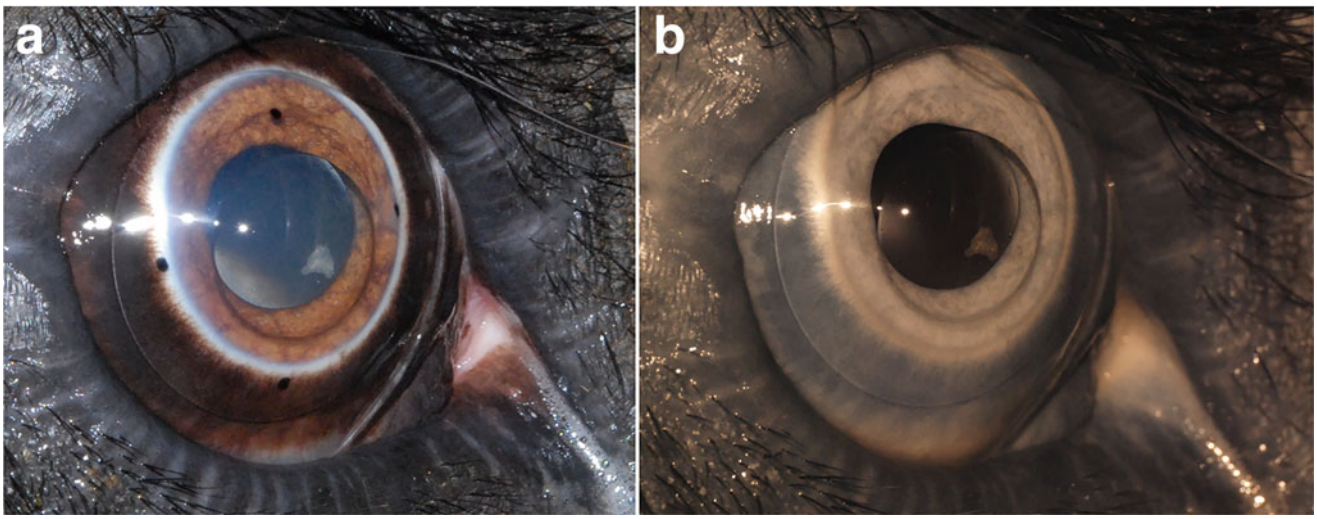

Fig. 30.19 (**a**) Color and (**b**) infrared images of a corrective contact lens placed for vision improvement in an African elephant *Loxodonta africana*

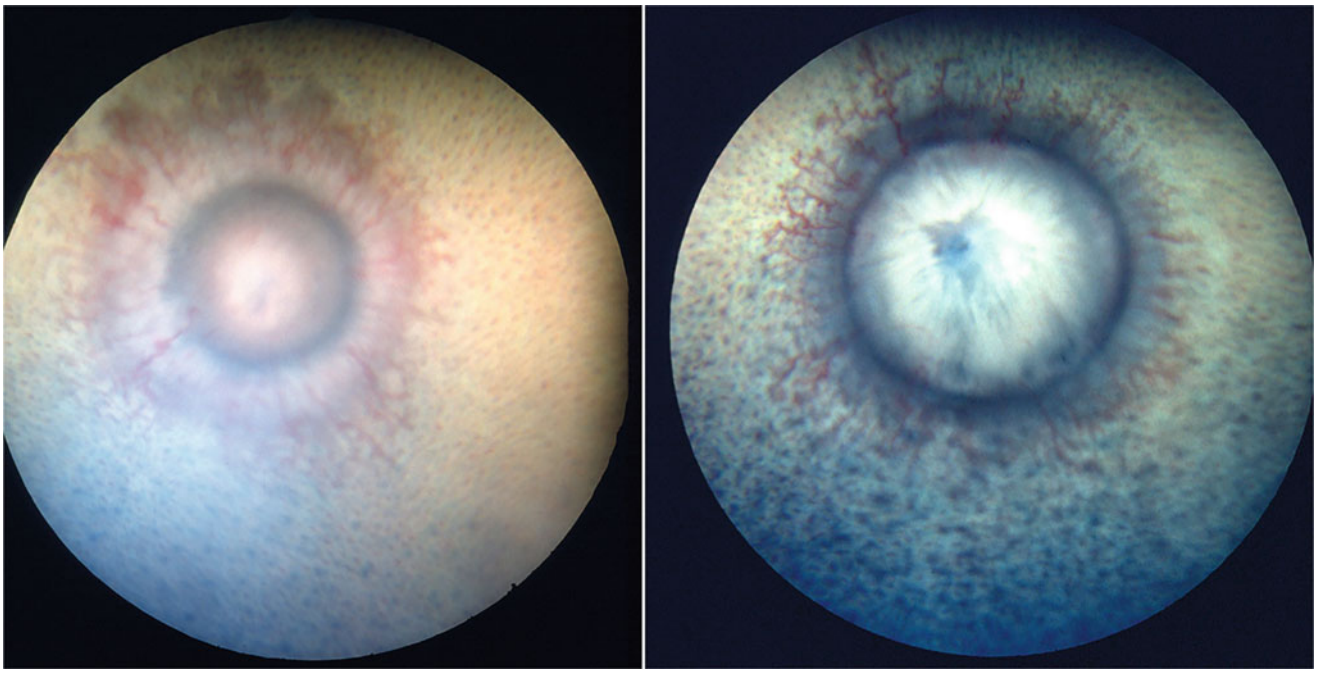

Fig. 30.20 Normal fundus images of elephants. Note the paurangiotic vascular pattern, a yellowish faint tapetum, and visible Stars of Winslow. Courtesy of the University of California Davis Comparative Ophthalmology Service

typical mammalian eyelids. Rather than the typical mammalian extraocular muscles, manatees have been shown to have four muscles in orbit, all associated with the palpebrae. There are two muscles that originate in the optic foramen, one that ends at the base of the upper eyelid and another that ends at the base of the lower eyelid. The other two muscles are attached to the third eyelid. All four of these muscles are skeletal muscles. The eyelids also have orbicularis oculi muscles. It thus appears that the manatee globe does not have much independent movement and that the eyelids are more designed to squint and can constrict into a small rounded point to reduce entering light to a pinpoint spot (Samuelson et al. 2010). Similar to other species, manatees have also been found to have orbital fat surrounding the optic nerve; unlike other species, it is proposed that this fat may be involved in eye positioning since there is no retractor bulbi muscle in these animals (Samuelson et al. 2009).

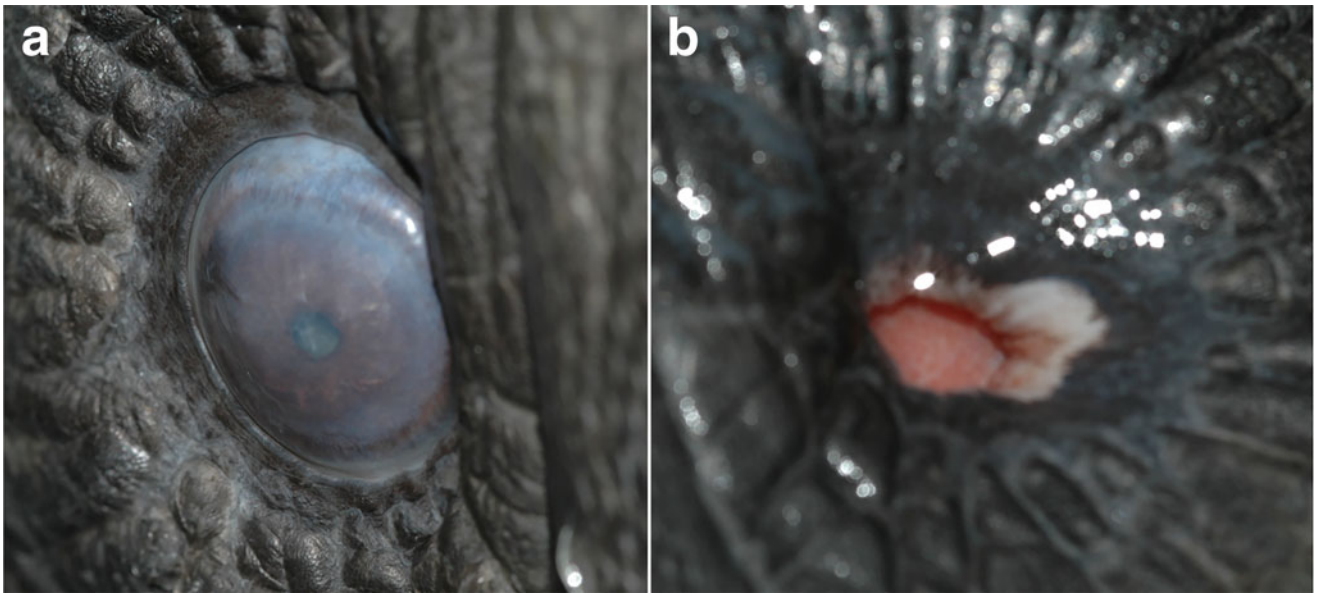

Fig. 30.21 (**a**) A normal manatee eye, small relative to body mass. (**b**) Retraction of the globe, making examination difficult. Courtesy of the University of Florida Ophthalmology Service

The manatee tear film, similar to other marine mammals, has a high carbohydrate concentration (Kelleher Davis). This was found to be even higher in animals in a rehabilitation setting than in captivity. Additionally, manatee tears, similar to other species, have been found to have antimicrobial activity (Davis and Argueso 2014).

The nasolacrimal system of these subungulate orders, the Sirenia, Hyracoidea, and Proboscidea, is unusual. These groups all lack traditional nasolacrimal systems and have missing lacrimal glands, lacrimal punctae, and nasolacrimal ducts. All of these groups lack lacrimal glands and tarsal glands in the upper and lower eyelids. The manatee eyelids contain accessory glands that are largely mucous producing, and the third eyelid has a tubuloalveolar gland that produces mucous (Samuelson et al. 2007). The third eyelid has also been found to have skeletal muscle and is capable of quick movement (Samuelson et al. 2009).

Cornea/Sclera/Conjunctiva

The scleral vasculature of the manatee has a two-tiered venous system (Hatfield et al. 2003). Manatees have been shown to have blood vessels and VEGF receptors in their corneas (Harper et al. 2004, 2005; Samuelson et al. 2004). This is unusual and not something that is present in other species. This has even been shown in a manatee fetus cornea. While the vessels are present, they are small and not dense and therefore unlikely to interfere with light transmission or vision in most cases. The cause of the blood vessel growth is unknown but does not appear to be associated with an acquired condition such as trauma or infection. It is more likely there is either a developmental or evolutionary cause behind the cornea vascularization. The manatee cornea has also been shown to have an irregular corneal surface, potentially allowing the manatee to live in both saltwater and freshwater environments (Ben-Shlomo et al. 2010). In the wild, it has been reported that manatees can suffer from corneal fibrosis and ulceration and trauma is not uncommon. Manatees can also suffer from oxidative damage and water temperature variation, particularly cold stress. These environmental changes can affect the corneas as well as eyelids (Kern and Colitz 2013, p. 1801).

Uvea

The manatee ciliary body is very unique among mammals in that it has a dense vascular system and no musculature (Samuelson et al. 2004). Like its relative the elephant, the manatee also lacks defined ciliary processes or a pars plana (Natiello et al. 2005). The manatee ciliary body is also unique in that there is a dual venous system present (Natiello and Samuelson 2005). While it is possible that manatees, due to their lack of ciliary body musculature, have no accommodative mechanism, it has also been proposed that they may use their vasculature to accommodate (Natiello and Samuelson 2005). To date, whether or not they accommodate is unknown, and if they cannot, this contributes to the data suggesting poor vision overall. The mean and median IOPs

with rebound tonometry (TonoVet) for animals without ocular disease were 8.5 and 9.5 mmHg (Ben-Shlomo et al. 2008).

Lens

The lens is spherical in shape, similar to other marine mammals such as pinnipeds and cetaceans. This allows the lens to have high refractive power and to be the main refractive structure in the eye. This is a necessary adaption for aquatic species as the corneal refractive power is largely negated by the similar refractive indices of cornea and water.

Retina/Vision/Optics

Manatees, particularly the West Indian Manatee, has been found to lack a tapetum. As they function mostly during the day (diurnal) and eat near the surface, this likely explains the lack of tapetum compared to other marine mammals (West et al. 1991). Manatees have traditionally been thought to have very poor vision, but there are some conflicting studies. An initial study published in 1981 found a mainly rod retina with a high photoreceptor to ganglion cell ratio and low refractive error (low hyperopia to emmetropia) underwater (Piggins et al. 1983). However, other reports in a very similar species, dugongs, find emmetropia in air and hyperopia underwater (Petit and Rochon-Duvigneaud 1929). Manatees are reported to have very limited binocular vision with about a 15-degree field (Piggins et al. 1983). This is in comparison to 120 deg. of binocular vision in people and 65 degrees in horses. A study by Mass et al. 1997 found that manatees had a limited visual resolution of about 20 min of visual arc (Bauer et al. 2003; Mass et al. 1997).

The conflicting data continues as the retinal appearance, and photoreceptor density does not match the vision behavior testing. An analysis of the photoreceptors themselves under light and electron microscopy reveals a low rod: cone ratio and higher cone cells than prior studies. This indicates that manatees have greater visual acuity than expected and are visual diurnally as well as nocturnally (Cohen et al. 1982). This fits their behavior as they are active both during the day and at night. Despite that, in vision behavior testing of two captive-born manatees, neither did as well as the retinal appearance would predict, and one did very poorly with near vision acting virtually blind up close. This could be due to individual variation or corneal vascularization differences, among others (Bauer et al. 2003). A psychophysical assessment of manatee vision by Bauer et al. determined that manatees use vision for larger objects seen at an intermediate or far distance but use the contact for objects up close (Bauer et al. 2003). This could account for the frequent boat strike injuries as they use touch as a sense up close. Therefore in sum, while the ganglion cell density recorded by Mass et al. (1997) indicates they should have good visual acuity, the resolving power is lower than expected. This may be due to the corneal vascularization and opacification of the ocular media (Bauer et al. 2003).

All marine mammals except for otters have historically been found to be lacking in a cone pigment and have been found to be monochromatic rather than dichromatic. However, further studies with manatees have since located two cone types on EM and found that manatees have a ventrally located central visual area, where there was a high density of ganglion cells. Manatees, unlike other marine mammals, but similar to their closest relatives the elephants and hyraxes have two opsin visual pigments that respond to short and long light wavelengths (Newman). One cone type is in the blue spectrum, and one is in the green spectrum (Griebel and Schmide 1996). They have three visual pigments, LWS, SWS, and rod, and the rod and LWS pigments are red-shifted from those of terrestrial mammals with maximal absorbance of 504 nm (Newman Robinson ARVO abstract). A proposed explanation for the manatee red-shifting and dichromatic vision vs. other marine mammals is their habitat and foraging range. Unlike other marine mammals who forage deeper, manatees are exposed to brackish waters and eat sea grasses high in the water column where it is murky and brighter, often with brownish and yellow-green hues; therefore, manatees can distinguish blue and green from grays but cannot distinguish red from certain grays (Griebel and Schmide 1996). A study evaluating brightness discrimination and determining shades of gray found that manatees have an ability to distinguish brightness on par with pinnipeds (Griebel and Schmid 1997). Unlike other animals like rodents and birds, they do not have UV sensitivity (Griebel and Schmid 1997).

References

Ahnelt PK, Kolb H (2000) The mammalian photoreceptor mosaic-adaptive design. Prog Retin Eye Res 9:711–777

Asher RJ, Lehmann T (2008) BMC biology. Dental eruption in afrotherian mammals. BMC Biol 6:14

Bapodra P, Bouts T, Mahoney P et al (2010) Ultrasonographic anatomy of the Asian elephant (Elephas maximus) eye. J Zoo Wildl Med 41(3):409–417. https://doi.org/10.1638/2009-0018.1

Bauer GB, Colbert DE, Gaspard JC, Littlefield B, Fellner W (2003) Underwater visual acuity of Florida manatee (*Trichechus manatus latirostris*). Int J Comp Psychol 16:130–142

Ben-Shlomo G, Brooks DE, Barrie K et al (2008) Tonometry in the Florida manatee. In: 39th Annual Meeting of the American College of Veterinary Ophthalmologists. Boston, MA

Ben-Shlomo G, Brooks DE, Plummer C et al (2010) A novel corneal anatomy observed in the Florida manatee. Vet Ophthalmol 13:418–419

Ben-Shlomo G, Plummer C, Barrie K et al (2012) Characterization of the normal dark adaptation curve of the horse. Vet Ophthalmol 15: 42–45

Cerreta AJ, McMullen RJ, Scott HE et al (2019) Bilateral phacoemulsification in an African elephant (*Loxodonta africana*). Case Rep Vet Med. https://doi.org/10.1155/2019/2506263

Cleland BG, Crewther DP, Crewther SG, Mitchell DE (1982) Normality of spatial resolution of retinal ganglion cells in cats with strabismic amblyopia. J Physiol 326:235–249

Cohen JL, Tucker GS, Odell DK (1982) The photoreceptors of the West Indian manatee. J Morphol 183:197–202

Curcio CA, Allen KA (1990) Topography of ganglion cells in human retina. J Comp Neurol 300:5–25. https://doi.org/10.1002/cne.903000103

Davis RK, Argueso P (2014) Composition of terrestrial and marine mammal tears is dependent on species and environment. IOVS 55:36

Dengler-Crish CM, Crish SD, O'Riain MJ et al (2006) Organization of the somatosensory cortex in elephant shrews (E. edwardii). Anat Rec 288:859–866

Duke Elder S (1958) The eye in evolution. In: System of ophthalmology. Henry Kimpton Publishers, London, p 470

Eisenberg JF, Gould E (1969) The tenrecs: a study in mammalian behavior and evolution. Smithson Contrib Zool 27:1–135

Fraunfelder FT, Finnegan M, Wilson DJ (2006) Conjunctival-corneal intraepithelial neoplasm in an Asia elephant (*Elephas Maximus*). J Zoo Wildl Med 37:424–426

Goldman C (1986) A review of the management of the Aardvark (Orycteropus afer) in captivity. Int Zoo Yearb 24/25:286–294

Gould E, Eisenberg JF (1966) Notes on the biology of the Tenrecidae. J Mammal 47:660–686

Griebel U, Schmid A (1997) Brightness discrimination ability in the West Indian manatee (*Trichechus manatus*). J Exp Biol 200:1587–1592

Griebel U, Schmide A (1996) Color vision in the Manatee (*Trichechus manatus*). Vision Res 36(17):2747–2757

Griffiths M (1968) Echidnas. Pergamon Press, Oxford

Harper JY, Lewis PA, Samuelson DA (2004) An examination of VEGFR-1 and VEGFR-2 in the Corneas of the Florida Manatee. IOVS 45:2344

Harper JY, Samuelson DA, Reep RL (2005) Corneal vascularization in the Florida manatee (Trichechus manatus) and threedimensional reconstruction of vessels. Vet Ophthalmol 8:89–99

Hatfield JR, Samuelson DA, Lewis PA (2003) Structure and presumptive function of the iridocorneal angle of the West Indian manatee (Trichechus manatus), short-finned pilot whale (Globicephala macrorhynchus), hippopotamus (Hippopotamus amphibius), and African elephant (Loxodonta africana). Vet Ophthalmol 6:35–43

Hayashi S, Osawa T, Tohyama K (2002) Comparative observations on corneas, with special reference to Bowman's layer and Descemet's membrane in mammals and amphibians. J Morphol 254:247–258

Hughes A (1977) The topography of vision in mammals. In: Crescitelli, handbook of sensory physiology, vol 7. Springer, Berlin

Johnson GL (1901) Contributions to the comparative anatomy of the mammalian eye, chiefly based on ophthalmoscopic examination. Philos Trans R Soc Lond B 194:22–112

Kern T, Colitz CMH (2013) Exotic animal ophthalmology. In: Gelat KN, Gilger BC, Kern TJ (eds) Veterinary ophthalmology, 5th edn. Ch 33. Wiley-Blackwell, pp 1750–1819

Kodikara DS, De Silva N, Makuloluwa CA et al (1992) Bacterial and fungal pathogens isolated from corneal ulcerations in domesticated elephants (Elephas maximus maximus) in Sri Lanka. Vet Ophthalmol 2(3):191–192. https://doi.org/10.1046/j.1463-5224.1999.00072.x

Kuhrt H, Bringmann A, Hartig W et al (2017) The retina of Asian and African elephants: comparison of newborn and adult. Brain Behav Evol 89:84–103. https://doi.org/10.1159/000464097

Lehmann T (2009) Phylogeny and systematics of the Orycteropodidae (Mammalia, Tubulidentata). Zool J Linnean Soc 155(3):649–702

Manchip KEL, Sayers G, Lewis JCM et al (2019) Unilateral phacoemulsification in a captive African elephant (*Loxodonta africana*). Open Vet J 9:294–300

Mass AM, Odell DK, Ketten DR, Supin AY (1997) Ganglion layer topography and retinal resolution of the Caribbean manatee Trichechus manatus latirostris. Dokl Biol Sci 355:392–394

Matas M, Wise I, Masters NJ et al (2010) Unilateral eyelid lesion and ophthalmologic findings in an aardvark (*Orycteropus afer*): case report and literature review. Vet Ophthalmol 13(Suppl. 1):116–122

McCullagh KG, Gresham GA (1969) Eye lesions in the African elephant (*Loxodonta africana*). Res Vet Sci 10:587–591. https://doi.org/10.1016/S0034-5288(18)34401-1

Mess A, Carter AM (2006) Evolutionary transformations of fetal membrane characters in Eutheria with special reference to Afrotheria. J Exp Biol 306B:140–163

Millar RP (1973) An unusual light-shielding structure in the eye of the dassie, Procavia capensis Pallas (Mammalia: hyracoidea). Ann Transvaal Mus 28:203–205

Murphy CJ, Kern TJ, Howland HC (1992) Refractive state, corneal curvature, accommodative range and ocular anatomy of the Asian elephant (*Elephas maximus*). Vis Res 32:2013–2121

Murphy WJ, Pringle TH, Crider TA et al (2007) Using genomic data to unravel the root of the placental mammal phylogeny. Genome Res 17:413–421

Natiello M, Lewis P, Samuelson D (2005) Comparative anatomy of the ciliary body of the west indian manatee (Trichechus manatus) and selected species. Vet Ophthalmol 8:375–385

Natiello N, Samuelson D (2005) Three-dimensional reconstruction of the angioarchitecture of the ciliary body of the West Indian manatee (Trichechus manatus). Vet Ophthalmol 8:367–373

Nei M, Zhang J, Yokoyama S (1997) Color vision of ancestral organisms of higher primates. Mol Biol Evol 14:611–618

Newman LA, Robinson PR (2006) The visual pigments of the West Indian manatee (*Trichechus manatus*). Vis Res 46:3326–3330

Nikolaev S, Montoya-Burgos JI, Margulies EH et al (2007) Early history of mammals is elucidated with the ENCODE multiple species sequencing data. PLoS Genet 3:e2

O'Day KJ (1952) Observations on the eye of the monotreme. Trans Ophthal Soc Aust 12:95–104

Peichl L, Künzle H, Vogel P (2000) Photoreceptor types and distributions in the retinae of insectivores. Vis Neurosci 17:943–948

Pettigrew JD, Bhagwandin A, Haagensen M et al (2010) Visual acuity and heterogeneities of retinal ganglion cell densities and the tapetum lucidum of the African elephant (*Loxodonta Africana*). Brain Behav Evol 75:251–261. https://doi.org/10.1159/000314898

Piggins D, Muntz WRA, Best RC (1983) Physical and morphological aspects of the eye of the manatee (*Trichechus inunguis*) natterer 1883: (Sirenia: Mammalia). Marine Behav Physiol 9:111–130

Petit G, Rochon-Duvigneaud A (1929) L'oeil et la vision de L'Halicore dugong ERXL. Bull Soc Zool Fr 54:129–138

Rahm U (1990) "Tubulidentates: Aardvark". In: Parker SP (ed) Grzimek's Encyclopedia of Mammals, vol 4. McGraw-Hill Publishing Company, New York, p 452

Rochon-Duvigneaud A (1943) Les yeaux et la vision des vertebres. Masson, Paris

Samuelson DA (2013) Ophthalmic anatomy. In: Gelatt KN, Gilger BC, Kern TJ (eds) Veterinary ophthalmology, 5th edn. John Wiley & Sons, Inc., Ames, pp 39–170

Samuelson DA, Travers A, Lewis PA, Young JH (2004) Corneal angiogenesis in the Florida manatee. Invest Ophthalmol Visual Sci 45: 4805

Samuelson DA, Reppas G, Wong M, Lewis PA, Barrie KP, Graham AR (2007) Re-invented nasolarimal system among selected subungulate species. IOVS 48:1214

Samuelson DA, McGee JL, Maciejewski K et al (2009) Description of uniquely devised extrinsic ocular musculature in the Florida manatee. IAAAM. Poster abstract

Samuelson DA, McGee JL, Maciejewski K, Strobel MM, Lewis PA (2010) A uniquely constructed extraocular myology in the Florida Manatee (*Trichechus manatus latirostris*). IOVS 51:6334

Shoshani J (2005) "Order Hyracoidea" In: Wilson DE, Reeder DM (eds) Mammal species of the world: a taxonomic and geographic reference, 3rd edn. Johns Hopkins University Press, pp 88–89

Siemen D (1976) Elektronenmikroskopische Untersuchungen zur Reduktion des Auges bei unterirdisch lebenden oder nachtaktiven Säugetieren. Diplomarbeit (diploma thesis), Sektion Biologie, Universität Kiel

Soemmering DW (1818) De oculorum hominis animaliumque sectione horizontali commentatio. Gottingen. An extract edited by Anderson, S. 8r Munk, 0. (1971). Lederle Labs, Copenhagen

Stetter MD (2003) Tubulidentata (Aardvarks). In: Fowler ME, Miler RE (eds) Zoo and wild animal medicine. Saunders, Missouri, pp 538–541

Stone J (1983) Topographical organization of the retina in a monotreme: Australian apiny anteater (Tachyglossus aculeatus). Brain Behav Evol 22:175–184

Stone J, Halasz P (1989) Topography of the retina in the elephant, *Loxodonta africana*. Brain Behav Evol 34:84–95

Suedmeyer W (2006) Special senses. In: Fowler ME, Mikota SK (eds) Biology, medicine and surgery of elephants. Blackwell Pub, Ames, pp 399–407

Svartman M, Stanyon R (2012) The chromosomes of Afrotheria and their bearing on mammalian genome evolution. Cytogen Genome Res 137:144–153

Walls G (1942) The vertebrate eye and its adaptive radiation. Cranbrook Institute of Science, Bloomfield Hills, Michigan

West JA, Sivak JG, Murphy CJ et al (1991) A comparative study of the anatomy of the iris and ciliary body in aquatic mammals. Can J Zool 69:2594–2260

Willis CK, Skinner JD, Robertson HG (1992) Abundance of ants and termites in the False Karoo and their importance in the diet of the aardvark (Orycteropus afer). Afr J Ecol 30:322–334

Wolfer J, Rich P (1992) Persistent corneal erosion in an Asian elephant. Can Vet J 33:337–339

Yokoyama S, Takenaka N, Agnew DW et al (2005) Elephants and human color-blind deuteranopes have identical sets of visual pigments. Genetics 170:335–344. https://doi.org/10.1534/genetics.104.039511

Ophthalmology of Whippomorpha: Hippopotamuses, Whales, and Dolphins

31

Carmen Colitz and Fabiano Montiani-Ferreira

Introduction

The suborder Whippormorpha is small by number but features the largest of all vertebrates, cetaceans (whales and dolphins), as well as hippopotamuses (Waddell et al. 1999). Despite previous consideration that hippopotamuses were more closely related to Suidae (pigs) (Geisler and Uhen 2005), common ancestry is to the Artiodactyla, or even-toed ungulates considering similar auditory structures, hairless bodies, dense subcutaneous fat, and molecular analysis (Gatesy 1997; Thewissen et al. 2007; Beck et al. 2006; Tsagkogeorga et al. 2015). Despite similarities, the ocular anatomy of cetaceans is quite distinct from that of hippopotamuses. Little is known about ocular disease and in hippopotamuses, however, there is a better understanding of how to manage and prevent ophthalmic conditions affecting cetaceans that are under human care. We provide here a review of Whippomorpha ocular anatomy and morphology, as well as the current state of clinical ophthalmology in these species.

Hippopotamuses

Molecular and morphological evidence has demonstrated that extant hippos are a sister group to Cetacea, belonging to the crown clade Cetancodonta within the order Cetartiodactyla, but gaps in the fossil record have presented some challenges in determining their shared ancestral traits (Maust-Mohl et al. 2019). The hippopotamus (*Hippopotamus amphibius*) also called the common hippo or river hippopotamus, is one of only two extant species in the family Hippopotamidae, the other being the pygmy hippopotamus (*Choeropsis liberiensis* or *Hexaprotodon liberiensis*). The IUCN Red List of Threatened Species considers hippos as a vulnerable species, while the pygmy hippopotamus is considered as endangered (Lewison and Pluháček 2017).

C. Colitz (✉)
All Animal Eye Care in Jupiter Pet Emergency and Specialty Center, Jupiter, FL, USA
e-mail: ccolitzacvo@gmail.com

F. Montiani-Ferreira
Comparative Ophthalmology Laboratory (LABOCO), Veterinary Medicine Department, Federal University of Paraná, Curitiba, PR, Brazil
e-mail: montiani@ufpr.br

F. Montiani-Ferreira et al. (eds.), *Wild and Exotic Animal Ophthalmology*, https://doi.org/10.1007/978-3-030-81273-7_6

Fig. 31.1 Skull of a common hippo (*Hippopotamus amphibious*). Note the narrow middle portion and the prominent supraorbital arch. Legend: 1. Zygomatic arch, 2. Supraorbital ridge of frontal, 3. Crest on the zygomatic bone, 4. Infraorbital foramina, 5. Eminentia canina, 6. Lacrimal bulla. Used with permission from David Kilpatrick, Alamy Stock Photo

The common hippo can be found in rivers throughout the savanna of Africa and the main rivers of Central Africa (Estes 1992; Lewison and Pluháček 2017; Pushkina 2007; Stevenson-Hamilton 1912). Pygmy hippos are native to the forests and swamps of West Africa, primarily in Liberia, with small populations in Sierra Leone, Guinea, and Ivory Coast (Stroman and Slaughter 1972). There are just over 350 pygmy hippopotamuses in the ex situ population worldwide, so it is an uncommon resident in zoological collections compared to the most common hippos (*Hippopotamus amphibius*).

Hippopotamuses are generally herbivores and their diet consists almost entirely of grass, supplemented by aquatic plants. Although there are occasional occurrences of hippopotami eating some meat or fish, this is mostly regarded as unusual behavior, possibly due to stress. They are thought to be quite visually dependent both underwater while submerged on rivers or lakes (sometimes inside turbid waters), but more importantly on land, where most foraging occurs. The pygmy hippo favors heavily forested regions and is considerably less aquatic, but just as the common hippo, it does depend on water and usually remains close to streams. Additionally, the pygmy hippo is more reclusive and nocturnal.

Anatomy and Physiology

Hippos have several adaptations indicative of semiaquatic lifestyle that include partially webbed feet (Fisher et al. 2007) and skin that is mostly hairless and glandular (Eltringham 1999). Their skull and cranial sensory system are no different, exhibiting valvular nostrils and ears and dorsally protruding nostrils, eyes, and ears (Eltringham 1999). Anatomically, hippo eyes, nostrils, and ears are positioned in the rostral aspect of the head, so they are able to see, hear, and breathe while mostly submerged, greatly facilitating vision while their body is totally submerged. The skull of the hippopotamus is quite large, with a greater splanchnocranium than neurocranium (Fig. 31.1). From the dorsal view, the skull has a narrow middle portion (at the region of the maxillae) and wide caudal and rostral portions (Lucy et al. 2018; Zorić et al. 2018). The pygmy hippo's skull is more rounded and the eyes are set more on the side of the head. Their bony orbits are enclosed (complete) and positioned dorsolaterally (Fig. 31.1). The angle of divergence between the two optic axes of the orbits is 120° (Prince 1956). The supraorbital ridge of the frontal bone is very pronounced in both hippo species. This feature gives these animals the conspicuous bilateral periscope-eye-like appearance (Fig. 31.2). Large rounded lacrimal bullae can be seen on the floor of their bony orbit (Fig. 31.1).

In mammals, the upper lid is typically more mobile and provides greater corneal coverage. Hippopotamuses are an exception because of the extensive lower eyelid movement, resulting in closure of the palpebral fissure nearly axially on the cornea (Fig. 31.2a). In addition, true eyelashes are nearly absent so in hippopotamuses (Walls 1942) (Fig. 31.2b, c). Their third eyelid is well developed (Fig. 31.2c) and very active in protecting their corneal surface from underwater debris. Besides the primary orbital lacrimal gland, a superficial and a deep gland of the third eyelid were identified in pigmy hippos (Klećkowska-Nawrot et al. 2021). In the upper and lower eyelids, numerous serous glands were identified,

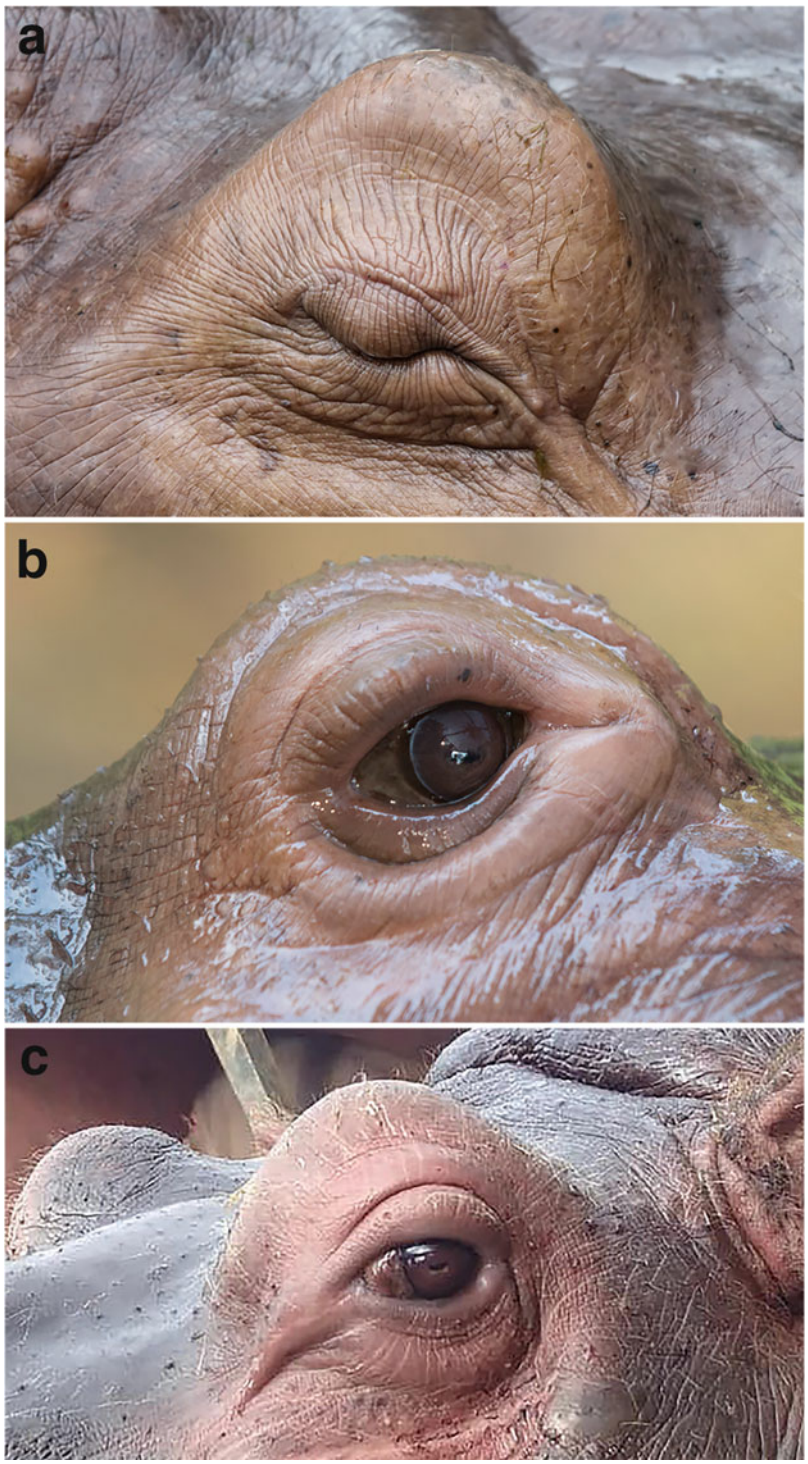

Fig. 31.2 Ocular adnexa of Hippopotamuses. (**a**) A hippopotamus blinking, displaying a mobile lower lid resulting in closure of the palpebral fissure nearly axially on the cornea. (**b**, **c**) Note the periscope-like appearance to the eye given by the prominent supraorbital ridge of the frontal bone and nearly absent eyelashes. Also, note the well-developed third eyelid exhibited in (**c**). **a**—Used with permission from MBLifestyle, Shutterstock.com. **b**—Used with permission from Perla Sofia, Shutterstock.com

which were typical for the pygmy hippopotamus and similar to those in Cetaceans. The cornea of most mammals is usually circular or almost so, but in cetaceans, ruminants, and hippopotamuses it is horizontally oval (Duke-Elder 1958). The hippo pupil is horizontal, almost rectangular when miotic (Fig. 31.3a) and slightly oval when mydriatic (Fig. 31.3b). The pupil margins possess discrete granular iridica, which is slightly more prominent in the ventral aspect of the pupil (Fig. 31.3b). The presence of frothy copious ocular discharge is commonly reported in this species. This is thought to be either a normal feature of this species' tear film but anecdotal reports also associate this type of secretion to stress, especially when it becomes more mucoid and whitish in color (Figs. 31.3b and 31.4). A similar feature has been observed in

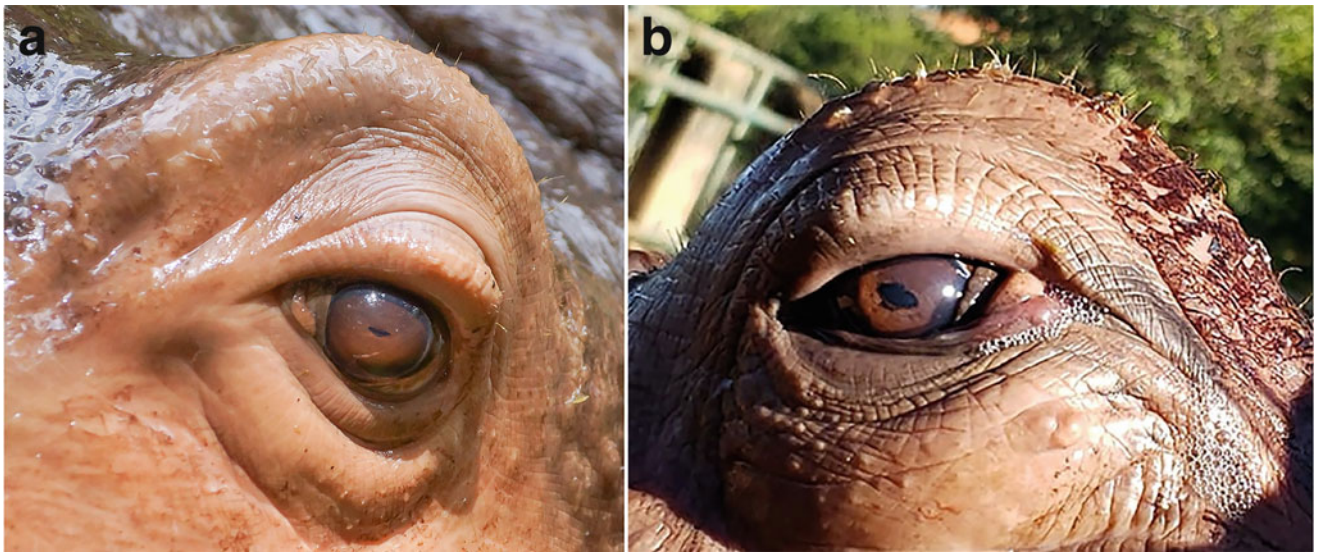

Fig. 31.3 The iris of Hippopotamuses is darkly pigmented. The pupil is horizontal, almost rectangular, when miotic (**a**), and slightly oval when mydriatic (**b**). Note that the pupillary margins possess discrete granular iridica, which is slightly more prominent in the ventral aspect of the pupil (**b**). A discrete amount of a frothy discharge can be observed in this picture, a common finding in hippopotamuses, likely due to the lack of a nasolacrimal duct. **a**—Used with permission from wk1003mike, Shutterstock.com. **b**—Courtesy of Ana Carolina Rodarte

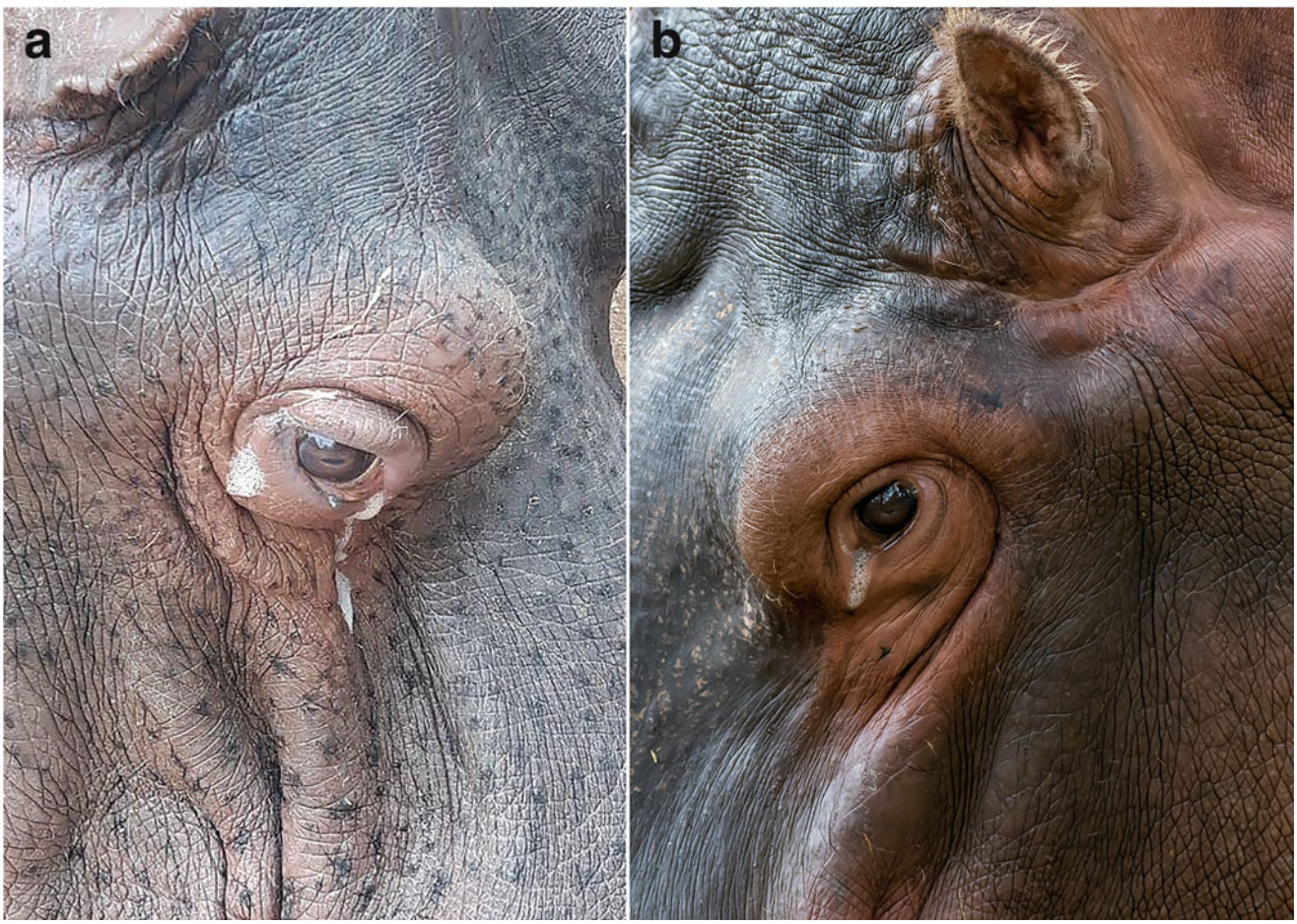

Fig. 31.4 Frothy ocular discharge is commonly noted in hippopotamuses. This is a normal finding, and most likely is related to the absence of a nasolacrimal duct. (**a**)—Courtesy of Fabiano Montiani-Ferreira; (**b**)—Used with permission from grafxart, Shutterstock.com

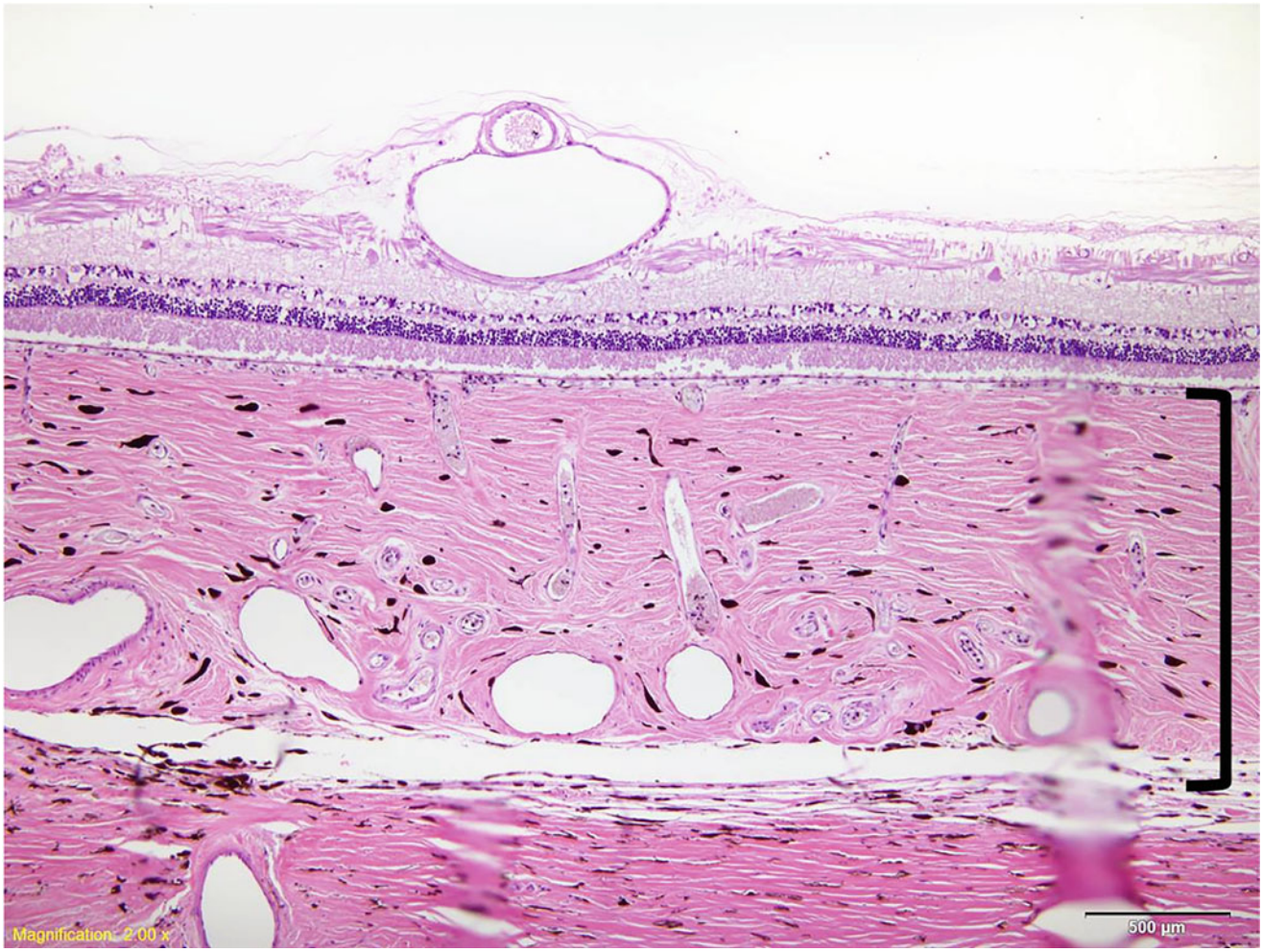

Fig. 31.5 Photomicrograph (H&E) of a section of the hippopotamus's posterior segment including the retina and the markedly fibrous choroid (denoted by the bracket). Courtesy of the Comparative Ocular Pathology Laboratory of Wisconsin. Magnification—200×

elephants (see Chap. 30: Ophthalmology of Afrotheria). One possible reason is the fact that hippopotamuses do not possess a nasolacrimal duct (Duke-Elder 1958).

Regarding the posterior segment, both species (*Hippopotamus amphibius* and *Choeropsis liberiensis*) possess a tapetum lucidum fibrosum (Hegner and Pilleri 1968). The hippo choroid is thick and markedly fibrous (Fig. 31.5). The retina of the hippopotamus possesses about 243,000 ganglion cells, of which 3.4% (8300) is composed of alpha cells. Alpha cells are thought to detect brisk transient visual stimuli. The distribution of both total and alpha cells reveals a dual topographic organization of a temporal and nasal area embedded within a well-defined horizontal streak. Enhanced resolution of the temporal area toward the frontal visual field may facilitate grazing, while resolution of the horizontal streak and nasal areas may help the discrimination of objects (predators, conspecifics) in the lateral and posterior visual fields, respectively. A specialized nasal area of the retina in the river hippopotamus retina supports the notion that this feature may enhance visual sampling in the posterior visual field to compensate for limited neck mobility as suggested for rhinoceroses and cetaceans (Coimbra et al. 2017). The optic nerve of the hippo has an enormously thick accessory sheath already noted to be present in whales and the elephant, with some of the fibers being non-myelinated (Duke-Elder 1958).

Diseases of the Eye and Adnexa

Only a few reports of ophthalmic disease have been reported in hippos. Signs of ocular hypertension were reported in a common hippo (*Hippopotamus amphibious*) diagnosed with pheochromocytoma (Duncan et al. 1994). *Oculotrema hippopotami* quite commonly parasitizes the eye of the hippopotamus (Tinsley 2013; Rubtsova et al. 2018), especially in the wild, causing conjunctivitis. This is the only monogenean (a class of parasitic flatworms that are commonly found on fishes and lower aquatic invertebrates) known to use a

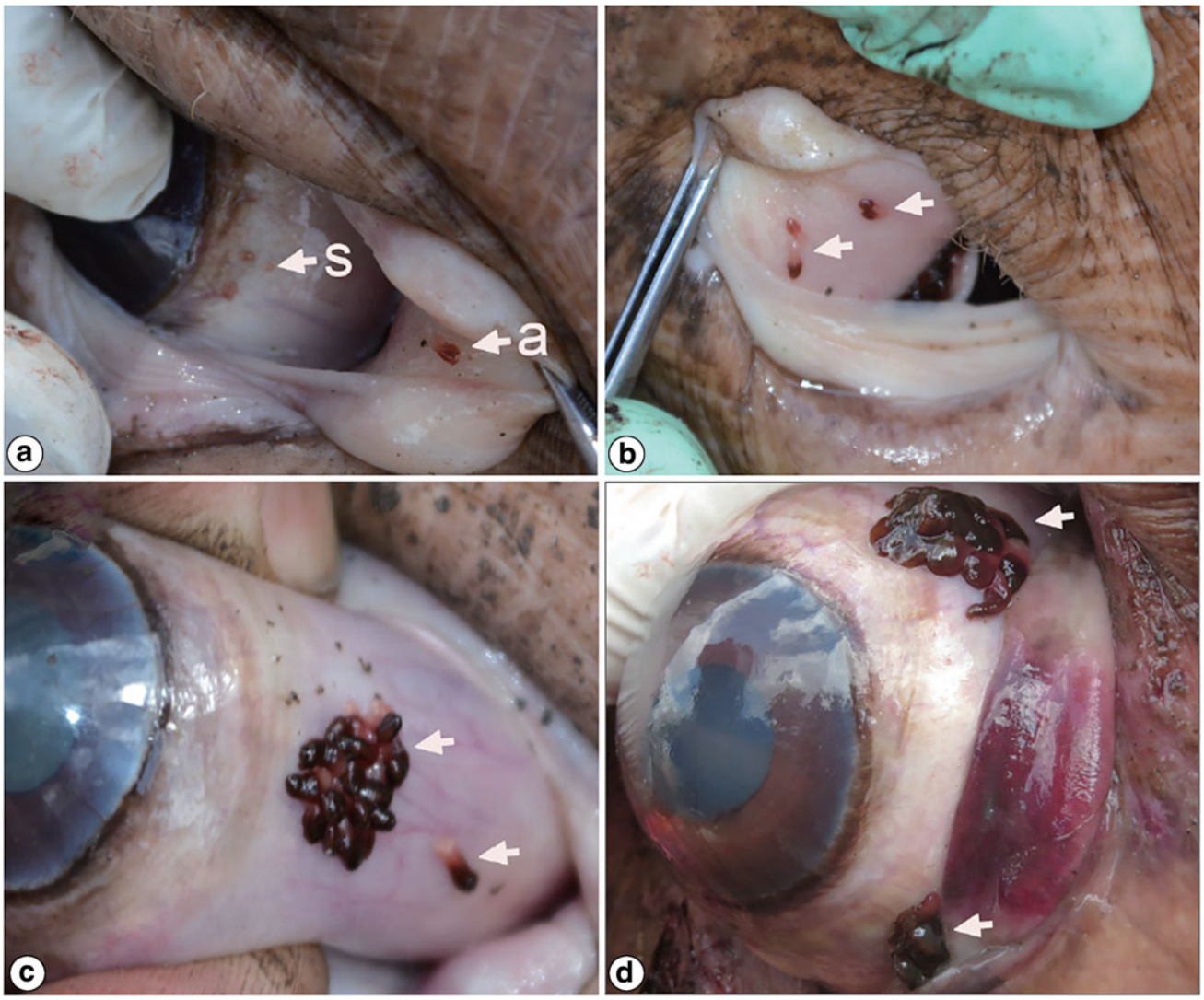

Fig. 31.6 *Oculotrema hippopotami* parasitism in common hippo (*Hippopotamus amphibious*) eyes. (**a**) Sub-adult forms of *O. hippopotami* (s) near the limbus and an adult (a) on the posterior surface of the third eyelid. (**b**) Four adults (arrows) on the third eyelid. (**c**) A cluster of adult forms and one isolated adult in the bulbar conjunctiva (arrows). (**d**) A rare case of the presence of two clusters of *O. hippopotami* attached to the same globe. Images used with permission from Rubtsova et al. 2018. Morphological Studies of Developmental Stages of Oculotrema hippopotami (Monogenea: Polystomatidae) Infecting the Eye of Hippopotamus amphibius (Mammalia: Hippopotamidae) Using SEM and EDXA with Notes on Histopathology. Korean J Parasitol. 2018 Oct;56(5):463–475

mammalian host (Fig. 31.6). Certainly, much is to be learned about ocular disease and its clinical management in hippopotamuses.

Cetaceans

The infraorder Cetacea contains whales, dolphins, and porpoises. Cetaceans are aquatic mammals that evolved from their terrestrial ancestors over 50 million years ago, and are the dominant group of marine mammals in terms of ecological and taxonomic diversity and geographic range (Encyclopedia of Marine Mammals 2008). Nearly 90 species of cetaceans exist, divided into two parvorders: the Mysticeti, or baleen whales, and the Odontoceti, or toothed whales. Of these, only a few species of Odontoceti are kept in human care and include Atlantic bottlenose dolphins (*Tursiops truncatus*), Pacific bottlenose dolphins (*Tursiops truncatus gilli*), Indopacific humpback dolphins (*Tursiops aduncus*), Beluga whales (*Delphinapterus leucas*), and orcas AKA killer whales (*Orcinus orca)* which are the largest species of oceanic dolphins.

Cetaceans are fascinating animals possessing both excellent sight and the ability to echolocate. Echolocation is a form of biological sonar that allows them to recognize objects and explore their environments, especially when foraging in

murky waters or at night where there is low visibility. In human care, cetaceans use their vision more than echolocation, as they are often training and feeding with their human trainers.

The following is a review of the current literature regarding the anatomy, physiology, and diseases of the cetacean eye.

Anatomy and Physiology

Various studies have described the glands responsible for the tear film in dolphins. A large circumorbital conjunctival gland is located within the eyelids deep to the palpebral musculature and is most developed medially (Waller and Harrison 1978; Tarpley and Ridgway 1991). The medial aspect of the orbital gland is often mistaken for the Harderian gland. Waller and Harrison (1978) divided the orbital gland into a conjunctival component and a medial component, which they termed the Harderian gland. The orbital gland has numerous excretory ducts that drain through pores randomly scattered across the conjunctival fornix. The gland is categorized as a compound seromucous tubular type. No other discrete lacrimal gland has been found; however, presumed remnants of lacrimal gland tissue were identified between the orbit and the palpebral musculature in the form of fatty lobules (Waller and Harrison 1978; Bolk et al. 1934). Cetaceans lack palpebral glands, such as meibomian glands and the glands of Moll and Zeiss, and they also lack a nictitating membrane (Tarpley and Ridgway 1991).

Since cetaceans spend their lives in the water, this has presumably modified their need for ocular adnexal structures. Similar to more recent studies, Tarpley and Ridgeway (1991) analyzed bottlenose dolphin tears, identified mucopolysaccharides, and negligible amounts of triglycerides and cholesterol. Cetacean tear film, like pinniped tear film, is not oily but rather is more hydrophilic, viscous, and mucus-like (Kelleher Davis and Sullivan 2009). Cetaceans produce copious amounts of thick mucinous tears and the mucin layer is significantly thicker in cetaceans compared to terrestrial mammals and pinnipeds. Mucins in the preocular tear film are essential for protection against pathogens, and very likely for protection against other environmental challenges in the aquatic environment. The mucins may serve to prevent evaporation and provide stability in the tear film of marine mammals including dolphins (Kelleher Davis and Sullivan 2009). In addition to a variety of mucins, cetacean tears also contain albumin and lysozyme (Colitz et al. 2007). Tear film samples from two dolphin species were shown to inhibit the growth of *E. coli*, supporting the antimicrobial function of the mucins (Kelleher Davis and Argueso 2015). The carbohydrates, N-acetylgalactosamine and N-acetylglucosamine, were present in higher amounts in dolphin tears than pinniped species, manatees, and humans (Kelleher Davis and Argueso 2014).

A PhD thesis by Nina Young described a variety of parameters from the tear film of three bottlenose dolphins (Young 1984). The mean ± SD tear film refractive index was 1.33682 ± 0.0007. The tear film osmolarity was very high, ranging from 408 to 557 with a mean of 470 ± 73 mOsm/kg. The pH was quite alkaline with a mean of 8.44 ± 0.19. Sodium ion concentration ranged from 133 to 170 mEq/L and potassium ranged from 28 to 37 mEq/L. The total protein ranged from 1.265 mg/ml to 2.583 mg/ml. Lysozyme was negligible, but present, with a mean of 0.0049 ± 0.0016 mg/ml. The total mean carbohydrate concentration was 3.031 ± 0.488 mg/ml and the total mean glucose was 26.58 ± 13.93 mg/100 ml. There was no significant difference between the refractive index, sodium level, and the ratio of tear potassium to plasma potassium in dolphins compared with human and rabbit tears. Prealbumin, albumin, and lactoferrin (a strong bacteriostatic protein) were most likely present based on the molecular weight of the protein bands. The parameters in dolphins that greatly differed from those in humans and terrestrial mammals included carbohydrates, total protein, glucose, cholesterol, lysozyme, osmolarity, and pH. The presence of even a tiny amount of lysozyme along with probable lactoferrin, and possibly immunoglobulins, establishes the dolphin tear film as having bacteriolytic properties, important for an environment teeming with a variety of bacteria. While there is still much to be learned from the study of cetacean tear film, it is clear that it serves an important protective role.

A recent study in Pantropical spotted dolphins (*Stenella attenuata*) confirmed the lack of a nasolacrimal duct in this species and in other cetacean species that were studied, including bottlenose dolphins (*Tursiops truncatus)*. Interestingly, by examining different stages of fetal development, it was found that formation of the nasolacrimal duct commenced at the same time as lacrimal bone formation, but the lacrimal foramen failed to develop (Rehorek et al. 2017).

Cetacean eyes are very mobile. They have dorsal, ventral, medial and lateral rectus muscles, dorsal and ventral oblique muscles, and a retractor bulbi muscle with similar innervation as that of terrestrial mammals. Cetaceans are able to move their left eye independent of the right eye (McCormick 1969; Dawson 1980). Dolphins have complete decussation at the optic chiasm (hence they do not have consensual pupillary light reflex) and lateral placement of the eyes, suggesting a predominantly panoramic mode of vision at the expense of depth perception (Tarpley et al. 1994). In addition, they also have independent eyelid movements (Lilly 1964; Supin et al. 2001). Additionally, cetaceans have unihemispheric sleep; i.e., dolphins shut down one hemisphere of their brain to sleep, and close the opposite eye. Thus, when the left half

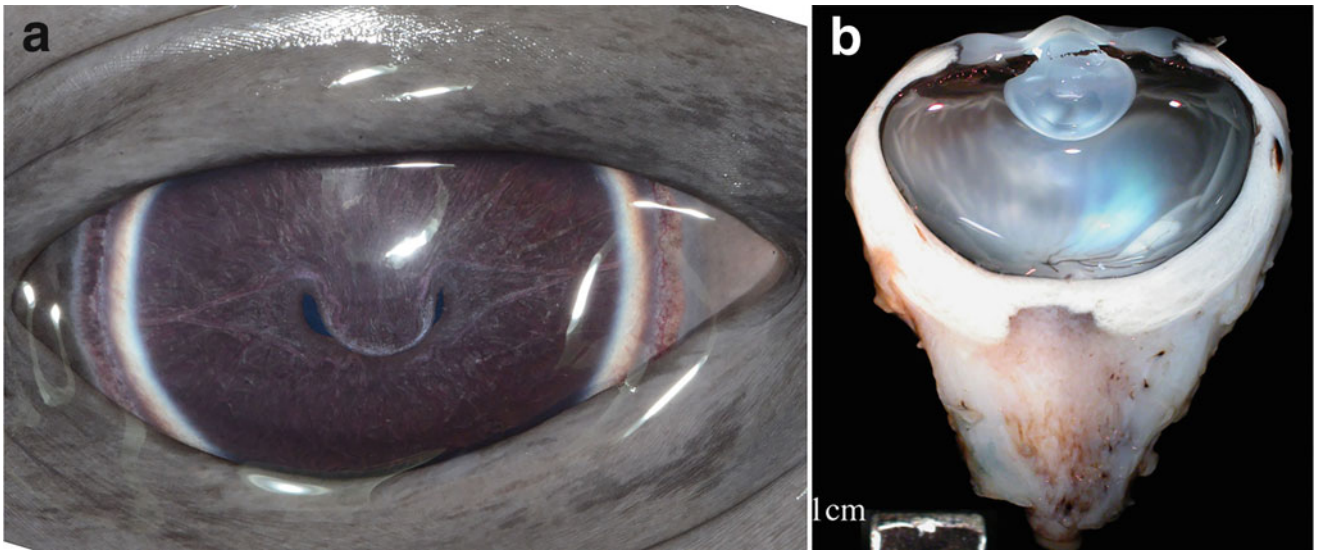

Fig. 31.7 (**a**) Normal right eye (OD) of a bottlenose dolphin (*Tursiops* spp.). This image demonstrates a constricted pupil with the operculum overlapping the ventral aspect of the pupil margin providing a medial and a temporal pupillary aperture. (**b**) Gross image of a normal bottlenose dolphin (*Tursiop*s spp) globe. Used with permission from Miller S, Samuelson D, Dubielzig R. Anatomic features of the cetacean globe. Vet Ophthalmol. 2013 Jul;16 Suppl 1:52–63

of the brain sleeps, the right eye will be closed. During sleep, the other half of the brain controls breathing functions and monitors the environment, including vision.

The globes of cetaceans are similar to the globes of terrestrial mammals, with some important functional differences (Miller et al. 2013). Figure 31.7 shows a clinical image of a normal bottlenose dolphin eye (Fig. 31.7a) and a gross image of the cross section of a normal bottlenose dolphin eye (Fig. 31.7b). The cornea and anterior segment have a relatively flattened curvature resulting in a globe that has a shorter axial length than its diameter (Mass and Supin 2007). The average axial length of the bottlenose dolphin globe was measured at 29.13 mm, the average scleral thickness measured 5.43 mm, the horizontal equatorial diameter measured 36.85 mm, and the vertical equatorial diameter measured 33.84 mm (Miller et al. 2013). The cetacean cornea is thinner axially and thicker peripherally (Supin et al. 2001; Miller et al. 2013, 2010). Similar to pinnipeds, the corneal layers from internal to external include the endothelium, Descemet's membrane, stroma, Bowman's layer, and the epithelium (Miller et al. 2010, 2013) (Fig. 31.8).

The Bowman's layer in cetaceans is similar in many ways to that of other species, though its thickness was measured at 16–22 microns, which was thicker than that found in giraffe, monkeys, and chickens (Samuelson et al. 2005). The Bowman's layer in dolphins also differs in that it possesses elastic fibers which react positively for the lectin wheat germ agglutinin (Samuelson et al. 2005).

The cetacean cornea has a refractive index similar to that of water and aqueous humor; while in the water the cornea is a negligible source of light refraction and focusing, divergent refraction does occur. The refractive index of the axial cornea is 1.37 and that of the peripheral thicker cornea is 1.53 (the refractive index of water is 1.33 to 1.34). The spherical lens has sufficient refractive power to focus images onto the retina and is positioned so that its center is almost in the center of the globe, which allows any incoming light rays to be almost identically focused on the retina (Mass and Supin 2007; Supin et al. 2001). The cetacean eye is emmetropic underwater (Kroger and Kirschfeld 1994). The cetacean lens eliminates spherical aberration via multifocal optics, which is achieved by a heterogeneous lens structure, wherein the outer layers have a lower refractive index than the inner nucleus (Rivamonte 1976; Kroger and Kirschfeld 1993). The pupil is horizontally shaped at its midposition, with two pupils forming (one medial and one temporal) when maximally constricted. The cetacean pupil and multifocal lens allow the use of different zones of the lens at once, and possibly allow some color vision in the blue-green spectrum, or improve differences in brightness.

The cetacean iris can adapt quickly to the rapid changes in brightness that occur when the animal dives from more lit surface water to the darker deeper depths of the ocean (Fig. 31.9). In addition, the shape of most cetacean pupils shape is unusual with the dorsal aspect having a protruberance called an operculum. In dim light, the operculum is raised giving the pupil an oval to almost round shape (Fig. 31.9d), like other mammals. As light increases, the operculum is lowered to give a U-shaped pupil that gradually closes (Fig. 31.9**b–d**) further until the operculum moves further ventrally to just cover its adjacent ventral pupil margin leaving 2 narrow apertures medially and temporally

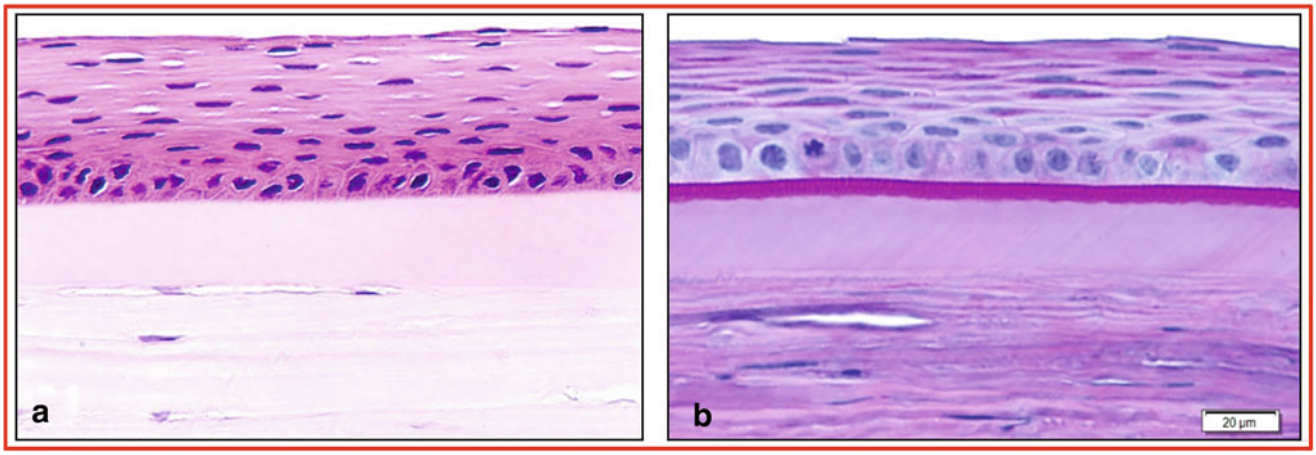

Fig. 31.8 (**a**) Histologic section of normal cornea from a bottlenose dolphin (*Tursiops* spp.) stained with H&E. (**b**) Histologic section of normal cornea from a bottlenose dolphin (*Tursiops* spp.) stained with periodic acid-Schiff (PAS). **a**—Courtesy of Comparative Ocular Pathology Laboratory of Wisconsin (COPLOW). **b**—Used with permission from Colitz CM, Walsh MT, and McCulloch SD. Characterization Of Anterior Segment Ophthalmologic Lesions Identified In Free-Ranging Dolphins and Those Under Human Care. J Zoo Wildl. Med. 2016 Mar;47(1):56–75

(Fig. 31.7a) (Mass and Supin 2007). Thus far, only the Amazon river dolphin (*Inia geoffrensis)* has been found to have a round pupil. The iris and ciliary body are highly vascular, with the iris having a robust musculature. The ciliary body musculature is poorly developed in all dolphin species and absent in most whales (Waller 1984; West et al. 1991; Bjerager et al. 2003; Miller et al. 2013). Instead of accommodation via change in lens shape, it has been proposed that accommodation is achieved by axial displacement (anterior translation) of the lens due to an increase in intraocular pressure (IOP), via contraction of the massive retractor bulbi muscle. When the retractor bulbi muscle subsequently relaxes, the globe recedes back into the orbit and the lens shifts posteriorly again (posterior translation) with a decrease in IOP (Kroger and Kirschfeld 1989; Supin et al. 2001). Specialized mechanoreceptors called encapsulated sensory corpuscles are present in the anterior uvea, the sclera surrounding the anterior uvea, and the trabecular meshwork (Miller et al. 2013). It is proposed that the function of encapsulated sensory corpuscles is in repositioning of the lens following the anterior translation, or they may detect IOP changes at the level of aqueous humor outflow (D. Samuelson, personal communication, 2020).

The normal IOPs of one male and one female bottlenose dolphin (*Tursiops truncatus)* and one Risso's dolphin (*Grampus griseus*) were published by Dawson, et al. (1992). The animals were administered diazepam and had their corneas topically anesthetized and their pupils pharmacologically dilated prior to measurements. An applanation tonometer (Tono-pen, Oculab) was used and the measurements were taken over a 30–38 min period for each animal. The mean ± SD IOP for the male bottlenose dolphin was 33.4 ± 2.4 mmHg OD and 33 ± 2.8 mmHg OS. The mean IOP for the female bottlenose dolphin was 24.6 ± 2.29 mmHg OD and 25.7 ± 3.47 mmHg OS. The mean IOP for the Risso's dolphin was 27.5 ± 3.4 mmHg OD and 28.7 ± 3.5 mmHg OS. More recently, the IOPs of a variety of cetacean species have been evaluated using two different tonometers (Colitz 2012). A Tono-Pen was used to measure the IOP in four Pacific bottlenose dolphins under behavioral restraint, and the mean IOP was 28.95 mmHg OD and 29.63 mmHg OS (Colitz 2012 and personal communication, Dr Maya Yamagata). These values are similar to those measured by Dawson, et al. (1992). The TonoVet is a newer, rebound tonometer that is easier to use and has a quieter beep and a smaller tip (Fig. 31.10); it has been used to measure IOPs in a variety of species including Pacific and Atlantic bottlenose dolphins, porpoises, and whales. In animals that were desensitized beforehand to the process of allowing IOP measurement, the average IOP was 28 mmHg OD and 27 mmHg OS, similar to the readings obtained with a TonoPen and to those measured by Dawson et al. (1992). In animals that were not desensitized, the IOPs were aberrantly higher, measuring between 36.5 and 40.57 mmHg. Tonometry was performed on a harbor porpoise and the IOP was 29 mmHg OD and 31 mmHg OS. In a Beluga calf, the IOPs measured 16 mmHg OU, and in an adult Beluga whale the IOPs measured 25 mmHg OU. Published accounts of intraocular pressure are available in Appendix 3.

The retina of all cetaceans evaluated to date is similar to that of terrestrial mammals with the same layers in the neural retina and the retinal pigment epithelium. However, the cetacean retina does differ in the thickness and numbers of pericarya and size of the cell types in some of the layers. The overall retinal thickness is 370 to 425 µm (Dral 1977; Dawson et al. 1982; Dawson et al. 1983; Murayama et al.

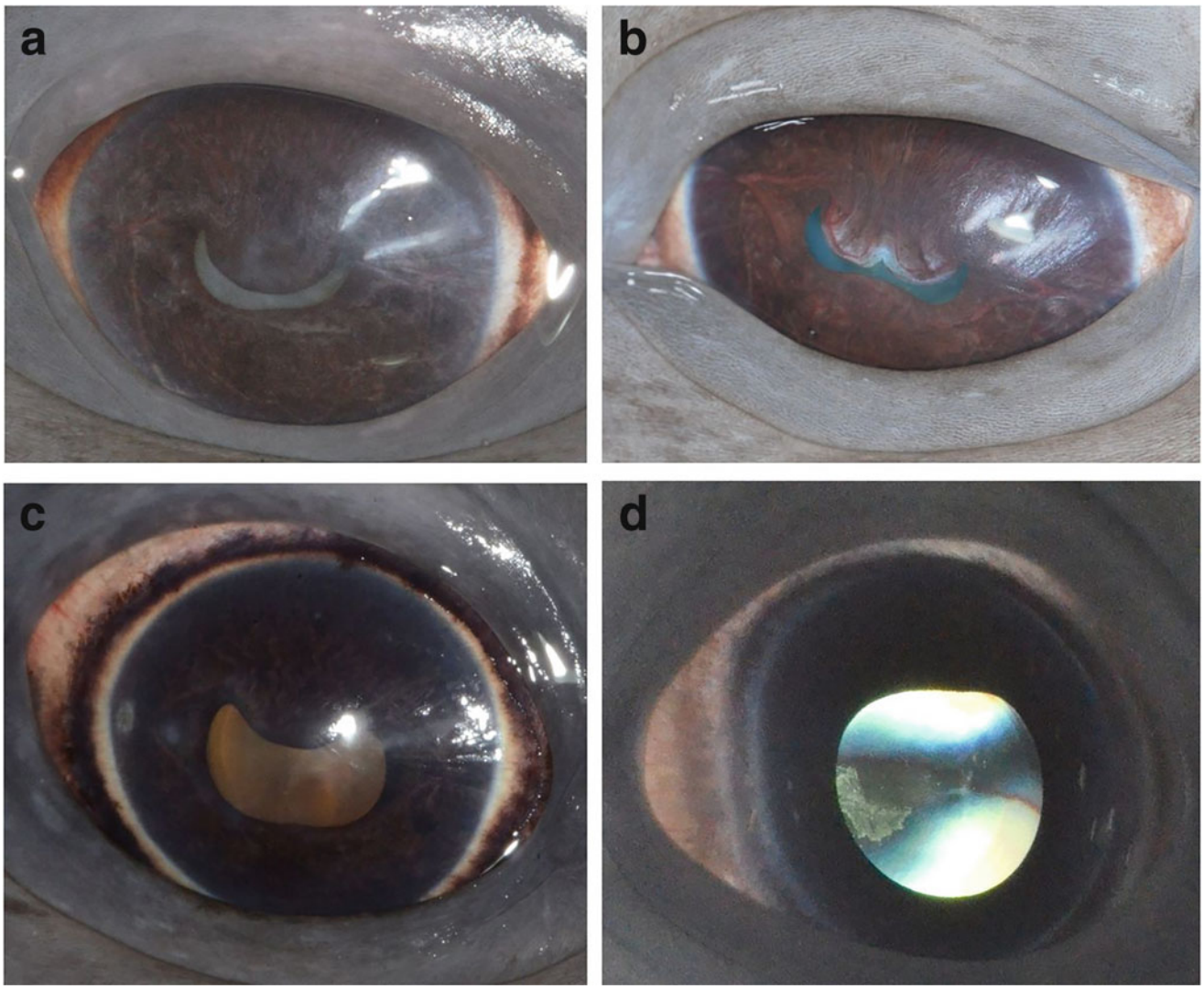

Fig. 31.9 Representation of pupil size changes in four different bottlenose dolphins (*Tursiops* spp.). (**a**) The top left is the pupil not completely constricted and U-shaped. (**b**) Another incompletely constricted pupil, but the operculum has an unusual bilobed appearance affording it a W-shape. (**c**) The bottom left is the pupil almost mydriatic with the operculum still evident. (**d**) The bottom right image is the pupil completely dilated under dim lighted conditions

1995). By comparison, the retinal thickness of the dog is 112–240 μm and the horse and cow are 110–220 μm (Prince et al. 1960).

The amacrine, bipolar, and horizontal cells are similar to those of terrestrial mammals. The differences are most prominent in the inner plexiform and ganglion cell layers. The ganglion cell layer has giant ganglion cells that measure 75 to 80 μm and some are larger, up to 100 μm (Dawson and Perez 1973; Perez et al. 1972; Dawson et al. 1982; Mass and Supin 1995a, b). In contrast, terrestrial mammals' "giant" ganglion cells measure 15 to 35 μm (Hebel and Hollander 1979). The ganglion cells are thought to be related to "Y" cells, which function to respond to movement as in cats (Fukada and Stone 1974). There are two clearly defined areas of higher ganglion cell density located nasally and temporally approximately 15 to 16 mm from the optic disk, with a thin band of ganglion cells that connect these two regions passing beneath the optic disk (Supin et al. 2001). The presence of two areas of high ganglion cell density exists in most cetacean species. When a dolphin looks at an object underwater, it positions itself sideways and observes the object with one eye using the nasal area of high ganglion cell density. Then, when the dolphin surfaces above the water, it uses the temporal area of high ganglion cell density to observe the object (Dral 1977, 1972; Dawson 1980). Overall, the ganglion cell layer has low cell density with the large cells separated by wide spaces; this is the case in the optic nerve as well (Dral 1977). To date, there is no explanation for the uncommonly large giant ganglion cells in cetaceans.

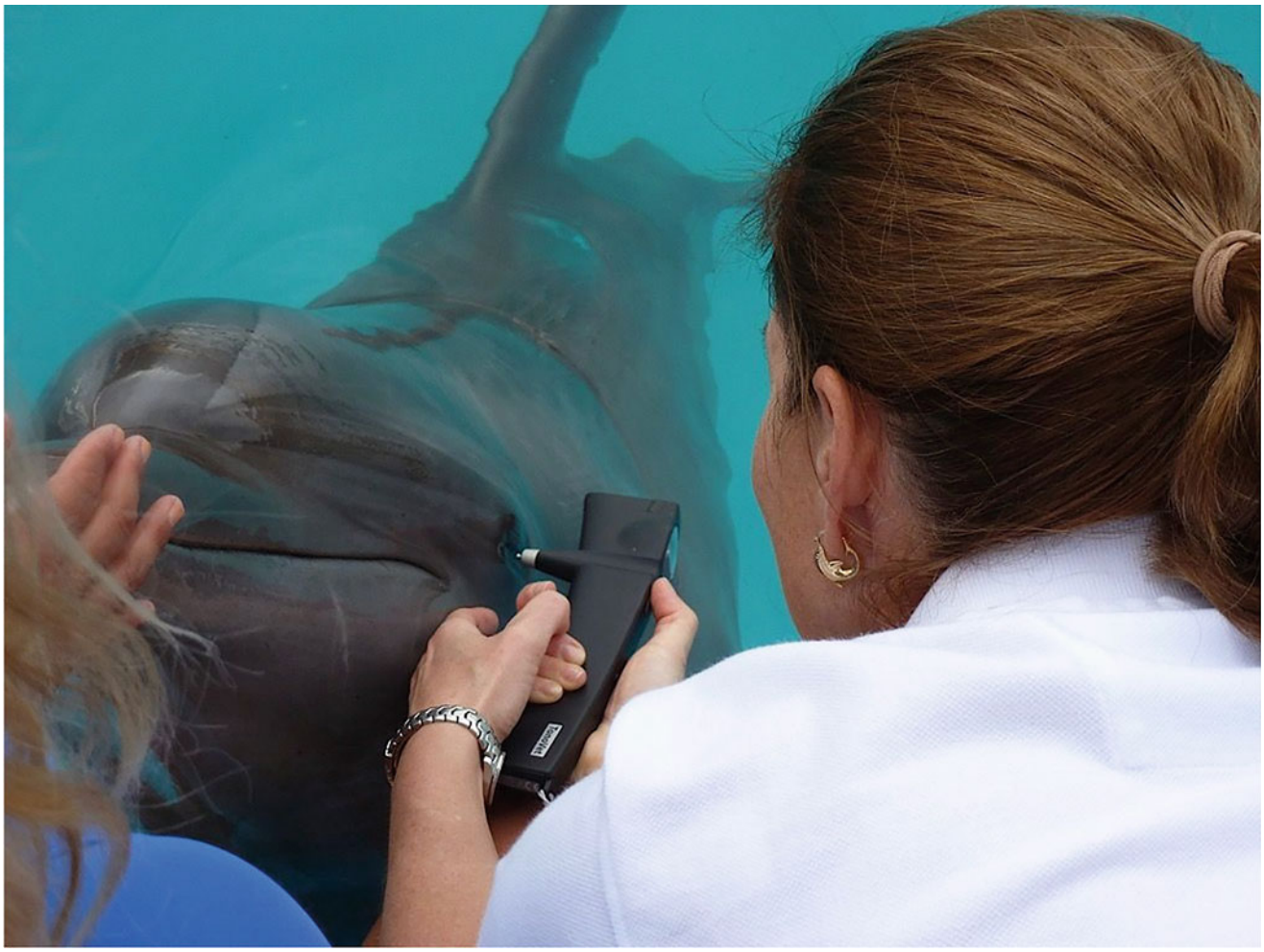

Fig. 31.10 Measurement of the intraocular pressure with a Tonovet tonometer in a bottlenose dolphin (*Tursiops* spp.)

The bottlenose dolphin has the best-described cetacean fundus. The cetacean retina is holangiotic and rod dominant (Dawson 1980). Unlike terrestrial ungulates, from which cetaceans are derived, the retinal vessels do not protrude into the vitreous. The tapetum encompasses the entire fundus in these species and is fibrous (tapetum fibrosum). The cetacean tapetum has far more layers than what is present in terrestrial species. The bottlenose dolphin's tapetum has a mean ± SD of 51 ± 7 layers, and the pygmy sperm whale's tapetum has 74 ± 14 layers. This implies that cetaceans' tapeta should function extremely efficiently (Young et al. 1988).

Despite the ability to echolocate, vision is still a very important special sense in these species despite often diving and foraging under low light conditions (Norris 1969). The need for color vision is thought to be of secondary importance.

As mentioned above in the cetacean retina, rod photoreceptors predominate with few cones. As in pinnipeds, cetaceans have long-wavelength-sensitive (LWS) cone opsin genes and have a mutated short-wavelength-sensitive (SWS) cone opsin gene causing a pseudogene (Fasick and Robinson 1998). Thus, cetaceans are cone monochromats. Cone densities were evaluated in six cetacean species, including bottlenose dolphins. The L-cone densities, in all but the harbor porpoise, were between 3000 and 7000/mm^2 and were comparatively close to those of nocturnal terrestrial mammals. All of the cetacean species lacked S-cones (Peichl et al. 2001). The L-cones and rods in marine mammals are more sensitive to shorter wavelengths than those of terrestrial mammals, extending the visual spectrum from the green spectrum into the blue spectrum. Molecular studies have found that the bottlenose dolphin possesses a short-wavelength-sensitive (SWS) pseudogene (Fasick and Robinson 1998). A larger-scale study confirmed the presence

of SWS pseudogenes in 16 species of cetaceans (Levenson et al. 2006). Sequencing the first exon of the SWS cone opsin genomic DNA identified the deletion mutation causing the nonfunctional SWS cone opsin or pseudogene (Newman and Robinson 2005). The noted absence of SWS-cones histologically supports the molecular study results (Peichl et al. 2001). The blue-shifting of LWS opsins occurs due to a replacement of serine at position 292 (Newman and Robinson 2005). This blue-shift may be an adaptation to the underwater light field (Peichl et al. 2001; Peichl and Moutairou 1998; Newman and Robinson 2005). Another study determined a correlation between the spectral sensitivity of rod opsins and the depths at which the different marine mammals forage (Fasick and Robinson 2000).

The ocular blood supply in marine species, including bottlenose dolphins, is delivered via an ophthalmic rete occupying most of the orbit, that has a very well-developed arterial network (Ninomiya et al. 2014). The ophthalmic rete's main blood supply is the basilar rete via the spinal rete. The choroidal and retinal arteries are derived from this rete. The proposed role of the ophthalmic rete is for ocular temperature conservation to provide the appropriate temperature for the function of photoreceptors, oculomotor muscles, ciliary muscles and iris, and the ocular vascular system. One other possible role is to dampen the flow of blood within the orbit (Ninomiya et al. 2014).

Diseases of the Eye and Adnexa

Eyelids

The appearance of hyperemia of the eyelids is normal in young bottlenose dolphins (Fig. 31.11a). However, as they age, the eyelids usually become gray like the rest of their bodies, though occasionally, a few adult dolphins will retain pink eyelids without disease (Fig. 31.11b) or other causes. This may be a lack of pigmentation that occurs with natural aging, though it is not definitively known. More commonly, eyelid hyperemia in adult dolphins is a result of self-trauma. Traumatic eyelid bruises or lacerations may occur from rough play or fighting (Fig. 31.12). Surgical repair of severe lacerations can be performed in 2-layers as in other species (Fig. 31.13). Eyelid tumors are uncommon but occur (Fig. 31.14).

Conjunctiva

Conjunctivitis is not common in cetaceans. However, conjunctival hyperemia and chemosis can occur secondary to keratopathy or self-trauma. A case of severe proliferative conjunctivitis (without active keratopathy) occurred in a bottlenose dolphin. While the cause was not definitively identified, ocular trauma, or self-trauma was the suspected cause (Fig. 31.15).

Orbit

No orbital diseases are known to have been reported in cetaceans.

Cornea

Common corneal diseases affecting cetaceans under human care have been described and include medial and temporal keratopathy, horizontal keratopathy, and axial keratopathy (Colitz et al. 2016). These are the four most common corneal diseases that affect cetaceans, and more than one of these can occur at the same time. Treatment for the keratopathies, including recommended medications, doses, and concentrations is detailed below in the section *Management of Active Keratopathy in Cetaceans.*

Medial Keratopathy

Medial keratopathy is the most common corneal disease of cetaceans with a prevalence of 53.9% of studied animals, and occurring bilaterally in 46.1% of animals (Colitz et al. 2016). Early in the disease, pigment just medial to the medial limbus begins to migrate toward the limbus, then crosses the limbus and migrates into the adjacent cornea (Fig. 31.16). Once pigment has established itself across the limbus, corneal fibrosis follows, along with vascularization (Fig. 31.17). Over time, the lesion may extend towards the axial cornea, linking horizontal or axial keratopathy when present. Medial keratopathy is often an incidental finding, and may be directly related to excessive ultraviolet (UV) exposure via the Coroneo effect (Coroneo et al. 1991) thought to be similar to the pathogenesis of pterygia in humans. These lesions are more common in animals exposed to higher UV indices in the experience of this author; a large epidemiological study is planned in order to test this hypothesis. Medial keratopathy is not painful unless a corneal ulcer or abscess develop within the medial keratopathy lesion causing severe pain and sometimes subtle cellular infiltrates (Fig. 31.18). Supportive care, including topical antibiotics, oral doxycycline, and pain management, leads to resolution of the ulcer or abscess and associated pain, but not the medial keratopathy lesion itself. Overall, diminished exposure to excessive UV radiation combined with daily UV–protective antioxidant support appears to slow progression of this disease (personal observation, Colitz).

Temporal Keratopathy

Temporal keratopathy is similar to medial keratopathy in presentation but occurs, as its name suggests, at the temporal conjunctiva, limbus, and cornea (Fig. 31.19). Temporal keratopathy has been reported to occur in 6.1% of animals and was bilateral in 5.6% of animals (Colitz et al. 2016). Temporal keratopathy appears to occur more frequently at higher latitudes, whereas, medial keratopathy is more common nearer the equator (personal observation Colitz and

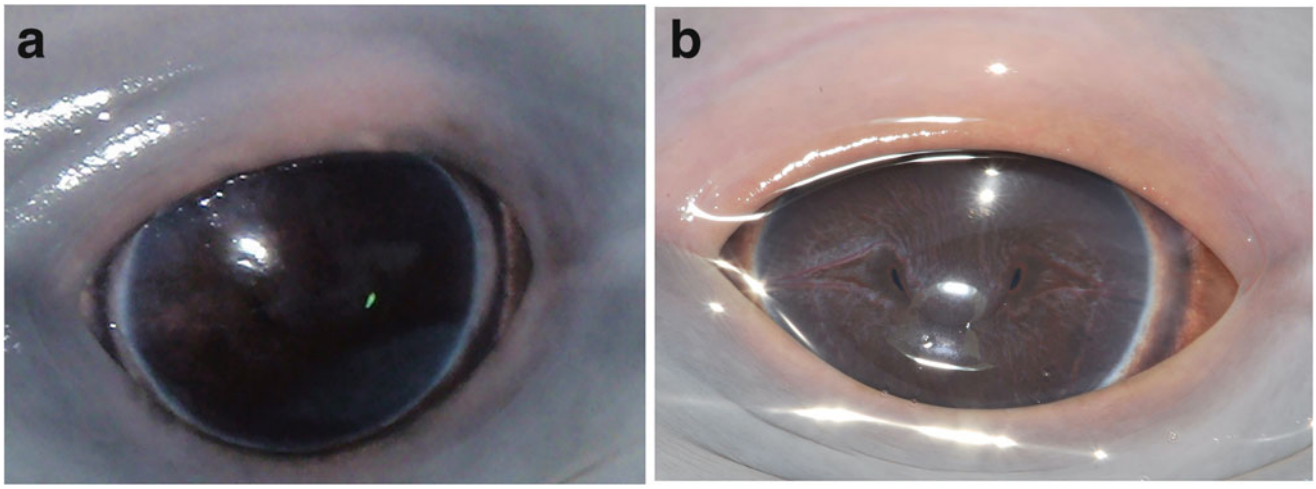

Fig. 31.11 (**a**) Young bottlenose dolphin (*Tursiops* spp.) with mild pink coloration to the upper and lower eyelids. (**b**) Adult bottlenose dolphin (*Tursiops* spp.) with diffuse pink coloration to the upper and lower eyelids that was normal for that animal

Alonso-Alegre). Additionally, the author has noted that temporal keratopathy is more common in animals that live indoors in the USA. However, since there are too few animals housed indoors, the true effect of indoor housing on this disease cannot be determined at this time. Similar to medial keratopathy, it is reasonable to assume that the Coroneo effect is a contributing factor to temporal keratopathy. Since cetaceans' eyes are very prominent, UV light can enter from either the medial or temporal aspects as the animals surface for feeding and other interactions, which occur more often than in the wild. Moreover, captive animals are kept in pools that are significantly shallower than the open sea, leading to higher UV exposure.

Horizontal Keratopathy

Horizontal keratopathy can be transient in its initial presentation and is the second most common ocular lesion affecting dolphins in human care. Horizontal keratopathy was reported to occur in 22.8% of animals and 15.6% had bilateral lesions (Colitz et al. 2016). This disease may develop in young animals even less than 1 year of age. The typical lesion occurs axially in the linear space on the superficial cornea where the superior and inferior eyelids appose. Lesions can be of any length and of variable width; they can be located more medially or temporally than just axially; and they may be straight or irregular (Fig. 31.20a,b). Early lesions can appear and disappear within a 24–48-hour time period, or

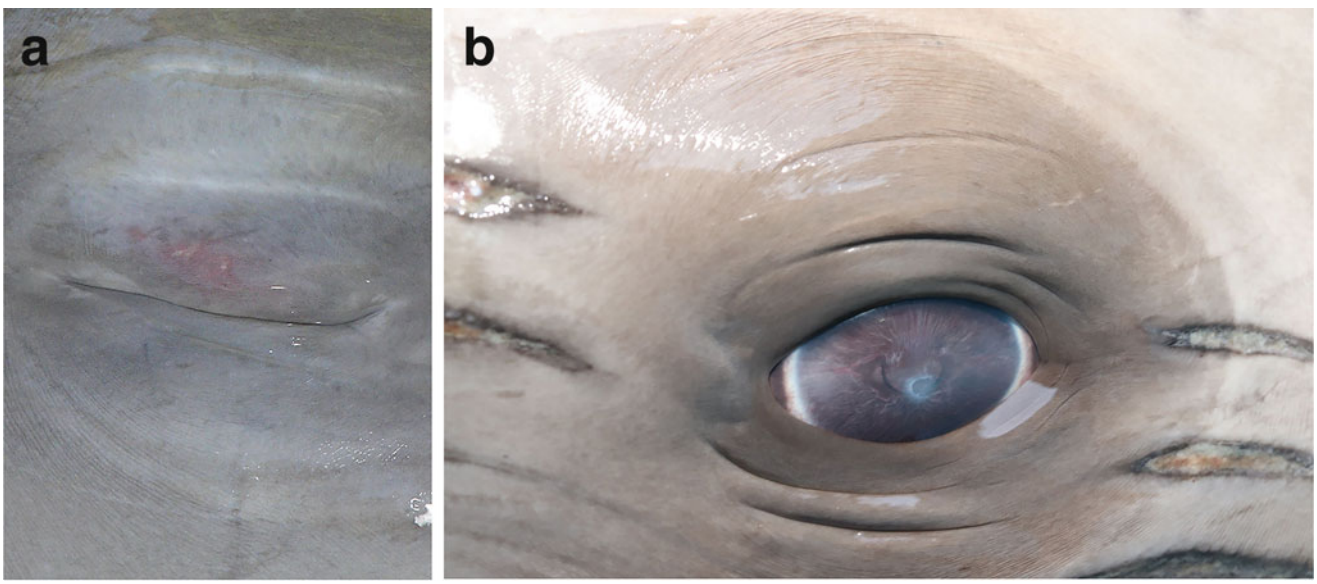

Fig. 31.12 (a) The right eye (OD) of a bottlenose dolphin (*Tursiops* spp.) with trauma to the upper eyelid causing hyperemia, mild bruising, and severe blepharospasm. (**b**) Periocular lacerations due to rough play with enclosure mate. **a**—Used with permission from Colitz CMH. Ocular Surface Diseases in Marine Mammals. Vet Clin North Am Exot Anim Pract. 2019 Jan;22(1):35–51

Fig. 31.13 The right eye (OS) of a bottlenose dolphin (*Tursiops* spp.) had a traumatic eyelid laceration, which was sutured. This image is 5 years after the trauma and repair occurred

resolve slowly. Over time, with repetitive insults, the lesions become permanent. New lesions can develop and be superimposed in the same site as the chronic lesions, and, some may develop corneal ulcers (Fig. 31.20). Histologically, the deeper corneal epithelial cells invade and penetrate Bowman's layer and eventually may invade the anterior corneal stroma (Fig. 31.21) (Colitz et al. 2012).

Predisposing factors of horizontal keratopathy include any nonspecific oxidative stress such as increases in UV exposure time or index, changes in water quality, and the use of most oral quinolone antibiotics for extended periods of time. Currently, there is no specific successful therapy for the initial time of presentation of this disease. While, as previously stated, in some cases the lesion will be resolved by the following day. If horizontal keratopathy has occurred once,

Fig. 31.14 The left eye (OS) of a bottlenose dolphin (*Tursiops* spp.). The lower eyelids had 2 tiny masses. The diagnosis is unknown. Use with permission from: Colitz CMH. Ocular Surface Diseases in Marine Mammals. Vet Clin North Am Exot Anim Pract. 2019 Jan;22 (1):35–51

Fig. 31.15 Left eye (OS) of a bottlenose dolphin (*Tursiops* spp.) with severe blepharoconjunctivitis. The cause was not identified. Used with permission from: Gulland, F.M. D., Dierauf, L.A., Whitman, K.L. (Eds.). CRC Handbook of Marine Mammal Medicine, third Edition, CRC Press, Boca Raton, pp. 377–412, figure 23.20

it will likely recur since the stressor is usually environmental. It is ideal to closely evaluate the water quality parameters for the two-week time period prior to the date of onset to see if there is an obvious stressor that can be better controlled. The use of oral quinolone antibiotics is common and necessary, depending on the infection. Knowing this, monitoring the eyes prior to their use and throughout the treatment protocol is suggested. Current recommendations include: (1) the use of daily oral UV-protective antioxidants including grapeseed extract, lutein, omega 3 fatty acids, and astaxanthin; (2) the use of topical 0.02 or 0.03% tacrolimus ophthalmic solution twice daily long term (the MCT diluent is preferred as it is more stable than the aqueous diluent; and (3) providing more shade or other form of lowering UV index such as changing the pool color to tan or sand (personal communication Latson and personal observation, Colitz).

Axial Keratopathy

Axial keratopathy is a close third in incidence; it was reported to occur in 24.4% of animals and was bilateral in 11.7% of cases (Colitz et al. 2016). The classic axial keratopathy lesion initially appears as a pinpoint gray-white opacity axially in

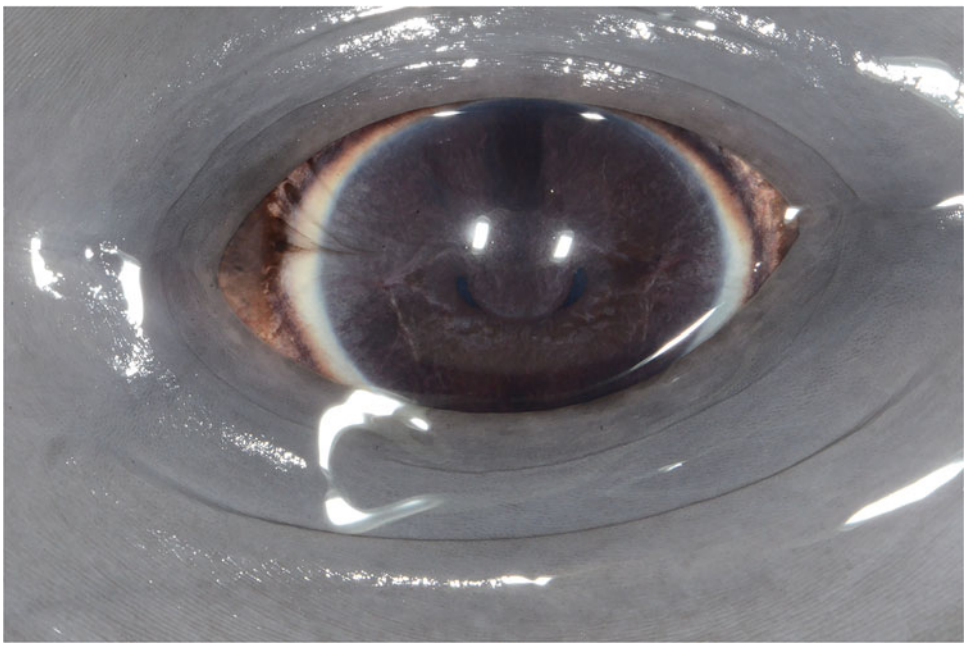

Fig. 31.16 Left eye (OS) of a bottlenose dolphin (*Tursiops* spp.) with early medial keratopathy. The medial limbus is beginning to have wispy migration of pigment from the conjunctiva crossing the limbus into the adjacent cornea

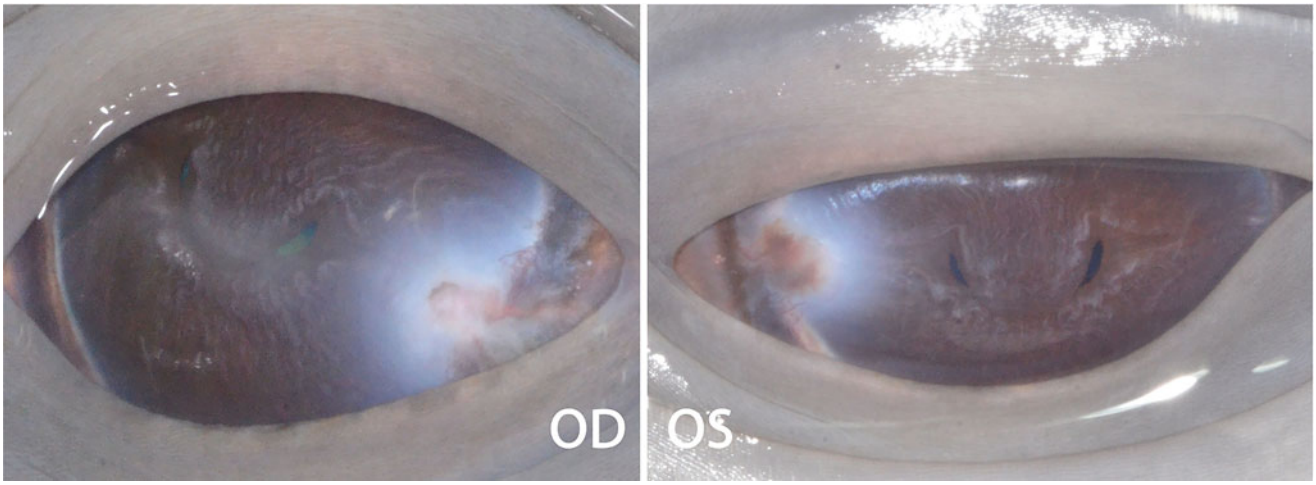

Fig. 31.17 Both eyes (OU) of a bottlenose dolphin (*Tursiops* spp.) with moderate medial keratopathy. There is pigment migration over each medial limbus into the adjacent cornea with severe focal edema, fibrosis, and vascularization

the anterior corneal stroma (Fig. 31.22a,b). The opacity often has a less dense grey halo surrounding the denser pinpoint opacity. This may remain unchanged for months to a few years and is not painful in its quiescent state. The underlying cause of axial keratopathy is not identified and nothing has been hypothesized as a possible cause. The initial lesion appears similar to a corneal disease termed "Florida Keratopathy," or "Florida Spots" that occurs in dogs and cats (personal observation, Colitz). It is possible that the two diseases share a similar initial cause. While Florida keratopathy does not cause clinical signs such as pain or infections in dogs and cats, the author hypothesizes that the lack of progression in dogs and cats may be due to stable immune function of the superficial cornea, and that cetaceans innately harbor additional threats to immune stability (e.g., water quality and other environmental factors) with subsequent infection by opportunistic pathogens. The immune system plays a role in the expression of diseases of the body, so it is logical that Florida Keratopathy and Axial Keratopathy could share a similar cause. The stimulus or trigger for progression in cetaceans is unknown, but secondary infection with opportunistic organisms appears to play a role in progression of the lesion (Figs. 31.22c,d and 31.23). Infection often causes stromal loss, resulting in clinical signs

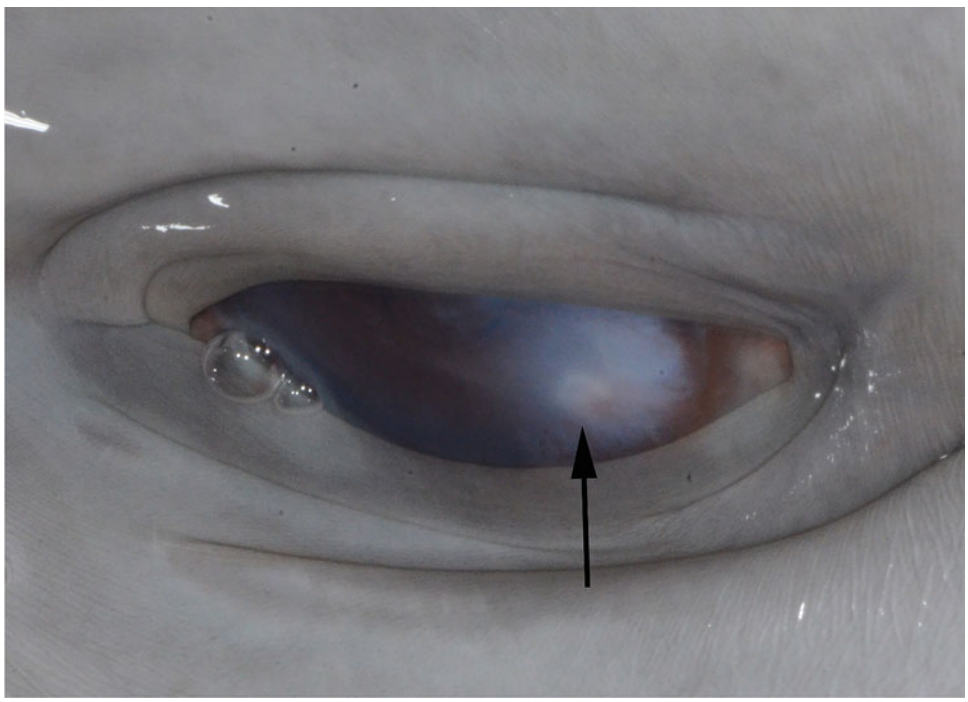

Fig. 31.18 Right eye (ODf) of a bottlenose dolphin (*Tursiops* spp.) with medial keratopathy and a concurrent stromal abscess. There is pigment migration over the medial limbus into the adjacent cornea with severe focal edema and vascularization. In addition, there is a dense opaque round lesion of cellular infiltrates consistent with a stromal abscess (arrow). Used with permission from: Colitz CMH, Walsh MT, McCulloch SD. Characterization of anterior segment ophthalmologic lesions identified in free-ranging dolphins and those under human care. J Zoo Wildl Med. 2016;47(1): 56–75

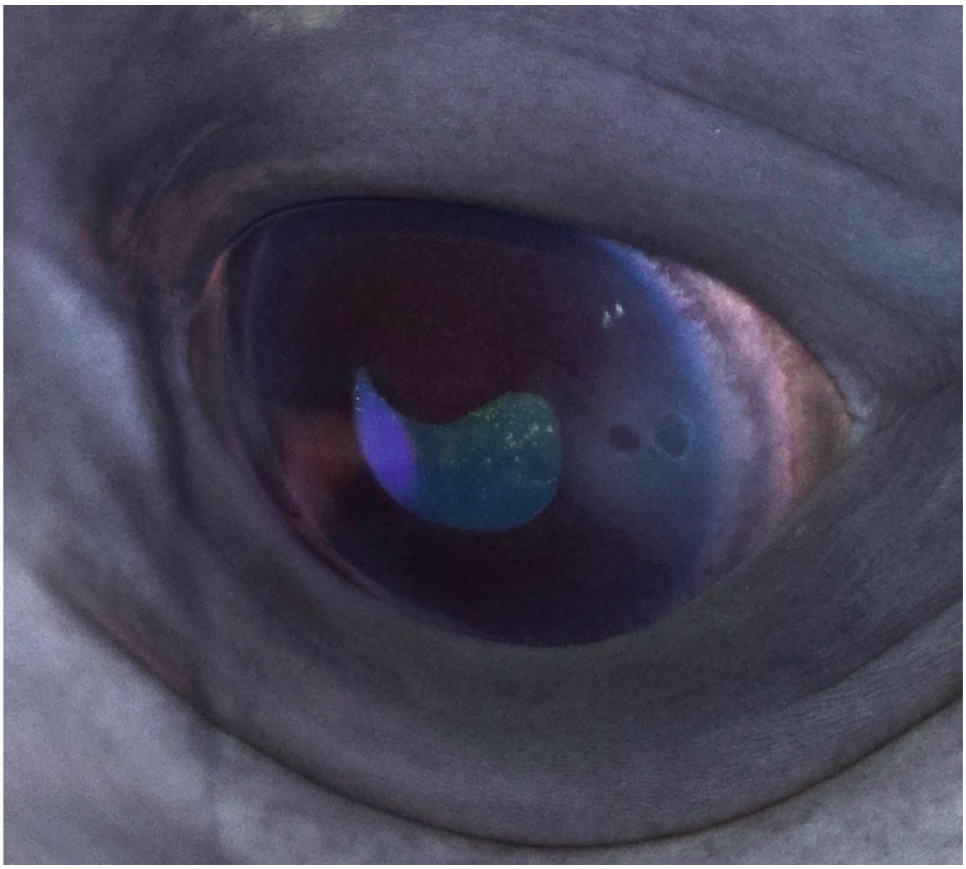

Fig. 31.19 Left eye (OS) of a bottlenose dolphin (*Tursiops* spp.) with temporal keratopathy. There is a triangular area of focal edema that has 2 round corneal ulcers within the keratopathy lesion. There is pigment migration over the limbus and hyperemia of the medial conjunctiva

of mild-to-severe pain. Topical and oral antibiotic therapy is important to control corneal infection; doxycycline is always included in the treatment plan, in addition to appropriate broad-spectrum bactericidal antibiotics.

A similar unusual keratopathy present in dogs and cats (without a defined name) is presumed to be caused by generalized immunodeficiency. Animals with immune-mediated disease or being treated with immunosuppressive medications, including systemic corticosteroids and cyclosporine, can develop an axial keratopathy with an associated intense bacterial infection that can even flourish in the presence of topical broad-spectrum antibiotics. In the author's experience, healing in dogs and cats occurs via corneal vascularization and presumed eventual rebalancing of the surface immunity. We hypothesize that Axial and chronic

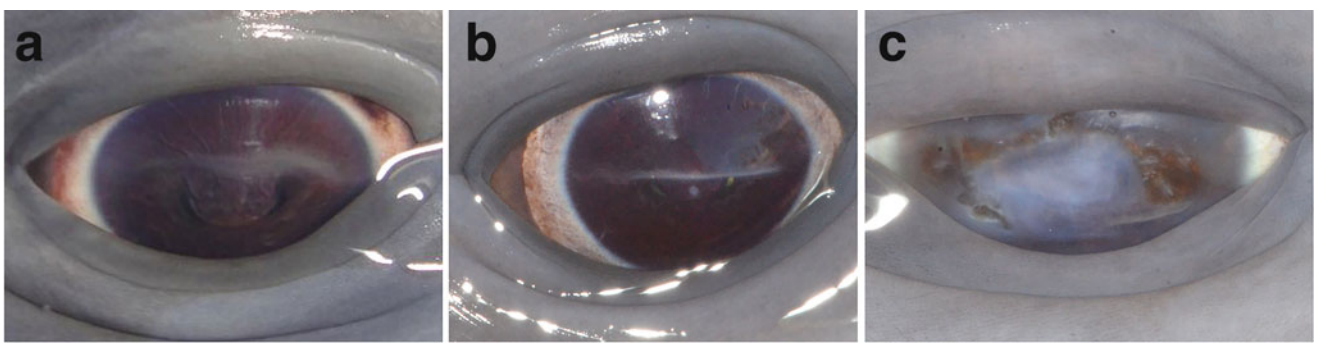

Fig. 31.20 Three examples of horizontal keratopathy in bottlenose dolphins (*Tursiops* spp.). (**a**) An initial lesion where the horizontal linear lesion is a diffuse superficial opacity. (**b**) Also, an acute to subacute example of horizontal keratopathy that is a discrete horizontal white superficial epithelial to anterior stromal lesion. (**c**) The left eye of a bottlenose dolphin (*Tursiops* spp.) with severe chronic horizontal and axial keratopathy. Large horizontally oval diffuse gray opacity and surrounding the gray opacity, there is a rust-colored irregular border with areas of stromal loss

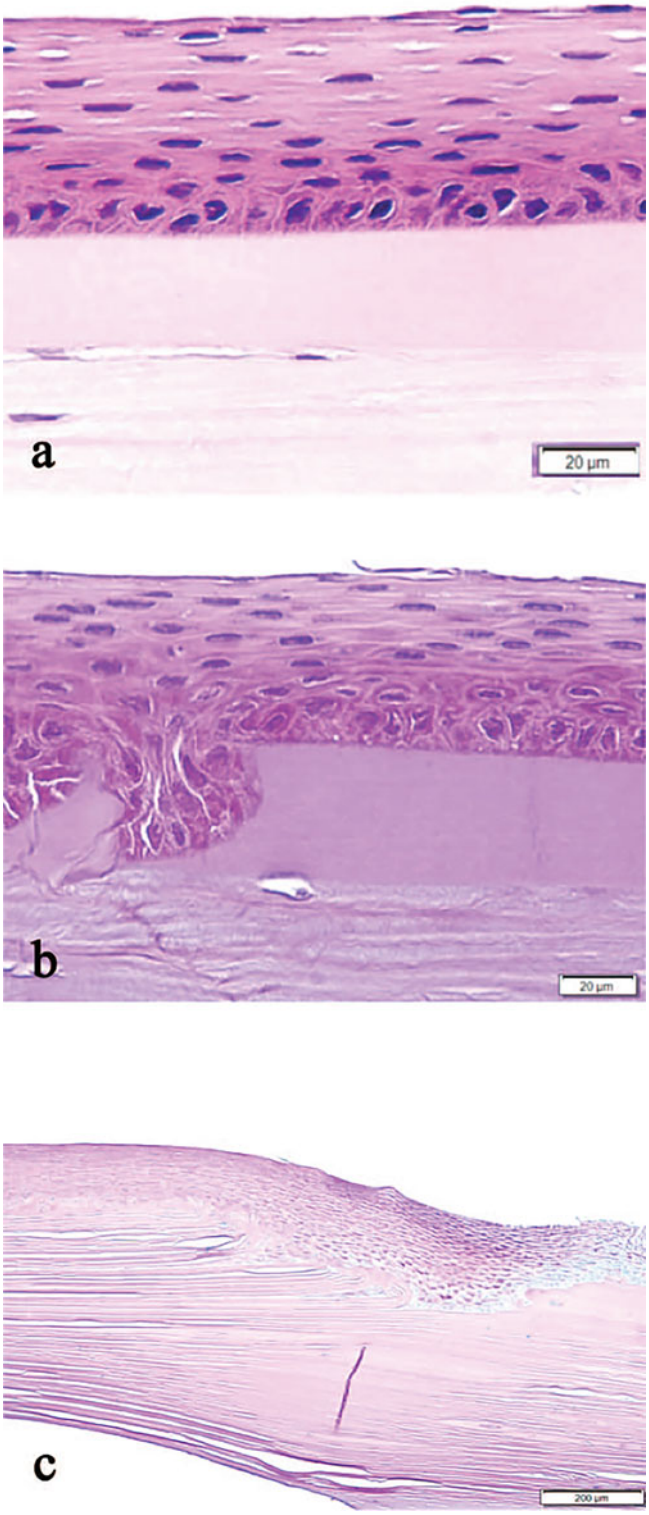

Fig. 31.21 (**a**) Histologic section from a bottlenose dolphin (*Tursiops truncatus*) with a normal cornea. (**b**) Histologic section from a bottlenose dolphin (*Tursiops truncatus*) with horizontal keratopathy. The basal epithelial cells are breaking through and into Bowman's layer. (**c**) Histologic section from a bottlenose dolphin (*Tursiops truncatus*) with horizontal keratopathy. The basal epithelial cells have broken through the entire Bowman's layer and into the anterior stroma.

Horizontal Keratopathy could be somewhat similar and possess a localized immunodeficiency component.

Axial Keratopathy and Horizontal Keratopathy may coexist, suggesting similar risk factors for their initiation and/or their progression as previously discussed. Chronic combination lesions have a smooth surface, variable stromal loss, and often have a rusty or brownish hue (Fig. 31.24). Animals with quiescent lesions do not show clinical signs of pain; however, flare ups will be painful, with lesions demonstrating perilesional diffuse edema with stromal ulceration or abscess formation within or at the edges of the lesion. These repetitive or recurrent lesions may be the result of immune imbalance.

Predisposing factors for Axial Keratopathy are unknown. However, similar to the other keratopathies, imbalances in water quality and excessive exposure to UV radiation are likely risk factors. Like the other keratopathies, the lesions will not completely resolve following treatment, and progression is variable over time. Secondary infections with opportunistic organisms will potentiate the rapidity and severity of corneal damage.

White Spot Keratopathy

There is an unusual keratopathy termed "White Spot Keratopathy" that only occurs in cetaceans living in regions exposed to the Pacific Ocean. This corneal disease is acute in onset; the lesion is initially superficial, white, sharply demarcated, and later deepens to invade the anterior stroma (Fig. 31.25). Many lesions have been diagnosed with a fungal infection; when the white tissue sloughs, the cornea then develops a strong vascular response with diffuse edema and pain. These lesions take a few months to resolve; supportive care includes topical and oral antibiotics, topical antifungals, and pain control.

Traumatic Corneal Lesions

Blunt and sharp trauma to the face, eyelids, and/or cornea commonly occurs as dolphins are very interactive with other animals in their habitat. Corneal lacerations (Fig. 31.26) are uncommon as the eyelids are protective.

Blunt trauma is more likely to cause bruising of the periocular tissues, including the eyelids, and often manifests as acutely closed (blepharospasm), swollen eyelids (blepharoedema) which may be transient or may persist for days to weeks or months. Medical attention should be paid the longer the eyelids remain closed. A bruised eyelid is not always associated with corneal damage (Fig. 31.12a). Like a horse or cow, dolphins have very strong eyelids; it is

Used with permission from: Colitz CM, Walsh MT, McCulloch SD. Characterization Of Anterior Segment Ophthalmologic Lesions Identified In Free-Ranging Dolphins and Those Under Human Care. J Zoo Wildl Med. 2016 Mar;47(1):56–75

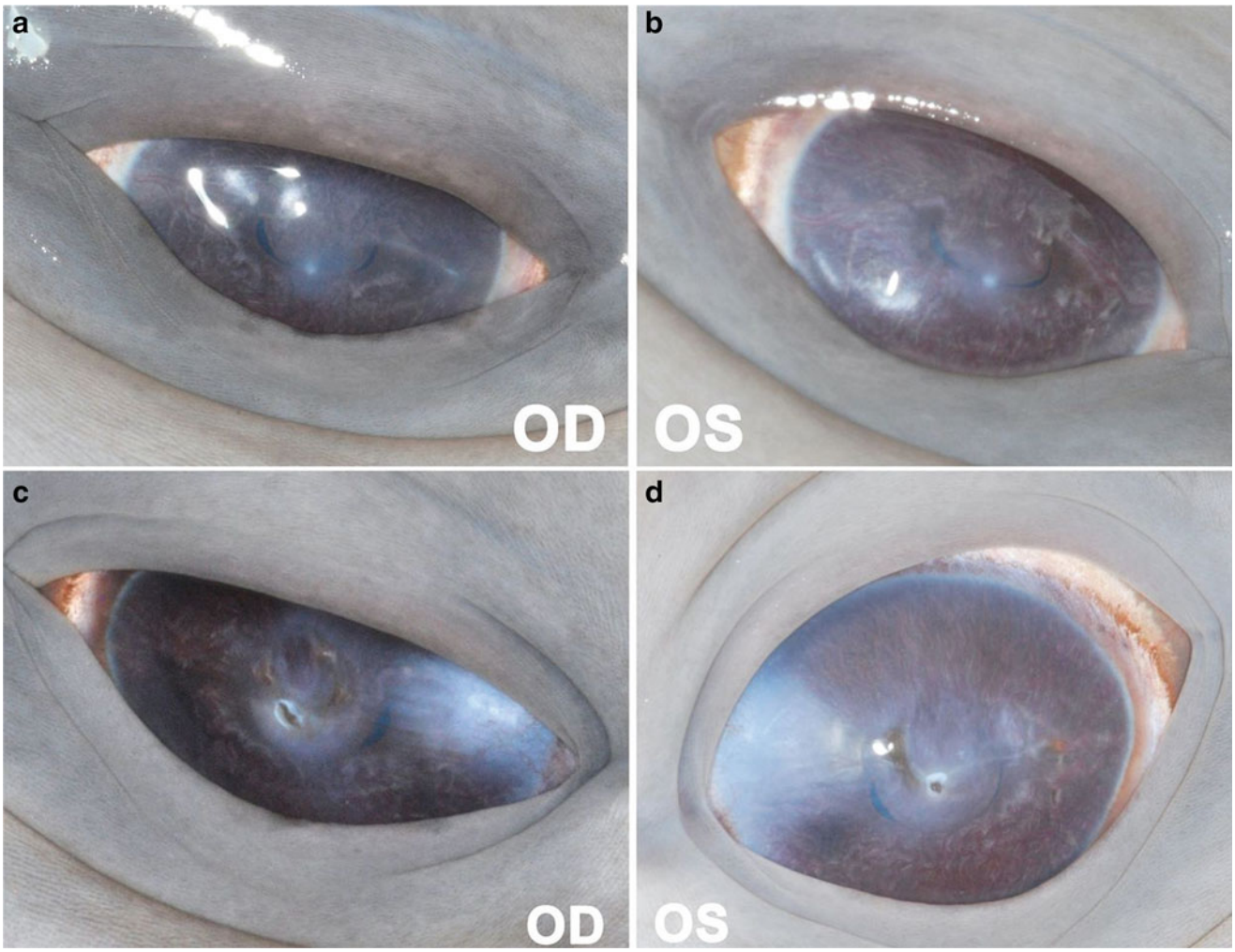

Fig. 31.22 (**a**, **b**) Both eyes of a bottlenose dolphin (*Tursiops truncatus*) with early axial keratopathy. Compare with **c**, **d**, demonstrating both eyes of a bottlenose dolphin with progressing axial keratopathy. The lesions are ulcerated with a dense rim of cellular infiltrates surrounding the ulcers margins. This animal also has moderate medial keratopathy with pigment that has crossed the medial limbus and diffuse edema and fibrosis in the medial corneas. The OD also has stippled pigment in the medial keratopathy lesion as well

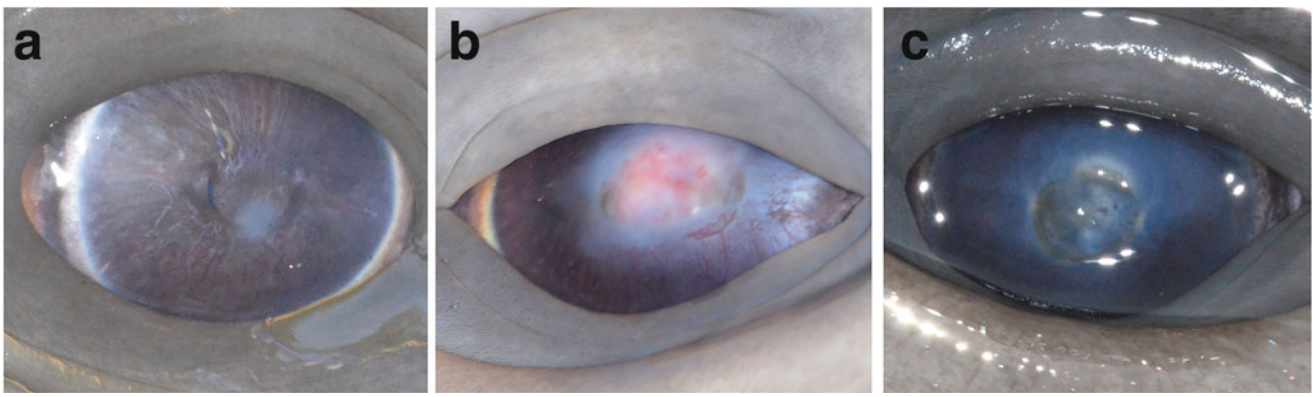

Fig. 31.23 (**a**) Left eye (OS) of a bottlenose dolphin (*Tursiops truncatus*) with early axial keratopathy. (**b**) Right eye (OD) of a bottlenose dolphin (*Tursiops truncatus*) with axial keratopathy that has a vascularized corneal ulcer with cellular infiltrates. There is an ulcerated rim at the medial and ventromedial rim of the ulcer. The vascularized area also has surrounding edema. The medial aspect has pigment that migrated across the limbus and is migrating into the adjacent cornea with associated edema that extends from the ulcer to the medial keratopathy lesion. (**c**) Right eye (OD) of a bottlenose dolphin (*Tursiops truncatus*) with axial keratopathy. There is an axial round gray to off-white opacity with rust colored rim and the axial lesion appears to have stromal loss. The remainder of the cornea has variable diffuse edema

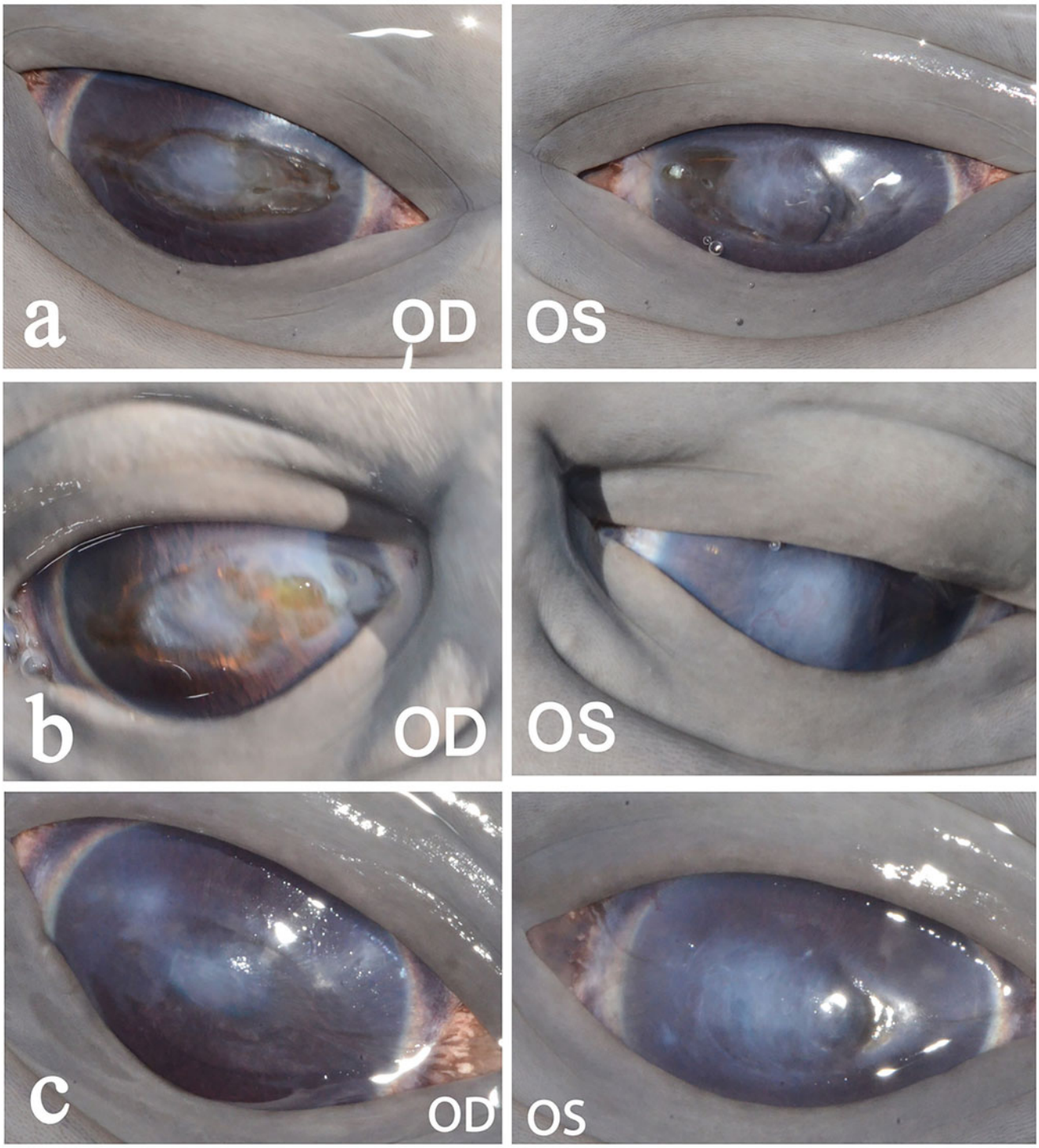

Fig. 31.24 Right (OD) and left (OS) eyes of one bottlenose dolphin (*Tursiops truncatus*) over a 3-year period demonstrating progression of the horizontal and axial keratopathy lesions from year 1 (**a**) to year 2 (**b**). Then, 1 year later, from year 2 (**b**) to year 3 (**c**), after administration of 0.02% tacrolimus drops twice daily. From year 1 to 2, there is visible worsening of the diffuse edema and, in OD, worsening of the irregularity of the rust coloration surrounding the axial opacity. The following year, the corneas are both less edematous and are smoother and appear improved

impossible to examine a dolphin's cornea if the animal will not open their eyelids voluntarily or upon command. Unfortunately, ocular ultrasonography through the closed eyelids cannot diagnose a corneal ulcer. If there is suspicion of a corneal ulcer or laceration being present, the lesion can rapidly become infected with opportunistic organisms (i.e.,

Fig. 31.25 Left eye (OS) of a bottlenose dolphin (*Tursiops* spp.) with white spot keratopathy. There is a dense white irregularly round corneal opacity surrounded by diffuse edema. This most likely has a fungal etiology

bacteria and/or fungi or yeast) and the corneal wound is at risk for progression and corneal perforation. Treatment with either oral ciprofloxacin or enrofloxacin for 5–10 days (i.e., until the eyelids begin to open) in combination with oral doxycycline (4–5 mg/kg BID) can diminish the incidence of severe corneal damage, scarring, and perforation in many dolphins with blepharospasm attributed to a traumatic event. The reason for choosing a quinolone antibiotic is to address *Pseudomonas* spp., which is the most pathogenic bacteria in the environment that causes keratomalacia, which may lead to deep corneal ulcerations and perforation in a matter of hours. The reason for the use of doxycycline is that it inhibits matrix metalloproteinase-9 (MMP9); it also has immunomodulatory, anti-inflammatory, and pro-healing effects (Van Vlem et al. 1996; Ralph 2000; Chandler et al. 2010). MMP9 is an enzyme released by certain bacteria (e.g., *Pseudomonas* and *Beta-streptococcus*), as well as by neutrophils and keratocytes, and is responsible for corneal stromal loss ("corneal melting") (Fukuda et al. 2017). Once the eyelids begin to open allowing visualization of the cornea, then appropriate topical therapy can be tailored to the condition and the oral fluoroquinolone can be discontinued. As mentioned earlier, Horizontal Keratopathy can occur due to the extended use of any of the oral quinolone antibiotics but, in these cases, quinolone use is necessary and always with oral doxycycline (personal observation, Colitz).

Management of Active Keratopathy in Cetaceans

The majority of cetacean keratopathies do not cause discomfort in their quiescent states, though they can rapidly progress depending on environmental factors and secondary infections. When the eye(s) become infected with secondary bacterial, yeast, and/or fungal infections, the animal will demonstrate clinical signs of pain including blepharospasm along with ocular discharge or change in the consistency of the tear film and discharge. Most normal dolphins will have a thick viscous layer of precorneal tear film on the surface of the cornea that usually extends onto the adjacent inferior eyelid. It can be more aqueous in consistency though the cause for this change is not known yet. Severe corneal infections may cause the tear film to have a pale-yellow tinge. When a change in corneal opacification is noticed, the first step is to photograph the eye to compare it to the clinical state prior to the new issue, note the clinical signs, and identify and attempt to correct any environmental factor (s) that may have initiated the flare up. The author suggests putting the animal in a shaded pool area and increase antioxidant support. If an infected corneal ulcer or abscess is also present, then treatment with antibiotics is important to

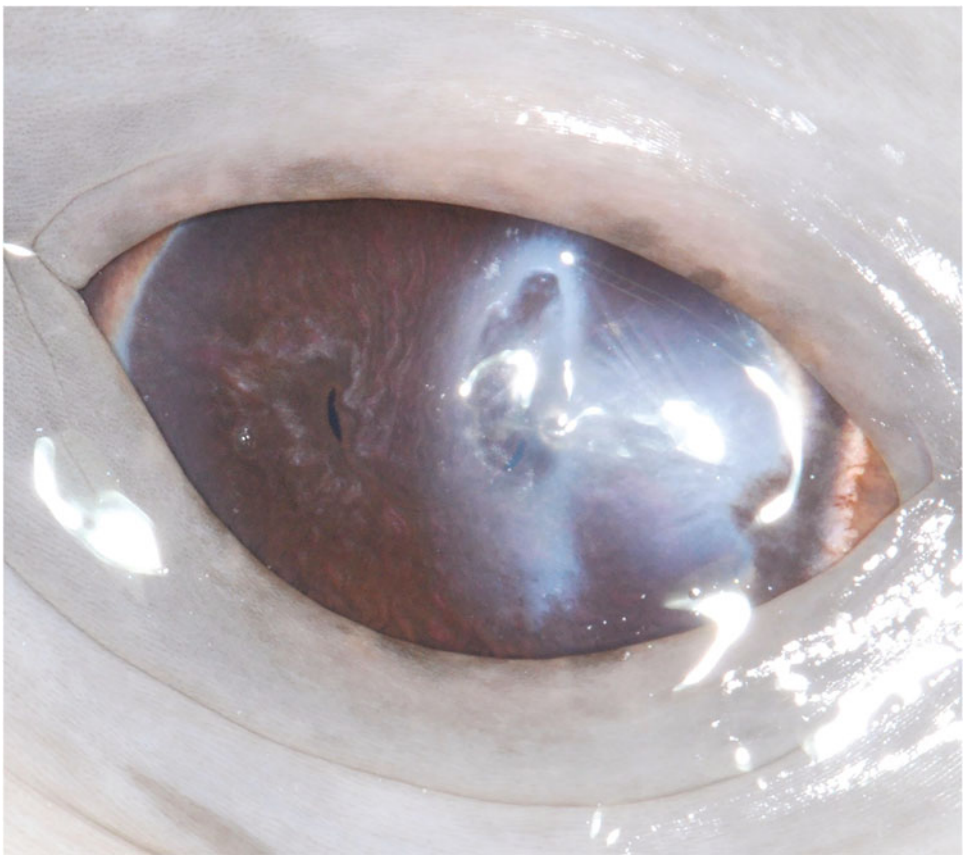

Fig. 31.26 Right eye (OD) of a bottlenose dolphin (*Tursiops* spp.) that had a vertical corneal laceration that has healed. The eye also has medial keratopathy

address the common opportunistic bacteria (e.g., *Pseudomonas* spp. and coliforms), as well as providing pain medications.

Topical ophthalmic solutions may penetrate the tear film better and possibly make the tear film a drug depot if 2–3% (final concentration) of acetylcysteine is added to the topical antibiotic solution or is applied 1 to 2 min prior to applying the latter. The current recommendations for initial treatment of a suspected corneal ulcer or abscess include:

- It is best to try to keep the eye above water for as long as possible. Some animals are trained for up to 2–3 min, and others do not tolerate this length of time in the lateral position. At least 1 to 2 min is advised and more, up to 3–4 min, if possible.
- The use of either topical compounded 0.1% doxycycline (used TID to QID) or oral doxycycline (4–5 mg/kg BID) to aid in healing and provide anti-inflammatory effects (Bahrami et al. 2012; Federici 2011).
- The use of a combination of topical neomycin-polymyxin-gramicidin (aka neopolygram) or trimethoprim-polymyxin ophthalmic solution either used TID to QID along with an aminoglycoside ophthalmic solution such as tobramycin or gentamicin. The combination of neopolygram or trimethoprim/polymyxin addresses the susceptibility spectrum of many coliforms. The aminoglycoside antibiotic addresses *Pseudomonas* spp. This combination is suggested as the first-choice combination arsenal for the common opportunistic and pathologic flora in the aquatic environment. If a fungal and/or yeast infection is suspected (which is less common than bacteria), then treatment with either topical 1% voriconazole or 0.1% terbinafine ophthalmic drops, used TID, have been practical and less expensive than oral fluconazole, voriconazole or terbinafine (Colitz et al. 2018).
- In some cases, a variety of oral antibiotics may be necessary as administration of topical medications may not be possible due to the animal not cooperating. The formulary in the *CRC Handbook of Marine Mammal Medicine*, third Edition, has doses for all medications commonly used in cetaceans. This author has used enrofloxacin, ciprofloxacin, amoxicillin-clavulanic acid, clindamycin, and others.
- Topical nonsteroidal anti-inflammatory drops should be avoided with cases of coreal ulceration and abscesses.
- If possible, collection of corneal cytology and culture samples is suggested. This may not be practical in most cases; therefore, response to therapy may be the only way to monitor progress. Collection of the tear film may provide a suggestive representative sample if there is an excess of a single microorganism and neutrophils.

- Pain control is also important. Oral meloxicam and/or tramadol are most often prescribed for cetaceans, under the guidance of an experienced marine mammal veterinarian.

Management of Quiescent Keratopathy in Cetaceans

Suggested management of medial, temporal, axial, and horizontal keratopathies:

- Lowering the UV index by providing increased shade, painting the pool with natural hues such as tan or sand colors, rather than bright, reflective ones, and/or other strategies.
- Control of water quality parameters, especially salinity, pH, free and total chlorine, ORP, and coliform count.
- Consistent use of UV-protective antioxidants, and antioxidants that increase or regenerate glutathione. See section about antioxidants at the end of this chapter.
- Topical immunomodulating medications; i.e., 0.02% or 0.03% tacrolimus solution applied BID to TID. Many lesions that were consistently treated for months to years had some improvement in lesion size, subjectively (personal observation, Colitz).

As previously mentioned, once lesions are present it is imperative to try to identify and improve the offending environmental factor(s), especially the amount of shade, pool color, and water salinity. The risk factors affecting pinnipeds causing corneal and lens abnormalities are likely the same in cetaceans. Knowing that the lesions will never resolve completely does not mean that management should not be attempted and consistent. The goal should be to slow the progression of the lesions and minimize the risk of secondary infection.

Lens

Cataracts in dolphins are more common than previously thought. They have been reported to have a 16% incidence (Fig. 31.27), but the incidence is likely higher. In most cases, the inability to examine dolphins in dim light conditions makes the diagnosis of incipient or early immature cataracts difficult. Unlike in pinnipeds, cataracts in cetaceans do not typically progress to impair sight and the ability of cetaceans to echolocate may impair the ability of veterinary ophthalmologists to assess their true visual function. Unlike in pinnipeds, lens instability is very rare in cetaceans. This author has diagnosed two dolphins with a unilateral lens luxation (Fig. 31.28). Lensectomy for cataracts that impair sight may be considered in future, as knowledge and experience in cetacean anesthesiology continues to evolve (Colitz et al. 2018).

Glaucoma

Primary or secondary glaucoma has not been reported in any cetacean species. It is interesting to note that their IOPs can be aberrantly elevated if they are positioned on their ventrums for medical procedures. This does not appear to cause clinical issues associated with glaucoma.

Retina

Clinical diagnoses of retinal detachment, retinal hemorrhages, chorioretinitis, or any other retinal diseases have not been reported in any live cetaceans to date. Histologic retinal lesions have been identified in two dolphin eyes with corneal perforations, including retinal detachments (Fig. 31.29).

Ocular Manifestations of Systemic Disease

A systemic storage disease with central photoreceptor atrophy and retinal pigment epithelium lipofuscinosis was diagnosed in a Beluga whale (R.R. Dubielzig personal communication). A systemic mycotic infection in a bottlenose dolphin caused severe pyogranulomatous and lymphoplasmacytic panophthalmitis and orbital cellulitis with suppurative endophthalmitis and orbital fibrinous vascular necrosis and thrombosis (Fig. 31.30). The suspected etiology was *Mucorales* species.

Ophthalmic Surgery

More extensive experience in cetacean anesthesiology has allowed surgical intervention. Surgical procedures common in other species, such as conjunctival grafts and cataract removal, are now a possibility for dolphins.

Nutraceutical Antioxidants

A variety of antioxidants that target the eye have been used for over a decade in marine mammals to alleviate damage from chronic exposure to oxidative stressors, such as sunlight and imbalances in water quality. UV-protective antioxidants

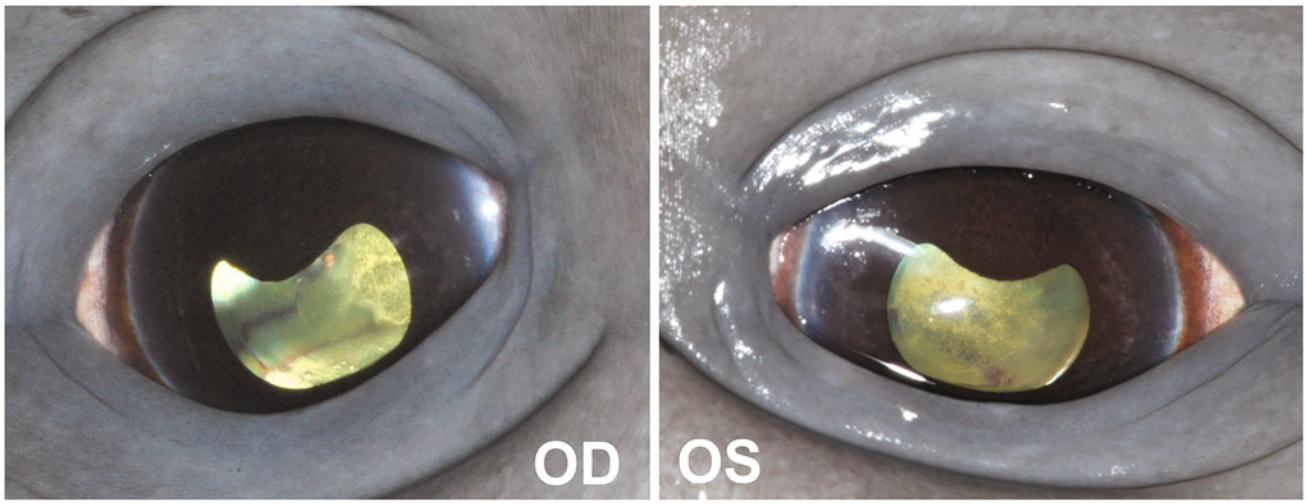

Fig. 31.27 Right (OD) and left (OS) eyes of one bottlenose dolphin (*Tursiops truncatus*) with bilateral posterior cortical incipient cataracts

are supportive for cetacean health; specifically, grapeseed extract, lutein, astaxanthin, milk thistle, and omega-3-fatty acids (Kidd 2011; Yoshihisa et al. 2014; Vaid and Katiyar 2010; Jia et al. 2011; Barden et al. 2008; Chandler and Colitz 2010). Combining these antioxidants (which also have anti-inflammatory properties) with green tea extract (EGCG) is an ideal strategy (Chandler and Colitz 2010; Souyoul et al. 2018; Grether-Beck et al. 2016; Roberts et al. 2009; Qin et al. 2014; Svobodova et al. 2007). Lutein has been shown to selectively accumulate in the lens and retina where it protects against light-induced oxidative damage and aging (Bernstein et al. 2001; Krinsky 2002; Seddon et al. 1994; Mejia-Fava and Colitz 2014; Koutsos et al. 2013). Omega-3 fatty acids (docosahexaenoic acid and eicosapentaenoic acid) protect the retina against phototoxic damage and a variety of other oxidative stressors (Seddon et al. 1994; Yee et al. 2010).

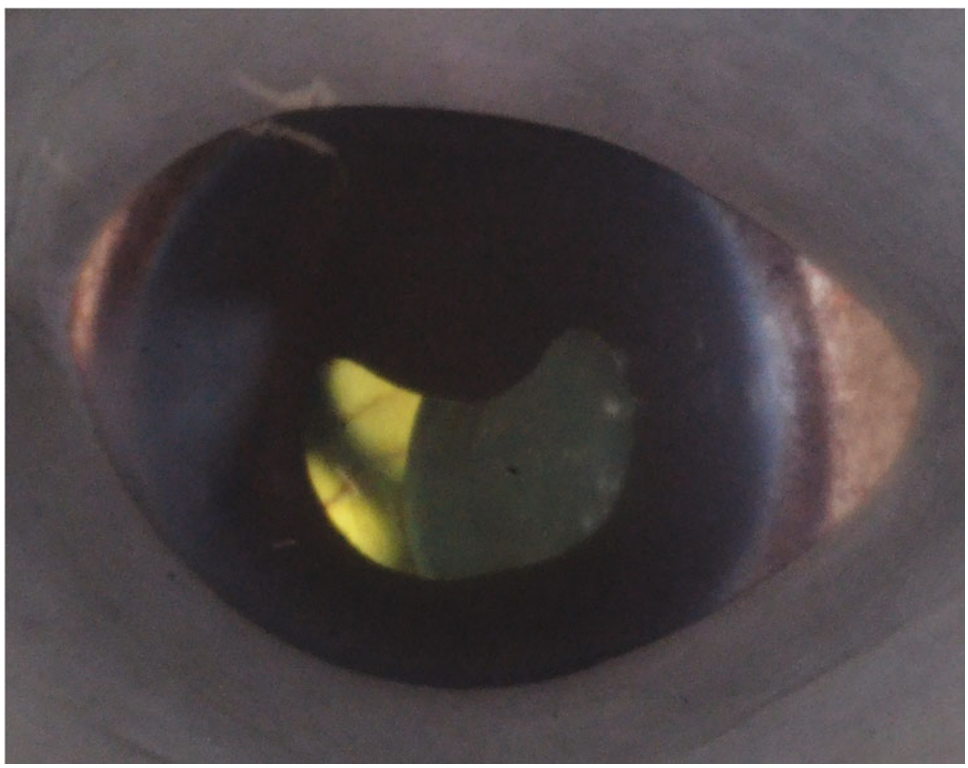

Fig. 31.28 Right (OD) eye of a bottlenose dolphin (*Tursiops truncatus*). In addition to temporal keratopathy, the lens has a few pinpoint incipient cataracts and the lens is subluxated

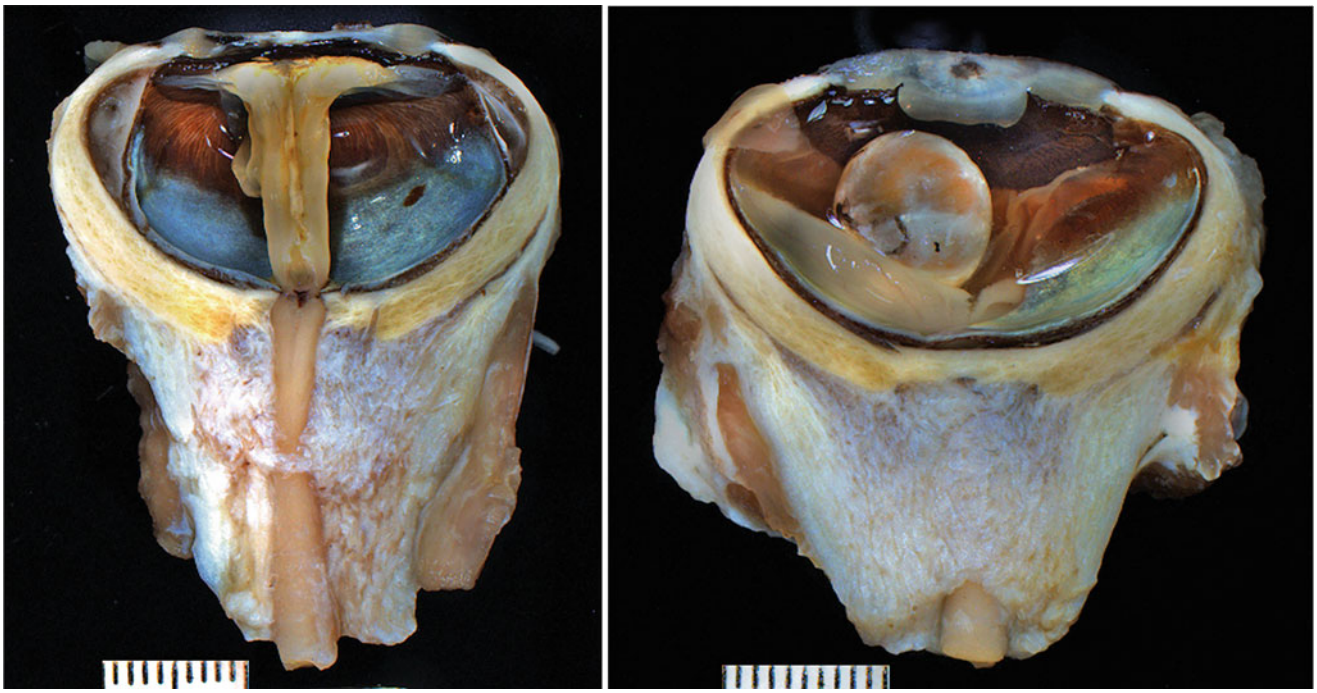

Fig. 31.29 Right (OD) and left (OS) eyes of a 50-year-old bottlenose dolphin (*Tursiops truncatus*) with horizontal keratopathy. Both eyes are phthisical, have retinal detachments, and have anterior and posterior synechia. OS has a posteriorly luxated lens, it is not known if it was luxated antemortem. Images and report courtesy of the Comparative Ocular Pathology Laboratory of Wisconsin (COPLOW)

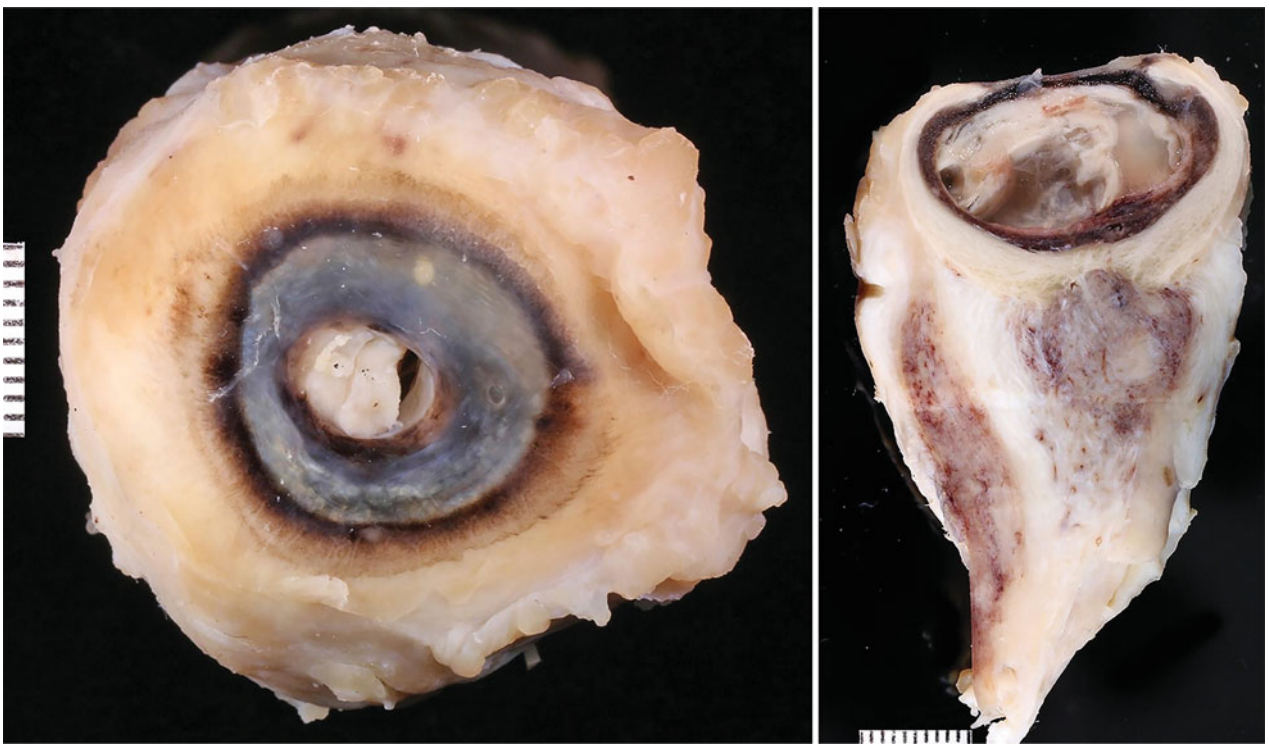

Fig. 31.30 Eye from a 37-year-old bottlenose dolphin (*Tursiops truncatus)* with suspected systemic fungal infection with *Mucorales* fungi. The eye had severe pyogranulomatous and lymphoplasmacytic panophthalmitis and orbital cellulitis with intralesional fungal hyphae. The cornea was perforated and there was suspected loss of the lens through the perforation. Image and report courtesy of Comparative Ocular Pathology Laboratory of Wisconsin (COPLOW)

It is thought that chronic exposure to UV light, disinfectants, and by-products of disinfection continually create damaging free radicals in the skin and on corneal surfaces. These stressors likely disrupt the precorneal tear film, making it less effective at protecting the cornea against bacteria and other damaging factors. The eyes and skin are the most UV-exposed organs of the body. Apoptosis, or programmed cell death, of keratocytes occurs secondary to chronic exposure to free radicals. The cornea is especially susceptible to free radical damage since it absorbs the majority of the UV radiation entering the eye. Chronic exposure to oxidative stress depletes endogenous antioxidants, including glutathione, catalase, and lactate dehydrogenase in the cornea and increases the risk of UV damage, specifically keratocyte loss and stromal degeneration (Newkirk et al. 2007; Cejkova et al. 2000; Lofgren and Soderberg 2001). UVB exposure to rabbit corneas decreased Na+-K+-dependent ATPase in the epithelium, then the endothelium resulting in edema (Cejkova and Lojda 1995). In addition to diminishing the exposure to exogenous oxidative stress by improving shade structures and balancing the water quality as much as possible, the consistent intake of antioxidants may contribute to protecting the cornea against oxidative stress, regenerating reduced glutathione, and others.

References

Bahrami F, Morris DL, Pourgholami MH (2012) Tetracyclines: drugs with huge therapeutic potential. Mini Rev Med Chem 12:44–52

Barden CA, Chandler HL, Lu P, Bomser JA, Colitz CMH (2008) The effect of grape polyphenols on oxidative stress in canine lens epithelial cells. Am J Vet Res 69:94–100

Beck RMD, Bininda-Emonds ORP, Cardillo M et al (2006) A higher-level MRP supertree of placental mammals. BMC Evol Biol 6:93

Bernstein PS, Khachik F, Carvalho LS, Muir GJ, Zhao DY, Katz NB (2001) Identification and quantification of carotenoids and their metabolites in the tissues of the human eye. Exp Eye Res 72:215–223

Bjerager P, Heengaard S, Tougaard J (2003) Anatomy of the eye of the sperm whale (*Physeter macroephalus L.*). Aquat Mammals 29:31–36

Bolk L, Goppert E, Kallius E, Lubosch W (1934) Handbuch der vergleichenden Anatomie der Wirbeltiere. Jena

Cejkova J, Lojda Z (1995) Histochemical study on xanthine oxidase activity in the normal rabbit cornea and after repeated irradiation of the eye with UVB rays. Acta Histochem 98:47–52

Cejkova J, Stipek S, Crkovska J, Ardan T (2000) Changes of antioxidant enzymes in the cornea of albino rabbits irradiated with UVB rays. Histol Histopathol 15:1043–1050

Chandler HL, Colitz CMH (2010) Protection of canine lens epithelial cells from ultraviolet radiation induced apoptosis with grape seed extract. In: 41st Annual Meeting of the American College of Veterinary Ophthalmologists, San Diego, CA, p 422

Chandler HL, Gemensky-Metzler AJ, Bras ID, Robbin-Webb TE, Saville WJA, Colitz CMH (2010) In vivo effects of adjunctive tetracycline treatment on refractory corneal ulcers in dogs. J Am Vet Med Assoc 237:378–386

Coimbra JP, Bertelsen MF, Manger PR (2017) Retinal ganglion cell topography and spatial resolving power in the river hippopotamus (Hippopotamus amphibius). J Comp Neurol 525(11):2499–2513

Colitz CMH (2012) Preliminary intraocular pressure measurements from 4 Cetacean species. Paper presented at the 43rd Annual International Association for Aquatic Animal Medicine Conference

Colitz CMH, Sessler RJ, Green-Church K, Renner MS, Rodriguez MM, Chandler HL, Newkirk K, Nichols KK, Nichols JJ (2007) Tear film analysis of *Orcinus orca*. Vet Ophthalmol 10:411

Colitz CMH, Dubielzig RR, Kelleher Davis R (2012) Horizontal keratopathy in dolphins analogous to keratoconus in humans. Paper presented at the Annual Conference of the Association for Reserach in Vision and Ophthalmology, Fort Lauderdale, May 6, 2012

Colitz CMH, Walsh MT, McCulloch SD (2016) Characterization of anterior segment ophthalmologic lesions identified in free-ranging dolphins and those under human care. J Zoo Wildl Med 47(1):56–75

Colitz CMH, Bailey JE, Mejia-Fava JC (2018) Cetacean and pinniped ophthalmology. In: Dierauf L, Gulland FMD (eds) CRC handbook of marine mammal medicine, 3rd edn. CRC Press Taylor & Francis Group, pp 517–536

Coroneo MT, Muller-Stolzenburg NW, Ho A (1991) Peripheral light focusing by the anterior eye and the ophthalmohelioses. Ophthalmic Surg 22:705–711

Dawson DD (1980) The cetacean eye. In: Harman LM (ed) Cetacean behavior: mechanism and function. John Wiley and Sons, New York, pp 53–100

Dawson WW, Perez JM (1973) Unusual retinal cells in the dolphin eye. Science 181:747–749

Dawson WW, Hawthorne MN, Jenkins RL, Goldston RT (1982) Giant neural system in the inner retina and optic nerve of small whales. J Comp Neurol 205:1–7

Dawson WW, Hope GM, Ulshafer RJ, Hawthorne MN, Jenkins RL (1983) Contents of the optic nerve of a small cetacean. Aquat Mammal 10(2):45–56

Dawson WW, Schroeder JP, Dawson JC, Nachtigall PE (1992) Cyclic ocular hypertension in cetaceans. Mar Mamm Sci 8:135–142

Dral ADG (1972) Aquatic and aerial vision in the bottle-nose dolphin. Neth J Sea Res 5:510–513

Dral ADG (1977) On the retinal anatomy of cetacea (mainly Tursiops truncatus). In: Harrison RJ (ed) Functional anatomy of marine mammals. Academic, London, pp 81–134

Duke-Elder S (1958) The eye in evolution. In: Duke-Elder S (ed) System ophthalmology. Mosby Company, St. Louis, p 902

Duncan M, Grahn B, Wilcock B, Boermans H, Johnson L, Smith D (1994) Pheochromocytoma associated with hypertensive lesions in a river hippopotamus (Hippopotamus amphibius). J Zoo Wildl Med 25(4):575–579

Eltringham SK (1999) The hippos. Academic Press, London

Encyclopedia of Marine Mammals (2008) 2 edn. Academic Press

Estes R (1992) The behavior guide to African mammals: including hoofed mammals, carnivores, primates. University of California Press, Los Angeles

Fasick JI, Robinson PR (1998) Mechanism of spectral tuning in the dolphin visual pigments. Biochemist 37:433–438

Fasick JI, Robinson PR (2000) Spectral-tuning mechanisms of marine mammal rhodopsins and correlations with foraging depth. Vis Neurosci 17(5):781–788

Federici TJ (2011) The non-antibiotic properties of tetracyclines: clinical potential in ophthalmic disease. Pharmacol Res 64:611–623

Fisher RE, Scott KM, Naples VL (2007) Forelimb myology of the pygmy hippopotamus (Choeropsis liberiensis). Anat Rec 290:673–693

Fukada Y, Stone J (1974) Retinal distribution and central projection of W,X, and Y cells of the cat's retina. J Neurophysiol 37:749–772

Fukuda K, Ishida W, Fukushima A, Nishida T (2017) Corneal fibroblasts as sentinel cells and local immune modulators in infectious keratitis. Int J Mol Sci 18(9):E1831
Gatesy J (1997) More DNA support for a Cetacea/Hippopotamidae clade: the blood-clotting protein gene gamma-fibrinogen. Mol Biol Evol 14:537–543
Geisler JH, Uhen MD (2005) Phylogenetic relationships of extinct cetartiodactyls: results of simultaneous analyses of molecular, morphological, and stratigraphic data. J Mam Evol 12:145
Grether-Beck S, Marini A, Jaenicke T, Stahl W, Krutmann J (2016) Molecular evidence that oral supplementation with lycopene or lutein protects human skin against ultraviolet radiation: results from a double-blinded, placebo-controlled, crossover study. Br J Dermatol 176:1231–1240
Hebel R, Hollander H (1979) Size and distribution of ganglion cells in the bovine retina. Vis Res 19:667–674
Hegner B, Pilleri G (1968) Eye morphology of Hippopotamus amphibius and Choeropsis liberiensis (Mammalia Artiodactyla Hippopotamidae) under various aspects of tapetum lucidum fibrosum and Schlemms canal. Acta Anat 69:458–461
Jia Z, Song Z, Zhao Y, Wang X, Liu P (2011) Grape seed proanthocyanidin extract protects human lens epithelial cells from oxidative stress via reducing NF-κB and MAPK protein expression. Mol Vis 17:210–217
Kelleher Davis R, Argueso P (2014) Composition of terrestrial and marine mammal tears is dependent on species and environment. In: ARVO Annual Meeting, p 36
Kelleher Davis R, Argueso P (2015) Antimicrobial activity detected in ocular and salivary secretions from marine mammals. In: Association for research in vision ophthalmology, Denver, Colorado
Kelleher Davis R, Sullivan DA (2009) What provides stability to the marine mammal tear film? In: ARVO Annual Meeting, p 4251
Kidd P (2011) Astaxanthin, cell membrane nutrient with diverse clinical benefits and anti-aging potential. Altern Med Rev 16(4):355–364
Klećkowska-Nawrot JE, Goździewska-Harłajczuk K, Paszta W (2021) Gross anatomy, histological, and histochemical analysis of the eyelids and orbital glands of the neonate pygmy hippopotamus (Suina: Choeropsis liberiensis or Hexaprotodon liberiensis, Morton 1849) with reference to its habitat. Anat Rec (Hoboken) 304(2): 437–455
Koutsos EA, Schmitt T, Colitz CMH, Mazzaro L (2013) Absorption and ocular deposition of dietary lutein in marine mammals. Zoo Biol 32:316–323
Krinsky NI (2002) Possible biological mechanisms for a protective role of xanthophylls. J Nutr 132:540S–542S
Kroger RH, Kirschfeld K (1989) Accomodation in the bottlenosed dolphin (*Tursiops truncatus*). Paper presented at the Fifth International Theriol Congr, Rome
Kroger RH, Kirschfeld K (1993) Optics of the harbor porpoise eye in water. J Opt Soc Am A 10(7):1481–1489
Kroger RH, Kirschfeld K (1994) Refractive index in the cornea of a harbor porpoise (*Phocoena phocoena)* measured by two-wavelengths laser inferometry. Aquat Mammal 20:99–107
Levenson DH, Ponganis PJ, Crognale MA, Deegan JF, Dizon A, Jacobs GH (2006) Visual pigments of marine carnivores: pinnipeds, polar bear, and sea otter. J Comp Physiol A 192:833–843
Lewison R, Pluháček J (2017) Hippopotamus amphibius. The IUCN Red List of Threatened Species 2017: e.T10103A18567364. https://doi.org/10.2305/IUCN.UK.2017-2.RLTS.T10103A18567364.en. Downloaded on 17 June 2021
Lilly J (1964) Animals in aquatic environment: adaptation of mammals to the ocean. In: Handbook of physiology: adaptation to the environment, vol 1. Am Physiol Soc, Washington, pp 741–747
Lofgren S, Soderberg PG (2001) Lens lactate dehydrogenase inactivation after UV-B irradiation: an in vivo measure of UVB penetration. Invest Ophthalmol Vis Sci 42:1833–1836
Lucy KM, Indu VR, Leena C, Fathima R, George C, Patki HS, Surjith S, Anneth AJ (2018) Gross anatomy of the skull of hippopotamus (Hippopotamus amphibius) Indian J. Anim Res 52(5):793–795
Mass AM, Supin AY (1995a) Ganglion cell topography of the retina in the bottlenose dolphin, Tursiops truncatus. Brain Behav Evol 45: 257–265
Mass AM, Supin AY (1995b) Retinal resolution in the bottlenose dolphin (Tursiops truncatus). In: Kastelein RA, Thomas JA, Nachtigall PA (eds) Sensory systems of aquatic mammals. De Spil, The Netherlands, pp 419–428
Mass AM, Supin AY (2007) Adaptive features of aquatic Mammals' eye. Anat Rec 290:701–715
Maust-Mohl M, Reiss D, Reidenberg JS (2019) A comparison of common hippopotamus (Artiodactyla) and Mysticete (Cetacea) nostrils: an open and shut case. Anat Rec (Hoboken) 302(5):693–702
McCormick JG (1969) Relationship of sleep, respiration and anesthesia in the porpoise: a preliminary report. Proc Natl Acad Sci U S A 62: 697–703
Mejia-Fava J, Colitz CMH (2014) Supplements for exotic pets. Vet Clin North Am Exot Anim Pract 17(3):503–525. https://doi.org/10.1016/j.cvex.2014.05.001
Miller S, Samuelson D, Dubielzig R (2013) Anatomic features of the cetacean globe. Vet Ophthalmol 16(Suppl):52–63
Miller SN, Colitz CMH, Dubielzig RR (2010) Anatomy of the California Sea lion globe. Vet Ophthalmol 13(Suppl 1):63–71
Murayama T, Somiya H, Aoki I, Ishii T (1995) Retinal ganglion cell size and distribution predict visual capabilities of Dall's porpoise. Mar Mamm Sci 11:136–149
Newkirk KM, Chandler HC, Parent AE, Young DC, Colitz CM, Wilkie DA, Kusewitt DF (2007) Ultraviolet radiation-induced corneal degeneration in 129 mice. Toxicol Pathol 35(6):819–826
Newman LA, Robinson PR (2005) Cone visual pigments of aquatic mammals. Vis Neurosci 22:873–879
Ninomiya H, Imamura E, Inomata T (2014) Comparative anatomy of the ophthalmic rete and its relationship to ocular blood flow in three species of marine mammal. Vet Ophthalmol 17(2):100–105
Norris KS (1969) The echolocation of marine mammals. In: Anderson HJ (ed) The biology of marine mammals. Academic, New York, pp 391–424
Peichl L, Moutairou K (1998) Absence of short-wavelength sensitive cones in the retinae of seals (Carnivora) and African giant rats (Rodentia). Eur J Neurosci 10:2586–2594
Peichl L, Berhmann G, Kroger RHH (2001) For whales and seals the ocean is not blue: a visual pigment loss in marine mammals. Eur J Neurosci 13(1520–1528)
Perez JM, Dawson WW, Landau D (1972) Retinal anatomy of the bottlenosed dolphin (Tursiops truncatus). Cetology 11:1–11
Prince JH (1956) Comparative anatomy of the eye. Charles C Thomas, Springfield
Prince JH, Diesen CD, Eglitis I (1960) Anatomy and histology of the eye and orbit in domestic animals. Charles, C. Thomas, Springfield, IL
Pushkina D (2007) The Pleistocene easternmost distribution in Eurasia of the species associated with the Eemian Palaeoloxodon antiquus assemblage. Mammal Rev 37(3):224–245
Qin YJ, Chu KO, Yip YW, Li WY, Yang YP, Chan KP, Ren JL, Chan SO, Pang CP (2014) Green tea extract treatment alleviates ocular inflammation in a rat model of endotoxin-induced uveitis. PLoS One 9(8):e103995
Ralph RA (2000) Tetracyclines and the treatment of corneal stromal ulceration: a review. Cornea 19:274–277
Rehorek SJ, Hillenius WJ, Lovano DM, Thewissen JGM (2017) Ontogeny of the orbital glands and their environs in the pantropical spotted dolphin (Stenella attenuata:Delphinidae). Dev Biol 301(1):77–87
Rivamonte A (1976) Eye model to account for comparable aerial and underwater acuities of the bottlenose dolphin. Neth J Sea Res 10: 491–498

Roberts RL, Green J, Lewis B (2009) Lutein and zeaxanthin in eye and skin health. Clin Dermatol 27:195–201

Rubtsova NY, Heckmann RA, Smit WJ, Luus-Powell WJ, Halajian A, Roux F (2018) Morphological studies of developmental stages of Oculotrema hippopotami (Monogenea: Polystomatidae) infecting the eye of Hippopotamus amphibius (Mammalia: Hippopotamidae) using SEM and EDXA with notes on histopathology. Korean J Parasitol 56(5):463–475

Samuelson DA, Ganesh KC, Miles SM, Zivotofsky AZ, Zivotofsky D Lewis PA (2005) Morphology and histochemistry of Bowmans' layer in selected vertebrates. In: ARVO Annual Meeting, p 2181

Seddon JM, Christen WG, Manson JE, Lamotte FS, Glynn RJ, Buring JE, Hennekens CH (1994) The use of vitamin supplements and risk of cataract among US male physicians. Am J Public Health 84:788–792

Souyoul SA, Saussy KP, Lupo MP (2018) Nutraceuticals: a review. Dermatol Ther (Heidelberg) 8:5–16

Stevenson-Hamilton J (1912) Animal life in Africa. E.P. Dutton and Company, New York

Stroman HR, Slaughter LM (January 1972) The care and breeding of the Pygmy hippopotamus (Choeropsis liberiensis) in captivity. Int Zoo Yearb 12(1):126–131

Supin AY, Popov VV, Mass AM (2001) Vision in aquatic mammals. In: The sensory physiology of aquatic mammals. Kluwer Academic Publishers, Boston, pp 229–284

Svobodova A, Zdarilova A, Maliskova J, Mikulkova H, Walterova D, Vostalova J (2007) Attenuation of UVA-induced damage to human keratinocytes by silymarin. J Dermatol Sci 46:21–30

Tarpley RL, Ridgway SH (1991) Orbital gland structure and secretions in the Atlantic bottlenose dolphin (Tursiops truncatus). J Morphol 207(2):173–184

Tarpley RL, Gelderd JB, Bauserman S, Ridgway SH (1994) Dolphin peripheral visual pathway in chronic unilateral ocular atrophy: complete decussation apparent. J Morphol 222:91–102

Thewissen JGM, Cooper LN, Clementz MT et al (2007) Whales originated from aquatic artiodactyls in the Eocene epoch of India. Nature 450:1190–1194

Tinsley RC (2013) The oncomiracidium of Oculotrema hippopotami Stunkard, 1924 and relationships within the Polystomatidae (Monogenea). Syst Parasitol 84(2):123–135

Tsagkogeorga G, McGowen MR, Davies KTJ et al (2015) A phylogenomic analysis of the role and timing of molecular adaptation in the aquatic transition of cetartiodactyl mammals. Royal Soc Open Sci 2:150156

Vaid M, Katiyar N (2010) Molecular mechanisms of inhibition of photocarcinogenesis by silymarin, a phytochemical from milk thistle (Silybum marianum L. Gaertn.) (review). Int J Oncol 36(5): 1053–1060

Van Vlem B, Vanholder R, De Paepe P, Vogelaers D, Ringoir S (1996) Immunomodulating effects of antibiotics: literature review. Infection 24(4):275–291

Waddell PJ, Okada N, Hasegawa M (1999) Towards resolving the interordinal relationships of placental mammals. Syst Biol 48:1–5

Waller G (1984) The ocular anatomy of cetacea: an historical perspective. In: Pilleri GV (ed) Investigation of cetacea, vol XVI. pp 138–148

Waller GH, Harrison RJ (1978) The significance of eyelid glands in delphinids. Aquat Mammal 6:1–9

Walls GL (1942) The vertebrate eye and its adaptive radiation. Cranbrook Institute of Science, Oxford

West JA, Sivak JG, Murphy CJ, Kovacs KM (1991) A comparative study of the anatomy of the iris and ciliary body in aquatic mammals. Can J Zool 69:2594–2607

Yee P, Weymouth AE, Fletcher EL, Vingreys AJ (2010) A role for omega-3 polyunsaturated fatty acid supplements in diabetic neuropathy. Invest Ophthalmol Vis Sci 51:1755–1764

Yoshihisa Y, Rehman MU, Shimizu T (2014) Astaxanthin, a xanthophyll carotenoid, inhibits ultraviolet-induced apoptosis in keratinocytes. Exp Dermatol 23(3):178–183

Young NM (1984) The ocular secretions of the bottlenosed dolphin Tursiops truncatus. PhD, University of Florida

Young NM, Hope GM, Dawson WW (1988) The tapetum fibrosum in the eyes of two small whales. Mar Mamm Sci 4:281–299

Zorić Z, Lozanče O, Marinković D, Blagojević M, Nešić I, Demus N and Đorđević M (2018) Skull bone anatomy of the young common Hippopotamus (Hippopotamus Amphibius). Acta Vet 68(3): 361–372

Ophthalmology of Ruminantia: Giraffe, Deer, Wildebeests, Gazelles, and Relatives

32

Caryn E. Plummer and Eric C. Ledbetter

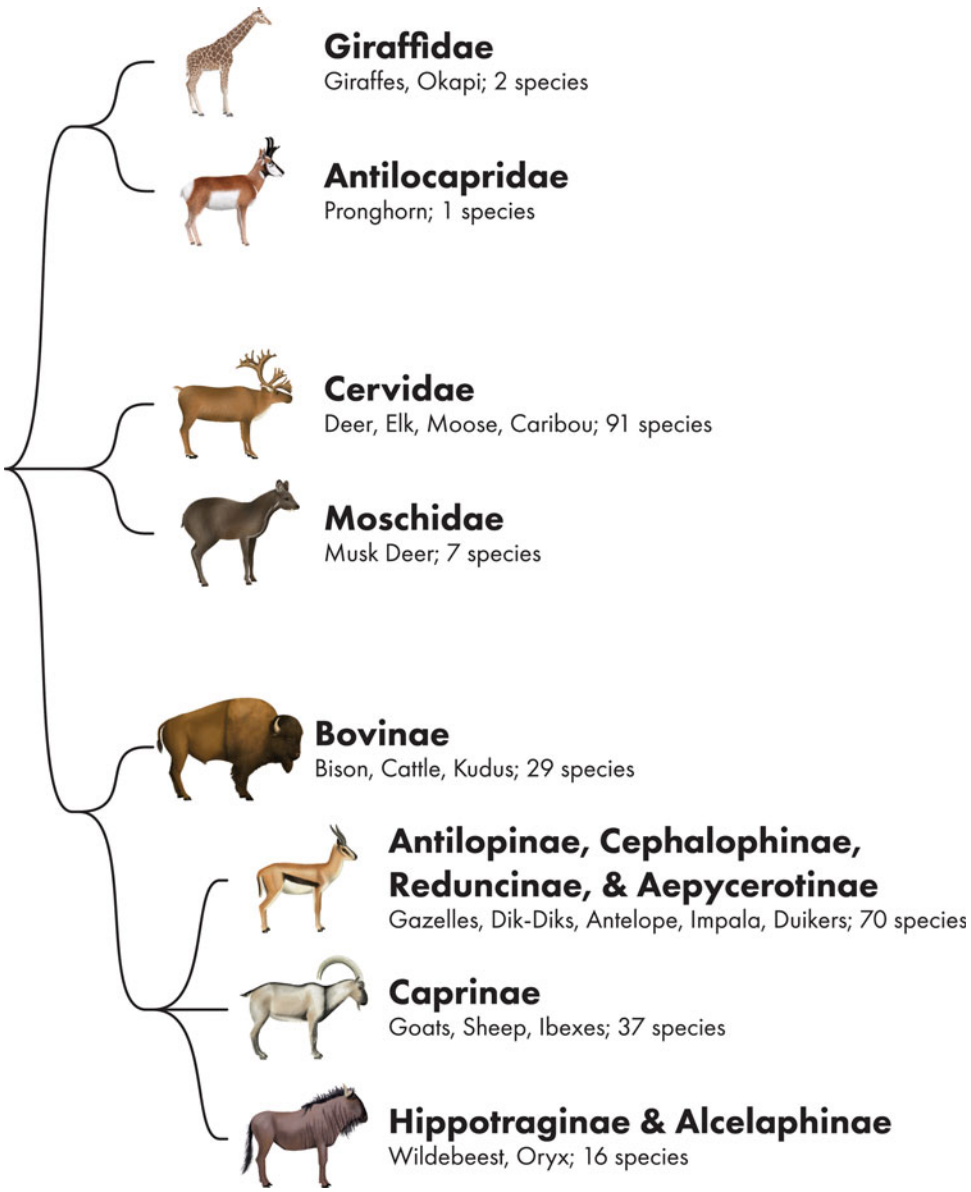

© Chrisoula Skouritakis

C. E. Plummer (✉)
Departments of Small and Large Animal Clinical Sciences, College of Veterinary Medicine, University of Florida, Gainesville, FL, USA
e-mail: plummerc@ufl.edu

E. C. Ledbetter
Department of Clinical Sciences, Cornell University College of Veterinary Medicine, Ithaca, NY, USA
e-mail: ecl32@cornell.edu

F. Montiani-Ferreira et al. (eds.), *Wild and Exotic Animal Ophthalmology*, https://doi.org/10.1007/978-3-030-81273-7_7

Introduction

Ruminantia is a clade of even-toed hoofed mammals with ruminant digestion, within the order Artiodactyla (Flower 1883), and includes two infraorders: Pecora and Tragulina. Chevrotains are the only extant members of Tragulina and due to lack of information about the ocular system of chevrotains, this chapter will focus on the infraorder Pecora. The Pecora, often referred to as horned livestock, include the Superfamilies Giraffidea, Cervoidae, and Bovidae. Defining characteristics of these species include a four-chambered stomach and a paraxonic foot that supports the animal's body weight on the third and fourth digits of the hoof (Flower 1883). Most Pecora have a distinguishing cranial appendage projecting from the frontal bones of the skull (Bubenik 1990). Modern Pecora have one of four types of cranial appendages: horns (cattle, sheep, goats, and antelope), antlers (Cervidae—deer and moose), ossicones (Giraffidae—giraffe and okapi), or pronghorns (Pronghorn antelope, *Antilocapra americana*, the only extant species with pronghorns) (Janis and Scott 1987; Gomez et al. 2019). The exceptions, members of the genus *Hydropotes* (water deer) and *Moschus* (musk deer), instead have long, saber-like teeth, or tusks instead of a cranial appendage (Gomez et al. 2019). Although varied, the eyes and adnexa of this exotic hoofstock have many characteristics in common with their domestic counterparts, although their susceptibility to certain infections may differ. Ocular surface disease, especially infectious keratoconjunctivitis, and uveal inflammation associated with systemic disease account for most ophthalmic disease in these animals.

Ophthalmic Anatomy and Physiology

While diversity can be found among the ocular structures of these species, the general anatomy of the pecoran eye shares much in common with other ungulate orders. As herbivorous mammals, Pecora species have relatively deep orbits with complete bony orbital rims. The enclosed, or complete, orbit provides protection to the globe and reinforcement of the skull during interactions with predators or during intraspecies dominance rituals. The orbits in most of these species are positioned laterally on the skull, which increases the monocular peripheral field of view and improves the ability to detect danger in the environment and scout for foraging opportunities. Most Pecora have large globes with prominent corneas, variably pigmented uveal tracts, horizontally elongated pupillary apertures (many with corpora nigra extensions along the pupil margins), and holangiotic retinal vasculature patterns. Most possess a tapetum lucidum.

Few studies exist comparing the unique characteristics of the orbital and ocular anatomy of wild hoofstock to each other or their domestic counterparts. A few examples of documented distinctions are noted below.

Orbit and Adnexa

Terrestrial artiodactyls inhabit some of the world's most extreme environments, including arid deserts and high elevations. As medium-to-large-bodied mammals, these even-toed ungulates have a variety of specialized physiologies that facilitate occupation of their ecosystems. Nearly all living artiodactyls possess a derived cranial arterial pattern that is highly distinctive from most other mammals. The majority of arterial blood entering the intracranial cavity is supplied by a large arterial meshwork called the carotid rete, which replaces the internal carotid artery. This interdigitating network branches from the maxillary artery and is housed within the cavernous venous sinus. As the cavernous sinus receives cooled blood draining from the nasal mucosa, heat rapidly dissipates across the high surface area of the rete to be carried away from the brain by the venous system (O'Brien et al. 2016). Extensive experimentation has demonstrated that the artiodactyl carotid rete drives one of the most effective selective brain cooling mechanisms among terrestrial vertebrates. This rete system does not, however, function in resistance or blood pressure mitigation in the few species studied (domestic goats *Capra hircus* and giraffe *Giraffa camelopardalis*) (O'Brien and Bourke 2015); the use of selective brain cooling contributes to the conservation of body water (Strauss et al. 2016).

Some artiodactyls also possess an orbital rete, a flat, triangular- or leaf-shaped arterial network, which consists of a complex of small arterioles that intermixes with a similar complex of the supraorbital vein at the base of the orbital cavity. Blood to the retina passes through the orbital rete. The orbital retinal arterioles leave the parent external ophthalmic artery at right angles forming T-shaped bifurcations, and follow a tortuous, undulating course. Each retinal arteriole is connected by side branches and forms a rope-ladder-like network. Some of the side branches are surrounded by a groove representing the intra-arterial cushion that regulates blood flow at branching sites. The central retinal artery supplying the retina originates from the orbital rete. The ciliary arteries supplying the choroid arise from the external ophthalmic artery proximal to the orbital rete. The anatomical specializations of the orbital rete may involve buffering the blood pressure and flow to the retina and regulating ocular tissue temperature as in the carotid rete. In addition, the orbital rete may help dampen the tension that the vessel exerts on the retina, by stretching in response to eyeball movement. This structure has been best described in the Japanese deer (*Cervus nippon*) (Ninomiya and Masui 1999).

The pronghorn (*Antilocapra Americana)* possesses a carotid rete with greater density and smaller caliber vessels overall and a more highly vascular orbital rete compared to the elk (*Cervus canadensis*) and the deer (*Odocoileus virginianus*). These anatomical differences may indicate differences in efficiency of heat exchange in the retina. It has been suggested that the orbital rete is anatomically in a position to moderate extremes of temperature by cooling arterial blood flowing specifically to the eyes and olfactory bulbs (Carlton and McKean 1977).

The nictitans and the Harderian glands are located in the anterior and inferior aspects of the orbit. They function to support and protect the globe. They were traditionally thought to be fundamentally distinct glands, however, recently they have been shown in the Chinese muntjac deer (*Muntiacus reevesi*) and the fallow deer (*Dama dama*) to be two different lobes of a single, heterogeneously developed gland, the anterior orbital gland (Rehorek et al. 2007); it is not known if this is the case for other Pecoran species. A few species have had light microscopic descriptions of these accessory glands. In the okapi (*Okapia johnstoni)*, the superficial gland of the third eyelid and lacrimal gland are complexly branched multilobar tubular glands formed by mucous units with tubular secretory portions and no plasma cells. The deep gland of the third eyelid (Harderian) was absent in the okapi and present in the Père David's deer (*Elaphurus davidianus)*. Organized lymphoid follicles are present within the upper and lower eyelids in the okapi and Père David's deer. The orbital glands in the Père David's deer had a multilobar tubuloacinar structure with numerous plasma cells and a mucoserous character (Klećkowska-Nawrot et al. 2019).

The lacrimal glands and tears of domestic cattle contain lactoferrin, which plays an important role in the health of the ocular surface through its antimicrobial action and anti-inflammatory activities. This protein has also been detected in the lacrimal gland and glands of the third eyelid in bison (*Bison bison*). Lysozyme has not been detected in the lacrimal gland of cattle or bison. The similarities between these species suggest that variability in the susceptibility to infectious corneal diseases that exists between bison and cattle is due to a difference in other tear components (such as transferrin, complement, or beta-lysin) rather than in lysozyme and lactoferrin (Pinard et al. 2003). Domestic sheep and goats have quantifiable levels of lysozyme in their tears; however, levels in exotic Caprinae have not been established (Brightman et al. 1991).

Cornea and Sclera

Reindeer reportedly have an unusually thick epithelial layer compared to oxen (*Bos taurus*) and other mammals (Winqvist and Rehbinder 1973). However, the corneas of three different cervidae: reindeer (*Rangifer tarandus tarandus*), elk (*Cervus canadensis*), and roe deer (*Capreolus capreolus*) are reported to be similar in structure and composition and appear to increase in thickness with increasing age (Rehbinder et al. 1977).

Aqueous Humor Dynamics

The aqueous humor dynamics of the enucleated eye of the white-tailed deer (*Odocoileus virginianus*) have been reported to be similar to that of other mammals, despite wide variations in globe size. The mean ± SD anterior chamber volume of the deer eye is 1400 ± 90 μl with a flow rate of 12.7 μl/minute and a turnover rate of 0.9% per minute per volume of the anterior chamber. The outflow facility is 1.29 ± 0.20 μl/minute/mmHg when the resting intraocular pressure was held at 9.8 ± 0.48 mmHg (Colasanti 1984).

Retina

Pecoran species have holangiotic retinal vascular patterns and most have a tapetum lucidum to assist with retinal capture of photons in dimly lit surroundings (Fig. 32.1). While not studied in great detail, the structure and electrophysiologic function of the retina of white-tailed deer (*Odocoileus virginanus*) has been found to be similar to that of other diurnal mammals such as sheep and pigs (Witzel et al. 1978). Electroretinogram (ERG) flicker photometry was used to study the spectral mechanisms in the retinas of white-tailed deer (*O. virginianus*) and fallow deer (*Dama dama*). In addition to having a rod pigment with a maximum sensitivity of about 497 nm, both species appear to have two classes of photopic receptors, a short-wavelength-sensitive cone mechanism having maximum sensitivity 450–460 nm and a cone having peak sensitivity in the middle wavelengths (537 nm in white-tailed deer; 542 nm in fallow deer). Deer resemble other ungulates and many other types of mammals in having two classes of cone pigment and, thus, the requisite retinal basis for dichromatic color vision (Jacobs et al. 1994).

Studies of the retinal topography in artiodactyls have revealed a common pattern of retinal specialization in cows (*Bos taurus*), goats (*Capra aegagrus hircus*), sheep (*Ovis aries*), fallow deer (*D. dama*), and giraffes (*Giraffa camelopardalis*) (Coimbra et al. 2013; Hebel and Hollander 1979; Hughes and Whittridge 1973; Gonzalez-Soriano et al. 1997; Hebel 1979; Shinozaki et al. 2010). Each species exhibits a horizontal visual streak formed by an elongated arrangement of high ganglion cell density which improves visual sampling across the horizon allowing detection of predators or conspecifics without extensive head or eye movements. The

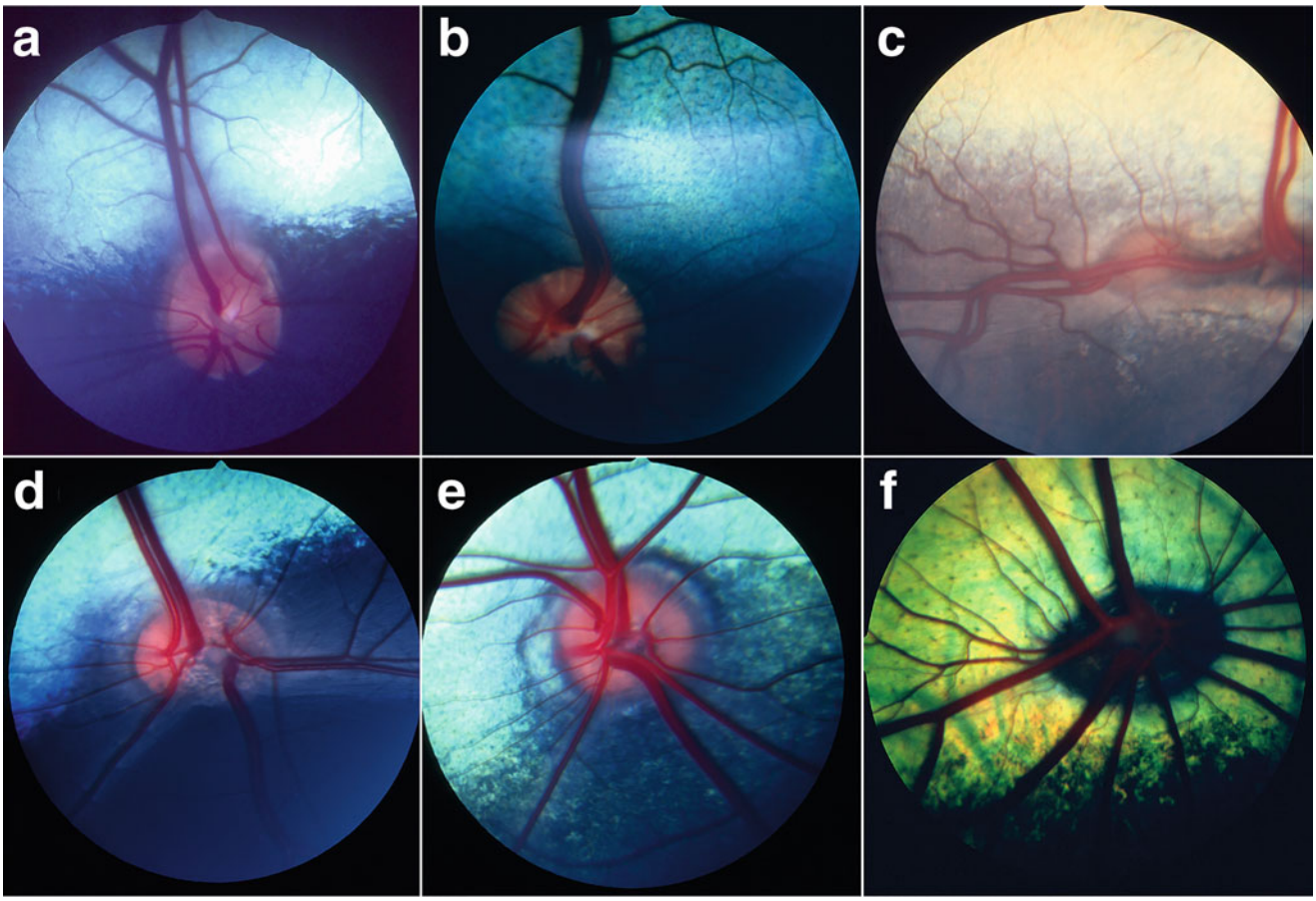

Fig. 32.1 Normal fundi of select species within the Ruminantia. Note the consistent presence of a tapetum lucidum and the holangiotic retinal vascular pattern. (**a**) Giraffe (*Giraffa camelopardalis*), (**b**) adult female Mouflon (*Ovis gmelini*), (**c**) Pere David's Deer (*Elaphurus davidianus*), (**d**) Domestic sheep (*Ovis aries*), (**e**) Domestic goat (*Capra aegagrus hircus*), and (**f**) Mouse deer (*Traugulus* sp.). **a**—Courtesy of Dr. Nicholas Millichamp. **b**–**f**—Courtesy of the University of California Davis Comparative Ophthalmology service

temporal area of the horizontal streak has a concentric arrangement of the retinal ganglion cells which is used for fixation and increases the animals' discrimination of fine detail in the frontal visual field which facilitates foraging tasks. A dorsotemporal extension is formed by an increase in neuronal density that runs perpendicularly from the temporal to the dorsal retina. This extension purportedly assists in detection of objects entering the inferior visual field and its magnitude is correlated with the height and size of the body of the individual species as a function of the distance of the head to the ground (Hughes and Whittridge 1973). This extension is most pronounced in the giraffe (Coimbra et al. 2013).

Vision

Vision is critical to the health, survival, and success of terrestrial vertebrates. Since most Pecora and artiodactyls are herbivorous and many are prey species, their vision is adapted to survey their environment looking for both foraging opportunities and predation threats. Most have wide, panoramic fields of view, good sensitivity to low light conditions, and good motion detection as well as dichromatic color vision. The particular aspects of visual perception vary between species and their environmental niches.

Vision and ecological studies show considerable differences in visual perception between species, even between closely related species such as the giraffe (*Giraffa camelopardalis*) and okapi (*Okapia johnstoni*). Giraffes are reported to have excellent vision while okapi exhibits poor eyesight and rely on the sense of smell and hearing. Some of the differences in visual acuity and capacity may be a function of their ecologies. Giraffes inhabit the open savannah while okapi lives in dense, low-light forests (Ishengoma et al. 2017).

The Arctic has extreme seasonal changes in light levels and is proportionally UV-rich because of scattering of the shorter wavelengths and their reflection from snow and ice. The cornea and lens in Arctic reindeer (*Rangifer tarandus*

tarandus) do not block all UV and, unlike in most mammals, the reindeer retina responds electrophysiologically to these wavelengths. Both rod and cone photoreceptors respond to low-intensity UV stimulation. Reindeer thus extend their visual range into the short wavelengths characteristic of the winter environment and periods of extended twilight present in autumn and spring. A specific advantage of this short-wavelength vision is the information provided by differential UV reflections known to occur in both Arctic vegetation and different types of snow. UV is normally highly damaging to the retina, resulting in photoreceptor degeneration, however, such damage appears not to occur in these animals. Reindeer may have evolved retinal mechanisms protecting against extreme UV exposure present in the daylight found in the snow-covered late winter environment (Hogg et al. 2011).

An additional Arctic reindeer adaption to the extreme seasonal fluctuations in environmental light levels occurs in the tapetum lucidum (Stokkan et al. 2013). During the summer the reindeer tapetum lucidum is a golden color, but in the winter it assumes a deep blue hue. The shift to a blue reflection scatters light through photoreceptors rather than directly reflecting it, resulting in increased photon capture and elevated retinal sensitivity. The change in wavelength reflection from the tapetum lucidum that increases retinal sensitivity during the winter also results in reduced visual acuity and may represent an adaption to assist Arctic reindeer in detecting predators during the dark winter months. This potentially unique phenomenon is mediated by changes in the collagen spacing within the tapetum lucidum. During the winter, intraocular pressure is increased in Arctic reindeer, which may explain the mechanism of the collagen compression (Stokkan et al. 2013).

The only species in which the development of the refractive state has been studied is the Thomson gazelle (*Gazella thomsoni*) (Ofri et al. 2004). Newborn Thomson gazelles were examined repeatedly retinoscopically as they matured. They were observed to be hyperopic at birth (mean ± SD refractive error of 3.44 ± 0.31 D) but rapidly became emmetropic (0.13 ± 0.21 D) by Day 50 of age and remained so through adulthood. Likely rapid development of emmetropia contributes to the survival of young gazelles by permitting them to detect and flee predators early in life.

Examination and Diagnostic Techniques

Observation Prior to manual restraint, if possible, the animal's activity and movement in its normal environment or other calm, safe location should be observed. The examiner should assess the animal's locomotion, posture, head movements, ability to navigate, and overall appearance. Animals with vision loss may be observed to spook or shy away on the affected side.

Restraint The need for restraint will vary depending upon the individual's size, temperament, and familiarity with humans. Small ruminants, especially those acclimated to human contact, may need only manual restraint. Chemical restraint is usually necessary for larger Pecorans. Please see a current reference for sedation and anesthesia protocols in ruminants. If chemical restraint is necessary, the examiner should be aware that it will confound the neuro-ophthalmic assessment of vision.

Vision and Neuro-Ophthalmic Assessment Evaluation of vision and the cranial nerves is a crucial initial step in the ophthalmic examination (Featherstone and Heinrich 2013). In the conscious patient, this can be performed quickly and efficiently with a menace response. Because anesthetic restraint precludes evaluation of the menace response, dazzle reflex, and may alter pupillary light reflexes, these should be performed prior to anesthesia whenever it is safe and possible to do so. As with other mammals, the menace response is learned and may not be present in neonates, even in precocial species such as pecorans.

Tear Film Evaluation Assessment of the aqueous portion of the tear film is an important component of any ophthalmic examination, especially in species prone to tear film and ocular surface disease. While dry eye has not been commonly described in exotic ruminants, tear testing is useful to detect developmental defects, nutritional deficiency, denervation injuries, inflammatory conditions, or other pathologies which may affect the function of the lacrimal gland. The few studies evaluating the tear film in percorans have employed the Schirmer tear test I, performed in the same manner as in dogs and cats. Reference ranges for available species have been included in Table 32.1 and Appendix 3. Significant interspecies differences in normal aqueous tear fraction exist, and these are likely related to habitat (Ofri et al. 1999, 2000, 2001; Villar et al. 2019; Somma et al. 2016; Martins et al. 2007; Oriá et al. 2015; Kvapil et al. 2018). As with other vertebrate species, any tear test should ideally be performed prior to anesthesia, instillation of topical liquids, or manipulation of the eyelids or cornea (Featherstone and Heinrich 2013). If this is not possible, a comparison to reference ranges of the same or similar species under the same sedation or anesthesia protocol and correlation of values with clinical signs of ocular surface disease should be made.

Intraocular Pressure Intraocular pressure (IOP) may be measured in the clinical setting by applanation or rebound tonometry. The majority of the studies estimating IOP in pecorans have employed applanation tonometry with the TonoPen® or TonoPen Vet®. Established reference ranges generally place pecoran IOPs in the middle to low teens (Ofri et al. 2000, 2001; Martins et al. 2007; Oriá et al. 2015; Kvapil

Table 32.1 Established aqueous tear production in Pecoran species as measured by Schirmer Tear Test I

Species	Schirmer tear test (mm/min) Mean ± SD	References	Notes
Nubian ibex (*Capra ibex nubiana*)	13.2 ± 5.1	Ofri et al. 1999	Sedated with etorphine hydrochloride and acepromazine maleate
Arabian oryx (*Oryx leucoryx*)	12.7 ± 4.8	Ofri et al. 1999	Sedated with etorphine hydrochloride and acepromazine maleate
Eland (*Taurotragus oryx*)	18.8 ± 5.9	Ofri et al. 2000	Sedated with etorphine hydrochloride and acepromazine maleate
Asian fallow deer (*Dama mesopotamica*)	10.5 ± 6.5	Ofri et al. 2000	Sedated with etorphine hydrochloride and acepromazine maleate
Brown brocket deer (*Mazama gouazoubira*)	8.9 ± 1.8	Martins et al. 2007	Manual restraint, no sedation
Sambar deer (*Rusa unicolor*)	18.8 ± 4.7	Oriá et al. 2015	Manual restraint, no sedation
Eland (*Taurotragus oryx*)	18.7 ± 5.9	Ofri et al. 2001	Sedated with etorphine hydrochloride and acepromazine maleate
Impala (*Aepyceros melampus*)	18.8 ± 1.8	Ofri et al. 2002	Sedated with etorphine hydrochloride and acepromazine maleate
White-tailed wildebeest (*Connochaetes gnou*)	19.6 ± 4.3	Ofri et al. 2002	Sedated with etorphine hydrochloride and acepromazine maleate
Fallow deer (*Dama dama*)	17.8 ± 3.16	Kvapil et al. 2018	Manual restraint, no sedation
Mouflons (*Ovis aries musimon*)	17.9 ± 3.87	Kvapil et al. 2018	Manual restraint, no sedation
Alpine ibex (*Capra ibex*)	11.7 ± 3.87	Kvapil et al. 2018	Manual restraint, no sedation
Alpine chamois (*Rupicapra rupicapra*)	14.5 ± 3.0	Kvapil et al. 2018	Manual restraint, no sedation
White-tailed deer–fawn (*Odocoileus virginianus*)	12.32 ± 4.46	Villar et al. 2019	Manual restraint, no sedation

et al. 2018; Villar et al. 2019) (Table 32.2, Appendix 3). To date, the Thomson gazelle has the lowest reported IOP estimate in any species (Ofri et al. 2000).

Culture and Cytology Corneal and conjunctival samples should ideally be collected for culture with a sterile swab prior to instillation of topical anesthetics. The commensal conjunctival microbiota naturally varies from species to species and between different geographical regions.

Conjunctival swabs collected from 44 live and 226 hunter-harvested mule deer (*Odocoileus hemionus*) in Wyoming and Utah revealed a number of bacteria and nematodes (Dubay et al. 2000a). *Staphylococcus* spp. and *Micrococcus* spp. were the most common of the 22 Gram-positive species isolated and *Enterobacter* spp., *Echserchia coli* and *Pseudomonas* spp. were the most common of the 29 species of Gram-negative bacteria isolated from asymptomatic, ophthalmoscopically normal animals (Dubay et al. 2000a). Non-piliated *Moraxella* spp. were only occasionally isolated in normal animals. *Thelazia californiensis* nematodes may be observed in 15–66% of hunter-harvested mule deer in the absence of overt clinical signs of keratoconjunctivitis (Dubay et al. 2000b). *Thelazia californiensis* has been observed in the fornices of normal white-tailed deer (*O. virginianus*) and black-tailed deer (*O. h. columbianus*) (Beitel et al. 1974).

Microbial isolation performed from conjunctival samples of normal brown brocket deer in Brazil revealed *Bacillus* spp. and *Diplococcus* spp. commonly. *Staphylococcus* spp., *Streptococcus* spp., and *Corynebacterium* spp. were isolated from the majority of animals as well (Martins et al. 2007).

Samples taken from the conjunctiva of healthy fallow deer (*Dama dama*), mouflons (*Ovis aries musimon*), Alpine ibex (*Capra ibex*), and Alpine chamois (*Rupicapra rupicapra*) revealed a predominance of Gram-positive organisms, especially *Staphylococcus* spp., *Streptomyces* spp., *Micrococcus* spp., and *Corynebacterium* spp. Gram-negative organisms were rarely isolated (Kvapil et al. 2018).

Seventeen species of bacteria were isolated from the conjunctiva of normal North American bison (*Bison bison*). The most prevalent bacteria were of the genus *Bacillus* (74.6%). *Mycoplasma* organisms were not observed. The bacteriological profile found in bison is similar to that found in domestic cattle (Davidson et al. 1999).

Table 32.2 Established IOP estimates in Pecoran species

Species	Method	IOP (mmHg) Mean ± SD	Notes	References
Eland (*Taurotragus oryx*)	Applanation	14.6 ± 4.0	Sedated with etorphine hydrochloride and acepromazine maleate	Ofri et al. 2001
Asian fallow deer (*Dama mesopotamica*)	Applanation	11.9 ± 3.3	Sedated with etorphine hydrochloride and acepromazine maleate	Ofri et al. 2001
Thomson gazelle (*Gazella thomsoni*)	Applanation	7.6 ± 1.6	Sedated with etorphine hydrochloride and acepromazine maleate	Ofri et al. 2000
Brown brocket deer (*Mazama gouazoubira*)	Applanation	15.3 ± 3.1	Manual restraint, no sedation	Martins et al. 2007
Sambar deer (*Rusa unicolor*)	Applanation	11.4 ± 2.8	Manual restraint, no sedation	Oriá et al. 2015
Arabian oryx (*Oryx leucoryx*)	Applanation	11.8 ± 3.4	Sedated with etorphine hydrochloride and acepromazine maleate	Ofri et al. 1998
Addax antelope (*Addax nasomaculatus*)	Applanation	11.2 ± 3.2	Sedated with etorphine hydrochloride and acepromazine maleate	Ofri et al. 2002
Impala (*Aepyceros melampus*)	Applanation	8.0 ± 1.2	Sedated with etorphine hydrochloride and acepromazine maleate	Ofri et al. 2002
Fallow deer (*Dama dama*)	Applanation	14.1 ± 2.48	Manual restraint, no sedation	Kvapil et al. 2018
Mouflons (*Ovis aries musimon*)	Applanation	14.9 ± 2.20	Manual restraint, no sedation	Kvapil et al. 2018
Alpine ibex (*Capra ibex*)	Applanation	13.1 ± 2.43	Manual restraint, no sedation	Kvapil et al. 2018
Alpine chamois (*Rupicapra rupicapra*)	Applanation	10.2 ± 2.5	Manual restraint, no sedation	Kvapil et al. 2018
White-tailed deer—adult (*Odocoileus virginianus*)	Applanation	15.57 ± 2.88	Sedated with xylazine, tiletamine and zolazepam	Villar et al. 2019
White-tailed deer—adult (*Odocoileus virginianus*)	Rebound	12.87 ± 2.57	Sedated with xylazine, tiletamine and zolazepam	Villar et al. 2019
White-tailed deer—fawn (*Odocoileus virginianus*)	Applanation	16.21 ± 4.97	Manual restraint, no sedation	Villar et al. 2019
White-tailed deer—fawn (*Odocoileus virginianus*)	Rebound	14.05 ± 5.03	Manual restraint, no sedation	Villar et al. 2019

Ophthalmic Diseases

Developmental Ocular Malformations

Multiple, nodular pigmented masses protruding from the cornea and adjacent sclera in a white-tailed deer (*O. virginianus*) were diagnosed as choristomas containing well-differentiated skin, cartilage, and bone (LaDouceur et al. 2012). Corneal and epibulbar dermoids are congenital anomalies of the cornea or conjunctiva characterized by well-differentiated tissues not usually located on the ocular surface, most commonly skin-like tissue. These lesions are often incidental although they may be associated with other ocular abnormalities, and clinically can cause considerable irritation for the affected animal. Keratectomy and reconstruction of the ocular surface are typically curative. One of the authors (CEP) has observed and treated a corneal dermoid in an okapi (*Okapia johnstoni*) calf (Fig. 32.2).

Congenital ocular abnormalities have been reported in white-tailed deer (*Odocoileus virginianus*) (Clarke et al. 2018). Most case reports and cases series describe bilateral ocular lesions in otherwise normal fawns that include microphthalmia, anophthalmia, congenital cataracts, dermoids, ectopic lacrimal tissue, colobomata, and anterior segment dysgenesis (Fig. 32.3). In 1977, there was a report of eight white-tailed deer fawns (*Odocoileus virginianus*) with abnormal eyes but no other apparent abnormalities of other organs (Fulton et al. 1977). The severity of the ocular abnormalities ranged from mild microphthalmia with functional globes to severe microphthalmia with cystic derangements to anophthalmia. Intraocular dermoid cysts were found in three animals, and anterior segment dysgenesis and retinal dysplasia or hypoplasia were present in all cases. The more severe manifestations occurred earlier in embryonic development, with either failure of normal invagination of the optic vesicle, incomplete invagination, or abnormal differentiation of neural ectoderm and surface ectoderm. The cause of the anomalous development in these cases was not apparent but

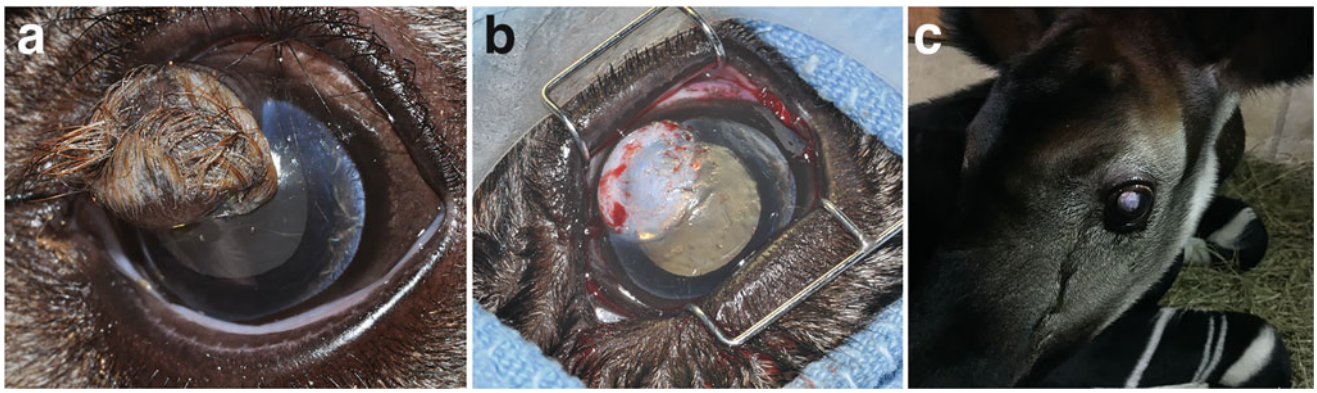

Fig. 32.2 (**a**) Corneal dermoid in an Okapi (*Okapia johnstoni*) calf. (**b**) Immediately following keratectomy to remove the dermoid. (**c**) Okapi calf immediately following recovery from anesthesia for keratectomy

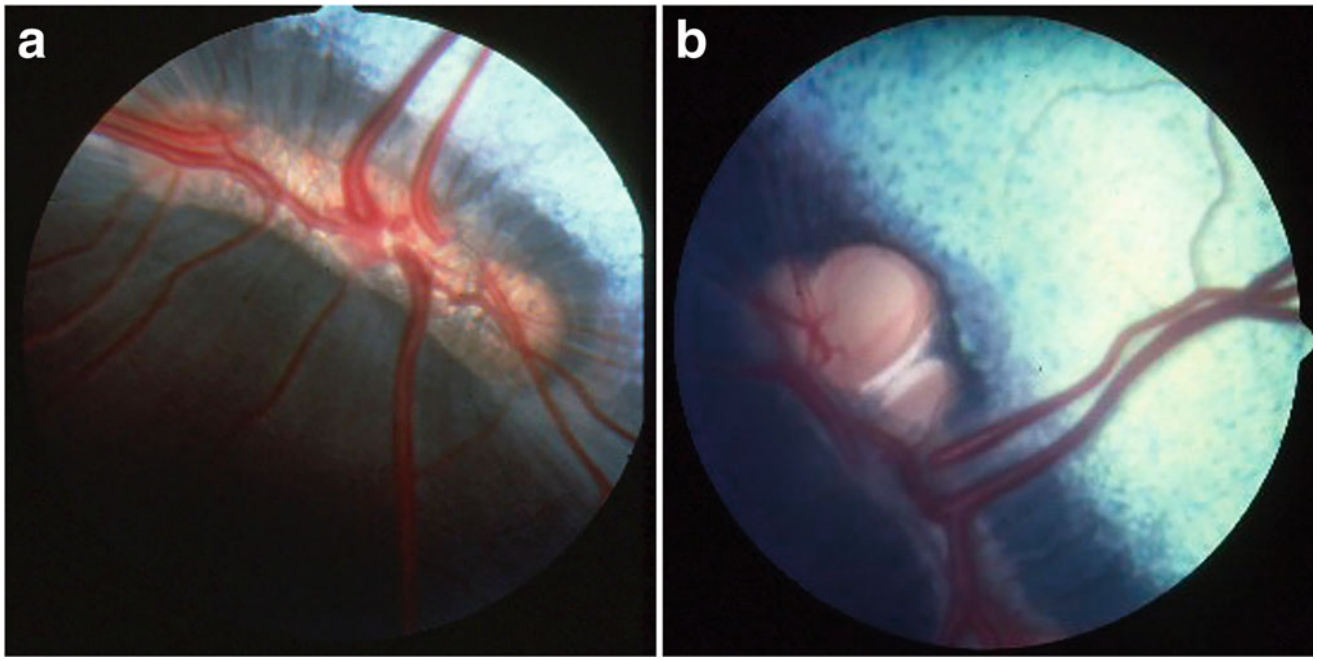

Fig. 32.3 (**a**) Fundus of a normal white-tailed deer (*Odocoileus virginianus*). (**b**) Fundus of a white-tailed deer with an optic nerve coloboma. Photographs courtesy of Dr. Nicholas Millichamp

was speculated to be the result of inheritance with or without chromosomal abnormalities, intrauterine infection, or exposure to an environmental or toxic factor at critical stages of ocular development. A number of other reports have described ocular and neurologic abnormalities that have resulted in visual deficits in white-tailed deer (Howard et al. 1976).

Complex microphthalmia with multiple ocular abnormalities and intraocular dermoid cyst in red deer (*Cervus elaphus*) has been reported (Gaudie et al. 2012; Gelmetti et al. 2010; Mutinelli et al. 2012). Affected animals, which had been found deceased or were euthanized due to blindness, had severe bilateral ocular dysgenesis with aphakia and dermoid metaplasia of the lens vesicle. An underlying etiology was not determined. Similar findings have been observed in Texel sheep (*Ovis ammon*) in which the condition has an autosomal recessive pattern of inheritance (van der Linde-Sipman et al. 2003; Becker et al. 2010). In these sheep, abnormal development of the lens vesicle and lack of lens capsule development gave rise to epithelial structures in the anterior chamber and the disorganized development of mesenchymal structures.

Congenital cataracts with persistent hyperplastic primary vitreous and persistent tunica vasculosa lentis have been observed in a sambar deer fawn (*Rusa unicolor*) (Somma

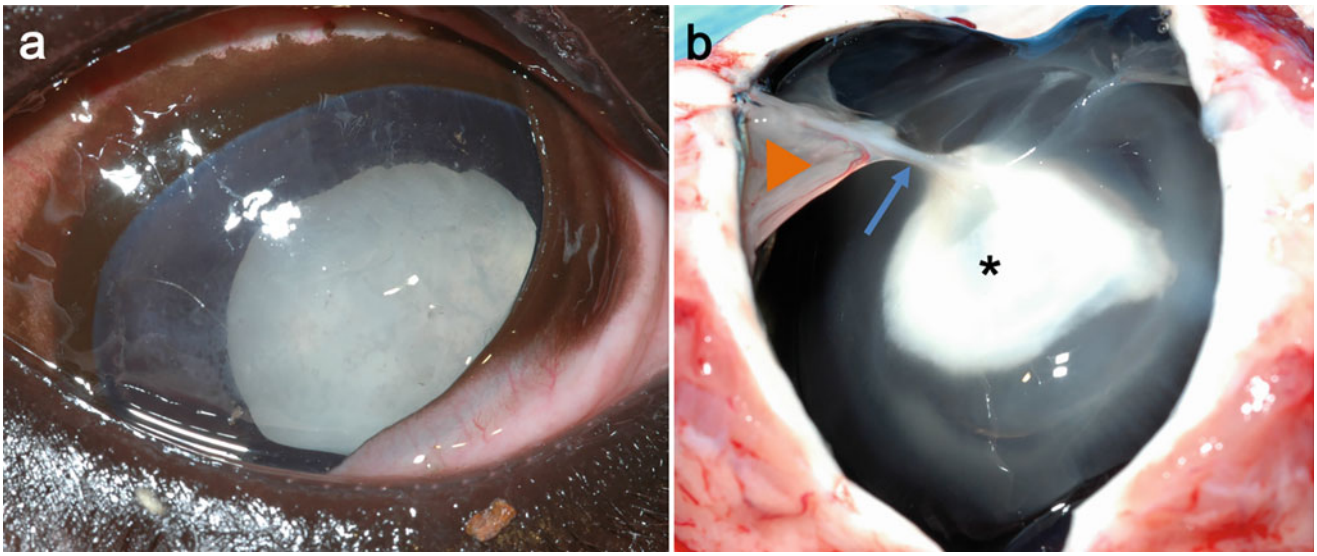

Fig. 32.4 (**a**) Giraffe (*Giraffa camelopardalis*) *calf with a congenital cataract.* (**b**) *Bisected posterior segment of a giraffe globe with posterior cataract, persistent hyperplastic primary vitreous and a retinal detachment.* Orange triangle—Retinal detachment; blue arrow—persistent hyperplastic primary vitreous; asterisk—Posterior cataract

et al. 2016). The same findings were also observed in white-tailed deer (O. *virginianus)* and giraffe (*Giraffa camelopardalis*) (Fig. 32.4) (C.E. Plummer, personal observation).

Acquired Ophthalmic Disease

Eyelid

A European bison (*Bison bonasus*) cow was observed to have developed papillomatous masses of the skin at the medial canthus during a period of stress. Cutaneous papillomatosis was confirmed histologically. Negative stain transmission electron microscopic examination revealed papillomavirus in the papillomas and papillomavirus DNA was also detected using the polymerase chain reaction with FAP59 and FAP64 primers (Literák et al. 2006).

A survey of ophthalmic abnormalities in North American bison (*Bison bison*) described individuals with healed eyelid lacerations (likely traumatically induced) and periocular blepharitis related to *Demodex* spp. infection (Davidson et al. 1999). Demodicosis has been reported to cause nodules with caseous centers in the periorbital areas, perineum, and ventral aspect of the tail in bison, as opposed to the pruritic, alopecic lesions observed in other species (Vestweber et al. 1999).

Cornea

Infectious keratoconjunctivitis (IKC) is the most common ocular disease in ruminants, especially domestic cattle and Caprinae, worldwide, particularly in the summer months in warm and humid climes. Its prevalence is associated with dust, debris, compromised hygiene, as well as UV radiation and mechanical vectors such as flies. Ocular trauma is also a common inciting factor for IKC in some domestic and wild ruminant species. This trauma can result from antler and horn damage to the ocular surface associated with the fighting behaviors that occur during dominance or territorial disputes (Fig. 32.5). Affected animals present with serous to mucopurulent exudate, conjunctival hyperemia, perilimbal and corneal vascularization, corneal edema, erosion, ulceration, and infiltration of neutrophils into the cornea (Fig. 32.6). Iridocyclitis may be observed as well. In the most advanced stages, corneal perforation, and anterior synechia may occur. A large number of different etiologic agents have been implicated including bacteria (*Moraxella* spp., *Neisseria* spp., *Listeria* spp., *Chlamydia*/*Chlamydophila* spp.), mycoplasmal organisms, viruses, and parasites. However, in cattle, the only organism to satisfy Koch's postulates is *Moraxella bovis*. In sheep and goats, *Mycoplasma conjunctivae* are considered to be the primary causative agent of IKC. Other agents may initiate or complicate the condition, however. In free-ranging wildlife, there are fewer reports of IKC than there are in domestic species and even less is known about potential etiologic agents. However, a variety of reports have speculated about potential causative agents. Most reports involve only a few individual cases or small groups of animals, especially mule deer (*Odocoileus hemionus*), white-tailed deer (*O. virginianus*), pronghorn antelope (*Antilocapra americana*), moose (*Alces alces*), reindeer (*Rangifer tarandus tarandus*), big-horn sheep (*Ovis canadensis*), and muskox (*Ovibos moschatus*) (Williams et al. 1985; Meagher et al. 1992; Kummeneje 1976; Handeland et al. 2020). While in domestic species IKC usually causes transient disease with modest to significant

Fig. 32.5 Eyelid laceration, infectious keratitis, corneal perforation, and endophthalmitis in a reindeer (*Rangife tarandus tarandus*) that developed following fighting behavior and antler ocular trauma

economic losses but limited mortality, pathogenicity in wild species is generally higher, causing outbreaks with morbidity and mortality up to 30% (Fernández-Aguilar et al. 2013; Handeland et al. 2020). Susceptibility varies dramatically between species.

Infectious keratoconjunctivitis associated with *Moraxella* spp., *Chlyamydia* spp., and the parasite *Thelazia californiesis* have been reported to cause blepharospasm, epiphora, and corneal opacity in mule deer (*Odocoileus hemionus*) in Utah (Taylor et al. 1996). Non-piliated *Moraxella ovis* has been isolated from mule deer (*O. hemionus*) and moose (*Alces alces*) with keratoconjunctivitis in Wyoming, however, it was not definitively implicated in clinical disease (Dubay et al. 2000b). Affected mule deer exhibit excessive lacrimation, mucopurulent conjunctivitis, keratitis, and corneal opacity. Affected moose develop severe conjunctivitis, keratitis, and corneal ulceration. *Moraxella bovis* has not been routinely isolated from white-tailed deer (*Odocoileus virginianus*) or red deer (*Cervus elaphus*) with or without keratoconjunctivitis (Pearson 1984; Webber and Selby 1981; Badger et al. 1980).

Severe infectious keratoconjunctivitis (IKC) epizootic in free-ranging alpine ibex (*Capra ibex ibex*) in Switzerland was attributed to *Mycoplasma conjunctivae* (Mayer et al. 1997). In mountain habitats, where domestic ruminants share grazing areas with susceptible wild mountain ungulates such as chamois (*Rupicapra* spp.), Alpine ibex (*Capra ibex*), and European mouflon (*Ovis aries musimon*) it appears that domestic sheep play a key role as a reservoir host for *M. conjunctivae* and can transmit the agent to the wild species (Fernández-Aguilar et al. 2013). That said, *Mycoplasma conjunctivae* was recently detected in asymptomatic Alpine ibex (*Capra ibex ibex*) and Alpine chamois (*Rupicapra rupicapra*). Mycoplasmal load was significantly lower in eyes from healthy carriers and animals with mild signs than from animals with moderate and severe signs. Although some strains were found in both asymptomatic and diseased animals of the same species, others apparently differed in their pathogenic potential depending on the infected species. Overall, there is widespread occurrence of *M. conjunctivae* in wild Caprinae with and without IKC signs. This suggests that an external source of infection may not be required for an IKC outbreak in wildlife and *M. conjunctivae* may persist in apparently healthy populations of wild Caprinae (i.e., carriers). *M. conjunctivae* plays a central role in outbreaks but other infectious agents may be involved in IKC cases in non-epidemic situations. The presence and severity of signs are related to the quantity of *M. conjunctivae* in the eyes rather than to the strain. Likely, individual or environmental factors influence the clinical expression of the disease and *M. conjunctivae* (Mavrot et al. 2012).

Keratitis and conjunctivitis in reindeer (*Rangifer tarandus tarandus*) in Sweden have been associated with introduction of the larval stages of the nostril fly (*Cephenomyia trompe*) into the conjunctival sac. Clinical signs associated with this aberrant location occur mostly in summer months which corresponds to the annual peak of solar UV radiation, similar to outbreaks of *Moraxella*-associated IKC in cattle

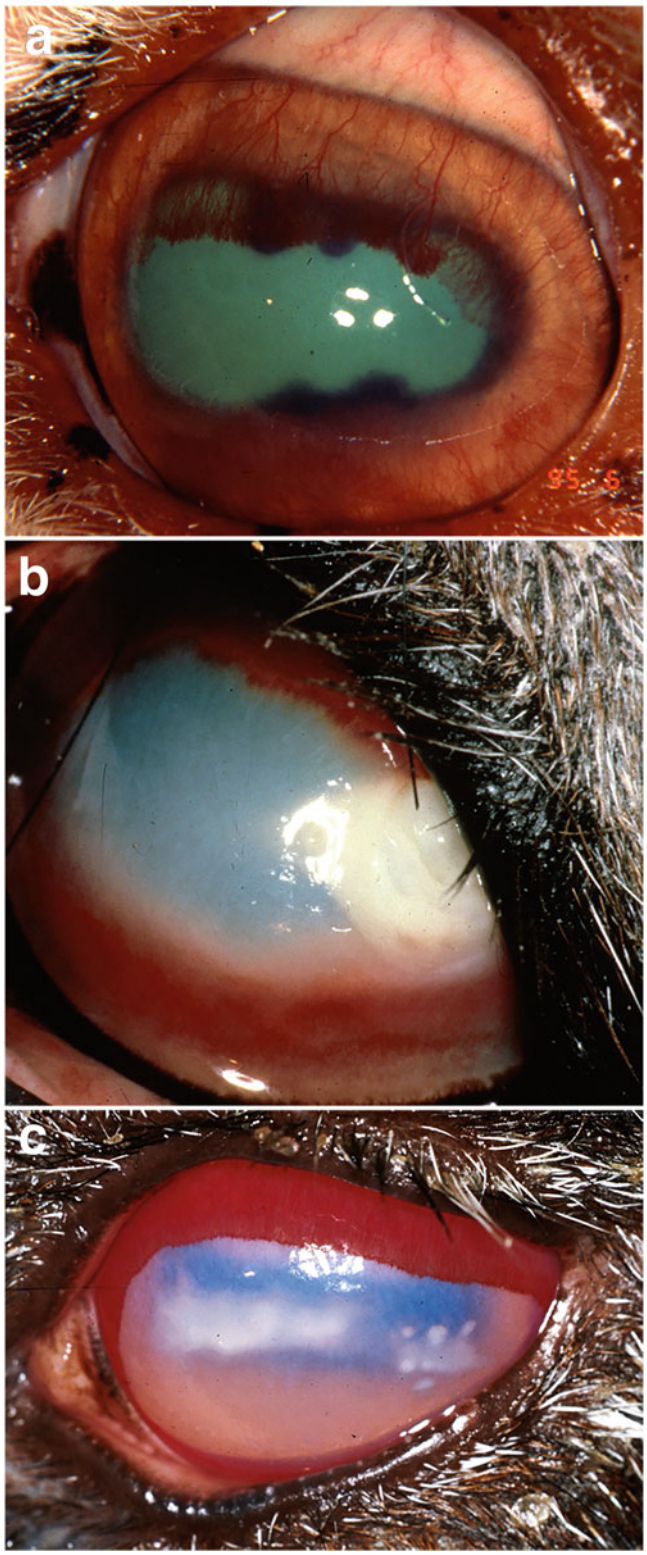

Fig. 32.6 Infectious keratoconjunctivitis in members of the Ruminantia. (**a**) A sheep (*Ovis aries*) with keratoconjunctivitis associated with *Mycoplasma conjunctivae*. Note the conjunctival hyperemia and corneal vascularization. (**b**) An adult steer (*Bos taurus*). Note the 360˚˜ peripheral vascularization, dense edema, and cellular infiltrate in the cornea. (**c**) An ibex (*Capra ibex).* Note the corneal vascularization, edema, and cellular infiltrate

(Rehbinder 1977). Documented clinical signs included conjunctival hyperemia and erosions, as well as corneal vascularization and ulcerations. Samples for bacterial culture obtained from reindeer with active keratoconjunctivitis exhibit greater growth of bacteria than those from clinically normal animals, however, the difference is not great. *Pasteurella multocida* is commonly isolated, however, its significance to the disease state is unclear (Rehbinder and Glatthard 1977). *Moraxella* spp. have not been routinely isolated from reindeer with keratoconjunctivitis. Forest reindeer are reported to have a higher prevalence of keratoconjunctivitis than do mountain reindeer, possibly due to marked differences in herding conditions (Rehbinder and Glatthard 1977).

Infectious keratoconjunctivitis in Eurasian tundra reindeer (*Rangifer tarandus tarandus*) is considered a multifactorial disease without a single causative pathogen. However, transmission studies have shown that cervid herpesvirus 2 may induce clinical signs in apparently healthy individuals of this species while *Moraxella bovoculi* alone does not (Sánchez Romano et al. 2018; Tryland et al. 2017). Cervis herpesvirus 2 has been associated with the development of keratoconjunctivitis in semi-domestic reindeer (*Rangifer tarandus tarandus*) in Norway (Tryland et al. 2009). The virus was isolated from the eye, nose, and vagina of clinically affected animals but not from clinically unaffected animals. Viral DNA was detected by PCR in all affected and five unaffected animals. In vitro cytopathic activity of virus isolated from affected animals increased with the severity of clinical signs experienced by the host. Secondary bacterial infections with *Moraxella* spp., particularly *Moraxella bovoculi* and *Staphylococcus aureus*, *Streptococcus* spp., and *Arcanobacterium pyogenes* were common. Clinical signs include blepharospasm, epiphora, corneal edema and vascularization, infiltration, and ulceration. Similar to the disease course of domestic cattle with infectious bovine keratoconjunctivitis, animals at this stage either healed uneventfully or had their corneal disease progress to perforation. Cervid herpesvirus 2 is endemic in reindeer and may be the primary agent for IKC in these animals (Tryland et al. 2009; Sánchez Romano et al. 2018). A report of IKC in reindeer in Norway described two novel viruses isolated from affected animals, a unique herpesvirus designated cervid herpesvirus 3 and a papillomavirus. It is not known if either virus was causative, contributing, or incidental (Smits et al. 2013). Recently, a report of an outbreak of IKC in reindeer in Sweden was found to be associated with *Chlamydia pecorum*. Many, but not all affected animals, exhibited concurrent seroprevalence of cervid herpesvirus 2 antibodies (Sánchez Romano et al. 2019).

Keratoconjunctivitis associated with infections of the conjunctival fornices and lacrimal ducts with nematode parasites has been reported in numerous species of Pecora. Most

reports have identified *Thelazia californiensis* as the offending organism. Eyeworm (*T. californiensis*) infections in Columbian black-tailed deer (*Odocoileus hemionus columbianus*) in Oregon and in mule deer (*Odocoileus hemionus*) in Utah are common and clinical signs correlate with the degree of nematode load. Conjunctivitis and corneal opacities are worse in animals with a greater number of nematodes (Beitel et al. 1974; Taylor et al. 1996). *Thelazia skriabini* have been isolated from the conjunctival fornices and behind the nictitans of white-tailed deer (*Odocoileus virginianus*) in North America (Kennedy et al. 1993). Keratoconjunctivitis associated with *Thelazia gulosa* has been reported in giraffe (*Giraffa camelopardalis angolensis*) (Walker and Becklund 1971).

Fungal keratitis occurs relatively commonly in domestic populations of reindeer (*Rangifer tarandus tarandus*) and in temperate climates is most common in the summer and fall months. The clinical appearance of reindeer keratomycosis is similar to other species and may include both ulcerative and nonulcerative corneal lesions (Fig. 32.7a). Confirmation of a diagnosis of fungal keratitis in reindeer or other ruminant species can be achieved by cytology, histopathology, in vivo confocal microscopy, fungal culture, or fungal PCR assay (E.C. Ledbetter, personal observation) (Fig. 32.7b).

Therapy for IKC in wild hoofstock depends not only on the cause but also on how amenable to treatment the individual is. For viral etiologies, supportive care is the only feasible option. If a bacterial, Mycoplasmal, or Chlamydial etiology is known or suspected, long-acting parenteral antibiotics are indicated. However, these may not eliminate a carrier state. Keratomycosis can be treated with topical ophthalmic antifungals in compliant individuals, but some cases may require anterior lamellar keratectomy and conjunctival grafting for resolution. If nematode organisms are present, they should be manually removed if possible. If an individual animal will tolerate medical therapy, topical antibiotics, and systemic analgesics, such as non-steroidal anti-inflammatory agents, should be utilized.

A novel gammaherpesvirus was identified in a conjunctival swab from a Reeves's muntjac (*Muntiacus reevesi*) associated with severe keratitis and intraocular inflammation. The eye had a 3-week history of opacity and discomfort. On examination, dense corneal edema and superficial vascularization were present. Limited view of the anterior chamber revealed hypopyon and miosis. The fellow eye was unremarkable. Phylogenetic analyses indicated that the virus is a member of the genus percavirus in the subfamily *Gammaherpesvirinae*. Supportive care resulted in the resolution of clinical signs (Fig. 32.8) (Monk et al. 2015).

Although plague is relatively rare in wild ungulates, it is reported on occasion. Mule deer (*O. hemionus*) in Wyoming and Oregon may develop ocular lesions including keratoconjunctivitis, panophthalmitis, and retinal detachment associated with Yersina pestis infection (Edmunds et al. 2008). Affected deer were killed when they were observed to be non-visual. Intralesional organisms, subsequently identified at *Y. pestis* were observed within the inflamed globes. In addition to the ocular signs, affected deer demonstrated evidence of septicemia, pneumonia, and lymphadenitis, with intralesional organisms.

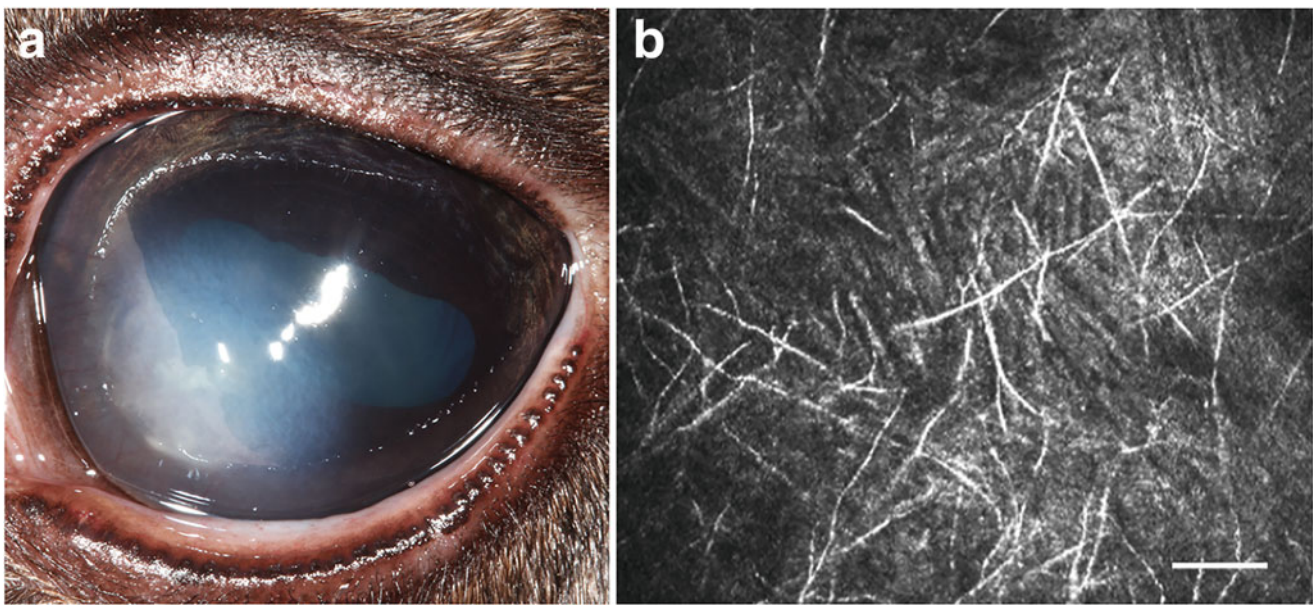

Fig. 32.7 Fungal keratitis in a reindeer (*Rangifer tarandus tarandus*). (**a**) Corneal vascularization, edema, cellular infiltrate, and keratomalacia are present. The diagnosis was confirmed by detection of hyphae on corneal cytology and during in vivo confocal microscopy examination of the cornea (**b**). Bar = 50 μm

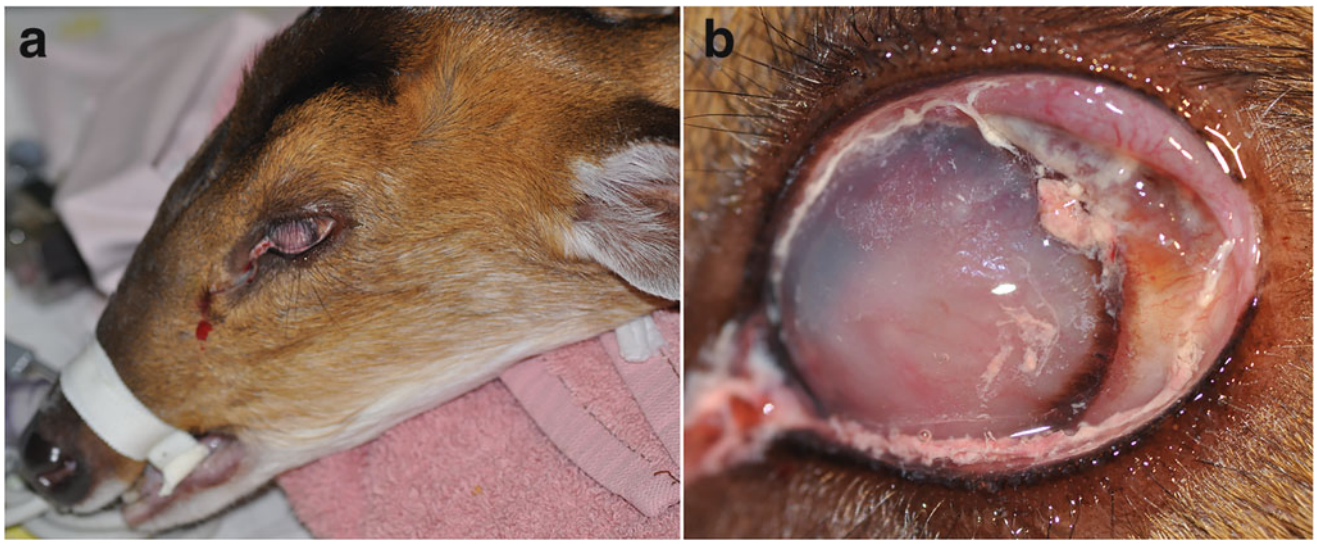

Fig. 32.8 (**a**) Reeve's muntjac (*Muntiacus reevesi*) under general anesthesia for examination and diagnostic testing. (**b**) Conjunctivitis, keratitis, and uveitis in an adult muntjac are potentially associated with a gammaherpesviral infection

A survey describing the incidence of ophthalmic abnormalities in North American bison (*Bison bison*) reported that the most frequently identified ocular lesions were corneal lesions, particularly opacities and evidence of inflammation (Davidson et al. 1999).

Neoplasia

Squamous cell carcinoma is a common tumor of the eye and adnexa in cattle, particularly minimally pigmented breeds that are exposed to high levels of UV radiation. This tumor was recently reported on the conjunctiva of a reindeer (*Rangifer tarandus tarandus*) (Gonzalez-Alonso-Alegre et al. 2013). The affected individual presented with a raised pink, papillomatous white mass of the temporal bulbar conjunctiva adjacent to the limbus. Excision was curative. The tumor exhibited significant nuclear p53 expression suggesting a p53 mutation may have initiated this primary tumor.

Lens

Elk (*Cervus Canadensis)* in Sweden are on occasion reported to behave as if they are blind. In the early 1970s 10 of 17 elk submitted for necropsy were observed to have bilateral cataracts. The cause of the lens lesions was not determined, but the presence of cataract in a fetus of a cataractous elk cow may indicate a congenital or hereditary etiology (Kronevi et al. 1977).

Cataracts may be observed in other pecorans on a sporadic basis. If bilateral and complete, affected individuals usually fail to thrive and have a greater susceptibility to predation. Cataract removal surgery has been attempted in white-tailed deer (*Odocoileus virginianus*) with mixed success. In two wild, rescue, white-tailed deer fawns with presumptive congenital cataracts, thick vitreal opacity was observed following lens extraction (G. Ben-Shlomo, personal communication). Postoperative uveitis may be difficult to control, and secondary glaucoma has occurred. Diligent preoperative investigations into the individual's overall health should be performed before attempting lens extraction (Fig. 32.9). Cataracts that develop secondary to uveitis may have a poorer prognosis with surgery than congenital cataracts.

Both congenital and acquired cataracts occur relatively commonly in domestic populations of reindeer (*Rangifer tarandus tarandus*) (Fig. 32.10), and successful cataract surgery has been performed on multiple reindeer, including both calves and mature individuals (E.C. Ledbetter, personal observation). The surgical techniques used for phacoemulsification in reindeer are predominantly similar to other large ruminants. The cataractous lenses are large, but generally relatively soft. Head positioning and the surgical approach must be carefully planned as their large antlers can interfere with operating microscope positioning and surgeon access to the eye. It is also advisable to avoid elective cataract surgery while the reindeer antlers are covered in velvet as manipulation of the velvet in anesthetized reindeer can result in clinically significant hemorrhage. Compared to white-tailed deer, postoperative uveitis is generally minimal in reindeer after cataract surgery and vision-threatening complications occur infrequently (E.C. Ledbetter, personal observation).

Uveitis

Uveitis in the Ruminantia usually occurs as a manifestation of a systemic disorder or infection. Any condition that results in septicemia or a systemic inflammatory response has the potential to induce uveitis in these species (Fig. 32.11). There are no specific reports of other underlying etiologies of

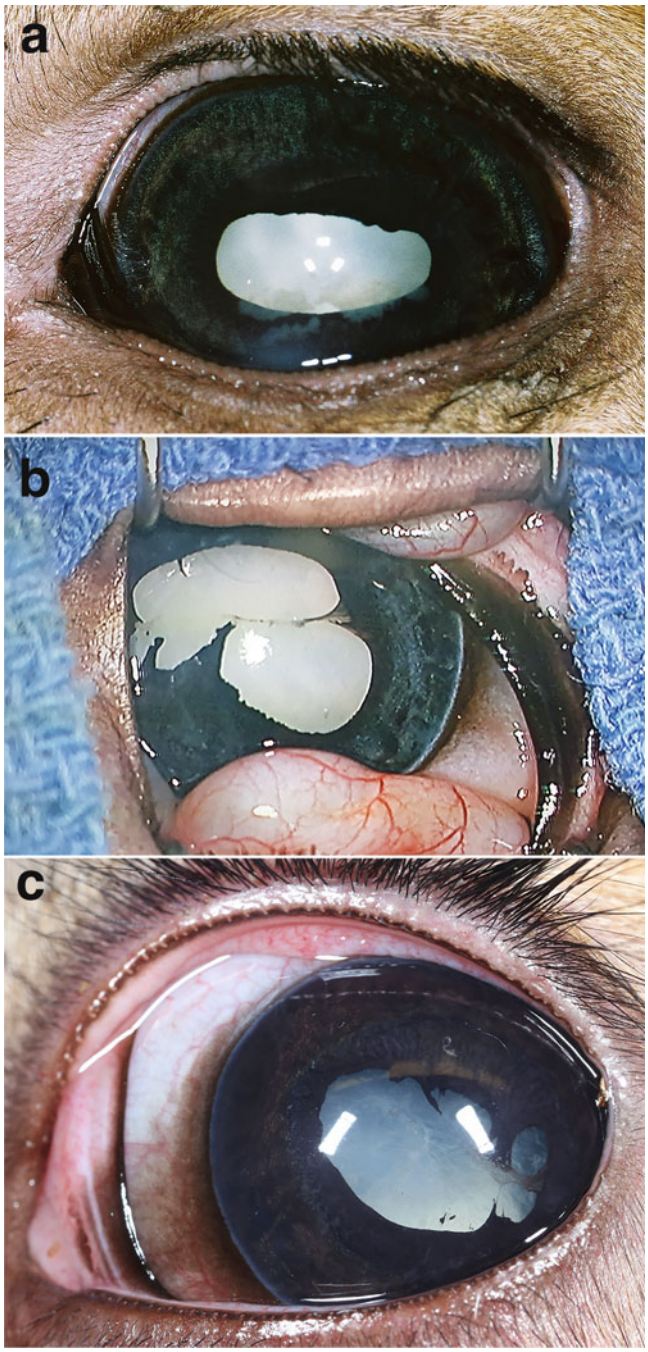

Fig. 32.9 (**a**) Mature cataract in a white-tailed deer (*Odocoileus virginianus*) fawn without clear indications of complications secondary to cataract formation. (**b**, **c**) Mature, intumescent cataract with moderate-to-severe lens-induced uveitis, shallow anterior chamber and posterior synechia in (**b**) a white-tailed deer (*Odocoileus virginianus*) fawn and (**c**) a black-tailed deer (*Odocoileus hemionus*) fawn. **b**—Courtesy of Gil Ben-Shlomo. **c**—Courtesy of Bret A. Moore

intraocular inflammation in pecorans, with the exception of reflex uveitis that may accompany corneal disease. However, most corneal disease that is not traumatically induced is associated with an infectious etiology. Cataracts of rapid

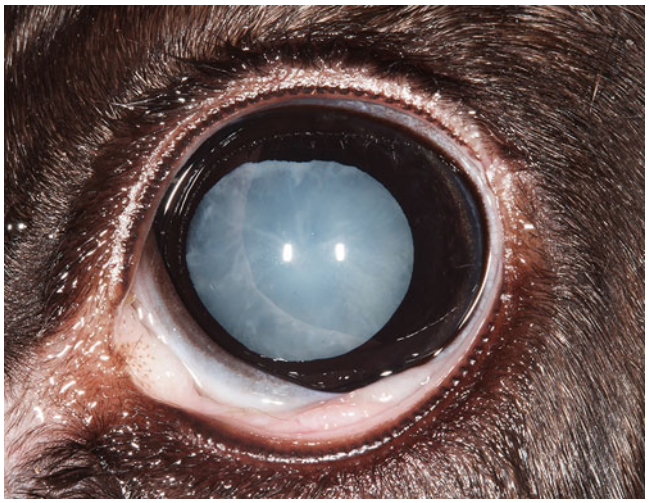

Fig. 32.10 *Mature cataract in a* reindeer (*Rangifer tarandus tarandus*)

onset or long duration may incite lens-induced uveitis or exacerbate pre-existing uveitis in exotic hoofstock (Fig. 32.12). If the individual is amenable to therapy, topical corticosteroids or non-steroidal anti-inflammatory agents and topical cycloplegic/mydriatic agents are indicated to address the uveitis. If topical therapy is not possible, systemic non-steroidal agents may be used.

Ocular disease associated with *Listeria monocytogenes* in fallow deer (*Dama dama*) fed silage has been reported (Welchman et al. 1997). Affected animals developed profuse epiphora and blepharospasm which accompanied severe anterior uveitis. Keratitis was present as well, but the majority of the signs and sequelae were attributable to intraocular inflammation. *L. monocytogenes* was isolated from the conjunctiva of affected animals. Most animals recovered following cessation of silage feeding, although two animals died after neurologic episodes and were observed to have listerial encephalitis.

Malignant catarrhal fever (MCF), a herpesvirus-induced disease mainly of ruminants, has been reported to cause an often fatal necrotizing vasculitis in many species of ungulates. Some species, such as the wildebeest (*Connochaetes gnou*) (alcelaphine herpesvirus-1) and sheep (*Ovis aries*) (ovine herpesvirus-2), appear to be carriers of the virus which is highly pathogenic in other species, especially bison and most cervid species (Schultheiss et al. 1998; Schultheiss et al. 2007; Palmer et al. 2013). Cases of MCF in deer and bison often occur with sudden death. Individuals that do not succumb immediately usually develop hemorrhagic diarrhea, bloody urine, and corneal opacity before expiring. High fever and depression accompany catarrhal inflammation, erosions, and mucopurulent exudation affecting the upper respiratory, ocular, and oral mucosa, swollen lymph nodes, lameness, central nerve system signs, and

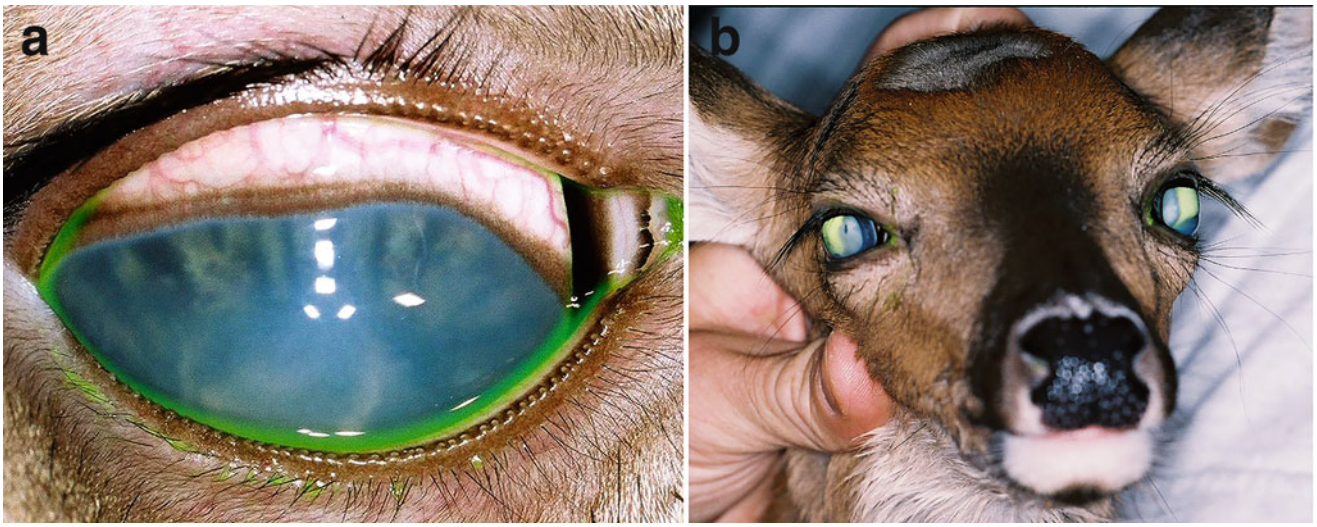

Fig. 32.11 (**a**) Anterior uveitis in a white-tailed deer (*Odocoileus virginianus*) fawn that was septicemic. Note the episcleral injection, corneal edema, miosis, and fibrin in the anterior chamber. (**b**) Same fawn as in (**a**). The uveitis was accompanied by vitritis and cataract development. This individual developed secondary glaucoma. Note the buphthalmos and mydriasis

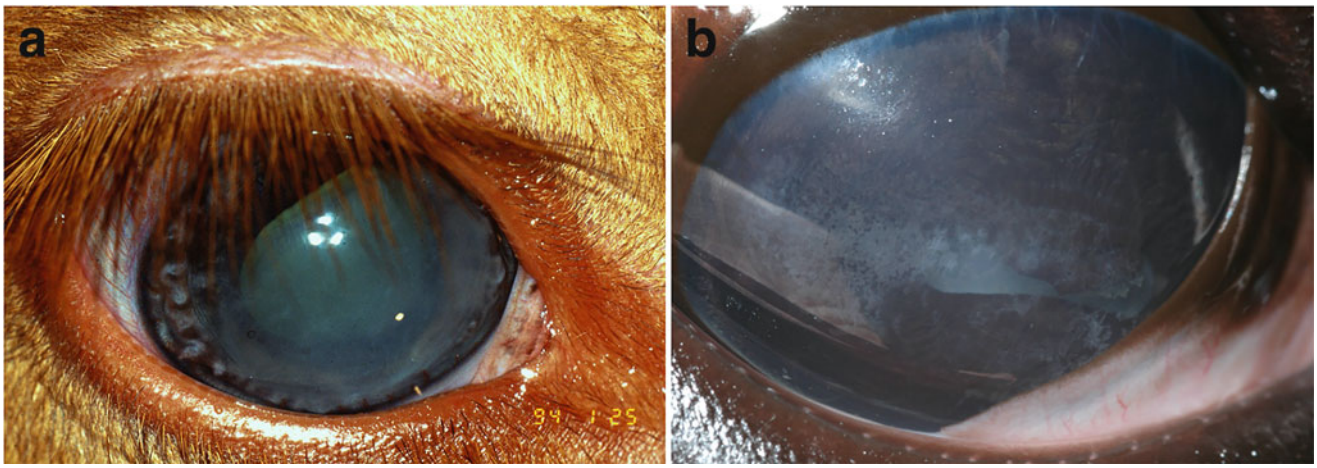

Fig. 32.12 (**a**) Anterior uveitis in a calf (Bos taurus) with septicemia. Note the corneal edema and anterior chamber fibrin. (**b**) Cataract and corneal degeneration in a giraffe (*Giraffa camelopardalis*) calf that had septicemia and uveitis

panophthalmitis. Sheep-associated MCF has been reported in free-ranging moose in Canada and Norway (Neimanis et al. 2009; Vikøren et al. 2015).

In Africa, cattle frequently become infected with malignant catarrhal fever virus following association with latently infected wildebeest. The virus may be isolated from the nasal and ocular secretions of apparently normal wildebeest calves (Mushi et al. 1980). Sika deer (*Cervus nippon*) exposed to wildebeest or infected domestic sheep have been reported to develop fulminant and lethal disease that includes conjunctival hemorrhage and panophthalmitis (Sanford and Little 1977; Zhu et al. 2019). Malignant catarrhal fever in Rusa deer (*Cervus timorensis*) in Australia is associated with a rapid and severe clinical course (Denholm and Westbury 1982). Affected animals develop a fibrinoid necrotizing vasculitis and exhibit acute enteritis with severe diarrhea and wasting and severe bilateral uveitis with marked hypopyon and corneal edema before succumbing or being euthanized. The origin of the infection was not determined but may have resulted from intermingling of sheep carriers with the affected deer. Indian gaur (*Bos gaurus*) and kudu (*Tragelaphus strepsiceros*) have also been reported to develop MCF (Castro et al. 1982).

Severe anterior uveitis associated with fever was found to be related to a bovine herpesvirus 1-related virus in red deer (*Cervus elaphus*) in Scotland (Inglis et al. 1983). Prior to this report, the only disease reported to cause ocular lesions in red deer was MCF. Affected calves in this outbreak did not exhibit classic MCF signs and most recovered with supportive care.

Fig. 32.13 *Parelaphostrongylus tenuis* central nervous system infection in a reindeer (*Rangifer tarandus tarandus*) with severe neurological disease. Ocular lesions included strabismus, facial nerve paralysis, and exposure keratitis

A case of unilateral uveitis due to intraocular nematodiasis caused by *Parelaphostrongylus tenuis*, also known as the meningeal worm, has been reported in an eland antelope (*Taurotragus oryx*) (Gandolf et al. 2003). Infection with this organism is common in white-tailed deer (*O. virginianus*), but is generally non-pathogenic in that species. The diagnosis in the eland calf was made upon histopathologic examination of the enucleated globe. The eland was later euthanized because of progressive, severe neurologic signs associated with its *P. tenuis* infection. *P. tenuis* can cause severe neurologic disease associated with aberrant migration in susceptible hoofstock. Central nervous systemic *P. tenuis* infection in reindeer (*Rangifer tarandu tarandus*) is not infrequent and can be associated with blindness, strabismus, and facial nerve paralysis (Fig. 32.13) (E.C. Ledbetter, personal observation).

Prion Disease

Prion diseases, also known as transmissible spongiform encephalopathies (TSE), are a group of slowly developing fatal neurodegenerations that include sheep and goat scrapie, chronic wasting disease (CWD) in white-tailed deer (*Odocoileus virginianus*), black-tailed deer (*O. hemionus columbianus*), mule deer (*Odocoileus hemionus*), and elk (*Cervus Canadensis*), bovine spongiform encephalopathy in cattle, feline spongiform encephalopathy in eland (*Taurotragus oryx*), nyala (*Tragelaphus angasi*) and kudu (*Tragelaphus strepsiceros)* (as well as cats) and zoological spongiform encephalopathy that occurs in a variety of species including nyala (*Tragelaphus angasii*), Greater kudu (*Tragelaphus strepsiceros*), gemsbok (*Oryx gazelle*), Arabian oryx (*Oryx leucoryx*), Scimitar-horned oryx (*Oryx dammah*), eland (*Taurotragus oryx*), and bison (*Bison bison*) (Ye 2009). In these diseases, a conformational change occurs in the normal prion protein that results in an abnormally folded isoform that accumulates in the nervous tissues and retinas of affected individuals causing vacuolation, gliosis, and neuronal degeneration.

Chronic wasting disease is the most common TSE reported in captive and free-ranging cervids. Clinical signs include behavior changes, mild-to-moderate aggression, excessive salivation, grinding of the teeth, and weight loss leading to emaciation. The disease results from accumulation of an abnormal protein, or prion, in the brains of affected animals. Affected animals become progressively more cognitively impaired in advanced stages of the disease, but often appear to be visually impaired as well. This likely is, at least in part, due to accumulation of the abnormal prion in the retina as well as the visual pathways of the brain in the later stages of the disease. This has been shown to be the case in Rocky Mountain elk (*Cervus elaphus nelson*) (Spraker et al. 2010), white-tailed deer (*O. virginianus*), and mule deer (*O. hemionus*) with CWD as well as in sheep with scrapie and cattle with bovine spongiform encephalopathy (Spraker et al. 2002; Keane et al. 2008; Hortells et al. 2006).

Species-Specific Surveys

A prospective study to establish ocular characteristics, determine the nature and prevalence of ocular lesions in North American bison (*Bison bison*) revealed 15 ocular abnormalities in 13 of the 63 bisons examined. Abnormalities observed included minor ocular discharge in 5 animals, 1 eyelid laceration, 1 periocular *Demodex* spp. infection, 6 corneal abnormalities, 1 anterior synechia, and 1 cataract (Davidson et al. 1999).

A report of the necropsy findings of free-living moose (*Alces alces*) in Canada revealed marked ocular lesions responsible for vision deficits or abnormal behavior in 9% of animals (7/74) submitted for necropsy between 1969 and 1994. Lesions included extensive keratitis and corneal scarring, lymphocytic-plasmacytic anterior uveitis, cataract, and retinal degeneration. An underlying etiology was not determined in any of the cases. The authors of that report surmise that ocular disease may have an important effect on the survival of individual moose (Kuiken et al. 1997).

References

Badger S, Jopp A, Wilson PR et al (1980) A “pinkeye-like” condition in deer. N Z Vet J 28(11):243

Becker D, Tetens J, Brunner A, Bürstel D, Ganter M, Kijas J, International Sheep Genomics Consortium, Drögemüller C (2010) Microphthalmia in Texel sheep is associated with a missense mutation in the paired-like homeodomain 3 (PITX3) gene. PLoS One 5 (1):e8689. https://doi.org/10.1371/journal.pone.0008689

Beitel RJ, Knapp SE, Vohs PA Jr. (1974) Prevalence of eyeworm in three populations of Columbian black-tailed deer in northwestern Oregon. J Parasitol 60(6):972–975. No abstract available

Brightman AH, Wachsstock RS, Erskine R (1991) Lysozyme concentrations in the tears of cattle, goats, and sheep. Am J Vet Res 52(1):9–11

Bubenik A (1990) Epigenetical, morphological, physiological, and behavioral aspects of evolution of horns, pronghorns, and antlers. In: Bubenik G, Bubenik A (eds) Horns, pronghorns, and antlers. Springer, New York

Carlton C, McKean T (1977) The carotid and orbital retia of the pronghorn, deer and elk. Anat Rec 189(1):91–107

Castro AE, Daley GG, Zimmer MA et al (1982) Malignant catarrhal fever in an Indian gaur and greater kudu: experimental transmission, isolation, and identification of a herpesvirus. Am J Vet Res 43(1): 5–11

Clarke LL, Niedringhaus KD, Carmichael KP et al (2018) Congenital ocular abnormalities in free-ranging white-tailed deer. Vet Pathol 55(4):584–590

Coimbra JP, Hart NS, Collin SP et al (2013) Scene from above: retinal ganglion cell topography and spatial resolving power in the giraffe (*Giraffa camelopardalis*). J Comp Neurol 521(9):2042–2057

Colasanti BK (1984) Aqueous humor dynamics in the enucleated deer eye. Comp Biochem Physiol A Comp Physiol 78(4):755–756

Davidson HJ, Vestweber JG, Brightman AH et al (1999) Ophthalmic examination and conjunctival bacteriologic culture results from a herd of North American bison. J Am Vet Med Assoc 215(8): 1142–1144

Denholm LJ, Westbury HA (1982) Malignant catarrhal fever in farmed Rusa deer (*Cervus timorensis*). 1. Clinico-pathological observations. Aust Vet J 58(3):81–87

Dubay SA, Williams ES, Mills K, Boerger-Fields AM (2000a) Bacteria and nematodes in the conjunctiva of mule deer from Wyoming and Utah. J Wildl Dis 36(4):783–787

Dubay SA, Williams ES, Mills K et al (2000b) Association of *Moraxella ovis* with keratoconjunctivitis in mule deer and moose in Wyoming. J Wildl Dis 36(2):241–247

Edmunds DR, Williams ES, O'Toole D et al (2008) Ocular plague (*Yersinia pestis*) in mule deer (*Odocoileus hemionus*) from Wyoming and Oregon. J Wildl Dis 44(4):983–987

Featherstone HJ, Heinrich CL (2013) Ophthalmic examination and diagnostics. In: Gelatt KN, Gilger BC, Kern TJ (eds) Veterinary ophthalmology, 5th edn. Wiley-Blackwell, Ames, Iowa

Fernández-Aguilar X, Cabezón O, Marco I et al (2013) *Mycoplasma conjunctivae* in domestic small ruminants from high mountain habitats in Northern Spain. BMC Vet Res 9:253

Flower W (1883) On the arrangement of the orders and families of existing Mammalia. Proc Zool Soc Lond, pp 178–186

Fulton AB, Albert DM, Buyukmihci N et al (1977) Spontaneous anophthalmia and microphthalmia in white-tailed deer. J Comp Pathol 87(4):557–568. No abstract available

Gandolf AR, Atkinson MW, Gemensky AJ et al (2003) Intraocular nematodiasis caused by *Parelaphostrongylus tenuis* in an eland antelope (*Taurotragus oryx*). J Zoo Wildl Med 34(2):194–199

Gaudie C, Fletcher J, Williams D et al (2012) Severe ocular dysplasia in British red deer (*Cervus elaphus*). Vet Rec 170(14):369–370

Gelmetti D, Bertoletti I, Giudice C (2010) Bilateral complex microphthalmia with intraocular dermoid cyst in a neonate red deer (*Cervus elaphus*). J Wildl Dis 46(3):961–965

Gomez W, Patterson TA, Swinton J et al. (2019) Bovidae: antelopes, cattle, gazelles, goats, sheep, and relatives. Animal Diversity Web. University of Michigan Museum of Zoology. Retrieved 3 September 2019

Gonzalez-Alonso-Alegre EM, Rodriguez-Alvaro A, Martinez-Nevado-E, Martinez-de-Merlo EM, Sanchez-Maldonado B (2013) Conjunctival squamous cell carcinoma in a reindeer (*Rangifer tarandus tarandus)*. Vet Ophthalmol 16(Suppl 1):113–116

Gonzalez-Soriano J, Mayayo-Vicente S, Martinez-Sainz P et al (1997) A quantitative study of ganglion cells in the goat retina. Anat Histol Embyol 26:39–44

Handeland K, Madslien K, Bretten T et al (2020) Mycoplasma conjunctivae-associated keratoconjunctivitis in Norewegian muskox (*Ovibos moschatus*). J Wildl Dis 56(2). https://doi.org/10.7589/2019-04-103

Hebel R (1979) Distribution of retinal ganglion cells in five mammalian species. Anat Embryol (Berl) 150:45–51

Hebel R, Hollander H (1979) Size and distribution of ganglion cells in the bovine retina. Vis Res 19:667–673

Hogg C, Neveu M, Stokkan KA et al (2011) Arctic reindeer extend their visual range into the ultraviolet. J Exp Biol 214(Pt 12):2014–2019

Hortells P, Monzon M, Monleon E et al (2006) Pathological findings in the retina and visual pathways associated to natural scrapie in sheep. Brain Res 1108:188–194

Howard DR, Krehbiel JD, Fay LD et al (1976) Visual defects in white-tailed deer from Michigan six case reports. J Wildl Dis 12(2): 143–147

Hughes A, Whittridge D (1973) The receptive fields and topographic organization of goat retinal ganglion cells. Vis Res 13:1101–1114

Inglis DM, Bowie JM, Allan MJ et al (1983) Ocular disease in red deer calves associated with a herpesvirus infection. Vet Rec 113(8): 182–183

Ishengoma E, Agaba M, Cavener DR (2017) Evolutionary analysis of vision genes identifies potential drivers of visual differences between giraffe and okapi. PeerJ 5:e3145

Jacobs GH, Deegan JF 2nd, Neitz J et al (1994) Electrophysiological measurements of spectral mechanisms in the retinas of two cervids: white-tailed deer (*Odocoileus virginianus*) and fallow deer (*Dama dama*). J Comp Physiol A 174(5):551–557

Janis C, Scott K (1987) The interrelationships of higher ruminant families with special emphasis on the members of the Cervoidea. Am Mus Novit 2893:1–85

Keane DP, Barr DJ, Boschler PN et al (2008) Chronic wasting disease in a Wisconsin captive white-tailed deer farm. J Vet Disgn Invest 20: 698–703

Kennedy MJ, Moraiko DT, Treichel B (1993) First report of immature *Thelazia skrjabini* (Nematoda: Thelazioidea) from the eye of a white-tailed deer, *Odocoileus virginianus*. J Wildl Dis 29(1): 159–160

Klećkowska-Nawrot JE, Goździewska-Harłajczuk K, Barszcz K (2019) Comparative study of the eyelids and orbital glands morphology in the okapi (*Okapia johnstoni*, Giraffidae), Père David's deer (*Elaphurus davidianus*, Cervidae) and the Philippine mouse-deer (*Tragulus nigricans*, Tragulidae). Histol Histopathol 18144. https://doi.org/10.14670/HH-18-144

Kronevi T, Holmberg B, Borg K (1977) Lens lesions in the elk. Acta Vet Scand 18(2):159–167

Kuiken T, Grahn B, Wobeser G (1997) Pathology of ocular lesions in free-living moose (*Alces alces*) from Saskatchewan. J Wildl Dis 33(1):87–94

Kummeneje K (1976) Isolation of *Neisseria ovis* and a *Colesiota conjunctivae*-like organism from cases of kerato-conjunctivitis in reindeer in northern Norway. Acta Vet Scand 17(1):107–108

Kvapil P, Pirš T, Slavec B, Luštrik R, Zemljič T, Bártová E, Stranjac B, Kastelic M (2018) Tear production, intraocular pressure and conjunctival bacterial flora in selected captive wild ruminants. Vet Ophthalmol 21(1):52–57. https://doi.org/10.1111/vop.12478

LaDouceur EE, Ernst J, Keel MK (2012) Unilateral corneoscleral choristomas (corneal dermoids) in a white-tailed deer (*Odocoileus virginianus*). J Wildl Dis 48(3):826–828

Literák I, Tomita Y, Ogawa T, Shirasawa H, Smíd B, Novotny L, Adamec M (2006) Papillomatosis in a European bison. J Wildl Dis 42(1):149–153

Martins BC, Oriá AP, Souza AL, Campos CF, Almeida DE, Duarte RA, Soares CP, Zuanon JA, Neto CB, Duarte JM, Schocken-Iturrino RP, Laus JL (2007) Ophthalmic patterns of captive brown brocket deer (*Mazama gouazoubira*). J Zoo Wildl Med 38(4):526–532

Mavrot F, Vilei EM, Marreros N, Signer C, Frey J, Ryser-Degiorgis MP (2012) Occurrence, quantification, and genotyping of *Mycoplasma conjunctivae* in wild Caprinae with and without infectious keratoconjunctivitis. J Wildl Dis 48(3):619–631

Mayer D, Degiorgis MP, Meier W, Nicolet J, Giacometti M (1997) Lesions associated with infectious keratoconjunctivitis in alpine ibex. J Wildl Dis 33(3):413–419

Meagher M, Quinn WJ, Stackhouse L (1992) Chlamydial-caused infectious keratoconjunctivitis in bighorn sheep of Yellowstone National Park. J Wildl Dis 28(2):171–176. https://doi.org/10.7589/0090-3558-28.2.171

Monk CM, Childress AL, Bercier M, Whitley RD, Wellehan JFX (2015) Identification of a novel gammaherpesvirus in the conjunctiva of a Reeve's muntjac (*Muntiacus reevesi)*. In: Proceedings of the American College of Veterinary Ophthalmologists Annual Meeting

Mushi EZ, Karstad L, Jessett DM (1980) Isolation of bovine malignant catarrhal fever virus from ocular and nasal secretions of wildebeest calves. Res Vet Sci 29(2):168–171

Mutinelli F, Vercelli A, Carminato A, Luchesa L, Pasolli C, Cova M, Marchioro W, Melchiotti E, Vascellari M (2012) Bilateral microphthalmia and aphakia associated with multiple eye abnormalities in a free-living European red deer calf (*Cervus elaphus*). J Vet Med Sci 74(4):527–529

Neimanis AS, Hill JE, Jardine CM, Bollinger TK (2009) Sheep-associated malignant catarrhal fever in free-ranging moose (*Alces alces*) in Saskatchewan, Canada. J Wildl Dis 45(1):213–217

Ninomiya H, Masui M (1999) Vasculature of the orbital rete in the Japanese deer (*Cervus nippon*). Vet Ophthalmol 2(2):107–112

O'Brien HD, Bourke J (2015) Physical and computational fluid dynamics models for the hemodynamics of the artiodactyl carotid rete. J Theor Biol 386:122–131

O'Brien HD, Gignac PM, Hieronymus TL, Witmer LM (2016) A comparison of postnatal arterial patterns in a growth series of giraffe (Artiodactyla: *Giraffa camelopardalis*). PeerJ 4:e1696. https://doi.org/10.7717/peerj.1696

Ofri R, Horowitz IH, Kass PH (1998) Tonometry in three herbivorous wildlife species. Vet Ophthalmol 1(1):21–24

Ofri R, Horowitz I, Kass PH (1999) Tear production in three captive wild herbivores in Israel. J Wildl Dis 35(1):134–136

Ofri R, Horowitz IH, Kass PH (2000) How low can we get? Tonometry in the Thomson gazelle (*Gazella thomsoni*). J Glaucoma 9(2): 187–189

Ofri R, Horowitz H, Levison M, Kass PH (2001) Intraocular pressure and tear production in captive eland and fallow deer. J Wildl Dis 37(2):387–390

Ofri R, Millodot S, Tadmor Y, Matalon E, Kass PH, Horowitz IH, Millodot M (2004) The development of the refractive state in the newborn Thomson gazelle. J Comp Physiol A Neuroethol Sens Neural Behav Physiol 190(10):831–835. Epub 2004 Aug 12

Oriá AP, Gomes Junior DC, Oliveira AV, Curvelo VP, Estrela-Lima A, Pinna MH, Meneses ÍD, Filho EF, Ofri R (2015) Selected ophthalmic diagnostic tests, bony orbit anatomy, and ocular histology in sambar deer (*Rusa unicolor*). Vet Ophthalmol 18(Suppl 1):125–131. https://doi.org/10.1111/vop.12221

Palmer MV, Thacker TC, Madison RJ, Koster LG, Swenson SL, Li H (2013) Active and latent ovine herpesvirus-2 (OvHV-2) infection in a herd of captive white-tailed deer (*Odocoileus virginianus*). J Comp Pathol 149(2–3):162–166

Pearson AB (1984) A possible cause for the 'pink-eye-like' condition in red deer. N Z Vet J 32(7):119

Pinard CL, Weiss ML, Brightman AH, Fenwick BW, Davidson HJ (2003) Evaluation of lysozyme and lactoferrin in lacrimal and other ocular glands of bison and cattle and in tears of bison. Am J Vet Res 64(1):104–108

Rehbinder C (1977) Keratitis in reindeer. Relation to the presence of 1st instar larvae of the nostril fly (*Cephenomyia trompe L*) in the conjunctival sac and to natural ultraviolet radiation. Acta Vet Scand 18(1):75–85

Rehbinder C, Glatthard V (1977) Keratitis in reindeer. Relation to bacterial infections. Acta Vet Scand 18(1):54–64

Rehbinder C, Winqvist G, Roos C (1977) Structure of the cornea in some cervidae. Acta Vet Scand 18(2):152–158

Rehorek SJ, Hillenius WJ, Sanjur J, Chapman NG (2007) One gland, two lobes: organogenesis of the "Harderian" and "nictitans" glands of the Chinese muntjac (*Muntiacus reevesi*) and fallow deer (*Dama dama*). Ann Anat 189(5):434–446

Sánchez Romano J, Mørk T, Laaksonen S, Ågren E, Nymo IH, Sunde M, Tryland M (2018) Infectious keratoconjunctivitis in semi-domesticated Eurasian tundra reindeer (*Rangifer tarandus tarandus*): microbiological study of clinically affected and unaffected animals with special reference to cervid herpesvirus 2. BMC Vet Res 14(1):15. https://doi.org/10.1186/s12917-018-1338-y

Sánchez Romano J, Leijon M, Hagström Å, Jinnerot T, Rockström UK, Tryland M (2019) *Chlamydia pecorum* associated with an outbreak of infectious Keratoconjunctivitis in semi-domesticated reindeer in Sweden. Front Vet Sci 6:14

Sanford SE, Little PB (1977) The gross and histopathologic lesions of malignant catarrhal fever in three captive sika deer (Cervus nippon) in southern Ontario. J Wildl Dis 13(1):29–32

Schultheiss PC, Collins JK, Austgen LE, DeMartini JC (1998) Malignant catarrhal fever in bison, acute and chronic cases. J Vet Diagn Investig 10(3):255–262

Schultheiss PC, Van Campen H, Spraker TR, Bishop C, Wolfe L, Podell B (2007) Malignant catarrhal fever associated with ovine herpesvirus-2 in free-ranging mule deer in Colorado. J Wildl Dis 43(3):533–537

Shinozaki A, Hosaka Y, Imagawa T, Uehara M (2010) Topography of ganglion cells and photoreceptors in the sheep retina. J Comp Neurol 518:2305–2315

Smits SL, Schapendonk CM, van Leeuwen M, Kuiken T, Bodewes R, Stalin Raj V, Haagmans BL, das Neves CG, Tryland M, Osterhaus AD (2013) Identification and characterization of two novel viruses in ocular infections in reindeer. PLoS One 8(7):e69711. https://doi.org/10.1371/journal.pone.0069711

Somma AT, Moura CM, Lange RR, Medeiros RS, Montiani-Ferreira F (2016) Congenital cataract associated with persistent hyperplastic primary vitreous and persistent tunica vasculosa lentis in a sambar deer (*Rusa unicolor*) - clinical, ultrasonographic, and histological findings. Clin Case Rep 4(7):636–642. https://doi.org/10.1002/ccr3.500

Spraker TR, Zink RR, Cummings BA, Sigurdson CJ, Miller MW, O'Rourke KI (2002) Distribution of protease-resistant prion protein and spongiform encephalopathy in free-ranging mule deer (*O. hemionus*) with chronic wasting disease. Vet Pathol 39:546–556

Spraker TR, O'Rourke KI, Gidlewski T, Powers JG, Greenlee JJ, Wild MA (2010) Detection of the abnormal isoform of the prion protein associated with chronic wasting disease in the optic pathways of the brain and retina of Rocky Mountain elk (*Cervus elaphus nelsoni*). Vet Pathol 47(3):536–546

Stokkan KA, Folkow L, Dukes J, Neveua M, Hogg C, Siefken S, Dakin SC, Jeffrey G (2013) Shifting mirrors: adaptive changes in retinal reflections to winter darkness in Arctic reindeer. Proc R Soc B 280: 20132451. https://doi.org/10.1098/rspb.2013.2451

Strauss WM, Hetem RS, Mitchell D, Maloney SK, Meyer LC, Fuller A (2016) Three African antelope species with varying water dependencies exhibit similar selective brain cooling. J Comp Physiol B 186(4):527–540

Taylor SK, Vieira VG, Williams ES, Pilkington R, Fedorchak SL, Mills KW, Cavender JL, Boerger-Fields AM, Moore RE (1996) *Infectious keratoconjunctivitis in free-ranging mule deer* (*Odocoileus hemionus*) from Zion National Park, Utah J Wildl Dis 32(2): 326–330

Tryland M, Das Neves CG, Sunde M, Mørk T (2009) Cervid herpesvirus 2, the primary agent in an outbreak of infectious keratoconjunctivitis in semidomesticated reindeer. J Clin Microbiol 47(11): 3707–3713. https://doi.org/10.1128/JCM.01198-09

Tryland M, Romano JS, Marcin N, Nymo IH, Josefsen TD, Sørensen KK, Mørk T (2017) Cervid herpesvirus 2 and not *Moraxella bovoculi* caused keratoconjunctivitis in experimentally inoculated semi-domesticated Eurasian tundra reindeer. Acta Vet Scand 59(1): 23. https://doi.org/10.1186/s13028-017-0291-2

van der Linde-Sipman JS, van den Ingh TSGAM, Vellema P (2003) Morphology and morphogenesis of hereditary microphthalmia in Texel sheep. J Comp Pathol 128(4):269–275. https://doi.org/10.1053/jcpa.2002.0632

Vestweber JG, Ridley RK, Nietfeld JC, Wilkerson MJ (1999) Demodicosis in an American bison. Can Vet J 40(6):417–418

Vikøren T, Klevar S, Li H, Hauge AG (2015) A geographic cluster of malignant catarrhal fever in moose (Alces alces) in Norway. J Wildl Dis 51(2):471–474

Villar T, Pascoli AL, Klein A et al (2019) Tear production, intraocular pressure, and central corneal thickness in white-tailed deer (*Odocoileus virginianus*). Vet Ophthalmol 15

Walker ML, Becklund WW (1971) Occurrence of a cattle eyeworm, Thelazia gulosa (Nematoda: Thelaziidae), in an imported giraffe in California and T. lacrymalis in a native horse in Maryland. J Parasitol 57(6):1362–1363

Webber J, Selby L (1981) A survey of white-tailed deer (*Odocoileus virginianus*) for evidence of *Moraxella bovis* infection. J Wildl Dis 17(1):9–10

Welchman D, Hooton JK, Low JC (1997) Ocular disease associated with silage feeding and *Listeria monocytogenes in fallow deer*. Vet Rec 140(26):684–685. No abstract available

Williams ES, Becerra VM, Thorne ET, Graham TJ, Owens MJ, Nunamaker CE (1985) Spontaneous poxviral dermatitis and keratoconjunctivitis in free-ranging mule deer (Odocoileus hemionus) in Wyoming. J Wildl Dis 21(4):430–433. https://doi.org/10.7589/0090-3558-21.4.430

Winqvist G, Rehbinder C (1973) Fine structure of the reindeer cornea in normal conditions and in keratitis. Acta Vet Scand 14(2):292–300. https://doi.org/10.1186/BF03547447

Witzel DA, Springer MD, Mollenhauer HH (1978) Cone and rod photoreceptors in the white-tailed deer *Odocoileus virginianus*. Am J Vet Res 39(4):699–701

Ye X (2009) Visual pathology in animal prion diseases. Histol Histopathol 24(12):1563–1577

Zhu H, Sun N, Li Y et al (2019) Malignant catarrhal fever: an emerging yet neglected disease in captive sika deer (Cervus nippon) herds in China. Transbound Emerg Dis 67(1):149–158

Ophthalmology of Tylopoda: Camels, Alpacas, Llamas, Vicunas, and Guanacos

33

Eric C. Ledbetter

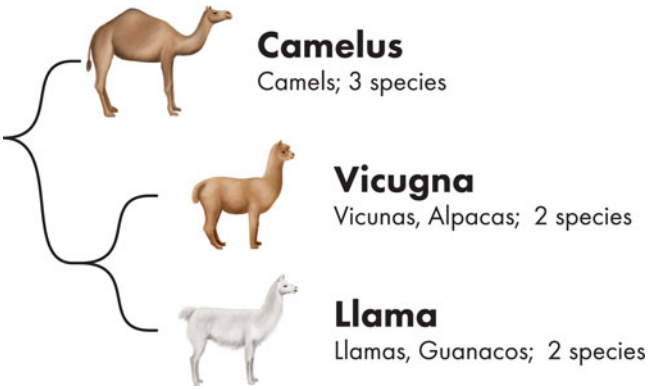

Introduction

The family Camelidae comprises the only extant members of the suborder Tylopoda and includes the Afro-Asian and South American camelid species. The Afro-Asian, or Old World, camelids include the domestic Bactrian camel (*Camelus bactrianus*), wild Bactrian camel (*Camelus ferus*), and domestic dromedary camel (*Camelus dromedaries*). Wild Bactrian camel populations are restricted to northern China and southern Mongolia and are genetically distinct species to their domesticated relatives. Although no true wild populations of dromedary camels exist, there are several feral populations present in different regions of the globe, with a notably large population residing in the Australian Outback. The South American, or New World, camelids include the domesticated alpaca (*Vicugña pacos*) and llama (*Lama glama*) and the wild guanaco (*Lama guanaco*) and vicuña (*Vicugña vicugña*). As the name implies, all South American camelids were originally native to South American.

Although each camelid species possesses unique characteristics, all are herbivorous, two-toed ungulates. In many regions of the world, the Afro-Asian camelids are used as transportation, pack animals, food sources (both meat and dairy), in sports racing, and camel hair is utilized in the textile industry. With their popularity growing as both fiber-producing and companion animals, South American camelids are now distributed worldwide. Ocular disease is encountered frequently by clinicians treating camelids and may be associated with a diverse array of potential etiologies. Congenital ocular abnormalities and ocular trauma are especially common and important ophthalmic conditions of the camelids.

E. C. Ledbetter (✉)
Department of Clinical Sciences, Cornell University, Ithaca, NY, USA
e-mail: ecl32@cornell.edu

F. Montiani-Ferreira et al. (eds.), *Wild and Exotic Animal Ophthalmology*, https://doi.org/10.1007/978-3-030-81273-7_8

Ocular Anatomy

Camelids possess prominent eyes, and their globes are relatively large relative to their head size. The eyes are laterally positioned on the skull, and this combined with their long and highly mobile neck, provides a broad field of view and protection from predators. Camelids have an enclosed orbit that is entirely bordered by bone. Prominent supraorbital ridges are present that provide additional protection for the globes.

Detailed gross and histologic investigations of many aspects of the ocular anatomy of dromedary camels are available; however, much less published information is obtainable for the other species of camelids. In an ocular ecobiometry study of dromedary camels, the mean axial globe length was 29.8 mm, and the mean sagittal globe length was 33.0 mm (El-Tookhy et al. 2012). The frontal bone forms the roof of the dromedary camel orbit and a portion of the medial wall, the zygomatic process of the frontal bone extends laterally and contributes a large portion of the roof and lateral wall of the orbit, the presphenoid bone forms the caudomedial aspect of the orbit, the palatine bone comprises a segment of the ventromedial wall, the maxilla contributes a small area to the rostral ventral part of the orbital wall, the lacrimal bone forms a portion of the medial and rostral wall, and the zygomatic bone forms the greater portion of the rostral and ventral margin of the orbital rim and the rostroventral part of the orbital wall (Abuagla et al. 2016). The principle arterial blood supply of the orbit and globe of the Bactrian and dromedary camels is described and includes the external ophthalmic artery, external ethmoidal artery, malar artery, ophthalmic rete mirabile, and the rostral epidural rete mirabile (Smuts and Bezquidenhout 1987; Wang 2002).

Similar to many other mammals, camelids possess seven ocular muscles that include dorsal rectus, ventral rectus, medical rectus, lateral rectus, dorsal oblique, ventral oblique, and retractor bulbi (Abuagla et al. 2016). Motor innervation of these muscles is also similar to other mammals that have been evaluated and includes the oculomotor, trochlear, and abducens nerves (Jaint et al. 2010). These nerves travel through the orbitorotundum foramen (Badawy and Eshra 2018).

An ultrasonographic and macroscopic biometric study of the dromedary camel globe was performed to provide reference anatomical measurements (Kassab 2012). In adult camels, the axial globe length was 31.4 mm when measured by ultrasound and 33.0 mm when measured by macroscopic evaluation. The anterior chamber depth was 5.8 mm by ultrasound and 6.5 mm by macroscopic evaluation. Vitreal chamber depth was 18.61 mm by ultrasound and 17.9 mm by macroscopic evaluation (Kassab 2012).

The dromedary camel Harderian gland (sometimes also referred to as the deep gland of the nictitans membrane) is located in the medial orbit and is a compound tubuloalveolar mucous gland. The gland is composed of glandular acini lined with pyramidal cells that can be differentiated into three distinct cell types on the basis of nuclear morphology: type I cells have round to oval nuclei with uniform distribution of fine chromatin material; type II cells contain smaller, round nuclei that stain darkly; and type III cells have the largest nuclei that stain lightly (Kumar et al. 2003). Myoepithelial cells and unmyelinated nerve terminals are present within the gland and together are believed to function as a unit of contractile elements and regulators of fluid transport (Abou-Elmagd 1992).

The camelid eyelids possess numerous long eyelashes and several sets of vibrissae (Fig. 33.1). South American camelids are unusual as their eyelids are devoid of meibomian glands. In these camelid species, sebaceous glands located in the medial canthi are believed to contribute to the lipid layer of the trilaminar tear film (Fig. 33.2). In contrast, dromedary camels are described as possessing meibomian glands, but they are restricted to the superior eyelid (Fahmy et al. 1971). These dromedary camel tarsal glands are simple branched mucous tubular glands with excretory ducts opening into the palpebral conjunctival along the posterior margin of the eyelid.

Although generally appearing histologically and clinically similar to other ungulates, the Afro-Asian camels' nictitans membranes are commonly described as semi-transparent, and this is speculated to be an adaptation at allowing ocular surface protection during sand storms while permitting

Fig. 33.1 Lateral view of a Bactrian camel's numerous long eyelashes and sets of vibrissae

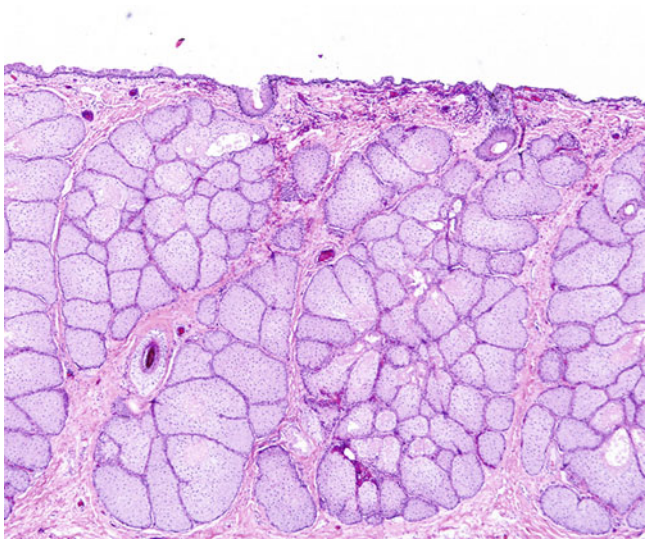

Fig. 33.2 Histologic photomicrograph of the sebaceous glands located in the medial canthus of a llama

some level of vision. Detail histologic studies of the dromedary camel nictitans membrane have been performed and found that both the bulbar and palpebral surfaces are covered with stratified squamous, nonkeratinized epithelium (Al-Ramadan and Ali 2012). The bulbar surface of the nictitans contains numerous goblet cells that are concentrated at their base. The nictitans cartilage is composed of two parts: A T-shaped segment within the membrane of the third eyelid that runs parallel to the free margin and a narrow root-shaped appendix embedded within the gland of the third eyelid (Al-Ramadan and Ali 2012). There are conflicting descriptions of the type of cartilage that is present in the dromedary camel nictitans membrane, including descriptions of both hyaline and elastic cartilage (Al-Ramadan and Ali 2012; Mohammadpour 2009). The oval-shaped gland of the nictitans membrane is a tubuloalveolar serous gland (Mohammadpour 2009). The gland contains two distinct types of secretory units that include acini with a small lumen lined with tall pyramidal cells and tubules with a large lumen lined with cuboidal epithelial cells (Al-Ramadan and Ali 2012). In prior studies, no muscle was found within the nictitating membrane, and movement was therefore determined to be passive (Al-Ramadan and Ali 2012; Mohammadpour 2009).

The highly unusual lacrimal apparatus of the dromedary camel has been extensively studied. The dromedary camel lacrimal gland is located dorsolateral to the globe on the inner surface of the supraorbital process of the frontal bone and the frontal process of the zygomatic bone (Mohammadpour 2008). The gland possesses an irregular flattened and elongated lobular shape and is relatively small for an animal of this size (Alsafy 2010). The camel lacrimal gland contains 2–4 excretory ducts that open into the superior conjunctival fornix (Awkati and Al-Bagdadi 1971; Ibrahim et al. 2006). A highly unusual feature of the dromedary camel eye is the absence of both superior and inferior lacrimal puncta (Abdalla et al. 1970; Alsafy 2010; Ibrahim et al. 2006). In these camels, the apparently nonfunctional nasolacrimal system starts blindly adjacent to both eyelid margins, the canaliculi open into the lacrimal sac, and then the nasolacrimal duct travels in an S-shaped course to the medial wall of the nasal vestibule at the junction between the mucous membrane and skin where a small opening (approximately 0.1 cm) has been described (Alsafy 2010; Ibrahim et al. 2006; Shokry et al. 1987). The physiologic and clinical significance of a non-patent nasolacrimal drainage system is unknown as only tear evaporation, and eyelid overflow appears to allow tear egress from the ocular surface in this species. This unusual anatomy has been speculated to be an adaptation to the adverse climates and sandy environments in which dromedary camels evolved, where continuous lacrimal flow is required to cleanse the ocular surface, and the absence of puncta prevents their occlusion by sand and other small environmental particles (Sadegh and Shadkhast 2007). If not representative of an ongoing evolutionary loss of the lacrimal drainage system, other authors have speculated that the presence of a well-developed lacrimal sac and nasolacrimal duct without patent puncta could suggest other possible and unidentified system functions (Ali et al. 2019).

In contrast to dromedary camels, large superior and inferior lacrimal puncta are located adjacent to the medial canthus in South American Camelids (Ali et al. 2019; Sapienza et al. 1992). These slit-like openings are 1–2 mm in diameter and located approximately 4–6 mm from the medial canthus. In llamas, the paired canaliculi are 2–4 mm in length and converge into a relatively poorly developed lacrimal sac that sits in the lacrimal fossa of the lacrimal bone (Sapienza et al. 1992). The nasolacrimal duct originates from the lacrimal sac, travels through the osseous lacrimal canal of the lacrimal bone for approximately 2 cm, and then transverses the nasal cavity in a sigmoid fashion covered only by soft tissue (Sapienza et al. 1992). The nasolacrimal duct ultimately ends in a 2–3 mm orifice at the caudoventral margin of the nasal vestibule near the mucocutaneous junction of the nares. The total length of the nasolacrimal duct in llamas varies from approximately 10 cm in young animals up to approximately 15 cm in mature llamas (Sapienza et al. 1992).

Similar too many other mammals, camel tears contain lysozyme, lipocalin, lactoferrin, serum albumin, and immunoglobulins (Gionfriddo et al. 2000; Shamsi et al. 2011). A gas chromatography-mass spectroscopy and inductively-coupled plasma mass spectroscopy study of camel tears reported that the major compounds detected in tears were alanine, valine, leucine, norvaline, glycine, cadaverine, urea, ribitol, sugars, and higher fatty acids (including octadecanoic acid and hexadecanoic acid) (Ahamad et al.

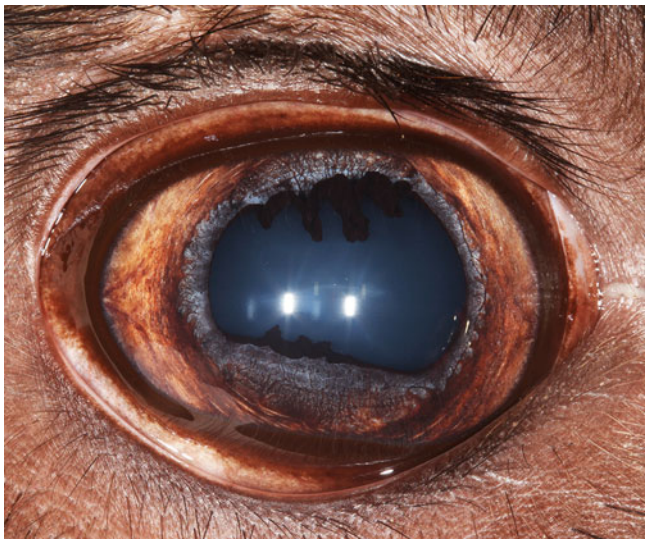

Fig. 33.3 Normal anterior segment of a Bactrian camel

2017). The precorneal tear film of dromedary camels contains oily droplet-like structures that may be an adaptation to dry climates (Am et al. 2018). A seasonal variation in tear proteins was also identified in dromedary camels in Saudi Arabia and thought to represent an adaptation to survival in the extreme desert conditions that are characterized by hot, dry, and dusty summer seasons with extremely cold and rainy winter seasons (Shamsi et al. 2011).

The camelid cornea is large with tightly adherent eyelids, which normally results in minimal conjunctiva visible through the palpebral fissure. Dense limbal and peripheral corneal epithelial pigmentation is a common finding in camelid species and may serve as protection from ultraviolent radiation (Fig. 33.3) (Abuagla et al. 2016). The characteristic peripheral corneal pigment is not an acquired ocular feature in dromedary camels, as its prenatal development has been characterized (Abdo et al. 2014). The basic anatomy of the camelid cornea is similar to other ungulates; however, several anatomical features of the dromedary camel are notable. The total corneal thickness in one study of dromedary camels was 629 μm; however, the epithelium was composed of approximately 13 cellular layers and was remarkably thick (227 μm and 36% of total corneal thickness) (Almubrad and Akhtar 2012). It was suggested that the thicker epithelium and thinner stroma might be an adaptation to hot and arid climates as this would theoretically decrease stromal fluid evaporation, require the endothelium to regulate the hydration of a smaller amount of tissue, and ultimately assist in the regulation of corneal hydration (Almubrad and Akhtar 2012). Corneal thickness measurements in alpacas performed in vivo using spectral-domain optical coherence tomography identified a relatively thinner corneal epithelium. In one study, the mean total corneal thickens in alpacas was 634.8 μm, and the mean corneal epithelium thickness was 147.4 μm (LoPinto et al. 2017b).

Descemet's membrane in the dromedary camel has been repeatedly noted to be remarkably thick and averaged 5.5 μm in one study (Rahi et al. 1980; Almubrad and Akhtar 2012). Evaluation of the ultrastructural features of the dromedary camel cornea determined that the proteoglycans within the posterior corneal stroma were significantly larger in size and greater in number those what was present in the anterior and midstroma (Almubrad and Akhtar 2012). A defined Bowman's layer was absent; however, a thin layer of dense and fine collagen fibrils was present below the epithelial basement membrane suggesting the presence of a rudimentary structure similar to Bowman's layer. The mean collagen fibril diameter in the camel cornea was measured at 25 nm (Almubrad and Akhtar 2012). A study comparing the propensity of the camel and bovine corneal stroma to swell when hydrated determined the camel cornea develops more rapid and prominent swelling under some conditions; however, the structural and biochemical reasons for this were not identified (Almubrad et al. 2010). Another study evaluated the ultrastructure alterations of the dromedary camel corneal stroma associated with hydration and determined the interfibrillar spacing of the anterior, mid-, and posterior stroma all increased in contrast to human corneas where the anterior stroma is spared (Akhtar 2013). The camel stromal hydration was associated with a fivefold increase in thickness in 24 h, which was much greater than the 2.33 increase noted in human corneas under similar conditions and suggesting a greater potential for the development of severe corneal edema (Muller et al. 2001).

The anterior chamber is deep, and iris pigmentation varies from light blue to dark brown in camelids. Heterochromia iridum and iridis are both common. Camelids possess a horizontal, oval pupil. The alpaca iris possesses an incomplete major arterial circle with bifurcation into superior and inferior components occurring prior to the arteries entry within the iris base. Long radial ciliary arteries emanate from the outer aspect of the major arterial circle of the iris, and the radial ciliary arteries bifurcate numerous times as they course toward the iris base (LoPinto et al. 2017a). There is a correlation between iris pigmentation and congenital deafness in alpacas and llamas, with a high frequency of bilateral deafness occurring in individuals with a pure white coat and blue iris pigmentation (Gauly et al. 2005). In one study, 78% of alpacas and llamas with a pure white coat coloration and bilateral blue irides assessed by brainstem auditory-evoked potential testing were found to be deaf (Gauly et al. 2005). The mechanism of the deafness in camelids with non-pigmented irides is suspected to be similar to other species where this correlation exists, such as domestic cats, and involves the absence of melanocytes leading to incomplete development of the inner ear.

The most striking feature of the camelid iris is the large pupillary ruff (Fig. 33.3). The pupillary rough is modified iris posterior pigment epithelium that is compromised of a series

of vertically-folded tissue. It is present on both the dorsal and ventral pupil margins, augments pupillary constriction, and is believed to be an adaptation to protect the eye from high levels of ultraviolet radiation. Evaluation of the alpaca pupillary ruff by contrast angiography identified complex vascular networks surrounding the pupillary ruff, but blood vessels were not detected within the pupillary ruff itself (LoPinto et al. 2017a). The dromedary camel iris is relatively thick along its entire length (443.68 μm total thickness at the pupillary border and 871.13 μm total thickness at the ciliary border) and consists of a well-defined anterior border layer, the middle layer of connective tissue stroma, and posterior pigmented epithelial layer (Aly et al. 2009). The development of the iris sphincter and dilator muscles has been described as being intermediate between the well-developed muscles of the dog and the poorly developed muscles of the donkey (Aly et al. 2009).

A basic description of the dromedary camel iridocorneal angle indicated a prominent angular aqueous plexus is present that communicates posteriorly with the vortex venous system and anteriorly with the subconjunctival venous system (Mahmood et al. 2013). The dromedary camel ciliary body is comprised of two distinct anatomical zones, the pars plicata and pars plana (Mahmood et al. 2013). The relatively large dromedary camel lens is supported by zonular ligaments arising from approximately 111 to 115 ciliary processes (Mahmood et al. 2013). The mean lens thickness in two studies of mature camels was 7.9 mm and 10.99 mm, respectively (Kassab 2012; Osuobeni and Hamidzada 1999). The mean diameter of the dromedary camel lens was 15.8 mm in one study (El-Tookhy et al. 2012). Zeta-crystallin, a protein previously believed to be unique to guinea pigs and related hystricomorph rodents, constitutes approximately 8–13% of the dromedary camel total lens protein (Garland et al. 1991). This presence of the same crystallin in species widely separated evolutionarily is surprising and might have arisen from a distant common ancestor or convergent evolution.

The camelid retina is holangiotic and atapetal (Figs. 33.4 and 33.5). The prenatal development of the dromedary camel retina has been the subject of multiple investigations that have determined that the photoreceptors are first observed at a 55 cm fetal crown vertebral rump length, and all ten layers of the retina are completely differentiated at a 98 cm fetal crown vertebral rump length (Osman et al. 2013, Abdel-Moniem 1992). The anatomical distribution and amount of pigmentation in the choroid and retinal pigment epithelial is highly variable between individual animals. A histologic and electronic microscope study of the dromedary camel choroid identified five distinct layers: suprachoroid, vessel layer, choriocapillaris, tapetum, and Bruch's membrane (Kotb et al. 2019). Like the choroid of other camelids, the dromedary camel is grossly atapetal; however, several layers of thin collagen bundles morphologically similar to a tapetum lucidum fibrosum are present microscopically in the central choroid (Kotb et al. 2019). The overlying retinal pigment epithelium is highly pigmented anterior to this choroidal region; however, this area has been postulated to represent a poorly developed and functionless tapetum lucidum.

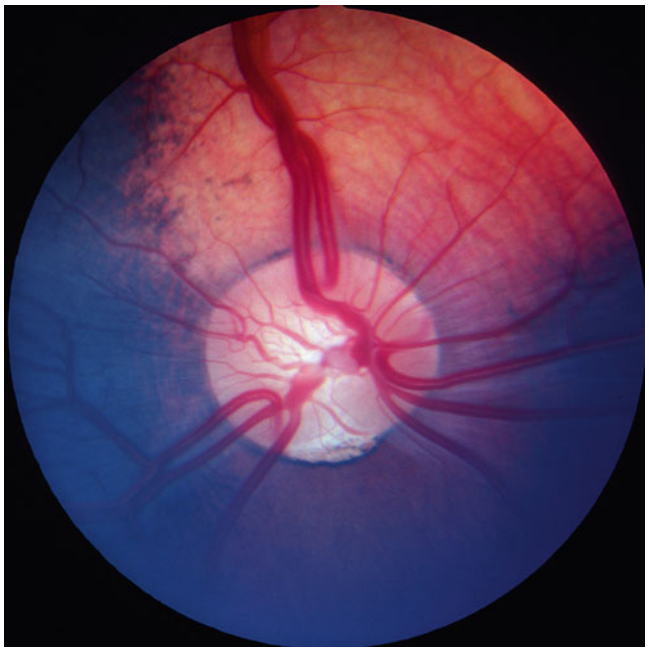

Fig. 33.4 Normal fundus of a llama

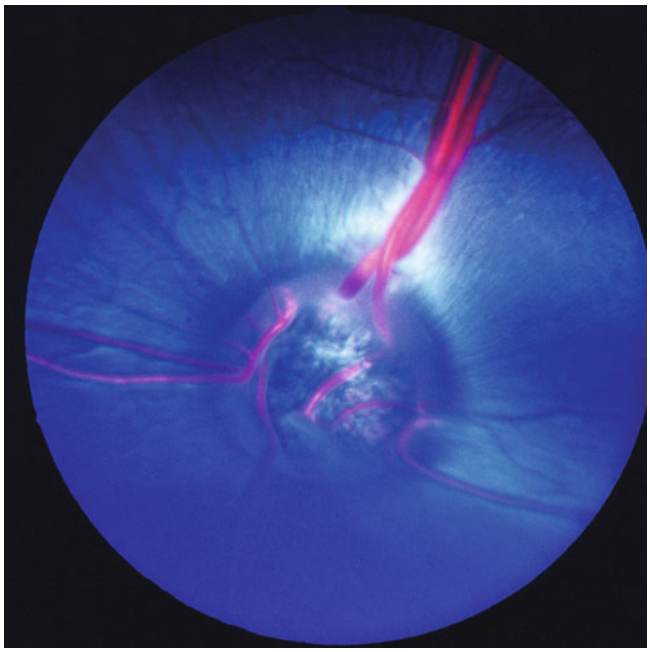

Fig. 33.5 Normal fundus of a dromedary camel

The morphology of the dromedary camel retinal pigment epithelium and choriocapillaris as observed with light and

electron microscopy was described (Altunay 2007). The retinal pigment epithelium was composed of a single layer of hexanocuboidal cells that, similar to other vertebrate species, were joined laterally by a series of apically-located tight junctions. An unexpected feature of the camel retinal pigment epithelium was the observation of an undefined structure at the level of the tight junctions throughout the inner side of the plasma membrane that resembled the myofibrillar organization of skeletal muscle (Altunay 2007). The function of this structure was unknown. Bruch's membrane was typically pentalaminate throughout the camel retina, and the layers included: the basement membrane of the retinal pigment epithelium, inner collagen layer, central discontinuous elastic fiber layer, outer collagen layer, and the basement membrane of the choriocapillaris endothelium. The endothelium of the camel choriocapillaris facing Bruch's membrane was extremely thin and heavily fenestrated (Altunay 2007). These fenestrations display typical single-layered diaphragm.

Three large and elevated pairs of retinal vessels are generally present in camelids, and the arterioles and venules frequently coil around each other (Fig. 33.6). The optic disc varies from pale pink to grey in coloration and is generally a slightly elongated horizontal oval shape. It is not uncommon for myelinated retinal nerve fibers to extend into the surrounding retina one or more optic disc diameters. The diameter of the adult dromedary optic nerve head was 13.66 mm when measured by ultrasound and 14.2 mm when measured by macroscopic evaluation (Kassab 2012).

Fig. 33.6 Normal fundus of a llama demonstrating the characteristic coiling of the retinal arterioles and venules

Camelid Vision

Camelids are diurnal and possess functionally excellent peripheral vision with a wide field of view. The lateral placement of the globes limits binocular vision; however, the coordinated movements of the long and agile neck further enhance functional vision in these species and their ability to cover the visual field. Observation of camels does indicate a limited region of binocular overlap where both pupils are visible simultaneously from in front of the animals (Harman et al. 2001).

Studies evaluating the visual ability of camelids are limited. A histological evaluation of the distribution of retinal ganglion cells and visual acuity in alpacas identified a horizontal streak of high ganglion cell density across the retinal meridian superior to the optic disc and with a temporal upward extension (Wang et al. 2015). The temporal upward extension of the horizontal streak is referred to as the anakatabatic area and is common among herbivores. The highest retinal ganglion cell densities were located in the temporal retina, where the maximal visual acuity was estimated to range between 12.5 and 133.4 cycles per degree (Wang et al. 2015).

A histologic evaluation of the retinal ganglion cell layer in dromedary camels determined the distribution of ganglion cells was highly unusual and that the camels lacked the typical horizontal streak observed in the retina of alpacas and many other ungulates (Harman et al. 2001). This study further determined that the dromedary camel retina possesses neither a single area centralis nor a typical visual streak but rather two regions of high ganglion cell density.

Estimates of total ganglion cells were around one million per camel retina, and they were arranged into two regions of high cell densities, one in the temporal retinal and one in the nasal retina (Harman et al. 2001). These high-density regions were located midway between the dorsal and ventral retina. The central regions of the retina had exceptionally low densities of ganglion cells. Mean retinal thickness was calculated to be 104 μm, with a range of 70–176 μm. An unusual feature was a vertical streak of higher cellular density present in the mid-retina slightly nasal to the optic disc and composed of small non-ganglion cells. These small non-ganglion cells were believed to be displaced amacrine cells. A similar vertical streak has only been previously described in the two-toed sloths. Approximately 900,000 axons were present within the optic nerves (Harman et al. 2001). A dense network of major blood vessels and capillaries was present across the retinal surface and located primarily between the ganglion cell layer and the inner nuclear layer. In contrast to many other animal species, the retinal vessels did not avoid regions of the retina such as an area centralis or visual streak (Harman et al. 2001).

Anatomical estimates of visual acuity in dromedary camels determined the maximum visual acuity to be 10.4 cycles per degree (Harman et al. 2001). This acuity was judged as reasonably good despite the lack of a visual streak and is comparable to reports of the domestic cat but lower than that of horses. Peak acuity in the nasal high cell density region and in the low-density central retina was estimated to be 9.5 and 2.7 cycles per degree, respectively (Harman et al. 2001). Behavioral estimations of visual acuity performed in a single Bactrian camel determined the camel's visual acuity to be 10 cycles per degree (Harman et al. 2001).

Examination Techniques

The ophthalmic examination of camelids is best performed in a quiet environment and a room or stall that can be darkened. The specific type and amount of restraint required to perform a complete ophthalmic examination are dictated by the individual animal. Most alpacas and llamas require only minimal manual restraint, and the examinations can be performed with the animal free-standing or with the assistance of stocks using a padded bar or towel to control head movements. For particularly fractious animals or those with potentially fragile ocular lesions (e.g., corneal perforations or lacerations), sedation is helpful to reduce anxiety, minimize head movements, and increase the efficiency of the examination process (Townsend 2010).

Wild South American camelids and the Afro-Asian camelids can be more difficult to examine. Although the temperament of many camels can be considered docile, the size, strength, and aggressiveness of some Afro-Asian camelids can make them potentially dangerous, and they are capable of inflicting serious injuries requiring appropriate precautious to be followed at all times (Al-Ali et al. 2019; Abu-Zidan et al. 2012). Depending on the individual camel, ophthalmic examinations can be performed either standing or with the camel in sternal recumbency. Camel holders, muzzles, and crush techniques are described for field examinations, and sedation may be required to safely and efficiently perform the ophthalmic examination (Tefera 2004). Auriculopalpebral nerve blocks are also helpful to facilitate complete ophthalmic examination in the Afro-Asian camelids (Naruka 1983), and orbital injection techniques for both motor and sensory anesthesia of the globe are described for these species (Badawy and Eshra 2018).

Following the collection of a complete and thorough medical history, the ophthalmic examination is performed in a systematic manner. Evaluation of the animal from a distance allows one to observe for blepharospasm and to determine how well the animal navigates in a potentially unfamiliar environment. Moving to within approximately an arm's length distance then allows one to visually examine the skull and periocular structures for size and symmetry. The globe size, position, and movement are concurrently evaluated. Vision can be assessed by the performance of the menace response and dazzle reflex. During menace response evaluation, care must be taken to avoid contact with the long vibrissae that are present superior and inferior to the globe in most camelids (Fig. 33.1). Palpebral reflexes are performed by lightly touching nasal and temporal to the eyelids. It is often helpful to examine pupil size, shape, and symmetry in both light and dark environments, and the direct and indirect pupillary light reflexes are determined.

The adnexa and anterior segments are examined with a strong focal light source, ideally with magnification. The ocular surface should be examined before and after the application of vital stains (i.e., sodium fluorescein, lissamine green, or rose bengal). Funduscopic examination can be performed with a direct ophthalmoscope or, preferably, indirect ophthalmoscopy is performed using a 20 diopter or 2.2 Pan Retinal® condensing lens. These lenses are recommended for initial evaluation of the camelid fundus as they provide a good balance between field of view and image magnification in these species. Pharmacologic mydriasis is required for a complete examination of the lens and posterior segment and can be achieved in camelids by the topical ophthalmic application of tropicamide 1% solution.

Ancillary ocular tests are indicated in many instances of camelid ocular disease and include Schirmer I tear testing and tonometry (see Appendix 3). Schirmer I tear tests to quantify basal and reflex tear production are performed in camelids with the same commercially available, standardized filter paper strips used in other animal species. Mean (± standard deviation) published reference values for animals free of ocular disease include 20.88 (± 4.04) mm/min for alpacas (McDonald et al. 2018) and 17.3 (±1.1) mm/min for llamas (Trbolova et al. 2012). In clinically normal dromedary camels, mean (± standard deviation) Schirmer I tear test values were 18.0 (± 3.2) mm/min for right eyes and 16.7 (±2.9) mm/min for left eyes in calves <6 months of age; 24.9 (±2.9) mm/min for right eyes and 25.0 (±2.8) mm/min for left eyes in immature camels >6 months, but <6 years of age; and 30.4 (±2.8) mm/min for right eyes and 30.7 (±2.2) mm/min for left eyes in mature camels that were 5–10 years of age (Marzok et al. 2017). In the camels, age was positively correlated with Schirmer tear test values, and no significant differences were found between genders.

Measurement of intraocular pressure can be performed in camelids with either applanation (e.g., TonoPen®) or rebound (e.g., TonoVet®) tonometers. Mean (± standard deviation) published reference values for alpacas free of ocular disease were 14.85 (±0.45) mmHg and 16.14 (±3.74) mmHg in two studies utilizing applanation tonometers (Nuhsbaum et al. 2000; Willis et al. 2000). In llamas, reported reference values

for intraocular pressure estimated by applanation tonometry include 13.1 (±0.35) mmHg and 16.96 (±3.51) mmHg (Nuhsbaum et al. 2000; Willis et al. 2000). A recent study (McDonald et al. 2017) comparing intraocular pressure measurements in the same clinically normal alpacas evaluated by both rebound and applanation tonometer determined that values obtained via rebound tonometry (mean: 14.21 mmHg) were significantly higher than the values obtained with applanation tonometry (mean: 12.51 mmHg). Regardless of which type of tonometer is used, it is always best practice to be consistent at each subsequent clinical examination. In dromedary camels, reported reference values for intraocular pressure estimated by applanation tonometry include 31.1 (±2.1) mmHg for right eyes and 30.8 (±1.9) mmHg for left eyes of immature camels (< 5 years of age) and 27.1 (±1.2) mmHg for right eyes and 28.2 (±1.2) mmHg for left eyes of mature camels (between 5 and 10 years of age) (Marzok and El-khodery 2015). In the dromedary camels, age was negatively correlated with intraocular pressure.

The tear ferning test has been evaluated in a small group of normal dromedary camels and determined the tear film grade in the camels was 0-1 using the Masmali tear ferning grading scale; however, no correlations of this test with the ocular surface disease have been reported as of this time (Am et al. 2018).

Cochet-Bonnet esthesiometry can be performed to evaluate corneal sensitivity in camelids, and reference values are reported from two populations of normal alpacas. Corneal sensitivity varied by corneal region, but when all regions were combined, the median corneal touch threshold was 2.8 g/mm^2 for adult alpacas and 0.8 g/mm^2 for crias (Rankin et al. 2012). Crias were found to have significantly greater corneal sensitivity compared with adult alpacas in all corneal regions that were evaluated. In a separate study of ophthalmologically normal adult alpacas, the central corneal region was also determined to be the most sensitive with a mean (± standard deviation) corneal touch threshold values (in mm filament length) reported to be 34.5 (± 7.1) mm (Welihozkiy et al. 2011).

Ocular Disease Prevalence

Previous studies have evaluated the overall prevalence and distribution of ocular disease in specific populations of camelids. Ophthalmic examination performed on a group of 29 alpacas determined that 38% had one or more ocular diseases (Gelatt et al. 1995). The most common ocular lesions in the alpacas were cataracts, signs of previous uveitis, corneal scarring, optic disc colobomas, and conjunctivitis. Trauma and hereditary causes were speculated to be the most common etiologies of the observed ocular lesions (Gelatt et al. 1995). A retrospective medical record study of ocular disease in llamas reported a 6% prevalence of ocular disease in an evaluated population of 3242 animals (Gionfriddo et al. 1997). Corneal disease, particularly ulcerative keratitis, was the most frequent ocular disease in the llamas, followed by uveal lesions and cataracts. Trauma was considered the most common etiology of llama ocular disease in the study (Gionfriddo et al. 1997).

A population of 17 llamas and 23 alpacas were examined, and the most common ocular findings included iris-to-iris persistent pupillary membranes (14 llamas and 5 alpacas) and various types of cataracts (11 llamas and 5 alpacas) ranging from capsular opacities to immature cortical cataracts (Webb et al. 2006). Corneal scarring, corneal dystrophy, conjunctival masses, and eyelid masses were less common finings. In a report of 56 sick neonatal alpacas and llamas presented over a 10-year period to one institution, 21% had ocular lesions that included ulcerative keratitis, congenital cataracts, conjunctivitis, and microphthalmia (Bertin et al. 2015).

The prevalence of ocular disease was investigated in a large Indian population of 3045 dromedary camels using both prospective examinations and retrospective medical records review (Bishnoi and Gahlot 2001a). In this population, 209 camels (6.86%) had one or more ocular lesions. A diverse group of lesions was identified, but abnormalities of the cornea and sclera, conjunctival, and eyelids were most frequently detected. A higher prevalence of ocular disease was found in camels >12 years of age relative to camels <6 years of age. The most common suspected etiologies of the ocular lesions were external trauma (55% of cases), chemical irritants (12%), foreign bodies (10%), infections (4%), and vitamin A deficiency (5%) (Bishnoi and Gahlot 2001a).

A study examining 2500 dromedary camels from Egypt identified 260 camels (10.4%) with ocular disease and determined that conjunctivitis, corneal disease, blepharitis, and panophthalmitis were the most prevalent conditions (Fahmy et al. 2003). A retrospective study of 910 dromedary camel cases examined in India reported that 22.5% had ocular disease and the most common ocular lesions were corneal opacities (32.7%), eyelid lacerations (21%), nonspecific eye injuries (12.7%), epiphora (11.2%), and conjunctivitis (9.3%) (Kumar et al. 2016).

A survey of ocular lesions was performed on a farm of 102 dromedary camels in India (Ranjan et al. 2016). The overall prevalence of ocular disease was 19.6% in the camels. Ocular lesions detected included corneal ulceration (4.9% of camels, ranging from superficial ulceration to corneal perforation), acute conjunctivitis (3.9%), blepharitis (2.9%), chronic conjunctivitis (2.0%), nonulcerative keratitis (2.0%), and nonspecific globe problems (3.9%) which were described as possibly being either orbital disease or glaucoma. In this survey, the frequency of ocular lesions

increased with age, and the most common underlying etiologies of the lesions were speculated to be infectious or resulting from trauma associated with grazing on thorny vegetation (Ranjan et al. 2016).

Orbital Disease

There are few published examples of orbital disease in camelids, but congenital anomalies, traumatic fractures of the orbital rim, and orbital cellulitis (often associated with orbital vegetative foreign bodies, such as wood slivers) do occur in these species, although on a relatively infrequent basis. Congenital anomalies such as synophthalmia (Fig. 33.7), where the embryonic prosencephalon fails to divide the orbital cavities, rarely occur in camelids and are usually present concurrently with other severe ocular abnormalities and additional systemic malformations that are incompatible with life. The orbital regrowth of a malignant nonteratoid ocular medulloepithelioma is described following enucleation in a llama (Schoeniger et al. 2006).

Eyelid Disease

Anatomical entropion is occasionally observed in both Afro-Asian and South American camelids and can be congenital in their calves and crias (Fig. 33.8), or acquired from cicatricial changes associated with trauma or severe blepharitis. The resultant trichiasis can lead to severe ocular irritation, conjunctivitis, keratitis, and often corneal ulceration. Uncomplicated cases of anatomical entropion can be surgically corrected with the Hotz-Celsus or similar procedure. Hereditary factors may be involved, and female dromedary camels

Fig. 33.7 Synophthalmia in a stillborn alpaca cria

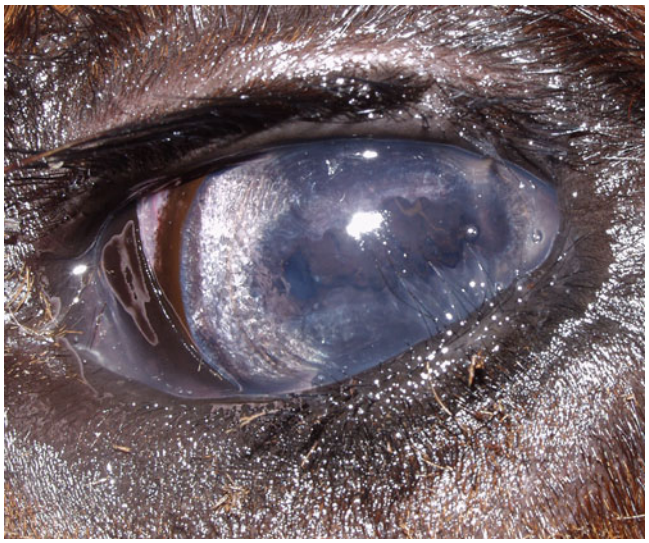

Fig. 33.8 Inferior eyelid entropion and trichiasis in a llama cria

with entropion have been described that also produced offspring with entropion (Yeruham et al. 2002).

Blepharitis is common in camelids and can result from numerous underlying causes, including infectious, allergic, and traumatic etiologies (Scott et al. 2011). Depending on the specific etiology, the eyelid lesions of blepharitis typically include various combinations of alopecia, erythema, blepharedema, crusts, scales, nodules, papules, pustules, pruritus, and ulceration. Due to the complex nature of dermatitis in camelids, skin scrapings, trichography, and biopsy for cytology, culture, and histopathology are often required to achieve a definitive diagnosis and to implement condition-specific therapy.

Bacterial blepharitis occurs relatively commonly in camelids and is often associated with multifocal or generalized dermatitis (Fig. 33.9). Staphylococcal folliculitis, dermatophilosis, and *Corynebacterium pseudotuberculosis* can all produce solitary, multifocal, or generalized dermatitis that may involve the eyelids (D'Alterio et al. 2006; Scott et al. 2011). Treatment involves antimicrobial therapy based upon culture and susceptibility testing. In one study, the most frequent bacteria isolated from 36 dromedary camels with blepharitis were *Staphylococcus aureus* ($n = 12$ isolates), *Bacillus* spp. ($n = 9$), *Corynebacterium pseudotuberculosis* ($n = 6$), *Escherichia coli* ($n = 6$), *Klebsiella pneumoniae* ($n = 3$), *Streptococcus faecalis* ($n = 3$), and *Staphylococcus epidermidis* ($n = 3$) (Fahmy et al. 2003). Severe bacterial blepharitis may interfere with normal eyelid structure and function with resultant secondary conjunctival and corneal disease. Treatment of eyelid disease in camelids should always involve frequent evaluation of the health of the ocular surface and supportive treatment when required. Dermatophytosis and cutaneous candidiasis can involve the periocular region and cause blepharitis in camelids but are

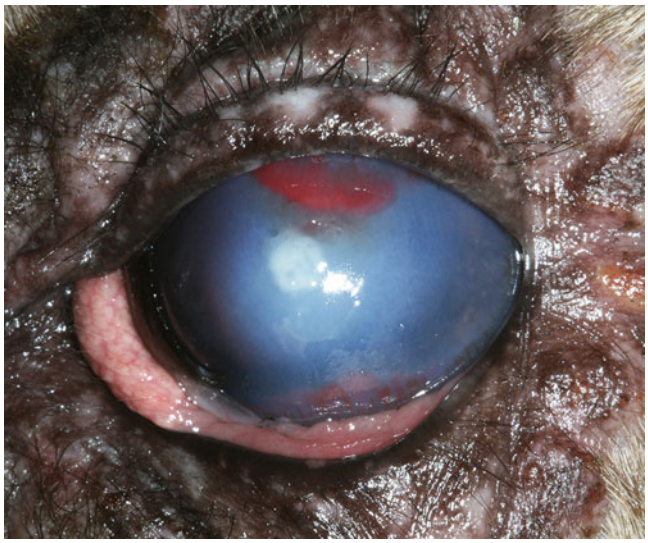

Fig. 33.9 Chronic bacterial blepharitis and secondary ocular surface disease in an alpaca

Fig. 33.10 Blepharitis and generalized dermatitis resulting from midge bite hypersensitivity in an alpaca

less frequently diagnosed than bacterial infections (Ho et al. 2017).

Allergic blepharitis can occur in response to numerous offending allergens, but insect bite (e.g., *Culicoides* spp. midges) hypersensitivity is among the most frequent cause of eyelid lesions in camelids (Fig. 33.10). A recurrent and seasonal pattern is common, and lesions are most frequently found on the periocular region, pinnae, nose, axillae, groin, ventral mid-line, and distal legs (Scott et al. 2011). Eosinophilic inflammation may be identified on cytologic or histologic examination of skin samples. Allergen identification and avoidance (e.g., protective housing, permethrin sprays) are the most critical components of therapy. Ectoparasitism, including sarcoptic mange, chorioptic mange, psoroptic mange, and pediculosis, are also relatively common causes of blepharitis in alpacas and llamas (Scott et al. 2011). Skin scraping or skin biopsies for histopathology are often required for the diagnosis of ectoparasites, and treatment includes appropriate topical or systemic antiparasitic agents. A case of sterile eosinophilic and neutrophilic folliculitis and furunculosis was described in an alpaca and was localized to the eyelids (Scott et al. 2011). The condition responded to oral prednisone administration and was speculated to be associated with insect envenomation. Severe tick infestation-associated blepharitis is described in dromedary camels (Ranjan et al. 2016; Fahmy et al. 2003).

Cutaneous periocular *Habronema* infection is reported in dromedary camels in endemic regions, but this condition appears to occur much less commonly in the camelid species than in other host species such as horses (Myers et al. 2010). Eyelid lesions are frequently located at the medial canthus and appear as ulcerative, fibrotic masses or plaques that are pruritic and non-healing. The pathogenesis of these lesions is believed to involve a hypersensitivity reaction to the dead or dying nematode larvae. Histological evaluation of dermal biopsies or skin scrapings is diagnostic and reveals eosinophilic granulomas with characteristic nematode larvae (Myers et al. 2010). Treatment is similar to equine habronemiasis and includes surgical debridement, prevention of self-trauma, subcutaneous ivermectin (as oral ivermectin may not be effective in camelids for this condition), anti-inflammatory therapies, and fly control to prevent recurrences (Jarvinen et al. 2002).

Camelpox, caused by an orthopoxvirus, is an important socioeconomic and clinical disease of dromedary camels. Camelpox virus infection can result in localized or generalized skin disease (i.e., development of papules, macules, pustules, vesicles, and scabs) and commonly involves the eyelids (Balamurugan et al. 2013). Camelpox virus is also noteworthy as it is a potential zoonotic agent.

Zinc-responsive dermatitis is a relatively common dermatologic disease of alpacas. Lesions are nonpruritic and appear as scales, papules, and thick crusty plaques that most commonly develop in relatively hairless areas but occasionally will also involve the periocular region (Scott et al. 2011). Response to zine supplementation is both therapeutic and can assist with establishing a diagnosis. Traumatic eyelid wounds are relatively common in camelids, and frequent causes include aggressive male interactions, dog bites, barbed wire fencing, and other sharp environmental objects. Eyelid lacerations and blunt trauma wounds are treated in a similar fashion to other species.

Eyelid neoplasms appear to be very uncommon in camelids. Nictitating membrane squamous cell carcinomas

in one alpaca and one llama were described in a study analyzing pathology and necropsy submissions (Valentine and Martin 2007), but no additional details were provided. An ossifying fibroma, a benign fibro-osseous lesion that presented in a llama as a firm mass rostral and inferior to the medial canthus, was reported (McCauley et al. 2000). The ossifying fibroma appeared to originate from the oral cavity and resulted in death by asphyxiation due to complete occlusion of the nasal passages. Multiple hamartomas that clinically presented as firm, smooth lesions of the eyelid, neck, and foot are reported in an alpaca (Scott et al. 2011).

Nasolacrimal Disease

Congenital disorders of the nasolacrimal system are relatively frequent ocular problems in South American camelids. One or more components of the nasolacrimal system may be absent, and conjunctival puncta atresia, nasolacrimal duct atresia, and nasal puncta atresia have all been described in alpacas and llamas (Sandmeyer et al. 2011; Mangan et al. 2008; Arnold et al. 2002; Sapienza et al. 1992). Lesions may be unilateral or bilateral. Ocular discharge, often beginning as epiphora and progressing to mucopurulent in nature with the development of secondary bacterial infection, conjunctivitis, facial wetting, and periocular dermatitis, are frequent presenting complaints in these young animals (Fig. 33.11).

The Jones fluorescein dye test, attempted nasolacrimal flushing, dacryocystorhinography, computed tomography, magnetic resonance imaging, rhinoscopy, and lacrimoscopy can be used to confirm the diagnosis and localize the site of atresia. Surgical correction of the atresia or the creation of an alternative tear drainage pathway (e.g., surgical creation of a punctal opening, conjunctivobuccostomy, conjunctivomaxillosinusotomy, conjunctivorhinostomy, canaliculorhinostomy, canaliculodacryocystorhinostomy, dacryocystorhinostomy, dacryocystomaxillorhinostomy, etc.) to establish functional patency is the treatment of choice (Fig. 33.12). Many of these procedures require the temporary placement of a surgical stent for several weeks to maintain the patency of the newly created tear pathway and to permit epithelialization. Post-operative topical antimicrobial and anti-inflammatory therapy helps to minimize the risk of infection and encourage uncomplicated healing. Complications associated with premature stent displacement or failure of the new tear draining pathway following stent removal can occur and require additional surgical interventions.

Fig. 33.11 Nasolacrimal duct atresia in an alpaca cria associate with mucopurulent ocular discharge, secondary bacterial conjunctivitis, and periocular dermatitis

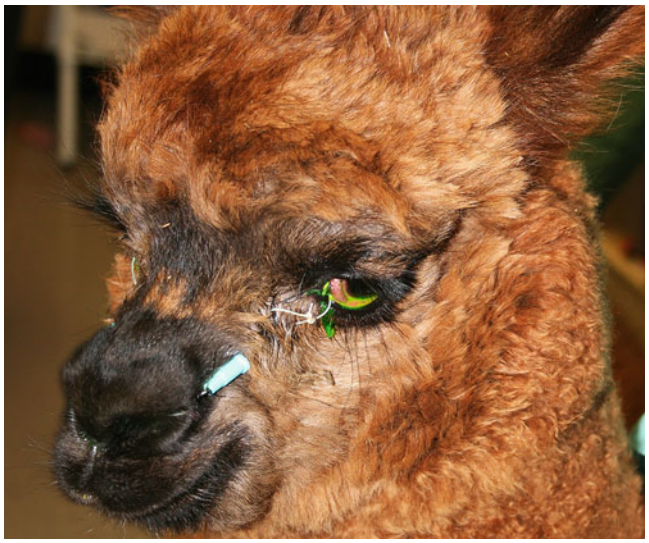

Fig. 33.12 Surgical treatment of nasolacrimal duct atresia in an alpaca cria by dacryocystorhinostomy with placement of an indwelling catheter

Acquired nasolacrimal obstructions and dacryocystitis can occur in camelids of any age and are often the result of nasolacrimal foreign bodies or *Thelazia* parasites. Unilateral mucoid or mucopurulent discharge, conjunctivitis, and periocular dermatitis are common clinical lesions. Treatment consists of removal of the obstruction, which can involve manual removal, nasolacrimal cannulation and flushing, or surgical exploration. Removal of the obstruction is followed by topical antimicrobial therapy to clear the opportunistic infection.

Conjunctival Disease

Congenital conjunctiva cysts appear to occur relatively commonly in crias and calves. Conjunctival cysts most frequently involve the bulbar conjunctiva, and some are large enough to displace the globe (Fig. 33.13). Conjunctival cysts can be

Fig. 33.13 Large conjunctival cyst in an alpaca displacing the globe and associated with multiple congenital ocular anomalies including posterior staphyloma and optic disc coloboma

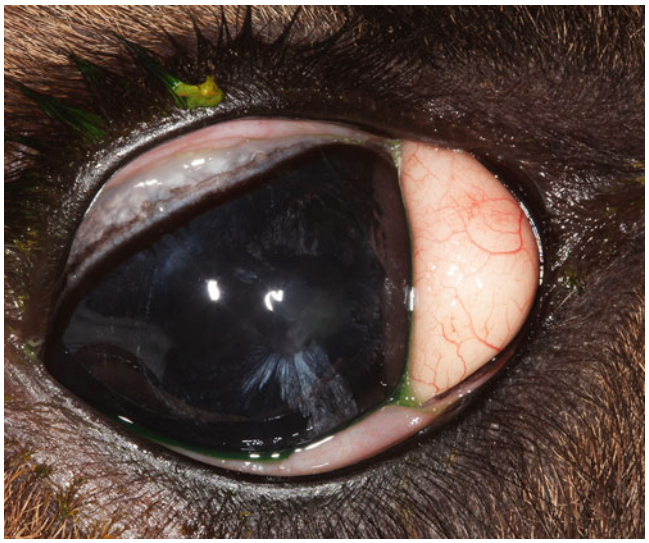

Fig. 33.14 Subconjunctival orbital fat prolapse in an alpaca presenting as a smooth surfaced, fluctuant, pink mass at the medial canthus

isolated lesions or associated with multiple additional congenital ocular anomalies (e.g., scleral ectasia, optic disc or peripapillary coloboma). Small conjunctival cysts that do not enlarge can be incidental finings that only require monitoring; however, surgical excision is recommended for those affecting vision or comfort. Prior to surgery, a complete ophthalmic examination and potentially ocular imaging studies (e.g., ocular ultrasonography) are indicated as some conjunctival cysts, particularly those associated with other congenital ocular anomalies can have intraocular communications (Schuh et al. 1991). Attempted excision, biopsy, or overzealous aspiration of fluid in cysts with intraocular communications can have dire consequences for the globe.

Conjunctival dermoids are described in camelids and can be surgically excised if irritating (Gionfriddo et al. 1997). Subconjunctival orbital fat prolapse is seen primarily in young camelids and appears as nonpainful, smooth surfaced, fluctuant, pink masses under the conjunctival surface (Fig. 33.14). Subconjunctival orbital fat prolapse in camelids is presumed to have similar pathophysiology to other species (i.e., defects in the orbital septum, Tenon's capsular, or muscular fasciae) and treatment, when required, involves surgical excision of the prolapsed fast with the repair of the defect to prevent recurrence (Klauss et al. 2005). Diffuse hyperkeratosis and conjunctivitis were described in a single llama cria with congenital ichthyosis, a condition caused by defects in the terminal differentiation of keratinocytes and defective desquamation (Belknap and Dunstan 1990). Subconjunctival hemorrhage is a common finding in camelids associated with external trauma and is reported in dromedary camel calves after difficult parturition and birth trauma (Bishnoi and Gahlot 2001a).

Conjunctivitis is a frequent condition in all camelid species. Clinical lesions may include blepharospasm, pruritus, ocular discharge, hyperemia, chemosis, ulceration, and conjunctival follicle formation with chronicity. Allergic conjunctivitis is seen in camelids and is typically associated with relatively mild clinical lesions and a seasonal or chronic history. The diagnosis of allergic conjunctivitis is suggested by the exclusion of other etiologies by ophthalmic examination and appropriate diagnostic testing. Conjunctivitis associated with environmental irritants or conjunctival foreign bodies is also relatively common. Vigorous flushing of the conjunctival surface with sterile eye wash, after the application of topical anesthetic, can be used to dislodge particulate conjunctival foreign material. Large conjunctival foreign bodies may require swabs or fine forceps for removal. Topical ophthalmic antimicrobial treatment for opportunistic bacterial infections is indicated concurrent with foreign body removal. An outbreak of conjunctivitis and ulcerative keratitis associated with weed seed-contaminated hay was reported in a herd of alpacas (Fischer and Hendrix 2012). In the described alpacas, the conjunctival foreign bodies were located in the temporal conjunctival fornix and manually removed with the resolution of clinical lesions.

Infectious conjunctivitis occurs in camelids due to bacterial, parasitic, fungal, and viral etiologies. Bacterial conjunctivitis is anecdotally described to be a common disease in camelids (Czerwinski 2019; Gionfriddo et al. 1997), but in published descriptions, it is often unclear if the bacterial infection was a primary or secondary lesion of the conjunctiva. The clinical lesions of bacterial conjunctivitis can be

Fig. 33.15 Chronic bacterial conjunctivitis and blepharitis in a llama

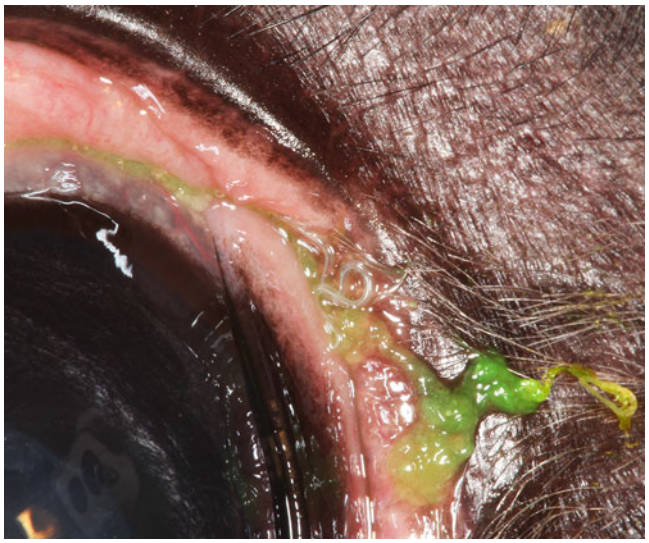

Fig. 33.16 Parasitic conjunctivitis in an alpaca associated with *Thelazia* spp. infection. Conjunctival hyperemia, chemosis, mucoid discharge, and a thin, threadlike, white, motile filaria on the conjunctival surface are present

severe and can be present with concurrent bacterial blepharitis (Fig. 33.15). The isolation of a variety of potentially pathogenic bacterial species from cases of conjunctivitis is described in both South American and Afro-Asian camelids (Gionfriddo 2013; Fahmy et al. 2003); however, conjunctival culture results must be interpreted cautiously in camelids as potentially pathogenic bacteria and fungi can be isolated from the conjunctival microflora in the absence of ocular disease (Storms et al. 2016; Fahmy et al. 2003; Gionfriddo et al. 1992; Gionfriddo et al. 1991). *Moraxella catarrhalis* and *Moraxella lacunata* have been associated with chronic exudative conjunctivitis in dromedary camels specifically (Fahmy et al. 2003).

A thorough ophthalmic examination is always indicated in cases of suspected bacterial conjunctivitis to exclude conjunctival foreign bodies or other underlying ocular diseases. Treatment is directed at the primary ocular disease when present, and topical antimicrobial therapy is instituted based upon culture and antimicrobial susceptibility testing of a conjunctival sample. Conjunctival bacterial abscesses are rarely observed in camelids and may be secondary to sharp penetrating conjunctival wounds. In the author's experience, these abscesses respond poorly to medical therapy alone, and surgical debridement is often required for resolution.

Parasitic conjunctivitis results from *Thelazia* spp. and is transmitted between animals by insect vectors (Sazmand and Joachim 2017). These thin, threadlike, white, motile filarial parasites reside within the conjunctival fornices and nasolacrimal duct (Fig. 33.16). The nematodes can be observed moving, often rapidly, within the tear film during the ophthalmic examination and most commonly produce a mild-to-moderate conjunctivitis. *Thelazia* are common ocular parasites of camelids in many geographic regions and often affect multiple individuals within a herd concurrently. Mild peripheral keratitis is occasionally present with conjunctivitis. Treatment is manual removal of parasites under topical anesthetic, which may need to be repeated multiple times if filariae are hidden within the nasolacrimal system. Alternatively, topical application of antiparasitic agents such as ivermectin or diethylcarbamazine can be used to eliminate the parasites (Gionfriddo 2013). All animals in a herd may require treatment, and fly control is important to prevent the recurrence of the parasitic infection.

Fungal conjunctivitis associated with *Candida* infection occurs uncommonly in camelids (Ho et al. 2017). The described clinical cases in alpacas varied from mild to severe conjunctivitis and were always associated with periocular cutaneous candidiasis and potential immunosuppressive conditions. Successful treatment of *Candida* blepharoconjunctivitis with topical antifungals (i.e., miconazole) and therapy to resolve the underlying immunosuppression condition is reported (Ho et al. 2017).

Viral conjunctivitis is described in South American camelids associated with cowpox virus infection (Goerigk et al. 2014). This orthopoxvirus can produce either mild, localized lesions characterized by pustules and crusts or generalized disease. Generalized cowpox virus infections are commonly associated with bilateral mucopurulent conjunctivitis, stomatitis, rhinitis, and a high mortality rate (Goerigk et al. 2014; Prkno et al. 2018). Cowpox virus infections in camelids may occur as herd outbreaks, and the cowpox virus is a potential zoonotic agent (Prkno et al. 2017).

Corneal Disease

Corneal disease is the most common ocular disease of camelids. The prominence of the camelid cornea combined with the potentially hazardous environments in which they reside account for many of these lesions and injuries. Many camelid corneal diseases, particularly those associated with trauma and infections, require prompt therapy to save both the globe and vision.

Non-inflammatory corneal masses are uncommon in camelids but can include dermoids, epithelial inclusion cysts, and viral papillomas. Corneal dermoids are occasionally detected in camelids and can be excised by lamellar keratectomy if they are irritating or obstructing vision (Moore et al. 1999). Corneal epithelial inclusion cysts result from the inoculation of viable corneal epithelial cells into the corneal stroma with subsequent proliferation and cyst formation. These lesions can be congenital or result from corneal surface trauma (either external or surgical). Corneal epithelial inclusion cysts are generally nonpainful, solitary, white-to-pink masses that can appear flat or slightly raised from the corneal surface. Surgical excision by lamellar keratectomy is generally curative. A limbal-based corneal epithelial inclusion cyst was described in a llama (Pirie et al. 2008). The epithelial inclusion cyst in the llama was nonpainful, smooth, raised, partially pigmented, and vascularized. A histopathologically-typical viral papilloma was removed by superficial keratectomy from the cornea of a dromedary camel that contained bovine papilloma virus-1 antigen and was speculated to be associated with cattle exposure and subsequent bovine papilloma virus infection (Kilic et al. 2010).

Corneal degeneration and corneal dystrophy are reported in alpacas and llamas (Webb et al. 2006), although the frequency of these conditions is presently unknown. Clinically, both corneal dystrophy and degeneration are identified by the presence of white, crystalline, refractile opacities within the cornea. Corneal dystrophy is a hereditary disease associated with the abnormal metabolism of lipids within the cornea and their subsequent deposition. In most instances, corneal dystrophy lesions are bilaterally symmetrical and occur in the absence of corneal vascularization. Corneal degeneration is an acquired condition where lipid or mineral is deposited into the cornea, most commonly associated with concurrent corneal vascularization. Corneal degeneration lesions can be unilateral or bilateral. Corneal degeneration can occur after any previous corneal insult, in association with other ocular diseases (e.g., keratitis, uveitis), or be associated with systemic abnormalities of lipid and mineral metabolism. A case of bilateral corneal degeneration was described in an alpaca, and the lipid deposits occurred in the presence of systemic hypercholesterolemia and atherosclerosis (Richter et al. 2006). Idiopathic calcific corneal degeneration in an alpaca (Pucket et al. 2014) and idiopathic corneal degeneration in a llama are described (Grahn and Cullen 2001a). In both the reported idiopathic camelid cases, the typical pattern of corneal degeneration being associated with a previous ocular insult or concurrent ocular disease was absent, suggesting further research of these conditions in camelids is warranted.

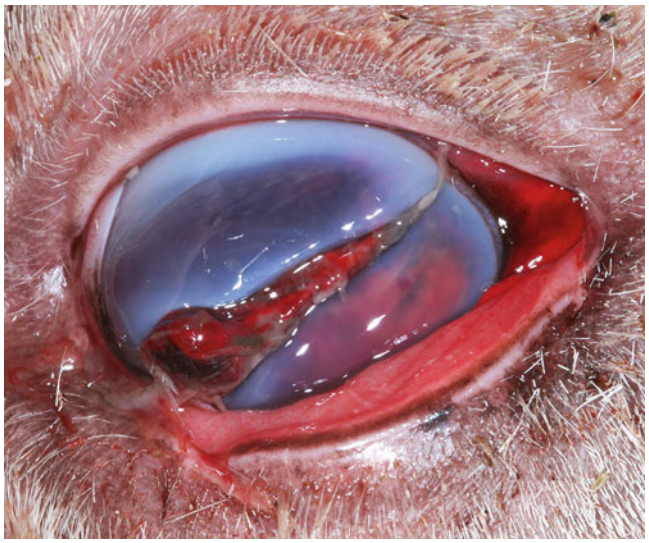

Fig. 33.17 Full-thickness corneal laceration, iris prolapse, and hyphema in a llama with ocular barbed wire trauma

Corneal lacerations can occur under a variety of circumstances in camelids, but interactions with sharp environment objects (such as barbed wire or thorny vegetation) are among the most common scenarios (Fig. 33.17). As with other species, the depth of the laceration guides the therapeutic approach. For relatively superficial corneal lacerations (i.e., <50% stromal depth), medical therapy is generally all that is indicated and includes topical ophthalmic broad-spectrum antimicrobials, topical ophthalmic atropine, and potentially systemic non-steroidal medications. Surgical repair concurrent with medical therapy is indicated for corneal lacerations that are ≥50% stromal depth.

Corneal foreign bodies are very common in camelids and most commonly involve plant materials. Similar to corneal laceration, treatment is dictated by the depth of the corneal foreign material. Superficial corneal foreign bodies can often be removed by a stream of eyewash, swabs, or fine forceps. Deep corneal foreign bodies may require keratectomy for complete removal. Following removal, topical ophthalmic broad-spectrum antimicrobials, topical ophthalmic atropine, and potentially systemic non-steroidal medications are indicated with frequent monitoring for the development of secondary infectious keratitis (Ledbetter et al. 2013). If the foreign body penetrated full-thickness into the anterior chamber, a course of a systemic antimicrobial is recommended to decrease the risk of infectious endophthalmitis.

Superficial, apparently noninfected corneal ulcers are occasionally encountered in camelids. Many of these represent acute, uncomplicated traumatic lesions. Treatment for this type of ulcerative keratitis should include topical ophthalmic broad-spectrum antimicrobials and atropine, with frequent monitoring for complications such as the development of secondary infection until healed. Chronic superficial corneal ulcers in camelids are most commonly associated with other ocular diseases (e.g., conjunctival foreign bodies, cilia or eyelid abnormalities, exposure keratitis, etc.) or infectious etiologies. Management of these chronic superficial ulcers is primarily directed toward identifying and correcting the underlying condition that is resulting in their development and persistence. An outbreak of conjunctivitis and superficial ulcerative keratitis associated with conjunctival plant foreign bodies was described in a herd of alpacas (Fischer and Hendrix 2012). Fan-shaped superficial corneal ulcers located at the temporal limbus were noted in all examined alpacas with corneal ulceration, a finding the authors considered suggestive of temporal conjunctival foreign bodies in this species. A case of an indolent corneal ulcer that was successfully treated by grid keratotomy was reported in a llama with clinical features reminiscent of canine spontaneous chronic corneal epithelial defects (Jones et al. 2007). Further investigation is required to determine the underlying pathophysiologic mechanisms involved in the development of indolent ulcers in camelids.

Infectious keratitis is a common, sight-threatening condition in all camelid species. Both bacterial and fungal pathogens frequently infect the camelid cornea, and prompt diagnostic evaluation to determine the underlying infectious agent and to permit implementation of microorganism-specific therapies are always indicated. Trauma, adnexal disease, or other ocular surface diseases are generally required to initiate infectious keratitis in camelids and serve to circumvent the normal corneal anatomic, immunologic, and physiologic defense mechanisms (Fig. 33.9) (Sumner et al. 2012). Once the corneal infection is initiated, ocular lesions in camelids often progress rapidly (Fig. 33.18) (Guyonnet et al. 2018). Infectious keratitis can be clinically recognized by the presence of one or more of the following: corneal infiltrates, corneal stromal loss, anterior uveitis (which may include hypopyon), and keratomalacia (Fig. 33.19). Corneal lesions associated with infectious keratitis may be ulcerative or nonulcerative with stromal abscess formation.

Potential bacterial pathogens of the camelid cornea are numerous and include both aerobic and anaerobic bacteria. Common aerobic bacteria isolated from infectious keratitis of camelids in general include *Staphylococcus*, *Streptococcus*, and *Pseudomonas* species. In one study, the most frequent bacteria isolated from dromedary camels with ulcerative keratitis or other corneal wounds were *Staphylococcus aureus*, *Staphylococcus epidermidis*, *Streptococcus pyogenes*,

Fig. 33.18 Keratomalacia and corneal perforation in a Bactrian camel

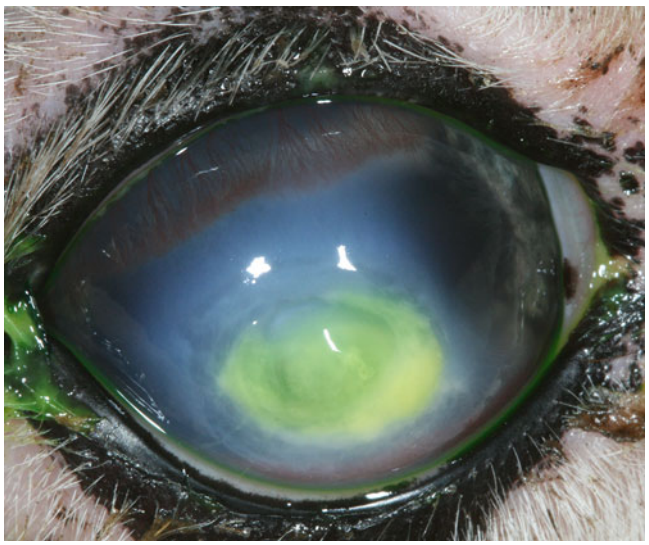

Fig. 33.19 Bacterial keratitis in an alpaca. A corneal stromal ulcer with infiltrates and keratomalacia are present

Arcanobacterium pyogenes, *Bacillus* spp., *Corynebacterium ulcerans*, *Escherichia coli*, *Proteus mirabilis*, and *Pseudomonas aeruginosa* (Fahmy et al. 2003). The frequency of anaerobic bacterial involvement in South American camelid corneal infection is also higher than many other animal species. In a study of septic corneal ulcers, 18.8% of alpacas had one or more obligate anaerobic bacteria isolated from their corneal samples, including *Clostridium*, *Peptostreptococcus*, and *Fusobacterium* species (Ledbetter and Scarlett 2008).

Diagnostic evaluation of suspected bacterial keratitis should include the collection of corneal samples for cytologic evaluation and both aerobic and anaerobic culture and

antimicrobial susceptibility determinations (Massa et al. 1999). While initial diagnostic test results are pending, topical ophthalmic broad-spectrum antimicrobials, topical ophthalmic atropine, topical ophthalmic matrix metalloproteinase inhibitors, systemic non-steroidal anti-inflammatory medications, and systemic antimicrobials (in cases of vascularized or perforated corneal lesions) are instituted. The utilization of subpalpebral lavage systems is recommended in camelids when frequent topical ophthalmic medication application is required in fragile or painful eyes (Borkowski et al. 2007). These lavage systems can also be connected to infusion systems to provide continuous treatment. Surgical grafting is recommended for rapidly progressing, deep (>50% depth) or perforated corneal lesions (Rodriguez-Alvaro et al. 2005; Bishnoi and Gahlot 2001b). Various graft options are available for camelids, including conjunctival grafts, corneal grafts, and processed biological grafting materials (e.g., amniotic membrane, swine intestinal submucosa, porcine urinary bladder extracellular matrix, etc.).

Moraxella canis has been associated with outbreaks of keratoconjunctivitis in herds of dromedary camels (Tejedor-Junco et al. 2010). The camel outbreaks were reported as being clinically very similar to infectious bovine keratoconjunctivitis associated with *Moraxella bovis* infection. Treatment with autogenous vaccination and subconjunctival amoxicillin (once per week for 4 weeks) resulted in complete recovery in the infected camels (Tejedor-Junco et al. 2010).

Similar to the horse, fungal keratitis occurs at a much higher frequency in camelids than in most other animal species. In a study of alpaca fungal keratitis, 10 of 11 cases occurred in the summer or fall months (Ledbetter et al. 2013) in a temperate climate. Corneal lesions associated with mycotic infection appeared highly variable in the alpacas but included stromal corneal ulcers, stromal abscesses, corneal perforations, and nonulcerative keratitis (Fig. 33.20). Specific corneal lesions suggestive of fungal keratitis in camelids may include white, yellow, brown, or black corneal plaques, often with a feathery or fluffy appearance; corneal satellite lesions; corneal furrowing; and deep stromal abscesses. Fungi isolated from corneal samples of alpacas with mycotic infection included species of *Aspergillus*, *Alternaria*, *Beauveria*, *Fusarium*, *Rhizomucor*, and *Verticillium* (Ledbetter et al. 2013). Confirmation of a diagnosis of fungal keratitis in camelids can be achieved by cytology, histopathology, in vivo confocal microscopy, fungal PCR assay, or fungal culture. Treatment is similar to bacterial keratitis but also includes topical ophthalmic antifungals (e.g., itraconazole, miconazole, voriconazole, or natamycin) and potentially anterior lamellar keratectomy to remove fungal plaques.

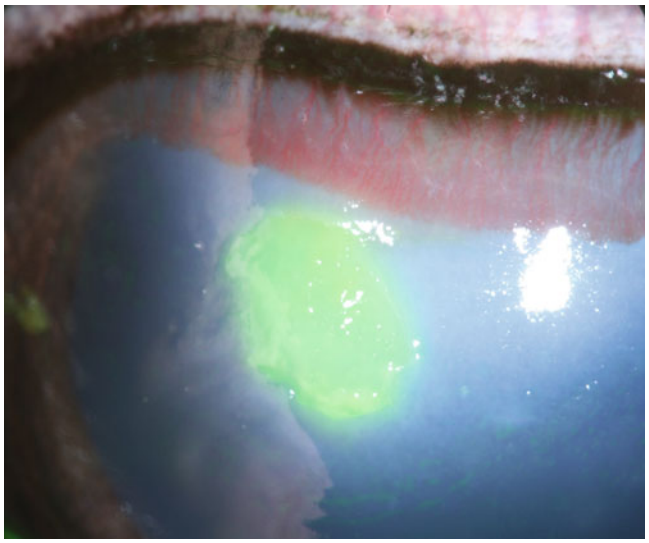

Fig. 33.20 Fungal keratitis in an alpaca with a yellow corneal plaque stained with fluorescein

Viral keratitis, potentially associated with herpesvirus infection, has been postulated to occur in camelids. The dendritic morphology of the observed corneal ulcers and the perceived response to topical antiviral agents has been cited as evidence for viral involvement, but the existence of this disease entity in camelids remains speculative at this point. Although typically a disease of small ruminants, Peste des Petits is also an infectious cause of keratoconjunctivitis in dromedary camels (Zakian et al. 2016). Peste des Petits is caused by infection with a Morbillivirus and is associated with severe conjunctivitis and ulcerative keratitis in camels occurring concurrently with diarrhea, stomatitis, pneumonia, sudden death, and abortion.

Historically, camelids have been cited as being relatively vulnerable to the development of marked corneal edema following a variety of insults to the corneal endothelium (Andrew et al. 2002). Aqueous humor analysis and specular microscopy evaluation of the corneal endothelium of alpacas and llamas did not provide a specific explanation for this clinical observation (Aubin et al. 2001); however, clinicians should be aware of the potential for endothelial degeneration in camelids with corneal or intraocular disease. Bullous keratopathy, with the formation of large stromal bullae, is described in alpacas as a potential complication of marked corneal edema and has been observed by the author on many occasions (Guyonnet et al. 2018). Endothelial dystrophy was suspected as the underlying etiology of corneal edema in a guanaco cria with multiple congenital ocular abnormalities (Barrie et al. 1978). Efforts should be made in camelids to protect the corneal endothelium during surgical interventions and to resolve any conditions that may damage these cells as rapidly as possible.

Anterior Uveal Disease

Congenital abnormalities of the anterior uvea are commonly encountered in camelids. Although pupillary membranes are frequently present in crias at birth that will resolve over the first few weeks of life, persistent pupillary membranes are also very common in older camelids (Webb et al. 2006). Persistent pupillary membranes can be present as single tissue strands or dense sheets of tissue. These membranes are most commonly iris-to-iris, but attachments to both the cornea and lens can occur as well. Persistent pupillary membranes most commonly appear as tissue with the same pigmentation pattern of the iris but may also be red when they contain patent vessels and blood (Fig. 33.21). Iris colobomas are observed in camelids and can be present as isolated lesions or associated with additional ocular development anomalies (Fig. 33.22) (Knickelbein et al. 2018).

In camelids, anterior uveitis may result in blepharospasm, conjunctival hyperemia, episcleral injection, ciliary flush, corneal edema, keratic precipitates, aqueous flare, anterior chamber fibrin, hyphema, hypopyon, and miosis (Fig. 33.23). Synechiae and cataracts are frequent sequelae. As in other animal species, uveitis may be associated with a variety of ocular and systemic conditions. A complete physical and ophthalmic examination is warranted in all cases of uveitis. General bloodwork, including hemogram and serum biochemistry panel, and urinalysis are indicated with additional diagnostic testing (e.g., serology, imaging studies, etc.) based upon the initial examination results and the specific clinical practice area. Although many cases of anterior uveitis in camelids are apparently idiopathic, traumatic, lens-induced, neoplastic, and infectious etiologies of uveitis also occur commonly in camelids (Grahn and Cullen 2001b; Madany et al. 2006). Systemic infectious disease that may be associated with uveitis in camelids include septicemia (which can result from failure of passive transfer in crias/calves or another tissue nidus of infection in any aged camelid), aspergillosis, brucellosis, listeriosis, *Mycoplasma haemolamae*, systemic mycosis (particularly coccidioidomycosis), equine herpesvirus-1, and toxoplasmosis (Coster et al. 2010; Rebhun et al. 1988; Pickett et al. 1985). Treatment of uveitis in camelids is similar to other species and includes topical and systemic ophthalmic anti-inflammatory medications, topical ophthalmic atropine, and systemic antimicrobials as indicated based upon the specific etiology of the uveitis (Madany et al. 2006).

Fig. 33.21 Numerous patent persistent pupillary membranes in a mature alpaca

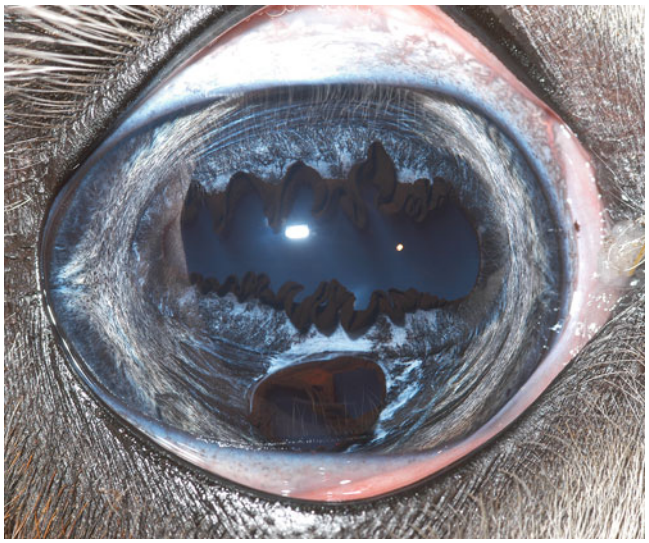

Fig. 33.22 Inferior iris coloboma in an alpaca

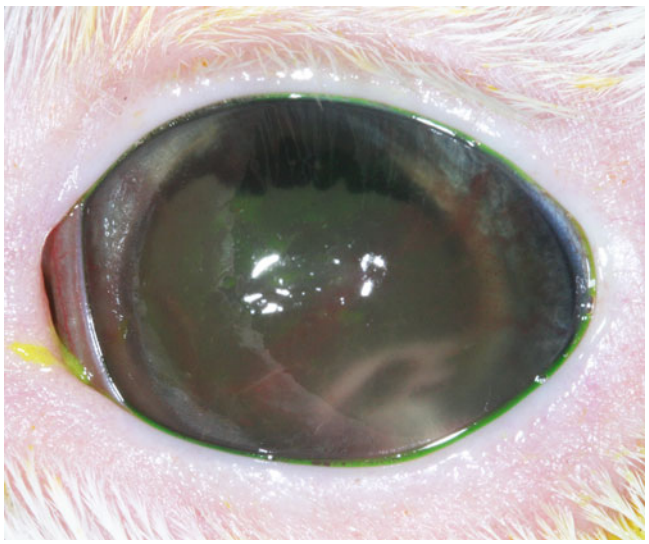

Fig. 33.23 Severe anterior uveitis in a septic alpaca cria with failure of passive transfer. Aqueous flare, anterior chamber fibrin, and hypopyon are present

Fig. 33.24 Extensive anterior uveal melanoma filling the anterior chamber and associated with secondary glaucoma. Buphthalmos and Haab's striae are present

Fig. 33.25 Congenital cataract in an alpaca cria

Anterior uveal neoplasia occurs relatively infrequently in camelids. Melanoma is the most common neoplasm of the iris and ciliary body in camelids and is reported in both alpacas and llamas (Tschoner et al. 2018; Hill and Hughes 2009; Hamor et al. 1999). Uveal melanomas can be heavily pigmented or amelanotic and clinically appear as light grey to black exophytic masses (Fig. 33.24). Secondary glaucoma, corneal opacities from contact with the mass, uveitis, and retinal detachments are common presenting complaints and associated ocular lesions. The biological behavior of uveal melanomas in camelids is not well established, but regional lymph node metastasis of uveal melanoma is described in a llama (Tschoner et al. 2018).

Lens Disease

Cataracts are the most common lens condition in camelids (Figs. 33.25 and 33.26). Congenital and acquired cataracts are reported in these species (Grahn and Cullen 2001b; Donaldson et al. 1992). Cataract etiologies that are suspected to occur in camelids include hereditary, those associated with other structural ocular abnormalities, post-inflammatory, toxins, and traumatic (Gionfriddo 2002). Cataracts may be present as isolated ocular lesions or in association with additional ocular abnormalities such as persistent pupillary membranes, persistent hyaloid artery, persistent hyperplastic primary vitreous, persistent tunica vasculosa lentis, choroidal coloboma, and optic nerve coloboma (Knickelbein et al. 2018; Gionfriddo and Blair 2002; Barrie et al. 1978). Sequelae of chronic cataracts in camelids may include lens-induced uveitis, lens subluxation, and secondary glaucoma.

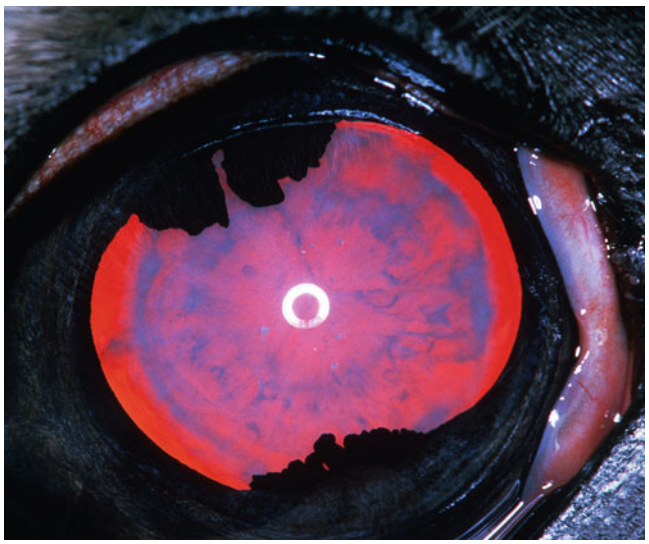

Fig. 33.26 Immature cataract in a llama viewed by retroillumination

Incipient and early immature cataracts may not have an appreciable effect on vision in camelids and can be monitored periodically for progression. Administration of a topical ophthalmic non-steroidal anti-inflammatory medication once or twice daily is recommended for cataracts that progress beyond the incipient stage to prevent, or to treat, lens-induced uveitis. Surgical cataract removal by phacoemulsification is the treatment of choice for cataracts that compromise vision. Historically, cataract surgery was considered to be a high-risk procedure in camelids and was generally discouraged due to the perceived guarded prognosis for a successful outcome. Numerous single animal case reports described serious post-operative complications and generally poor outcomes of cataract surgery in the South American camelids. Severe corneal

edema, corneal perforation, aqueous misdirection and ciliary block glaucoma, severe uveitis, and development of phthisis bulbi have been reported as complications and outcomes of cataract surgery in camelids (Gionfriddo 2002; Powell et al. 2002; Ingram and Sigler 1993).

More recently, successful cataract surgery in camelids has also been reported (Gionfriddo and Blair 2002). The author of this chapter has performed several phacoemulsification procedures on South American camelids, with the majority being uncomplicated and having favorable long-term outcomes. The utilization of atraumatic surgical techniques; balanced salt solution with bicarbonate, dextrose, and glutathione as the intraocular irritating solution; and copious intraocular instillation of high viscosity hyaluronic acid viscoelastic materials to protect the corneal endothelium and uvea contributes to a successful outcome in camelids (Gionfriddo 2002). Complete and thorough pre-operative assessment of the general health of the eye is important in camelids as additional ocular abnormalities are common in these species. Complete ophthalmic examination, electroretinography, and ocular ultrasonography (including color Doppler imaging to detect patent persistent fetal vascular structures) are recommended to screen for additional abnormalities that might result in intraoperative complications or preclude a successful visual outcome after surgery.

Lens luxations are uncommon in camelids. Lens subluxation (partial displacement of the lens from the patellar fossa) or complete luxation (either anterior or poster) occur as a result of zonular ligament damage. Primary lens luxations associated with genetic factors have not been described in camelids, but secondary lens luxations occur in association with chronic uveitis, hypermature cataracts, trauma, and chronic glaucoma (Fig. 33.27).

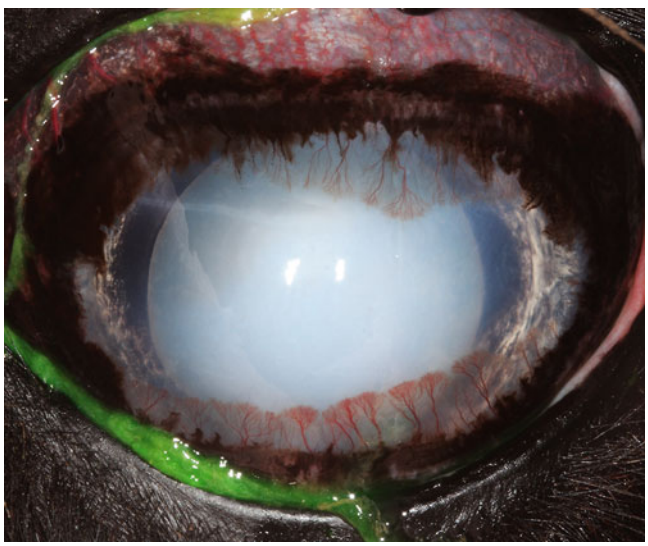

Fig. 33.27 Anterior lens luxation and a mature cataract in an alpaca with chronic lens-induced uveitis and buphthalmos

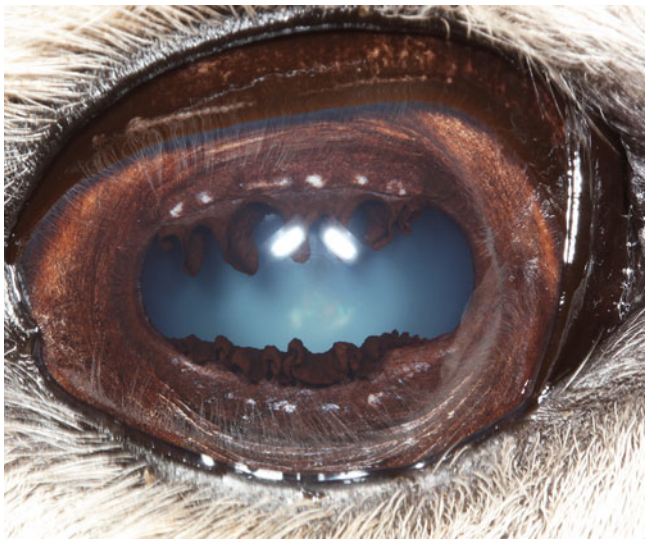

Fig. 33.28 Nuclear sclerosis in an elderly llama

Nuclear sclerosis is an expected finding in older camelids and is clinically recognized as a visible accentuation of the lens nucleus with a bluish-grey appearance (Fig. 33.28). Nuclear sclerosis results from new lens fiber growth throughout life and the resultant compression of lens fibers within the central lens. As in other animal species, nuclear sclerosis does not typically cause clinically important vision loss, the fundus is visible through the sclerotic lens, and treatment is not required.

Vitreous Disease

Congenital abnormalities of the vitreous frequently occur in camelids. Persistent hyaloid artery, persistent hyperplastic primary vitreous, and persistent tunica vasculosa lentis can all be observed. These vasculature structures can be patent or devoid of blood (Hostnik et al. 2012; Gionfriddo and Blair 2002). Congenital vitreal abnormalities have a variable effect on the vision, which largely depends on the extent and location of the persistent tissue, as well as if it is associated with cataract formation. The development of apparently spontaneous vitreous hemorrhage can result from the presence of any of these persistent fetal vascular structures.

The most common acquired vitreal disease in camelids is vitritis associated with panuveitis (Grahn and Cullen 2001b). Although vitritis can occur with any etiology of intraocular inflammatory disease, in some conditions (such as equine herpesvirus-1 infection), this lesion can be dramatic (Rebhun et al. 1988). Intraocular nematodiasis with a mobile intravitreal parasite was reported in a single llama with paralaphostrongylosis (Dunkel et al. 2011).

Posterior Segment Disease

Congenital abnormalities of the posterior segment are common in camelids. Colobomas of the retinal pigment epithelium, choroid, and optic disc are frequently encountered and described in publications (Schuh et al. 1991) (Fig. 33.29). Retinal dysplasia, choroidal dysplasia or hypoplasia, retinal non-attachment, optic nerve hypoplasia, and scleral ectasia also occur (Knickelbein et al. 2018; Leipold et al. 1994). These abnormalities range from incidental findings to blinding conditions. The etiology of these abnormalities is presently unknown, but genetic factors have been suggested, and related animals with multiple congenital ocular defects are reported (Knickelbein et al. 2018). The use of camelids with these congenital abnormalities for breeding should be discouraged.

Chorioretinitis and optic neuritis in camelids may result from a variety of conditions, including idiopathic, infectious, immune-mediated, and neoplastic diseases (Paulsen et al. 1989). In general, the differential diagnosis and diagnostic approached are the same as for anterior uveitis. Systemic infectious diseases that are specifically associated with posterior segment inflammation in camelids include equine herpesvirus-1, aspergillosis, toxoplasmosis, septicemia, and paralaphostrongylosis (Gionfriddo 2013; Dunkel et al. 2011; Coster et al. 2010; Rebhun et al. 1988; Pickett et al. 1985).

Equine herpesvirus-1 infection is acquired from contact with its natural equid hosts. Herd outbreaks and isolated cases of infection occur in alpacas and llamas (Rebhun et al. 1988). Severe panuveitis, sometimes concurrent with encephalitis and neurologic disease, is observed. Ocular lesions may include mydriasis, anterior uveitis, vitritis, retinal vasculitis, chorioretinitis, retinal detachment, and optic neuritis (House et al. 1991; Rebhun et al. 1988) (Figs. 33.30 and 33.31). Vitreal and retinal hemorrhages are common. Blindness may result from the ocular or central nervous system lesions associated with equine herpesvirus-1 infection, and the prognosis for the return of vision is poor (Rebhun et al. 1988). Infection in animals with the severe neurologic disease may be fatal. It is currently unclear how medically important and common this viral pathogen is in wild camelid populations, but serologic surveys of wild guanacos and vicuñas have not identified evidence of exposure to equine herpesvirus-1 (Marcoppido et al. 2010; Karesh et al. 1998).

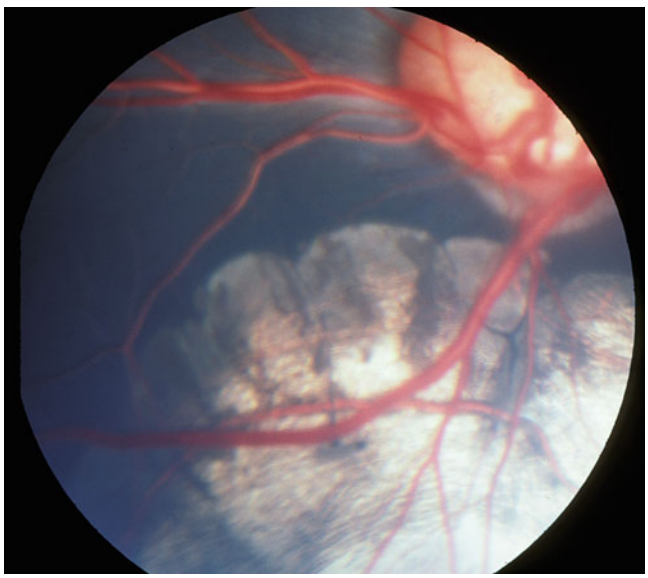

Fig. 33.29 Optic disc coloboma, choroidal hypoplasia, and scleral ectasia in an alpaca cria

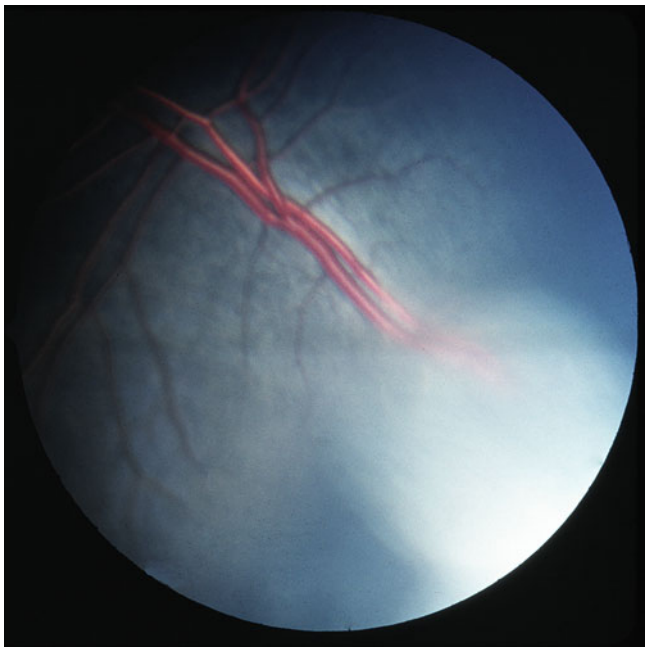

Fig. 33.30 Posterior vitritis, chorioretinitis, and optic neuritis in an alpaca cria with equine herpesvirus-1 infection. The optic disc is obscured from view by the massive posterior vitreal inflammatory response

Aspergillosis is described as causing pneumonia, neurologic disease, and bilateral chorioretinitis in camelids (Pickett et al. 1985). Toxoplasmosis is anecdotally described to cause chorioretinitis and panophthalmitis in llamas, sometimes concurrent with late-term abortions (Gionfriddo 2010). In camelids, septicemia occurs most commonly in neonates with failure of passive transfer and can result in blindness, chorioretinitis, and retinal detachment (Dolente et al. 2007; Adams and Garry 1992). Intraocular nematodiasis was described in a single llama associated with the *Paralaphastrongylus tenuis* migration into the posterior segment of the eye (Dunkel et al. 2011). The llama presented with blepharospasm, and a mobile helminth was identified within the

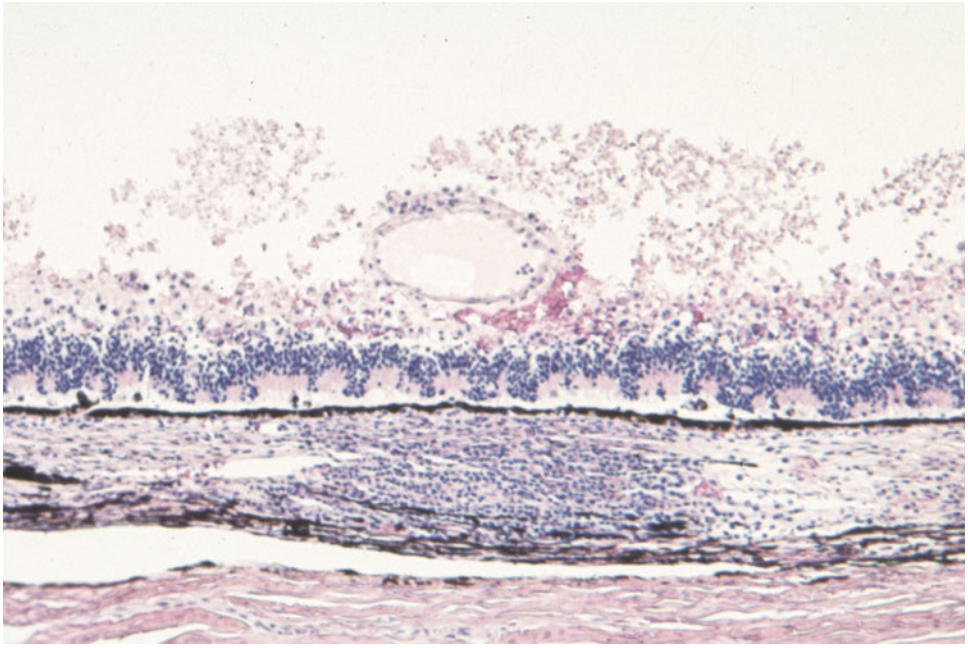

Fig. 33.31 Histologic photomicrograph of equine herpesvirus-1 retinitis in a llama. Characteristic histopathologic findings include acute necrotizing retinitis and eosinophilic intranuclear

vitreous. The affected eye was nonvisual, presumably from central nervous system lesions. The nematode appeared to have migrated along the optic chiasm and optic nerve into the vitreal cavity of the eye.

Although they are believed to develop rarely, neoplasia of the camelid posterior segment has been reported several times in South American camelids (Schoeniger et al. 2006; Fugaro et al. 2005; Hendrix et al. 2000). The masses were identified as a malignant teratoid medulloepithelioma, malignant nonteratoid medulloepithelioma, and retinoblastoma. The presenting ocular signs and lesions in the animals were varied and included anterior uveitis, buphthalmos, corneal perforation, visible intraocular mass, and subretinal mass. The ultrasonographic features of a posterior segment neoplasm were described in a dromedary camel, including the presence of a hyperechoic mass with well-defined boundaries, but the mass was not further identified (El-Tookhy and Tharwat 2012).

Glaucoma

Glaucoma infrequently occurs in camelids. Congenital glaucoma is rare in camelids and is usually associated with multiple congenital ocular defects (Cullen and Grahn 1997). Secondary glaucoma, resulting from chronic uveitis, intraocular masses, or lens-induced uveitis, is the most common type of glaucoma encountered in clinical practice (Fig. 33.24) (Grahn and Cullen 2001b). There are few literature descriptions of glaucoma in camelids. A llama with idiopathic chronic uveitis, iris bombé, and buphthalmos is described, and a case of multiple congenital ocular anomalies with concurrent congenital glaucoma in a llama is reported (Grahn and Cullen 2001a; Cullen and Grahn 1997). Primary glaucoma has not been described to occur in camelids.

Ocular Toxicities

Presumptive enrofloxacin-induced retinopathy is reported in a guanaco (Harrison et al. 2006). The guanaco developed vision loss several days after being treated with a 14-day course of enrofloxacin. Optic disc pallor and white infiltrates temporal to the optic disc were observed bilaterally on fundus examination, but the retinas otherwise appeared normal. No clinical improvements or examination changes were noted after 5 months. During the histopathologic evaluation of the eyes, outer retinal atrophy of the central retina was noted, similar to what occurs in feline enrofloxacin retinal toxicity.

Topical ophthalmic corticosteroids administration can induce abortion in camelids. In llamas, administration of neomycin-polymyxin B-dexamethasone ophthalmic ointment resulted in systemic absorption, detectable serum concentrations within 24 h of administration, and abortions in some animals (Graham et al. 2002). As the application of topical corticosteroids can induce abortions in some camelids and late-gestation animals are at greatest risk, the judicious use of topical ophthalmic corticosteroids and avoidance when possible in pregnant animals is recommended.

References

Abdalla O, Fahmy MF, Arnautovic I (1970) Anatomical study of the lacrimal apparatus of the one-humped camel. Acta Anat (Basel) 75(4):638–650. https://doi.org/10.1159/000143474

Abdel-Moniem ME (1992) Prenatal development of the retina in one humped camel. Assiut Vet Med J 27:45–55

Abdo M, Hosaka YZ, Erasha A et al (2014) Prenatal development of the eye tunics in the dromedary camel (Camelus dromedarius). Anat Histol Embryol 43(4):257–264. https://doi.org/10.1111/ahe.12069

Abou-Elmagd A (1992) Ultrastructural observations on myoepithelial cells and nerve terminals in the camel Harderian gland. Anat Embryol (Berl) 185(5):501–507. https://doi.org/10.1007/bf00174087

Abuagla IA, Ali HA, Ibrahim ZH (2016) An anatomical study on the eye of the one-humped camel (Camelus dromedarius). Int J Vet Sci 5(3): 137–141

Abu-Zidan FM, Hefny AF, Eid HO et al (2012) Camel-related injuries: prospective study of 212 patients. World J Surg 36(10):2384–2389. https://doi.org/10.1007/s00268-012-1673-2

Adams R, Garry FB (1992) Gram-negative bacterial infection in neonatal New World camelids: six cases (1985-1991). J Am Vet Med Assoc 201(9):1419–1424

Ahamad SR, Raish M, Yaqoob SH et al (2017) Metabolomics and trace element analysis of camel tear by GC-MS and ICP-MS. Biol Trace Elem Res 177(2):251–257. https://doi.org/10.1007/s12011-016-0889-7

Akhtar S (2013) Ultrastructure alteration in the corneal stroma of hydrated camel corneoscleral button and corneal button. Microsc Res Tech 76(1):86–93. https://doi.org/10.1002/jemt.22140

Al-Ali MA, Hefny AF, Abu-Zidan FM (2019) Head, face and neck camel-related injuries: biomechanics and severity. Injury 50(1): 210–214. https://doi.org/10.1016/j.injury.2018.11.029

Ali MJ, Rehorek SJ, Paulsen F (2019) A major review on disorders of the animal lacrimal drainage systems: evolutionary perspectives and comparisons with humans. Ann Anat 224:102–112. https://doi.org/10.1016/j.aanat.2019.04.003

Almubrad T, Akhtar S (2012) Ultrastructure features of camel cornea--collagen fibril and proteoglycans. Vet Ophthalmol 15(1):36–41. https://doi.org/10.1111/j.1463-5224.2011.00918.x

Almubrad T, Khan MFJ, Akhtar S (2010) Swelling studies of camel and bovine corneal stroma. Clin Ophthalmol 4:1053–1060. https://doi.org/10.2147/opth.s12576

Al-Ramadan SY, Ali AM (2012) Morphological studies on the third eyelid and its related structures in the one-humped camel (Camelus dromedarius). J Vet Anat 5(2):71–81

Alsafy MAM (2010) Comparative morphological studies on the lacrimal apparatus of one humped camel, goat and donkey. J Biol Sci 10:224–230

Altunay H (2007) Fine structure of the retinal pigment epithelium, Bruch's membrane and choriocapillaris in the camel. Anat Histol Embryol 36(2):116–120. https://doi.org/10.1111/j.1439-0264.2006.00736.x

Aly KH, Abd-Elhafez E, Ali M et al (2009) Histomorphometric analysis of the irides of dogs, camels, buffalos and donkeys. Res Vet Sci 86(1):1–6. https://doi.org/10.1016/j.rvsc.2008.05.004

Am M, Ra F, El-Naggar AH et al (2018) Structure and microanalysis of tear film fering of camel tears, human tears, and refresh plus. Mol Vis 24:305–314

Andrew SE, Willis AM, Anderson DE (2002) Density of corneal endothelial cells, corneal thickness, and corneal diameters in normal eyes of llamas and alpacas. Am J Vet Res 63(3):326–329. https://doi.org/10.2460/ajvr.2002.63.326

Arnold CE, Baird AN, Reilly LK (2002) Surgical correction of atresia of the nasolacrimal duct in the new world camelids: 3 cases. New England J Large Anim Health 1:15–18

Aubin ML, Gionfriddo JR, Mama KR et al (2001) Analysis of aqueous humor obtained from normal eyes of llamas and alpacas. Am J Vet Res 62(7):1060–1062. https://doi.org/10.2460/ajvr.2001.62.1060

Awkati A, Al-Bagdadi F (1971) Lacrimal gland of the camel (Camelus dromedarius). Am J Vet Res 32(3):505–510

Badawy AM, Eshra EA (2018) Development of an ultrasound-guided technique for retrobulbar nerve block in dromedary camels: a cadaveric study. Vet Anaesth Analg 45(2):175–182. https://doi.org/10.1016/j.vaa.2017.09.039

Balamurugan V, Venkatesan G, Bhanuprakash V et al (2013) Camelpox, an emerging orthopox viral disease. Indian J Virol 24(3):295–305. https://doi.org/10.1007/s13337-013-0145-0

Barrie KP, Jacobson E, Peiffer RL Jr (1978) Unilateral cataract with lens coloboma and bilateral corneal edema in a guanaco. J Am Vet Med Assoc 173(9):1251–1252

Belknap EB, Dunstan RW (1990) Congenital ichthyosis in a llama. J Am Vet Med Assoc 197(6):764–767

Bertin FR, Squires JM, Kritchevsky JE et al (2015) Clinical findings and survival in 56 sick neonatal New World camelids. J Vet Int Med 29(1):368–374. https://doi.org/10.1111/jvim.12478

Bishnoi P, Gahlot TK (2001a) Descemetocele and subconjunctival haemorrhage in camels (Camelus dromedarius). J Camel Pract Res 8(1):87

Bishnoi P, Gahlot TK (2001b) Note on incidence and occurrence of diverse ophthalmic affections in camels (Camelus dromedarius). J Camel Pract Res 8(1):73–75

Borkowski R, Moore PA, Mumford S et al (2007) Adaptations of subpalpebral lavage systems used for llamas (Lama glama) and a harbor seal (Phoca vitulina). J Zoo Wildl Med 38(3):453–459

Coster ME, Ramos-Vara JA, Vemulapalli R et al (2010) Coccidioides posadasii keratouveitis in a llama (Lama glama). Vet Ophthalmol 13(1):53–57. https://doi.org/10.1111/j.1463-5224.2009.00747.x

Cullen CL, Grahn BH (1997) Congenital glaucoma in a llama (Lama glama). Vet Comp Ophthalmol 7:253–257

Czerwinski SL (2019) Ocular surface disease in New World camelids. Vet Clin North Am Exot Anim Pract 22(1):69–79. https://doi.org/10.1016/j.cvex.2018.09.001

D'Alterio GL, Knowles TG, Eknaes EI et al (2006) Postal survey of the population of South American camelids in the United Kingdom in 2000/01. Vet Rec 158(3):86–90. https://doi.org/10.1136/vr.158.3.86

Dolente BA, Lindborg S, Palmer JE et al (2007) Culture-positive sepsis in neonatal camelids: 21 cases. J Vet Int Med 21(3):519–525. https://doi.org/10.1892/0891-6640(2007)21[519,csincc]2.0.co;2

Donaldson LL, Holland M, Koch SA (1992) Atracurium as an adjunct to halothane-oxygen anesthesia in a llama undergoing intraocular surgery. A case report. Vet Surg 21(1):76–79

Dunkel B, Sweeney RW, Habecker PL et al (2011) Intraocular nematodiasis in a llama (Lama glama). Can Vet J 52(2):181–183

El-Tookhy O, Tharwat M (2012) Clinical and ulstrasonopgraphic findings of some ocular affections in dromedary camels. J Camel Pract Res 19(2):183–191

El-Tookhy O, Al-Sobayil F, Ahmed AF (2012) Normal ocualr ecobiometry of the dromedary camels. J Camel Pract Res 19(1): 13–17

Fahmy MF, Arnautovic I, Abdalla O (1971) The morphology of the tarsal glands and the glands of the third eyelid in the one-humped camel. Acta Anat (Basel) 78(1):40–46. https://doi.org/10.1159/000143572

Fahmy LS, Hegazy AA, Abdelhamid MA, Hatem ME, Shamaa AA (2003) Studies on eye affections among camels in Egypt: Clinical and bacteriological studies. Sci J King Faisal Univ (Basic Appl Sci) 4:159–176

Fischer K, Hendrix D (2012) Conjunctivitis and ulcerative keratitis secondary to conjunctival plant foreign bodies in a herd of alpacas (Lama Pacos). Vet Ophthalmol 15(2):110–114. https://doi.org/10.1111/j.1463-5224.2011.00939.x

Fugaro MN, Kiupel M, Montiani-Ferreira F et al (2005) Retinoblastoma in the eye of a llama (Lama glama). Vet Ophthalmol 8(4):287–290. https://doi.org/10.1111/j.1463-5224.2005.00407.x

Garland D, Rao PV, Del Corso A et al (1991) Zeta-Crystallin is a major protein in the lens of Camelus dromedarius. Arch Biochem Biophys 285(1):134–136. https://doi.org/10.1016/0003-9861(91)90339-k

Gauly M, Vaughan J, Hogreve SK et al (2005) Brainstem auditory-evoked potential assessment of auditory function and congenital deafness in llamas (Lama glama) and alpacas (L. pacos). J Vet Int Med 19(5):756–760. https://doi.org/10.1892/0891-6640(2005)19[756,bapaoa]2.0.co;2

Gelatt KN, Otzen Martinic GB, Flaneig JL et al (1995) Results of ophthalmic examinations of 29 alpacas. J Am Vet Med Assoc 206(8):1204–1207

Gionfriddo JR (2002) Cataracts in New World camelids (llamas, alpacas, vicunas, and guanacos). Vet Clin North Am Exot Anim Pract 5(2):357–369. https://doi.org/10.1016/s1094-9194(01)00006-8

Gionfriddo JR (2010) Ophthalmology of South American camelids. Vet Clin North Am Food Anim Pract 26(3):531–555. https://doi.org/10.1016/j.cvfa.2010.08.004

Gionfriddo JR (2013) Ophthalmology of new world camelids. In: Gelatt KN, Gilger BC, Kern TJ (eds) Veterinary ophthalmology, 5th edn. John Wiley & Sons Inc., pp 1675–1691

Gionfriddo JR, Blair M (2002) Congenital cataracts and persistent hyaloid vasculature in a llama (Lama glama). Vet Ophthalmol 5(1):65–70. https://doi.org/10.1046/j.1463-5224.2002.00207.x

Gionfriddo JR, Rosenbusch R, Kinyon JM et al (1991) Bacterial and mycoplasmal flora of the healthy camelid conjunctival sac. Am J Vet Res 52(7):1061–1064

Gionfriddo JR, Gabal MA, Betts DM (1992) Fungal flora of the healthy camelid conjunctival sac. Am J Vet Res 53(5):643–645

Gionfriddo JR, Gionfriddo JP, Krohne SG (1997) Ocular diseases of llamas: 194 cases (1980-1993). J Am Vet Med Assoc 210(12):1784–1787

Gionfriddo JR, Davidson H, Asem EK et al (2000) Detection of lysozyme in llama, sheep, and cattle tears. Am J Vet Res 61(10):1294–1297. https://doi.org/10.2460/ajvr.2000.61.1294

Goerigk D, Theuss T, Pfeffer M et al (2014) Cowpox virus infection in an alpaca (Vicugna pacos) - clinical symptoms, laboratory diagnostic findings and pathological changes. Tierarztl Prax Ausg G Grosstiere Nutztiere 42(3):169–177. doi:14030169 [pii]

Graham BP, Powell CC, Gionfriddo JR et al (2002) Evaluation of neomycin, polymixin B, dexamethasone ophthalmic ointment as a cause of abortion in llamas. Abstracts of 33rd Annual Meeting of the American College of Veterinary Ophthalmologists, p 301

Grahn BH, Cullen CL (2001a) Diagnostic ophthalmology. Can Vet J 42(9):735–736

Grahn BH, Cullen CL (2001b) Diagnostic ophthalmology. Bilateral idiopathic uveitis in a llama. Can Vet J 42(7):575–576

Guyonnet A, Bourguet A, Donzel E et al (2018) Bilateral bullous keratopathy secondary to melting keratitis in a Suri alpaca (Vicugna pacos). Clin Case Rep 6(4):626–630. https://doi.org/10.1002/ccr3.1389

Hamor RE, Severin GA, Roberts SM (1999) Intraocular melanoma in an alpaca. Vet Ophthalmol 2(3):193–196. https://doi.org/10.1046/j.1463-5224.1999.00075.x

Harman A, Dann J, Ahmat A et al (2001) The retinal ganglion cell layer and visual acuity of the camel. Brain Behav Evol 58(1):15–27. https://doi.org/10.1159/000047258

Harrison TM, Dubielzig RR, Harrison TR et al (2006) Enrofloxacin-induced retinopathy in a guanaco (Lama guanicoe). J Zoo Wildl Med 37(4):545–548. https://doi.org/10.1638/05-114.1

Hendrix DV, Bochsler PN, Saladino B et al (2000) Malignant teratoid medulloepithelioma in a llama. Vet Pathol 37(6):680–683. https://doi.org/10.1354/vp.37-6-680

Hill FI, Hughes SM (2009) Osteogenic intraocular melanoma in an alpaca (Vicugna pacos). J Vet Diagn Invest 21(1):171–173. https://doi.org/10.1177/104063870902100132

Ho K, Cobiella D, Walz H et al (2017) Cutaneous candidiasis infection in two alpacas. Vet Rec Case Rep 4:e000354. https://doi.org/10.1136/vetreccr-2016-000354

Hostnik ET, Wickins SC, Conway JA, Dark MJ (2012) Ocular and olfactory forebrain abnormalities within a neonatal alpaca (Vicugna pacos). J Vet Med Sci 74(7):945–947. https://doi.org/10.1292/jvms.11-0558. Epub 2012 Mar 8

House JA, Gregg DA, Lubroth J et al (1991) Experimental equine herpesvirus-1 infection in llamas (Lama glama). J Vet Diagn Investig 3(2):137–143

Ibrahim ZH, Abdalla AB, Osman DI (2006) A gross anatomical study of the lacrimal apparatus of the camel (Camelus dromedarius). Sudan J Sci Technol 9:1–8

Ingram KA, Sigler RL (1993) Cataract removal in a young llama. Proceedings of the Annual Meeting of the American Association of Zoo Veterinarians, pp 95–97

Jaint RK, Kumar P, Singh AD (2010) Topographic anatomy, blood supply and nerve supply of the extrinsic muscles of the eyeball in camel (Camelus dromedarius). J Camel Pract Res 17:167–171

Jarvinen JA, Miller JA, Oehler DD (2002) Pharmacokinetics of ivermectin in llamas (Lama glama). Vet Rec 150(11):344–346. https://doi.org/10.1136/vr.150.11.344

Jones ML, Gilmour MA, Streeter RN (2007) Use of grid keratotomy for the treatment of indolent corneal ulcer in a llama. Can Vet J 48(4):416–419

Karesh WB, Uhart MM, Dierenfeld ES et al (1998) Health evaluation of free-ranging guanaco (Lama guanicoe). J Zoo Wildl Med 29(2):134–141

Kassab A (2012) Ultrasonographic and macroscopic anatomy of the enucleated eyes of the buffalo (Bos bubalis) and the one-humped camel (Camelus dromedarius) of different ages. Anat Histol Embryol 41(1):7–11. https://doi.org/10.1111/j.1439-0264.2011.01097.x

Kilic N, Toplu N, Aydogan A et al (2010) Corneal papilloma associated with papillomavirus in a one-humped camel (Camelus dromedarius). Vet Ophthalmol 13(Suppl):100–102. https://doi.org/10.1111/j.1463-5224.2010.00795.x

Klauss G, Suedmeyer WK, Galle LE et al (2005) Surgical resection of an orbital fat prolapse in a California sea lion (Zalophus californianus). Vet Ophthalmol 8(4):277–281. https://doi.org/10.1111/j.1463-5224.2005.00396.x

Knickelbein KE, Maggs DJ, Reilly CM et al (2018) Multiple ocular developmental defects in four closely related alpacas. Vet Ophthalmol 21(5):544–551. https://doi.org/10.1111/vop.12540

Kotb AM, Ibrahim IA, Aly KH et al (2019) Histomorphometric analysis of the choroid of donkeys, buffalos, camels and dogs. Int Ophthalmol 39(6):1239–1247. https://doi.org/10.1007/s10792-018-0932-0

Kumar P, Jain RK, Gupta AN (2003) Histoarchitecture of Harderian gland of Camel (Camelus dromedarius). Indian J Anim Sci 73(9):972–975

Kumar P, Purohit NR, Gahlot TK (2016) Retrospective analysis of ocular affections in dromedary camels. J Camel Pract Res 23(2):247–250

Ledbetter EC, Scarlett JM (2008) Isolation of obligate anaerobic bacteria from ulcerative keratitis in domestic animals. Vet Ophthalmol 11(2):114–122. https://doi.org/10.1111/j.1463-5224.2008.00610.x

Ledbetter EC, Montgomery KW, Landry MP et al (2013) Characterization of fungal keratitis in alpacas: 11 cases (2003-2012). J Am Vet Med Assoc 243(11):1616–1622. https://doi.org/10.2460/javma.243.11.1616

Leipold HW, Hiraga T, Johnson LW (1994) Congenital defects in the llama. Vet Clin North Am Food Anim Pract 10(2):401–420. https://doi.org/10.1016/S0749-0720(15)30572-7

LoPinto AJ, Pirie CG, Ayres SL et al (2017a) Comparison of indocyanine green and sodium fluorescein for anterior segment angiography of ophthalmically normal eyes of goats, sheep, and alpacas performed with a digital single-lens reflex camera adaptor. Am J Vet Res 78(3):311–320. https://doi.org/10.2460/ajvr.78.3.311

LoPinto AJ, Pirie CG, Bedenice D et al (2017b) Corneal thickness of eyes of healthy goats, sheep, and alpacas manually measured by use of a portable spectral-domain optical coherence tomography device. Am J Vet Res 78(1):80–84. https://doi.org/10.2460/ajvr.78.1.80

Madany J, Nowakowski H, Pepiak A et al (2006) Uveitis anterior in a camel - the clinical case. Bull Vet Inst Pulawy 50:131–135

Mahmood S, Razak JM, Al-Maliki SH (2013) Histomorpholgical study of ciliary body and ciliary process in one humped camel (Camelus Dromedarius). Bas J Vet Res 12(2):228–236

Mangan BG, Gionfriddo JR, Powell CC (2008) Bilateral nasolacrimal duct atresia in a cria. Vet Ophthalmol 11(1):49–54. https://doi.org/10.1111/j.1463-5224.2007.00595.x

Marcoppido G, Parreno V, Vila B (2010) Antibodies to pathogenic livestock viruses in a wild vicuna (Vicugna vicugna) population in the Argentinean Andean altiplano. J Wildl Dis 46(2):608–614. https://doi.org/10.7589/0090-3558-46.2.608

Marzok MA, El-Khodery SA (2015) Intraocular pressure in clinically normal dromedary camels (Camelus dromedarius). Am J Vet Res 76(2):149–154. https://doi.org/10.2460/ajvr.76.2.149

Marzok MA, Badawy AM, El-Khodery SA (2017) Reference values and repeatability of the Schirmer tear tests I and II in domesticated, clinically normal dromedary camels (Camelus dromedarius). Vet Ophthalmol 20(3):259–265. https://doi.org/10.1111/vop.12411

Massa KL, Murphy CJ, Hartmann FA et al (1999) Usefulness of aerobic microbial culture and cytologic evaluation of corneal specimens in the diagnosis of infectious ulcerative keratitis in animals. J Am Vet Med Assoc 215(11):1671–1674

McCauley CT, Campbell GA, Cummings CA et al (2000) Ossifying fibroma in a llama. J Vet Diagn Investig 12(5):473–476. https://doi.org/10.1177/104063870001200517

McDonald JE, Knollinger AM, Dustin Dees D et al (2017) Comparison of intraocular pressure measurements using rebound (TonoVet((R))) and applanation (TonoPen-XL((R))) tonometry in clinically normal alpacas (Vicugna pacos). Vet Ophthalmol 20(2):155–159. https://doi.org/10.1111/vop.12384

McDonald JE, Knollinger AM, Dees DD et al (2018) Determination of Schirmer tear test-1 values in clinically normal alpacas (Vicugna pacos) in North America. Vet Ophthalmol 21(1):101–103. https://doi.org/10.1111/vop.12466

Mohammadpour AA (2008) Anatomical characteristics of dorsal lacrimal gland in one humped camel (Camelus dromedarius). J Biol Sci 8(6):1104–1106

Mohammadpour AA (2009) Morphological and histological study of superior lacrimal gland of third eyelid in camel (Camelus dromedarius). Iran J Vet Res 10(4):334–338

Moore CP, Shaner JB, Halenda RM et al (1999) Congenital ocular anomalies and ventricular septal defect in a dromedary camel (Camelus dromedarius). J Zoo Wildl Med 30(3):423–430

Muller LJ, Pels E, Vrensen GF (2001) The specific architecture of the anterior stroma accounts for maintenance of corneal curvature. Br J Ophthalmol 85(4):437–443. https://doi.org/10.1136/bjo.85.4.437

Myers DA, Smith CD, Greiner EC et al (2010) Cutaneous periocular Habronema infection in a dromedary camel (Camelus dromedarius). Vet Dermatol 21(5):527–530. https://doi.org/10.1111/j.1365-3164.2009.00795.x

Naruka NS (1983) Studies on some of the regional anaesthesia of the head of the camel (Camelus dromedarius). M.V.Sc. Thesis, Sukhadia University, Udaipur

Nuhsbaum MT, Gionfriddo JR, Powell CC et al (2000) Intraocular pressure in normal llamas (Lama glama) and alpacas (Lama pacos). Vet Ophthalmol 3(1):31–34. https://doi.org/10.1046/j.1463-5224.2000.00103.x

Osman AHK, Eidaroos H, Metwally E (2013) Histogenesis of the camel retina (Camelus dromedarius). Cell Dev Biol 2(1):1–7. https://doi.org/10.4172/2168-9296.1000109

Osuobeni EP, Hamidzada WA (1999) Ultrasonographic determination of the dimensions of ocular components in enucleated eyes of the one-humped camel (Camelus dromedarius). Res Vet Sci 67(2):125–129. https://doi.org/10.1053/rvsc.1998.0288

Paulsen ME, Young S, Smith JA et al (1989) Bilateral chorioretinitis, centripetal optic neuritis, and encephalitis in a llama. J Am Vet Med Assoc 194(9):1305–1308

Pickett JP, Moore CP, Beehler BA et al (1985) Bilateral chorioretinitis secondary to disseminated aspergillosis in an alpaca. J Am Vet Med Assoc 187(11):1241–1243

Pirie CG, Pizzirani S, Parry NM (2008) Corneal epithelial inclusion cyst in a llama. Vet Ophthalmol 11(2):111–113. https://doi.org/10.1111/j.1463-5224.2008.00608.x

Powell CC, Nuhsbaum TM, Gionfriddo JR (2002) Aqueous misdirection and ciliary block (malignant) glaucoma after cataract removal in a llama. Vet Ophthalmol 5(2):99–101. https://doi.org/10.1046/j.1463-5224.2002.00214.x

Prkno A, Hoffmann D, Goerigk D et al (2017) Epidemiological investigations of four cowpox virus outbreaks in Alpaca Herds, Germany. Viruses 9(11):344. https://doi.org/10.3390/v9110344

Prkno A, Kaiser M, Goerigk D et al (2018) Clinical presentation of cowpox virus infection in South American camelids - A review. Tierarztl Prax Ausg G Grosstiere Nutztiere 46(1):50–56. https://doi.org/10.15653/TPG-170502

Pucket JD, Boileau MJ, Sula MJ (2014) Calcific band keratopathy in an alpaca. Vet Ophthalmol 17(4):286–289. https://doi.org/10.1111/vop.12097

Rahi AH, Sheikh H, Morgan G (1980) Histology of the camel eye. Acta Anat (Basel) 106(3):345–350. https://doi.org/10.1159/000145199

Ranjan R, Nath K, Naranware S et al (2016) Ocular affections in dromedary camel - a prevalence study. Intas Polivet 17(II):348–349

Rankin AJ, Hosking KG, Roush JK (2012) Corneal sensitivity in healthy, immature, and adult alpacas. Vet Ophthalmol 15(1):31–35. https://doi.org/10.1111/j.1463-5224.2011.00910.x

Rebhun WC, Jenkins DH, Riis RC et al (1988) An epizootic of blindness and encephalitis associated with a herpesvirus indistinguishable from equine herpesvirus I in a herd of alpacas and llamas. J Am Vet Med Assoc 192(7):953–956

Richter M, Grest P, Spiess B (2006) Bilateral lipid keratopathy and atherosclerosis in an alpaca (Lama pacos) due to hypercholesterolemia. J Vet Intern Med 20(6):1503–1507. https://doi.org/10.1892/0891-6640(2006)20[1503:blkaai]2.0.co;2

Rodriguez-Alvaro A, Gonzalez-Alonso-Alegre EM, Delclaux-Real del Asua M et al (2005) Surgical correction of a corneal perforation in an alpaca (Lama pacos). J Zoo Wildl Med 36(2):336–339. https://doi.org/10.1638/04-031.1

Sadegh AB, Shadkhast M (2007) Lacrimal apparatus system in one-humped camel of Iran (Camelus dromedarius): anatomical and radiological study. Iran J Vet Surg 2(5):75–80

Sandmeyer LS, Bauer BS, Breaux CB et al (2011) Congenital nasolacrimal atresia in 4 alpacas. Can Vet J 52(3):313–317

Sapienza JS, Isaza R, Johnson RD et al (1992) Anatomic and radiographic study of the lacrimal apparatus of llamas. Am J Vet Res 53(6):1007–1009

Sazmand A, Joachim A (2017) Parasitic diseases of camels in Iran (1931-2017) - a literature review. Parasite 24:21. https://doi.org/10.1051/parasite/2017024

Schoeniger S, Donner LR, Van Alstine WG (2006) Malignant nonteratoid ocular medulloepithelioma in a llama (Lama glama). J Vet Diagn Investig 18(5):499–503. https://doi.org/10.1177/104063870601800517

Schuh JCL, Feruson JG, Fisher MA (1991) Congenital coloboma in a llama. Can Vet J 32:432–433

Scott DW, Vogel JW, Fleis RI et al (2011) Skin diseases in the alpaca (Vicugna pacos): a literature review and retrospective analysis of 68 cases (Cornell University 1997-2006). Vet Dermatol 22(1):2–16. https://doi.org/10.1111/j.1365-3164.2010.00918.x

Shamsi FA, Chen Z, Liang J et al (2011) Analysis and comparison of proteomic profiles of tear fluid from human, cow, sheep, and camel eyes. Invest Ophthalmol Vis Sci 52(12):9156–9165. https://doi.org/10.1167/iovs.11-8301

Shokry M, Abdel Hamid MA, Ahmed AS (1987) Radiogrphay of the nasolacrimal duct in the dromedary (Camelus dromedarius). J Zoo Anim Med 18:94–95

Smuts MMS, Bezuidenhout AJ (1987) Anatomy of the dromedary. Oxford University Press, Oxford

Storms G, Meersschaert C, Farnir F et al (2016) Normal bacterial conjunctival flora in the Huacaya alpaca (Vicugna pacos). Vet Ophthalmol 19(1):22–28. https://doi.org/10.1111/vop.12248

Sumner JP, Mueller T, Clapp KS et al (2012) Modified ear canal ablation and lateral bulla osteotomy for management of otitis media in an alpaca. Vet Surg 41(2):273–277. https://doi.org/10.1111/j.1532-950X.2011.00904.x

Tefera M (2004) Observations on the clinical examination of the camel (Camelus dromedarius) in the field. Trop Anim Health Prod 36(5):435–449. https://doi.org/10.1023/b:trop.0000035006.37928.cf

Tejedor-Junco MT, Gutierrez C, Gonzalez M et al (2010) Outbreaks of keratoconjunctivitis in a camel herd caused by a specific biovar of Moraxella canis. J Clin Microbiol 48(2):596–598. https://doi.org/10.1128/JCM.02329-09

Townsend WM (2010) Examination techniques and therapeutic regimens for the ruminant and camelid eye. Vet Clin North Am Food Anim Pract 26(3):437–458. https://doi.org/10.1016/j.cvfa.2010.08.001

Trbolova A, Gionfriddo JR, Ghaffari MS (2012) Results of Schirmer tear test in clinically normal llamas (Lama glama). Vet Ophthalmol 15(6):383–385. https://doi.org/10.1111/j.1463-5224.2012.01002.x

Tschoner T, Voigt K, Falkenau A et al (2018) Intraocular melanoma in a 10-year-old female llama (Lama glama). Tierarztl Prax Ausg G Grosstiere Nutztiere 46(5):334–339. https://doi.org/10.15653/TPG-180093

Valentine BA, Martin JM (2007) Prevalence of neoplasia in llamas and alpacas (Oregon State University, 2001-2006). J Vet Diagn Investig 19(2):202–204. https://doi.org/10.1177/104063870701900213

Wang HH, Gallagher SK, Byers SR et al (2015) Retinal ganglion cell distribution and visual acuity in alpacas (Vicugna pacos). Vet Ophthalmol 18(1):35–42. https://doi.org/10.1111/vop.12131

Wang JL (2002) The arterial supply to the eye of the bactrian camel (Camelus bactrianus). Vet Res Commun 26(7):505–512. https://doi.org/10.1023/a:1020310213203

Webb AA, Cullen CL, Lamont LA (2006) Brainstem auditory evoked responses and ophthalmic findings in llamas and alpacas in Eastern Canada. Can Vet J 47(1):74–77

Welihozkiy A, Bedenice D, Price LL et al (2011) Measurement of corneal sensitivity in 20 ophthalmologically normal alpacas. Vet Ophthalmol 14(5):333–336. https://doi.org/10.1111/j.1463-5224.2011.00895.x

Willis AM, Anderson DE, Gemensky AJ et al (2000) Evaluation of intraocular pressure in eyes of clinically normal llamas and alpacas. Am J Vet Res 61(12):1542–1544

Yeruham I, Van Straten M, Elad D (2002) Entropion, corneal ulcer and corneal haemorrhages in a one-humped camel (Camelus dromedarius). J Vet Med 49:409–410

Zakian A, Nouri M, Kahroba H et al (2016) The first report of peste des petits ruminants (PPR) in camels (Camelus dromedarius) in Iran. Trop Anim Health Prod 48(6):1215–1219. https://doi.org/10.1007/s11250-016-1078-6

Ophthalmology of Perissodactyla: Zebras, Tapirs, Rhinoceroses, and Relatives

34

Brian C. Gilger and Andrew G. Matthews

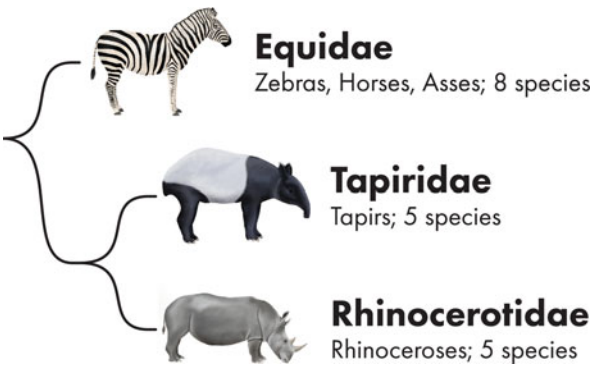

Introduction

In phylogenetic systematics, Perissodactyla represents an order of the class Mammalia and comprises the odd-toed ungulates. The order is conventionally divided into two Sub-Orders; Hippomorpha and Ceratomorpha (Table 34.1). Hippomorpha comprises the family Equidae with eight extant species of horses, asses, and zebras in the single genus *Equus*. Ceratomorpha comprises the monogeneric family Tapiridae, with five extant species, and the Rhinocerotidae, with five currently surviving species of rhinoceros in four genera (Table 34.1).

In terms of conservation status, with the exception of the domestic horse and the kiang, the members of the order represent some of the planet's more threatened species, with some being classed currently as critically endangered (IUCN Red List of Threatened Species: https://www.iucnredlist.org).

The early ancestors of modern Perissodactyls divided into Hippomorphs and Ceratomorphs during the early Eocene period (58-52 million years ago; mya), at which time they appear to have been an abundant and highly successful group of mammals with extensive speciation widely distributed across North America, Europe, and Asia. The subsequent division of the Ceratomorphs into Tapiridae and Rhinocerotidae occurred during the late Eocene and Oligocene periods (50-25 mya) and in the case of the tapir species, evolution continued into the Miocene and late Pliocene (11-2 mya). As radiation and speciation progressed within the order, the fossil record shows concurrent extinctions and geographic migration of vulnerable species, influenced by climate change, habitat loss, competition for nutrients and, possibly, human predation, resulting in the distribution and population types now extant. In the case of the Hippomorphs, both fossil records and karyotyping studies (Trifonov et al. 2008) have shown extensive evolutionary radiation during the Miocene, but the modern horse (*Equus* spp.), the only

B. C. Gilger (✉)
College of Veterinary Medicine, North Carolina State University, Raleigh, NC, USA
e-mail: brian_gilger@ncsu.edu

A. G. Matthews
Bents Cottage, LunanBay, Inverkeilor, Angus, Scotland, UK

F. Montiani-Ferreira et al. (eds.), *Wild and Exotic Animal Ophthalmology*, https://doi.org/10.1007/978-3-030-81273-7_9

Table 34.1 Species diversity of currently extant members of Order Perissodactyla (After Steiner and Ryder 2011)

Sub-order	Family	Species	Common name
Hippomorpha	Equidae	*Equus caballus* *E. przewalskii* *E. asinus* *E. kiang* *E. hemionus* *E. zebra* *E. quagga*[a] *E. grevyi*	Domestic horse Przewalski's wild horse African wild ass Kiang Asiatic wild ass (Onager) Mountain zebra Plains zebra[a] Grevy's zebra
Ceratomorpha	Tapiridae	*Tapirus indicus* *T. terrestris* *T. pinchaque* *T. bairdii*	Malayan/Asian tapir Lowland/Brazilian tapir Mountain tapir Baird's tapir
	Rhinocerotidae	*T. kabomani* *Diceros bicornis* *Ceratotherium simum* *Rhinoceros unicornis* *Dicerorhinus sumatrensis* *Rhinoceros sondaicus*	Little black tapir Black rhinoceros White rhinoceros Indian rhinoceros Sumatran rhinoceros Javanese rhinoceros

[a]Formerly known as *E. burchellii.* Burchell's zebra is now classed a subspecies of *E. quagga*

Table 34.2 Defining anatomical and physiological characteristics of members of the order Perissodactyla

	Molar dentition	Alimentary tract	Forelimb phalanges (no)	Hindlimb phalanges (no)
Equidae	Hypsodont	Simple stomach and fermentative hindgut	1	1
Tapiridae	Brachydont	Simple stomach and fermentative hindgut	4	3
Rhinocerotidae	Hypsodont	Simple stomach and fermentative hindgut	3	3

extant genus, appeared relatively late, during the Pliocene (2-4 mya) (Steiner and Ryder 2011).

All Perissodactyls are characteristically mesaxonic, where the sagittal plane of symmetry of the distal limb passes through the third phalanx. Their geographic range in the wild is restricted to mainly subtropical or tropical lowland habitats, ranging from grassland savannahs to rainforests. Outliers are the Mountain tapir, found in the central Andean cloud forest, the Mountain zebra, whose preferred habitat is the more mountainous areas of southern Africa, and the Kiang found on the Tibetan Plateau. All members of the order are herbivores, either predominantly grazers (Equidae), predominantly browsers (Tapiridae) or both grazers and browsers (Rhinocerotidae), this representing anatomical and physiological adaptation to their preferred habitats (Coimbra and Manger 2017). The defining anatomical and physiological characteristics of the Perissodactyls are shown in Table 34.2.

Ocular Anatomy and Function

In terms of foraging behavior, Perissodactyla are either cathemeral (i.e., irregularly active at any time) or diurnal (Equidae, Rhinocerotidae, *T. terrestris* and *T. pinchaque*), or are nocturnal crepuscular (i.e., twilight active) feeders (other Tapiridae) (García et al. 2012; Banks et al. 2015). These patterns of feeding activity reflect the nature of the habitat and the need to avoid potential predatory threats and will determine to a significant extent visual requirement and ocular structure and function (Peichl 2005; Veilleux and Lewis 2011; Veilleux and Kirk 2014; Banks et al. 2015).

In general, terrestrial mammal visual systems reflect specialization for habitat variation in ambient light intensity (Veilleux and Lewis 2011). Decreasing corneal diameter relative to the axial length of the eye reduces visual sensitivity but enlarges the retinal image and ameliorates peripheral distortion of the image, and is recognized as potentially conferring some survival advantage in open habitat prey ungulates. However, studies on Perissodactylae have failed to identify differences in corneal diameter: ocular axial length ratios, irrespective of their occupying primarily either open or afforested habitats (Veilleux and Lewis 2011; Veilleux and Kirk 2014).

Like the domestic horse, non-domestic *Equidae* have relatively large, laterally placed eyes with horizontal pupils and well-developed *granula iridica* (Johnson 1901; Banks et al. 2015). The horizontal, oblate pupil increases the horizontal depth of field and minimizes blurring of peripheral vision resulting from astigmatism of oblique incidence (Banks et al. 2015) (Fig. 34.1), resulting in increased image quality both of

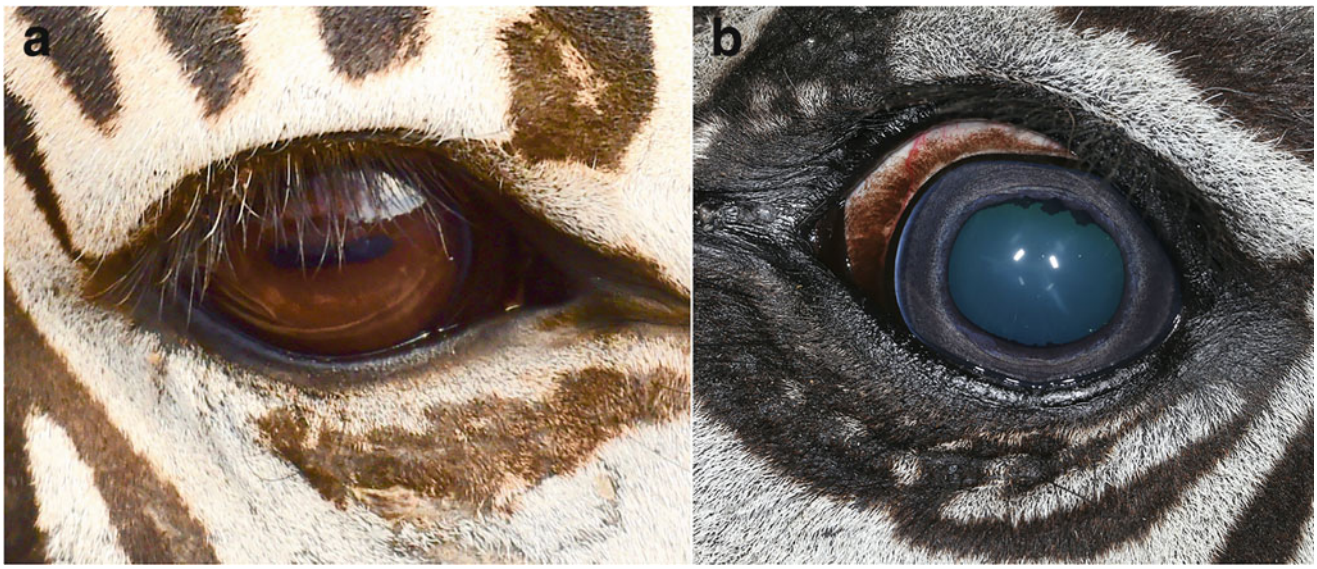

Fig. 34.1 Zebra eye. (**a**) Note the horizontal, oblate pupil similar to that observed in a domestic horse. (**b**) Dilated zebra eye, with the pupil maintaining only a slightly ovoid shape upon full mydriasis. (**a**) Courtesy of Dr. Ronald K. Cott. (**b**) Courtesy of Dr. Bret A. Moore

the ground immediately in front and of the area behind. In addition, using head pitch, the animal appears able to align the long axis of the pupil with the horizon (Banks et al. 2015). These evolutionary adaptations will confer a significant survival advantage to a cathemeral prey species occupying open grasslands.

The anatomic ocular dimensions, including anterior chamber depth, lens thickness, axial length and corneal curvature, have been measured in 12 eyes of eight Grevy's zebra, aged 4–14 years, using ultrasound biometry (Evans et al. 2009). The mean (± SD) axial length (40.7 ± 1.1 mm), anterior chamber depth (6.9 ± 0.30 mm), and lens thickness (13.83 ± 4.24 mm) were essentially similar to those recorded in the domestic horse (Grinninger et al. 2010). Mean intraocular pressure (IOP) using applanation tonometry was 21.77 mmHg (Evans et al. 2009) (Appendix C). In another study using applanation tonometry, IOP recorded in six eyes of Plains zebras (*Equus burchellii*) was 29.5 ± 3.4 mmHg (Ofri et al. 1998) (Appendix C).

The *Equidae* fundus is paurangiotic and with an extensive fibrous tapetum. The tapetal reflex in non-domestic *Equidae* varies from blue-yellow to green-yellow (Johnson 1901) (Fig. 34.2). The neurosensory retina is rod dominated, with increasing cone and ganglion cell numbers in the photoreceptor dense macular areas. These comprise the near contiguous *area centralis* and the visual streak, which are located dorsotemporally to the optic disc and in outline approximate to the shape of the horizontal pupil (Sandmann et al. 1996; Ehrenhofer et al. 2002; Peichl 2005). The macular areas are thought to be used for binocular vision and will permit high acuity dichromic blue/yellow, color vision.

The *Rhinocerotidae* eye is small relative to the domestic horse, with an ultrasonographically measured mean axial length of 2.61 ± 0.11 cm (Bapodra and Wolfe 2014) compared with 4.05 ± 0.27 cm in the horse (Grinninger et al. 2010). The rounded pupil of *Rhinocerotidae* spp. is typically associated with cathemeral foraging and the absence of significant predation risk (Banks et al. 2015). Anecdotal commentary, presumably made by smug survivors of a close encounter, has it that rhinoceroses are notoriously short sighted. However, rhinoceroses are mildly hyperopic (Howland et al. 1993), and ganglion cell topographic studies on both the black and the white rhinoceros have shown the presence of a visual streak with an *area centralis* both temporally and nasally. In the white rhinoceros, the visual streak lies dorsal to the optic disc, and in the black the optic disc lies within the visual streak (Pettigrew and Manger 2008; Coimbra and Manger 2017) (Fig. 34.3). It is thought that the appearance of a nasally located *area centralis* may compensate for limited lateral head movement in these species (Coimbra and Manger 2017). Calculations based on peak ganglion cell density and axial length of the eyes indicate that *Rhinocerotidae* has a visual resolution of 6–7 cycles/degree. This compares to 60 cycles/degree in humans, 25 cycles/degree in horses and 6 cycles/degree in rabbits, and allows for the prediction that rhinoceroses, in optimal conditions of contrast and luminance, can discern an adult human at between 100–200 m (Pettigrew and Manger 2008; Coimbra and Manger 2017). The greater visual resolution in the horse is likely to be a consequence of larger eye size rather than increased ganglion cell density (Coimbra and Manger 2017). *Rhinocerotidae* have heavily pigmented

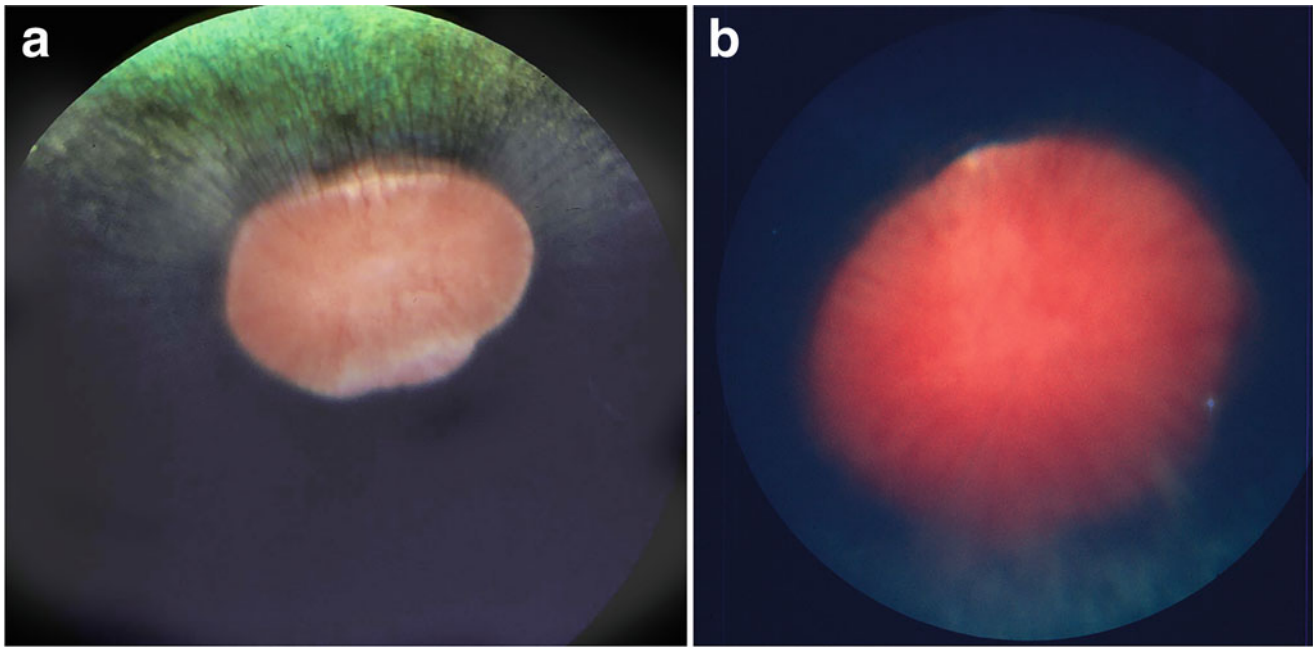

Fig. 34.2 Normal fundus images of an (**a**) adult and (**b**) foal zebra. Note the paurangiotic vasculature pattern. The blood vessels are fine and present only in the direct area of the optic disc and cross its margin to extend a short distance into the retina. The optic disc is horizontally oval, and the tapetal reflex is green to green-yellow. In the foal, the optic nerve is hyperemic

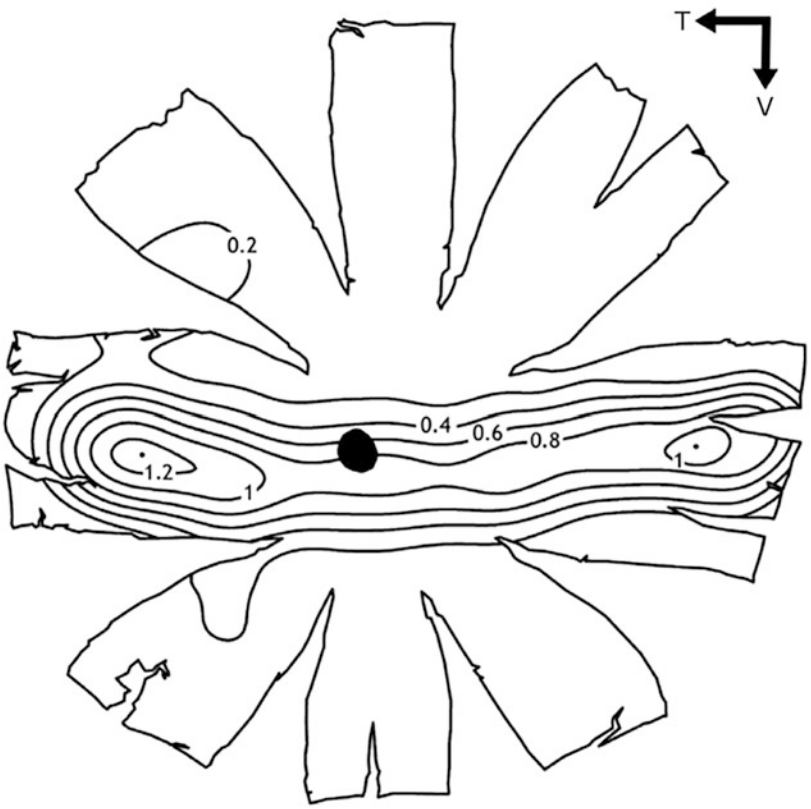

Fig. 34.3 Topographic flat-mount retinal map demonstrating retinal ganglion cell densities in the White Rhinoceros (*C. simum*). There is a well-defined horizontal streak of increased retinal density from 200 cells/mm^2 to a peak density temporally (approximately 2000 cells/mm^2 and nasally (approximately 1800 cells/mm^2). The black circle near the center of the figure represents the optic disc. T temporal, V ventral. Modified, with permission, from Coimbra and Manger (2017) Journal of Comparative Neurology 525: 2484–2498

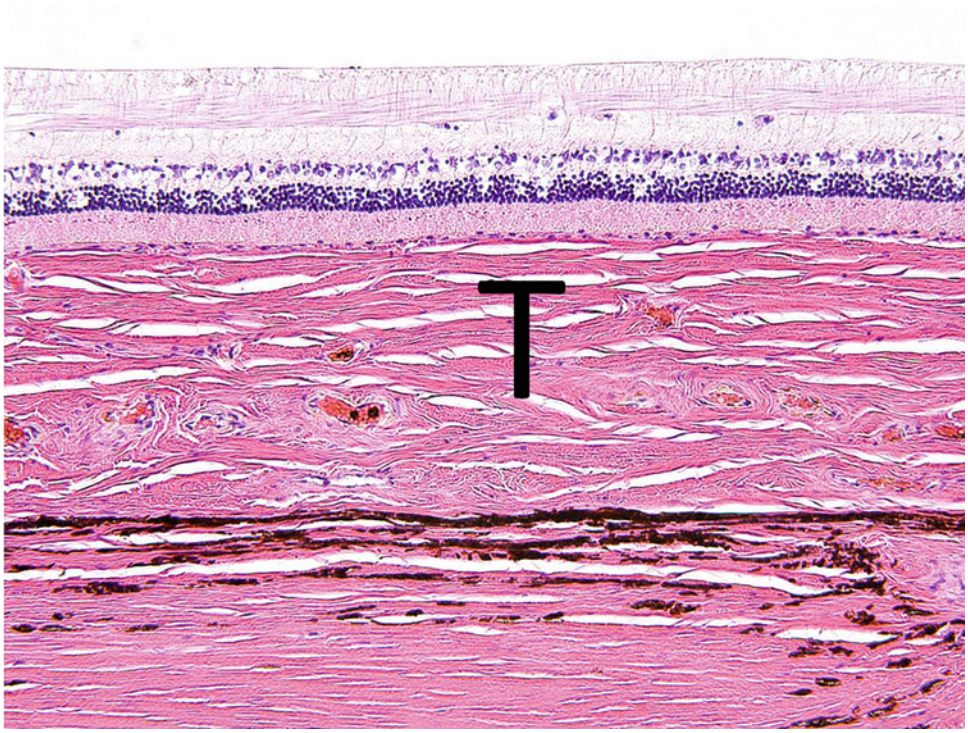

Fig. 34.4 Histologic micrograph of Tapir retina. Note the massive fibrous tapetum lucidum (T). (Courtesy of the Comparative Ocular Pathology Laboratory of Wisconsin)

atapetal and paurangiotic fundi (Johnson 1901; Coimbra and Manger 2017). The mean IOP measured by means of applanation tonometry in five adult rhinoceroses sedated with an alpha-2 agonist and opiate combination was 31.2 ± 6.62 mmHg, and the mean Schirmer tear test was 18.2 ± 3.49 mm/min (Bapodra and Wolfe 2014) (Appendix C).

Very little is known specifically about the eyes of *Tapiridae* other than that they have a rounded pupil (Banks et al. 2015) and a paurangiotic fundus with a fibrous tapetum (Fig. 34.4) (Johnson 1901; Francois and Neetens 1962).

Both the *Rhinocerotidae* and the *Tapiridae*, like the equids, will have a dichromatic vision in the blue green spectrum. This represents a neuroecological adaptation to habitat and activity patterns (Gerkema et al. 2013).

Ocular Disease

Although the ocular disease in the domestic horse is relatively common, with the exception of traumatic or other injury, ocular disease amongst captive Perissodactyl populations appears to be relatively uncommon (Greenwood A, personal communication). Immunoinflammatory, including autoimmune, diseases of the cornea and the uveal tract in the domestic horse are frequent and challenging causes of blindness or serious visual compromise (Gilger and Hollingsworth 2017; Brooks et al. 2017), and given the highly conserved nature of innate immunity and the individual diversity of adaptive immune responses in mammalian species (Holmes and Ellis 1999; Muraille 2014; Kumar et al. 2017), it is likely that the potential exists for these diseases to occur in non-domestic Perissodactyla. However, the frequency of permissive immunogenotypes, conferring susceptibility to disease is likely to have been reduced in non-domesticated populations by selective predation of affected individuals. Furthermore, wide-ranging foraging activity in these populations is likely to restrict exposure to microbial pathogens or other natural agents capable of initiating disease, e.g., *Leptospira* spp. in Equine Recurrent Uveitis. As anthropogenic pressures on wild populations prevail, loss of genetic diversity and increased exposure to potential pathogens in conjunction with increasing environmental and social stressors will inevitably skew population immunological dynamics and may result in an increased incidence of immunoinflammatory and autoimmune disease (Martin et al. 2010; Archie 2013; Ujvari et al. 2018).

Beyond the domestic horse, there is very little published data on ophthalmic physiology and disease amongst members of this order. Given the common early phylogenetic origin of the members of the order and the conserved nature of mammalian immunopathological responses, the clinical approach to managing ocular disease should be based upon the protocols current in dealing with domestic horses. This approach, however, will be constrained by compliance issue which may be overcome to some degree using local depot medications or, in the case of corneal ulceration or keratomalacia, by early recourse to conjunctival grafting

procedures. Captive tapirs appear susceptible to UV exposure associated with keratomalacia, similar to that seen in captive marine pinnipeds. This may also be the case with rhinoceros.

Non-Domestic Equidae (Wild Horse, Wild Ass, and Zebra)

Very little information exists in the literature regarding the ocular disease in Grevy's zebra (*E. grevyi*), mountain zebra (*E. zebra*), or the Plains zebra (*E. quagga*). There is a single report of intracapsular lens extraction performed in an 11.5-year-old Przewalski's wild horse mare that had presented with unilateral blepharitis, corneal edema, and anterior lens luxation (Kenny et al. 2003).

Rhinocerotidae

There are a few isolated reports of ocular disease in Rhinocerotidae, most of which describe the consequences of ocular surface trauma. A 40-year-old white rhinoceros (*C. simum*) sustained repeated injuries to the right lower eyelid from a female pasture mate at a zoological park. The affected rhinoceros subsequently developed intractable uveitis and infectious keratitis resulting in enucleation (Fig. 34.5). Other than dehiscence of the skin incision, the rhinoceros recovered without incident (Gilger B, personal communication). In another zoological facility, a 34-year-old male with greater one-horned rhinoceros (*R. unicornis*), developed blepharospasm, corneal opacity, and a deep corneal ulcer with a central descemetocele. The corneal lesion was repaired surgically using a free island tarsoconjunctival graft following the initial failure of a conjunctival pedicle graft, resulting in a central corneal scar and a comfortable eye (Esson et al. 2006). A 19-month-old male with greater one-horned rhinoceros (*R. unicornis*) with severe keratomalacia in the left eye involving more than 80% of the corneal surface was managed using surgical debridement followed by a 360 conjunctival graft. The graft was removed 6 weeks later, resulting in a comfortable eye with a central corneal scar (Gandolf et al. 2000). A 3-year-old male rhinoceros in a zoological facility suffered from chronic keratitis with intermittent ulceration (Fig. 34.6). It was suspected that the ocular surface disease was immune-mediated and triggered by UV light, similar to the condition seen in tapirs (see below). The condition was partially controlled by increasing the shaded area in the enclosure and by a long-term application of topical cyclosporine and tacrolimus once to twice daily, although compliance was challenging (Ben-Shlomo G, personal communication).

A female white rhinoceros (*C. simum*) presented with intermittent, bilateral conjunctivitis, and severe conjunctival proliferation, ultimately extending across both corneas and causing loss of vision. The eyes were normal otherwise except for signs of bilateral chronic keratitis (corneal fibrosis, pigmentation, and superficial vascularization). Conjunctival habronemiasis was diagnosed based on histopathology of excised tissue, and the disease was controlled using oral ivermectin and topical antibiotics, although subsequently recurrence was recorded (Horowitz et al. 2016) (Fig. 34.7).

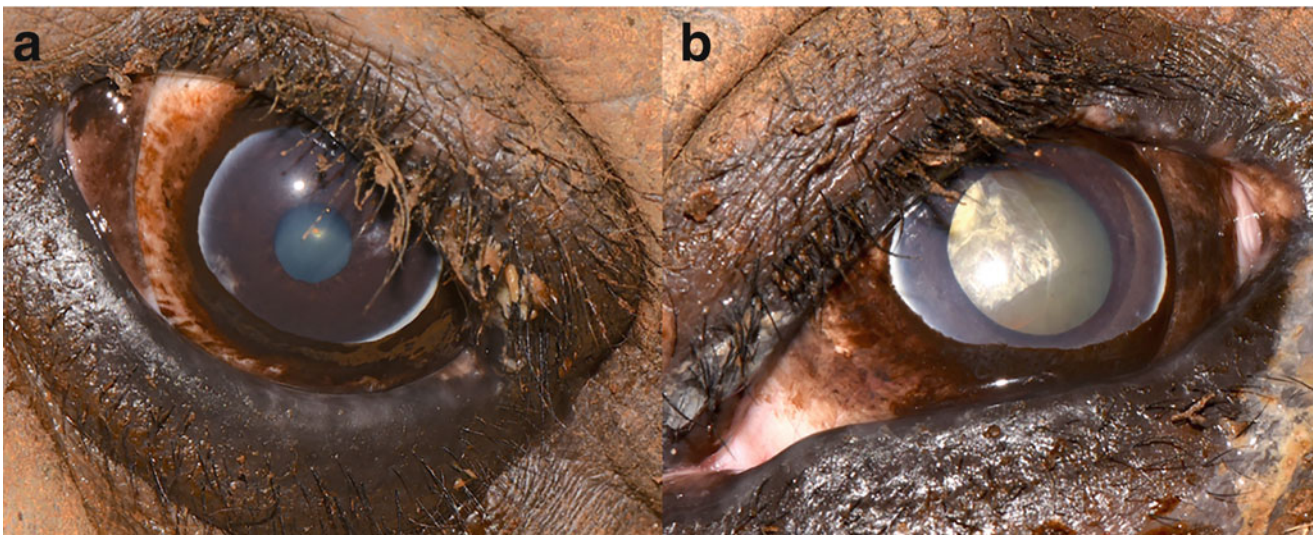

Fig. 34.5 Image of eyes of a 40-year-old white rhinoceros (*C. simum*). (**a**) The right eye appeared normal except for small white corneal scars. (**b**) The left eye had epiphora, diffuse corneal edema, and a cortical cataract. In addition, this eye had signs of active uveitis, including mild aqueous flare and low intraocular pressure (this eye has been pharmacologically dilated using topical 1% tropicamide HCL). Treatment with topical dexamethasone helped control the uveitis, but the eye was eventually enucleated following the development of a deep corneal ulcer

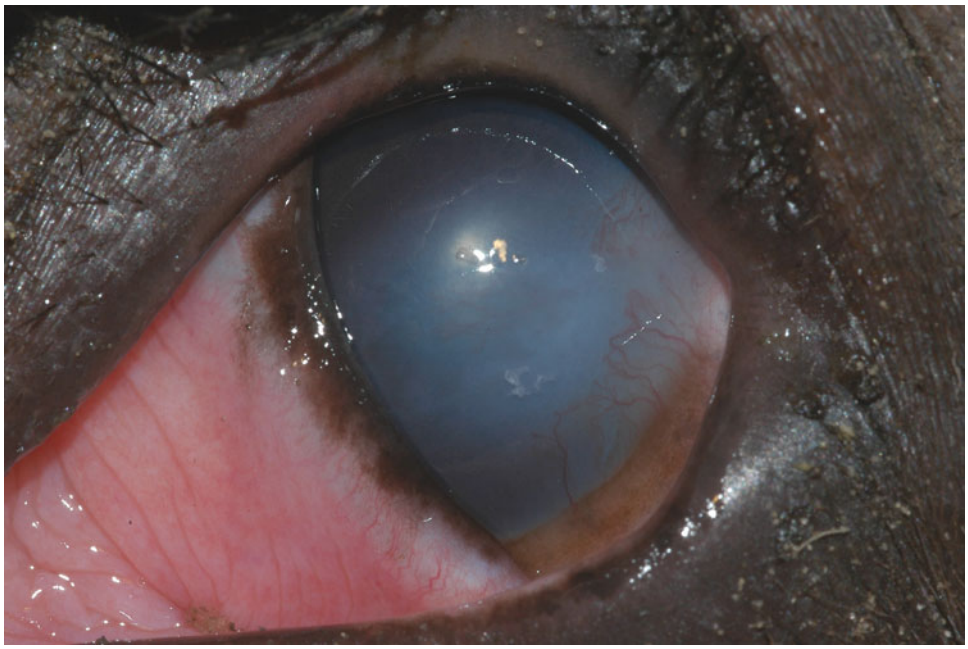

Fig. 34.6 Rhinoceros with a chronic, intermittently ulcerative, keratitis, which was suspected to be immune-mediated and triggered by UV light exposure. (Photograph courtesy of Dr. Gil Ben-Shlomo)

Fig. 34.7 White rhinoceros with a presumptive diagnosis of eyelid Habronemiasis resulting in granulomatous blepharitis and conjunctivitis. (Photograph courtesy of Dr. José Ricardo Pachaly)

Tapiridae

Ocular surface inflammation, especially ulcerative keratitis and conjunctivitis, is reported to be common in captive tapir most likely caused by trauma and exposure to UV light, which free-ranging tapirs have little exposure to since their natural habitat is primarily dense jungles (Montiani-Ferreira 2001; Da Silva et al. 2013).

Two female South American Tapirs (*T. terrestris*) at a zoological park were observed to have unilateral blepharospasm and epiphora as a result of deep central corneal ulcers. Successful treatment consisted of topical tobramycin and serum. Medication of ocular surface within the deep-set

Fig. 34.8 Chronic ulcerative keratitis in a Malayan tapir (*T. indicus*). Chronic ulcerative stromal disease developed bilaterally (**a**). Two months following placement of an episcleral cyclosporine implant (**b**) demonstrating a central corneal scar, but the resolution of the stromal keratitis. This chronic keratitis is suspected to be caused or perpetuated by excessive UV light exposure

orbits was facilitated by use of a flexible intravenous catheter inserted into the medial canthus (Da Silva et al. 2013).

Malayan tapirs (*T. indicus*) at a zoological park in South Florida develop chronic, proliferative, and bilateral corneal changes typically by one year of age or within one year of arrival at the park. Biopsy of the raised irregular corneal lesions suggested a diagnosis of papilloma. In a 26-year-old, wild caught, male Malayan tapir, presenting with similar corneal lesions, 5-fluorouracil (25 mg in 0.5 mL) was injected subconjunctivally and repeated at 3, 7, 12, and 17 weeks. The lesions decreased in size, and an improvement in visual function was present for up to 2 years following the series of injections (Karpinski and Miller 2002).

Malayan tapirs (*T. indicus*) have also been observed (Karpinski L, personal communication) to develop chronic bilateral keratopathy, including opacification and ulceration, associated with excessive UV exposure, similar to that observed in marine pinnipeds (Miller et al. 2013). As in the case of the affected pinnipeds, the Malayan tapirs responded to topical or episcleral cyclosporine (Fig. 34.8).

Summary

Very little objective information has been published on the incidence and management of ocular diseases among members of the order Perissodactyla. In terms of general clinical guidance, given the common early phylogenetic origin of the order's species and their likely broad similarity in immunopathological responses to ocular injury or insult, any approach to the diagnosis and therapy of ocular disease should be based upon protocols used at present in the domestic horse (*E. caballus*) (Gilger 2017). In the case of captive tapirs and possibly rhinoceros, the clinician should be alert to the potential role of UV exposure in the genesis of chronic destructive keratitis, as described in captive marine pinnipeds in the USA (Miller et al. 2013). In any event, the principles guiding the clinical management of the acute ocular disease are:

- Prompt and accurate diagnosis of the generic nature of the disease process and the ocular tissues involved in that process.
- Where appropriate, identify any extraneous causal agent, *e.g.*, fungi or other microbial pathogens, foreign material. This may involve microbial sampling, biopsy, or aspiration of intraocular content (Stoppini and Gilger 2017; Dwyer 2017).
- Formulate and implement an effective therapeutic strategy targetting the affected tissue and directed towards the elimination of any causal agent or other impediments to healing, e.g., foreign body, necrotic corneal or other tissue, or towards suppression of aberrant or dysregulated immunoinflammatory responses, e.g., keratolysis and ulceration driven by innate hydrolases derived from leucocytes and macrophages sequestered on the ocular surface.
- Promote ocular repair, directed towards restoring the physical integrity and normal function of the injured ocular tissues.

In the case of most non-domestic species, the above must be accomplished within the constraints imposed by limited patient contact and compliance and the perceived risks to

the patient of multiple general anesthesia events. In circumstances of good management facilities and relatively tractable patients, effective topical therapy may be possible via a transpalpebral lavage system allowing remote administration of the agent. However, in many cases, effective topical therapy typically requires short interval dosing, which may limit its suitability for use. Continuous delivery pumps can be used in conjunction with subpalpebral lavage systems and may have a benefit in enhancing the bioavailability of some topical medication such as hydrolase inhibitor preparation in corneal ulceration. However, some medications, such as ophthalmic suspensions (e.g., natamycin), or drugs that require refrigeration (e.g., voriconazole, cefazoline), are not suitable to be used in continuous delivery systems, and the clinician should consider this where such systems are considered.

With the probable exception (in some instances) of the inflamed uveal tract or ocular surface, most systemically administered therapeutic agents, including those administered orally, cannot be relied upon alone to achieve and maintain therapeutic levels within the eye or on the ocular surface (Matthews 2004, 2009). This necessitates early consideration of the use of depot formulated drug preparations, where appropriate and where available, administered by local administration techniques such as subconjunctival, intracorneal, or intracameral injection. Consideration should also be given to the use of slow-release embedded devices, e.g., suprachoroidal or episcleral Cyclosporine A implants, in managing immune-mediated uveal or corneal disease, or cisplatin beads as adjunctive therapy in managing periocular tumors.

When addressing a severe corneal wound condition (e.g., keratomalacia, deep stromal ulcer, descemetocele), early recourse to single intervention conjunctival grafting surgeries (Brooks et al. 2017) in managing corneal ulceration is likely to accelerate corneal healing and repair and may preserve the eye, albeit at the expense of end-stage corneal clarity, and should be a primary consideration in any therapeutic strategy.

References

Archie EA (2013) Wound healing in the wild: stress, sociality and energetic costs affect wound healing in natural populations. Parasite Immunol 35(11):374–385

Banks MS, Sprague WW, Schmoll J et al (2015) Why do animal eyes have pupils of different shapes? Sci Adv. https://doi.org/10.1126/sciadv.1500391

Bapodra P, Wolfe BA (2014) Baseline assessment of ophthalmic parameters in the greater one-horned rhinoceros (*Rhinoceros unicornis*). J Zoo Wildl Med 45:859–865

Brooks D, Matthews A, Clode A (2017) Diseases of the equine cornea (Chapter 7). In: Gilger B (ed) Equine ophthalmology, 3rd edn. Wiley Blackwell, Philadelphia, pp 1252–1368

Coimbra JP, Manger PR (2017) Retinal ganglion cell topography and spatial resolving power in the white rhinoceros (Ceratotherium simum). J Comp Neurol 525:2484–2498

Da Silva M-AO, Hermoza C, Rojas G, Freundt JM (2013) Identifying an effective treatment for corneal ulceration in captive tapirs. Tapir Conserv 22:12–14

Dwyer A (2017) Practical field ophthalmology (Chapter 3). In: Gilger B (ed) Equine ophthalmology, 3rd edn. Wiley Blackwell, Philadelphia, pp 72–111

Ehrenhofer MCA, Deeg CA, Reese S et al (2002) Normal structure and age-related changes of the equine retina. Vet Ophthalmol 5:39–47

Esson DW, Wellehan JFX, Lafortune M et al (2006) Surgical management of a malacic corneal ulcer in a greater one-horned Asian rhinoceros (Rhinoceros unicornis) using a free island tarsoconjunctival graft. Vet Ophthalmol 9:65–69

Evans AL, Carter RT, Marlar AB, Citino SB (2009) Determination of the appropriate size intraocular lens for cataract surgery in the Grevy's zebra (Equus Grevyi). In: Proceedings AAZV AAWV Joint Conference

Francois J, Neetens A (1962) Vascularisation of the retino-optic block. In: Davson H (ed) Vegetative physiology and biochemistry: the eye, vol 1. Academic Press, New York, pp 372–380

Gandolf AR, Willis AM, Blumer ES, Atkinson MW (2000) Melting corneal ulcer management in a greater one-horned rhinoceros (Rhinoceros unicornis). J Zoo Wildl Med 31:112–117

García MJ, Medici EP, Naranjo EJ et al (2012) Distribution, habitat and adaptability of the genus tapirus. Integr Zool 7:346–355

Gerkema MP, Davies WL, Foster RG et al (2013) The nocturnal bottleneck and the evolution of activity patterns in mammals. Proc R Soc B Biol Sci 280:20130508. https://doi.org/10.1098/rspb.2013.0508

Gilger BC (2017) Equine ophthalmology, 3rd edn. Wiley Blackwell, Philadelphia

Gilger BC, Hollingsworth SR (2017) Diseases of the uvea, uveitis, and recurrent uveitis. In: Equine ophthalmology, 3rd edn. Wiley Blackwell, Philadelphia

Grinninger P, Skalicky M, Nell B (2010) Evaluation of healthy equine eyes by use of retinoscopy, keratometry, and ultrasonographic biometry. Am J Vet Res 71:677–681

Holmes EC, Ellis SA (1999) Evolutionary history of MHC class I genes in the mammalian order Perissodactyla. J Mol Evol 49:316–324

Horowitz IH, Dubielzig RR, Botero-Anug AM et al (2016) Conjunctival habronemiasis in a square-lipped rhinoceros (Ceratotherium simum). Vet Ophthalmol 19:161–166

Howland HC, Rowland M, Murphy CJ (1993) Refractive state of the rhinoceros. Vision Res 33:2649–2651

Johnson GL (1901) I. Contributions to the comparative anatomy of the mammalian eye, chiefly based on ophthalmoscopic examination. Philos Trans R Soc Lond Ser B. https://doi.org/10.1016/1352-2310(95)00219-7

Karpinski LG, Miller CL (2002) Fluorouracil as a treatment for corneal papilloma in a Malayan tapir. Vet Ophthalmol 5:241–243

Kenny DE, Dugan SJ, Knightly F, Baier J (2003) Intracapsular lens removal in a Przewalski's wild horse (Equus caballus przewalskii). J Zoo Wildl Med 34:284–286

Kumar A, Suryadevara N, Hill TM et al (2017) Natural killer T cells: an ecological evolutionary developmental biology perspective. Front Immunol 8(1858):1–19

Martin LB, Hopkins WA, Mydlarz LD, Rohr JR (2010) The effects of anthropogenic global changes on immune functions and disease resistance. Ann N Y Acad Sci 1195:129–148

Matthews AG (2004) Ophthalmic therapeutics (Chapter 13). In: Bertone JJ, Horspool LJ (eds) Equine clinical pharmacology. WB Saunders, Philadelphia, pp 217–246

Matthews AG (2009) Ophthalmic antimicrobial therapy in the horse. Equine Vet Educ 21:271–280

Miller S, Colitz CM, St Leger J, Dubielzig R (2013) A retrospective survey of the ocular histopathology of the pinniped eye with emphasis on corneal disease. Vet Ophthalmol 16:119–129

Montiani-Ferreira F (2001) Ophthalmology. In: Fowler M, Cubas Z (eds) Biology, medicine and surgery of South American wild animals. Iowa State University Press, Ames, pp 437–456

Muraille E (2014) Generation of individual diversity: a too neglected fundamental property of adaptive immune system. Front Immunol 5(208):1–7

Ofri R, Horowitz IH, Kass PH (1998) Tonometry in three herbivorous wildlife species. Vet Ophthalmol 1:21–24

Peichl L (2005) Diversity of mammalian photoreceptor properties: adaptations to habitat and lifestyle? Anat Rec A Discov Mol Cell Evol Biol 287A:1001–1012

Pettigrew JD, Manger PR (2008) Retinal ganglion cell density of the black rhinoceros (Diceros bicornis): calculating visual resolution. Vis Neurosci 25:215–220

Sandmann D, Boycott BB, Peichl L (1996) Blue-cone horizontal cells in the retinae of horses and other equidae. J Neurosci 16:3381–3396

Steiner CC, Ryder OA (2011) Molecular phylogeny and evolution of the Perissodactyla. Zool J Linnean Soc. https://doi.org/10.1111/j.1096-3642.2011.00752.x

Stoppini R, Gilger B (2017) Equine ocular examination basic techniques (Chapter 1). In: Gilger B (ed) Equine ophthalmology, 3rd edn. Wiley Blackwell, Philadelphia, pp 1–39

Trifonov VA, Stanyon R, Nesterenko AI et al (2008) Multidirectional cross-species painting illuminates the history of karyotypic evolution in Perissodactyla. Chromosome Res 16:89–107

Ujvari B, Klaassen M, Raven N et al (2018) Genetic diversity, inbreeding and cancer. Proc R Soc B 285:20172589. https://doi.org/10.1098/rspb.2017.2589

Veilleux CC, Kirk EC (2014) Visual acuity in mammals: effects of eye size and ecology. Brain Behav Evol 83:43–53

Veilleux CC, Lewis RJ (2011) Effects of habitat light intensity on mammalian eye shape. Anat Rec (Hoboken) 49:316–324

Ophthalmology of Felidae: Cats

35

Francesca Corsi, Adolfo Guandalini, João Luiz Rossi Junior, Gil Ben-Shlomo, Fabiano Montiani-Ferreira, and Bret A. Moore

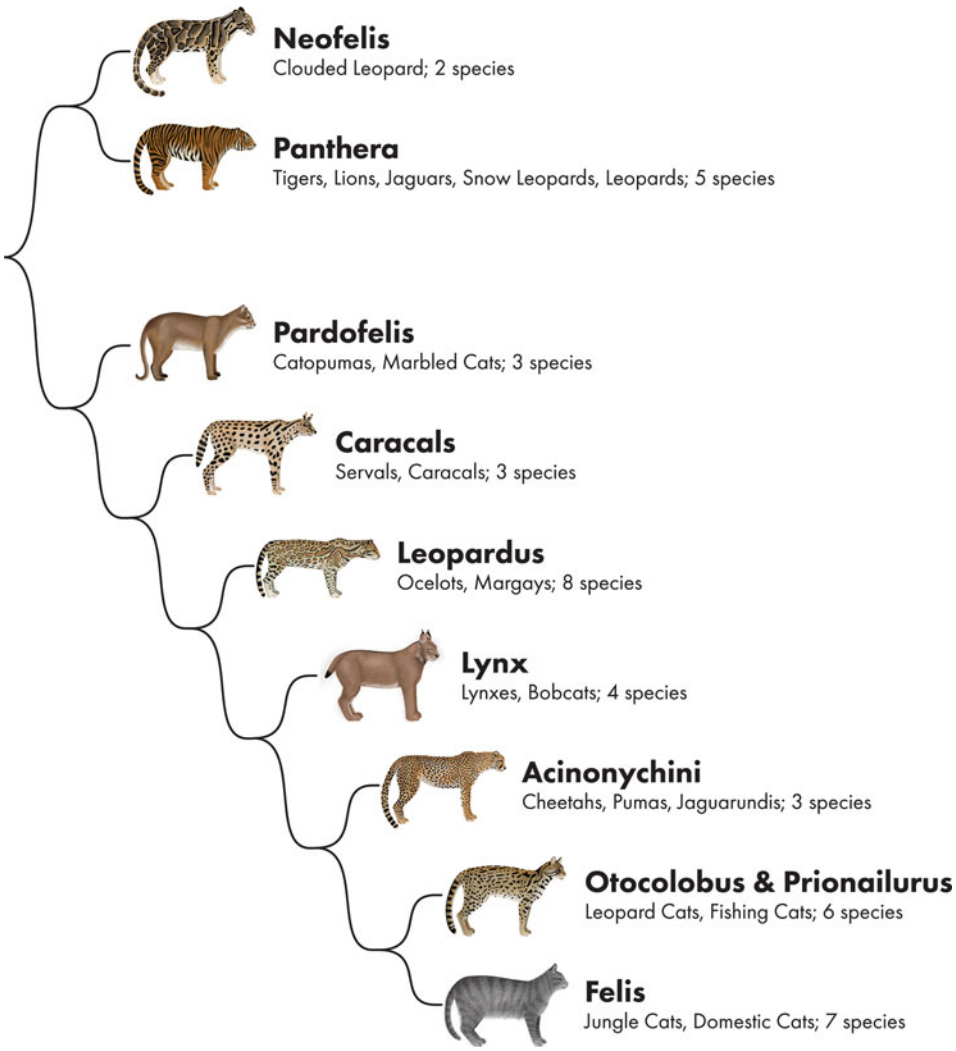

© Chrisoula Skouritakis

F. Corsi · A. Guandalini (✉)
Centro Veterinario Specialistico (CVS), Rome, Italy

J. L. Rossi Junior
Programa de Pós-Graduação em Ciência Animal e Graduação em Medicina Veterinária da Universidade Vila Velha-UVV, Espírito Santo, Brazil

G. Ben-Shlomo
Cornell University College of Veterinary Medicine, Ithaca, NY, USA
e-mail: gb473@cornell.edu

F. Montiani-Ferreira
Comparative Ophthalmology Laboratory (LABOCO), Veterinary Medicine Department, Federal University of Paraná, Rua dos Funcionários, Curitiba, PR, Brazil
e-mail: montiani@ufpr.br

B. A. Moore
College of Veterinary Medicine, University of Florida, Gainesville, FL, USA
e-mail: bretthevet@dvm.com

F. Montiani-Ferreira et al. (eds.), *Wild and Exotic Animal Ophthalmology*, https://doi.org/10.1007/978-3-030-81273-7_10

Introduction

Over 65 million years ago, squirrel-sized creatures that ran after insects gave rise to all modern carnivores, ranging from bears, wolves, ferrets, raccoons, cats, hyenas, gynets, and meerkats. There were, of course, descendants that did not survive to this day, such as the saber-toothed tiger and bear-sized raccoons. Exactly when the cat story began depends on which primitive mammal one considers as the first "cat." The fossorial record for Felidae is incomplete, as early cats lived in forests where fossils are rarely found, and only a few remains, such as the tiny middle ear bones, are able to potentially distinguish felids from other animals of the Carnivora. Nevertheless, it is generally accepted that the first "cat-like" carnivores belong to two lineages that lived about 40 million years ago in the Eocene forests of North America. One lineage was represented by Hoplophoneus and another by Dinictis, both are prehistoric "feliform" mammalian carnivores belonging to an extinct genus of the family Nimravidae. These lineages shared a feature that is now a hallmark of modern cats: sharp butcher teeth (Turner 1997; Macdonald 1992).

Systematics and Vision

Within the Carnivora, only the Felidae family consists exclusively of specialized killers: from the Siberian tiger (*Panthera tigris tigris*) weighing up to 320 kg to the 1 kg black-footed cat (*Felis nigripes*), all are formidable, efficient predators. Variations in hunting abilities do exist among the 38 feline species in the world, with some species relying primarily on speed (cheetah *Acinonyx jubatus*), pursuit (jaguar *Panthera onca*), or fishing (fishing cat *Prionailurus viverrinus*). Some species hunt primarily on land (lion *Panthera leo*) or even climbing and hunting in trees (*margay Leopardus wiedii*), whereas others hunt in the water (fishing cat *Prionailurus viverrinus*). A flexible spine and muscular pelvic limbs provide speed, agility, and strength. Additionally, all cats are digitigrade (i.e., they walk on their fingertips), a feature that enables fluid movement due to balanced distribution of body weight. Their carnivorous lifestyle and hunting strategies are exemplified in their digestive anatomy and protein requirements. The skull is highly vaulted and the zygomatic arches are wide while the rostrum is shortened. Strong sagittal ridges provide anchorage for the powerful masseter muscles. The mechanical advantage of a shortened face and powerful jaw muscles increases the bite force of the canine teeth. Felids can be classified as hypercarnivores in their natural state because they need a much higher proportion of animal protein in their diet. For a domestic cat to stay healthy, its diet must contain about 12% protein (by weight) for adults and 18% for kittens. In comparison, domestic dogs can survive on much less. In general, adult dogs can survive on only 4% protein. Felids have the smallest number of teeth among land carnivores (only a few mustelids come close to having the same number of teeth, approximately 30), but these are highly specialized for meat processing, especially carnassial teeth. Scissor-like paired upper and lower teeth played a crucial role in the evolution of all carnivores, but it was in the felids whose teeth were sharpened to the thinnest point. Thus, felids can swallow whole pieces of meat without much chewing and rely on their strong digestive enzymes to digest it. Finally, felids have a rough surface on their tongues, with which they can remove the skin or muscles from the surface of their prey's bones. Add to this arsenal of weapons a set of retractable claws (except for the *Acinonyx jubatus*) hidden in the fingers, and a complete and fearsome predator is exemplified (Macdonald 1992; De La Rosa and Nocke 2000).

Predators depend on adept sensory abilities to efficiently locate and subdue their prey. In felids, some sensory abilities appear to be more developed than in other carnivores, as well as between other members of Felidae, differences that are largely reflecting in activity pattern and their hunting grounds (Ewer 1998). Felids do rely on olfaction to locate and approach potential prey, but their sense of smell is no match for canids. One commonality across Felidae sensory system is the presence of touch-sensitive hair called vibrissae or whiskers on both sides of the muzzle, around the eyes, below the chin, and on the wrists. These whiskers act as a "tactile third eye" or "touch vision," which is critical for some felids to hunt at night by helping them to move through small spaces and avoid obstacles in the dark. These whiskers are extremely sensitive to movement, enough to detect slight changes in air current, and even allow blindfolded cats to avoid obstacles. A hunting felid holds its whiskers on both sides of its face like a fan. Just before attacking the prey, the cat moves its whiskers forward, extending them like a net in front of its mouth to provide directional information about the movements of its prey prior to even coming in contact. After capture, Felids wraps its whiskers around the prey, sensitive to any tremor that indicates that the prey may twitch (Ewer 1998).

Felids predominantly rely on their sense of vision to help them catch prey. Their eyes are wonderful examples of those adapted for visual success at both day and night, a common finding among nocturnal carnivores (Walls 1942). That is not to say that their eyes are not more nocturnal than diurnal, but that they can succeed in a wide range of luminances. In photopic conditions, visual success is dominated by acuity and color vision. Visual acuity refers to the ability to resolve individual objects with detail, and ultimately depends on both optical and retinal properties. Acuity in cats is not high, at least compared to other mammals, such as primates, likely

being limited by retinal properties rather than visual optics or central processing (Blake et al. 1974). Visual acuity has been measured to be between 5 and 6 cycles per degree by visual evoked potentials (the equivalent of 20/100–20/120 on the Snellen chart) in the lynx *Lynx europea* (Maffei et al. 1990), similar to acuity in domestic cats (Blake et al. 1974).

Visual acuity is largely a factor of eye size and the density of photopic retinal cells (cone photoreceptors and their associated retinal ganglion cells). Although cat eyes are large relative to body size, the increased size of their eyes is not particularly for the benefit of increasing visual acuity, but rather to improve light capture with the intent of producing a smaller, brighter retinal image (Walls 1942). Eye size varies with large felids having eyes nearly twice the size of the domestic cat (Malmstrom and Kroger 2006). The density of retinal cells is heterogenous across the retina, and uniformly in cats a retinal specialization consisting of an area centralis in the superotemporal to the optic nerve provides high-resolution sampling of a small portion of the visual space. Cats also have a prominent nasal and a slight temporal extension of the area centralis, forming a "streak like" modification to their area centralis (of which differs from a traditional visual streak) that provides extended high acuity sampling along the horizontal meridian (Stone 1978; Hughes 1977; Rowe and Stone 1976). This tail or extension of the area centralis contains not only numerous small X-type ganglion cells for high spatial resolution as in the area centralis, but principally it contains W-type ganglion cells important for the detection of small, moving objects which may improve the detection of weak visual cues rather than enhance spatial resolution (Rowe and Stone 1976).

Despite having a rod-dominated retina, cone photoreceptors are present and are largely responsible for a cat's success in light. At night, the ability, or inability, of cats to detect color is probably of little consequence, as in dim light cone stimulation to distinguish one color from another is absent or limited. Color vision in domestic cats has been widely examined but remains controversial (Ringo and Wolbarsht 1986). Initially, cats were thought to lack discriminative color vision, but since have been shown to have peak sensitivities of 450 nm and 556 nm. Additionally, a third photopic spectral sensitivity has been noted near the rod-like 500 nm spectrum. Overall, the cat has the theoretical machinery for trichromatic vision, but thus far evidence of only drichromacy has been shown behaviorally (Ringo and Wolbarsht 1986).

Variation in cone photoreceptor populations across the retina also exists. In domestic cats, the proportion of S-cones is particularly rich in the ventral retina, generally a shared feature among wild cats, including the African lion and tiger (Ahnelt et al. 2006). The European lynx also has an S-cone-rich dorsal retina, making a large portion of the retinal periphery highly populated by S-cones, a design that likely enables earlier detection of spectrally distinct items (Ahnelt et al. 2006). The cheetah, however, is an exception whereby the population of M-cones matches that of the S-cones, and in combination with the horizontal tails of the streak-like extensions of the *area centralis* provides optimal visual conditions for hunting along the horizontal meridian in a horizon dominated savannah habitat (Hughes 1977; Ahnelt et al. 2006). This would seem important for arguably the most specialized open-terrain hunter with regard to speed (Ahnelt et al. 2006).

Being strictly carnivorous and specialized hunters, felids have perhaps the greatest degree of binocular vision within the Carnivorous Order. The position of the eyes is frontal and comparatively higher in the skull than other members of the Carnivora, enabling stereopsis, or the perception of depth based on spatial disparity cues to accurately observe and calculate the distance of prey (Ptito et al. 1991. In domestic cats, the total visual field is approximately 200° with a binocular overlap of 140° (Miller 2018). This visual field is changed through visual behaviors such as eye movements and head movements. Cats have an oculomotor range of about 50°, compared to nearly 100° in humans, but have a greater propensity for head movements to modify the visual field. This pattern of visual behaviors is directly related to the configuration of retinal areas of high acuity, where the fovea of humans occupies a smaller area (1° of visual arc) compared to the area centralis and or visual streak of cats (5° of visual arc).

Most felids are largely nocturnal, or at least are somewhat active in dim light (although limited in the cheetah). With large eyes relative to other carnivores, characterized by large curved corneas, a lens that is positioned more posteriorly due to a deeper anterior chamber, and the ability to create a large pupillary aperture, cat eyes are well adapted for vision in dim light, producing a smaller but brighter retinal image (Walls 1942). The minimum threshold of light for vision, or sensitivity to light, is about six times greater than that of the human eye! First, slit pupils have the ability to open considerably more than round pupils, providing the aperture required for capturing photons when scant at night. In addition, a slit-shaped pupil can close completely. This way the eye is protected from too much light even becoming nearly closed leaving only a pair of pinpoint holes (i.e., Scheiner's Disc). Many smaller felids have slit-shaped pupils but round pupils are more common in larger species. The Eurasian lynx is intermediate, where an oval or rhomboid pupil shape is noted. Large felids with round pupils have monofocal lenticular optics, whereas those with slit pupils have multifocal optics. The slit pupil enables use of the full lens diameter such that there is limited loss of a well-focused image due to chromatic defocus negated by the peripheral zones of the multifocal lens (Malmstrom and Kroger 2006). The clouded leopard is the only large felid with a definitive slit pupil. The

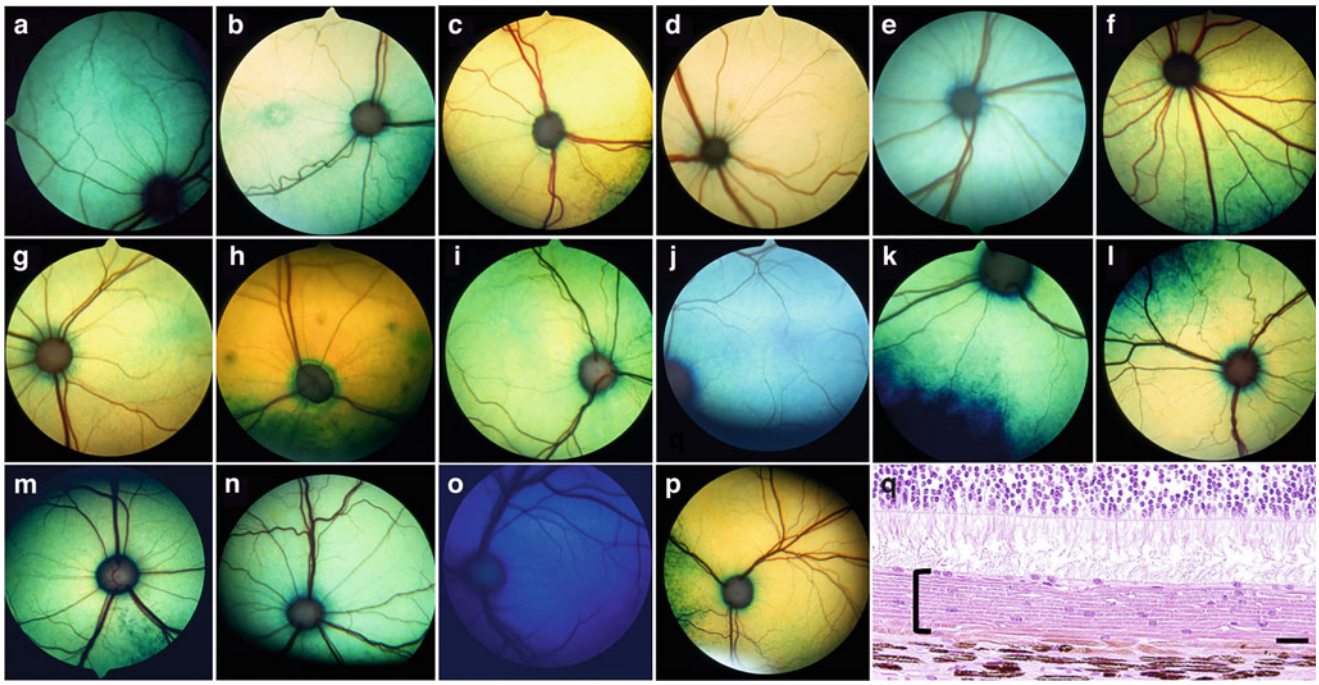

Fig. 35.1 Normal fundi of wild and exotic felids. (**a**) An adult jungle cat *Felis chaus*, (**b**) adult bobcat *Lynx rufus*, (**c**) adult serval *Leptailurus serval*, (**d**) adult margay *Leopardus wiedii*, (**e**) 10-week-old ocelot *Leopardus pardalis*, (**f**) adult ocelot, (**g**) adult clouded leopard *Neofelis nebulosa*, (**h**) adult snow leopard *Panthera uncia*, (**i**) adult leopard *Panthera pardus*, (**j**) 12-week-old cougar *Puma concolor*, (**k**) 24-week-old cougar, (**l**) adult cougar, (**m**) juvenile Siberian tiger *Panthera tigris altaica*, (**n**) adult Bengal tiger *Panthera tigris*, (**o**) 6-week-old African lion *Panthera leo*, (**p**) adult African lion, (**q**) histological cross-section of the retina of an adult African lion showing the thick cellular tapetum (bracket) imparting the highly reflective tapetum present in adults. Scale bar—20 μm. Note the immature, blue tapetum of young felids (**e**, **j**, **k**, **o**). (**a**-**p**) Courtesy of the University of California Davis Comparative Ophthalmology Service. (**q**) Courtesy of the Comparative Ocular Pathology Laboratory of Wisconsin

fact that only smaller felids and the clouded leopard have a slit pupil by itself may suggest that these species are more active at night, and that their night vision is better than their larger relatives.

The retina, however, is the primary determinant of visual success in scotopic conditions. The retina of felids is exquisitely rod-dominant, providing high sensitivity yet has a dichromatic cone population providing the ability to discern colors as previously discussed (Blake 1979). However, compared to diurnal species that possess a fovea (essentially birds and primates), which is consisted of pure cone photoreceptors, the felid *area centralis* is dominated by rod photoreceptors (though it has the greatest density of cone photoreceptors compared to other retinal areas) (Walls 1942). However, compared to diurnal species, where their respective retinal specialization may be complete devoid of rods, the felid *area centralis* is dominated by rod photoreceptors, approaching nearly ten-fold the density of cones, to provide low luminance spatial resolution. To deal with low light levels, the eyes of nocturnal animals have another refinement in the form of a reflective layer behind the retina, known as *tapetum lucidum*. The cat *tapetum lucidum* is of the cellular types, and is of particular brilliance, such that ancient Egyptians thought that it represented a reflection of the sun at night. The color of the *tapetum* is heterogenous and varies with age and species, probably due to differences in tapetal rodlet spacing with iridocytes, refractive index, and light-tapetum interactions (Fig. 35.1). Young animals with a developing *tapetum* have a funduscopic blue appearance, which generally becomes progressively more yellow with age. Adult tapetal coloration can vary in cats from light orange to green (Fig. 35.1). The felid *tapetum* is composed of cellular layers that of many other carnivores (15–20 layers centrally, compared to about 10 in Canids) resulting in increased reflectance (nearly 130 times that of humans) and providing retinal photoreceptors a "second chance" to absorb photons of light at the expense of visual acuity due to light scatter, enhancing visual sensitivity at night (or in low luminosity conditions).

Additional known clinically relevant anatomical differences between wild and domestic felids are minimal; however, approaching the examination and therapeutic management in wild and captive exotic felids can be a major challenge clinically.

The Felidae family is under severe pressure due to human encroachment on natural environments, competition for prey, and the action of infectious diseases. Data from the International Union for Conservation of Nature—IUCN (2016)

categorizes in the Red List of Threatened Species 12 feline species as least worrying, 12 as vulnerable, 7 as almost threatened, and 7 as threatened. The future of these species depends on the understanding that felines play a fundamental role in nature, regulating the number of prey as ungulates and rodents, which can cause serious damage to food production for humanity (Kitchener et al. 2017). We have taken over the image of felids countless times to represent imperial coats of arms, to bear symbols of power and wealth; but what have we given back to the animals in return? We provide below an approach to exotic felid ophthalmology as a means to facilitate and encourage better care for this magnificent group of carnivores. We place specific focus on the aspects differing from that of domestic cats, and thus for more information about general ophthalmology in members of the Felidae, we encourage review of domestic feline texts.

Ophthalmic Examination

Approaching ophthalmic examination and treatment of ocular disease in wild animals is challenging, especially when it comes to managing species that can inflict serious injury to the caregiver, like non-domestic felids. When examination, diagnostic, and therapeutic options, the training (if any) and treatability of the patient must be carefully considered. Some captive felids are trained to look upward in a box chute to enable examination and administrations of topical medications. There are instances when a squeeze cage might be extremely useful for examination and administering topical medications from a distance (sprayed) onto the eyes from a small sterile spray bottle. This type of bottle can be ordered from a compounding pharmacy. Such approaches help reduce the use of a chemical restraint for each repetition of the treatment. In some cases, with very tamed and/or trained felids, zookeepers may attach the eye drop bottle to a long forceps so they can reach the animal eye usually of a cage or through the cage mesh, without the risk of having their hands scratched or bitten. Subconjunctival injection of antibiotic or anti-inflammatory medication may be the best solution for patients who cannot be treated otherwise following the initial evaluation and/or surgical procedure, under chemical restraint. Additionally, a more aggressive and decisive surgical approach may be elected if one is faced with an, "only one chance to fix" scenario. Oral medications can also be given for some ocular conditions and should be considered, when appropriate. The use of systemic enrofloxacin is known to cause retinal toxicity in domestic cats. However, a retrospective study with 81 eyes from 14 lions (*Panthera leo*) and 33 tigers (*Panthera tigris*) showed no evidence of enrofloxacin-associated thinning of the outer nuclear layer in the lions and tigers evaluated by comparing animals that had not received enrofloxacin ($n = 11$) with treated animals ($n = 36$), suggesting that enrofloxacin can be used safely in these animals (Newkirk et al. 2017).

The basic eye examination techniques are similar to other species. However, in most cases, a thorough eye examination is performed under chemical restraint (usually anesthesia), as the patient can easily inflict harm or death to the examiner (Holzer and Solomon 2003). In fact, the use of remote chemical-restraint delivery systems (darts) and squeeze cages (Fig. 35.2) are standard practices with large wild Felids for human and animal safety. However, even under general anesthesia, the eye examination may be challenging due to the sub-ideal environment, i.e., the position of the animal (commonly on the ground), the level of ambient light (in the open or in the animal's enclosure), which is usually bright. Additionally, the need to perform multiple examinations and/or procedures simultaneously, by different specialists and veterinarians, in order to decrease the overall time that the patient is maintained under anesthesia, may also pose some challenges. Hence, the examiner has to be flexible (at times literally) and adjust to the specific environment and examination technique. In some cases, a limited eye examination can be performed on a captive conscious animal, with a barrier between the patient and the examiner. In these instances, a squeeze cage may be useful. Nevertheless, it does require some training and some level of cooperation by the patient. Training is as challenging and it takes patience. In the author's experience, offering the animal a distractor, such as chunks of meat or squirts of milk (sprayed out of a spray bottle) through the barrier, are effective and facilitate that examination (Fig. 35.3). Needless to say, the examination has to be performed in a quiet environment, away from the public, and when the patient is the only animal in the enclosure. The trust between the animal and the zookeeper is paramount for the success of this examination technique (Fig. 35.3). The examiner should approach the barrier very slowly and be attuned to the keeper, and readily responsive to the keeper's instructions to stop/continue the approach to the barrier, and to begin, pause or stop the examination altogether. A minimum number of personnel should participate in this type of examination, and ideally, only the zookeeper and examiner should be present. In facilities with an attending veterinarian who is engaged with routine procedures and examinations of the animal over a long period of time, greater patient cooperation may be achieved when the attending veterinarian is not present. Regardless, a thorough eye examination under chemical restraint or anesthesia may still be needed (Fig. 35.4), and is almost certainly required for additional diagnostic testing and sample collection including tear testing, nasolacrimal patency, and tonometry (Fig. 35.5). Lack of animal conditioning, presence of new or inexperienced zookeepers make

Fig. 35.2 A squeeze cage is being used to physically restraint a jaguar. This type of cage has adjustable sidewalls, which can gently press the side of the animal against the other fixed wall so it cannot move its limbs. Such cages are standard equipment for veterinary hospitals, zoos and very useful for handling large cats without chemical immobilization. Courtesy of Dr. Fabiano Montiani-Ferreira

the ocular examination in conscious felids a very challenging and dangerous procedure. Thus, on these occasions, chemical restraint is the only viable option to perform an eye exam.

When employing a basic eye examination on a conscious animal through a barrier, a valuable information can be attained for different portions of the eyes, from the eyelids to the back of the lens and even, to some degree, the vitreous. The examiner can assess the symmetry between the eyes, anatomic and physiologic (i.e., blinking) integrity of the eyelids, and clarity of the cornea and anterior chamber. The size, shape and color of the pupils, and pupillary light reflexes (direct and consensual) can be assessed. The large felids have round pupils in all light conditions, whereas moderately sized felids (e.g., bobcats) have pupils that are somewhat vertically elongated when miotic, and small felids and domestic cats have vertical slit pupils (Fig. 35.6). The exception is the clouded leopard (Fig. 35.6c), who has vertical slit pupils when miotic. Beyond the iris, the clarity of the lens, and clarity of the vitreous (i.e., can tapetal reflection be seen easily or not) can be assessed. Initial examination should be performed under ambient light, and a bright light source (e.g., a slit lamp, Finoff transilluminator, and penlight) should be used once the animal had acclimated to the presence of the examiner. It is helpful to have the evaluated animal on an elevated bench, if available, so the eye of the examiner and examinee are approximately at the same height (Fig. 35.4). Photography can also be utilized to complement the physical examination, especially when optical zoom and digital magnification are utilized. When used, photography should be taken at the highest resolution possible, to allow effective digital magnification.

Ocular Diseases

Ocular diseases in wild felids are commonly presented, particularly in animal sanctuaries and rehabilitation centers. Unfortunately, sometimes these conditions are irreversible, and since these animals heavily depend on vision for their ability to hunt, completely blind felids should not be released in the wild (Fig. 35.7). Binocularity allows stereopsis by horizontal disparity and is important for hunting. However, even the loss of one eye might complicate significantly their survival after the release depending on the species. The visual ecology of a given animal must be considered prior to releasing an animal with unilateral visual deficits.

Fig. 35.3 (**a**) An adult lioness laying on a bench and being fed chunks of meat by the familiar zookeeper, when the examiner is slowly approaching the barrier. The source of light (a slit-lamp in this case) was held in a position where the lion can see it and get used to it. At this time, the examination was performed under ambient light and the slit-lamp is turned off. (**b**) Once the lioness is acclimated to the presence of the examiner, the light source was turned on to assess the pupillary light reflexes and complete the eye examination. During the whole time of the examination, the lioness is being fed meat in a slow, steady paste, to distract her from the eye examination. (**c**) A young adult male Snow leopard being examined through a barrier, utilizing a similar technique. In this case, squirts of milk and chunks of meat are used to distract the leopard. Incipient cataracts can be easily seen in both eyes. Apart from the cataracts, no opacities were noted in the ocular media, including the cornea, anterior chamber, and vitreous; the tapetal reflection can be seen with no interference. The color of the iris and the shape and size of the pupils can also be assessed. This Snow leopard was born with bilateral eyelid agenesis that was corrected surgically. (**d**) The picture in **c** was digitally magnified to better demonstrate the incipient cataracts. Courtesy of Dr. Gil Ben-Shlomo and the Blank Park Zoo, Des Moines, Iowa

Fig. 35.4 Eye examination in wild felids. (**a**) Slit-lamp biomicroscopy procedure in an African lion (*Panthera leo*). The examination was performed on the floor and under bright ambient light conditions, after induction of anesthesia, and while other medical procedures were being performed. As the lioness was laying on the floor, the examiner had to hover over the eye, from the back, to facilitate the use of the slit-lamp (without laying on the floor). An infected corneal ulcer was found on examination. (**b**, **c**) Gonioscopy with digital photography being performed with a slit-lamp biomicroscope similarly, in a jaguar (*Panthera onca*). (**d**, **e**) Indirect ophthalmoscopy being performed on a snow leopard (**b**) and a Bengal tiger (**c**) as they were prepared for additional medical procedures. As such, the examination was conducted under bright light condition and with a space shared with other personnel. (**a**, **d**, **e**) Courtesy of Dr. Gil Ben-Shlomo. (**b**, **c**) Courtesy of Dr. Ana Carolina Rodarte de Almeida

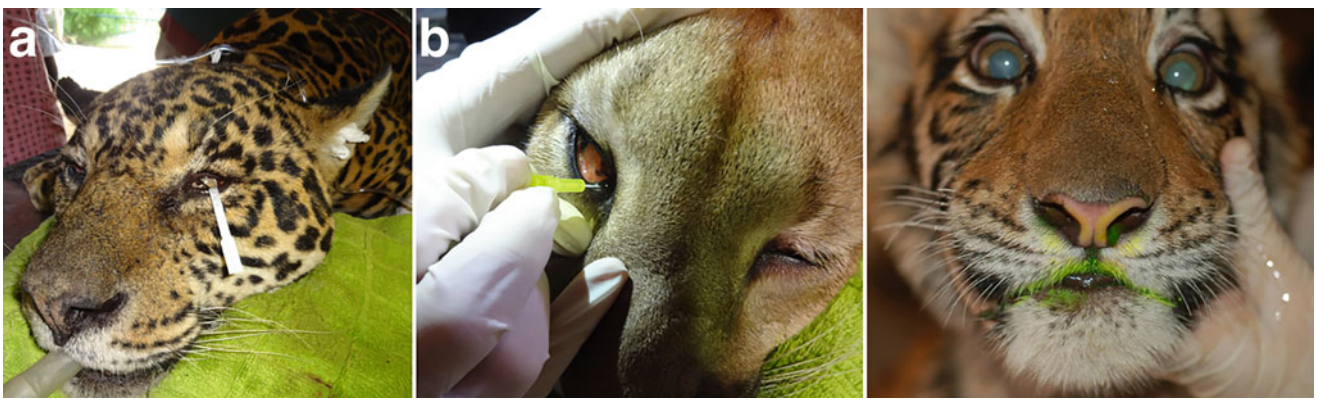

Fig. 35.5 Ophthalmic diagnostic testing in large felids under chemical restraint. (**a**) A Schirmir's tear test being performed in a jaguar (*Panthera onca*). (**b**) Nasolarcimal punctal cannulation in a puma (*Puma concolor*). A positive Jones test in a young tiger (*Panthera tigris*). Courtesy of Dr. Ana Carolina Rodarte de Almeida

Fig. 35.6 Pupil shapes in non-domestic felids. (**a**) The round pupil of an African lion (*Panthera leo*), (**b**) the intermediately round pupil of the bobcat (*Lynx rufus*), and (**c**) the vertical slit pupils of the clouded leopard (*Neofelis nebulosa*). (**a**) Courtesy of Ana Carolina Rodarte de Almeida. (**b**) Courtesy of Bret A. Moore. (**c**) Courtesy of Rogerio R. Lange

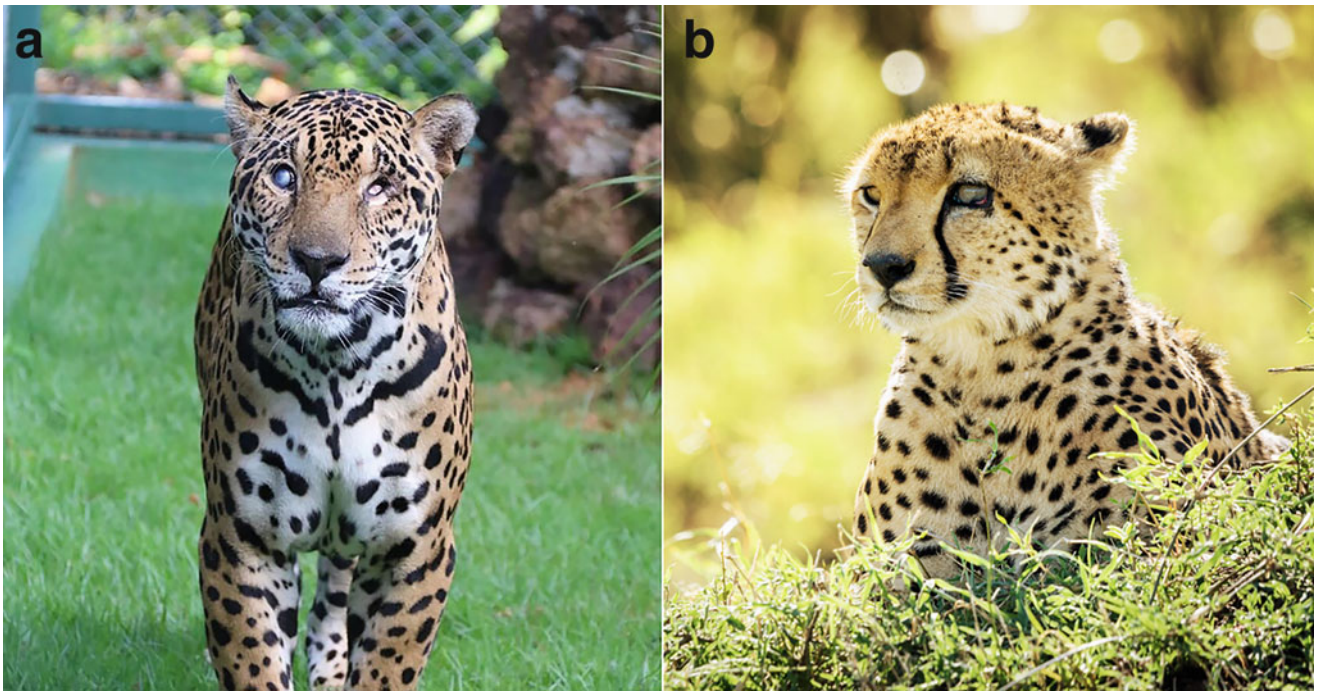

Fig. 35.7 (**a**) An adult jaguar (*Panthera onca*) rescued by a Brazilian wild felid sanctuary presenting phthisis bulbi in the left eye and severe ocular disease in the right eye. (**b**) An adult cheetah (*Acinonyx jubatus*) with visually impairing ocular disease of the left eye. (**a**) Courtesy of Raul Coimbra and Cristina Gianni—Nex—No Extinction, Brazil. (**b**) Used with permission from JossK, Shutterstock.com

For the remainder of this chapter, we will focus on ocular disease in exotic felids. In wild cats, ocular and systemic symptoms are superimposable to those observed in domestic cats (Millichamp 1997). Considering, only conditions with specific importance to exotic felids, and those that have been reported in the literature, will be discussed to avoid overlap with domestic cats of which ample other resources exist.

Eyelids

Eyelid agenesis, or eyelid coloboma, has been described in numerous mammalian species, and among the Felidae in domestic cats, snow leopards *Panthera uncial* (Hamoudi et al. 2013), Texas cougars *Puma concolor* (Cutler 2002) and cheetahs (Boucher et al. 2016) (Fig. 35.8). Persistent pupillary membranes frequently accompany eyelid agenesis, and less frequently choroidal and optic nerve coloboma, retinal dysplasia, iris hypoplasia, and cataracts (Martin et al. 1997; Hamoudi et al. 2013) (Fig. 35.9), although these ophthalmic abnormalities may also exist alone without agenesis of the eyelid (an iris to cornea persistent pupillary membrane has been described in a 2-month-old tiger cub with a corneal opacity; Buddhirongawatr et al. 2015). This condition is particularly prevalent in snow leopards. It was first reported in a snow leopard cub at the Helsinki zoo with multiple ocular colobomas (MOC) (Gripenberg et al. 1985), followed by others (Schäffer et al. 1988; Hamoudi et al. 2013). This complex of MOC is considered to be a specific clinical entity characterized by the superior eyelid coloboma and variable microphthalmia, uveal, retinal and optic nerve coloboma, persistent hyperplastic primary vitreous, cataracts, retinal dysplasia, and hydrocephalus. However, superior eyelid coloboma is the single consistent feature in affected animals (Gripenberg et al. 1985). All occurrences of eyelid coloboma in the snow leopard have been located temporal to central on the superior eyelid of one or both eyes (Gripenberg et al. 1985; Barnett and Lewis 2002). The relationship between eyelid coloboma and the development of MOC is not understood, considering that the uvea and retina largely develop from the neuroectoderm and neural crest, whereas the eyelids are derived from mesoderm and surface ectoderm and during a later stage of development (Barnett and Lewis 2002).

Identification of a genetic element as the cause of eyelid coloboma and MOC is important moving forward. Pedigree analysis of the snow leopard in the Helsinki study was unable to provide evidence of a genetic link (Gripenberg et al. 1985, Barnett and Lewis 2002). A teratogenic effect caused by a virus or abnormal nutrition (e.g., hyper- and hypovitaminosis A, and folic acid deficiency) has been suggested, although no evidence exists to substantiate these claims (Barnett and Lewis 2002). Additionally, the high and increasing prevalence among different institutions housing snow leopards suggests a genetic link. Further studies are

Fig. 35.8 Degrees of eyelid agenesis. (**a**) Snow leopard (*Panthera uncial*) with a short but deep superior eyelid coloboma that was able to be closed primarily in two layers (**b**). (**c**) A snow leopard with a larger and deeper defect and significant trichiasis causing keratitis. The patient was able to fully blink as an adult, and thus cryoepilation was elected, which provided good results with no residual discomfort and improvement in keratitis (**d**—3 months post-cryoepilation). (**e**) Subtle eyelid coloboma of a domestic feline without the need of correction. (**f**) Severe eyelid coloboma in a domestic feline causing marked keratitis. (**a**, **b**, **e**) Courtesy of the University of California Davis Comparative Ophthalmology Service. (**c**, **f**) Courtesy of Bret A. Moore. (**d**) Courtesy of Brian C. Leonard

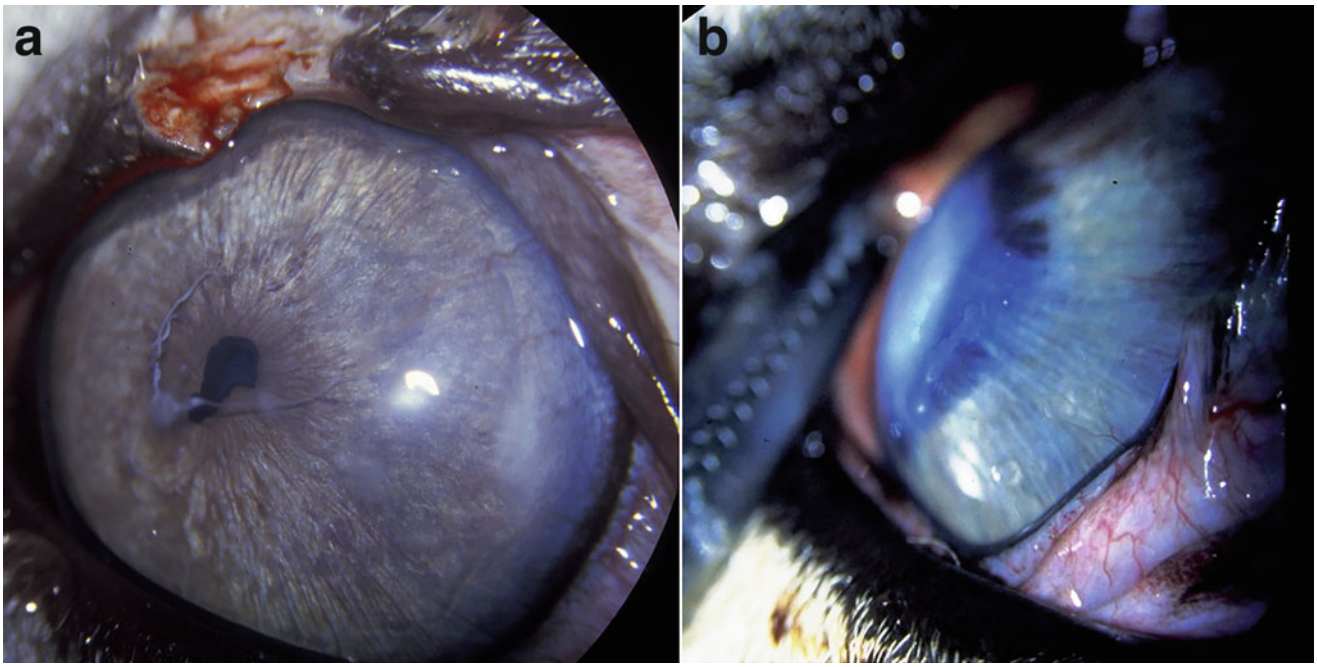

Fig. 35.9 Ocular anomalies in snow leopards (*Panthera uncial*) associated with superior eyelid colobomata. (**a**) An iris-to-iris persistent pupillary membrane. Note the notch in the superior eyelid that was freshened prior to primary closure of the mild defect. (**b**) Peter's Anomaly featuring severe iris-to-cornea persistent pupillary membranes and leukocoria axially due to the iris adhesions. Courtesy of Hannes Meissel

important to help identify the cause and enable institution of better breeding practices, a major challenge for a population of animals that may benefit from captive breeding due to natural population decline.

The severity of eyelid coloboma can vary both in extent of the eyelid margin involved and the proximodistal depth of the defect (Fig. 35.8), and the severity of clinical signs at near and adult size must be evaluated prior to definitive treatment. Additionally, as with all therapeutic options in this chapter, the treatability of the animal must be carefully considered. In all but the mildest cases, trichiasis characterized by variable ocular discharge, blepharospasm, and secondary keratitis is a prominent source of irritation even if complete eyelid closure can be achieved. Short but deep defects (Fig. 35.8a) can sometimes be closed primarily in two layers after creating new wound edges, similar to a wedge resection or a four-sided technique (Fig. 35.8b). If a larger portion of the eyelid margin is involved, but complete eyelid closure can be achieved, cryoepilation can provide desirable results (Fig. 35.8c, d). In the authors' experience, facial skin of larger felids is sometimes looser and more mobile than that of domestic felids, and complete closure can be achieved in cases that one would not expect based on work with pet cats. Cryoepilation consisting of 2 cycles of 25–30 second freeze at −80 °C followed by a slow thaw works well. A good contact of the cryotherapy probe to the skin is important. Hairs should epilate easily; otherwise, a third freeze-thaw cycle may be necessary. Oral nonsteroidal anti-inflammatory therapy is recommended postoperatively. A second cryoepilation may be necessary if significant hair regrowth is noted, which may occur even if the procedure was sufficiently performed, due to hairs being in the anagen phase at the time of surgery. On one far end of the spectrum, subtle agenesis without trichiasis does not need to be repaired, although tear film quality should be monitored when possible throughout life (Fig. 35.8e). On the other end, cases of severe coloboma causing significant keratitis and discomfort due to exposure must be corrected by a definitive blepharoplastic procedure (Fig. 35.8f). We encourage review of the domestic felid literature for complete information regarding definitive blepharoplastic repair, and recommend that the type of procedure be chosen based on not only its ability to produce the desired anatomic outcome but also on the comfort and experience of each procedure in the hands of the surgeon (Modified Robert-Bistner procedure, Mustarde techinique, cross eyelid-flaps, lip commissure transposition, other sliding grafts, etc.) (Munger and Gourley 1981; Roberts and Bistner 1968; Esson 2001; Dziezyc and Millichamp 1989; Whittaker et al. 2010; Hunt 2006).

Eyelid agenesis has also been described a 4-month-old Texas cougar and in a 3-month-old cheetah. The Texas cougar was born in captivity, and suffered from chronic ocular discomfort and mucoid discharge. Extensive bilateral eyelid colobomas located dorsolaterally were diagnosed, with only a 4–5 mm wedge of normal eyelid margin medially. Persistent pupillary membranes and a typical inferopapillary coloboma were present bilaterally, while an atypical (12 o'clock position) iris coloboma was also present

in the right eye. A rotational pedicle flap and sliding conjunctival relocation produced a functionally effective result A recipient bed was created in the upper eyelid by sharp dissection of conjunctiva and separation of the globe. A 20-X 5-mm skin and orbicularis lower eyelid pedicle flap were created near the margin. The pedicle was undermined to the lateral canthus, where a releasing incision was made and the flap was rotated into position dorsally. A tacking suture apposed the pedicle flap and eyelid after a sharp incision of the margins. The pedicle and eyelid bed were opposed with 6/0 polyglactin 910 in a buried interrupted pattern. Mobilized dorsal conjunctiva was sutured to the pedicle flap in a slightly overriding continuous pattern (Cutler 2002). In the cheetah, bilateral superior eyelid colobomas have been described, each affecting about 50% of the temporal eyelid. Multiple ocular defects were also noted, including a lateral perilimbal dermoid OD in the lateral perilimbal area, persistent pupillary membranes OU, bilateral immature posterior cortical cataracts OU, a peripapillary coloboma in the dorsolateral region of the optic disc OD, and choroidal hypoplasia in the dorsolateral region of the optic disc OS. An intrauterine cause could not be excluded as the cause of clinical signs in this case (Boucher et al. 2016).

Various eyelid neoplasms have been reported. A rare case of sebaceous carcinoma has been described in an Amur tiger (*Panthera tigris altaica*). The erythematous and irregular mass was 5 mm in diameter and was located at the lateral canthus where it involved the skin and the palpebral conjunctiva. For surgical excision, a lateral canthoplasty was performed using 3-0 poliglecaprone absorbable suture in a two-layer closure using a simple continuous pattern to close the tarsoconjunctival layer and a running subcuticular pattern to close the skin at the lateral canthus. Recurrence was suspected 3 months later, and a second excision via lateral canthoplasty was followed by intralesional bevacizumab (2.5 mg each at 4 sites) due to the typical aggressive and malignant behavior of this type of neoplasm. The surgical wound was closed in two layers using 3-0 poliglecaprone absorbable suture, in a continuous subcuticular pattern to close the tarsoconjunctival layers, in a figure-eight pattern at the lid margin, and in a simple interrupted pattern to close the skin along the remainder of the incision (Edelmann et al. 2013). Recurrence was confirmed histologically, but following the second procedure, no further recurrence or metastasis was noted. Another case of a sebaceous carcinoma was described in a Bengal tiger (*Panthera tigris tigris*), although it was located at the medial caruncle and was completely excised via medial canthoplasty (Iaquinandi et al. 2017). A large eyelid epidermoid carcinoma of the medial canthus has been described in a white tiger (*Panthera tigris*) causing the inability to open the eye (Bose et al. 2002). The mass involved about 50% of the upper and lower eyelids. Surgical resection was performed. A skin incision was given at the palpebral border and separated from the growth. Then the growth along with palpebral conjunctiva, which was also involved, was removed. The medial edge of the skin flap was pulled towards the inner canthus and fixed with an interrupted nylon suture. The growth on lower eyelid was excised along with skin and orbicularis oculi muscle, which were involved and ulcerated. Skin was incised at the outer canthus to mobilize the remaining portion of the eyelids toward the inner canthus to its maximum extent and fixed to medial canthus area (Bose et al. 2002). Postoperatively complete palpebral closure was able to be achieved, although a detailed description of the surgical approach, the histologic margins, or extent of follow-up were not described. A squamous cell carcinoma of nearly the entire inferior eyelid margin of a white tiger has also been described (Gupta et al. 2013). Simple excision was performed, although histologic margins were not described. No adjunctive therapy was administered, and the mass recurred within 1 month. A two-round chemotherapy treatment was administered (cyclophosphamide and prednisolone, with Vincristine sulfate added to the second treatment regime) was administered. Recurrence was noted 1 month later, and the animal was given two cycles of chemotherapy. The tiger died 3 months later, and postmortem examination revealed metastasis to the lungs, liver, pancreas, and spleen (Gupta et al. 2013).

Squamous cell carcinoma of the eyelids is the most frequent tumor of the appendages in domestic cats; it originates from the epidermis and is a type of malignant and locally invasive tumor. Although the eyelid margin is the most common site of origin, this type of tumor can also involve the conjunctiva and the cornea, primarily or secondarily (Caligiuri et al. 1988). A case of corneal squamous cell carcinoma in a 5-year-old cheetah (*Acynonyx jubatus*) presenting corneal opacity and mucopurulent discharge has been reported. By examining the animal's affected eye under general anesthesia, it was also possible to observe a thickening of the lower eyelid, the third eyelid, and the conjunctiva; furthermore, the latter two were also hyperemic. The corneal neoformation was circular, vascularized and whitish-pink in color. The diagnosis of corneal squamous cell carcinoma was made after biopsy and histological examination. Following the histopathological diagnosis an orbital exenteration was performed (Caligiuri et al. 1988).

Plaque-like lesions have been reported on the eyelid margins in a 3-month-old cheetah cub with herpesvirus type 1 rhinotracheitis and cutaneous ulcers. The lesions were self-limiting and regressed over a period of 1 month (Junge et al. 1991).

Conjunctiva

Conjunctival developmental ocular anomalies are infrequent. A dermoid located in the bulbar conjunctiva without corneal involvement was reported in an African lion (*Panthera leo*

leo). The only clinical sign noted was epiphora at the medial canthus. The dermoid had an irregular shape, was pigmented with hair present, and measured about 7 × 4 mm. The mass was surgically removed following sterile irrigation and two drops of epinephrine injection U.S.P. were applied to the dermoid tissue to effect hemostasis. Hemorrhage was minimal and completely controlled by the additional application of adrenalin chloride on a sterile cotton-tipped applicator stick (Robinson and Benirschke 1981).

Although infectious conjunctivitis is very common in domestic cats, it is infrequently reported in exotic felids. In domestic felids, the most frequent viral cause is feline herpesvirus 1 (FHV-1), with ocular manifestations most consistently including conjunctivitis and keratitis (Shahzad et al. 2015). The most frequent bacterial cause is *Chlamydophila felis* (Shahzad et al. 2015), with clinical signs including conjunctival hyperemia, prominent chemosis, often unilaterally prior to progressing to bilateral (Marti et al. 2019). A Puma (*Puma concolor*) in Pakistan showed protrusion of the third eyelid, ocular discharge, conjunctival hyperemia, and a slight bilateral corneal opacity (Shahzad et al. 2015) and a Eurasian lynx (*Lynx lynx*) had pronounced unilateral conjunctivitis with hyperemia, chemosis, and a yellow, turbid and mucopurulent discharge (Marti et al. 2019). In both cases, conjunctival swabs were positive for *Chlamydophila felis*. Systemically administered broad-spectrum antibiotics, but preferably tetracyclines, are indicated in cases of animals that are hard to manage with topical medications (Millichamp 1997). Accordingly, cephalosporin was administered in the first case and tetracycline in the second case, both orally. In a fishing cat (*Felis viverina*), a pale-yellow color of the conjunctiva and sclera (among other organs) was noted on necropsy. In this case, *Chlamydia psittaci* was diagnosed by direct immunofluorescence (Kik et al. 1997) and was suspected to lead to the death of the animal (Kik et al. 1997). In a study carried out on 72 conjunctival swabs from non-domestic cats (*Leopardus pardalis*, *Leopardus tigrinus*, *Panthera tigris*, *Puma concolor*, *Puma yagouaroundi*, *Oncifelis colocolo*, *Panthera onca*), only in an ocelot (*Leopardus pardalis*) was the conjunctival swab positive for *Chlamydophila* sp. The same animal was also positive for FHV-1 via PCR. According to the same study, the transmission of FHV-1 and *C. felis* occurs more easily when a group of animals lives in close contact; indeed, non-domestic cats with solitary habits such as those sampled in this study are less frequently in contact with other animals and this limits the transmission of the pathogen (Seki et al. 2016). However, results from one survey investigating the presence of neutralizing antibodies against FHV-1 in Brazilian captive wild felids (*Leopardus tigrinus*, *Leopardus wiedii*, *Herpailurus yaguarondi*, *Puma concolor*, *Leopardus pardalis*, and *Panthera onca*) showed a low percentage of seropositivity and low antibody titers, suggesting that the virus does not circulate extensively among these animals (Ruthner Batista et al. 2005).

To date, canine distemper (CDV) has been reported in all families of terrestrial carnivores: Canidae, Felidae, Hyaenidae, Mustelidae, Procyonidae, Ursidae, and Viverridae. CDV infection can occur in wild and captive felids, being already reported in leopards (*Panthera pardus*), tigers (*Panthera tigris*), lions (*Panthera leo*), jaguar (*Panthera onca*), Asiatic lions (*Panthera leo persica*) (Appel et al. 1994; Deem et al. 2000; Mourya et al. 2019). No investigation was performed regarding the specific ocular signs the affected animals present. However, affected animals have been observed presenting conjunctival hyperemia and lacrimation besides respiratory and central nervous system signs (Mourya et al. 2019). Vaccines seem to work, since an attenuated Onderstepoort strain was used successfully in captive African lions in Maasai Mara National Reserve in Kenya and a live attenuated canine vaccine was used in a vaccine trial in tigers (Sadler et al. 2016).

Thelazia callipaeda is a nematode that can be found in the conjunctival sac of domestic and wild carnivores (Mihalca et al. 2016). During the post-mortem, examination of an imported Eurasian lynx (*Lynx Lynx*) found dead in Japan, *Thelazia callipaeda* was identified in the conjunctival sac and under the third eyelid of both eyes. The parasites had a thin, straight, whitish appearance and their length was between 1 cm and 1.8 cm (El-Dakhly et al. 2012). In another study carried out on 89 wild carnivores in Romania, three animals—including a wild cat (*Felis silvestris*) were found infested with *Thelazia callipaeda*; it was located in the conjunctival sac in this case too (Mihalca et al. 2016).

Three other wild cats (*Felis silvestris*) in southern Italy have been found infested with *T.callipaeda* (Mihalca et al. 2016). No treatment or outcome was fully described as they were all wild animals. All of these cases were diagnosed as part of a wildlife survey and none was treated in captivity.

Cornea

Corneal ulceration in wild felids exhibits a wide variety of causes, but trauma is probably the most common. Perhaps the greatest clinical challenge is treatment. Topical medications are often not able to be consistently administered, or are of substantial safety risk, and thus in many cases uncomplicated superficial ulcers are rarely treated medically unless proper training has been implemented to enable it. When deep, surgical stabilization by conjunctival grafting (i.e., pedicel flaps and advancement flaps) is recommended because it reduces or eliminates the need for frequent topical medications (a subconjunctival antibiotic can be administered while under anesthesia for surgery) and stabilizes the defect while providing a vascular supply

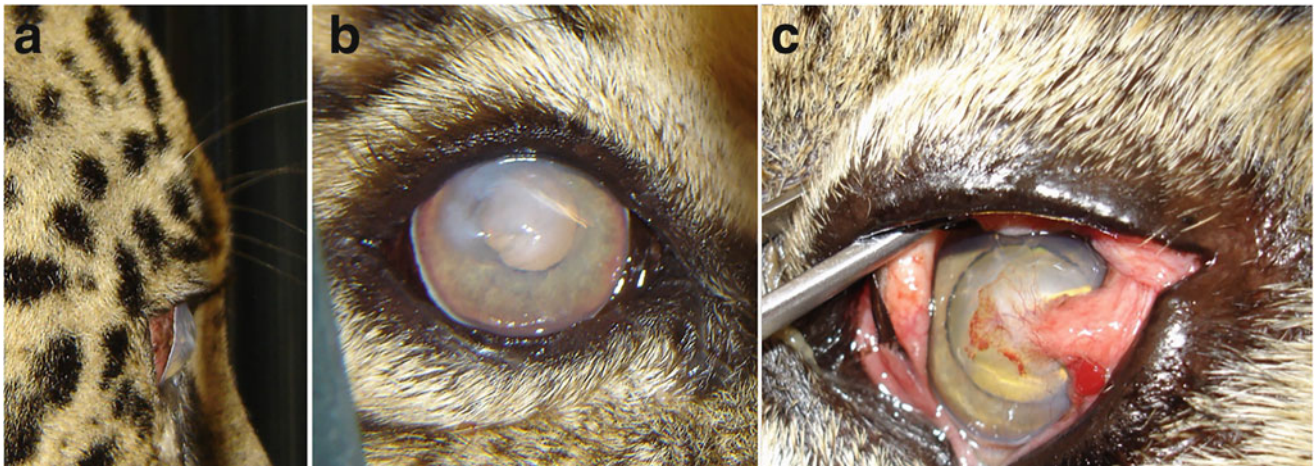

Fig. 35.10 A 10-year-old male jaguar (*Panthera onca*) with an extensive corneal ulceration. *Pseudomonas aeruginosa* was isolated from corneo-conjunctival swabs. (**a**) Lateral view. (**b**) Frontal view. Note the gelatinous texture, a typical sign of corneal malacia (melting) and stromal edema. For treatment of this ulcer, a pedicle graft was performed, followed by topical therapy with 0.3% ciprofloxacin four times a day (delivered through a small spray bottle while the animal was in a squeeze cage). (**c**) Appearance of the graft 21 days after surgery. Courtesy of Dr. Fabiano Montiani-Ferreira

(Fig. 35.10). This technique, however, may result in some scars, although thin grafts can clear substantially. Wild felids should not be challenged by a small opacity in 1 eye in regards to hunting, and especially in those captive individuals, visual compromise should not be encumbering. In the snow leopard (*Panthera uncia*), free-island grafts of equine amniotic membrane were used to treat a deep corneal ulcer caused by temporal trichiasis of the upper eyelid following a cryotherapy treatment for the eyelid agenesis of the animal. A midstromal keratectomy was performed in the area of corneal ulceration. One layer of equine amnion was placed stromal side down into the corneal defect and sutured using 8-0 polyglactin-910 in a simple interrupted pattern followed by an over-sewn 8-0 polyglactin-910 in a simple continuous pattern (Knollinger et al. 2018).

Indolent corneal ulcers are encountered, although the pathology is not well defined similarly to those in domestic cats (i.e., compared to dogs where an anterior stromal abnormality is implicated). During examination, topical fluorescein stain frequently undermines the redundant epithelium bordering the ulcer. Epithelial debridement with a cotton-tipped applicator (Fig. 35.11), with consideration for anterior

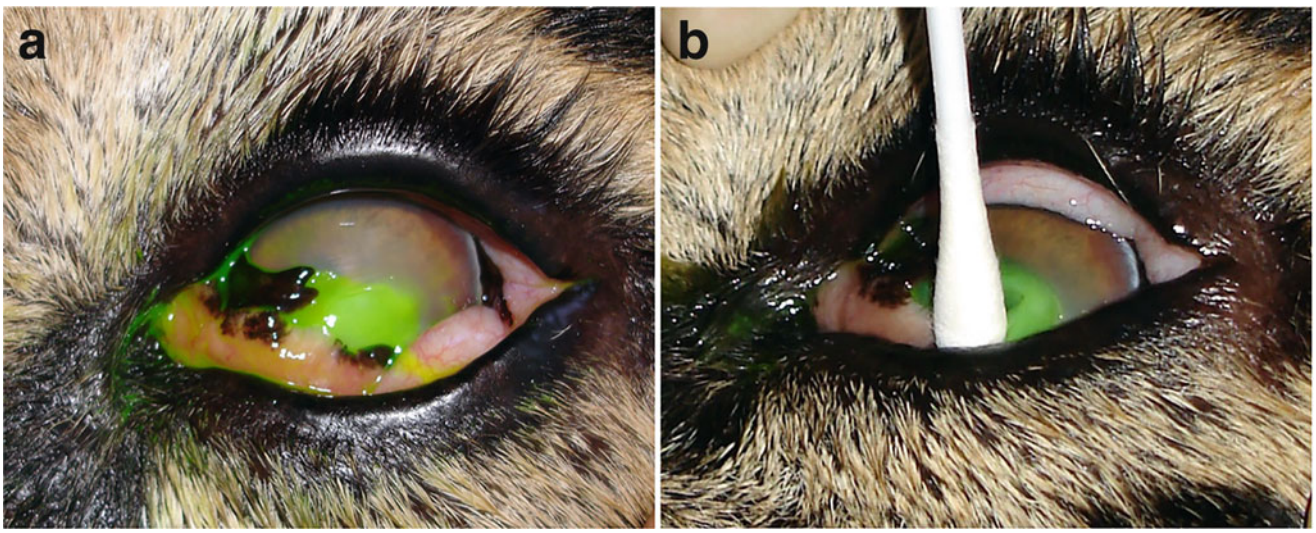

Fig. 35.11 A 2-year-old jaguar (*Panthera onca*) presented a healed third eyelid laceration and a corneal ulcer (**a**). After several attempts to treat the condition with topical therapy, the corneal ulceration was determine to be indolent as evidenced by remaining superficial and having a redundant epithelial edge. (**b**) Debridement of the ulcer promoted healing by removing the outer non-adhering layer of the cornea with a cotton swab. Courtesy of Dr. Fabiano Montiani-Ferreira

stromal keratotomy (with a diamond burr) or keratectomy, are the typical treatments. The authors have not faced similar concerns with the development of sequestra as may occur in domestic felines.

A case of B-cell lymphoma involving the cornea, conjunctiva, and sclera in a jaguar (*Panthera onca*) has been reported. Bilateral corneal samples were taken for histological evaluation, which suggested that bilateral lamellar keratectomy and the removal of the scleral-conjunctival mass may be curative. Although infrequent, ocular B-cell lymphoma should be considered as an important differential diagnosis for growths/plaques on the corneal surface (Prando et al. 2017).

Glaucoma

In wild cats, glaucoma has been observed in a male lion cub (*Panthera leo*) aged 8 weeks (Gerding et al. 1987). It was a primary, unilateral glaucoma, associated with a widespread and well-differentiated infiltration of lymphocytes and mast cells in the uveal stroma (Gerding et al. 1987). A tiger from a circus was diagnosed with bilateral secondary glaucoma that was thought to be linked to traumas provoked by the circus training (Thomas et al. 2006). Otherwise, little is known about glaucoma in exotic felids, nor is their aqueous dynamics and normal intraocular pressure. In a study on the intraocular pressure (IOP) of Angola lions (*Panthera leo bleyenbergi*) and African lions (*Panthera leo*) using a Tono-Pen XL applanation tonometer, it was observed that the average intraocular pressure of animals aged less than or equal to 1 year was significantly lower (12.8 ± 3.5 mmHg) than the average IOP of those aged more than 1 year (23.9 ± 4.1 mmHg). Moreover, the average IOP of adult African lions (24.2 ± 4.00 mmHg) was significantly higher than the one of adult Angola lions (20.6 ± 3.9), although the average age of African lions was lower than the age of the Angola lions. Furthermore, it was observed that IOP significantly increased in the first 20 months of life, showed a plateau between 20 and 40 months, and then decreased gradually (Ofri et al. 2008). Additionally, based on the detected progesterone levels, mature lionesses (*Panthera leo*) in "luteal" phase and therefore with progesterone levels >5 ng ml^{-1} reported a significantly higher intraocular pressure (27.1 ± 2.1 mmHg) than immature, non-luteal lionesses (*Panthera leo*) with progesterone levels <5 ng ml^{-1} and a pressure of 21.0 ± 2.4 mmHg (Ofri et al. 1999). All reference values are available in Appendix C.

Uvea

A range of uveal diseases (from uveitis to tumors) have been reported and various wild felids. Many other infectious and systemic conditions are likely able to cause uveitis in wild felids, and those considered a possible cause in domestic species should remain on the differential list of exotic cats (e.g., systemic hypertension; Fig. 35.12). Infectious causes of uveitis in exotic felids exist, but do not seem to be nearly as prevalent as in domestic cats. One example is toxoplasmosis,

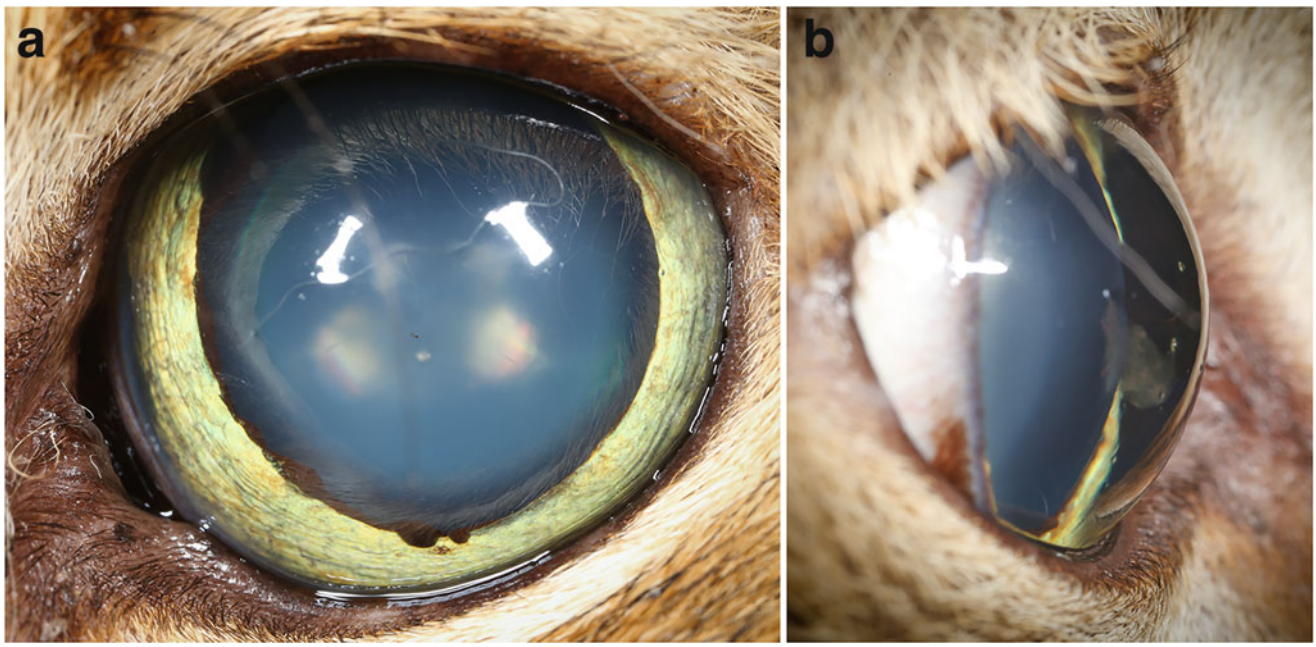

Fig. 35.12 A geriatric savannah cat (a cross between a serval and a domestic cat) with renal disease presented with cloudy eyes. Nuclear sclerosis was a large contributor to the presenting complaint (**a**), but a fibrinohemorrhagic clot was found in the anterior chamber associated with the anterior lens capsule along with moderate anterior uveitis (**b**). Uveal cysts are also visible at the ventral pupillary margin in (**a**). The retina demonstrated both intra- and pre-retinal hemorrhages but no detachment was detected. Courtesy of Dr. Bret A. Moore

which may be diagnosed in all vertebrates and might be spread by wild felids (Kaandorp 2012). While *Toxoplasma gondii* can be associated with uveitis in domestic cats, this may not be the case in wild cats. Cañón-Franco et al. (2013) detected *T. gondii* in ocular tissues (eyeball, extraocular muscles, and vitreous body) of various wild small felids from Brazil (Pampas cat *Leopardus colocolo*, Geoffroy's cat *Leopardus geoffroyi*, Ocelot *Leopardus pardalis*, Oncilla *Leopardus tigrinus,* Margay *Leopardus wiedii*, Jaguarondi *Puma yagouaroundi*) without any signs of ophthalmic disease. Similarly, Bartonella spp. have been detected in free-ranging African lions (*Panthera leo*) and cheetahs (*Acinonyx jubatus*) without ocular abnormalities (Cunningham and Yabsley 2012). However, other infectious diseases have been shown to cause ocular signs, as with feline infectious peritonitis (FIP). A case of bilateral panuveitis caused by FIP has been observed in an African lion (*Panthera leo*). Post-mortem examination revealed an irregular pupillary margin, uveal edema, and a white, gelatinous membrane that covered the retina (Fig. 35.13). Histology confirmed bilateral panuveitis with retinal detachment (Mwase et al. 2015).

A few different uveal neoplasms have been described in wild cats. A case of bilateral anterior uveitis has been observed in the caracal (*Caracal caracal*) for the first time as an unusual manifestation of a granular lymphoma. The animal had severe chemosis, conjunctival hyperemia, and moderate episcleral vascular injection, hypopyon, hyphema, iritis, anisocoria. Secondary glaucoma had developed in the right eye due to uveitis. By means of paracentesis of the aqueous humor, granular lymphoma was diagnosed, subsequently confirmed by a cytologic evaluation of a neoformation located at the level of the jejunum (Aitken-Palmer et al. 2011). Ocular melanoma has been reported in an African lion (*Panthera leo*). Clinical signs included conjunctival hyperemia, a moderate serous epiphora, and buphthalmos. The neoplasm, with a diameter of 1.5 cm, infiltrated the anterior uvea, occupying about 30% of the anterior chamber, with pulmonary and pleural metastases. In addition to the primary melanoma, mammary mucinous carcinoma was also noted in this animal (Cagnini et al. 2012).

Lens

Cataracts are the most common lenticular abnormality in exotic felids (Kern and Glaze 2000), and have been described in many species including the Siberian tiger (*Panthera tigris altaica*) (Seitz and Weisse 1979), the Bengal tiger (*Panthera tigris tigris*) (Lange et al. 2017; Kleiner et al. 2014), the jaguar (*Panthera onca*) (Zarza et al. 2015), the clouded leopard (*Neofelis nebulosa*) (Cooley 2001), the African lion (*Panthera leo*) (Sardari et al. 2007; Viñas et al. 2019), the snow leopard (*Panthera uncia*) (Scurrell et al. 2015) and the Angola lion (*Panthera leo bleyenberghi*) (Steinmetz et al. 2006).

Congenital cataracts may be found alone or in conjunctival of multiple ocular anomalies, as was diagnosed in a 5-month-old Siberian tiger (*Panthera tigris altaica*) that

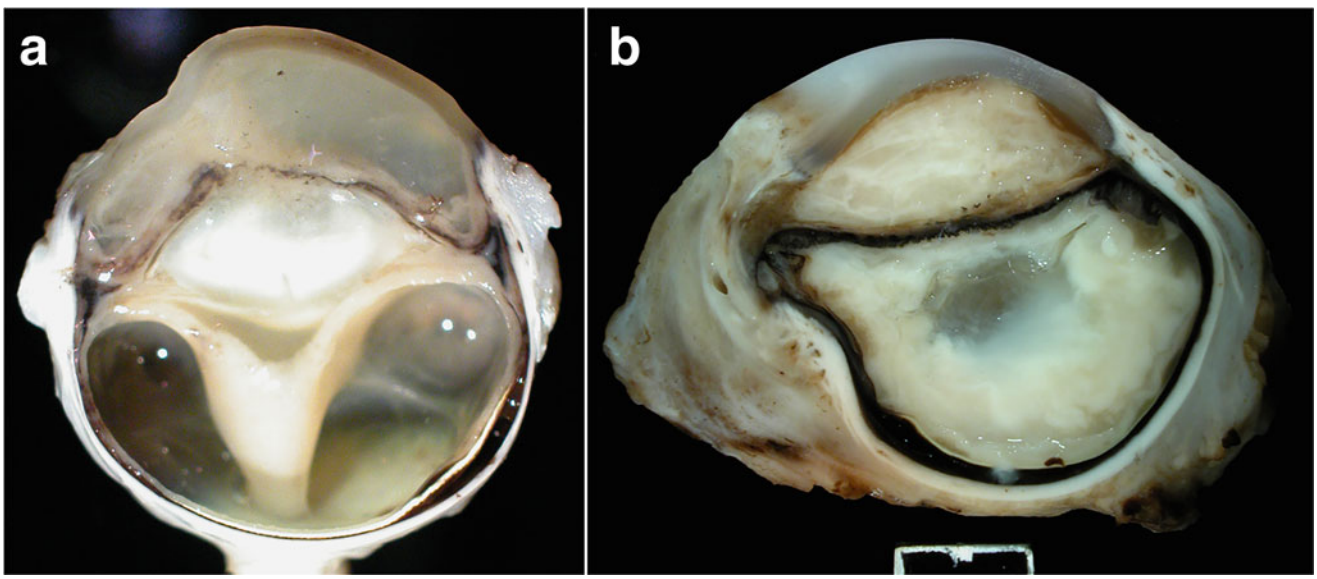

Fig. 35.13 Gross pathology of large felid eyes with infectious uveitis. (**a**) An ocelot (*Leopardis pardalis*) with feline infectious peritonitis (FIP), demonstrating severe anterior and posterior uveitis with carpeting of the retinal with inflammatory cells. (**b**) A cougar (*Puma concolor*) with endophthalmitis of unknown cause. Note that the entire vitreous cavity of filled with inflammatory cells. Courtesy of the Comparative Ocular Pathology Laboratory of Wisconsin

Fig. 35.14 (**a**) A representative cub from a litter fed with artificial milk that ended-up presenting bilateral cataracts and strabismus. (**b**) Another cub was also fed with artificial milk presenting severe alopecia. (**a**) Courtesy of Fabiano Monitiani-Ferreira. (**b**) Used with permission from: Lange RR, Lima L, Frühvald E, et al. Cataracts and strabismus associated with hand rearing using artificial milk formulas in Bengal tiger (*Panthera tigris* spp. tigris) cubs. *Open Veterinary Journal.* 2017;7: 23–31

was found blind. Examination revealed bilateral persistent pupillary membranes, anterior subcapsular cataracts, and nuclear cataracts. The animal underwent unilateral intracapsular extraction of the lens and, after the operation, it behaved with only mild visual deficit (Seitz and Weisse 1979). Familial cataracts thought to have a heritable basis have been described in Angolan lions (*Panthera leo bleyenberghi*). Feline microsatellites and SNPs were developed for evaluating primary cataract candidate genes in the lions, although no gene was found as causative (Philipp et al. 2010). Additionally, unilateral cataract of probable hereditary origin has been described in the clouded leopard (*Neofelis nebulosa*). The animal, only 3 months of age, underwent phacoemulsification and preventive transscleral diode laser retinopexy. Two months after the first operation, it developed an incipient anterior cortical cataract in the other eye, which progressed in the following 3 weeks, and the animal underwent another phacoemulsification surgery. Even if the hereditary origin is the most probable cause, a nutritional one cannot be excluded; indeed, it was observed that the persistence of nutritional deficiencies can also cause the formation of cataracts in more adult animals (Cooley 2001).

A study was carried out on the Bengal tiger (*Panthera tigris* tigris) to explain the nutritional factors that potentially contribute to ophthalmological and dermatological changes (Lange et al. 2017). Four tigers fed with artificial milk were examined and compared to two tigers fed naturally by their mother. Artificially fed tigers developed bilateral cataracts, strabismus, and alopecia (Fig. 35.14), while those fed naturally did not develop ophthalmologic or dermatological abnormalities. The concentration of taurine, arginine, phenylalanine, tryptophan, and histidine was very low in artificial milk compared to natural milk, which could explain cataract development. Taurine might have played an important role since it has already been described in other species, and since taurine is the most abundant intraocular amino acid. In this case, taurine deficiency is likely to expose the lens to an oxidative stress (Lange et al. 2017). Two of the tigers underwent cataract surgery using an ancillary phaco-fragmentation instrument with a nylon loop to fragment the lens nucleus with good outcomes. Additionally, two four-month-old cubs were operated in the same manner. In all cases, the lens nucleus detached from the lens cortex and moved anteriorly to the anterior chamber in the transoperative period. The authors opted to use an ancillary phaco-fragmentation instrument with a nylon loop that wraps around the nucleus and when pulled (like a snare) can fragment the lens nucleus (Fig. 35.15). The phaco-fragmentation instrument was developed by the authors and works similarly to the miLOOP (Carl Zeiss Meditec, Inc., Dublin, CA) (Fig. 35.16). Vision was restored postoperatively with no signs of taurine deficiency retinopathy were observed funduscopically, such as the focal lesion at the *area centralis* observed in the domestic cat (feline central retinal degeneration). Similarly, a two-and-a-half-year-old Bengal tiger (*Panthera tigris tigris*) underwent bilateral phacoemulsification and foldable acrylic lens implant (30 diopters) for presumably nutritional cataracts. The young tiger had been fed with bovine milk at an early stage of life, which has an amino acid and vitamin deficiency and an excess sugar for this species, which probably led to the cataract formation (Kleiner et al. 2014).

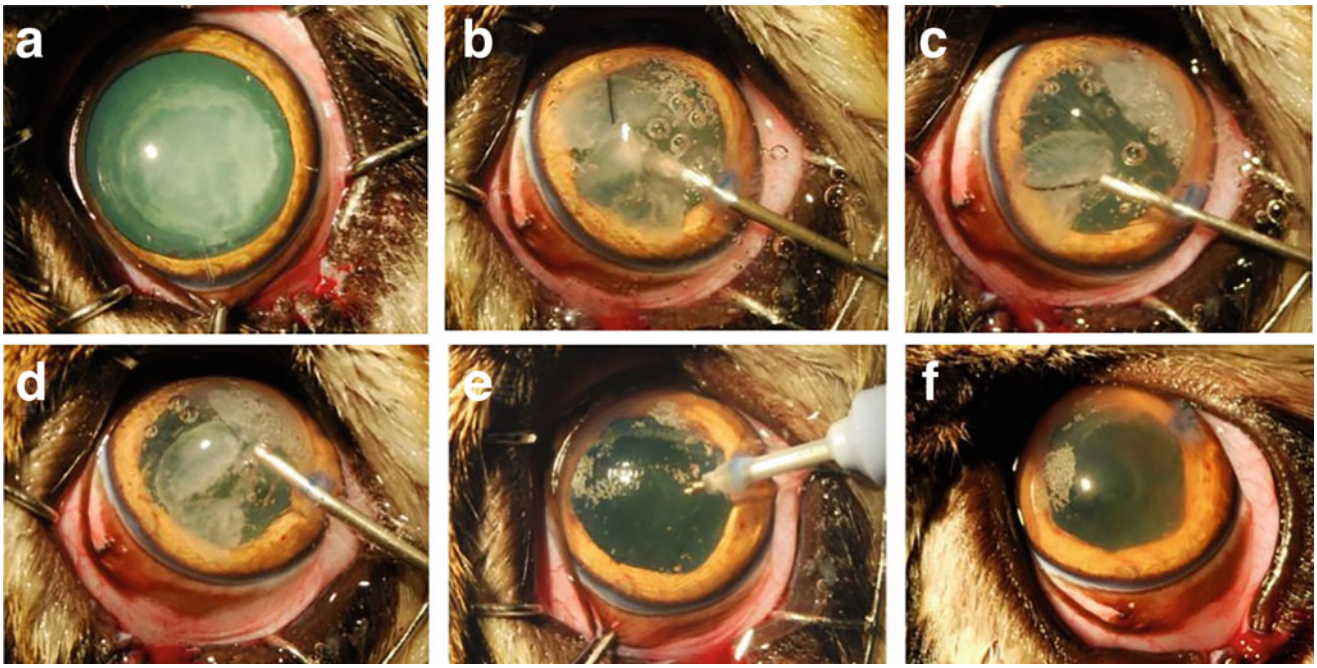

Fig. 35.15 Sequence of pictures of the phacoemulsification surgery performed in one of the previously mentioned artificially fed cubs (4-month-old male) (Fig. 35.14) that had developed bilateral cataracts, strabismus, and alopecia. (**a**) Preoperative aspect of the animal's eye. (**b**) Beginning phaco-fragmentation of the lens nucleus with a nylon loop (Fig. 35.16), after capsulorhexis and spontaneous anterior dislocation of the lens nucleus to the anterior chamber. (**c**) A large lens nucleus fragment wrapped by the nylon loop. (**d**) Lenticular fragment after phacofragmentation. (**e**) End of the phacoemulsification procedure with irrigation and aspiration of the remaining lens material in the capsular bag and anterior chamber. (**f**) Polyglactin 910 absorbable suture (9-0) was used for closure of the corneal incision. Used with permission from: Montiani-Ferreira F, Lima L. Oftalmología de animales exóticos y salvages. In: Oftalmología clínica en animales de compañia. Herrera D (ed). Intermédica, Buenos Aires, Argentina, 2015, 240–276

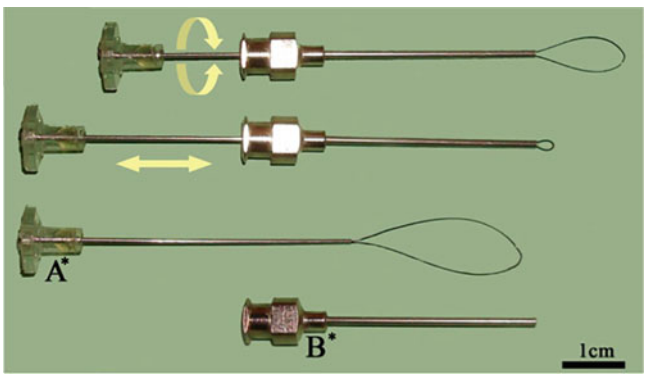

Fig. 35.16 Photograph of phaco-fragmentation instruments used in cataract surgery. (A^*) Movable controlling internal handpiece. (B^*) Stable external guide hand piece. The nylon loop is a component of the control piece. The instrument is used with both hands. The external guide piece (B^*) is held with one hand of the surgeon, while the internal piece (A^*) can be moved with the other hand until it wraps around the lens nucleus (or particular fragment). Subsequently, the internal piece is pulled so the diameter of the loop gets progressively smaller until it crushes the lens fragment. Used with permission from: Lima, L. Contribuições para oftalmologia clínica, cirúrgica e investigativa de animais domésticos, selvagens e de mascotes não convencionais. M. S., Thesis. Universidade Federal do Paraná, Curitiba-PR, Brazil. 2011

A 2.5-year-old tigress (*Panthera tigris tigris*) affected by a bilateral immature cataract was treated with bilateral phacoemulsification and implantation of an artificial lens (Fig. 35.17). The 21 mm artificial lenses, with a dioptric power of 30D, were created specifically for the animal using the Binkhorst equation following measurements with an B-mode ultrasound to determine the antero-posterior axial length and lens thickness.

Other cases of reported cataracts in exotic felids have had various causes and presentations. A unilateral cataract was diagnosed in a wild, male jaguar (*Panthera onca*) with leishmaniasis, aged between 10 and 12 years. In addition to an altered lens, it also showed skin ulcers caused by the leishmania itself (Zarza et al. 2015). A case of cataract associated with an anterior lens dislocation solved with an intracapsular lens extraction has been described in the African lion (*Panthera leo*) (Sardari et al. 2007). One study on a group of Angola lions (*Panthera leo bleyenberghi*) revealed that cataracts were the most commonly observed ocular abnormality (Steinmetz et al. 2006). Bilateral crystalline lens dislocation has been identified in an adult male African lion (*Panthera leo*), causing glaucoma and corneal striae. The

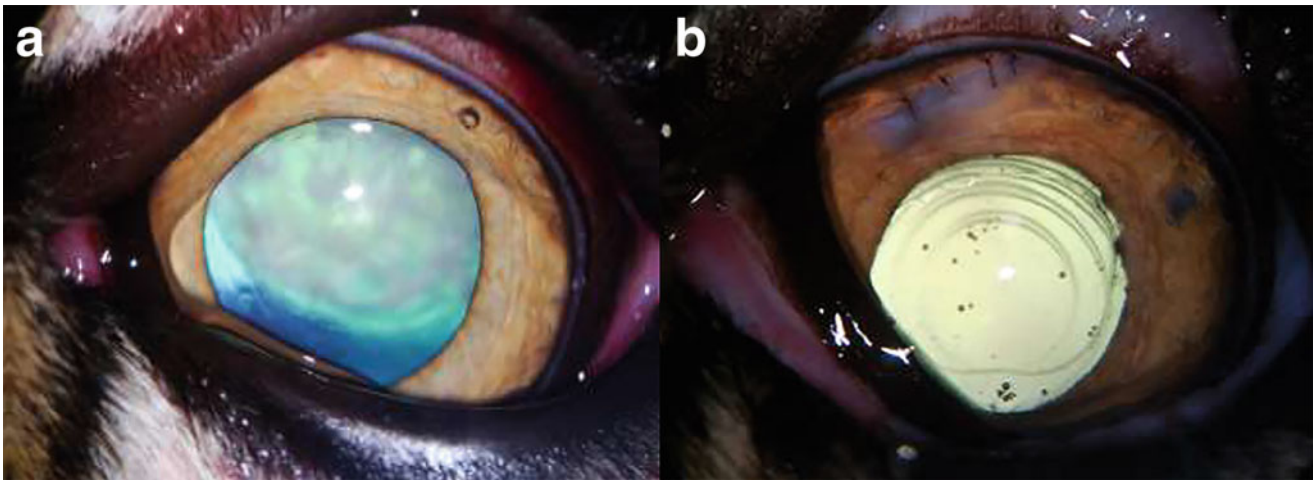

Fig. 35.17 (**a**) The left eye of a 2.5-year-old tigress (*Panthera tigris tigris*) is affected by an immature cataract. (**b**) The same eye after surgery demonstrated a biconvex foldable hydrophilic acrylate intraocular lens (30 diopters) that was implanted. Used with permission from Kleiner, J.A., Watanabe, E.K. and Bettini, C. (2014). Facoemulsificação bilateral seguida de implante de lentes acrílicas dobráveis em uma Tigresa-de-Bengala (*Panthera tigris tigris*)—relato de caso. *Clinica Veterinaria*, 19(109): 68–78, used with permission

posteriorly dislocated lenses were surgically removed to try and preserve the residual vision (Bush and Koch 1976). *Encephalitozoon cuniculi* was found to be the cause of bilateral hypermature cataracts associated with capsular rupture and marked phacoclastic uveitis in a snow leopard (*Panthera uncia*). In the anterior and posterior lens cortex A large number of *E.cuniculi* spores were detected, both extracellularly and within macrophages, in the anterior and posterior lens cortex. A definitive diagnosis was confirmed by Immunohistochemistry and PCR on both globes (Scurrell et al. 2015).

Vitreous, Chorioretina, and Optic Nerve

Other than direct and indirect funduscopy, electroretinography (ERG) can be utilized for the evaluation of retinal function. In the author's experience, the ERG amplitudes of felids (domestic or wild) are significantly higher compared to canines (Fig. 35.18). The normal scotopic ERG waveforms have differences between felid species, and thus normal parameters should be established to enable accurate interpretation of results. Reference values for scotopic ERG measurements were reported in a fishing cat (*Prionailurus viverrinus*) and leopard cat (*Prionailurus bengalensis*) (Sussadee et al. 2017).

Optic nerve hypoplasia (ONHp) or atrophy has also been described in a blind 1-year-old cheetah (*Acinonyx jubatus*) (Walser-Reinhardt et al. 2010). It is a non-progressive condition that causes visual deficit and pupillary light reflex (PLR) abnormalities. The tapetal area around the optic nerve head contained multiple hyperpigmented linear lesions and the optic nerve head appeared dark grey and about half of its normal size (Walser-Reinhardt et al. 2010). Additionally, coloboma of the optic nerve head was reported in Bengal tiger kittens (*Panthera tigris tigris*) (Dietz et al. 1985).

Central retinal degeneration and cataracts are the most common lesions found in non-domestic cats (Kern and Glaze 2000) (Fig. 35.19), Three cheetahs (*Acynonyx jubatus*) from the Jerusalem Zoo, with no genetic link among them, presented a progressive loss of vision, until they reached complete blindness. In one of the three animals, an ellipsoid and hyperreflective lesion was found in the dorsolateral region of the optic disc in both eyes, corresponding to a grade 2 Feline Central Retinal Degeneration (FCRD). In one of the other two animals, there was a large area with a hyperreflective band that extended through the retina, dorsally to the optic disc, consistent with FCRD grade 4. In the cheetah, this pathology may be associated with a taurine deficiency, may have a hereditary cause or may be acquired.

In a mountain lion (*Puma concolor*) cub, photoreceptor degeneration has been described. The cub, which was completely blind, showed widespread tapetal hyperreflectivity in both eyes a marked decrease in retinal vasculature and the presence of slightly pigmented areas in the non-tapetal fundus. A genetic or nutritional etiology was suspected, with the former etiology more strongly supported, based on the cub's signalment, history, and histopathology (DiSalvo et al. 2016). In an African black-footed cat (*Felis Nigripes*), a progressive retinal atrophy was found at 3 months of age. According to this study, cats homozygous for a 2-base pair deletion within IQCB1, the gene that encodes NPHP5, showed loss of vision. The variant segregated concordantly in other related individuals in the pedigree supporting the identification of a recessively inherited early feline PRA (Oh et al. 2017).

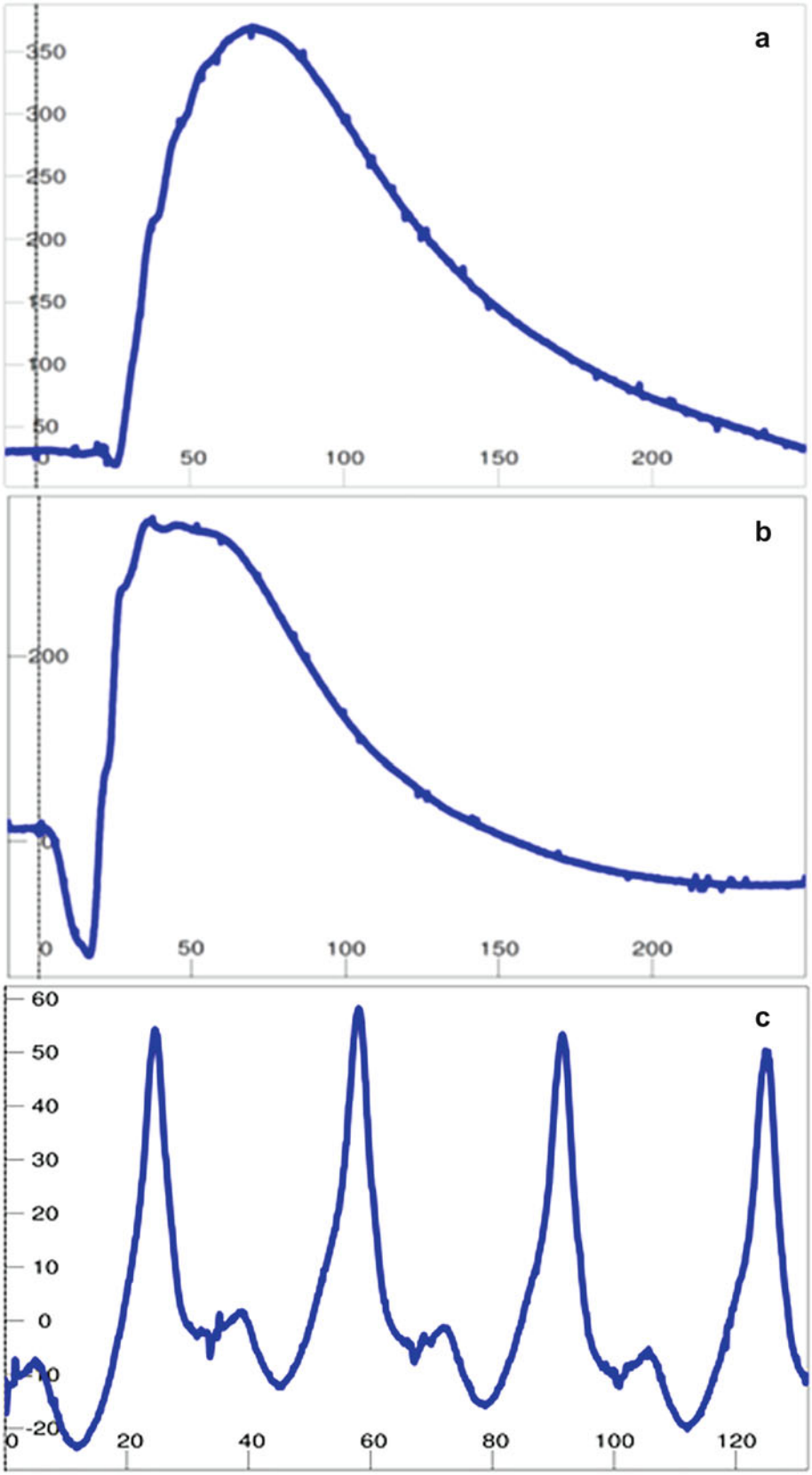

Fig. 35.18 Electroretinography (ERG) was performed on a Bengal tiger (*Panthera tigris tigris*) with a Handheld Multi-species Electroretinography, HMsERG, (Ocuscience, Henderson, NV). The ERG tracings were recorded after the zookeeper suspected that the tiger had scotopic visual impairment. The ERG recording demonstrated normal retinal function under scotopic (dark-adapted for 20 min) and photopic (light-adapted for 10 min at 30 cd/m^2) conditions, ruling out retinal disease. (**a**) Pure rod response using a dim stimulus (average of 10 flashes, 0.5 Hz, −2 log cds/m^2); (**b**) Combined rod-cone response (average of 32 flashes, 2 Hz, 1 log cds/m^2); (**c**) Flicker response (128 flashes, 31 Hz, 1 log cds/m^2). Note the high amplitudes of the flash ERG recordings, which is about double than canine ERG amplitude in this author's experience. Courtesy of Dr. Gil Ben-Shlomo

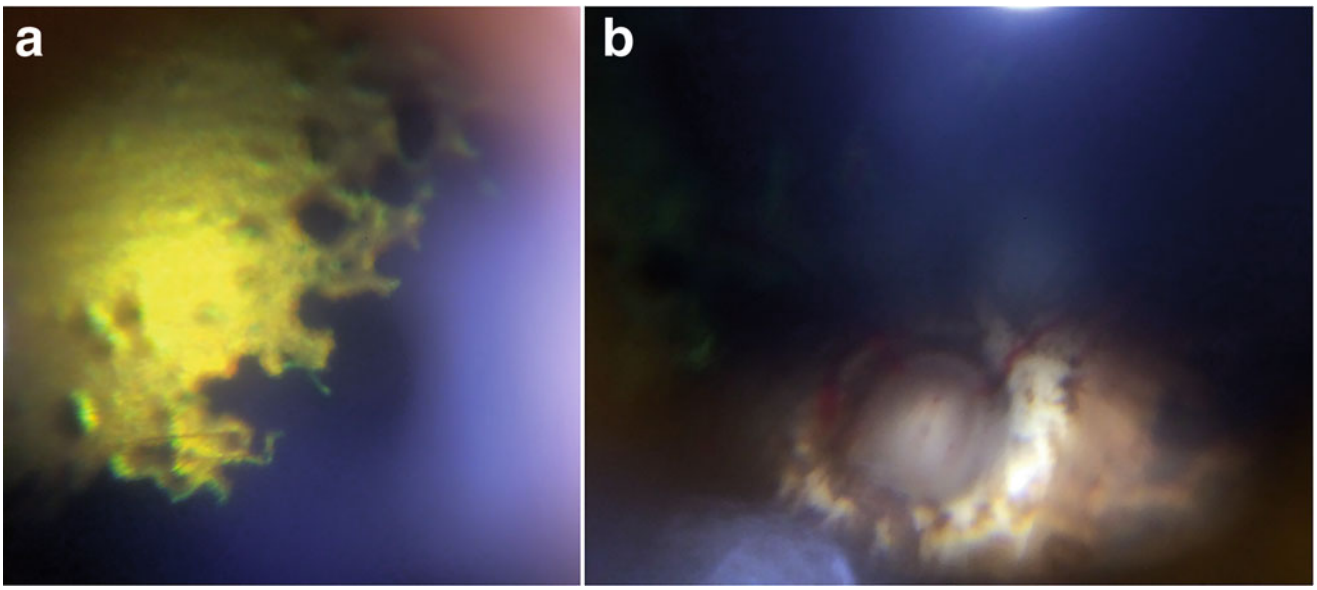

Fig. 35.19 A jaguar (*Panthera onca*) with retinal degeneration, showing (**a**) marked tapetal hyperreflectivity and absence of retina vessels, and (**b**) a pale and small optic disc. Courtesy of Dr. Ana Carolina Rodarte de Almeida

Several cases of chorioretinitis in wild felids have been anecdotally reported, usually occurring as an ocular manifestation of systemic disease. To properly treat it and prevent further eye damage and vision loss, the underlying cause must be identified, with special emphasis on infectious agents. Indeed, several infectious organisms, including viral (such as FIP, coronavirus, feline leukemia virus, and feline immunodeficiency virus) and fungal (like histoplasmosis and blastomycosis) can induce retinal damage (Ofri et al. 1996). The cheetah has been reported to be highly sensitive to FIP (Ofri et al. 1996; Walser-Reinhardt et al. 2010). A chorioretinal scar was detected in a tiger (*Panthera tigris tigris*) that tested positive for *Toxoplasma gondii* (Buddhirongawatr et al. 2016). The authors examined a 13-year-old jaguar (*Panthera onca*) that tested positive for *Toxoplasma gondii* and *Hemoplasma* spp. that had an extensive chorioretinal scar involving the optic nerve and its ventrolateral aspect of the left eye (Fig. 35.20) causing blindness.

Mycobacterium bovis has been described as a cause of tuberculosis in domestic and wild animals, but ocular tuberculosis is rare in animals. It was diagnosed in an adult male wild cat with a history of blindness. Fluorangiography showed signs of chronic posterior uveitis, extensive non-perfused chorioretinal areas, neovascularization of the optic disc, vasculitis, and hemorrhage. The presence of choroidal nodules suggests a hematogenous infection, whereas vasculitis and choroiditis are often the results of immune hypersensitivity (Martın-Suarez et al. 2012).

Neuroophthalmic Conditions

Strabismus is commonly observed in captive exotic felids (Fig. 35.21). In fact, a popular movie in the 1960s titled "Clarence" featured the cross-eyed lion that later became the basis for a popular television series called Daktari. Strabismus may lead to abnormal vision (amblyopia) in the deviating or strabismic eye, due to the difference between the images projecting to the brain from the two eyes. Possible causes of strabismus were an adaptation to genetically determined abnormal visual pathways related to lack of pigment, abnormalities of the abducens nerves, and mechanical restricting conditions of the medial rectus muscles (Bernays and Smith 1999). Mammals with hypopigmentation of the retinal pigment epithelium have an altered visual system. Albino mammals have reduced numbers of uncrossed optic fibers projecting to all visual centers, disorganization of the pattern (lamination) in the dorsal lateral geniculate nucleus, and disorganization of projections from the dorsal lateral geniculate nucleus to the visual cortex. Therefore, individuals with oculocutaneous albinism show hypopigmentation, decreased visual acuity, and nystagmus (Creel et al. 1990). White Bengal tigers (*Panthera tigris tigris*) have been observed to have convergent strabismus and reduced vision (Guillery and Kaas 1973; Bernays and Smith 1999; Pachaly and Montiani-Ferreira 2003) (Fig. 35.21c). White tigers have the gray-brown to black stripes seen in normal tigers, but the normal yellow striping is replaced by an off-white to cream

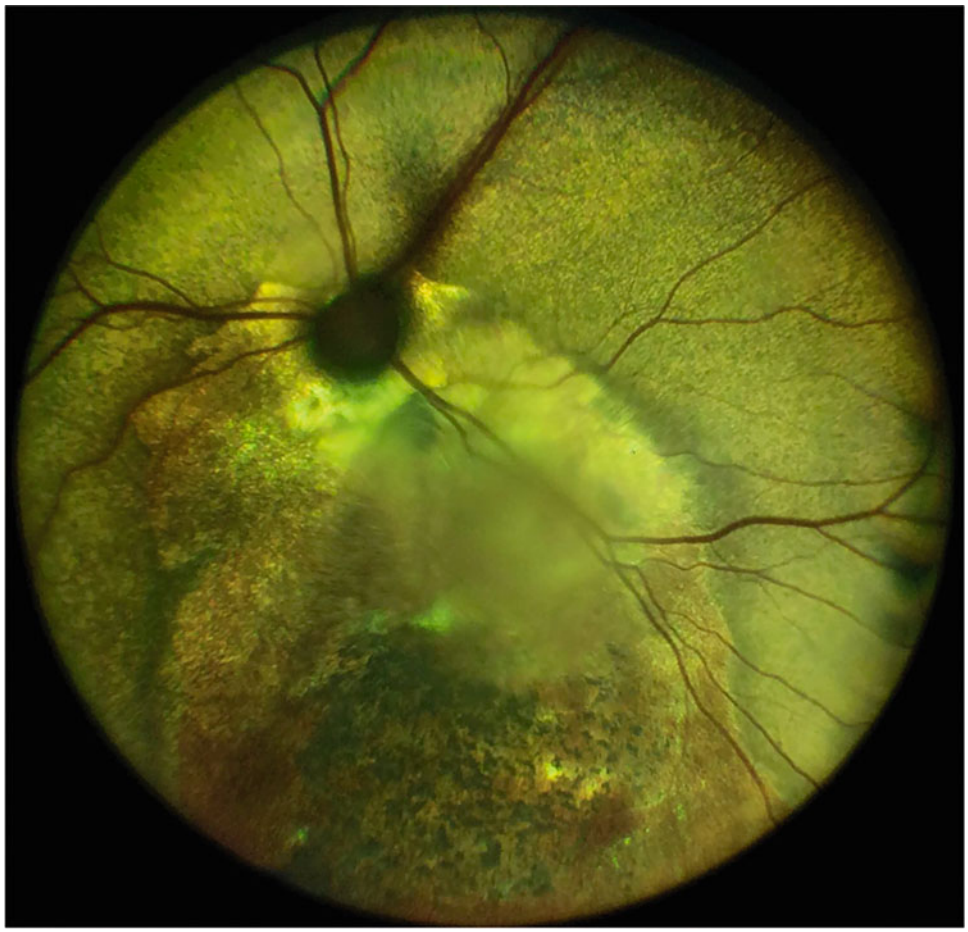

Fig. 35.20 Fundus photograph was taken with a Volk InView (Volk Optical Inc., Mentor, OH, USA) of a 13-year-old jaguar (*Panthera onca*) that tested positive for *Toxoplasma gondii* and *Hemoplasma* spp. An extensive chorioretinal hyperreflective scar is present involving the optic nerve and the entire ventrolateral aspect of this left eye. Note the moderate focal retinal detachment and edema below the optic disc. Courtesy of Dr. Ana Carolina Rodarte de Almeida

color. A fundus typical of color-dilute cats was observed in all these patients. No other significant abnormalities were found on ocular examination. Guillery and Kaas (1973) demonstrated some evidence that white tigers possess the same visual pathway abnormalities seen in Siamese cats.

Central disease can also cause visual deficits and other neuroophthalmic abnormalities. Large felid leucoencephalomyelopathy can cause visual deficits, and has been described in a number of species including a Sumatran tiger (*Pathera tigris sumatrae*) with vision loss, cataracts, and ataxia

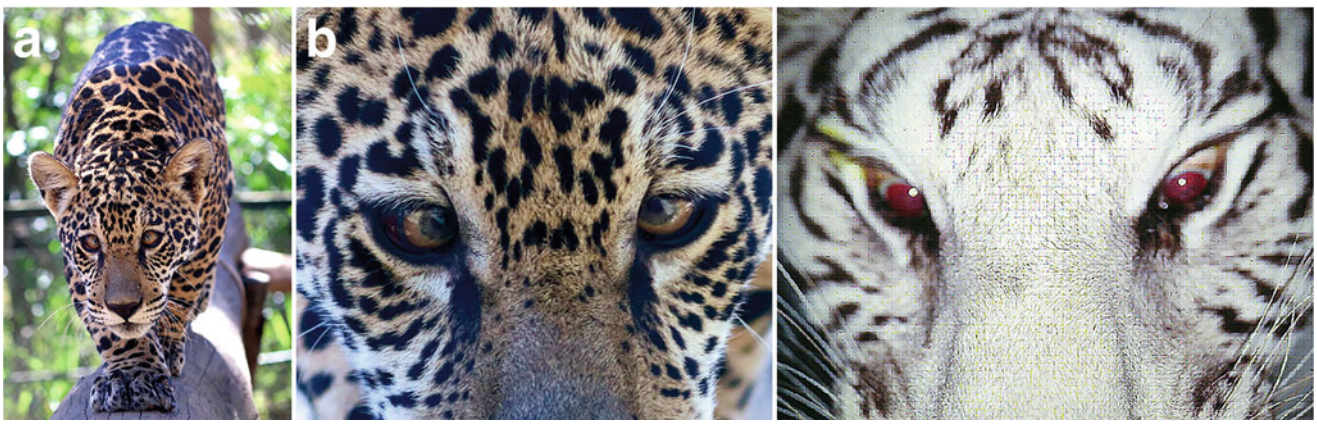

Fig. 35.21 (**a**, **b**) A captive jaguar (*Panthera onca*) with strabismus of undefined etiology. (**c**) A white Bengal tiger (*Panthera tigris*) with convergent strabismus and a red fundic reflex indicating absence of a *tapetum lucidum* and poorly pigmented RPE in the non-tapetal area. (**a**) Courtesy of Raul Coimbra and Cristina Gianni—Nex—No Extinction, Brazil

(Junginger et al. 2015; Hanshaw et al. 2019), another tiger of unknown subspecies (*Panthera tigris*) (de Lahunta and Glass 2009), and cheetahs (*Acinonyx jubatas*) and other large felids (Brower et al. 2014). Additionally, feline ischemic encephalopathy was described as causing acute right mydriasis and left hemiparesis in an African lion (*Pathera leo*) that was euthanized (Raymond et al. 1998).

Orbit

A case of malignant papillary adenocarcinoma with pulmonary metastases has been described in the jaguar (*Panthera onca*). The neoformation, about 10 cm in diameter, occupied the orbital fossa causing a corneal opacity and the total blindness of the animal. This tumor was histologically composed of spherical to low cuboidal and columnar cells occurring in solid mass, as well as in papilliform proliferation (Muraleedharan et al. 2010).

In a Bengal tiger (*Panthera tigris tigris*), which had been blind for about a year, a meningioma was diagnosed. In histological terms, it appeared as a neoformation attached to the left frontal bone and associated with the left frontal lobe. In domestic cats, meningioma is the most frequently described intracranial tumor, comprising 58% of cases. Clinical signs caused by an intracranial tumor include convulsions, circling seizures, altered level of consciousness, and blindness. In histological terms, the retinas were diffusely thin and hypocellular, with a loss of ganglion cells. The optic tracts were 3 mm wide. Every alteration was consistent with severe chronic retinal atrophy; hence, meningioma was probably not the cause of blindness (Akin et al. 2013).

References

Ahnelt PK, Schubert C, Kubber-Heiss A et al (2006) Independent variation of retinal S and M cone photoreceptor topographies: a survey of four families of mammals. Vis Neurosci 23:429–435

Aitken-Palmer C, Isaza R, Dunbar M et al (2011) Anterior uveitis as an atypical presentation of large granular lymphoma in a caracal (Caracal caracal). Vet Ophthalmol 14:337–340

Akin EY, Baumgartner WA, Lee JK, Beasley MJ (2013) Meningioma in a Bengal tiger (Panthera tigris tigris). J Zoo Wildl Med 44(3): 761–764

Appel MJ, Yates RA, Foley GL et al (1994) Canine distemper epizootic in lions, tigers, and leopards in North America. J Vet Diagn Investig 6:277–288

Barnett KC, Lewis JC (2002) Multiple ocular colobomas in the snow leopard (*Uncia uncia*). Vet Ophthalmol 5:197–199

Bernays ME, Smith RI (1999) Convergent strabismus in a white Bengal tiger. Aust Vet J 77:152–155

Blake R (1979) The visual system of the cat. Percept Psychophys 26(6): 423–448

Blake R, Cool SJ, Crawford MLJ (1974) Visual resolution in the cat. Vis Res 14:1211–1217

Bose VSC, Nath I, Mohanty J, Panda SK, Rao AT (2002) Epidermoid carcinoma of the eyelid in a tiger (Panthera tigris). Zoos' Print J 17(12):965–966

Boucher CJ, Venter IJ, Janse van Rensburg D, Sweers L (2016) Eyelid agenesis and multiple ocular defects in a captive cheetah cub (*Acinonyx jubatus*). Vet Record Case Rep 4:e000301

Brower AI, Munson L, Radcliffe RW et al (2014) Leucoencephalomyelopathy of mature captive Cheetahs and other large felids: a novel neurodegenerative dis- ease that came and went? Vet Pathol 51:1013–1021

Buddhirongawatr R, Kongcharoen A, Tungsaudjai S et al (2015) Persistent pupillary membranes in a Bengal tiger. Annual meeting of the European College of Veterinary Ophtalmologists, Veterinary Ophtalmology, Poster 12, E9

Buddhirongawatr R, Kongcharoen A, Tangsudjai S et al (2016) Ophtalmic findings in 29 tigers (Panthera tigris tigris) in a private zoo in Thailand. Annual Meeting of the European College of Veterinary Ophthalmologists, Veterinary Ophthalmology, ORAL14, 19, E10

Bush M, Koch SA (1976) Surgical correction of bilateral lens luxation in an African lion. J Am Vet Med Assoc 169:987–988

Cagnini DQ, Salgado BS, Linardi JL et al (2012) Ocular melanoma and mammary mucinous carcinoma in an African lion. BMC Vet Res 8: 176–181

Caligiuri R, Carrier M, Jacobson ER et al (1988) Corneal squamous cell carcinoma in a cheetah (Acinonyx jubatus). J Zoo Anim Med 19: 219–222

Cañón-Franco WA, Araújo FA, López-Orozco N et al (2013) Toxoplasma gondii in free-ranging wild small felids from Brazil: molecular detection and genotypic characterization. Vet Parasitol 197(3–4): 462–469

Cooley PL (2001) Phacoemulsification in a clouded leopard (Neofelis nebulosa). Vet Ophthalmol 4:113–117

Creel DJ, Summers CG, King RA (1990) Visual anomalies associated with albinism. Ophthalmic Paediatr Genet 11(3):193–200

Cunningham M, Yabsley MJ (2012) Primer on tick-borne diseases in exotic carnivores. In: Miller RE, Fowler ME (eds) Fowler's zoo and wild animal medicine current therapy, vol 7. Saunders, St. Louis, pp 458–464

Cutler TJ (2002) Bilateral eyelid agenesis repair in a captive Texas cougar. Vet Ophthalmol 5:143–148

De La Rosa CL, Nocke CC (2000) The wild cats. In: A guide to the carnivores of Central America. University of Texas Press, Austin, pp 19–73. 262 pp

de Lahunta A, Glass E (2009) Veterinary neuroanatomy and clinical neurology, 3rd edn. Saunders Elsevier, St Louis, p 426

Deem SL, Spelman LH, Yates RA, Montali RJ (2000) Canine distemper in terrestrial carnivores: a review. J Zoo Wildl Med 31(4):441–451

Dietz HH, Ericksen E, Jensen OA (1985) Coloboma of the optic nerve head in Bengal tiger kittens (Panthera tigris tigris). Acta Vet Scand 26:136–139

DiSalvo AR, Reilly CM, Wiggans KT, Woods LW, Wack RF, Clifford DL (2016) Photoreceptor degeneration in a mountain lion cub (*Puma concolor*). J Zoo Wildl Med 47(4):1077–1080

Dziezyc J, Millichamp NJ (1989) Surgical correction of eyelid agenesis in a cat. J Am Anim Hosp Assoc 25:513–516

Edelmann ML, Utter ML, Klein LV, Wotman KL (2013) Combined excision and intralesional bevacizumab for sebaceous carcinoma of the eyelid in an Amur tiger (panthera tigris altaica). Vet Ophthalmol 16(3):219–224

El-Dakhly K, El-Hadid SA, Shimizu H, El-Nahass ES, Murai A, Sakai H, Yanai T (2012) Occurrence of *Thelazia callipaeda* and *Toxocara cati* in an imported EUROPEAN lynx (*Lynx lynx*) in Japan. J Zoo Wildl Med 43(3):632–635

Esson D (2001) A modification of the Mustardé technique for the surgical repair of a large feline eyelid coloboma. Vet Ophthalmol 4:159–160

Ewer RF (1998) The special senses. In: The carnivores. Cornell University Press, New York, pp 120–138. 500pp

Gerding PA, Brightman AH, McLaughlin SA, Helper LC, Whiteley HE, Render LA (1987) Glaucoma associated with a high number of mast cells in the uveal tract of an African lion cub. J Am Vet Med Assoc 191:1013–1014

Gripenberg U, Blomqvist L, Pamilo P, Soderlund V, Tarkkanen A, Wahlberg C, Varvio-Aho SL, Ranta-Knowles KV (1985) Multiple ocular coloboma (MOC) in snow leopards (*Panthera uncia*). *Hereditas* 103:221–229

Guillery RW, Kaas JH (1973) Genetic abnormality of the visual pathways in a "white" tiger. *Science* 180(92):1287–1289

Gupta A, Jadav K, Nigam P, Swarup D, Shrivastava AB (2013) Eyelid neoplasm in a white tiger (*Panthera tigris*)—a case report. Veterinarski Arhiv 83(1):115–124

Hamoudi H, Rudnick J-C, Prause JU et al (2013) Anterior segment dysgenesis (Peters' anomaly) in two snow leopard (Panthera uncial) cubs. Vet Ophthalmol 16(Supplement 1):130–134

Hanshaw DM, McLelland DJ, Finnie JW (2019) Large felid leucoencephalomyelopathy in a Sumatran tiger (Panthera tigris sumatrae) from an Australian zoo. Aust Vet J 97:277–282

Holzer MP, Solomon KD (2003) Bobcat bite injury of the eye and ocular adnexa. Arch Ophthalmol 121:918–919

Hughes A (1977) The topography of vision in mammals of contrasting life style: comparative optics and retinal organization. In: Crescitelli F (ed) The visual system of vertebrates, vol VII, 5th edn. Springer, Heidelberg, pp 613–756

Hunt GB (2006) Use of lip-to-lid flap for replacement of the lower eyelid in five cats. Vet Surg 35:284–286

Iaquinandi A, Lois F, Falzone M, Sande P (2017) Sebaceous carcinoma in a Bengal tiger (*Panthera tigris tigris*) in captivity. 48th Annual Meeting of the American College of Veterinary Ophthalmologists, Veterinary ophthalmology, abstracts E14

IUCN (2016) International Union for Conservation of Nature. Classification of cat species in the 2016 IUCN red list of threatened SpeciesTM. http://www.catsg.org/index.php?id=74. Assessed 22 Oct 2019

Junge RE, Miller RE, Boever WJ et al (1991) Persistent cutaneous ulcers associated with feline herpesvirus type 1 infection in a cheetah. J Am Vet Med Assoc 198:1057–1058

Junginger J, Hansmann F, Herder V et al (2015) Pathology in captive wild felids at German zoological gardens. PLoS One 10:e0130573

Kaandorp J (2012) Veterinary challenges of mixed species exhibits. In: Fowler ME, Miller RE (eds) Zoo and wild animal medicine: current therapy, vol 7, pp 24–31

Kern TJ, Glaze MB (2000) Ocular disorderds of captive non-domestic felids. 31st Annual Meeting of the American College of Veterinary Ophthalmologists, *Veterinary Ophthalmology*, Abstract No. 027, 3, pp 247–257

Kik MJL, Van der Hage MH, Putten SWM (1997) Chlamydiosis in a Fishing Cat (Felis viverrina). J Zoo Wildl Med 28(2):212–214

Kitchener AC, Breitenmoser-Würsten CH, Eizirik E et al (2017) A revised taxonomy of the Felidae. The final report of the Cat Classification Task Force of the IUCN/SSC Cat Specialist Group. Cat News Special Issue 11, 80 pp

Kleiner JA, Watanabe EK, Bettini C (2014) Facoemulsificação bilateral seguida de implante de lentes acrílicas dobráveis em uma Tigresa-de-Bengala (*Panthera tigris tigris*) - relato de caso. Clin Vet 19(109):68–78

Knollinger AM, McDonald JE, Carpenter NA et al (2018) Use of equine amniotic membrane free-island grafts for treatment of a midstromal corneal ulcer and descemetocele in a snow leopard *(Panthera uncia)*. *J Am Vet Med Assoc* 253:1623–1629

Lange RR, Lima L, Frühvald E et al (2017) Cataracts and strabismus associated with hand rearing using artificial milk formulas in Bengal tiger (*Panthera tigris* spp tigris) cubs. Open Vet J 7:23–31

Macdonald D (1992) Sharpening the tooth. In: The Velvet claw – a natural history of the carnivores. Butler & Tanner Ltd, London, pp 43–77. 256pp

Maffei L, Fiorentini A, Bisti S (1990) The visual acuity of the lynx. Vis Res 30:527–528

Malmstrom T, Kroger RHH (2006) Pupil shapes and lens optics in the eyes of terrestrial vertebrates. J Exp Biol 209:18–25

Marti I, Pisano SRR, Wehrle M et al (2019) Severe conjunctivitis associated with *Chlamydia felis* infection in a free-ranging Eurasian Lynx (*Lynx lynx*). J Wildl Dis 55:522–525

Martin CL, Stiles J, Willis M (1997) Feline Colobomatous Syndrome. Vet Comp Ophthalmol 7:39–43

Martɲn-Suarez EM, Guisado A, Galan A et al (2012) Ocular manifestations of tuberculosis in a wildlife feline. European Society of Veterinary Ophthalmologists, Veterinary Ophthalmology, Abstract No. 12, 16(1):E23

Mihalca AD, Ionică AM, D'Amico G, Daskalaki AA, Deak G, Matei IA, Simonca V, Iordache D, Modry D, Gherman CM (2016) *Thelazia callipaeda* in wild carnivores from Romania: new host and geographical records. Parasit Vectors 9:350

Miller PE (2018) The eye and vision. In: Maggs DJ, Miller PE, Ofri R (eds) Slatter's fundamentals of veterinary ophthalmogy. Elsevier, St. Louis, p 9

Millichamp NJ (1997) Management of ocular disease in exotic species. Semin Avian Exotic Pet Med 6(3):152–159

Montiani-Ferreira F, Lima L (2015) Oftalmología de animales exóticos y salvages. In: Herrera D (ed) Oftalmología clínica en animales de compañia. Intermédica, Buenos Aires, pp 240–276

Mourya DT, Yadav PD, Mohandas S et al (2019) Canine distemper virus in Asiatic Lions of Gujarat State, India. Emerg Infect Dis 25(11):2128–2130

Munger RJ, Gourley IM (1981) Cross lid flap for repair of large upper eyelid defects. J Am Vet Med Assoc 178:45–48

Muraleedharan K, SESHADRI SJ, GOWDA RNS, APPAJI P (2010) Cancer of eye in a jaguar (Panthera onca). Zoos' Print (webversion) 25:33

Mwase M, Shimada K, Mumba C, Yabe J, Squarre D, Madarame H (2015) Positive Immunolabelling for feline infectious peritonitis in an African Lion (*Panthera leo*) with bilateral Panuveitis. J Comp Pathol 152:265–268

Newkirk KM, Beard LK, Sun X et al (2017) Investigation of Enrofloxacin-associated retinal toxicity in nondomestic felids. J Zoo Wildl Med 48(2):518–520

Ofri R, Barishak RY, Eshkar G, Aizenberg T (1996) Feline central retinal degeneration in captive cheetahs (Acinonyx jubatus). J Zoo Wildl Med 27:101–108

Ofri R, Shore LS, Kass PH et al (1999) The effect of elevated progesterone levels on intraocular pressure in lions (Panthera leo). Res Vet Sci 67:121–123

Ofri R, Steinmetz A, Thielebein J et al (2008) Factors affecting intraocular pressure in lions. Vet J 177:124–129

Oh A, Pearce JW, Gandolfi B et al (2017) Early-onset progressive retinal atrophy associated with an IQCB1 variant in African black-footed cats (*Felis nigripes*). Sci Rep 7:43918

Pachaly JR, Montiani-Ferreira F (2003) Convergent strabismus in a white Bengal tiger (*Panthera tigris*) - case report. In: JOVET, UMUARAMA Arquivos de Ciências Veterinárias e Zoologia da UNIPAR, vol 6, pp 176–187

Philipp U, Steinmetz A, Distl O (2010) Development of feline microsatellites and SNPs for evaluating primary cataract candidate genes as a cause for cataract in Angolan lions (*Panthera leo bleyenberghi*). J Hered 101:633–638

Prando FAS, Pereira JS, Pereira NG et al (2017) Bilateral ocular B-cell lymphoma in a jaguar (Panthera onca, Linnaeus, 1758)-a case report. Annual Meeting of the European College of Veterinary Ophthalmologists, *Veterinary Ophthalmology, 2017,* E6 ABSTRACTS, Poster 15

Ptito M, Lepore F, Guillemot JP (1991) Steropsis in the cat: behavioral demonstration and underlying mechanism. Neuropsychologia 29: 443–464

Raymond JT, Butler TC, Janovitz EB (1998) Unilateral cerebral necrosis resembling feline ischemic encephalopathy in an African lion (Panthera leo). J Zoo Wildl Med 29:328–330

Ringo JL, Wolbarsht ML (1986) Spectral coding in cat retinal ganglion cell receptive fields. J Neurophysiol 55:320–330

Roberts SR, Bistner SI (1968) Surgical correction of eyelid agenesis: an improved surgical technique designed to enable lid closure. Mod Vet Pract 49:40–43

Robinson PT, Benirschke K (1981) Removal of a conjunctival dermoid in an African Lion (Panthera Leo). J Zoo Anim Med 12(3):85–88

Rowe MH, Stone J (1976) Properties of ganglion cells in the visual streak of the cat's retina. J Comp Neurol 169:99–125

Ruthner Batista HB, Kindlein Vicentini F, Franco AC et al (2005) Neutralizing antibodies against feline herpesvirus type 1 in captive wild felids of Brazil. J Zoo Wildl Med 36(3):447–450

Sadler RA, Ramsay E, McAloose D, Rush R, Wilkes RP (2016) Evaluation of two canine distemper virus vaccines in captive tigers (Panthera Tigris). J Zoo Wildl Med 47:558–563

Sardari K, Emami MR, Tabatabaee AA, Ashkiani A (2007) Cataract surgery in an African lion (Panthera leo) with anterior lens luxation. Comp Clin Pathol 16:65–67

Schäffer E, Wiesner H, von Hegel G (1988) Multiple okulare Kolobome (MOC) mit persistierender Pupillarmembran beim Schneeleopard (Panthera uncia) [Multiple ocular coloboma (MOC) with persistent pupillary membrane in the snow leopard (Panthera uncia)]. Tierarztl Prax 16(1):87–91

Scurrell EJ, Holding E, Hopper J, Denk D, Fuchs-Baumgartinger A, Silbermayr K, Nell B (2015) Bilateral lenticular Encephalitozoon cuniculi infection in a snow leopard (*Panthera uncia*). *Vet Ophthalmol* 18:143–147

Seitz R, Weisse I (1979) Operation on a congenital cataract in a Siberian tiger. Ophthalmologica 178:56–65

Seki MC, André MR, Carrasco AOT, Machado RZ, Pinto AA (2016) Detecção de *Chlamydophila felis* e Herpesvirus felino tipo 1 em felídeo não doméstico no Brasil. Braz J Vet Res Anim Sci 53(2): 169–176

Shahzad S, Saleem MB, Mahmood AK, Shelly SY, Ahmad SS, Tariq Z, Qadir Z (2015) Treatment of conjunctivitis in puma cubs in Lahore Zoo, Pakistan. J Anim Plant Sci 25:735–737

Steinmetz A, Eulenberger K, Thielebein J, Buschatz S, Bernhard A, Wilsdorf A, Ofri R (2006) Lens-anomalies and other ophthalmic findings in a group of closely-related Angola lions (Panthera leo bleyenberghi). Zoo Biol 25:433–439

Stone J (1978) The number and distribution of ganglion cells in the cat's retina. J Comp Neurol 180:753–772

Sussadee M, Vorawattanatham N, Pinyopummin A, Phavaphutanon J, Thayananuphat A (2017) Scotopic electroretinography in fishing cat (Prionailurus viverrinus) and leopard cat (Prionailurus bengalensis). Vet Ophthalmol 20(3):266–270

Thomas R, Navin S, Singh T, Chakrabarti S (2006) A tiger with glaucoma. Br J Ophthalmol 90:1549

Turner A (1997) Anatomy and action. In: The big cats and their fossil relatives. Columbia University Press, New York, pp 93–150. 234pp

Viñas M, D'Anna N, Guandalini A, Capasso M, Nocerino M, Guerriero A, Sapienza J (2019) Bilateral phacoemulsification and intraocular lens implantation in a young African lion (Panthera leo). Can Vet J 60(2):186–192

Walls GL (1942) The vertebrate eye and its adaptive radiation. Hafner, New York, 814pp

Walser-Reinhardt L, Wernick MB, Hatt JM et al (2010) Bilateral vision loss in a captive cheetah (Acinonyx jubatus). Vet Ophthalmol 13: 128–133

Whittaker CJG, Wilkie DA, Simpson DJ et al (2010) Lip commissure to eyelid transposition for repair of feline eyelid agenesis. Vet Ophthalmol 13:173–178

Zarza H, Arias-Alzate A, González-Maya JF et al (2015) First record of Leishmaniasis in wild Jaguars (Panthera onca) from Mexico. Notas mastozoològicas 2(1)

Ophthalmology of *Canidae*: Foxes, Wolves, and Relatives

36

Freya M. Mowat and Leo Peichl

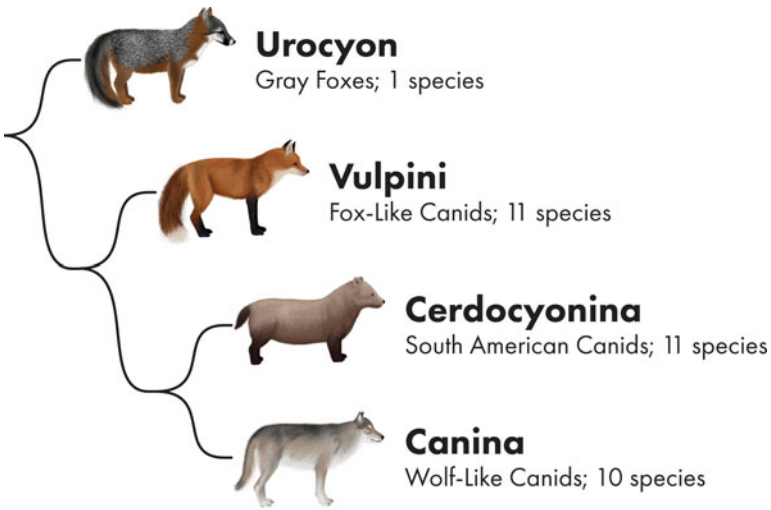

Introduction

Canidae are a diverse family, occupying many continents and ecosystems. They range from insectivores to carnivores, diurnal to nocturnal, and solitary to social. An overview of the phylogeny of each genus is given in Fig. 36.1, and details on the number of species, range, habitat preference, and behavior are given in Table 36.1, along with their International Union for Conservation of Nature and Natural Resources Red List of Threatened Species status. Because these varied habitats and behaviors likely had an adaptive impact on visual performance in the different species, we start this chapter with some basic information on the current knowledge of the visual system in canids.

The ocular anatomy and visual capacity of the domestic dog (*Canis familiaris*) have been extensively studied and are summarized in well-referenced reviews. The majority of studies into canid ocular anatomy, physiology, and clinical medicine have been performed in this species (Miller and Murphy 1995; Byosiere et al. 2018). Not all species of canids have been studied in detail, and this chapter reviews both published and the authors' unpublished findings of normal anatomy and physiology primarily in the gray wolf (*Canis lupus*), red fox (*Vulpes vulpes*), Arctic fox (*Vulpes lagopus*), side-striped jackal (*Canis adustus*), golden jackal (*Canis aureus*), coyote (*Canis latrans*), bat-eared fox (*Otocyon megalotis*), and raccoon dog (*Nyctereutes procyonoides*). In

F. M. Mowat (✉)
Department of Ophthalmology and Visual Sciences, School of Medicine and Public Health, Madison, WI, USA

Department of Surgical Sciences, School of Veterinary Medicine, University of Wisconsin-Madison, Madison, WI, USA
e-mail: mowat@wisc.edu

L. Peichl
Institute of Cellular and Molecular Anatomy, Dr. Senckenbergische Anatomie, Goethe University, Frankfurt am Main, Germany

Institute of Clinical Neuroanatomy, Dr. Senckenbergische Anatomie, Goethe University, Frankfurt am Main, Germany
e-mail: peichl@em.uni-frankfurt.de

F. Montiani-Ferreira et al. (eds.), *Wild and Exotic Animal Ophthalmology*, https://doi.org/10.1007/978-3-030-81273-7_11

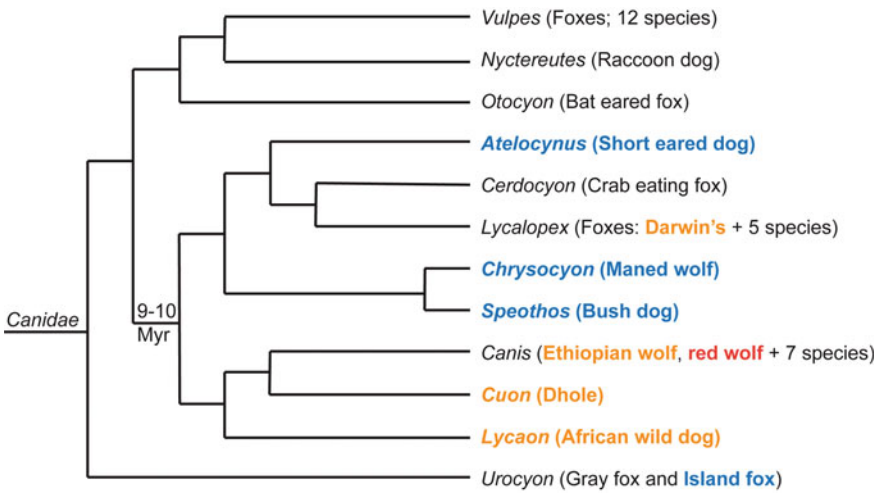

Fig. 36.1 The phylogeny of extant genera of the Canid family. Bolded and colored species are listed on the International Union for Conservation of Nature and Natural Resources Red List of Threatened Species (International Union for Conservation of Nature 2020), as near threatened (blue), endangered (orange), or critically endangered (red). Myr million years [Adapted from information provided in Lindblad-Toh et al. (2005)]

this chapter, normal ocular and retinal anatomy, ophthalmic examination techniques, and reported disorders of the ocular system in wild canid species are discussed, with comparisons to findings in domestic dogs where applicable. In the later description of the clinical aspects of canid ophthalmology, we present observations on additional species, including material provided by the authors and a number of veterinary ophthalmologist colleagues, as well as brief descriptions of pertinent disorders of the domestic canine.

Superimposed on a common ocular blueprint, there are species-specific differences, e.g., in pupil shape, photoreceptor properties, and retinal ganglion cell topographies that indicate evolutionary adaptations to different habitats and lifestyles. However, variability in anatomy and vision has been noted on an individual and breed level in domestic dogs and suggests a strong influence of selective breeding. It can be assumed that wild canid species are more homogeneous in their ocular anatomy and visual performance. Hence the information presented in this chapter, albeit mostly obtained from only a few specimens, is expected to be representative.

Canid Ocular Anatomy

Eye Dimensions and Orientation

Canid eyes are nearly spherical, their axial length (the distance between cornea and posterior pole) and equatorial diameter are very similar (Table 36.2). The optic nerve exit point (blind spot) is located near the geometric posterior pole. The eye's axial length is an important factor in specifying the visual acuity of a species. It is a proxy for the focal length (posterior nodal distance, PND) of the eye's optics and thus determines the image size on the retina, the retinal magnification factor (see the below section "Visual Acuity Estimates" and Hughes 1977).

All Canidae have frontally oriented eyes. In the dog, the divergence of the optical axes is 15–25° [for an overview of optical axes divergence across mammals, see Plate 30 in Johnson (1901), reproduced as Fig. 1 in Hughes (1977)]. For other canid species, facial images available on the Internet show very similar frontal eye orientations. This is quantified by skull measurements showing rather similar orbit orientations across canid species (Casares-Hidalgo et al. 2019). Compared to species with more laterally positioned eyes (e.g., many rodents and ungulates), frontal eyes provide a larger binocularly viewed field in front of the animal and thus improved depth perception (stereopsis), but with a lesser extent of the monocular fields to the sides, i.e. a smaller panoramic field of view. This is advantageous for hunting animals that need to accurately judge prey distance for a strike, but do not have to fear predators approaching from behind or the side. Behavior testing suggests that the dog's panoramic field of view is about 240°, and the binocularly viewed frontal segment subtends 30–60° (Sherman and Wilson 1975). There is some apparent individual breed variability in the extent of the dog's binocular field (Mowat, unpublished observations).

Orbit and Adnexa

The canid adnexa comprise the eyelids, conjunctiva, and orbital tissues. Detailed anatomy of the domestic dog is described elsewhere (Evans and de Lahunta 2013). Published comparative anatomy studies between canids do not identify substantial differences in adnexal anatomy, although limited studies have been reported, namely in the crab-eating fox (Lantyer-Araujo et al. 2019). Facial features including coat

Table 36.1 Canid biology. Genus subgroups within the Canidae family, describing habitat and behavior traits pertinent to ocular and visual function (Sources: Myers 2014; Nowak and Walker 1991; International Union for Conservation of Nature 2020)

Genus	Extant species	Common name	Continent	Habitat	Behavior	Conservation status (IUCN)
Vulpes	12	Fox: Arctic, cape, Tibetan, Blandford's, swift, Bengal, Rüppel's red, fennec, kit, etc.	Various; red fox is most widely distributed	Various; e.g., open tundra (Arctic fox), forested, heterogeneous & fragmented landscapes (red fox), desert (fennec)	Omnivore, scavenger, and predator ("mousing jumps"); usually nocturnal; Arctic fox more diurnal during Arctic summer; hierarchical society, silver fox has been semi-domesticated in Russia	Least concern
Nyctereutes	1	Raccoon dog	Asia	Forested streams, river valleys, lake shores, with thick underbrush, marshes or reedbeds	Omnivore, scavenger; nocturnal (some studies show diurnal and crepuscular activity); pairs/small family groups; the only canid hibernating in winter	Least concern (invasive in Europe)
Otocyon	1	Bat-eared fox	Africa	Savanna and short grass habitats in arid and semi-arid regions; hides in tall grass and shrubs	Insectivore; mostly nocturnal in northern locations, seasonally nocturnal or diurnal in southern locations; family groups; highly social, use vision for communication	Least concern
Atelocynus	1	Short-eared dog	South America	Lowland rainforests, preferring swamps and areas along rivers	Carnivore/omnivore; diurnal/nocturnal/ crepuscular; mostly solitary; possibly partially aquatic, having partial interdigital membrane	Near threatened
Cerdocyon	1	Crab-eating fox	South America	Woodland and wooded savanna	Omnivore; nocturnal/ crepuscular; monogamous pairs	Least concern
Lycalopex	6	Foxes: Pampas, culpeo, hoary, Darwin's, South American gray, Sechuran	South America	Various; forest, scrub, grassland, heath, desert	Omnivore; nocturnal (pampas, Culpeo, South American gray), diurnal (hoary), diurnal/nocturnal/ crepuscular (Darwin's); solitary, family groups (Darwin's, South American gray)	Least concern; endangered (Darwin's)
Chrysocyon	1	Maned wolf	South America	Grassland, scrub forest	Omnivore; nocturnal/ crepuscular; solitary	Near threatened
Speothos	1	Bush dog	Central/South America	Forests, wet savannas, near rivers	Carnivore; diurnal/ crepuscular; partially webbed toes for swimming; pack hunting; live in small hierarchical packs	Near threatened
Canis	9	Dingo, side-striped jackal, domestic dog, red wolf, Ethiopian wolf, coyote, gray wolf, black-backed	Australia (dingo); Africa (e.g., jackals); Europe (golden jackal, gray wolf); Asia (golden jackal, gray wolf); North America	Various; arctic tundra to forest, prairie, and arid landscapes (gray wolf); open grassland, woodland, mangroves (golden jackal); open	Omnivore (side-striped jackal, black-backed jackal, golden jackal, domestic dog, coyote), carnivore (dingo, red wolf, Ethiopian wolf,	Least concern; endangered (Ethiopian wolf); critically

(continued)

Table 36.1 (continued)

Genus	Extant species	Common name	Continent	Habitat	Behavior	Conservation status (IUCN)
		jackal, golden jackal	(coyote, gray wolf, red wolf)	and brushy areas, pine stands (coyote)	gray wolf); diurnal (Ethiopian wolf), nocturnal (side-striped jackal, red wolf, coyote, black-backed jackal); monogamous pairs (side-striped jackal, black-backed jackal, golden jackal/ small family groups/ hierarchical packs)	endangered (red wolf)
Cuon	1	Dhole	Asia	Various; mountainous, dense forest, scrub jungle, open country	Omnivore, persistence hunter for large artiodactyls; diurnal; highly social, rigid hierarchy, complex visual communication (will wag tail for communication)	Endangered
Lycaon	1	African wild dog	Africa	Grassland, savannah, open woodland, semi-desert	Carnivore, persistence hunter; diurnal; highly social with hierarchical pack (independent male/female) with dominant monogamous pair	Endangered
Urocyon	2	Gray fox	North America/ northern South America	Deciduous forest, wooded, brushy, and rocky habitats	Omnivore; nocturnal/ crepuscular; tree climbing (retractable claws); solitary, mostly monogamous	Least concern
		Island fox	North America (Channel Islands off California)	Various, all island habitats including forest, grassland, cactus scrub, marshland, dunes	Omnivore; diurnal/ nocturnal; relatively solitary	Near threatened

color, eye position, and iris color reflect the level of visual communication between individuals within different species in the canid family, therefore small differences in anatomy might be expected based on different behaviors in divergent species (Ueda et al. 2014).

The eyelids are haired and contain modified cilia on the upper eyelid, with no visible lower cilia. Upper eyelid motion is comparably larger than lower eyelid motion during blinking. Eyelid (and corneal) sensation is derived from branches of the trigeminal nerve, and eyelid movement is controlled by striated muscles innervated by branches of the facial nerve. Smooth muscles of the eyelid and orbit are also present. There are some differences in eyelid and facial muscle anatomy between domestic dogs and gray wolves, which are hypothesized to be related to the evolutionary drive to develop communication between domestic dogs and humans (Kaminski et al. 2019).

Conjunctiva lines the inside of the eyelids (palpebral conjunctiva) and the globe (bulbar conjunctiva) and contain goblet cells for mucus production. Canids possess two lacrimal punctae situated in the upper and lower palpebral conjunctiva close to the medial canthus. The punctae drain tears down the nasolacrimal system to the nasolacrimal punctum, close to the opening of the nares.

The canid bony orbit is incomplete, similar to most carnivores, to facilitate a wide mandibular range of motion. A ligament connects the zygomatic and frontal bones, forming the anterior boundary of the orbit. The orbit narrows in a cone shape toward the skull, forming the basis for the visual axis.

The orbit contains extraocular muscles, ligaments and fascia, branches of cranial nerves, fat, and glandular tissue. The domestic dog has six extraocular muscles and one retrobulbar muscle that coordinate ocular movement (Evans and de Lahunta 2013).

Table 36.2 Canid eye dimensions. Comparative ocular dimensions for available canid species

Species	Act.[a]	Pupil shape[a]	AL (mm)	ED (mm)	CD (mm)	LD/LT (mm)	CD:ED	LD:ED	LT:AL
Domestic dog[b]	P	Round	13–25	20–26	n.d.	n.d.	n.d.	n.d.	n.d.
Gray wolf[c]	P	Round	23.6	24.9	18.0	12.6/7.1	0.72	0.51	0.30
Coyote	P	Round	21.1	22.0	16.1	11.3/6.6	0.73	0.51	0.31
Golden jackal	P	Round	19.0	20.6	15.2	10.8/6.1	0.74	0.52	0.32
Side-striped jackal	N	Round	19.4	20.8	14.8	10.4/5.1	0.71	0.50	0.26
Red fox[c]	P	Vert	19.1	19.4	15.7	11.5/6.7	0.81	0.59	0.34
Arctic fox[c]	P	Vert	18.0	18.2	13.7	10.3/6.5	0.74	0.56	0.36
Bat-eared fox	N	Vert	17.0	16.7	13.1	9.3/6.4	0.78	0.56	0.38
Gray fox[d]	N/P	Vert	17.4	17.4	13.9	n.d.	0.80	n.d.	n.d.
Crab-eating fox[d,e]	N	Vert	16.6	17.1	14.0	n.d.	0.82	n.d.	n.d.
Raccoon dog	N	Vert	n.d.	15.0	n.d.	n.d.	n.d.	n.d.	n.d.

Key: Act. predominant diel activity, AL axial globe length, ED equatorial globe diameter, CD corneal diameter, LD lens diameter, LT lens thickness, CD:ED relative corneal diameter with respect to the eye's equatorial diameter, LD:ED relative lens diameter with respect to the eye's equatorial diameter, LT:AL relative lens thickness with respect to the eye's axial length. Alternate eye dimensions of several of these species are reported in a publication (Kirk 2006) which slightly differ from those reported here. Data are from unpublished measurements (Peichl) unless referenced:

[a]N nocturnal, P polyphasic, vert vertical slit pupil or vertically elongated oval pupil (Banks et al. 2015)

[b]AL data summarized from Howland et al. (2004) and Peichl (1992b), ED data from Peichl (1992b). The corresponding cornea and lens sizes were not available

[c]Eye data from Malkemper and Peichl (2018)

[d]Eye data from Kirk (2006)

[e]Eye data from Lantyer-Araujo et al. (2019). For the crab-eating fox the two studies report somewhat different dimensions, their mean is given here

Tear Film

Glands that contribute to the canid tear film include the lacrimal and nictitans glands (aqueous portion), goblet cells of the conjunctiva (mucus portion), and the meibomian glands of the eyelids (lipid portion). Although comparative studies are relatively lacking, there is evidence for shared anatomy between different members of the canid family, based on similarities in gland anatomy and histology between the domestic dog and crab-eating fox (Lantyer-Araujo et al. 2019) with only minor anatomic differences identified between species.

Cornea

The canine cornea is a transparent extension of the fibrous tunic of the eye. It is composed of four layers and forms the primary refractive structure of the eye. The epithelium is formed of nonkeratinized stratified squamous epithelium derived from stem cells situated at the corneal limbus. The stroma is the thickest element of the cornea. It is relatively acellular, has a high water content, and is composed of glycosaminoglycans and collagen fibers in a highly oriented structure. Descemet's membrane is a thin acellular basement membrane of the deepest layer, the corneal endothelium—a single cell layer of endothelial cells that limit corneal hydration by the action of the sodium-potassium ATPase pump. This action aids in maintenance of corneal clarity. Although few comparative studies have been performed, there is no evidence of dramatic differences in corneal anatomy between different species within the canid family (Lantyer-Araujo et al. 2019).

Iris and Pupil Shape

Pupil shape differs between canid species. Members of the genera *Canis*, *Chrysocyon*, *Cuon*, *Lycaon,* and *Speothos* have round pupils, whereas *Vulpes*, *Cerdocyon*, *Lycalopex*, *Urocyon*, *Otocyon,* and *Nyctereutes* species have vertical slit pupils or vertically oval pupils [supplement in Banks et al. (2015); Table 36.2]. Slit pupils have long been considered advantageous for crepuscular to arrhythmic (cathemeral, polyphasic) species because they allow greater changes of pupil area and hence greater modulation of light admission to the retina. These species need large pupils with a correspondingly large sphincter muscle (*sphincter pupillae*) for vision at low light levels, but also need to constrict their pupils to a small aperture at diurnal light levels, for which the necessary compression of the large sphincter volume is a problem. A slit pupil has additional iris muscles that laterally compress the opening, providing a small aperture with less compression of the sphincter (Detwiler 1956). This, for example, allows a cat's slit pupil to change its aperture area by a factor of ~135, whereas the human circular pupil only changes by a factor of ~15 [reviewed in Banks et al. (2015)].

However, this hypothesis has shortcomings. It does not explain why among mammals with relatively similar activity patterns there are species with slit pupils and species with

round pupils. It also does not explain why some mammals (mostly Carnivora) have vertically and some (mostly Artiodactyla and Perissodactyla) have horizontally elongated pupils. Two additional hypotheses have been proposed. The first hypothesis is that slit pupils allow corrections for longitudinal chromatic aberration (Malmström and Kröger 2006). This group found that slit pupils are only present in species that have multifocal optical systems. A multifocal lens can only compensate for chromatic aberration when the full diameter of the lens is used for imaging at low light levels with a dilated pupil. At high light intensities a constricted round pupil would shade the peripheral zones of the lens, losing their compensatory effects. In contrast, a slit pupil would allow the use of the peripheral lens zones even at bright light. The red fox is a canid example for the correlation of a slit pupil with a multifocal lens. Future studies will have to establish whether canid species with circular pupils have monofocal lenses, and those with slit pupils have multifocal lenses.

The second hypothesis proposes that vertically elongated pupils are useful for arrhythmic ambush predators, whereas horizontally elongated pupils are advantageous for prey animals with laterally oriented eyes (Banks et al. 2015). The authors find that "vertically elongated pupils create astigmatic depth of field such that images of vertical contours nearer or farther than the distance to which the eye is focused are sharp," whereas "horizontally elongated pupils create sharp images of horizontal contours ahead and behind, creating a horizontally panoramic view that facilitates detection of predators from various directions." Among canids, they find a particularly strong correlation between an ambush mode of foraging and a vertically elongated pupil. They conclude that vertically elongated pupils facilitate stereopsis, which is particularly relevant for ambush predators that need to precisely judge the distance to their prey. However, the correlation does not hold for all canids. Within the foxes, two species with vertical pupils do not exhibit ambush feeding methods: firstly, the bat-eared foxes (which feed exclusively on termites), and secondly raccoon dogs (which have a scavenger feeding pattern). A proposed alternative explanation has been suggested (Banks et al. 2015): the optical advantage of a vertical slit pupil depends on eye height, being larger for smaller and less relevant for larger animals. This could have led to round pupils in the larger canids and vertically elongated pupils in the smaller canids.

Lens

Canid lenses are transparent and colorless. They are larger relative to the size of the eye compared with humans, with a diameter of more than half the eye's equatorial diameter, and a thickness of one quarter to one third of the eye's axial length (Table 36.2). This indicates an evolutionary adaptation to low light vision, as a larger and thicker lens allows more light to reach the retina, provided there is a correspondingly large pupil and cornea. In canids, the corneal diameter is large, covering about three quarters of the eye's equatorial diameter (Table 36.2). By comparison, in the diurnal human eye the corneal diameter is only half, and the lens diameter only ~40% of the eye's equatorial diameter; the lens thickness is only 17% of the eye's axial length.

The lenses of many mammals, particularly diurnal ones like primates and squirrels, contain filters that block UV light (i.e., wavelengths <400 nm), but an unexpectedly large number of species have UV-transmissive lenses that allow variable amounts of UV light to reach the retina (Douglas and Jeffery 2014). The dog belongs to the latter group, its lens transmits 61% of the incident light between 315 and 400 nm, with a 50% transmission at 335 nm (Douglas and Jeffery 2014). No such measurements exist for other canids, but it is suspected that their lenses are similarly UV-transparent, suggesting that canids can perceive UV light if their retinae contain UV-sensitive photoreceptors. This aspect is discussed below.

Chromatic aberration, i.e. the differential refraction of light based on wavelength, is a physical problem of natural lenses. One study found that the lenses of a number of terrestrial vertebrates, including some mammals, are multifocal (Malmström and Kröger 2006). They have concentric zones of different focal length with each zone focusing a different spectral range on the retina, thus compensating for the chromatic aberration. This correlates with the pupil shape (see previous section "Iris and Pupil Shape"). Among their studied species with a multifocal lens was the red fox. Their results obtained from domestic dogs and gray wolves were inconclusive. A multifocal lens was seen in some dog individuals and in specific breeds, whereas others had a monofocal lens. The gray wolf lenses showed refractive irregularities in the central zone that might indicate multifocality. Therefore, no generalizations can be made regarding refractive properties of canid lenses.

Tapetum Lucidum

The tapetum lucidum is a reflective layer behind the retina that provides the photoreceptor cells with a second opportunity for photon absorption, which is particularly useful for enhancing visual sensitivity at low light levels [for reviews, see Schwab et al. (2002); Ollivier et al. (2004)]. Tapeta are present in the eyes of many vertebrates. As the anatomical structure and hence physical basis for the reflection differ between animal groups, it is concluded that a tapetum independently evolved several times (Schwab et al. 2002). Among the mammals, the presence of a tapetum is largely

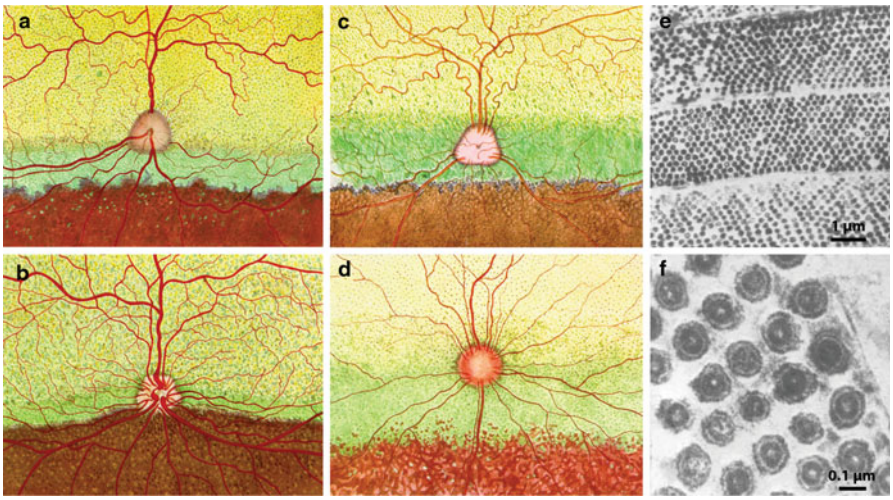

Fig. 36.2 Comparative anatomy of the canid tapetum. Fundus drawings of gray wolf (**a**), red fox (**b**), coyote (**c**), and raccoon dog eyes (**d**). The drawings show the yellow-green tapetum lucidum with its speckled appearance due to the many dots (termed "stars of Winslow") representing end-on views of large choroidal capillaries penetrating the tapetum. The position of the sharp horizontal ventral boundary of the tapetum relative to the optic disc differs between the species, as does the shape of the optic disc and the retinal blood vessel pattern. (**e**) Electron micrograph of beagle dog tapetum cells, showing the densely packed and regularly spaced electron-dense rodlets in cross-section. (**f**) Higher power electron micrograph of the rodlets, showing their substructure with two concentric rings of zinc [(**a**–**d**) adapted from Johnson and Whitteridge (1968) with permission by The Royal Society, (**e**, **f**) adapted from Wen et al. (1982) with permission by the Association of Research in Vision and Ophthalmology (ARVO)]

restricted to the Carnivora, Artiodactyla, and Perissodactyla; it is a rare feature in other orders. In terrestrial mammals, including the canids, the tapetum is restricted to the dorsal half of the fundus. This is thought to compensate for the difference between the brighter light from the sky, perceived by the ventral retina and the less bright light reflected from the ground, perceived by the dorsal retina. In all canids, the retinal area centralis (region of highest visual acuity) and visual streak are located within the tapetal region. The tapetum has a relatively sharp horizontal lower boundary against the normally pigmented ventral fundus. Depending on the canid species, the boundary may be located at the level of the optic disc, above it, or below it. Examples are shown in Figs. 36.2 and 36.3; fundus images of further canid species are shown in Johnson (1901); Johnson and Whitteridge (1968). It is unclear whether this difference has any functional significance.

The tapetum of the domestic canine is located between the choroid and the retinal pigment epithelium (RPE). In the tapetal region, the RPE cells are unpigmented and thus do not block tapetal reflection. The domestic dog central tapetum is composed of up to 20 layers of specialized rectangular cells. Other authors have reported as few as nine layers, although this may relate to differences between dog breeds. The tapetum gradually thins to fewer layers toward its periphery and has the appearance of a brick wall in cross-section (see Fig. 36.4). Dog tapetum cells are densely packed with rodlets of approximately 4 µm length and approximately 0.15 µm thickness that are oriented in parallel within the cell, with a spacing of about 0.2 µm (Fig. 36.2e, f) (Wen et al. 1982, 1985), review: (Ollivier et al. 2004). The rodlets have a higher refractive index than the surrounding cytoplasm, which leads to constructive interference. The rodlet spacing defines the spectral reflectance and hence the color appearance of the tapetum, which in canid species is commonly yellowish to greenish. The orientation of the rodlets differs between neighboring tapetum cells, producing an overall diffuse reflection. In the dog, the tapetum matures postnatally and only attains its adult appearance by four months of age; the immature tapetum of a puppy appears blue (Ollivier et al. 2004). It can be assumed that this is similar in other Canidae, although the time course of maturation may differ between species.

Canid rodlets are very rich in zinc cysteine, with highest zinc levels found in the red fox, slightly lower levels in the Arctic fox, and relatively lowest levels in the dog (Weitzel et al. 1955). The zinc is a major contributor to the rodlets' high refractive index. It also makes the rodlets electron-dense, showing their substructure of concentric rings [Fig. 36.2f; (Wen et al. 1982)]. An absence of zinc is the cellular basis for the hereditary tapetum abnormality found in certain beagles, in which the tapetal cells are degenerated and have lost their regular rodlet arrangement (Wen et al. 1982). For other canid species, no studies are available on the detailed structure and biochemical properties of the tapetum cells. However, zinc deficiency could be a consideration for tapetal abnormalities observed in other species.

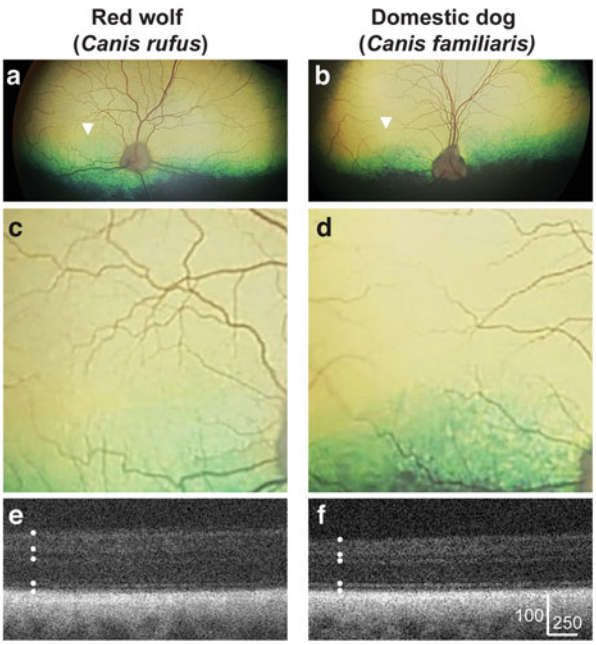

Fig. 36.3 Comparative in vivo canid retinal anatomy. The retinae of a red wolf (*Canis rufus*, **a**, **c**, **e**) and a domestic dog (*Canis lupus familiaris*, **b**, **d**, **f**) are shown. Images are shown of the right eye of 10-year-old females of each species. The domestic dog was of mixed breed (German Shepherd mix). Both canids have retinal blood vessels approximately delineating a visual streak dorsal to the optic nerve with a temporally located area centralis (white arrowheads in **a** and **b**). However, when the area centralis is viewed at higher magnification (**c**, **d**), the wolf has a more prominent blood vessel pattern that arcs around the area centralis (**c**), compared with the dog which has a relatively irregular blood vessel pattern (**d**). Similarly, optical coherence tomography (OCT) images of the area centralis of each species highlight that the retinal layers are overall thicker in the wolf (**e**), compared with the dog (**f**). Dots delineate individual retinal layers in **e** and **f**, scale in **f** is in microns

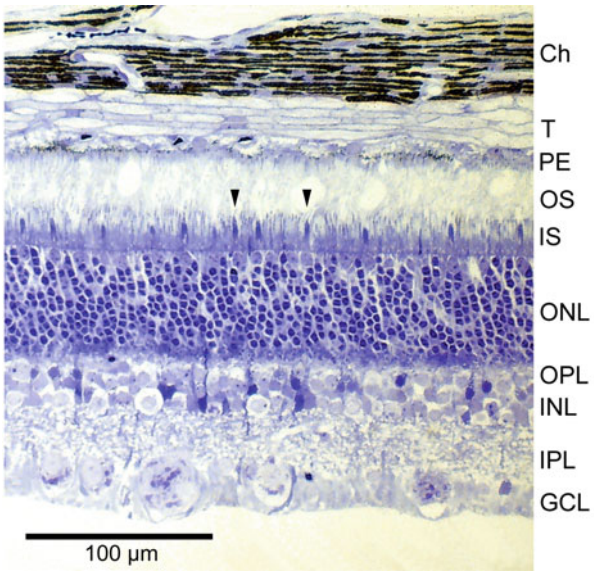

Fig. 36.4 The dog retina in transverse section. Transverse section through a dog retina as a typical example of a canid retina. Toluidine blue stained semi-thin Epon section from dorsal midperipheral retina. [Note that the tapetum only has 5 cell layers here, less than the central maximum of 20 layers, see text.] Ch pigmented choroid, T tapetum lucidum, PE retinal pigment epithelium with only few pigment granules in this region, OS photoreceptor outer segments, IS photoreceptor inner segments, ONL outer nuclear layer containing the photoreceptor somata, OPL outer plexiform layer, INL inner nuclear layer, IPL inner plexiform layer, GCL ganglion cell layer. Arrow heads indicate two of the cone photoreceptors that can be distinguished from the more numerous rods by a darkly stained thick inner segment and a soma that is larger and paler than the rod somata

Retina

Canid retinae, as far as they have been studied, conform to the basic blueprint of the mammalian retina (Fig. 36.4). They are vascularized (holangiotic), with the main vessels entering the retina within or close to the optic nerve head and then ramifying in the optic nerve fiber layer to supply the retina (see Figs. 36.2 and 36.3). Smaller vessels and capillaries branch off vertically to penetrate the inner retinal layers. The outer retina (i.e., the outer nuclear layer with the photoreceptor somata) is supplied with oxygen via nutrient diffusion from the choroidal vasculature. Note that in retinae with a pronounced visual streak (see section "Retinal Ganglion Cells" below), the smaller blood vessels of the inner retina approach the visual streak from the dorsal and ventral side, but hardly ever cross the streak line (Figs. 36.2 and 36.3). This vascular pattern has the appearance of a "watershed" as seen in river systems and is a feature that also is apparent in in vivo fundus imaging.

The canid retinae contain both rod and cone photoreceptors, and a variety of bipolar and ganglion cell types in the inner retina. A range of modulating interneurons modify the signal transmission in both plexiform layers: two horizontal cell types in the outer plexiform layer (OPL) and a range of amacrine cell types in the inner plexiform layer (IPL). The thickness of the retinal layers differs somewhat between canid species (Figs. 36.3e, f and 36.4), and in each species, the retina is thickest at the area centralis and thins toward the periphery. The mammalian retinal circuitry has been extensively studied in a few model species [e.g., mouse, cat, rabbit, primates; reviewed by Masland (2001); Wässle (2004); Demb and Singer (2015)]. For the dog and other canids, relatively few data are available, except for studies of the photoreceptors and ganglion cells in some species. This allows a more detailed account of these two neuron classes, representing the input and output stage of retinal processing, respectively, in the next sections.

Rod Photoreceptors

The mammalian outer retina generally contains rods and cones. Most species have rod dominated retinae, but the rod-to-cone ratio roughly correlates with the diel activity of

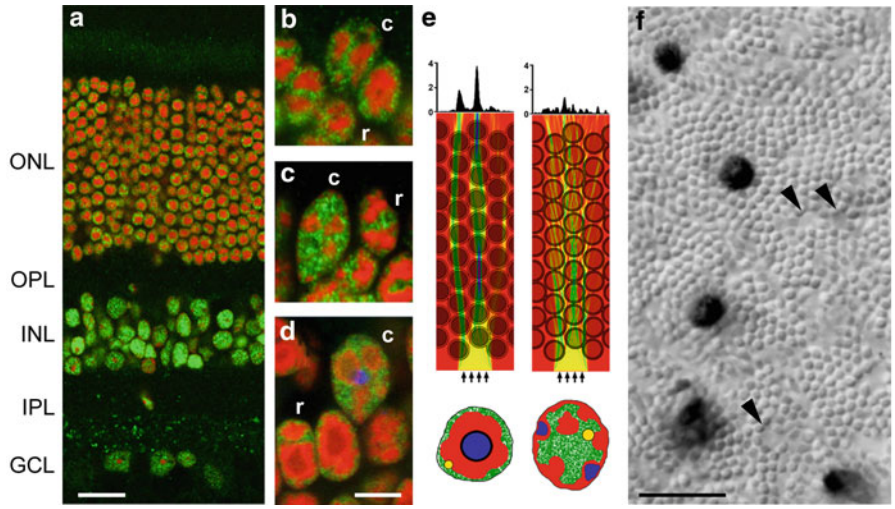

Fig. 36.5 Canid rod photoreceptors. Rod properties in some Canidae. (a) Transverse section of raccoon dog retina, stained for euchromatin (anti-H3K4me3 immunolabel, green) and for heterochromatin (DAPI, red). The cell nuclei in the INL and GCL show dominant euchromatin label and distributed heterochromatin, whereas the rod nuclei in the ONL show a compacted heterochromatin lump in the center and euchromatin in the nuclear periphery. (b–d) High power micrographs of the label in rod and cone nuclei of raccoon dog (b), dog (c), and Arctic fox (d). The rod nuclei (r) have an inverted architecture with compacted heterochromatin in the center, whereas the cone nuclei (c) have a conventional architecture with smaller heterochromatin aggregates distributed throughout the nucleus. Some rods have a nuclear fold filled with euchromatin, giving them a coffee bean-like appearance. (e) Modeling of light transmission through an ONL made up of rods with inverted nuclei as found in nocturnal mammals (left) and of rods with conventional nuclei as found in diurnal mammals (right); the respective nuclear organization is shown schematically at the bottom. The light intensity graphs at the top show the light distribution where it exits the ONL columns to enter the rod inner and outer segments. With inverted nuclei the light is focused, with conventional nuclei it is scattered (light intensity axis in arbitrary units), for details see text. (f) Rod mosaic in a flat-mounted red fox retina, differential interference contrast (DIC) image with focus on the level of the rod inner segments. The retina had been immunolabeled for S cone opsin, the few S cones appear in black. The scattered unlabeled L cones have larger inner segments than the rods (three marked by arrowheads). Abbreviations of retinal layers as in Fig. 36.4. Scale bar in image **a** is 20 µm, scale bar in image **d** is 5 µm for images **b**–**d**, scale bar in image **f** is 10 µm. Images **a**–**d** kindly provided by Irina Solovei, image **e** modified from Solovei et al. (2009) with permission, image **f** by Peichl, unpublished

a species [reviewed by Peichl (2005)]. The canids studied to date have rod dominated retinae with a low percentage of cones (see below), fitting their mostly nocturnal to crepuscular activity. As with the tapetum lucidum, a high proportion of the more sensitive rods represents an adaptation to vision at low light levels. However, it should be noted that most predominantly diurnal mammals, including humans and other primates, also have rod dominated retinae with just a few percent of their photoreceptors being cones; only the fovea of diurnal primates is free of rods to allow a denser cone packing and high acuity daylight vision. Hence, humans have adequate scotopic vision, even though we are foveally night-blind. The rod dominated retinae of most mammals are thought to represent the evolutionary heritage of a "nocturnal bottleneck" in the early mammals. Compared to their sauropsid ancestors, all mammals also have a reduced set of spectral cone types (see section "Spectral Cone Types and Color Vision"), similarly arguing for an adaptive emphasis on nocturnal, rod-based vision.

Because the rod outer segments are slender, with a diameter of about 2 µm, their dense packing requires that the rod somata with their larger diameter of about 5 µm need to be stacked in several tiers in the outer nuclear layer (ONL), hence a thick ONL is a hallmark of a nocturnally adapted retina. The canids certainly fall into that category (Fig. 36.5). Depending on the species, the number of ONL tiers in the central to midperipheral retina ranges from 8 to 13. Actual rod densities are only available for a few species and in most cases have only been assessed in selected retinal regions. A detailed analysis of six beagle dog retinae revealed a centroperipheral rod density gradient with a peak density of 501,000 rods/mm^2 in the central area and 305,000 rods/mm^2 in ventral peripheral retina (Mowat et al. 2008). In two beagle dog retinae, Peichl found a similar rod density range, but found a local minimum rather than a maximum in the central area (Fig. 8 in Peichl 1991; Peichl, unpublished). Rod densities of 200,000–540,000/mm^2 were also reported for mixed breed dogs (Yamaue et al. 2015). Red fox rod densities range from approximately 400,000/mm^2 to 700,000/mm^2, and Arctic fox rod densities from approximately 290,000/mm^2 to 470,000/mm^2; both species show large local rod density variations without a clear centroperipheral gradient (Malkemper and Peichl 2018). Limited rod density estimates obtained from transverse sections of the midperipheral retina yielded 220,000–300,000 rods/mm^2 in the gray wolf and 240,000–380,000 rods/mm^2 in the raccoon

Table 36.3 Canid photoreceptor densities

Species	Act.	L cone density range (1000/mm^2)	S cone density range (1000/mm^2)	S cone % of cones	Rod density range (1000/mm^2)	Cone % of PRs
Domestic dog[a,b,c]	P	3.1–26.3	0.6–1.8	10–18%	200–540	2.5–4.0%
Gray wolf[d]	P	5.7– >50.0[e]	0.4–1.7[e]	7–9%	220–300[f]	~2–6%[f]
Red fox[g]	P	3.3–23.4	0.5–3.4	5–35%	400–700	0.7–5.0%
Arctic fox[g]	P	3.7–44.8	0.5–2.9	4–16%	290–470	1.3–11.0%
Raccoon dog[d]	N	6.3–26.7	1.2–6.6	14–24%	240–380[f]	~3%[f]

Key: Act. predominant diel activity pattern, N nocturnal, P polyphasic
[a]Domestic dog rods and cones (Mowat et al. 2008)
[b]Domestic dog rods and cones (Klein et al. 2014)
[c]Domestic dog rod photoreceptors (Yamaue et al. 2015)
[d]Gray wolf and raccoon dog, Peichl unpublished
[e]High densities from temporal streak, area centralis densities could not be counted but were certainly higher
[f]Limited estimates from midperipheral retina
[g]Red fox and arctic fox (Malkemper and Peichl 2018)

dog. The available data are summarized in Table 36.3, although rod topographic maps are not currently available for any canids.

Nocturnal retinae, including those of the canids, have a high rod density for increased sensitivity, but the resulting thick ONL increases light scatter and diffusion, thus reducing the number of photons reaching the rod outer segments. As an evolutionary adaptation to compensate for this disadvantage, the rods of nocturnal mammals have a unique inverted nuclear architecture, where the more compacted heterochromatin with its higher refractive index is condensed in the nuclear interior, whereas the less compacted and less refractive euchromatin forms the peripheral shell of the nucleus (Solovei et al. 2009) (Fig. 36.5). This turns the rod nuclei into minute collecting lenses. The columns of rod nuclei in the ONL form strings of such micro-lenses and guide the light to the rod outer segments with only minimal loss. One major benefit of the inverted rod nuclei is an improved contrast sensitivity at low light levels (Subramanian et al. 2019).

The rods of diurnal species, and the cones and other retinal neurons of all mammals have a conventional nuclear architecture, with the active euchromatin located in the nuclear interior where it can interact more freely with neighboring gene loci and the transcription apparatus in three dimensions, whereas the non-active heterochromatin is dispersed across the nucleus. From a cell-biological point of view this is the better arrangement, as the conventional nuclear architecture is prevailing in nearly all higher organisms since 500 million years. Apparently, the need to improve optical transmission in nocturnal retinae was the unique adaptive pressure resulting in the inverted rod nuclear architecture.

An inverted rod nuclear architecture is found in the red fox and Arctic fox [supplement to Solovei et al. (2009)], and also in the raccoon dog, domestic dog, and gray wolf (Fig. 36.5; Irina Solovei, personal communication). These studies used antibodies against specific histone modifications to visualize euchromatin and heterochromatin, respectively (Solovei et al. 2009), but the nuclear architecture can also be highlighted with 4′,6-diamidino-2-phenylindole (DAPI) staining, as DAPI preferentially binds to heterochromatin. Depending on the species, the inverted rod nuclei either have a single central heterochromatin aggregate or they have a fold suggesting incomplete fusion of two heterochromatin clusters, with the appearance of a coffee bean (Fig. 36.5).

An electroretinographic study reported the spectral sensitivity peak of domestic dog rods as 508 nm (Jacobs et al. 1993). This wavelength is slightly longer than what is commonly seen in mammals (approximately 500 nm). In a similar study, the scotopic sensitivity of the coyote peaked at 500 nm (Horn and Lehner 1975). For other canids, no corresponding data are available.

Cone Photoreceptors

Spectral Cone Types and Color Vision

All canid species studied to date possess a consistent population of cones. Conforming to the basic mammalian pattern, the canids have two spectral cone types, one containing a long wavelength-sensitive (LWS) cone visual pigment, the other a short wavelength-sensitive (SWS1) cone visual pigment. For convenience, these are termed L cones and S cones here. The two cone types are the basis for dichromatic color vision. Behavioral tests showed that domestic dogs have dichromatic color vision, with peak sensitivities at 555 nm for the L cone pigment and at 429 nm for the S cone pigment (Neitz et al. 1989). Electroretinographic flicker photometry, performed in the dog, red fox, Arctic fox, and Island gray fox, confirmed that in all these canids the peak spectral sensitivities were at 555 nm for the L cones, and at 430–435 nm for the S cones [Fig. 36.6a; (Jacobs et al. 1993)]. It is a reasonable assumption that this cone pigment tuning and hence type of color vision is similar across canids,

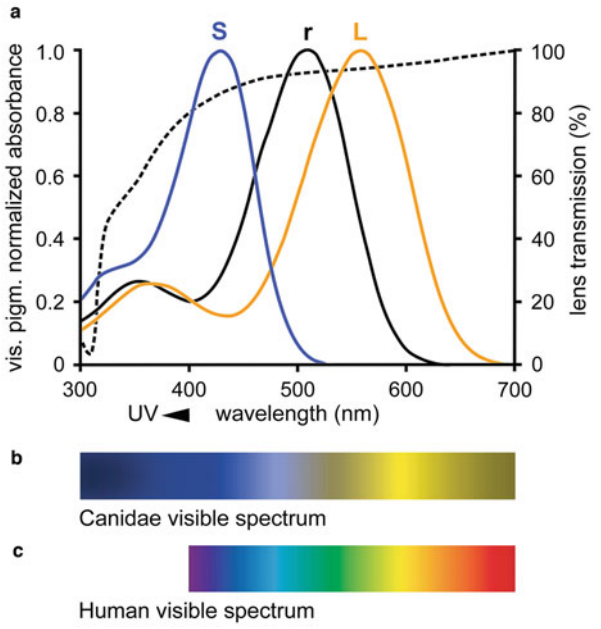

Fig. 36.6 Canid photopigment spectral sensitivity. (**a**) Semi-schematic graph of the spectral tuning curves of canid L cone visual pigments (L, absorption maximum at 555 nm, orange curve), S cone visual pigments (S, absorption maximum at 430–435 nm, blue curve), and rod visual pigments (r, absorption maximum at 508 nm, black curve), together with the spectral transmission curve of the dog lens (50% transmission at 335 nm, broken black curve). Wavelengths below 400 nm are termed ultraviolet (UV). The canid photoreceptor sensitivity peaks have been reported by Jacobs et al. (1993); the shapes of the pigment tuning curves and the dog lens transmission curve are modified from Figs. 1 and S3d in Douglas and Jeffery (2014). See text for details. (**b**) Presumed color range seen by the dichromatic canids, similar to that seen by deuteranope humans, but extending into the UV. (**c**) Color range seen by a normal human trichromat; the human lens blocks UV wavelengths (<400 nm)

as it appears consistent across carnivores (Jacobs 1993; Jacobs et al. 1993). A molecular study of the SWS1 opsin genes across mammals has shown the presence of a blue-to-violet tuned SWS1 opsin in additional canid species (Emerling et al. 2015).

Compared to humans, the 555 nm tuning of the canid L cone pigment is closer to that of human red cone pigment (560 nm) than to that of human green cone pigment (530 nm). Hence the color vision of canids most likely is similar to that of a human deuteranope (dichromacy due to hereditary absence of the green cone pigment): short wavelengths, i.e., blue to violet hues, can be discriminated from longer wavelengths, but all green to red hues appear as the same orange-brownish color. This is schematically illustrated in Fig. 36.6b. The spectral absorption curves of the cone and rod pigments are bell-shaped and thus sensitive, with decreasing absorption, to a wavelength window around the tuning peak. The shortwave flank of the curves extends down into the ultraviolet (UV, <400 nm) and even shows a small secondary peak there, termed the β-band, which is a property of the protein moiety of each visual pigment (Fig. 36.6a). The canid S cone pigment is more sensitive to UV than the other visual pigments, and as the canid lens is quite UV-transmissive (Fig. 36.6a; see previous section "Lens"), canids probably can see UV with their S cones, perceiving it as a blue-violet hue (Douglas and Jeffery 2014).

The spectral cone types can also be identified immunohistochemically with antibodies directed against the L and S cone opsins, respectively. This allows for post-mortem assessment in paraformaldehyde-fixed retinal tissue, i.e. without the need for physiological experiments on live animals. Applied to flattened whole retinae, the staining also gives information about the density and topographic distribution of the cone types, which cannot be obtained at present from electroretinographic recordings or molecular analysis of the opsin genes. Immunohistochemical analysis of the cones in various canids demonstrates that they have a majority of L cones and a more irregularly arranged minority of S cones, examples are shown in Fig. 36.7. Interestingly, across the wolf retina, nearly all S cones coexpress various amounts of L opsin. In the raccoon dog, there is coexpression of L opsin in practically all S cones of central and ventral retina, but no coexpression in dorsal S cones (Fig. 36.7). Small amounts of L opsin in the S cones are also found across the retina in the red and Arctic fox (Malkemper and Peichl 2018) and in the domestic dog (Peichl, unpublished observation). The L opsin in the S cones does not appear to have a marked influence on the spectral tuning, because the S cone sensitivity curves of the dog and foxes appear normal and not broadened or longwave-shifted (Jacobs et al. 1993).

Cone Densities and Topographies

Canid cone density data are summarized in Table 36.3. A study of cone densities in nine beagle dogs showed a strong central-peripheral density gradient (Mowat et al. 2008), with the area centralis located temporal and dorsal to the optic nerve head. In the central area the cone density individually ranged from 20,600/mm^2 to 29,800/mm^2 (mean 26,300/mm^2), and in peripheral retina from 1870/mm^2 to 4080/mm^2 (mean 3050/mm^2). The percentage of S cones among the cones was 9–12% in the central area and 15–18% in the ventral peripheral retina. Cones comprised about 4% of the photoreceptors in the central area and about 2.5% in the ventral periphery (rod:cone ratios 23:1 and 41:1, respectively). In contrast, another focal study of the dog area centralis found across the studied individuals, a local increase of cone density to 64,000–212,000/mm^2 (average 127,000/mm^2), with a concomitant local reduction in rod density (Beltran et al. 2014). Because this approaches human foveal cone densities (100,000–324,000/mm^2, average 199,000/mm^2; Curcio et al. 1990) the authors termed it a fovea-like area, although the region was not determined to be rod-free,

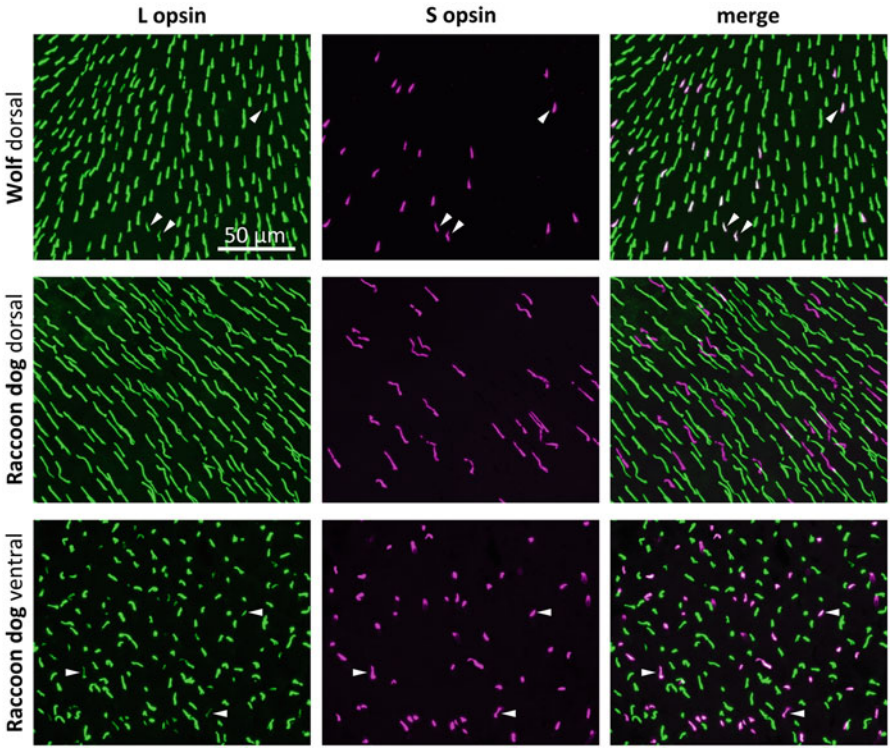

Fig. 36.7 Canid cone mosaics. Spectral cone types in the wolf (*Canis lupus*) and raccoon dog (*Nyctereutes procyonoides*). Double immunofluorescence labeling for L opsin (rendered in green; left column) and S opsin (rendered in magenta; middle column) in flat-mounted retinal pieces. The merge of the two labels is shown in the right column. The focus is on the opsin-containing cone outer segments. Illustrated regions are from wolf dorsal midperiphery (top row), raccoon dog dorsal midperiphery (middle row), and raccoon dog ventral periphery (bottom row, less good outer segment preservation). L cones are more numerous than S cones, and the S cones form a less regular mosaic than the L cones. Across the wolf retina, and in ventral but not dorsal raccoon retina, there is L opsin coexpression in most S cones (some indicated by arrow heads). The scale bar applies to all images

unlike the human fovea. Similarly in one beagle retina (Peichl, unpublished), a very focal cone density peak of 114,000/mm^2 and a concomitant rod density minimum of 53,000/mm^2 were noted in the central area, i.e. a rod:cone ratio of 1:2. The retina was methacrylate-embedded and densities are not corrected for shrinkage, but the rod:cone ratio would not be affected by shrinkage. It is possible that there are large inter-individual differences in dog peak cone density. In any case, such an extremely high cone density is an enigma that remains to be solved. The area centralis of the dog, in contrast to the primate fovea, does not have correspondingly high ganglion cell densities to convey the high visual resolution of the cone mosaic to the brain (see section below "Ganglion Cell Topographies" and Table 36.4), hence there appears to be no adaptive advantage.

Cone densities in the red and Arctic fox have been assessed (Malkemper and Peichl 2018). Both species have a strong centro-peripheral density gradient, from a central area peak of 22,600 cones/mm^2 to a peripheral minimum of 3300 cones/mm^2 in the red fox, and a central area peak of 44,800 cones/mm^2 to a peripheral minimum of 3700 cones/mm^2 in the Arctic fox (see previous section "Rod Photoreceptors"). With the lower rod densities in the Arctic fox (see above), its cones constitute 7–11% of the photoreceptors in central retina, whereas red fox cones only constitute 4–5% of the photoreceptors in central retina. The peak cone density of the red fox is within the range found across nocturnal to cathemeral carnivores, including domestic dogs (Mowat et al. 2008), whereas that of the Arctic fox is nearly twice as high and among the cone densities found in diurnal carnivores [summary in (Malkemper and Peichl 2018)]. The Arctic fox is described as having a nocturnal to crepuscular lifestyle, but during the long Arctic summer days, it likely has to forage extensively in daylight to secure enough food. We hypothesize that the higher cone and lower rod density are adaptations to the light conditions during the Arctic summer.

In both fox species, the S cone density does not peak in the central area, but shows highest values in the ventral retina (Malkemper and Peichl 2018). In the red fox, the S cone proportion among the cones is approximately 3.5–8% in the central area and along the visual streak, 12–15% in dorsal midperipheral retina, and up to 35% in the ventral retina. This pattern is qualitatively similar in the Arctic fox. Such a topography with highest S cone proportions in the ventral retina and no obvious S cone peak in the central area also is seen in a number of other carnivores, including some felids [summary and references in Malkemper and Peichl (2018)]. It was suggested that in domestic dogs, there is a higher proportion of S-cones in the ventral retina compared with the dorsal retina area centralis (Mowat et al. 2008), but further work is needed to verify this finding. The most intuitive adaptive explanation for a ventral S cone increase is the uneven distribution of wavelengths across the visual field. In ground-dwelling animals, the dorsal retina will mainly be excited by longer wavelengths reflected from the ground

Table 36.4 Canid ganglion cell topographies and estimated visual acuities

Species	Habitat	Visual streak	Peak RGC density (cells/mm^2)	RMF (mm/deg)	Estimated maximal vis. acuity (cpd)	Estimated vis. acuity of β cells (cpd)
Beagle dog[a]	Varied	++/+	9100–14,400	0.184–0.195	8.8–11.7	7.1–9.4
Gray wolf[b]	Varied	++	14,000	0.230	13.6	11.0
Coyote	Varied	++	11,000	0.216	11.3	9.1
Golden jackal	Varied	++	16,700	0.195	12.6	10.2
Side-striped jackal	Varied	++	7600	0.198	8.6	7.0
Red fox[b]	Varied	+	7900	0.195	8.7	7.0
Arctic fox[b]	Open	++	10,000	0.184	9.2	7.4
Bat-eared fox	Varied	+	9000	0.174	8.3	6.7
Raccoon dog[c]	Closed	0	8300	0.153	7.0	5.6

Key: Retinal magnification factor (RMF) given as the mean of that calculated from the posterior nodal distance (PND) with a PND/AL ratio of 0.54 for nocturnal to crepuscular mammals (Pettigrew et al. 1988), and of that calculated with the equation RMF = 0.011 × AL given by (Hughes 1977). Acuity of β cells calculated with the assumption that β cells constitute 65% of the RGCs in these species. Data sources: all unpublished by the author (Peichl) unless referenced:
[a]Peichl (1992b)
[b]Malkemper and Peichl (2018)
[c]For the raccoon dog, no eye axial length was available (see Table 36.2), the RMF was calculated with the assumption that the axial length equals the equatorial diameter. Visual streak: ++, pronounced; +, moderate; 0, none. cpd, cycles per degree of visual angle. For details see text

(grass, soil, leaf litter, etc.), whereas the ventral retina will receive a considerably higher amount of short wavelength light from the sky. However, as the canids and other large carnivores do not have to fear aerial predators, the benefits of this arrangement are unclear. The evolutionary drive for the ventral S cone bias in these species therefore remains to be discovered.

In one studied raccoon dog (Peichl, unpublished), L cone density peaked at 26,700/mm^2 in the central area and decreased to 6300/mm^2 in peripheral retina; S cone density ranged from 6600/mm^2 centrally to 1200/mm^2 peripherally. The S cone proportion was higher in the ventral than in the dorsal retina (approximately 24% vs. 14%). With the rod density estimate given above, the raccoon dog would have a cone proportion of about 3%. For the gray wolf, there is limited cone density data from selected regions from one retina (Peichl, unpublished). L cone density decreased from more than 50,000/mm^2 near the central area to 5300–6000/mm^2 in the peripheral retina. S cone density in the corresponding locations decreased from 1700/mm^2 to 440–570/mm^2; across the retina S cones comprised 7–9% of the cones, without any difference between the ventral and dorsal regions. Cone densities in the area centralis could not be quantified precisely, but exceeded 50,000/mm^2. The gray wolf, like the Arctic fox, thus has a peak cone density within the range found in diurnal carnivores, suggesting an adaptation to polyphasic activity with a strong diurnal component. This is in line with observations that gray wolves, although generally considered nocturnal, can be diurnal or bimodal depending on region and season (Theuerkauf 2009).

Cryptochrome 1 in Canid S Cones

An intriguing finding is that the canid S cones contain cryptochrome 1 (Cry1) in their outer segments (Niessner et al. 2016). Cryptochromes are blue light-absorbing flavoproteins that in animals have an important function in the circadian rhythms, particularly those involving circadian nuclear transcription regulation. However, the Cry1 located in the outer segment is not suited for this function, for which a nuclear or perinuclear location is required, and its function remains enigmatic. Adding to the puzzle is the fact that this localization was only found in canids and some Primates, but not in felids or any of the other 90 studied mammals (Niessner et al. 2016). Cry1a, the avian homolog of mammalian Cry1, has similarly been found in the S cone outer segments of robins and chickens, where it is hypothesized to have a role in light-dependent magnetic orientation [review: (Wiltschko and Wiltschko 2019)]. It is possible that canids also possess a light-dependent magnetic sense based on retinal Cry1. Behavioral evidence suggests that red foxes and dogs are magnetosensitive (Cerveny et al. 2011; Hart et al. 2013; Martini et al. 2018), but it is unknown whether that capability is associated with a retinal cryptochrome mechanism or with a non-light-dependent magnetite-based system [review: (Begall et al. 2014)].

Retinal Ganglion Cells

Ganglion Cell Types

Mammalian retinal ganglion cells (RGCs) can be classified into a number of distinct types with different morphologies

and functions. Canid RGC types, as far as they have been studied, conform to the types found across carnivores. The most extensive studies of carnivore RGCs have been conducted in the cat and have revealed a dozen or more types [reviews: (Kolb 2011; Peichl 2009; Masland 2001)]. This diversity of RGC types with different morphological and functional properties shows the complexity of retinal image processing before the information is passed on to the visual centers of the brain. The main types, which are also present in canids, are briefly presented in the following paragraphs.

Alpha ganglion cells have the largest soma, the largest-caliber, most rapidly conducting axons; and a large dendritic field. The dendritic tree is roughly circular with stout radially oriented, relatively densely branched dendrites. Alpha cell dendrites contain large amounts of neurofibrils and can be stained by classical neurofibrillar staining [reduced silver staining; Peichl et al. (1987); Peichl (1992a)] and immunolabeled with antibodies against neurofilament proteins. The alpha cells are the brisk-transient (Y) cells of physiology and comprise two functional subtypes, ON alpha and OFF alpha, as defined by their response to light. Alpha/Y cells show a vigorous transient (phasic) response whenever there is a stimulus change; their response to stationary, constant stimuli decays within the first few tenths of a second following stimulus onset. Alpha/Y cells respond best to rapid spatial or temporal changes of coarse patterns, hence they can be considered as "novelty detectors." Alpha cells represent roughly 5–15% of the RGCs, with some regional variation (see below).

Beta ganglion cells have a medium-sized soma and a medium-caliber axon. The dendritic tree is very small and roughly circular, with radial, relatively densely branched dendrites. In fact, beta cells look like miniature versions of alpha cells. Accordingly, they collect input from only a few bipolar cells and are the high-resolution (visual acuity) system of the carnivore retina. Beta cells are the brisk-sustained (X) cells of physiology. Like the alpha/Y cells, the beta/X cells comprise two functional subtypes, ON and OFF. Their response to visual stimuli is sustained (tonic). Beta/X cells respond well to small, high-contrast, stationary stimuli. They represent roughly 50% of the RGCs, with some regional variation (see below section "Ganglion Cell Topographies").

Other cat RGC types that have small somata and thin axons were originally subsumed under the term gamma cells. Based on differences in dendritic tree morphology they have since been classified as several distinct types and termed by letters from delta to theta (Isayama et al. 2000). As far as is known, they also differ in their light responses and in their projection targets in the brain. Each of these types only makes up a small proportion of the RGCs, but as a group the RGCs with small somata represent roughly 40% of the RGCs, with some regional variation.

Alpha and beta cells have been identified in the retinae of dogs, gray wolves, and foxes (Peichl 1992a; Malkemper and Peichl 2018), examples are shown in Fig. 36.8. The RGC soma sizes seen in the jackals, the coyote, the bat-eared fox, and the raccoon dog that we have studied clearly indicate that alpha and beta cells also are present in these canids (Peichl, unpublished). In addition, the canid retinae contain RGCs with smaller soma sizes and dendritic morphologies that fit gamma cell types.

Mammalian retinae possess an additional special RGC type, the intrinsically photosensitive RGCs (ipRGCs). These cells express the photopigment melanopsin and are directly light-sensitive, i.e. they are photoreceptors as well as RGCs, even though they also receive light information via the rods and cones [reviews: (Berson 2003; Bailes and Lucas 2010)]. They have been found across mammalian species, including the domestic dog (Yeh et al. 2017) and it can be assumed that they are also present in the other canids. The sluggish and non-adapting light responses of ipRGCs and their major projection targets (the suprachiasmatic nucleus containing the master clock of the mammalian circadian system, and the olivary pretectal nucleus that governs the pupillary light reflex), particularly those involving rhythms, indicate their role in measuring ambient light intensities and thus providing input to circadian photoentrainment and to the pupillary response. The low population density of ipRGCs (maximally a few percent of the RGCs) argues against a significant contribution to image-forming vision and visual acuity.

Ganglion Cell Topographies

In the studied canids, as in most mammals, the topographic distribution of RGCs across the retina shows a distinct density peak in a small area located in the temporal retina, termed the area centralis [reviews: (Hughes 1977; Moore et al. 2017)]. From there, the RGC density declines toward the periphery. As the density of each RGC type decreases, the individual cells increase in soma and dendritic field size. This serves to maintain a complete coverage of the retina by each type. RGCs in the area centralis have the smallest dendritic fields and hence functional receptive fields, making the area centralis the region of highest visual acuity (see below section "Visual Acuity Estimates"). Toward the retinal periphery, image processing becomes coarser. The behavioral visual acuity of an animal commonly corresponds to the peak acuity of its area centralis, as the area centralis is used to fixate objects of interest.

Some mammals show a horizontal band of increased RGC density that extends from the area centralis into temporal and nasal retina and is termed a "visual streak" [reviews: (Moore et al. 2017; Hughes 1977)]. Among the wild canids, a pronounced visual streak is present in the gray wolf, the Arctic fox, the jackals, and the coyote, a more moderate visual streak

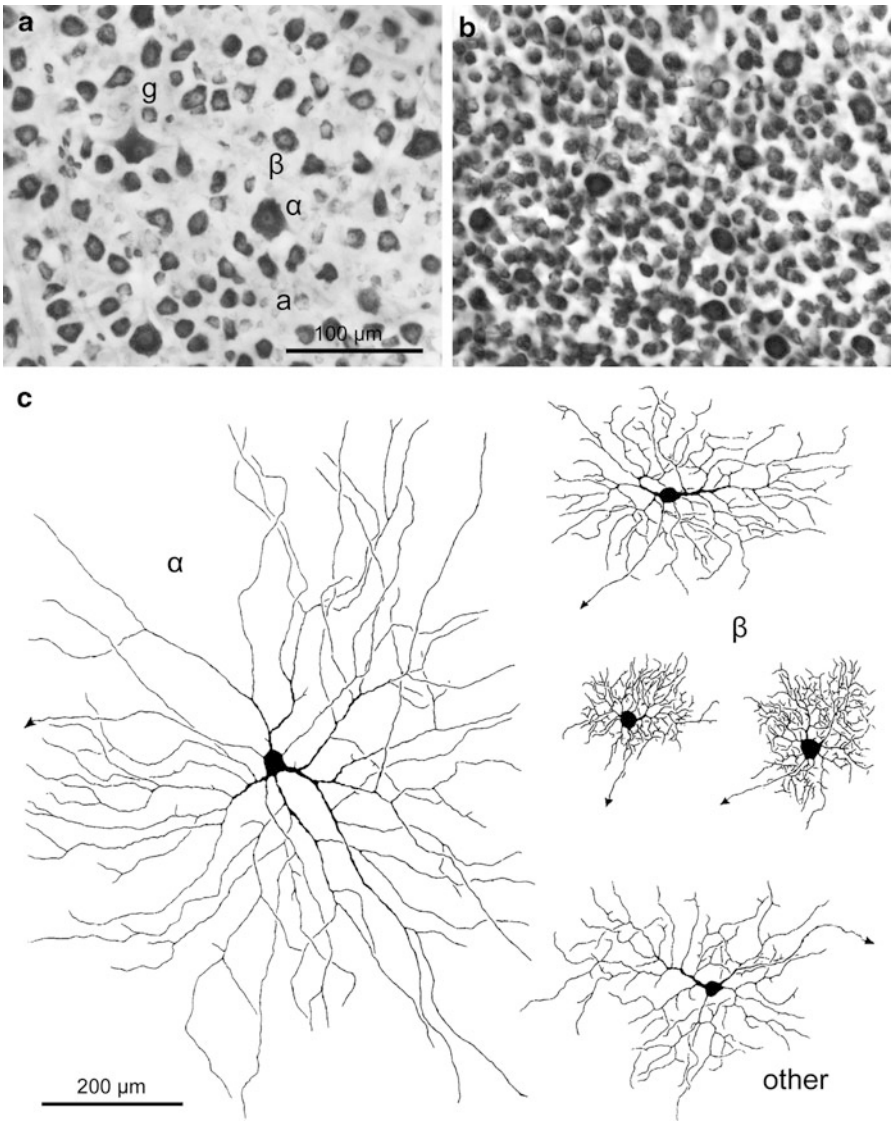

Fig. 36.8 Canid retinal ganglion cell morphologies. Morphologies of fox and wolf retinal ganglion cells (RGCs). (**a**, **b**) Cresyl violet "Nissl" staining of the ganglion cell layer of a red fox retinal flat mount. (**a**) Field in dorsal midperiphery, examples of an alpha RGC with large soma (α), of a beta RGC with medium-sized soma (β), of a non-alpha, non-beta RGC with smaller soma (g), and of an amacrine cell with small soma and less Nissl substance (a) are indicated. (**b**) Field near the area centralis with high RGC density and overall smaller somata. (**c**) Drawings of lucifer yellow-injected individual RGCs of the gray wolf. The cells are from nasal far periphery and drawn at the same magnification. Axons are marked by arrowheads. Of the three beta cells the two smaller ones are from the visual streak region, the larger one is from outside the visual streak. Scale bar in (**a**) applies to (**a**, **b**) [(**a**, **b**) adapted from Malkemper and Peichl (2018) and (**c**) from Peichl (1992a), all with permission by John Wiley & Sons]

in the red fox and the bat-eared fox, and no visual streak in the raccoon dog (Peichl 1992b; Malkemper and Peichl 2018; Peichl unpublished), examples are shown in Fig. 36.9.

In domestic dogs, some breeds have pronounced visual streaks, while other breeds have less prominent visual streaks; the peak RGC density in the area centralis also differs between breeds (Gonzalez-Soriano et al. 1995; Peichl 1992b; McGreevy et al. 2004). This is likely a consequence of the extensive inbreeding of dogs for specific desired features, unrelated to their visual capabilities. RGC topography differences are also seen between individuals within a breed (Peichl 1992b; Gonzalez-Soriano et al. 1995). This suggests that only small genetic changes may be responsible for the expression of a visual streak.

In retinae with a pronounced visual streak, the smaller blood vessels surround the visual streak line temporal and nasal to the optic nerve head, giving the impression of a "watershed." This is the case for example in the wolf, the coyote, and the Arctic and red fox (Fig. 36.3a–c), and also in dogs that have a pronounced visual streak (Fig. 10 in Peichl 1992b). This vascular feature is directly visible via routine funduscopy.

The location of the horizontal visual streak corresponds to the retinal location onto which the horizon is projected, the visual streak enables the animal to see the horizon with enhanced visual resolution. New objects, either predators or potential prey, generally first appear at the horizon. In fact, in an open terrain the retinal images of most objects—except very close ones—are contained in a small horizontal sector of the visual field (Fig. 36.10). Hence, a visual streak is advantageous for prey as well as predatory species if they live in an open environment where the horizon is a relevant visual feature, and when their field of view is not obscured by nearby vegetation (e.g., when they are large enough to see

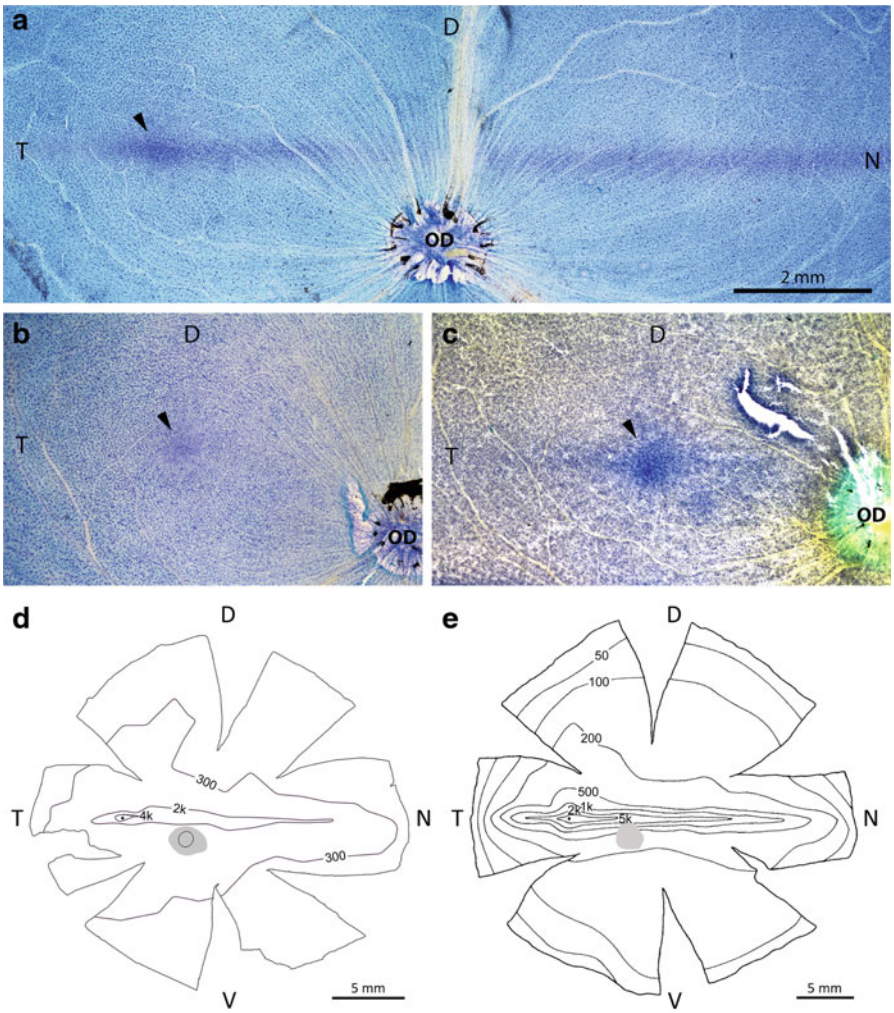

Fig. 36.9 Canid retinal ganglion cell topographies. Topographic distribution of RGCs determined in Nissl-stained canid retinae. (**a–c**) Low-power micrographs of flat-mounted retinae of the Arctic fox (**a**), raccoon dog (**b**), and bat-eared fox (**c**). (**a**) The pronounced visual streak of the Arctic fox appears as a dark blue horizontal band of higher RGC density extending from temporal to nasal retina dorsal of the optic disc (OD), it includes the temporal area centralis of highest RGC density (arrow head). The major retinal blood vessels appear brighter, because they displace the RGC somata. (**b**) The raccoon dog has no visual streak, RGC density drops uniformly in all directions from the temporal area centralis (arrow head). (**c**) The bat-eared fox has a visual streak extending temporal and nasal of the area centralis (arrow head). (**d**) Topographic RGC density map of the Arctic fox with the outline of the retinal whole mount, the RGC isodensity lines (numbers indicating the RGC density in cells/mm^2), a dot marking the position of the RGC density peak in the area centralis. The optic nerve head is indicated by the elliptical outline, the shaded area indicates where RGC counts were not possible. (**e**) Topographic RGC density map of the gray wolf, conventions as in (**d**). The scale bar in (**a**) applies to (**a–c**), note the different scales in (**d**) and (**e**). T temporal, N nasal, D dorsal, V ventral [(**d**) adapted from Malkemper and Peichl (2018) (**e**) adapted from Peichl (1992b) both with permission by John Wiley & Sons]

the horizon above the grass). This has been proposed most prominently by Hughes in his widely accepted "terrain hypothesis." (Hughes 1977).

Some of the studied canids conform to the prediction of the terrain hypothesis. The very pronounced visual streak of the Arctic fox matches its open tundra and Arctic habitats, the more forest-dwelling red fox has only a moderate visual streak (Malkemper and Peichl 2018). The raccoon dog inhabits forested streams, river valleys and lake shores, where thick underbrush, marshes, or reedbeds provide dense cover (Ward and Wurster-Hill 1990); the absence of a visible horizon fits the lack of a visual streak. Bat-eared foxes mostly inhabit short grass habitats and savanna in arid and semi-arid regions, but hide in tall grass and thick shrubs (Clark 2005); the moderate visual streak appears to be a suitable adaptation.

Some species do not show an obvious correlation between RGC topography and habitat [discussed in Hughes (1977) and Moore et al. (2017)]. Among the canids, this is the case in the gray wolf, the coyote, and the jackals. They have pronounced streaks, but they utilize a wide range of habitats of which some are not really open. Gray wolves occupy habitats from arctic tundra to forest, prairie, and arid landscapes (Smith 2002). Side-striped jackals inhabit moist wooded areas, savannahs and thickets, marshes, bushlands, grasslands, and swamps (Brensike 2000). Golden jackals

Fig. 36.10 Visual field and horizon. In an open terrain with a visible horizon, here illustrated by grazing wildebeests in the Serengeti, the retinal images of most objects except very close ones are contained in a rather narrow horizontal band (gray bar on the right). A horizontal visual streak processes this relevant sector of the visual field with enhanced resolution. Photo: Leo Peichl

often live in open grassland, but are also found in woodlands and mangroves (Moehlman and Hayssen 2018). Coyotes prefer pine stands and brushy areas as well as open areas (Magee 2008). For these species it remains unclear what the driving adaptive force is for a visual streak.

Canid RGC distributions show one peculiarity that is not present in other carnivores: alpha cells are absent from a large region of temporal retina. This has been observed in the dog and gray wolf (Peichl 1992b), red and Arctic fox (Malkemper and Peichl 2018), coyote, golden jackal, side-striped jackal and bat-eared fox (Peichl, unpublished). The region lacking alpha cells starts a few millimeters temporal to the area centralis and extends to the temporal periphery. The functional consequence of the absence of alpha cells is not understood. The alpha cells are considered to play important roles in flicker and motion perception, and to be involved in global form vision and stereopsis. The temporal retina represents central parts of the panoramic visual field, and the region lacking alpha cells is located in the binocular segment of the visual field, hence this region is also perceived by the nasal retina of the contralateral eye where the alpha cells are present. This implies that alpha cell tasks that could be performed monocularly may not be severely impaired, whereas binocular tasks like stereopsis would be expected to be impaired [see discussion in Peichl (1992b)]. Physiological studies at various levels of the canid visual system would be required to assess such potential deficits.

Visual Acuity Estimates

For wild canids, no behavioral or electrophysiological studies of visual acuity are available, so we are limited to anatomical estimates of their acuity. At any retinal location, the RGC density and RGC receptive fields can be considered as the "pixel density" and "pixel size" of image capture, respectively. RGC density is highest, and receptive field size smallest, in the area centralis. Hence this region sets the limit of retinal resolution, the visual acuity. An anatomical estimate of visual acuity can be calculated from the axial length of the eye and the peak RGC density, the corresponding equations are given in Malkemper and Peichl (2018). Table 36.4 lists the peak RGC densities and acuity estimates for the canids we have studied.

Before discussing these acuities, several provisos have to be mentioned. First, the image size on the retina, specified by the retinal magnification factor (RMF), is set by the posterior nodal distance (PND) of the eye's optical system consisting of the cornea and lens. In the absence of schematic eyes for the wild canids, the PND can only be estimated. For the ratio of PND to eye axial length (AL), estimates of 0.51–0.54 for nocturnal eyes and of 0.54–0.6 for crepuscular eyes have been published (Pettigrew et al. 1988). We have used a ratio of 0.54 in our calculations. From measurements across many vertebrate eyes (Fig. 9b in Hughes 1977), Hughes has derived a constant PND/AL ratio of 0.6 for nocturnal as well as diurnal eyes, resulting in a general equation $RMF = 0.011 \times AL$. The two approaches give somewhat different values, and we give the resulting mean RMF values in Table 36.4.

Secondly, peak RGC density counts may include a certain proportion of displaced amacrine cells, so they represent upper limits. Furthermore, the peak RGC densities of the coyote, golden and side-striped jackal, bat-eared fox, and raccoon dog were obtained in only one retina per species, and inter-individual density differences are to be expected like those seen in the gray wolf (Peichl 1992b), and the red and Arctic fox (Malkemper and Peichl 2018).

Finally, not all RGC types contribute to visual resolution. Nevertheless, total RGC peak densities are commonly used for species where no RGC classification is available. In carnivores, only the small beta cells are considered to be relevant. In the cat area centralis, beta cells make up about 65% of the RGCs, and we assume that this also holds for the canids (Malkemper and Peichl 2018). Table 36.4 gives visual acuity estimates based on total RGC peak density and on assumed beta cell peak density.

Visual acuity is commonly expressed in cycles per degree (cpd), giving the spatial frequency of a black-and-white grating (stripe pattern), i.e. the number of black and white stripe pairs per degree of visual angle, that can be resolved. Table 36.4 lists beagle data for comparison with the wild canids. We have specified the beagle to narrow down the larger range of eye sizes and RGC densities seen across dog breeds, but even among beagles there is variation. A study using visual evoked potentials reported beagle visual acuities of 7.0–9.5 cpd (Murphy et al. 1997). This is a surprisingly good match to our beta cell-derived anatomical estimate of

7.1–9.4 cpd, giving some confidence to the anatomical estimates for the wild canids.

Among the wild canids in Table 36.4, the gray wolf has the highest and the raccoon dog the lowest visual acuity, a difference by a factor of two. Probably the pack hunting of wolves requires more emphasis on vision than the omnivorous and often scavenging feeding habit of the raccoon dog. Most interesting are comparisons between closely related species. The red fox and Arctic fox have rather similar visual acuities (7.0 vs. 7.4 cpd), as the higher peak RGC density of the Arctic fox makes up for its smaller eye. Here it appears that the different visual environments did not exert adaptive pressure on acuity, and that the common feeding strategies were more influential. The golden jackal and side-striped jackal acuities differ markedly, with 10.2 vs. 7.0 cpd. These species have different feeding habits, the golden jackal is a more active hunter and ambush predator (Moehlman and Hayssen 2018), while the side-striped jackal is less predatory and carnivorous than other jackals, often scavenging (Brensike 2000). Nevertheless, the acuity of the side-striped jackal is as good as that of the red fox. The visual acuity of the bat-eared fox (6.7 cpd) is slightly lower than that, it can be assumed that feeding on termites does not require very good vision.

Overall, this range of anatomically estimated visual acuities across the studied wild canids is not particularly large if one considers that even among domestic dog breeds and individuals between 5.5 and 19.5 cpd have been estimated behaviorally (Lind et al. 2017). Finally, it should be stated that spatial detail and color are not the only visual features captured and processed by the retina. For example, movement detection, depth perception, dim light vision, and the entrainment of circadian rhythms are equally important retinal tasks (Miller and Murphy, 1995; Byosiere et al. 2018). As far as we know, these features are processed by dedicated ganglion cell types and circuitries about which we have no information in the wild canids.

Although there are no published reports of ametropia in nondomestic canids, there is considerable variation in refractive index between different domestic dog breeds (Kubai et al. 2008). Certain domestic dog breeds (toy poodle, Rottweiler and collie) had a higher proportion of myopes, whereas other breeds (Alaskan malamute, Australian shepherd) had a higher proportion of hypermetropes. The effect of refractive index on visual acuity remains to be determined in wild canid species.

Clinical Ophthalmic Examination of Canids

Because the canid family contains the domestic dog, ophthalmic examination and diagnostic techniques suitable for dogs can generally be utilized in other canids. The reader is referred to excellent books covering domestic canine ophthalmology in detail (Gelatt et al. 2013; Maggs et al. 2017). A brief overview of commonly used techniques and tools for examination and published reference values for unsedated domestic dogs is provided below (also see Appendix C).

Anterior Segment (Adnexa, Cornea, Anterior Chamber, Lens) Examination

- Color photography: can be used to document changes in lesions affecting the surface of the eye or adnexa over time.
- Slit-lamp biomicroscopy (Fig. 36.11a): Portable handheld slit lamps suitable for human pediatric ophthalmology offer a greater degree of maneuverability, and magnification up to 16×. They are commonly utilized in veterinary ophthalmology and can provide a magnified view of structures anterior to the posterior lens/anterior vitreous.
- Magnified view using an otoscope head or direct ophthalmoscope: if a slit lamp is not available, a magnified view of the anterior structures of the eye can be achieved using readily available instrumentation. A light source in parallel with the angle of view is advantageous for optimal viewing.
- Schirmer tear test: (STT) Normal STT value reported in unsedated domestic dogs is 21 mm/min (± standard deviation 4.2 mm) (Gelatt et al. 1975). Use of systemic sedatives and anesthetics, topical anesthetics, and/or topical or systemic medications with anticholinergic effects can reduce tear production.
- Tonometry: Bilateral tonometry should be performed as part of any routine ophthalmic examination, particularly if elevated intraocular pressure (IOP) is suspected. Care with restraint and eye/eyelid manipulation should be taken during measurement to avoid exogenous influences on intraocular pressure. Tonometers validated and commonly used for domestic dogs are listed below with reference ranges, and some advantages and disadvantages of their particular use:
  - Applanation method: TonoPen™; mean 19.2 mmHg ± standard deviation 5.9 mmHg (Gelatt and MacKay 1998). Disadvantages: application of topical anesthetic is required, larger footplate less advantageous for smaller eyes; underestimates IOP at high values (Dziezyc et al. 1992).
  - Rebound method: TonoVet™; mean 10.8 mmHg ± standard deviation 3.1 mmHg (Knollinger et al. 2005). Advantages: no topical anesthetic required, greater correlation with true intraocular pressure at higher pressures, small footplate is an advantage in smaller eyes. Disadvantage: The probe must be

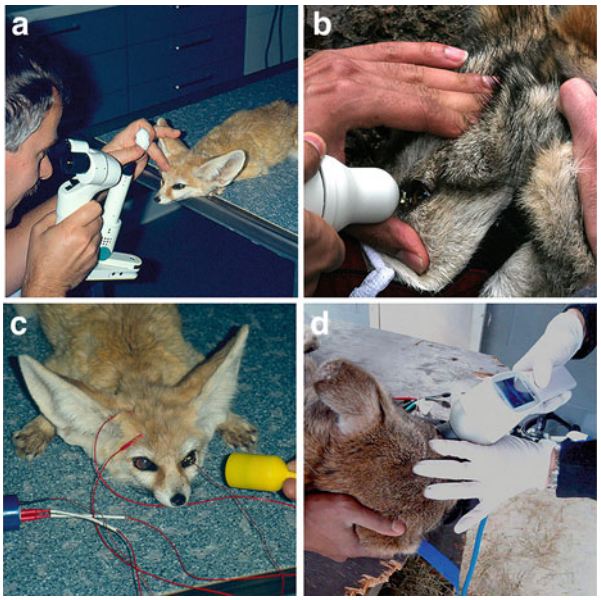

Fig. 36.11 Examination techniques. Slit-lamp biomicroscopy of a sedated fennec fox (*Vulpes zerda*) (**a**). Fundus photography in a manually restrained Mexican wolf (*Canis lupus baileyi*) (**b**). Unilateral electroretinography of a sedated fennec fox (*Vulpes zerda*) (**c**). Hand-held electroretinography in a manually restrained red wolf (**d**). Images **a** and **c** courtesy of Dr. med. Vet. Uwe Gränitz, Tierärtzliche Praxis für Augenheilkunde, Chemnitz, Germany. Image **b** courtesy of Dr. Simon Petersen-Jones, Michigan State University. Image **d** courtesy of Suzie Buzzo, Tallahassee Museum

maintained parallel to the ground, which can be practically more difficult.
  - Indentation method: Schiotz tonometer; mean 4.9 ± 1.5 tonometer scale units (Miller and Pickett 1992). Disadvantage: eye must be facing upwards for measurement. Values obtained must be calculated using human calibration chart.
- Fluorescein staining: Fluorescein is a hydrophilic fluorescent dye. When corneal ulceration is present, and the hydrophilic corneal stroma is exposed, fluorescein will bind to the exposed stroma, and the ulcer is delineated. Fluorescein is best observed using a blue light source. Corneal epithelium (superficial cornea) and Descemet's membrane (deep cornea) do not bind fluorescein. It is important to remember that very deep ulcers (descemetoceles) will not stain with fluorescein. Similarly, certain types of chronic ulcer (indolent forms) may also not stain well with fluorescein.
- Radiography: rarely useful in investigation of diseases of the eye due to bony structure superimposition. Can be useful to visualize fractures or radio-opaque foreign bodies such as gunshot.
- Ultrasound: can be used to examine the anterior and posterior segments through opaque ocular media. Useful to identify retinal detachment, masses or foreign bodies affecting the iris, vitreous, retina, or orbit. Can aid in sample acquisition (e.g., fine needle aspiration of orbit).
- Computed tomography or magnetic resonance imaging: best resolution imaging options for evaluation of the globe and orbital structures.

Posterior Segment (Vitreous, Retina) Examination

Mydriasis is recommended for optimal observation of the peripheral lens, vitreous, and retina. In domestic dogs, a commonly used mydriatic is tropicamide (0.5–1% ophthalmic solution) applied topically to the eye. Onset is within 10–20 min in unsedated dogs, and duration is up to 12 h, although effects can begin to wane after 2 h (Rubin and Wolfes 1962). Consideration should be made when sedation is administered prior to mydriatic application (see below section "Special Considerations for Wild Canid Clinical Ophthalmic Examination"). Commonly used methods to examine the posterior segment in canine ophthalmology:

- Ophthalmoscopy: for visualization of the retina and optic nerve.
  - Direct ophthalmoscope: upright and highly magnified. In the domestic dog, with the wide aperture beam, the field size has been calculated as 2.5 mm, lateral magnification of 17.24, and axial magnification of 405 (Murphy and Howland 1987).
  - Indirect ophthalmoscopy with lenses (20 diopter) ± binocular headset: inverted and low magnification. In contrast to direct ophthalmoscopy lateral magnification is calculated as 1.74 and axial magnification as 4.04, approximately 10 times lower magnification than direct ophthalmoscopy (Murphy and Howland 1987). A subsequently wider field of view is also achieved, allowing a more optimal "screen" of the whole fundus to be achieved: with a 48 mm diameter, 20D lens, field size is 12.48 mm, 5 times that of direct ophthalmoscopy (Murphy and Howland 1987).
  - Panoptic ophthalmoscope: upright and moderately magnified. This more recent addition to ophthalmoscopy tools offers an intermediate magnification and field of view, and has an additional advantage of placing the observer more distant from the corneal surface (as opposed to the proximity of the observer's head and hand to the eye in direct ophthalmoscopy and the proximity of the observer's hand holding the indirect lens in indirect ophthalmoscopy). This may offer advantages for both safety of the observer and stress management of the animal during fundic examination.

- Fundus photography can be performed using specialized cameras (Fig. 36.11b), which usually requires consultation with a veterinary ophthalmologist. However, with practice, adequate fundus photography can be achieved with good mydriasis using an indirect lens and a smartphone (Haddock et al. 2013). Using the smartphone as the light source for indirect ophthalmoscopy, videos can be generated of the fundus, and individual frames can be captured for documentation.
- Electroretinography (ERG; Fig. 36.11c, d): for determination of retinal function through measurement of electrical response to lights of different intensity. Handheld, battery powered versions are available for use in the field. Adequate restraint is necessary (manual or sedation), and a darkened facility is optimal to prevent ambient light contamination of the stimuli.
- Optical coherence tomography (OCT, Fig. 36.3e, f): this is a specialized technique that provides near-histologic resolution of the retina in cross-section. The principle is similar to ultrasound, except that light is used instead of sound. This technique requires sedation or anesthesia due to relatively long acquisition times and is impractical at present for use in the field. It is predominantly used as a research tool in current veterinary ophthalmology practice, although with the advent of hand-held technology, its use may become more widespread.

Special Considerations for Wild Canid Clinical Ophthalmic Examination

Due to the anticipated lack of patient compliance, examination of wild canids is typically performed under sedation or anesthesia. Therefore, values obtained for diagnostic tests such as STT, IOP, and ERG should be interpreted with consideration for the anesthetic or sedative protocol used. In dogs, sedation with alpha-2 agonists/opioids or general anesthesia with propofol and isoflurane reduces the ERG a- and b-wave amplitude and also lengthens the implicit time of the responses (Freeman et al. 2013). Sedation with alpha-2-agonists/opioids in dogs also reduces STT values (Sanchez et al. 2006) and reduces IOP (Rauser et al. 2012). Ideally, non-diseased animals administered identical drug combinations will be available as comparators, although this is rarely feasible in clinical practice. The contralateral eye in unilaterally affected animals can also be used as a comparator. Examinations are commonly performed in field conditions, and it may also be difficult to achieve adequate darkness for slit-lamp biomicroscopy and retinal examination. Despite these challenges, diagnostic ophthalmologic examination and accompanying diagnostic testing is feasible in this family of animals (Fig. 36.11) and may be prompted by obvious clinical signs such as ocular discomfort, ocular discharge, opacity (or other changes in globe appearance), or vision disturbances.

Sedation protocols frequently incorporate high doses of alpha-2 agonist sedative agents, which cause miosis in dogs (Artigas et al. 2012) and wolves (Mowat, personal observation). To remedy this, it is recommended to combine 0.5–1% tropicamide with 2.5% phenylephrine in a 50:50 ratio, and administer this topically to each eye at the earliest opportunity during the capture process, and if feasible, before the administration of sedatives. Often multiple doses of mydriatics must be applied to achieve sufficient mydriasis to perform an adequate lens and posterior segment examination. Consideration must be made to the finding in dogs that topical phenylephrine can cause or exacerbate systemic hypertension (Pascoe et al. 1994). Animals should be provided with access to shade for at least 12 h after the examination to mitigate the duration of mydriasis. In *Canis lupus familiaris*, tropicamide is described to last 12 h and phenylephrine 12–18 h (Gelatt et al. 2013), although the duration of a combination of the two drugs has not been described. In addition to mydriasis, application of parasympatholytics will inhibit the activity of ciliary musculature, inhibiting accommodative capacity of the eye. Although the extent of accommodation in canines is hypothesized to be small (approximately 2–3 diopters) (Miller and Murphy 1995), physiologic evidence for ciliary body muscular activity in response to parasympathetic neurotransmitters has been demonstrated (Yoshitomi and Ito 1986). For wild predators, the visual consequences of the paralysis of accommodation should be considered when planning ophthalmic examinations with mydriasis.

Ophthalmic Disorders of Canids

General Considerations

There is a relative paucity of ophthalmic conditions described in the canid family (aside from domestic dogs), which may reflect lower disease frequency compared with domestic canines, or the limited opportunity to examine wild canids. Certain populations are likely to be over-represented in the literature as they represent valuable fur species in some countries (e.g., silver foxes, a melanistic variant of the red fox; *Vulpes vulpes*). Similarly, species that are endangered in the wild and are under species management plans in captivity may also be over-represented in the literature, as husbandry practices and health monitoring are performed on captive individuals frequently, allowing detection of disease that may go unmonitored in either wild individuals or in species with fewer numbers in captivity. In addition, managed species in captivity may also not reside in their native habitat,

and environmental influences on ocular health (such as temperature, relative humidity, ultraviolet light exposure, and novel exposure to locally endemic canid diseases) should be considered. Canids in captivity may also receive routine wellness care including antiparasitic administration, and vaccination against infectious diseases common in domestic dogs. Finally, the lifespan of individuals in captivity is longer than in the wild, which may lead to a higher prevalence of certain diseases with late-life onset in captive individuals.

Inbreeding occurs in a number of endangered canid species, which limits genetic diversity. In particular, inbreeding can restrict variability in the major histocompatibility (MHC) locus, and may thereby impair the ability to combat infectious diseases such as distemper and parvovirus (Hedrick et al. 2003). Inbreeding also serves to increase the likelihood that founder effect mutations will be spread throughout populations. In captive populations, the selective pressure against deleterious ocular gene mutations is likely to be minimal, especially if diseases are identified after breeding has been successful. When species survival planning utilizes inbred captive populations for the purposes of reintroduction, the potential for deleterious heritable ophthalmic mutations should be considered, to limit release of animals with the potential to develop visual deficits, thus affecting their breeding and survival potential in the wild (Mowat 2019).

Despite these factors, it is likely that many conditions affecting wild canids are similar to those seen in the domestic dog. The reader is again referred to veterinary ophthalmology texts in which domestic canid ophthalmic conditions are described in detail, beyond the scope of this chapter (Gelatt et al. 2013; Maggs et al. 2017).

Orbit and Adnexal Disorders

The ocular adnexa are defined as the supporting tissues of the eye and include the eyelids, conjunctiva, third eyelid, lacrimal system, and orbit. Although theoretically, any condition described in domestic dogs could affect wild canids, common adnexal conditions in the domestic canine, that might be predicted to (or have been reported to) affect wild canids are discussed.

Clinical Signs of Adnexal Disorders

Clinical signs of ocular discomfort are common with adnexal disease, as the eyelids, tear film, and conjunctiva are important for corneal lubrication and protection. Signs of ocular discomfort in canines include:

- excessive tearing (epiphora),
- mucoid or purulent ocular discharge,
- blepharospasm (squinting of one or both eyes),
- redness of the eyelids or conjunctiva,
- alopecia or excoriation of the eyelids due to self-trauma,
- opacity of the ocular surface.

Although these signs can signify adnexal disease, ocular discomfort can manifest as a consequence of corneal or intraocular conditions such as uveitis and glaucoma and are therefore nonspecific in nature.

Examination Findings and Diagnostic Testing in Adnexal Disorders

When signs of ocular surface irritation are present, in addition to general clinical examination, eyes should undergo STT of both eyes, followed by fluorescein staining to evaluate the eye for presence of corneal ulceration. If surface disease is not evident, tonometry should also be performed to rule in or out the possibility of intraocular disorders such as uveitis or glaucoma. Further sampling (cytology, fine needle aspiration) may be warranted. Advanced imaging should be considered for extensive lesions, or those involving the orbit.

Common Canine Adnexal Disorders and Their Management

Entropion

Entropion is an inrolling of the eyelids, caused by abnormal eyelid anatomy (excessive eyelid length, cicatricial influences on eyelid margin position). When entropion is extensive or causes corneal disease (including ulceration), surgical management of entropion is recommended. The reader is referred to texts describing appropriate surgical management of entropion (Maggs et al. 2017; Gelatt et al. 2011). Appropriate technique for eyelid margin apposition is critical to prevent corneal trauma related to inadequate surgical technique.

Eyelid Neoplasia

Although most canine eyelid neoplasms are benign compared with malignant (Wang et al. 2019), masses that are rapidly growing should be addressed promptly. Fine needle aspiration can yield important prognostic and/or presurgical information that can guide margin planning. It is recommended to submit excised masses for histopathological evaluation. A maximum of 25% of the eyelid length should be excised for mass removal and primary closure—removal of additional lid length requires utilization of reconstructive techniques.

Neoplasia affecting the orbit is more commonly malignant. Clinical signs include changes in globe position, corneal irritation or ulceration due to exposure, and/or inappetence secondary to impingement of the mandibular ramus on the orbital contents. It is recommended to pursue advanced imaging techniques to evaluate local invasion into surrounding tissues and rule out distant metastasis prior to

formulating a diagnostic and therapeutic treatment plan for suspected orbital neoplasia.

Keratoconjunctivitis Sicca (KCS)

The preocular tear film is essential to maintain corneal health. Deficiency of the aqueous tear component frequently causes corneal discomfort and opacity in domestic dogs. Clinical signs include mucoid ocular discharge, redness, and corneal opacity. Corneal ulcers can occur due to desiccation or self-trauma and can rapidly deepen due to infection and inflammation.

The most common cause of KCS in domestic dogs is immune-mediated (T-cell) destruction of the lacrimal tissue and manifests bilaterally and symmetrically in middle aged dogs. This type of KCS is frequently responsive to cyclosporine. KCS responsive to topical cyclosporine has been reported in a male red wolf (*Canis rufus*). Presenting clinical signs included periocular alopecia and mucopurulent ocular discharge with an initial STT value of 0 mm/min (Acton et al. 2006). Following 1 week of topical 0.2% cyclosporine once daily, discharge was markedly improved, and STT values had increased to >15 mm/min in both eyes. Subconjunctival cyclosporine slow release implants were placed in both eyes under sedation to limit the need for continued daily therapy. Twelve months following implantation, STT values remained >13 mm/min in both eyes. In dogs, these subconjunctival implants have been shown to improve clinical signs of KCS for >480 days, and STT values for a median of 330 days (Barachetti et al. 2015). Yearly monitoring of clinical signs and Schirmer values is recommended, and replacement or augmentation of implants can be implemented as needed.

Conjunctival Disease

Conjunctival disease is common in domestic dogs and can be broadly divided into noninfectious and infectious forms. Non-infectious forms include inflammation (conjunctivitis) and neoplasia. Conjunctival disease in wild canid species has been reported with some frequency, usually in association with infectious etiologies as described below.

A species of bacteria (*Arcanobacterium phocae*) has been described associated with conjunctivitis and periocular pyoderma in the blue fox (*Vulpes lagopus*) in Finland and other European countries (Nordgren et al. 2014). This bacterium has also been associated with superficial dermal infections in sea and freshwater mammals (Nonnemann et al. 2017). *A. phocae* is a Gram-positive coccobacillus that occasionally morphs into a short rod and is susceptible to all tested antibiotics (Johnson et al. 2003), although clinical response to parenteral broad-spectrum antibiotics was reported as poor. The disease manifests in foxes initially as serous ocular discharge and anorexia, progressing to purulent discharge and subsequent periocular pyoderma. Clinical sequelae noted were entropion (3/19 cases), keratoconjunctivitis (19/19 cases), and less commonly uveitis or retrobulbar cellulitis. Lymphoplasmacytic conjunctivitis with neutrophilic inflammation was present on histopathology. *A. phocae* was cultured in 6/19 cases and in 6/11 cases with purulent ocular discharge, commonly as part of a mixed bacterial culture with *Staphylococcus* and *Streptococcus* species. *A. phocae* was present by PCR identification in all foxes and viruses were not identified. *A. phocae* was detected in significantly more diseased foxes compared with healthy foxes (Nordgren et al. 2014). Husbandry practices such as high-density housing may contribute to the incidence of disease, but the epidemiology is not fully understood.

Bilateral mucopurulent ocular discharge can be an early sign of distemper virus infection, related to the viral replication in conjunctival goblet cells. Although cytologic evidence of viral inclusions can occur in canine distemper, the correlation with more sensitive methods (PCR/immunofluorescence) is relatively poor, and it is not recommended that cytology be used exclusively for diagnosis (Athanasiou et al. 2018). All canidae, including wild species are susceptible to distemper virus infection [for a review, see Deem et al. (2000)]. Similar to domestic canids, ocular signs in wild canids are typically associated with other systemic signs including diarrhea, emaciation, neurologic signs, and mortality (Deem et al. 2000; Woo et al. 2010).

Foxes (*Vulpes* spp.) and wolves (*Canis* spp.) are reported to be susceptible to the conjunctival parasites *Thelazia callipaeda* and *Thelazia californiensis* (Otranto et al. 2004, 2007, 2009; Seixas et al. 2018; Cabanova et al. 2018). Parasites are transmitted to the eye by secretophagous flies (*Diptera*). Clinical signs range from mild (conjunctivitis, epiphora) to severe (keratitis, corneal ulceration). The disease is most prevalent in Europe and Asia. Wild canids may provide a reservoir for infection of domestic canines and vice versa (Otranto et al. 2009; Cabanova et al. 2018). Treatment of *Thelazia* spp. includes mechanical removal and/or use of ectoparasiticides such as moxidectin or imidacloprid (Tahir et al. 2019).

Anterior Segment Disorders

Cornea

Corneal disorders in dogs can be broadly categorized into nonulcerative and ulcerative forms.

Clinical Signs of Corneal Disease

Clinical signs of ulcerative corneal disease are commonly those associated with discomfort, as detailed previously in section "Orbit and Adnexal Disorders." Purulent or mucopurulent ocular discharge frequently occurs if there is corneal infection or inflammation.

Examination Findings and Diagnostic Testing in Corneal Disease

Careful examination of the adnexa should be performed to determine if corneal disease is related to adnexal disease. The extent of corneal vascularization can indicate the chronicity of disease—vascularization is initiated at the time of trauma and can take days to weeks to progress to the axial cornea. When corneal disorders are suspected, STT and fluorescein staining will provide useful information. In addition, sampling of suspected inflamed or infected ulcers for bacterial/fungal culture and cytology will help to inform treatment decisions.

Nonulcerative Keratitis Causes and Treatment

Chronic Superficial Keratitis (CSK; Pannus)

A common condition affecting the domestic dog is chronic superficial keratitis (CSK; also known as pannus), which is presumed to have a hereditary component (Barrientos et al. 2013; Cheng et al. 2016), and is particularly common in German Shepherd dogs and Greyhounds. The condition is characterized by bilateral, laterally focused areas of superficial corneal vascularization and pigmentation. Patients typically show fewer clinical signs of ocular pain than with ulcerative keratitis. The condition is exacerbated by exposure to ultraviolet radiation and high altitude. Chronic superficial keratitis mirroring the lesions seen in domestic dogs has been described in a 6.5-year-old male Mexican wolf (*Canis lupus baileyi*) (Harwell et al. 1985). Clinical signs were bilateral serous ocular discharge with no blepharospasm. Clinical examination revealed conjunctival hyperemia, superficial corneal vascularization on the dorsal cornea and pigmentation on the ventral aspect. Schirmer tear test was reported as normal and fluorescein staining was negative. Initial treatment with subconjunctival dexamethasone (1 mg) resulted in partial regression of vascularization and pigmentation. To achieve longer-term control, the corneas were treated with beta radiation (strontium 90–6000 rads in 2 sites per cornea). This resulted in resolution of vascularization and reduction in pigmentation. Underlying etiology was not determined, although the wolf was housed in a partially shaded enclosure with year-round sunshine, indicating that ultraviolet light exposure may have been a contributing factor.

Corneal Edema

Corneal edema can be a manifestation of corneal disease (e.g., corneal ulceration) or intraocular disease (e.g., uveitis). It is important to note that there is an infectious cause of diffuse corneal edema that may have relevance for wild canid ophthalmology. In domestic dogs, infection with canine adenovirus-type 1 (CAdV-1; the cause of infectious canine hepatitis) can cause corneal edema (Andrew 2008). Other systemic signs of infection include depression, anorexia, jaundice, and petechiae. Ocular clinical signs include mild conjunctival hyperemia (presumed due to mild anterior uveitis), varying degrees of anterior uveitis, and delayed onset corneal edema that develops 1–3 weeks following infection. Natural infection results in corneal edema in approximately 20% cases, and 0.4% of dogs vaccinated with modified live CAdV-1 vaccines can develop corneal edema. Edema is attributable to immune complex (arthus type III) deposition. Incidence with CAdV-2 vaccines is substantially lower. A recent report in domestic canines indicates that when multiple viral infections (such as Canine Distemper Virus, CAdV-1, Canine papillomavirus) are diagnosed in the same individual, corneal edema remains exclusively associated with CAdV-1infection. Figure 36.12 shows a fox kit (*Vulpes vulpes*) found moribund in the North Eastern United States. The fox was euthanized and histopathologic lesions consistent with distemper were identified. However, additional testing for CAdV-1 was not reported, and the bilateral corneal edema evident might support this as an additional co-infection.

Ulcerative Keratitis: Causes and Treatment

Corneal ulcers are common in domestic dogs and can become secondarily infected with bacteria (and in rarer cases fungi), necessitating medical and sometimes surgical intervention. Onset of ulceration is associated with clinical signs of discomfort (squinting, ocular discharge, redness). Proteases released by bacteria or inflammatory cells can contribute to rapid progression and stromal loss. Diagnostic testing, including obtaining samples for cytology, and bacterial (± fungal) culture and antibiotic drug sensitivity testing is encouraged. Because frequently administered topical medications are typically required to treat bacterial infections, systemic antibiotics are sometimes considered, to limit animal handling for topical medication application. However, very few systemic antibiotics penetrate the tear film and achieve minimum inhibitory concentrations, and therefore are typically not effective in treating corneal bacterial infection unless the cornea is substantially vascularized. Orally administered tetracyclines (such as doxycycline and minocycline) can penetrate the tear film in humans (Doughty 2016) and therefore could be considered, provided there is bacterial sensitivity to that class of antibiotics. A secondary advantage of tetracyclines are their antiproteolytic activity through their inhibition of matrix metalloproteinases and their anti-inflammatory activity (Perret and Tait 2014). Subconjunctival injection of parenteral antibiotics may provide an alternative option, although few studies have evaluated the pharmacokinetics of this approach, and drugs may only be delivered at therapeutic levels for a brief period of time. In addition, there is much focus in medicine to develop more options for sustained topical ocular drug delivery which may have application in management of canid corneal disease (Jumelle et al. 2020).

Fig. 36.12 Bilateral corneal edema in a wild fox (*Vulpes vulpes*). The fox kit was found moribund in the North Eastern USA and was euthanized. Ocular examination revealed marked bilateral corneal edema; interior structures could not be visualized although an intact dazzle reflex was present. Histopathology (images not available) revealed systemic lesions consistent with canine distemper virus infection. Image courtesy of Dr. Stephanie Pumphrey, Tufts Cummings University School of Veterinary Medicine

In general, similar treatment modalities to domestic dogs are appropriate, and if an ulcer is non-healing or progressive, prompt consultation with a veterinary ophthalmologist is recommended, as deep ulcers can rapidly progress to perforation. Surgical treatment (most commonly conjunctival pedicle graft placement) should be performed using magnification. A deep stromal ulcer presumed to be traumatic in origin was diagnosed in a Fennec fox (*Vulpes zerda*) and successfully treated surgically using a rotational flap conjunctival graft (Fig. 36.13). Scant growth of an alpha-hemolytic *Streptococcus* species was present on aerobic bacterial culture. Medical management included topical antibiotics at high frequency (fluoroquinolone, 4–6 times daily), topical mydriatics (atropine ointment once daily), and systemic pain management (non-steroidal anti-inflammatories and opioids as indicated). Healing was uneventful. Case information courtesy of Jenessa Gjeltema and Jb Minter, North Carolina State University.

Lens

The crystalline lens is avascular and transparent to facilitate transmission of focused rays of light to the retina; diseases commonly cause opacity (i.e., cataract) of the lens. Cataract has been reported in wild canid species from captive populations in the USA and Europe. Hereditary lens dislocation (luxation) has been reported in domestic dogs, but no reports exist in wild canids.

Clinical Signs of Lens Disorders

Cataract will cause visual disturbance when it affects a large proportion of the lens. Unilateral visual disturbance is difficult to determine in domestic dogs, therefore bilateral disease

Fig. 36.13 Conjunctival graft surgery to address a deep stromal ulcer of the left eye in a fennec fox (*Vulpes zerda*). A deep stromal ulcer with a malacic base was identified, associated with mucopurulent ocular discharge (**a**). A rotational flap conjunctival graft was performed, shown here at 10 days postoperative (**b**). Healing and graft incorporation into the corneal stroma had progressed as expected at 4 weeks postoperatively (**c**), and 12 weeks following surgery only a small, minimally vascularized corneal leukoma remained (**d**). Images courtesy of Dr. Jenessa Gjeltema, North Carolina State University

is usually necessary for clinically detectable vision impairment. A white opacity of the lens can be observed in more advanced forms of cataract, even from a distance.

Examination Findings and Diagnostic Testing for Lens Disorders

A white opacity will be present in the lens with cataract. Distant examination (transilluminator or direct ophthalmoscope) can be used to visualize the tapetal reflection: this is useful to observe the extent of blockade of the tapetal reflection created by a cataract. Advanced forms of cataract can be associated with uveitis, because of release of foreign lens proteins into the anterior chamber. Clinical findings can include low IOP, miosis, iridal hyperpigmentation, aqueous flare, and in severe cases, visible anterior chamber cells (hypopyon or hemorrhage) and/or fibrin. Secondary glaucoma (resulting in increased intraocular pressure) can occur as a consequence of chronic lens-induced uveitis in domestic dogs.

Primary Cataract: Causes and Treatment

Although breed-related cataract is common in domestic dogs, the underlying genetics of breed-associated cataract are not currently well defined. The only gene definitively associated with cataract formation in specific purebred domestic dog

breeds (Australian Shepherd dogs, Boston Terriers, and Staffordshire Bull Terriers) is a mutation in the gene *HSF4* (Mellersh et al. 2007, 2009). Inbreeding in certain captive canids could predispose to primary cataract formation; high incidence of cataract formation in the absence of other predisposing factors and ocular abnormalities in a specific breeding group should be explored as a potential hereditary disease.

Phacoemulsification and lens implantation has been performed to treat bilateral, mature, vision impairing cataracts of suspected genetic etiology in three sibling gray wolves (*Canis lupus*). Cataracts were noted at approximately four months of age in three wolf pups in a litter of four born in captivity. Pups were nursed normally by the dam, and no other systemic health concerns were identified in pups or dam that could have predisposed to cataract formation. Dam and sire were unaffected. All three affected wolves were male, and the related female pup had incipient (non-vision threatening) cataracts which did not progress with follow-up. The breeding pair had not bred previously, and because of the potential for genetic etiology of cataract, the pair were not subsequently bred again. One affected male also suffered from pulmonic stenosis which was treated with balloon valvuloplasty. Pupil responses and dazzle reflex were present in all affected eyes. Cataract surgery was performed at seven months of age, following a period of acclimation to topical ophthalmic medication application. Electroretinography was performed with full mydriasis preoperatively under general anesthesia (Retiport 32, Roland Consult, Brandenburg, Germany, with Kojiman electrode). The following settings were used in two wolves with no dark adaptation (due to anesthesia considerations): 0 dB flash intensity at 0.3 Hz with no background light, average of eight responses, high pass filter 1 Hz, low-pass filter 300 Hz. Results showed a mean electroretinogram a-wave amplitude (both eyes) of 58.2 and 24.5 μV and a mean b-wave amplitude (of both eyes) of 70.5 and 70.2 μV. Ocular b-mode ultrasonography did not reveal any retinal, vitreal, or lens abnormalities precluding surgery. Routine phacoemulsification with placement of 41 diopter foldable intraocular lenses was performed. Postoperatively, animals received oral non-steroidal anti-inflammatories (carprofen) and oral antibiotics (cephalexin) in addition to topical ocular dorzolamide (antiglaucoma) three times daily, and steroid-antibiotic combination (neomycin polymyxin dexamethasone) four times daily. Wolves did not wear an Elizabethan collar, but were housed singly for approximately 2 weeks. Oral and topical medications were tapered with improvements in ocular health. At 6 months postoperatively, intraocular pressures were controlled with mild corneal fibrosis, no aqueous flare and moderate corneal degeneration, maintained on every other day topical antibiotic-steroid. Long-term yearly follow-up was performed since surgery in 2012 (at least 5 years), and wolves remained visual. Case description courtesy of Dr. Wendy Townsend, Purdue University College of Veterinary Medicine.

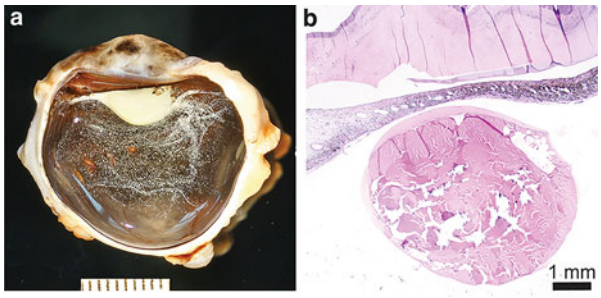

Fig. 36.14 Cataract in an African wild dog (*Lycaon pictus*) presumed secondary to uveitis or trauma. Pigmentary keratitis, a small lens with cataract and asteroid hyalosis are visible using gross histology (**a**). Histology revealed a preiridal fibrovascular membrane, hypermature cataract (note focal dark blue areas of mineralization) within a small lens (**b**). The posterior segment revealed histologic evidence of chronic secondary glaucoma (not shown). Images courtesy of Dr. Richard Dubielzig, Comparative Ocular Pathology Laboratory of Wisconsin

A bilaterally blind 7-year-old coyote (*Canis latrans*) affected with cataract in Texas was published as a single case report (Pence and Meinzer 1977). Anecdotally, additional coyotes in the surrounding area were also visually impaired, although clinical or histologic data were not presented. Histology revealed unilateral corneal vascularization and ulceration, iris hyperpigmentation, a mature cataract, and mild lymphoplasmacytic anterior uveitis and vitritis. Underlying etiology was not determined for the cataract. The contralateral eye had phthisis bulbi, presumed to be secondary to penetrating trauma as an orbital foreign body was found. The etiology of cataract was hypothesized to be genetic, but further studies have not been performed to support this.

Secondary Cataract: Causes and Treatment

Similar to dogs, cataract formation secondary to other conditions is described in some wild canids. Any condition that disrupts the intraocular environment has the potential to interfere with lens metabolism and cause cataract. Common secondary lens conditions in the domestic canine that may affect wild canids are included in the sections below.

Uveitis

Unilateral cataract has been identified, related to uveitis and glaucoma in an African wild dog (*Lycaon pictus*, Fig. 36.14), although the causative nature of the cataract was uncertain due to the advanced stage of cataract at the time of enucleation and histopathological evaluation. It is possible that the cataract formed secondary to uveitis or trauma, or that uveitis was a consequence of the cataract, as hypermature cataracts will leak substantial protein into the aqueous humor, resulting in inflammation.

Nutritional Imbalance

Cataracts of presumed nutritional etiology have been described in gray (Timber) wolves (*Canis lupus*) (Vainisi et al. 1981). Initial findings in wolf pups ($n = 5$) raised on commercial milk replacer from the age of 9 days to beyond 30 days found that two pups had partial resolution after diet normalization (dry dog food) at 1 year. Histology in six eyes (three pups) revealed iris hyperpigmentation, evidence of anterior uveitis, and cataractous lenses with liquefaction and loss of normal architecture. Subsequent prospective studies were completed to investigate the cause of the cataract. Pups raised on the commercial milk replacer developed cataract, whereas pups allowed to remain with the mother did not. When normal diet was introduced at an earlier stage, progression to mature cataract did not occur, and cataracts regressed to faint nuclear opacities. Addition of animal fat (lard) and/or vitamin C to commercial milk replacer did not prevent cataract formation. The milk replacer and milk from a lactating wolf were compared, and marked disparity was found in protein content (liquid analysis: 5.6% in milk replacer versus 12.6% in wolf milk). A particular disparity was found in arginine (liquid analysis: 1.24% in milk replacer versus 7.34% in wolf milk) and methionine (liquid analysis: 0.32% in milk replacer versus 2.65% in wolf milk), although numerous other proteins were lower in concentration in milk replacer than wolf milk. Supplementation of milk replacer with arginine ($n = 3$), but not methionine ($n = 1$) prevented cataract formation. Lactose supplementation also prevented cataract formation ($n = 2$). It was hypothesized that lactose may facilitate the absorption of arginine.

Infectious Disease

The protozoan *Encephalitozoon cuniculi* has been associated with uveal arteritis and cataract in farmed Arctic foxes (*Vulpes lagopus*) in Norway (Arnesen and Nordstoga 1977). Systemic lesions include polyarteritis nodosa in young foxes, manifesting as growth retardation, ataxia and paresis, and in some cases seizures. Some animals were noted to be blind clinically, and on histopathology ($n = 17$ eyes, 10 animals), arteritis was found affecting the short and long posterior ciliary arteries in the anterior and posterior uvea. Cataracts of varying stages were also documented, frequently associated with lens capsule rupture. Modified Gram stain revealed slightly elongated Gram-positive organisms 1–3 μm in length within artery walls and cataractous lenses.

Retinal Degeneration

Cataracts presumed to be associated with progressive retinal atrophy have been described in three related Fennec foxes (*Vulpes zerda*) (Granitz et al. 1999). Cataracts ranged from incipient to late immature/early mature and different stages of cataract maturity were present in the same individual animal (Fig. 36.15). Intraocular pressure was 10 mmHg in mature cataract affected eyes, compared with a range between 10–15 mmHg in three unaffected animals. No signs of lens-induced uveitis were detected by slit-lamp biomicroscopy. The two affected foxes had not been administered any milk replacement products in early development, limiting the possibility of a nutritional etiology. There was no known history of toxicant exposure, trauma, or metabolic derangements. Blood glucose levels in the two affected animals were normal compared with three other sampled foxes with normal ophthalmic examination findings. The cataracts were presumed to be related to retinal degeneration (discussed below in section "Posterior Segment Disorders"). Case information courtesy of Dr. med. Vet. Uwe Gränitz, Tierärtzliche Praxis für Augenheilkunde, Chemnitz, Germany.

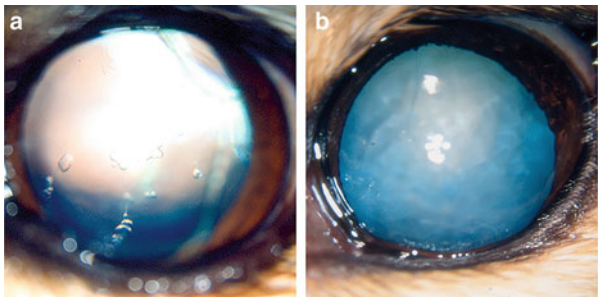

Fig. 36.15 Cataracts in adult fennec foxes (*Vulpes zerda*) associated with progressive retinal atrophy. Cataracts in this related group of individuals ranged from incipient punctate vacuoles in the anterior and posterior cortex (**a**) to late immature/early mature cataract (**b**). Both eyes shown had no detectable uveitis and absent retinal function on electroretinography. Images courtesy of Dr. med. Vet. Uwe Gränitz, Tierärtzliche Praxis für Augenheilkunde, Chemnitz, Germany

Uvea

The uvea includes the iris, ciliary body, and the choroid posteriorly. The most common condition affecting the uvea in domestic dogs is uveitis (inflammation).

Clinical Signs of Uveitis

Clinical signs of uveitis include ocular redness, corneal edema (blue/gray haze to eye), ocular discharge, miosis, and/or dyscoria.

Examination Findings and Diagnostic Testing in Uveitis

Cells, protein, and blood can collect in the anterior chamber and be visible as aqueous flare or cell consolidation. Secondary glaucoma is a common sequel of chronic uveitis. Intraocular pressure should be monitored in eyes with uveitis. Aqueocentesis can be utilized in rare cases where exfoliative ocular neoplasia is suspected (e.g., lymphoma). There is minimal utility in aqueocentesis for diagnosis of inflammatory or infectious disease in domestic dogs (Linn-Pearl et al. 2015). Because an underlying cause is present in many cases, further systemic diagnostic testing in cases of uveitis is commonly indicated.

Uveitis: Causes and Treatment

Uveitis occurs commonly in association with intraocular or systemic diseases, although idiopathic causes represent a substantial proportion of cases described in the literature (Bergstrom et al. 2017). Ocular or intraocular causes of uveitis include blunt or sharp trauma, reflex uveitis secondary to ulcers, lens-induced (secondary to lens trauma or cataract), neoplasia (primary ocular tumors, metastatic or multicentric neoplasia, or paraneoplastic syndromes), and retinal detachment. Systemic causes include various infections, neoplastic, toxic, metabolic and immune-mediated conditions (Maggs et al. 2017). In wild canids, uveitis related to infectious or traumatic etiologies would be predicted to be the most common forms, although no definitive reports exist.

Treatment of uveitis should address any specific underlying causes using the appropriate topical or systemic medications. Symptomatic therapy is also commonly utilized, which includes systemic anti-inflammatories (non-steroidal anti-inflammatories or corticosteroids, every 12–24 h, tapering with effect), topical anti-inflammatories (non-steroidal anti-inflammatories or corticosteroids, every 6–24 h, tapering with effect), and (if secondary glaucoma is absent) topical ocular cycloplegics (atropine, every 8–24 h, to effect). Topical ophthalmic medication administration may be challenging in wild species, therefore subconjunctival injection of long acting corticosteroids could be considered (e.g., 10 mg methylprednisolone acetate, reported to last at least 21 days) (Regnier et al. 1982). Side effects such as adrenocortical suppression and poor healing of corneal abrasions or ulcerations should be considered when adopting this approach.

Glaucoma

Glaucoma is defined as progressive loss of the ganglion cells of the retina. In domestic dogs, this is most commonly associated with increased IOP.

Clinical Signs of Glaucoma

Domestic dogs with glaucoma typically present acutely with unilateral signs of ocular discomfort (ocular redness, squinting, ocular discharge), corneal edema (gray/blue hue to the cornea), mydriasis, blindness (when unilateral may be difficult to identify even in pet dogs). Because the pain in glaucoma is more diffuse in origin, overt signs of ocular pain may be absent, and lethargy may be a defining clinical sign.

Examination Findings and Diagnostic Testing in Glaucoma

Acute glaucoma is commonly associated with acute onset elevation in IOP, diffuse corneal edema, mydriasis, and optic nerve swelling. Wedge-shaped areas of retinal necrosis can occur secondary to choroidal ischemia. Chronic glaucoma can have many sequelae including phthisis bulbi, buphthalmos (and corresponding corneal disease due to exposure), lens subluxation, cataract, and retinal degeneration.

Glaucoma: Causes and Treatment

Glaucoma is classified into primary (hereditary) forms, common in purebred dogs, and secondary forms. Secondary forms occur most commonly as a consequence of uveitis, and this would be anticipated to be the most prevalent cause in wild canids, due to the association between both trauma and infectious agents (common entities in wildlife) and uveitis. Primary glaucoma has not been described in wild canids, but uveitis and presumed secondary glaucoma have been described, related to cataract formation (see previous section "Lens").

If identified in the acute stage, medical treatment could be considered to attempt to preserve sight. Typical medications in domestic dogs involve frequent (2–3 times daily) application of topical medications to reduce intraocular pressure (e.g., prostaglandin analogues, beta blockers, carbonic anhydrase inhibitors). Although side effects are rare, bradycardia has been reported in domestic dogs secondary to the use of topical beta blockers (Smith et al. 2010) and local irritation and keratitis have been reported with the use of topical carbonic anhydrase inhibitors [for a review, see Maslanka (2015)].

The frequency of application for topical ophthalmic antiglaucoma medications may not be feasible in wild canids. Use of oral carbonic anhydrase inhibitors is associated with significant systemic side effects in domestic dogs (Maslanka 2015). Newer advances in implant-based drug delivery may offer novel alternatives in the future, delivering antiglaucoma drugs via inert subconjunctival implants, nanoparticles or gelling ophthalmic solutions (Yadav et al. 2019). Alternatively, surgical options for intraocular pressure reduction have been described (Komaromy et al. 2019), although the relatively short duration of IOP control and intensity of medical management in the immediate postoperative period limits the long-term benefit of these approaches for wild canids at present.

In chronic cases, if intraocular pressure remains high for a prolonged period, the eye may swell (buphthalmos), causing corneal disease (corneal vascularization, ulceration), cataract, and/or significant degeneration of the retina. Sight restoration at this stage is not possible, and if the eye is causing discomfort, enucleation should be considered.

Posterior Segment Disorders

The posterior segment includes the vitreous, retina, and choroid.

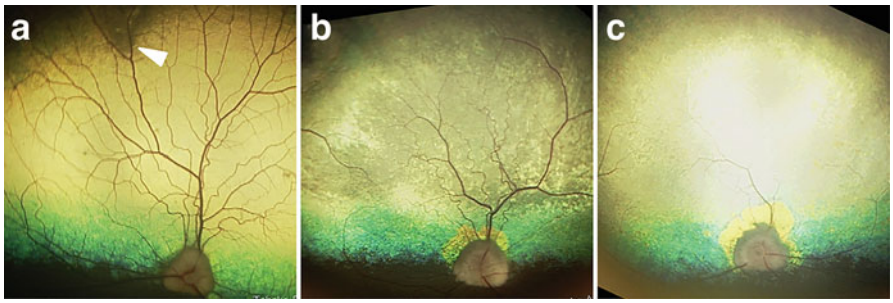

Fig. 36.16 Suspected hereditary retinal degeneration in adult Mexican wolves (*Canis lupus baileyi*). Of the four wolves examined, one had normal fundi apart from a small unilateral focal peripheral area of altered tapetal reflectivity (arrowhead in **a**). The other three wolves had bilateral multifocal coalescing areas of tapetal hyperreflectivity (**b**), particularly centered around the optic nerve head, and vascular attenuation. One wolf had bilateral diffuse tapetal hyperreflectivity and more prominent retinal vascular attenuation (**c**). Images courtesy of Michigan State University Ophthalmology Service

Clinical Signs of Posterior Segment Disorders

Vision impairment is the primary clinical sign in diffuse retinal disorders affecting both eyes. Unilateral or focal disease may not result in vision impairment. Cataract can be a sequel to retinal degeneration and may be initially interpreted as the cause of vision loss.

Examination Findings and Diagnostic Testing in Posterior Segment Disorders

Fundus examination following pharmacologic mydriasis is recommended when evaluating animals for vision loss. Evaluation of menace response, dazzle reflex, and pupillary light reflexes may be informative, but may also be inhibited by the stress of handling. If retinal dysfunction is debated on fundic examination, or if the view of the fundus is impaired by ocular opacity, electroretinography is indicated to objectively assess retinal function.

Inherited Retinal Disorders: Causes and Treatments

Mutations in genes affecting retinal structure or function are detected with relative frequency in purebred domestic dogs, with over 20 causative genetic mutations described to date (Palanova 2016; Petersen-Jones and Komaromy 2015). The reason for the relative frequency of genetic retinal disorders is unknown, but is hypothesized to be related to inbreeding within breeds to maintain or enhance certain physical traits consistent with breed standards. Because endangered captive canids must commonly be maintained in small groups and with limited breeding individuals available, there is potential for the propagation of genetic mutations causative for retinal disease (Mowat 2019). Detection, monitoring, and elimination of these potentially blinding traits is essential if reintroduction efforts are to be successful.

Hereditary retinal disorders in dogs most commonly present as bilaterally symmetrical, slowly progressive vision loss, usually manifesting initially as night blindness (rod photoreceptor dysfunction) and progressing to night and day blindness (rod and cone photoreceptor dysfunction). The majority of genes mutated in domestic canine retinal degenerative disorders are involved in the development or function of the photoreceptors or retinal pigmented epithelium. In many purebred domestic dog breeds, the causative mutation for retinal degeneration has been identified and genetic tests are available to guide breeding efforts. To date, no causative genes have been identified for wild canid retinal degenerative disorders.

There are no published effective therapies to address inherited retinal degenerative disease in dogs, although progress in gene augmentation has been made in purebred dog models of human retinal disease (Petersen-Jones and Komaromy 2015). Eliminating causative mutations from the breed line is the primary goal to address hereditary retinal disorders population-wide.

A group of four captive Mexican wolves (*Canis lupus baileyi*) were examined for suspected retinal disease-causing vision impairment. One wolf had minimal fundus abnormality (Fig. 36.16a), whereas the other three had diffuse/multifocal areas of tapetal hyperreflectivity and retinal vascular attenuation indicative of retinal degeneration (Fig. 36.16b, c). The mutation in the gene *prcd* (Zangerl et al. 2006) was excluded as causative for the retinal degeneration by genomic DNA sequencing of affected and unaffected wolves (Petersen-Jones, unpublished observation).

A potential hereditary retinal degenerative disease was identified in three related fennec foxes (*Vulpes zerda*) (Fig. 36.17) (Granitz et al. 1999). Retinal degeneration and/or extinguished retinal function was identified in a male fox (at least 8 years old) and two of his male offspring (littermates, 4.5 years old). The female littermate offspring examined (4.5 years old) was unaffected, as was the dam (at least 8 years old). Fundus examination in some cases was limited by cataract formation (see previous section "Lens"), but when fundus examination was feasible, normal foxes had

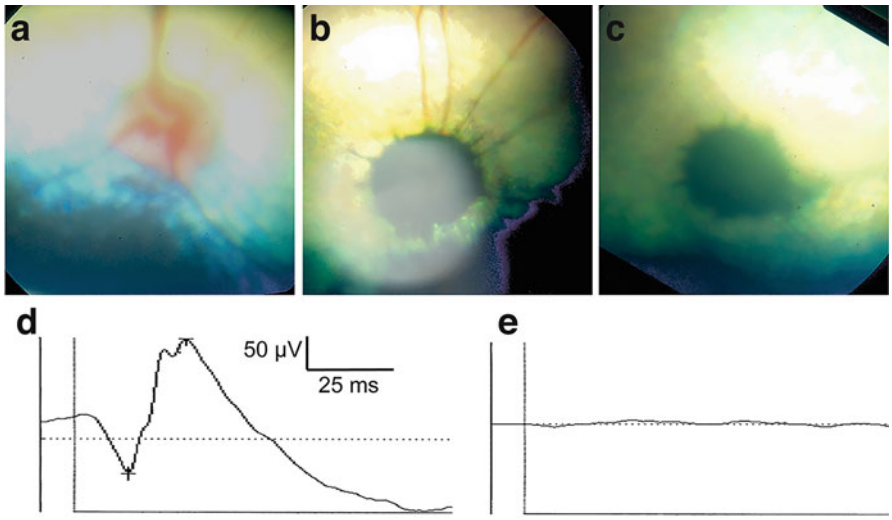

Fig. 36.17 Retinopathy in a group of related fennec foxes (*Vulpes zerda*). Normal central fundus appearance is similar to other canids, with a dorsally located tapetum, myelinated optic nerve head and incomplete venous circle on the optic nerve, with three main venule branches serving the superficial retina (**a**). Affected foxes had moderate vascular attenuation with marked optic nerve degeneration (**b**, artifact on lower aspect of image from incipient cataract obscuring view) or marked vascular attenuation with marked optic nerve degeneration (**c**). Electroretinography of an unaffected fennec fox with distinct a- and b-waves (**d**), compared with no detectable responses in an affected fox (**e**). Images courtesy of Dr. med. Vet. Uwe Gränitz, Tierärtzliche Praxis für Augenheilkunde, Chemnitz, Germany

a normal canid-like appearance (Fig. 36.17a), whereas blind foxes had varying degrees of retinal vascular attenuation and optic nerve degeneration (Fig. 36.17b, c). Electroretinography performed under sedation (medetomidine 100 µg/kg and ketamine 4 mg/kg intramuscularly) showed normal dog-like waveforms in unaffected foxes (Fig. 36.17d; mean a-wave amplitude of 2 eyes: 64.5 µV, mean b-wave amplitude of 2 eyes: 148.2 µV) and extinguished responses in affected foxes (Fig. 36.17e). Based on the relationships between affected individuals, a hereditary etiology was proposed; an X-linked mode of inheritance may be responsible based on the presence of affected males and lack of affected females.

A suspected hereditary retinal degenerative disorder has also been identified in red wolves (*Canis rufus*) (Acton et al. 2000; Seeley et al. 2016; Ring and Kearns 1997). Red wolves are a critically endangered species, and only approximately 300 remain in captive or managed populations throughout North America. The captive population was created from a small number of individuals in the 1970s, and therefore the current population is substantially inbred, with reduced genetic diversity. In contrast to the normal canid-like fundus appearance in unaffected wolves (Fig. 36.18a), retinopathy is characterized by tapetal hyperreflectivity and vascular attenuation, with patchy discoloration and/or loss of the tapetum and frequently, substantial optic nerve degeneration (Fig. 36.18b). Males are more frequently affected than females, indicating a possible X-linked mode of inheritance (Mowat, unpublished observations). Genetic studies have excluded a mutation in *cGMP PDE6B*, causative for retinal degeneration in the Irish Setter breed of domestic dog (Aguirre et al. 1999), and also a mutation in *RPGR*, causative for X-linked hereditary retinal degeneration in the Samoyed, Siberian Husky and mixed-breed domestic dog breeds (Zangerl et al. 2007).

Secondary Retinal Disorders: Causes and Treatment

Secondary disorders affecting the retina are commonly related to systemic hypertension, inflammation, tumors, and/or infection of the neighboring choroid. Infectious causes of uveitis should be considered if signs of inflammation are noted (e.g., white colored lesions in the nontapetal fundus, vitreal inflammation, subretinal exudate), particularly when associated with signs of anterior uveitis. Diagnostic testing should be fully utilized to facilitate specific treatment of any underlying cause, particularly in the face of an outbreak of disease affecting multiple animals. Common secondary disorders in domestic dogs, or those reported in wild canids are listed below.

Infectious Causes of Secondary Retinal Disorders

Systemic mycoses (such as *Blastomyces*, *Histoplasma*, *Cryptococcus,* and *Coccidioides* species) commonly cause chorioretinitis in domestic dogs. Although they can also cause anterior uveitis, the choroid appears to be preferentially affected.

Viral diseases (such as distemper, herpesvirus, and rarely, rabies virus) have infrequently been reported to cause retinal disease. A publication described that in a group of 15 rabies infected red foxes (*Vulpes vulpes*), three foxes had evidence

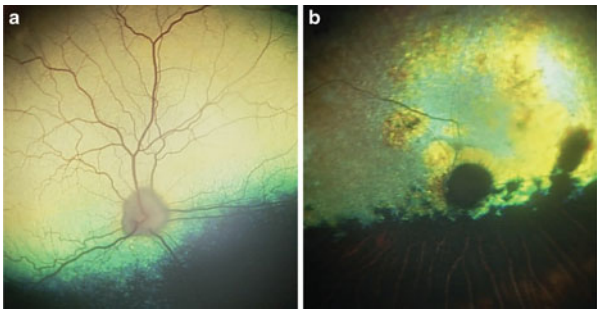

Fig. 36.18 Retinopathy in red wolves. A 9-year-old unaffected female red wolf fundus shows a typical canid-like vascular tree, optic nerve and tapetum (**a**). In contrast, a 6-year-old affected male red wolf fundus shows marked vascular attenuation, tapetal hyperreflectivity and focal coalescing areas of altered tapetal coloration, with marked optic nerve degeneration (**b**). Images courtesy of Freya Mowat, unpublished

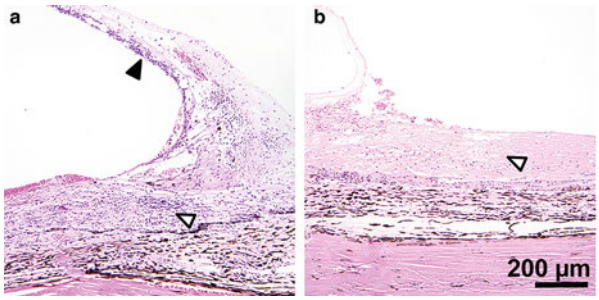

Fig. 36.19 Retinal detachment and inflammation in an African wild dog (*Lycaon pictus*). (**a**) Both eyes were affected with multiple retinal detachments with significant diffuse retinal atrophy (black arrowhead). There was significant choroidal lymphoplasmacytic infiltrate in some areas (white arrowhead). (**b**) Adjacent areas had choroidal and subretinal fibrosis (white arrowhead). Images courtesy of Dr. Richard Dubielzig, Comparative Ocular Pathology Laboratory of Wisconsin

of ocular Negri bodies typical of rabies (Ravisse and Blancou 1981). Negri bodies were identified in the ganglion cells of the retina, and in sympathetic ganglia close to the optic nerve. Uveitis, retinitis, and ganglion cell rabies antigen have been described in a case report of rabies in a human (Haltia et al. 1989). Clinically, there were multiple neurologic deficits, and post-mortem histopathologic examination identified severe encephalitis and multifocal neuritis.

Parasitic migration can cause retinal disease (e.g., *Toxocara* and *Angiostrongylus* spp.). An African wild dog (*Lycaon pictus*), imported from the Netherlands to Sweden 6 months previously, developed bilateral visual deficits. Eyes were submitted post-mortem for histopathological analysis. Both eyes showed retinal detachment, multiple retinal tears and diffuse retinal atrophy, most prominent in the periphery. There were multiple small choroidal neovascular foci. One eye showed lymphoplasmacytic and granulomatous retinitis and choroiditis (Fig. 36.19a) with multifocal areas of dense fibrosis (Fig. 36.19b). Anterior and posterior subcapsular cataract was assumed to be secondary to inflammation. Pathology was suggested to be consistent with infection or parasite migration although no organisms were observed. Case details courtesy of Dr. Richard Dubielzig, Comparative Ocular Pathology Laboratory of Wisconsin.

Tick-borne diseases (e.g., *Ehrlichia*, *Rickettsia* and *Anaplasma* spp.) are common causes of uveitis in domestic dogs (Massa et al. 2002). One paper determined that 8.9% of dogs with ocular forms of *Ehrlichia canis* had fundus lesions manifesting as retinal vascular tortuosity, chorioretinitis, retinal degeneration, optic nerve atrophy, or serous/hemorrhagic/exudative retinal detachment (Komnenou et al. 2007)

Non-infectious Causes of Secondary Retinal Disorders

Dietary deficiency of either vitamin A (Lanska 2010) or Vitamin E (Davidson et al. 1998) can cause visual deficits and blindness as a result of retinal degeneration. Commercial dog foods contain adequate levels of nutrients, but consideration for possible nutrient deficiency should be made if captive animals are fed non-commercial foods.

Dogs with hypertension can exhibit bilateral retinal hemorrhage, retinal detachment and tortuosity of the retinal vessels. Differential diagnosis for retinal or intraocular hemorrhage includes forms of coagulopathy. A female geriatric (approximately 13 years old) fennec fox (*Vulpes zerda*) was examined for blindness. Clinical examination revealed bilateral complete retinal detachments. Systemic blood pressure was not evaluated, but the animal had a low body condition score and serum biochemistry testing revealed elevated blood urea nitrogen concentration, supportive of kidney disease. Subsequent clinical examination was performed several months later following onset of pain in the right eye. This eye had corneal edema, elevated intraocular pressure (25 mmHg), corneal vascularization, and a suspected corneal abscess. Histopathology was performed following unilateral right eye enucleation. Suppurative keratitis was present consistent with the clinical corneal abnormalities. The eye had hyphema and vitreous hemorrhage, in addition to complete retinal detachment and prominent PAS-positive thickening of the retinal and choroidal vasculature (Fig. 36.20). The vascular changes were consistent with systemic hypertension. A dense preiridal fibrovascular membrane was present on the anterior surface of the iris, presumed to have contributed to secondary glaucoma. Case details courtesy of Dr. Richard Dubielzig, Comparative Ocular Pathology Laboratory of Wisconsin.

Infrequently, neoplasia is identified in the retina and can be primary or, more commonly secondary in nature. Enucleation should be considered for large or rapidly enlarging masses.

Fig. 36.20 Hypertensive retinopathy in a fennec fox. There is complete retinal detachment, and significant retinal atrophy with vitreal hemorrhage and fibrosis (asterisk). The lens (white arrowhead) contains a small amount of remnant cataractous cortex, and mostly nucleus (morgagnian cataract). The ciliary body vasculature is dilated and there is intrastromal hemorrhage (black arrowhead). Similar changes to retinal and choroidal vasculature were present (not shown). The choroid and sclera (#) appear atrophied. Images courtesy of Dr. Richard Dubielzig, Comparative Ocular Pathology Laboratory of Wisconsin

Acknowledgements We are grateful to Professor Dieter Kruska (University of Kiel, Germany) and Dr. Ulf Wenzel (Leipzig, Germany) for providing eyes of various canids. The skilled technical assistance of Heide Ahmed is most gratefully acknowledged. Professor Jeremy Nathans (Johns Hopkins University, Baltimore) provided cone opsin antibodies. Dr. Suzanne Kennedy-Stoskopf provided assistance with red wolf retinopathy description. Additional thanks go to several colleagues who have provided images; they are named in the text or figure legends.

References

Acton AE, Munson L, Waddell WT (2000) Survey of necropsy results in captive red wolves (Canis rufus), 1992–1996. J Zoo Wildl Med 31 (1):2–8. https://doi.org/10.1638/1042-7260(2000)031[0002:SONRIC]2.0.CO;2

Acton AE, Beale AB, Gilger BC et al (2006) Sustained release cyclosporine therapy for bilateral keratoconjunctivitis sicca in a red wolf (Canis rufus). J Zoo Wildl Med 37(4):562–564. https://doi.org/10.1638/06-021.1

Aguirre GD, Baldwin V, Weeks KM, Acland GM, Ray K (1999) Frequency of the codon 807 mutation in the cGMP phosphodiesterase beta-subunit gene in Irish setters and other dog breeds with hereditary retinal degeneration. J Hered 90(1):143–147

Andrew SE (2008) Immune-mediated canine and feline keratitis. Vet Clin North Am Small Anim Pract 38(2):269–290., vi. https://doi.org/10.1016/j.cvsm.2007.11.007

Arnesen K, Nordstoga K (1977) Ocular encephalitozoonosis (nosematosis) in blue foxes. Polyarteritis nodosa and cataract. Acta Ophthalmol 55(4):641–651

Artigas C, Redondo JI, Lopez-Murcia MM (2012) Effects of intravenous administration of dexmedetomidine on intraocular pressure and pupil size in clinically normal dogs. Vet Ophthalmol 15(Suppl 1): 79–82. https://doi.org/10.1111/j.1463-5224.2011.00966.x

Athanasiou LV, Kantere MC, Kyriakis CS, Pardali D, Adamama Moraitou K, Polizopoulou ZS (2018) Evaluation of a direct immunofluorescent assay and/or conjunctival cytology for detection of canine distemper virus antigen. Viral Immunol 31(3):272–275. https://doi.org/10.1089/vim.2017.0101

Bailes HJ, Lucas RJ (2010) Melanopsin and inner retinal photoreception. Cell Mol Life Sci 67(1):99–111. https://doi.org/10.1007/s00018-009-0155-7

Banks MS, Sprague WW, Schmoll J, Parnell JA, Love GD (2015) Why do animal eyes have pupils of different shapes? Sci Adv 1(7): e1500391. https://doi.org/10.1126/sciadv.1500391

Barachetti L, Rampazzo A, Mortellaro CM et al (2015) Use of episcleral cyclosporine implants in dogs with keratoconjunctivitis sicca: pilot study. Vet Ophthalmol 18(3):234–241. https://doi.org/10.1111/vop.12173

Barrientos LS, Zapata G, Crespi JA et al (2013) A study of the association between chronic superficial keratitis and polymorphisms in the upstream regulatory regions of DLA-DRB1, DLA-DQB1 and DLA-DQA1. Vet Immunol Immunopathol 156(3–4):205–210. https://doi.org/10.1016/j.vetimm.2013.10.009

Begall S, Burda H, Malkemper EP (2014) Chapter two - Magnetoreception in mammals. In: Naguib M, Barrett L, Brockmann HJ et al (eds) Advances in the study of behavior, vol 46. Academic Press, pp 45–88. https://doi.org/10.1016/B978-0-12-800286-5.00002-X

Beltran WA, Cideciyan AV, Guziewicz KE et al (2014) Canine retina has a primate fovea-like bouquet of cone photoreceptors which is affected by inherited macular degenerations. PLoS One 9(3):e90390. https://doi.org/10.1371/journal.pone.0090390

Bergstrom BE, Stiles J, Townsend WM (2017) Canine panuveitis: a retrospective evaluation of 55 cases (2000–2015). Vet Ophthalmol 20(5):390–397. https://doi.org/10.1111/vop.12437

Berson DM (2003) Strange vision: ganglion cells as circadian photoreceptors. Trends Neurosci 26(6):314–320. https://doi.org/10.1016/S0166-2236(03)00130-9

Brensike J (2000) Canis adustus. https://animaldiversity.org/accounts/Canis_adustus. Accessed 17 Jan 2020

Byosiere SE, Chouinard PA, Howell TJ, Bennett PC (2018) What do dogs (Canis familiaris) see? A review of vision in dogs and implications for cognition research. Psychon Bull Rev 25(5):1798–1813. https://doi.org/10.3758/s13423-017-1404-7

Cabanova V, Miterpakova M, Oravec M et al (2018) Nematode *Thelazia callipaeda* is spreading across Europe. The first survey of red foxes from Slovakia. Acta Parasitol 63(1):160–166. https://doi.org/10.1515/ap-2018-0018

Casares-Hidalgo C, Perez-Ramos A, Forner-Gumbau M et al (2019) Taking a look into the orbit of mammalian carnivorans. J Anat 234(5):622–636. https://doi.org/10.1111/joa.12953

Cerveny J, Begall S, Koubek P et al (2011) Directional preference may enhance hunting accuracy in foraging foxes. Biol Lett 7(3):355–357. https://doi.org/10.1098/rsbl.2010.1145

Cheng S, Wigney D, Haase B, Wade CM (2016) Inheritance of chronic superficial keratitis in Australian greyhounds. Anim Genet 47(5): 629. https://doi.org/10.1111/age.12446

Clark HO (2005) Otocyon megalotis. Mamm Species 766:1–5. https://doi.org/10.2307/3504550

Curcio CA, Sloan KR, Kalina RE, Hendrickson AE (1990) Human photoreceptor topography. J Comp Neurol 292(4):497–523. https://doi.org/10.1002/cne.902920402

Davidson MG, Geoly FJ, Gilger BC et al (1998) Retinal degeneration associated with vitamin E deficiency in hunting dogs. J Am Vet Med Assoc 213(5):645–651

Deem SL, Spelman LH, Yates RA, Montali RJ (2000) Canine distemper in terrestrial carnivores: a review. J Zoo Wildl Med 31(4):441–451. https://doi.org/10.1638/1042-7260(2000)031[0441:CDITCA]2.0.CO;2

Demb JB, Singer JH (2015) Functional circuitry of the retina. Annu Rev Vis Sci 1:263–289. https://doi.org/10.1146/annurev-vision-082114-035334

Detwiler SR (1956) The eye and its structural adaptations. Am Sci 44(1): 45–72

Doughty MJ (2016) On the prescribing of oral doxycycline or minocycline by UK optometrists as part of management of chronic Meibomian gland dysfunction (MGD). Cont Lens Anterior Eye 39(1):2–8. https://doi.org/10.1016/j.clae.2015.08.002

Douglas RH, Jeffery G (2014) The spectral transmission of ocular media suggests ultraviolet sensitivity is widespread among mammals. Proc Biol Sci 281(1780):20132995. https://doi.org/10.1098/rspb.2013.2995

Dziezyc J, Millichamp NJ, Smith WB (1992) Comparison of applanation tonometers in dogs and horses. J Am Vet Med Assoc 201(3):430–433

Emerling CA, Huynh HT, Nguyen MA, Meredith RW, Springer MS (2015) Spectral shifts of mammalian ultraviolet-sensitive pigments (short wavelength-sensitive opsin 1) are associated with eye length and photic niche evolution. Proc Biol Sci 282(1819). https://doi.org/10.1098/rspb.2015.1817

Evans HE, de Lahunta A (2013) The eye. In: Evans HE, de Lahunta A (eds) Miller's anatomy of the dog, 4th edn. Elsevier Health Sciences, pp 746–781

Freeman KS, Good KL, Kass PH et al (2013) Effects of chemical restraint on electroretinograms recorded sequentially in awake, sedated, and anesthetized dogs. Am J Vet Res 74(7):1036–1042. https://doi.org/10.2460/ajvr.74.7.1036

Gelatt KN, MacKay EO (1998) Distribution of intraocular pressure in dogs. Vet Ophthalmol 1(2–3):109–114. https://doi.org/10.1046/j.1463-5224.1998.00024.x

Gelatt KN, Peiffer RL Jr, Erickson JL, Gum GG (1975) Evaluation of tear formation in the dog, using a modification of the Schirmer tear test. J Am Vet Med Assoc 166(4):368–370

Gelatt KN, Gelatt JP, Plummer C (2011) Veterinary ophthalmic surgery, 2nd edn. Elsevier Health Sciences

Gelatt KN, Gilger BC, Kern TJ (2013) Veterinary ophthalmology: two volume set, 5th edn. Wiley

Gonzalez-Soriano J, Rodriguez-Veiga E, Martinez-Sainz P et al (1995) A quantitative study of ganglion cells in the German shepherd dog retina. Anat Histol Embryol 24(1):61–65. https://doi.org/10.1111/j.1439-0264.1995.tb00010.x

Granitz U, Woitow J, Thielebein J, Randt A, Spretke T (1999) Retinal degeneration and cataracts in genetically related Fenneks - *Fennecus zerda* (Abstract). Vet Ophthalmol 2:255–266

Haddock LJ, Kim DY, Mukai S (2013) Simple, inexpensive technique for high-quality smartphone fundus photography in human and animal eyes. J Ophthalmol 2013:518479. https://doi.org/10.1155/2013/518479

Haltia M, Tarkkanen A, Kivela T (1989) Rabies: ocular pathology. Br J Ophthalmol 73(1):61–67. https://doi.org/10.1136/bjo.73.1.61

Hart V, Novakova P, Malkemper EP et al (2013) Dogs are sensitive to small variations of the Earth's magnetic field. Front Zool 10(1):80. https://doi.org/10.1186/1742-9994-10-80

Harwell GM, Angell JA, Merideth RE, Carley C (1985) Chronic superficial keratitis in a Mexican wolf. J Am Vet Med Assoc 187(11): 1268

Hedrick PW, Lee RN, Buchanan C (2003) Canine parvovirus enteritis, canine distemper, and major histocompatibility complex genetic variation in Mexican wolves. J Wildl Dis 39(4):909–913. https://doi.org/10.7589/0090-3558-39.4.909

Horn SW, Lehner PN (1975) Scotopic sensitivity in coyotes (Canis latrans). J Comp Physiol Psychol 89(9):1070–1076

Howland HC, Merola S, Basarab JR (2004) The allometry and scaling of the size of vertebrate eyes. Vision Res 44(17):2043–2065. https://doi.org/10.1016/j.visres.2004.03.023

Hughes A (1977) The topography of vision in mammals of contrasting life style: comparative optics and retinal organisation. In: Crescitelli F (ed) Handbook of sensory physiology, vol VII/5. Springer, Berlin, pp 613–756

International Union for Conservation of Nature. https://www.iucn.org/. Accessed 25 Feb 2020

Isayama T, Berson DM, Pu M (2000) Theta ganglion cell type of cat retina. J Comp Neurol 417(1):32–48. https://doi.org/10.1002/(sici)1096-9861(20000131)417:1<32::aid-cne3>3.0.co;2-s

Jacobs GH (1993) The distribution and nature of colour vision among the mammals. Biol Rev Camb Philos Soc 68(3):413–471. https://doi.org/10.1111/j.1469-185x.1993.tb00738.x

Jacobs GH, Deegan JF 2nd, Crognale MA, Fenwick JA (1993) Photopigments of dogs and foxes and their implications for canid vision. Vis Neurosci 10(1):173–180

Johnson GL (1901) I. Contributions to the comparative anatomy of the mammalian eye, chiefly based on ophthalmoscopic examination. Philos Trans R Soc Lond Ser B 194(194–206):1–82. https://doi.org/10.1098/rstb.1901.0001. Containing Papers of a Biological Character

Johnson GL, Whitteridge D (1968) Ophthalmoscopic studies on the eyes of mammals. Philos Trans R Soc Lond B Biol Sci 254(794): 207–220. https://doi.org/10.1098/rstb.1968.0016

Johnson SP, Jang S, Gulland FM et al (2003) Characterization and clinical manifestations of Arcanobacterium phocae infections in marine mammals stranded along the Central California coast. J Wildl Dis 39(1):136–144. https://doi.org/10.7589/0090-3558-39.1.136

Jumelle C, Gholizadeh S, Annabi N, Dana R (2020) Advances and limitations of drug delivery systems formulated as eye drops. J Control Release 321:1–22. https://doi.org/10.1016/j.jconrel.2020.01.057

Kaminski J, Waller BM, Diogo R et al (2019) Evolution of facial muscle anatomy in dogs. Proc Natl Acad Sci U S A 116(29):14677–14681. https://doi.org/10.1073/pnas.1820653116

Kirk EC (2006) Eye morphology in cathemeral lemurids and other mammals. Folia Primatol (Basel) 77(1–2):27–49. https://doi.org/10.1159/000089694

Klein D, Mendes-Madeira A, Schlegel P, Rolling F, Lorenz B, Haverkamp S, Stieger K (2014) Immuno-histochemical analysis of rod and cone reaction to RPE65 deficiency in the inferior and superior canine retina. PLoS One 9(1):e86304. https://doi.org/10.1371/journal.pone.0086304

Knollinger AM, La Croix NC, Barrett PM, Miller PE (2005) Evaluation of a rebound tonometer for measuring intraocular pressure in dogs and horses. J Am Vet Med Assoc 227(2):244–248. https://doi.org/10.2460/javma.2005.227.244

Kolb H (2011) Morphology and circuitry of ganglion cells. https://webvision.med.utah.edu. Accessed 15 Apr 2020

Komaromy AM, Bras D, Esson DW et al (2019) The future of canine glaucoma therapy. Vet Ophthalmol 22(5):726–740. https://doi.org/10.1111/vop.12678

Komnenou AA, Mylonakis ME, Kouti V et al (2007) Ocular manifestations of natural canine monocytic ehrlichiosis (Ehrlichiacanis): a retrospective study of 90 cases. Vet Ophthalmol 10(3):137–142. https://doi.org/10.1111/j.1463-5224.2007.00508.x

Kubai MA, Bentley E, Miller PE et al (2008) Refractive states of eyes and association between ametropia and breed in dogs. Am J Vet Res 69(7):946–951. https://doi.org/10.2460/ajvr.69.7.946

Lanska DJ (2010) Chapter 29: historical aspects of the major neurological vitamin deficiency disorders: overview and fat-soluble vitamin

a. Handb Clin Neurol 95:435–444. https://doi.org/10.1016/s0072-9752(08)02129-5
Lantyer-Araujo NL, Silva DN, Estrela-Lima A et al (2019) Anatomical, histological and computed tomography comparisons of the eye and adnexa of crab-eating fox (Cerdocyon thous) to domestic dogs. PLoS One 14(10):e0224245. https://doi.org/10.1371/journal.pone.0224245
Lind O, Milton I, Andersson E, Jensen P, Roth L, Borges RM (2017) High visual acuity revealed in dogs. PLOS ONE 12(12):e0188557. https://doi.org/10.1371/journal.pone.0188557
Lindblad-Toh K, Wade CM, Mikkelsen TS et al (2005) Genome sequence, comparative analysis and haplotype structure of the domestic dog. Nature 438(7069):803–819. https://doi.org/10.1038/nature04338
Linn-Pearl RN, Powell RM, Newman HA, Gould DJ (2015) Validity of aqueocentesis as a component of anterior uveitis investigation in dogs and cats. Vet Ophthalmol 18(4):326–334. https://doi.org/10.1111/vop.12245
Magee C (2008) Coyote (Canis latrans). https://www.cfr.msstate.edu/wildlife/mammals/. Accessed 17 Jan 2020
Maggs D, Miller P, Ofri R (2017) Slatter's fundamentals of veterinary ophthalmology, 6th edn Elsevier - Health Sciences Division
Malkemper EP, Peichl L (2018) Retinal photoreceptor and ganglion cell types and topographies in the red fox (Vulpes vulpes) and Arctic fox (Vulpes lagopus). J Comp Neurol 526(13):2078–2098. https://doi.org/10.1002/cne.24493
Malmström T, Kröger RH (2006) Pupil shapes and lens optics in the eyes of terrestrial vertebrates. J Exp Biol 209(Pt 1):18–25. https://doi.org/10.1242/jeb.01959
Martini S, Begall S, Findeklee T et al (2018) Dogs can be trained to find a bar magnet. PeerJ 6:e6117. https://doi.org/10.7717/peerj.6117
Masland RH (2001) The fundamental plan of the retina. Nat Neurosci 4(9):877–886. https://doi.org/10.1038/nn0901-877
Maslanka T (2015) A review of the pharmacology of carbonic anhydrase inhibitors for the treatment of glaucoma in dogs and cats. Vet J 203(3):278–284. https://doi.org/10.1016/j.tvjl.2014.12.017
Massa KL, Gilger BC, Miller TL, Davidson MG (2002) Causes of uveitis in dogs: 102 cases (1989–2000). Vet Ophthalmol 5(2):93–98. https://doi.org/10.1046/j.1463-5224.2002.00217.x
McGreevy P, Grassi TD, Harman AM (2004) A strong correlation exists between the distribution of retinal ganglion cells and nose length in the dog. Brain Behav Evol 63(1):13–22. https://doi.org/10.1159/000073756
Mellersh CS, Graves KT, McLaughlin B et al (2007) Mutation in HSF4 associated with early but not late-onset hereditary cataract in the Boston terrier. J Hered 98(5):531–533. https://doi.org/10.1093/jhered/esm043
Mellersh CS, McLaughlin B, Ahonen S et al (2009) Mutation in HSF4 is associated with hereditary cataract in the Australian shepherd. Vet Ophthalmol 12(6):372–378. https://doi.org/10.1111/j.1463-5224.2009.00735.x
Myers (2014) Animal Diversity Web. https://animaldiversity.org. Accessed 30 Jan 2020
Miller PE, Murphy CJ (1995) Vision in dogs. J Am Vet Med Assoc 207(12):1623–1634
Miller PE, Pickett JP (1992) Comparison of the human and canine Schiotz tonometry conversion tables in clinically normal dogs. J Am Vet Med Assoc 201(7):1021–1025
Moehlman PD, Hayssen V (2018) Canis aureus (Carnivore: Canidae). Mamm Species 50(957):14–25. https://doi.org/10.1093/mspecies/sey002
Moore BA, Tyrrell LP, Kamilar JM et al (2017) 1.19 - Structure and function of regional specializations in the vertebrate retina. In: Kaas JH (ed) Evolution of nervous systems, 2nd edn. Academic Press, Oxford, pp 351–372. https://doi.org/10.1016/B978-0-12-804042-3.00008-7
Mowat FM (2019) Naturally occurring inherited forms of retinal degeneration in vertebrate animal species: a comparative and evolutionary perspective. Adv Exp Med Biol 1185:239–243. https://doi.org/10.1007/978-3-030-27378-1_39
Mowat FM, Petersen-Jones SM, Williamson H, Williams DL, Luthert PJ, Ali RR, Bainbridge JW (2008) Topographical characterization of cone photoreceptors and the area centralis of the canine retina. Mol Vis 14:2518–2527
Murphy CJ, Howland HC (1987) The optics of comparative ophthalmoscopy. Vision Res 27(4):599–607. https://doi.org/10.1016/0042-6989(87)90045-9
Murphy CJ, Mutti DO, Zadnik K, Ver Hoeve J (1997) Effect of optical defocus on visual acuity in dogs. Am J Vet Res 58(4):414–418
Neitz J, Geist T, Jacobs GH (1989) Color vision in the dog. Vis Neurosci 3(2):119–125. https://doi.org/10.1017/s0952523800004430
Niessner C, Denzau S, Malkemper EP et al (2016) Cryptochrome 1 in retinal cone photoreceptors suggests a novel functional role in mammals. Sci Rep 6:21848. https://doi.org/10.1038/srep21848
Nonnemann B, Chriel M, Larsen G, Hansen MS, Holm E, Pedersen K (2017) Arcanobacterium phocae infection in mink (Neovison vison), seals (Phoca vitulina, Halichoerus grypus) and otters (Lutra lutra). Acta Vet Scand 59(1):74. https://doi.org/10.1186/s13028-017-0342-8
Nordgren H, Aaltonen K, Sironen T et al (2014) Characterization of a new epidemic necrotic pyoderma in fur animals and its association with Arcanobacterium phocae infection. PLoS One 9(10):e110210. https://doi.org/10.1371/journal.pone.0110210
Nowak RM, Walker EP (1991) Walker's mammals of the world, 5th edn. Johns Hopkins University Press, Baltimore
Ollivier FJ, Samuelson DA, Brooks DE et al (2004) Comparative morphology of the tapetum lucidum (among selected species). Vet Ophthalmol 7(1):11–22. https://doi.org/10.1111/j.1463-5224.2004.00318.x
Otranto D, Lia RP, Buono V, Traversa D, Giangaspero A (2004) Biology of Thelazia callipaeda (Spirurida, Thelaziidae) eyeworms in naturally infected definitive hosts. Parasitology 129(Pt 5):627–633
Otranto D, Cantacessi C, Mallia E, Lia RP (2007) First report of Thelazia callipaeda (Spirurida, Thelaziidae) in wolves in Italy. J Wildl Dis 43(3):508–511. https://doi.org/10.7589/0090-3558-43.3.508
Otranto D, Dantas-Torres F, Mallia E et al (2009) Thelazia callipaeda (Spirurida, Thelaziidae) in wild animals: report of new host species and ecological implications. Vet Parasitol 166(3–4):262–267. https://doi.org/10.1016/j.vetpar.2009.08.027
Palanova A (2016) The genetics of inherited retinal disorders in dogs: implications for diagnosis and management. Vet Med (Auckl) 7:41–51. https://doi.org/10.2147/VMRR.S63537
Pascoe PJ, Ilkiw JE, Stiles J, Smith EM (1994) Arterial hypertension associated with topical ocular use of phenylephrine in dogs. J Am Vet Med Assoc 205(11):1562–1564
Peichl L (1991) Catecholaminergic amacrine cells in the dog and wolf retina. Vis Neurosci 7(6):575–587
Peichl L (1992a) Morphological types of ganglion cells in the dog and wolf retina. J Comp Neurol 324(4):590–602. https://doi.org/10.1002/cne.903240411
Peichl L (1992b) Topography of ganglion cells in the dog and wolf retina. J Comp Neurol 324(4):603–620. https://doi.org/10.1002/cne.903240412
Peichl L (2005) Diversity of mammalian photoreceptor properties: adaptations to habitat and lifestyle? Anat Rec A Discov Mol Cell Evol Biol 287(1):1001–1012. https://doi.org/10.1002/ar.a.20262
Peichl L (2009) Retinal ganglion cells. In: Binder MD, Hirokawa N, Windhorst U (eds) Encyclopedia of neuroscience. Springer,

Heidelberg, pp 3507–3513. https://doi.org/10.1007/978-3-540-29678-2_5106
Peichl L, Ott H, Boycott BB (1987) Alpha ganglion cells in mammalian retinae. Proc R Soc Lond B Biol Sci 231(1263):169–197. https://doi.org/10.1098/rspb.1987.0040
Pence DB, Meinzer WP (1977) Blindness in a coyote, Canis latrans, from the rolling plains of Texas. J Wildl Dis 13(2):155–159
Perret LJ, Tait CP (2014) Non-antibiotic properties of tetracyclines and their clinical application in dermatology. Australas J Dermatol 55(2): 111–118. https://doi.org/10.1111/ajd.12075
Petersen-Jones SM, Komaromy AM (2015) Dog models for blinding inherited retinal dystrophies. Hum Gene Ther Clin Dev 26(1):15–26. https://doi.org/10.1089/humc.2014.155
Pettigrew JD, Dreher B, Hopkins CS, McCall MJ, Brown M (1988) Peak density and distribution of ganglion cells in the retinae of microchiropteran bats: implications for visual acuity. Brain Behav Evol 32(1):39–56. https://doi.org/10.1159/000116531
Rauser P, Pfeifr J, Proks P, Stehlik L (2012) Effect of medetomidine-butorphanol and dexmedetomidine-butorphanol combinations on intraocular pressure in healthy dogs. Vet Anaesth Analg 39(3): 301–305. https://doi.org/10.1111/j.1467-2995.2011.00703.x
Ravisse P, Blancou J (1981) Histological ocular lesions of rabies in foxes (author's transl). Comp Immunol Microbiol Infect Dis 4(1): 101–105
Regnier A, Toutain PL, Alvinerie M et al (1982) Adrenocortical function and plasma biochemical values in dogs after subconjunctival treatment with methylprednisolone acetate. Res Vet Sci 32(3): 306–310
Ring R, Kearns K (1997) Retinal degeneration in red wolves. Proceedings of the American College of Veterinary Ophthalmologists, 1
Rubin LF, Wolfes RL (1962) Mydriatics for canine ophthalmoscopy. J Am Vet Med Assoc 140:137–141
Sanchez RF, Mellor D, Mould J (2006) Effects of medetomidine and medetomidine-butorphanol combination on Schirmer tear test 1 readings in dogs. Vet Ophthalmol 9(1):33–37. https://doi.org/10.1111/j.1463-5224.2005.00432.x
Schwab IR, Yuen CK, Buyukmihci NC, Blankenship TN, Fitzgerald PG (2002) Evolution of the tapetum. Trans Am Ophthalmol Soc 100: 187–199. discussion 199–200
Seeley KE, Garner MM, Waddell WT, Wolf KN (2016) A survey of diseases in captive red wolves (Canis Rufus), 1997–2012. J Zoo Wildl Med 47(1):83–90. https://doi.org/10.1638/2014-0198.1
Seixas F, Travassos P, Coutinho T et al (2018) The eyeworm Thelazia callipaeda in Portugal: current status of infection in pets and wild mammals and case report in a beech marten (Martes foina). Vet Parasitol 252:163–166. https://doi.org/10.1016/j.vetpar.2018.02.007
Sherman SM, Wilson JR (1975) Behavioral and morphological evidence for binocular competition in the postnatal development of the dog's visual system. J Comp Neurol 161(2):183–195. https://doi.org/10.1002/cne.901610204
Smith J (2002) *Canis lupus*. https://animaldiversity.org/accounts/Canis_lupus. Accessed 17 Jan 2020
Smith LN, Miller PE, Felchle LM (2010) Effects of topical administration of latanoprost, timolol, or a combination of latanoprost and timolol on intraocular pressure, pupil size, and heart rate in clinically normal dogs. Am J Vet Res 71(9):1055–1061. https://doi.org/10.2460/ajvr.71.9.1055
Solovei I, Kreysing M, Lanctot C et al (2009) Nuclear architecture of rod photoreceptor cells adapts to vision in mammalian evolution. Cell 137(2):356–368. https://doi.org/10.1016/j.cell.2009.01.052
Subramanian K, Weigert M, Borsch O et al (2019) Rod nuclear architecture determines contrast transmission of the retina and behavioral sensitivity in mice. Elife 8. https://doi.org/10.7554/eLife.49542
Tahir D, Davoust B, Parola P (2019) Vector-borne nematode diseases in pets and humans in the Mediterranean Basin: an update. Vet World 12(10):1630–1643. https://doi.org/10.14202/vetworld.2019.1630-1643
Theuerkauf J (2009) What drives wolves: fear or hunger? Humans, diet, climate and Wolf activity patterns. Ethology 115(7):649–657. https://doi.org/10.1111/j.1439-0310.2009.01653.x
Ueda S, Kumagai G, Otaki Y et al (2014) A comparison of facial color pattern and gazing behavior in canid species suggests gazecommunication in gray wolves (Canis lupus). PLoS One 9(2):e98217. https://doi.org/10.1371/journal.pone.0098217
Vainisi SJ, Edelhauser HF, Wolf ED, Cotlier E, Reeser F (1981) Nutritional cataracts in timber wolves. J Am Vet Med Assoc 179(11):1175–1180
Wang SL, Dawson C, Wei LN, Lin CT (2019) The investigation of histopathology and locations of excised eyelid masses in dogs. Vet Rec Open 6(1):e000344. https://doi.org/10.1136/vetreco-2019-000344
Ward OG, Wurster-Hill DH (1990) Nyctereutes procyonoides. Mamm Species 358:1–5. https://doi.org/10.2307/3504213
Wässle H (2004) Parallel processing in the mammalian retina. Nat Rev Neurosci 5(10):747–757. https://doi.org/10.1038/nrn1497
Weitzel G, Buddecke E, Fretzdorff AM, Strecker FJ, Roester U (1955) Structure of zinc compound in tapetum lucidum of dog and fox. Hoppe Seylers Z Physiol Chem 299(5–6):193–213
Wen GY, Sturman JA, Wisniewski HM et al (1982) Chemical and ultrastructural changes in tapetum of beagles with a hereditary abnormality. Invest Ophthalmol Vis Sci 23(6):733–742
Wen GY, Sturman JA, Shek JW (1985) A comparative study of the tapetum, retina and skull of the ferret, dog and cat. Lab Anim Sci 35(3):200–210
Wiltschko R, Wiltschko W (2019) Magnetoreception in birds. J R Soc Interface 16(158):20190295. https://doi.org/10.1098/rsif.2019.0295
Woo GH, Jho YS, Bak EJ (2010) Canine distemper virus infection in fennec fox (Vulpes zerda). J Vet Med Sci 72(8):1075–1079. https://doi.org/10.1292/jvms.09-0510
Yadav KS, Rajpurohit R, Sharma S (2019) Glaucoma: current treatment and impact of advanced drug delivery systems. Life Sci 221:362–376. https://doi.org/10.1016/j.lfs.2019.02.029
Yamaue Y, Hosaka YZ, Uehara M (2015) Spatial relationships among the cellular tapetum, visual streak and rod density in dogs. J Vet Med Sci 77(2):175–179. https://doi.org/10.1292/jvms.14-0447
Yeh CY, Koehl KL, Harman CD et al (2017) Assessment of rod, cone, and intrinsically photosensitive retinal ganglion cell contributions to the canine chromatic pupillary response. Invest Ophthalmol Vis Sci 58(1):65–78. https://doi.org/10.1167/iovs.16-19865
Yoshitomi T, Ito Y (1986) Pre-synaptic actions of noradrenaline on the dog ciliary muscle tissue. Exp Eye Res 43(1):119–127. https://doi.org/10.1016/s0014-4835(86)80050-1
Zangerl B, Goldstein O, Philp AR et al (2006) Identical mutation in a novel retinal gene causes progressive rod-cone degeneration in dogs and retinitis pigmentosa in humans. Genomics 88(5):551–563. https://doi.org/10.1016/j.ygeno.2006.07.007
Zangerl B, Johnson JL, Acland GM, Aguirre GD (2007) Independent origin and restricted distribution of RPGR deletions causing XLPRA. J Hered 98(5):526–530. https://doi.org/10.1093/jhered/esm060

Ophthalmology of Ursidae: Bears

37

Claudia Hartley and Rui Pedro Rodrigues Oliveira

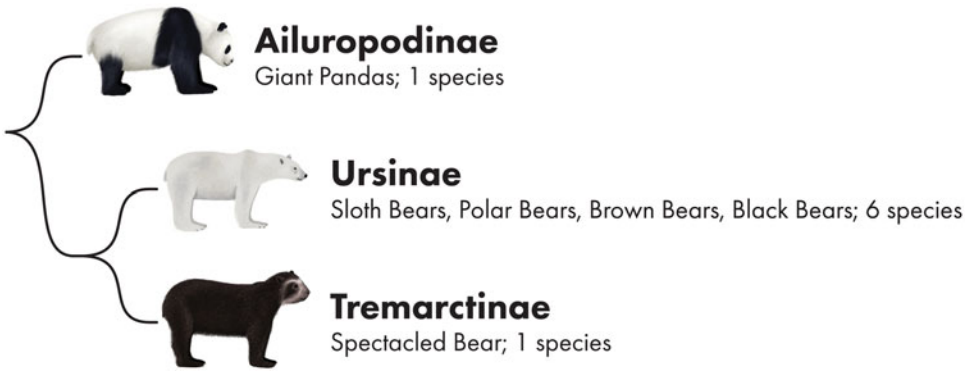

© Chrisoula Skouritakis

Introduction

Bears belong to the order Carnivora, suborder Caniformia. Caniformia means "doglike". Their family is called Ursidae. Modern bears comprise eight species in three subfamilies: Ailuropodinae (monotypic with the giant panda), Tremarctinae (monotypic with the Andean spectacled bear), and Ursinae (containing six species: brown bear, American black bear, Polar bear, Asiatic black bear, sloth bear, sun bear). Bears' closest living relatives are the pinnipeds, canids, and musteloids (Wesley-Hunt and Flynn 2005).

Ursinae

The American black bear (*Ursus americanus*) population outnumbers all other bear species combined, extending from Canada to Mexico, and are classified as of least concern on the IUCN Red List and populations are considered to be increasing (Garshelis et al. 2016). They have a bodyweight from 41 kg to 250 kg with males generally larger than females, and have an average lifespan in the wild is approximately 18 years but may exceed 30 years, and in captivity 40 years. They are omnivorous and adaptable to their habitat with diets including vegetative matter from buds to roots, to nuts and seeds, fleshy fruits, insects, fish and meat, both of their own killing and carrion. They will also readily raid human-related foods from garbage to crops, as well as birdseed. They are active during the day and night, varying with location and proximity to competitors (e.g., brown bears). Hibernation varies with geographical location and may occur for up to 7 months of the year in more northern climates, but be absent where food is readily available year round. Bodyweight pre-hibernation can be 25–60% heavier to sustain them over this period. They may reproduce every other year or, where food is scarcer, interbirth intervals may reach 3 years.

Brown bears are the most widely distributed ursid species, occupying three continents and 45 countries. They occupy a wide range of habitats, and their range overlaps with the

C. Hartley (✉)
University of Edinburgh, Edinburgh, UK

R. P. R. Oliveira
Universidad Autónoma de Barcelona (UAB), Instituto Oftalmológico Veterinário, Lisbon, Portugal

F. Montiani-Ferreira et al. (eds.), *Wild and Exotic Animal Ophthalmology*, https://doi.org/10.1007/978-3-030-81273-7_12

American black bear (*Ursus americanus*) in North America, polar bear (*Ursus maritimus*) in North America, Greenland, Norway and Russia, and the Asiatic black bear (*Ursus thibetanus*) in Asia. Forty-four subpopulations of brown bear have been identified worldwide, and many are small, isolated, and require conservation strategies. However, overall, the Brown bear (*Ursus arctos*) is categorized as of least concern on the IUCN Red List, and their population is considered stable (McLellan et al. 2017). They have a body mass ranging from 115 kg (females) and 273 kg (males) in Europe, but this varies with time of year and hibernation (Swenson et al. 2007). In Alaska and northern latitudes, much larger body masses have been recorded, even up to 600 kg (Pasitschniak 1993). Lifespan in the wild has been recorded up to 28 years, while in captivity, the oldest recorded bear was 47 years old. The diet of the Brown bear is omnivorous with a wide variety of foods, including grasses, flowers, berries, roots, shoots, nuts, and fungi, as well as insects, grubs and beehives (honey), carrion, fish and meat (live kills). They are diurnal but are known to forage and also hunt nocturnally (Klinka and Reimchen 2002).

The Polar bear (*Ursus maritimus*) presides over the ice-covered waters of the circumpolar Arctic basin, extending south into Canada, Greenland (Denmark), Norway, Russia, Siberia, and Alaska. They are classified as vulnerable on the IUCN Red List (Wiig et al. 2015), with the greatest threat believed to be loss of Arctic sea ice, climate change, and pollution (Dybas 2012). They are the largest of the ursid species at 200–250 cm in body length, 170 cm at shoulder height, with body weight ranges of 150–800 kg (Demaster and Stirling 1981) and a height of up to 4 m when stood on hind feet (Amstrup 2003). Lifespan is approximately 20–25 years in the wild but may reach 30 years. The mean lifespan of Polar bears in captivity in one study was 24 years (LaDouceur et al. 2014), and the most common cause of death or euthanasia was the end-stage renal disease, with a prevalence of 20%. The longest lifespan recorded in captivity for a Polar bear is 43 years (Weigl 2005). They are mostly carnivorous ("hypercarnivore") and hunt from sea ice, so during summer months, when confined to land, they subsist largely on fat stores and carrion (Whiteman et al. 2018). The majority of their diet is, therefore, marine mammal kills (ringed and bearded seals predominate, but also harp, hooded and ribbon seals, walrus, and beluga whales), although they have been reported to eat some vegetation (e.g., kelp), birds and their eggs, fish, and occasionally small mammals, although these sources are not considered calorie-dense enough to sustain Polar bears. At the time of spring birthing, the mother may not have eaten for up to 8 months, the longest food deprivation period recorded of any mammal. They are diurnal (Ware et al. 2020), and in bright light, they appear white, an artifact due to light scattering, considering that their hairs are actually transparent against black skin. Their dense coat consisting of a thick underfur (5 cm in length) with longer guard hairs (15 cm) and the hairs have a hollow core helps with thermoregulation both by insulation and by harnessing solar radiation to heat the subcutaneous and skin surface layers by means of the hollow core conducting energy to the black skin (Khattab and Tribursch 2015). They are powerful swimmers with webbing of their feet and have been shown to have prolonged stamina for swimming (up to 9 days and 687 km) recorded by radiotelemetry (Pagano et al. 2012).

The Asiatic black bear (*Ursus thibetanus*) is distributed from Iran to Japan, extending North into Russia. They are classified as vulnerable on the IUCN Red List (Garshelis and Steinmetz 2016), with population declines everywhere other than China of about 30% in the past 30 years (IUCN 2020). Their bodyweight varies from 40–200 kg, and they have been recorded living to more than 30 years in captivity, but lifespan is shorter in the wild. Their diet may vary according to the availability of food, and they appear able to adapt somewhat to habitat change. They most consistently eat succulent vegetation in spring, with insects, a variety of fruits in summer and nuts in autumn, with meat supplementation from mammalian ungulates that they either predate or scavenge (Hwang et al. 2002; Panthi et al. 2019; Hashimoto et al. 2003; Reid et al. 1991; Huygens et al. 2003; Koike 2010). Asiatic black bears are considered diurnal, with the greatest activity during daylight hours in spring, summer and fall. However, increased nocturnal activity is evident in the autumn and occurs even in animals that did not retreat to dens in winter (Hwang and Garshelis 2007). In northern latitudes, they hibernate during periods of food unavailability (varying from October through to May).

The last two Ursinae species, the Sun bear (*Helarctos malayanus*) and Sloth bear (*Melursus ursinus*) are sympatric. The Sun bear, of which two subspecies exist [Borneo sun bear (*Helarctos malayanus euryspilus*) and Malayan sun bear (*Helarctos malayanus malayanus*)], is distributed across Southeastern Asia from Bangladesh to Indonesia. Populations are in decline, by about 35% in the last 30 years due to habitat loss and hunting and they are categorized as vulnerable on the IUCN Red List (Scotson et al. 2017). They are the smallest of the Ursid family, with a bodyweight of 30–90 kg. They are omnivorous, and their diet includes insects and honey, along with a variety of fruit species. Both diurnal and nocturnal behavior in the Sun bear has been reported. Hibernation is not evident in Sun bears, and this is hypothesized to be due to the year round availability of food in their home ranges.

The Sloth bear (*Melursus ursinus*) is found across India, Nepal, Bhutan and Sri Lanka and is classified as vulnerable on the IUCN Red List (Dharaiya et al. 2020). They are slightly larger than Sun bears, with a bodyweight of 55–192 kg (Garshelis et al. 1999b), as well as a longer shaggy black coat with a cream-colored crescent on the chest. The

Sloth bear also has a mane around the face and neck and has a long lower lip and palate advantageous for sucking up insects (ants and termites) as well as well-developed nasal alar cartilages that are capable of closing the nostrils during feeding. Two subspecies (*Melursus ursinus inornatus* and *Melursus ursinus ursinus*) have been described with a sparser and shorter coat with the smaller build of the *Melursus ursinus inornatus* subspecies found only on the island of Sri Lanka. It is estimated that 90% of the Sloth bear range occurs in India, also crossing into Nepal, Sri Lanka and very rarely in Bhutan (Garshelis et al. 1999a; Yoganand et al. 2006). Populations are believed to be in decline due to habitat destruction, poaching and capture for exploitation. Sloth bears are myrmecophagous and have smaller home ranges than other ursid species. They are insectivorous and frugivorous, but the proportions of fruits to insects in their diets vary during the year according to the fruiting season. They are reported to be the most aggressive of extant bear species; however, this may be a reflection of the larger human populations close to their ranges. Sloth bears are reported to be the most nocturnal of the bear species, although nursing mothers may be more active during the daytime (Ramesh et al. 2013).

Termarctinae

The Andean spectacled bear (*Tremarctos ornatus*) is the only bear species naturally found in South America, and they are found in mountainous regions from Venezuela to Bolivia, including the Andean mountain ranges of Colombia, Ecuador, and Peru. Populations are believed to be decreasing predominantly through loss of habitat due to expansion of agriculture frontiers and mining and oil exploration, but also through bear killings in human-animal conflicts. They are classed as vulnerable on the IUCN Red List (Velez-Liendo and García-Rangel 2017). They have a black to brown coat with distinctive beige to ginger facial and upper chest markings, which do not always include "spectacles," but are distinctive to each individual bear, allowing identification. Bodyweight varies from 35 kg to 200 kg, with males (mean 115 kg) heavier than females (mean 65 kg) (Soibelzon and Tarantini 2009; Cavelier et al. 2011). They have a shorter and broader nose than other bear species. They are arboreal and largely herbivorous, although approximately 5% of the diet is compromised of meat (Nowak 1999). They have the largest muscles of mastication of the bear species (even surpassing those of the Giant Panda; *Ailuropoda melanoleuca*), thought to be related to their highly fibrous diet (Davis 1955). The Andean spectacled bear is usually solitary, although groups have been encountered at sites of abundant food and are shy of human contact. They are active both during the day and night, and activity levels vary with the environment (in the Peruvian desert, bears shelter under shrubs during the day). Lifespan in captivity has been recorded up to 36 years, but is estimated to exceed 20 years in the wild in the absence of human conflict (Nowak 1999).

Ailuropodinae

The Giant Panda bear (*Ailuropoda melanoleuca*) is found in China; 75% of the population inhabits Sichuan Province, at elevations of 800–3900 m in forested areas with a dense understory of bamboo and frequent rain, mist, and cloud cover (Boedeker et al. 2010). The population remains fairly isolated across the total range of approximately 30,000 km^2. Two-thirds of wild giant pandas are found within nature reserves (SFAC 2015). The species is now found in only six mountain ranges at the eastern edge of the Tibetan plateau, distributed in as many as 30–40 distinctive populations. The Min Shan Mountains are the heart of panda numbers and activities, probably sustaining half the remaining wild individuals (Lumpkin and Seidensticker 2002; Wildt et al. 2006). They are classified as vulnerable on the IUCN Red List (Swaisgood et al. 2016, *The IUCN Red List of Threatened Species* 2016).

The Giant Panda bear is an iconic animal for conservationists; it is also the symbol of WWF "World Wildlife Fund" since its creation in 1961 and is one of the most recognizable logotypes in the world. Today, they are an emerging conservation success story that demonstrates the benefits of comprehensive planning and extensive collaboration that can conserve a species (Traylor-Holzer and Ballou 2016), but it was not always like this. Population size remained at 100–115 pandas for many years despite several intensive breeding programs, with most of the population being wild-born, largely due to a 1–3-day oestrus period, delayed implantation, behavioral ineptitude, and extremely altricial cubs with low total survival rate. But in 1997, the number of captive-born Giant Panda bear in captivity exceeded the number of wild-born individuals (Traylor-Holzer and Ballou 2016). Over the past 20 years, the captive giant panda population has developed into a demographically stable population, expanding from 152 pandas in 19 institutions in 2002 to a population of 423 individuals in 78 institutions worldwide in November 2015 (Traylor-Holzer and Ballou 2016). Furthermore, the most recent survey indicates a total wild population of approximately 1864 individuals, excluding dependent young. The population is divided into approximately 33 subpopulations, only 6 of which have more than 100 individuals. However, it is believed that the population has stabilized and begun to increase in parts of the range due to habitat protections (SFAC 2015).

Most adult male Giant Panda bears in the wild weigh from 85 kg to 125 kg, while females range between 70 kg and

100 kg. At birth, cubs weigh only 85–140 g (Hechtel 2020). The average lifespan in the wild is approximately 18–20 years but may exceed 30 years in captivity (the oldest Giant Panda bear recorded in captivity was 38 years when she died in 2016). Despite being members of the order Carnivora and having a simple gastrointestinal tract, they are primarily herbivorous and consume bamboo (*Bambusoideae*) as 99% of their diet. Bamboo contains very little nutritional value, so an individual adult Giant Panda bear can consume 6–10 kg of bamboo per day (Wildt et al. 2006). Such a fibrous diet, in part, explains some of its unique morphology, including the large head relative to body mass, the skull's expanded zygomatic arches, and the associated powerful muscles for mastication (Nowak 1999). The remaining 1% of their diet consists of other plants and even meat (pikas and other small rodents). Unlike its bear counterparts, the Giant Panda bear does not hibernate, probably because of the need to forage throughout the year for its low-energy diet of bamboo, spending 14h each day searching, selecting and consuming bamboo (Lumpkin and Seidensticker 2002; Wildt et al. 2006).

Human Interactions

Despite near global decline in or vulnerability of bear populations, aside from the American black bear, bears are unfortunately a target of inhumane treatment in many parts of the world.

Asiatic black bears, Brown bears and Sun bears are used in "bile farming," which is used in traditional Chinese medicine. There are an estimated 10,000 Asiatic black bears in captivity in China, where bile farming is a legal enterprise under licensed conditions. These bears are kept on legal bile farming enterprises in crates (some with insufficient room to stand or turn around). Farms vary in number of bears kept, from one to more than a thousand. The bile is milked daily via abdominal free drip stomas to their gall bladders after metal catheters were banned under regulations (although these are still seen). Bile farming is a high-value enterprise. Campaigns promoting herbal and synthetic alternatives to bear bile for traditional Chinese medicine are also an important route to reducing demand. Although it has been illegal since 1989 to capture wild Asiatic black bears, many young farmed bears that have entered rescue establishments have snare wounds, including amputated limbs suggesting they have come from wild populations. Bile farming is not legal in Vietnam, but it is legal to keep a bear or bears in captivity as "pets" (an estimated 1000 in captivity), from which bile draining has been reported. However, legitimate seizure of captive bears requires undercover filming of bile drainage procedures. In 2017, a memorandum of understanding (MOU) was signed by the Forestry department of the Vietnamese government to end bear farming in Vietnam, as well as promote the welfare of captive bears in the country and conservation of wild bear populations. Another MOU, signed in 2015, with the Vietnamese Traditional Medicine Association, had already committed traditional medicine practitioners to cease prescribing bear bile by 2020 completely.

American black bears are legally hunted for sport (under strict license and control), and this is permitted in USA, Canada, Sweden, and other countries but is prohibited in Mexico. A growing concern is the poaching of bears for their paws and gallbladders for sale to enter the lucrative traditional Chinese medicine market (Williamson 2002). The value of certain bear parts by weight, in some Asian countries, exceeds the price of gold, thereby creating a market that places a price on the head of every wild bear. As well as gallbladders and bile, bear paws are considered a "tonic" food and gourmet delicacy in China, Korea, Taiwan and Japan. The pet trade for ursid infants is also rife and may represent a spin-off from poaching of a wild mother for paws or gallbladder and taking the cub to sell on. Bear cubs can be extremely appealing, and when larger or adult may be traded into the bile farming industry. The trade includes Asiatic black bears, Sun bears, Brown bears, and Sloth bears in Asia.

Bear species (usually American black bear, Asiatic black bear, or Brown bear) have been used for bear baiting for many centuries across the world. The practice of tormenting a bear with dogs is still a spectator blood sport that occurs in some regions of Pakistan and Eastern Europe. Within Pakistan, the practice continues most commonly in the provinces of Sindh and Punjab in the winter months. Events range from one bear and few dogs to 10 or more bears and more than 40 dogs. Pakistan's Bioresource Research Centre is working in the field to break up events, to rescue bears and to end the practice through education, provision of alternative livelihoods, and the support and encouragement of law enforcement. Illegal bear baiting was documented in Ukraine in 2013, and the Humane Society provided evidence from undercover work in South California, USA, in 2010. While still legal in South Carolina, it was effectively banned when the South Carolina Department of Natural Resources indicated it would not issue any new permits for the private possession of black bears in 2013.

The USA, Canada, and Greenland allow and manage a subsistence harvest of Polar bears, while hunting and harvest are prohibited in Norway and Russia. Subsistence purposes include consumption of meat, use of hides for clothing and small-scale handicrafts. Whole hides may also be kept as trophies or sold on open markets (Obbard et al. 2010). The financial return can provide important income for local people in Canada and Greenland. Sport hunting of Polar bears only occurs in Canada and must be guided by local Inuit hunters (Simpson 2019). The harvest level has been deemed to be sustainable in most subpopulations, although illegal

hunting in eastern Russia has been reported to be high enough to pose a threat to the population (Belikov et al. 2005).

Sloth bears kept for "dancing" as a popular entertainment was traditional in India dating back to the thirteenth century. The practice was banned in 1972 but bears remained on the streets often within the Kalandar community, and the income from one dancing bear was able to support an extended family. Sloth bear cubs would be trained from an early age and later fitted with a nose ring (running through a stoma created via the skin and nasal bone) attached to a four-foot leash. Some had teeth removed or broken to reduce the risk of injury to handlers, and most handlers also used sticks to coerce their bears into submission. The last dancing bear on Indian streets was rescued in 2009 by a coalition of Indian and International welfare groups. Kalandars were supported in finding alternative sources of income, and some employed by sanctuaries caring for the rescued bears. Bears are also used in circuses and in unaccredited roadside zoos/tourist attractions, including cub-petting operations in the USA. They are also killed across their ranges with increasing human-bear conflict if designated as a "nuisance bear." There are increasing numbers of bears ending up in rescue/rehab facilities because of these human activities.

Vision in Bears

Very little is known about the sensory capabilities of bears. It is believed that Giant panda bears, similar to Brown bears and Polar bears are cone dichromats, having short-wave sensitive (S–) cones and middle-to-long-wave sensitive (L–) cones. Overall cone densities and S-cone proportions in the Ursidae studied are higher than in most other mammals indicating an adaptation to specific modes of diurnal vision (Peichl et al. 2005).

American black bears are reported to have good eyesight and have been able to learn color discrimination experimental tasks faster than chimpanzees and just as fast as domestic dogs. They were also capable of rapidly learning to distinguish different shapes such as small triangles, circles and squares (Bacon and Berghard 1974). Picture recognition has been demonstrated in one study of a single 11-year-old female American black bear (Johnson-Ulrich et al. 2016) and in another study of two Sloth bears (Tabellario et al. 2020).

A previous hypothesis suggested that Giant panda bear vision is not well developed and is similar to that of nocturnal mammals (Schaller 1993). However, they are not nocturnal, and tend to be polycyclic, with activity peaks in the early morning and late afternoon (Schaller et al. 1985), suggesting the possibility of color discrimination (Kelling et al. 2006). Discrimination between shades of green, red, and blue stimuli from numerous shades of gray has been shown, and because the brightness was eliminated as a cue, these discriminations can be attributed to color vision, thus providing experimental evidence that the giant panda's visual capabilities, including color vision, are comparable to those of other bears (Bacon and Berghard 1974). Additionally, pandas use visual signals as a means of communication. They communicate with body postures (Schaller et al. 1985) and visual markings such as bark stripping and clawing (Laidler and Laidler 1992; Schaller et al. 1985).

Color vision in pandas may not be as salient a cue for bamboo selection as it is for other bears that forage for fruits and a wide range of vegetation types. On the other hand, color may indeed contribute to more effective foraging for bamboo. Color variation may guide leaf choice or indicate nutrient content and may be especially important for Giant panda bears when they select bamboo patches from a distance. For example, color discrimination may help Giant panda bears avoid dying bamboo on the basis of visual changes accompanying periodic bamboo flowering and death, which can occur in small regions or on entire mountainsides (Schaller et al. 1985).

Bony Orbit and Globe

Anatomy of the Bony Orbit and Globe

Bear species have proportionally small eyes for their body weight, and forward-facing orbits. The forward-facing orbit is postulated to be evolutionarily advantageous for enhanced binocular vision and predatory behavior (compared to lateralized eyes with enhanced panoramic predator-spotting ability). All the bear species have forward-facing orbits, and this seems to be unrelated to their carnivorous (e.g., *Arctos maritimis*), omnivorous (*Ursus thibetanus*, *Helarctos malayanus*, *Melursus ursinus*, *Tremarctos ornatus, Ursus arctos*) or herbivorous (*Ailuropoda melanoleuca*) dietary preference.

The skull of all bear species possesses a sagittal crest, which is a ridge of bone running lengthwise along the midline of the top of the skull (at the sagittal suture) (Fig. 37.1a, c). The sagittal crest serves primarily for attachment of the temporalis muscle, which is one of the primary chewing muscles. Thus, the prominence of this bone indicates that there are remarkably strong jaw muscles in Ursids.

The orbit in Giant Panda bears (*Ailuropoda melanoleuca*), as in other ursids, is an open, elongate cone with the base formed by the incomplete bony ring of the eye socket (completed by the orbital ligament) and the apex by the orbital fissure. On its medial wall (the only complete boney wall), the dorsal and ventral boundaries, separating the orbit from the temporal fossa above and the infratemporal fossa

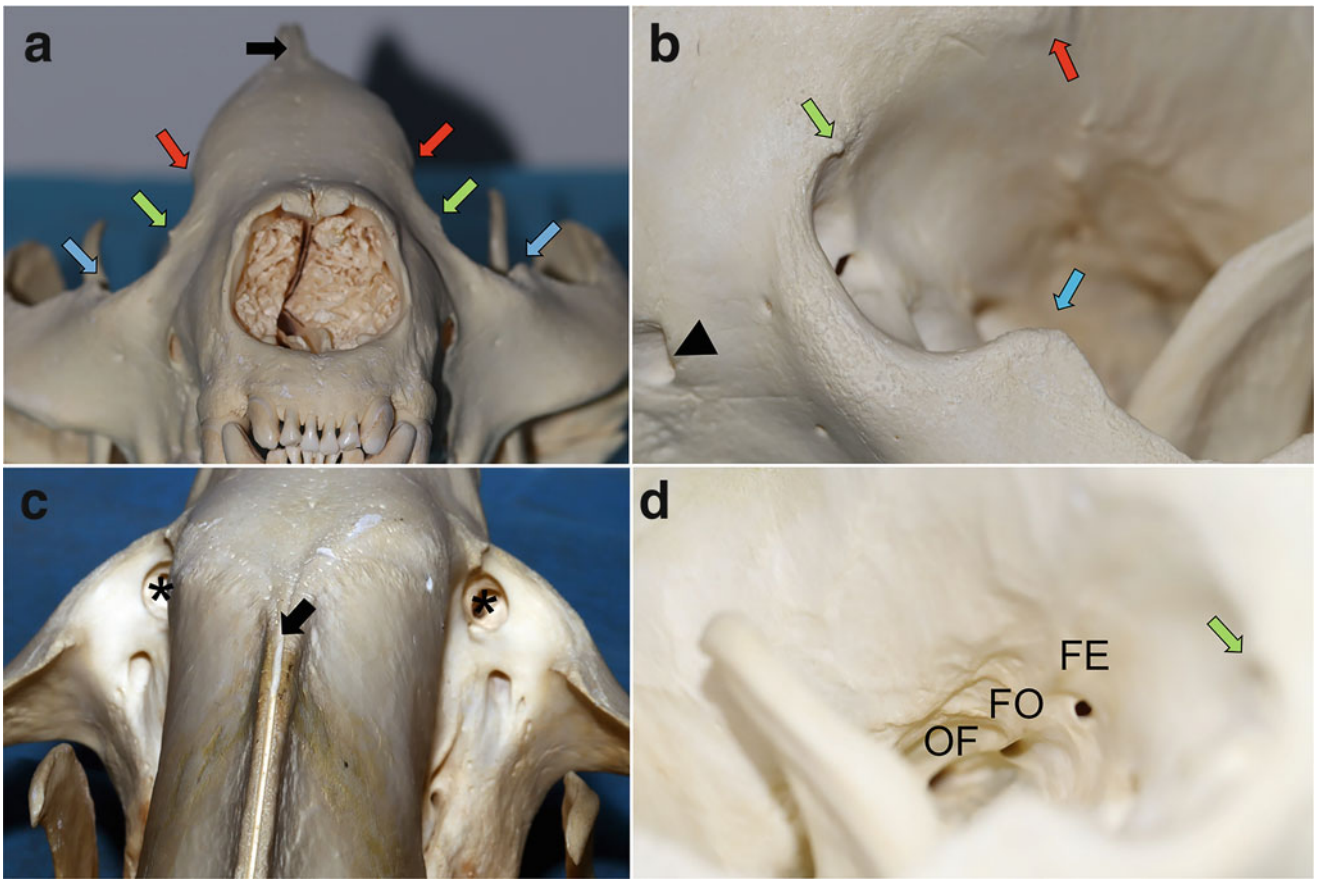

Fig. 37.1 Representative macerated skulls of the Giant Panda bear (*Ailuropoda melanoleuca*). (**a**) Rostral view: Note the presence of a sagittal crest and how the zygomatic arch substantially projects laterally. Zygomatic process of the frontal bone (red arrow); Frontal process of zygomatic bone (blue arrow); Lacrimal process (green arrow); Sagittal crest (black arrow) (**b**) Rostrolateral view: Note that bony orbit is open. Zygomatic process of the frontal bone (red arrow); Frontal process of zygomatic bone (blue arrow); Lacrimal process (green arrow); Sagittal crest (black arrow); infraorbital foramen (black arrowhead). (**c**) Dorsal, slightly caudal view: Note the funnel-shaped lacrimal fossa located medially on the ventral wall of the bony orbit, bilaterally (asterisks), which lodges the lacrimal sac. Also, note that the rostral surface of the zygomatic arch is wide. Sagittal crest. (**d**) Lateral, slightly rostral view: FE foramen ethmoidal (most rostral), FO optic foramen, OF Orbital fissure (most caudal). Photo credit: Rui Oliveira

below, are well marked by the superior and inferior orbital ridges. These ridges are less prominent in other ursids. Elsewhere the boundaries of the orbit are poorly marked on the skull; because of the feebly developed postorbital processes on both frontal and jugal bones, even the anterior limits are poorly indicated in *Ailuropoda* as compared with those of other ursids.

The lacrimal fossa, which lodges the lacrimal sac, is a large funnel-shaped pit at the anteromedial corner of the orbit (Fig. 37.1c). The nasolacrimal canal opens into the bottom of the fossa. The canal is only a millimeter or two long, opening almost at once into the nasal cavity, immediately beneath the posterior end of the maxilloturbinal crest. Bears are unique in having the nasolacrimal canal open into the maxillary sinus (Davis 1964). Immediately behind the lacrimal fossa is a shallow pit, the fossa muscularis, in which the ventral oblique muscle of the eye arises; the thin floor of this pit is usually broken through on dry skulls and then resembles a foramen. In bears and other arctoids the lacrimal fossa is much smaller than in *Ailuropoda*, but otherwise similar. The fossa muscularis in *Ailurus* is very similar to that of *Ailuropoda*; in bears, it is relatively massive—as large as the lacrimal fossa and several millimeters deep. The *fossa muscularis* is completely absent in the Canidae and Procyonidae (Davis 1964).

Three foramina in a row, about equidistant from each other, pierce the medial wall of the posterior half of the orbit (Fig. 37.1b). Each leads into the cranial fossa via a short canal directed posteriorly, medially, and ventrally. The most anterior is the ethmoidal foramen, which conducts the external ethmoidal nerves and vessels into the anterior cranial fossa. Behind this is the optic foramen (optic nerve, ophthalmic vessels), and most posteriorly and the largest foramina is the combined orbital fissure and foramen rotundum (which carries the oculomotor, trigeminal, trochlear, and abducens nerves, the anastomotic and accessory

meningeal arteries, and orbital vein). Except for the confluence of the orbital fissure and foramen rotundum, which is peculiar to *Ailuropoda*, the pattern of these three foramina is similar in all arctoids. The foramen ovale, in forms in which it is separate from the orbital fissure, transmits the third (mandibular) branch of the trigeminus and the middle meningeal artery (Davis 1964).

Additionally, the vertical diameter of the infratemporal fossa is much less in *Ailuropoda* than in Ursidae, and the orbit is rotated slightly ventrally compared with that of *Ursus*. Reduction of the infratemporal fossa in *Ailuropoda* is correlated with the more ventral position of the eye, and thus secondarily with the ventral expansion of the temporal fossa. The tremendously enlarged maxillary tuberosity, associated with the enlargement of the molar teeth, further reduces the volume of the fossa (Davis 1964). The orbital long axis (from the orbital fissure to the center of the eye socket) forms an angle of about 10° with the long axis of the skull in *Ursus*, whereas in *Ailuropoda,* the axes are parallel. At the ventral boundary of the orbital opening, there is a prominent crescent-shaped depression, which in life lodges a cushion of extraocular fat (Davis 1964).

The shape of the Giant panda bear globe is nearly spherical (antero-posterior long axis: 18.2 mm; equatorial axis: vertical 17.3 mm, horizontal 19.2 mm). In a histopathological study of a Giant panda bear from the Smithsonian National Zoological Park at the gross examination, the left eye measured 18 × 18 × 19 mm and the right eye measured 19 × 20 × 20 mm (McLean et al. 2003). Ultrasonographic B scan measurements of axial globe length of an Asiatic black bear were recorded as 15.9 ± 1.6 mm, with an axial lens diameter of 5.9 ± 0.5 mm (Hartley et al. 2013a). SB axial globe measurements of 43 individuals revealed 15.4 ± 1.9 mm with an axial lens diameter of 4.7 ± 0.3 mm (Hartley et al. 2014).

Diseases of the Bony Orbit and Globe

Retrobulbar fat prolapse to the subconjunctival space has been encountered in one Asiatic black bear in captivity. Although the cause of the prolapse was not clear, the resected material was confirmed as adipose tissue on histopathology (Fig. 37.2).

Phthisis bulbi occurs as a chronic sequel to uveitis in bears and has been particularly witnessed in those bears previously kept in captivity until aged as dancing bears (Fig. 37.3). Phthisis bulbi was identified in 12 Sloth bears (19 eyes) in a population of 43 Sloth bears examined at two sanctuaries in India. Grievous trauma to the globe by "correction" sticks used to placate or manipulate the bear to perform was proposed as the mechanism of phthisis development (Stades et al. 1995; Hartley et al. 2014).

Fig. 37.2 Subconjunctival location of retrobulbar fat prolapse in an adult female Asiatic black bear (*Ursus thibetanus*). Photo credit: Claudia Hartley

Enucleation in the bears is similar to that in dogs and can be undertaken by either transconjunctival or transpalpebral approaches. Conjunctival pseudocyst formation as a complication following enucleation with incomplete conjunctival removal leading to recurrent and persistent seromucinous discharging fistula has been observed in bears (Hartley et al. 2013b) as described in other species (Fig. 37.4) (Ward and Neaderland 2011; Spiess and Pot 2013).

Adnexa

Anatomy of the Adnexa

Bears are born with closed eyelids, with some variation between species as to when they open. Brown bear cubs open their eyelids at day 30–35 of age (Tumanov 1998), whereas polar bear cubs open their eyelids at 30–42 days of age (Kenny and Bickel 2005). The eyelids of the *Ursidae* family are very similar to most of the terrestrial mammalians. They represent a composite structure composed of skin and cutaneous appendages, including hair follicles and glandular structures. Bears have eyelashes only on the upper lid. The skin on the outer surface of the Giant panda bear eyelids is slightly thinner and more delicate than skin elsewhere on the body, but to a less extent compared to most domestic animals. There is a strong and encircling orbicularis oculi muscle anchored at the medial canthus. The eyelid margins are thick, with a well-developed fibrous tarsus, which contains the sebaceous tarsal (meibomian) glands. There is a large caruncle area usually with several hairs on the medial canthus. There is thin and flexible palpebral and bulbar conjunctiva, which is continuous, forming the upper and lower

Fig. 37.3 (**a**) Bilateral phthisis bulbi in an adult female sloth bear (*Melursus ursinus*). (**b**, **c**) Right and left phthisical eyes respectively of the same bear. Photo credit: Claudia Hartley

conjunctival fornix. The lower conjunctival fornix is critical to tear collection and movement to the lacrimal punctum.

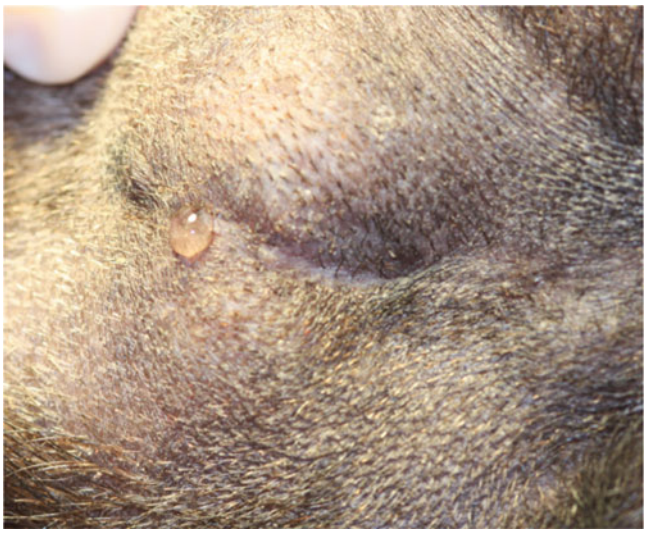

Fig. 37.4 Conjunctival pseudocyst formation with persistent drainage of seromucinous discharge (resolved with orbital debridement of conjunctival tissue) in an Asiatic black bear (*Ursus thibetanus*). Photo credit: Claudia Hartley

The palpebral fissure size in a Giant panda bear is just enough to accommodate the eyeball with an excellent blinking capability and good corneal coverage. In other bear species such as Asiatic black bear, sun bear, brown bear and sloth bear, the eyelids are well fitted, but the globe can be semi-prolapsed through the palpebral fissure with gentle posterior pressure on the lids under general anesthesia (Fig. 37.5). There is usually little bulbar conjunctiva exposed laterally, and this conformation together with a thick and nicely developed third eyelid, are very protective for the globe (Fig. 37.6).

Diseases of the Adnexa

Eyelid disease in an unpublished study of 135 captive Asiatic black bears and Asiatic black bear-Brown bear crossbred animals was common ($n = 45$), with 19 bears displaying blepharitis and 16 with entropion. Most cases of entropion were considered secondary to obesity (rather than conformational). Evidence of eyelid trauma was seen in 7 bears, with a single bear appearing to have small eyelid colobomata (notch defects). However, in these latter cases, acquired (traumatic)

Fig. 37.5 Partial prolapse of the globe in an adult Asiatic black bear (*Ursus thibetanus*) in Vietnam. Photo credit: Claudia Hartley

disease was not completely ruled out. Two bears had benign eyelid masses.

Entropion as a conformational or developmental issue is rare in bears, but an adult-onset entropion due to obesity is seen, akin to that seen in Vietnamese pot-bellied pigs (Linton and Collins 1993; Allbaugh and Davidson 2009). The fatty eyelids and periorbita impinge on the cornea (Fig. 37.7). Surgical correction to reduce the entropion can be achieved using both Hotz-Celsus and modified Stades' procedures, although repeat surgeries were sometimes warranted (Fig. 37.7b, c). More extensive face-lift procedures could be considered (Allbaugh and Davidson 2009), however, due to the fibrotic healing response seen in bears and the inability to protect the surgical site from self-trauma (bears will pick at surgical wounds), this could potentially result in disastrous dehiscence complications. Weight loss regimes are recommended but can be hard to achieve in captive bears due to skeletal pathology and/or restricted environments limiting activity. As bears are highly resource driven, group housing can complicate weight loss programs without provoking bear to bear aggression.

Eyelid trauma is reasonably common in bears in captivity due to fighting (Fig. 37.8) and injuries associated with climbing or by vegetable matter/feeds (e.g., bamboo). Despite the excellent ocular protection provided by the eyelids and orbital bone structures, ocular trauma is also encountered in ursid species. In one study (Miller et al. 2020), cornea and conjunctiva were the first and the second anatomical structures traumatized and were the first and second most prevalent eye conditions observed in captive Giant panda bears. In a rescued Giant panda bear from the wild, an old lesion compatible with an extensive upper and lower eyelid laceration and corneal trauma was documented (Fig. 37.9). The existing ocular abnormalities observed (corneal keratitis with fibrosis and extensive upper and lower eyelid scars) were compatible with a presumed old ocular trauma and eyelid laceration that had healed with notched lids.

Cicatricial ectropion in captive bears, secondary to traumatic injuries, is encountered, with perhaps a higher prevalence than wild bears due to greater bear to bear contact (group housing and conspecific aggression) than would be expected in the natural environment. Bears tend to heal with a fibrotic response, and therefore cicatricial effects can be more profound, and this should be carefully considered when attempting reparative surgeries (Fig. 37.10).

Eyelid masses are not commonly seen in bears, but when present, have generally been of a benign nature (tarsal adenoma, papilloma). In a captive Ursidae study (Blake and Collins 2002), a melanoma of the eyelid was diagnosed.

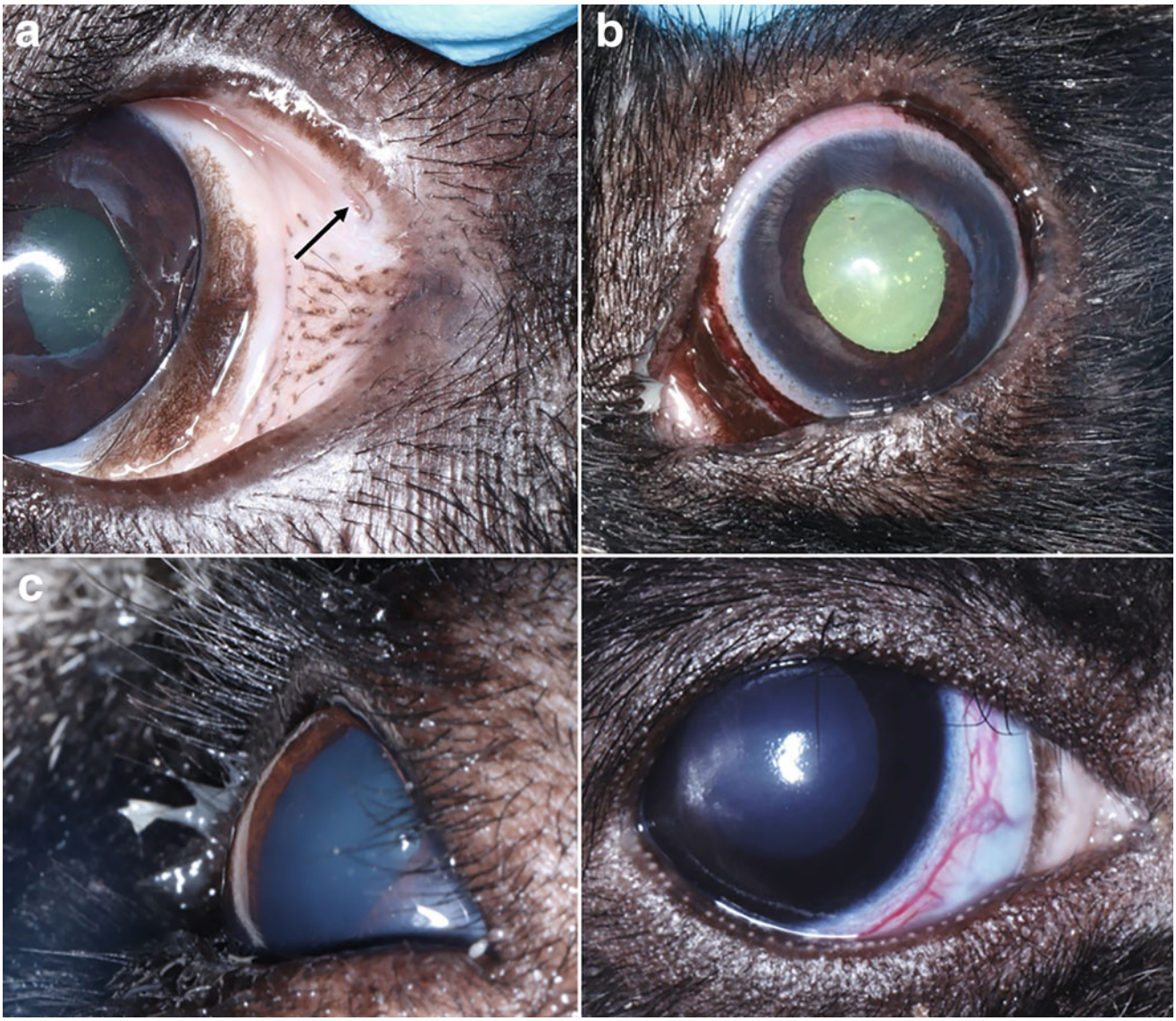

Fig. 37.6 The ocular adnexa of the Giant panda bear (*Ailuropoda melanoleuca*) (**a**) A right eye showing details of the eyelids and third eyelid, caruncula and superior lacrimal punctum opening (black arrow). (**b**, **c**) Left eyelid margins demonstrating that they are thick with a well-developed fibrous tarsus and contain the sebaceous meibomian glands. There is a large caruncle area with several hairs at the medial canthus (**b**). Some mild mucous discharge can be seen in (**c**). A newborn showing obvious upper eyelid eyelashes, and there are prominent meibomian gland duct openings on the lower eyelid. There are also some signs of corneal superficial keratitis and a very prominent Circle of Hovius. Photo credits: Rui Oliveira

Cutaneous hemangioma was diagnosed ventral to the eye on a 13-year-old, 102-kg, male Giant panda bear in a zoological collection. Initially, the case was presented with a small amount of blood on the left side of the face, with no pruritus observed. This animal had previously suffered superficial cuts on its pseudo thumb caused by sharp bamboo stems; thus the blood was initially attributed to trauma while feeding on bamboo. A small, round, dark gray, alopecic and ulcerated mass (less than 1 cm in diameter) was observed. The mass was excised under general anesthesia 3 months after presentation. Histopathology sections demonstrated a circumscribed, non-encapsulated superficial dermal proliferation of irregular dilated thin-walled vessels, many filled with blood and some showing intravascular papillary endothelial hyperplasia. The endothelial cells of the lesion did not have cytological atypia or mitotic activity, nor was there any evidence of destructive local tissue infiltration to suggest malignant behavior. The histologic appearance was considered to represent that of a cavernous type of hemangioma, and excision was complete. Four years after surgery, no sign of recurrence was observed (Mauroo et al. 2006). Dermal hemangioma may appear as solitary or multiple masses. The overlying epidermis is usually alopecic; ulceration and hemorrhage are frequent findings. Chronic

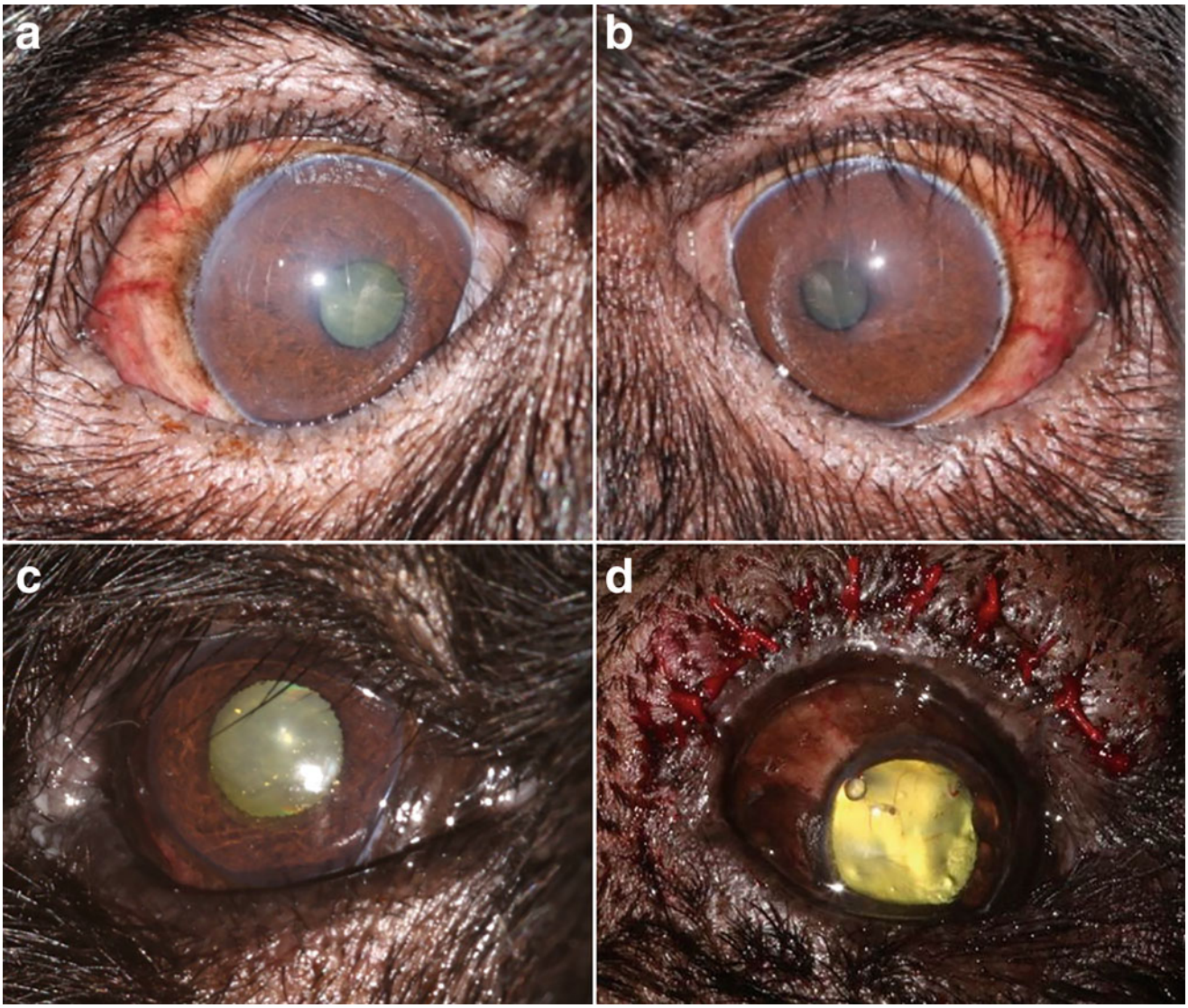

Fig. 37.7 Entropion in bears. Right (**a**) and left (**b**) lower eyelid entropion in adult female Asiatic black bear (*Ursus thibetanus*) from a sanctuary, resulting in chronic epiphora and conjunctival hyperemia. (**c**) Upper eyelid entropion (lid lightly retracted) on right eye of an adult female Asiatic black bear—note mucopurulent discharge at lateral canthus also. (**d**) Hotz-Celsus procedure on the upper eyelid of the same right eye as (**c**). Photo credit: Claudia Hartley

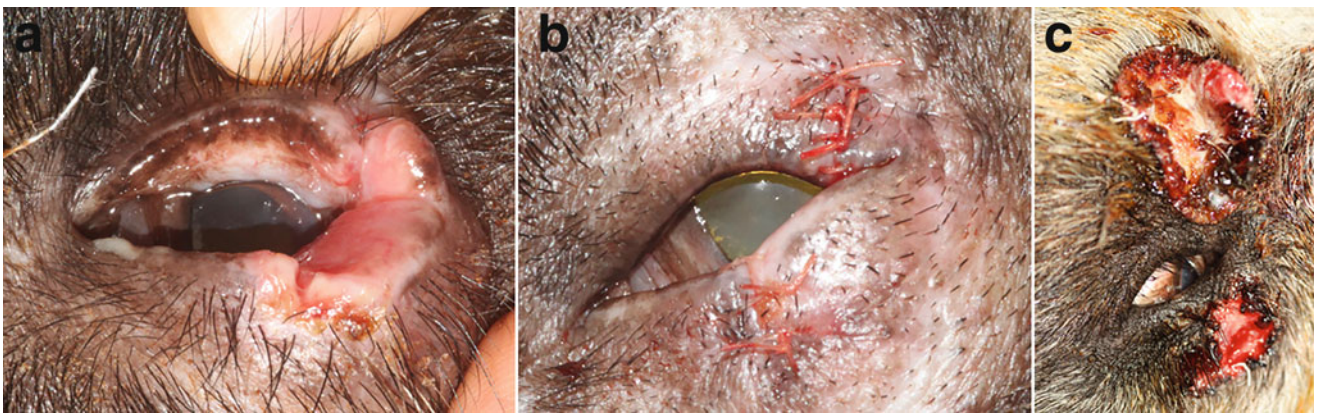

Fig. 37.8 (**a**, **b**) Eyelid laceration due to fighting in a group-housed Asiatic black bear (*Ursus thibetanus*); before (**a**) and after repair (**b**). (**c**) Periocular wounds in an adult sloth bear (*Melursus ursinus*) from presumed fighting with a conspecific (sanctuary in India). Photo credit: Claudia Hartley

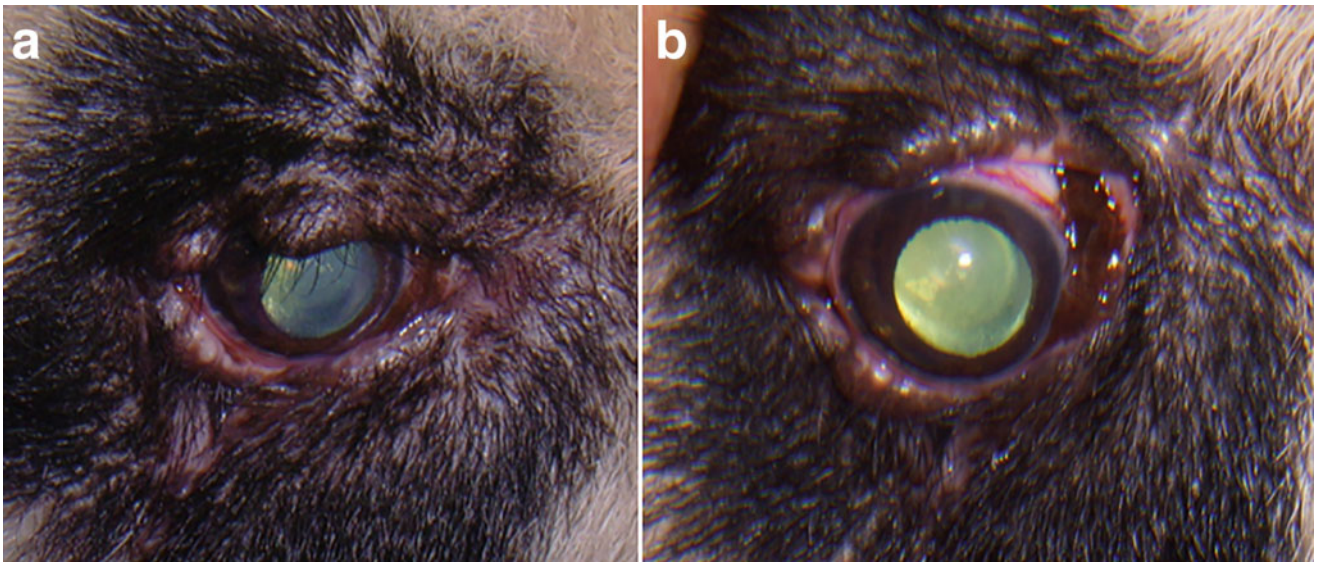

Fig. 37.9 Ocular trauma in Giant panda bears (*Ailuropoda melanoleuca*) (**a**) A presumed old ocular trauma causing extensive eyelid laceration on the right eye. (**b**) A presumed old ocular trauma causing extensive eyelid laceration on the right eye. OD presented with mild conjunctivitis, mild keratitis, with areas of corneal fibrosis, and extensive loss of tarsal margin, on both upper and lower eyelids, close to the lateral canthus. On the periocular area, there were large areas of eyelid scarring compatible with previous ocular trauma and eyelid laceration. Photo credit: Rui Oliveira

solar exposure has been reported to be a contributory factor in domestic dogs. This giant panda had been previously housed in an outdoor exhibit at high altitude; however, cutaneous neoplasia has not been reported among large captive populations of giant pandas also housed at high altitudes in China. The etiology, in this case, is unknown.

Blepharitis is seen commonly in bears and may have a number of etiologies. It is seen secondary to entropion and increased eyelid wetting because of epiphora. *Demodex* and *Sarcoptes* spp. have not been encountered in periocular hair plucks and skin scrapes, respectively, in Asiatic black bears, Sun bears, or Brown bears examined by one of the authors, but a generalized disease caused by both parasite infestations have been reported in wild American brown bear populations (Manville 1978; Foster et al. 1998; Forrester et al. 1993; Peltier et al. 2018; Van Wick and Hashem 2019; Niedringhaus et al. 2020). There are several reports of sarcoptic mange in other Ursidae, including the Polar bear (*Ursus maritimus*), Brown bear (*Ursus arctos*) (Jedlicka and Hojovcova 1972) and also in *Procyonidae* including the Red panda *Ailurus fulgens* (Bornstein et al. 2001).

Ursicoptes americanus mange has been reported in an American black bear and was associated with alopecia and pruritis (Yunker et al. 1980), similar to animals affected by Demodex and Sarcoptes infestations. The chewing louse *Trichodectes pinguis* has been reported in wild Asiatic black bears, Brown bears, and American black bears (Yokohata et al. 1990; Fandos-Esteruelas et al. 2016).

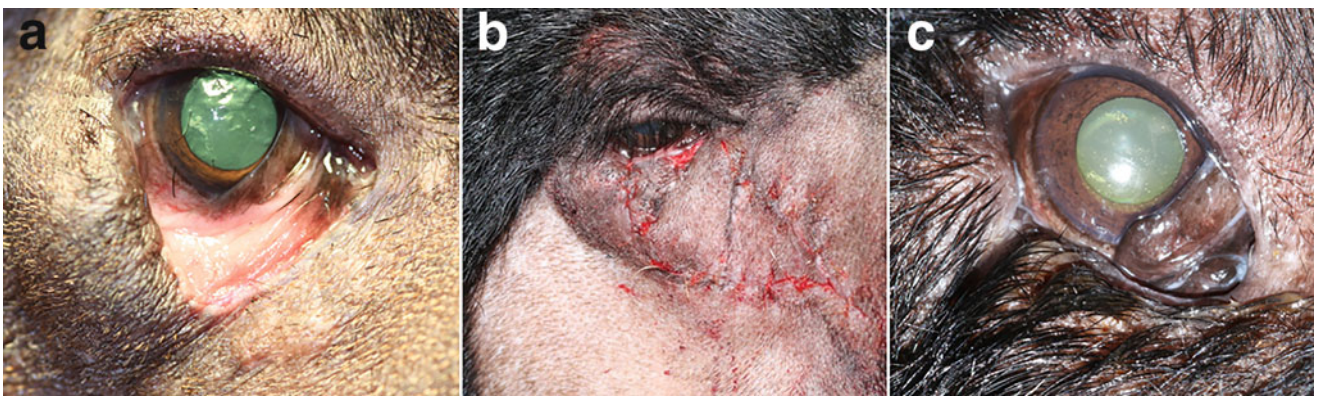

Fig. 37.10 Cicatricial entropion in an adult female Asiatic black bear (*Ursus thibetanus*), which occurred following a fight with conspecific (**a**) Prepared for surgery (H-plasty). (**b**) Appearance after second surgery due to postoperative contracture (V to Y plasty). (**c**) Final appearance after blepharoplastic repair, some mucoid ocular discharge remains despite the reduction of exposure. Photo credit: Claudia Hartley

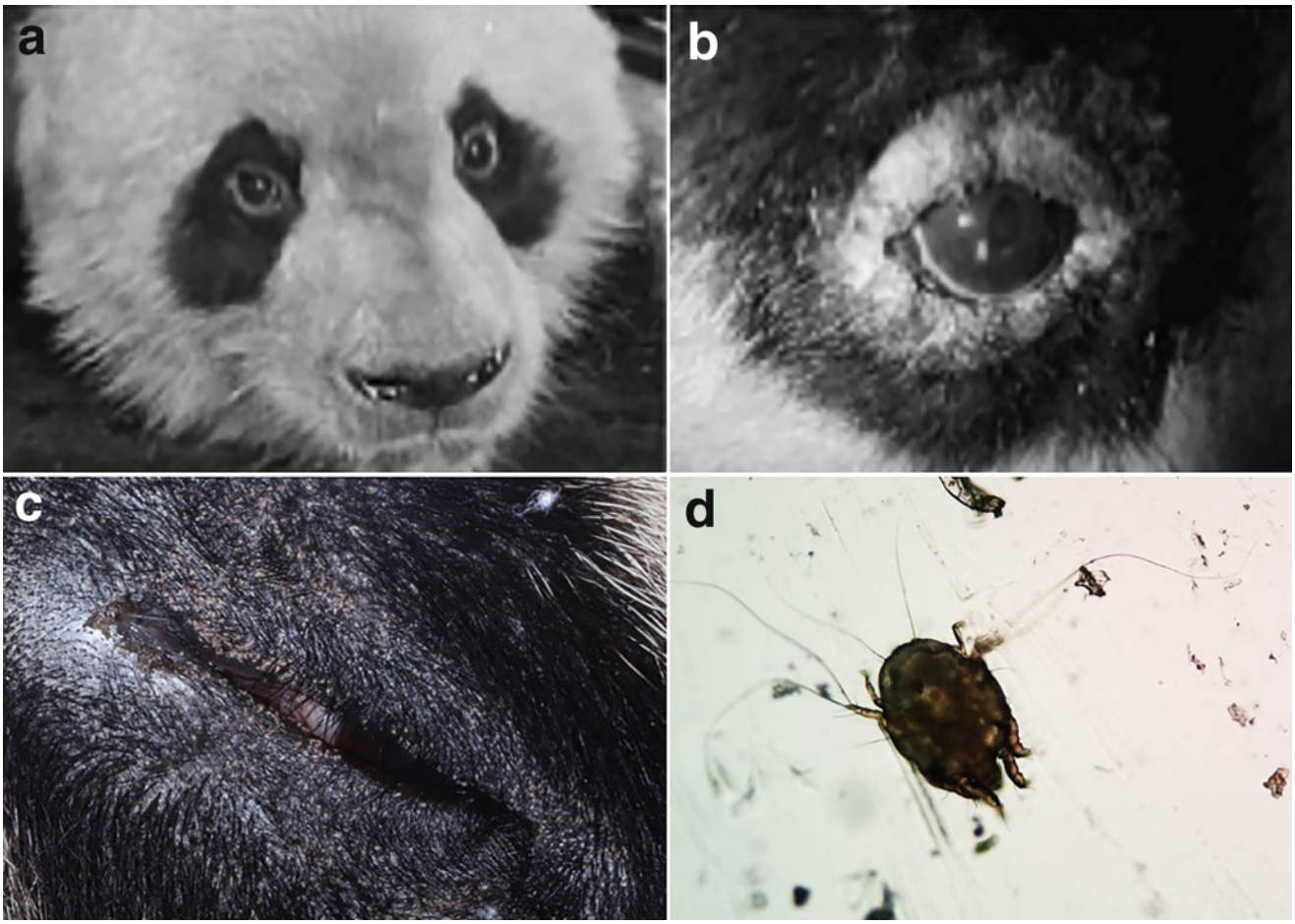

Fig. 37.11 Infectious anterior blepharitis in Giant panda bears (*Ailuropoda melanoleuca*). (**a**, **b**) A male with hair loss, skin crusting, and swelling around the eyelid margins caused by *Demodex* sp. mites. (**c**, **d**) Sarcoptic mange causing alopecia and pruritis (**c**) with a parasite seen on cytology (**d**). (**a**, **b**) Used with permission from Wildt, DE, Zhang A, Zhang H, Janssen D, Ellis S (2006). Giant pandas: biology, veterinary medicine and management. Cambridge University Press. (**c**, **d**) Photo credit: Rui Oliveira

Several causes of parasitic blepharitis have been diagnosed in Giant panda bears, including *Demodex* sp. and *Sarcoptes scabiei* (Fig. 37.11). We also diagnosed three cases of Thelaziosis, causing mucopurulent discharge with potential dacryocystitis and conjunctivitis in several Giant panda bears. Medical treatment in these cases included topical neomycin and polymyxin B sulfates and dexamethasone ophthalmic eye drops (Maxitrol, Alcon) twice daily for 3–5 days and one dose of spot-on dermal application of 10% imidacloprid and 2.5% moxidectin (Advocate Spot-On; Bayer HealthCare).

Wildt et al. (2006) describe 6 of 61 Giant panda bears (9.8%) had clinical disease associated with *Demodex* sp. skin mites (Fig. 37.11a, b). Diagnosis was made by performing a skin scraping of the affected area followed by a microscopic examination. All but one affected panda was an adult, and four had been captive-born. The most typical lesions were mild alopecia associated with crusting and swelling of the eyelids. In one case, a 5.5-year-old male had severe, generalized demodicosis with widespread alopecia, erythema, pyoderma and lichenification of the skin (Wildt et al. 2006). Mild alopecia (hair loss) on the eyelid border attributed to *Demodex* sp. mites was seen in five animals, with one additional individual experiencing severe demodicosis with extensive hair loss and pyoderma (Wildt et al. 2006).

Alopecia and pruritus have been observed in giant pandas in association with renal failure (Li et al. 2001), stereotypical behaviors (Zhang et al. 2000) and ectoparasitism (Leclerc-Cassan 1985). At the workshop on Diagnostic and Clinical Pathology in Zoo and Wildlife Species (Beijing, June 2002), demodicosis was recognized as a significant skin disease in the giant panda. Periocular and generalized demodicosis were also observed during the CBSG Giant Panda Biomedical Survey, with one animal being severely affected with alopecia, erythema, pyoderma and skin lichenification (Zhang

et al. 2000). References to *Demodex* sp. in the giant panda also appear in the literature (Xu et al. 1986). Although no data are available, we suspect that demodicosis in the giant panda is associated with a compromised immune status, as it is in the domestic dog.

Several Giant panda bears observed with recurrent blepharitis were confirmed to have sarcoptic mange caused by the *Sarcoptes scabiei* mites (Fig. 37.11c, d). In our examinations, several animals (3/26) we found having mild to severe blepharitis caused by *Sarcoptes scabiei*. Sarcoptic mange is a globally distributed, infectious disease of wildlife that is emerging in some species and has been reported in greater than 100 species of mammals. The sarcoptic mite burrows deep into the epidermis, causing inflammation, intense pruritis and, in advanced cases, a perturbed skin barrier that may result in death secondary to infection, dehydration and impaired thermoregulation (Rowe et al. 2019). Treatment for this condition in the Giant panda bears has been undertaken using one dose of "spot-on" dermal application of selamectin 6% (Stronghold® "spot-on"). This treatment is usually done monthly on animals that are conditioned for "spot-on" applications, and whenever is necessary and possible in animals that are not conditioned for this procedure.

Periocular alopecia in the captive Giant panda bear population was a very common problem. Swabs for bacterial and fungal cultures, eyelid scrapings and skin biopsies were all inconclusive as to the cause of this abnormality, and further investigation was necessary to try to find the cause for this condition (Fig. 37.12). Possible involvement of *Demodex* and/or *Sarcoptes scabiei* mites was also investigated through microscopic examination of multiple deep skin scrapings as well as from hair plucked from adjacent eyelid skin, but these examinations were negative for the presence of mites. On a few skin biopsies conducted on a couple of most severe cases of alopecia by the local veterinary team, the histopathology results were also inconclusive (non-specific inflammation), and no diagnosis was obtained. This condition was not considered related to husbandry or a particular place or enclosure, as animals at different facilities and in different countries were displaying signs of this problem, while others in the same location did not show it. Based on this information, we hypothesized that the cause for this periocular alopecia was a multifactorial condition with hormonal components and a possible immunodeficiency role. Periocular alopecia has also been seen in Asiatic black bears in China.

An alopecic syndrome in Polar bears has been described as affecting the head, neck and shoulders, but the cause remains elusive. It does not appear to affect the periocular area. However, the loss of the heat-insulating effect of their coat has been hypothesized to have a detrimental effect on survival for those affected (Atwood et al. 2015). Another alopecic syndrome has been reported in Andean spectacled bears, but this is largely manifested with flank alopecia. Some authors have speculated that this may represent a stress response to group housing (Van Horn et al. 2018).

One Giant panda bear was presumptively diagnosed with vitiligo. Although there are no previous descriptions of this condition in bears, the skin lesions and location of these were considered very typical of this condition as described in other species (Fig. 37.13). The animal in question developed several areas of non-ulcerated, non-pruritic depigmentation in the palmar, plantar footpads and digital pads, interdigital skin, lips, nares, ventral tail, and perineal region. Furthermore, these areas were not painful or inflamed, and no pustules, crusts or scales were observed, but a few superficial erosions on the palmar pads were noted. Unfortunately, skin biopsies of the affected areas to confirm the diagnosis of this condition by histopathology (very restricted sampling allowed in this case) were not possible. Given this limitation, a presumed diagnosis of cutaneous vitiligo was made for this case. Other possible differential diagnoses to consider are *discoid lupus erythematosus*, zinc-responsive dermatosis, cutaneous epitheliotrophic lymphoma, *Pemphigus foliaceus* or other autoimmune skin diseases like uveodermatological syndrome (absence of intraocular signs like uveitis makes this an improbable differential). Vitiligo has been described in domestic animals, including cattle, horses, cats, dogs and chickens; there is also a single case report in a black rhinoceros (*Diceros bicornis michaeli*) (Takle et al. 2010) and another recent case report of cutaneous vitiligo associated with hypovitaminosis D in Malayan flying foxes (*Pteropus vampyrus*) and Island flying foxes (*Pteropus hypomelanus*) (Stringer et al. 2016). Recently, a connection has been made between human autoimmune diseases, including vitiligo and Vitamin D deficiency (Saleh et al. 2013).

Conjunctiva

Anatomy of the Conjunctiva

The conjunctiva of bears is very similar to that in dogs, with bulbar and palpebral portions reflecting at a conjunctival fornix dorsally and ventrally. The conjunctiva also lines the surface of the third eyelid and is continuous with both bulbar and palpebral components. To the authors' knowledge, based on published information and on previous Giant panda bear examinations, no conjunctival congenital abnormalities have been observed or reported (Fig. 37.14a).

Diseases of the Conjunctiva

In a study examining 135 bears (Asiatic black bears, Sun bears, and Brown bears) at sanctuaries in China and Vietnam (rescued from the bile farming trade), conjunctival hyperemia

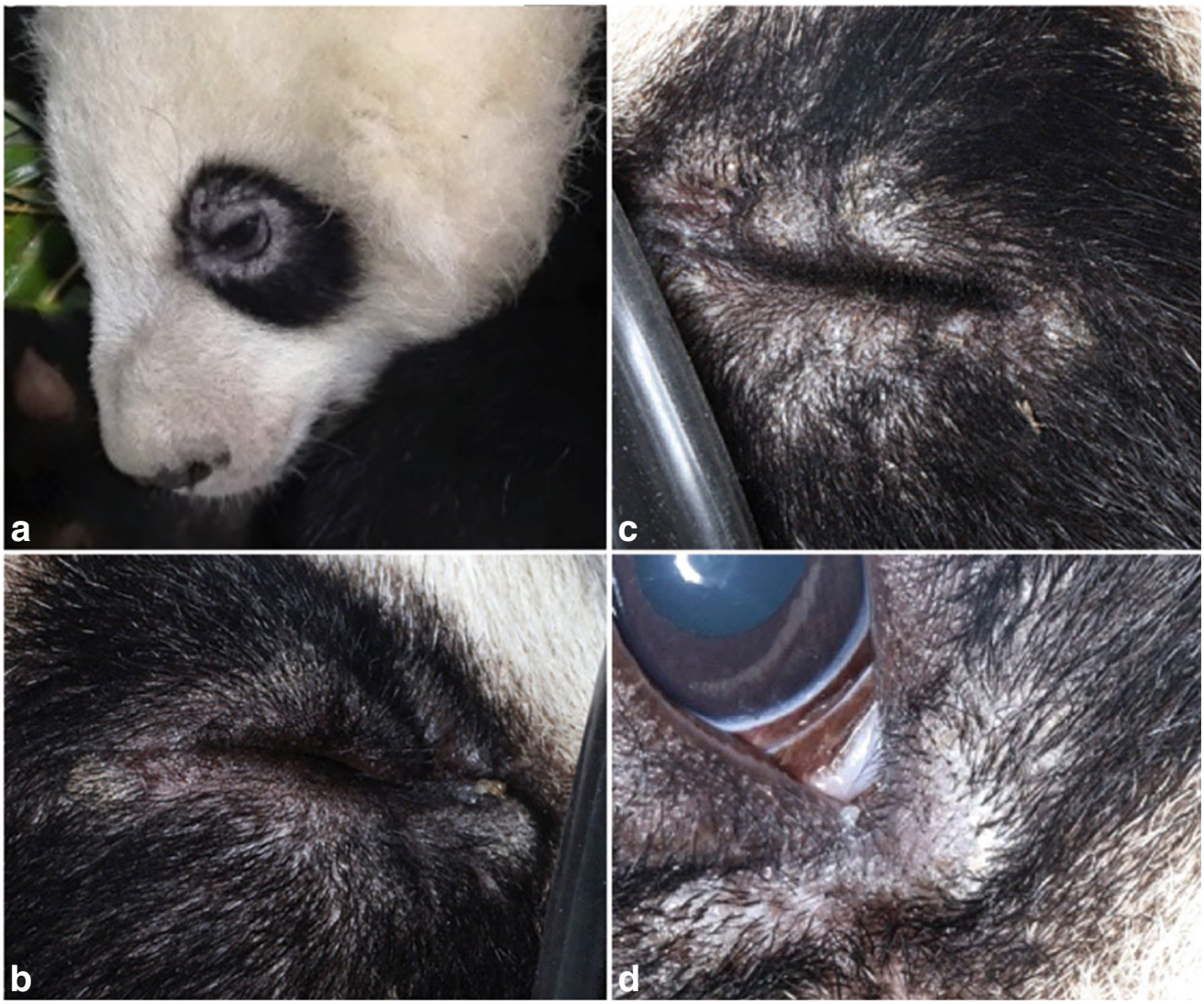

Fig. 37.12 (a) and (b) Left eye. (c) and (d) Right eye. Periocular alopecia was observed in several captive Giant panda bears (*Ailuropoda melanoleuca*). These lesions were frequently observed, and no diagnosis was obtained. This condition needs further investigation in order to try to reach a definitive diagnosis. Photo credit: Rui Oliveira

(Fig. 37.14b) was reported in 20 bears. Conjunctival masses were seen in six animals, but only two of these had concurrent hyperemia. Subjectively it appeared that these bears were more resistant to displaying hyperemia under anesthesia than dogs, but no provocative tests have been undertaken to verify this. Non-specific signs of conjunctivitis with hyperemia (Fig. 37.14b), mild thickening, follicular hyperplasia and ocular discharge can be seen in bears (including Asiatic black bears, Sun bears, Brown bears, and Sloth bears examined at various sanctuaries) and specific causes included: secondary to presumed atopy (biopsies and dermatological workups suggestive), secondary to conjunctival exposure (cicatricial ectropion, phthisis bulbi) or irritation from dusty conditions (largely seasonal—dry seasons combined with wind). Surgical correction of the ectropion or enucleation of a phthisical eye is usually sufficient to resolve conjunctivitis associated with these conditions.

Conjunctival flora sampled between 2010 and 2019 from captive or rescued Asiatic black bears in China with conjunctivitis or corneal disease ($n = 40$) revealed a preponderance of Gram-positive cocci (50% of bacterial colonies), followed by Gram-positive rods (12.5%), Gram-negative rods (12.5%) and yeasts (12.5%). Gram-negative cocci and no growth were obtained in 6% each. Species identification was not attempted. Sensitivity testing revealed: sensitivity to enrofloxacin in 32% (resistance 41%; intermediate 26%, $n = 34$), sensitivity to amoxicillin-clavulanate in 28% (resistance 64%, intermediate 7%, $n = 39$), sensitivity to cephalexin in 39% (resistance 50%, intermediate 11%, $n = 36$), sensitivity to clindamycin in 42% (resistance 46%,

Fig. 37.13 Areas of symmetrical depigmented patches in a giant panda bear (*Ailuropoda melanoleuca*) on the nasal planum (**a**), periocular region (**b**), footpads (**c**) and third eyelid (**d**). Photo credit: Rui Oliveira

intermediate 11.5%, $n = 26$), sensitivity to gentamicin in 72% (resistance 17%, intermediate 10%, $n = 29$), sensitivity to metronidazole in 3% (resistance 97%, $n = 32$), sensitivity to trimethoprim in 33% (resistance 64%, intermediate 3%, $n = 33$), sensitivity to penicillin in 18% (resistance 68%, intermediate 15%, $n = 34$), and sensitivity to doxycycline in 44% (resistance 54%, intermediate 3%, $n = 39$).

Conjunctival flora sampled between 2010 and 2017 from captive or rescued Asiatic black bears and Sun bears in Vietnam with conjunctivitis, or corneal disease ($n = 18$) revealed a preponderance of Gram-positive cocci that were not speciated by the microbiology lab (29% of bacterial colonies), followed by *Enterococci* (21%), *Staphylococci* (7%) and *Acinetobacter* (7%). No growth was recorded in 36% of samples. Sensitivity testing was not undertaken on all bacterial colonies but revealed: sensitivity to amoxicillin-clavulanate in 100% ($n = 6$), sensitivity to cephalexin in 25% (resistance 50%, intermediate 25%, $n = 4$), sensitivity to clindamycin and doxycycline in 20% (resistance 60%, intermediate 20%, both $n = 5$), sensitivity to gentamicin in 75% (resistance 12.5%, intermediate 12.5%, $n = 8$), sensitivity to ciprofloxacin in 29% (resistance 57%, intermediate 14%), and resistance to metronidazole and oxytetracycline in 100% (both $n = 4$). It is very difficult to draw accurate conclusions with such small data samples. It should also be noted that most of these animals are not able to receive topical medication (not drop-trained captive animals).

Within a previous study (Blake and Collins 2002), including 512 animals in the family Ursidae (with the exception of Giant panda bear), sun bears had the highest prevalence of ocular disease (13%), and four bears of 17 (23.5%) were listed as conjunctivitis, with three (75%) found in spectacled

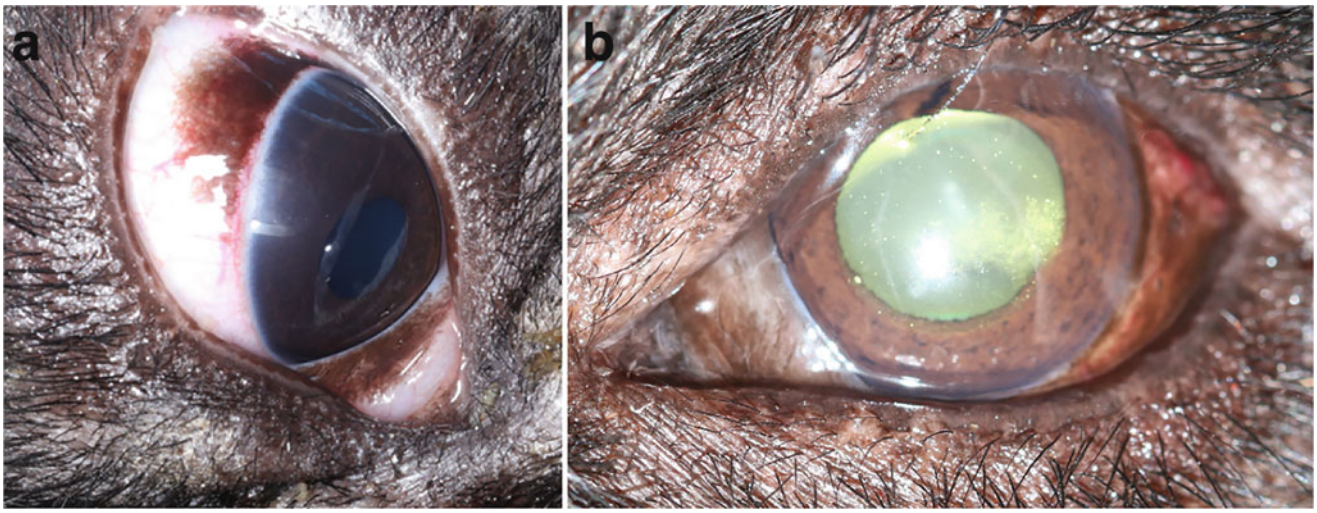

Fig. 37.14 (**a**) Normal partially pigmented bulbar conjunctiva and third eyelid in the giant panda bear (*Ailuropoda melanoleuca*). (**b**) Bulbar conjunctival hyperemia in an adult female Asiatic black bear (*Ursus thibetanus*). (**a**) Photo credit: Rui Oliveira. (**b**) Photo credit: Claudia Hartley

bears and one polar bear. In this study, there was also a case of chronic contact conjunctival irritation (Blake and Collins 2002).

Conjunctivitis and/or ocular discharge was the second most-reported ocular abnormality reported in captive ursids (Miller et al. 2020). This is similar to the results of another survey of captive ursids, in which conjunctivitis was the second-most-common ocular abnormality, affecting 23.5% (4 of 17) animals.

Nematodes belonging to the genus Thelazia (Spirurida, Thelaziidae) are parasites inhabiting the eyes and associated tissues of mammals (Anderson 2000). At least 16 species have been identified in different hosts (Otranto and Traversa 2005), and among them, the eyeworm *Thelazia callipaeda* affects both animals and humans. This zoonotic parasite that lives in the conjunctival sac, under the lids and the nictitating membrane of dogs, cats and wildlife, may induce a range of clinical signs, such as epiphora, photophobia, keratitis, conjunctivitis, etc. (Otranto and Traversa 2005; Soares et al. 2013; Motta et al. 2014). This larval nematode is transmitted between animals by face flies. It is small and may be seen moving across the surface of the eye or hiding beneath the third eyelid. Occasionally, its presence can cause enough irritation that the animal will self-traumatize, which can lead to a secondary corneal ulcer (Gionfriddo 2013).

During author's examinations of three adult Giant panda bears living in the breeding facility in Chengdu, China, were diagnosed with ocular thelaziosis. Ophthalmological examination revealed mild unilateral bulbar and nictitating membrane conjunctival hyperemia with the serous or mucopurulent discharge of the affected eyes. STT and IOP values were within the bear reference ranges in all eyes. Several adult nematode worms were retrieved using delicate conjunctival serrated forceps from three Giant panda bear eyes that presented with the previous history of intermittent unilateral ocular discharge and epiphora (left and right eyes affected). The white worms were observed close to the caruncle, under the third eyelid and on conjunctival or corneal surface with undulating movements that increased with light intensity (Fig. 37.15a, b). In total five worms were collected and morphologically identified as adults of *Thelazia callipaeda*. All specimens were identified as *T. callipaeda* according to several morphological features: size, presence of a buccal capsule, transversally striated cuticle, the position of the vulva (located anterior to the esophagus-intestinal junction), presence of numerous rounded first-stage larvae in the distal uterus in female worms, and the presence of two dissimilar spicules in the caudal bursa of the male worm (Otranto et al. 2003; Caron et al. 2013).

In affected Giant panda bears, all worms observed were removed using dedicated conjunctival forceps. The nasolacrimal patency was also tested by normograde flushing of saline via both upper and lower puncta of both eyes. When testing the nasolacrimal patency of one individual's left eye, one worm was flushed out to the nostril. Medical treatment included topical neomycin and polymyxin B sulfates and dexamethasone ophthalmic eye drops (Maxitrol, Alcon) twice daily for 3–5 days (trained to receive topical medications) and one dose of spot-on dermal application of 10% imidacloprid and 2.5% moxidectin (Advocate Spot-On; Bayer HealthCare).

Thelazia callipaeda has an indirect life cycle. After mating, female *Thelazia* nematodes produce first-stage larvae (L1) that are released in the lacrimal secretions. A non-biting fly is the intermediate host that is attracted to the eyes and ingests L1s that develop to second (L2) and third-

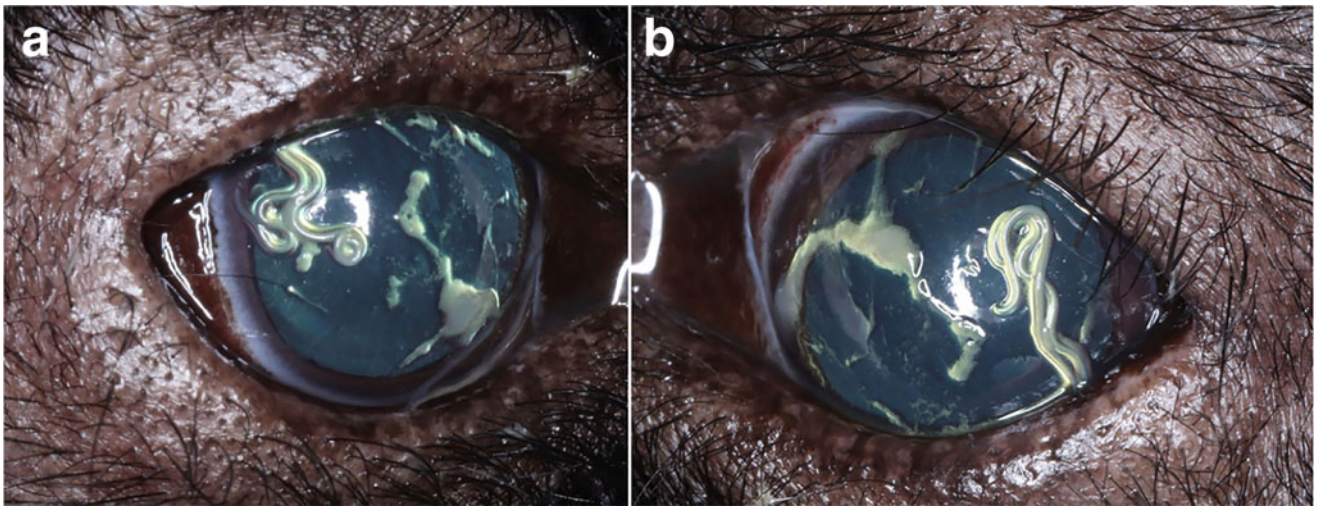

Fig. 37.15 (**a**) (right eye) and (**b**) (left eye)—Giant panda bear (*Ailuropoda melanoleuca*) eyes with *Thelazia callipaeda* and mucopurulent discharge. Photo credit: Rui Oliveira

stage larvae (L3). Finally, L3s are transmitted by the infected flies into the eyes of the definitive host and subsequently, develop to adulthood. In Europe, the intermediate host for *T. callipaeda* is the zoophilic fruit fly *Phortica variegata*, which feeds on plant juices and lacrimal secretions of animals and humans (Otranto et al. 2006). The first-stage larvae L1s are released by the adult worms into the conjunctival secretions of infected animals, and they are ingested by *P. variegata* flies, where undergoing two molts, they develop into the infective third-stage larvae (L3) within about 3 weeks. The third-stage larvae are transferred back to the eye when the fly feeds on ocular secretions (Bianciardi and Otranto 2005; Motta et al. 2014). The face fly *Musca autumnalis* in North America, and *Phortica variegata* in Asia (and Europe) are known intermediate hosts (Bowman 2010; Otranto et al. 2006). Foxes and wolves may be important in the spread and maintenance of disease (Dorchies et al. 2007; Otranto and Traversa 2005).

The adult whitish nematodes (about 0.5–2 cm) and first-stage larvae (L1) localize under the third eyelid provoking lacrimation, conjunctivitis or even keratitis and corneal ulceration. The lateral serrations of the cuticle of the nematodes cause mechanical damage to the conjunctiva and cornea, leading to lacrimal secretions upon which non-biting Diptera feed (Bianciardi and Otranto 2005). In affected wild animals, *T. callipaeda* adult and larval stages may cause mild ocular manifestations (conjunctivitis, epiphora, and ocular discharge) to severe disease (keratitis and corneal ulcers) (Otranto and Traversa 2005). The most common symptoms in affected dogs and foxes in Switzerland were conjunctivitis and epiphora, while keratitis was present only in a low number of animals.

Both adult and larval stages of the eye worm are responsible for symptoms ranging from mild (e.g., lacrimation, ocular discharge, epiphora) to severe (e.g., conjunctivitis, keratitis and, corneal opacity or ulcers), also related to the load of parasites inhabiting the conjunctival sacs (Shen et al. 2006). The most common clinical signs observed in all species are conjunctival hyperemia and serous ocular discharge; the parasite is easily removed from the conjunctival fornix with forceps, although continued exposure to the vector will result in reinfection.

The parasitic stages of *T. callipaeda* (i.e., adults and larvae) may be removed mechanically by rinsing the conjunctival sac with sterilized saline fluids or by collecting the adults with fine forceps or cotton swab; however, worm removal may be incomplete. Successful treatment of eye worm infection also includes topical instillation of organophosphates (Rossi and Peruccio 1989) ormoxidectin 1% (Lia et al. 2004), which were effective against *T. callipaeda*. For compliance reasons, it may be recommended to use systemic macrocyclic lactones licensed for dogs and cats, such as the spot-on formulation containing moxidectin (Advocate®, Bayer HealthCare AG). Additionally, milbemycin oxime/praziquantel tablets (Milbemax®, Novartis-Animal Health) at the minimal dose of 0.5 mg/kg milbemycin oxime (InterceptorW, MilbemaxW, Program PlusW, SentinelW, Novartis Animal Health) (Ferroglio et al. 2008) Interceptor W was reported to have good therapeutic and prophylactic efficacy in treating thelaziosis in naturally infested dogs (Ferroglio et al. 2008; Motta et al. 2012) and was shown to reduce infection rate in naturally infected dogs and cats significantly. Meanwhile, imidacloprid 10% and moxidectin 2.5% spot-on formulation was shown to

be effective for the treatment and prevention of canine thelaziosis (Bianciardi and Otranto 2005; Lechat et al. 2015).

There are two cases reported of conjunctival tumors in the Giant panda bear, one of ocular squamous cell carcinoma (SCC) at the limbus and another of a haemangiosarcoma of the conjunctiva. In the Miller et al. (2020) study, a single case of ocular SCC at the limbus is described, which resolved after the second surgical removal of the tumor. Previously published ocular neoplasia in the giant panda included a retinal hamartoma and conjunctival hemangiosarcoma (Lopez et al. 1996; McLean et al. 2003).

The conjunctival hemangiosarcoma case was diagnosed in a 13-year-old male Giant panda bear from the Zoo de la Casa de Campo, Madrid, Spain. In this case, a small (5 mm diameter) circular, the reddish-pink discrete lesion was present on the bulbar conjunctiva at the lateral limbus of the left eye. Other ocular signs were slight intermittent hemorrhage originating from this mass. Under general anesthesia, the tumor was excised by superficial keratectomy/sclerectomy, with a margin of approximately 2 mm. The mass appeared to be completely confined to the conjunctiva without invasion of the underlying bulbar tissue. Postoperative treatment was topical gentamicin/dexamethasone eye drops BID-TID for 1 week (Lopez et al. 1996). Histopathology showed a superficial lesion consisting of vascular spaces and clefts lined by plump, hyperchromatic endothelial cells with small dark nuclei. There was good cellular differentiation and a low mitotic rate. The mass was hemorrhagic with small quantities of hemosiderin and inflamed with neutrophilic infiltrates. The conjunctival epithelium was ulcerated. A diagnosis of well-differentiated haemangiosarcoma was made. Six weeks after surgery, the panda was in good health with no signs of mass recurrence (Lopez et al. 1996). The animal lived in an enclosure that provided two fairly open grassy paddocks, an indoor dormitory, and a shady air-conditioned semi "open pavilion," Although the panda, one of two at the location, did spend much of the day during summer in his shaded pavilion, he was exposed to high levels of sunlight when out and about in the paddock even though there were trees and bushes giving some cover. It should be remembered that the natural habitat of giant pandas is cool, wet mountain forests, where they tend to prefer regions with a canopy coverage of 90% or more (Schaller et al. 1985). A recommendation was made to increase the amount of shade in the grass paddocks used by the pandas in Spain, and this probably should extend to all enclosures for Giant panda bears in the world, especially in sunny locations with elevated UV exposure.

Conjunctival masses encountered in bears by the authors include squamous cell carcinoma (Sun bear) (Fig. 37.16a), a pigmented non-neoplastic mass in an Asiatic black bear (Fig. 37.16b), lymphoplasmacytic plaques (presumed immune-mediated; Asiatic black bear) (Fig. 37.16c, d), retrobulbar fat prolapse that produced a subconjunctival mass (Asiatic black bear), and a benign non-neoplastic conjunctival pigmented mass (Asiatic black bear).

Third Eyelid

Anatomy of the Third Eyelid

The third eyelid (or nictitating membrane) is a mobile, modified conjunctival fold that protrudes from the medial canthus, lying between the cornea and the lower eyelid in the medial portion of the inferior conjunctival sac. It has glandular and protective functions. The nictitating membrane in the Giant panda bear is very prominent. Its free border is nearly square, with a slight concavity at the center and rounded corners. This border is typically heavily pigmented on both its outer and inner surfaces. The membrane is supported by a broad central strip of cartilage, the nictitating cartilage, which begins medially with a rounded tip, then extends along with the eyeball in a gentle dorsally concave arc, and terminates by expanding slightly in the free border of the membrane. The width of the cartilage is rather uniform, about 4 mm (Davis 1964).

A lacrimal gland surrounds the base of the cartilage plate, extending upwards on the inner surface. It secretes an aqueous film. Clusters of lymphoid follicles are normally present on the bulbar surface of the membrane (Boedeker et al. 2010). Blood supply to the nictitating membrane is from a branch of the internal maxillary artery located between the inferior and medial rectus muscles. Afferent innervation is from the infratrochlear branch of the ophthalmic nerve (branch of the trigeminal cranial nerve). Efferent innervation is sympathetic via the cranial cervical ganglia (Boedeker et al. 2010).

Movement of the membrane across the cornea in a dorsolateral direction is dependent on the action of the retractor bulbi muscles. When extended across the globe, the nictitating membrane is protective in nature, preventing environmental debris from direct contact with the cornea. Motion of the membrane mechanically removes particulate matter and assists in the distribution of the precorneal tear film (Boedeker et al. 2010).

Diseases of the Third Eyelid

It appears that Ursidae is less prone than domestic small animals to diseases of the nictitating membrane such as eversion of the cartilage or prolapse of the third eyelid gland ("cherry eye"). During authors' examinations there were no recorded congenital abnormalities of the third eyelids except perhaps for a unilateral incompletely formed third eyelid of a Giant panda bear (Fig. 37.17a). As a differential, the possibility of a previous traumatic laceration

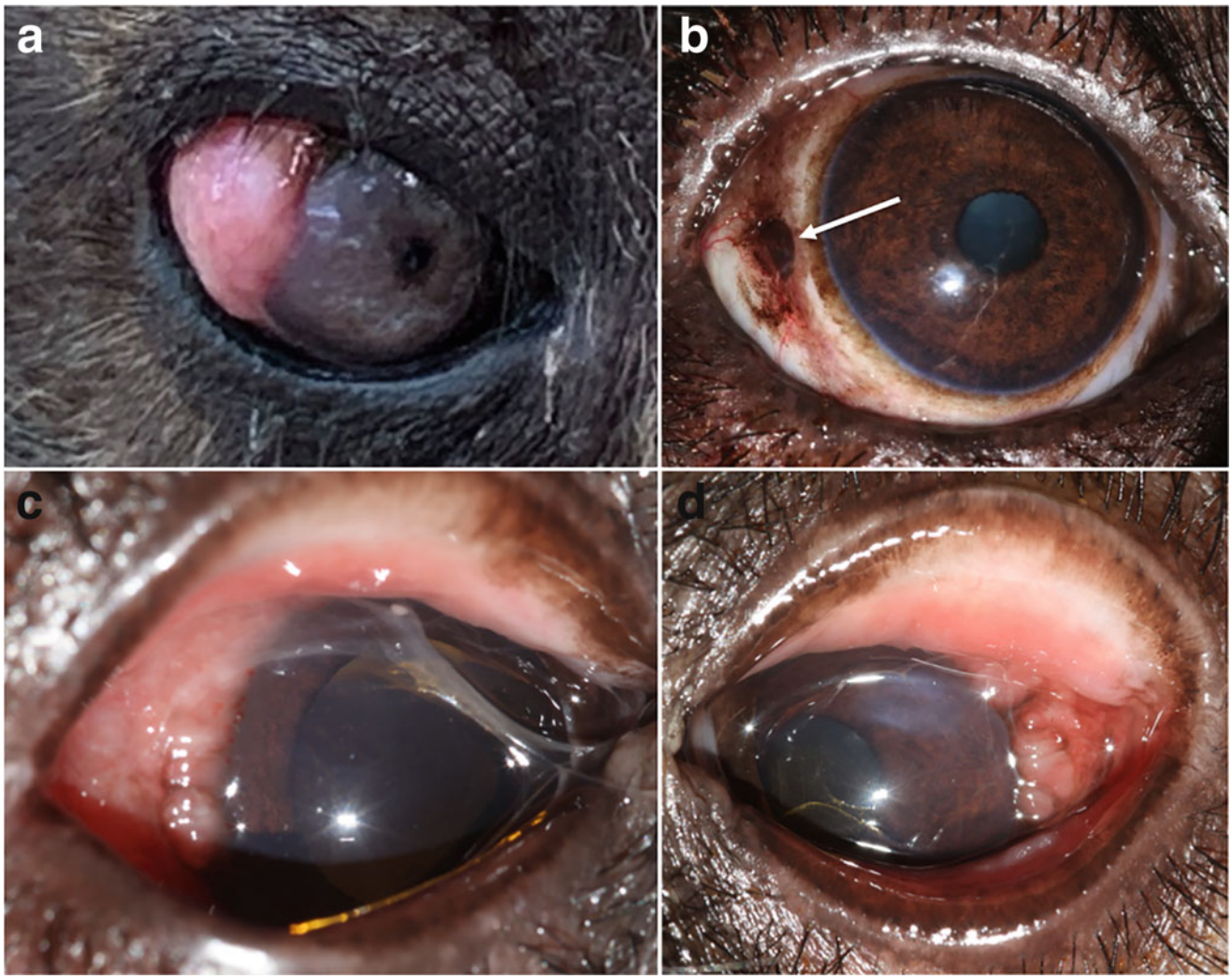

Fig. 37.16 Conjunctival masses in bears. (**a**) Squamous cell carcinoma in an adult female Sun bear (*Helarctos malayanus*). (**b**) A pigmented, plaque-like, subtly raised conjunctival lesion (white arrow) in the right eye of an adult female Asiatic black bear (*Ursus thibetanus*; Vietnam) prior to excisional biopsy. Histopathology reported a benign non-neoplastic pigmented tissue. (**c**) Right and (**d**) Left eyes of an adult Asiatic black bear in Vietnam showing bilateral lymphoplasmacytic plaques. They were treated with subconjunctival cyclosporine implants following histopathological diagnosis. Photo credits: Claudia Hartley

(Fig. 37.17b), that may have occurred very early in life and healed with round borders was considered and was not completely excluded.

A case report of a Giant panda bear described in detail by (Boedeker et al. 2010) diagnosed with suppurative, necrotizing conjunctivitis, had concurrent dacryoadenitis requiring removal of the third eyelid and associated gland (Fig. 37.18a). Although the histologic analysis was consistent with the presence of a seromucous gland, removal of the third eyelid did not result in iatrogenic keratoconjunctivitis sicca (Boedeker et al. 2010). In this case, a 10-year-old 123 kg male giant panda with no significant prior medical history presented for severe, acute swelling and protrusion of the right nictitating membrane (Fig. 37.18a). Topical treatment was initiated with gentamicin ophthalmic solution (Alcon Laboratories, Inc., Fort Worth, TX) BID OD and flurbiprofen ophthalmic solution 0.03% (Pacific Pharma, Irvine, CA) BID OD and application of lubricant ophthalmic ointment (Artificial Tears; Bausch & Lomb, Inc., Tampa, FL) twice daily to the protruding tissue of the right nictitating membrane using a large cotton-tipped applicator. The panda tolerated the administration of the medications well. Positioning the animal in a metal mesh chute facilitated eye drop instillation while feeding him preferred food items (Fig. 37.18b). Previous conditioning of the panda by its trainers to undergo voluntary procedures in the chute system was requisite to success. The third eyelid was excised and submitted for histopathology. After surgery, treatment with topical gentamicin and flurbiprofen solutions was discontinued, and treatment with tobramycin 0.3% and dexamethasone 0.1%

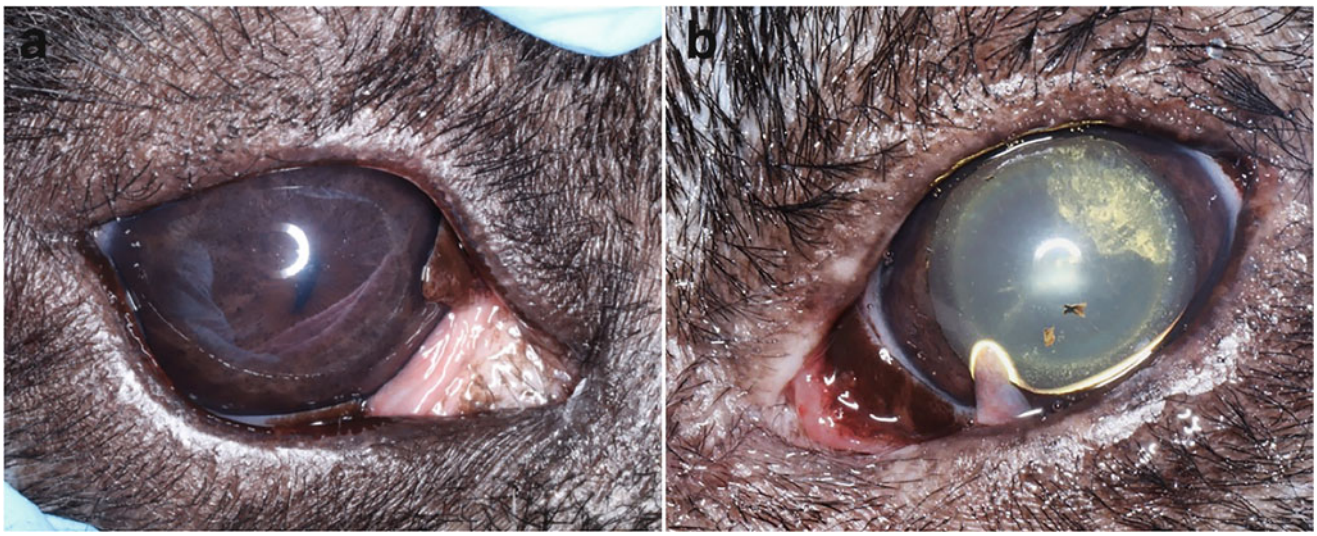

Fig. 37.17 Congenital malformation (**a**) and trauma (**b**) of the third eyelid in Giant panda bears (*Ailuropoda melanoleuca*). (**a**) Incomplete third eyelid, with a large portion of leading or free edge margin missing in the right eye of a captive Giant panda bear (*Ailuropoda melanoleuca*). Also, note the vertically elongated pupils typical in the Giant panda bear. (**b**) Giant panda bear with a third eyelid laceration close to base insertion and ventral bulbar conjunctiva under the lower eyelid. This laceration was an existing old lesion (incidental finding), and the most probable cause was traumatic. Also present—immature anterior cortical cataracts at a 12 to 3 o'clock position and two small iris pigment adhesions to the lens on an axial position measuring approximately 1 mm in size each. Nuclear sclerosis was also observed in the lens. Photo credits: Rui Oliveira

ophthalmic suspension (TobraDex; Alcon Laboratories, Inc., Fort Worth, TX) twice daily for 7 days was initiated. From the histopathologic evaluation of the excised abnormal nictitating membrane, the presence of glandular material of the nictitating membrane could be confirmed. The morphology and staining characteristics were consistent with a seromucous gland in this panda. No evidence of neoplasia was present in the tissues examined from this panda diagnosed with necrotizing and suppurative conjunctivitis, dacryoadenitis, and fibrinoid vasculitis of the nictitating membrane.

This condition was considered most likely to have resulted from foreign body irritation or trauma, possibly from bamboo or other plant material in its exhibit, a conspecific enclosure mate, or accidental self-trauma. As already mentioned in this case report (Boedeker et al. 2010), and noting the fact that

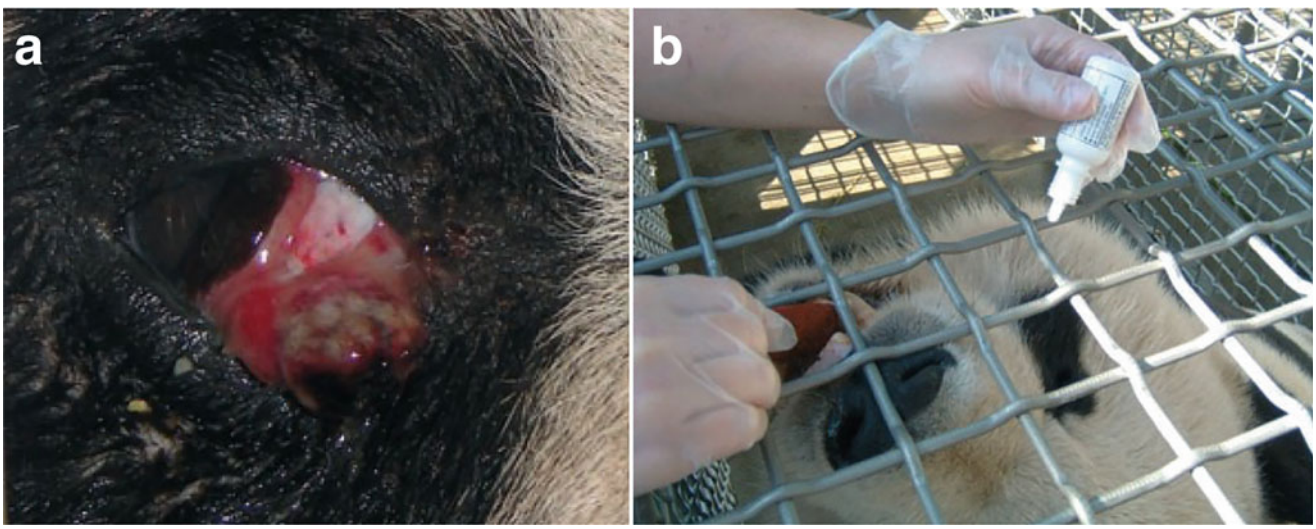

Fig. 37.18 (**a**) Severe inflammation and protrusion of right nictitating membrane in a Giant panda bear (*Ailuropoda melanoleuca*). (**b**) Administration of topical ophthalmic medications. Used with permission from Boedeker NC, Walsh T, Murray S, Bromberg N. Medical and surgical management of severe inflammation of the nictitating membrane in a Giant Panda (*Ailuropoda melanoleuca*). Vet Ophthalmol. 2010 Sep;13 Suppl:109–115

vegetative foreign material was found in the excised third eyelid tissue, it is hypothesized that ocular trauma caused by bamboo is a more frequent condition than we might initially predict. In fact, when seeing a Giant panda bear chewing bamboo, they constantly manipulate the bamboo shoots sideways to their head and to the back of the mouth, where the molar and premolar teeth are located to chew the hard bamboo, but also very close to the eyes so they could conceivably cause ocular trauma (cornea, conjunctiva, eyelids and third eyelids). In support of this hypothesis, although rare in humans, there are several human ophthalmology case reports that easily demonstrate bamboo leaves and splinters can be very traumatic for the eye (Kawashima et al. 2009).

There is an unpublished report of surgical excision of a basosquamous carcinoma of the nictitating membrane in an Andean bear (*Tremarctos ornatus*), also without clinical evidence of postoperative development of keratoconjunctivitis sicca (Gamble KC, 2020, Lincoln Park Zoo, personal communication).

Nasolacrimal System

Anatomy of the Nasolacrimal System

The *Ursidae* nasolacrimal system is very similar to the ones we find in most carnivores. The lacrimal gland is situated on the dorsolateral aspect of the orbit, below the *levator palpebrae superioris* and behind (outside) the tendinous expansion of that muscle. The bulk of the gland lies directly beneath the postorbital ligament. It has a thick, moderately elongated body. Its dimensions are 15 mm in length by 10 mm in its greatest width (Davis 1964). Inferior and superior puncta are positioned on the inner conjunctival surface of the eyelids, near the nasal limit of the tarsal glands. Two lacrimal puncta and two canaliculi are usually present per eye, which opens independently into the lacrimal sac, and this continues to the nasolacrimal duct. The lacrimal sac is an inconspicuous, vertically elongated sac. The superior lacrimal duct opens at its upper tip so that there is no fornix (Davis 1964).

Diseases of the Nasolacrimal System

Micropuncta was suspected in one Asiatic black bear with chronic epiphora; the nasolacrimal system was patent, and saline flushing did not reveal parasites or bacterial infection, and surgical enlargement of the lower eyelid punctum appeared to ameliorate (but not resolve) the epiphora.

In our Giant panda bear ocular examinations, we found one animal with congenital aplasia, of the upper nasolacrimal puncta, in both eyes, but we could not find this in any other animal we examined. In this case, a lower puncta nasolacrimal cannulation and flushing with saline was performed, and patency of the nasolacrimal ducts was confirmed in both eyes. Fluorescein passage or Jones test was also positive after 1 min bilaterally, but we could not differentiate if the condition present was aplasia of the punctum and canaliculus or a simple imperforate superior punctum. Furthermore, to the authors' knowledge, it is the first time this congenital abnormality in Ursidae is reported.

Three cases of mild dacryocystitis with mucopurulent discharge and conjunctivitis were observed in Giant panda bears diagnosed with Thelaziosis. In one giant panda bear with suppurative, necrotizing conjunctivitis and concurrent dacryoadenitis requiring removal of the third eyelid and the associated gland was described in detail by (Boedeker et al. 2010). Culture grew *Stenotrophomonas maltophilia* and *Enterococcus* spp. with extensive antibiotic resistance. Treatment with topical (neomycin/polymyxin B/gramicidin ophthalmic solution and later doxycycline) and systemic (doxycycline) antibiotics based on sensitivity results was initiated. All treatments were well tolerated. Healing was uncomplicated with no recurrence of the lesion. Although the histologic analysis was consistent with the presence of a seromucous gland, removal of the third eyelid did not result in iatrogenic keratoconjunctivitis sicca (Boedeker et al. 2010).

In a study examining 135 Asiatic black bears, Sun bears, and Brown bears at sanctuaries in China and Vietnam (rescued from the bile farming trade), conjunctival hyperemia was recorded in 20 bears (see "Conjunctiva" section). Quantitative keratoconjunctivitis sicca (KCS) was uncommon in the same population, with two bears demonstrating low Schirmer tear readings in conjunction with compatible clinical signs (hyperemia/tacky ocular discharge/secondary keratitis). The diagnosis was somewhat impeded by the testing of tear production under anesthesia. Normal STT readings in the 135 bears were 10.5 $\pm$ 5.6 mm/min; median 10 mm/min. Therefore, STT readings of 4 mm/min or less in conjunction with compatible signs were considered suggestive of KCS in this population. A total of 11 bears ($n = 135$) had STT below this cut-off, but only two had compatible clinical signs or history. Qualitative tear deficiency was also suspected in some bears with conjunctivitis or ocular discharge based on slit-lamp biomicroscopy assessment of the tear film (e.g., punctate appearance or mucoid debris suspended in tear film).

Normal STT reading in 43 Sloth bears at two sanctuaries in India revealed a mean STT of 11.6 ± 6.0; median11 mm/min. Quantitative KCS was not recorded in this population; however, qualitative tear deficiency was suspected in some cases with non-specific signs of conjunctivitis (punctate appearance to tear film, mucus debris in tear film on slit-lamp biomicroscopy).

To the best of our knowledge, Schirmer tear test (STT) for quantitative abnormalities is not routinely performed in the existing captive bear populations. Results of ophthalmic examinations of Giant panda bear have been mentioned in very few studies, but no studies have focused specifically on Schirmer tear test (STT) procedures in the Giant panda bear. To authors knowledge, no data is present in the veterinary literature about normal reference ranges for STT values in Giant panda bears, nor is it known whether or not there is a significant difference between their STT values regarding age and sex variations and comparing it to others species of bears. Therefore, one of the purposes of the author's previous examinations was to perform this test in clinically normal Giant panda bears in order to determine the normal reference range of STT values for this species. In a previous study using a group of eight captive Giant panda bears (4 females and 4 males) with ages that ranged from 10 to 31 years (mean ± SD; 8.7 ± 4.6 years) and residents of the China Conservation & Research Centre for the Giant Panda, Wolong Nature Reserve, Sichuan, China. For each test (STT I), no differences were observed between readings for the right and left eyes ($P \ddagger 0.05$). The mean ± SD STT I value for the right eye was 15.9 ± 4.5 mm/min (range, 8–21 mm/min), and the mean ± SD STT I value for the left eye was 14.9 ± 3.8 mm/min (range, 7–19 mm/min). The mean ± SD STT I value for both eyes was 15.4 ± 4.1 mm/min (range, 7–21 mm/min). No animal gender or age variations were compared because the sample population was much reduced (unpublished data, Rui Oliveria).

In another group of 15 Giant panda bears of the Chengdu Research Base of Giant Panda Breeding, Chengdu, China (age ranged from 1 to 26 years). All animals in both male and female groups were captured using a dart with intramuscular ketamine in doses ranging from 70 mg/kg to 80 mg/kg. All animals were transported to the surgical center deeply sedated and then were intubated following a short period of volatile gas mask anesthesia. Anesthesia was maintained using isoflurane and oxygen with all animals in sternal recumbency and head slightly elevated to a horizontal position. In all GPB, Schirmer tear tests (STT) I were performed by using a sterile Schirmer tear test standardized strip (MSD previous Schering-Plough Animal Health, Union, NJ, USA) placed in the lower conjunctival fornix for 1 min (Fig. 37.19), most of the times just before intubation, and when volatile gas mask anesthesia was administered.

Cornea

Anatomy of the Cornea

The cornea shows a typical vertebrate morphology, and there is a perilimbal girdle of pigmentation within the basal layer of the conjunctival epithelium. The epithelium of the cornea is 8–11 layers thick and lies directly on the corneal stroma since no Bowman's membrane is present. The stroma, which shows no abnormality, is lined by a substantial Descemet's membrane and a somewhat attenuated endothelium (Ashton 1976). The cornea measures vertical 13.0 mm; horizontal 13.5 mm (Ashton 1976). In another histopathological study of a GPB from the Smithsonian National Zoological Park at the gross examination, the cornea measuring 15 × 15 mm in both eyes (McLean et al. 2003).

Diseases of the Cornea

No corneal congenital abnormalities have been described, although the authors have observed one persistent pupillary membrane. In a study of 135 bears in a Vietnam and two China sanctuaries (largely Asiatic black bears, some Sun bears and Brown bears) corneal disease was common ($n = 89$) in the three populations, with vascularization ($n = 22$), and opacities that mostly resembled fibrotic lesions ($n = 18$), and corneal edema ($n = 12$) (Fig. 37.20). Corneal ulceration was present in three bears, to the level of Descemet's membrane in two. Scarring consistent with previous corneal perforation (along with anterior synechiae) was present in one bear. Ghost vessels were encountered frequently and were assumed to be a sequela of the previous keratitis. Corneal scarring from presumed previous ulceration/injury was largely fibrotic in appearance and not commonly pigmented in these bears.

Incidents of corneal ulceration are common in bears in captivity and may take many forms from superficial, including indolent (resembling spontaneous chronic corneal epithelial defects (SCCED) in dogs) (Fig. 37.21), to stromal and descemetoceles (Fig. 37.22). Full-thickness perforations that have healed with anterior synechiae and corneal fibrosis have been seen in captive rescued Asiatic black bears. One adult female Giant panda bear presented with an indolent ulcer or SCCED spontaneous chronic corneal epithelial defects. Commonly referred to as SCCED in dogs, canine indolent ulcers are characterized by an abnormal superficial stroma and lack of adhesion complexes within the basement membrane (Bentley et al. 2001). Corneal structural analysis was not available in this animal. Descemetocoeles can be encountered in bears and have been successfully treated using procedures used in domestic species (e.g., conjunctival

Fig. 37.19 Schirmer tear test (STT-1) in Giant panda bears (*Ailuropoda melanoleuca*) was performed by using a sterile Schirmer tear test standardized strip (MSD Animal Health, Union, NJ, USA) placed in the lower conjunctival fornix for 1 min. Photo credit: Rui Oliveira

pedicle grafts). Indolent ulcerations have been successfully managed with simple debridement followed by grid keratotomy or diamond burr debridement (a similar protocol to that for dogs). Topical medications were largely not possible in the examined populations of bears (Asiatic black bears, Sun bears, Brown bears, and Sloth bears) in China, Vietnam, Cambodia, Laos, and India. Oral doxycycline and analgesic agents (meloxicam/carprofen/paracetamol/tramadol) have been used with apparent success in many cases. Superficial vascularization was common in ulcerated corneas

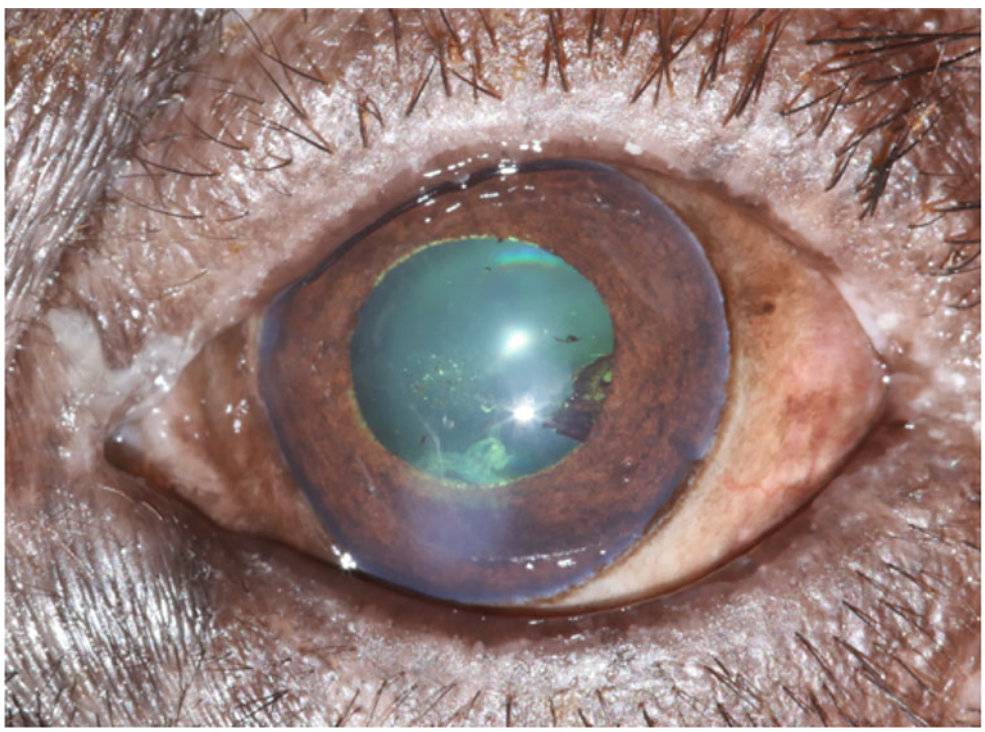

Fig. 37.20 An adult female Asiatic black bear (*Ursus thibetanus*; China) with an area of focal endothelial fibrosis and attendant edema, along with posterior synechia and cataract formation, suspected from blunt trauma. This eye has been pharmacologically dilated (full dilation was achieved later). Fellow eye enucleated due to recurrent hyphema and secondary glaucoma. Photo credit: Claudia Hartley

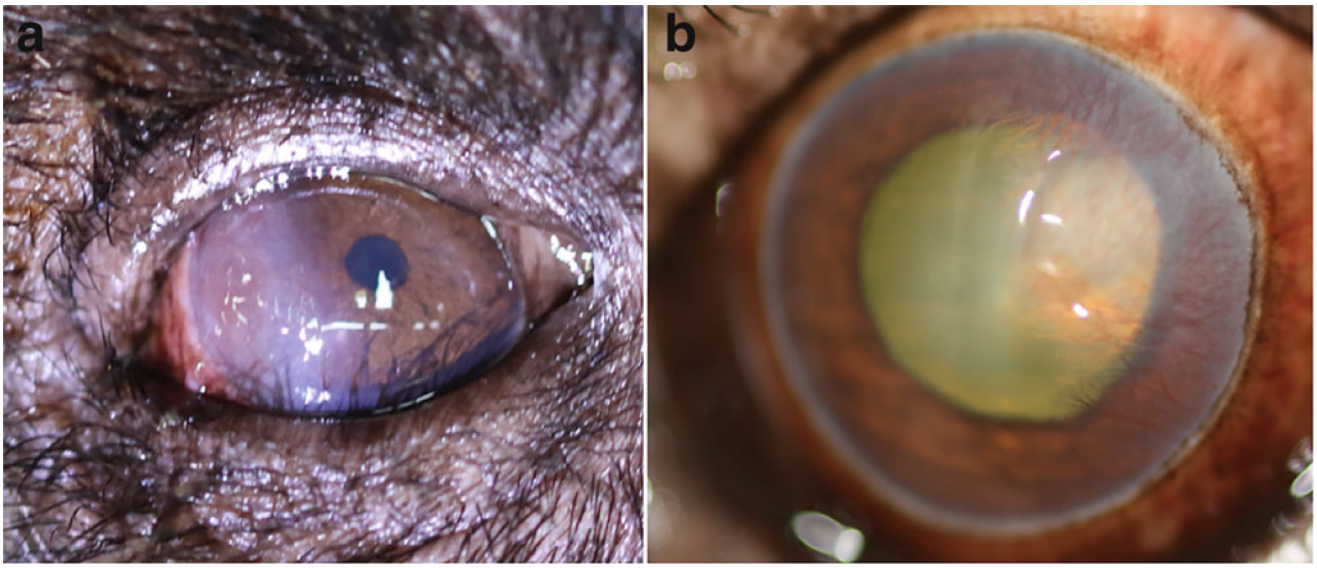

Fig. 37.21 Indolent corneal ulcers in adult Asiatic black bears (*Ursus thibetanus*). (**a**) An indolent ulcer in the lateral cornea of the right eye. Vascularization of the area was extensive. Healed following debridement and grid keratotomy. (**b**) An indolent ulcer and superficial corneal vascularization. Photo credits: Claudia Hartley

(Fig. 37.23) that later progressed to ghost vessels after epithelization had occurred.

Although the authors have not observed a confirmed case of keratomycosis in the Giant panda bear, Polar bear, Asiatic black bear, Sun bear, Brown bear or Sloth bear, there are two presumed reported cases of this condition in Giant panda bears, although there was no definitive diagnosis of the agent responsible for the supposed fungal infection. In both cases, there was an ongoing corneal infection with keratitis, corneal neovascularization, corneal edema and variably sized yellowish stromal cellular infiltrate or abscessation. In both cases, topical and systemic medications, including different antibiotics combinations were used, but the response of the lesion to treatment was poor, and improvement was only achieved once antifungal medications were commenced. Based on the appearance of the corneal lesions and the fact there was significant improvement once antifungal treatment was commenced, keratomycosis was suspected.

A presumed keratomycosis case of a Giant panda bear in Japan refers to a 22-year-old female giant panda, 88 kg weight, with severe keratitis of the left eye, which did not respond to antimicrobial (0.5% levofloxacin, Nipro, Osaka) and hyaluronate (0.1% sodium hyaluronate) or pranoprofen (0.1% pranoprofen) ophthalmic solutions. Systemic enrofloxacin 450 mg by subcutaneous injection once daily was also administered for 2 weeks. Complete ophthalmic examination under sedation or general anesthesia was not performed because the animal was pseudopregnant and in poor physical condition. At 46 days after this condition was noted, treatment was revised, and additional topical fluconazole 0.2% and oral itraconazole 400 mg PO SID was given

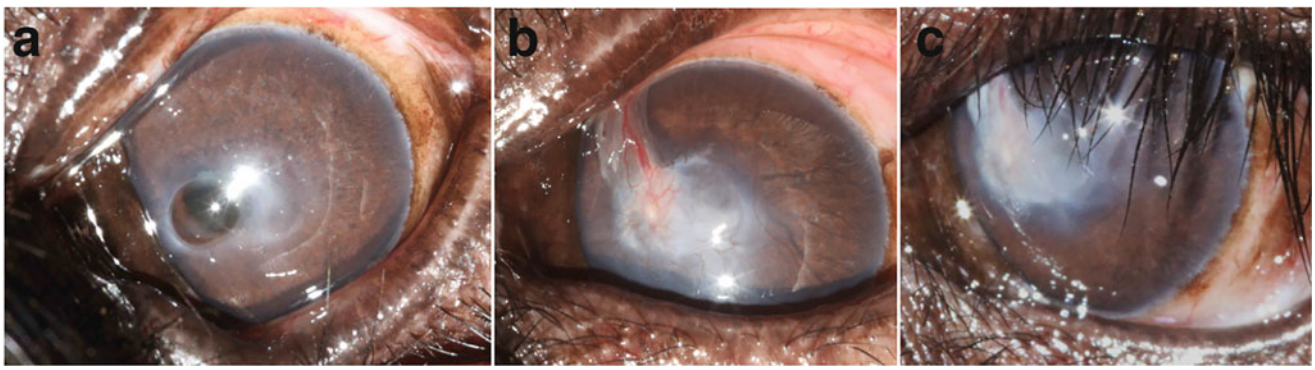

Fig. 37.22 A descemetocele in an adult Asiatic black bear (*Ursus thibetanus*). (**a**) Note the clear area surrounded by stroma edema that signifies a very deep stromal ulcer, in this case, a descemetocele. (**b**, **c**) Postoperative appearance 18 months later both under anesthesia (**b**) and conscious in den (**c**). Photo credits: Claudia Hartley

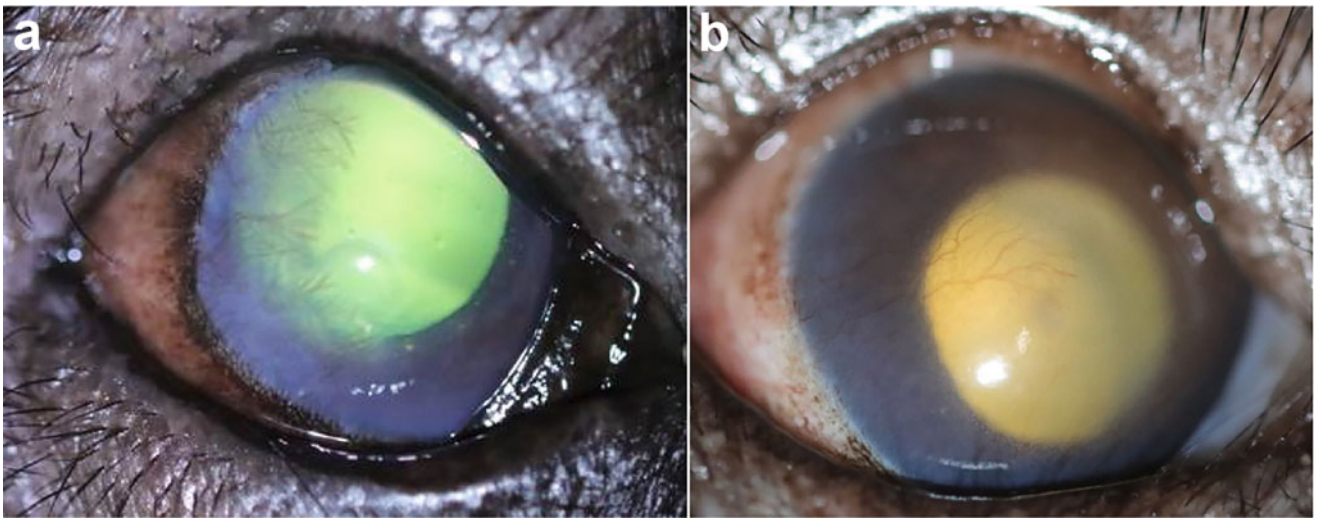

Fig. 37.23 (**a**) and (**b**) Arborising vascularisation and corneal edema associated with previous superficial corneal ulceration in the lateral cornea of two adult Asiatic black bears (*Ursus thibetanus*) in China. Photo credits: Claudia Hartley

for several weeks until corneal lesions were noted to be much improved.

A case observed in the USA was a 12-year-old male, which was treated using moxifloxacin 0.5% ophthalmic solution three times daily for 14 days, and thereafter twice a day for 14 days, flurbiprofen 0.03% ophthalmic solution twice daily for 7 days, neomycin, polymyxin, bacitracin ophthalmic ointment twice daily for 7 days and atropine 1% ophthalmic solution once daily for 4 days. Once keratomycosis was suspected, natamycin 5% ophthalmic suspension was given three times daily for 18 days, and thereafter twice daily for 14 days. Oral flunixin meglumine 130 mg twice daily for 4 days and itraconazole 5 mg/kg once daily for several days until the corneal lesion improved.

It should also be noted that ocular trauma is the most frequently implicated cause of fungal keratitis and, specifically, bamboo-related trauma leading to the development of keratomycosis has been reported in humans (Gopinathan et al. 2002; Lin et al. 2005; Lan et al. 2013; Qiu and Yao 2013; Volk et al. 2018). A keratitis case with the suspected fungal component in a 12-year-old male Giant panda bear is shown in Fig. 37.24.

In a study of 43 Sloth bears in two sanctuaries in India, corneal opacities were identified in 18 bears (24 eyes) (Fig. 37.25). These appeared to be very similar to some of the findings in other bear species in China, Vietnam, Cambodia and Laos, although superficial corneal pigmentation was slightly more common, subjectively associated with phthisis bulbi (Fig. 37.25b, c).

Perilimbal haze or opacity was the most common corneal change identified in four bear species examined (Asiatic black bear, Sun bear, Brown bear, Sloth bear), and appeared to occur in aged (> ~ 20 years) animals (Figs. 37.26 and 37.27). This resembled arcus senilis in humans, which is described as a peripheral opaque ring in the cornea (composed of cholesterol, phospholipids and triglycerides), and is more common in males, and those over 40 years of age (Cooke 1981). It is associated with hypercholesterolemia, alcohol consumption, blood pressure, cigarette smoking, obesity, diabetes, age and coronary heart disease, although it appears to be equivocal as to whether it is an independent risk factor for coronary heart disease (Fernandez et al. 2007). In bears, increased serum cholesterol levels were not linked to disease (based on routine bloodwork), although extended lipid profiles were not undertaken.

Within a previous study on Ursidae (Blake and Collins 2002), captive Sun bears had the highest prevalence of ocular disease and were the only species diagnosed with keratitis. In this study, 9 of these 17 (53%) cases of eye disease were found in Sun bears, with 7 of 9 cases reported as chronic keratitis, one as corneal neoplasia (squamous cell carcinoma of the left eye, keratitis of the right eye, and melanoma of the eyelid), and one as a probable lacrimal duct aplasia. Chronic keratitis was only reported in Sun bears and not in other bear species. 4 of 17 (23.5%) total cases were listed as conjunctivitis, with three of those (75%) found in Spectacled bears, and one case of chronic conjunctivitis was found in an American black bear. Of the four remaining cases, the distribution was as follows: two cases of corneal trauma in Asiatic black bears, one case of chronic contact irritation in a Polar bear, and one case of diabetic cataracts in a Brown bear (Blake and Collins 2002).

The cause of this apparent Sun bear predisposition to chronic keratitis is unknown, but it is speculated that a genetic predisposition may be present or that chronic sun exposure in this rainforest species may influence this

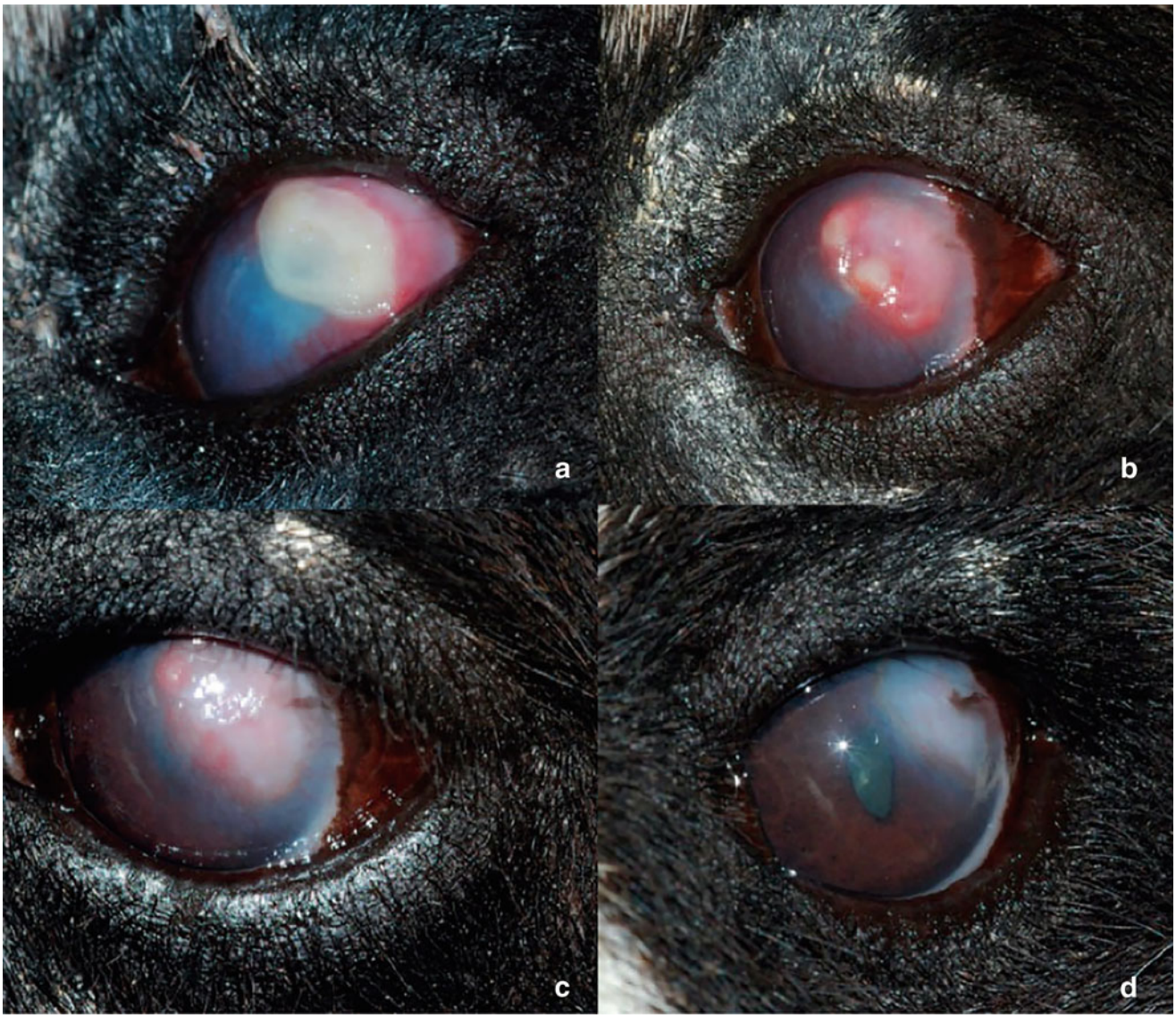

Fig. 37.24 Ulcerative keratitis in a 12-year-old male Giant panda bear with suspected fungal component. Photographs are taken (**a**) 4, (**b**) 11, (**c**) 18, and (**d**) 32-days after initiation of topical antifungal drops to illustrate the changes during resolution of disease. Medication was discontinued at the time point shown in **d**, and the patient continues to have a scar present. Used with permission from Miller S, Whelan N, Hope K, Nogueira Marmolejo MG, Knightly F, Sutherland-Smith M, Rivera S. Survey of clinical ophthalmic disease in the giant panda (Ailuropoda Melanoleuca) among North American zoological institutions. J Zoo Wildl Med. 2020 Jan 9;50(4):837–844

development. One case, as examined by a veterinary ophthalmologist, was described as solar-induced corneal dysplasia and/or endothelial dysplasia of unknown cause. The syndrome was described in this case as ulcerative with progression to permanent white scarring with eventual vision impairment. (Blake and Collins 2002) Additionally, one case of ocular nodular fasciitis, similar to canine fibrous histiocytoma, affecting conjunctiva, sclera, and cornea (see also Diseases of the Sclera) has been reported and successfully removed in an Asiatic black bear (Mainka and Christmas 1987).

According to Miller et al. (2020), the cornea was the most commonly affected ocular structure in Giant panda bear ophthalmic pathology. The relatively high prevalence of ocular disease in the giant panda and sun bear could indicate a genetic or anatomic predisposition. Corneal haze was noted in several cases, most often diffuse and associated with ocular discomfort. Multiple disease episodes were reported in four animals, with 20 clinical episodes and one additional animal that presented with corneal scarring from historic keratitis. Age at presentation varied from 0.4 to 26 years (mean, 11.8 years; median, 10.4 years) (Miller et al. 2020). Multiple cases with previous episodes of ocular lesions compatible

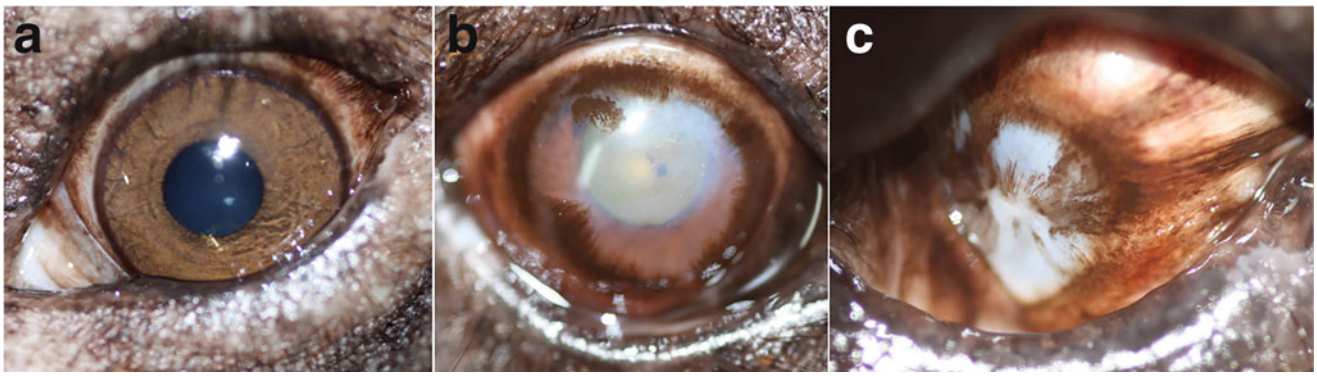

Fig. 37.25 (**a**) Normal ocular appearance for an adult Sloth bear (*Melursus ursinus*). (**b**) Circumferential superficial corneal pigmentation along with some fibrosis, especially dorsolaterally to centrally in an adult Sloth bear (India). Wrinkled Descemet's membrane could be appreciated (particularly notable at 8 o'clock paracentrally) as an indication of early phthisis bulbi. Peripheral anterior synechia (at 10–12 o'clock) and cataract was also present. (**c**) Corneal fibrosis and pigmentation and contracture associated with phthisis bulbi. Photo credits: Claudia Hartley

with keratitis were observed in 6/30 Giant panda bears, with recurrent episodes in some of them, and one additional animal who presented with corneal scarring and superficial neovascularization in one eye and a mass on the corneal surface of his contralateral eye. The age of animals observed with keratitis varied from 2 months to 26 years (mean, 11.8 years; median, 10.4 years). Due to the difficulty in obtaining diagnostic samples for culture and sensitivity testing, empirical therapy with broad-spectrum antimicrobials was often provided in cases that developed ulcerative keratitis. Such aggressive medical management was initiated given the rapid deterioration and melting of corneal ulcers seen in some Giant pandas (Miller et al. 2020; Rivera S, personal communication, 2020).

Bullous keratopathy, corneal edema resulting in the formation of subepithelial and/or stromal bullae, was reported in a 5-month-old captive female giant panda (Miller et al. 2020). Bullous keratopathy can be a result of endothelial disease or traumatic injury that results in the accumulation of fluid in the stroma. The giant panda cub affected in this study had no concurrent inflammatory disease and has shown no recurrence since resolution, supporting trauma as the most likely inciting cause.

One 25-year-old female Giant panda bear developed perilimbal corneal lipid deposition, commonly referred to as arcus senilis in humans or lipid keratopathy in veterinary medicine (Cogan and Kuwabara 1959; Ledbetter and Gilger 2013; Miller et al. 2020).

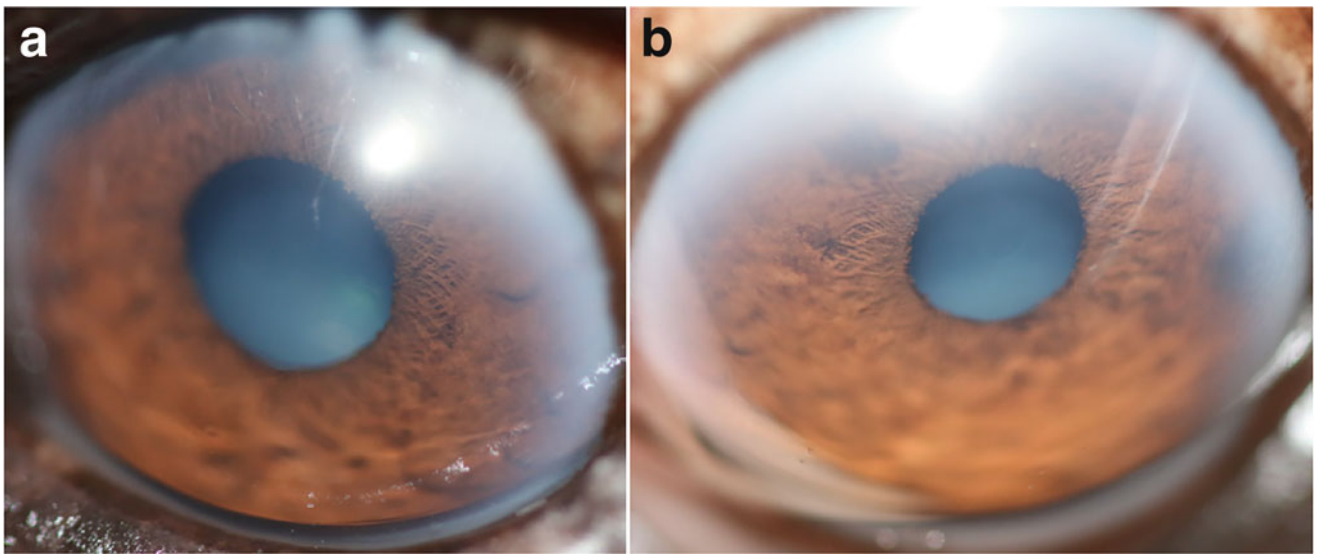

Fig. 37.26 Marked bilateral (**a, b**) perilimbal haze in an aged (27 year old) brown bear (*Ursus arctos*) in captivity in the UK. Photo credit: Claudia Hartley

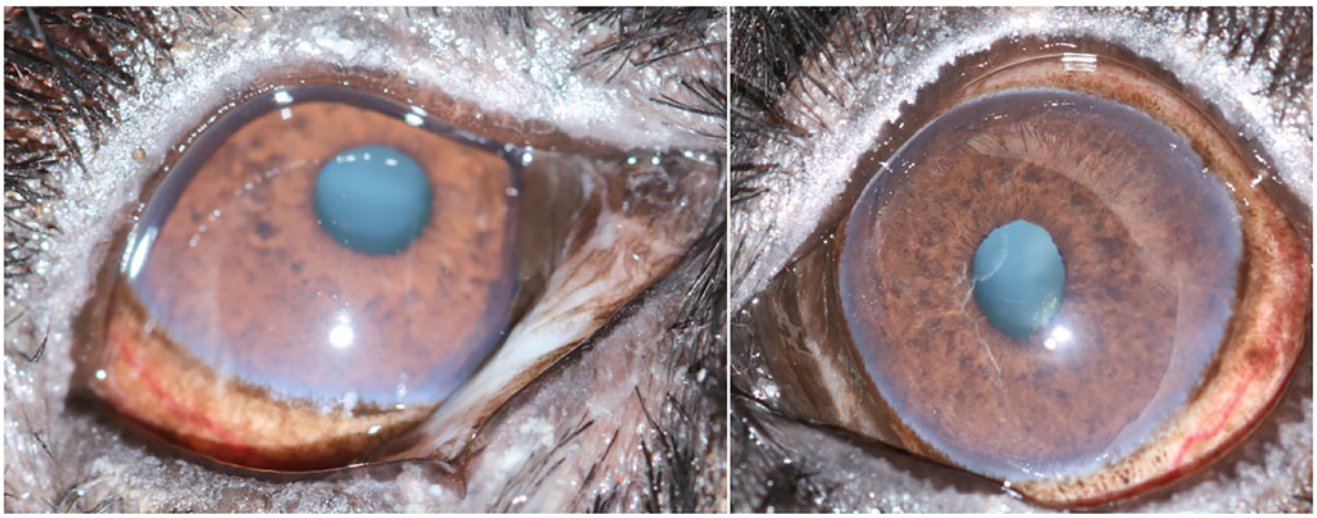

Fig. 37.27 Mild-moderate bilateral perilimbal haze in an adult Asiatic black bear (*Ursus thibetanus*) in China. Note also lower eyelid "notch" in the right eye. Photo credit: Claudia Hartley

Corneal neoplasia is relatively uncommon in animals but has been reported in several species. Corneal, limbal, and corneoscleral neoplasia, in general, are rare in dogs and include neoplasms such as SCC (squamous cell carcinoma), melanoma, papilloma, lymphoma, and hemangioma/hemangiosarcoma (Ledbetter and Gilger 2013). Corneal squamous cell carcinoma (SCC) has also been identified in a Sun bear (*Helarctos malayanus*) (Blake and Collins 2002). Ultraviolet (UV) radiation, lack of pigmentation, and chronic irritation are predisposing factors to developing SCC. (Dugan et al. 1991; Dreyfus et al. 2011; Montiani-Ferreira et al. 2008). This patient had no reported history of keratitis before the development of the tumor (Miller et al. 2020). Oral SCC has been reported in Sun bears associated with a novel gammaherpesvirus infection (Lam et al. 2013).

One case of a limbal haemangiosarcoma in a Giant panda bear (Lopez et al. 1996) and one case of corneal squamous cell carcinoma (SCC) in a Giant panda bear (authors'

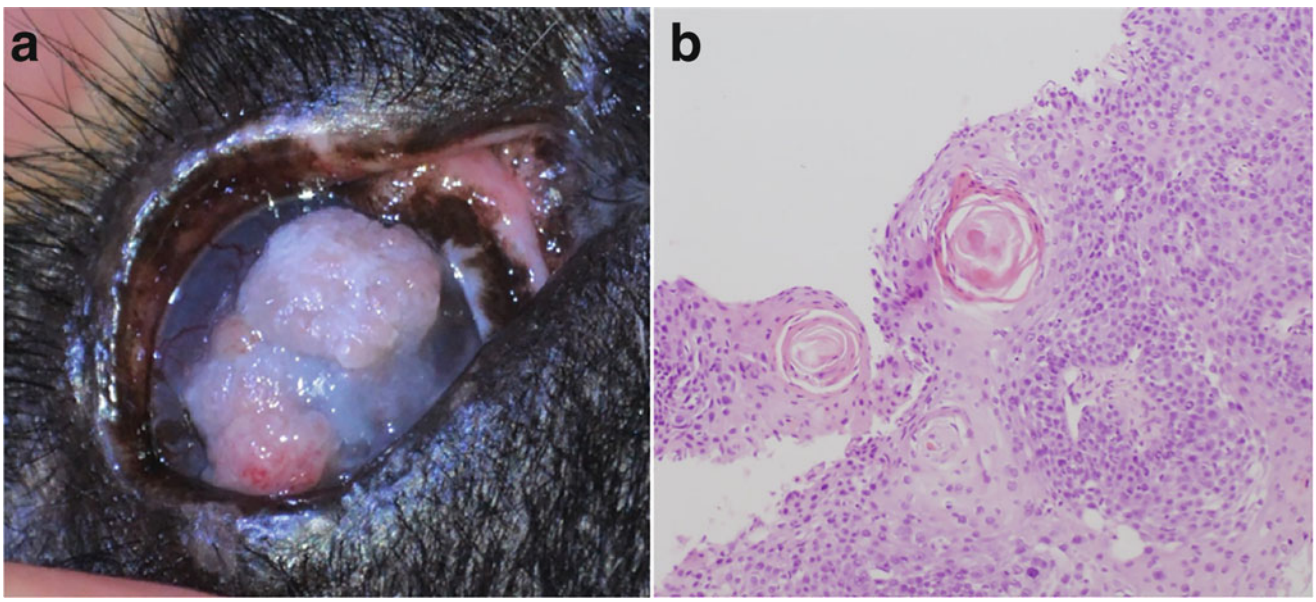

Fig. 37.28 Corneal squamous cell carcinoma in a Giant panda bear (*Ailuropoda melanoleuca*). (**a**) Photograph of the right eye demonstrating an exophytic, irregular multilobulated, white to reddish-pink mass occupying approximately 60% of the total corneal surface. The cornea surrounding the mass was edematous and vascularized. (**b**) Photomicrograph of the neoplasm showing keratin pearls surrounded by polygonal cells, many of which show prominent nucleolus. Hematoxylin and eosin, original magnification 10×. Photo credits: (**a**) Rui Oliveira, (**b**) Carolina Naranjo

unpublished observation) (Fig. 37.28). An 18-year-old male Giant panda bear from Chengdu, China, was examined for assessment of a right corneal lesion that was progressing over the last 8–9 months and had significantly increased in size over the last few months. The corneal lesion had become large in size, elevated on the corneal surface and recently affecting almost half of the corneal surface. Upon ophthalmic examination, two exophytic irregular pink masses were present—the larger was approx. 8 × 7 mm and the other measured 3 × 4 mm—occupying approx. 50% of the total corneal central and para-central corneal surface of the right eye. The cornea surrounding these lesions appeared oedematous, with moderate haziness and considerable corneal superficial neovascularization (Fig. 37.28). A preliminary diagnosis of a corneal neoplasm was made. Under general anesthesia using isoflurane inhalation, excisional biopsy samples were obtained by superficial keratectomy, with all the abnormal tissue being removed and subsequently submitted for histopathological examination. Following the excision, the affected cornea was treated with topical ofloxacin every 12 h for 2 weeks after the surgery. Unfortunately, at the facilities where the procedure was done, there was no surgical loupes availability or any other magnification available, so total excision of the mass could not be guaranteed.

Multiple tissue fragments were examined histopathologically. Some tissue fragments showed ulceration of the surface and healing by reactive fibrovascular granulation tissue formation. Sections showed proliferation of infiltrating columns of epithelial cells with squamous differentiation, with some areas of necrosis and infiltration of the stromal tissue by large numbers of neutrophils, lymphocytes and plasma cells (Fig. 37.28b). These findings suggested the neoplasm was a relatively aggressive corneal SCC, a neoplasm uncommonly found at this site. The tissue showed solid sheets of tumor cells with central keratinization and formation of keratin pearls, which are the common features of SCC (Fig. 37.28b). Mitotic figures were occasionally seen, indicating aggressive growth of the carcinoma. Considering that the neoplasm might not have been completely excised on the day of surgery, we recommended the affected eye be treated again either by doing a new surgery using cryotherapy on the corneal surface areas where the mass was present and/or by using topically chemotherapeutic agents such as topical mitomycin or 5-fluorouracil solutions as adjunctive therapy. According to the veterinary team where this animal was located, the mass did not recur in the 5 months following the surgery; no further information on long-term outcome of this case or if further treatments were necessary was available. Similar to some published cases in dogs (Montiani-Ferreira et al. 2008), this tumor had no involvement of the limbus, suggesting the tumor originated within the corneal epithelium itself.

The occurrence of areas of corneal irritation evidenced microscopically by the presence of an inflammatory cell infiltrate, neovascularization, hyperplasia, and dysplasia, as well as an increase in epithelial thickness surrounding the tumor site, may give some support to the theory that chronic microtrauma may have contributed to the initiation of the SCC. Kim et al. postulated the origin of a corneal papilloma in a dog was due to chronic corneal irritation (keratoconjunctivitis sicca and pigmentary vascular keratitis) (Montiani-Ferreira et al. 2008). Other associations might include cellular damage by UV light and possible recurrent corneal ulcerations, herpesvirus infections, or trauma induced by bamboo leaves. For us to be able to further explore this possibility, more cases of corneal SCC in Giant panda bears need to be diagnosed and studied in detail, so we can confirm our suspicions if a similar pathogenesis of this condition exists as is described for dogs. Further argument in support of this hypothesis is the fact that the Giant panda bear also displayed a predisposition to corneal disease, particularly keratitis.

Another ocular mass excised in a Giant panda bear, further aggravating our suspicions that UV light may be a confounding factor of ocular cellular damage, was determined histopathologically to be a low-grade hemangiosarcoma that was removed from the outer ocular limbus of a 13-year-old male giant panda at Madrid Zoo (Lopez et al. 1996). The tumor appeared to be painless and was confined to the conjunctiva with no invasion of the underlying tissues (see “Conjunctiva” section). Haemangiosarcomas are not uncommon in a variety of species, and their development is potentially stimulated by sunlight (Lopez et al. 1996). It is not unusual for captive pandas to be exposed to ultraviolet radiation far in excess of levels in their native habitat of foggy, wet mountain forests. The panda in Madrid was moved to a more shaded enclosure, which is probably a good suggestion for all giant pandas housed in sunny areas (Wildt et al. 2006). However, the housing of giant pandas is uniform because strict housing guidelines are set by China, and facilities are inspected before the arrival of the giant pandas (Ellis et al. 2006).

Endothelial fibrosis can be extensive following intraocular surgery in ursid species, and care to avoid iatrogenic trauma is imperative. Diffuse corneal edema and endothelial fibrosis secondary to anterior lens luxation and uveitis is encountered in bears (Asiatic black bear, Sun bear, Sloth bear and Brown bear examined by one author) and is often in older individuals (Fig. 37.29). In time, some of these eyes may develop glaucoma (and display corneal edema associated with this) or progress to phthisis (and the attendant corneal opacification). Keratitis and corneal endothelial lesions were observed in several Giant panda bears with lens luxation and cataracts. In Giant panda bears, three of four animals diagnosed with anterior lens luxation (usually older animals

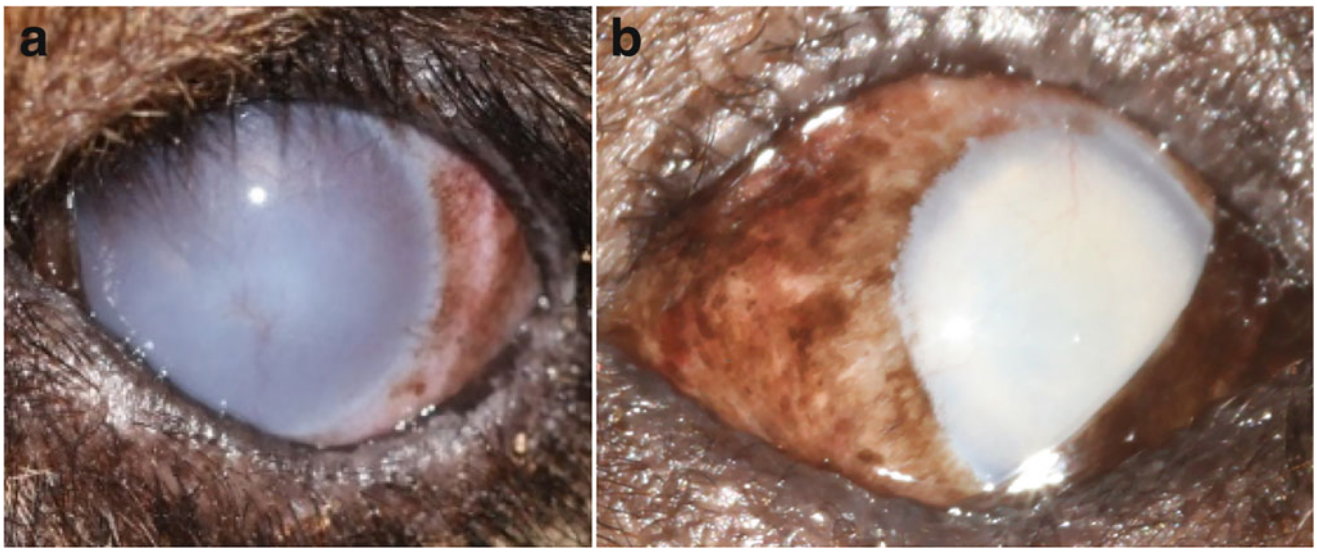

Fig. 37.29 Keratitis secondary to lens luxation in bears. (**a**) Diffuse corneal edema and arborizing superficial vascularisation in all quadrants secondary to lens luxation (posterior) and uveitis in an adult Sun bear (*Helarctos malayanus*) in Cambodia sanctuary. (**b**) Diffuse marked corneal edema with superficial neovascularization from the dorsal limbus, a dilated pupil, and hypermature anteriorly luxated cataract in an adult Sun bear in Cambodia. The corneal edema remained after lens extraction in this animal. Photo credits: Claudia Hartley

with hypermature cataracts) there was associated corneal fibrosis and/or keratitis lesions. Regardless of species, physical contact between lens and corneal endothelium may compromise the latter (Ledbetter and Gilger 2013). Corneal disease secondary to lens luxation is a common problem in aging *Ursidae*. Traumatic endothelial damage with permanent focal corneal edema may occur with anterior lens luxation. Usually, corneal edema and fibrosis secondary to anterior lens luxation are permanent unless the lens is removed immediately. Unfortunately, chronic lens luxations are common (see Disease of the Lens). Corneal pathology includes endothelial attenuation, rupture of Descemet's membrane, hypercellularity of the stroma with fibroblasts, and variable vascularization (Kern and Colitz 2013).

Sclera

Anatomy of the Sclera

The sclera is essentially similar in all Ursidae family. Histological examination of the Giant panda bear eye revealed scattered pigment cells and the sclera to be thickest anteriorly and posteriorly but thin equatorially. Perforating arteries and nerves may be seen near the optic disc. (Ashton 1976). The sclera contained a plexus of vessels (circle of Hovius) adjacent to the ciliary body, which drained the aqueous humor into the surface veins (McLean et al. 2003).

Disease of the Sclera

No scleral congenital abnormalities have been reported or observed by the authors. Acquired scleral abnormalities, we have observed several Giant panda bears and a few Asiatic black bears with secondary glaucoma and marked episcleral congestion. Usually, these are cases of lens subluxation or anterior/posterior lens luxation, and hypermature cataracts that develop secondary glaucoma where the episcleral congestion is caused by the marked IOP elevation.

There is one case published of ocular nodular fasciitis in a captive Asiatic black bear (*Selenarctos thibetanus*) that was treated by keratectomy and subconjunctival corticosteroid administration (Mainka and Christmas 1987). In this case, a 24-year-old male Asiatic black bear was noted to have a unilateral clear ocular discharge from the right eye, and a small red raised lesion on the lateral edge of the cornea was visible. Under general anesthesia, the cornea was examined, and a raised red mass approximately 5 mm in diameter was found that involved both cornea and sclera in the area of the lateral canthus. The rest of the eye appeared normal, and there was no obvious etiology such as ectopic cilia, distichia, or eyelid abnormalities to explain the lesion. In gross appearance, the mass resembled a fibrous histiocytoma or squamous cell carcinoma. A superficial keratectomy was performed using a #15 scalpel blade was used to do a triangle-shaped keratectomy extending 1–2 mm beyond the margins of the mass. The cornea beneath the mass appeared grossly normal and clear (Mainka and Christmas 1987). Postsurgical medication included 10 mg of methylprednisolone acetate and 10 mg of gentamicin sulfate given subconjunctivally, and

chloramphenicol ophthalmic ointment administered topically (at the end of surgery only). No postoperative medications were prescribed due to the difficulty of treating a conscious bear (although palatable oral medications in the feed are relatively easy to administer to bears, particularly analgesic drugs). Mucoid ocular discharge was seen for 5 days post-surgery. The wound healed uneventfully, and only a small corneal opacity remains visible on the cornea 1 year postoperatively (Mainka and Christmas 1987). The lesion was submitted for histopathologic examination, which revealed the mass to be composed of an edematous haphazard mixture of plump fibroblasts, capillaries, macrophages, and lymphocytes. No granulocytes were present, and no etiologic agent was identified. Considering the location and macroscopic appearance of the mass, the histology was consistent with nodular fasciitis/fibrous histiocytoma of dogs.

The lesion in dogs is of unknown etiology but typically presents as a firm painless solitary proliferation of fibroblasts and mononuclear leukocytes below the bulbar conjunctiva at or near the limbus. Surgical excision, even if incomplete, is usually curative in the cases that have been reported in dogs. This appears to be true of this Asiatic black bear case as well. Treatment of ophthalmologic conditions often requires topical eye drops treatment several times daily. This method of administration is not possible in most of the large carnivores in a zoo collection unless they have been trained to accept eye drops—which is possible but clearly requires resources that not all zoo/sanctuaries have. In this case, the authors felt the use of a single dose of subconjunctival medication plus topical provided adequate treatment (Mainka and Christmas 1987).

Uvea

Anatomy of the Uvea

To authors' knowledge, there are limited studies of bear's uvea or iris. In a histopathological study of Giant panda bear globes, which possess vertically elongated pupils, the iris was found to be heavily pigmented and a continuous mesodermal layer upon its anterior surface characteristic of the placental eye. Posteriorly there is a layer of pigmented epithelium, which is cystic in its inner one third. Other species with slit pupils like the Giant panda bear are able to increase their aperture by 135- and 300-fold (Hammond and Mouat 1985), whereas humans' circular pupil changes by ~15-fold (De Groot and Gebhard 1952). Species that are active at night and day need to dilate sufficiently under dim conditions while constricting enough to prevent dazzle in daylight. A slit pupil provides the required dynamic range. (Banks et al. 2015). On functional grounds, a variable-aperture vertical pupil allows for excellent mydriasis but avoids dazzle by also providing excellent miosis (Banks et al. 2015) (See also "Vision in Bears" section).

Giant Panda bears possess vertically elongated pupils (Fig. 37.30a), similar to the shape of a domestic cat pupil. In fact, the word for Giant Panda bear in Chinese is "*Da xiong mao* – 大熊猫", that literally means "large bear-cat." Some local people believe that its name originated because of its cat-like facial features: slit eyes and a round face (Fig. 37.30 (a)). There is a striking correlation between terrestrial species' pupil shape and ecological niche (that is, foraging mode and time of day they are active). Species with vertically elongated pupils are very likely to be ambush predators and be active day and night. Species with horizontally elongated pupils are very likely to be prey and to have laterally placed eyes (Banks et al. 2015). For the case of Giant Panda bears, even though they are technically carnivores, 99% of their diet consists of bamboo leaves (Wei et al. 2015); we hypothesize that its vertical pupil may have evolved as an adaptation to enhance vision in low light conditions, typical of temperate forest habitat with dense bamboo understories.

In all other ursid species (Asiatic black bear, Sun bear, Sloth bear, American black bear, Brown bear, Polar bear and Andean spectacled bear), the pupil is round and reminiscent of canids. The iris stroma, which is attenuated towards the iris root, contains numerous nerve fibers and shows well-developed sphincter and dilator smooth muscle fibers. The ciliary processes are well developed and covered by pigmented and non-pigmented epithelium, which in some areas is proliferative and in others cystic.

The choroid is of the standard vertebrate type. It is heavily pigmented and shows a cellular tapetum as seen in the upper half of the fundus of all carnivores, but in bears, more commonly present in both ventral and dorsal fundus, with a non-tapetal zone peripherally, and in this region, the pigment epithelium is not pigmented. (Ashton 1976).

Disease of the Uvea

Chi-Chi, a Giant panda bear, who was wild captured in Sichuan, China in 1955 before moving to Beijing for 2 years, then to Moscow zoo, Russia, and later Berlin, Frankfurt and Copenhagen, before being sold to London zoo in 1958. She died at the London zoo in 1972. Upon her death, following an 8-year history of increasingly frequent seizures, her eyes were examined histologically (Ashton 1976). The only pathological changes seen in these eyes were the presence of cysts in the iris, pars plana and peripheral retina, which was also degenerate, and these findings, together with a minimally sclerotic lens, were considered attributable to old age. (Ashton 1976). Cases of dyscoria (Fig. 37.30b)

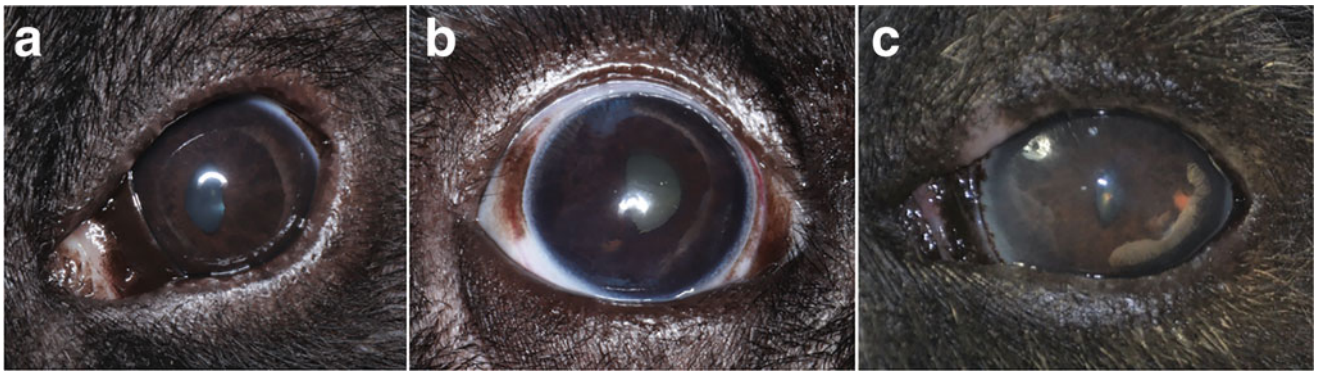

Fig. 37.30 (**a**) Normal eye of Giant Panda bear (*Ailuropoda melanoleuca*) with detail of the slit shape pupil, one of the anatomical characteristics responsible for the cat-like facial features. (**b**) Right iris of a Giant panda bear with a "D-shape pupil" and dyscoria. There was no iris mass present or obvious signs of inflammation, so the cause was suspected to be a partial dysfunction of the iris dilator muscle or its innervation. (**c**) Left iris of a Giant panda bear with a peripheral iris discoloration. There was no mass present on the iris thickness or any signs of previous uveitis present that could explain this color change. Monitoring the size and thickness of the lesion was recommended, and if any growth was detected, an iris biopsy was recommended. Note the white linear perilimbal coloration is a reflection artifact off the corneal surface. Photo credit: Rui Oliveira

and partial iris discoloration (Fig. 37.30c) have also been observed in the Giant panda bear.

Developmental and senile abnormalities have been observed. Persistent pupillary membranes have been encountered in a Giant panda bear (Fig. 37.31a) but not thus far in Asiatic black bears, Sun bears, Sloth bears, or Brown bears examined by the authors. A single case of suspected iris coloboma was seen in one adult female Asiatic black bear and monitored over a period of over 6 years during which time it did not change in appearance (Fig. 37.31b). Evidence of previous uveitic episodes with posterior and anterior synechiae, vitreal membranes and vitreoretinal traction bands have been witnessed in multiple ursid species (Asiatic black bear, Sun bear, Sloth bear and Brown bear) examined. Subtle iris atrophy was encountered in some older Asiatic black bears, Brown bears, and Sloth bears, most typically with a mild transillumination of the pupillary margin, but was not as marked as it can be in some canine breeds. More marked iris atrophy has been seen in Giant panda bears by one of the authors (Fig. 37.31c).

Cases of partial iris discoloration and iris dyscoria were also observed in the Giant panda bear, and both thought to be caused by penetrating and blunt trauma with anterior synechia and iris tears (Fig. 37.32). Vascular changes of the iris compatible with aneurysms were seen in two bears with suspected systemic hypertension. In one of these bears, recurrent episodes of hyphema and subsequent development of glaucoma prompted enucleation, and histopathology revealed signs typical of hypertension. In the other bear, there were multiple retinal hemorrhages, vascular beading as well as an iris aneurysm (Fig. 37.33), which subsequently resolved with anti-hypertensive medications (enalapril and amlodipine).

A pigmented raised plaque-like iris mass was observed in an adult female Asiatic black bear and was considered a possible melanoma. This bear was euthanased due to

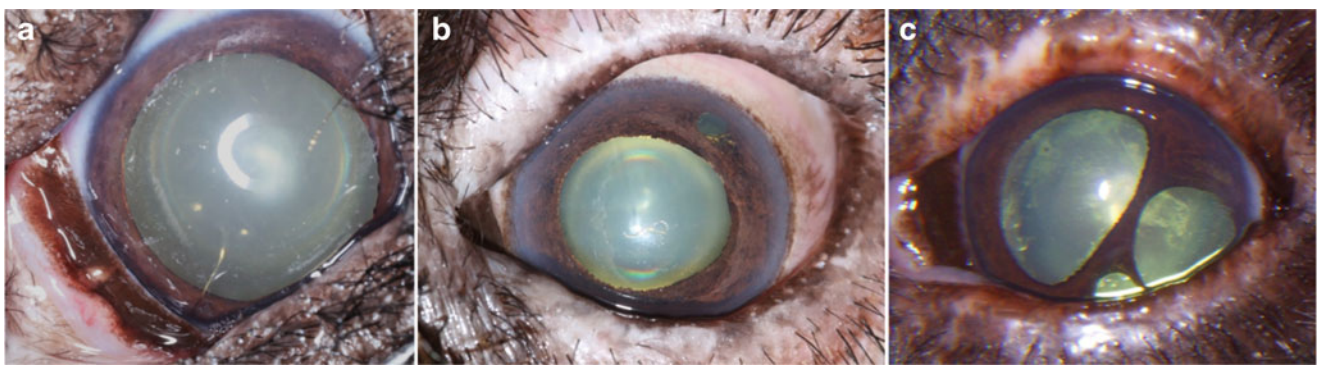

Fig. 37.31 Developmental and senile iris changes in bears. (**a**) A Giant panda bear (*Ailuropoda melanoleuca*) eye with an iris to cornea persistent pupillary membrane at the 7 o'clock position. (**b**) Mild-moderate perilimbal haze, nuclear sclerosis of the lens, and presumed iris coloboma (2 o'clock) in the left eye of an adult female Asiatic black bear (*Ursus thibetanus*) from China. (**c**) Severe iris atrophy and dyscoria/pseudopolycoria in an adult Giant panda bear. Photo credits: (**a**, **c**) Rui Oliveira, (**b**) Claudia Hartley

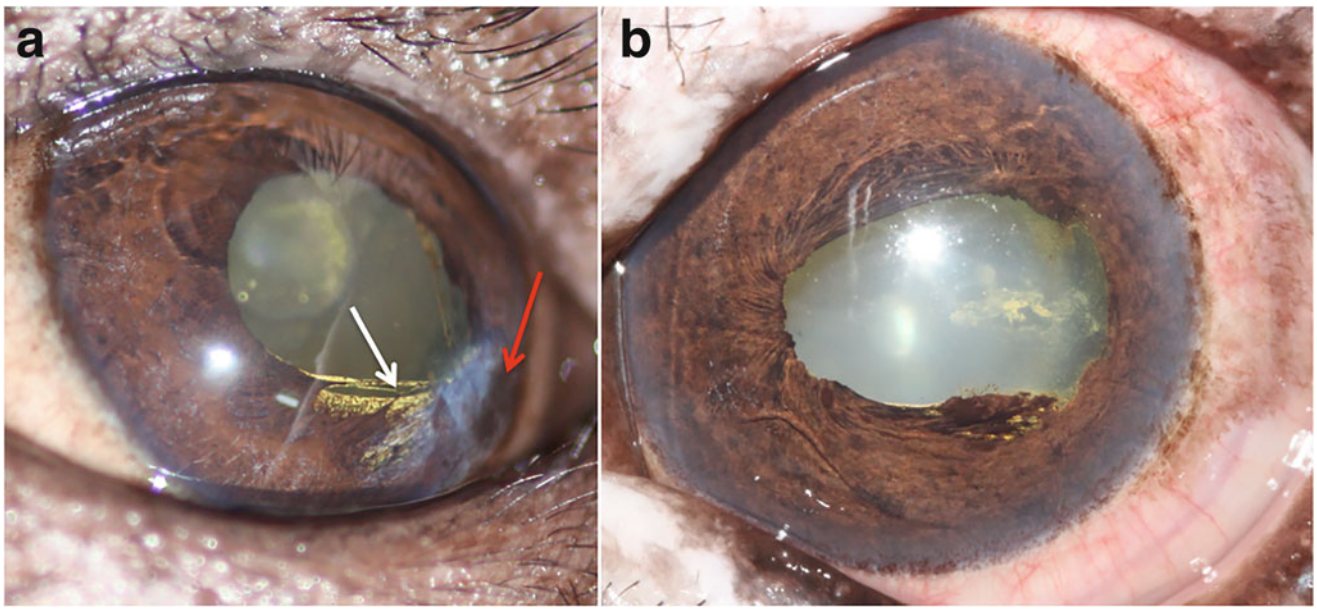

Fig. 37.32 Traumatic iris changes in adult Asiatic black bears (*Ursus thibetanus*). (**a**) Dyscoria, anterior synechia (white arrow) and corneal scarring (fibrosis and pigment; red arrow) secondary to a presumed perforating injury in an. (**b**) Traumatic iris tear and dyscoria with incipient cataract formation. Note also perilimbal haze, conjunctival hyperemia and fine neovascularization of cornea through 360°. Photo credits: Claudia Hartley

mobility issues and cardiomegaly with signs of pulmonary edema identified on radiography (quality of life considered poor), but histopathology of post-mortem obtained samples (multiple tissues/organs) were reported as "non-diagnostic."

Active uveitis is somewhat more elusive in bears as aqueous flare appears to be less dramatic and most often absent in cases where uveitis is suspected (e.g., reduced intraocular pressure, episcleral hyperemia). Aqueous flare was identified in 3 bears in a population of 135 bears examined in Vietnam and China. Keratic precipitates are also rarely encountered. Vitreal haze, debris and membranes can be witnessed and are often frustrating to treat successfully.

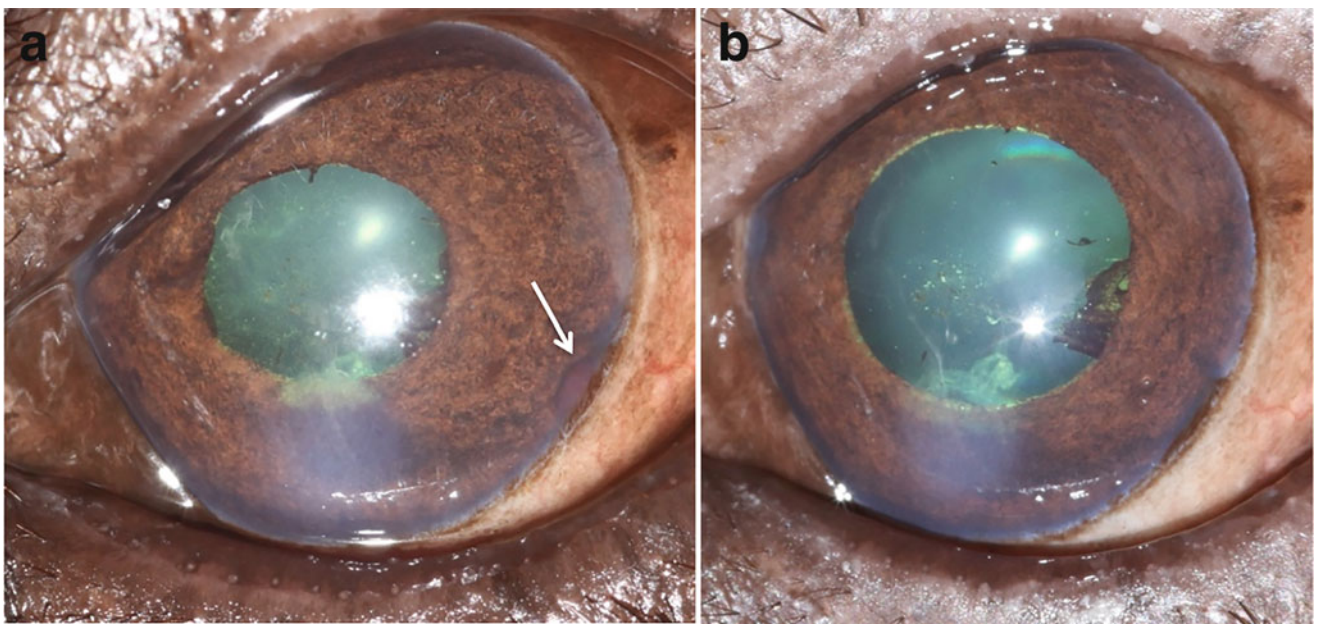

Fig. 37.33 A peripheral iris aneurysm in an adult female Asiatic black bear (*Ursus thibetanus*). (**a**) Appearance of peripheral iris aneurysm (as seen in 2012) in an adult female Asiatic black bear (4 o'clock, white arrow). (**b**) Absence of iris aneurysm (as seen in 2014) following anti-hypertensive medications. Photo credits: Claudia Hartley

Lens

Lens Anatomy

There are limited studies on the *Ursidae* lens. In a histopathological study of a Giant panda (Ashton 1976), the lens was found to measure 9.0 × 7.0 mm. It has a sharply delineated capsule, which was thick anteriorly, suddenly tapers at the equator and becomes extremely thin posteriorly. Beneath the capsule anteriorly lies a monolayer of epithelial cells, which extends to the equator where numerous nucleated lens fibers may be seen (Ashton 1976). The panda in this study (Chi-Chi London Zoo) was also found to have bilateral retinal degeneration and lenticular sclerosis attributed to old age, but there was no evidence of cataract formation. The only pathological changes seen in this eye were the presence of cysts in the iris, pars plana and peripheral retina, which was also degenerate, and these findings, together with a doubtfully sclerotic lens, were probably attributable to old age (Ashton 1976).

Lens Diseases

There are no reports on congenital cataracts or other congenital lens anomalies in *Ursidae* (e.g., aphakia, microphakia, spherophakia, lenticonus, or lenticular coloboma). Except for one case of diabetic cataracts in a brown bear, reported in a previous study on *Ursidae* (Blake and Collins 2002), only senile cataracts, or those secondary to lens luxation, have been identified in the *Ursidae*. In that regard, lens disease is common in bears and has been diagnosed by the authors in Asiatic black bears, Sun bears, Sloth bears, Brown bears, and Giant panda bears. Lens luxation has also been reported in an Andean spectacled bear in a zoological collection in the UK (Bacon, personal communication 2021).

In a study of 135 bears (largely Asiatic black bears, also Sun bears and few Brown Bears) examined at rescue facilities in China and Vietnam, lens disease was encountered in 46 bears. Cataract was the most common ocular abnormality identified ($n = 38$) (Fig. 37.34), followed by lens luxation ($n = 17$, 9 of which had concurrent cataracts). In Giant panda bears, however, several animals ranging in age from 10 to 37 years had acquired cataracts [from Chengdu, Dejuan and OPC (Ocean Park Corporation), Hong Kong]. The prevalence of lens opacity was noteworthy in animals older than 10–12 years. Many of these animals had incipient or immature cataracts (numbers and ages), and the majority of these occurred in older animals (Fig. 37.35a). A small proportion was mature or hypermature cataracts often seen in the oldest animals. In animals older than 25 years, the incidence of fully mature cataracts was more frequent, and in some cases, they developed hypermature cataracts with associated lens-induced uveitis. In another study of Sloth bears rescued from the dancing trade in India, cataract was recorded in 16 bears (27 eyes) (Fig. 37.35b) and lens luxation in 14 bears (16 eyes), although phthisis bulbi precluded diagnosis of lens disease conclusively in 12 animals. Phacoemulsification of cataracts was undertaken in one elderly bear (bilaterally), but unfortunately, this bear succumbed to tuberculosis within a few months of surgery. Cataract surgery in another bear was planned but postponed due to tuberculosis (and rupture of an axillary lymph node), and she did not recover from this disease to pursue surgical treatment to restore vision, despite systemic triple antibiotic therapy for several months.

Lens luxation seen by the authors in individuals presumed to be older/geriatric animals based on dental examinations and verbal histories as bile farm records were largely non-existent or unreliable at the time of rescue. Lens luxation in combination with a retinal detachment was seen in nine bears, and it is hypothesized by the authors that vitreal disruption due to lens luxation leads to retinal detachment (see Diseases of the Retina). Lens luxation was seen as subluxation, posterior luxation, anterior luxation, and rarely with vitreal prolapse into the anterior chamber (Fig. 37.36). Additionally, the authors have observed four Giant panda bears with hypermature cataracts, with associated lens-induced uveitis, and three of these with secondary lens subluxation (3 animals, 5 eyes), or complete lens luxation (Fig. 37.37a). In two of these Giant panda bears, the subluxated lens eventually progressed to full anterior or posterior luxation and was followed by secondary glaucoma bilaterally over the period of observation (Fig. 37.37b). Glaucoma was seen less commonly in bears with lens luxation in China and Vietnam with an IOP >30 mmHg only recorded in one Asiatic black bear with lens subluxation, while 17 bears had lens luxation/subluxation in the same population. Even in the face of anterior lens luxation (and the potential for pupil block glaucoma), raised IOP was not a feature in Asiatic black bears, Sun bears, or Brown bears as might have been expected.

Considering, to the authors knowledge, there are no publications definitively describing primary lens luxation or primary glaucoma (and/or goniodysgenesis) in the *Ursidae* it could be hypothesized that these cases of secondary glaucoma are caused by the presence of lens luxation, at least in the GPB. The presence of lens luxations of non-cataractous lenses in Asiatic black bears and Sun bears could argue toward a primary lens luxation etiology, but this cannot be assumed.

There is one published case report of lens surgery reported in an Asiatic black bear (Maehara et al. 2020). A 20-year-old male Asiatic black bear (*Ursus thibetanus*) with a 10-year history of bilateral blindness and cataracts underwent extracapsular lens extraction by phacoemulsification and

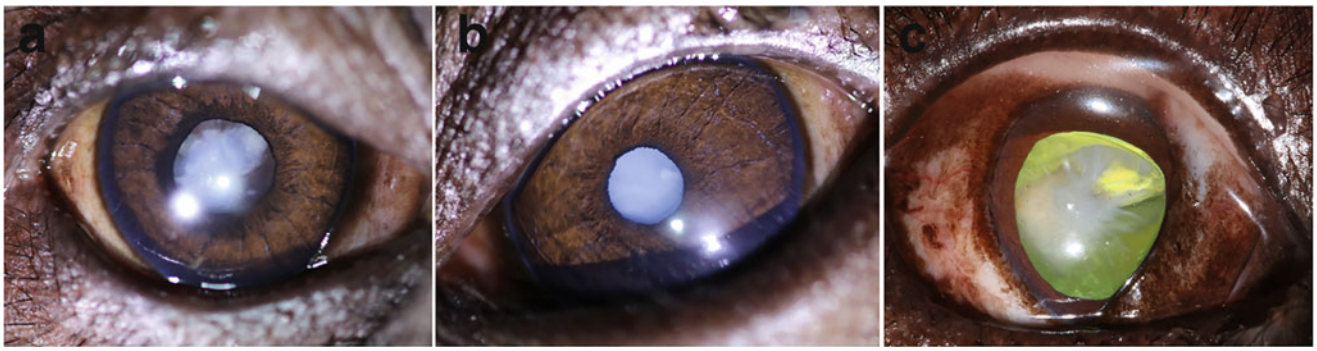

Fig. 37.34 Cataracts in Asiatic black bears (*Ursus thibetanus*). (**a, b**), Bilateral cataracts in 2-year-old Asiatic black bear in Vietnam—this bear underwent successful bilateral phacoemulsification. (**c**) Nuclear and cortical cataract in an adult Asiatic black bear in China with a small dorsal aphakic crescent. Photo credits: Claudia Hartley

aspiration (PEA) under general anesthesia. After surgery, systemic prednisolone, a gastro-protective drug and ofloxacin were administered. The bear had recovered vision, and good quality vision was maintained for 15 months (Maehara et al. 2020).

Successful bilateral surgery phacoemulsification for congenital/juvenile cataracts in a black bear (*Ursus americanus*) has been reported in a scientific abstract (Uhl 2019). In this report, bilateral hypermature cataracts with subjective microphthalmia and microphakia was diagnosed. Postoperative medications included subconjunctival triamcinolone (8 mg) and cefazolin (100 mg), oral meloxicam (0.1 mg/kg, once daily) and amoxicillin/clavulanic acid (16.67 mg/kg, twice daily). Intraoperative findings included shallow anterior chambers, irregular lens capsules with plaque formations, soft cataractous lenses in both eyes, and elongated ciliary processes in the left eye. At 281-days post-surgery, the bear was visual, comfortable, and interacting well with other bears (Uhl 2019).

The first case report of successful cataract surgery in a Giant panda bear was reported in 2003 (Yucun et al. 2003). In another case report (Hung 2018) an emergency intracapsular lens extraction (ICLE) performed for an anterior lens luxation (with secondary glaucoma that was non-responsive to topical medication) was performed. After successful removal of the entire lens, the IOP returned to normal after surgery. Unfortunately, the animal did not recover vision, which was believed to be due to irreparable retinal and optic nerve damage secondary to glaucoma. Another case of cataract surgery in a Giant panda bear was reported by Jin et al. (2010), where vision was restored "to a certain degree." Lastly, a Giant panda bear was examined by one of the authors (RO) with bilateral retinal detachment (confirmed by B-mode ultrasound) and a hypermature cataract in the right eye and an aphakic left eye. To the authors' knowledge,

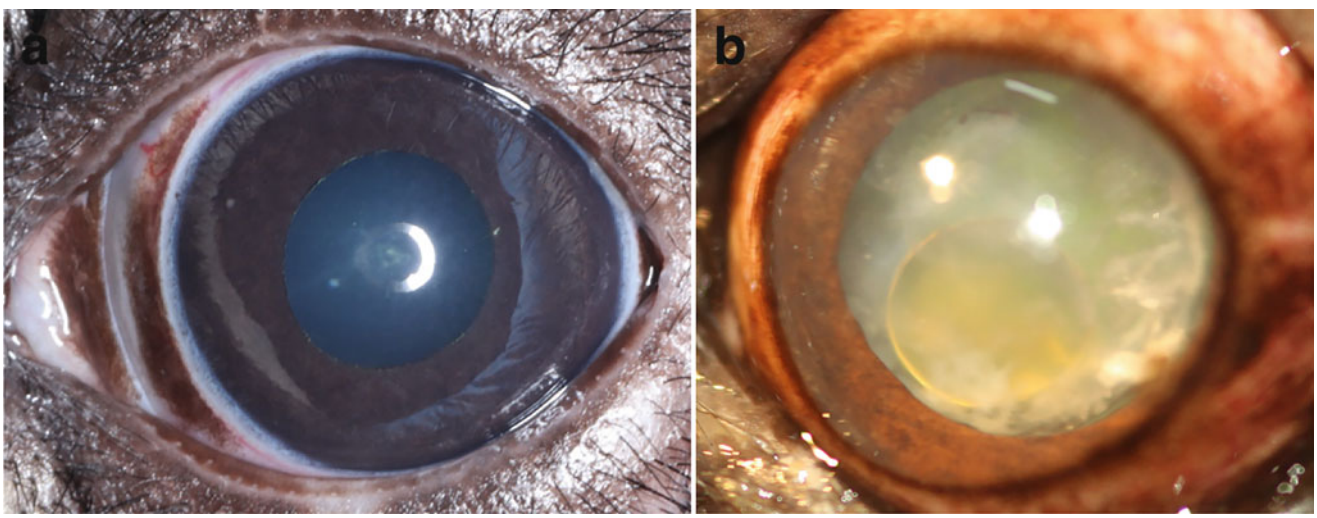

Fig. 37.35 (**a**) Small incipient cataract, triangular shape, located on the posterior cortex in an 18-year-old Giant panda bear (*Ailuropoda melanoleuca*). (**b**) Brunescent nucleus sitting ventrally in a hypermature cataract (Morgagnian) in an adult Sloth bear (*Melursus ursinus*) from India. Photo credits: (**a**) Rui Oliveira, (**b**) Claudia Hartley

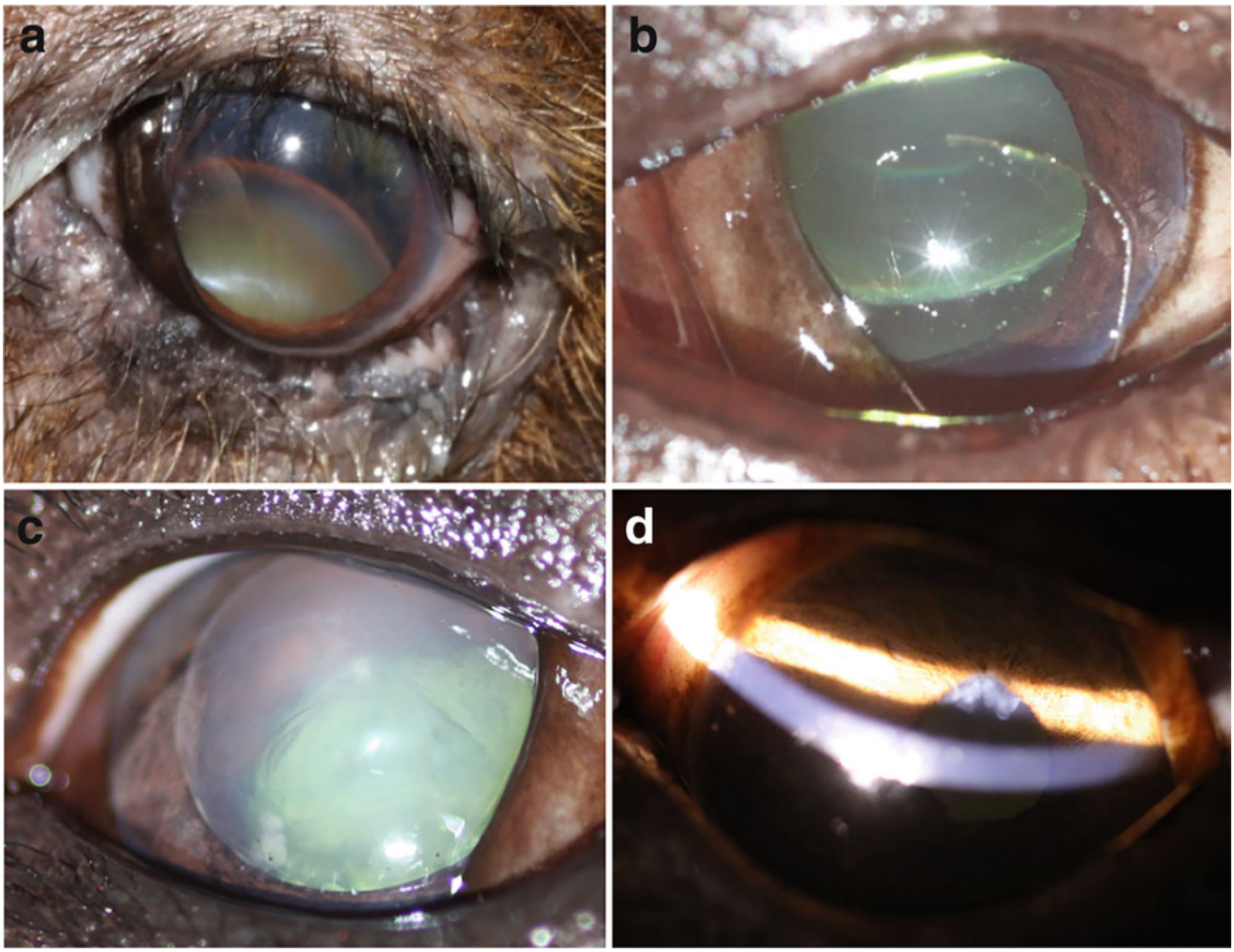

Fig. 37.36 (**a**) Posterior lens luxation and uveitis, with a dilated pupil due to retinal detachment in a Sun bear (*Helarctos malayanus*) in Cambodia. Conjunctivitis also presents secondary to the intraocular disease with mucopurulent discharge. (**b**) Lens luxation (posterior) in an adult Asiatic black bear (*Ursus thibetanus*) in China. Note that the bear was in dorsal recumbency; hence aphakic crescent was ventral. Note also the absence of cataract formation (non-cataractous lenses may also luxate in bears). (**c**) Anterior lens luxation in an adult Asiatic black bear with early cataract formation and central diffuse corneal edema (China). (**d**) Deep anterior chamber and vitreal prolapse in an adult Asiatic black bear with posterior lens luxation in China. Photo credits: Claudia Hartley

there is no published data on this case, but we were able to confirm this was an animal in which a physician ophthalmologist had performed, unfortunately unsuccessfully, cataract surgery in the left eye.

Given the significant presence of cataracts in the older Giant panda bear population (12/48) and the potential for severe complications once these reach hypermature stage (lens luxation and secondary glaucoma) we propose it is preferable to consider undertaking earlier phacoemulsification surgery. Obviously, a cost/benefit evaluation must always be considered for each one of these precious animals, but we would suggest that if there is no particular health limitation or contraindication for short general anesthesia then phacoemulsification surgery should be considered for all existing cases of mature cataracts. These cases should be performed by qualified and experienced veterinary ophthalmologists with appropriate microsurgical equipment. It is also recommended that thought and preparation for how postoperative medications will be administered are prioritized (pre-operative training of individuals to be compliant for topical and/or systemic medications) as success can rely heavily on these factors.

As yet, unpublished case report of successful cataract surgery (by phacoemulsification or extracapsular lens extraction) exists in ten Asiatic black bears and one juvenile Sun bear, and three adult Sun bears in China, Vietnam and Cambodia (Fig. 37.38). Complications included: dislocation of an artificial intraocular lens (IOL) haptic onto the anterior iris in one Asiatic black bear, endothelial fibrosis adjacent to the wound in one bear (poor compliance with anti-

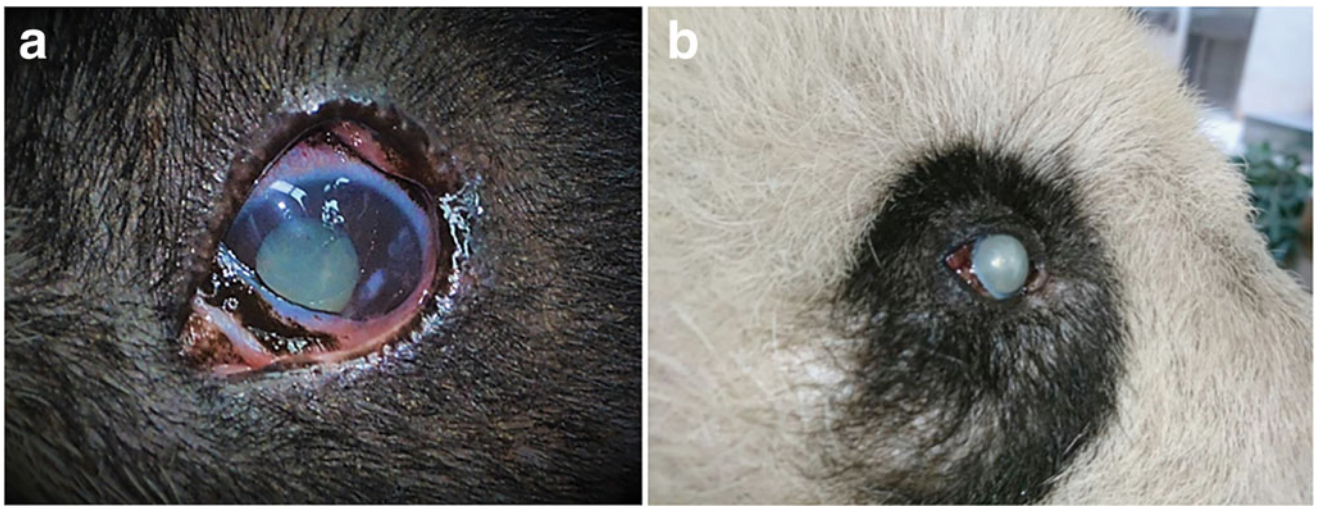

Fig. 37.37 Lens luxations in Giant panda bears (*Ailuropoda melanoleuca*). (**a**) In this Giant panda bear, the left eye was diagnosed with hypermature cataract, an aphakic crescent with posteriorly subluxated lens and vitreous herniation in the anterior chamber. Multifocal keratitis and corneal superficial neovascularization was also present in the ventrocentral cornea. (**b**) A 37-year-old female Giant panda bear with anterior lens luxation and hypermature cataract with secondary glaucoma in the right eye. The animal was comfortable, and there was no blepharospasm present. The eye was visual despite IOP measurement of 41–45 mmHg. Additional findings included a slight corneal edema, mild conjunctivitis and mild episcleral congestion. Photo credits: (**a**) Rui Oliveira, (**b**) Ocean Park Corporation (OPC) Hong Kong

inflammatory drugs postoperatively) and medial strabismus in one Asiatic black bear, excessive posterior capsular opacification reducing vision (corrected with a second surgery involving posterior capsulorhexis and anterior vitrectomy) in another Asiatic black bear and medial strabismus in a juvenile Sun bear, although all were visual. One Asiatic black bear underwent unsuccessful cataract surgery in Vietnam, where multiple ocular defects were present, despite positive electroretinography (a retrobulbar optic nerve lesion was suspected).

Additionally, unsuccessful cataract surgery was recently performed on one Asiatic black bear in the country of Laos in 2019, where the surgery was without complication, but retinal degeneration had advanced between initial assessment (including ultrasound and electroretinography), and surgical intervention (4 years). This illustrates the need to perform surgery earlier where possible. Finally, bilateral

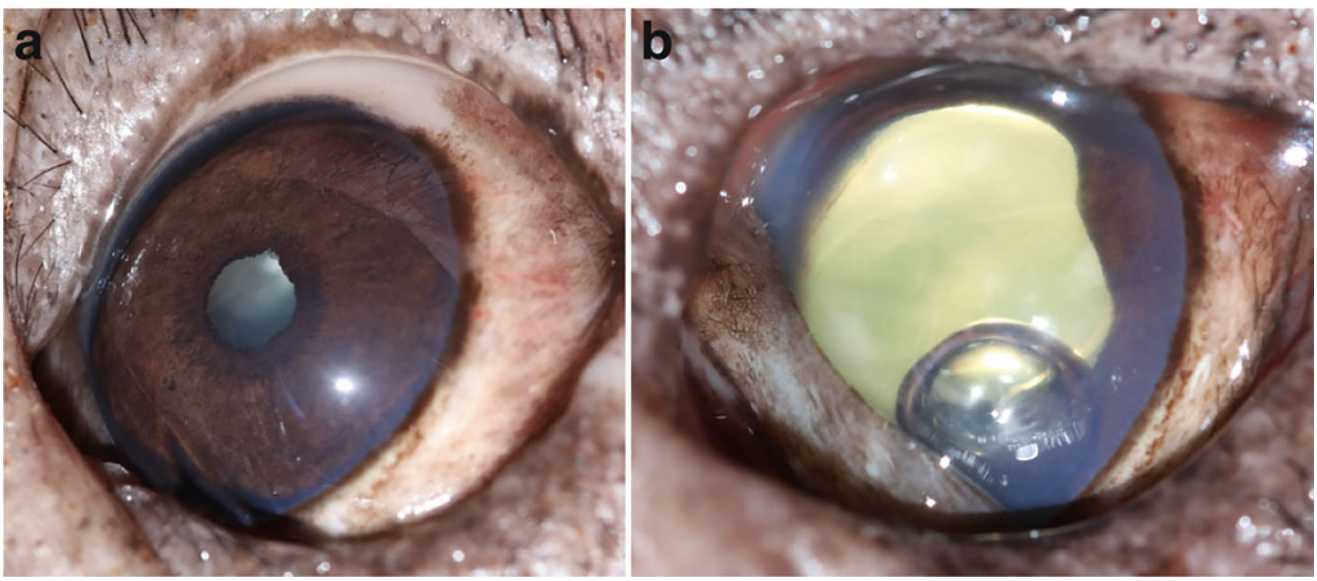

Fig. 37.38 (**a**) Mature cataract in an adult Asiatic black bear (*Ursus thibetanus*) prior to phacoemulsification (and prior to pre-operative pupil dilation). (**b**) Immediately following successful phacoemulsification in the same eye and animal in Cambodia. Photo credit: Claudia Hartley

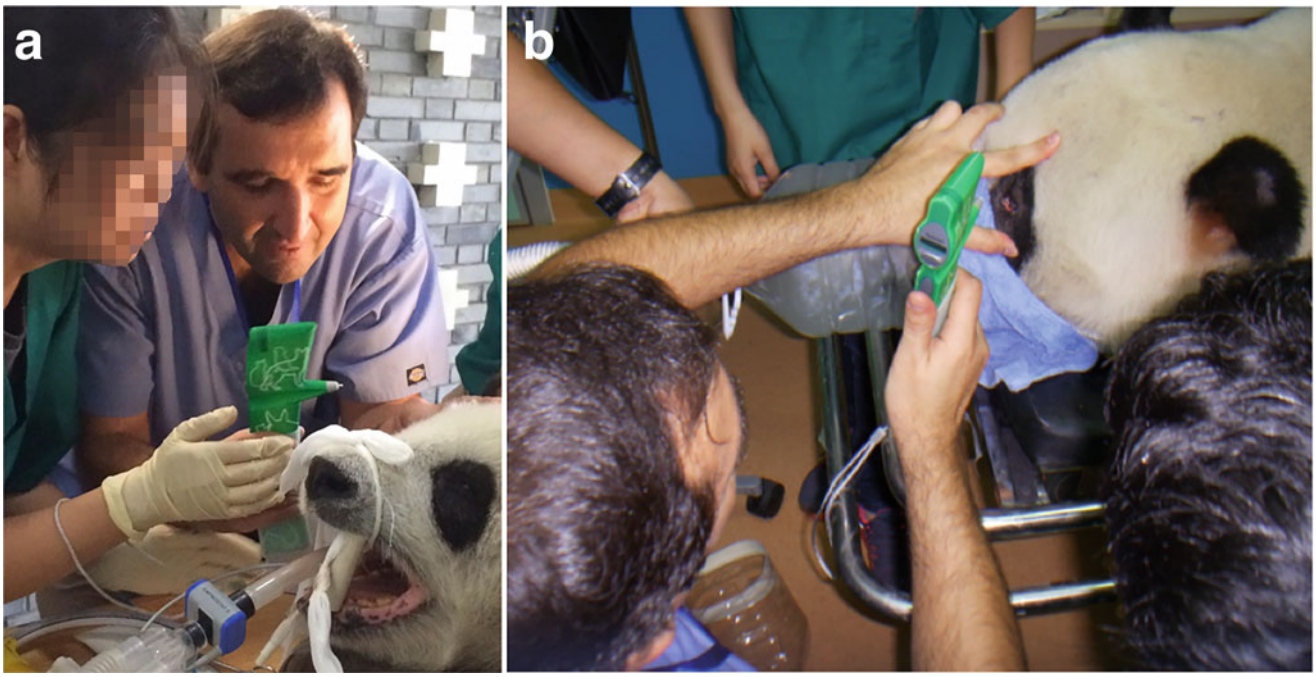

Fig. 37.39 A male Giant panda bear (*Ailuropoda melanoleuca*) (**a**) and female Giant panda bear (**b**) during rebound tonometry (Icare® TonoVet, Helsinki, Finland) procedure as part of a training program on ophthalmic examination for local veterinarians (Workshop of worldwide experts in Giant Panda Medical Husbandry Skill International Exchange Training in China Conservation and Research Center for Giant Panda (CCRCGP), Wolong Nature Reserve, Dujiangyan, Sichuan, China in 2015). Photo credit: Rui Oliveira

phacoemulsification was successfully performed in a single Sloth bear in India, but sadly, this elderly individual succumbed to tuberculosis a few months after surgery.

Glaucoma

In an ocular histopathology study of the Giant panda (Ashton 1976), the filtration angles in Giant panda bears are of the type seen in other carnivores, the ciliary body is split into two leaves to form a wide and deep ciliary cleft. The anterior leaf of the ciliary body predominantly consists of meridional muscle fibers, which are continuous with the inner aspect of the corneosclera and terminate through the trabecular meshwork in the peripheral cornea. Muscle fibers in the inner leaf terminate in the iris root. The cleft is bridged by delicate pectinate fibers enclosing the spaces of Fontana, which connect with the trabecular meshwork lying at the corneoscleral junction; several large nerve bundles are seen in this meshwork. Externally within the adjacent sclera lies a plexus of channels ("circle of Hovius"; "angular aqueous plexus") which communicates via the intrascleral collector vessels with the surface veins. Scattered pigment cells are present within the trabeculae and related sclera (Ashton 1976).

Tonometry was performed in 23 Giant panda bears between the ages of 1 and 26 years (average age of 10.6 years, 46 clinically normal eyes) using rebound tonometry (TonoVet, Icare, Finland) (Fig. 37.39). Animals examined (15 females and 8 males) were clinically normal and anaesthetized via intramuscular dart with ketamine in doses ranging from 70 mg/kg to 80 mg/kg. All animals were transported to the surgical center deeply sedated and then were intubated following a short period of volatile gas mask anesthesia. Anesthesia was maintained using isoflurane and oxygen, and animals were all in sternal recumbency with the head positioned in a straight/extended position and using a vacuum pillow in order not to cause compression in the neck area.

Procedures to measure IOP (intraocular pressure) in all Giant panda bears were performed by using a rebound tonometer (Icare® TonoVet, Helsinki, Finland) in "dog mode", placed perpendicularly to each of the animal's eyes and with the distance from the probe to the corneal surface of 4–6 mm. The mean IOP by rebound tonometry was 16.43 mmHg (mean) with a standard deviation (SD) of ±3.011. The mean IOP value for the right eye was 15.78 ± 2.90, and the mean IOP value for the left eye was 17.07 ± 3.05 mmHg. Statistical analysis was performed using Shapiro–Wilk Normality Test and general IOP descriptive statistics (all included, left, right, male and female) and no significant differences in eye side, gender or age were observed (*T*-test between eye side (R × L)—not significantly different $P = 0.26$ and *T*-test between sex (M × F)—not significantly different $P = 0.60$).

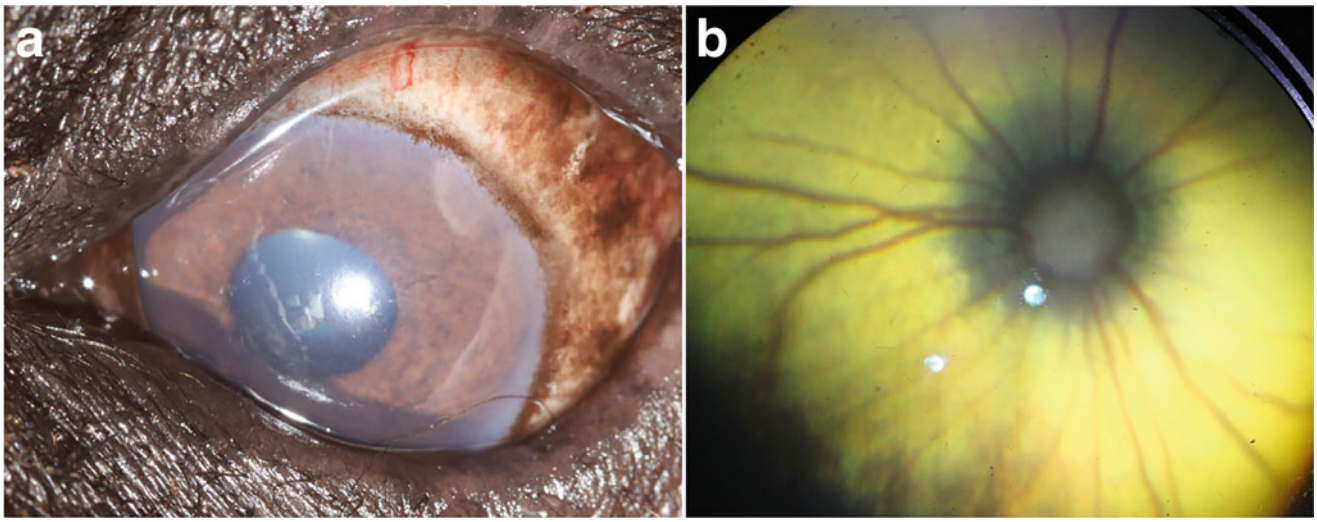

Fig. 37.40 (**a**) Mild diffuse corneal edema in Asiatic black bear (*Ursus thibetanus*) in China with an IOP of 69 mmHg. (**b**) Appearance of the fundus of the same eye, note optic nerve atrophy. Photo credit: Claudia Hartley

The mean IOP of 135 bears (Asiatic black bear, Sun bear and Brown bear population) was 19.6 ± 5.6 mmHg under general anesthesia (medetomidine, tiletamine and midazolam induction, isofluorane maintenance); median 19 mmHg. Glaucoma was seen in 7 Asiatic black bears of 135 examined, where a glaucoma diagnosis was considered with IOP above 30 mmHg (range 30–69 mmHg). However, in six of these Asiatic black bears, systolic blood pressure was also raised (above 160 mmHg, range 173–251 mmHg), and in five Asiatic black bears, IOP readings were subsequently below 25 mmHg when systolic blood pressure was reduced to less than 140 mmHg. In the remaining one Asiatic black bear with raised IOP and systolic blood pressure, the IOP reduced to 60 mmHg (from 69 mmHg) when the systolic blood pressure reduced below 140 mmHg (124 mmHg). This globe had mild diffuse corneal edema, a subluxated lens, and a grey atrophied appearing optic nerve head (Fig. 37.40). The globe was enucleated as a treatment for presumed glaucoma and a painful ocular condition that was permanently non-visual.

To the author's knowledge, no cases of congenital or primary glaucoma have been diagnosed in Giant panda bears. Bilateral chronic glaucoma was diagnosed in one Asiatic black bear, although intraocular pressures were normal at time of enucleation. This animal had bilateral hydrophthalmos, lens luxation, cataract and retinal detachment. The mean axial globe diameter was 21.8 mm for both eyes (normal 15.9 ± 1.6 mm) (Hartley et al. 2013a, b). Gonioscopy was performed in 30 Asiatic black bears and was normal (fine hair-like pectinate ligament and open angle) in the majority (28/30). One Asiatic black bear had a slightly narrow angle with a poorly rarefied ligament (fibrae latae, 50–100%) in both eyes but a normal intraocular pressure. In another Asiatic black bear, a broad area of peripheral anterior synechia was identified in one eye, presumed secondary to uveitis. Therefore, it appears that goniodysgenesis is rare in Asiatic black bears.

The examination of 43 Sloth bears in two sanctuaries in India revealed a mean IOP of 12.5 ± 5.2 mmHg, median12 mmHg. Similar to cases in Giant panda bears and Asiatic black bears, the Sloth bears also had cataracts and lens luxation/subluxation concurrently. Unilateral glaucoma has been reported in two Sloth bears examined as members of a population residing in sanctuaries following rescue from the dancing bear trade. This appeared to be linked to the development of hypermature cataract, lens luxation and presumed secondary glaucoma (Fig. 37.41a) (Hartley et al. 2014).

Secondary glaucoma was diagnosed in two Giant panda bears and both were associated with hypermature cataracts and anterior lens luxation (Fig. 37.41b). These animals only developed ocular hypertension after the lens had become completely luxated in the anterior chamber, causing a pupillary blockage, with no aqueous passing to the anterior chamber, resulting in an acute IOP elevation in these eyes. Luxation or subluxation of the lens in the posterior chamber or into the vitreous is also a risk factor for glaucoma, but the mechanism for secondary glaucoma is not as obvious.

In the author's experience, the cases observed with glaucoma in Giant panda bears were caused by anterior lens luxation and hypermature cataracts. In these cases, despite intraocular pressures being elevated at 70–80 mmHg, only mild ocular signs of mild episcleral congestion and mild corneal edema were observed. Usually, these eyes look comfortable and open, only presenting with mild photophobia and very little conjunctival redness. This stoicism was also evident in other bear species examined by the authors

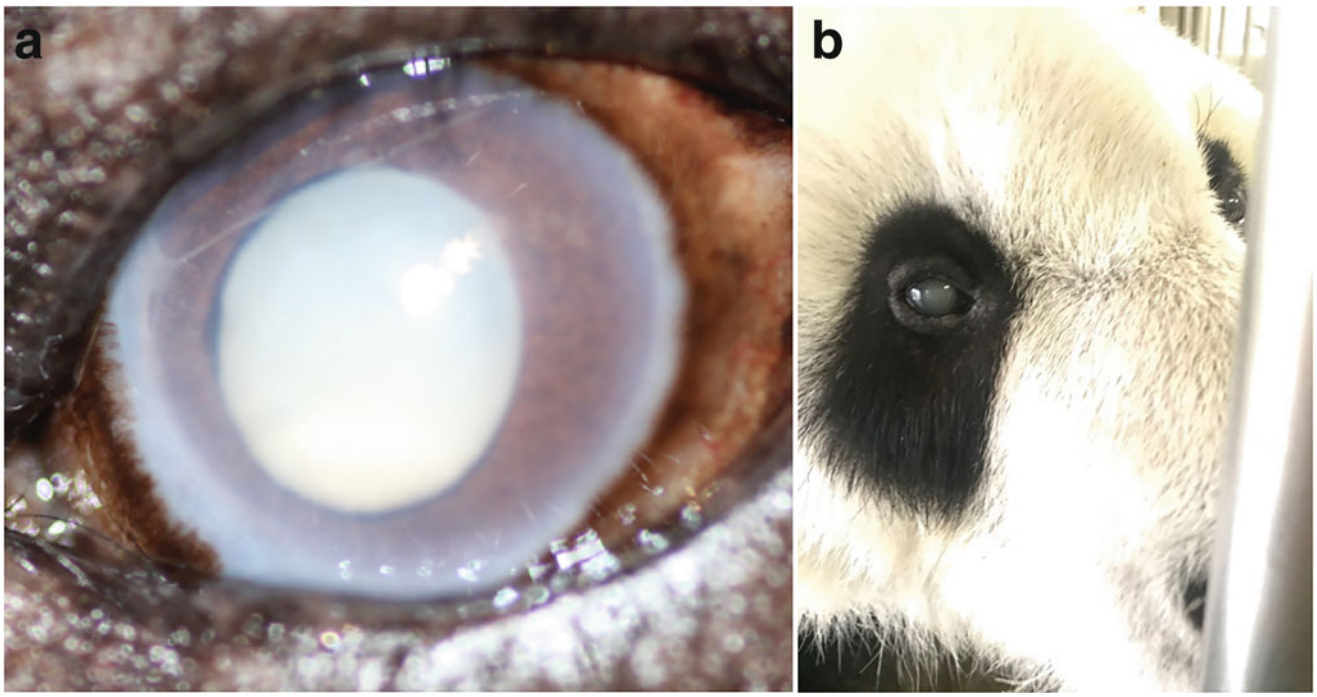

Fig. 37.41 (**a**) Unilateral buphthalmos in an adult male Sloth bear with hypermature highly mobile luxated cataractous lens. (**b**) A 31-year-old, Male Giant panda bear (*Ailuropoda melanoleuca*) with right anterior lens luxation and mature cataract with secondary glaucoma OPC (Ocean Park Corporation) Hong Kong. Photo credits: (**a**) Claudia Hartley, (**b**) Rui Oliveira

(Asiatic black bears, Sun bears, Brown bears, Sloth bears and a Polar bear). This is an important factor to be aware of when considering both diagnoses and analgesia in *Ursidae*, as signs may be subtler and should not be overlooked.

In Giant panda bear cases with lens luxation we observed it is hypothesized that anterior lens luxation, in a similar mechanism to dogs, results in a pupillary blockage (physically, the lens completely blocks the pupil), which impairs aqueous passage to the anterior chamber and/or obstructs the pupil and outflow pathways of the drainage angle. This triggers an IOP elevation and secondary glaucoma. Another possible explanation and contributing factor would be the presence of concomitant and chronic uveitis, caused by mature (or hypermature) cataracts in the aging Giant panda bear. In cases of chronic uveitis, like advanced lens-induced uveitis (LIU), the presence of inflammatory mediators in the posterior chamber may weaken the lens zonules. In addition, the ciliary cleft may be densely infiltrated with inflammatory cells obstructing outflow by their physical presence and/or by producing cytokines that adversely affect trabecular endothelium function. This is the proposed most common mechanism of glaucoma secondary to feline lymphoplasmacytic uveitis or uveodermatologic syndrome in dogs. Macrophages are too large to pass through the trabecular pores readily and, on occasion, accumulate within the cleft to cause obstructive secondary glaucoma (Grahn and Peiffer 2007).

Unfortunately, we have not been able to provide evidence for these hypotheses by histopathological analysis (due to enormous restrictions to collect tissues samples in many bear species covered under CITES legislation), but we strongly suspect glaucoma is secondary to a previous lens luxation condition. The lens luxation is potentially caused by chronic and progressive lens-induced uveitis, causing zonular gradual weakening and inevitable zonular breaking, subsequently resulting in complete lens luxation and secondary glaucoma. It is interesting that subluxation is often associated with increased IOPs in dogs but apparently not in Giant panda bears. This theory is supported by the fact that all Giant panda bear eyes initially diagnosed with subluxation and cataracts alone were normotensive (IOPs were within the normal range in both eyes of all animals prior to complete lens luxation occurred).

In two Giant panda bears from Hong Kong, one of the authors (RO) was able to observe, diagnose, and try to manage two cases (three eyes in total) of glaucoma secondary to lens luxation together with the Ocean Park Corporation (OPC) Hong Kong veterinary team. The first animal to develop glaucoma secondary to lens luxation was a female Giant panda bear 36–37 years when she first presented with anterior lens luxation and secondary glaucoma in her left eye (Fig. 37.41). Over approximately 1.5 years, we tried to manage this condition using medication only, as general anesthesia was not an option, considering her advanced age (she was

the oldest Giant panda bear ever recorded when she died at 38 years old) and some pre-existing health concerns. Thus, lens luxation and glaucoma had to be managed medically, to the detriment of the author's preferred option, which was to perform surgery to remove the lens (either by intracapsular lens extraction (ICLE) or phacoemulsification) or by couching and using miosis-inducing eye drops. This was considered as the best option after a posterior luxation of the lens was achieved, so initially topical tropicamide solution 1% eye drops (Mydriacyl, Alcon) was applied and repeated after 5 min to obtain total mydriasis. Furthermore, by using food treats and conditioning the animal to look up in her cage, eventually, we manage to dislocate the lens back to the vitreous chamber (converting the anterior luxation to a posterior luxation), at which time a topical prostaglandin analog, latanoprost 0.05 mg/ml (Xalatan 0.005%, Pfizer), was used to cause miosis. By inducing tight miosis, the lens was trapped in the posterior segment of the eye and theoretically reducing the risk of the lens luxating anteriorly again. Additionally, the prostaglandin analogs are powerful anti-glaucoma drugs and might prevent or delay an increase in IOP, such as secondary glaucoma, a common sequela of lens luxation. Assuming that the pharmacokinetics of the prostaglandin analog in bears is similar to that in dogs, because no studies are available of this drug use in *Ursidae*.

By the time the second application of latanoprost was administered, the IOP had measured 23–24 mmHg, and the lens remained in the vitreous chamber. Additionally, on a careful examination of the contralateral right eye using tropicamide solution 1% eye drops to induce mydriasis and slit-lamp, there were already some areas of zonular weakness dorsally a very slightly subluxated lens (approximately one quadrant subluxation). Topical prostaglandin analogs, such as latanoprost or travoprost, were used twice a day in this animal for the purpose of inducing miosis and maintaining the lens in the vitreous chamber during a long period and reducing the potential for anterior lens luxation recurrence. Pupillary constriction increases the lens-iris contact area and can provide enhanced support to the lens, also reducing the risk of anterior lens luxation in dogs (Binder et al. 2007). In that report, vision was maintained for 1 year in 16 of 20 (80%) eyes and for 2 years in 11 of 19 (58%) of eyes. Miotic therapy delayed anterior lens luxation in eyes with lens instability.

The animal was managed medically for several months, using a combination of prostaglandin analogs like latanoprost 0.05 mg/ml BID, and dorzolamide hydrochloride 2% and timolol maleate 0.5% eye drops twice/three times daily, for glaucoma and lens luxation in combination with Nepafenac 0.1% eye drops twice/three times daily, and prednisolone acetate twice/three times daily, for the lens-induced uveitis caused by the existing hypermature cataracts.

Approximately 6 months after the left eye was diagnosed with lens luxation and glaucoma, the contralateral eye had signs of more advanced lens subluxation. With time, the right lens also luxated, and despite topical medical treatment, eventually, some episodes of pressure spikes and anterior lens re-luxation were present, resulting in further deterioration of her vision. Despite all treatments and efforts to save her vision, regretfully, she ended up having a much-reduced vision in her right eye and completely losing vision in her left eye more than 1 year after this condition was initially diagnosed.

A 31 year-old-male Giant panda bear from OPC, Hong Kong, underwent emergency intracapsular lens extraction (ICLE) for anterior lens luxation and secondary glaucoma in the right eye, which was non-responsive to medication. On initial ocular examination, there was an anterior lens luxation in the right eye, a mature cataract and mild corneal edema. Initially, the IOP could not be measured as the animal was not conditioned for IOP measurements, but dazzle and indirect PLR were present, and the eye was apparently comfortable without signs of blepharospasm or pain. Topical tropicamide solution 1% drops were applied to obtain mydriasis and to try to avoid glaucoma by a pupillary block. On the following day, the lens had dislocated back to the vitreous chamber, at which time a topical prostaglandin analog, latanoprost 0.05 mg/ml, was used as a potent miotic agent to promote miosis. By inducing tight miosis, the lens was trapped in the vitreous chamber and so, this way, was less likely to luxate anteriorly again. Additionally, the prostaglandin analogs are powerful anti-glaucoma drugs and were speculated to prevent or delay an increase in IOP, such as secondary glaucoma, a common sequela of lens luxation.

Unfortunately, on the fourth day after the initial diagnosis of lens luxation, and despite the use of latanoprost, the lens was again partially luxated in the anterior chamber, at which time the animal was sedated and examined for possible ILCE surgery referral. At this time right IOP measurement was 77–85 mmHg by rebound tonometry (Tonovet™), but dazzle reflex, menace response and indirect PLR were all negative. The left ophthalmic examination was normal except for the presence of a posteriorly subluxated lens with immature cataract and IOP measured 11–14 mmHg. During the following days, the lens was intermittently observed partially luxated in the anterior chamber or in the posterior segment but, because this was not a sustainable situation long term, it was decided to remove the lens by ICLE despite the guarded prognosis to recover vision in the right eye. On the day of surgery, the right lens was successfully removed under general anesthesia by performing an ICLE and subtotal anterior automated vitrectomy. This re-established a normal fluid flow through the pupil, thus returning the IOP to normal after surgery. Unfortunately, the animal did not recover vision from the eye. This was speculated to be due to previous

pressure spikes of IOP, resulting in permanent neuroretinal and optic nerve damage, with irreversible loss of vision. Perioperative fluids and single injections of potentiated amoxicillin at 8 mg/kg by subcutaneous injection and cefovecin sodium (Convenia®, Zoetis) at 8 mg/kg by subcutaneous injection were administered. Post-surgically, the Giant panda bear was medicated topically using prednisolone acetate eye drops, Nepafenac 0.1% eye drops, dorzolamide hydrochloride 2% and timolol maleate 0.5% eye drops, moxifloxacin (as HCl) 0.5% all four times daily, and latanoprost 0.05 mg/ml. Orally were administered carprofen (Rimadyl®, Zoetis) at 2 mg/kg twice daily for a month and doxycycline at 300 mg once daily (3 mg/kg) for 7 days. Twenty days after surgery, the right eye was comfortable, the surgical wound was healing fine, and there was no flare. The IOP measured in the low teens (readings taken in conscious bear), PLRs and dazzle reflex were absent, and the menace response remained negative on this side. At 60 days after surgery, the right eye IOP measured 50 mmHg and topical brimonidine tartrate three times daily was added to previous medications. This case continues to be monitored for IOP control and, if medications alone are not enough to reduce values measured to a normotensive range, additional surgical options are being regarded as the next step for this bear.

Considering the significant presence of cataracts in the oldest Giant panda bear population (12/48) and the existing potential of severe complications once these reach a hypermature state (lens luxation and secondary glaucoma), we believe it i's preferable to consider earlier phacoemulsification surgery. Thus, once these animals develop mature cataracts, it is better to proceed to phacoemulsification surgery and not to wait for much more challenging surgical cases and with a guarded surgical prognosis (see "Lens" section). This condition is probably going to be a recurrent ophthalmic problem in the aging GPB population, and we suspect we will see more of these cataract cases reported in the near future as the existing animal population ages. Obviously, risk/benefit evaluation must always be considered for each and every of these precious animals, but we would say that if there is no particular health limitation or any contraindication for short general anesthesia, phacoemulsification surgery should be considered without restrictions in all existing cases of mature cataracts or lens luxations above 180° (see "Lens" section).

Another very important consideration to address in the future is the need to train captive Giant panda bear populations for basic ophthalmic examination (ocular light illumination/transillumination, tonometry and slit-lamp examination). Lens subluxations and secondary glaucoma are an expected occurrence in geriatric pandas. Medical and surgical management of both conditions, including conditioning training of the animal for long-term eye monitoring and treatment of these ophthalmic conditions, is essential for a successful outcome in vision-threatening conditions. Husbandry training for ophthalmic examination, eye drops, and tonometry should be initiated in pandas before reaching old age so we can try to prevent or treat lens subluxation, luxation and secondary glaucoma. In the case of the 37-year-old female Giant panda bear, we managed to involve the OCP Hong Kong trainers/keepers to train her for the use of most ophthalmic examination equipment, and after a few months, she voluntarily allowed us to perform tonometry and slit-lamp examinations.

Retina and Optic Nerve

Anatomy of the Retina and Optic Nerve

There is very little information available on normal bear funduscopic studies or documented retinal or optic nerve head abnormalities. It is known that the Giant panda bear retina possesses rods and cones in a typical mammalian architecture: the visual cell layer is rod-rich as in nocturnal animals. Large ganglion cells and the thick ganglion cell layer are a feature of the bear retina (Fig. 37.42a). As to be expected, there is no true macula or fovea. The choroid is of the standard vertebrate type. It is heavily pigmented and shows a cellular tapetum as seen in the upper half of the fundus of all carnivores, and in this region, the pigment epithelium is not pigmented (Ashton 1976).

The optic nerve leaves the globe slightly below and lateral to the posterior pole. The eye is surrounded by the usual incomplete bony ring, which is completed posteriorly by a stout orbital ligament. The orbital ring is nearly circular in outline, measuring 40 mm in anteroposterior diameter by 37 mm in dorsoventral diameter. A prominent and well-marked cushion of fat, situated outside the periorbita, occupies the anteroinferior corner of the orbit (Davis 1964). In the Giant panda bear, the optic nerve (CNII) emerges from the optic foramen to pursue a faintly S-shaped course to the globe. It has a diameter of approximately 2.5 mm, and its length from the optic foramen to the posterior globe is 50 mm. On funduscopic examination, the circular optic nerve head is poorly myelinated and of variable size. There are defined tapetal and non-tapetal areas, with an individual variation regarding the size of non-tapetal retina according to melanin pigment intensity levels in the retinal pigment epithelium (Fig. 37.42b, c). On histopathological examination, there is a normal lamina cribrosa area where the optic nerve enters the eye. Regarding its vascular supply, the retina is

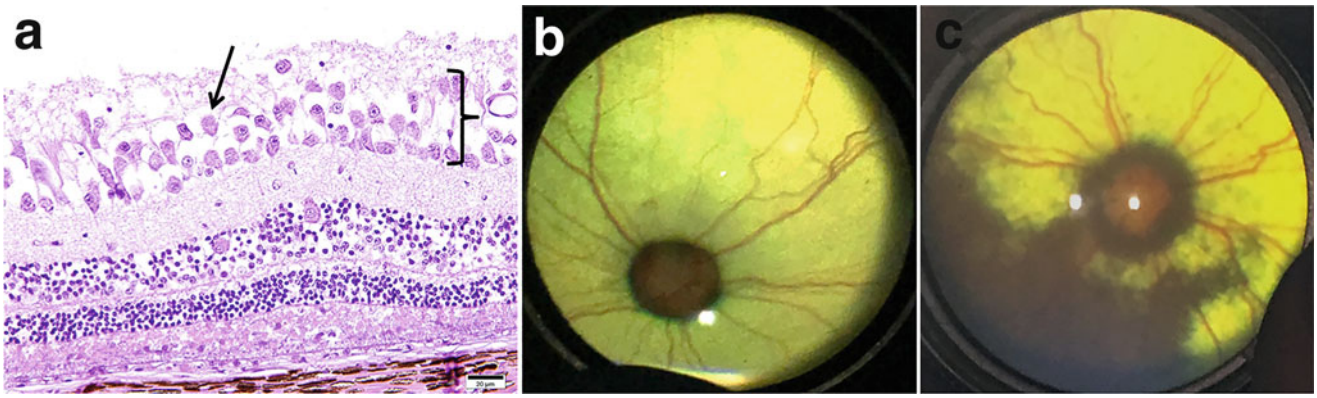

Fig. 37.42 (**a**) Photomicrograph of a retinal section from an American black bear cub (*Ursus americanus*). Note the large ganglion cells (black arrow) and the thick ganglion cell layer (black bracket). HE. Bar size = 20 μm. (**b**, **c**) Normal fundus pictures of two different Giant panda bears (*Ailuropoda melanoleuca*), showing a central poorly myelinated circular optic nerve head of variable size. Retina vascular pattern is holangiotic with no blood vessels crossing the optic nerve head (**b**) and exiting optic disc margin, similarly to what is seen on the feline fundus. Usually, the tapetal area is very extensive (**b**). However, there is a variability in the size of the non-tapetal area, which in the most pigmented fundus reaches the optic nerve head and in some cases even surrounds the optic nerve head (**c**). Picture taken with a 20 Diopter indirect lens. Photo credits: (**a**) Comparative Ocular Pathology Laboratory of Wisconsin, (**b**) Rui Oliveira

holangiotic, but there is no evidence of a central retinal artery, and the retinal vessels derive from the ciliary arteries at the disc margin (Ashton 1976).

The normal retinal appearance in ursid species is holangiotic with a large circular central area of tapetum lucidum and a peripheral rim of non-tapetal retina reaching to the ora serrata. The retinal venules appear wider and slightly darker than their arteriole counterparts, which also often have a more tortuous path. The optic nerve head is round and poorly myelinated, resembling that of cats (Fig. 37.43).

Diseases of the Retina and Optic Nerve

Congenital abnormalities were rarely encountered in the authors' examinations of ursid species. One Asiatic black bear with optic nerve coloboma had presented with blindness since rescue (and history reported of blindness on the bile farm) and wandering nystagmus. Both optic nerve heads were deeply cupped with a typical grey coloration to the optic nerve excavations suggesting coloboma rather than glaucomatous cupping (intraocular pressures were normal). A severe optic atrophy secondary to hypovitaminosis-A in utero or early post-natally (and bilateral bony optic canal

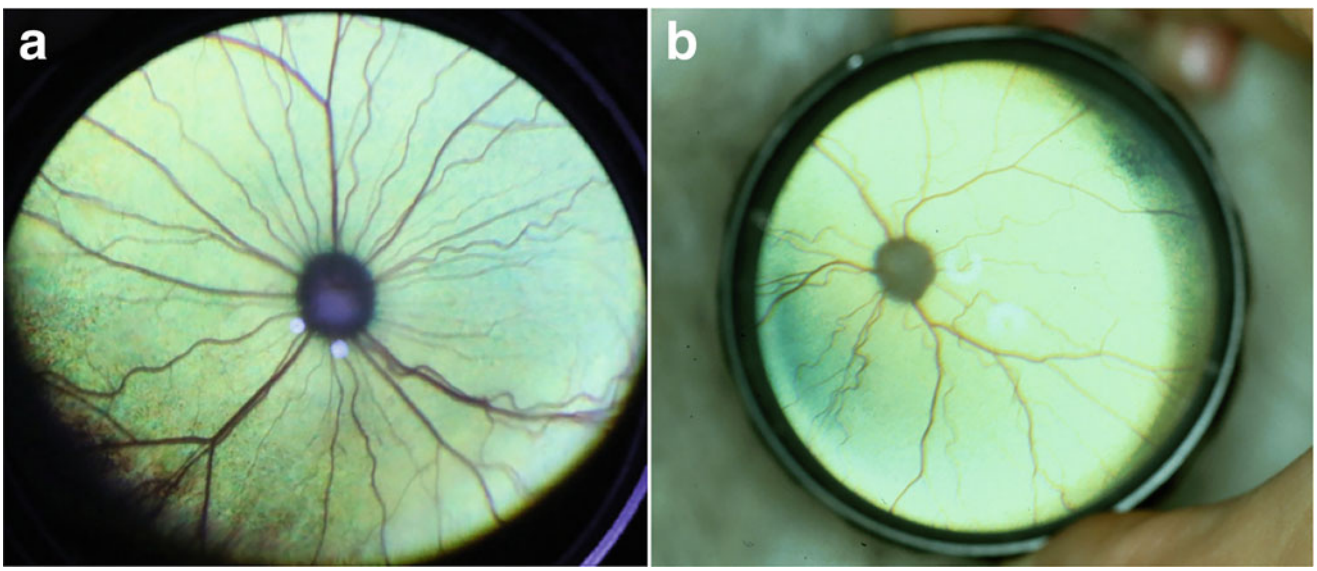

Fig. 37.43 (**a**) Normal retinal appearance in an adult Asiatic black bear (*Ursus thibetanus*). Photograph taken using a digital SLR camera (Canon 7D) and 40 diopter indirect lens. (**b**) Normal funduscopic appereance of an adult male Polar Bear (*Ursus maritimus*). Photograph taken using a 20 diopter indirect lens. Photo credits: (**a**) Claudia Hartley, (**b**) Rui Oliveira

malformation) could not be excluded. Advanced diagnostic imaging was sought but was ultimately not possible for this bear before his death.

There are only a few published reports describing ocular fundus abnormalities in bears. One instance is a wild American black bear cub (*Ursus americanus*) that was found blind (Dombrowski et al. 2016). This case report describes optic nerve degeneration, retinal dysplasia, and blindness in an American black bear cub (*Ursus americanus*). Clinical examination of this case confirmed an inability to navigate a photopic maze, bilateral tapetal hyperreflectivity, fundi devoid of retinal vessels, and small pale optic nerve papillae. The bear's aggressive temperament precluded a complete neuro-ophthalmic assessment without sedation. Observation of the bear within a cage determined that direct and consensual pupillary light reflexes (PLRs) were present, menace responses were absent, and the bear walked directly into the cage walls. Single-flash electroretinography revealed A and B-wave amplitudes of approximately 40 μV and 140 μV, respectively, in both eyes. Histologic abnormalities found in this case included bilateral optic papillary mineralization and bilateral segmental optic nerve degeneration, with occasional intralesional lymphocytes confirmed with immunohistochemistry for CD3+. There was also bilateral multifocal retinal dysplasia, gliosis, lymphocytic retinitis, a complete lack of retinal blood vessels, an intravitreal vascular membrane, and a mild lymphocytic–plasmacytic uveitis with small pre-iridal cellular membranes. The presence of a positive ERG in a blind bear with numerous retinal ganglion cells and degenerative changes in the optic nerve are most consistent with vision loss due to optic nerve injury, which given the young age of the bear, likely occurred during ocular development. The presence of ocular inflammation suggests this injury resulted from an inflammatory/infectious process. The etiology could not be determined (Dombrowski et al. 2016).

A peculiar syndrome of retinal changes has emerged within the older population of rescued Asiatic black bears in China and Vietnam. These changes include retinal and vitreal hemorrhages (Fig. 37.44a, b), and vascular caliber changes (Fig. 37.44c, d), or perivascular infiltrates (generally grey in appearance, Fig. 37.44c, d). In a study of 135 bears in China and Vietnam, retinal vascular changes, including perivascular infiltrates ($n = 23$), hemorrhages ($n = 35$) or vascular beading or aneurysm formation ($n = 33$) was identified in 54 bears and was the commonest ocular abnormality identified. Most of these bears had combinations of the three vascular abnormalities. Investigation for infectious causes including *Toxoplasma*, *Neospora*, *Ehrlichia*, *Borrelia*, *Babesia*, *Bartonella*, Aspergillosis, Candidiasis, Blastomycosis, Histoplasmosis, Cryptococcosis and Cocciodiomycosis was not rewarding. Treatment trials against infectious disease (doxycycline, clindamycin, itraconazole, ketoconazole and terbinafine) were also not encouraging (most lesions remained static, some deteriorated).

Treatment for presumed systemic hypertension in a few cases gave gratifying improvements and was widened to include all such cases. During the same period, a number of bears succumbed to ruptured/dissecting aortic aneurysms (Bando et al. 2018) and cardiovascular investigation by specialist cardiology and diagnostic imaging colleagues identified left ventricular hypertrophy and aortic aneurysms in a larger number of individuals. Systemic hypertension was regarded as a likely contributing factor in the development of aortic aneurysms in these bears (Bando et al. 2018).

Lesions of retinal hemorrhage with a central grey or white "tuft" were seen in many cases and strongly resembled "Roth's spots" reported in humans (Fig. 37.44a). These occur through retinal vessel rupture with whole blood extravasation and fibrin plug development at the site of vessel rupture. Retinal endothelial dysfunction appears to be the cornerstone of white-centered retinal hemorrhage. Historically, these spots were linked to bacterial endocarditis in humans, and this was a consideration for these bears given their frequent concurrent dental disease (from bar chewing causing tooth fractures and root abscessation) and cholangiohepatitis (due to the bile harvesting methods with cholecystostomies). However, in humans, Roth's spots have also been linked to leukemia, anemia, anoxia, carbon monoxide poisoning, prolonged intubation during anesthesia, pre-eclampsia, hypertension, diabetic retinopathy, HIV retinopathy, complicated labor and traumatic delivery in mothers and neonates, shaken baby syndrome, intracranial hemorrhage from arteriovenous malformations or aneurysm, and acute reduction of intraocular pressure following trabeculectomy surgery (Ruddy et al. 2019). Most of these differentials could be excluded in the bear population, either as not applicable (e.g., shaken baby or traumatic birthing) or with hematological examinations (e.g., anemia, diabetes).

Additionally, grey-white retinal exudates, often multifocal, were encountered in many of these Asiatic black bears (Fig. 37.44b, d). These strongly resemble "cotton wool spots" reported in humans. In humans, these are considered a sign of "serious vascular damage" (Schmidt 2008). They are seen at the borders of retinal ischemic zones and have been described in hypertensive, diabetic, and acquired immunodeficiency (AIDS) human patients. They are also reported associated with central retinal artery occlusion, retinal vein occlusion, carotid artery obstruction, high altitude retinopathy, radiation retinopathy, systemic lupus erythematosus, polyarteritis nodosa, giant cell arteritis, amongst other collagen vascular and immunological diseases. They have also been described in conjunction with infectious diseases (such as Leptospirosis, Rickettsial disease and Onchocerciasis), neoplastic disease (e.g., metastatic carcinoma and leukemia), as well as

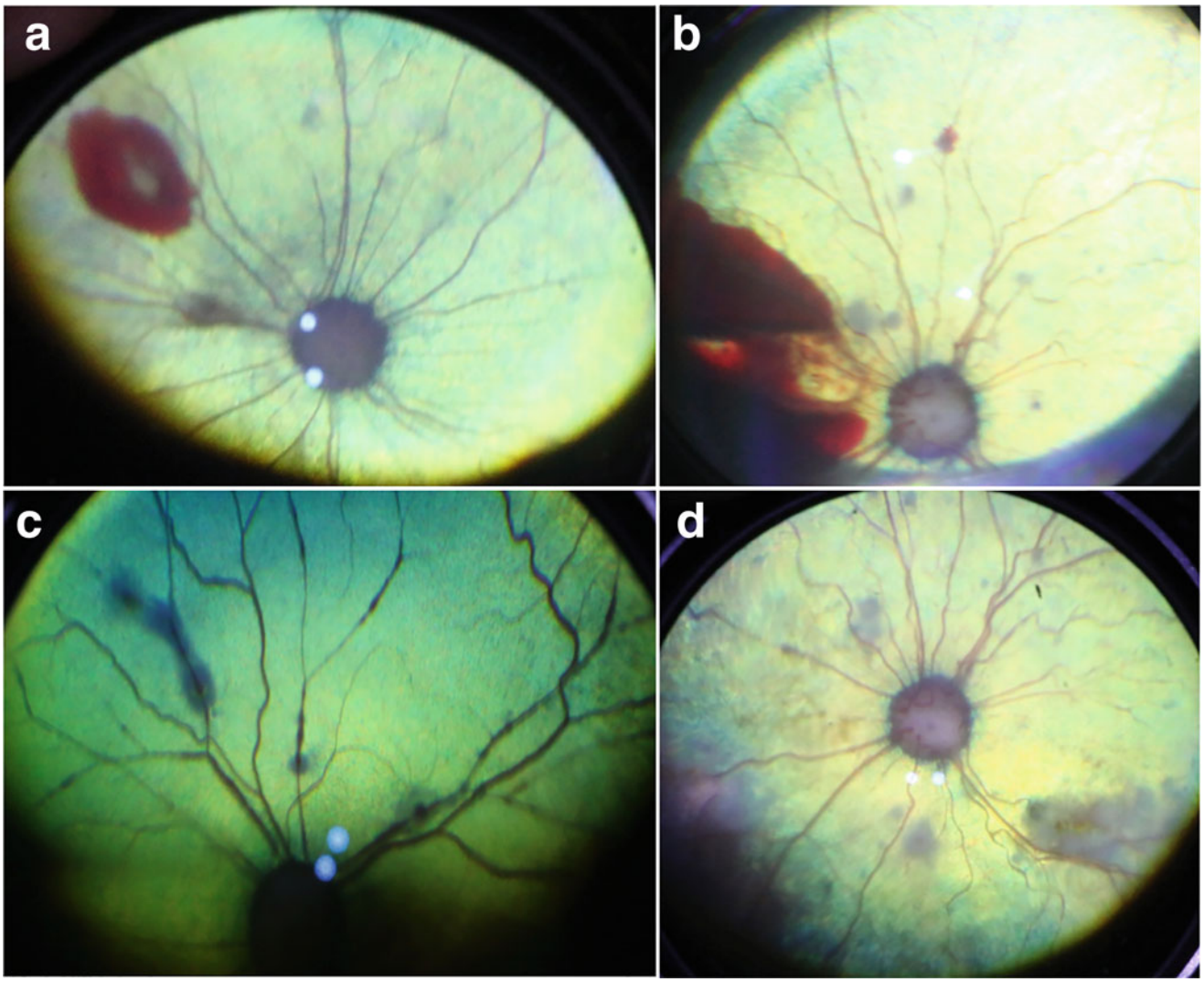

Fig. 37.44 A peculiar syndrome of retinal changes has emerged in Asiatic black bears (*Ursus thibetanus*). (**a**) Large retinal hemorrhage with central white "tuft" pushing into vitreous (resembling "Roth's spots" in humans). (**b**) Large vitreal hemorrhage between 7 and 10 o'clock with multifocal grey exudates in the dorsal tapetal fundus. Single small spot of intraretinal hemorrhage at 12 o'clock overlying a retinal arteriole. Note also the beading of many of the retinal arterioles. (**c**) Perivascular exudates and vascular beading. (**d**) Multifocal grey-white retinal exudates (similar to cotton wool spots), some appearing to be subretinal (e.g., peripapillary at 11 o'clock) while others more superficial in the retina or into vitreous (e.g., at 4 o'clock). Note also the beading of retinal arterioles. Photo credits: Claudia Hartley

septicemia, dysproteinemias, severe anemia and acute blood loss (Schmidt 2008).

No ocular signs of confirmed systemic hypertension are described in the Giant panda bear except for one case, a 29-year-old male that developed moderate, compensated renal insufficiency that progressed over 6 months to renal failure associated with degenerative cystic renal disease. This giant panda had a long history of infrequent epistaxis episodes that became more severe as hyposthenuria, moderate azotemia and moderate non-regenerative anemia (hematocrit, 25%) developed. After 6 months of therapy, with intermittent fluid therapy and human recombinant erythropoietin use, the animal was euthanized due to worsening epistaxis, at which time retinal hemorrhages associated with chronic kidney disease and secondary renal hypertension where observed (Wildt et al. 2006).

On post-mortem, histopathology findings in a geriatric Giant panda bear (male 28 years old), some of the retinal arterioles were found to be sclerotic, which was considered most likely secondary to hypertension (McLean et al. 2003). A macroaneurysm and thrombosis in the left retina were probably also associated with hypertension (Wildt et al. 2006). The findings of metastatic calcification, hypertension (retinal arteriolar sclerosis and aneurysm), and infection (corneal ulcers and cyclitis) are all sequelae of renal failure and contributed to the panda's debilitated condition (McLean et al. 2003).

One 16-year-old male and a 24-year-old female Giant panda bear were trained to allow measurement of arterial blood pressure by non-invasive oscillometry. Average values for the female were 241/135 mmHg, and mean arterial pressure was 176 mmHg. Based on comparison with the male panda housed at the same facility, with normal values of domestic species and anecdotal data from another geriatric panda, a tentative diagnosis of systemic hypertension was made in the female giant panda (Mauroo et al. 2003). No fundus abnormalities compatible with systemic hypertension were observed in this female Giant panda bear. Hypertensive retinopathy in the Giant panda bear does not appear to be a common condition in the author's experience, but further investigation (including systemic blood pressure measurements and detailed fundus examinations) are necessary for all geriatric Giant panda bear populations, especially considering this is a very common problem in other bear species.

Retinal detachment has been frequently diagnosed by the authors in Asiatic black bears, a Sun bear and a Sloth bear, seemingly associated with lens luxation or cataract. Retinal detachment was not always directly observable but diagnosed using ocular ultrasound. In a study of 135 bears (Asiatic black bears, Sun bears, and Brown bears), 21 bears had a retinal detachment. In a study of 43 Sloth bears in two rescue sanctuaries in India, the retinal detachment was identified in 15 bears (20 eyes). In the authors' experience, retinal detachment is a common condition observed in bears, accompanying mature or hypermature cataracts, especially if left untreated for lens-induced uveitis.

A 16 year-old-male Giant panda bear from Chengdu, China, was diagnosed with a left hypermature cataract, an aphakic crescent with posteriorly subluxated lens, and vitreous herniation in the anterior chamber. Ocular ultrasound revealed a complete retinal detachment in the left eye, and a hypermature cataract and subluxated lens were confirmed. Regrettably, because of the existing retinal detachment, phacoemulsification surgery to remove the existing cataract was not appropriate (Fig. 37.45a). In this Giant panda bear, the right eye was already aphakic with a complete retinal detachment at the time of his examination. This animal had been previously submitted to right-sided phacoemulsification, (by an unknown Chinese medical ophthalmologist surgeon) a few years before (unfortunately unsuccessful as vision was never recovered after surgery was performed) (see Diseases of the Lens).

Intracapsular lens extraction was also associated with a high risk of retinal detachment in Asiatic black bears. An initial extracapsular approach using phacoemulsification followed by slow, gentle traction to remove the lens capsule was associated with a much higher success rate (lower rate of retinal detachment). This was only feasible in subluxated lenses (as opposed to completely luxated, either anteriorly or posteriorly). The authors speculate that in this species, more adherent vitreal base and tension on this at luxation or surgery may result in retinal detachment. Partial retinal detachment due to a peripheral giant retinal tear (>2 clock hours) was successfully halted from propagation using 810 nm diode laser retinopexy in one adult male Asiatic black bear (Fig. 37.45b).

Retinal degeneration was also commonly diagnosed. In the study of 135 bears (Asiatic black bears, Sun bears, Brown bears) mentioned earlier, 21 had a diagnosis of retinal degeneration (Fig. 37.46). In 10 cases, this was diagnosed on direct visualization of a degenerate retina, while in 11 the diagnosis was made based on electroretinography findings (Hartley et al. 2013a). Previous histopathology reports from enucleated globes demonstrating these changes were suggestive of retinal pigment epithelial (RPE) lipofuscinosis (Dubielzig RR, 2020, Comparative Ocular Pathology Laboratory of Wisconsin, personal communication). It could be hypothesized that Vitamin E deficiency as a result of chronically inappropriate diets on the bile farms prior to rescue or increased Vitamin E loss through bile harvesting (including the enterohepatic circulation of fat-soluble vitamins) could have led to the deficiency. In a study of 43 Sloth bears in two rescue sanctuaries in India, retinal degeneration was present in 18 bears (23 eyes) (Hartley et al. 2014).

Ocular histopathology performed on a case of a 23-year-old female Polar bear (*Ursus maritimus*) revealed retinal degeneration, retinal atrophy, multifocal detachment and peripheral retinal tear associated with hypermature cataract, lens-induced uveitis and vitreous degeneration (Dubielzig RR, 2020, Comparative Ocular Pathology Laboratory of Wisconsin, personal communication). Chorioretinal scars with tapetal hyperreflectivity or focal pigment deposition (possibly retinal pigment epithelium hypertrophy) have been seen in some bears (Asiatic black bears, Sun bears, Brown bears, and Sloth bears) examined by the authors, although identifying etiology in these chronic cases was not usually fruitful.

Previously published ocular neoplasia in the retina of the Giant panda bear include one report of a retinal astrocytic hamartoma of unknown cause in both eyes of a 28-year-old male giant panda (Hsing-Hsing, Smithsonian's National Zoological Park), euthanized because of advanced renal failure, with several degenerative conditions including degenerative joint disease, chronic epistaxis, decreased mobility, progressive keratitis, and bilateral corneal ulcers with reduced vision. Both retinas had small nodules of proliferated astrocytes, indicative of hamartomas and similar to the congenital lesions found in humans, which arise from abnormal tissue development and maturation (McLean et al. 2003). Although the evidence is conclusive that these two tumors were astrocytic in origin, the question of whether they were congenital or acquired tumors was not as well answered.

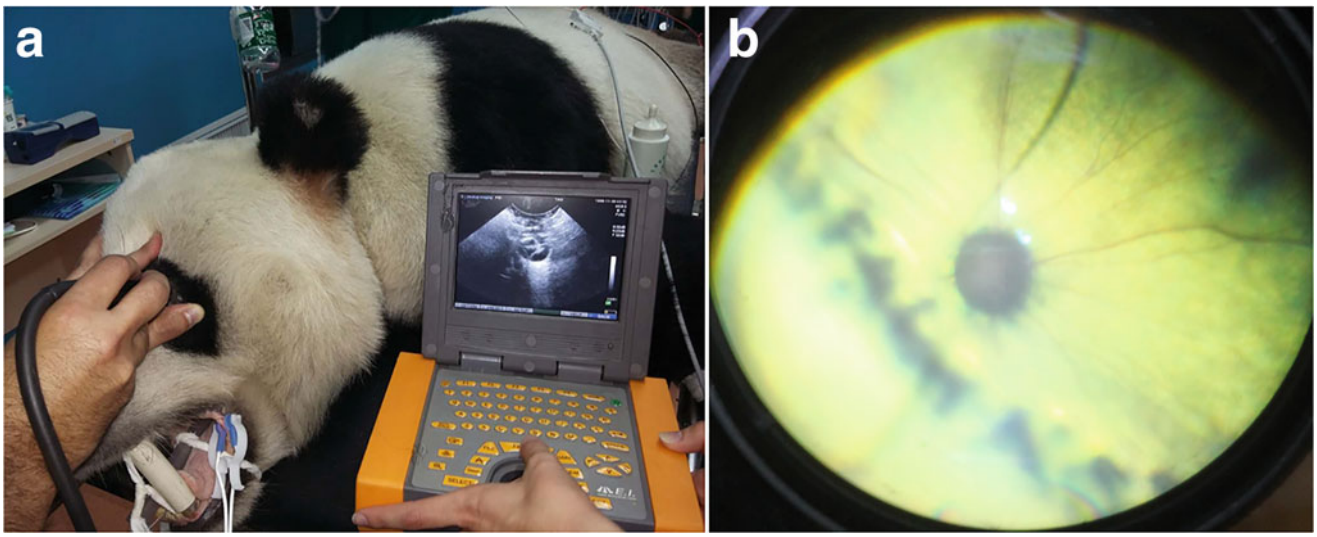

Fig. 37.45 (a) B-mode ocular ultrasonography being performed in a 16-year-old Giant panda bear (*Ailuropoda melanoleuca*) in Chengdu. It was confirmed by an eye ultrasound there was a left hypermature cataract with posterior lens subluxation, vitreous herniation and complete retinal detachment, so phacoemulsification surgery was not considered. (**b**) Two-line diode laser retinopexy scars along the margin of a partial retinal detachment associated with a giant retinal tear in an adult male Asiatic black bear (*Ursus thibetanus*). Photo credits: (**a**) Rui Oliveira, (**b**) Claudia Hartley

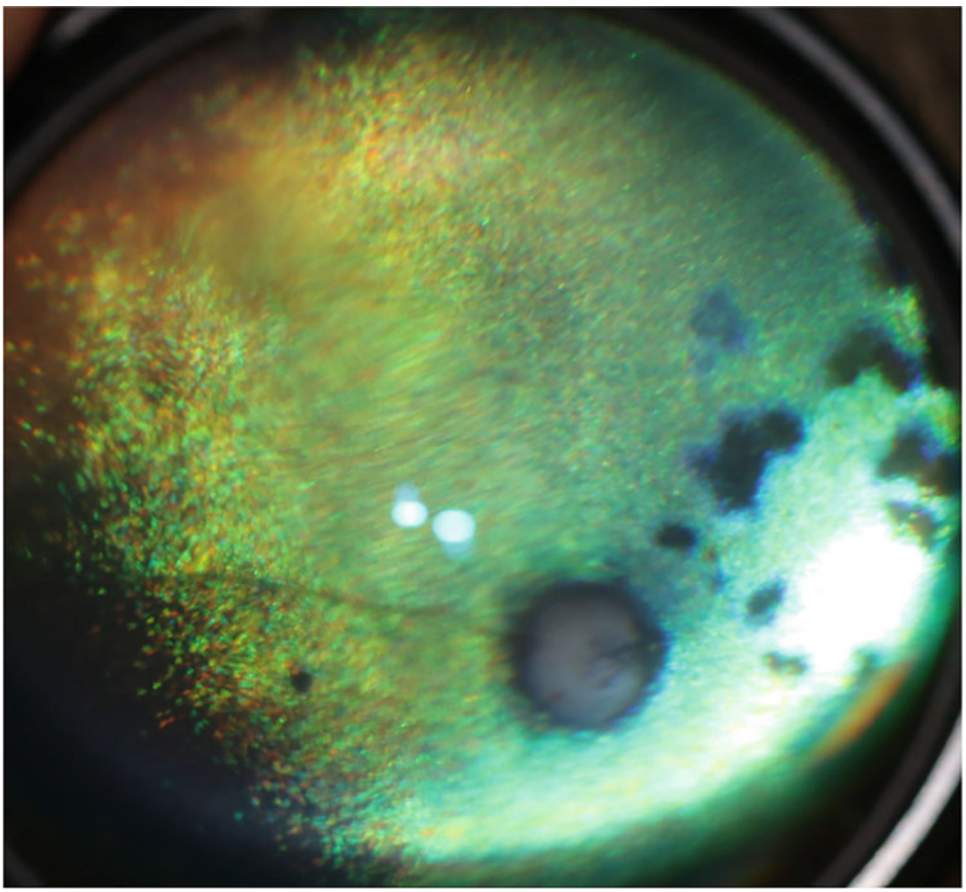

Fig. 37.46 Advanced retinal degeneration and optic nerve atrophy in an adult female Asiatic black bear (*Ursus thibetanus*). Photo credit: Claudia Hartley

Acknowledgements

- Veterinary Team of the Chengdu Research Base of Giant Panda Breeding in China, especially Dr. Wang Cheng Dong and Dr. Lou Li.
- Veterinary Department of the Ocean Park Hong Kong, especially Dr. Paolo Martelli, Dr. Lee Foo Khong and nurse Wendy Chan.
- Veterinary Team of the China Conservation and Research Center for Giant Panda (CCRCGP), Wolong Nature Reserve, Sichuan, China.
- Veterinary Team of the Singapore Zoo, Wildlife Reserves Singapore (WRS), especially Dr. Serena Oh, for welcoming us to their facilities in Singapore.
- Dr. Eva Lam (Macau Giant Panda Information Centre, IAM - Governo da Região Administrativa Especial de Macau).
- Dr. Cedric Tutt, for his help and great companionship during our trips to Chengdu, China.

References

Advani NK (2017) WWF wildlife and climate change series: giant panda. World Wildlife Fund, Washington, DC

Allbaugh RA, Davidson HJ (2009) Surgical correction of periocular fat pads and entropion in a potbellied pig (Sus scrofa). Vet Ophthalmol 12(2):115–118

Amstrup SC (2003) Polar bear, Ursus maritimus. In: Feldhamer GA, Thomson BC, Chapman JA (eds) Wild mammals of North America: biology, management, and conservation. John Hopkins University Press, Baltimore, pp 587–610

Anderson RC (2000) Nematode parasites of vertebrates: their development and transmission, 2nd edn. CABI Publishing, Guilford, pp 404–407

Andley UP, Sawardekar MA, Burris JL (1997) Action spectrum for photocross-linking of human lens proteins. Photochem Photobiol 65(3):556–559

Andrew SE (2003) Corneal fungal disease in small animals. Clin Tech Small Anim Pract 18:186–192

Arbuckle JB (1977) Thelazia worms in the eyes of British cattle. Vet Rec 100:477

Arbuckle JB, Khalil LF (1978) A survey of thelazia worms in the eyelids of British cattle. Vet Rec 102:207–210

Ashton NH (1976) Chi-Chi the giant panda: scientific study: the eye. Trans Zool Soc Lond 33:127–131

Atwood TC, Young JK, Beckmann JO, Breck SW, Fike J, Rhodes OE, Bristow KD (2011) Modeling connectivity of black bears in a desert sky island archipelago. Biol Conserv 144:2851–2862

Atwood T, Peacock E, Burek-Huntingdon K, Shearn-Boschler V, Bodenstein B, Beckmen K, Durner G (2015) Prevalence and spatio-temporal variation of an Alopecia Syndrome in polar bears (Ursus maritimus) of the Southern Beaufort Sea. J Wildl Dis 51(1): 48–59

Bacon ES, Berghard GM (1974) Learning and colour discrimination in the American black bear bears: their biology and management. In: Third international conference on bear research and management, Binghamton, New York, USA, and Moscow, U.S.S.R., June 1974. IUCN Publications New Series 40, pp 411–430

Bando MKH, Nelson LO, Webster N, Ramsay NJD, Bacon HJ, Sellon R (2018) Aortic aneurysm, dissection, and rupture in six bile-farmed bears. J Zoo Wildl Med 49(3):738–747

Banks MS, Sprague WW, Jürgen S, Parnell JAQ, Love GD (2015) Why do animal eyes have pupils of different shapes? Sci Adv 1(7): e1500391–e1500391

Belikov SE, Boltunov AN, Ovsianikov NG, Belchanskiy GI, Kochnev AA (2005) Polar bear management and research in Russia 2001–2004. In: Proceedings of the 14th working meeting of the IUCN/SSC Polar Bear Specialist Group, Seattle, Washington, USA, 20–24 June 2005. IUCN, Gland, Switzerland/ Cambridge, UK

Bentley E, Abrams GA, Covitz D, Cook CS, Fischer CA, Hacker D, Stuhr CM, Reid TW, Murphy CJ (2001) Morphology and immunohistochemistry of spontaneous chronic corneal epithelial defects (SCCED) in dogs. Invest Ophthalmol Vis Sci 42(10): 2262–2269

Bernays ME, Flemming D, Peiffer RL Jr (1999) Primary corneal papilloma and squamous cell carcinoma associated with pigmentary keratitis in four dogs. J Am Vet Med Assoc 214(2):215–217, 204

Bhaibulaya M, Prasertsilpa S, Vajrasthira S (1970) Thelazia callipaeda Railliet and Henry, 1910, in man and dog in Thailand. Am J Trop Med Hyg 19:476–479

Bhuyan KC, Bhuyan DK (1984) Molecular mechanism of cataractogenesis: III. Toxic metabolites of oxygen as initiators of lipid peroxidation and cataract. Curr Eye Res 3(1):67–82

Bianciardi P, Otranto D (2005) Treatment of dog thelaziasis caused by Thelazia callipaeda (Spirurida, Thelaziidae) using a topical formulation of imidacloprid 10% and moxidectin 2.5%. Vet Parasitol 129(1–2):89–93

Binder DR, Herring IP, Gerhard T (2007) Outcomes of nonsurgocal management and efficacy of demecarium bromide treatment for primary lens instability in dogs: 34 cases (1990–2004). J Am Vet Med Assoc 231(1):89–93

Blake CN, Collins D (2002) Captive ursids: results and selected findings of a multi-institutional study. In: Proceedings American Association of Zoo Veterinarians Annual Conference, Milwaukee, Wisconsin, pp 121–126

Blix AS, Lentfer JW (1979) Modes of thermal protection in polar bear cubs – at birth and on emergence from the den. Am J Phys Regul Integr Comp Phys 236(1):67–74

Boedeker NC, Walsh T, Murray S, Bromberg N (2010) Medical and surgical management of severe inflammation of the nictitating membrane in a giant panda (Ailuropoda melanoleuca). Vet Ophthalmol 13(Suppl):109–115

Bornstein S, Mörner T, Samuel WM (2001) Sarcoptes scabiei and sarcoptic mange. In: Samuel WM, Pybus MJ, Kocan AA (eds) Parasitic diseases of wild mammals. Iowa State University Press, Ames, pp 107–109

Bowman DD (2010) Parasitologia Veterinária de Georgis, 9th edn. Elsevier, Rio de Janeiro, 448 pp

Bridge AS, Vaughan MR (2011) Reproductive ecology of American black bears in the Alleghany Mountains of Virginia, USA. J Wildl Manag 75(5):1137–1144

Brooks DE, Greiner EC, Walsh MT (1983) Conjunctivitis caused by Thelazia sp. in a Senegal parrot. J Am Vet Med Assoc 183:1305–1306

Busse C, Sansom J, Dubielzig RR, Hayes A (2008) Corneal squamous cell carcinoma in a Border Collie. Vet Ophthalmol 11(1):55–58

Calero-Bernal R, Otranto D, Pérez-Martín JE, Serrano FJ, Reina D (2013) First report of Thelazia callipaeda in wildlife from Spain. J Wildl Dis 49:458–460. https://doi.org/10.7589/2012-10-268

Caron Y, Premont J, Losson B, Grauwels MJ (2013) Thelazia callipaeda ocular infection in two dogs in Belgium. J Small Anim Pract 54:205–208. https://doi.org/10.1111/jsap.12003

Cavelier J, Lizcano D, Yerena E, Downer C (2011) Ch17: The Mountain Tapir (Tapirus pinchaque) and Andean Bear (Tremarctos ornatus): two sharismatic, large mammals in South American tropical montane cloud forests. In: Bruijnzeel LA, Scatena FN, Hamilton LS (eds) Tropical montane cloud forests: science for conservation and management. Cambridge University Press

Chandler HL, Kusewitt DF, Colitz CM (2008) Modulation of matrix metalloproteinases by ultraviolet radiation in the canine cornea. Vet Ophthalmol 11(3):135–144

Clode A, Davis J, Davidson G, Salmon J, Lafevers H, Gilger B (2011) Aqueous humor and plasma concentrations of a compounded 0.2% solution of terbinafine following topical ocular administration to normal equine eyes. Vet Ophthalmol 14:41–47

Cogan DG, Kuwabara T (1959) Arcus senilis, its pathology and histochemistry. Arch Ophthalmol 61:553–560

Colitz CM, Saville WJ, Renner MS, McBain JF, Reidarson TH, Schmitt TL, Nolan EC, Dugan SJ, Knightly F, Rodriguez MM, Mejia-Fava JC, Osborn SD, Clough PL, Collins SP, Osborn BA, Terrell K (2010) Risk factors associated with cataracts and lens luxations in captive pinnipeds in the United States and the Bahamas. J Am Vet Med Assoc 237(4):429–436

Colwell DD, Dantas-Torres F, Otranto D (2011) Vector-borne parasitic zoonoses: emerging scenarios and new perspectives. Vet Parasitol 182:14–21

Cooke NT (1981) Significance of arcus senilis in Caucasians. J R Soc Med 74:201–204

Davidson MG, Nelms SR (1999) The canine lens. In: Gelatt KN (ed) Veterinary ophthalmology. Lea & Febiger, Malvern, pp 429–460

Davis DD (1955) Masticatory apparatus in the spectacled bear (Tremarctos ornatus). Fieldiana Zool 37:25–46

Davis DD (1964) The giant panda. A morphological study of evolutionary mechanisms. Fieldiana zoology memoirs, vol 3. Chicago Natural History Museum, Paris, pp 41–124

De Groot SG, Gebhard JW (1952) Pupil size as determined by adapting luminance. J Opt Soc Am 42:492–495

Demaster DP, Stirling I (1981) Ursus maritimus (polar bear). American Society of Mammalogists, Mammalian Species, No 145, pp 1–7, 8 May 1981

Derocher AE, Andriashek D, Arnould JPY (1993) Aspects of milk composition and lactation in Polar bears. Can J Zool 71:561–567

Dharaiya N, Bargali HS, Sharp T (2020) Melursus ursinus (amended version of 2016 assessment). The IUCN Red List of Threatened Species 2020. https://doi.org/10.2305/IUCN.UK.2020-1.RLTS.T13143A166519315.en

Diakou A et al (2015) Thelazia callipaeda (Spirurida: Thelaziidae): first report in Greece and a case of canine infection. Parasitol Res 114(7): 2771–2775

Dombrowski E, McGregor GF, Bauer BS, Parker D, Grahn BH (2016) Blindness in a wild American black bear cub (Ursus americanus). Vet Ophthalmol 19(4):340–346

Dorchies P, Chaudieu G, Simeon LA et al (2007) First reports of autochthonous eyeworm by Thelazia callipaeda (Spirurida, Thelaziidae) in dogs and cats from France. Vet Parasitol 149:294–297

Dreyfus J, Schobert CS, Dubielzig RR (2011) Superficial corneal squamous cell carcinoma occurring in dogs with chronic keratitis. Vet Ophthalmol 14(3):161–168. https://doi.org/10.1111/j.1463-5224.2010.00858.x. PMID: 21521439

Dubielzig RR (2002) Tumors of the eye (Chapter 15). In: Meuten DJ (ed) Tumors in domestic animals, 4th edn. Iowa State, Ames, pp 739–754

Dugan SJ, Roberts SM, Curtis CR, Severin GA (1991) Prognostic factors and survival of horses with ocular/adnexal squamous cell carcinoma: 147 cases (1978–1988). J Am Vet Med Assoc 198(2): 298–303. PMID: 2004996

Dybas CL (2012) Polar bears are in trouble – and ice melt's not the half of it: 'Ice bears' are the most polluted mammals on earth. Bioscience 62(12):1014–1018

Ellis S, Pan W, Xie Z, Wildt D (2006) The giant panda as a social, biological and conservation phenomenon. In: Wildt D, Zhang A, Zhang H, Janssen D, Ellis S (eds) Giant pandas: biology, veterinary medicine and management. Cambridge University Press, Cambridge, pp 1–16. https://doi.org/10.1017/CBO9780511542244.002

Fandos-Esteruelas N, Malmsten J, Brojer C, Grandi G, Lindstrom A, Brown P, Swenson JE, Evans AL, Arnemo JM (2016) Chewing lice Trichodectes pinguis pinguis in Scandinavian brown bears (Ursus arctos). Int J Parasitol Parasit Wildl 5:134–138

Fernandez A, Sorokin A, Thompson PD (2007) Corneal arcus as coronary artery disease risk factor. Atherosclerosis 193:235–240

Ferroglio E, Rossi L, Tomio E, Schenker R, Bianciardi P (2008) Therapeutic and prophylactic efficacy of milbemycin oxime (interceptor) against Thelazia callipaeda in naturally exposed dogs. Vet Parasitol 154:351–353

Forrester DJ, Spalding MG, Wooding JB (1993) Demodicosis in black bears (Ursus americanus) from Florida. J Wildl Dis 29(1):136–138

Foster GW, Cames TA, Forrester DJ (1998) Geographical distribution of Demodex ursi in black bears in Florida. J Wildl Dis 34:161–164

Garner MH, Spector A (1980) Selective oxidation of cysteine and methionine in normal and senile cataractous lenses. Proc Natl Acad Sci U S A 77(3):1274–1277

Garshelis DL (2002) Misconceptions, ironies, and uncertainties regarding trends in bear populations. Ursus 13:321–334

Garshelis D, Steinmetz R (2016) Ursus thibetanus (errata version published in 2017). The IUCN Red List of Threatened Species 2016. https://doi.org/10.2305/IUCN.UK.2016-3.RLTS.T22824A45034242.en

Garshelis DL, Joshi AR, Smith JLD (1999a) Estimating density and relative abundance of sloth bears. Ursus 11:87–98

Garshelis DL, Joshi AR, Smith JVD, Rice CG (1999b) Chapter 12: Sloth bear conservation action plan, pp 225–240

Garshelis DL, Scheick BK, Doan-Crider DL, Beecham JJ, Obbard ME (2016) Ursus americanus (errata version published in 2017). The IUCN Red List of Threatened Species 2016. https://doi.org/10.2305/IUCN.UK.2017-3.RLTS.T41688A121229971.en

Ginn PE, Mansell JEKL, Rakich PM (2007) Skin and appendages. In: Maxie MG (ed) Jubb, Kennedy and Palmer's pathology of domestic animals, vol I, 5th edn. Elsevier, London, p 538

Gionfriddo JR (2013) Ophthalmology of new world camelids. In: Gellat KN (ed) Veterinary ophthalmology, 5th edn. Lippincott Williams and Wilkins, Philadelphia, pp 1675–1692

Gong J, Harris RB (2006) Chapter 13: The status of bears in China. In: Understanding Asian bears to secure their future. Japan Bear Network, Ibaraki, pp 50–56

Gopinathan U, Garg P, Fernandes M, Sharma S, Athmanathan S, Rao GN (2002) The epidemiological features and laboratory results of fungal keratitis: a 10-year review at a referral eye care center in South India. Cornea 21(6):555–559

Gould SJ (1982) The Panda's thumb: more reflections in natural history. W. W. Norton & Co., New York

Grahn BH, Peiffer RL (2007) Fundamentals of veterinary ophthalmic pathology. In: Gelatt KN (ed) Veterinary ophthalmology, 4th edn. Blackwell, Oxford, pp 355–437

Hammond P, Mouat GS (1985) The relationship between feline pupil size and luminance. Exp Brain Res 59(3):485–490

Hartley C, Donaldson D, Bacon HJ, Officer K, Bando M, O'Dwyer J, Reynard J, Leadbeater W, Field N, Nelson C, Hall K, Elliot V, Gorman E, Walters H, Ryan F, Perrin K, Kingston R, Gasson J, Weegenaar WF, Meilvang AS, Quine H, Bendixsen T, Robinson J (2013a) Ocular findings in Asiatic black bears (Ursus thibetanus), Malayan sun bears (Helarctos malayanus), Eurasian brown bears

(ursus arctos arctos), and a Tibetan brown bear (Ursus arctos pruinosus) rescued from the bile farming industry & wildlife trade in Asia. 44th annual meeting of the American College of Veterinary Ophthalmologists, Puerto Rico. Vet Ophthalmol 6(6):E26–E50
Hartley C, Donaldson D, Bacon H, Officer K, Bando M, O'Dwyer J, Reynard J, Leadbeater W, Field N, Nelson C, Hall K, Elliot V, Gorman E, Walters H, Ryan F, Perrin K, Kingston R, Gasson J, Weegenaar A, Wicker F, Meilvang AS, Quine H, Bendixsen T, Robinson J (2013b) Ocular surgeries in Asiatic black bears (Ursus Thibetanus) and a Malayan sun bear (Helarctos Malayanus) rescued from the Bile Farming Industry & Wildlife Trade in Asia. 44th annual meeting of the American College of Veterinary Ophthalmologists, Puerto Rico. Vet Ophthalmol 6(6):E26–E50
Hartley C, Busse C, Matas Reira M, Bacon HJ, Arun AS, Khadekar Y, Selvaraj I, Satyanarayan K, Seshamani G, Knight A (2014) Ocular findings in sloth bears (Melursus ursinus) rescued from the dancing bear trade in India. Abstracts: 45th annual meeting of the American College of Veterinary Ophthalmologists, Ft Worth, Texas. Vet Ophthalmol 17(6):E31–E49
Hashimoto Y, Kaji M, Sawada H, Takatsuki S (2003) Five-year study on the autumn food habits of the Asiatic black bear in relation to nut production. Ecol Res 18:485–492
Hechtel J (2020) The International Association for Bear Research and Management (IBA). https://www.bearbiology.org/iba-publications. Downloaded 06 Feb 2021
Hermosilla C, Herrmann B, Bauer C (2004) First case of Thelazia callipaeda infection in a dog in Germany. Vet Rec 154(18):568–569
Hertz JC, Ferree Clemons BC, Lord CC, Allan SA, Kaufman PE (2017) Distribution and host associations of ixodid ticks collected from wildlife in Florida, USA. Exp Appl Acarol 73:223–236
Hilderbrand GV, Schwartz CC, Robbins CT, Hanley TA (2000) Effect of hibernation and reproductive status on body mass and condition of coastal brown bears. J Wildl Manag 64(1):178–183
Hodžić A, Latrofa MS, Annoscia G, Alić A, Beck R, Lia RP, Dantas-Torres F, Otranto D (2014) The spread of zoonotic Thelazia callipaeda in the Balkan area. Parasit Vectors 30:352
Hull V et al (2011) Evaluating the efficacy of zoning designations for protected area management. Biol Conserv 144:3028
Hung G (2018) Ocean Park celebrates the birthdays of its most beloved ambassadors. https://www.oceanpark.com.hk/en/press-release/ocean-park-celebrates-birthdays-of-its-most-beloved-ambassadors
Huygens OC, Miyashita T, Dahle B, Carr M, Izumiyama S, Sugawara T, Hayashi H (2003) Diet and feeding habits of Asiatic black bears in the Northern Japanese Alps. Ursus 14(2):236–245
Hwang M-H, Garshelis DL (2007) Activity patterns of Asiatic black bears (Ursus thibetanus) in the Central Mountains of Taiwan. J Zool 271:203–209
Hwang M-H, Garshelis DL, Wang Y (2002) Diets of Asiatic black bears in Taiwan, with methodological and geographical comparisons. Ursus 13:111–125
Islam MA, Uddin M, Aziz MA, Muzaffar SB, Chakma S, Chowdhury SU, Chowdhury GW, Rashid MA, Mohsanin S, Jahan I, Saif S, Hossain MB, Chakma D, Kamruzzaman M, Akter R (2013) Status of bears in Bangladesh: going, going, gone? Ursus 24:83–90
IUCN (2020) The IUCN Red List of Threatened Species. Version 2020-3. https://www.iucnredlist.org. Downloaded 06 Feb 2021
Jedlicka J, Hojovcova M (1972) Sarcoptesräude bei Bären im Zoologischen Garten Brno. Erkrankungen der Zootiere 14:257–260
Jin X, Ma Q, Meng Y, Ren J, Pan G, Zhao P, Zhang Q (2010) Treatment of cataract in giant panda. Prog Vet Med:S858–S859
Johnson-Ulrich Z, Vonk J, Humbyrd M (2016) Picture object recognition in an American black bear (*Ursus americanus*). Anim Cogn 19:1237–1242
Joshi A, Smith J, Garshelis D (1999) Sociobiology of the myrmecophagous sloth bear in Nepal. Can J Zool 77(11):1690–1704
Kawashima M, Kawakita T, Shigeyasu C, Shimazaki J (2009) Lamellar corneal injury by bamboo splinters: a case report. J Med Case Rep 3(1):1–3
Kelling AS, Snyder RJ, Marr MJ et al (2006) Color vision in the giant panda (Ailuropoda melanoleuca). Learn Behav 34:154–161
Kennedy MJ (1992) The efficacy of ivermectin against the eyeworm, Thelazia skrjabini, in experimentally infected cattle. Vet Parasitol 45:127–131
Kennedy MJ (1993) Prevalence of eyeworms (Nematoda: Thelazioidea) in beef cattle grazing different range pasture zones in Alberta, Canada. J Parasitol 79:866–869
Kennedy MJ (1994) The effect of treating beef cattle on pasture with ivermectin on the prevalence and intensity of Thelazia spp. (Nematoda: Thelazioidea) in the vector, Musca autumnalis (Diptera: Muscidae). J Parasitol 80:321–326
Kennedy MJ, MacKinnon JD (1994) Site segregation of Thelazia skrjabini and Thelazia gulosa (Nematoda: Thelazioidea) in the eyes of cattle. J Parasitol 80:501–504
Kennedy MJ, Moraiko D (1987) The eyeworm, Thelazia skrjabini in cattle in Canada. Can Vet J 28:254–265
Kennedy MJ, Phillips FE (1993) Efficacy of doramectin against eyeworms (Thelazia spp.) in naturally and experimentally infected cattle. Vet Parasitol 49:61–66
Kennedy MJ, Moraiko DT, Goonewardene L (1990) A study on the prevalence and intensity of occurrence of Thelazia skrjabini (Nematoda: Thelazioidea) in cattle in Central Alberta, Canada. J Parasitol 76:196–200
Kennedy JJ, Moraiko DT, Treichel B (1993) First report of immature Thelazia skrjabini (Nematoda: Thelazioidea) from the eye of a white-tailed deer, Odocoileus virginianus. J Wildl Dis 29:159–160
Kennedy M, Kim KH, Harten B, Brown J, Planck S, Meshul C, Edelhauser H, Rosenbaum JT, Armstrong CA, Ansel JC (1997) Ultraviolet irradiation induces the production of multiple cytokines by human corneal cells. Invest Ophthalmol Vis Sci 38(12):2483–2491
Kenny DE, Bickel C (2005) Growth and development of Polar bear (Ursus maritimus) cubs at Denver Zoological Gardens. Int Zoo Yearb 39:205–214
Kern TJ, Colitz CMH (2013) Exotic animal ophthalmology (Chapter 33). In: Gelatt KN et al (eds) Veterinary ophthalmology. Wiley-Blackwell, Hoboken, pp 1750–1819
Khattab MQ, Tribursch H (2015) Fibre-optical light scattering technology in polar bear hair: a re-evaluation and new results. J Adv Biotechnol Bioeng 3(2):1–14
Li D, Hu D, Tang C, Sutherland-Smith M, Rideout B (2001) Diagnosis and treatment of acute renal failure in an 8 month old giant panda (Ailuropoda melanoleuca). In Proceedings of the American Association of Zoo Veterinarians, pp 239–41
Kleiman NJ, Spector A (1993) DNA single strand breaks in human lens epithelial cells from patients with cataract. Curr Eye Res 12(5):423–431
Klinka DR, Reimchen TE (2002) Nocturnal and diurnal foraging behaviours of brown bears (Ursus arctos) on a salmon stream in coastal British Colombia. Can J Zool 80:1317–1322
Koike S (2010) Long-term trends in food habits of Asiatic black bears in the Misaka Mountains on the Pacific coast of Central Japan. Mamm Biol 75:17–28
Kozlov DP (1962) The life cycle of nematode, Thelazia callipaeda parasitic in the eye of the man and carnivores. Dokl Akad Nauk SSSR 142:732–733
Ladouceur EEB, Garner MM, Davis B, Tseng F (2014) A retrospective study of end-stage renal disease in captive polar bears (Ursus Maritimus). J Zoo Wildl Med 45(1):69–77
Laidler K, Laidler L (1992) Pandas: giants of the bamboo forest. BBC Books, London

Lam L, Garner MM, Miller CL et al (2013) A novel gammaherpesvirus found in oral squamous cell carcinomas in sun bears (*Helarctos malayanus*). J Vet Diagn Investig 25(1):99–106
Lan L, Wang F-Y, Zeng G (2013) Staining with methylthioninium chloride for the diagnosis of fungal keratitis. Exp Ther Med 6:229–1232
Laurie A, Seidensticker J (1977) Behavioural ecology of the Sloth bear (Melursus ursinus). J Zool 182:187–204
Leclerc-Cassan, M., 1985. The giant panda Li-Li: history and pathological findings. In Proceedings of the international symposium on the giant panda (Vol. 10, pp. 169–174). Chengdu, China: Sichuan Science & Technology Press.
Lechat C, Siméon N, Pennant O, Desquilbet L, Chahory S, Le Sueur C, Guillot J (2015) Comparative evaluation of the prophylactic activity of a slow-releaseinsecticide collar and a moxidectin spot-on formulation against infection innaturally exposed dogs in France. Parasit Vectors 8:93
Ledbetter EC, Gilger BC (2013) Diseases and surgery of the canine cornea and sclera. In: Gelatt KN, Gilger BC, Kern TJ (eds) Veterinary ophthalmology, vol 2, 5th edn. Wiley-Blackwell, Oxford, pp 976–1049
Li R et al (2015) Climate change threatens giant panda protection in the 21st century. Biol Conserv 182:93–101
Lia RP, Traversa D, Agostini A et al (2004) Field efficacy of moxidectin 1 per cent against Thelazia callipaeda in naturally infected dogs. Vet Rec 154(5):143–145
Linton LL, Collins BK (1993) Entropion repair in a Vietnamese pot-bellied pig. J Small Exotic Anim Med 2:124–127
Lin HC, Chu PH, Kuo YH, Shen SC (2005) Clinical experience in managing Fusarium solani keratitis. Int J Clin Pract 59(5):549–554
Liu J (2015) Promises and perils for the panda. Science 348(6235):642
Loeffler K et al (2006) Diseases and pathology of giant pandas. In: Giant pandas: biology, veterinary medicine and management, pp 377–409
Lopez M, Talavera C, Rest JR, Taylor D (1996) Haemangiosarcoma of the conjunctiva of a giant panda. Vet Rec 138(1):24. PMID: 8825333
Lumpkin S, Seidensticker J (2002) Smithsonian book of giant pandas. Smithsonian Press, Washington, DC
Macdonald D (2001) The new encyclopedia of mammals. Oxford University Press, Oxford
Maehara S, Matsumoto N, Takiyama N et al (2020) Surgical removal of cataract in an Asiatic black bear (Ursus thibetanus) by phacoemulsification and aspiration. J Vet Med Sci 82(6):740–744
Magnis J, Naucke TJ, Mathis A et al (2010) Local transmission of the eye worm Thelazia callipaeda in southern Germany. Parasitol Res 106(3):715–717
Mainka S, Christmas R (1987) Ocular nodular fasciitis in an Asiatic black bear (Selenarctos thibetanus). J Zoo Anim Med 18(4):156–158
Manville AM (1978) Ecto- and endoparasite of the Black Bear in Northern Wisconsin. J Wildl Dis 14:97–101
Mauroo NF, Routh A, Hu W (2003) Diagnosis and management of systemic hypertension in a giant panda (Ailuropoda melanoleuca). Joint Conference-American Association of Zoo Veterinarians, pp 289–290
Mauroo NF, Rourke NL, Chan WK (2006) Cutaneous hemangioma in a giant panda (Ailuropoda melanoleuca). J Zoo Wildl Med 37(1): 59–60
McDonald JE, Fuller TK (2001) Prediction of litter size in American black bears. Ursus 12:93–102
McLean IW, Bodman MG, Montali RJ (2003) Retinal astrocytic hamartomas: unexpected findings in a giant panda. Arch Ophthalmol 121(12):1786–1790
McLellan BN, Proctor MF, Huber D, Michel S (2017). Ursus arctos (amended version of 2017 assessment). The IUCN Red List of Threatened Species 2017. https://doi.org/10.2305/IUCN.UK.2017-3.RLTS.T41688A121229971.en
Miller PE, Campbell BG (1992) Subconjunctival cyst associated with Thelazia gulosa in a calf. J Am Vet Med Assoc 201:1058–1060
Miller S, Whelan N, Hope K, Nogueira Marmolejo MG, Knightly F, Sutherland-Smith M, Rivera S (2020) Survey of clinical ophthalmic disease in the giant panda (Ailuropoda Melanoleuca) among North American zoological institutions. J Zoo Wildl Med 50(4):837–844
Miró G, Montoya A, Hernández L et al (2011) Thelazia callipaeda: infection in dogs: a new parasite for Spain. Parasit Vectors 4:148
Montiani-Ferreira F, Kiupel M, Muzolon P, Truppel J (2008) Corneal squamous cell carcinoma in a dog: a case report. Vet Ophthalmol 11(4):269–272. https://doi.org/10.1111/j.1463-5224.2008.00622.x. PMID: 18638354
Moolenbeek WJ, Surgeoner GA (1980) Southern Ontario survey of eyeworms, Thelazia gulosa and Thelazia lacrymalis in cattle and larvae of Thelazia spp. in the face fly, Musca autumnalis. Can Vet J 21:50–52
Motta B, Schnyder M, Basano FS, Nägeli F, Nägeli C, Schiessl B, Mallia E, Lia RP, Dantas-Torres F, Otranto D (2012) Therapeutic efficacy of milbemycin oxime/praziquantel oral formulation (Milbemax®) against Thelazia callipaeda in naturally infested dogs and cats. Parasit Vectors 5:85
Motta B, Nägeli F, Nägeli C et al (2014) Epidemiology of the eye worm Thelazia callipaeda in cats from southern Switzerland. Vet Parasitol 203(3–4):287–293
Murata K, Asakawa M (1999) First report of Thelazia sp. from a captive oriental white stork (Ciconia boyciana) in Japan. J Vet Med Sci 61: 93–95
Nevile JC, Hurn SD, Turner AG (2016) Keratomycosis in five dogs. Vet Ophthalmol 19(5):432–438
Ngopraset D, Reed DH, Steinmetz R et al (2012) Density estimation of Asian bears using photographic capture-recapture sampling based on chest marks. Ursus 23(2):117–133
Niedringhaus KD, Brown JD, Ternent M et al (2020) Serology as a tool to investigate Sarcoptoic Mange in American black bears (Ursus americanus). J Wildl Dis 56(2):350–358
Nowak RM (1999) Carnivora: Ursidae: Tremarctos ornatus. Walker's mammals of the world, vol 1, 6th edn. Johns Hopkins University Press, Baltimore, pp 680–681
Obbard ME, Thiemann GW, Peacock E, DeBruyn TD (2010) Polar bears. Proceedings of the 15th working meeting of the IUCN/SSC Polar Bear Specialist Group, Copenhagen, Denmark, 29 June–3 July 2009. IUCN, Gland/Cambridge
Otranto D, Traversa D (2005) Thelazia eyeworm: an original endo- and ecto-parasitic nematode. Trends Parasitol 21(1):1–4
Otranto D, Ferroglio E, Lia RP et al (2003) Current status and epidemiological observation of Thelazia callipaeda (Spirurida, Thelaziidae) in dogs, cats and foxes in Italy: a "coincidence" or aparasitic disease of the Old Continent? Vet Parasitol 116:315–325
Otranto D, Cantacessi C, Testini G et al (2006) Phortica variegate as an intermediate host of Thelazia callipaeda under natural conditions: evidence for pathogen transmission by a male arthropod vector. Int J Parasitol 36(10–11):1167–1173
Overend DJ (1983) Thelazia gulosa in cattle. Aust Vet J 60:126–127
Pagano AM, Dumer GM, Amstrup SC, Simac KS, York GS (2012) Long-distance swimming by Polar bears (Ursus maritimus) of the southern Beaufort Sea during years of extensive open water. Can J Zool 90:663–676
Panthi S, Aryal A, Coogan SCP (2019) Diet and macronutrient niche of Asiatic black bear (Ursus thibetanus) in two regions of Nepal during summer and autumn. Ecol Evol 9:3717–3727
Pasitschniak M (1993) Mammalian species. Ursus arctos. Am Soc Mammal 439:1–10
Peichl L, Dubielzig RR, Kübber-Heiss A, Schubert C, Ahnelt PK (2005) Retinal cone types in Brown Bears and the Polar Bear indicate dichromatic color vision. ARVO Annual Meeting Abstract, Volume 46, Issue 13

Peltier SK, Brown JD, Ternent MA, Fenton H, Niedringhaus KD, Yabsley MJ (2018) Assays for detection and identification of the causative agent of mange in free-ranging black bears (Ursus Americanus). J Wildl Dis 54(3):471–479
Pimenta P, Cardoso L, Pereira MJ, Maltez L, Coutinho T, Alves MS, Otranto D (2013) Canine ocular thelaziosis caused by Thelazia callipaeda in Portugal. Vet Ophthalmol 16:312–315
Plummer CE, Regnier A, Gelatt KN (2013) The canine glaucoma. In: Gelatt KN, Gilger BC, Kern TJ (eds) Veterinary ophthalmology, 5th edn. Wiley Blackwell, Ames, pp 1050–1145
Prange H, Kokles R, Zimmermann G (1968) Clinical observations and studies regarding the etiology of enzootically occurring bovine keratoconjunctivitis, with particular consideration of Thelazia. Monatshefte fur Veterinarmedizin 23:692–698
Qiu WY, Yao YF (2013) Mycotic keratitis caused by concurrent infections of Exserohilum mcginnisii and Candida parapsilosis. BMC Ophthalmol 13(1):37
Ramesh T, Kalle R, Sankar K, Qureshi Q (2013) Activity pattern of sloth bear Melursus ursinus (Mammalia: Ursidae) in Mudumalai Tiger Reserve, Western Ghats, India. J Threat Taxa 5(5):3989–3992
Rampazzo A, Kuhnert P, Howard J, Bornand V (2009) Hormographiella aspergillata keratomycosis in a dog. Vet Ophthalmol 12(1):43–47
Reid D, Jiang M, Teng Q, Qin Z, Hu J (1991) Ecology of the Asiatic black bear in Sichuan, China. Mammalia 55(2):231–237
Ríos-Uzeda B, Gomez H, Wallace RB (2006) First density estimation of spectacled bear (Tremarctos ornatos) using camera trapping methodologies. Ursus 18:124–128
Rios-Uzeda B, Gomez H, Wallace RB (2007) A preliminary density estimate for Andean bear using camera-trapping methods. Ursus 18(1):124–128
Robbins CT, Ben-David M, Fortin JK, Nelson OL (2012) Maternal condition determines birth date and growth of newborn bear cubs. J Mammal 93(2):540–546
Rogers LL, Rogers SM (1976) Parasites of bears: a review. Bears: their biology and management: third international conference on bear research and management, Binghamton, New York, USA, and Moscow, U.S.S.R., June 1974. IUCN Publications New Series 40, pp 411–430
Rossi L, Bertaglia PP (1989) Presence of Thelazia callipaeda Railliet & Henry, 1910, in Piedmont, Italy. Parassitologia 31:167–172
Rossi L, Peruccio C (1989) Thelaziosi oculare nel Cane, aspetti clinici e terapeutici. Veterinaria 2:47–50
Rowe ML, Whiteley PL, Carver S (2019) The treatment of sarcoptic mange in wildlife: a systematic review. Parasit Vectors 12(1):99
Ruddy SM, Bergstrom R, Tivakaran VS (2019) Roth spots. In: StatPearls. StatPearls Publishing, Treasure Island. http://www.ncbi.nlm.nih.gov/books/NBK482446/
Saleh HM, Abdel Fattah NS, Hamza HT (2013) Evaluation of serum 25-hydroxyvitamin D levels in vitiligo patients with and without autoimmune diseases. Photodermatol Photoimmunol Photomed 29(1):34–40. https://doi.org/10.1111/phpp.12016. PMID: 23281695
Samuelson DA, Andresen TL, Gwin RM (1984) Conjunctival fungal flora in horses, cattle, dogs, and cats. J Am Vet Med Assoc 184(10):1240–1242
Sargo R, Loureiro F, Catarino AL, Valente J, Silva F, Cardoso L, Otranto D, Maia C (2014) First report of Thelazia callipaeda in red foxes (Vulpes vulpes) from Portugal. J Zoo Wildl Med 45:458–460
Schaller G (1993) The last panda. University of Chicago Press, Chicago
Schaller G, Hu J, Pan W et al (1985) The giant pandas of Wolong. University of Chicago Press, Chicago
Schmidt D (2008) The mystery of cotton-wool spots. A review of recent and historical descriptions. Eur J Med Res 13:231–266
Schwartz CC, Keating KA, Reynolds HV et al (2003) Reproductive maturation and senescence in the female brown bear. Ursus 14(2):109–119
Scotson L, Fredriksson G, Augeri D, Cheah C, Ngoprasert D, Wai-Ming W (2017) Helarctos malayanus (errata version published in 2018). The IUCN Red List of Threatened Species 2017. https://doi.org/10.2305/IUCN.UK.2017-3.RLTS.T9760A45033547.en
Servheen C, Herrero S, Peyton B (1999) Bears: status survey and conservation action plan. IUCN/SSC Bear and Polar Bear Specialist Groups, IUCN, Gland, Switzerland and Cambridge, UK
SFAC (2015) State Forestry Administration of China, 2015. Release of the fourth national survey report on giant panda in China. State Forestry Administration, Beijing
Shen J, Gasser RB, Chu D, Wang ZX, Yuan X, Cantacessi C, Otranto D (2006) Human thelaziosis—a neglected parasitic disease of the eye. J Parasitol 92:872–875
Simpson M (2019) Polar bear sports hunting: Canada's flawed interpretation of the International Polar Bear Agreement. J Int Wildl Law Policy 22(2):145–158
Skinner D, Mitcham JR, Starkey LA et al (2017) Prevalence of Babesia spp, Ehrlichia spp, and tick infestations in Oklahoma black bears (Ursus americanus). J Wildl Dis 53(4):781–787
Skrjabin KI, Sobolov AA, Ivashkin VM (1971) Essentials of nematodology. Spirurata of animals and man and the diseases caused by them, part 4, Thelazioidea, vol 16. Israel program for translations, Jerusalem (ISBN978-0706511796)
Soares C, Ramalho Sousa S, Anastácio S, Goreti Matias M, Marquês I, Mascarenhas S, João Vieira M, de Carvalho LM, Otranto D (2013) Feline thelaziosis caused by Thelazia callipaeda in Portugal. Vet Parasitol 196:528–531. https://doi.org/10.1016/j.vetpar.2013.03.029
Soibelzon LH, Tarantini VB (2009) Estimación de la masa corporal de las especies de osos fósiles y actuales (Ursidae, Tremarctinae) de América del Sur. Revista del Museo Argentino de Ciencias Naturales 11(2):243–254
Soll MD, Carmichael IH, Scherer HR et al (1992) The efficacy of ivermectin against Thelazia rhodesii (Desmarest, 1828) in the eyes of cattle. Vet Parasitol 42:67–71
Spiess BM, Pot SA (2013) Diseases and surgery of the canine orbit. In: Gelatt KN (ed) Veterinary ophthalmology, 5th edn. Wiley-Blackwell Publishing, Ames, pp 793–831
Stades FC, Dorrestein GM, Boeve MH et al (1995) Eye lesions in Turkish dancing bears. Vet Q 17(Suppl 1):45–46. https://doi.org/10.1080/01652176.1995.9694591
Steinmetz R, Garshelis DL (2008) Distinguishing Asiatic black bears and sun bears by claw marks on climbed trees. J Wildl Manag 72:814–821
Steinmetz R, Garshelis DL (2010) Estimating ages of bear claw marks in southeast Asian tropical forests as an aid to population monitoring. Ursus 21:143–153
Stringer E, Han S, Larsen RS (2016) Cutaneous vitiligo associated with hypovitaminosis D in Malayan flying foxes (Pteropus vampyrus) and island flying foxes (Pteropus hypomelanus). Veterinary Record Case Reports 4:e000297
Swaisgood RR, Lindburg DG, Zhou X (1999) Giant pandas discriminate individual differences in conspecific scent. Anim Behav 57(5):1045–1053
Swaisgood RR, Wang D, Wei F (2016) Ailuropoda melanoleuca. In IUCN Red List of Threatened Species. See http://www.iucnredlist.org/details/712/0
Swenson JE, Adamic M, Huber D, Stokke S (2007) Brown bear body mass and growth in northern and southern Europe. Oecologia 153:37–47
Tabellario S, Babitz MA, Bauer EB, Brown-Palsgrove M (2020) Picture recognition of food by sloth bears (*Melursus ursinus*). Anim Cogn 23:227–231
Takle GL, Suedmeyer WK, Garner MM (2010) Diagnosis and treatment of vitiligo in a sub-adult eastern black rhinoceros (Diceros bicornis michaeli). J Zoo Wildl Med 41(3):545–549

Tasić-Otašević S, Gabrielli S, Trenkić-Božinović M et al (2016) Eyeworm infections in dogs and in a human patient in Serbia: a one health approach is needed. Comp Immunol Microbiol Infect Dis 45:20–22

Taylor HR (1995) Ocular effects of UV-B exposure. Doc Ophthalmol 88:285–293

Teel PD, Ketchum HR, Mock DE, Wright RE, Strey OF (2010) The Gulf Coast tick: a review of the life history, ecology, distribution, and emergence as an arthropod of medical and veterinary importance. J Med Entomol 47(5):707–722

Traylor-Holzer K, Ballou JD (2016) 2016 breeding and management recommendations and summary of the status of the giant panda ex situ population. Apple Valley, IUCN Conservation Breeding Specialist Group

Tsubota T, Kanagawa H (1993) Morphological characteristics of the ovary, uterus and embryo during the delayed implantation period in the Haokkaido brown bear (Ursus arctis yesoensis). J Reprod Dev 39:325–331

Tumanov IL (1998) Reproductive characteristics of captive European brown bears and growth rates of their cubs in Russia. Ursus 10:63–67

Tweedle DM, Fox MT, Gibbons LM et al (2005) Change in the prevalence of Thelazia species in bovine eyes in England. Vet Rec 157: 555–556

Uhl L (2019) Phacoemulsification in a 1.5-year old American black bear (*Ursus americanus*) with congenital/juvenile cataracts. The 50th Annual Scientific Meeting of the American College of Veterinary Ophthalmologists, Maui, Hawaii, 6–9 Novermber 2019, Veterinary Ophthalmology, pp E28–E80

Van Horn RC, Sutherland-Smith M, Sarcos AEB et al (2018) The Andean bear alopecia syndrome may be caused by social housing. Zoo Biol 38:434–441

Van Wick M, Hashem B (2019) Treatment of sarcoptic mange in an American black bear (Ursus americanus) with a single oral dose of Fluralaner. J Wildl Dis 55(1):250–253

Velez-Liendo X, García-Rangel S (2017) Tremarctos ornatus (errata version published in 2018). The IUCN Red List of Threatened Species 2017. https://doi.org/10.2305/IUCN.UK.2017-3.RLTS.T22066A45034047.en

Vieira L, Rodrigues FT, Costa A, Diz-Lopes D, Machado J, Coutinho T, Tuna J, Latrofa MS, Cardoso L, Otranto D (2012) First report of canine ocular thelaziosis by Thelazia callipaeda in Portugal. Parasit Vectors 5:124. https://doi.org/10.1186/1756-3305-5-124

Vohradsky F (1970) Clinical course of Thelazia rhodesii infection of cattle in the Accra plains of Ghana. Bull Epizoot Dis Afr 18:159–170

Volk HA, O'Reilly A, Bodley K, McCracken H (2018) Keratomycosis in captive red pandas (Ailurus fulgens): 2 cases. Open Vet J 8(2): 200–203. https://doi.org/10.4314/ovj.v8i2.14. Epub 2018 Jun 1. PMID: 29911025; PMCID: PMC5987353

Ward AA, Neaderland MH (2011) Complications from residual adnexal structures following enucleation in three dogs. J Am Vet Med Assoc 239(12):1580–1583

Ward DA, Latimer KS, Askren RM (1992) Squamous cell carcinoma of the corneoscleral limbus in a dog. J Am Vet Med Assoc 200(10): 1503–1506. PMID: 1612986

Ware JV, Rode KD, Robbins CT et al (2020) The clock keeps ticking: circadian rhythms of free-ranging Polar bears. J Biol Rhythm 35(2): 180–194

Wei F et al (2014) Giant pandas are not an evolutionary cul-de-sac: evidence from multidisciplinary research. Mol Biol Evol 32(1):4–12

Wei F, Swaisgood R, Hu Y et al (2015) Progress in the ecology and conservation of giant pandas. Conserv Biol 29(6):1497–1507

Weigl R (2005) Longevity of mammals in captivity. In: Living Collections of the World. Kleine Senckenberg-Reihe, Stuttgart. http://genomics.senescence.info/species

Wesley-Hunt GD, Flynn JJ (2005) Phylogeny of the Carnivora: basal relationships among the Carnivoramorphans, and assessment of the position of 'Miacoidea' relative to Carnivora. J Syst Palaeontol 3(1): 1–28

Whiteman JP, Harlow HJ, Durner GM, Regehr EV, Amstrup SC, Ben-David M (2018) Phenotypic plasticity and climate change: can Polar bears respond to longer Arctic summers with an adaptive fast? Oecologia 186:369–381

Wiig Ø, Amstrup S, Atwood T, Laidre K, Lunn N, Obbard M, Regehr E, Thiemann G (2015) Ursus maritimus. The IUCN Red List of Threatened Species

Wilcock BP (1993) The eye and ear. In: Jubb KVF, Kennedy PC, Palmer N (eds) Pathology of domestic animals, vol I, 4th edn. Academic Press, Inc., San Diego, pp 512–515

Wildt DE, Zhang A, Zhang H, Janssen D, Ellis S (2006) Giant pandas: biology, veterinary medicine and management. Cambridge University Press, Cambridge, 586p

Williams DL, Heath MF, Wallis C (2004) Prevalence of canine cataract: preliminary results of a cross-sectional study. Vet Ophthalmol 7(1): 29–35

Williamson DF (2002) In the black: status, management, and trade of the American black bear (Ursus americanus) in North America. TRAFFIC North America. World Wildlife Fund, Washington D.C.

Xu YH, Xie HX, Liu SL, Zhou ZY, Shi XQ (1986) A new species of the genus Demodex (Acariformes: Demodicidae) Acta Zool Sin 32: 163–167

Yabsley MJ, Nims TN, Savage MY, Durden LA (2009) Ticks and tick-borne pathogens and putative symbionts of black bears (Ursus americanus floridanus) from Georgia and Florida. J Parasitol 95(5): 1125–1128

Yang CH, Tung KC, Wang MY et al (2006) First Thelazia callipaeda infestation report in a dog in Taiwan. J Vet Med Sci 68(1):103–104

Yoganand K, Rice CG, Johnsingh AJT, Seidensticker J (2006) Is the Sloth bear in India secure? A preliminary report on distribution, threats and conservation requirements. J Bombay Nat Hist Soc 103(2–3):172–181

Yokohata Y, Fujita O, Kamiya M et al (1990) Parasites from the Asiatic black bear (*Ursus thibetanus*) on Kyushu Island, Japan. J Wildl Dis 26(1):137–138

Yucun C, Guangjian Z, Yuanyuan D (2003) Cataract operation on a giant panda. Chin J Zool 38(3):47–49

Yunker CE, Binninger CE, Keirans JE, Beecham J, Schlegel M (1980) Clinical mange of the black bear, Ursus americanus, associated with Ursicoptes americanus (Acari:Audycoptidae). J Wildl Dis 16:347–356

Zhang GQ, Swaisgood RR, Wei RP, Zhang HM, Han HY, Li DS et al (2000) A method for encouraging maternal care in the giant panda. Zoo Biol 19(1):53–63

Zhang A, Zhang H, Zhang J et al (2000) 1998–2000 CBSG Giant Panda Biomedical Survey Summary. Apple Valley, MN: IUCN/SSC Conservation Breeding Specialist Group

Ophthalmology of Pinnipedimorpha: Seals, Sea Lions, and Walruses

38

Carmen Colitz

Introduction

Pinnipeds are a clade of semi-aquatic carnivorous fin-footed marine mammals that descended from the superfamily Arctoidea within the suborder Canifornia. This is the same suborder that gave rise to bears (Ursidae) and weasels (mustilidae) (Arnason et al. 2006; Delisle and Strobeck 2005). The Mustilidae are thought to be the most closely related species to pinnipeds (Arnason and Widegren 1986). Approximately 33 million years ago, the Otariidae (eared seals) and Obinidae (walruses) split from the Phocidae (true seals). A later split occurred, separating Otariidae and Obinidae (Arnason et al. 2006). The transition of pinnipeds from land to water evolved simultaneously with their ability to see in air and underwater equally well (Hanke et al. 2009a; Schusterman 1981; Schusterman and Balliet 2006). Many anatomical and physiological adaptations occurred to allow pinnipeds these amazing visual abilities.

Ocular Anatomy

Like most mammals, pinnipeds have three eyelids: the dorsal and ventral eyelids, and the nictitating membrane, or the third eyelid (Kelleher Davis et al. 2013a). The dorsal and ventral eyelids primarily consist of an orbicularis oculi muscle that lacks a distinct tarsus. Pinnipeds lack meibomian glands and the associated lipid layer of the tear film (Kelleher Davis et al. 2013b). Tear film interferometry has shown that the lipid layer of the tear film is absent in pinnipeds, although a very thin layer could have been present yet undetectable by the assay (Kelleher Davis et al. 2013a). The lid margin has solitary sebaceous glands without associated hair follicles.

C. Colitz (✉)
All Animal Eye Care in Jupiter Pet Emergency and Specialty Center, Jupiter, FL, USA
e-mail: ccolitzacvo@gmail.com

F. Montiani-Ferreira et al. (eds.), *Wild and Exotic Animal Ophthalmology*, https://doi.org/10.1007/978-3-030-81273-7_13

The dermal layer of the eyelids consists of small sebaceous glands with associated hair follicles (Kelleher Davis et al. 2013a). There are two lacrimal glands in all pinnipeds and a third in walrus that most likely secrete the aqueous component of the tear film. These glands are comprised of tubuloacinar bundled arrangements, similar to those of terrestrial mammalian lacrimal glands. One is located dorsotemporally beneath the dorsal eyelid, and the other is associated with the nictitating membrane (Kelleher Davis et al. 2013a). Walruses, unlike phocids and otariids, have a Harderian gland located ventrally within the orbit that generates a significant volume of the tear film (author's personal observation). Its secretions were aqueous in appearance (author's personal observation). An older reference states that the Harderian gland lies rostro-ventral to the globe and produces an oily mucus; recent observations confirm that while this location is correct, the secretions are not oily in nature. Pinnipeds, as well as cetaceans, lack a nasolacrimal excretory system, which is likely an adaptation to their aquatic lifestyles.

Evaluation of the tear film of pinnipeds identified numerous proteins ranging between 30 and 120 kilodaltons in size, similar to those of human tears. However, the protein and carbohydrate concentration ratios in pinniped tears, including sea lion, harbor seal, and fur seal, were generally greater than those of humans (Kelleher Davis et al. 2013a) Based on these findings, the authors of this study hypothesized that mucins are present in the aqueous phase of marine mammal pre-ocular tear film and that the mucins are important for ocular surface protection. They hypothesized that these differences in the tear film, compared to human tears, were due to an evolutionary adaptation to the aquatic environment of marine mammals. The precorneal tear film is of vital importance for the health of the ocular surface of all species; however, much is still to be learned about the unique tear film of pinnipeds and other marine mammals.

All pinnipeds have strong extraocular muscles and significant ocular mobility. Studies of visual field and eye movement in harbor seals found that the animals were able to move their eyes 12° (+/−2°) medially and laterally, and 64° dorsally, with visual fields of 210° in the horizontal plane and 121° dorsally (Hanke et al. 2006b). Their strong extraocular muscles also allow pinnipeds to retract their globes deep into the orbit. Their eyelid muscles are equally strong, making the act of opening their eyelids by an examiner all but impossible in an awake or lightly sedated patient. Walruses can contract their extraocular muscles more than other pinnipeds, resulting in impressive anterior positioning ("bulging") of their globes (Kastelein et al. 1993). It is thought that maximal protrusion of the globes increases the monocular visual field; additionally, dorsal and frontal eye positioning enhances binocular vision (Kastelein et al. 1993). The visual acuity of walruses is less than in other pinnipeds, being more specialized for short-range and shallow underwater feeding on bottom-dwelling molluscs (Kastelein et al. 1993). Walruses possess a large amount of adipose-rich connective tissue between the recti and retractor bulbi muscles (Kastelein et al. 1993).

The ocular anatomy and physiology of marine mammal eyes, including those of pinnipeds, is similar to that of terrestrial mammals, although with some important functional differences (Figs. 38.1, 38.2) (Miller et al. 2013). Otariid and phocid globes are large, and the corneas are relatively flattened. In the California sea lion (*Zalophus californianus*), the peripheral convex aspect of the corneal surface has refraction of 21.7D (Dawson et al. 1987). The obinid eye is smaller, although walruses still possess a relatively flattened cornea (Fig. 38.2). All of the pinniped species evaluated to date have a visible flattened corneal plateau, also called the emmetropic window, located just inferonasal to the axial cornea (Fig. 38.3). This makes the eyes capable of focusing incoming light through the stenopeic (pinhole) pupil directly to the cone-rich area centralis of the retina (Miller et al. 2010; Hanke et al. 2006a). The emmetropic window reduces aerial myopia, making the optical features of the corneal surface similar in both aquatic and terrestrial environments (Hanke et al. 2006a; Mass and Supin 2007). The shape of the emmetropic window is oval in most phocids and round in otariids and obinids. The emmetropic window measures 6.5 mm in diameter in the California sea lion (Dawson et al. 1987). In all pinnipeds, the cornea is thinner axially and thicker peripherally (Miller et al. 2013; Miller et al. 2010). From external to internal, the corneal layers include epithelium, Bowman's layer, stroma, Descemet's membrane, and endothelium (Fig. 38.4) (Miller et al. 2010; Miller et al. 2013). It is unusual for Bowman's layer to be present in carnivorous species such as pinnipeds.

The pectinate ligaments in the iridocorneal drainage angle are prominent, and in phocids, they extend across the surface of the iris (Fig. 38.5). Unlike in humans and domestic mammals, topical anticholinergic agents (i.e., tropicamide and atropine) do not readily dilate pinniped pupils. Topical sympathomimetic agents (phenylephrine and epinephrine), slightly dilate pinniped pupils and take at least 20 minutes to get 4 mm dilation (personal observation, Colitz). It is unknown if the lack of response in pinniped pupils to topical mydriatics is due to the inability of these drugs to penetrate the sclera and cornea or due to the absence of adequate cholinergic and adrenergic receptors in uveal tissue(Barnes and Smith 2004). Subconjunctival atropine administration in a fur seal dilated the pupil 5–6 mm for up to 4 days (Barnes and Smith 2004). The most consistent pharmacologic pupillary dilator agent in pinnipeds is 1:1000 epinephrine injected intracamerally (personal observation, Colitz).

In the California sea lion, the iris dilator muscle is located more posteriorly than in other mammalian species, being more developed at the iris base and extending posteriorly to the pars plicata. The iris dilator muscle is absent near the pupillary margin (Fig. 38.1) (Miller et al. 2010), suggesting that in pinnipeds, this muscle functions primarily for

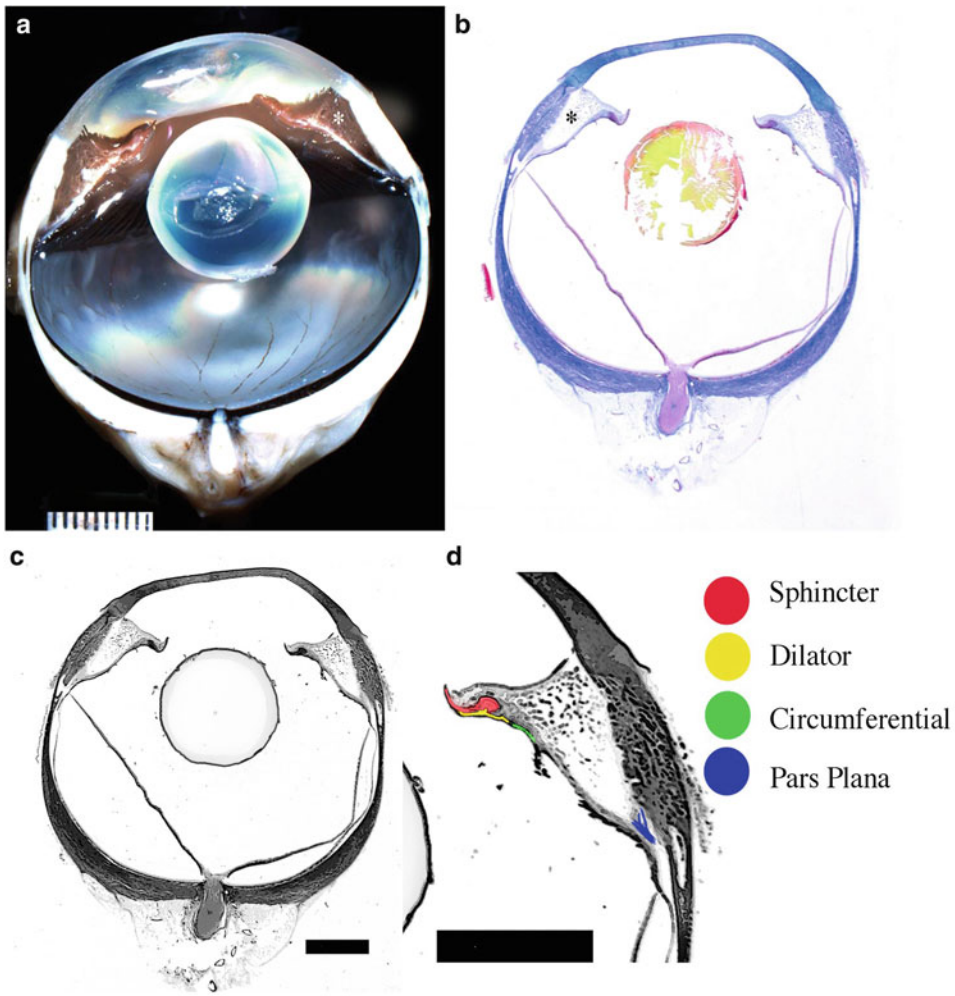

Fig. 38.1 Images of dorsoventrally sectioned globe and photomicrographs showing the locations of musculature in the iris and ciliary body of the California sea lion (*Zalophus californianus*). (**a**) Gross image. (**b**) Subgross image of the same grobe stained with Masson's trichrome. Note thin sclera at the equator and the axial thinning of the cornea. The round lens and the wide ciliary cleft (*) are also apparent. (**c**) Entire globe. (**d**) Close up of the ciliary cleft and localization of the musculature and the pars plana. (Both bars for **c** and **d** = 1 cm). Used with permission from Miller et al. 2020: Anatomy of the California sea lion globe. Veterinary Ophthalmology 13: 63–71

accommodation rather than mydriasis. In response to intracameral epinephrine administration, the pinniped lens shifts anteriorly, possibly indirectly facilitating mydriasis (personal observation, Colitz). In the California sea lion, the iris sphincter muscle extends from the pupillary margin to slightly posterior to the iris base. This muscle is thickest at both the iris base and also immediately posterior to the insertion points of the pectinate ligaments (Miller et al. 2010). The location of the iris sphincter muscle suggests dual functions both in accommodation and miosis (Fig. 38.1). A third muscle is speculated to be involved in pinniped accommodation; it is a thin smooth muscle located circumferentially within the ciliary body at the base of the ciliary processes Fig. 38.1) (Miller et al. 2010). When contracted, this muscle moves the lens by compressing the posterior chamber space surrounding the lens equator (West et al. 1991). The ciliary muscle is located in the ciliary body, similar to humans and most other mammalian eyes (Miller et al. 2010). Both the hypothesized accommodative abilities as well as the round and rigid features of pinniped lenses make translocation (i.e., anterior and posterior movement of the lens) with concomitant mydriasis as the lens glides anteriorly the likely method of accommodation (personal observation, Colitz). When not in active accommodation, the center of the lens is equidistant between the cornea and the retina; thus, the optics of pinniped vision is presumed to be centrally symmetrical (Mass and Supin 2007).

The pinniped lens is suspended by both zonules and direct attachments to the ciliary processes, an interesting combination of terrestrial and avian anatomic traits.

Harbor seals, and most likely all pinnipeds, have multifocal lenses. Multifocal lenses have been described in fishes and terrestrial vertebrates with slit pupils (Malmstrom and Kroger 2006; Kroger et al. 1999; Karpestam et al. 2007). A non-circular pupil (Fig. 38.5) appears to be an adaptation in order to create a multifocal optical system (Malmstrom and Kroger 2006). A non-circular pupil allows the eye to employ multiple refractive zones, with different refractive powers, in the imaging process (Malmstrom and Kroger 2006; Kroger et al. 1999). Pinnipeds have teardrop-shaped pupils in ambient light. As light becomes brighter, their pupils can constrict progressively to a keyhole shape and then to a pinhole. As the

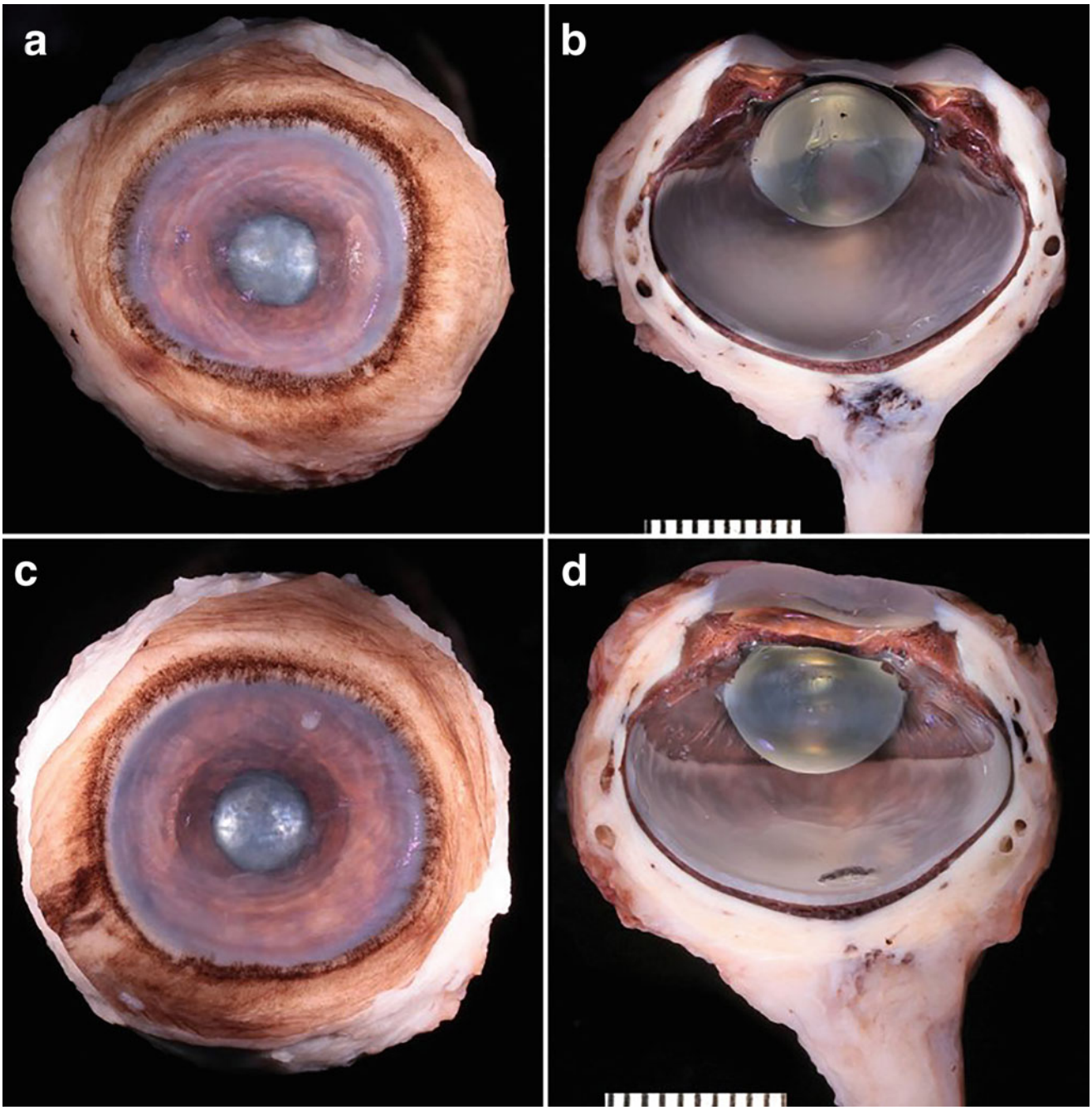

Fig. 38.2 Gross images of normal walrus (*Odobenus rosmarus*) eyes. (**a**, **b**) and (**c**, **d**) are of the same eyes, respectively. Frontal views (**a, c**) show pigmented conjunctiva with a relatively small corneal diameter. Cross-sections (**b, d**) show a flattened cornea and a semi-spherical lens. Courtesy of the Comparative Ocular Pathology Laboratory of Wisconsin

pupil becomes more miotic in bright light, the lens becomes more monofocal (Hanke et al. 2008). It was suggested that multiple focal lengths may be useful in seals with mesopic color vision and may increase the depth of focus when the pupil is dilated (Hanke et al. 2008). When dilated in darkness, the pupil of walruses is oval, and the pupils of phocids and otariids are round (Kastelein et al. 1993).

The vitreous body in the northern fur seal (*Callorhinus ursinus*) has been described as rigid rather than gelatinous. The author agrees that the vitreous of most pinniped eyes (observed intraoperatively during lens surgery) is stiff, with a firm vitreous base that does not allow absorption of surgical fluids or blood into the vitreous (personal observations, Colitz).

Fig. 38.3 Right eye of a California sea lion (*Zalophus californianus*). This eye is normal, and the flash artifact is enhancing the flattened plateau used for focusing on land and in shallow water

The tapetum lucidum is a layer of tissue lying directly posterior to the neural retina that acts as a retroreflector to efficiently capture and reflect light rays back through the retina a second time, thereby enhancing night vision in the central visual field. The tapetum lucidum is 20 to 34 cell layers thick, depending on the species (Miller et al. 2010; Nagy and Roland 1970;˙ Nagy and Roland 1970; Jamieson and Fisher 1971). Pinnipeds have a thick and extensive tapetum lucidum that covers all but the most peripheral retina (Fig. 38.6). As with other mammals with tapeta, there are no pigment granules in the tapetal zone of the retinal pigment epithelium (Jamieson and Fisher 1972). The robust thickness of the tapetum lucidum in pinnipeds has not yet been correlated to its relative ability to recapture light, although the pinniped eye likely utilizes the entire tapetum to view the underwater world, which is dimly perceived in both the superior and inferior visual fields (Hanke et al. 2009a; Walls 1942). It has been found that when Weddell seals hunt for fish, they use backlighting to stalk their prey (Davis et al. 1999).

Pinniped retinas have the same layers as terrestrial mammals, possessing both rods and cones with rods predominating (Fig. 38.7). (Griebel and Schmid 1992; Lavigne and Ronald 1975; Mass and Supin 2007) The outer nuclear layer is the thickest layer, with a depth greater than 20 pericarya (Mass and Supin 2007). When five species of seals and sea lions were evaluated using immunohistochemical analysis, it was found that cones comprise only approximately 1% of all photoreceptors (Peichl et al. 2001). Depending on the species, cone density varied between 3000/mm^2 and 10,000/mm^2 (Peichl et al. 2001), which approximates the cone density of nocturnal terrestrial mammals. In an immunohistochemical study evaluating L-cones and S-cones in marine mammals and their close terrestrial relatives, L-cones were present in all species, but functional S-cones were absent in all of the marine species, including three otariid species (*Arctocephalus pusillus* or Australian fur seal, *Callorhinus ursinus* or Northern fur seal, and *Otaria byronia* or Southern sea lion) and four phocid species (*Halichoerus grypus* or Grey seal, *Cystophora cristata* or hooded seal, *Phoca vitulina* or harbor seal, and *Phoca hispida* or ringed seal). Messenger RNA of middle-to-long-wavelength sensitive L cone opsin is present in pinnipeds, but no pinnipeds, including phocids, otariids, and walruses, have messenger RNA for S cone opsin sequences (Peichl and Moutairou 1998; Levenson et al. 2006; Newman and Robinson 2005). The absence of S-cones in pinnipeds reflects a mutational loss at a critical

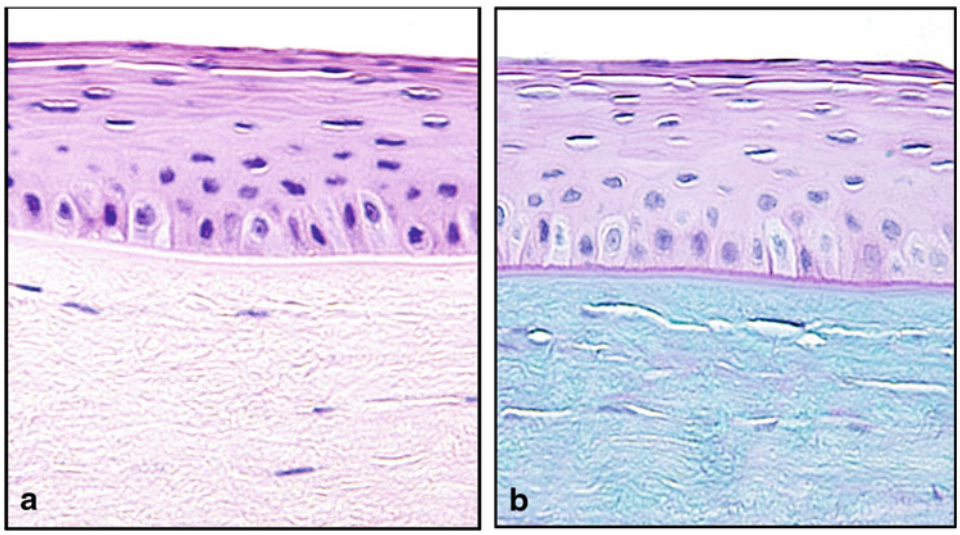

Fig. 38.4 Histological sections through the normal pinniped anterior cornea. (**a**) H & E. (**b**) Alcian blue and PAS photomicrograph showing showing the corneal epithelium and a thin Bowman's layer overlying normal stroma. Images courtesy of the Comparative Ocular Pathology Laboratory of Wisconsin

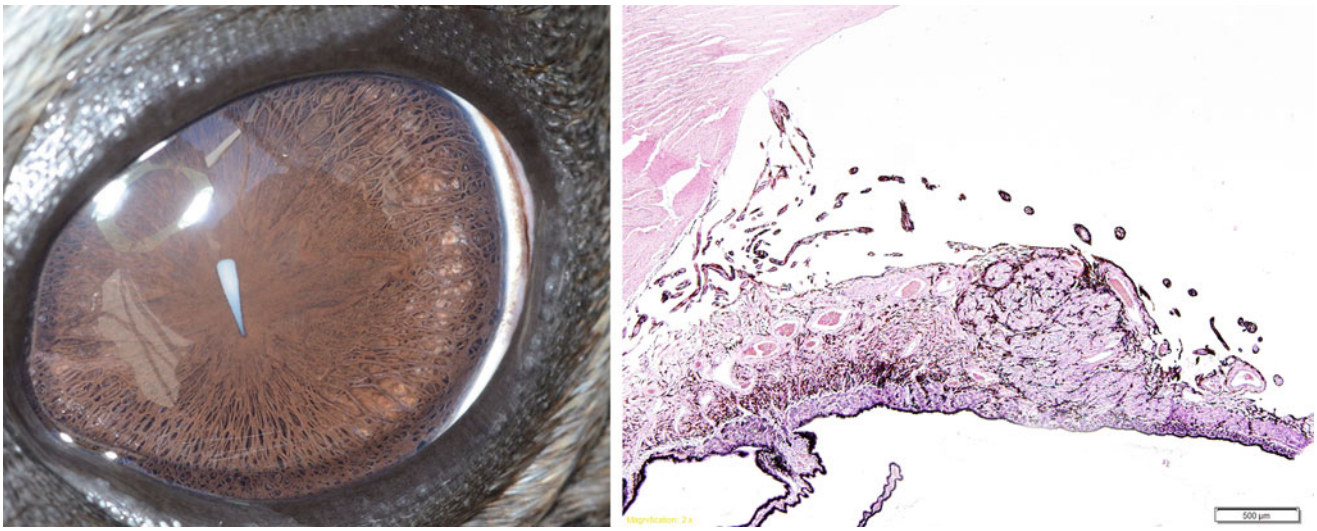

Fig. 38.5 Clinical image of the left eye of a harbor seal (*Phoca vitulina*) and a histological image of the pectinate ligaments. The relatively constricted pupil is a slim teardrop shape. The pectinate ligaments are numerous and extend onto the anterior surface of the iris to the approximate location of the iris collarette. The eye also has a cataract

point in pinniped adaptation to the aquatic environment. A deletion mutation in the structural short-wavelength S cone opsin gene was found in the harp seal (*Phoca groenlandica),* causing it to be a pseudogene (Newman and Robinson 2005). Additionally, electroretinographic studies to date in pinnipeds have not identified cone responses (Levenson et al. 2006). Rod opsins were found to be similar between pinniped and terrestrial mammals, with the exception of the elephant seal, indicating that pinnipeds continue to require good vision on land (Levenson et al. 2006). Deep-diving elephant seals have rod opsins relatively sensitive to short-wavelength light (Levenson et al. 2006). Good correlation was found between rod opsin sequences and electroretinogram measurements. In a study evaluating color vision, three California sea lions were trained to discriminate between two shades of grey and a colored stimulus. The findings suggested that sea lions are dichromats, as they were able to discriminate between green and grey and between blue and

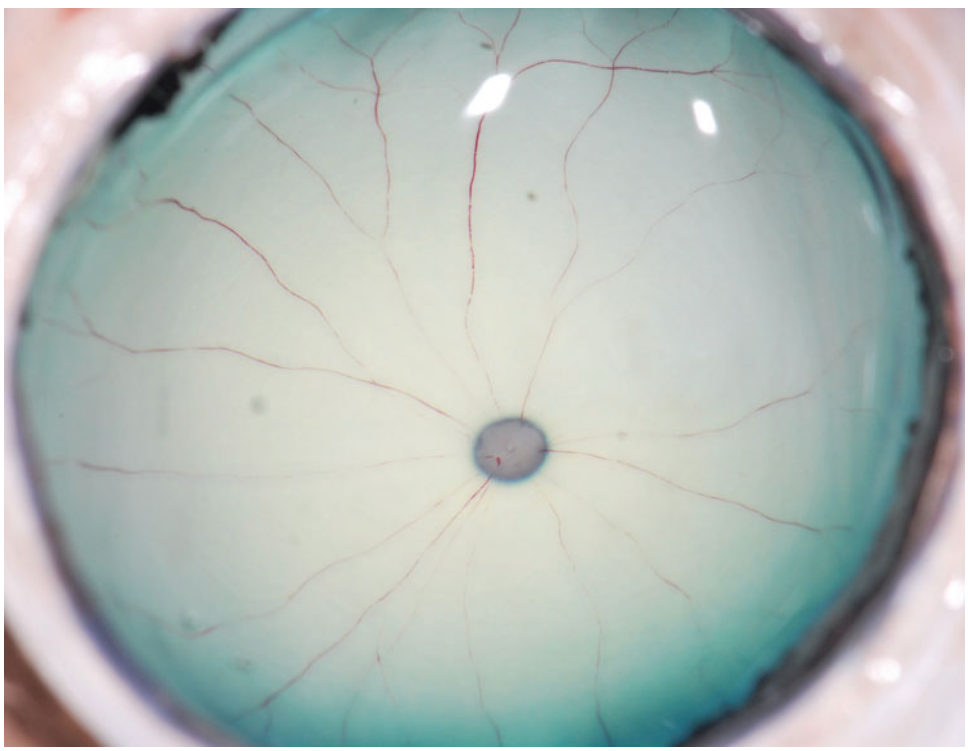

Fig. 38.6 Gross dissection of an eye from a California sea lion (*Zalophus californianus*). The cornea, iris, lens have been excised to show the holangiotic fundus. Note that the tapetal area is complete, and the optic nerve is round with radiating vasculature extending to the peripheral fundus. Image from KN Gelatt, BC Gilger and TJ Kern (Eds) Veterinary Ophthalmology. fifth Ed, Wiley Blackwell, Iowa, USA. Fig. 33.37. Page 1785 with permission

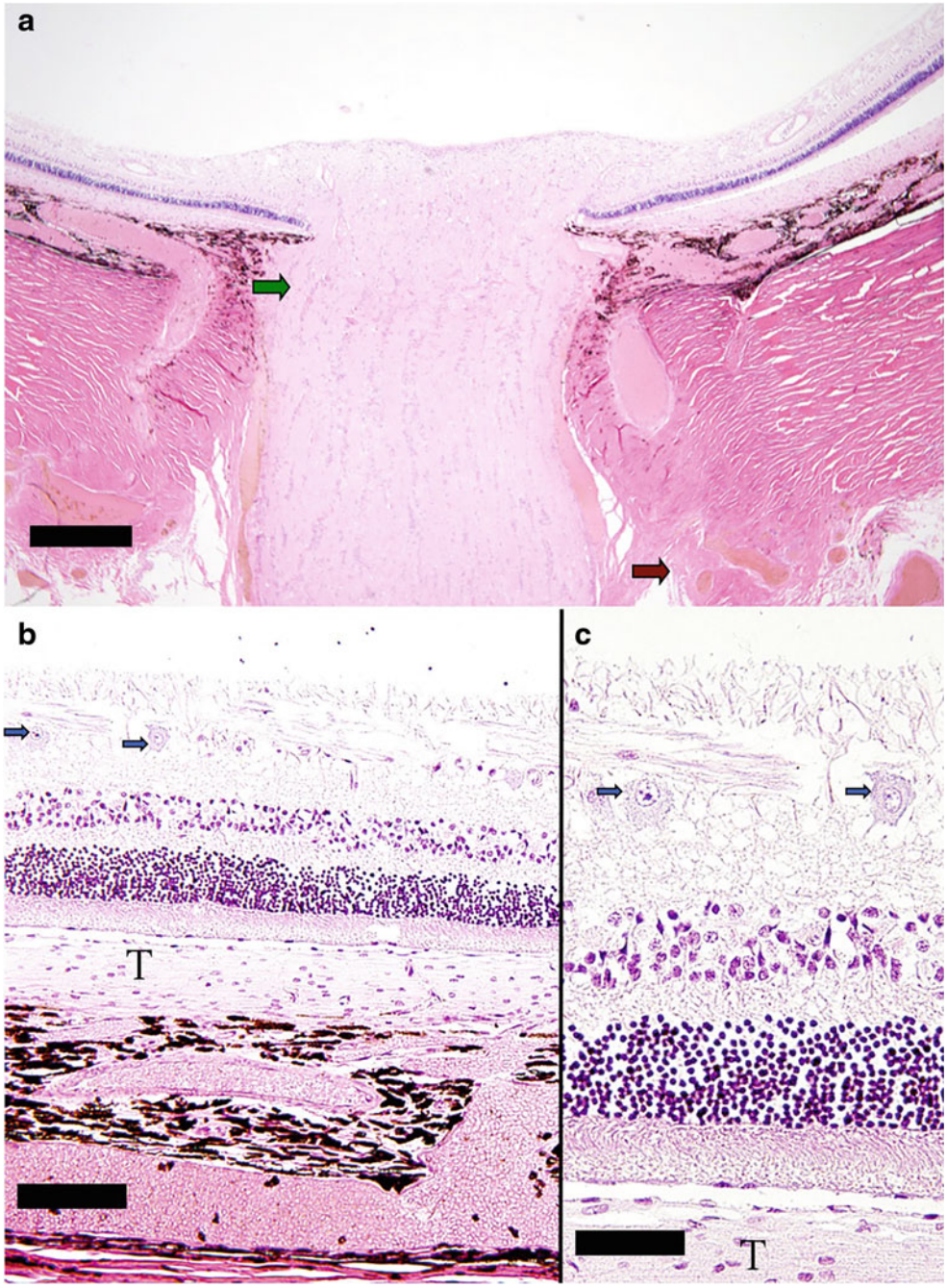

Fig. 38.7 Photomicrographs showing the retina and optic nerve of a California sea lion (*Zalophus californianus*): (**a**) Low magnification. The delicate lamina cribrosa (green arrow) and the beginning of the vascular plexus beyond the sclera (red arrow) are labeled (bar = 2 μm). (**b, c**) The exceptionally large but sparse ganglion cells (blue arrows) are labeled. Layers of the retina are similar to other canids, except the tapetum is thicker (T). (**b** bar = 50 μm and **c** bar = 25 μm). Used with permission from Miller et al. 2020: Anatomy of the California sea lion globe. Veterinary Ophthalmology 13:63–71

grey, but not between red and grey (Griebel and Schmid 1992).

The inner nuclear layer of the pinniped retina is poorly organized, relatively thin, and does not have clear boundaries. Giant horizontal cells are present, as well as bipolar and amacrine cells that are diffusely distributed as compared to the strict order present in terrestrial mammals (Supin et al. 2001). Ganglion cells are variably large, with most ranging between 10 and 30 μm in northern fur seals (*Callorhinus ursinus*), Steller sea lions (*Eumetopias jubatus*), harp seals (*Pagophilus groenlandicus*), Caspian seals (*Pusa caspica)* and walrus (*Odobenus rosmarus*), although cell size can extend up to 60 μm (Nagy and Roland 1970; Mass 1992; Mass and Supin 1992; Mass and Supin 2010). A well-defined circular area of ganglion cell density is present in the temporal retinal quadrant in various pinniped species with the exception of walrus, with a peak cell density of 1000–1250 cells/mm^2. This area corresponds to the area of highest visual resolution and binocular vision and is likely analogous to the area centralis of terrestrial mammals (Mass and Supin 2007; Mass and Supin 2003; Mass and Supin 2005). However, in walrus and harbor seals, the high-density area of ganglion

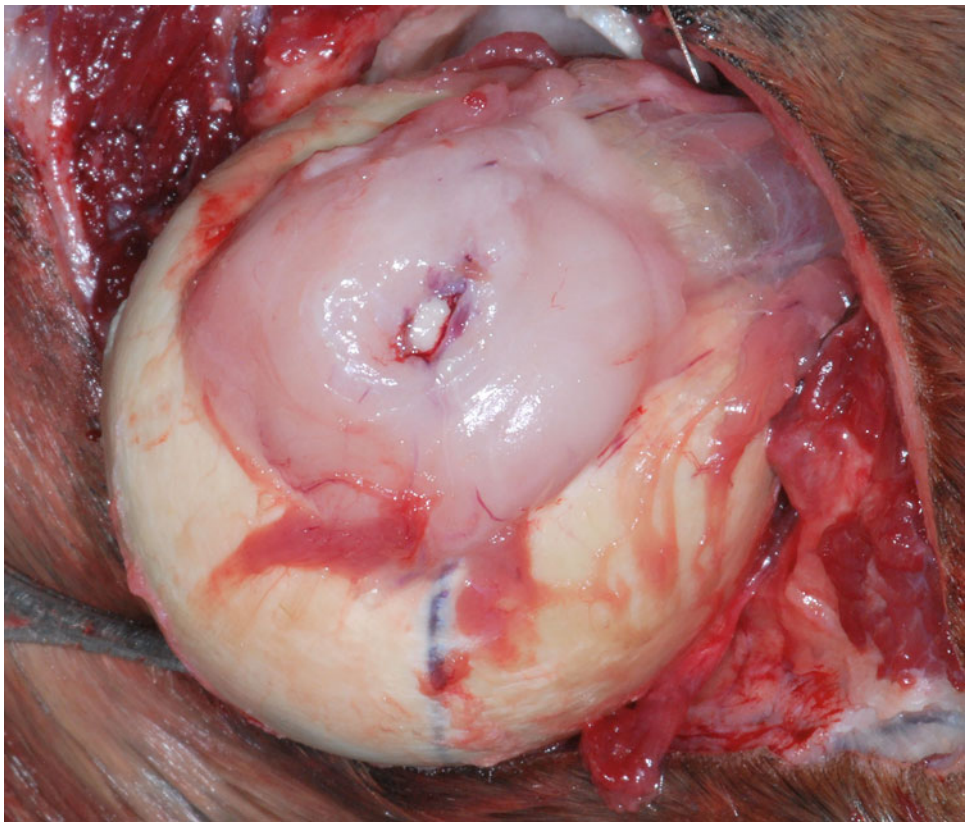

Fig. 38.8 Posterior aspect of a globe from a California sea lion (*Zalophus californianus*). Surrounding the optic nerve, there is a pale pink smooth structure that is the extensive vascular plexus, also called the ophthalmic rete

cells is an elongated prominent nasal streak (Mass 1992; Hanke et al. 2009b). In walruses, the area of the retina providing optimal vision resembles that of animals with a visual streak rather than an area centralis (Supin et al. 2001).

An extensive vascular plexus is located posterior to the globe in pinnipeds (Fig. 38.8) (Miller et al. 2010). A similar ophthalmic rete exists in cetaceans, with its proposed function being the maintenance of temperature and oxygen concentration (Ninomiya and Yoshida 2007). The vascular plexus in pinnipeds may have similar functions. The lamina cribrosa within the optic nerve is delicate, and the optic nerve is devoid of myelin (Miller et al. 2010). The optic nerve is very long and coiled in walruses when the globe is retracted within the orbit. Adipose-rich connective tissue surrounds the optic nerve (Kastelein et al. 1993).

Congenital Ocular Abnormalities

Microphthalmia and anomalies of phalanges and the ilium have been reported in a Hawaiian monk seal (*Monachus schauinslandi*), and congenital cataracts have been described in two other Hawaiian monk seals. A stranded male yearling harp seal (*Phoca groenlandica*) was blind bilaterally, with concurrent bilateral pendular vertical nystagmus and dyscoria (Erlacher-Reid et al. 2011). Ocular ultrasonography revealed bilateral hyper mature resorbed cataracts with a retrolental cone-shaped hyperechoic structure suggestive of persistent hyperplastic primary vitreous. Dyscoria was present, in addition to an altered iridal surface with an excess of iridogonial membranes, which may have been persistent pupillary membranes or simply an excessive number of the strand-like iridal structures that are normally present only in the ciliary region of the phocid iris (Erlacher-Reid et al. 2011). A female South African fur seal (*Arctocephalus pusillus pusillus*) initially presented with diffuse corneal edema, bullous keratopathy, and corneal ulcers but did not respond to medical management. The seal was diagnosed with persistent tunica vasculosa lentis and persistent hyperplastic primary vitreous. Bilateral resorbed hyper mature cataract and retinal detachment with dysplastic retinal rosette formation were also noted (Colitz et al. 2014).

Only one pinniped with presumed bilateral congenital or otherwise anomalous eyelid abnormalities has been identified. A juvenile female California sea lion was noted to have an unusual congenital lesion in which the medial aspect of the superior eyelid was fused to the nictitating membrane. This was either a congenital anomaly or a cicatricial postnatal lesion. The defect impeded the normal movement of the third eyelid and was repaired, restoring normal movement of the third eyelid (Fig. 38.9).

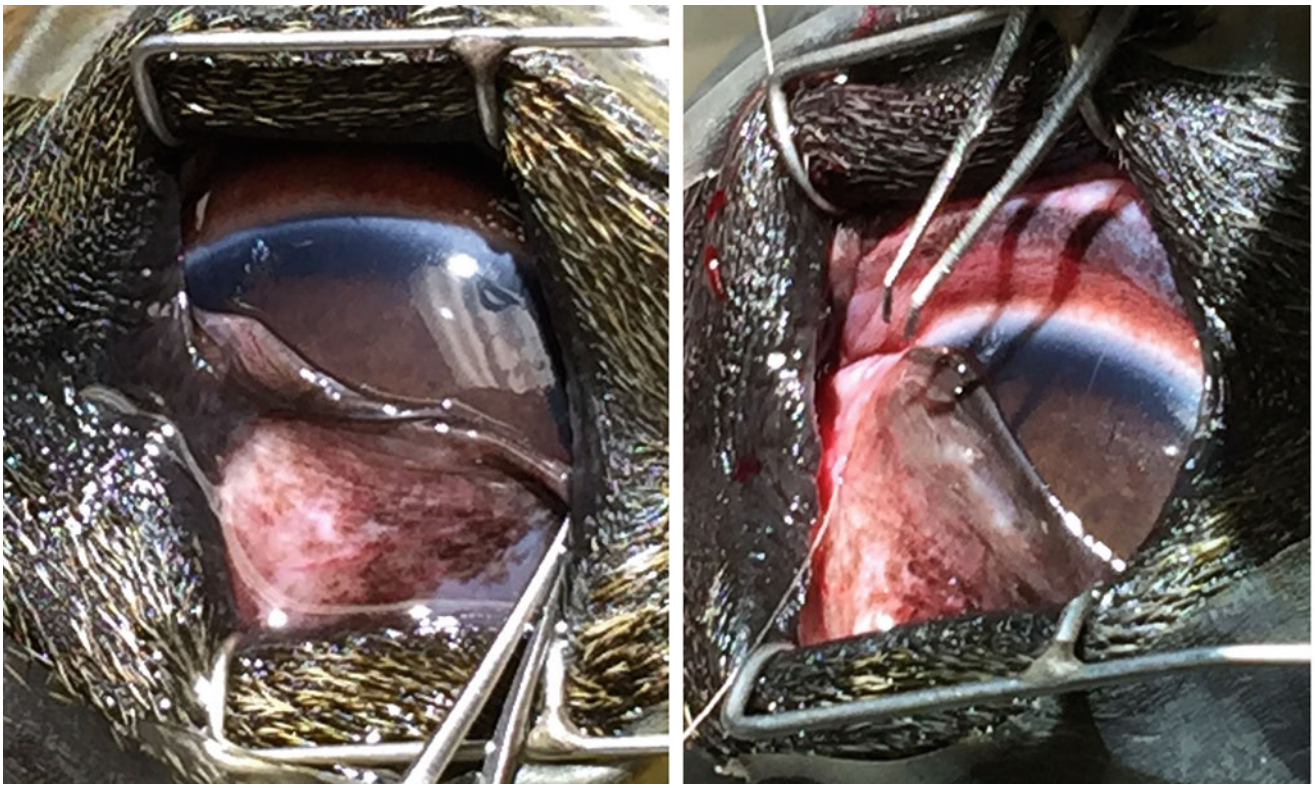

Fig. 38.9 Left eye of a juvenile California sea lion (*Zalophus californianus*). A bilateral congenital anomaly was identified and corrected in this animal. The medial aspect of the dorsal eyelid was still adhered to the adjacent margin of the nictitating membrane impeding the normal movement of the third eyelid. This was resected and the third eyelid sutured to its normal location. The animal regained normal function of its third eyelid. Image from Gulland, F.M.D., Dierauf, L.A., Whitman, K.L. (Eds.). CRC Handbook of Marine Mammal Medicine, third Edition, CRC Press, Boca Raton, pp. 377–412. Fig. 23.14 Left eye of a juvenile California sea lion (Zalophus californianus) with permission

Non-Congenital Abnormalities

Eyelids

The grey seal is the only species, identified thus far, that normally has partially elevated nictitating membranes (Fig. 38.10). Even in the presence of ocular pain, other pinniped species do not elevate their nictitating membranes as grey seals do. This phenomenon does not appear to be linked with pain, although keratopathy can enhance the degree of elevation of the nictitating membrane.

South American sea lions can develop dermatitis that may affect periocular skin (Fig. 38.11). The cause has not been identified, although a fungus, *Malassezia pachydermatis,* was isolated from the skin of one animal (Nakagaki et al. 2000). Water temperature or other environmental factors may be either risk factors or the direct cause of dermatitis (Dr. Michael Walsh, personal communication, 2016).

Eyelid inflammation or masses and trauma appear to be the most common eyelid lesions in pinnipeds. Slow growing masses on the lower eyelid and the medial canthus in a South American fur seal (*Arctocephalus australis)* were diagnosed as papillomas induced by otarine herpesvirus-1 (Oliveira et al. 2019). A Hawaiian monk seal developed a pedunculated corrugated mass of the upper eyelid (Fig. 38.12a), and later developed a mass of the lower eyelid (not shown). These masses were diagnosed histologically as idiopathic ulcerative dermatitis. The same monk seal had a diffusely green algal biofilm evident on its skin. This was histologically confirmed (Fig. 38.12b). A few California sea lions have developed smooth pigmented or nonpigmented masses adjacent to eyelid margins (Fig. 38.12c). One mass was diagnosed as an intradermal round cell tumor with no detectable mitotic activity, with a differential diagnoses of mast cell tumor or plasmacytoma; however, special histologic staining did not yield mast cell granules.(Kern and Colitz, 2013) Another California sea lion developed an ulcerated hyperemic lower eyelid mass (Fig. 38.12d), diagnostics were not performed. A harbor seal had an eyelid mass diagnosed as a myxoma.

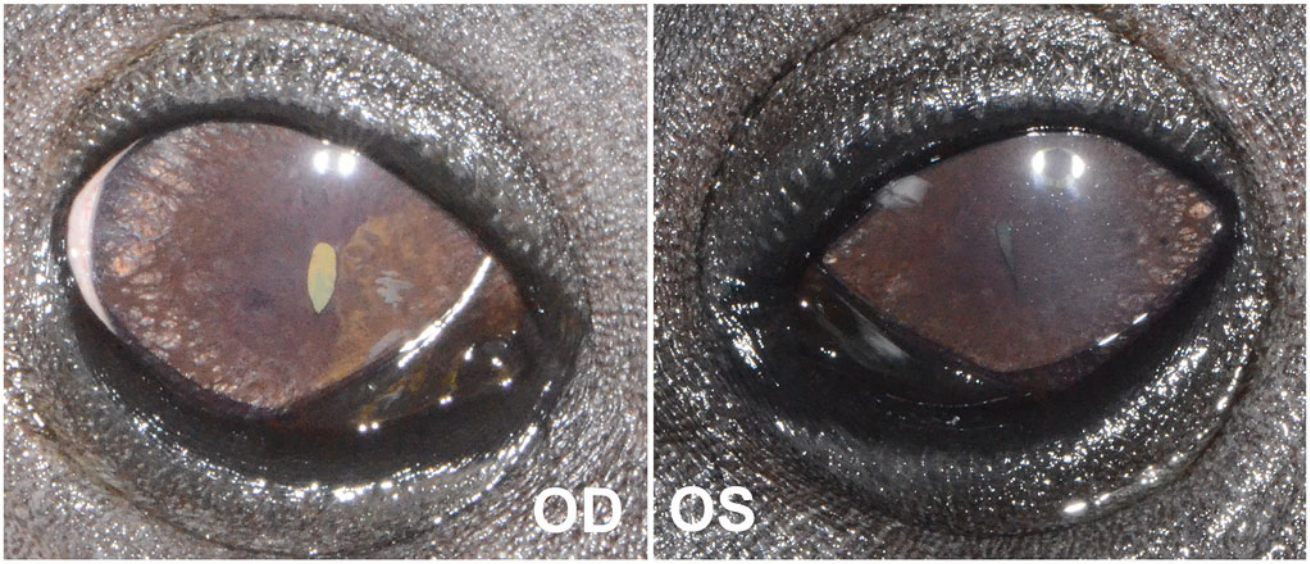

Fig. 38.10 Both eyes of a Grey seal (*Halichoerus grypus*) with mildly elevated third eyelids. Normally, the third eyelids are not evident in most pinniped species. However, Grey seals often have their third eyelids slightly to moderately elevated. These globes also have immature cataracts, and the right eye has lateral limbal hyperemia

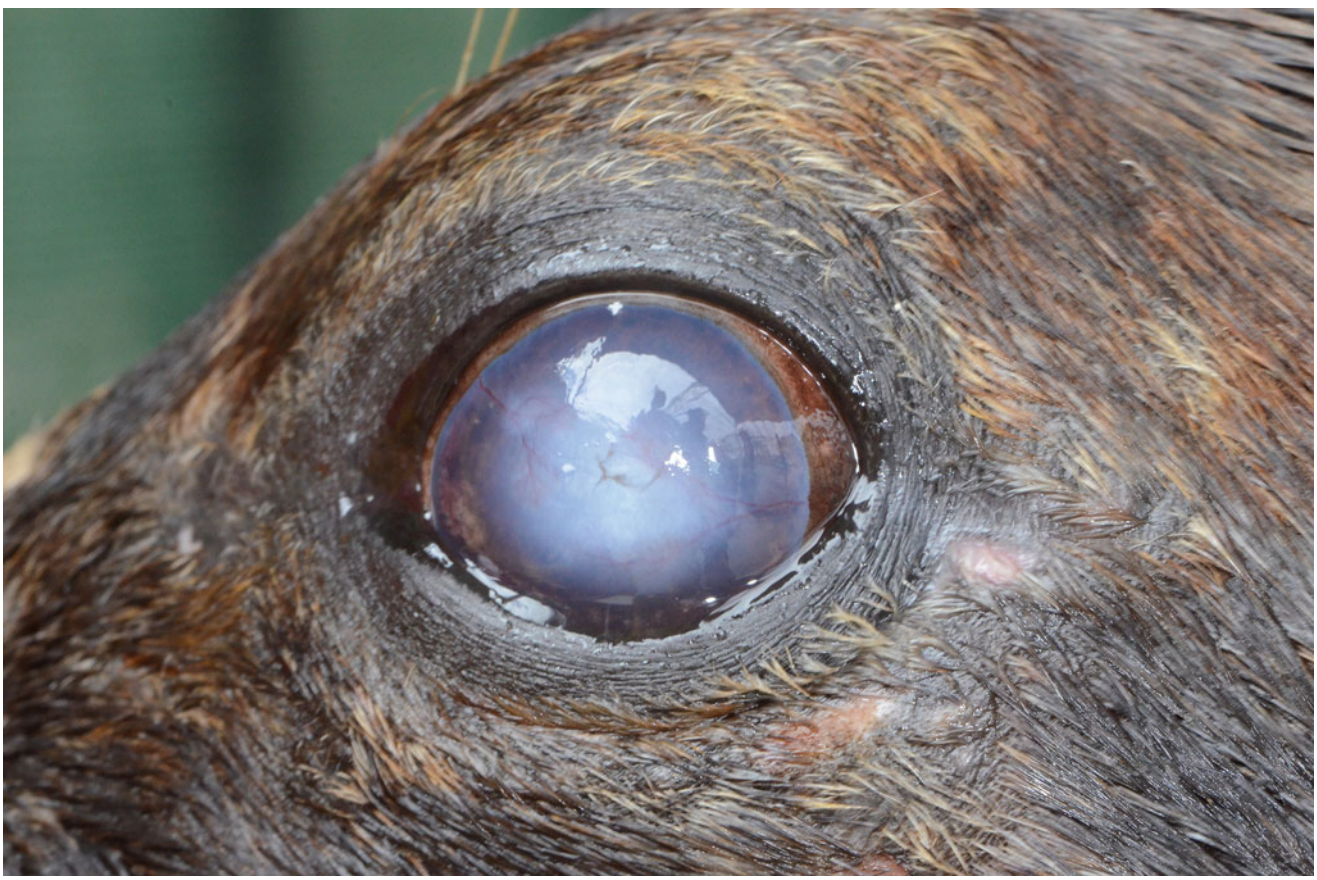

Fig. 38.11 Left eye of a South American sea lion (*Otaria flavescens*). The periocular skin has multifocal pale pink lesions with alopecia due to dermatitis. The cornea also has stage 3 pinniped keratopathy. There is perilimbal edema, and the pigment has migrated over the entire limbus

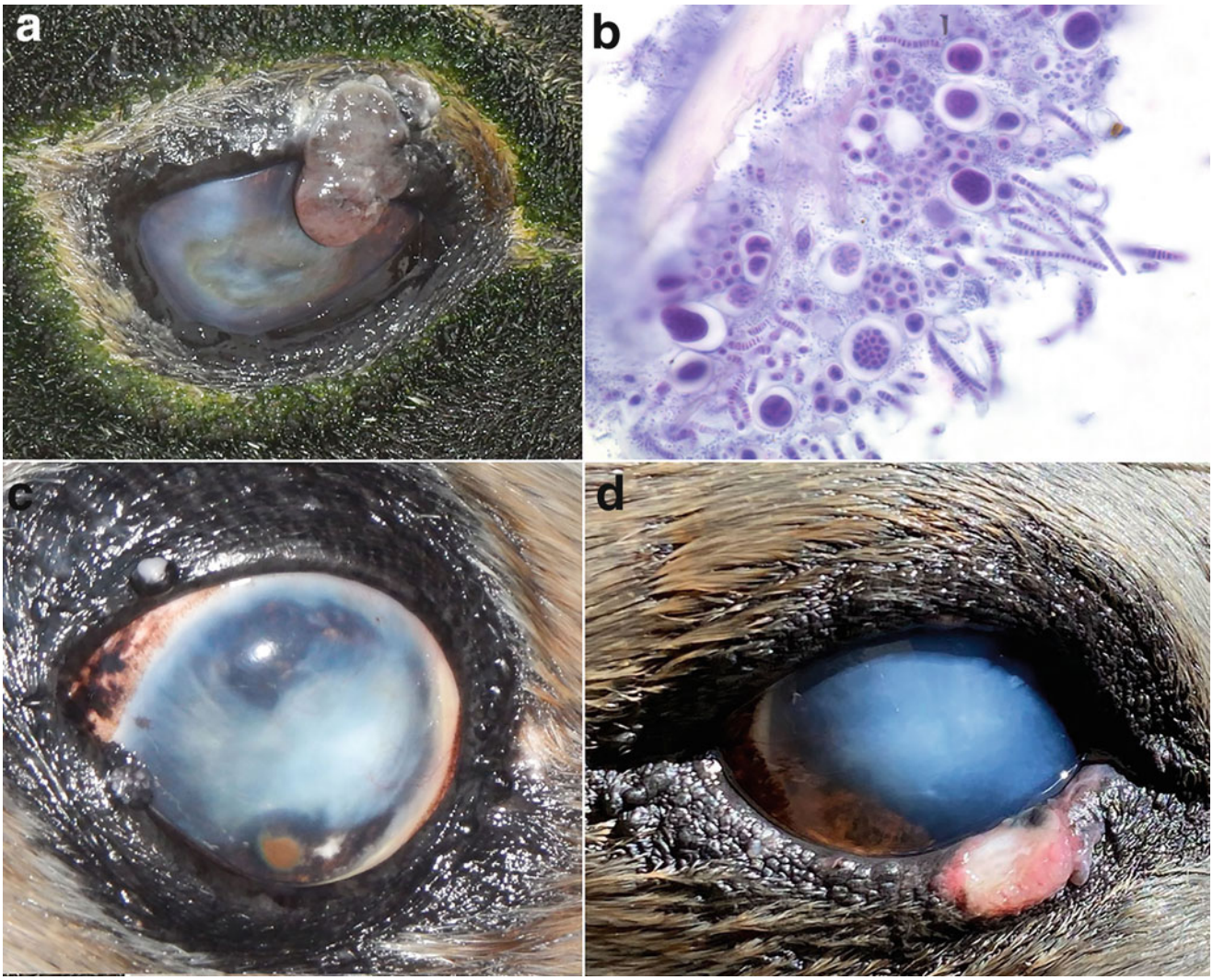

Fig. 38.12 Images from three animals with different eyelid masses and histopathology of algal biofilm. (**a**) Right eye from a Hawaiian monk seal (*Monachus schauinslandi*) with chronic stage 3 pinniped keratopathy. The upper eyelid has a pedunculated pink and pigmented mass. The periocular skin has a green algal biofilm growing on it and this extends over most of this animal's body. (**b**) Histopathology of the green algal biofilm on the skin of this animal. (**c**) Left eye from a California sea lion (*Zalophus californianus*) with chronic stage 3 pinniped keratopathy and one tan round lesion ventrally, likely amyloid. There is a smooth white and pigmented mass on the medial upper eyelid and another at the medial aspect of the inferior eyelid. (**d**) Right eye from a Hawaiian monk seal with chronic stage 3 pinniped keratopathy. The lesion is pink raised and ulcerated. (**a**)—Courtesy of Dr. Beth Doescher and the Comparative Ocular Pathology Laboratory of Wisconsin

Eyelid trauma in pinnipeds usually results from playing or sparring with other animals. In the author's experience, all lesions evaluated thus far have healed without surgical intervention (Fig. 38.13) (Colitz et al. 2018a). While the eyelids of walruses naturally depigment with age, this condition can appear as an unusual finding in young walruses (Fig. 38.14).

Orbit

Fat pad prolapse is occasionally seen in California sea lions and in walrus. The orbital fat prolapse, occurring inferotemporally, was resected and confirmed to be orbital fat in a 23-year-old California sea lion (Klauss et al. 2005). In walrus, the prolapse has been located temporally (Fig. 38.15).

Conjunctiva

Primary conjunctivitis is rare in pinnipeds. One harbor seal has been reported with moderate to severe conjunctival hyperemia and chemosis (Fig. 38.16). Histopathological findings suggested an allergic reaction, but no specific allergen was identified. Conjunctival hyperemia is a typical secondary development in pinnipeds with anterior lens luxation or keratopathy, though the natural pigmentation of pinniped

Fig. 38.13 Right eye of a young California sea lion (*Zalophus californianus*). There is a relatively acute traumatic eyelid laceration at the temporal aspect. The cornea has a focal grey-white opacity that was present prior to the eyelid laceration. Image from Gilger and TJ Kern (Eds) Veterinary Ophthalmology. fifth Ed, Wiley Blackwell, Iowa, USA. Fig. 33.38. Page 1786, with permission

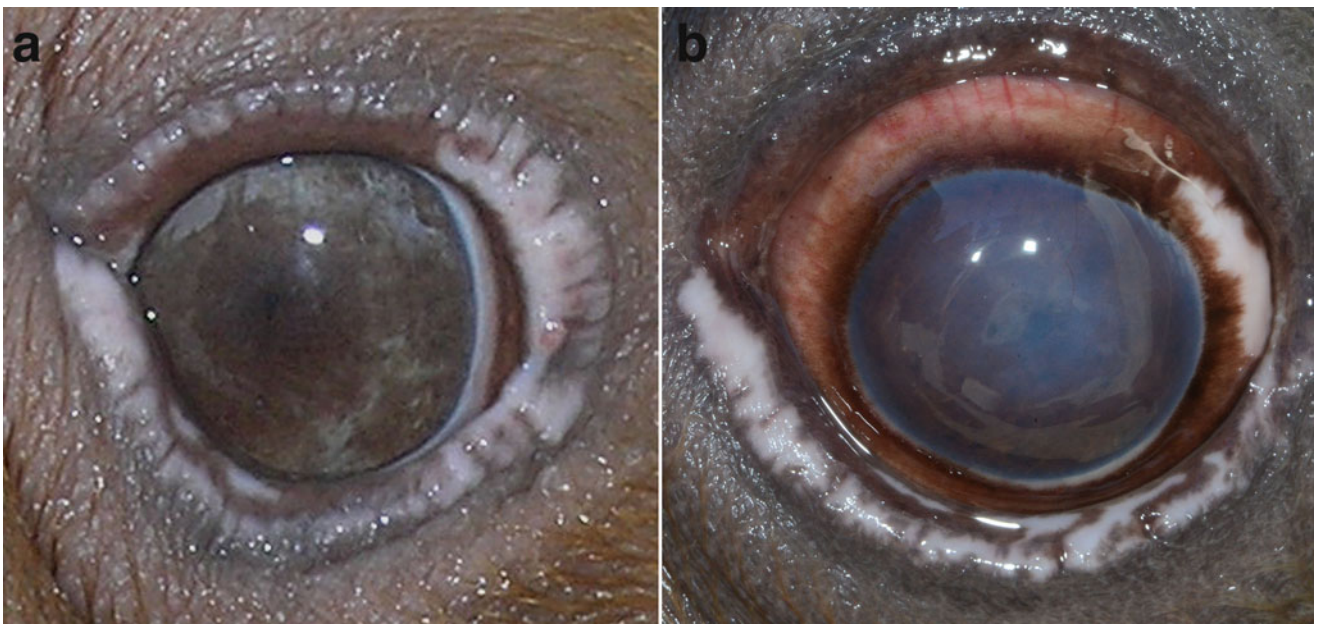

Fig. 38.14 Left eyes from two walruses (*Odobenus rosmarus*) (**a**) Superior and inferior eyelid depigmentation. (**b**) Inferior eyelid depigmentation, lateral conjunctival depigmentation, and diffuse corneal edema with vascularization due to stage 3 pinniped keratopathy

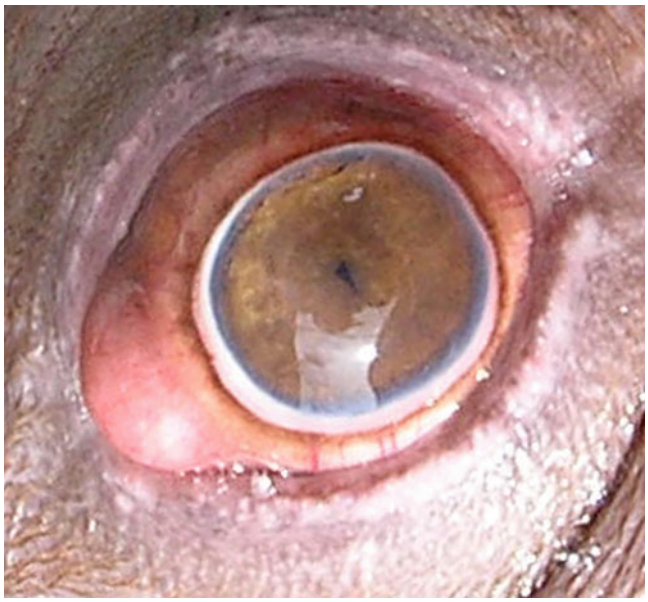

Fig. 38.15 Right eye from a walrus (*Odobenus rosmarus*). There is a smooth oval swelling beneath the conjunctiva temporally consistent with fat prolapse

Fig. 38.16 Left eye of a harbor seal (Phoca vitulina). There is moderate to severe conjunctival hyperemia and thickening ventrally. There is a focal grey-white corneal opacity of the dorsolateral paraxial cornea and a mature cataract

conjunctiva can mask the presence of hyperemia. The dorsotemporal and temporal conjunctiva often become depigmented in walruses and sea lions, respectively. While this may be a normal sign of aging, conjunctival depigmentation is more commonly encountered in eyes with chronic Pinniped Keratopathy (Fig. 38.14, 38.18a, and 38.30c).

Cornea

Corneal disease affects both pinnipeds in the wild and those in human care. In a retrospective study of over 6000 pinnipeds from two stranding facilities in California, the majority of identified ocular lesions were present in the cornea (Colitz et al. 2011b). In pups, corneal edema, nonspecific corneal opacities, and corneal ulcers were the most common ophthalmic diagnoses, with the most common systemic abnormality being malnutrition. The juvenile age group had the fewest ophthalmologic lesions and systemic abnormalities. Corneal perforations and phthisis bulbi were the most common ocular lesions, with gunshot wounds being the most common systemic abnormality. In subadults, phthisis bulbi was the most common eye lesion, and domoic acid toxicosis was the most common systemic abnormality. In adult pinnipeds, corneal edema and corneal ulcers were the most common ophthalmologic lesions, and domoic acid toxicosis was the most common systemic abnormality.

Grey seals are a larger phocid species commonly found in coastal waters of the United Kingdom. Similar to pinnipeds of coastal California, corneal ulcers and perforations are common in grey seals. A study evaluated the conjunctival flora from stranded grey seals with healthy eyes and those with corneal lesions (Fleming and Bexton 2016). Of 32 animals with normal eyes, 35 of 58 eyes yielded bacterial growth. The most common bacterial isolates were *Gemella haemolysans, Escherichia coli, Clostridium perfringens, Streptococcus oralis, and Streptococcus mitis*. Animals with abnormal eyes grew similar bacteria. Cultures from two eyes with corneal perforations grew *Gemella haemolysans* and *Streptococcus mitis*. Two seals had superficial corneal ulcers, with one seal affected bilaterally. The bacterial culture from the seal with a unilateral ulcer grew *Clostridium perfringens*. The cultures from the seal with bilateral ulcers grew *Escherichia coli* and *Streptococcus agalactiae*. Nine seals with normal eyes at the time of stranding developed a variety of corneal ulcers. Bacterial isolates from the corneal ulcers that were not melting (malacic) included *Acinetobacter Iwoffii, Klebsiella pneumoniae, Proteus spp, Bifidobacterium sp,* and *Clostridium testosterone*. Five seals developed melting corneal ulcers, all yielding *Pseudomonas aeruginosa* isolates (Fleming and Bexton 2016).

Besides Pinniped Keratopathy (see below for discussion), pinnipeds in human care can also develop traumatic corneal ulcers and, rarely, tumors involving the cornea. One elderly harbor seal developed a progressively enlarging red mass initially affecting the dorsal aspect of the cornea, extending

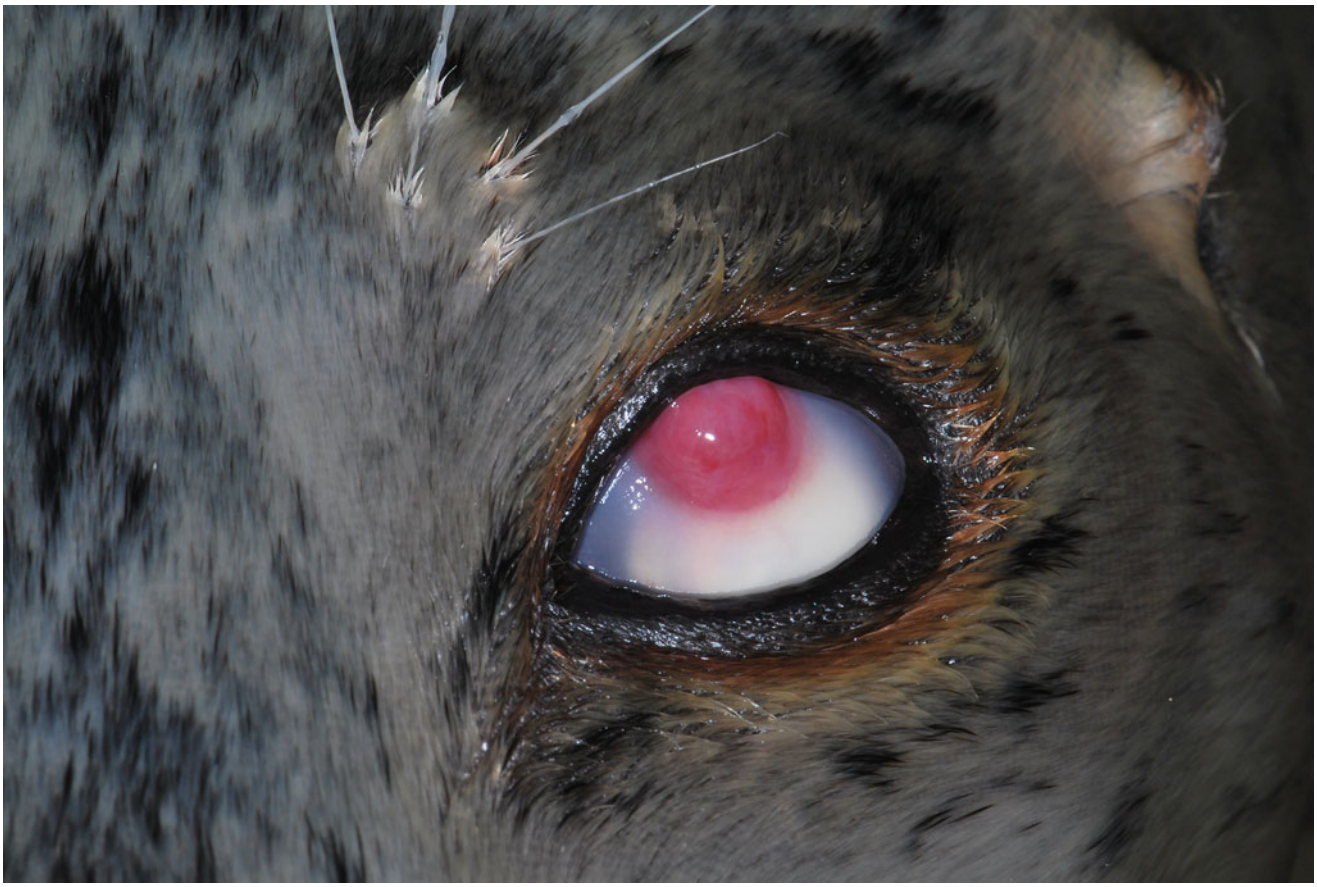

Fig. 38.17 Left eye of a harbor seal (*Phoca vitulina*). There is a raised smooth red mass at the dorsal aspect of the cornea with severe diffuse corneal edema. The pupil is mydriatic, and a mature cataract evident as well. The cataract was anteriorly luxated

both intrastromally and ventrally (Fig. 38.17). Over a two-year period, the mass widened and became more raised. The eye also had a cataract that subsequently luxated anteriorly. The histological diagnosis was histiocytic sarcoma. An elderly California sea lion developed a peripheral nerve sheath tumor that affected the deep corneal stroma and invaded the anterior chamber with extension into the ciliary cleft (Fig. 38.18). Clinically, the cornea was opaque with an irregular surface. The presumptive clinical diagnosis was Pinniped Keratopathy. However, deep corneal vascularization with large, broad vessel arborization was present. This is an unusual finding, as corneal vascularization is typically impaired in pinnipeds; when present, the vessels are attenuated with numerous fine vascular branching.

Pinniped Keratopathy

Pinniped Keratopathy (PK) occurs in all species of pinnipeds in human care evaluated to date (Colitz et al. 2018a; Colitz et al. 2010a; Kern and Colitz 2013). Keratopathy is used instead of keratitis due to the paucity of inflammation in these cases. A recently published worldwide epidemiological study found that 56.7% of pinnipeds were affected; of these animals, 51.4% were affected bilaterally (Colitz et al. 2018b). Significant risk factors were found to be: lighter or reflective pool paint colors, water salinity less than 29 g/L (ppt), a history of previous ocular disease, a history of previous trauma or injury, and having been tested for leptospirosis. Factors diminishing the risk of PK included an ultraviolet (UV) index of less than or equal to 6.0 and being younger than 20 years of age (Colitz et al. 2018b). The UV index is a numerical forecast of the expected risk of overexposure to sunlight (Agency 2016). Humans exposed to a UV index of 6.0 can develop sun-related damage, especially without the use of sunblock or a wide-brimmed hat. Since eyewear and visor-like headwear are unfortunately not available for pinnipeds, providing adequate, useful shade structures is one of the most important ways to protect pinnipeds from chronic UV damage. Facilities located closer to the equator

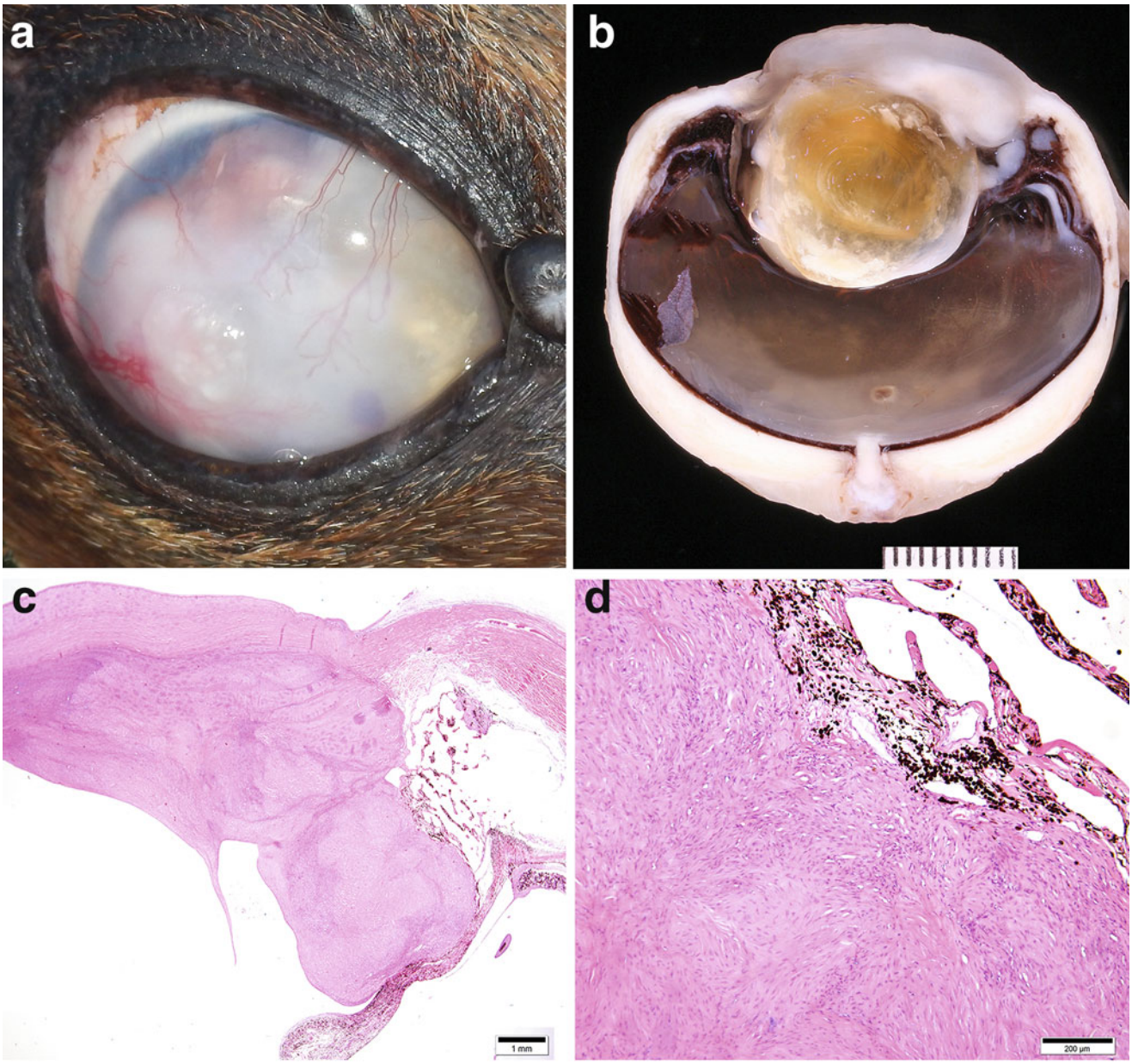

Fig. 38.18 The right eye of a California sea lion (*Zalophus californianus*) with a peripheral nerve sheath tumor, gross image of the globe and two histological images of the mass. (**a**) The left eye had almost complete depigmentation of the lateral conjunctiva, diffuse corneal edema with vascularization, ventrolaterally the cornea is thickened with an intrastromal mass that extends into the anterior chamber and ciliary body. The lens is anteriorly luxated as well. In addition, here is also a smooth pigmented and white mass of the dorsomedial eyelid. (**b**) Gross image of the globe showing the corneal stromal and anterior chamber mass adherent to the anteriorly luxated cataractous lens. (**c**, **d**) Histological sections of the mass with highly cellular spindle cells with a swirling pattern, and in other areas a storiform pattern. (**c**) bar = 1 mm, (**d**) bar = 200 µm. Image and report courtesy of Comparative Ocular Pathology Laboratory of Wisconsin

can have a consistently high UV index of up to 10 or 11 through many months of the year. The presence of a higher UV index means that it takes less exposure time to cause sun-related damage. The UV index is not only dependent on direct sun exposure in the pools or other animal enclosure areas but is also influenced by the paint colors of the pools, enclosure walls, and the floors surrounding the pools. Less reflective colors, such as tan or sand protect against PK because they lower the UV index. When the days are longer during late spring through early fall, animals often have a higher incidence of PK flare-ups during those months, even in areas with a lower UV index. It is important

to remember that UV damage is cumulative; because of this fact, it is logical that being younger is a protective factor and that older animals are more likely to have PK lesions. Training and feeding sessions should be held under adequate shade structures and/or having the animals face away from the sun with the goal of minimizing reflectivity from the water or surrounding areas.

In addition to minimizing UV exposure, water quality and environmental factors are of utmost importance to eye health in pinnipeds. There are many known parameters, and many not yet specifically identified, that must be considered. In the study mentioned earlier, water salinity under 29 g/L was the only water quality parameter identified as a risk factor for PK. The importance of freshwater as a risk factor for PK has been reported (Dunn et al. 1996). The majority of facilities have naturally or synthetically salinated water in the animals' pools. However, there are still, unfortunately, a few facilities that house pinnipeds in freshwater. The pH of the water (specifically higher than 7.6) was associated with a higher incidence of PK, though the difference was not statistically significant (Colitz et al. 2018b). This may only imply that pH is important when extreme changes in pH occur. This value must be considered along with the other water quality abnormalities when PK is observed.

There are three general types of life support systems (LSS) for captive pinnipeds: open, semi-closed, and closed. These LSS may, in turn, use different filtration systems for disinfection, including chlorine, bromine, ozone, or UV. Unfortunately, there is much variability globally between the various LSS; their details of design, while extremely important, are quite difficult to compare statistically.

Some important parameters to consider when one or more animals have a PK flare-up include coliform count and oxidative reduction potential (ORP) and total and free chlorine concentration, depending on the disinfection system used. The coliform count should be kept low but not zero as this suggests excessive chemicals in the system. Other parameters include water temperature, the specific type of disinfection system (mechanical filtration, biological filtration, chemical filtration, and UV sterilization), environmental pollution, water source, the creation of by-products of disinfection, the effect of sunlight on the by-products of disinfection, and many others (Colitz et al. 2018b). The most common chemical disinfection systems use ozone and/or chlorine. Though not statistically significant, the study found that an ozone system, when well regulated, generated the lowest incidence of PK and the combination of ozone and chlorine systems yielded the highest incidence of PK. Ozone is ten times more powerful than chlorine as a disinfection agent and is easier, safer, and cleaner than chlorine. Ideally, an ozone system should de-gas before it returns to the pinniped exhibit. The range of ORP associated with the least eye issues in pinnipeds was between 451 and 600 mV. The suggested threshold for total and free chlorine was 0.5 mg/L; corneal edema can occur at higher levels. Chlorine in the presence of ammonia will produce harmful chloramines and bromamines. System circulation is also very important, with higher system turnover being better than lower turnover.

When corneal edema and blepharospasm occur in more than one animal or in an animal with a history of PK, there is likely an LSS or environmental imbalance. Animals with a history of PK are much more sensitive to mild environmental or water quality changes, with affected animals often being unfortunate sentinels for LSS degradation or subtle environmental changes. The author typically suggests reviewing LSS parameters for the past 10 to 14 days to see if there were any obvious change(s) in the parameters over a prolonged period. The ammonia level can become uncontrolled because it is typically not consistently measured in LSS. Acute elevations in ammonia have resulted in severe PK with significant effects including severe corneal edema, epiphora, blepharospasm and stromal malacia (personal communication V. Fravel, personal observation, Colitz).

Unfortunately, once an animal develops PK, the cornea will never return to its normal state. This is surmised to be due to a permanent imbalanced surface immunity and an inability to vascularize well. Other observations are that a cornea with a history of active PK will be exquisitely more sensitive to minor changes in the environment than an unaffected cornea. Animals with underlying health problems, including systemic infection, neoplasia, or advanced age, appear to be more likely to have poorly controlled PK that does not respond to traditional therapy (personal observation, Colitz). Clinical signs of PK have not been identified in wild pinnipeds. However, once pinnipeds are placed in human care, PK may develop likely due to differences between the ocean environment and the animals' new captive environment. Their health status may be stressed and/or immunocompromised as well and may contribute to the development of PK.

Stages of Pinniped Keratopathy

There are three well-described stages of clinical PK, with each species having unique disparities, which will be further described in the next sections (Colitz et al. 2010a). The earliest stage, Stage 1, affects less than 10% of the cornea and initially presents with mild perilimbal corneal edema in all species. Some animals may have mild limbal/perilimbal pigment migration from the conjunctiva to the cornea. With chronicity, some eyes will diffusely depigment the

conjunctiva. Clinical signs of pain are variable but usually are noted when a corneal ulcer is present. The ulcers, as described further below, have indolent characteristics, even at Stage 1 of the disease. The onset of Stage 1 is almost always due to a change in one or more environmental factors discussed earlier (personal observation, Colitz). Sometimes the limbal and perilimbal corneal changes are an incidental finding, and the environmental factor(s) may not be obvious. Periocular black crusty discharge, due to epiphora, is evident in some animals. Despite being in a marine environment, this suggests that the tear quality is abnormal, causing it to collect and accumulate in the periocular fur (Fig. 38.19).

The second stage, Stage 2, involves 10 to 20% of the corneal surface area. Affected Stage 2 eyes in most pinniped species demonstrate perilimbal corneal edema (with more diffuse axial or paraxial edema in some eyes), limbal/perilimbal hyperemia, and pigment migration that can be mild or may obscure the limbus. If corneal ulceration is present, it is always an indolent ulcer (i.e., a chronic nonhealing corneal ulcer, Fig. 38.20) (personal observation, Colitz). Even ulcers that appear focal will have loose epithelium overlying and surrounding the ulcer. This has been confirmed histologically as a consistent change (Fig. 38.21). As per COPLOW, the epithelium is histologically attenuated and not attached, with minimal to no inflammation; there is also loss of polarity with rare keratinocyte apoptosis/necrosis and epithelial edema. In the author's experience, animals exhibiting signs of ocular pain in conjunction with negative corneal fluorescein retention always have a variably sized nonadherent, or indolent, corneal epithelium (Fig. 38.21). The cause of indolent ulceration in this species is unknown. Unfortunately, debriding the ulcer is not typically practical as the intense pain does not make the debridement simple, and sedation or anesthesia may be risky for the animal and/or the handlers. Stromal loss occurs with chronicity due to prolonged infection and exposure to UV (Newkirk et al. 2007). Because corneal vascularization in pinnipeds does not progress significantly over time, as it does in other species such as cetaceans, healing is very slow to impossible without addressing the component of defective corneal epithelialization. Opportunistic infection with bacteria and/or fungi or yeast appear to be the main component of

Fig. 38.19 Left eye of a California sea lion (*Zalophus californianus*). There is periocular debris adhered to the fur due to chronic epiphora. The globe has perilimbal edema and pigmentation of the limbus indicative of stage 1 pinniped keratopathy. There is mild heterochromia iridis and an immature cataract

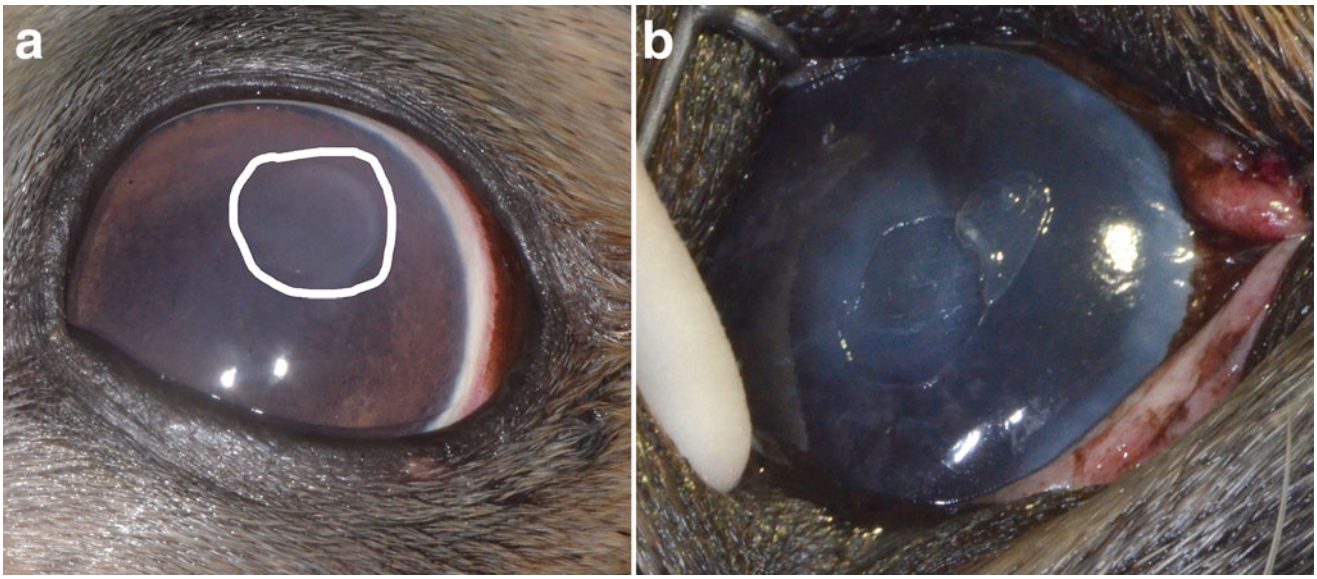

Fig. 38.20 Left eyes of a California sea lion (*Zalophus californianus*) and an Australian sea lion (Neophoca cinerea) with indolent corneal ulcers. (**a**) There is diffuse corneal edema and a round area dorsolateral paraxially where the corneal epithelium is not adherent to the stroma though is not an obvious ulcer (white circle). (**b**) The corneal epithelium in this eye was easily debrided, and the underlying stroma was edematous. There is also more pronounced perilimbal corneal edema

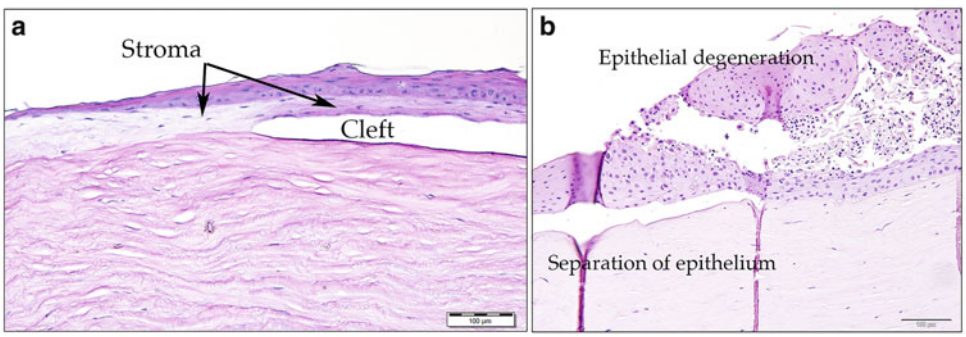

Fig. 38.21 Histopathological images of two indolent ulcers from two postmortem globes from California sea lions (Zalophus californianus). There is separation of the epithelium from the underlying stroma as well as epithelial attenuation (**a**) and degeneration (**b**). The stromal keratocytes are sparse. Used with permission from Gulland, F.M.D., Dierauf, L.A., Whitman, K.L. (Eds.). CRC Handbook of Marine Mammal Medicine, third Edition, CRC Press, Boca Raton, pp. 377–412

progression from Stage 1 to Stage 2 and, eventually, to Stage 3 in some cases.

The most advanced stage of PK is Stage 3, in which at least 20% of the cornea is affected; in some animals, the entire ocular surface is engulfed. As mentioned, Stage 3 is usually the result of an opportunistic infection that is aggressive and difficult to control. In some cases, even with oral and topical antibiotics and anti-inflammatory and pain medications, progression to stromal loss (with or without malacia), descemetocele formation, or even corneal perforation may occur (Fig. 38.22a, c). Corneal abscessation may occur and is usually due to a coliform or fungal/yeast infection. Very commonly, a corneal abscess will be accompanied by overlying nonadherent epithelium, thus combining stromal ulceration/abscessation with an indolent ulcer. Surgical repair using BioSIS and/or amniotic membrane graft material covered with a conjunctival pedical flap has been successfully performed to address progressing corneal ulcers or perforations. Clinically, conjunctival grafts may not adhere well due to the poor vascularization in pinnipeds and necrose from the distal portion towards the pedical, though the BioSIS portion usually adheres and integrates into the corneal defect. Histologically, this has been confirmed as the conjunctival grafts do not embed into the corneal stroma (personal communication, Dr. Richard Dubielzig). Conjunctival graft failure has occurred in approximately 50% of grafts performed to date and entails blanching of the distal portion of the graft or complete dehiscence (Fig. 38.22b). Since the BioSIS has remained in almost all eyes, it appears to promote repair of the perforation or descemetocele. Healing is best if

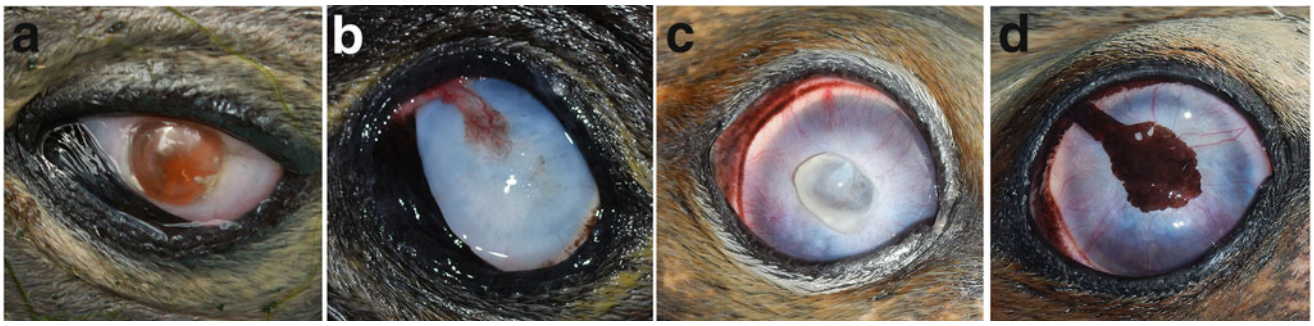

Fig. 38.22 Corneal perforations and healed repairs from a Hawaiian monk seal (*Neomonachus schauinslandi*) and a California sea lion (Zalophus californianus). (**a**) Left eye with a chronic gradually enlarging corneal perforation that was plugged with the brunescent lens nucleus from the anteriorly luxated cataractous lens. The remaining cornea was densely edematous and vascularized throughout the stroma. (**b**) Left eye of the same animal 5 months post-operatively. The eye underwent lensectomy and flushing of the anterior chamber debris, and then the cornea was repaired using a BioSIS graft and covered with a conjunctival pedical flap. The majority of the conjunctival graft became ischemic though the BioSIS material was integrated into the cornea. The contralateral eye also underwent lensectomy, and each eye had two cyclosporine implants placed. (**c**) Right eye with a chronic descemetocele that perforated. The cornea is diffusely vascularized, has severe edema, and the axial corneal descemetocele had a small leak that would seal intermittently. There was also an unstable lens still in the patellar fossa at the time of surgery. (**d**) Right eye of the same animal 9 months post-operatively. The eye underwent intracapsular cataract extraction, and the cornea was repaired using BioSIS graft and covered with a conjunctival pedicle flap. The other eye also underwent lensectomy, and each eye had two cyclosporine implants placed

infections are controlled. If cataract and/or anterior lens luxation is also present, lensectomy has been performed in conjunction with corneal repair with cyclosporine implants placed as well (Colitz et al. 2014). The use of oral NSAIDs is important, but the dose appropriate for the animal's weight appears to inhibit vascularization of the conjunctival graft, therefore, a quarter to a third of the oral dose is suggested. Oral tramadol+/− gabapentin is/are used to control pain.

Of course, avoidance of ulcer progression is best, if possible. First, the clinician should try to identify and correct the offending factor or factors. If a corneal ulcer is present, it should be treated with topical broad-spectrum antibiotics that address opportunistic coliforms and *Pseudomonas* spp. as well as oral or topical compounded doxycycline. Additionally, systemic nonsteroidal anti-inflammatory pain medications and tramadol are usually needed. Long-term topical tacrolimus drops are helpful in controlling the disease (note that it is never too early to start their use once lesions are identified). Episcleral subconjunctival cyclosporine implants have been used for over 10 years in many animals to effectively help control PK (Fig. 38.23) (Colitz et al. 2016). The control of PK with topical tacrolimus or cyclosporine implants definitely relies on controlling the variables that contribute to PK as much as reasonably possible. Younger animals that had cyclosporine implants placed before developing PK appear to have delayed onset of the disease (personal observation, Colitz). A new product, EyeQ amnion eyedrops (Vetrix), has shown promise in the more rapid improvement of acute onset of PK, infectious ulcerative keratitis, and indolent-type ulcers following debridement (personal observation, Colitz). While oral nonsteroidal anti-inflammatory medications and either cyclosporine or tacrolimus inhibit vascularization, pinniped corneas typically have negligible ingrowth of vascularization in the absence of these medications. Therefore, their use does not appear to slow or inhibit the healing of corneal ulcers or abscesses, except with conjunctival grafts. The control of infection and exogenous factors is most important.

Quiescence can be achieved, in most cases, regardless of the stage of PK with appropriate therapy and control of environmental factors. Quiescence is characterized by ocular comfort, resolved or minimized corneal edema, healed corneal ulcer or abscess, and resolved infection. For PK to be controlled, three important factors must be addressed: 1) control the infection rapidly; 2) support proper re-epithelialization of an ulcer using debridement and burr keratotomy or grafting surgery; and, 3) the most important factors for attaining ideal control is to control the imbalanced environment, provide adequate and significant shade, and change pool and surrounding colors to a darker or natural-colored UV absorptive shade. The indolent component of ulcerative PK often makes this the most frustrating part of the disease. Sometimes, debridement, with burr keratotomy if appropriate, may need to be performed. Most currently, the concurrent use of Amnion drops appears to improve healing.

Pinniped Keratopathy by Species

Pinniped Keratopathy (PK) was initially described in otariids (eared seals) (Colitz et al. 2010a). However, it was later realized that all pinniped species evaluated are susceptible

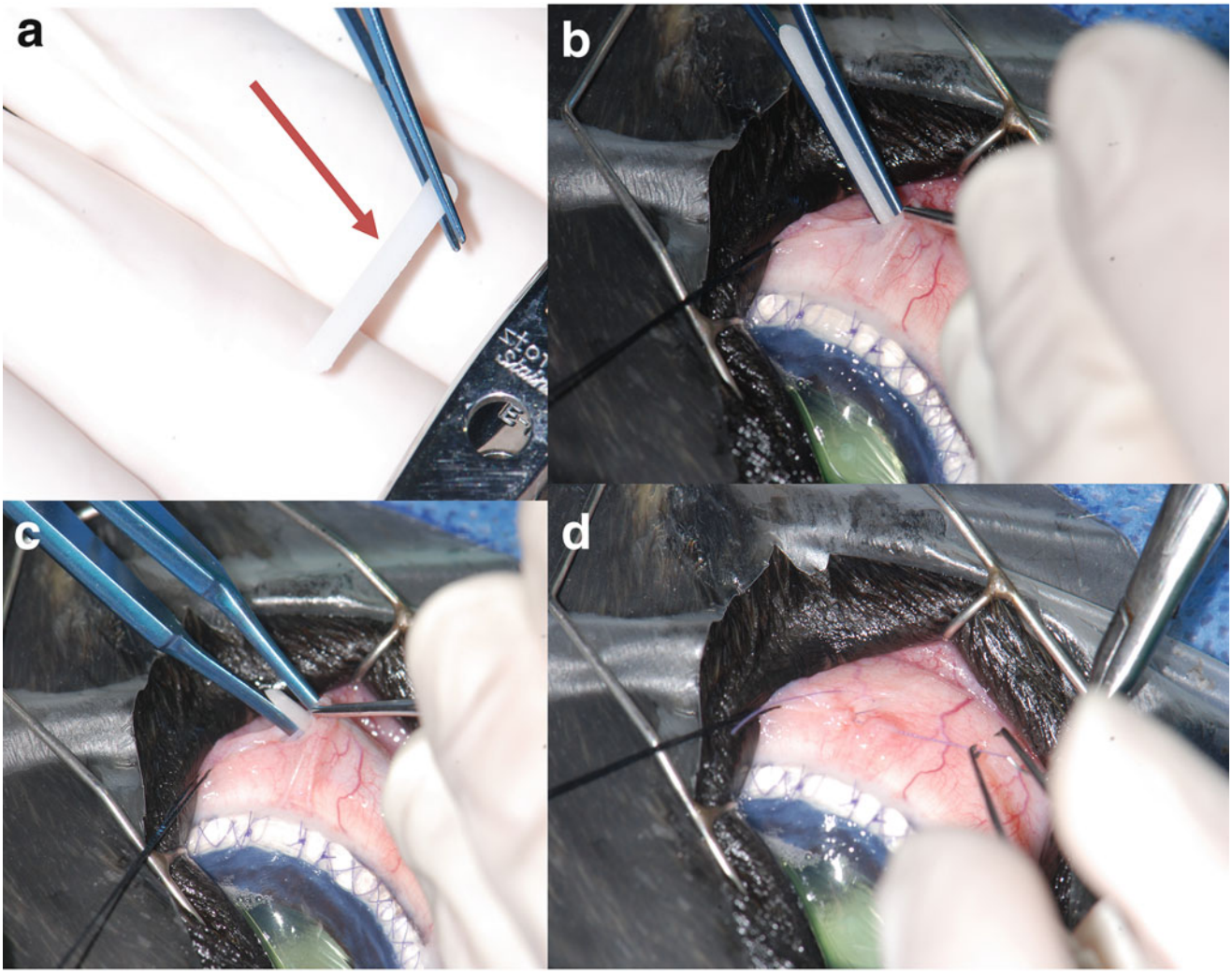

Fig. 38.23 Episcleral subconjunctival cyclosporine implants. (**a**) Cyclosporine implant shown prior to placement. (**b**) Cyclosporine implant being inserted into the subconjunctival tunnel approximately 5 mm posterior to the dorsal limbus. (**c**) The implant almost completely inserted into the subconjunctival tunnel. (**d**) Suturing of the incision using 7–0 Vicryl. The eye shown in these images had just had a lensectomy, and the incision is closed with 7–0 Vicryl using a simple sawtooth pattern

to this disease. The initial description included 113 pinnipeds, which were predominantly California sea lions, although other reported species included one northern fur seal, one Guadalupe fur seal, seven brown fur seals, and six Steller sea lions. PK can affect pinnipeds of any age, noted as young as six-month-old pups.

Sea Lions

California Sea Lions (*Zalophus Californianus*)

Normal eyes from a California sea lion are shown for comparison purposes (Fig. 38.24). The initial lesions in affected California sea lions occur in the dorsotemporal corneal quadrant as a focal grey opacity (Fig. 38.25a) or superficial corneal ulcer (i.e., loss of epithelium with nonadherent epithelial margins). Mild to moderate perilimbal corneal edema is typically present. Many will also have aberrant pigmentation crossing the limbus or depigmentation of the conjunctiva. The pigment migration may blur the limbal demarcation (Fig. 38.25b). Over time, the focal ulcer becomes infected due to opportunistic bacteria infiltrating under the nonadherentepithelium. In addition, chronic UV and exposure to environmental stressors exacerbate the edema and pain. Stage 2 progresses to stage 3 at a variable speed depending on the environmental factors and, likely also due to the animal's innate immune system (Fig. 38.25b, c).In some eyes, the pigment becomes sparse, i.e., depigmentation, while in others, it progresses. California sea lions with chronic PK can also develop amyloid deposition in the cornea and

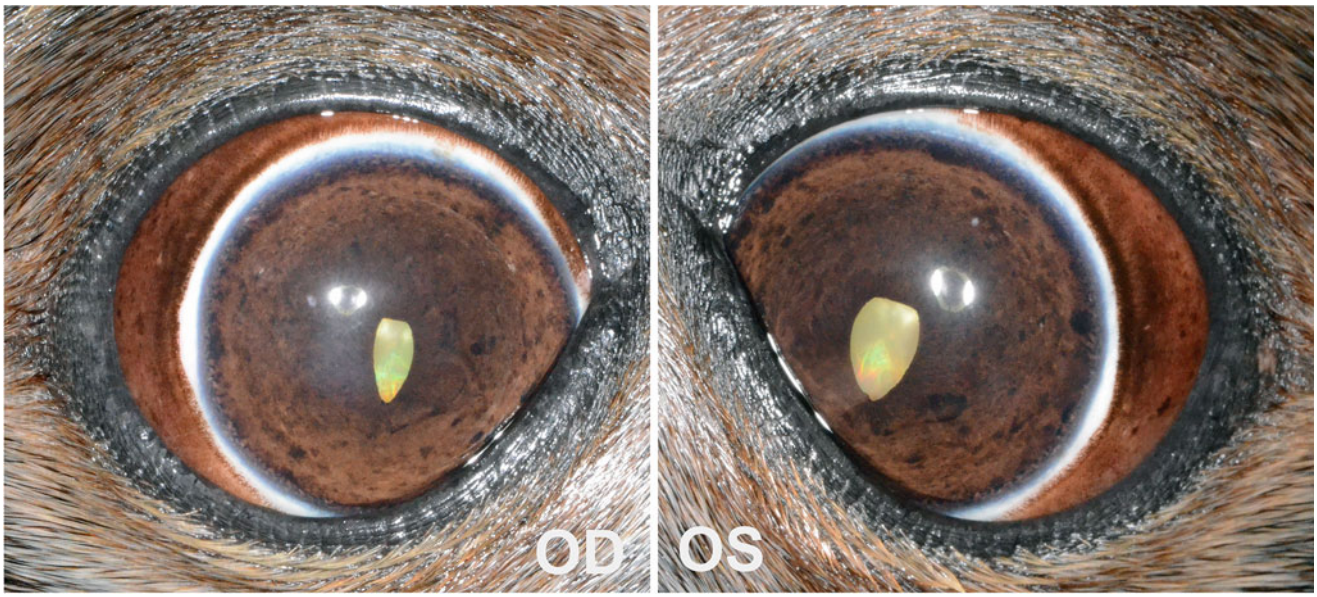

Fig. 38.24 Normal cornea and limbus in each eye of a California sea lion (*Zalophus californianus*). There is an incipient cataract in each eye

Fig. 38.25 Three right eyes from three California sea lions (*Zalophus californianus*) with PK. (**a**) Stage 1 PK. Right eye with a focal grey corneal opacity located dorsolateral paraxially. There is medial perilimbal edema, and temporally there is pigment beginning to migrate across the limbus and mild hyperemia of the limbus as well. (**b**) Stage 2 PK. Left eye with an irregular dense white corneal opacity with mild corneal vascularization. There is severe pigment migration across the limbus into the adjacent cornea and perilimbal edema. (**c**) Stage 3 PK. There is severe diffuse corneal edema encompassing approximately 75–80% of the cornea with an axial area of stromal loss and cellular infiltrates. The limbus is hyperemic, and medially, there is pigment migration across the limbus

ciliary body (Fig. 38.26). Amyloid is only diagnosed onhistopathologic evaluation.

South American Sea Lions (*Otaria Flavescens*)

South American sea lions develop very similar lesions and progression as Australian sea lions. Perilimbal corneal edema is the initial lesion with migrating pigment over the limbus and eventual loss of demarcation of the limbus by pigmentation. The cornea develops a faint diffuse grey superficial opacity that progresses over time. Corneal ulceration and progression with stromal loss are similar to other species' changes.

Australian Sea Lions (*Neophoca Cinerea*)

In general, the initial lesions in affected Australian sea lions are more similar to those of affected South American sea lions and fur seals. The first lesion evident is perilimbal corneal edema followed by migration of conjunctival pigment; this pigment eventually first covers the temporal limbus and later obscures the entire limbus (Fig. 38.27). In some cases, a mild amount of pigment will migrate into the adjacent cornea. Pinniped keratopathy appears less common and aggressive in Australian sea lions. Factors may or may not be related to the species and possibly related to husbandry.

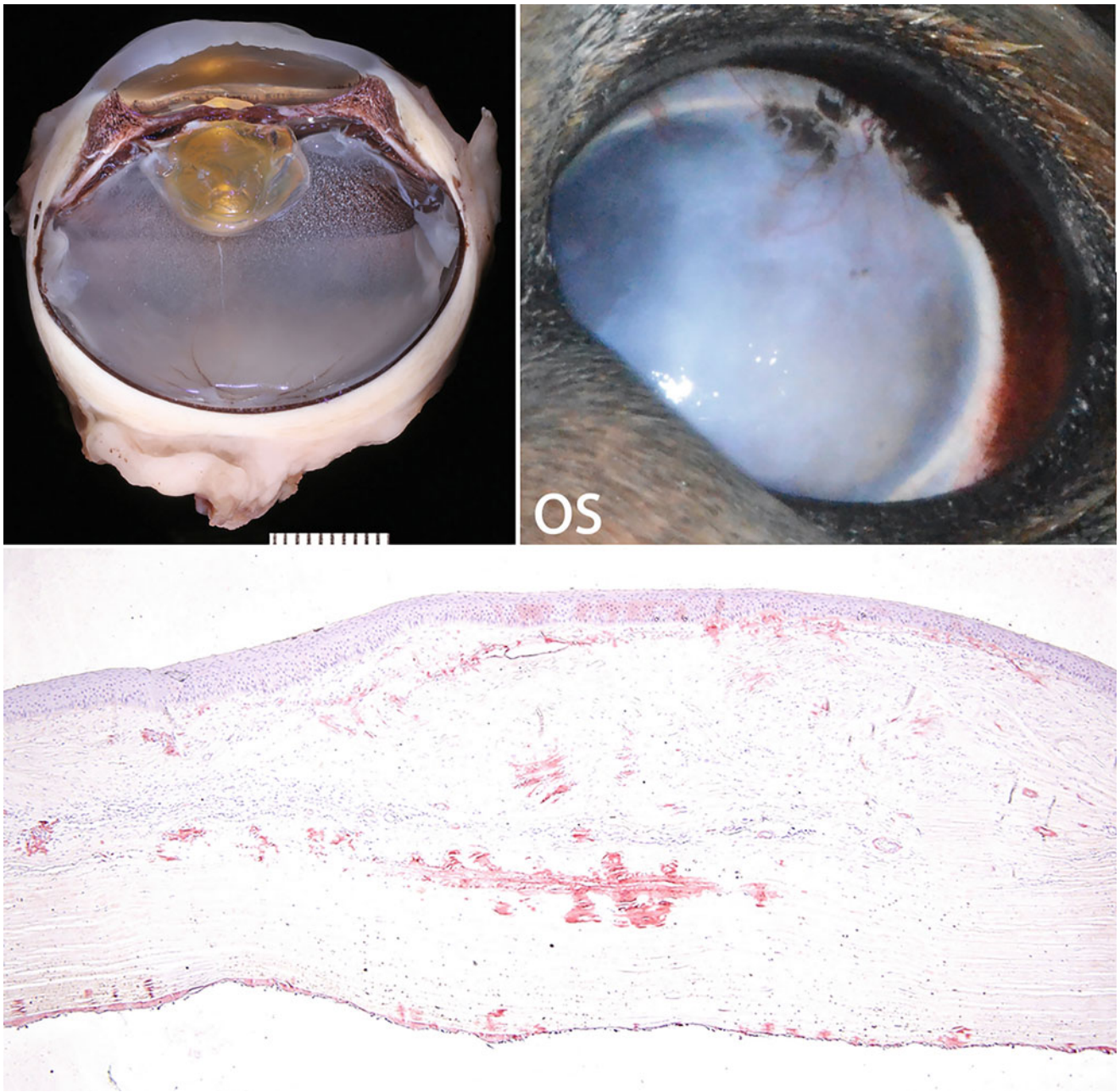

Fig. 38.26 Left eye from a California sea lion (*Zalophus californianus*). Gross image of the globe with numerous abnormalities including a hypermature cataract with lens capsule rupture, a cyclitic membrane causing the lens capsule to be adhered to the pars plicata. The cornea is fibrotic and thickened with a hypereosinophilic acelluar protein material throughout the stroma down to just adjacent to Descemet's membrane. The same material is present in the ciliary body epithelium. The material stained positive with Congo red stain showing a green birefringence typical of amyloid. Images and report courtesy of Comparative Ocular Pathology Laboratory of Wisconsin

Fur Seals

Northern Fur Seals (*Callorhinus Ursinus*)

Very few Northern fur seals are under human care, so their eyes in different environments are not available for comparison with other pinnipeds. One group of Northern fur seals lives in a completely roofed enclosure without excessive, or even mild, exposure to sunlight. Most of the eyes in this colony have minimal PK lesions. The initial identifiable lesion is perilimbal corneal edema. In some affected animals, migration of pigment later ensues over the entire limbus (not just dorsotemporally and temporally as in sea lions) (Fig. 38.28).

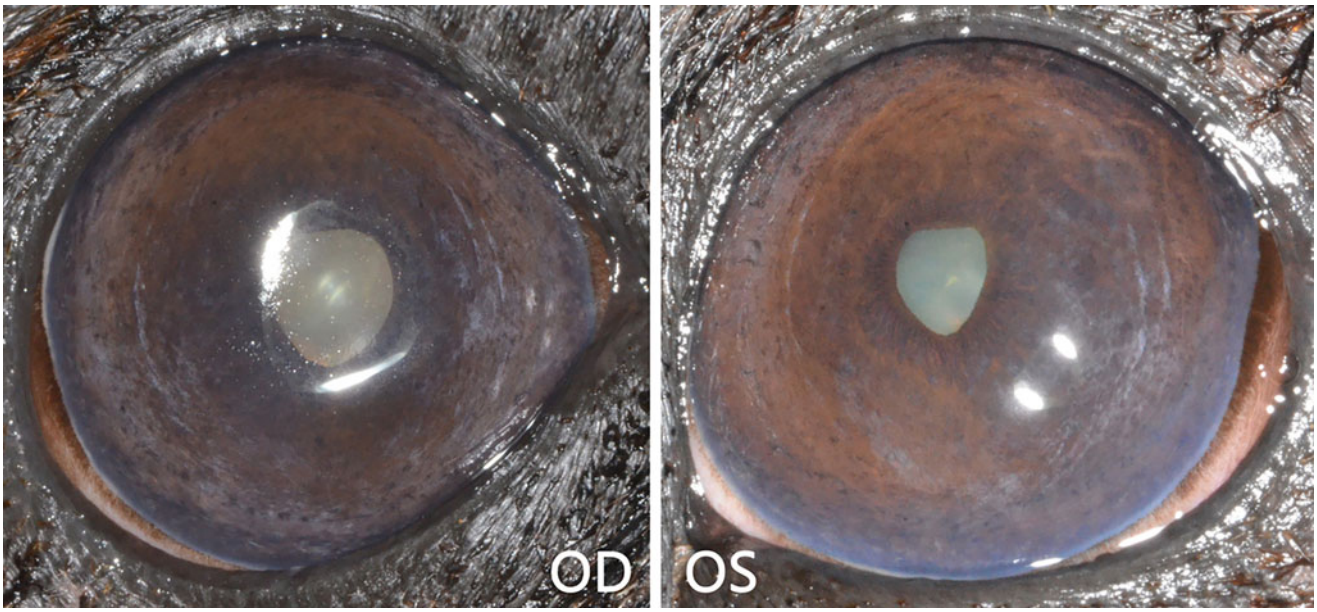

Fig. 38.27 Eyes of an Australian sea lion (*Neophoca cinerea*). There is mild perilimbal corneal edema bilaterally indicative of stage 1 PK. There is also an incipient cataract OU

New Zealand Fur Seals (*Arctophoca Forsteri*)

New Zealand fur seals appear to have similar keratopathy initiation and progression as Northern fur seals. The pigment migration consistently migrates over the limbus with perilimbal edema. As keratopathy progresses, the dorsotemporal corneal quadrant may develop progressive edema, vascularization, ulceration, and mild pigment migration (Fig. 38.28). Diffuse axial corneal edema may also develop. Conjunctival depigmentation is common.

South African Fur Seals (*Arctocephalus Pusillus*)

Of all the fur seals evaluated around the world, South African fur seals appear to be the species that can be more aggressively affected by PK (Fig. 38.28). Certainly, the variables of UV index, water quality, and shade are suspected to be important, however, species susceptibility is also on the list of possibilities.

Their initial clinical signs are similar to those of Northern fur seals and New Zealand fur seals with perilimbal edema. The dorsolateral edema progresses, and there can be ulceration and stromal loss in some eyes, similar to all species with infection and excessive UV exposure. Thin superficial corneal vessels may gradually grow towards the axial cornea within the edematous region. Pigmentation can migrate, even into the axial cornea (Fig. 38.28).

Subantarctic Fur Seals (*Arctocephalus Tropicalis*)

Similar to most other species, perilimbal corneal edema is a subtle initial clinical sign. However, Subantarctic fur seals appear to progress differently from other fur seals. There are very few individual seals of this species in human care, so this description is based only on these few animals. The stage 2–3 lesions are diffuse axial corneal edema that may wax and wane (Fig. 38.28). Further progression to a more advanced stage has not been documented. This subantarctic fur seal developed bilateral corneal edema, and a single cyclosporine implant was placed OU. The OD's axial corneal edema resolved completely, and the OS's edema improved. Then, the OS edema worsened again, and the animal had bilateral cataracts. At the time of bilateral lensectomy surgery at age 12 years, 2 cyclosporine implants replaced the single initial implant. She has been stable since that time 8 years ago (personal communication, Dr. David Blyde).

True Seals

True seals (phocids) were found to have a 51.4% incidence of PK in a recently published worldwide epidemiological study (Colitz et al. 2018b). This incidence is similar to that of otariids.

Harbor Seals (*Phoca Vitulina*)

Harbor seals are the most common phocid species in human care. Normal eyes from a harbor seal are shown for comparison in Fig. 38.5. Harbor seal PK also commonly demonstrates perilimbal to diffuse corneal edema. The next change is dorsolateral to lateral paraxial corneal edema.

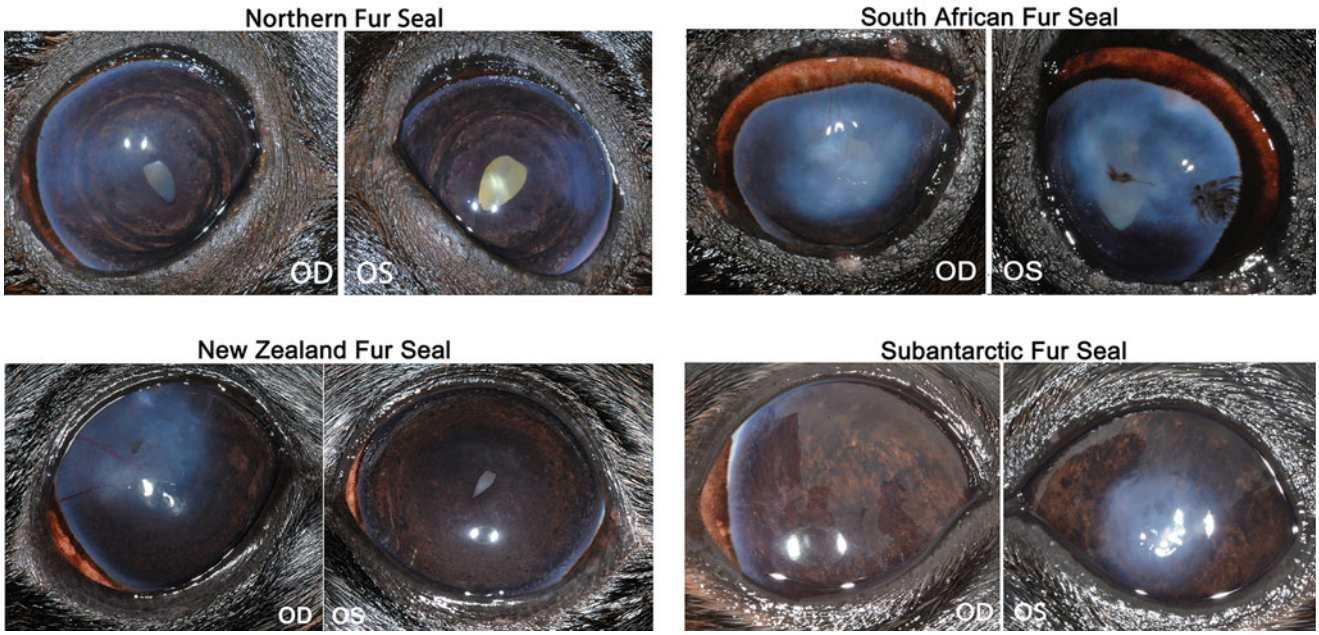

Fig. 38.28 Eyes from 4 different types of fur seals with PK. Northern fur seal *(Callorhinus ursinus)* eyes with perilimbal corneal edema that extends into the adjacent cornea worse in OD than in OS. OD is stage 3 and OS is stage 2 PK. There is also an incipient cataract OU. South African fur seal *(Arctocephalus pusillus)* eyes with stage 3 PK. There is diffuse corneal edema, pigment migration obliterating the limbus, OS has pigment migration into the adjacent and axial cornea, and the conjunctiva is hyperemic. New Zealand fur seal *(Arctophoca forsteri)* eyes with stage 3 pinniped keratopathy OD. There is diffuse corneal edema originating from dorsotemporal to dorsal limbus and extending to the axial cornea with pigment migration across limbus and into the cornea. OS has perilimbal edema as well as an immature cataract. Subantarctic fur seal *(Arctocephalus tropicalis)* eyes with stage 1 PK OD and stage 2 PK OS. OD has perilimbal corneal edema as well as pigment migration across the temporal limbus. OS has dense axial corneal edema and the limbus is not evident. Used with permission from Gulland, F.M.D., Dierauf, L.A., Whitman, K.L. (Eds.). CRC Handbook of Marine Mammal Medicine, third Edition, CRC Press, Boca Raton, pp. 377–412

Separation of the epithelium, often without an obvious ulcer, is also common in harbor seal PK, causing chronic pain. Corneal vascularization is more common in phocids than otariids but still requires a significant infection to initiate this change (Fig. 38.29).

Harp Seals (*Pagophilus Groenlandicus*)

Harp seals are not as numerous in human care as harbor seals. Both species develop corneal lesions similar to California sea lions, i.e., dorsotemporal paraxial grey opacities consistent with fibrosis, perilimbal edema, loss of limbal demarcation due to pigment migration, bullae, and ulcers with or without abscessation (Fig. 38.30).

Hawaiian Monk Seals (Monachus Schauinslandi)

PK in Hawaiian monk seals differs from lesions in other phocid species. Affected animals have extensive loss of epibulbar conjunctival pigmentation with patchy migration of pigment crossing the adjacent limbus, in addition to mild perilimbal vascularization.

Progressive corneal fibrosis and edema result in increased generalized opacification due to already discussed risk factors (Fig. 38.30).

Grey Seals (*Halichoerus Grypus*)

Grey seals, unfortunately, have the most severe PK lesions of not only all phocid species, but also all the pinniped species, with limbal hyperemia and vascularization crossing the limbus into the adjacent cornea. The cornea develops dense corneal edema and fibrosis, as well as a chalky white corneal opacity. Pigmentation may progress to involve the majority of (or even the entire) cornea (Fig. 38.30).

Leopard Seals (*Hydrurga Leptonyx*)

Very few leopard seals have been rescued and maintained in human care. The lesions observed were minimal and included limbal hyperemia and perilimbal edema (Fig. 38.30). No corneal lesions were identified (personal observation, Colitz).

Walruses (*Odobenus Rosmarus*)

There are fewer walruses in human care than other species. The reported incidence of keratopathy is 62.5%. Clinical signs include perilimbal corneal edema, limbal hyperemia, and some pigmentation that crosses the limbus (Fig. 38.31). Clinical signs are similar to those present in phocids. The

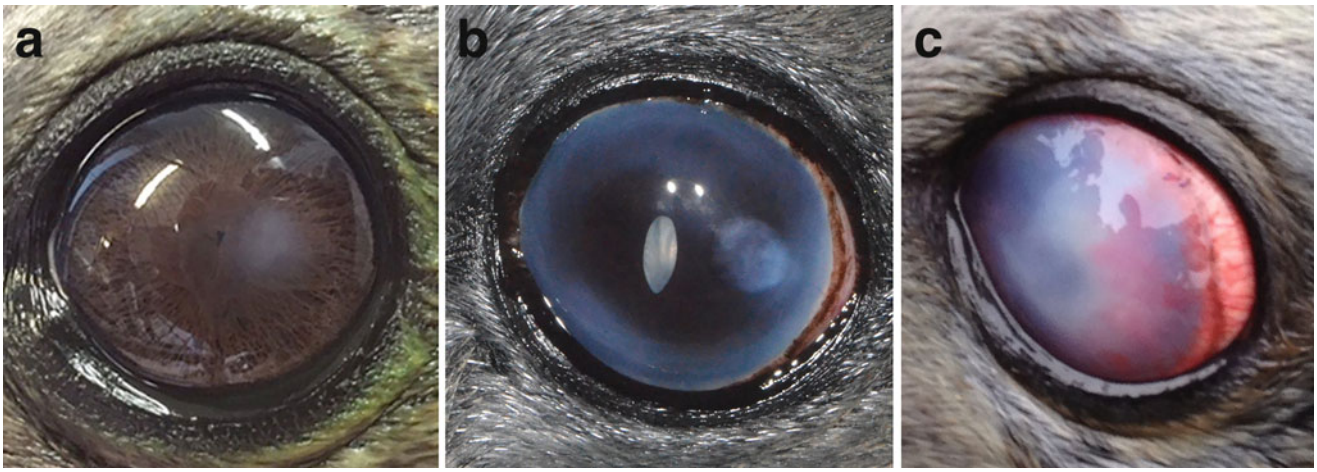

Fig. 38.29 Three eyes from 3 harbor seals (*Phoca vitulina*). (**a**) Stage 1 PK with a small area of focal mild corneal edema. (**b**) Stage 2–3 PK. The eye has severe perilimbal corneal edema, pigment migration across the limbus and conjunctival depigmentation. The cornea has a dense round grey-white opacity located temporally. There is also a late immature to mature cataract. (**c**) Stage 3 PK. There is severe diffuse corneal edema with intense vascularization. The limbus has pigment migration as well as intense hyperemia, and the temporal conjunctiva is depigmented

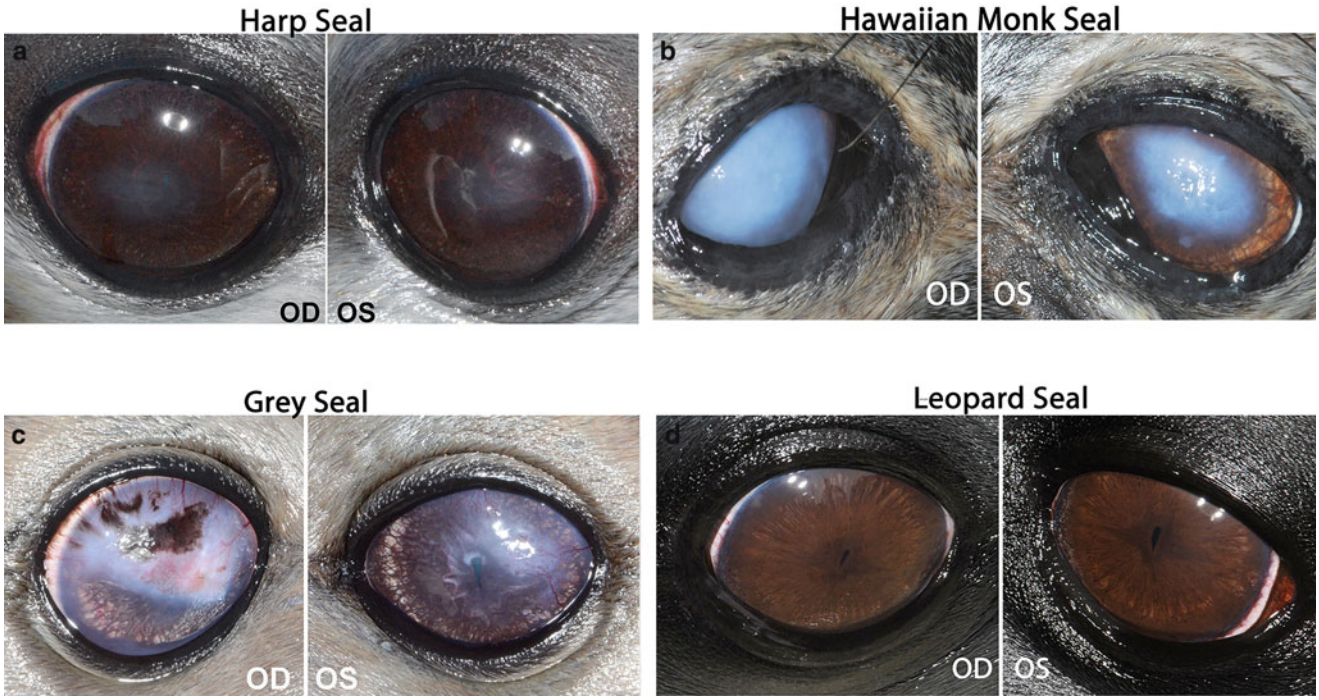

Fig. 38.30 Eyes from 4 species of phocids. (**a**) Stage 1 PK in a Harp seal (*Pagophilus groenlandicus*). There is lateral conjunctival depigmentation, pigment migration over the limbus, and faint oval grey corneal opacities located just dorsotemporal to the axial cornea. (**b**) Stage 3 PK in a Hawaiian monk seal (*Neomonachus schauinslandi*). Both eyes have severe diffuse corneal edema and presumed fibrosis. OD appears worse than OS. No other changes can be seen due to eyes not being completely open. (**c**) Stage 3 OD and stage 2 OS PK in a Grey seal (*Halichoerus grypus atlantica*). OD has severe corneal edema and vascularization with sparse, dense pigmentation. The limbus is hyperemic. The OS has mild to moderate corneal edema and vascularization. (**d**) Stage 1 PK in the earliest stage from a Leopard seal (*Hydrurga leptonyx*). There is limbal hyperemia with mild perilimbal corneal edema. Used with permission from Gulland, F.M.D., Dierauf, L.A., Whitman, K.L. (Eds.). CRC Handbook of Marine Mammal Medicine, third Edition, CRC Press, Boca Raton, pp. 377–412

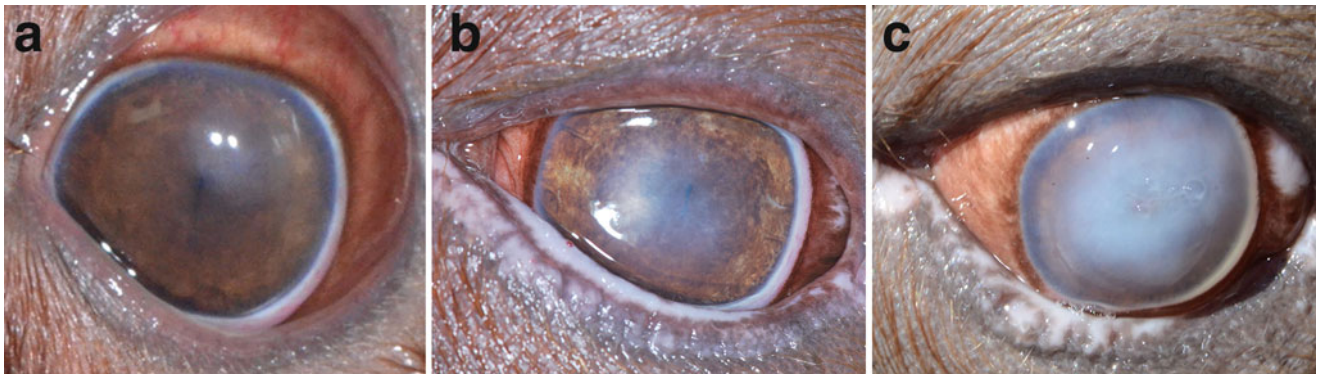

Fig. 38.31 Three eyes from 3 walrus (*Odobenus rosmarus*). (**a**) Stage 1 PK OS. There is mild perilimbal corneal edema, mild pigment migration across the limbus, and a small focal area of corneal edema located dorsotemporal to the axial cornea. (**b**) Stage 2 PK OS. There is hyperemia of the temporal limbus and perilimbal corneal edema of the medial limbus. There is diffuse edema of the axial cornea encompassing approximately 20–30% of the cornea. (**c**) Stage 3 PK OS. There is severe corneal edema encompassing the entire cornea, with numerous superficial bullae evident. The temporal limbus has pigment migration, and the temporal conjunctiva is depigmented. The ventral eyelid is also depigmented

initial lesion is a small axial diffuse grey corneal opacity, and it usually progresses in size. Some eyes will develop a corneal ulcer and/or a stromal abscess. If the underlying problem is not addressed, such as environmental issues, for example, the opacity will eventually encompass a significant portion of the cornea.

Juvenile California Sea Lions

Younger California sea lions (approximately two to three years of age) maintained on the west coast of the United States may develop a unique variant of PK termed Juvenile Pinniped Keratopathy (JPK). Manifestation in affected eyes starts with an acute onset of severe diffuse corneal edema with few to numerous medium to large-sized bullae (Fig. 38.32). Only animals on the west coast of the United States, and one animal that had been transported from California to the east coast, have developed JPK. Clinical improvement is gradual, and it can take up to one year for affected eyes to become relatively stable (Fig. 38.32). Supportive medical care includes broad-spectrum topical and oral antibiotics to address opportunistic bacteria, oral or compounded topical doxycycline to avoid malacia, and pain control as needed. Once stabilized, topical 0.02% or 0.03% tacrolimus ophthalmic drops administered twice daily appear to induce quiescence (Colitz et al. 2018a) (Colitz personal observation). Affected eyes will develop typical PK within a few years of JPK becoming quiescent. The cause of JPK is unknown though may be due to the same reasons as other previously discussed causes of PK. However, identifiable stressors may be very minimal and not affect other juvenile sea lions. Therefore, individual susceptibility may also be a factor. Subconjunctival cyclosporine implants (two per eye) have worked well to control the disease and have been documented to last up to two years before the eyes require new implants.

Medical Management of Active Pinniped Keratopathy

Clinical signs of active PK include blepharospasm, epiphora, periocular crusty brown-black debris adhered to eyelid fur, perilimbal to diffuse corneal edema, corneal bullae, pinpoint to the large indolent ulcer with or without subjacent corneal stromal ulcer, and corneal abscessation. It is important to address secondary bacterial, fungal, and/or yeast infections in order to diminish the risk of progression with possible descemetocele formation or corneal perforation. Concurrent fungal or yeast infections appear to be more common in colder months of the year (personal observation, Colitz). Pain and inflammation must be addressed with the administration of oral nonsteroidal-antiinflammatory medication such as carprofen or meloxicam; tramadol and/or gabapentin are often needed as well. Thus far, every phocid and otariid patient has had an indolent ulcer (chronic corneal erosion, with nonadherent epithelium) component (personal observation, Colitz). Therefore, training the patient to tolerate debridement under topical anesthesia is ideal, though not always possible. The optimal procedure for an uncomplicated indolent ulcer is debridement with a dry sterile cotton-tipped applicator followed by diamond burr keratotomy. If this is not possible, then epithelial debridement with a sterile cotton-tipped applicator alone is recommended. Debridement may be needed more than once. A new medication called EyeQ Amniotic Eye Drops (by VETRIX) contains many beneficial growth factors, including epidermal growth factor, basic

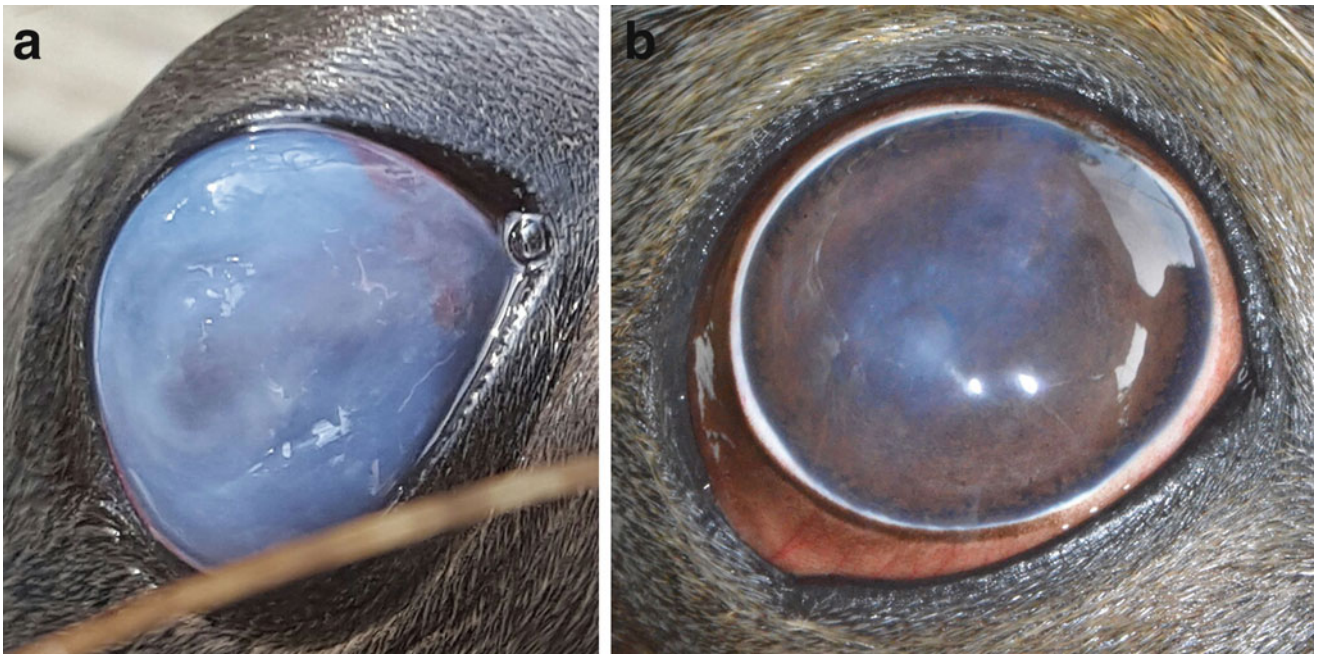

Fig. 38.32 Right eye of a juvenile California sea lion (*Zalophus californianus*). (**a**) At the most severe, the cornea was severely edematous, and the stroma was very irregular throughout. There was vascularization growing in from the medial aspect. (**b**) A year later, the cornea had recovered impressively and showed mild to moderate corneal edema and mild fibrosis. There was very mild pigment migration into the temporal limbus

fibroblast growth factor, and transforming growth factor-beta. These growth factors have antimicrobial properties, help decrease inflammation, and increase limbal stem cell activity and cellular differentiation (Baradaran-Rafii et al. 2017).

The most common bacteria present in a closed or semi-closed LSS include *Pseudomonas* spp. and coliforms; in addition, fungal and yeast organisms including *Candida albicans and Aspergillus* spp. have also been isolated. Bacteria that have been cultured from corneal ulcers include *Vibrio* spp., *Pasteurella* spp., *Morganella morgani, Acinetobacter baumannii, Klebsiella pneumoniae, Enterococcus sp, Plesiomonas shigelloides, Aeromonas hydrophila, and Edwardsiella tarda*. The conjunctival flora from healthy and diseased grey seal (*Halichoerus grypus)* eyes was identified in one study in the United Kingdom (Fleming and Bexton 2016). The most common bacteria isolated from healthy eyes included *Gemella haemolysans, Escherichia coli, Clostridium perfringens, Streptococcus oralis, and Streptococcus mitis*. A variety of other microorganisms were also isolated from normal eyes, although 23 samples did not yield any bacterial growth. Microorganisms from superficial corneal ulcers included *Bifidobacterium* spp., *Clostridium perfringens, Escherichia coli, Streptococcus agalactiae, Klebsiella pneumoniae, Proteus* spp., and *Acinetobacter lwoffii*. Melting ulcers were all infected with *Pseudomonas aeruginosa*. Perforated corneas were infected with *Streptococcus mitis, Gemella haemolysans, and Comamonas testosterone* (Fleming and Bexton 2016).

Bacterial multidrug resistance is common, specifically by *Pseudomonas aeruginosa* and *Acinetobacter baumannii* (Potron et al. 2015). Gram-negative organisms acquire resistance to quinolones due to mutations in the efflux pump regulation systems or chromosomal mutations in genes that encode topoisomerases. Quinolone resistance genes have been identified in Enterobacteriaceae.(Potron et al. 2015) Since resistance to quinolones is so prevalent, the author usually avoids topical quinolones unless aminoglycosides are ineffective or poorly effective. Following cataract surgery, when the animal will be dry docked, quinolones may be used as part of the recovery regimen.

Antibiotic Treatment

Overall, there are few major differences in the topical antibiotics chosen for pinniped ocular therapy when compared to other species. However, *Pseudomonas* spp. have the potential for resistance to quinolones or can acquire resistance after a few weeks, as discussed previously. Therefore, long-term quinolone use is not recommended. Instead, an aminoglycoside such as tobramycin should be chosen. Compounded amikacin is also used when tobramycin or gentamicin are ineffective. Coliforms are typically sensitive

to neomycin-polymyxin-gramicidin (aka triple antibiotic solution or neopolygram). Polymyxin B sulfate and Trimethoprim ophthalmic solution, is a viable option for pinnipeds as an alternative to neopolygram as it also will address some coliforms and other bacteria. If the eye is held closed and drops are not feasible, then oral antibiotics to address the same spectrum are chosen, such as enrofloxacin or ciprofloxacin with amoxicillin-clavulanic acid as a good combination. Oral or topical compounded doxycycline is always included in the treatment regimen, more for its healing properties than its antibiotic properties as it inhibits keratomalacia, speeds re-epithelialization, and has anti-inflammatory properties. (Perry et al. 1986; Chandler et al. 2005; Bahrami et al. 2012) Topical solutions or suspensions are used in pinnipeds because ointments may be more difficult to administer in some patients.

Antifungal Treatment

If a fungal or yeast infection is diagnosed or suspected, antifungal medications can be used topically or orally. The most common antifungals that have been used include oral fluconazole and oral or topical voriconazole. However, since the triazoles are static antifungal medications, the use of compounded topical terbinafine ophthalmic drops has been used to successfully treat fungal keratitis in pinnipeds and other species. Oral terbinafine, which is a cidal antifungal, is safe and would be an excellent choice, though it is not yet routinely used in pinnipeds.

Pain Management

Oral carprofen and meloxicam are the most commonly used nonsteroidal anti-inflammatory medications (NSAID) and are indicated for pain and inflammation associated with PK. Topical nonsteroidal anti-inflammatory medications such as ketorolac and nepafenac should be avoided or used judiciously, as they may slow healing and may be associated with malacia.(Gaynes and Onyekwuluje 2008) Pinnipeds do not develop corneal vascularization to a significant degree compared with other species, so the use of oral NSAID medications has not made a significant difference in corneal vascularization or in corneal ulcer healing compared with not using oral NSAIDs. Oral tramadol or gabapentin is also important therapies when significant pain is present. Tramadol dosing depends on the individual, so initial under-dosing is advised with a gradual increase of the dose, as needed. A benefit of tramadol use is it allows for a lower dosage of oral NSAIDs.

Procedures

Since PK has a consistent indolent ulcer component, the lesions should be addressed using debridement and diamond burr keratotomy (Dawson et al. 2017), if appropriate for patient and infection controlled. Some animals have been desensitized to allow this procedure while awake, utilizing topical anesthesia, behavioral control, and premedication with tramadol. If this is not possible, the risk of anesthesia should not be taken lightly without an experienced anesthesiologist or marine mammal veterinarian. Pinnipeds have very strong retrobulbar muscles, therefore, application of topical anesthesia prior to manipulation of the globe is important.

Pinniped Keratopathy Control

For the past 15 years, topical immunomodulators tacrolimus and cyclosporine have been used to control PK. Currently, the optimal therapy is tacrolimus 0.02% or 0.03% topical emulsion in MCT, at a frequency of one drop two or three times daily. The aqueous formulation of tacrolimus is available but unstable, as per the manufacturer, therefore, the emulsion is more commonly used. Episcleral subconjunctival cyclosporine implants have also been beneficial for long-term PK control (Fig. 21) (Colitz et al. 2016; Staggs et al. 2013). Two implants per eye are inserted, lasting approximately two years, at which time they can be replaced. In pinnipeds that have not yet developed PK, the implants delay the onset of disease by at least six years (personal observation, Colitz). It must be emphasized that if the environmental factors are not addressed, particularly water quality and shade, the immunomodulators will not be as efficacious. They are not a miracle therapy.

Other Considerations about Keratopathy

Corneal lesions directly related to excessive exposure to ultraviolet radiation (UV) include loss of keratocytes (corneal stromal fibroblasts), development of corneal vascularization and fibrosis, corneal stromal thinning, and corneal perforation, without active or obvious infection (Newkirk et al. 2007). Exposure to UV up-regulates the production of matrix metalloproteinases 2 and 9 (Chandler et al. 2008). Matrix metalloproteinase-9 is released by keratocytes, some bacteria and fungi, and by neutrophils resulting in stromal loss and infected corneal ulcers and abscess formation. The combination of chronic exposure to UV, imbalances in the environmental factors, and recurrent infected corneal ulcers or abscesses explains why the corneas of marine mammals often have many of these abnormalities.

So far, viruses have not been isolated from active PK lesions. However, many viruses have been isolated from pinniped eyes. In one study, phocine herpesvirus-1 (PhHV-1) DNA was recovered from six percent of the eyes tested (Roth et al. 2013). All of these animals were under one year of age and were asymptomatic. Another study attempted to assess whether corneal lesions in stranded pinnipeds had a viral cause (Wright et al. 2015). Three pinniped species were evaluated, including California sea lions ($n = 29$), Northern elephant seals ($n = 18$), and Pacific harbor seals ($n = 34$).

The majority of the animals with ocular lesions had keratoconjunctivitis. A variety of bacterial organisms were cultured from the conjunctivas of affected and unaffected animals. Viral DNA from a variety of viruses was detected in 58% of ocular samples from affected and unaffected animals. Three novel adenoviruses and two novel herpesviruses were detected. While viruses appear to be common in the eyes of pinnipeds, there was no correlation found between viral infection and the presence of ocular lesions. A significant limitation of this study was not having a veterinary ophthalmologist perform ophthalmic examinations using slit-lamp biomicroscopy to better describe lesions (Wright et al. 2015). Therefore, subtle ocular lesions may have been overlooked. It is still possible that viral infections may have some role in ocular diseases in pinnipeds, and further investigation is warranted.

Anterior Uvea

The irides of pinnipeds are typically brown. However, some pinniped eyes have heterochromia iridis, or areas of iridal hypopigmentation ranging from trace to extensive (Fig. 38.33). It is unclear if these hypopigmented sites are areas of iris hypoplasia. Progressive iridal depigmentation has been identified in a few pinniped eyes, and was suspected to be secondary to uveitis. In another pinniped, a traumatic iris laceration was caused by a sea urchin spine (Fig. 38.34). In this animal, a fibrous band extended medially from the temporal iridocorneal angle to attach adjacent to the iridal laceration and was unchanged over several years. Two elderly pinnipeds were diagnosed with systemic hypertension clinically manifested as prominent iridal vessels and hyphema (Fig. 38.35).

Lens

Lens diseases, i.e., cataract and lens instability (subluxation or luxation), are common both in pinnipeds in the wild and in human care. The identified risk factors for pinniped cataracts in human care include aging ($\geq$ 15 years of age), a history of fighting, a history of any eye disease (most commonly PK), and lack of shade (i.e., exposure to excessive UV light or sunlight) (Colitz et al. 2010b). In one study, pinnipeds had a 46.8% incidence of lens diseases, including cataracts and lens instability. This study also showed a gradual increase in the incidence of cataracts as the animals aged. There was a 21% incidence of cataracts in pinnipeds as young as six to ten years of age; those between 11 and 15 years of age had a 58% incidence of cataracts; those between 21 to 25 years of age had an 87% incidence of cataracts, and animals over 25 years of age had a 100% incidence of cataracts (Colitz et al. 2010b). If this study

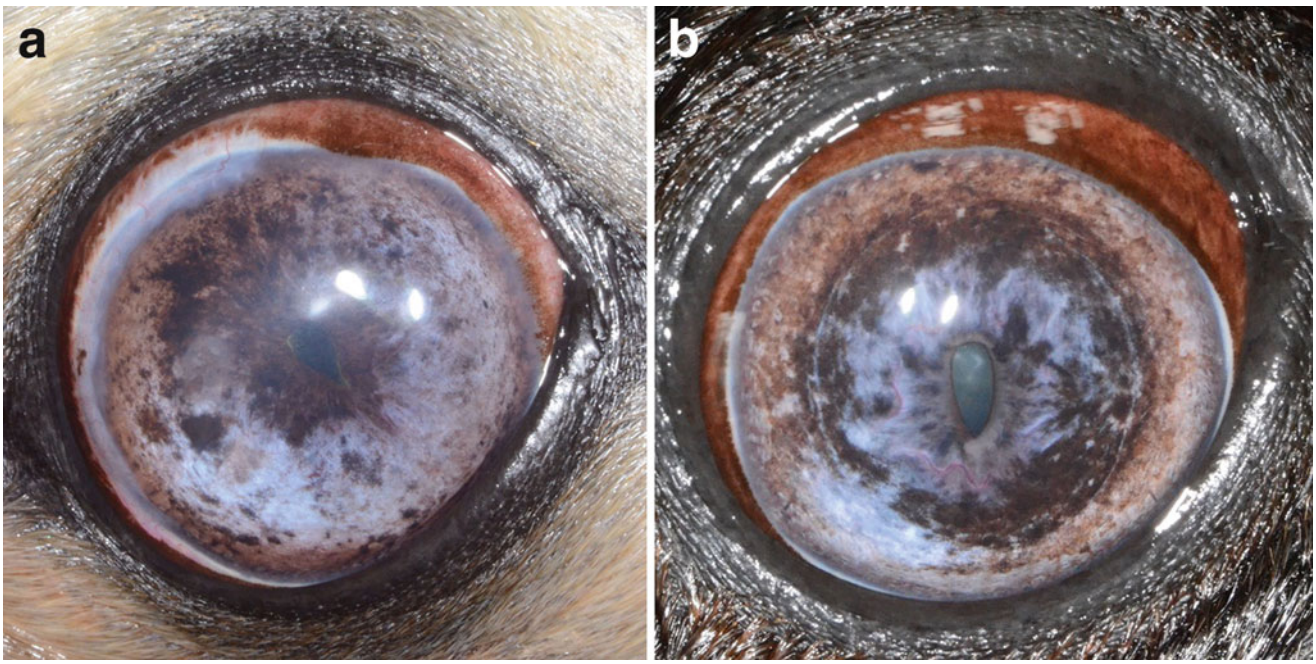

Fig. 38.33 Two eyes from two different sea lion species. (**a**) Right eye from a California sea lion (*Zalophus californianus*) that had undergone lensectomy for a progressing cataract. There is limbal incisional fibrosis with inactive vascularization. The iris has diffuse heterochromia. (**b**) Right eye from a South American sea lion (*Otaria flavescens*). There is perilimbal corneal edema pigment migration over the limbus and an early immature cataract. The iris has diffuse heterochromia

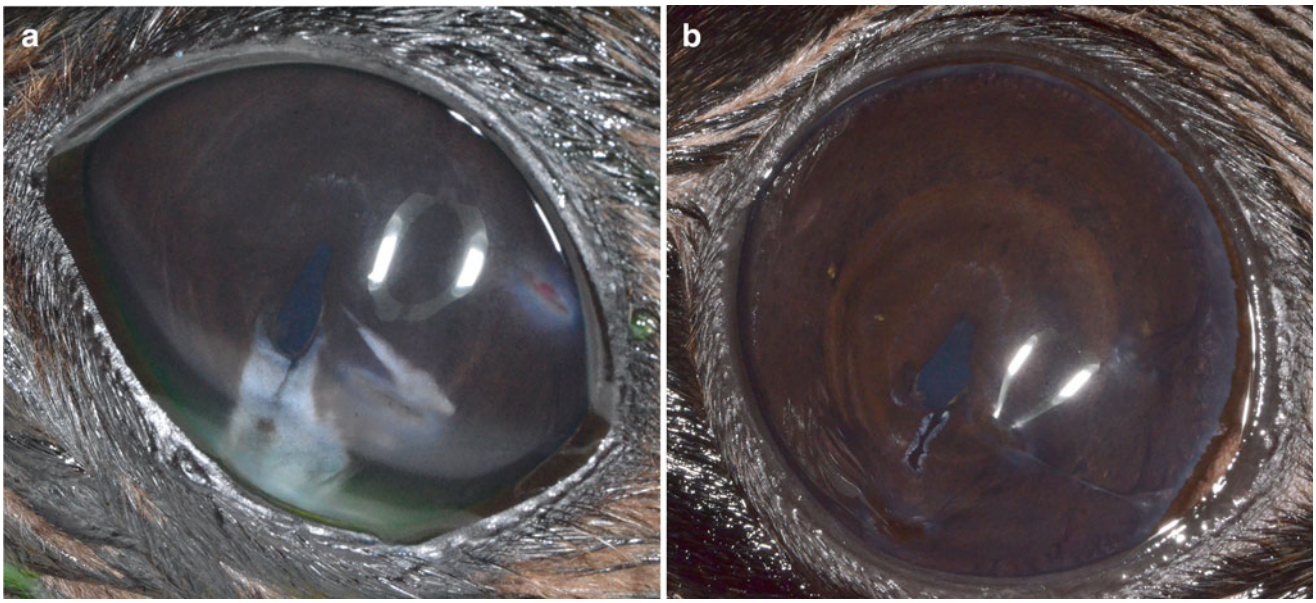

Fig. 38.34 Left eye from a young New Zealand fur seal (*Arctocephalus forsteri*) at presentation and 2 years later. (**a**) Left eye with a subacute full-thickness corneal penetrating injury that lacerated the ventral and temporal iris. The corneal injury is located dorsotemporally and still has a small amount of fibrin in the wound. (**b**) Left eye of the same animal 2 years later

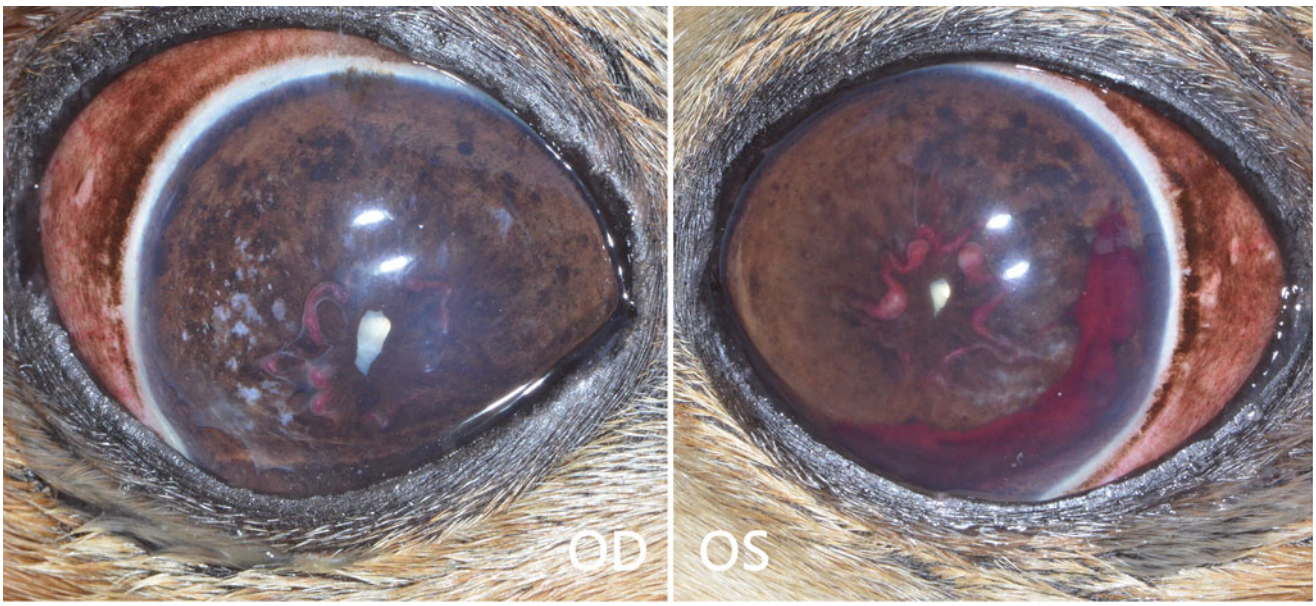

Fig. 38.35 Both eyes from a California sea lion (*Zalophus californianus*) with systemic hypertension. OD has mild pigment at dorsal limbus and adjacent cornea. The arterial circle is prominent and engorged and mild dyscoria, and there is a mature cataract. OS also has a prominent engorged arterial circle, dyscoria, and settled hyphema as well as a mature cataract

were to be repeated with more animals being evaluated, even the 0–5 year of age group would include animals with cataracts. The most important significant variable was that lack of adequate shade increased the risk of cataracts tenfold (Colitz et al. 2010b).

Cataracts and lensinstability (Fig. 38.36) tend to occur in high-risk animals; as a result of advancements in anesthetic protocols for pinnipeds, intracapsular or extracapsular lensectomy surgeries are now commonly performed (Colitz et al. 2018a; Colitz and Bailey 2019). Surgical lensectomy

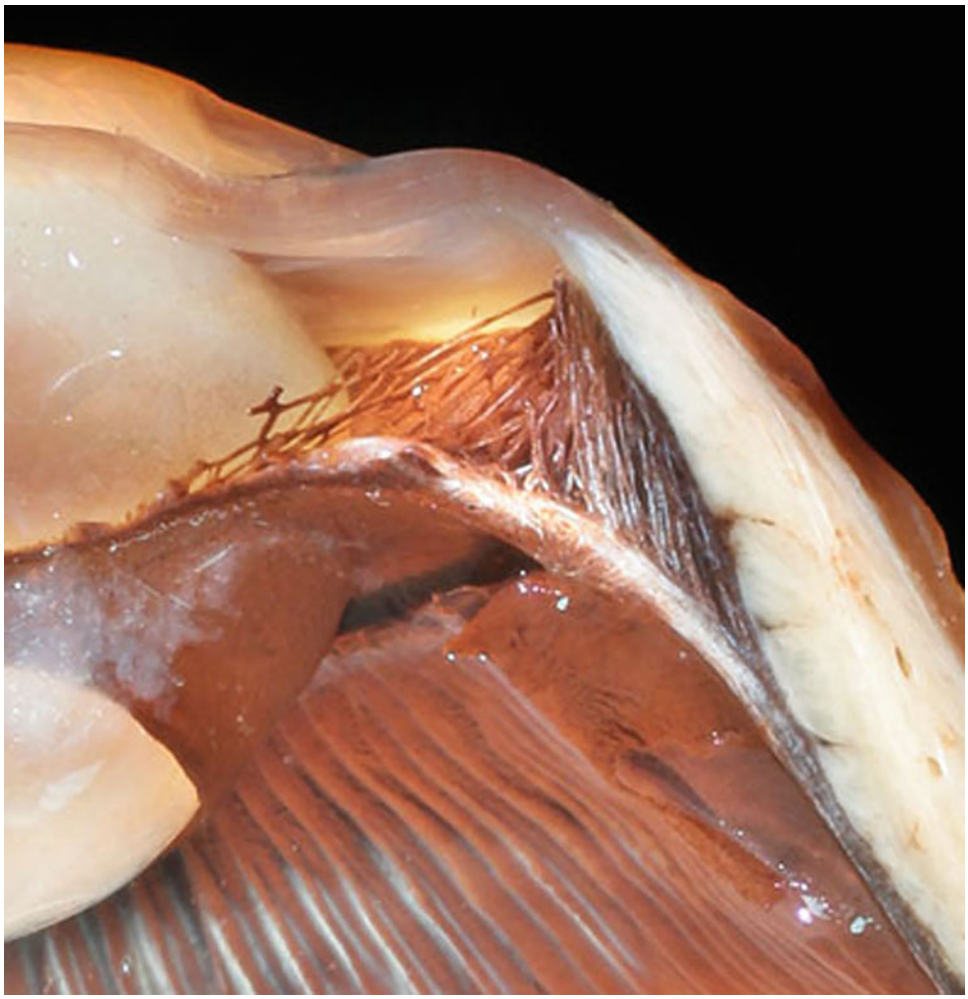

Fig. 38.36 Subgross image of a harbor seal (*Phoca vitulina*). This globe has an anterior lens luxation, and the lens is seen to be suspended on the anterior surface of the iris. The pectinate ligaments are evident on the anterior face of the iridocorneal angle and extending onto the iridal surface. The ciliary bodies are long and slim. Courtesy of the Comparative Ocular Pathology Laboratory of Wisconsin

has beenshown to improve visual confidence, successfully return the animal to routine training programs, and regain their status in socialgroups (Grubb et al. 2011). Surgery has been successfully performed on hundreds of pinnipedswith cataracts, with or without anterior lens luxations (Colitz et al. 2018a). However, finding a way to delay the onset of visually impairing cataracts, by even five years, may allow affected animals to avoid surgery and have longer productive functional lives.

Many factors impact the successful outcome of any ocular surgery in pinnipeds. An experienced and skilled ophthalmologist, anesthesiologist, and support team are essential. Controlling stress in the patient is very important, and this requires thoughtful foresight in preparing the patient for the events of the surgery day. The stress level of the patient on surgery day will be lessened by training and desensitization prior to surgery day, i.e., training to enter the squeeze-cage and allow the cage to squeeze the animal, training to allow an injection with or without squeezing in the squeeze-cage, and training the animal to breathe anesthetic gas (i.e., sevoflurane) through an anesthetic cone mask without avoidance of the cone. Training the animal for a successful postoperative period is essential, including the animal must be acclimated to being dry docked for up to three weeks without incurring excessive anxiety, consistently targeting for eye drops, making sure the animal will eat during the dry-dock period, consistently stationing the animal for eyedrop administration as well as high-resolution ocular photographs and physical examinations, consistently stationing the animal for tonometry using an Icare® TonoVet tonometer, training the animal to tolerate ocular examination with a slit-lamp biomicroscope under dimmed conditions, if possible. Other important useful medical behaviors include voluntary blood sampling, ocular ultrasound, and other tasks. Trainers are essential in the entire process due to the strong bond of trust between trainer and animal.

The ideal patient is one with progressive cataracts that have not luxated anteriorly (Fig. 38.37) and is either unaffected by PK or has controlled PK. Post-operatively, these eyes will have healthy, clear corneas. The goal of

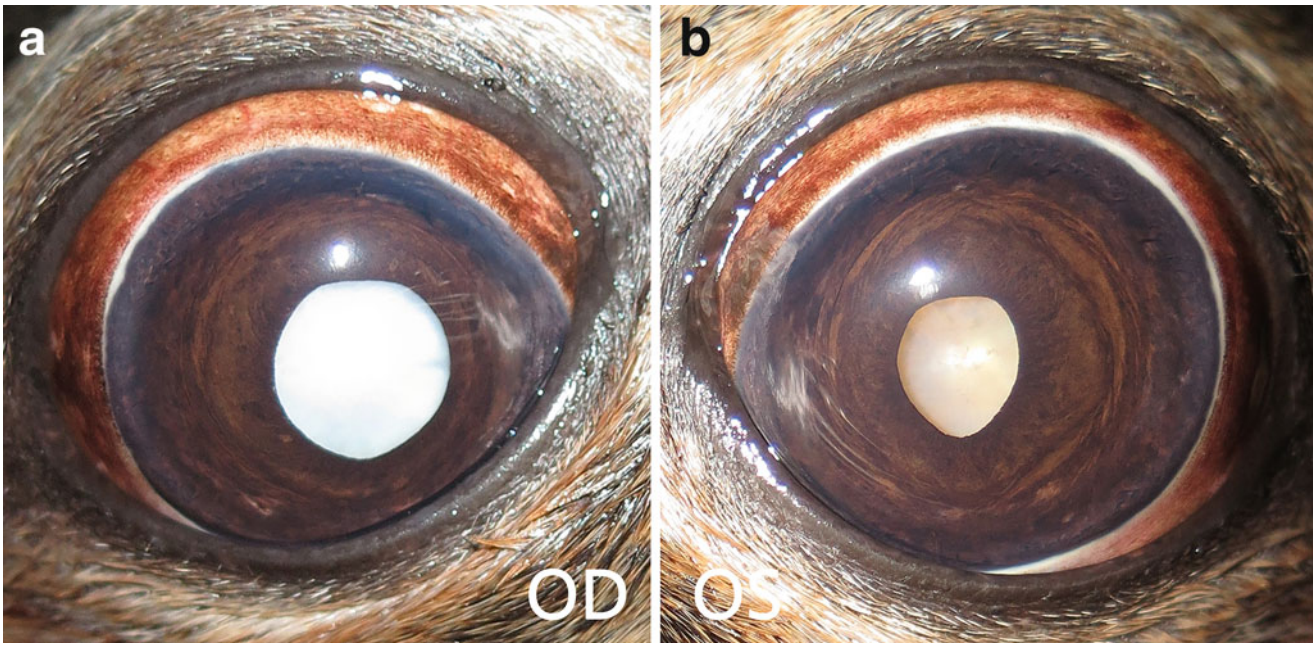

Fig. 38.37 Both eyes from an Australian sea lion (*Neophoca cinerea*) with cataracts. (**a**) OD has a mature cataract, and its pupil is more mydriatic than OS under the same light conditions. The pupil's mydriasis is significant as it indicates that the cataract is likely unstable. (**b**) OS has a late immature cataract. Neither retina was detached

intracapsular lensectomy with an anteriorly luxated lens is to alleviate pain and to regain sight (Fig. 38.38). Once animals with acute to subacute anterior lens luxations have undergone lensectomy surgery, the eyes heal with minimal to no corneal damage inflicted by the prior lens luxation. Most animals with chronic anterior lens luxations will still regain sight post-operatively and will have a resolution of pain. However, these eyes will have variably sized regions of corneal fibrosis but will have sight (Fig. 38.38).

Concurrent corneal ulceration is relatively common (personal observation, Colitz). In some cases, corneas did not retain fluorescein dye preoperatively, but the separation of the corneal epithelium from its underlying stroma is present and debrides as an indolent ulcer. In these patients, the entire superficial epithelium is loose and easily debrided, then, a diamond burr keratotomy was usually performed following the lensectomy (personal observation, Colitz). This allows successful re-epithelialization in most eyes, though some still require a second debridement. The recent addition of EyeQ amnion eyedrops (Vetrix) has been beneficial in patients with corneal ulcers at the time of surgery.

Medial strabismus is a species-specific abnormality that occurs only in blind California sea lions (Fig. 38.39). If medial strabismus is identified in the early stages, physiotherapy to keep the medial rectus muscle from contracting has stopped its progression. This occurs only in blind pinniped patients and is thought to be due to lack of visual stimulus (personal observation, Colitz, and comment from Richard R. Dubielzig). In two severely affected patients, the medial rectus muscle was transected at the time of lensectomy to allow improved globe movement. However, at rest, the globe reverted back to its medial position.

Pinniped lenses are spherical, very dense, and large. A two-year-old California sea lion that had stranded and was rescued had a cataract that was already so dense that phacoemulsification was unsuccessful. The lens was also luxated, requiring conversion to an open sky extracapsular lensectomy. The vitreous in this animal was severely degenerated. This patient had a chronic cataract with either underlying uveitis or secondary uveitis, causing vitreal synaeresis. Successful phacoemulsification has been performed on pups and one yearling pinniped (Colitz et al. 2011a; Esson et al. 2015).

While retinal detachment is a risk of chronic cataracts in other species, it is not common in adult pinnipeds born in human care that developed cataracts due to aging, exposure to UV, or other risk factors previously described (Colitz, personal observation). However, retinal detachments have been diagnosed in many stranded California sea lions, regardless of age at the time of stranding. The eyes from these animals had liquefied (i.e., degenerated) vitreous at the time of surgery and developed retinal detachments within months to a few years following surgery. Lensectomy in pinnipeds with known preoperative retinal detachments has been

Fig. 38.38 Both eyes from a 17-year-old California sea lion (*Zalophus californianus*) before and after lensectomy surgery. (**a**) OD with the anteriorly luxated lens that has age-appropriate nuclear sclerosis. There is perilimbal corneal edema and vascularization. The cornea is also edematous where the lens is touching. (**b**) OS with anteriorly luxated cataractous lens and moderate to severe corneal vascularization and limbal hyperemia as well as diffuse edema. (**c**) OD post-operatively with limbal fibrosis and moderate corneal fibrosis where the lens had been touching for a few months. (**d**) OS post-operatively with limbal fibrosis and vascularization and dense corneal fibrosis where lens had been touching longer than in OD

performed in order to retain a cosmetic globe despite being blind. Similar to other species, eyes with retinal detachment are predisposed to secondary glaucoma (personal observation, Colitz).

An important aspect of lensectomy in pinnipeds is that the lens capsules must be removed in their entirety, if possible. Post-operative anterior and posterior capsular opacification is aggressive in pinnipeds resulting in diminished sight or blindness (Fig. 38.40). In those patients in which a second

Fig. 38.39 Left eye of a California sea lion (*Zalophus californianus*) with medial strabismus and an anteriorly luxated cataractous lens

surgery was required, removal of the retained lens capsule has been successful, and sight was regained.

Ketorolac and nepafenac are the most commonly used topical nonsteroidal anti-inflammatory medications, with nepafenac being superior to ketorolac for immediate post-operative use. Commonly used oral nonsteroidal anti-inflammatory medications include carprofen and meloxicam. Topical corticosteroids are reserved for immediate pre- and post-operative care of lensectomy patients. Oral prednisone is used in patients post-operatively that are known for not eating well under stress and in patients without known corneal ulcers.

Post-Operative Complications

Harbor seals appear to be predisposed to lipid keratopathy post-operatively, and the concurrent use of topical corticosteroids may promote lipid deposition. The cause is unknown, and anecdotally, affected animals tend to be heavier (Fig. 38.41). It is possible that they have hypertriglyceridemia, although this has not been investigated. Recently, a harbor seal had cataract surgery, and corticosteroids were not used at all due to concurrent bilateral corneal ulcers. The corneas in that animal did not develop lipid infiltrates suggesting that the use of topical steroids may have played a role in the deposition of lipid in the other seals. Harbor seals with anterior lens luxations are unique in that at the time of surgery, the cornea surrounding axial corneal edema and fibrosis may develop progressive corneal endothelial degeneration post-operatively. This is different from other pinnipeds where peripheral corneal edema resolves in the area surrounding the permanent corneal fibrosis, thereby regaining transparency.

Hyphema is an uncommon clinical sign and has been seen as an intraoperative and post-operative complication. The use of dexmedetomidine as part of the preanesthetic protocol has been associated with mild to moderate intraoperative hyphema, even if the drug is reversed prior to starting surgery. Post-operative traumatic hyphema has occurred as well. While most cases resolve in a few days, an intracameral injection of tissue plasminogen activator (tPA) was used in one affected animal and was successful in resolving hyphema. One eye with hyphema, where tPA was suggested but not performed, developed phthisis bulbi (personal

Fig. 38.40 OS of a harbor seal (*Phoca vitulina*). Extracapsular lensectomy had been performed, and the lens capsule was not removed completely. Severe posterior capsule opacification resulted in diminish sight again

observation, Colitz). A very rare post-operative complication has been endophthalmitis (n = one eye).

Other Considerations about Cataracts and Uveitis

Anterior uveitis (inflammation inside the anterior segment of the eye) secondary to chronic PK occurs subclinically and is not clinically apparent in most pinnipeds. Anterior uveitis results in the secretion of matrix metalloproteinases-2 and 9 into the aqueous humor. In humans, the samples from patients with moderately active uveitis correlated with more MMP2 and 9 and increased levels of IL-1ß, IL-12, and IL1ra (El-Shabrawi et al. 2009). Since MMPs cause release of proinflammatory cytokines, MMPs may contribute to the chronicity of uveitis. Many MMPs, including MMP-2 and -9, cleave fibrillin proteins which contribute to lens instability. Exposure to UV-B irradiation can lead to lens instability by direct damage to fibrillin-based microfibrils, which compose the ciliary zonules hypothetically due to MMP-2 activation (Shiroto et al. 2017). Over time with aging and cumulative exposure to UV, zonular degradation results in lens instability, i.e., subluxation and luxation. In addition, chronic anterior uveitis contributes to cataractogenesis. Cataracts commonly form after a period of chronic PK. Potential ways to inhibit the inevitable activity of matrix metalloproteinase-9 include the use of oral doxycycline and a variety of supplements including grapeseed extract, bromelain, green tea extract, and turmeric.(Bahrami et al. 2012; Federici 2011; Jia et al. 2011; Yen et al. 2018; Demeule et al. 2000; Rathnavelu et al. 2016; Dai and Mumper 2010).

Uveitis and Glaucoma

The most common cause of uveitis in pinnipeds is lens-induced uveitis (personal observation, Colitz). The clinical signs of uveitis in pinnipeds include perilimbal corneal edema, diffuse corneal edema, perilimbal hyperemia, and miosis. Since corneal edema is common due to concurrent PK, its presence is difficult to blame solely on lens-induced uveitis. Pinnipeds rarely demonstrate aqueous flare as a

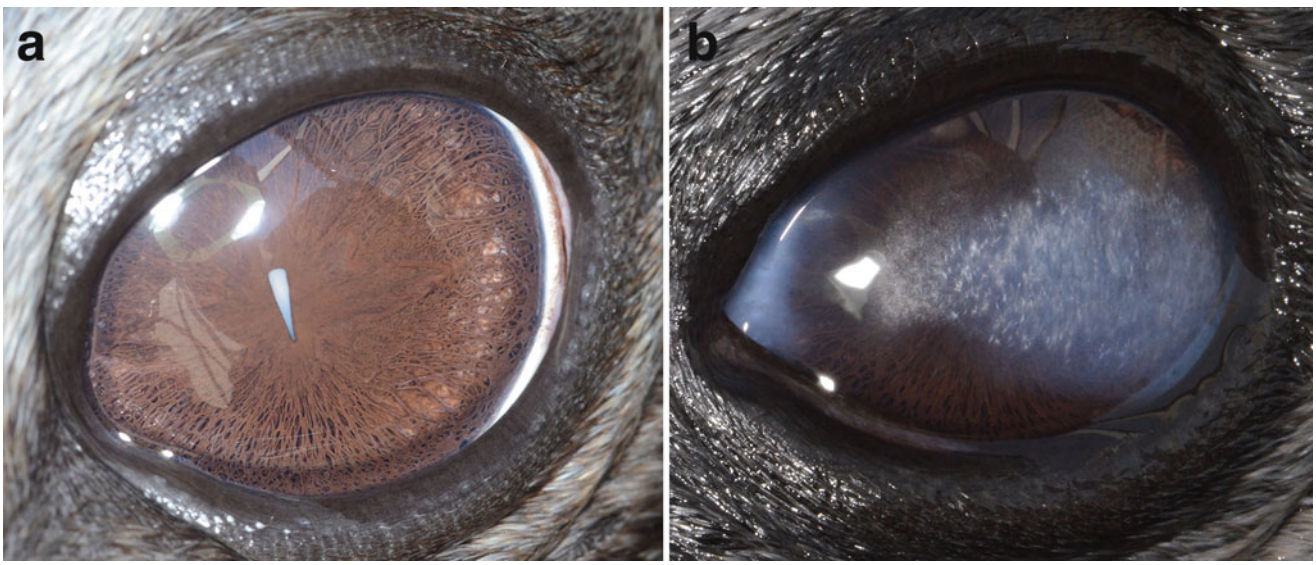

Fig. 38.41 OS of a harbor seal (*Phoca vitulina*) before cataract removal and post-operatively. (**a**) OS with a mature cataract and very mild pigment migration over the temporal limbus. (**b**) OS 2 years post-operatively. The cornea has dorsal limbal incisional fibrosis, and diffuse lipid infiltrates

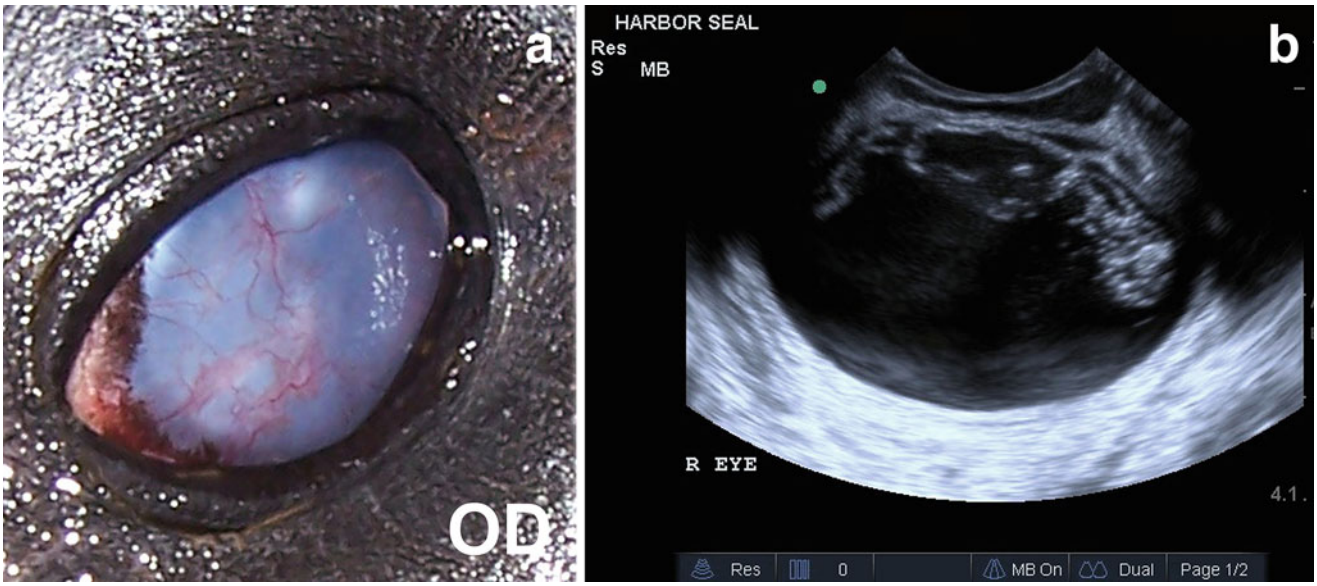

Fig. 38.42 The right eye of a harbor seal (*Phoca vitulina*) with chronic lens-induced uveitis. (**a**) The cornea developed diffuse edema with active vascularization. (**b**) Ultrasound image of the same eye shows the lens capsule that has resorbed lens material with disintegrated lens capsule and lens material located in the peripheral vitreous. The nucleus is not evident in this image but was in the vitreous

clinical sign of uveitis. With chronicity and without treatment, pre-iridal fibrovascular membranes with entropion or ectropion uvea may develop, increasing the risk of secondary glaucoma. Thus far, phocids, including harbor seals and grey seals, have been diagnosed with severe keratopathy associated with chronic and severe lens-induced uveitis (Fig. 38.42a). These eyes have had disintegrated lens capsules with the lens nucleus falling into the vitreous (Fig. 38.42b). The cortex has been either mostly resorbed or becoming thick and yellow.

Secondary glaucoma is not common but, when it does occur, it is secondary to chronic lens-induced uveitis, usually with concurrent anterior cataractous lens luxation. Control of lens-induced uveitis, even if clinical signs are not apparent, is important. Clinical signs of glaucoma in pinnipeds is mydriasis relative to the normal eye and diffuse corneal edema (Fig. 38.43). Histologically, the globes have had broad anterior synechia, full-thickness retinal atrophy with loss of ganglion cells and loss of photoreceptor nuclei. The optic nerve head was gliotic and atrophied, which extended deep into the optic nerve tissue (Courtesy of the Comparative Ocular Pathology Laboratory of Wisconsin).

Primary glaucoma is rare in pinnipeds. Only one California sea lion has been diagnosed with unilateral primary glaucoma, based on young age and lack of other clinical signs such as cataract (personal observation, Colitz). The normal range of intraocular pressure (IOP) in pinnipeds is 24 to 39 mmHg (Mejia-Fava et al. 2009). It is not uncommon to measure artifactually elevated IOPs depending on the animals' temperament and demeanor. This is why training and desensitization to this test are important for accurate measurements. Histological changes are described below under Fundus. Pre-iridal fibrovascular membranes are evident in some patients with glaucoma.

Pinnipeds with secondary glaucoma respond well to topical and/or oral carbonic anhydrase inhibitors (CAIs) in combination with appropriate anti-inflammatory medications to control underlying uveitis (personal observation, Colitz). Topical prostaglandin analog medications such as latanoprost are not as consistently effective as CAIs in pinnipeds (personal communication, R. Marrion and personal observation, Colitz).

Specific CAIs commonly used in pinnipeds are 2% dorzolamide or 2% dorzolamide combined with 0.5% timolol; brinzolamide is also an option, though it is currently much more expensive in the United States. The initial recommended dosage is 1–2 drops TID or QID. Oral CAIs including methazolamide and dichlorphenamide are also an option at a dose of 2 mg/kg PO BID. As mentioned previously, control of underlying uveitis should be addressed, in addition to performing a lensectomy especially if visually impairing cataract and/or anterior lens luxation are present.

Vitreous

Vitreal degeneration and asteroid hyalosis have been identified in many pinnipeds (Fig. 38.44). It appears that stranded animals with cataracts are more likely to have liquified vitreous (i.e. syneresis) compared to captive-born animals with cataracts (personal observation, Colitz).

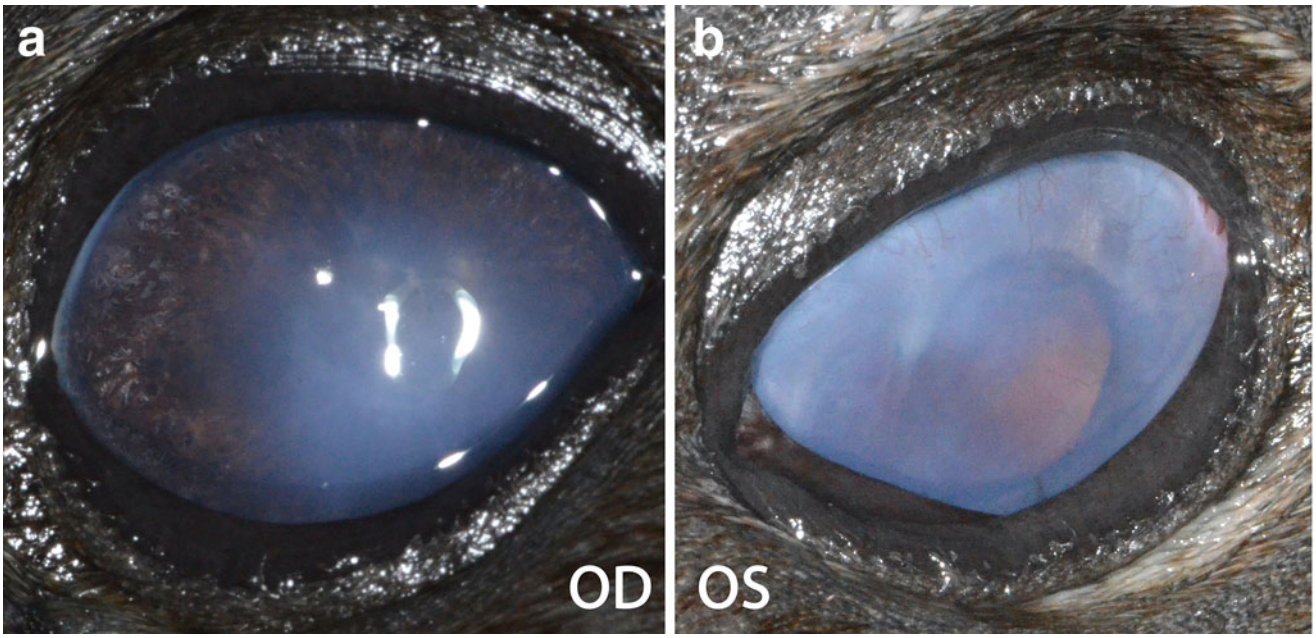

Fig. 38.43 OU from a harbor seal (*Phoca vitulina*) that had undergone surgical lensectomy 5 years prior. (**a**) OD has perilimbal corneal edema and diffuse corneal edema. (**b**) OS developed secondary glaucoma, was buphthalmic with diffuse corneal edema and vascularization. The pupil is mydriatic with ectropion uvea

Fundus

Fundic lesions are rare in pinnipeds. Unfortunately, dilated fundic evaluations are impossible in awake pinnipeds unless they are trained to be examined in a dark room. However, intraoperatively during lensectomy, the fundus is easily visible. Thus far, no lesions have been identified using this technique other than retinal detachments that were already diagnosed preoperatively via ultrasonography (personal observation, Colitz). Retinal detachments are common in eyes with chronic cataracts in stranded animals taken into human care.

Systemic hypertension has occurred in elderly pinnipeds (mentioned earlier). One that had undergone bilateral lensectomies developed systemic hypertension-related

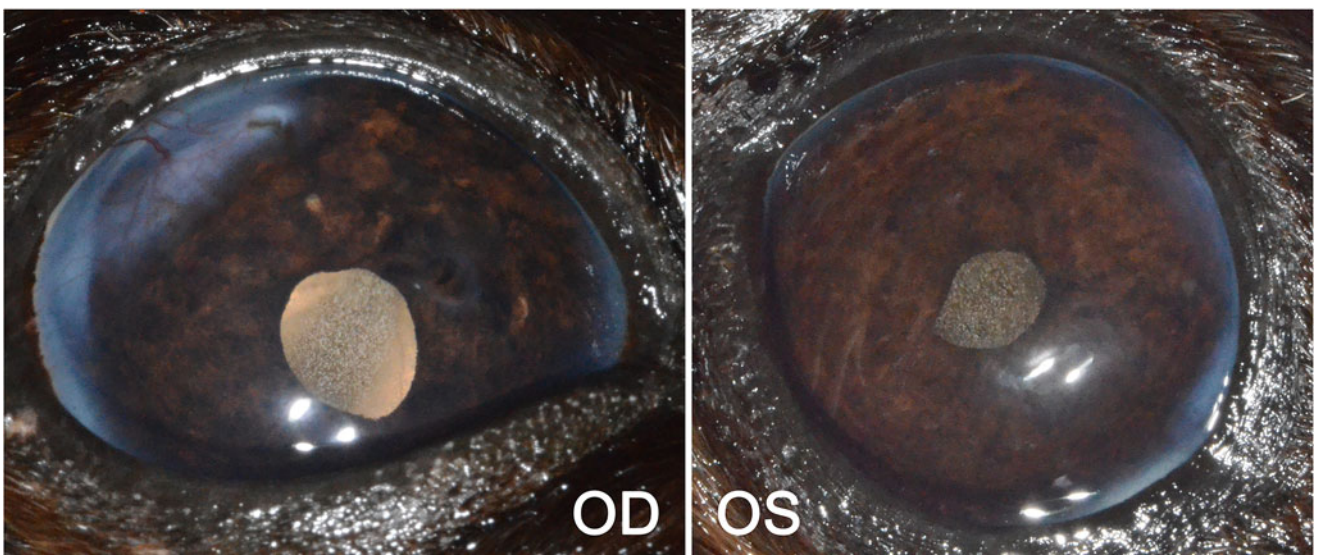

Fig. 38.44 OU from a New Zealand fur seal (*Arctophoca forsteri*) that had undergone bilateral lensectomies. Both eyes have perilimbal fibrosis from healed incisions. There is asteroid hyalosis evident in both eyes

Fig. 38.45 Subgross image of the OD of a South African fur seal (*Arctocephalus pusillus*) with retinal detachment and vitreal hemorrhage. The eye had undergone lensectomy, and the animal was suspected to have systemic hypertension. Courtesy of the Comparative Ocular Pathology Laboratory of Wisconsin

retinal detachments (Fig. 38.45). Histologically, there was loss of outer retinal tissue with intermittent thickening of Bruch's membrane and small artery thickening with a diminished lumen suggestive of hypertensive vasculopathy in an elderly sea lion (courtesy of the Comparative Ocular Pathology Laboratory of Wisconsin).

Histologically, there have been a variety of fundic lesions in pinniped identified by the Comparative Ophthalmic Pathology Laboratory of Wisconsin (COPLOW) (personal communication, Richard R. Dubielzig). One subadult harbor seal with chronic hypermature cataracts had complete retinal atrophy and optic nerve atrophy, with replacement of retina by collagen-rich connective tissue with low cellularity. The significance of these changes is unknown. A mature California sea lion with bilateral chronic hypermature luxated cataracts, and chronic keratopathy also had one buphthalmic eye with diffuse inner and outer retinal layer atrophy with gliosis and atrophy of the optic nerve. Other pinniped globes evaluated with chronic secondary glaucoma had decreased numbers of ganglion cells in the inner retinal layer. An elderly California sea lion that had undergone bilateral lensectomies had a pre-iridal fibrovascular membrane, dense and collagenous cyclitic membrane, and tractional retinal detachment with outer retinal atrophy. The retinal detachment was interpreted to be secondary to traction caused by the dense cyclitic membrane.

Other Neoplasia

A geriatric monk seal underwent enucleation for presumed chronic keratopathy and cataract with possible lens luxation. Histopathological evaluation found a neoplastic population of cells free floating in the posterior chamber, vitreous and multifocally carpeting the iris, ciliary body and choroid. The diagnosis was an intraocular round cell neoplasia with extensive necrosis. The lens capsule was ruptured with extrusion of lens material with moderate secondary lymphoplasmacytic phacoclastic panuveitis and histiocytic endophthalmitis. The relationship of the uveitis and round cell neoplasia is unknown, however, the pathologists at COPLOW have seen ocular lymphomas arise in the midst of chronic lymphoplasmacytic uveitis, especially in cats.

Ophthalmic Surgical Procedures in Pinnipeds

Since safer anesthetic protocols for pinnipeds have been developed over the past 10 years (personal observation and communication, Dr. James Bailey, DACVA), ophthalmic and other types of surgical procedures are now more commonly performed (Colitz and Bailey 2019). Besides

Fig. 38.46 A fur seal having underwent enucleation of the OS. Shutterstock.com

intracapsular and extracapsular lensectomy and phacoemulsification, corneal repair procedures for mid to deep stromal ulcers and corneal perforations have been successfully performed with or without concurrent lensectomy. BioSIS, A-Cell, and amniotic tectonic grafts have been placed then covered by a conjunctival flap (Fig. 38.23). Episcleral cyclosporine implant placement is performed in all lensectomy procedures (Fig. 38.24). Eyelid mass removal and enucleations have also been performed in pinnipeds (Fig. 38.46).

There are a few differences in ophthalmic surgery in pinnipeds compared to dogs and cats. The positioning of pinnipeds is typically sternal and slightly tilted, or laterally recumbent, with the head turned to position the eye appropriately for the surgical approach. Intravenous catheters are placed peripherally in the flippers. Intra-arterial catheters are placed in the median artery of the pectoral flipper or saphenous artery of the pelvic flipper. Jugular catheters are also commonly placed in the external jugular. An anesthesiologist well experienced in pinnipeds should be in charge of the animals' anesthetic event to avoid issues that are unique to these species.

Neoplasia in Pinnipeds

Carcinomas are common tumors in pinnipeds. An elderly female California sea lion had a history of chronic PK for over ten years. She had undergone bilateral lensectomies almost two years previously and was sighted until her death. Necropsy revealed that the right eye had metastatic intraocular carcinoma. Another older female California sea lion had bilateral intravascular metastatic adenocarcinoma. Metastatic lymphoma was diagnosed in the choroid of one California sea lion. Thank you to COPLOW for sharing these reports.

Antioxidant Support

The reader is referred Chap. 31: Ophthalmology of Whippomorpha for a discussion of antioxidants and their benefits for eye health.

References

Agency, U. S. E. P. 2016. Uv Index

Arnason U, Widegren B (1986) Pinniped phylogeny enlightened by molecular hybridizations using highly repetitive Dna. Mol Biol Evol 3:356–365

Arnason U, Gullberg A, Janke A, Kullberg M, Lehman N, Petrov EA, Vainoia R (2006) Pinniped phylogeny and a new hypothesis for their origin and dispersal. Mol Phylogenet Evol 41:345–354

Bahrami F, Morris DL, Pourgholami MH (2012) Tetracyclines: drugs with huge therapeutic potential. Mini Rev Med Chem 12:44–52

Baradaran-Rafii A, Asl NS, Ebrahimi M, Jabbehdari S, Bamdad S, Roshandel D, Eslani M, Momeni M (2017) The role of amniotic membrane extract eye drop (Ameed) in in vivo cultivation of Limbal stem cells. Ocul Surf 16:146–153

Barnes JA, Smith JS (2004) Bilateral Phacofragmentation in a New Zealand fur seal (Arctocephalus Forsteri). J Zoo Wildl Med 35:110–112

Chandler HL, Colitz CMH, Miller WW, Kusewitt DF (2005) Role of Tetracyclines in healing canine refractory ulcers. Invest Ophthalmol Vis Sci 46. E-Abstract 2597

Chandler HC, Kusewitt DF, Colitz CMH (2008) Modulation of matrix metalloproteinases by ultraviolet radiation in canine cornea. Vet Ophthalmol 11:135–144

Colitz CMH, Bailey JE (2019) Lens diseases and Anesthetic considerations for ophthalmologic procedures in pinnipeds. In: Miller RE, Lamberski N, Calle PP (eds) Fowler's zoo and wild animal medicine current therapy. Elsevier, St. Louis

Colitz CMH, Renner MS, Manire CA, Doescher B, Schmitt TL, Osborn SD, Croft L, Olds J, Gehring E, Mergl J, Tuttle AD, Sutherland-Smith M, Rudnick JC (2010a) Characterization of progressive keratitis in Otariids. Vet Ophthalmol 13:47–53

Colitz CMH, Saville WJA, Renner MS, Mcbain JF, Reidarson TH, Schmitt TL, Nolan EC, Dugan SJ, Knightly F, Rodriguez MM, Mejia-Fava JC, Osborn SD, Clough PL, Collins SP, Osborn BA, Terrell K (2010b) Risk factors associated with cataracts and lens Luxations in captive pinnipeds in the United States and the Bahamas. J Am Vet Med Assoc 237:429–436

Colitz CMH, Grubb C, Razner K (2011a) Objective and Behavioral results following cataract removal in 52 pinnipeds. Vet Ophthalmol 14:422

Colitz CMH, Gulland F, Palmer L (2011b) Retrospective Report of Ocular Problems in Wild Pinnipeds. *J Zoo Wildlife Med,* In Preparation For Submission

Colitz CMH, Bowman M, Cole G, Budelsky C, Doescher B, Anderson E (2014) Surgical Repair of a Corneal Perforation or Descemetocele with Concurrent Lensectomy in Three Pinnipeds. *International Association Of Aquatic Animal Medicine*

Colitz CMH, Gilger BC, Grundon R, Anderson E, Berliner A, Blyde D, Bowman M, Buchanan S, Chua F, Doescher B, Menchaca M, March D, Olds J, Phillips W, Reidarson T, Seruca C, Soborb A, Staggs L, Wells R (2016) The Use of Episcleral Subconjunctival Cyclosporine Implants to Control Otariid Keratopathy. Annual Conference of the International Association of Aquatic Animal Medicine, 2016 Virginia Beach, VA

Colitz CMH, Bailey JE, Mejia-Fava JC (2018a) Cetacean and pinniped ophthalmology. In: Dierauf L, Gulland FMD (eds) Crc handbook of marine mammal medicine, 3rd edn. CRC Press Taylor & Francis Group, Boca Raton

Colitz CMH, Saville WJA, Walsh MT, Latson E (2018b) Epidemiologic Study Of Risk Factors Associated With Corneal Disease In Pinnipeds. *J Am Vet Med Assoc,* In Press

Dai J, Mumper RJ (2010) Plant Phenolics: extraction, analysis and their antioxidant and anticancer properties. Molecules 15:7313–7352

Davis RW, Fuiman LA, Williams TM, Collier SO, Hagey WP, Kanatous SB, Kohin S, Horning M (1999) Hunting behavior of a marine mammal Beaneath the Antarctic fast ice. Science 283:993–996

Dawson WW, Schroeder JP, Sharpe SN (1987) Corneal surface properties of two marine mammal species. Mar Mamm Sci 3:186–197

Dawson C, Naranjo C, Sanchez-Maldonado B, Fricker GV, Linn-Pearl RN, Escanilla N, Karafnik C, Gould DJ, Sanchez RF, Matas-Riera M (2017) Immediate effects of diamond Burr debridement in patients with spontaneous chronic corneal epithelial defects, light and electron microscopic evaluation. Vet Ophthalmol 20:11–15

Delisle I, Strobeck C (2005) A phylogeny of the Caniformia (order carnivore) based on 12 complete protein-coding mitochondrial genes. Mol Phylogenet Evol 37:192–201

Demeule M, Brossard M, Page M, Gingras D, Beliveau R (2000) Matrix metalloproteinase inhibition by green tea Catechins. Biochim Biophys Acta 1478:51–60

Dunn JL, Overstrom NA, St.Aubin DJ (1996) An epidemiologic survey to determine factors associated with corneal and lenticular lesions in Captive Harbor seals and California Sea lions. Annual Meeting Of The Iaaam:108–109

El-Shabrawi Y, Christen WG, Foster CS (2009) Correlation of Metalloproteinase-2 and −9 with Proinflammatory cytokines interleukin-1ß, Interleukin-12 and the Interleukin-1 receptor antagonist in patients with chronic uveitis. Curr Eye Res 20:211–214

Esson DW, Nollens HH, Schmitt TL, Fritz KJ, Simeone CA, Stewart BS (2015) Aphakic phacoemulsification and automated anterior vitrectomy, and Postreturn monitoring of a Rehabilitated Harbor seal. J Zoo Wildl Med 46:647–651

Federici TJ (2011) The non-antibiotic properties of Tetracyclines: clinical potential in ophthalmic disease. Pharmacol Res 64:611–623

Fleming M, Bexton S (2016) Conjunctival Flora of healthy and diseased eyes of Grey seals (*Halichoerus Grypus):* implications for treatment. Vet Rec 179:99–103

Gaynes BI, Onyekwuluje A (2008) Topical ophthalmic Nsaids: a discussion with focus on Nepafenac ophthalmic suspension. Clinical Ophthalmol 2:355–368

Griebel U, Schmid A (1992) Color vision in the Californa Sea lion (Zalophus Californianus). Vis Res 32:477–482

Grubb CM, Razner KT, Colitz CMH (2011) Let Sea Lions Be See Lions! Analysis of Behavior in California Sea Lions Before and After Cataract Removal Surgery. *Annual Meeting Of The International Marine Animal Trainers Association.* Miami, FL

Hanke FD, Dehnhardt G, Schaeffel F, Hanke W (2006a) Corneal topography, refractive state, and Accomodation in harbor seals (*Phoca Vitulina*). Vis Res 46:837–847

Hanke W, Romer R, Dehnhardt G (2006b) Visual fields and eye movements in a harbor seal (*Phoca Vitulina)*. Vis Res 46:2804–2814

Hanke FD, Kroger RH, Siebert U, Dehnhardt G (2008) Multifocal lenses in a Monochromat: the harbour seal. J Exp Biol 211:3315–3322

Hanke FD, Hanke W, Scholtyssek C, Dehnhardt G (2009a). Basic Mechanisms in Pinniped Vision. *Exp Brain Res,* Epub Ahead Of Print

Hanke FD, Peichl L, Dehnhardt G (2009b) Retinal ganglion cell topography in Juvenile Harbor seals (*Phoca Vitulina)*. Brain Behavior And Evolution 74:102–109

Jamieson GS, Fisher HD (1971) The retina of the harbor seal, Phoca Vitulina. Can J Zool 49:19–23

Jamieson GS, Fisher HD (1972) The pinniped eye: a review. In: Harrison RJ (ed) Functional anatomy of marine mammals I. Academic Press, London, New York

Jia Z, Song Z, Zhao Y, Wang X, Liu P (2011) Grape seed Proanthocyanidin extract protects human lens epithelial cells from oxidative stress via reducing Nf-Kb and Mapk protein expression. Mol Vis 17: 210–217

Karpestam B, Gustafsson J, Shashar N, Katzir G, Kroger RH (2007) Multifocal lenses in coral reef fishes. J Exp Biol 210:2923–2931

Kastelein RA, Zweypfenning J, Spekreijse H, Dubbeldam JL, Born EW (1993) The anatomy of the walrus head (*Odobenus Rosmarus).* Part 3: the eyes and their function in walrus ecology. Aquat Mamm 19: 61–92

Kelleher Davis R, Colitz CMH, Staggs L, Argueso P (2013a) Carbohydrate profiles in ocular secretions from cetaceans and pinnipeds. International Association Of Aquatic Animal Medicine, Sausalito, California

Kelleher Davis R, Doane MG, Knop E, Knop N, Dubielzig RR, Colitz CMH, Argueso P, Sullivan DA (2013b) Anatomy of ocular gland morphology and tear composition of pinniped. Vet Ophthalmol 16: 269–275

Kern TJ, Colitz CMH (2013) Exotic animal ophthalmology. In: Gelatt KN, Gilger BC, Kern TJ (eds) Veterinary ophthalmology, 5th edn. John Wiley & Sons, Inc, Hoboken

Klauss G, Suedmeyer WK, Galle LE, Giuliano EA, Castaner LJ (2005) Surgical resection of an orbital fat prolapse in a California Sea lion (Zalophus Californianus). Vet Ophthalmol 8:277–281

Kroger RHH, Campbell MCW, Fernald RD, Wagner HJ (1999) Multifocal lenses compensate for chromatic defocus in vertebrate eyes. J Comp Physiol 184:361–369

Lavigne DM, Ronald K (1975) Pinniped Visual Pigments. Comp Biochem Physiol 52b:325–329

Levenson DH, Ponganis PJ, Crognale MA, Deegan JF, Dizon A, Jacobs GH (2006) Visual pigments of marine carnivores: pinnipeds, polar bear, and sea otter. J Comp Physiol A 192:833–843

Malmstrom T, Kroger RHH (2006) Pupil shapes and lens optics in the eyes of terrestrial vertebrates. J Exp Biol 209:18–25

Mass AM (1992) Retinal topography in the walrus (*Odobenus Rosmarus Divergrns*) and fur seal (*Callorhinus Ursinus).* In: Thomas JA, R. A, K, Supin AY (eds) Marine mammal sensory systems. Plenum, New York

Mass AM, Supin AY (1992) Peak density, size and regional distribution of ganglion cells in the retina of the fur seal *Callorhinus Ursinus*. Brain Behavior And Evolution 39:69–76

Mass AM, Supin AY (2003) Retinal topography of the harp seal *Pagophilus Groenlandicus*. Brain Behavior And Evolution 62: 212–222

Mass AM, Supin AY (2005) Ganglion cell topography and retinal resolution of the Steller Sea lion (*Eumetopias Jubatus).* Aquat Mammal 31:393–402

Mass AM, Supin AY (2007) Adaptive features of aquatic Mammals' eye. Anat Rec 290:701–715

Mass AM, Supin AY (2010) Retinal ganglion cell layer of the Caspian seal *Pusa Caspica*: topography and localization of the high-resolution area. Brain Behavior And Evolution 76:144–153

Mejia-Fava JC, Ballweber L, Colitz CMH, Clemons-Chevis CL, Croft LA, Dalton LM, Dold C, Gearhart SA, Hoffman EM, Osborn SD, Jack SW, Renner MS, Schmitt TL, Rodriguez M, Romano TA, Tuttle AD (2009) Use of rebound tonometry as a diagnostic tool to diagnose glaucoma in the captive California Sea lion. Vet Ophthalmol 12:405

Miller SN, Colitz CMH, Dubielzig RR (2010) Anatomy of the California Sea lion globe. Vet Ophthalmol 13:63–71

Miller S, Samuelson D, Dubielzig R (2013) Anatomic features of the cetacean globe. Vet Ophthalmol 16:52–63

Nagy AR, Roland K (1970) The harp seal, *Pagophilus Groenlandicus*. Can J Zool 48:367–370

Nakagaki K, Hata K, Iwata E, Takeo K (2000) Malassezia Pachydermatis isolated from a south American Sea lion (Otaria Byronia) with dermatitis. J Vet Med Sci 62:901–903

Newkirk KM, Chandler HC, Parent AE, Young DC, Colitz CM, Wilkie DA, Kusewitt DF (2007) Ultraviolet radiation-induced corneal degeneration in 129 mice. Toxicol Pathol 35:819–826

Newman LA, Robinson PR (2005) Cone visual pigments of aquatic mammals. Vis Neurosci 22:873–879

Ninomiya H, Yoshida E (2007) Functional anatomy of the ocular circulatory system: vascular corrosion casts of the cetacean eye. Vet Ophthalmol 10:231–238

Oliveira R, Martielli P, Chelysheva M, Naranjo C, Romero C (2019). Presumed Papilloma Eyelid Lesion Induced by an Otarine Herpesvirus (Othv)-1 Infection in a Seal

Peichl L, Moutairou K (1998) Absence of short-wavelength sensitive cones in the retinae of seals (Carnivora) and African Giant rats (Rodentia). Eur J Neurosci 10:2586–2594

Peichl L, Berhmann G, Kroger RHH (2001) For whales and seals the ocean is not blue: a visual pigment loss in marine mammals. Eur J Neurosci 13:1

Perry HD, Kenyon KR, Lamberts DW, Foulks GN, Seedor JA, Golub LM (1986) Systemic Tetracycyline hydrochloride as an adjunctive therapy in the treatment of persistent epithelial defects. Ophthalmology 93:1320–1322

Potron A, Poirel L, Nordmann P (2015) Emerging broad-Spectrum resistance in pseudomonas aeruginosa and Acinetobacter Baumannii: mechanisms and epidemiology. Int J Antimicrob Agents 45:568–585

Rathnavelu V, Alitheen NB, Sohila S, Kanagesan S, Ramesh R (2016) Potential role of bromelain in clinical and therapeutic applications. Biomedical Reports 5:283–288

Roth SJ, Tischer BK, Kovacs KM, Lydersen C, Osterrieder N, Tryland M (2013) Phocine herpesvirus 1 (Phhv-1) in harbor seals from Svalbard, Norway. Vet Microbiol 164:286–292

Schusterman RJ (1981) Visual acuities in pinnipeds. Psychol Rec 31: 125–143

Schusterman RJ, Balliet RF (2006) Aerial and underwater visual acuity in the California Sea lion (Zalophus Californianus) as a function of luminance. Ann NY Acad Sci 188:37–46

Shiroto Y, Terashima S, Hosokawa Y, Oka K, Isokawa K, Tsuruga E (2017) The effect of ultraviolet B on Fibrillin-1 and Fibrillin-2 in human non-pigmented ciliary epithelial cells in vitro. Acta Histochem Cytochem 50:105–109

Staggs LA, Colitz CMH, Holmes-Douglas S (2013) The Use of Subconjunctival Cyclosporine Implants in a California Sea Lion (Zalophus Californianus) Prior to Cataract Surgery. *International Association for Aquatic Animal Medicine*

Supin AY, Popov VV, Mass AM (2001) Vision in aquatic mammals. *The sensory physiology of aquatic mammals*. Kluwer Academic Publishers, Boston

Walls GL (1942) The vertebrate eye and its adaptive radiation. Hafner Press, New York

West JA, Sivak JG, Murphy CJ, Kovacs KM (1991) A comparative study of the anatomy of the iris and ciliary body in aquatic mammals. Can J Zool 69:2594–2607

Wright EP, Waugh LF, Goldstein T, Freeman KS, Kelly TR, Wheeler EA, Smith BR, Gulland FM (2015) Evaluation of viruses and their association with ocular lesions in pinnipeds in rehabilitation. Vet Ophthalmol 18:148–159

Yen YH, Pu CM, Liu CW, Chen YC, Chen YC, Liang CJ, Hsieh JH, Huang HF, Chen YL (2018) Curcumin accelerates cutaneous wound healing via multiple biological actions: the involvement of Tnf-A, Mmp-9, A-Sma, and collagen. Int Wound J 15:605–617

Ophthalmology of Mustelidae: Otters, Ferrets, Skunks, Raccoons, and Relatives

39

Fabiano Montiani-Ferreira and Katie Freeman

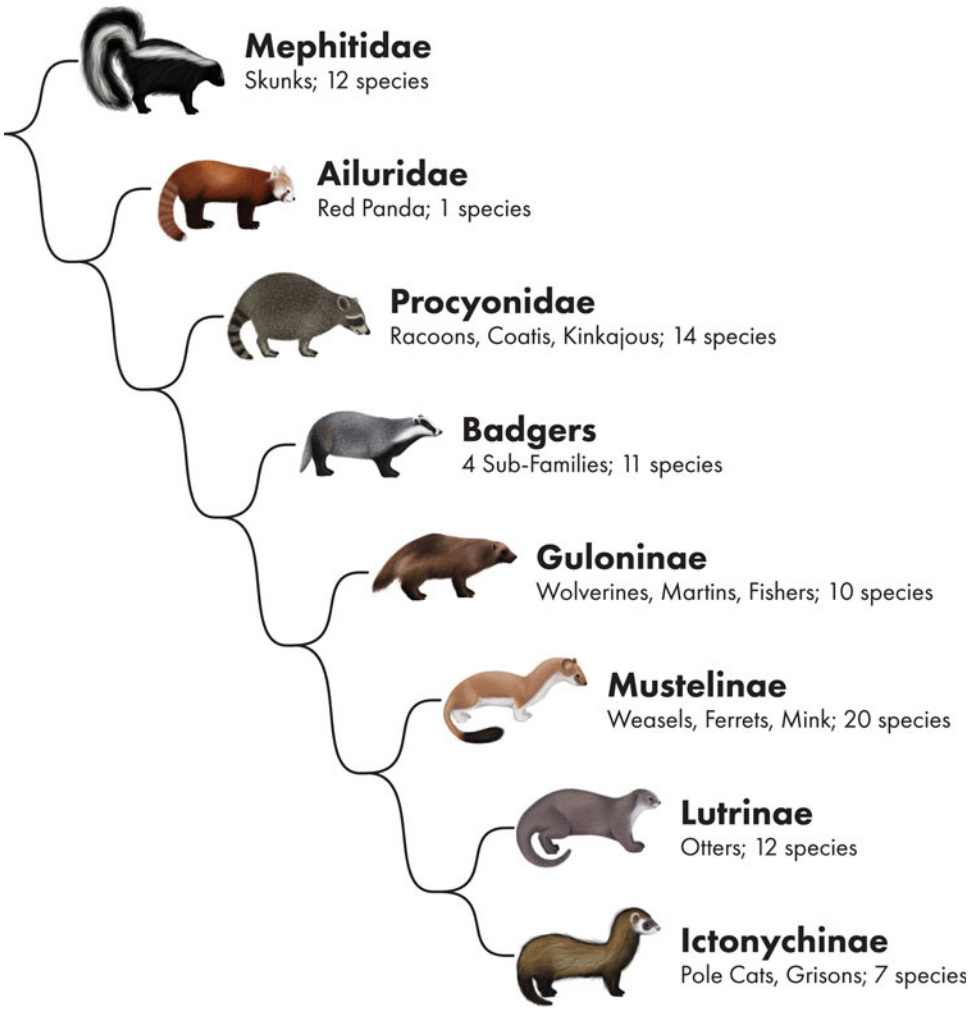

F. Montiani-Ferreira (✉)
Comparative Ophthalmology Laboratory (LABOCO), Veterinary Medicine Department, Federal University of Paraná, Curitiba, PR, Brazil
e-mail: montiani@ufpr.br

K. Freeman
Veterinary Vision, San Carlos, CA, USA

Introduction

The Musteloidea superfamily of carnivoran mammals consists of the families Ailuridae (red pandas), Mustelidae (mustelids: weasels, otters, martens, and badgers), Procyonidae (procyonids: raccoons, coatis, kinkajous, olingos, olinguitos, ringtails, and cacomistles), and

F. Montiani-Ferreira et al. (eds.), *Wild and Exotic Animal Ophthalmology*, https://doi.org/10.1007/978-3-030-81273-7_14

Mephitidae (skunks and stink badgers). The Mustelidae family, whose members are collectively known as mustelids, includes terrestrial forms (such as ferrets and skunks), arboreal species (such as martens), burrowing species (such as badgers), semiaquatic species (such as minks), and aquatic species (such as otters) (Burnie and Wilson 2001). The main physical links between all mustelids are shared characters of the skull and teeth, usually short legs and elongated bodies (Fujishiro et al. 2014).

Ferrets

Of all the species in the mustelidae family, the domestic ferret is certainly the species of greatest veterinary importance, since domestic ferrets are becoming more popular as pets and are increasingly been seen as a patient in different veterinary services. The complete scientific name for the domestic ferret is *Mustela putorius furo*. *Mustela* is a hybrid word meaning "long mouse," and is a combination of *mus*, which means mouse in Latin, and *theon* [*telos*], which means long in Greek. The term was originally used to refer to the weasel. The word *putorius* comes from the Latin, meaning "stench," referring to the musky odor of the ferret. The word *furo* also comes from the Latin *fur* meaning thief, and *furittus* meaning little thief. Therefore, a loose translation for the scientific name of the ferret would be "stinky weasel thief" and for the English name, ferret, would be just "little thief." It is believed that ferrets were domesticated approximately 2000 years ago, primarily for hunting purposes, becoming more popular worldwide as pets in the 1980s (Burnie and Wilson 2001; Huynh et al. 2017).

Ferrets also are commonly used as animal models for medical research initially for influenza and later for other diseases, including several ophthalmic investigations, such as particularly glaucoma, retinal morphology, and central vision pathways (Liets et al. 2003; Hoffmann et al. 2004; Aboelela and Robinson 2004; Manger et al. 2004; Chen et al. 2005; Hoar 1984; Fujishiro et al. 2014). Knowledge of normal parameters for the main ocular tests, fundamentals of ocular examination, basic anatomical features and the most common ocular diseases of the domestic ferret became a necessity for practicing veterinary ophthalmologists. Normal ocular values for selected ophthalmic tests and ocular biometry have been documented (Gaarder and Kern 2001; Montiani-Ferreira et al. 2006; Hernández-Guerra et al. 2007). Case reports of ferrets presenting different ocular conditions also have been published (Miller and Pickett 1989; Miller et al. 1993; Lipsitz et al. 2001; McBride et al. 2009; Ropstad et al. 2011; DiGirolamo et al. 2013; Verboven et al. 2014; Lindemann et al. 2016). Literature reviews concerning ferret vision, ocular examination, anatomical features of the eye as well as general ophthalmology are available (Miller 1997; Good 2002; van der Woerdt 2003; Gaarder and Kern 2001; Montiani-Ferreira 2009; Myrna and Girolamo 2019).

Basic Anatomical Features of the Ferret Eye

One important anatomical aspect of the ferret eye concerns the globe size, which is proportionally and absolutely small (approximately 7 mm of axial length) (Hernández-Guerra et al. 2007; Fujishiro et al. 2014). Ferrets possess a relatively large lens (about 3.5 mm) and a wide cornea for optimal light gathering in dim light conditions (Williams 2012). However, ferrets eyeballs are absolutely larger than those of rodents (Fujishiro et al. 2014). The globes are placed somewhat laterally in the skull (32° from the midline) giving a field of view of around 270°, but with a very limited binocular vision (approximately 40° frontally) (Fig. 39.1a) (Good 2002; Garipis et al. 2003; Williams 2012).

Ferret newborns are called kits and similarly to puppies are born with closed eyelids. Canine eyelids open at approximately 2 weeks after birth in most breeds (Montiani-Ferreira et al. 2003), whereas the eyelids of ferrets do not open until after 20 days after birth (Miller 1997; Gaarder and Kern 2001; Good 2002; Williams and Gum 2013).

Similar to other carnivores, ferrets have a well-developed third eyelid (semilunar fold of the conjunctiva) that is reinforced by a T-shaped cartilage. A lacrimal gland is present and is responsible for secreting a significant portion of the aqueous layer of the tear film. A firmly adherent conjunctiva is present on both the bulbar and the palpebral surfaces of the third eyelid. The ferret's third eyelid can be non-pigmented (whitish) or pigmented at the margin. There is no deep gland (Harderian gland) of the third eyelid in the ferret. Exposure of the palpebral (external) surface of the third eyelid can be obtained by manually retracting the globe back into the orbit (gentle digital retropulsion).

As in most species adapted for night vision, the corneal surface of the ferret is large, compared to dogs and cats. As in most species adapted for night vision, the corneal surface of the ferret is large, compared to dogs and cats. The mean central corneal thickness in the adult ferret is about 0.34 mm (Montiani-Ferreira et al. 2006). The corneal epithelium is nonkeratinized stratified squamous and approximately 4–5 cell layers thick, and is avascular (Montiani-Ferreira 2009). The other corneal layers are comparable to that of other carnivores but total about half the thickness of an adult dog cornea (Montiani-Ferreira et al. 2003, 2006).

The iris of ferrets are thin and most commonly heavily pigmented (Fig. 39.1a) with the exception of albino ferrets in which the iris is usually red-pink in color (Montiani-Ferreira 2009). The pupil is round when mydriatic but is peculiarly horizontally ovoid when miotic (Fig. 39.1b).

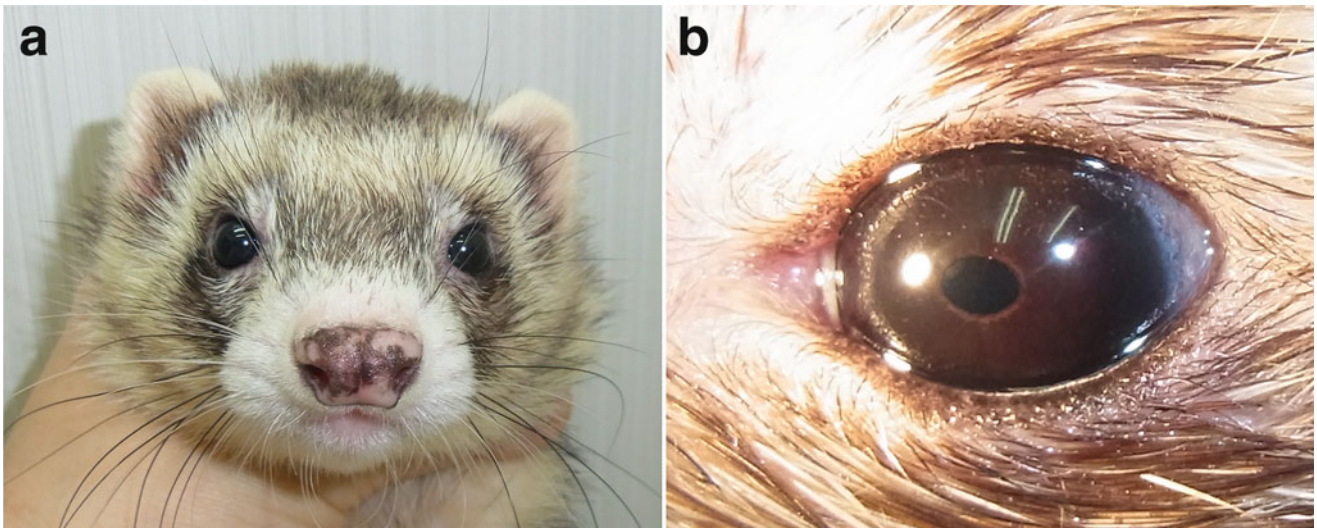

Fig. 39.1 (**a**) Note that the eyes of the ferret are positioned slightly laterally in the skull providing a limited binocular vision. (**b**) Note that the pupil of this *brown*-eyed ferret is oval, horizontally oriented, when in miosis. (Courtesy of Yasutsugu Miwa)

Phylogenetically close wild mustelids possess crepuscular habits, hunting typically at dusk and dawn (Williams 2012). Consequently, evolutionary speaking the ferret eye has a predominantly rod-dominated retina, specialized for function in dim light. The threshold of light needed for vision in the ferret is estimated to be five to seven times lower than in humans (Williams and Gum 2013). Darkly pigmented ferrets possess a brightly reflective choroidal and cellular tapetum lucidum of variable size and color. The color of the tapetal area seems to be influenced by coat color and age, with tapetal colors ranging from bluish (in young individuals) to yellow-green to dark orange (in brown, gray, black-coated individuals) (Fig. 39.2a, c). Albino and subalbinotic ferrets may lack partially or totally a tapetum, and when present they tend to be more of a light orange color. However, histologically, lightly colored individuals were reported to have a tapetum lucidum similar to that of the pigmented wild-type ferret (Tjalve and Frank 1984) (Fig. 39.2b, d). The ferret tapetum is rich in zinc and cysteine (Tjalve and Frank 1984; Braekevelt 1981). The retina is vascular in a holangiotic pattern with a small and poorly myelinated optic disc (Gaarder and Kern 2001) (Fig. 39.2c, d). In pigmented ferrets, 6000 retinal ganglion cells project ipsilaterally from the temporal area to the brain, whereas in albino ferrets only 1500 do so (Morgan et al. 1987). The impact of this difference has yet to be investigated. Overall, the axon count and density of optic nerve of the pigmented ferret is 82,000–88,000 (Henderson 1985). The Ferret retina possesses a prominent horizontal streak with the highest cellular density at the area centralis (Henderson 1985; Williams 2012), which is an area of increased photoreceptor and ganglion cell density, located superiorly and temporally to the optic disc. In terms of Snellen acuity, the pigmented ferret's visual resolution is 20/170 in bright light and 20/350 in dim light (Williams 2012). Ferrets are dichromats, thus possess two different cone populations within the retina, with a peak cone density of about 26,000/mm^2 with a peak rod density of 350,000/mm^2. They can detect moving objects (at the speed of a running mouse) better rather than stationary ones, and objects moving at 25–45 cm/s are optimally visualized (Hupfeld et al. 2006).

Knowledge of the ferret skull's intricate gross and radiographic anatomy is crucial for radiographic positioning, interpretation, as well as planning for safe surgical approaches. Descriptive and illustrated radiographic anatomy of the ferret is available elsewhere (Silverman and Tell 2005). The bony orbit of the ferret is deep and incomplete (open) (Fig. 39.3). As a result, it can be challenging for owners or keepers to detect a space-occupying lesion until it has reached a significant size (He and Killiaridis 2004). Ferrets possess a noticeable frontal process of the zygomatic bone and a salient lacrimal process, close to the maxilolacrimal suture line. The bony orbital margin has an outline that resembles an incomplete circle interrupted only by the prominent lacrimal process rostrally**.** The domestic ferret has an oval-shaped infraorbital foramen. At the orbital aspect of the lacrimal bone lies the fossa (or pit) of the lacrimal sac ventral to the lacrimal process. Only two foramina are present caudally at the medial wall of the orbit, the optic canal and, caudoventrally to this one, the orbitorotundum foramen. The orbitorotundum foramen is considered to be the result of the fusion of the orbital fissure and round foramen, and it is not present in other species of carnivores. One or two ethmoidal foramina may be present. As in dogs, a maxillary foramen is found at the orbital aspect of the maxillary bone, and two other foramina, the sphenopalatine and caudal

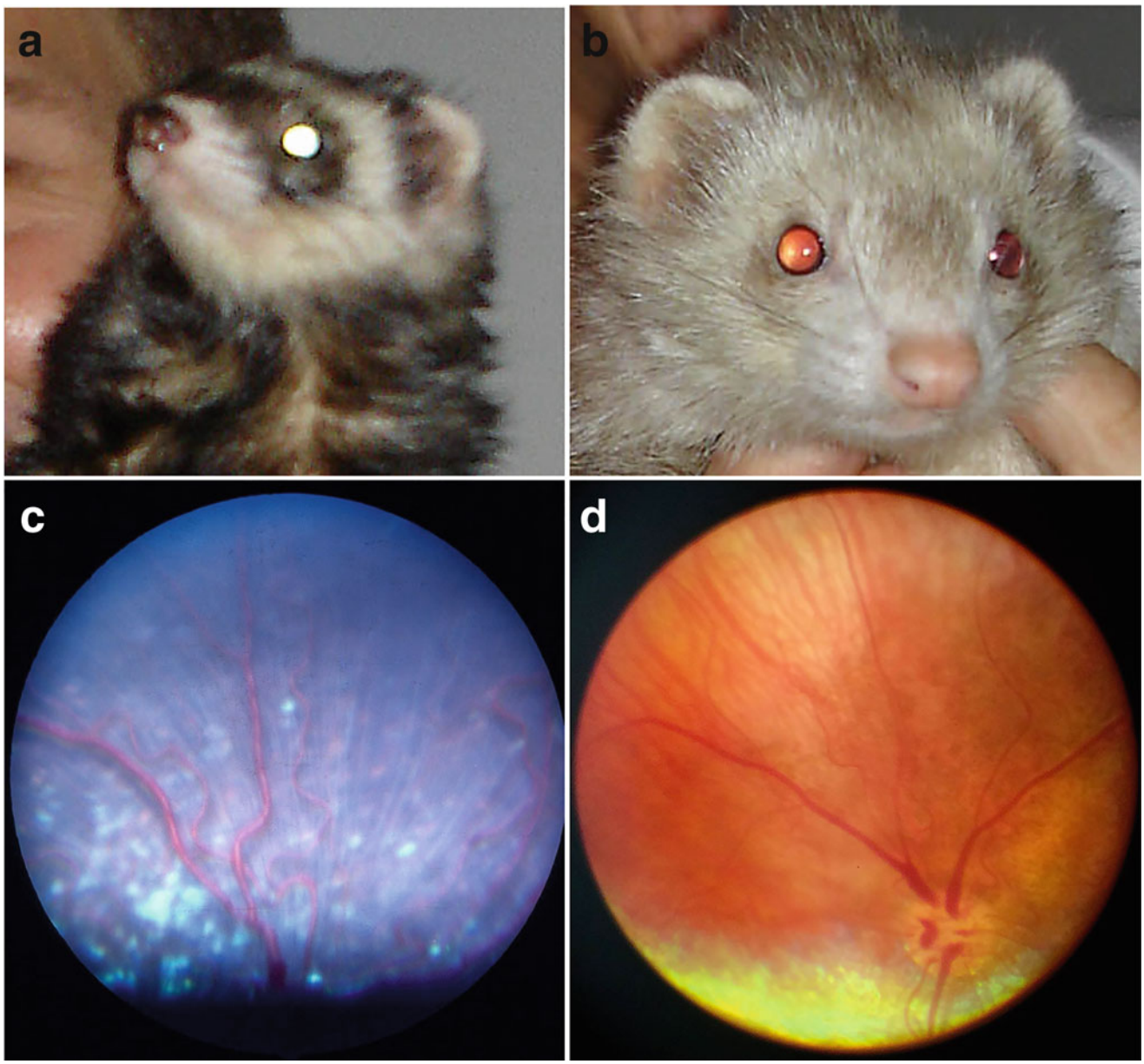

Fig. 39.2 Darkly pigmented ferrets possess a brightly reflective tapetum lucidum of variable size and color. (**a**) Note the *dark orange* reflex in this *black*-coated individual. (**b**) Note the presence of the holangiotic retina with a blueish tapetum lucidum in this young individual. (**c**) Note the small and poorly myelinated optic disc in this subalbinotic ferrets that lack melanosomes in the retinal pigment epithelium of the non-tapetal area and possess a tapetum lucidum of a *light yellow* to *orange color*. (**d**) (Courtesy Ana Carolina Rodarte de Almeida)

palatine, are found at the medial wall of the pterygopalatine fossa. Figure 39.3 provides an anatomic comparison of the orbit of two morphologic similar mustelids: the domestic ferret and the wild, free-ranging lesser grison *Galictis cuja*. In Spanish, the lesser grison is referred to as a huroncito (little ferret) or grisón. In Portuguese, this wild mustelid is called "furão selvagem" (wild ferret).

Ferrets possess a pronounced retrobulbar venous plexus that has been suggested as an alternative site for drawing blood (Fox et al. 1984; Good 2002; Davidson 1985; Wen et al. 1985). The authors do not recommend this procedure, since it is easier to collect blood from other locations and because of the possibility of damaging the globe with this technique. The clinical relevance for this observation is that hemorrhages from this venous plexus often occurs during enucleation procedures. If this happens, it should be carefully controlled by direct pressure, packing with gelatin sponges, or applying bovine thrombin at a concentration of 1000 IU/mL (Miller 1997; Williams and Gum 2013).

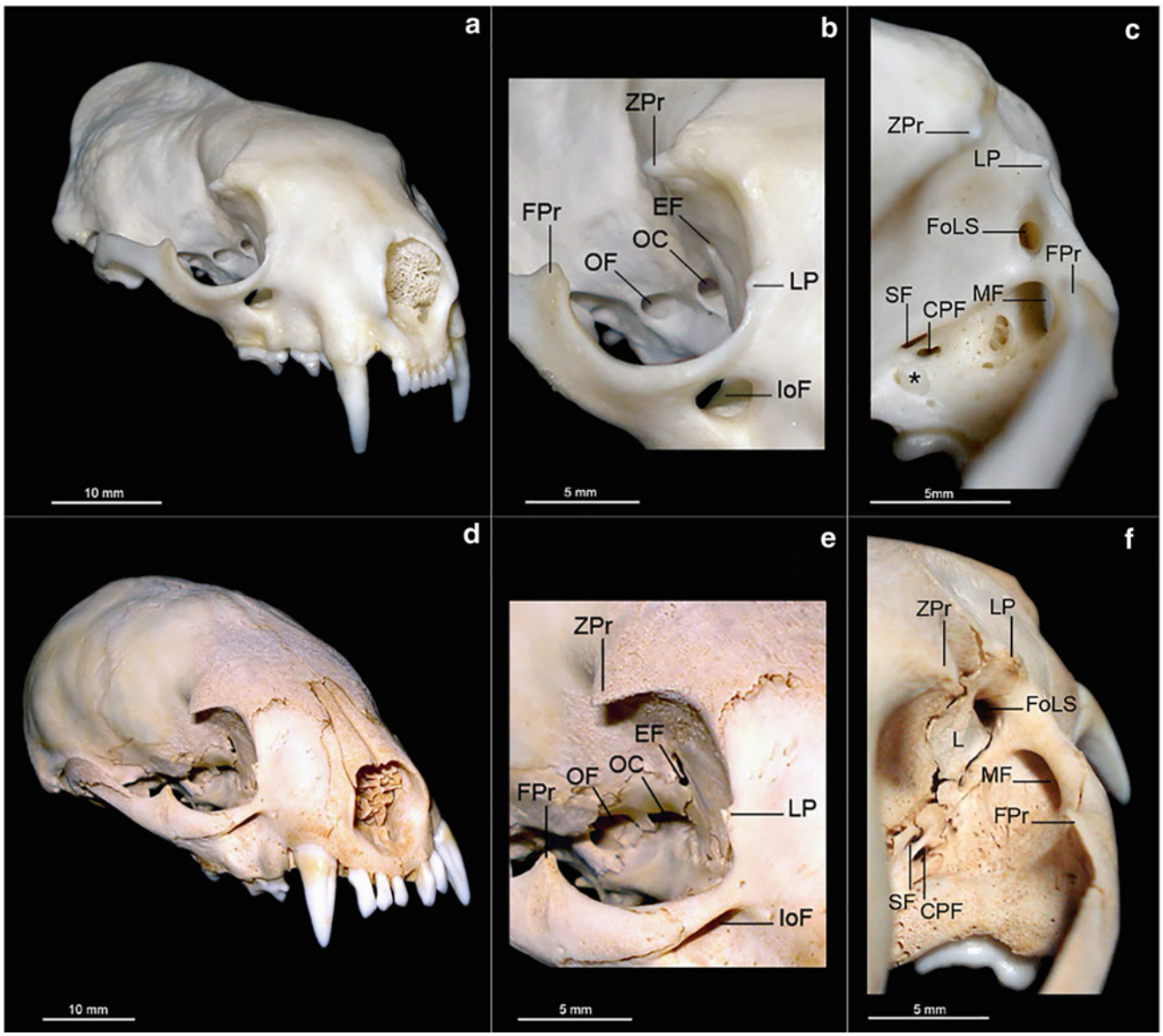

Fig. 39.3 Comparative anatomy of the bony orbit between a domestic and a wild mustelid. Views of an adult male domestic ferret (*Mustela putorius furo*) skull (**a**, **b**, and **c**) and of a male wild mustelid called lesser grison (*Galictis cuja*) skull (**d**, **e**, and **f**). (**a** and **d**) right rostrodorsolateral view of the two species; (**b** and **e**) close right rostrodorsolateral view of the orbit; (**c** and **f**) caudodorsolateral view of the orbit. *EF* ethmoidal foramen, *FPr* frontal process of the zigomatic bone, *IoF* infraorbital foramen, *L* lacrimal bone, *LP* lacrimal process, *FoLS* fossa for lacrimal sac, *MF* maxillary foramen, *OC* optic canal, *OF* orbitorotundum foramen, *PcF* caudal palatine foramen, *SF* sphenopalatine foramen, *ZPr* zigomatic process of the frontal bone. Note the exposure of the apical end of the root (*asterisk*) of the superior first (and unique) molar tooth through the pterygopalatine surface of the maxillary bone, on the floor of the pterygopalatine fossa. (Courtesy of Marcello Z. Machado)

Restraint and ophthalmic examination

Ferrets usually are fast and curious animals, which can make performing a complete ophthalmic examination a challenge. Other individuals may be quieter and calm and some may be even aggressive. Scruffing is the most common way of physically restraining ferrets during ophthalmic examination. The person scruffing the ferret should support some of the animal's weight, in order to avoid applying too much pressure in the neck itself, and to prevent iatrogenic elevation of intraocular pressure (IOP). Breaks during periods of restraint may help to decrease stress of the patient.

The palpebral fissures in young ferrets do not accommodate the width of the standard 5 mm Schirmer tear tests strips. The standard strip, nevertheless, fits most adult ferrets (Fig. 39.4a).

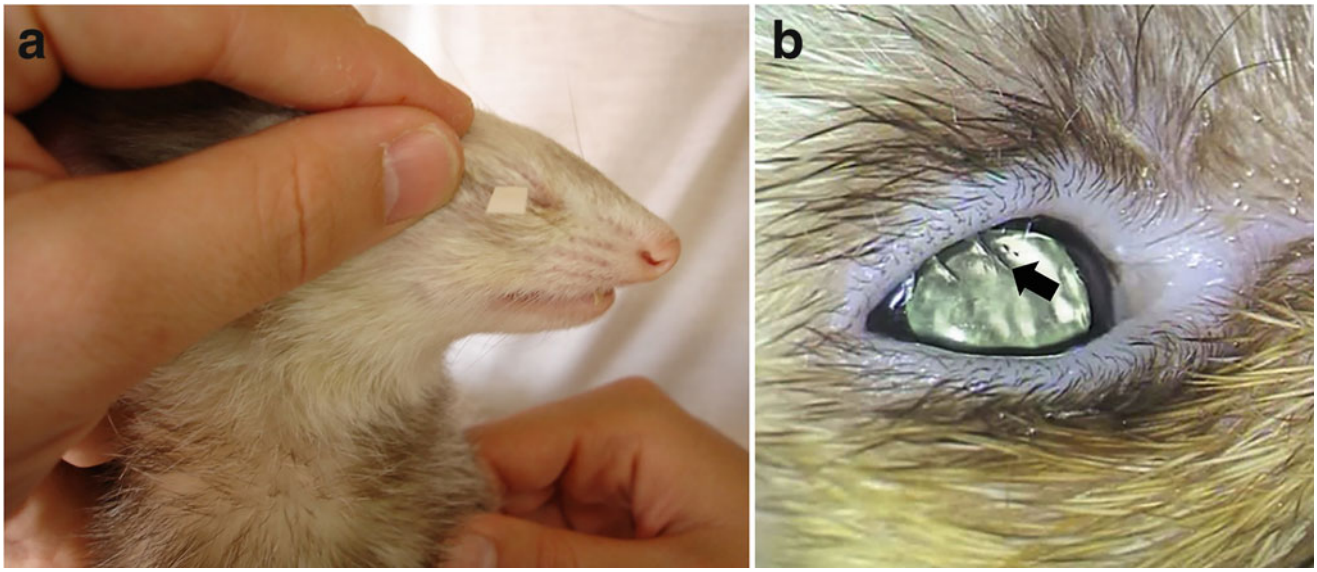

Fig. 39.4 (**a**) Note that the 5-mm Schirmer tear tests strip fits most adult ferrets (*arrow*). (**b**) Distichiasis in the right upper eyelid of a ferret. Note the three large distichia (*arrow*) in the upper eyelid of the right eye of a ferret with chronic epiphora and blepharospasm. Verboven CA, Djajadiningrat-Laanen SC, Kitslaar WJ, et al. Distichiasis in a ferret (*Mustela putorius furo*). Vet Ophthalmol. 2014;17:290–293

Ophthalmic Diseases

Eyelids

Entropion occurs due to the inversion of the eyelid margin (usually resulting in secondary trichiasis). It is a common ophthalmic condition in many domestic species and it has been documented in ferrets as well (Williams 2012). Anatomical (primary) entropion is the most common form in the ferret but it has been documented as a secondary condition due to conjunctival foreign bodies (Johnson-Delaney 2016). Serious corneal lesions can develop in some cases. Surgical correction requires most commonly the use of a modified Hotz-Celsus procedure. This involves excision of an ellipse-shaped stripe of skin parallel to the eyelid margin, the width, and length of which are dependent on the severity and extent of the entropion. Sutures of 6–0 polyglactin 910, silk, or braided nylon are frequently used to close the surgical wound.

Distichiasis has been diagnosed in ferrets (Verboven et al. 2014) (Fig. 39.4b). In this condition, cilia arise from Meibomian gland openings and both upper and lower eyelids can be affected. Animals with distichiasis must be evaluated carefully. The mere presence of distichiasis is not justification for surgical intervention. Treatment is indicated only when cilia are inducing corneoconjunctival irritation (ulceration, vascularization, fibrosis, pigmentation, epiphora, and/or blepharospasm). Possible treatment protocols include electroepilation or cryoelilation. Manual epilation is effective only temporarily but may aid in determining if the cilia are really causing a problem.

Congenital Ocular Conditions

Microphthalmia, cataracts, dermoids, and persistent fetal intraocular vasculature (PFIV) although uncommon, have been reported in the ferret (Miller 1997; Good 2002; Lipsitz et al. 2001; Kern 1989; Ryland and Gorham 1978). Microphthalmos has been reported in ferrets as part of an autosomal dominant multiple ocular anomaly syndrome (Dubielzig and Miller 1995) with cataract and retinal dysplasia (Williams and Gum 2013).

Neonatal Ocular Disorders

Ophthalmia neonatorum is a common condition in ferrets. A possible explanation for the relatively high prevalence is the long period of eyelid closure after bird. This disease occurs when an eye surface infection (often bacterial) occurs prior to lid separation. Clinically the eyelids appear distended (bulged) with or without the presence of external discharge. More than one individual in a litter frequently is affected. This disease is often diagnosed in kits aged a few days up to 3–4 weeks of age (Bell 1997; Good 2002; Williams 2012). Kits may stop nursing due to the pain related to pressing their head and eyes against the dam's nipple. It appears that *E. coli* mastitis in the jill may contribute to the disease development in kits (Besch-Williford 1987; Miller 1997; Good 2002). However, several other bacteria had been isolated in this disease. If possible, a sample of the exudate should be collected by aspiration or using a sterile swab and then submitted for culture and antimicrobial sensitivity tests. A feasible treatment option is to gently separate the eyelids (by cutting along the palpebral suture line by blunt dissection or by carefully with a small scalpel blade, then flushing the ocular

surface and conjunctival sac with sterile saline. Subsequently start topical antibiotic therapy guided by the sensitivity test results or, when culture was not performed, a broad-spectrum antibiotic ointment such as bacitracin zinc + polymyxin B sulfate + neomycin sulfate, could be used instead, three to four times a day for 10–12 days. Possible sequelae include symblepharon, corneal perforation, and even blindness.

Eyelid Masses

Neoplasia is the most common cause of skin masses in the ferret. Ferrets can develop a wide variety of skin cancers including mastocytomas, histiocytomas, sebaceous gland adenomas and adenocarcinomas, basal cell tumors, lymphoma, leiomyomas, lipomas, fibromas, fibrosarcomas, and hemangiomas. Anecdotal reports of the occurrence of neoplastic disease in the skin of the eyelids of ferrets are somewhat common. Mast cell tumor has been diagnosed in eyelids of both eyes of a 6-year-old spayed female ferret (personal communication, 2019). Another case report describes the presence of an ulcerated 1–2 cm mass located at the lower eyelid margin of a 3-year-old ferret. Histopathologic diagnosis revealed a malignant fibrous histiocytoma (Dillberger and Altman 1989).

Conjunctivitis

Conjunctivitis is commonly seen in ferrets. Prognosis varies, depending on the etiology (Miller 1997). Unilateral conjunctivitis is often associated with foreign bodies whereas bilateral conjunctivitis can be caused by improper bedding due to accumulation of dust and debris in the tear film and conjunctival fornix (Moody et al. 1985) or by a primary bacterial disease (Gaarder and Kern 2001) and these have a good prognosis. Conjunctivitis also is commonly associated with systemic diseases in the ferret, such as distemper virus infection (Fig. 39.5), human influenza virus, erythema multiforme, salmonellosis, or mycobacteriosis (Miller 1997; Good 2002; Hernández-Guerra et al. 2007, Hoefer et al. 2012; Orcutt and Tater 2012. Distemper cases usually have a poor prognosis (Fig. 39.5) (Deem et al. 2000; Langlois 2005; Perpiñán et al. 2008; van der Woerdt 2012). Mortalities following canine distemper virus infection have been described also in colonies and wildlife populations of other mustelids, including martens (Fig. 39.5), polecats, badgers, ferret-badger, otters, and weasels, leading to the assumption that all members of the family are susceptible (Beineke et al. 2015). Influenza-related conjunctivitis has a good prognosis. There are reports of *Salmonella* species-related conjunctivitis in ferrets but these are often accompanied by fever and hemorrhagic diarrhea (Good 2002; Marini et al. 1989; Gorham 1949; Morris and Coburn 1948).

Bacteria can normally be cultured at low numbers from the conjunctival sac (as in most mammals commensal isolates usually are Gram positive) (Montiani-Ferreira et al. 2006). Secondary bacterial conjunctivitis is more common than primary disease and often results from a predisposing factor. Blepharospasm, ocular discharge, and conjunctival hyperemia are common clinical signs of bacterial conjunctivitis. Conjunctival cytological scrapings using the non-cutting end of a scalpel blade can help in the process of diagnosis, since neutrophils, bacteria, and white blood cells with intracellular bacteria are frequently observed in these cases (Gaarder and Kern 2001). For diagnosing influenza-related conjunctivitis virus isolation and serological titers are indicated. Topical triple antibiotic ointment (bacitracin zinc + polymyxin B sulfate + neomycin sulfate) 4–6 times a day is usually curative (Gaarder and Kern 2001).

The ophthalmic signs of distemper include mucopurulent oculonasal discharge, blepharitis (Fig. 39.5), corneal ulcers, ankyloblepharon, anterior uveitis, photophobia, and keratoconjunctivitis sicca (Miller 1997; Good 2002; Hernández-Guerra et al. 2007; Kern 1989; van der Woerdt 2012). Conjunctivitis with a mucopurulent ocular discharge develops in 7–10 days after being infected with the virus (Gaarder and Kern 2001) and occurs during the initial phase of the disease, along with anorexia, fever, and nasal discharge (Deem et al. 2000; Langlois 2005; Perpiñán et al. 2008; van der Woerdt 2012). During a distemper infection, conjunctivitis, and ocular discharge are a direct result of a decreased tear production and secondary bacterial infection. Other clinical signs the ferrets with distemper may present are erythematous skin rash, including the foot pads. Serum antibody titers or immunofluorescent antibody testing of conjunctival or blood smears can aid the diagnosis Affected ferrets usually die within 12–35 days postinfection a regardless of symptomatic therapy (Gaarder and Kern 2001).

Human influenza virus-related conjunctivitis in ferrets usually is self-limiting and runs its course in about 5 days even without treatment. However, it can be accompanied in some cases by pneumonia, complicating the clinical picture (Miller 1997; Gaarder and Kern 2001).

Systemic infection with *Mycobacterium genavense* has been reported to cause generalized lymphadenopathy and conjunctivitis in two ferrets (Lucas et al. 2000). Treatment is challenging and may include: chloramphenicol ophthalmic ointment, 3 times a day for up to 90 days associated with systemic rifampicin, clofazimine, or clarithromycin (Lucas et al. 2000).

In ferrets, conjunctivitis may be a consistent clinical sign in systemic mycoplasmosis (Williams and Gum 2013).

Conjunctival foreign bodies causing conjunctivitis and corneal irritation or ulcers are common. Gentle removal of the foreign body with forceps and treating the ocular surface with topical broad-spectrum antibiotics seem to be the best treatment protocol. Foreign bodies may penetrate through the conjunctiva leaving a sinus that discharges into the conjunctival sac. Treatment includes removal of the foreign body,

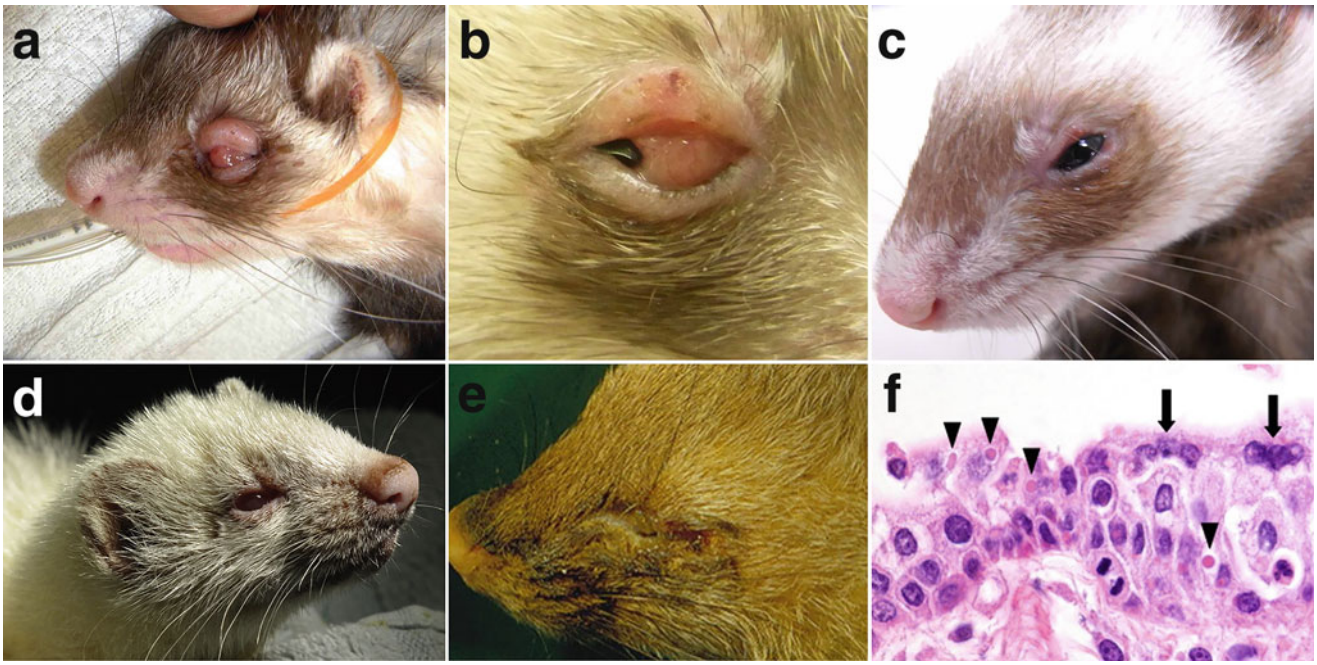

Fig. 39.5 Eyelid lesions in ferrets. (**a**–**c**) Multiple mast cell tumors of the eyelid and third eyelid of a 6-year-old spayed female ferret. Histopathologic analysis of biopsy samples from both locations on revealed multiple mast cell tumors. After oral prednisone administration, the eye lesions improved but recurred several weeks later. (**a**) Left eye at initial presentation. (**b**) Right eye at initial presentation. (**c**) Left eye 7 days after starting oral prednisone. (**d**) A case of conjunctivitis in a young ferret with a canine distemper virus infection. Note the oculonasal discharge, hyperemia, and blepharitis. (**e**) Canine distemper virus infection in a marten species. Note the presence of severe ocular discharge. (**f**) Photomicrography showing the conjunctival tissue with epithelial syncytial cells (*arrows*) and cytoplasmic eosinophilic viral inclusion bodies (*arrowheads*); hematoxylin–eosin, magnification ×600. (**a**)—Courtesy of Yasutsugu Miwa. (**d**)—Courtesy of Nicola Di Girolamo. (**e**, **f**)—Used with permission from: Beineke A, Baumgärtner W, Wohlsein P. Cross-species transmission of canine distemper virus-an update. One Health. 2015 Sep 13;1:49–59

surgical curettage, as well as treating with systemic and topical broad-spectrum antibiotics.

Corneal Diseases

Corneal Ulcers

A corneal ulcer is a lesion where there is a full-thickness defect in the corneal epithelium. The term can refer to a defect that just involves epithelium or one where there is loss of corneal stroma as well. Corneal ulcers are common in the ferret (Fig. 39.6), as it is for other species; the etiology is frequently multi-factorial, such as trauma, chemical irritants, eyelid defects (i.e., entropion and distichiasis), tear film defects, and secondary to corneal dystrophies and degenerations. Initial indications of the presence of corneal ulcers include an elevated third eyelid and corneal edema (Myrna and Girolamo 2019). The use of fluorescein dye (Fig. 39.6a, b) will demonstrate if the corneal epithelium has been ruptured and the stroma has been exposed. Fluorescein dye is also useful in assessing tear drainage via lacrimal puncta to the nares.

A broad-spectrum antibiotic (e.g., triple antibiotic solution) should be instilled q 6 h. It is important that the corneal ulcer specifically, the underlying abnormality or a given predisposing factor. If the response to treatment is not adequate, it is recommended to re-evaluate the diagnosis.

A topical parasympathetic blocking agent such as a 1% atropine solution, once a day for about 3–5 days, can be added to the protocol if iridocyclospasm is present. Culture and sensitivity tests can be used to direct the antibiotic choice. Chronic non-healing ulcers (also known as indolent ulcers or recurrent erosions) may necessitate an additional corneal epithelium debridement procedure with a cotton swab or diamond burr to promote corneal healing. Some serious ulcers are associated with a liquefaction (melting) of the corneal stroma. In this condition (melting ulcers) (Fig. 39.6c), corneal liquefaction (malacia) is caused by enzymatic (proteases) activity. The ulcer may rapidly (over hours) progress from a superficial to a deep ulcer. The enzymes originate from microorganisms (e.g., *Pseudomonas aeruginosa*, other Gram-negative rods, streptococci), PMN's, and from the cornea itself.

Deep or melting ulcers should be treated with surgery, usually a conjunctival pedicle graft technique, combined with aggressive antibiotic and anti-collagenase topical therapy (Montiani-Ferreira 2009).

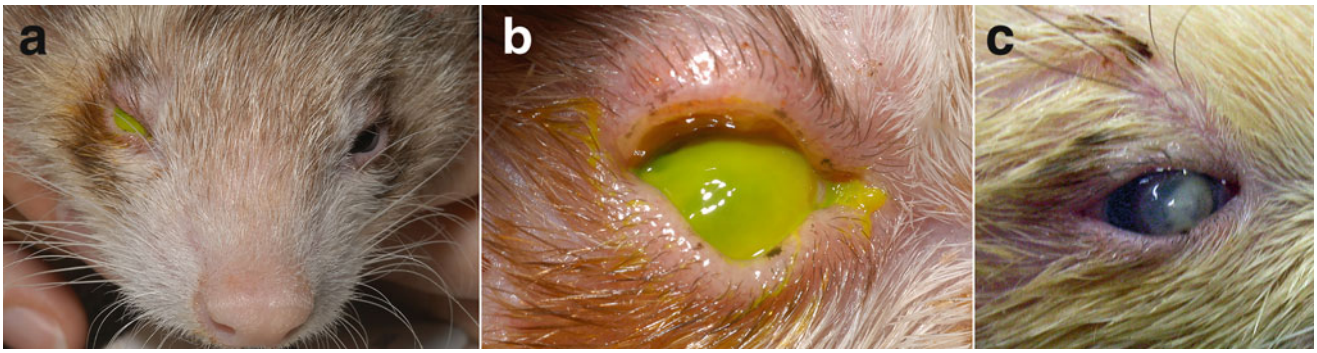

Fig. 39.6 A case of stromal ulcerative keratitis in the right eye of a ferret. Note the blepharospasm (**a**) and the fluorescein staining (**b**), demonstrating if the corneal epithelium has been ruptured and the stroma has been exposed. (**c**) A large corneal ulcer with an expanding white malacic gelatinous "melt." (Courtesy of Yasutsugu Miwa)

Other Corneal Diseases

Several other corneal diseases have been reported in the ferret and other mustelids. Intraocular disease can cause corneal edema and should be differentiated from corneal surface disease (Myrna and Girolamo 2019). Exposure keratitis secondary to exophthalmos has been reported (Miller and Pickett 1989; Good 2002). Ferrets with diets deficient in riboflavin were reported to develop corneal vascularization and opacification (Miller 1997; Good 2002). Degeneration of corneal endothelium leading to progressive corneal edema has been reported in mink (Hadlow 1987; van der Woerdt 2003). Some cases seem to respond to a symptomatic treatment using 5% sodium chloride solution, 2–4 times a day (van der Woerdt 2003; Montiani-Ferreira 2009).

Lymphoplasmacytic keratitis with multicentric lymphoma has been reported in a 2-year-old ferret (van der Woerdt 2003; Ringle et al. 1993). The keratitis in this ferret was unresponsive to topical steroids. In addition, systemic coronavirus was diagnosed in a patient with lethargy, weight loss, pruritus, and a yellowish corneal opacity (Lindemann et al. 2016). Anterior uveitis was evident in a similar fashion similar to cats with feline infectious peritonitis (Lindemann et al. 2016). The infiltrative corneal lesion in this ferret was similar to the corneal lesions described in a mink with Aleutian disease, a generalized parvoviral immune complex disease. The presence of antibodies against Aleutian Disease Virus (ADV) in ferrets is believed to increase susceptibility due to immunosuppression (Ringle et al. 1993). The mechanism by which ADV affects the immune system is not well-understood. Immunodepression could cause the ferret to be more vulnerable to viral enteritis, canine distemper virus, lymphoma, and other conditions. Degeneration of corneal endothelial cells leading to progressive corneal edema and cloudiness of the cornea is seen in older mink (8–11 years of age). Royal pastel females are predisposed. Unlike the disease in dogs, these mink do not develop corneal ulceration, pigmentation, or vascularization. There is no specific treatment for this condition, but symptomatic treatment with 5% sodium chloride solution or ointment two to four times a day may or may not improve corneal clarity (van der Woerdt 2012).

Congenital dermoids have been documented in the ferret showing the classic appearance of a patch of haired skin on the corneal surface (Myrna and Girolamo 2019).

Uveitis

Uveitis is not commonly diagnosed, even severe lens-induced uveitis (which is common in small animals); seems to be infrequent and mild when it happens. When the disease is diagnosed in the ferret, usually is secondary to trauma or ulcerative keratitis (reflex axonal pathway) (Miller 1997; Good 2002).

Aleutian disease might be considered in the differential diagnosis of ferrets presenting uveitis because experimentally induced Aleutian disease in minks produces uveitis as the primary ocular lesion (Miller 1997; Good 2002). Other causes of uveitis in ferrets include sepsis and neoplastic diseases, such as lymphosarcoma. If uveitis is present and a primary ocular origin cannot be found, diagnostic testing for systemic disease should be investigated (Good 2002). Thus, conjunctival cytology, complete blood count, serum biochemistry panel, urinalysis, thoracic radiographs, abdominal ultrasonography, PCR, and serology for infectious agents as well as other diagnostic testing modalities should be performed when uveitis is recognized in the ferret (Good 2002; Montiani-Ferreira 2009).

Topical steroids are used when corneal ulceration is not present. The frequency of application varies directly with the severity of the uveitis. Typically, it is applied 2–4 times a day. Lens-induced uveitis can usually be controlled with topical application of 1% prednisolone acetate 2 times a day (van der Woerdt 2003). Topical nonsteroidal solutions can be used with attention in cases of corneal ulceration as they have been associated in delay of corneal healing and promoting secondary infections. To relieve uveitis pain and to minimize the potential for posterior synechia in a miotic eye, topical

atropine can be used typically once or twice a day. Its use is contraindicated when glaucoma is suspected (Montiani-Ferreira 2009). Systemic steroids at anti-inflammatory doses or nonsteroidal anti-inflammatory drugs (when steroids are contraindicated) still are the foundation of the treatment of uveitis (Montiani-Ferreira 2009) but the underlying cause should always be identified and treated.

Since glaucoma can be a blinding and painful sequela to uveitis, treatment for uveitis should be meticulous and anti-glaucoma therapy should be considered if intraocular pressure begins to increase (Good 2002).

Cataracts

Cataracts are somewhat common in ferrets. The incidence of cataracts in young ferrets may be as high as 47% in certain populations (Miller et al. 1993). Some young individuals may present cataracts associated with microphthalmos (Miller et al. 1993). The etiology of cataracts in ferrets, however, is not fully understood and may be multifactorial. Probable causes for cataracts include genetic and nutritional (Miller et al. 1993). Congenital cataracts and senile cataracts (Fig. 39.7) have been reported in ferrets (Good 2002; Bakthavatchalu et al. 2016). Clinically, most cataracts are seen in older ferrets (more than 5 years of age) (Fig. 39.7). Diets high in fat or deficient in vitamins, such as vitamin E, vitamin A and/or protein may lead to cataract formation in ferrets (Miller 1997; Good 2002). In addition to conjunctivitis and cataracts, vitamin A deficiency is reported to cause night blindness in ferrets (Fox and McLain 1998).

Successful surgical treatment of cataracts in ferrets using extracapsular or phacoemulsification technique has been reported (van der Woerdt 2003). Surgical planning needs to take into account that ferrets have small eyes and shallow anterior chambers. Primary and secondary lens luxations and subluxations can occur in ferrets (Miller 1997; Good 2002; Kern 1989). The condition is somewhat common, especially the ones secondary to chronic cataracts (Fig. 39.8).

Glaucoma

Glaucoma is actually a group of conditions and not a single disease entity. These conditions lead to an impairment of the aqueous humor outflow, which leads to an elevation of intraocular pressure (IOP) that is detrimental to axoplasmic flow in the optic disc resulting in retinal degeneration and blindness. Glaucoma in humans is very common; the commonest form in humans (primary glaucoma) is a chronic disease and causes a slow loss of visual fields. Both, primary and secondary glaucoma have been reported in ferrets. Fortunately, primary glaucoma is not very common in this species (Good 2002; Boyd et al. 2007). Glaucoma is a very painful condition and the eye quickly develops irreversible blindness. Thus, acute glaucoma is a medical emergency, and urgent action or referral to a veterinary ophthalmologist should be pursued. Unfortunately, glaucoma can be difficult to diagnose during the early stages without proper equipment and very difficult to manage successfully. Glaucoma also should be part of the differential diagnosis of the red eye and should be differentiated from uveitis and conjunctivitis. In fact, post-uveitis and post-synechia secondary glaucomas have been reported in ferrets (Good 2002; Boyd et al. 2007) (Fig. 39.9a, b). Secondary glaucoma as a result of anterior or posterior lens luxations also has been reported in ferrets (Miller 1997; Good 2002). In these cases, surgical extraction of the lens is feasible but somewhat difficult due to the small size of the eye (Good 2002). Intraocular neoplasia also can cause glaucoma in ferrets by infiltrating the drainage angle or by causing inflammation and adhesions (Fig. 39.9c, d).

Presently, veterinary ophthalmologists use three types of indirect (noninvasive) IOP estimations: indentation, applanation, and rebound tonometry. The two most frequently used types of tonometers are the Tono-Pen applanation tonometer (Fig. 39.10) and the TonoVet® rebound tonometer (Icare Finland Oy, Helsinki, Finland). Tonometry is essential in the diagnosis and treatment of glaucoma. Digital tonometry (palpating the eye with fingers to estimate "normal" versus "high" pressure) is inaccurate and should not be used to diagnose glaucoma or monitor response to treatment. The size of the cornea of adult ferrets is large enough to fit the tip of the applanation tonometer such as Tono Pen XL (Mentor, Santa. Barbara, CA, USA) (diameter = 3 mm) for intraocular pressure (Fig. 39.10). The rebound tonometer *TonoVet* (Icare, Oy, *Finland*) presents an even smaller probe (diameter = 1.3 mm) and the examiner can avoid the contact of the eyelids more efficiently (Leiva et al. 2006; DiGirolamo et al. 2013).

The normal values of IOP in the ferret as measured with a Tono Pen XL is 12–17 mmHg (Montiani-Ferreira et al. 2006) and 14.07 ± 0.35 as measured with a TonoVet (DiGirolamo et al. 2013). Normal IOP values, as well as other parameters for ophthalmic tests, are available in Appendix 3.

An increase in globe volume can take place with chronicity of glaucoma. This condition is called buphthalmos (Fig. 39.9) and when present usually indicates that the eye is irreversibly blind. In these cases, nucleation should be discussed with the owners.

To treat glaucoma in ferrets the use of topical β-blockers (0.5% timolol maleate), carbonic anhydrase inhibitors (2.0% dorzolamide), parasympathomimetic agents (1.0% pilocarpine), and prostaglandin analogues (0.005% latanoprost) have been reported. Alternatively, the use of a fixed combination of dorzolamide-timolol (Cosopt®, Merck & Co., Inc., Whitehouse Station, NJ, USA) one drop in the affected eye with an 8- or 12-h interval has been proposed (Montiani-Ferreira 2009). The efficacy of all these agents, however, still has not been completely proved in this species (Good 2002).

In most cases, medical treatment is only temporarily effective and will fail at some time. If glaucoma is not controlled permanently with medication, a surgical procedure might be

Fig. 39.7 Cataract in an older ferret. (**a**) A castrated male, 6-year-old ferret presenting bilateral cataracts, in the right eye (**b**) note the hypermature cataract and in the left eye (**c**) Note a Morgagnian hypermature cataract, formed by liquefaction of the cortex and sinking of the dense nucleus to the bottom of the capsular bag. (Courtesy of Adolfo Guandalini)

indicated. Diode laser has been used to perform a transscleral cyclophotocoagulation to control the pressure in one case of glaucoma in a 7-year-old neutered male ferret. The intraocular pressure was controlled with alternate-day application of a topical steroid after (Good 2002). Animals with glaucoma should be referred for surgical treatment of glaucoma, when there is still some hope of vision. Early referral or emergency referral should always be considered when dealing with glaucoma. Once the eye is irreversibly blind, the animal's comfort is the main consideration.

Retinal Atrophy

Progressive retinal atrophy (PRA) has been anecdotally reported in ferrets (Gaarder and Kern 2001; Williams and Gum 2013). PRA is a collective term used to describe several hereditary retinopathies that are similar clinically. Since this disease initially targets rods that function in dim light and are most abundant in the peripheral retina, nyctalopia, and poor peripheral vision initially occur but may not be noticed until the disease is advanced. Progressive loss of day vision follows. Eyes appear "brighter" because tapetal reflectivity

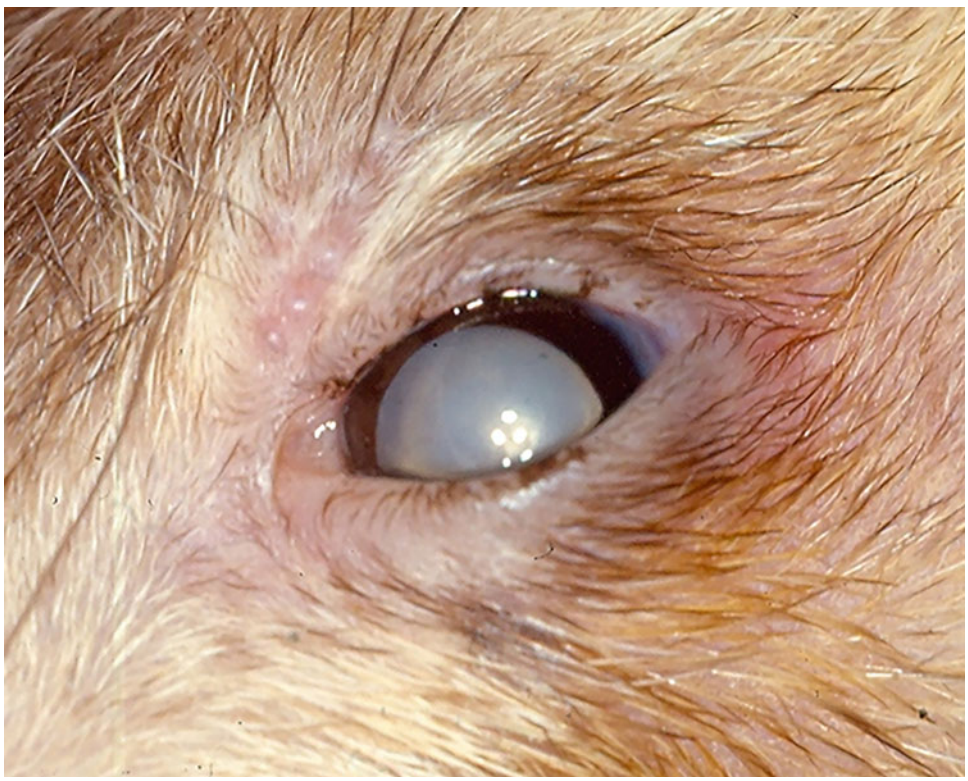

Fig. 39.8 Anterior lens luxation secondary to chronic cataracts in the left eye of an adult male ferret. (Courtesy of Adolfo Guandalini)

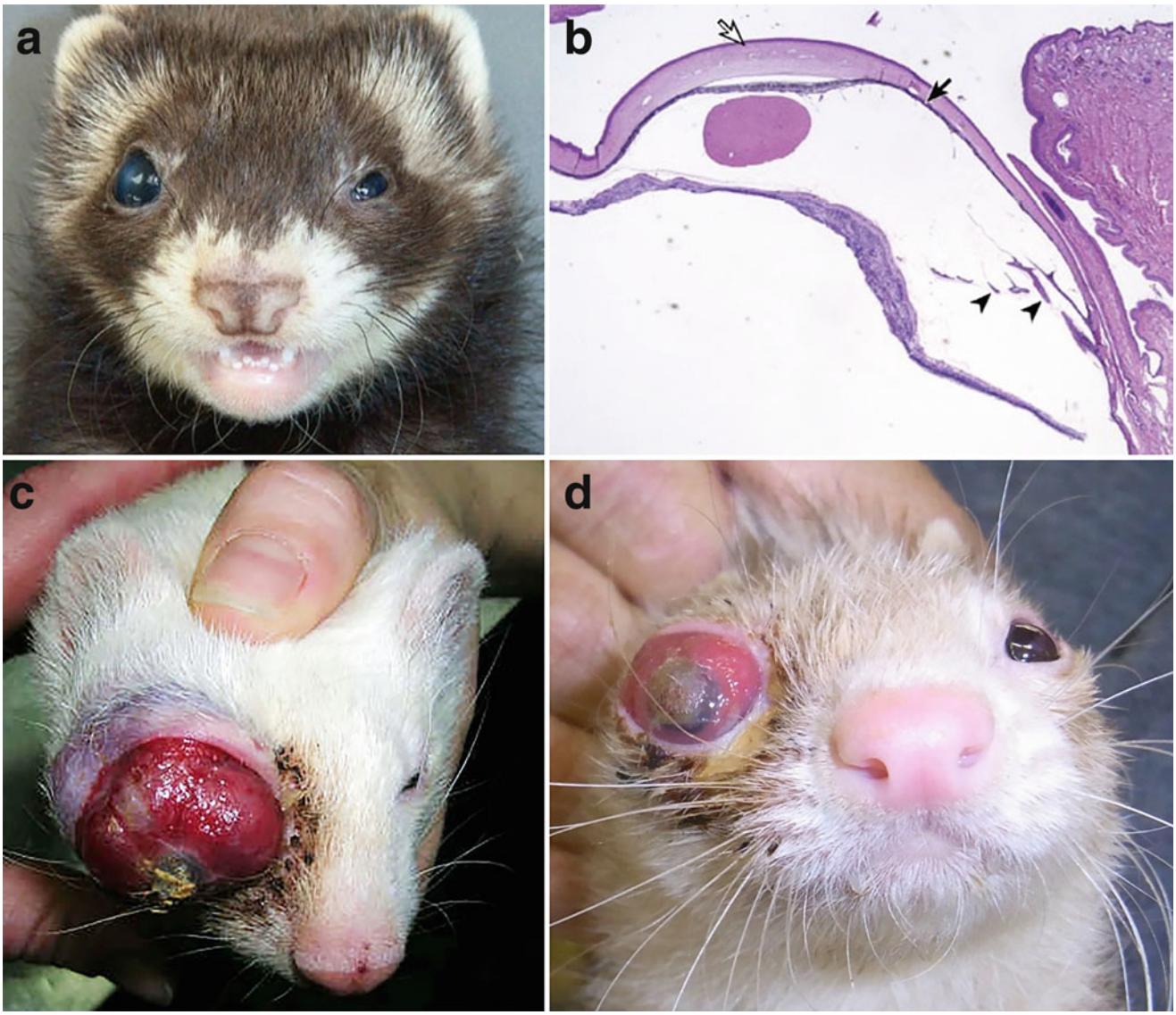

Fig. 39.9 Chronic secondary glaucoma cases presenting buphthalmos. (**a**) An 8-week-old male ferret with mild buphthalmos due to secondary glaucoma. (**b**) Low-power photomicrograph of the whole anterior segment of the same right eye (as in **a**). The white arrow indicates the cornea at three times the normal thickness with numerous (abnormal) corneal blood vessels. Peripherally the iris is attached to the cornea resulting in broad anterior synechiae (*black arrow*). *Black arrow* heads point to retracted ciliary processes. It is likely this ferret had secondary glaucoma caused by synechial-induced obstruction of the aqueous humor drainage system. (**c** and **d**) are representative cases of ferrets presenting more severe buphthalmos and forward displacement of the globe. In both cases, the condition was believed to be due to an intraocular neoplastic disease. In addition, in both of these cases, the owners were scheduled for bringing the patients for enucleation and failed to show up for the surgery. Thus, a definitive diagnosis was never reached. (**a**, **b**) Boyd K, Smith RS, Funk AJ, Rogers TD, Dobbins RM. A closer look: secondary glaucoma more likely. Lab Anim (NY). 2007;36(1):13–14 (with permission). (**c**) Courtesy of Angela Duke. (**d**) Courtesy of Yasutsugu Miwa)

is increased and pupils tend to remain dilated. Often first discovered by the owner when dog is taken to unfamiliar surroundings. Cataracts may or may not be present (van der Woerdt 2003). Increased tapetal reflectivity, granular texture to tapetum lucidum, depigmented non-tapetal fundus, attenuation of retinal blood vessels, demyelinated optic papilla, decreased pupillary light reflexes (particularly late in disease), and mydriasis also are common clinical features. Secondary cataracts may develop concurrently particularly in the later-onset forms. Genetic factors and nutritional (e.g., taurine and vitamin A) deficiencies have been suggested in different reviews but not reported in the primary literature are being investigated (Gaarder and Kern 2001; Good 2002; Williams and Gum 2013). Since there is no effective cure clinically available for this condition, the affected animals should be removed from breeding programs.

Fig. 39.10 An applanation tonometer (Tono-Pen XL, Mentor, USA) being used in the left eye of an adult ferret. Note that the size of the cornea of adult ferrets is large enough to fit the tip of the applanation tonometer

Exophthalmos

Exophthalmos is a pathological rostral protrusion of a normal-sized globe within the orbit. Retrobulbar diseases are occasionally seen in ferrets causing exophthalmos. Other clinical signs of retrobulbar disease include protrusion of the third eyelid and examiners' failure to retropulse the eyeball. There are case reports in the literature and several cases submitted to the Comparative Ocular Pathology Laboratory of Wisconsin (COPLOW) (Dubielzig, personal communication, 2019) of zygomatic salivary gland mucocele and orbital neoplastic disease (such as lymphosarcoma) causing exophthalmos in ferrets (Fig. 39.11) (Miller and Pickett 1989; McCalla et al. 1997; van der Woerdt 2003). Ultrasonography and fine-needle aspiration of the retrobulbar space followed by cytology may help diagnosing the exophthalmos-causing condition. Other diagnostic imaging modalities also may help, such as computed tomography scan and magnetic resonance.

Otters

There are 13 species of otter in the subfamily Lutrinae distributed across the globe. Most of the otters are insufficiently known, and most are rapidly disappearing along with the clean wetlands they inhabit worldwide. The IUCN Red List of Threatened Animals (IUCN 1988) lists eight otters as either "Vulnerable" or "Insufficiently Known." The five "Vulnerable" species include the marine otter (*Lutra felina*), Neotropical otter (*L. longicaudis*), giant otter (Pteronura brasiliensis) of South America, and the Eurasian otter (Lutra lutra) in Europe and northern Asia. In Asia, the Asian small-clawed otter (*Aonyx cinerea*), smooth otter (*Lutra perspicillata*), and hairy-nosed otter (*L. sumatrana*) are listed as "Insufficiently Known" (Foster-Turley et al. 1990).

Otters are amphibious (sea otters) or semiaquatic (river otters) carnivorous mammals who must adapt their visual processes to survive in both an aquatic environment and a terrestrial environment. They must see well in both environments as they mostly feed and breed in the water, including different water depths up to about 100 m (Bodkin et al. 2004). While sea otters can spend their entire lives in the water, they will keep their heads above water throughout the day and need to have an acute vision in both air and water. Sea otters, specifically Southern sea otters (*Enhydra lutris nereis*), are listed as a threatened species under the ESA. Threats to their livelihood historically included the fur trade and more recently include climate change/pollution, predation, and loss of their prey species the sea urchin, among other causes. They are a keystone species and sentinel animal of ocean health and one of the only marine animals to use tools as devices, which they use to open shells of mollusks such as mussels while foraging. In addition to the below-mentioned ocular adaptations to a marine environment, otters have developed long whiskers for sensation in murky waters and the densest fur of any mammal, allowing for survival

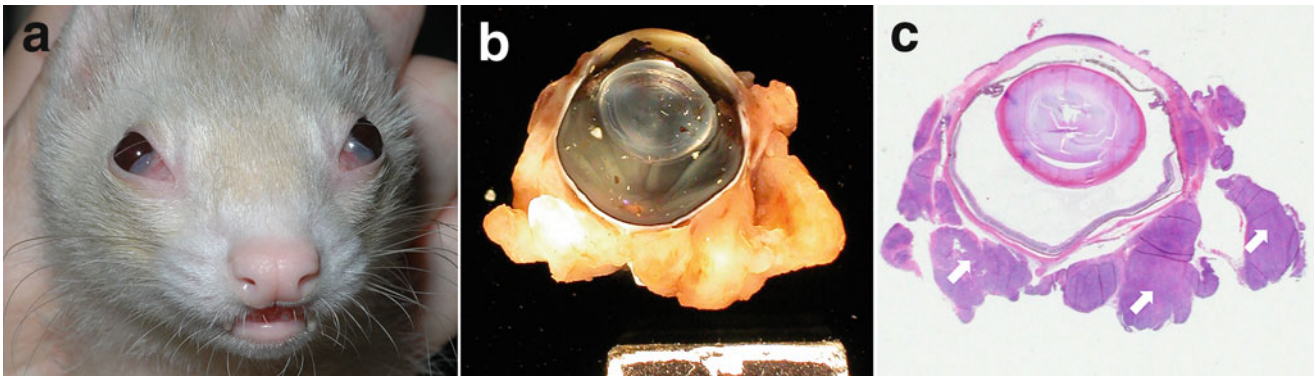

Fig. 39.11 An example of lymphosarcoma as a retrobulbar disease-causing exophthalmos. Note the rostral protrusion of a normal-sized globe and the protrusion of the third eyelid (**a**). Gross anatomy (**b**) and histologic (**c**) aspects of an enucleated globe diagnosed. Note the retrobulbar hypercellular proliferation causing compression of the globe. (Courtesy of Richard Dubielzig, Comparative Ocular Pathology Laboratory of Wisconsin (COPLOW))

without blubber in cold temperatures. Some of the ocular adaptations involve the cornea, lens, and accommodation. In a terrestrial environment, the cornea provides a significant amount of refractive power, bending light to focus on the retina because of the refractive indices differences between air and the cornea. In water, however, this corneal refractive power is lost due to the refractive indices of water and the cornea being very similar. For this reason, otters have to have a mechanism to adjust to vision in both environments. Both sea and river otters do this in a manner similar to some aquatic birds, with lens anterior movement allowing for an accommodative range of 60 D for the sea otter (Murphy et al. 1990; Ballard et al. 1989).

Morphological Features of the Globe and Orbit

In the same way as ferrets, the otters' bony orbit is incomplete. Using fixed globes, the horizontal limbal diameter was measured at 9 mm and the vertical diameter was 8 mm. The axial diameter of the globe was about 14 mm and equatorial diameter was 14.5 mm (Murphy et al. 1990). An image of a normal otter eye can be found in Fig. 39.12.

Otters possess a corneoscleral venous plexus within the sclera. The axial cornea is nearly 0.3 mm thick with very developed anterior epithelium composed of a layer of basal cells than a couple of layers of wing cells and about a dozen layers of superficial squamous cells. The stroma is 0.2 mm thick and has regularly aligned lamellae. Similar to other mammals, there is a thin Descemet's membrane and a posterior layer or endothelium with cuboidal cells (Murphy et al. 1990).

The iris stroma is mostly smooth muscle fibers. There is a circumferential smooth muscle sphincter extending from within 1 mm of the iris root to the pupillary margin. The radial iris dilator muscle occupies most of the iris extending from the root to within 0.2 mm of the pupillary margin. Otters also have an oblique smooth muscle fiber at the iris root and a well-developed ciliary muscle that is smooth muscle in composition (Murphy et al. 1990).

Otters have been shown to dilate partially with tropicamide. Anesthesia, particularly opioids, can counteract this, so dilating for a procedure such as cataract surgery can be challenging depending on the anesthetic used. Multiple drops may be needed including tropicamide, phenylephrine, and if intraocular surgery, epinephrine, and viscoelastic. Figure 39.13 shows an otter eye after receiving multiple drops of tropicamide versus the same otter the following day once the effects have worn off. As can be observed in Fig. 39.13a, a minor pharmacological dilation did occur, but more would be needed for a surgical procedure.

The lenses from fixed samples measured 7.4 mm. Unlike other marine mammals, otter lens anatomy is more similar to their terrestrial relatives and the rest of the *Mustelidae* family and they maintain a lenticular shaped lens rather than a spherical lens (Mass and Supin 2000). The retina is holangiotic (Fig. 39.14) with vessels extending throughout the retina and onto the optic nerve head, similar to other mustelids. The otter retina (*Enhydra lutris)* has three different opsins (Rod, M/L cone, S cone) (Levenson et al. 2006). There is an extensive cellular-type tapetum located in the choroid. Similar to terrestrial retinas, the otter retina has a nasotemporal area of high density of ganglion cells, or a visual streak, where there are relatively small and dense cells about 4000 cells/mm^2 (Mass and Supin 2000).

Vision an Optics

Anatomical and behavioral studies suggest that sea otter visual acuity is comparable although underwater acuity is possibly slightly worse than other marine mammals (Mass

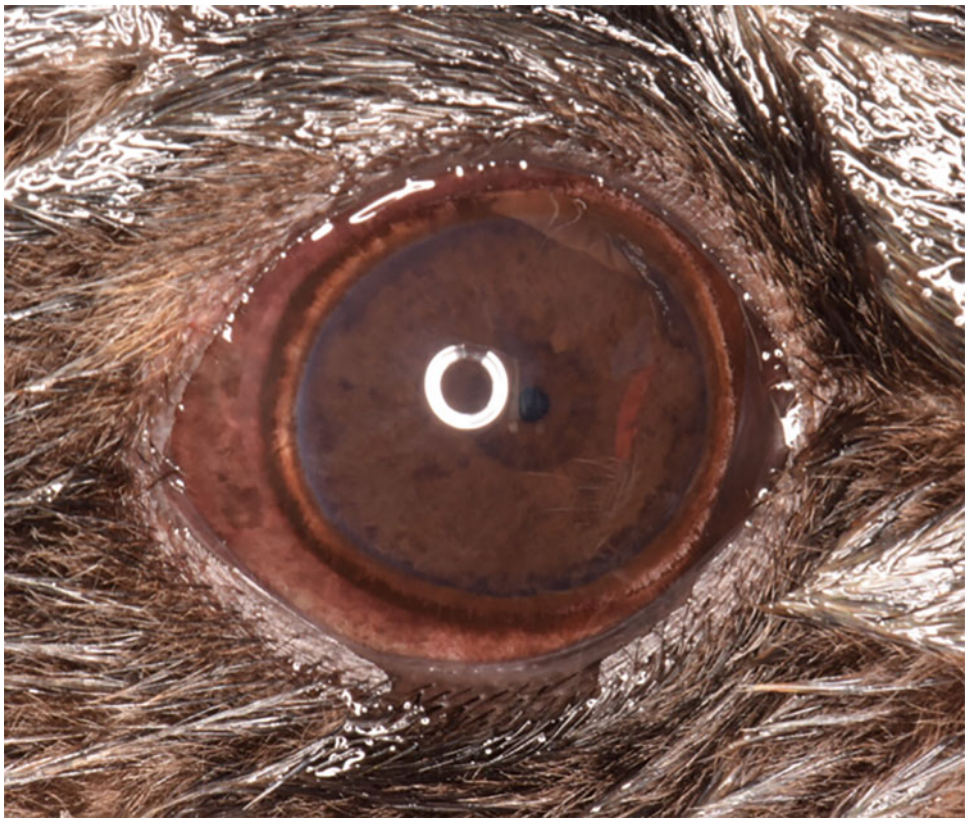

Fig. 39.12 Image of normal sea otter (*Enhydra lutris*) eye. (Image courtesy of K. Freeman and taken under USFWS MA 186914–2)

and Supin 2000; Gentry and Peterson 1967). The accommodative range of the otter is reported to be 3–4 times greater than any terrestrial mammal (Walls 1967). The sea otter and the Asian clawless otter both maintain equivalent visual acuities in air and water (Schusterman and Barrett, Ballet and Schusterman). They use the refractive

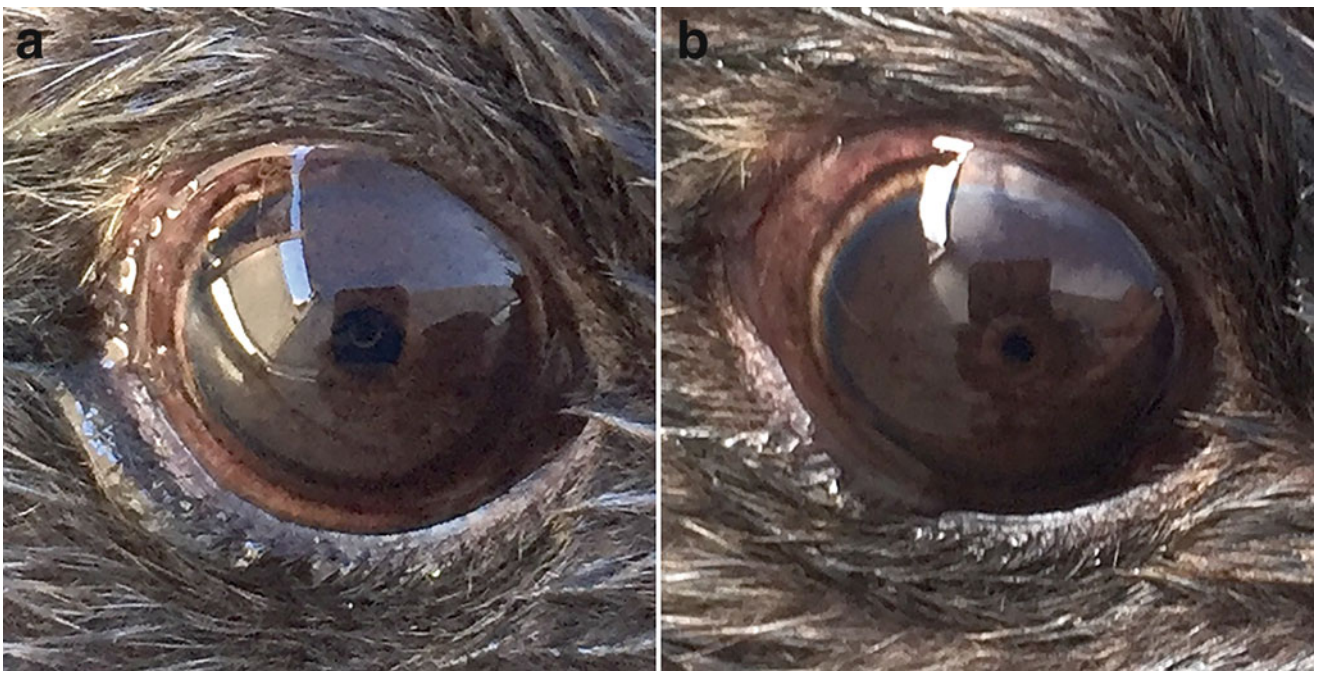

Fig. 39.13 Pupil dilation in otters. (**a**) Sea otter (*Enhydra lutris*) eye post-tropicamide. (**b**) Same otter eye 24 h following dilation

Fig. 39.14 Holangiotic retina of a normal sea otter (*Enhydra lutris*) eye. (Image by K. Freeman taken under USFWS MA 186914–2)

power of the curved cornea and lens, similar to other *Mustilidae* in air (Balliet and Schusterman 1971). The special adaptations are useful for water acuity where they have adapted to develop a large accommodative range similar to what cormorants accomplish with a very large movement and lens curvature change. This probable lens curvature change likely occurs with the aid of the iris and iris musculature forming a ring through which the lens is squeezed and moved anteriorly. A proposed mechanism in the sea otter involves the ciliary muscles, which may aid to move the ciliary body anteriorly and dilate the inner wall of the corneoscleral venous plexus, thereby causing an outflow of aqueous from the anterior chamber and an influx into the posterior segment, which would further propel the lens anteriorly. Murphy et al. 1990 also proposed that the unique uveal-uveal fibers contraction could draw the root of the iris posteriorly and the ciliary body anteriorly, further helping to move the lens anteriorly.

Ophthalmic Diseases

Corneal ulcers are approached similarly to those in ferrets and other carnivores. Ulceration from flaking mineral/lipid due to corneal degeneration/dystrophy has been diagnosed in an Asian small-clawed otter *Aonyx cinereus* (Bret A. Moore, personal communication). The right cornea was mildly affected axially (Fig. 39.15a), however, the left eye developed a deep facet with continued ulceration from ruptured epithelial bullae secondary to suspected endothelial decompensation (Fig. 39.15b, c). A conjunctival pedicle graft was elected to (1) provide stability over the deep corneal defect, and (2) act as an active source of edema removal from the corneal stroma (Fig. 39.15d). The graft was prepared very thin, and was secured onto the cornea with 10–0 Polyglactin 910 absorbable (Vicryl) following debridement of the epithelium within the defect.

Keratitis initiating at the lateral aspect of the cornea has been reported in otters. The origin of this is yet unknown but it is possible it is similar to a pinniped keratopathy and may have either an autoimmune or UV-induced or combination of both causes. Figure 39.16 shows an example of lateral keratitis. Figure 39.16a shows the pre-treatment corneal appearance and 16b shows continued fibrosis but more hypoperfused vessels post-NSAID treatment.

Otters in captivity have been shown to develop cataracts. Like other species, cataracts are likely due to a variety of causes including age-related, UV related, inherited, and metabolic/drug induced. Anecdotal evidence indicated that steroid use in cases of immune-mediated diseases has been linked to cataract development. Cataract surgery can be successfully performed with phacoemulsification. The lenses have been subjectively reported to be relatively soft and to aspirate easily with a short phacoemulsification time. Cataracts themselves can cause lens-induced uveitis and topical anti-inflammatory medications are needed when the cataracts are advanced and either late immature, mature, or hypermature. Figure 39.16a shows a mature cataract in a partially dilated sea otter and Fig. 39.16b is the same eye with the pupil not dilated. Figure 39.17a shows a mature cataract causing lens-induced uveitis in a partially dilated sea otter. Figure 39.17b is the same eye after treatment with topical ketorolac twice a day for a month showing resolution of the lens-induced uveitis.

Otters with systemic disease can develop anterior uveitis and/or corneal edema. For example, there was a case in Scotland of a wild malnourished Eurasian otter who developed bilateral corneal edema about 2 weeks after being admitted to a rehabilitation center. This otter died about 10 days later of *Clostridium piliforme* infection, Tyzzer's disease. While the iris appeared to have no more leukocytes than a normal iris, there was marked inflammation in the cornea and posterior cornea, including endothelium (Simpson et al. 2008). Uveitis involving the iris and ciliary body has also been reported in otters naturally infected with Aleutian Disease Virus (ADV) (Williams 2012).

Otters infected with the fatal parasite *Sarcocystis neurona* can have retinal damage starting at the retinal pigment epithelium and throughout all layers of the retina. In one case, this included damage to the inner and outer nuclear layers. In this same case, the damage was worse at the outer retina and inner surface of the tapetum. There was also hemorrhage in the choroid and vitreous. *S. neurona* causes a protozoal

Fig. 39.15 Corneal degeneration/dystrophy in an Asian small-clawed otter (*Aonyx cinereus*). (**a**) Mild axial corneal degeneration without complication. (**b**, **c**) Corneal mineral or lipid deposits sitting with a deep facet with several pinpoint ulcerations due to ruptured bullae. Note the severe corneal edema, thought to be due to endothelial decompensation. (**d**) A conjunctival pedicle graft was successfully placed, providing tectonic support as well as drawing fluid from the edematous stroma. (Courtesy of Bret A. Moore)

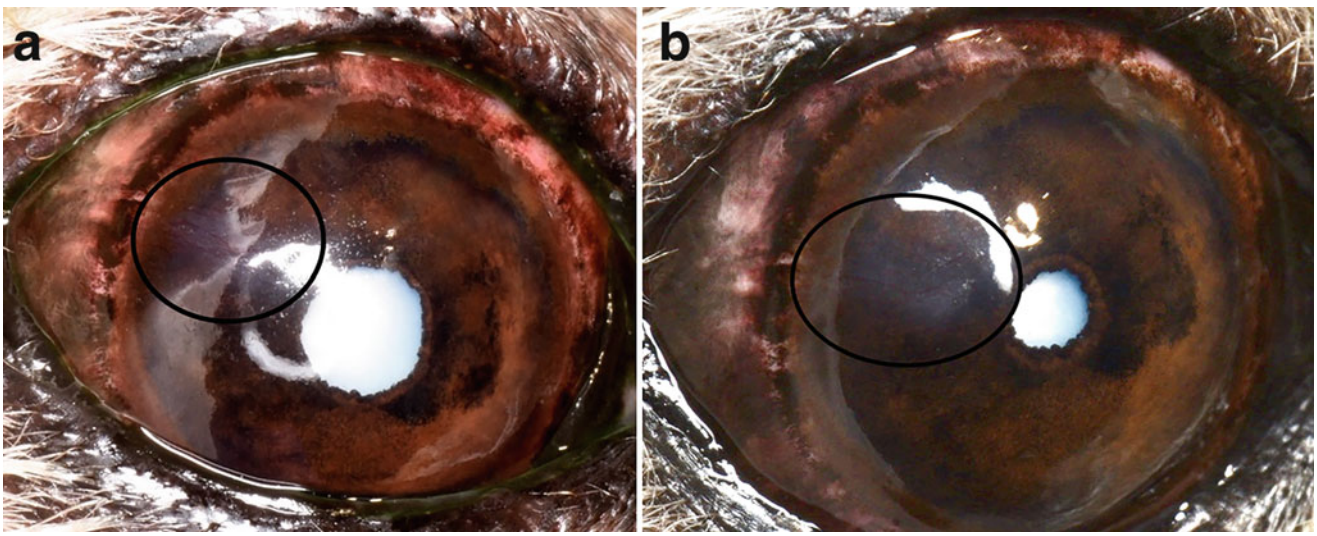

Fig. 39.16 Lateral keratopathy including vessels and fibrosis in older sea otters (*Enhydra lutris).* (**a**) is pre-treatment where more active inflammation can be seen and (**b**) is post weeks of ketorolac where reduced inflammation (hypoperfused vessels, less hyperemia) can be seen. In addition is possible to see a mature cataract in partially dilated otter (**a**) with mild LIU, best seen as conjunctival and episcleral injection. (**b**) Mature cataract, undilated eye treated with ketorolac. Note less conjunctival and episcleral injection

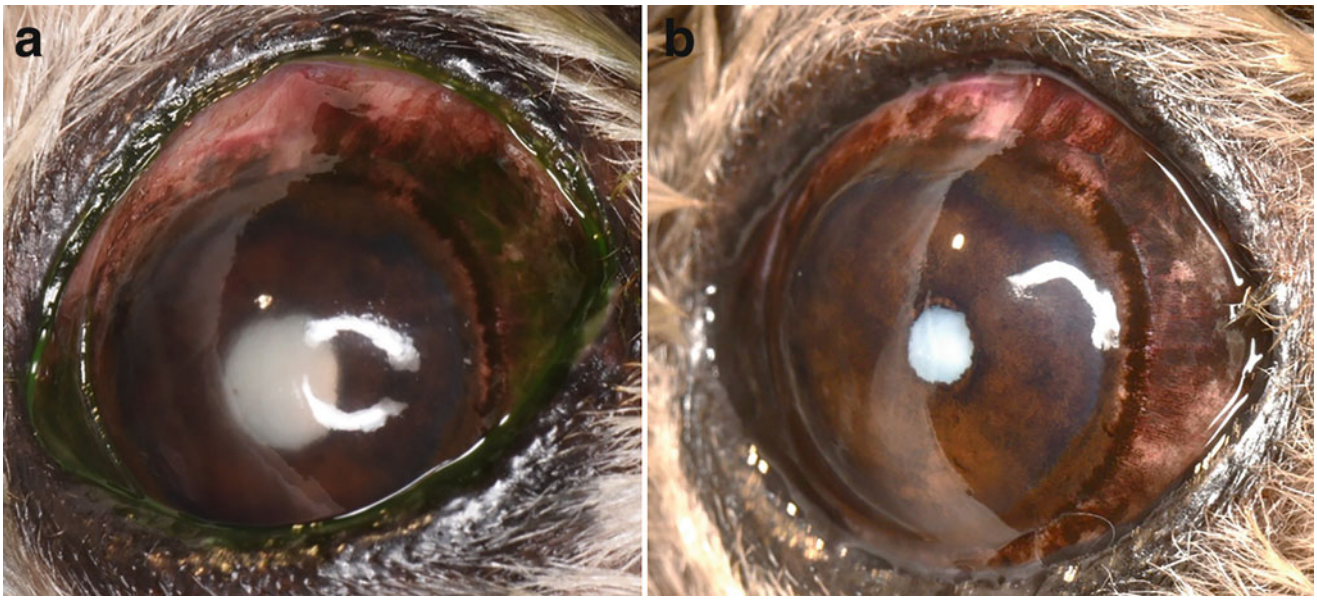

Fig. 39.17 Mature cataract with lens-induced uveitis in a sea otter (*Enhydra lutris*). (**a**) Note the hazy appearance of the pupillary margin obscured by flare and cell. Pigment on ALC also noted (**b**) is the same eye treated with ketorolac and undilated pupil. Note the much clearer anterior chamber and now well-defined pupillary margin

meningoencephalitis that does not always, but can have chorioretinal involvement. Pinnipeds have been successfully treated with ponazuril at 10 mg/kg for 3 months (Mylniczenko et al. 2008).

The finding of free-ranging blind otters appears to be relatively common (Williams 1989). A case of sudden reported blindness in a river otter Neotropical Otter (*Lontra longicaudis*) from the Curitiba Zoo (Brazil) was recently seen. During the examination, the animal appeared bright but not detectable menace response. No significant lesions were observed in the globe or adnexa. Pupillary reflexes were normal. A mini portable Ganzsfield (HMsERG model 1000, Ocuscience®, Michigan, USA) was used to perform the flash electroretinogram (FERG). ERGs were performed using chemical restraint isoflurane delivered by mask. The otter was placed in sternal recumbency with the active electrode (ERG-Jet, Fabrinal SA, La Chaux-de-Fonds, Switzerland) positioned on the cornea and hypodermic platinum needles (Model E2, Grass Technologies, Warvick, USA) positioned as reference and ground electrodes. The reference electrode was positioned about 2 cm from the lateral canthus, and the ground electrode was positioned at the base of the neck. The protocol used was a short protocol, consisting of light flash intensities of 10 mcd.s/m^2, 3000 mcd.s/m^2, and 10,000 mcd.s/m^2. a- and b-wave amplitudes, and implicit times (ITs), were measured by ERGVIEW 4.380 V software (Ocuscience®, Michigan, USA). Electroretinographic responses seemed compatible with normal retinal function (contained a- and b-waves with adequate amplitudes and implicit times) (Fig. 39.18). A presumptive diagnosis of central blindness was given at the time. On the same night of the examination, the otter had several seizures and died. At necropsy, a lesion compatible with occipital lobe infarction was observed (Fig. 39.18) confirming the suspicion of central blindness.

Very little is known about the giant otter, *Pteronura brasiliensis*, besides being the longest member of the Mustelidae family, endemic to wetlands and river systems in forests of South America (Eisenberg 1989). Vision has not been studied in detail yet, but it is known that the animal has large eyes and long whiskers to help detect prey in the water, with and nostrils and ears that close in the water. The giant is exclusively active during the day and hunts by sight and rest in their burrows at night. Giant Brazilian Otters are piscivores (prefer to eat fish), but when fish supplies are low they will also hunt crustaceans, small snakes, and small caiman (Wilson and Mittermeier 2009). There are several anecdotal reports of eye diseases observed in giant otters in the wild. One animal has been seen with phthisis bulbi apparently thriving in the Pantanal wetland, Brazil (Fig. 39.19).

Other members of the Musteloidea superfamily (red pandas, raccoons, coatis, kinkajous, olingos, olinguitos, ringtails, cacomistles, skunks, and stink badgers).

Compared to the members of the Mustelidae family, relatively little is known about the eye as well as its role in health and disease of the members of Ailuridae, Mephitidae, and Procyonidae families. Musteloids share diseases between species, such as mustelid herpes virus, canine distemper, and infectious hepatitis viruses, along with a range of nematodes and protozoans presenting a contagion risk when

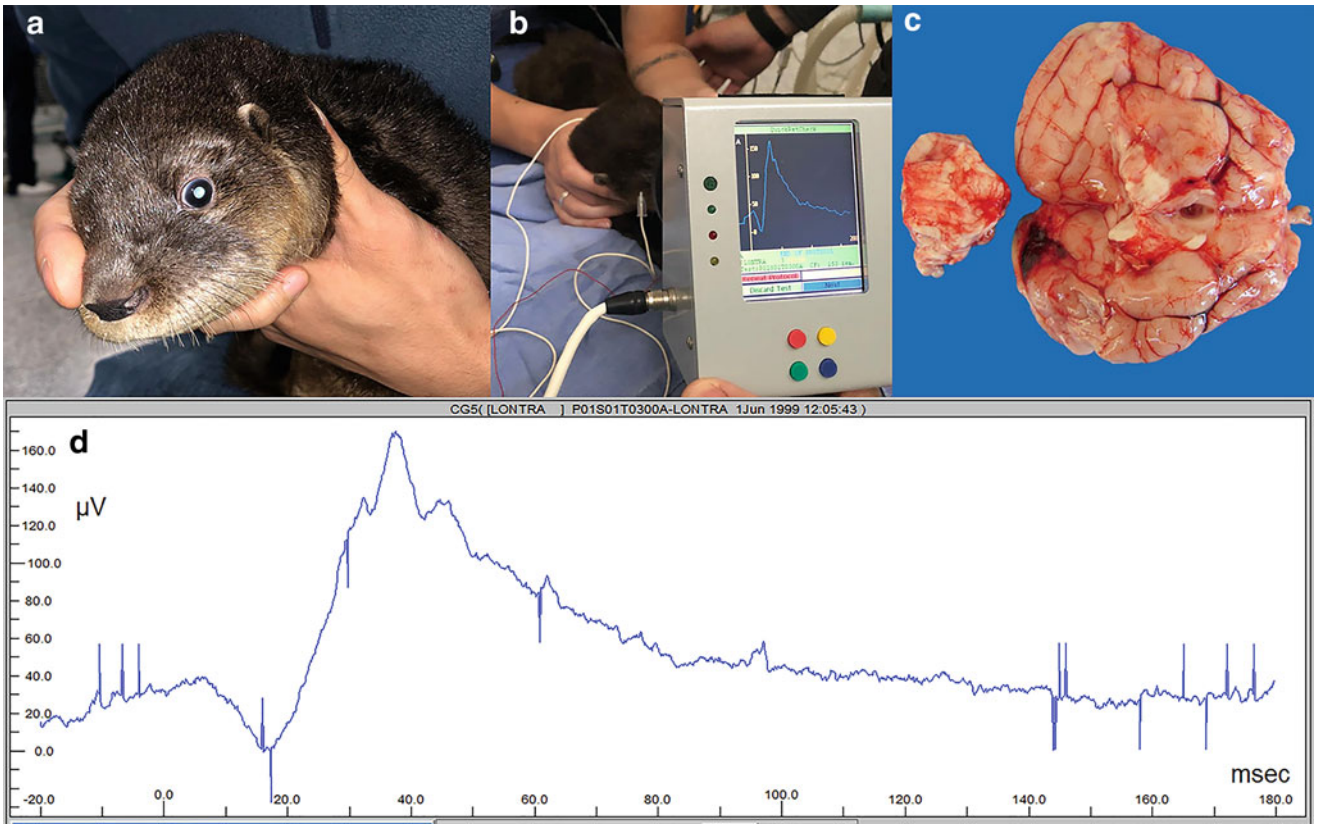

Fig. 39.18 A river otter from the Curitiba Zoo was examined with the chief complaint of blindness. No lesion was detected in the globe (**a**) and retinal function was not impaired based on electroretinographic results (**b**, **d**). On necropsy, a large area of parenchymal hemorrhage on the occipital lobe (**c**). (Image by Fabiano Montiani-Ferreira)

vulnerable musteloids are being conserved or reintroduced. Skunks and raccoons are major rabies hosts in North America and because both are considered synanthropic species, they can pose substantial zoonotic risks (Newman and Byrne 2017). In addition, raccoon roundworm larvae (*Baylisascaris procyonis*) should be considered as a probable cause of cular larva migrans and diffuse neuroretinitis in humans (Kazacos et al. 1985).

Red Pandas

The red panda (*Ailurus fulgens*) is an arboreal mammal species native to the eastern Himalayas and southwestern China. They eat mostly bamboo, but also may occasionally eat small mammals, birds, eggs, flowers, and berries. In captivity, they were observed to eat birds, flowers, maple and mulberry leaves, and bark and fruits of maple, beech, and mulberry (Roberts and Gittleman 1984; Panthi et al. 2015).

The red panda cubs start to open their eyes at about 18 days of age. After about 90 days, they achieve full adult fur and coloring and begin to venture out of the nest. They also start eating solid foods at this point, weaning at around 6–8 months of age. Conjunctivitis in newborn cubs delaying the eyelid opening, called ophthalmia neonatorum, has been observed in a patient with signs of ocular and respiratory infection (Fig. 39.20).

Red pandas are known to be highly susceptible to canine distemper virus (Deem et al. 2000; Qin et al. 2007) and to a number of protist and helminth disease-causing organisms from domesticated companion animals, including *Toxoplasma gondii*, *Neospora caninum*, and heartworm infections with *Dirofilaria immitis* (Lan et al. 2012). In addition, ascarid nematodes such as *Baylisascaris ailuri* (Xie et al. 2011) and several genera of metastrongylid nematodes such as *Angiostrongylus vaso*rum (Patterson-Kane et al. 2009) have been strongly implicated in inducing pneumonia and visceral, ocular, and neural larval migrans in red pandas.

It is believed that both its arboreal lifestyle and plant-based diet may have been contributing factors to the development of fungal keratitis, which was already reported in this species (Volk et al. 2018). Fungal keratitis was diagnosed and treated in two captive red pandas at a zoo in Melbourne, Australia (Fig. 39.21).

Fig. 39.19 A giant other with phthisis bulbi in its left eye, captured in this picture while eating a fish. (Courtesy of Nathalie Foerster and Grazielle Soresini, Brazil)

The diagnosis of fungal keratitis was confirmed with either cytology or histopathology. Severe unilateral ocular pain and stromal abscessation were observed. A superficial keratectomy was performed in both cases. Following surgery, a combination topical (topical silver sulfadiazine ointment), subconjunctival (atropine) as well as systemic medical therapy that included oral doxycycline (25 mg PO BID), carprofen (10 mg PO), and fluconazole (50 mg PO SID), contributed to a successful outcome (Volk et al. 2018). Bamboo-related trauma leading to the development of keratomycosis has been reported in humans (Gopinathan et al. 2002; Lin et al. 2005; Lan et al. 2012; Qiu and Yao 2013).

Raccoons

The presence of bushy ringed tails is an outstanding anatomical feature of raccoons. The most common species is the North American raccoon (*Procyon lotor*), also called common raccoon or northern raccoon, which ranges from northern Canada and most of the United States southward into South America. It has a noticeable black "mask" around the eyes and the tail has 5–10 black bands. The other two most common species of raccoon are the Crab-eating raccoon (*P. cancrivorus*) and the Cozumel raccoon (*P. pygmaeus*).

Normal conjunctival bacterial flora was investigated in 10 raccoons (Procyon lotor). The most common isolate in raccoons was *Bacillus* spp. Other isolates included *Streptococcus* spp., *Staphylococcus* spp., non-hemolytic *Escherichia coli*, and *Enterococcus faecalis*. *Mycoplasma* culture was negative in all samples (Pinard et al. 2002). In another investigation using five Crab-eating raccoons (*P. cancrivorus*) no microorganisms were isolated from 10 eyes. In the remaining 10 eyes, *Staphylococcus* spp. was the most common microorganism isolated from conjunctival sac. *Shigella* spp. comprised the Gram-negative genera isolated (Spinelli et al. 2010).

Raccoons eat in the upright position, using the front paws and digits to wash, hold, and examine its food at close range. These behavioral and morphological features prompted structural and functional studies of the raccoon's accommodative capability. These investigations showed that the raccoon exhibits the greatest accommodative capability of any

Fig. 39.20 A 19-day-old red panda cub with ophthalmia neonatorum and a respiratory infection. Note the dried ocular discharge sealing the palpebral fissure of both eyes closed. Also, note the presence of nasal secretion. (Courtesy of Bret A. Moore)

non-primate terrestrial mammal so far studied. Parasympathetic stimulation of the meridional muscle fibers of the ciliary body results in forward lens movement induces accommodation of up to 19 D in the raccoon, which is 6 times more than in the dog (Rohen et al. 1989).

Similar to dogs (Wen et al. 1985), young raccoons exhibit a strong bluish reflection from their tapetal area (Fig. 39.22). The retina of the raccoon is of the holangiotic type. The meridian region of the eye, which lies in the horizontal plane and passes around the optic disc, had a markedly sparse capillary network. This horizontal sparse vascular band may correspond to a visual streak (Fig. 39.22). The sparse retinal capillary network in raccoons is extremely beneficial for photon capture, thereby allowing the raccoon to see well at night, as the retinal vessels restrict the inflow of photons toward the photoreceptors (Ninomiya et al. 2005).

Regarding developmental disorders of the eye, anophthalmos and microphthalmos were associated with nasomaxillary and central nervous system abnormalities in two unrelated raccoons (Render et al. 1983). In addition, another raccoon with a unilateral micro-ophthalmia has been documented (Hamir 2011). As for acquired ocular conditions, several systemic diseases may affect the raccoon eye. Mucus secretion was visible on the conjunctival in two juvenile raccoons (*Procyon lotor*) with disseminated histoplasmosis (*H. capsulatum*) (Clothier et al. 2014). Signs of canine distemper virus in raccoons may vary, but classically it starts with a mild green to yellow conjunctival discharge (due to a resulting *keratoconjunctivitis sicca*) (Fig. 39.23) from one or both eyes. Raccoons and striped skunks (*Mephitis mephitis*) have been investigated for rabies and canine distemper virus co-infections during a concurrent rabies and canine distemper outbreak in Ontario, Canada in 2015–2016. Several animals that were investigated presented ocular signs. Virus was detected using real-time PCR of conjunctival swabs in rabies positive raccoons (22/32) and skunks (7/34). Coinfections with both viruses should be considered, particularly in distemper endemic areas that are at risk of rabies incursion (Jardine et al. 2018).

Horner syndrome results from interruption of the oculosympathetic pathway. While Horner's Syndrome is a somewhat common neuro-ophthalmologic disorder in small

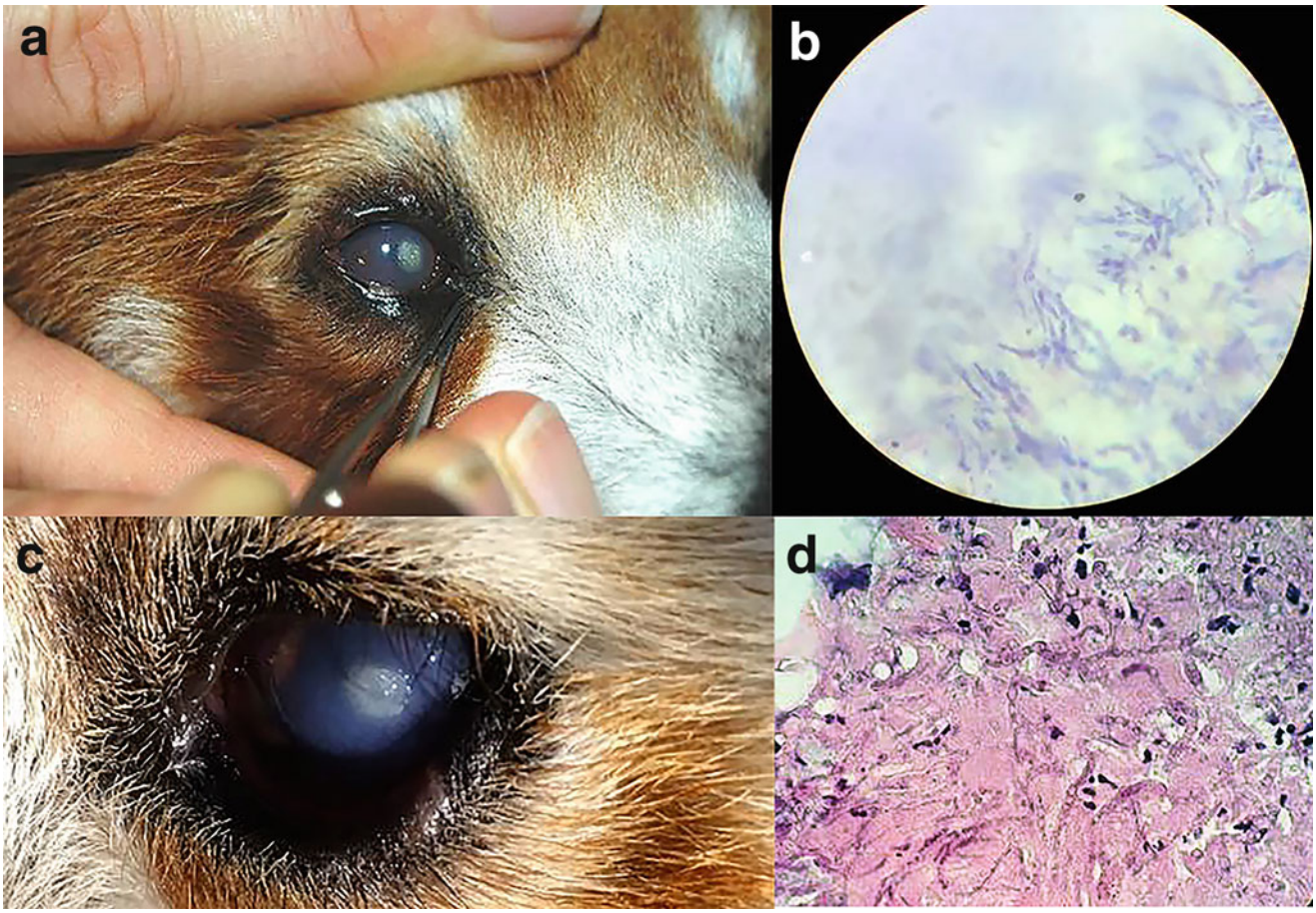

Fig. 39.21 Fungal keratitis in two captive red pandas. (**a**) Epithelial plaque and stromal abscessation in the right eye of a male red panda; (**b**) Cytology of affected corneal tissue from the same case, demonstrating filamentous fungal hyphae typical in appearance of *Aspergillus* spp. (**c**) Epithelial plaque and stromal abscessation in the left eye of a female red panda; (**d**) Histopathology of affected corneal tissue from the same case, demonstrating filamentous fungal hyphae, 100x magnification, oil immersion. From Volk HA, O'Reilly A, Bodley K, McCracken H. Keratomycosis in captive red pandas (*Ailurus fulgens*): 2 cases. Open Vet J. 2018;8(2):200–203 with permission

animal clinics, it is more complicated to detect in wild carnivores, yet diagnostic and therapeutic techniques applied e to domestic animals can be equally used as a reference for small carnivores of the Procyonidae family. A three-year-old male raccoon (*Procyon lotor*), castrated, from La Lajita Oasis Park Zoological Park (Spain) demonstrated a lack of appetite, state of mental depression, and mild dehydration. During physical examination, an abscess was observed in the left ventrolateral area of the neck as well as clinical signs compatible with Horner's Syndrome in the left eye, such as miosis, ptosis, enophthalmia, protrusion of the third eyelid (Fig. 39.24), anisocoria. A hypersensitivity test was performed by topical instillation of epinephrine 0.0001% on the left eye. Results suggested the presence of second-order Horner's Syndrome, probably caused by pressure from the abscess on the sympathetic innervation to the left eye. A radiologic study of the neck was carried out and blood samples and material from the abscess exudates were obtained. A culture of the exudates revealed the presence of *Escherichia coli*. Initial treatment was introduced according to indications resulting from the previously obtained antibiogram. Symptoms disappeared 6 days after the initial treatment (Nájera and Suarez 2012).

Coatis

Coatis, also are known as coatimundis, are members of the family Procyonidae in the genera *Nasua* and *Nasuella.* The two main (most common) species of coatis have are the South American ring-tailed coati (*Nasua nasua*), and the Central American white-nosed coati (*Nasua narica*). They are diurnal mammals native to South America, Central America, Mexico, and the southwestern United States. Coatis use

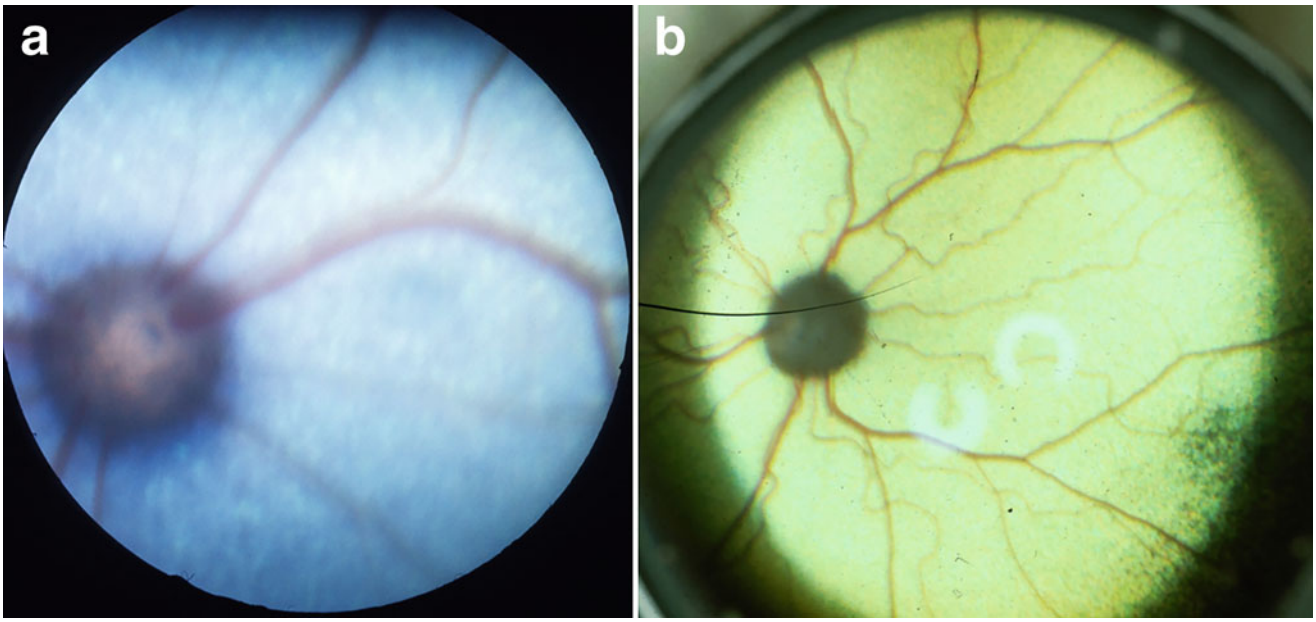

Fig. 39.22 Funduscopic images evidencing the holangiotic retina of raccoons (*Procyon lotor*) of different age groups. Note the bluish reflection from their tapetal area in a 6–8 week-old female raccoon (**a**). In this young adult raccoon, a yellowish reflection from their tapetal area is evident. Note the horizontal band of sparsely distributed retinal blood vessels corresponding to the raccoon retinal streak (*asterisks*) (**b**). (Courtesy of Christopher J. Murphy)

their long and flexible noses to push objects and rub parts of their body. The facial markings include white markings around the eyes and on the ears and snout. Kittens (coati babies) have their eyes closed at birth and usually only open them when they are about 10-days old. One interesting morphological features of the coati eye are the horizontally ovoid pupil (at rest), which when constricted becomes teardrop shaped, with the temporal edge being narrower than the

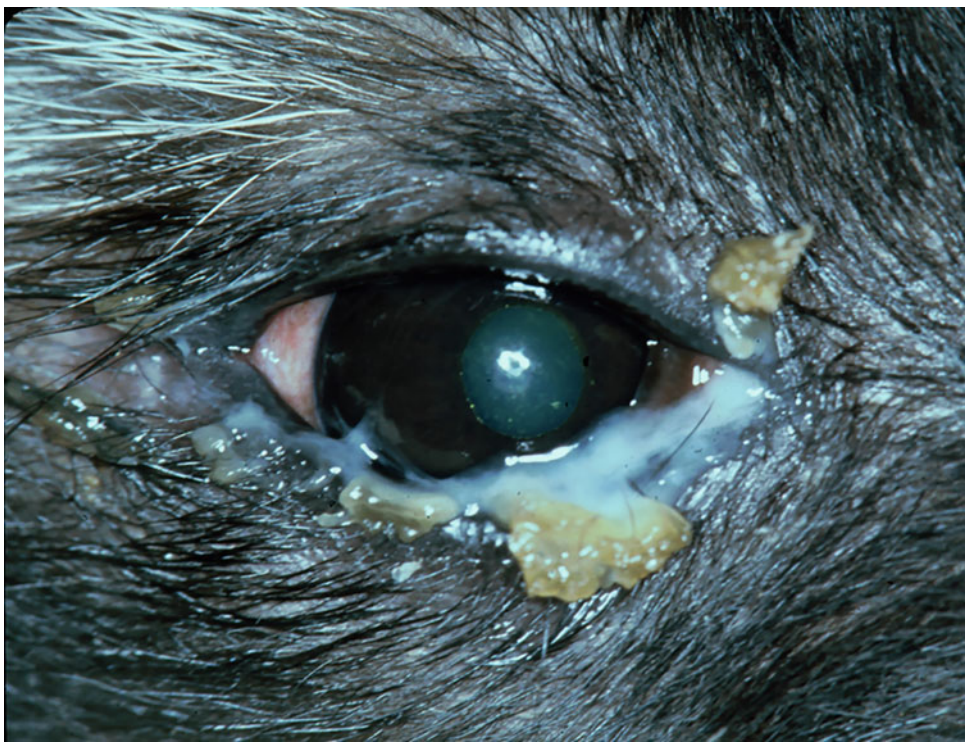

Fig. 39.23 A raccoon showing the classic ocular sign of canine distemper virus infection, a *green* to *yellow* conjunctival discharge. (Courtesy of Christopher J. Murphy)

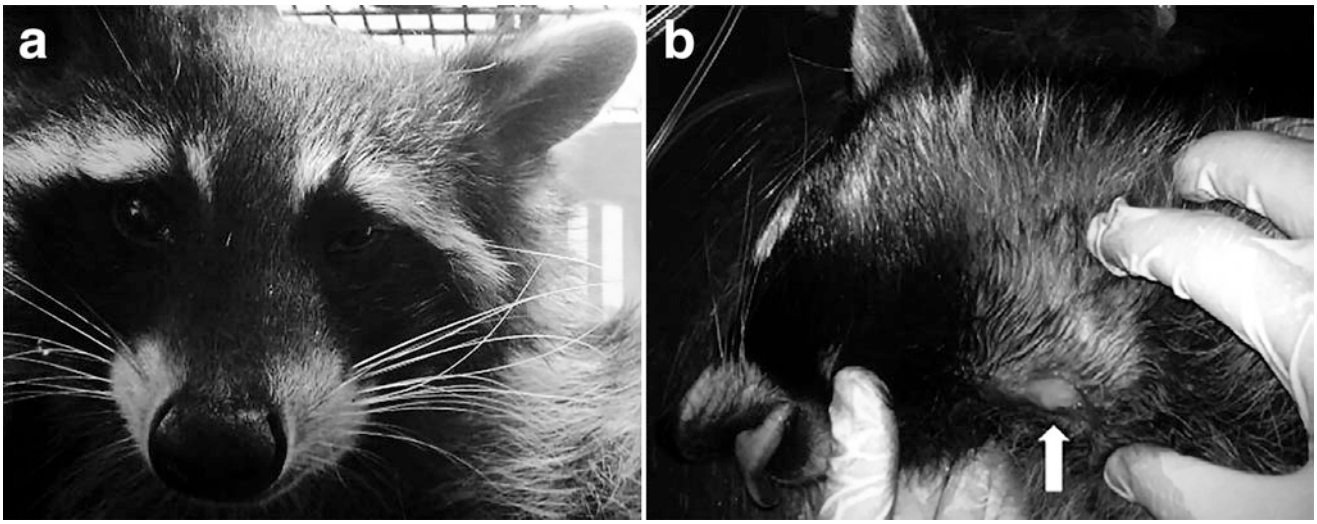

Fig. 39.24 Horner's syndrome in the left eye in a raccoon (*Procyon lotor*), associated with *Escherichia coli* neck abscess. (**a**) Note the ptosis, enophthalmia, slight protrusion of the third eyelid in the left eye. (**b**) Left ventrolateral view of the neck. Notice incision and exudate (*white arrow*). From: Nájera, F. and Suarez, A. 2012. "Horner's Syndrome associated with Escherichia coli Infection in a Raccoon (Procyon lotor)—A Case Report" Thai J Vet Med 42(3): 367–372. Figures 1 and 3. Used with permission

nasal and obliquely tilted ventrally (Fig. 39.25). The iris color in adults presents a dark brown color, while juveniles had a light brown. The fundus possesses a large tapetum lucidum, located dorsally. Its color varied with age, with adults having a green to yellow tapetum (Fig. 39.26) and juveniles being greenish-blue (Carvalho et al. 2021). The non-tapetal region is black. The optic disk is round, located in the tapetal region. No vascular ring was noted overlying the disk. The retina was holangiotic, with three to seven main veins emerging from the optic nerve, and several arterioles (Fig. 39.26).

A previous investigation with coatis describes the normal conjunctival microbiota. Results of this research showed that *Staphylococcus s*pp. was the most common microorganism isolated from conjunctival sac of coatis. *Escherichia coli* was isolated from the right eye of one coati that had no growth at contralateral eye. Nine eyes from coatis had no microorganisms isolated from the conjunctiva (Spinelli et al. 2010).

Severe inflammatory disease of the ciliary body (uveitis) associated with histopathologic detection of schizonts of the protozoan parasite *Sarcocystis neurona* in a White-nosed coati (*Nasua narica molaris*) has been reported (Dubey et al. 2017).

A coati was diagnosed with a unilateral dysfunction of the facial nerve-inducing exposure keratopathy (Fig. 39.27). On a survey performed by Carvalho et al. (2021), coatis aged 8–10 years of age commonly presented mild iris atrophy and nuclear sclerosis, with no predominance perceived among males or females (Fig. 39.28).

Kinkajou

Kinkajou, (*Potos flavus*), also called honey bear, is an unusual and elusive member of the Mustelidae family, notable by its long, prehensile tail that can curl around branches like a hand, short muzzle, and rounded ears. Native to the tropical rainforests of Central America and parts of South America. There are two possible theories to explain their other name "honey bears." The first one is because they like to lap up the honey from bees' nests with their long, narrow tongues. The second possibility refers to the typical golden color of the animal's soft fur (Crampton 2020). Kinkajous as part of the Musteoidea family, belonging to the family Procyonidae are classified as carnivores, mainly because of their skull structure and teeth. However, kinkajous in the wild are exclusively (or almost) vegetarian, feeding on fruit, leaves, flowers, and nectar. Kinkajous are important pollinators. As they travel from flower to flower to drink nectar, the flower's pollen sticks to their face and then smears off at the next flower. An interesting investigation on kinkajous diet described from analyses of feces and observations of habituated individuals showed the following results: Ripe fruit is the primary food comprising 90.6% of

Fig. 39.25 Note the horizontal ovoid pupil of a coati (*Nasua nasua*). Note that when constricted the pupil becomes teardrop shaped, with the temporal edge being narrower than the nasal and obliquely tilted ventrally. (Courtesy of Ana Carolina Rodarte)

feeding bouts and present in 99% of feces. Leaves and flowers made up <10% of the diet. No animal prey was eaten. Seventy-eight species of fruit from 29 families were detected. Moraceae was the main plant family in the diet and Ficus was the most important plant genus. Kinkajous is preferentially fed in large fruit patches. Selection indices were calculated for 37 fruit species. Compared with other large mammalian frugivores in central Panama the diet of kinkajous is most similar to the spider monkey (*Ateles geoffroyi*) (Kays 1999).

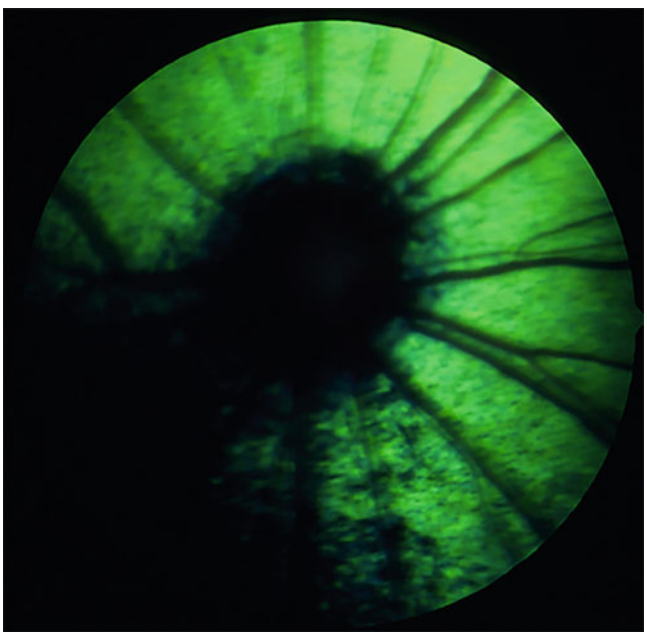

Fig. 39.26 Funduscopic image evidencing the holangiotic retina of the coati (*Nasua nasua*). Note the *bright green* tapetal shine and the retina richly vascularized with superficial blood vessels

Being arboreal and primarily active at night, the eyes of the kinkajous are adapted for nocturnal vision. In comparison to other members of the family Procyonidae, kinkajous possess a skull with a shorter rostrum. Their bony orbits and globe face more rostrally. Their eyes are comparatively bigger as well, with a wider corneal surface. Their vision has excellent brightness acuity and not so good color perception compared to coatis (Nasua nasua) (Chausseil 1992). This can be explained by the fact that in the family Procyonidae, the nocturnal raccoons (*Procyon lotor* and *P. cancrivorous*) and the nocturnal kinkajous (*Potos flavus*) lack S-cones while the diurnal coati (Nasua nasua) has L- and S-cones (Jacobs and Deegan 1992). There are one anecdotal report of a corneal ulcer diagnosed in one kinkajou.

Kinkajous are sometimes kept as exotic pets because they are generally playful, quiet and have little odor. Nevertheless, they can sometimes be aggressive. Kinkajous dislike sudden movements, loud noises, and being awake during the day. An agitated kinkajou may emit a loud noise and may attack,

Fig. 39.27 Photograph of a case of chronic epithelized (fluorescein-negative) exposure keratopathy in an adult coati (*Nasua nasua*) (Courtesy of Ana Carolina Rodarte)

usually clawing its victim and sometimes biting deeply. Kinkajous are captured for the exotic pet trade and hunted for their fur or meat. The fur is often used to make wallets or saddles. Despite these facts, the animal is not endangered at the moment (Crampton 2020). Kinkajou bites have a high risk of causing soft tissue infection in humans. There are reports of hand cellulitis and abscess after kinkajou bites (Hadvani and Dutta 2020). Pet kinkajous in the United States can be carriers (fecal–oral route) of the raccoon roundworm *Baylisascaris procyonis*, which is capable of causing severe morbidity and even death in humans, if the brain is infected (Kazacos 2001; Taira et al. 2018). A case of a novel rabies variant was discovered in a rabid wild kinkajou from Mato Grosso, Brazil, indicating a public health risk following exposure to either of the two animals (Dell'Armelina Rocha et al. 2020). Thus, kinkajous are not suitable pets for most people, because the species takes considerable resources to accommodate their needs (Wright and Edwards 2009).

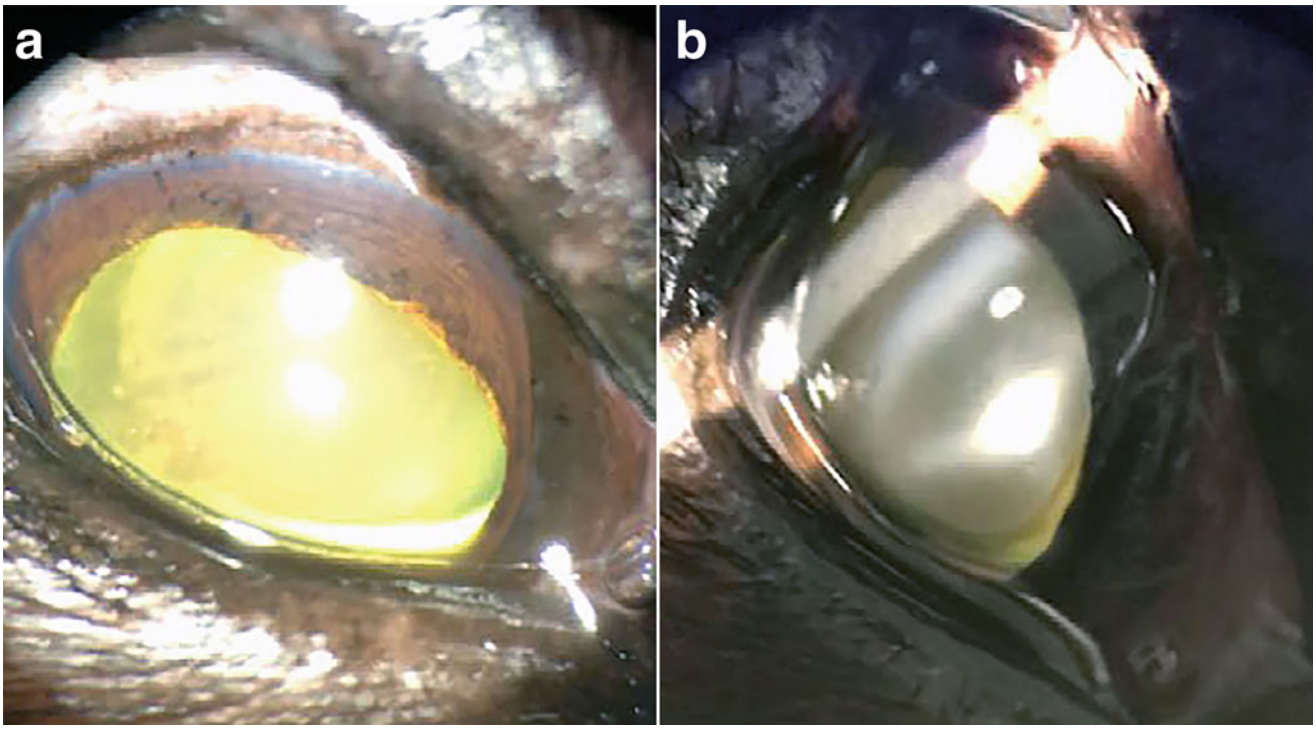

Fig. 39.28 Mild iris atrophy (**a**) and nuclear sclerosis in the left eye of an adult individual. (**b**) A better view of the mild nuclear sclerosis in the same animal depicted in (**a**) with the aid of a slit lamp. From: Carvalho CM, Rodarte-Almeida ACV, Moore BA, Borges BP, Machado MTS, Galera PD. Ocular examination findings and measurements of tear production and tonometry of ring-tailed coatis (Nasua nasua). Vet Ophthalmol. 2020. Epub ahead of print. PMID: 33547755. Used with permission

References

Aboelela SW, Robinson DW (2004) Physiological response properties of displaced amacrine cells of the adult ferret retina. Vis Neurosci 21: 135–144

Bakthavatchalu V, Muthupalani S, Marini RP, Fox JG (2016) Endocrinopathy and Aging in Ferrets. Vet Pathol 53(2):349–365

Ballard KA, Sivak JG, Howland HC (1989) Intraocular muscles of the Canadian river otter and Canadian beaver and their optical function. Can J Zool 67:469–474

Balliet RF, Schusterman RJ (1971) Underwaater and Aerial Visual Acuity in the Asian "Clawless" Otter (*Amblonyxx cineria cineria*). Nature 234:305–306

Beineke A, Baumgärtner W, Wohlsein P (2015) Cross-species transmission of canine distemper virus-an update. One Health 1:49–59

Bell JA (1997) Periparturient and neonatal diseases. In: Hillyer EV, Quesenberry KE (eds) Ferrets, Rabbits, and Rodents. WB Saunders, Philadelphia, pp 53–55

Besch-Williford (1987) Biology and medicine of the ferret. The Veterinary Clinics of North America. Small Anim Pract 17:1155–1183

Bodkin JL, Esslinger GG, Monson DH (2004) Foraging depths of sea otters and implications to coastal marine communities. Mar Mamm Sci 20:305–321

Boyd K, Smith RS, Funk AJ, Rogers TD, Dobbins RM (2007) A closer look: secondary glaucoma more likely. Lab Anim (NY) 36: 13–14

Braekevelt CR (1981) Fine structure of the tapetum lucidum in the domestic ferret. Anat Embryol 163:201–214

Burnie D, Wilson DE (2001) Animal. Dorling Kindersley, London

Carvalho CM, Rodarte-Almeida ACV, Moore BA, Borges BP, Machado MTS, Galera PD (2021) Ocular examination findings and measurements of tear production and tonometry of ring-tailed coatis (Nasua nasua). Vet Ophthalmol. https://doi.org/10.1111/vop.12866

Chausseil M (1992) Evidence for Color Vision in Procyonides: Comparison between Diurnal Coatis (Nasua) and Nocturnal Kinkajous (Potos flavus). Anim Learn Behav 20(3):259–265

Chen B, Boukamel K, Kao JP (2005) Spatial distribution of inhibitory synaptic connections during development of ferret primary visual cortex. Exp Brain Res 160:496–509

Clothier KA, Villanueva M, Torain A, Reinl S, Barr B (2014) Disseminated histoplasmosis in two juvenile raccoons (Procyon lotor) from a nonendemic region of the United States. J Vet Diagn Investig 26(2):297–301

Crampton L (2020) The Kinkajou: A tropical rainforest animal and an exotic pet. https://pethelpful.com/exotic-pets/The-Kinkajou-or-Honey-Bear-Rainforest-Mammal-and-Exotic-Pet. Assessed 15 Feb 2021

Davidson MGD (1985) Ophthalmology of exotic pets. Compend Contin Edu Pract Veterin 7:724–737

Deem SL, Spelman LH, Yates RA et al (2000) Canine distemper in terrestrial carnivores: a review. J Zoo Wildl Med 31(4):441–451

Dell'Armelina Rocha PR, Velasco-Villa A, de Lima EM, Salomoni A, Fusaro A, da Conceição SE, Negreiros RL, Zafino VL, Zamperin G, Leopardi S, Monne I, Benedictis P (2020) Unexpected rabies variant identified in kinkajou (Potos flavus), Mato Grosso, Brazil. Emerg Microbes Infect 9(1):851–854

DiGirolamo N, Andreani V, Guandalini A et al (2013) Evaluation of intraocular pressure in conscious ferrets (*Mustela putorius furo*) by means of rebound tonometry and comparison with applanation tonometry. Vet Rec 172:396

Dillberger JE, Altman NH (1989) Neoplasia in ferrets: eleven cases with a review. J Comp Pathol 100(2):161–176
Dubey JP, Trupkiewicz JG, Verma SK et al (2017) Atypical fatal sarcocystosis associated with Sarcocystis neurona in a White-nosed coati (*Nasua narica molaris*). Vet Parasitol 247:80–84
Dubielzig RR, Miller PE (1995) The morphology of autosomal dominant microphthalmos in ferrets. Proceedings of the 26th American college of veterinary ophthalmologists. Newport,RI, p 62
Eisenberg IF (1989) Mammals of the Neotropics. The northern Neotropics: Panama, Colombia, Venezuela, Guyana, Suriname, French Guiana, vol 1. The University of Chicago Press, Chicago, IL, pp 1–449
Foster-Turley P, Macdonald S, Mason C (eds) (1990) Otters: An Action Plan for their Conservation. IUCN/SSC Otter Specialist Group. IUCN and Kelvyn Press, Inc., Broadview, IL
Fox JG, McLain DE (1998) Nutrition. In: Fox JG (ed) Biology and diseases of the ferret, 2nd edn. Lippincott Williams & Wilkins, Baltimore, MD, pp 149–172
Fox JG, Hewes K, Niemi SM (1984) Retro-orbital technique for blood collection from the ferret (*Mustela putorius furo*). Lab Anim Sci 34: 198–199
Fujishiro T, Kawasaki H, Aihara M et al (2014) Establishment of an experimental ferret ocular hypertension model for the analysis of central visual pathway damage. Sci Rep 4:6501
Gaarder JE, Kern TJ (2001) Ocular disease in rabbits, rodents, reptiles and other small exotic animals. In: Slatter D (ed) Fundamentals of Veterinary Ophthalmology, 3rd edn. W.B. Saunders Company, Philadelphia, pp 593–599
Garipis N, Hoffmann KP (2003) Visual field defects in albino ferrets (Mustela putorius furo). Vis Res 43(7):793–800
Gentry R, Peterson R (1967) Underwater Vision of the Sea Otter. Nature 216:435–436
Good KL (2002) Ocular disorders of pet ferrets. The Veterinary Clinics of North America. Exotic Animal. Practice 5:325–339
Gopinathan U, Garg P, Fernandes M et al (2002) The epidemiological features and laboratory results of fungal keratitis—a 10-year review at a referral eye care center in south India. Cornea 21:555–559
Gorham JR (1949) Salmonella infections in mink and ferret. Am J Vet Res 10:183–192
Hadlow WJ (1987) Chronic corneal oedema in aged ranch mink. Vet Pathol 24:323–329
Hadvani T, Dutta A (2020) Hand Cellulitis and Abscess From a Kinkajou Bite: a Case Report and Review of Kinkajou Bites in Humans. Pediatr Infect Dis J 39(7):e151–e154
Hamir AN (2011) Pathology of neurologic disorders of raccoons (Procyon lotor). J Vet Diagn Investig 23(5):873–884
He T, Killiaridis S (2004) Craniofacial growth in the ferret (Mustela putorius furo)—a cephalometric study. Arch Oral Biol 49:837–848
Henderson Z (1985) Distribution of ganglion cells in the retina of adult pigmented ferret. Brain Res 358:221–228
Hernández-Guerra AM, Rodilla V, López-Murcia MM (2007) Ocular biometry in the adult anesthetized ferret. *Mustela putorius furo*. Vet Ophthalmol 10:50–52
Hoar RM (1984) Use of ferrets in toxicity testing. J Am Coll Toxicol 3: 325–330
Hoefer HL, Fox JG, Bell JA (2012) Ferrets. Gastrointestinal diseases. In: Quesenberry KE, Carpenter JW (eds) Ferrets, Rabbits and Rodents: Clinical Medicine and Surgery, 3rd edn. Elsevier, St Louis, pp 27–45
Hoffmann KP, Garipis N, Distler C (2004) Optokinetic deficits in albino ferrets (*Mustela putorius furo*): a behavioral and electrophysiological study. J Neurosci 24:4061–4069
Hupfeld D, Distler C, Hoffmann KP (2006) Motion perception deficits in albino ferrets (Mustela putorius furo). Vis Res 46:2941–2948
Huynh M, Chassang L, Zoller G (2017) Evidence-Based Advances in Ferret Medicine. Vet Clin North Am Exot Anim Pract 20(3): 773–803
Jacobs GH, Deegan JF 2nd (1992 Oct) Cone photopigments in nocturnal and diurnal procyonids. J Comp Physiol A 171(3):351–358
Jardine CM, Buchanan T, Ojkic D, Campbell GD, Bowman J (2018 Jul) Frequency of Virus Coinfection in Raccoons (Procyon lotor) and Striped Skunks (Mephitis mephitis) During a Concurrent Rabies and Canine Distemper Outbreak. J Wildl Dis 54(3):622–625
Johnson-Delaney C (2016) Ferret Medicine and Surgery. CRC Press, Boca Raton, FL, p 514
Kays R (1999) Food Preferences of Kinkajous (Potos flavus): A Frugivorous Carnivore. J Mammal 80(2):589–599
Kazacos KR (2001) Baylisascaris procyonis and related species. In: Samuel WM, Pybus MJ, Kocan AA (eds) Parasitic diseases of wild mammals, 2nd edn. Iowa State University Press, Ames, Iowa, pp 301–341
Kazacos KR, Raymond LA, Kazacos EA et al (1985) The raccoon ascarid. A probable cause of human ocular larva migrans. Ophthalmology 92(12):1735–1744
Kern TJ (1989) Ocular disorders of rabbits, rodents and ferrets. In: Kirk RW, Bonagura JD (eds) Current veterinary therapy X. WB Saunders, Philadelphia, pp 681–685
Lan J, Fu Y, Yang Z et al (2012) Treatment and prevention of natural heartworm (Dirofilaria immitis) infections in red pandas (*Ailurus fulgens*) with selamectin and ivermectin. Parasitol Int 61(2):372–374
Langlois I (2005) Viral diseases of ferrets. Vet Clin North Am Exot Anim Pract 8(1):139–160
Leiva M, Naranjo C, Peña MT (2006) Comparison of the rebound tonometer (ICare®) to the applanation tonometer (Tonopen XL®) in normotensive dogs. Vet Ophthalmol 9:17–21
Levenson DH, Ponganis PJ, Crognale MA, Deegan JF, Dizon A, Jacobs GH (2006) Visual pigments of marine carnivores: pinnipeds, polar bears, and sea otters. J Comp Physiol A 192:833–843
Liets LC, Olshausen BA, Wang GY et al (2003) Spontaneous activity of morphologically identified ganglion cells in the developing ferret retina. J Neurosci 23:7343–7350
Lin HC, Chu PH, Kuo YH, Shen SC (2005) Clinical experience in managing Fusarium solani keratitis. Int J Clin Pract 59:549–554
Lindemann DM, Eshar D, Schumacher LL, Almes KM, Rankin AJ (2016 Mar) Pyogranulomatous panophthalmitis with systemic coronavirus disease in a domestic ferret (Mustela putorius furo). Vet Ophthalmol 19(2):167–171
Lipsitz L, Ramsey DT, Render JA, Bursian SJ, Auelrich RJ (2001) Persistent fetal intraocular vasculature in the European ferret (*Mustela putorius*): clinical and histological aspects. Vet Ophthalmol 4:29–33
Lucas J, Lucas A, Furber H, James G, Hughes MS, Martin P, Chen SCA, Mitchell DH, Love DN, Malik R (2000) Clinical *Mycobacterium genavense* infection in two aged ferrets with conjunctival lesions. Aust Vet J 78:685–689
Manger PR, Nakamura H, Valentiniene S (2004) Visual areas in the lateral temporal cortex of the ferret (Mustela putorius). Cereb Cortex 14:676–689
Marini RP, Adkins JA, Fox JG (1989) Proven or potential zoonotic diseases of ferrets. J Am Vet Med Assoc 195:990–994
Mass AM, Supin AY (2000) Ganglion cells density and retinal resolution in the sea otter, Enhydra lutris. Brain Behav Evol 55:111–119. https://doi.org/10.1159/000006646
McBride M, Mosunic CB, Barron GH, Radlinsky MG, Frank PM, Carmichael KP, Moore PA, Roberts RE, Divers SJ (2009) Successful treatment of a retrobulbar adenocarcinoma in a ferret (Mustela putorius furo). Vet Rec 165(7):206–208
McCalla TL, Erdman SE, Kawasaki TA et al (1997) Lymphoma with orbital involvement in two ferrets. Vet Comp Ophthalmol 7:36–38
Miller PE (1997) Ferret ophthalmology. Sem Avian Exotic Pet Med 6: 146–151
Miller PE, Pickett JP (1989) Zygomatic salivary gland mucocele in a ferret. J Am Vet Med Assoc 194:1437–1438

Miller PE, Marlar AB, Dubielzig RR (1993) Cataracts in a laboratory colony of ferrets. Lab Anim Sci 43:562–568
Montiani-Ferreira F (2009) Ferrets: Ophthalmology. In: Keeble E, Meredith A (eds) BSAVA manual of rodents and ferrets. BSAVA, Gloucester, pp 311–319
Montiani-Ferreira F, Petersen-Jones S, Cassotis N, Ramsey DT, Gearhart P, Cardoso F (2003) Early postnatal development of central corneal thickness in dogs. Vet Ophthalmol 6:19–22
Montiani-Ferreira F, Mattos BC, Russ HH (2006) Reference values for selected ophthalmic diagnostic tests of the ferret (*Mustela putorius furo*). Vet Ophthalmol 9(4):209–213
Moody KD, Bowman TA, Lang CM (1985) Laboratory management of the ferret for biomedical research. Lab Anim Sci 35(3):272–279
Morgan JE, Henderson Z, Thompson ID (1987) Retinal decussation patterns in pigmented and albino ferrets. Neuroscience 20:519–535
Morris JA, Coburn DR (1948) The isolation of Salmonella typhimurium from ferrets. J Bacteriol 55:419–420
Murphy CJ, Bellhorn RW, Williams T et al (1990) Refractive state, ocular anatomy, and accommodative range of the sea otter (Enhydra lutris). Vis Res 30:23–32
Mylniczenko ND, Kearns KS, Melli AC (2008) Diagnosis and treatment of *Sarcocystis neurona* in a captive harbor seal (*Phoca vitulina*). J Zoo Wildlife Med 39:228–235
Myrna KE, Girolamo ND (2019 Jan) Ocular Examination and Corneal Surface Disease in the Ferret. Vet Clin North Am Exot Anim Pract 22(1):27–33
Nájera F, Suarez A (2012) Horner's Syndrome associated with Escherichia coli Infection in a Raccoon (Procyon lotor)—a case report. Thai J Vet Med 42(3):367–372
Newman C, Byrne A (2017) Musteloid diseases: implications for conservation and species management. In: Biology and conservation of musteloids. Oxford University Press. https://oxford.universitypressscholarship.com/view/10.1093/oso/9780198759805.001.0001/oso-9780198759805-chapter-9. Accessed 25 Jan 2021
Ninomiya H, Inomata T, Kanemaki N (2005 Jun) Microvasculature of the retina, ciliary processes and choroid in the North American raccoon (Procyon lotor) eye: a scanning electron microscopic study of corrosion casts. J Vet Med Sci 67(6):547–554
Orcutt C, Tater K (2012) Ferrets. Dermatologic disease. In: Quesenberry KE, Carpenter JW (eds) Ferrets, Rabbits and Rodents: Clinical Medicine and Surgery, 3rd edn. Elsevier Saunders, St. Louis, MO, pp 122–131
Panthi S, Coogan SC, Aryal A, Raubenheimer D (2015) Diet and nutrient balance of red panda in Nepal. Naturwissenschaften 102:54
Patterson-Kane JC, Gibbons LM, Jefferies R et al (2009) Pneumonia from Angiostrongylus vasorum infection in a red panda (*Ailurus fulgens fulgens)*. J Vet Diagn Investig 21:270–273
Perpiñán D, Ramis A, Tomás A et al (2008) Outbreak of canine distemper in domestic ferrets (Mustela putorius furo). Vet Rec 163:246–250
Pinard CL, Brightman AH, Yeary TJ, Everson TD, Cox LK, Chengappa MM, Davidson HJ (2002 Oct) Normal conjunctival flora in the North American opossum (Didelphis virginiana) and raccoon (Procyon lotor). J Wildl Dis 38(4):851–855
Qin Q, Wei F, Li M, Dubovi EJ, Loeffler IK (2007) Serosurvey of infectious disease agents of carnivores in captive red pandas (Ailurus fulgens) in China. J Zoo Wildlife Med 38:42–50
Qiu WY, Yao YF (2013) Mycotic keratitis caused by concurrent infections of exserohilum mcginnisii and candida parapsilosis. BMC Ophthalmol 13:37. https://doi.org/10.1186/1471-2415-13-37
Render JA, Kazacos EA, Vestre WA et al (1983) Ocular, nasomaxillary, and neural anomalies in raccoons, Procyon lotor. J Wildl Dis 19:234–243
Ringle MJ, Lindley DM, Krohne SG (1993) Lymphoplasmacytic keratitis in a ferret with lymphoma. J Am Vet Med Assoc 203:670–672
Roberts MS, Gittleman JL (1984) Ailurus fulgens. Mamm Species 222:1–8
Rohen JW, Kaufman PL, Eichhorn M et al (1989) Functional morphology of accommodation in the raccoon. Exp Eye Res 48:523–527
Ropstad EO, Leiva M, Peña T, Morera N, Martorell J (2011 Jul) Cryptococcus gattii chorioretinitis in a ferret. Vet Ophthalmol 14(4):262–266
Ryland LM, Gorham JR (1978) The ferret and its diseases. J Am Vet Med Assoc 173:1154–1158
Silverman S, Tell L (2005) Radiology of Rodents, Rabbits and Ferrets: An Atlas of Normal Anatomy and Positioning. Saunders Elsevier, Philadelphia
Simpson VR, Harhreaves J, Birtles RJ, Marsden H, Williams DL (2008) Tyzzer's disease in an Eurasian otter (*Lutra lutra*) in Scotland. Vet Rec 165:539–543
Spinelli TP, Oliveira-Filho EF, Silva D et al (2010) Normal aerobic bacterial conjunctival flora in the Crab-eating raccoon (*Procyon cancrivorus*) and Coati (*Nasua nasua)* housed in captivity in pernambuco and paraiba (Northeast, Brazil). Vet Ophthalmol 13 (Suppl):134–136
Taira K, Nakamura S, Tokiwa T et al (2018 Aug) Larva Migrans of Baylisascaris potosis In Experimental Animals. J Parasitol 104(4):424–428
Tjalve H, Frank A (1984) Tapetum lucidum in the pigmented and albino ferret. Exp Eye Res 38:341–351
Verboven CA, Djajadiningrat-Laanen SC, Kitslaar WJ et al (2014) Distichiasis in a ferret (Mustela putorius furo). Vet Ophthalmol 17:290–293
Volk HA, O'Reilly A, Bodley K et al (2018) Keratomycosis in captive red pandas (Ailurus fulgens): 2 cases. Open Vet J 8(2):200–203
Walls GL (1967) The vertebrate eye and its adaptive radiation. Hafner, New York
Wen GY, Sturman JA, Shek JW (1985 Jun) A comparative study of the tapetum, retina and skull of the ferret, dog and cat. Lab Anim Sci 35(3):200–210
Williams J (1989) Blindness in Otters IUCN Otter Spec. Group Bull 4:29–30
Williams DL (2012) The ferret eye. In: Williams DL (ed) Ophthalmology of Exotic Pets. Weiley, pp 73–85
Williams DL, Gum GG (2013) Laboratory animal ophthalmology. In: Gelatt KN, Gilger BC, Kern TJ (eds) Veterinary Ophthalmology, 5th edn. Ames-IA, Wiley-Blackwell, pp 1692–1724
Wilson DE, Mittermeier RA (2009) Handbook of The Mammals of The World, vol 1. Carnivores, Lynx Editions, Barcelona, p 641
van der Woerdt A (2003) Ophthalmologic diseases in small pet mammals. In: Quesenberry KE, Carpenter JW (eds) Ferrets, Rabbits and Rodents. Clinical Medicine and Surgery, 2nd edn. WB Saunders Company, Philadelphia, pp 421–428
van der Woerdt A (2012) Ophthalmologic diseases in small pet mammals. In: Quesenberry KE, Carpenter JW (eds) Ferrets, Rabbits and Rodents Clinical Medicine and Surgery, 3rd edn. Elsevier Saunders, St Louis, pp 523–531
Wright K, Edwards MS (2009) Considerations for kinkajou captive diets. Vet Clin North Am Exot Anim Pract 12:171–185
Xie Y, Zhang Z, Wang C et al (2011) Complete mitochondrial genomes of *Baylisascaris schroederi, Baylisascaris ailuri* and *Baylisascaris transfuga* from giant panda, red panda and polar bear. Gene 482:59–67

Ophthalmology of Chiroptera: Bats

40

Fabiano Montiani-Ferreira, Caryn E. Plummer, and Elizabeth Adkins

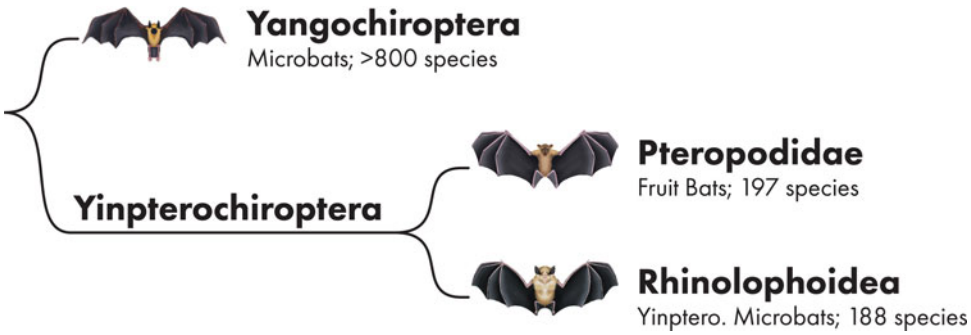

Introduction

Bats (order Chiroptera) are the only mammals that can truly fly rather than glide (Graham 1994; Peracchi et al. 2011). Their forelimbs are adapted as wings and they possess very peculiar sensory adaptations. Bats are one of the most diverse groups of mammals, existing on every major landmass, except the Polar region and a few oceanic islands. With over 1230 species, making nearly 1 in 5 mammal species (21%) a bat, they are exceeded in number only by the order Rodentia (Simmons 2005; Reis et al. 2007; Fenton and Ratcliffe 2010; Hassi 2018). Bats are divided into two suborders: (1) Yinpterochiroptera (or Pteropodiformes), formerly known as megabats (old world fruit bats, or flying foxes), comprising seven families distributed in Africa, Asia, and Oceania; and (2) Yangochiroptera (or Vespertilioniformes), which includes most of those formerly known as microbat families, except for the Rhinopomatidae, Rhinolophidae, Hipposideridae, and Megadermatidae. These latter four Old World microbat families are now classified as Yinpterochiroptera, which is currently comprised of 14 families distributed worldwide (Graham 1994; Rojas et al. 2016).

F. Montiani-Ferreira (✉)
Comparative Ophthalmology Laboratory (LABOCO), Veterinary Medicine Department, Federal University of Paraná, Curitiba, Brazil
e-mail: montiani@ufpr.br

C. E. Plummer
Department of Small Animal Clinical Sciences, College of Veterinary Medicine, University of Florida, Gainesville, FL, USA
e-mail: plummerc@ufl.edu

E. Adkins
Hope Advanced Veterinary Center, Vienna, VA, USA

F. Montiani-Ferreira et al. (eds.), *Wild and Exotic Animal Ophthalmology*, https://doi.org/10.1007/978-3-030-81273-7_15

Bats and Their Interactions with the Environment, Human, and Animal Health

Due to highly specialized habitat requirements and complex interactions with the environment, bats are considered a sentinel species whose populations and welfare inform the status of their ecosystems and the efficacies of conservation efforts (Jones et al. 2009). They have adapted to thrive in a variety of ecosystems and on a variety of diets, including insects, small mammals, fish, blood, nectar, fruit, and pollen (Teeling et al. 2018). Many insectivorous bats are highly mobile predators and often are cited as significant agents for the suppression of agricultural pests in natural and agricultural environments (Kunz et al. 2011). A single bat is capable of consuming up to 600 mosquitoes per hour (Gonsalves et al. 2013). Mosquito consumption by bats has been linked to a significant reduction of disease vectors. For instance, a 32% reduction in oviposition by Culex spp., a genus of mosquitoes that serve as a vector for several human and animal diseases, has been associated with bat predation (Reiskind and Wund 2009; Farajollahi et al. 2011). Bats also are critically important pollinators, being responsible for the dissemination of many of the nearly 300,000 flowering plants that require animal pollinators worldwide (Ollerton et al. 2011). Additionally, many species of frugivorous bats help to disperse tree seeds in their environment (Koopman 1993; Shilton et al. 1999).

According to the Centers for Disease Control (CDC), bats are responsible for roughly 7 in 10 rabies deaths among people who are infected with the rabies virus in the U.S.A. (CDC 2019). Bats are the leading rabies vector in the USA (more than raccoons, foxes, and skunks) and account for one-third of the 5000 rabid animals that are reported each year (CDC 2019). Even though bats are indispensable for our ecosystems and most species are harmless, it is important to remember that in some situations, bats can be a serious threat to human health. Relative to their total numbers, few bats become infected with rabies; however, when they do, the risk of exposure to humans and domestic animals is great. A possible reason for the high rate of transmission is that bats testing positive for rabies typically are those that are already found sick and often grounded and uncoordinated, making them enticing for dogs, cats, and children to play with. Any possible contact with bats by people or other animals needs to be taken very seriously, and appropriate personal protective equipment should be worn at all times. Rabies is almost universally fatal within one to two weeks following infection, although it is preventable if people take swift action after being bitten or scratched by an animal. Vaccinating pets, avoiding contact with wildlife, and seeking medical care if one is bitten or scratched by an animal are the most effective ways to prevent rabies (Pieracci et al. 2019). Pre-exposure prophylaxis is strongly recommended for people, including veterinarians, who are at high risk of exposure to rabies virus because of professional activities (WHO 2018). Compared with terrestrial mammals, bats have a greater capacity to co-exist with a variety of viruses. One of the possible reasons for this is a species-specific dampened interferon response (Xie et al. 2018). Another possibility is the fact that the immune systems of bats do not overreact to infections, which keeps them from falling ill from the many viruses they carry (Subudhi et al. 2019). They are the natural reservoir for the Marburg virus, and Nipah and Hendra viruses, which have caused human disease and outbreaks in Africa, Malaysia, Bangladesh, and Australia. Bats are thought to be the natural reservoir for the Ebola virus. Some of these viruses can spill over to other animals, such as the Swine Acute Diarrhea Syndrome (SADS), caused by a coronavirus. Other viruses can affect humans, which can have devastating consequences. People in many parts of the world eat bats and sell them in live animal markets, which was likely the source of a large number of viruses that have a close genetic relationship with coronaviruses. Examples are Middle East respiratory syndrome (MERS), severe acute respiratory syndrome (SARS), and possibly the recent coronavirus outbreak that began in Wuhan-China, the SARS-CoV-2. The latter virus is a betacoronavirus, like MERS-CoV and SARS-CoV. All three of these viruses have their origins in bats (Xie et al. 2018; Fan et al. 2019; CDC 2020).

Special Senses

Many species of bats, particularly those belonging to the suborder Yangochiroptera, possess echolocation systems that aid in flight orientation and hunting across different ecological niches (Fenton 1995). They use different types of vocalization soundwaves with constant or modulated frequency portions ranging from 1 to >50 ms (Neuweiler 1983). Other animals that use echolocation, such as cetaceans (Au 1993), and cave swiftlets and oilbirds (Griffin 1953; Suthers and Hector 1985; Fullard et al. 1993), receive echolocation signals by employing short-duration impulsive clicks (Fenton 1984). Among the Yinpterochiroptera bats, only the genus *Rousettus* possess echolocation abilities. The Egyptian fruit bat (*Rousettus aegyptiacus*) does so by emitting sound signals (clicks) using the tongue and analyzing returning echoes (Möhres and Kulzer 1956). Pteropodidae bats do not use echolocation but instead possess large eyes specialized for nocturnal vision (Simões et al. 2019).

Recently it has been revealed that some species of bats possess a sensory mechanism that acts as a magnetic compass, enabling them to detect the Earth's magnetic field in order to navigate (Holland et al. 2006, 2010). Birds and

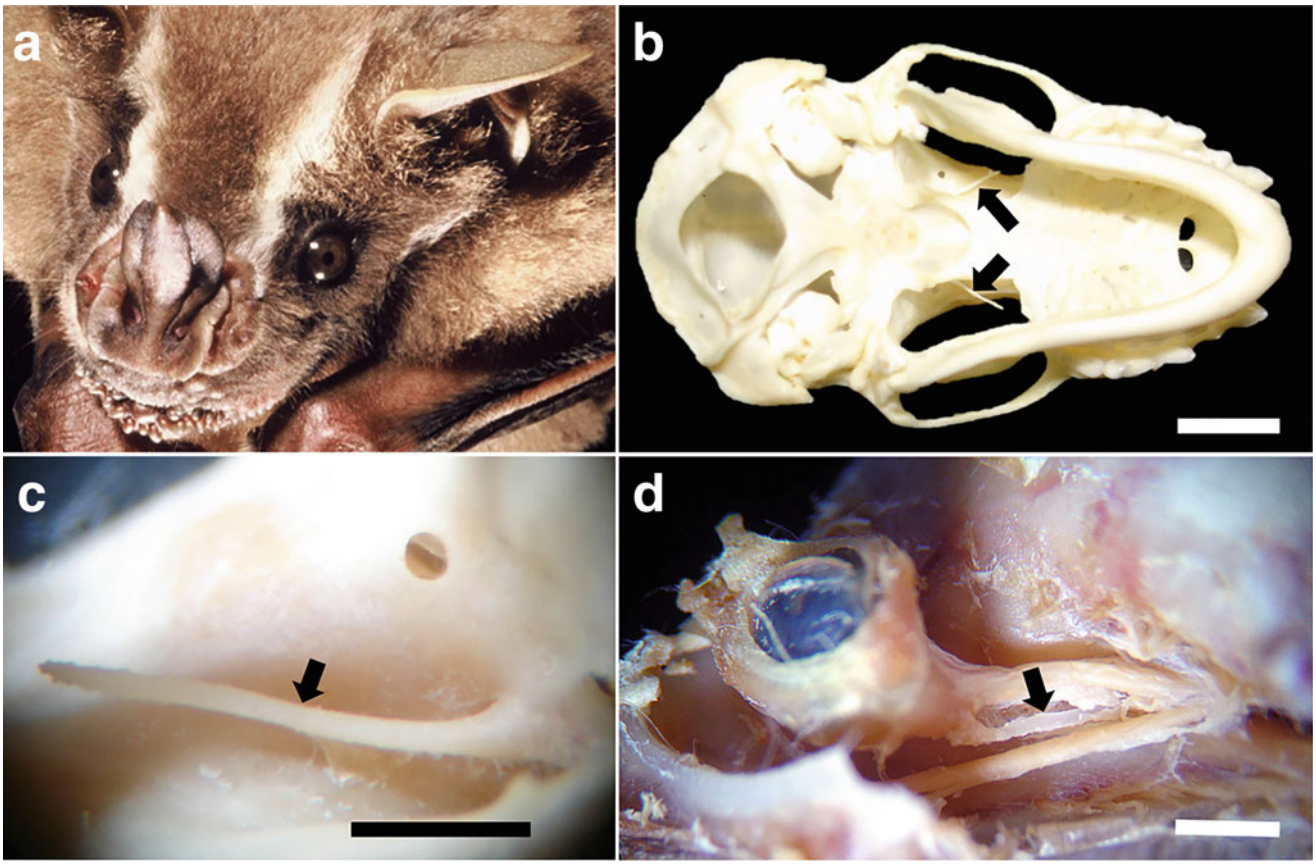

Fig. 40.1 The intraorbital optic spine of the alisphenoid bone in large fruit-eating bats (*Artibeus lituratus*). (**a**) An adult large fruit-eating bat. In a macerated skull, the spine is visible between the optic canal and the sphenorbital fissue on the alisphenoid bone (black arrows) (**b**—scale bar 5 mm, **c**—10 mm). (**d**) Dissection of the periorbita to expose the intraorbital optic spine and surrounding structures. Note the cylindrical bony structure (black arrow) immediately ventral to the optic nerve and dorsal to the mandibular branch of the trigeminal nerve (Scale bar—10 mm). (Figure courtesy of Zig Koch)

rodents that have been shown with the ability to recognize magnetic fields do so by possessing an inclination-based magnetic compass in retinal photoreceptive molecules (Mouritsen 2012; Malkemper et al. 2015). Whether or not bats possess the same retinal mechanism is yet to be determined.

Some fruit bats have evolved superior olfactory abilities that compete with those of canids. For instance, the Eastern tube-nosed fruit bat (*Nyctimene robinsoni*) possesses nostrils that function independently from one another, or stereo olfaction (similar to binocular vision or stereo hearing from two ears). This feature enables them to precisely locate and follow an odor trail three dimensionally (Schwab and Pettigrew 2005).

Bony Orbit

The bony orbits of some bats contain a unique elongated, bony process. The process has been shown to be extremely long in the phyllostomid fruit-eating bat (*Artibeus lituratus*) (Machado et al. 2007) (Fig. 40.1) and has since been observed in several other bats from the Yinpterochiroptera family (data not published). A similar but shorter anatomical structure has been described in megachiropteran bats (*Pteropus* spp.) (Giannini et al. 2006; Starck 1943), as well as in the European hedgehog (*Erinaceus europaeus*) (Fawcett 1918), manatee (*Trichechus* sp.) (Matthes 1921), and common shrew (*Sorex araneus*) (De Beer 1937). The shorter version of this osseous structure in other animals has been referred to as "processus paropticus" or "lamina hypochiasmatica" (Starck 1943), or "ala hypochiasmatica" (i.e., "process", De Beer 1937; Dorland 1994). However, we suggest that the term "intraorbital optic spine" is a more accurate term than "ala, or process", as it is both descriptive and instructive and indicates such an elongated bone formation that is also thin and sharp (NAV 1994). The intraorbital optic spine is speculated to not only serve as an attachment to one or more extraocular muscles (Machado et al. 2007), but it may also contribute to the structural support of other periorbital tissues (Fig. 40.1d). The precise function of this

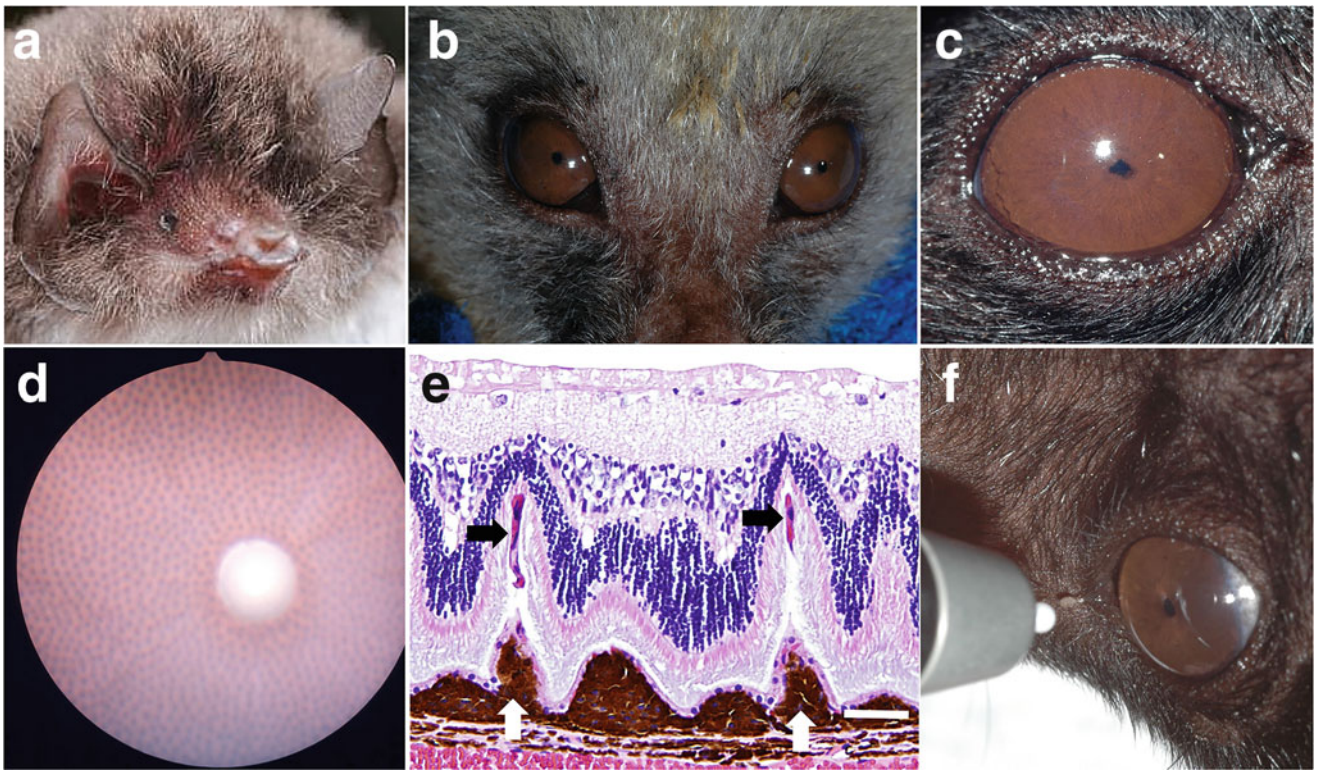

Fig. 40.2 Normal ocular anatomy and examination in bats. (**a**) Normal appearance of a very small "degenerated" eye of a Spix's disk-winged bat (*Thyroptera tricolor*). (**b**) A normal adult Island Flying Fox (*Pteropus hypomelanus*). Note the forward-facing eyes providing a large binocular field. (**c**) Normal appearance of the eye of an adult Malayan flying fox, or large flying fox (*Pteropus vampyrus*). Note the marked miosis in bright luminance. (**d**) A normal funduscopic image of a fruit bat *Nyctimene robinsoni* showing an anangiotic retinal vascular pattern and spotted appearance caused by numerous choroidal papillae as shown histologically in (**e**). Note the choroidal papillae (white arrows) bringing blood vessels into the retina (black arrows). Scale bar 20 μm. (**f**) Measurement of intraocular pressure in an adult Malayan flying fox using a rebound tonometer (Tonovet, Icare Oy, Finland) in a hanging position. (**a**—Courtesy of Zig Koch. **d**—Courtesy of the University of California Davis Comparative Ophthalmology Service. **e**—Courtesy of the Comparative Ocular Pathology Laboratory of Wisconsin)

osseous structure is not entirely known and further investigation is warranted.

Eyes and Visual System of Bats

"As blind as a bat" is a popular saying and English idiom, commonly used to imply that someone has very poor eyesight or that they pay little attention to their surroundings, respectively. This rather unfair assertion is based on the erroneous notion that bats cannot see well. However, most bat species have a very well-developed visual system. Members of Yinpterochiroptera bats generally have a more developed visual system, but even most of the Yangochiroptera bats see fairly well, with visual acuity comparable to that of the mouse (*Mus musculus*) or the hamster (*Mesocricetus auratus*) (Kirk and Kay 2004). It is true, however, that some small species of bats indeed have very small eyes (absolutely and relatively speaking), probably favoring other sensorial skills such as echolation and even olfaction. Some authors even dubbed these types of globes as "degenerated" (Prince 1956). However, these "degenerated" globes are more like exceptions than a general rule even for the small Yangochiroptera bats (Fig. 40.2a). Visual acuity varies in accordance with the requirements of a species' own specialized niche. Therefore, generalizations about bat vision in any sense may be incorrect. In fact, it has been reported that certain small insectivorous bats may have vision equivalent to that of larger-eyed frugivorous and nectarivorous bats (Bell and Fenton 1986).

The activity pattern of a given bat species provides a lot of information about their visual capabilities. Yinpterochiroptera bats are generally crepuscular or nocturnal while Yangochiroptera bats are nocturnal. Thus, the retina of both Yinpterochiroptera and Yangochiroptera bats is rod-dominated (Schwab and Pettigrew 2005). Both species have long been considered to have pure rod retinas, although both do contain a small population of cones (Müller and Peichl 2005, 2006; Müller et al. 2007a, 2009; Kim et al. 2008). Most bats possess dichromatic color discrimination

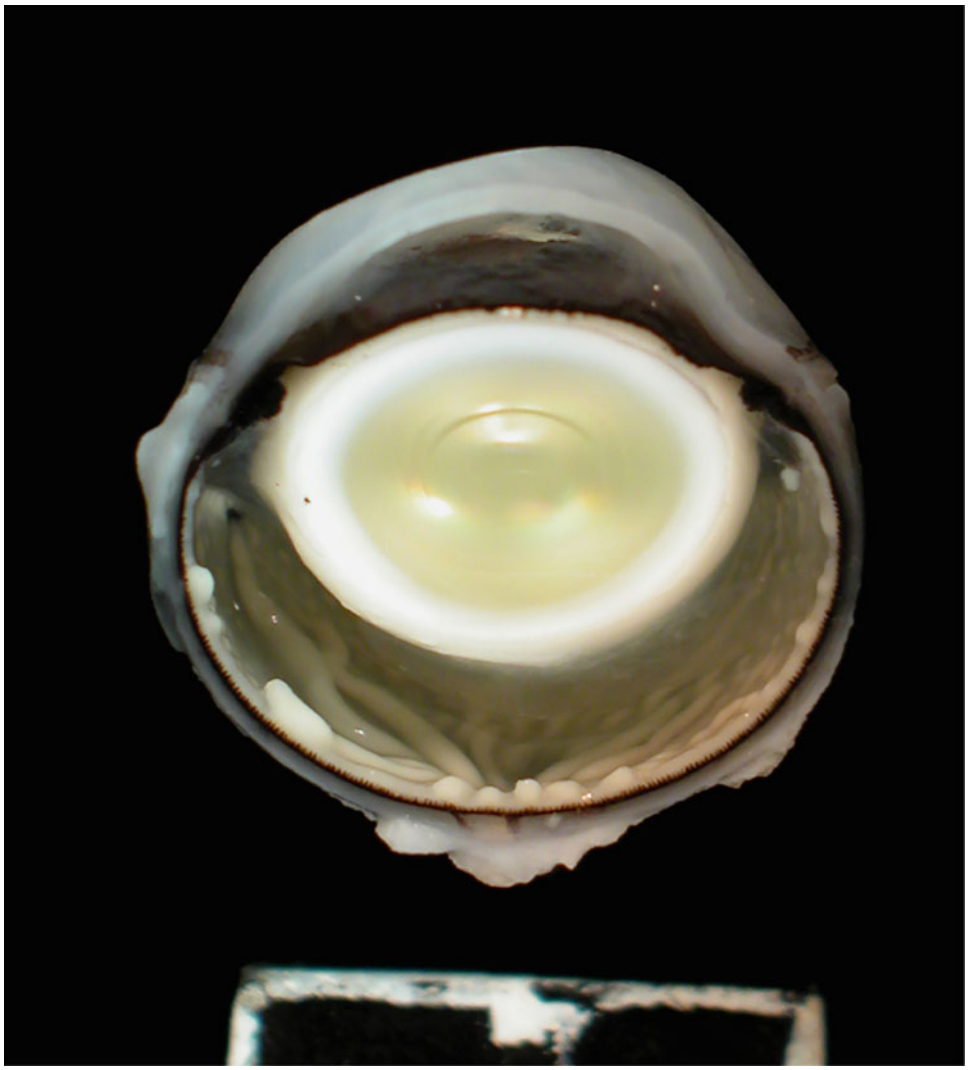

Fig. 40.3 Photograph of the cut surface of the right half of a formalin-fixed right eyeball of a fruit bat *Nyctimene robinsoni*. Note the remarkably spherical globe, large corneal surface, and the proportionally very large lens size (in its axial thickness). (Courtesy of the Comparative Ocular Pathology Laboratory of Wisconsin)

(Müller et al. 2009), although a small cohort of species is monochromatic (Müller et al. 2007a). Molecular analysis of opsin genes has shown that some Yinpterochiroptera bats even have the potential for trichromatic vision (Schwab and Pettigrew 2005). In fact, the visual pigments that are responsible for color vision for some frugivorous bats include a short wavelength opsin with a sensitivity that extends into the ultraviolet and a long-wavelength opsin with sensitivity to red color (Schwab and Pettigrew 2005; Müller et al. 2007b; Fujun et al. 2012).

In general, bat globes are small and positioned well forward in the orbit (Figs. 40.1a and 40.2b, c), with a binocular overlap of 40–50° in the horizontal visual field, typical of predatory animals and similar to that of canids (Prince 1956). There is a tight approximation of the eyelids to cornea and the third eyelid is visible in the ventromedial orbit with a pigmented leading edge (Blackwood et al. 2010) (Fig. 40.2b, c). Their eyeballs are remarkably spherical, and the cornea is usually very large with the limbus nearing the equator of the globe in some species (Prince 1956; Blackwood et al. 2010) (Fig. 40.3). The irides are usually darkly pigmented with a prominent iris collarette (Fig. 40.2c) (Blackwood et al. 2010). Pupils are round to horizontal ovoid when constricted, depending on the species, and typically, pupil size has a great size range depending on the ambient lighting conditions (Prince 1956; Blackwood et al. 2010) (Fig. 40.2c).

Funduscopy is challenging due to extremely small pupil size in bright light, although when viewed an anangiotic retina with a homogenously red reflex and evenly spaced gray spots are noted (Fig. 40.2d). Generally, animals with an anangiotic retinal vascular pattern have very thin retinas (<140 μm) to allow for adequate diffusion of oxygen from the choroid (Brudenall et al. 2007; Chase 1982). The retinas of Yinpterochiroptera species, such as the tube-nosed fruit bat *Nyctimene robinsoni*, have surprisingly thick retinae (250–350 μm) despite being avascular. A unique morphologic adaptation is present to ensure that the requisite oxygen

delivery occurs, consisting of numerous choroidal spike-like projections or papillae (Suthers 1970) (Fig. 40.2e). The tip of each evenly spaced papilla (125–150 μm apart) projects into the retina, bringing with it choroidal vasculature such that all portions of the retina are no more than 100 μm away from a blood supply (Schwab and Pettigrew 2005). The choroidal papillae are observable clinically as the heterogenous gray dot pattern described on funduscopy (Fig. 40.2d), a pattern that was once thought to represent innumerous foveae (Prince 1956). Additionally, this adaptation permits the retina to receive more light, since the presence of retinal vasculature blocks some light exposure, thus potentially improving visual acuity (Schwab and Pettigrew 2005).

Normative Data for Ophthalmic Diagnostic Tests

Information about the ocular anatomy and normal ophthalmic diagnostic parameters may serve as an important reference for practitioners in the diagnosis and management of ocular diseases in bats as well as provide a normal baseline for future investigations. This is especially important in the Yinpterochiroptera bats due to their reliance on vision for survival. A few investigations established normative ocular data has been established in relatively few species of bats. Reports of aqueous tear production, intraocular pressure, horizontal palpebral fissure length, and horizontal and vertical corneal diameters are available for select Yinpterochiroptera and Yangochiroptera species (Appendix C).

Among Yinpterochiroptera bats, aqueous tear production, palpebral fissure length, horizontal and vertical corneal diameters, and intraocular pressure (both upright and hanging upside-down) has been reported in three species: Malayan flying foxes *Pteropus vampyrus* (Fig. 40.2f), little golden-mantled flying foxes *Pteropus pumilus*, island flying foxes *Pteropus hypomelanus* (Blackwood et al. 2010). Phenol red thread: 20.23 ± 1.28 mm/15s; Palpebral fissure length: 13.34 ± 0.33 mm; Horizontal corneal diameter: 10.72 ± 0.32 mm; Vertical corneal diameter: 9.90 ± 0.30 mm. Interestingly, the IOP while in the hanging position 19.38 ± 0.77 mmHg which was significantly higher than the IOP of bats in an upright position, which was 13.95 ± 0.60 mmHg. The position of the bat should be considered when taking intraocular pressure measurements.

In Yangochiroptera bats, aqueous tear production, intraocular pressure, and horizontal palpebral fissure length have been reported (Somma et al. 2019). Aqueous tear production with endodontic paper points was 2.53 ± 1.65 mm/min for *Artibeus lituratus* and 1.89 ± 0.62 for *Anoura caudifer*. Intraocular pressure measured by rebound tonometry (Tonovet®, Icare Vantaa, Finland) in the upright position was 11.0 ± 3.28 mmHg for *Artibeus lituratus* and 7.28 ± 2.70 for *Anoura caudifer*. Horizontal palpebral fissure length was 5.04 ± 0.45 mm for *Artibeus lituratus* and 3.92 ± 0.51 for *Anoura caudifer* (Somma et al. 2019). In an investigation of the bacterial microbiota of the ocular surface of captive and free-ranging Yangochiroptera bats, three different species (*Desmodus rotundus*, *Diameus youngi*, and *Artibeus lituratus*), were analyzed. Seventeen bats had positive bacterial cultures in one or both eyes (Leigue Dos Santos et al. 2014). The number of positive samples in the bats evaluated was surprisingly low (29%) compared to the frequency of positive bacterial growth from the ocular surface of other mammals (45–91%) (Wang et al. 2008; Lima et al. 2010). Of all the isolates, Gram-positive bacteria, especially *Staphylococcus* spp., were more common than Gram-negative bacteria. In the majority of mammalian species, Gram-positive bacteria are the most common isolate (Cullen 2003). Coagulase-negative staphylococci (30.4%) was the most isolated genus, followed by *Bacillus* spp. (26%) and *Corynebacterium* spp. (21%). Only four Gram-negative species were isolated: *Shigella* spp., *Hafnia alvei*, *Morganella morganii*, and *Flavobacterium odoratu* (Leigue Dos Santos et al. 2014).

Ophthalmic Disease

Few scientific reports about ocular abnormalities in bats exist, and information pertaining to the diagnosis and treatment of ophthalmic disease in both captive and wild populations of bats is limited. This may suggest that individual bats with ocular conditions have a low survival rate in the wild. Alternatively, ocular lesions may be considerably underdiagnosed or under-reported.

Population surveys and evaluation of free-living individuals offer an important view into the prevalence and types of ophthalmic disease occurring naturally in the wild. In general, ocular lesions in free-living bats are rare, with ocular discharge, conjunctivitis, and chemosis being the most common findings (Fig. 40.4a). An infectious etiology should certainly be considered for these cases. Additionally, developmental abnormalities have been described with some frequency. In a survey of 8718 wild Yangochiroptera bats captured using mist nets in Mexico, nine (0.10%) of these had ocular lesions, reportedly consisting of corneal opacities (2), unclassified eye injuries and/or infections (4), microphthalmia (1), and anophthalmia (2). Six different species were represented in this study, across the Phyllostomidae and Molossidae families: *Desmodus rotundus*, *Glossophaga soricina*, *Artibeus jamaicensis*, *Artibeus lituratus*, *Sturnira parvidens*, and *Tadarida brasiliensis* (Sánchez-Hernández et al. 2018). Clinical anophthalmia was also reported in a greater bulldog bat (*Noctilio leporinus*) in the state of Colima, Mexico (Sánchez-Hernández et al. 2016). The bats described to be anophthalmic are suspected by the current authors to be

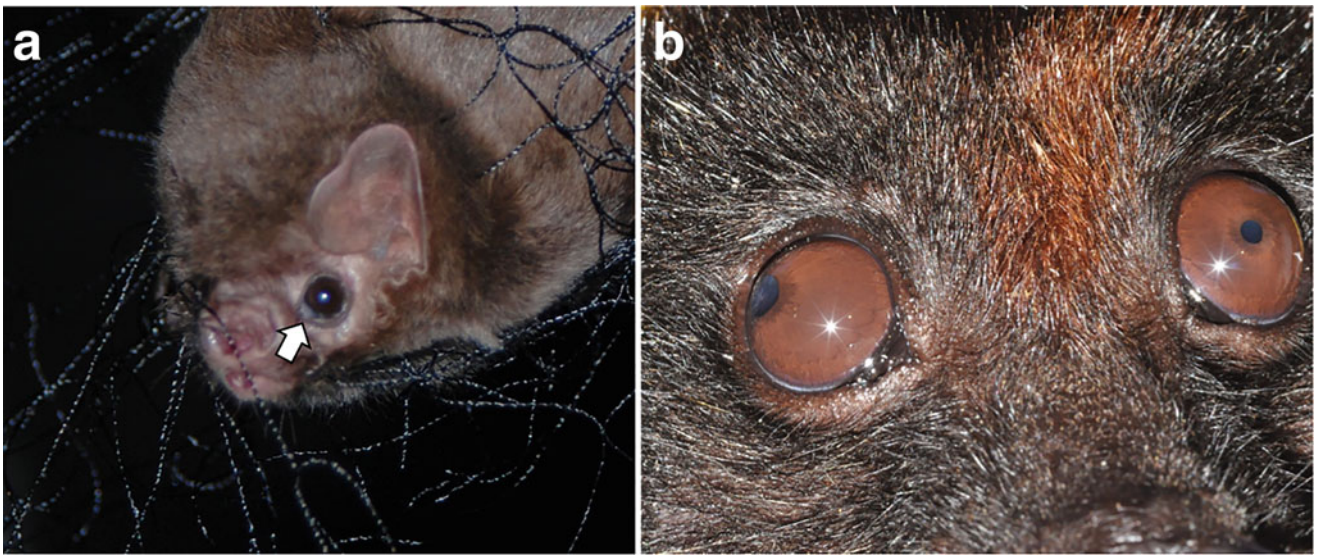

Fig. 40.4 (**a**) Mucoid ocular secretion at the medial canthus (arrow) and along the inferior lid margin of an adult white-winged vampire bat (*Diaemus youngi*) caught in a mist net for unrelated research purposes in South Brazil. (**b**) An adult Malayan flying fox (*Pteropus vampyrus*) with corectopia of the right pupil. Since pupil position in this eye was always present and not associated with other ocular abnormalities, it was deemed to be congenital

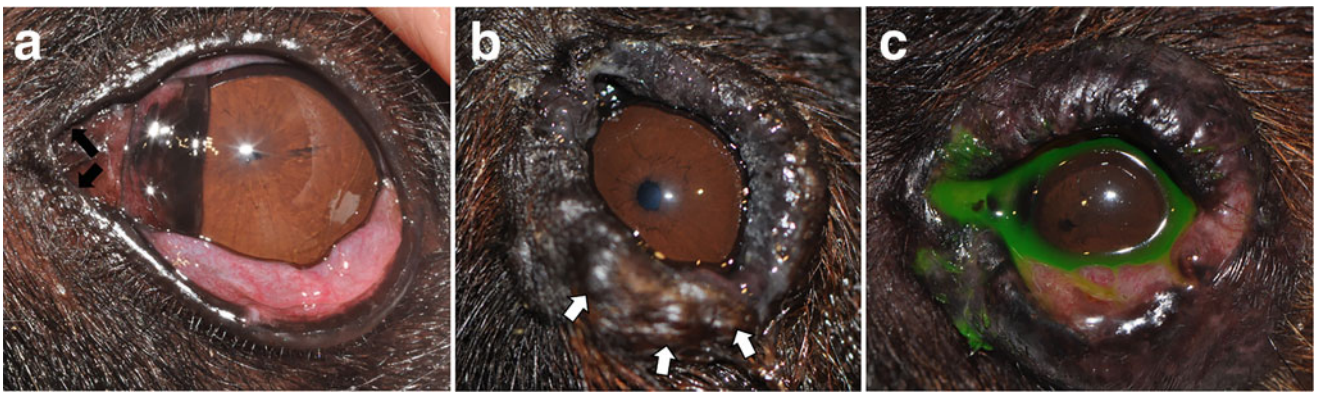

Fig. 40.5 (**a**) Conjunctivitis and chemosis of the left eye of an adult Malayan flying fox (*Pteropus vampyrus*). These signs were suspected to be due to an ocular surface infection (origin unknown). (**b**) Serous ocular discharge, periocular pruritus, chronic conjunctivitis, blepharitis, and meibomianitis (arrows) in the left eye of an 11-year-old, intact, male Malayan flying fox (*Pteropus vampyrus*). (**c**) A full-thickness wedge biopsy of the inferior eyelid was performed. Nested polymerase chain reaction amplification, sequencing, and phylogenetic analyses of DNA were used to identify a novel herpesvirus in the resulting tissue sample, a member of the genus *Percavirus* in the subfamily *Gammaherpesvirinae*

severely microphthalmic. Regardless, it is interesting to consider that free-living bats without appreciable eyes of species that typically are believed to depend on vision at least to some degree had success without vision. This speaks to the dominance of other sensory systems in some species of bats. Without major reliance on vision in the wild, the persistence of visually impairing developmental lesions may be possible.

Similar ocular abnormalities are found in captive bats, consisting most commonly of traumatic, developmental, and suspected infections etiologies (Fig. 40.5b). Kunz and Chase (1983) studied juvenile big brown bats (*Eptesicus fuscus*) Yangochiroptera, from a nursery colony in Massachusetts, USA. Some abnormalities found by this group include atypically small eyes, fused eyelids, choroidal changes, undifferentiated retinas, and underdeveloped lenses. In an ophthalmic examination survey of Yinpterochiroptera bats that included Malayan flying foxes (*Pteropus vampyrus*), little golden-mantled flying foxes (*Pteropus pumilus*), and island flying foxes (*Pteropus hypomelanus*), several ocular abnormalities were found and described including eyelid defects and eyelid masses, mucopurulent discharge, defects of the third eyelid, dull dry corneas, corneal scars, iris to iris persistent pupillary membranes, cystic dilation of iris posterior pigmented epithelium at the pupillary margin, prominent greater arterial circles, flat

hyperpigmented foci of the iris, iris masses, nuclear sclerosis and incipient cataracts (Blackwood et al. 2010).

Since bats generally live in large colonies, individual interactions may affect their ophthalmic health due to trauma, and infectious organisms can easily be transmitted to one another. Traumatic ocular surface abnormalities (lacerations and swelling) and infectious conjunctivitis and chemosis of unknown etiology (Fig. 40.5a) also are somewhat commonly observed in individuals belonging to bat sanctuaries. Most of these eyelid lesions were actually scars. In most of these cases, the eyelids were functioning properly even with a structural abnormality. This is somewhat surprising, given that the eyelids fit so tightly over the cornea. Captive bats in the southeastern United States often develop influenza-like symptoms in the spring. The symptoms do not respond to symptomatic therapy and appear to be self-limiting. The presumptive cause of these symptoms is viral. (Personal observation, E. Adkins). A novel gammaherpesvirus was identified in a large flying fox (*Pteropus vampyrus*) with conjunctivitis, blepharitis, and meibomianitis (Fig. 40.5b, c) by nested polymerase chain reaction and sequencing (Brock et al. 2013). The isolated virus, a member of the genus *Percavirus* in the subfamily *Gammaherpesvirinae*, was suggested as a possible causative agent, since different herpesviruses have been associated with conjunctivitis, keratitis, and meibomianitis in other mammalian species, including humans (Pfaller et al. 1984; Singh et al. 2007). A treatment protocol using Cidofovir (1 drop OU q12h for 28 days) was implemented. No significant improvement was noted and the antiviral medication was discontinued. Prednisolone (1 mg/kg PO q24h) was successful in suppressing the pruritus and conjunctivitis, although slight persistence of blepharitis was noted. No recurrence of the conjunctivitis was noted after prednisolone was discontinued. Additional research is still needed to prove the association of this virus as the causative agent for the ocular signs.

During the breeding season, males in particular may present with traumatic injuries due to competition for resources and mates. Lacerations of the eyelids, third eyelid, and cornea, as well as proptosis of the globe, may occur. Traumatic proptosis carries with it a guarded prognosis, depending on the severity and the duration of exposure. If possible, re-positioning of the globe followed by supportive tarsorrhaphy should be performed on an emergent basis in an attempt to salvage the globe. Eyes that have ruptured or have developed endophthalmitis, severe exposure keratitis with chronic corneal desiccation, persistent or intractable uveitis, or glaucoma should be considered candidates for enucleation. Even though enucleation in bats has been reported since the times of Lazaro Spallanzani (1794) in his experiments to prove echolocation, it is still a challenging surgical procedure due to the small size of the anatomic structures (Fig. 40.6) especially in those bats belonging to the suborder Yangochiroptera. Absorbable sutures (e.g., polyglactin 910 6-0, Vicryl, Ethicon Inc. Johnson and Johnson) are recommended to minimize post-operative handling. Nevertheless, the clinician should bear in mind that bats frequently exhibit complications following enucleation, especially persistent swelling and infections within the orbit, likely associated with dependent positioning when they rest in an inverted posture.

The most commonly observed ophthalmic lesions in captive bats, both Yinpterochiroptera and Yangochiroptera, are those of the cornea. Crystalline stromal dystrophy (lipid dystrophy) has been observed. Typically, there is a central grayish-white, crystalline deposit in the anterior corneal stroma (Fig. 40.7a). The corneal deposits are often circular or oval and can be unilateral or bilateral. The lesions typically do not cause discomfort. Non-ulcerative keratitis, suspected to be immune-mediated, is rather common in some bat populations such as in flying foxes (Fig. 40.7b). Treatment with topical anti-inflammatory or immunomodulatory medications such as 0.2% cyclosporine to dampen the response is usually curative in 4–6 weeks, and a maintenance dose is often not required (Fig. 40.7b).

Traumatic corneal ulcerations and lacerations are particularly common (Fig. 40.8). They are largely due to aggression between conspecifics, and the incidence of traumatic injuries increases during the breeding season. Treatment is similar to that recommended for domestic species with corneal injuries. However, the frequency recommended for other species may not be possible due to the stress of handling that accompanies frequent medication administration. When possible, appropriate medical therapy at an initial high frequency can substantially improve infected ulcers within days (Fig. 40.9). If such treatment is unable, or if initial presentation for treatment was delayed, corneal abscessation and rupture can occur. However, this can also be managed successfully medically, as demonstrated below in a young Malayan flying fox (*Pteropus vampyrus*) (Fig. 40.10). In this case, a corneal injury presumably induced a stromal infection followed by rapid healing of the corneal epithelium. Corneal vascularization was marked and almost the entire stromal tissue was affected with the abscess. In addition, the volume of the affected globe was smaller than the unaffected one, most likely due to the marked accompanying uveitis resulting in early phthisis bulbi. Vision was lost but the corneal infection healed with surgical excision of the abscess, topical and systemic antibiotic therapy, combined with tarsorrhaphy. Surgical excision of the abscess usually gives the best chance of a successful outcome in these cases.

Acute onset unilateral exophthalmos has been associated with retrobulbar abscesses and cellulitis in bats (Fig. 40.11). The most notable clinical signs are typically exophthalmos, elevation of the third eyelid, and a variable degree of conjunctival hyperemia and chemosis. Pain might be apparent

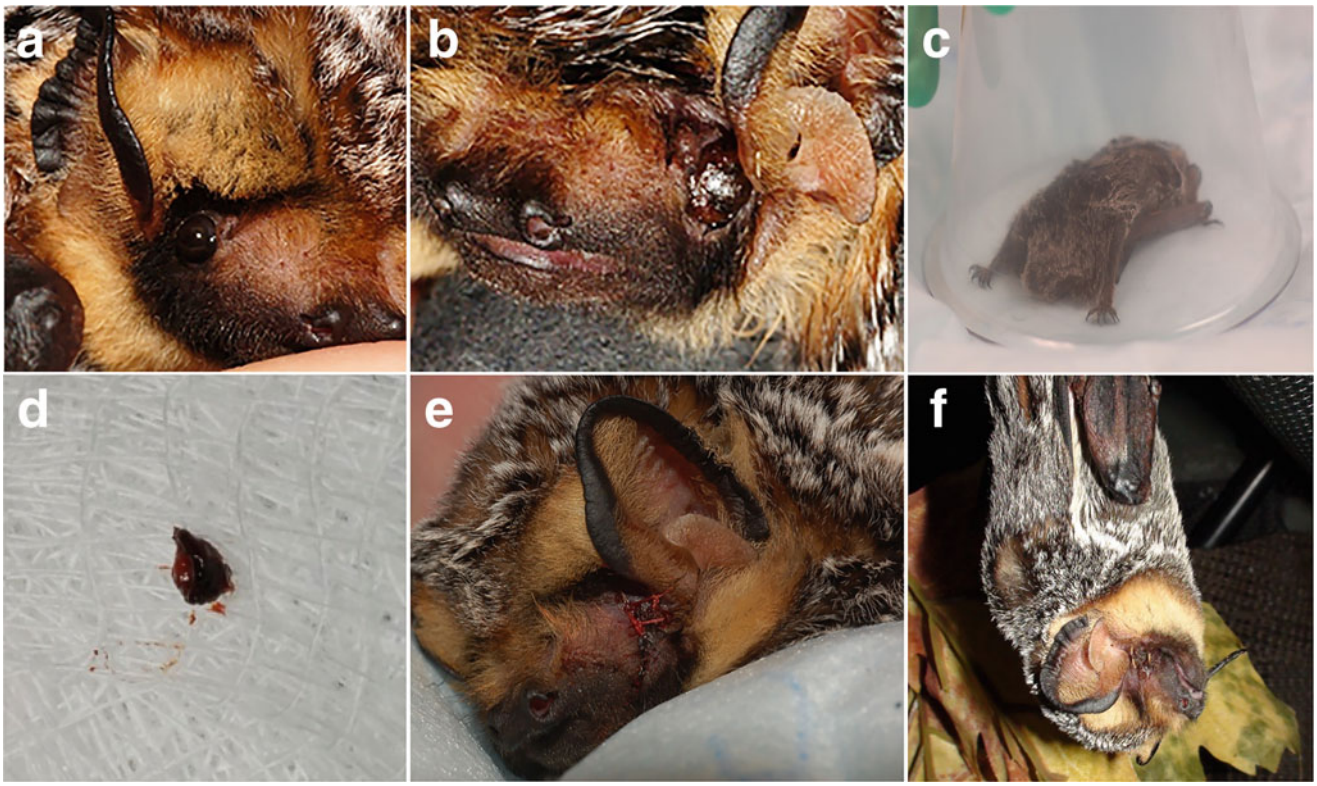

Fig. 40.6 An adult, male, hoary bat (60 g) with a normal right eye (**a**) but a chronically desiccated left cornea (**b**) that was unresponsive to treatment. Enucleation was elected because the bat stopped eating. (**c**) Mask induction of general anesthesia for enucleation OS. (**d**) Globe OS post-enucleation. (**e**) Postoperative enucleation OS. Histopathology of the globe revealed idiopathic profound anterior segment inflammation with loss of corneal structure and obliteration of the anterior chamber. (**f**) The sutures remained intact at two weeks post-enucleation

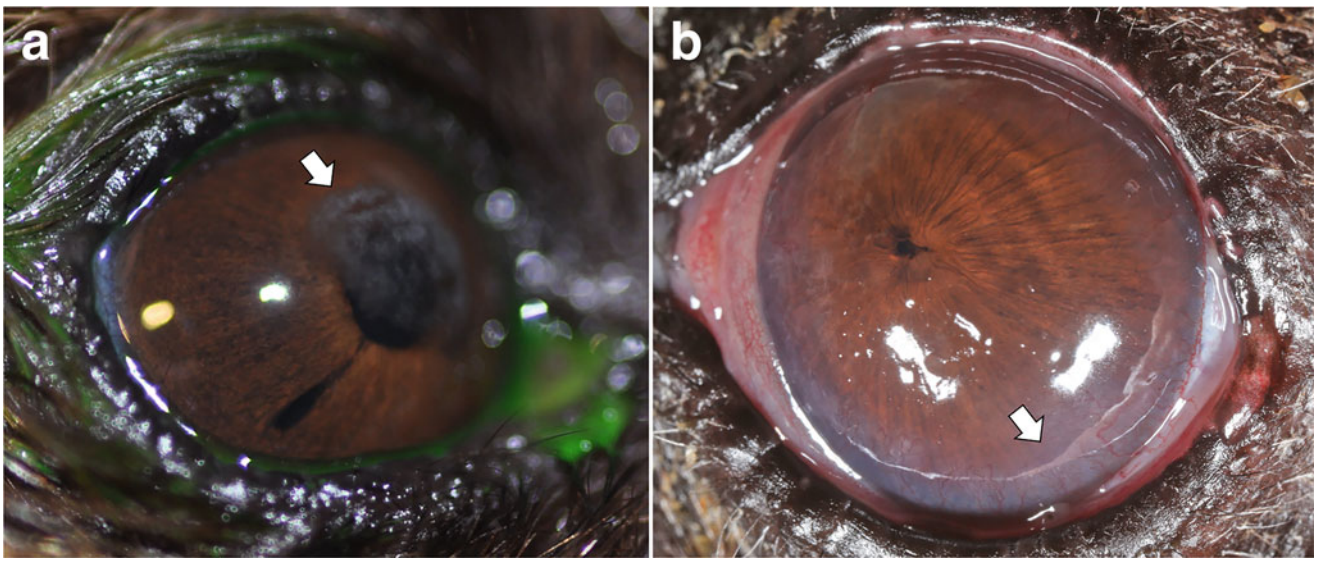

Fig. 40.7 Superficial corneal disease in bats. (**a**) Crystalline stromal dystrophy (lipid dystrophy) in the right eye of this adult Malayan flying fox (*Pteropus vampyrus*). Note the circular crystalline opacity in the axial corneal stroma (white arrow). Unless an underlying nutritional imbalance or an endocrine condition is diagnosed, these lesions are often benign and do not typically cause discomfort and require no treatment. (**b**) Non-ulcerative keratitis in an adult Malayan flying fox, suspected to be immune-mediated in origin. Administration of topical 0.2% Cyclosporine ointment twice daily resulted in significant improvement in 2 weeks and clearance within 1 month. Recurrence was not evident after stopping the medication. (**b**—Courtesy of Bret A. Moore)

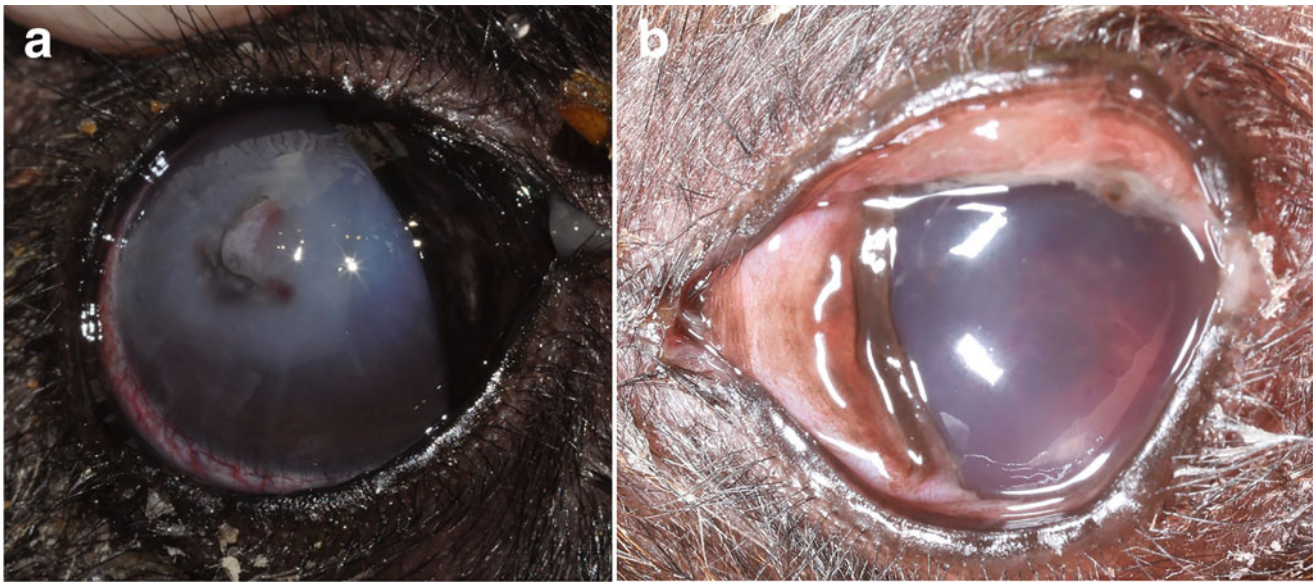

Fig. 40.8 Traumatic corneosceral laceration in bats. (**a**) A corneal laceration in a Malayan flying fox (*Pteropus vampyrus*) that resulted in collapse of the anterior chamber. The dark area within the wound bed was prolapsed iris. Note the presence of episcleral congestion and periocular crusting. (**b**) A dorsotempral limbal laceration in a Malayan flying fox is evidenced by a small, pigmented spot within a fibrin plug just beneath the dorsal conjunctiva. Hyphema is present, further suggesting a full-thickness laceration. The laceration extended posteriorly along the sclera past the globe equator. Substantial chorioretinal prolapse resulted in the decision to enucleate the eye. (**b**—Courtesy of Bret A. Moore)

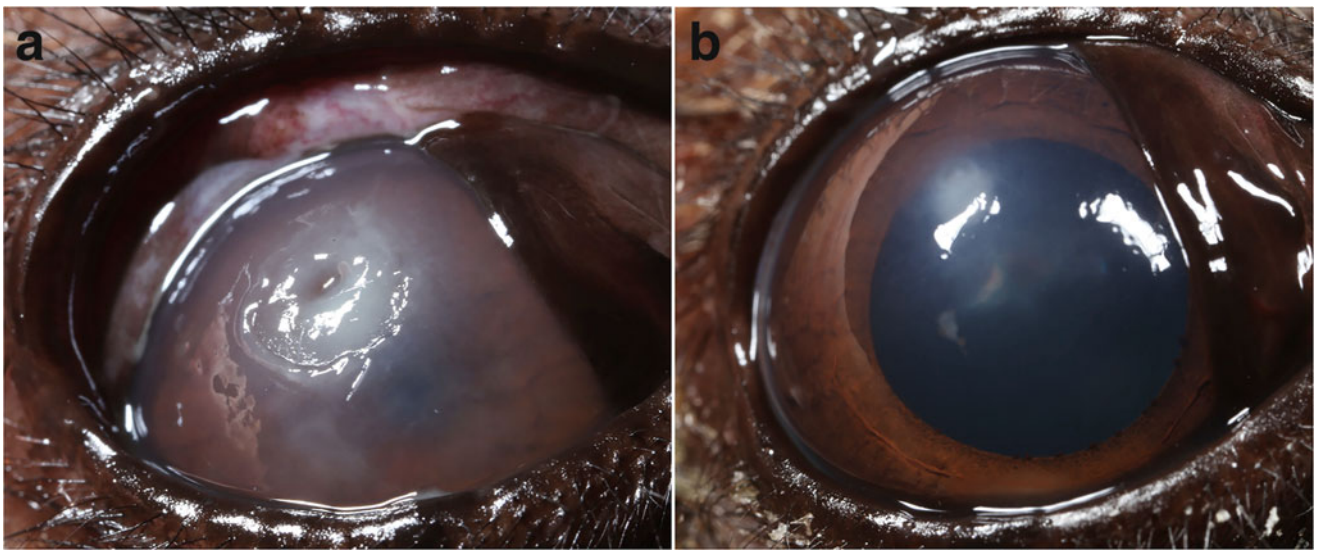

Fig. 40.9 The effects of aggressive and appropriate treatment of severe ulcerative keratitis in a Malayan flying fox (*Pteropus vampyrus*). (**a**) Note the deep (~85%) stromal ulcer with marked cellular infiltrate in the dorsolateral paraxial cornea at initial presentation. The bat was hospitalized and aggressive medical therapy consisting of q2 hour ofloxacin, tobramycin, serum (equine), and q12 atropine and oral meloxicam was initiated. (**b**) By day 3, the ulcer was nearly healed and only minimal cellular infiltrate remained. (Images courtesy of Bret A. Moore)

upon opening of the mouth. Possible causes are trauma, foreign body, tooth root abscess, sinus infection, and other undetermined causes. Orbital ultrasound or other diagnostic imaging modalities may be helpful in identifying retrobulbar abscesses. Dental examination, fine needle aspiration through oral mucosa behind the last molar, followed by microbiological culture and sensitivity testing may also help identify the etiology.

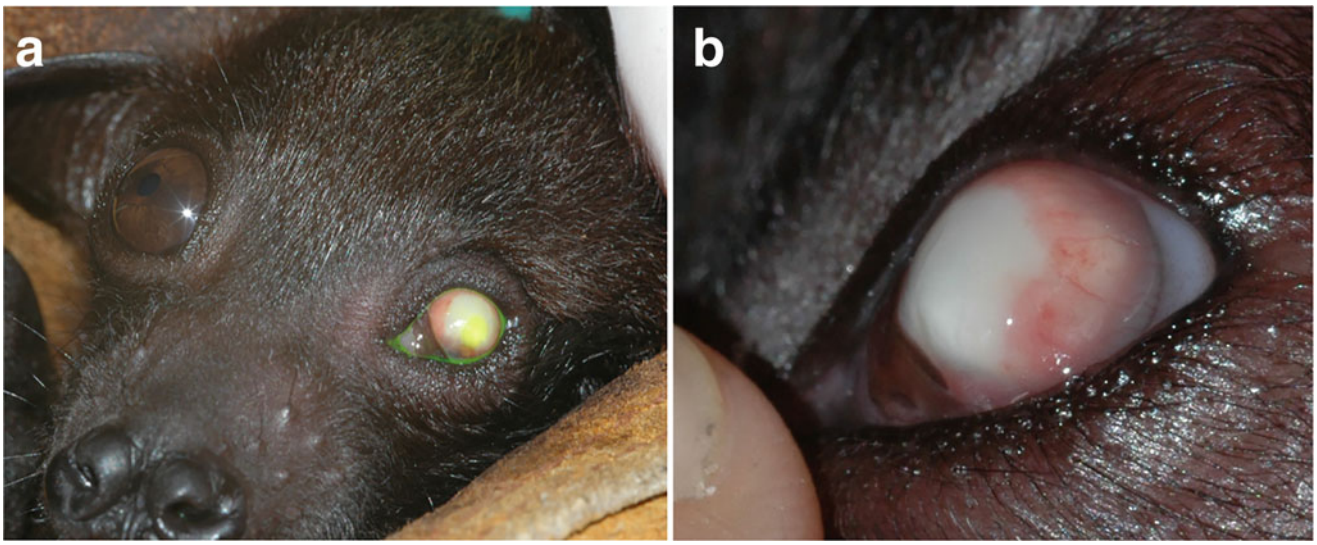

Fig. 40.10 A severe corneal abscess in a young Malayan flying fox (*Pteropus vampyrus*). (**a**) Note the relatively small area of fluorescein uptake (yellow) indicating ulceration. The volume of the affected globe was smaller than the right eye, most likely due to early phthisis bulbi. (**b**) Note the robust corneal vascularization with nearly complete abscessation of the entire stroma

Fig. 40.11 A case of retrobulbar abscess resulting in an acute onset unilateral exophthalmos in the right eye of an adult little golden-mantled flying fox (*Pteropus pumilus*). (**a**) Note marked swelling of the third eyelid as well as conjunctival hyperemia and chemosis. The inability to completely close the eyelids (lagophthalmos) resulted in exposure keratitis and corneal ulceration (detected by positive fluorescein staining). (**b**) Pain was apparent upon opening the mouth. The retrobulbar abscess was identified ultrasonographically and drained by making a small incision in the oral mucosa behind the last molar (black arrow), followed by blunt dissection through the pterygoid muscle into the orbit. This procedure was followed by systemic antibiotics (amoxicillin + clavulanic acid) administration and topical tobramycin, which caused the resolution of the problem

The authors have observed cataracts in a significant number of captive individuals of various species, most without an underlying etiology. Although a few were aged individuals, most were middle-aged, making a senile change less likely. The development of cataract secondary to chronic uveitis was highly suspected in a few individuals, and in some cases, chronic lens-induced uveitis was evident following cataract development. Chronic uveitis led to zonular degeneration

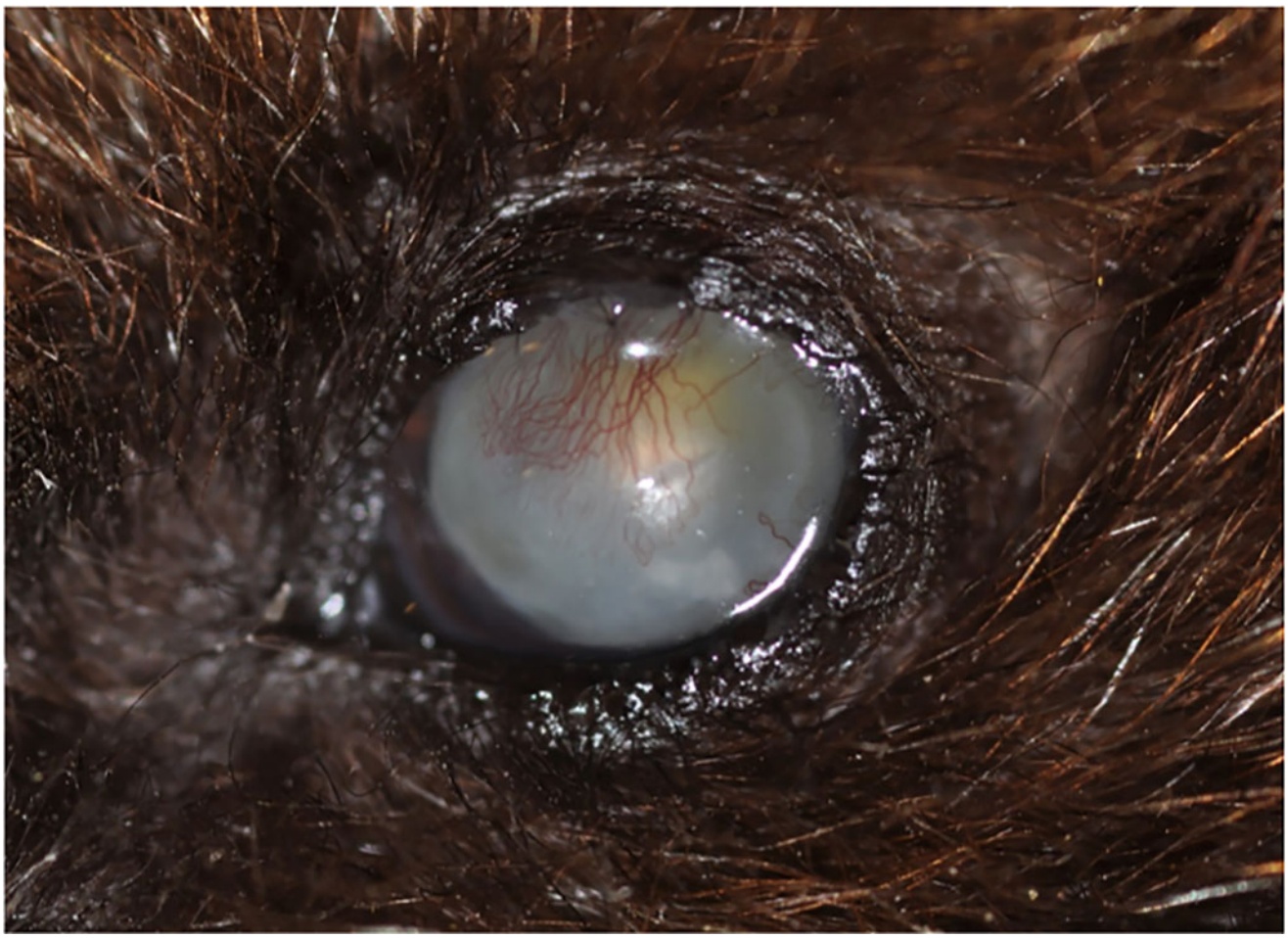

Fig. 40.12 Anterior luxation of a cataractous lens with secondary keratitis and glaucoma in an adult Malayan flying fox, or large flying fox (*P. vampyrus*). Corneal neovascularization and edema were evident due to direct endothelial damage secondary to the lens luxation and dysfunction secondary to elevated intraocular pressure

with anterior lens luxation and secondary glaucoma in one individual (Fig. 40.12). A report of cataracts in a group of Indian flying foxes (*Pteropus giganteus*) found that exposure to fluorescent light predisposed the bats to developing cataracts (DiGeronimo et al. 2018). This was not likely to be causative in our cases. Glaucoma has been observed in several bats, both Yinpterochiroptera and Yangochiroptera, and was deemed to be secondary in all instances due to evidence of antecedent injury or ocular disease. Medical therapy with topical anti-inflammatory medications and anti-glaucoma medications (carbonic anhydrase inhibitors and prostaglandin analogs), when feasible, has been successful in managing the majority of cases in the short term, although persistence and progression of disease may require more aggressive intervention with surgery. One individual experiencing anterior lens luxation did well in the short term following intracapular lens extraction, although some uveitis persisted. This individual became lost (being unreachable) at the point of follow-up.

Another clinical case report described exposure keratitis secondary to glaucoma and buphthalmos in an 11-year-old, 30 g fruit bat (*Cynopterus brachyotis*) (Greenberg et al. 2011). Treatment with frequent topical medications was not feasible due to unacceptable stress for the animal, and enucleation was not pursued initially due to concern of death by exsanguination. Therefore, chemical ciliary body ablation was elected using a combination of dexamethasone sodium phosphate (1 mg/kg) and gentamicin sulfate (3 mg/kg) injected into the vitreous chamber. It is worth mentioning that bat's lenses are large (Fig. 40.3). Thus, the vitreous injection procedure could be somewhat challenging. The authors' goal of the procedure was to reduce the eyeball size so that the animal could blink appropriately. However, the procedure did not reduce intraocular pressure and keratitis persisted, so enucleation was eventually performed.

References

Au WWL (1993) The sonar of dolphins. Springer, New York

Bell GP, Fenton MB (1986) Visual acuity, sensitivity and binocularity in a gleaning insectivorous bat, *Macrotus californicus* (Chiroptera: Phyllostomidae). Anim Behav 34:409–414

Blackwood SE, Plummer CE, Crumley W et al (2010 Sep) Ocular parameters in a captive colony of fruit bats. Vet Ophthalmol 13 (Suppl):72–79

Brock AP, Cortes-Hinojosa G, Plummer CE et al (2013) A novel gammaherpesvirus in a large flying fox (*Pteropus vampyrus*) with blepharitis. J Vet Diagn Invest 25:433–437

Brudenall DK, Schwab IR, Lloyd W et al (2007) Optimized architecture for nutrition in the avascular retina of Megachiroptera. Anat Histol Embryol 36:382–388

Centers for Disease Control and Prevention (2019) Bats lead in U.-S. rabies risk. https://www.cdc.gov/media/releases/2019/p0611-bats-rabies.html. Accessed 15 Oct 2019

Centers for Disease Control and Prevention (2020) Coronavirus (COVID-19). https://www.cdc.gov/coronavirus/2019-nCoV/index.html. Accessed 22 Apr 2020

Chase J (1982) The evolution of retinal vascularization in mammals, a comparison of vascular and avascular retinae. Ophthalmology 89: 1518–1525

Cullen CL (2003) Normal ocular features, conjunctival microflora and intraocular pressure in the Canadian beaver (*Castor canadensis*). Vet Ophthalmol 6:279–284

De Beer GR (1937) The development of the vertebrate skull. Clarendon Press, Oxford

DiGeronimo PM, Pisano SRR, Girolamo ND et al (2018) Selected ophthalmic parameters and potential risk for light-induced cataracts in two colonies of captive Indian flying foxes (*Pteropus* giganteus). J Zoo Wildl Med 49:129–133

Dorland W (1994) Dorland's: illustrated medical dictionary, 28th edn. W.B. Saunders Co. Process, Philadelphia, p 246

Fan Y, Zhao K, Shi Z-L, Zhou P (2019) Bat Coronaviruses in China. Viruses 11:210

Farajollahi A, Fonseca DM, Kramer LD et al (2011) "Bird biting" mosquitoes and human disease: a review of the role of Culex Pipiens complex mosquitoes in epidemiology. Infect Genet Evol 11:1577–1585

Fawcett E (1918) The primordial cranium of *Erinaceus europaeus*. J Anat Pt 2:211

Fenton MB (1984) Echolocation; implications for the ecology and evolution of bats. Q Rev Biol 59:33–53

Fenton MB (1995) Natural history and biosonar signals. In: Popper AN, Fay RR (eds) Hearing by bats. Springer, New York, pp 37–86

Fenton MB, Ratcliffe JM (2010) Quick guide: bats. Curr Biol 20:1060–1062

Fujun X, Kailiang H, Tengteng Z et al (2012) Behavioral evidence for cone-based ultraviolet vision in divergent bat species and implications for its evolution. Fortschr Zool 29:109–114

Fullard JH, Barclay RMR, Thomas DW (1993) Echolocation in free-flying Atiu swiftlets (*Aerodramus sawtelli*). Biotropica 25:334–339

Giannini NP, Wible JR, Simmons NB (2006) On the cranial osteology of Chiroptera. I. Pteropus (Megachiroptera: Pteropodidae). Bull Am Mus Nat Hist 295:1–134

Gonsalves L, Bicknell B, Law B et al (2013) Mosquito consumption by insectivorous bats: does size matter? PLoS One 8:e77183

Graham GL (1994) Introducing bats. In: In: Graham GL, Reid FA. (ed) Bats of the world – a golden guide. Western Publishing Company, Racine, pp 4–5

Greenberg SM, Barrie KP, Plummer CE et al (2011) Ciliary body ablation in a fruit bat (Cynopterus brachyotis). 42nd annual meeting of the American College of Veterinary Ophthalmologists, Hilton Head, SC, USA. Vet Ophthalmol 14:406–422

Griffin D (1953) Acoustic orientation in the oilbird, Steatornis. Proc Natl Acad Sci U S A 39:884–893

Hassi U (2018) Importance of bats (Order Chiroptera) in agricultural services. J Plant Sci Crop Protect 1:1–4

Holland RA, Thorup K, Vonhof MJ et al (2006) Bat orientation using Earth's magnetic field. Nature 444:702

Holland RA, Borissov I, Siemers BM (2010) A nocturnal mammal, the greater mouse-eared bat, calibrates a magnetic compass by the sun. Proc Natl Acad Sci U S A 107:6941–6945

Jones G, Jacobs DS, Kunz TH et al (2009) Carpe noctem: the importance of bats as bioindicators. Endangered Species Res 8(1–2);93: 115

Kim TJ, Jeon YK, Lee JY (2008) The photoreceptor populations in the retina of the greater horseshoe bat *Rhinolophus ferrumequinum*. Mol Cells 26:373–379

Kirk EC, Kay RF (2004) The evolution of high visual acuity in the Anthropoidea. In: Ross CF, Kay RF (eds) Anthropoid origins: new visions. Kluwer Academic/Plenum Publishers, New York, pp 539–602

Koopman KF (1993) Order Chiroptera. In: Wilson DE, Reeder DM (eds) Mammal species of the world: a taxonomic and geographic reference, 2nd edn. Smithsonian Institution Press, Washington, DC, pp 137–241

Kunz TH, Chase J (1983) Osteological and ocular anomalies in juvenile big brown bats (*Eptesicus fuscus*). Can J Zool 61:365–369

Kunz TH, Braun de Torrez E, Bauer D et al (2011) Ecosystem services provided by bats. Ann N Y Acad Sci 1223:1–38

Leigue Dos Santos L, Montiani-Ferreira F, Lima L et al (2014) Bacterial microbiota of the ocular surface of captive and free-ranging microbats: Desmodus rotundus, *Diameus youngi* and *Artibeus lituratus*. Vet Ophthalmol 17:157–161

Lima L, Montiani-Ferreira F, Tramontin M et al (2010) The chinchilla eye: morphologic observations, echobiometric findings and reference values for selected ophthalmic diagnostic tests. Vet Ophthalmol 13:14–25

Machado M, Schmidt EMS, Margarido TC (2007) A unique intraorbital osseous structure in the large fruit-eating bat (*Artibeus lituratus*). Vet Ophthalmol 10:100–105

Malkemper EP, Eder SHK, Begall S et al (2015) Magneto-reception in the wood mouse (*Apodemus sylvaticus*): influence of weak frequency-modulated radio frequency fields. Sci Rep 5:9917

Matthes E (1921) Das Primordialcranium von Halicore dugong. Z Anat:1–306

Möhres FP, Kulzer E (1956) Über die Orientierung der Flughund (Chiroptera Pteropodidae). Z Vergl Physiol 38:1–29

Mouritsen H (2012) Sensory biology: search for the compass needles. Nature 484:320–321

Müller B, Peichl L (2005) Retinal cone photoreceptors in microchiropteran bats. Invest Ophthalmol Vis Sci 46:2259

Müller B, Peichl L (2006) Cone photoreceptor diversity in the retinae of flying foxes (Megachiroptera). FENS Abstr 3:A072.014

Müller B, Goodman SM, Peichl L (2007a) Cone photoreceptor diversity in the retinas of fruit bats (megachiroptera). Brain Behav Evol 70: 90–104

Müller B, Peichl L, Winter Y et al (2007b) Cone photoreceptors and ultraviolet vision in the flower bat Glossophaga soricina (Microchiroptera, Phyllostomidae). Invest Ophthalmol Vis Sci 48: E-Abstract 5951

Müller B, Glösmann M, Peichl L et al (2009) Bat eyes have ultraviolet-sensitive cone photoreceptors. PLoS One 4:e6390

Neuweiler G (1983) Echolocation and adaptivity to ecological constraints. In: Huber F, Markle H (eds) Neuroethology and behavioural physiology. Springer, Berlin, pp 280–302

Nomina Anatomica Veterinaria (NAV) (1994) 4th edn. Zurich and New York: World Association of Veterinary Anatomists

Ollerton J, Winfree R, Tarrant S (2011) How many flowering plants are pollinated by animals? Oikos 120:321–326

Peracchi AL, Lima IP, Reis NR et al (2011) Ordem Chiroptera. In: Reis NR, Peracchi AL, Pedro AW, Lima IP (eds) Mamíferos do Brasil, 2nd edn. Londrina, pp 155–234

Pfaller K, Zirm M, Lalouette P et al (1984) Entzundliche Augenveranderungen bei der Maus durch das Herpes-Virus. Veranderungen durch den zytopathogenen Effekt. Ein Tiermodell. Klin Monbl Augenheilkd 184:549–552

Pieracci EG, Pearson CM, Wallace RM et al (2019) Vital signs: trends in human rabies deaths and exposures – United States, 1938–2018. MMWR Morb Mortal Wkly Rep 68:524–528

Prince JH (1956) Comparative anatomy of the eye. Charles C Thomas, Springfield

Reis NR, Shibatta OA, Peracchi AL et al (2007) Sobre os morcegos brasileiros. In: Reis NR, Peracchi AL, Pedro AW, Lima IP, do Brasil M (eds) , 1st edn. Londrina, pp 17–25

Reiskind MH, Wund MA (2009) Experimental assessment of the impacts of northern long-eared bats on ovipositing Culex (Diptera: Culicidae) mosquitoes. J Med Entomol 46:1037–1044

Rojas D, Warsi OM, Davalos LM (2016) Bats (Chiroptera: Noctilionoidea) challenge a recent origin of extant neotropical diversity. Syst Biol 65:432–448

Sánchez-Hernández C, Romero-Almaraz ML, Schnell GD et al (2016) Bats of Colima, Mexico (Animal Natural History Series). University of Oklahoma Press, Norman, OK, xvi + 321 pp

Sánchez-Hernández C, Zalapa SS, Guerrero S et al (2018) Ocular lesions and diseases in bats from Jalisco and Oaxaca, Mexico. Acta Chiropterologica 20:485–492

Schwab IR, Pettigrew J (2005) A choroidal sleight of hand. Br J Ophthalmol 89:1398

Shilton LA, Altringham JD, Compton SG et al (1999) Old world fruit bats can be long-distance seed dispersers through extended retention of viable seeds in the gut. Proc Biol Sci 266:219

Simmons NB (2005) Order Chiroptera. Mammal species of the world: a taxonomic and geographical reference. Smithsonian Institution Press, Washington, DC

Simões BF, Foley NM, Hughes GM et al (2019) As blind as a bat? Opsin phylogenetics illuminates the evolution of color vision in bats. Mol Biol Evol 36:54–68

Singh MP, Sharma A, Ratho RK (2007) Herpetic meibomianitis: an unusual case report. Southeast Asian J Trop Med Public Health 38: 466–468

Somma AT, Coimbra CM, Lange RR et al (2019) Reference values for selected ophthalmic diagnostic tests in two species of microchiroptera bats (*Artibeus lituratus* and *Anoura caudifer*). Vet Ophthalmol:1–6. https://doi.org/10.1111/vop.12690

Spallanzani L (1794) Lettere sopra il sospetto di un nuovo senso nei pipistrelli (Letters on the suspicion of a new sense in bats). Stamperia Reale (Royal Press), Torino (Turin), (Italy). [in Italian]

Starck D (1943) Beitrag zur Kenntnis der Morphologie und Entwicklungsgeschichte des Chiropterencraniums. Das Chondrocranium von Pteropus semindus. Anat Embryol 112:588–633

Subudhi S, Rapin N, Misra V (2019) Immune system modulation and viral persistence in bats: understanding viral spillover. Viruses 11(2): 192

Suthers RA (1970) A comment on the role of choroidal papillae in the fruit bat retina. Vision Res 10:921–923

Suthers RA, Hector DH (1985) The physiology of vocalization by the echolocating Oilbird, Steatornis caripensis. J Comp Physiol A 156: 243–266

Teeling E, Vernes S, Davalos LM et al (2018) Bat biology, genomes, and the Bat1K Project: to generate chromosome-level genomes for all living bat species. Annu Rev Anim Biosci 6:11–12.24

Wang L, Pan Q, Zhang QX et al (2008) Investigation of bacteria microorganisms in the conjunctival sac of clinically normal dogs and dogs with ulcerative keratitis in Beijing, China. Vet Ophthalmol 11:145–149

WHO Expert Consultation on Rabies, third report. Geneva: World Health Organization (2018) (WHO Technical Report Series, No. 1012). Licence: CC BY-NC-SA 3.0 IGO

Xie J, Li Y, Shen X et al (2018) Dampened STING-dependent interferon activation in bats. Cell Host Microbe 23(3):297–301.e4

Ophthalmology of Eulipotyphla: Moles, Shrews, Hedgehogs, and Relatives

41

Bradford J. Holmberg

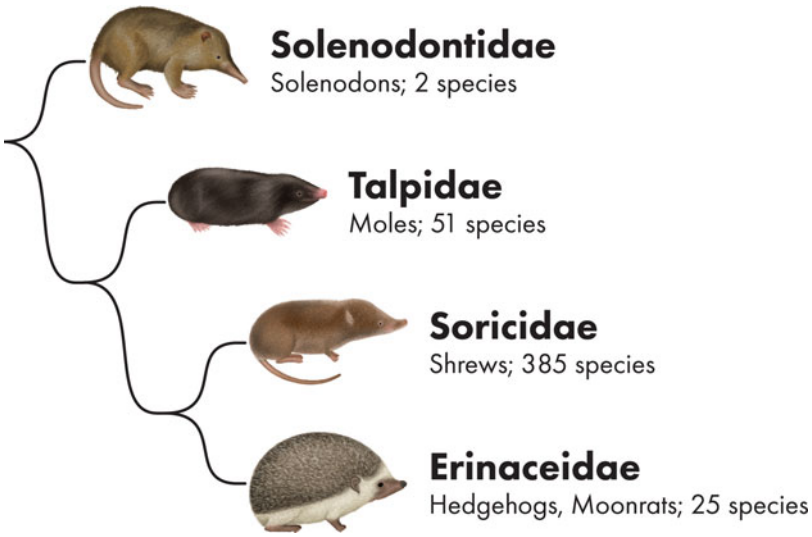

Introduction

Eulipotyphla is one of the newest orders of animals of the Mammalia class with some of the oldest and most primitive placental mammals. This order includes the families Solenodontidae, Talpidae, Soricidae, Erinaceidae, and the extinct Nesophontidae or West Indian shrews. These mammals were previously grouped in the now defunct order Insectivora (Bowdich 1821; Haeckel 1866), considered by taxonomists to be a "wastebasket" of primordial groups of placental mammals with uncertain relationships. The Macroscelididae, Tupaiidae, Chrysochloridae, and Tenrecidae families were also members of Insectivora. Gregory (1910) renamed Insectivora to Lipotyphla and removed the suborder Menotyphla (Macroscelididae and Tupaiidae). Lipotyphla remained a valid order until molecular studies revealed that the families Chrysochloridae (golden moles) and Tenrecidae (tenrecs) were not evolutionarily related to the other families. Chrysochloridae and Tenrecidae were moved to the order Afrotheria, and in 1999, Waddell et al. coined the name Eulipotyphla for the remaining families finally restoring monophyly. Understanding the diverse evolution of some of these placental mammals can be intellectually overwhelming and as the field of molecular phylogenetics expands many of the accepted taxon will continue to evolve.

Accounting for approximately 8–10% of all placental mammals and including more than 500 species worldwide, Eulipotyphla is a very pervasive order with species found on all continents except Antarctica (Woodman 2018). By definition, Eulipotyphla means "truly fat and blind." As this nomenclature suggests, most species have small eyes and poor vision. With minimal change over millions of years, these species provide a powerful model to study evolutionary adaption and the progression or regression of anatomic and

B. J. Holmberg (✉)
Animal Eye Center of New Jersey, Little Falls, NJ, USA

F. Montiani-Ferreira et al. (eds.), *Wild and Exotic Animal Ophthalmology*, https://doi.org/10.1007/978-3-030-81273-7_16

physiologic properties. The peer reviewed literature citing ophthalmic disease in this order of mammals is sparse to non-existent with the exception of some members of the Erinaceidae family.

Solenodontidae (Solenodons)

The order Solenodontidae encompasses four species including *Solenodon cubanus, Solenodon paradoxus, Solenodon arredondoi*, and *Solenodon marconi* with the last two species extinct (Nowak 1999). *S. cubanus* is native to Cuba, while *S. paradoxus* is native to Hispaniola (Haiti and Dominican Republic). Both species are endangered and considered functionally extinct due to accelerating habitat destruction as well as predation by dogs, cats, and mongooses (Turvey et al. 2008).

Meaning "slotted-tooth," solenodons are nocturnal, venomous, burrowing mammals. They are approximately 400–500 mm in total length and weigh up to 1 kg with *S. cubanus* the more diminutive of the two. The skull is long and slender with constriction between the orbits. The orbit is further narrowed due to expansion of the maxillary bone (Ottenwalder 2001). The zygomatic processes are blunted and the zygomatic arch is absent (Fig. 41.1a; Wible 2008, Derbridge et al. 2015). There are numerous long, large vibrissae lateral to the nostrils, with coarse hair on the sides of the snout with an additional 1–3 vibrissae located between the eye and mouth. These vibrissae are suspected to be tactile in nature (Derbridge et al. 2015). The eyes are small (Fig. 41.1b) and protected by hairless eyelids. There is no available literature describing normal ocular anatomy, physiology, or visual capabilities. One can infer visual capabilities based on behavioral observations. Solenodons move with zigzag, sideways, plantigrade motion moving the snout side to side searching for prey (Eisnberg and Gould 1966). When prey is detected, likely via olfaction and tactile cues from their vibrissae, they trap it between their forepaws and slide their head forward with an open mouth to engulf it. This behavior suggests visual acuity is poor. With a small globe they are also likely severely hyperopic. However, in captivity *S. paradoxus* is able to catch large prey such as mice (Eisnberg and Gould 1966), suggesting that vision may be more similar to Erinaceidae than Talpidae or Soricidae.

Talpidae

Many mammalian species have derived characteristics similar to moles due to convergent evolution and have subsequently been called moles. While marsupial moles (*Notoryctes sp.*), golden moles (Afrotheria), blind mole rats (Spalacidae), and mole rats (Bathyergidae) are commonly referred to as moles, they are evolutionarily unrelated. True moles are members of the Talpidae family consisting of 51 species. All species are fossorial with most living a completely subterranean existence. Exceptions include the Russian desman (*Desmana moschata*) that is almost entirely aquatic other than excavating a sleeping compartment, and the star-nosed mole (*Condylura cristata*) that is semiaquatic. They live throughout the Northern Hemisphere as well as southern Asia, but are absent in Ireland and South America. As burrowing animals, they have a relatively conserved body shape; cylindrical with short dense fur, strong laterally placed forelimbs with claws for digging, and numerous sensory vibrissae on their snout, head, and legs (Gruppe 2010).

Talpidae have evolved over millions of years to live in a subterranean environment without an abundance of light cues. This unique ecotope has promoted selective regression or altered development of several aspects of the eye. All basic eye structures are present and the majority of ocular genes are conserved. Therefore, it is important to distinguish this selective regression from degeneration. As the eye is a very metabolically active organ, this selective regression may play an advantageous evolutionary role allowing conservation of energy. Interestingly, injection of high concentrations of thyroxine in the neonatal European mole, *T. europaea*, will prevent this selective regression and stimulate normal ocular development (Tusques 1954).

The mole eye is one of the smallest of all mammals, measuring approximately 1 mm in diameter (Quilliam 1966). Depending on species, the eyelids may be closed and completely covered by a thin layer of skin (*T. occidentalis, T. stankovici, T. caeca, T. romana*) or they may be open (*T. europaea*) but lacking the ability to close (Figs. 41.2, 41.3; Carmona et al. 2010b). As a fossorial species, the lack of eyelid opening may be an adaptive function to protect against the dry soil these species inhabit. The European mole (*T. europaea*) inhabits a more humid climate with different soil properties possibly explaining this anatomic difference. *T. europaea* is also capable of extending the globe through the eyelids (Glösmann et al. 2008), although the physiologic mechanism for this process is not known.

The typical mammalian cornea contains a stratified epithelium with protective and sensory function, a hypocellular, avascular collagenous stroma, and an endothelium with both barrier and transport functions to regulate corneal hydration and maintain corneal transparency. The European mole (*T. europaea*) has this classic phenotype, while the Iberian mole (*T. occidentalis*) has a divergent phenotype (Fig. 41.4). The corneal epithelium of *T. europaea* is 2–3 layers thick with both basal and cuboidal cells with typical adhesions. It contains a superficial eosinophilic keratinized layer on the epithelial surface, possibly serving a protective function due to the lack of eyelid closure. The stroma is poorly organized

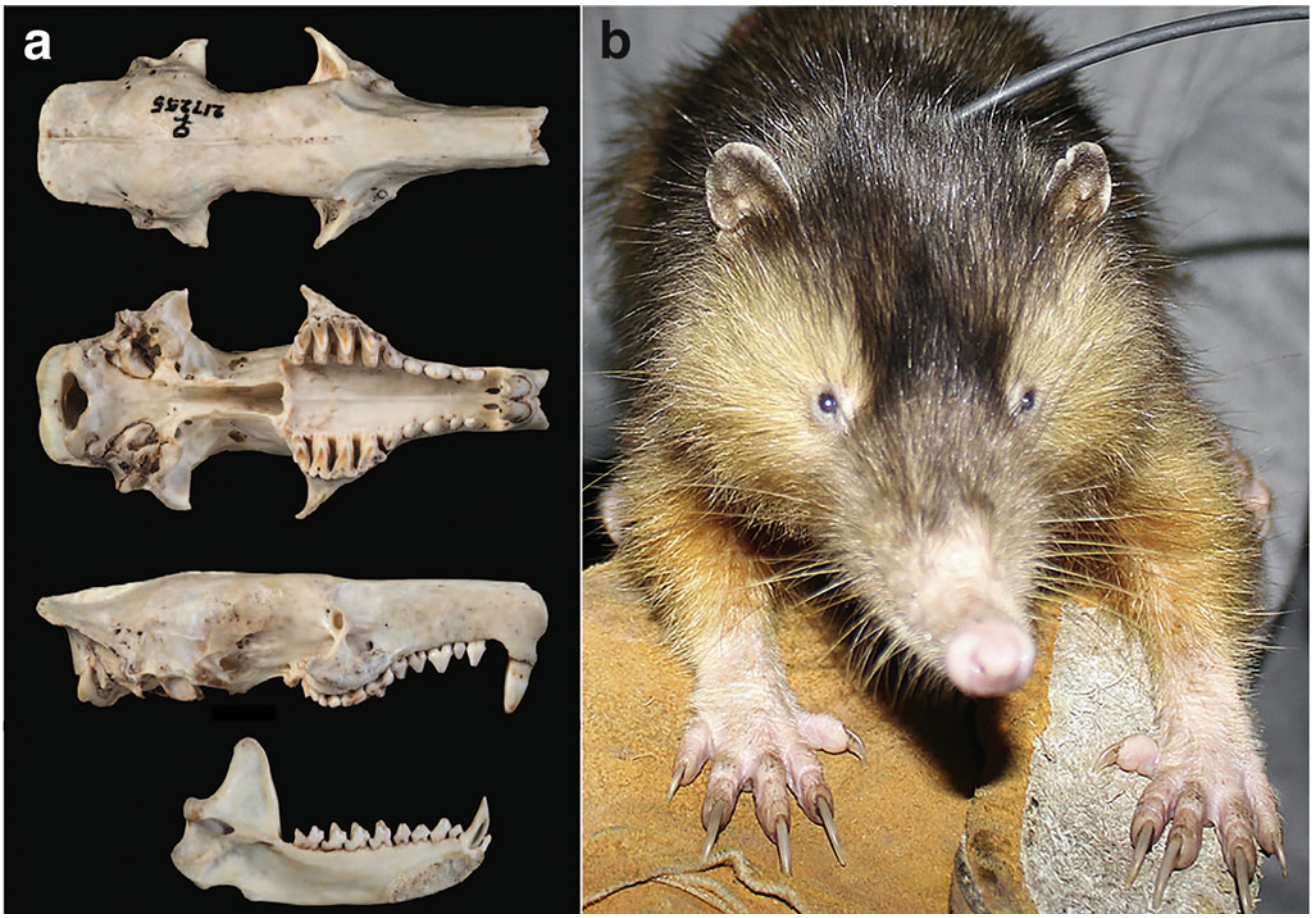

Fig. 41.1 (**a**) Dorsal, ventral, and lateral views of skull and lateral view of right mandible, respectively, of an adult female *Solenodon paradoxus*. Greatest length of skull is 86.6 mm (Used with permission from Derbridge et al. *Solenodon paradoxus* (Soricomorpha: Solenodontidae). Mammalian Species. 2015;47:100–106). (**b**) Hispaniolan solenodon (*S. paradoxus*). Note the small eye and numerous vibrissae along the snout (Used with permission from Kennerley et al. Home range and habitat data for Hispaniolan mammals challenge assumptions for conservation management. Global Ecology and Conservation 2019;18:1–10)

with more keratocytes compared to other rodents. Descemet's membrane and corneal endothelium are present (Carmona et al. 2010b). Iberian moles (*T. occidentalis*) have a more regressed corneal anatomy. The corneal epithelium is 1–2 layers thick and composed of flattened cells with prominent nuclei and typical cell–cell attachments. The stroma is well organized with standard collagen fibril structure and numerous keratocytes. However, the corneal endothelium and Descemet's membrane are absent (Carmona et al. 2010b). As the cornea is transparent, one must wonder how deturgescence is maintained without a functioning endothelium. This may be explained by the presence of significant corneal stromal vascularization in *T. occidentalis*, although all moles studied to date have corneal vascularization (Carmona et al. 2010b). To the author's knowledge, the Florida manatee (*Trichechus manatus latirostris*) is the only other mammal with a vascularized cornea (Harper et al. 2005). Corneal nerves are present, but disorganized and without the classic radial pattern of distribution seen in other mammals (Marfurt et al. 2001; He et al. 2010). Corneal curvature is regular in *T. occidentalis*, but is conical shaped in *T. europaea* (Figs. 41.3d, f and 41.4c; Carmona et al. 2010b) resembling that of the keratoconus phenotype in some humans. This corneal adaptation may aid in globe protraction or may be a result of this action.

The anterior segment of the mole eye is the most dysgenic of all ocular structures. The iris is pigmented with numerous protrusions from the anterior surface (Fig. 41.3c). There is no iris or ciliary body muscle present, resulting in a fixed pupil. The posterior iris adheres to the anterior lens capsule, replacing the lens zonules that are noticeably absent (Fig. 41.3d). The lens is approximately 0.5 mm in diameter, irregularly biconvex, semitransparent, and appears to float within the eye (Glösmann et al. 2008). It contains numerous disorganized, nucleated lens fibers (Fig. 41.3e) that continue to have some normal "ball and socket" connections (Carmona et al. 2008). With traditional lens development the lens vesicle detaches from the surface ectoderm,

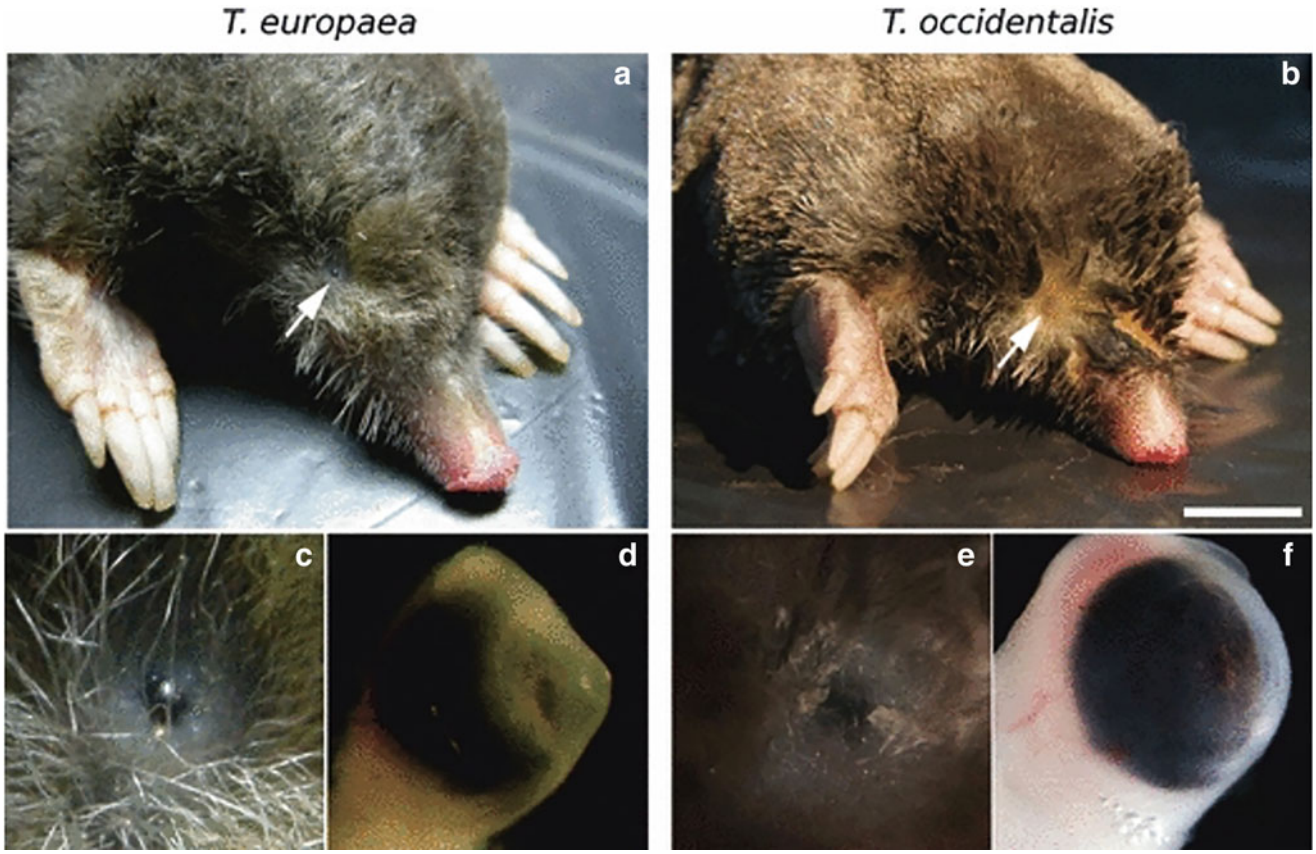

Fig. 41.2 External morphological features of the eye of *T. europaea* and *T. occidentalis*. Unlike *T. europaea*, which has open eyes (**a**), the Iberian mole shows permanently enclosed eyes under the skin (**b**). The minute eye of *T. europaea* (**c**) exhibits a cone-shaped cornea (**d**). In *T. occidentalis*, the skin enclosing the eye is relatively thin (**e**) and the cornea has the typical curved shape (**f**). *Scale bar* in (**b**) represents: (**a**, **b**) 10 mm, (**c**, **e**) 2 mm, and (**d**, **f**) 500 μm (Used with permission from Carmona et al. Development of the cornea of true moles (Talpidae): morphogenesis and expression of *PAX6* and cytokeratins. J Anat. 2010;217:488–500)

polarizes, and then cuboidal cells lining the vesicle elongate to form primary lens fibers. This process begins normally in moles, but is not completed. *PAX6* is an important gene involved in lens development. Its expression is normally maintained in proliferating cells of the anterior lens epithelium and down regulated in posterior lens fibers to allow terminal differentiation (Grindley et al. 1995). In moles, there is ectopic expression of *FOXE3*, a downstream effector of *PAX6*. This promotes posterior lens cell proliferation and anterior epithelial cell apoptosis, the opposite of normal development. This abnormal expression leads to a disorganized mass of immature and nuclear fiber cells with disrupted epithelium (Carmona et al. 2008). *PAX6* also regulates expression of crystallins that are required for light transparency, refraction, and maintenance of lens integrity (Cvekl and Piatigorsky 1996). Interestingly, even with abnormal expression of PAX6, α, ß, and γ-crystallin gene expression is present (Carmona et al. 2008), suggesting that the control of lens gene regulation in the mole is not conserved in this species.

In contrast to the lens, moles contain a well-conserved retina including all retinal cell types typically present in other placental mammals. In *T. europaea*, retinal cells are organized in a regular fashion. The photoreceptor layer contains 4–6 layers of uniform cells with several distinct features: receptors are relatively short along their radial axis, the inner and outer segments are of similar length, and the outer segments have signs of significant structural degeneration (Glösmann et al. 2008, Fig. 41.5). However, in *T. occidentalis* horizontal and amacrine cell organization is disrupted within the inner nuclear layer that may be induced by abnormal *FOXE3* expression in the lens (Carmona et al. 2010a). In both species, the retina is rod dominant with approximately 99,000–127,000 cells/mm^2. Cones number 10,300–17,750 cells/mm^2 and account for 9–15% of all photoreceptors (Glösmann et al. 2008). Nocturnal animals tend to possess 0.5–3% cones (Peichl 2005). The percentage of cones in moles is similar to that of some diurnal animals, suggesting that the mole eye is not adapted to low-light vision. Moles possess a rod opsin and two cone opsins. Cone opsins include a short wavelength sensitive cone (S cone) and a medium wavelength sensitive cone (M cone). Dual pigment cones are present with 30% of S

Fig. 41.3 Morphological characteristics of the eye of the Iberian mole. The eyes of the Iberian mole are largely hidden in the fur (**a**) and permanently closed due to the absence of eyelids (**b**). The cornea is transparent and the iris has numerous bulges (**c**). Hematoxylin and eosin staining of wax sections showed that the eye had the main structures and looked functional (**d**) but undeveloped due to the presence of nuclei in the disorganized lens fibers (**e**). The mole lens exhibited some transparency (**f**). Wild-type mouse eye (**g**) and lens (**h**) are shown as a model of normal mammalian eye phenotype. *Scale bar* represents 7 mm in A, 1.5 mm in B, 800 μm in C and D, 170 μm in E, 400 μm in F, and 2 mm in G and H (Used with permission from Carmona et al. The molecular basis of defective lens development in the Iberian mole. BMC Biol. 2008;6:44)

cones coexpressing M opsin. Genetic analysis of the S cone demonstrates the presence of phenylalanine residue at site 86 (Glösmann et al. 2008), implying that the functional S pigment is UV sensitive (Carvalho et al. 2007). This spectrum would be consistent with the UV transmittance of the mole lens. The S cones are present in a dorsoventral gradient, with higher densities in the ventral retina. This pattern appears to be conserved among Eulipotyphla (Peichl 2005). These cones in the inferior retina receive light from the upper visual field, a potential advantage for detecting breaches in the tunnel network or playing a role in anti-predatory behavior.

The mole has a holangiotic retina (Duke-Elder 1958) with a small, bright red optic disk (Lund and Lund 1965). The optic nerve has a diameter of 50 μm, consisting of axons from 2000 to 3000 ganglion cells of which 15% are myelinated (Quilliam 1966; Glösmann et al. 2008). There is incomplete decussation at the optic chiasm with vestigial retinocentral

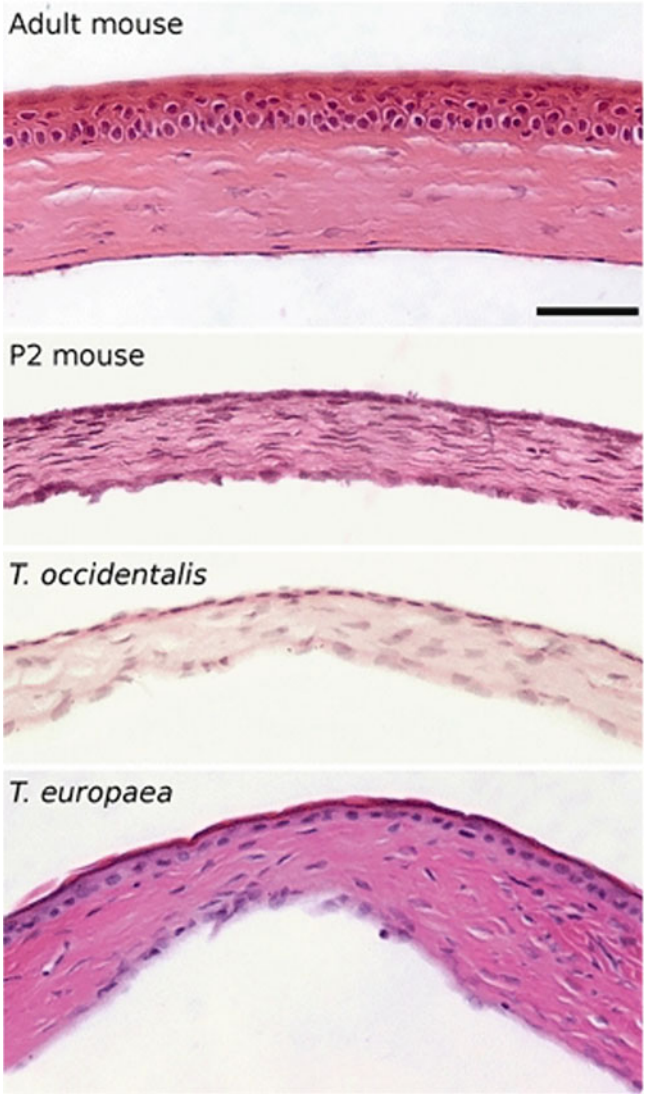

Fig. 41.4 Hematoxylin and eosin staining on corneal wax sections. (Adult mouse) Normal healthy adult mouse cornea with a multilayered epithelium (composed of six to seven cell layers), a stroma of connective tissue, and a monolayer endothelium. (P2 mouse) Developing cornea from a 2-day post-partum infant mouse with an underdeveloped monolayered epithelium. (*Talpa occidentalis*) The adult Iberian mole cornea is very similar to that of P2 mice. (*Talpa europaea*) The cornea of the European mole shows an intermediate status. The stroma is thicker and a two-to-three-layer epithelium with cuboidal basal cells is observed. However, the corneal surface is bulged, there is a considerable thinning in the central area, and a keratinized eosinophilic outermost layer is observed. *Scale bar*: 50 μm in all images (Used with permission from Carmona et al. Development of the cornea of true moles (Talpidae): morphogenesis and expression of *PAX6* and cytokeratins. J Anat. 2010;217:488–500)

projections. Sparse projections to the superior colliculus, lateral geniculate nucleus, nucleus of the accessory optic tract, pretectum, and visual cortex persist. The presence of two cone opsins along with intact retinocentral projections suggests photopic vision is present. Behavioral studies in *T. europaea* revealed withdrawal responses to high intensity light and successful performance of light/dark discrimination tasks (Lund and Lund 1965; Johannesson-Gross 1988). Whatever degree of light or hue discrimination that may be discernable, overall functional vision is likely very poor to absent. While other projections are diminished, projections arising from melanopsin containing retinal ganglion cells to the suprachiasmatic nucleus (SCN) of the hypothalamus remain normally developed. Approximately one percent of mouse retinal ganglion cells express melanopsin (Hattar et al. 2002) while a significantly higher proportion of cells express melanopsin in *T. occidentalis* (Carmona et al. 2010a). These SCN projecting retinal ganglion cells are intrinsically sensitive to light, independent of synaptic input from rod and cone photoreceptors. They maintain an essential role in circadian photoentrainment (Brown and Robinson 2004). Photoperiodicity is important for moles, as they are seasonal breeders with a cycle length that varies with latitude (Jiménez et al. 1990). Therefore, this increase in melanopsin containing retinal ganglion cells may be an adaptive trait.

There is no peer reviewed literature describing acquired ophthalmic disease in Talpidae.

Soricidae

Soricidae comprise over 85% of all animals in Eulipotyphla with 26 genera and 385 species separated into three subfamilies including Crocidurinae (white-toothed shrews), Soricinae (red-toothed shrews), and Myosoricinae (African shrews). They inhabit all major land masses except Australia, Tasmania, New Zealand, Antartica, Greenland, Iceland, the Arctic Islands, Ungava, West Indies, and some pacific islands. Most species favor moist, terrestrial environments where there is an abundance of vegetation cover and a wealth of invertebrate prey. Similar to the Hispaniolan solenodon (*Solenodon paradoxus*), the American short-tailed shrew (*Blarina brevicauda*), Mediterranean shrew (*Neomys anomalous*), and European water shrew (*Neomys fodiens*) are venomous (Kita et al. 2004). Most shrews are terrestrial, but approximately 11% are semifossorial, 6% are scansorial, and 4% are semiaquatic. They tend to be crepuscular, but some species are polyphasic or nocturnal. Shrews are some of the smallest placental mammals, with the Etruscan shrew (*Suncus etruscus*) weighing only 2 grams with a body length of 35 mm. With such a small body, it is of no surprise that the eye is also quite small, measuring 1.2 mm in diameter in the European common shrew (*Sorex araneus*). In some species, such as the greater white-toothed shrew (*Crocidura russula*) and African dark forest shrew (*Crocidura poensis*) the globe is egg-shaped with a longer anterior-posterior diameter than width; 1.4 mm × 1.35 mm for *C. russula* and 1.65 mm × 1.5 mm for *C. poensis* (Peichl et al. 2000).

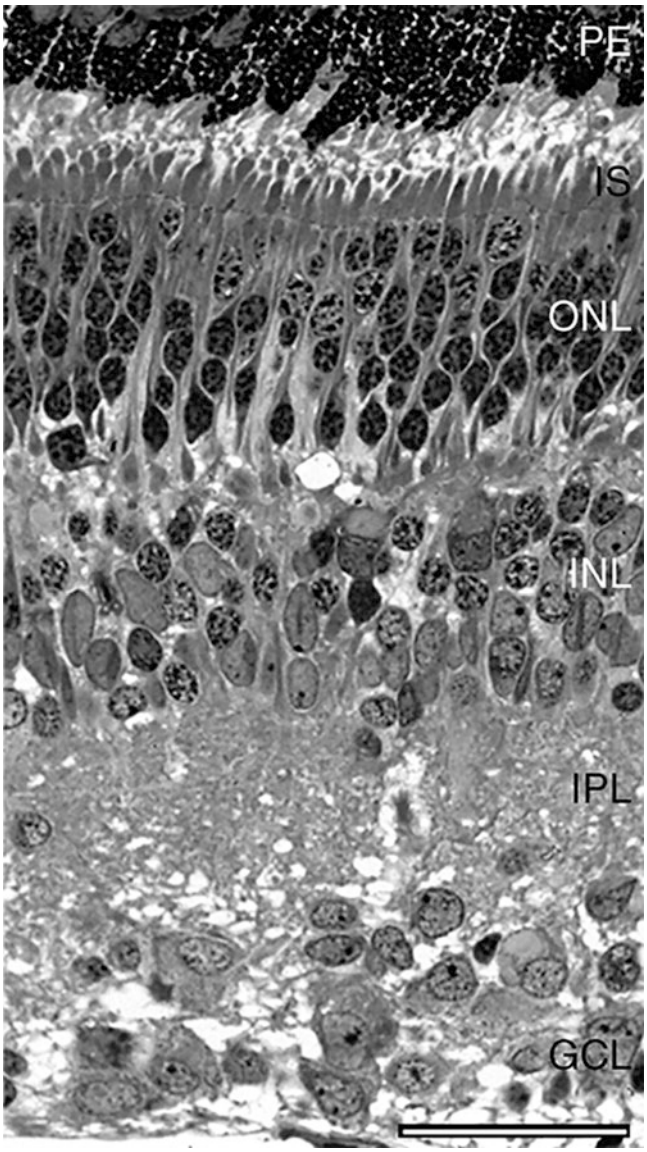

Fig. 41.5 Retina of *Talpa europaea*. Toluidine-blue-stained semi-thin section. *PE* pigment epithelium, *IS* photoreceptor inner segments, *ONL* outer nuclear layer, *INL* inner nuclear layer, *IPL* inner plexiform layer, *GCL* ganglion cell layer. *Scale bar*: 30 μm (Used with permission from Glösmann et al. Cone photoreceptors and potential UV vision in a subterranean insectivore, the European Mole. Journal of Vision 2008;8:23)

Shrews have long pointed snouts with numerous vibrissae covering the muzzle and top of head, with mystacial vibrissae on the sides of the snout and submental vibrissae below the jaw to aid in spatial orientation. The trigeminal nerve ganglia and central nuclei are well developed in shrews suggesting that tactile sensation received by these specialized hairs is considerable (Leitch et al. 2014). The small eye is laterally positioned in a long, narrow skull (Fig. 41.6). The orbit is open with an absent zygomatic arch similar to solenodons. The small eye may be visible in terrestrial species such as *Sorex araneus*, may be largely obscured by fur in semifossorial species such as *Cryptotis mexicanus*, or may be covered by skin in semiaquatic species such as *Nectogale elegans* (Churchfield 1990). Shrewlets are born blind and hairless with the eyes opening in some species around day 14 of life.

The structure of the cornea is conserved in Soricidae with all examined species containing five layers including the epithelium, Bowman's layer, stroma, Descemet's membrane, and endothelium. The corneal epithelium contains 3–4 layers of long, thin, nucleated cells linked by a network of adhesion junctions, especially desmosomes. Covering the epithelium is a thick multilaminar birefringent structure, consisting of several layers of dead epithelial cells. This layer was thickest in adults, thinner in juveniles, and absent in neonates (Lluch et al. 2009), suggesting that the oldest epithelial cells are not shed but retained. The purpose of this structure may be protective, although unlikely as it is absent in the cornea of other fossorial mammals, except the mole, *Talpa europaea*, that has an eosinophilic keratinized layer on the corneal surface (Carmona et al. 2010a). Similar to the mole, the structure in shrews contains a high level of protein, with that protein being keratin (Branis and Burda 1994). The keratin layer may function to thicken the cornea and increase its refractive power, thereby improving the optical properties of the eye. The corneal stroma is thin without any regular arrangement of the collagen fibrils. Descemet's membrane and the endothelium have the typical mammalian configuration (Lluch et al. 2009).

The shrew lens is biconvex with the anterior surface more curved than the posterior (Lluch et al. 2009). It measured 0.75 mm × 0.35 mm (diameter × anterior-posterior length) in *Sorex araneus*, 0.9 mm × 0.5 mm in *Crocidura poensis*, and 0.8 mm by 0.6 mm in *Crocidura russula* (Peichl et al. 2000). This lens structure minimizes spherical aberration.

Soricidae have a holangiotic retinal vascular pattern and a conserved retinal structure with no evidence of regression as seen in blind mole rats (*Spalax spp*). The retinal pigmented epithelium contains a significant number of melanin granules, with a similar expression to humans (Lluch et al. 2009). These granules likely absorb light and reduce scatter. The retina is rod dominant, but contains both rod and cone photoreceptors. Immunostaining for cone opsins revealed the presence of medium to long wavelength cones (M/L cones) as well as short wavelength cones (S cones) with a higher concentration of M/L cones compared to S cones (Peichl et al. 2000). Dual pigment cones are not present in Soricidae. The ratio of rods:cones varies among shrew species, with *Sorex araneus* having 13% cones consistent with its polyphasic lifestyle. Similar to moles (Peichl 2005), the distribution of S cones in shrews follows a dorsoventral gradient with the highest concentration of S cones in the ventral retina. The location of these S cones may allow

Fig. 41.6 The small eye of a Lesser white-toothed shrew *Crocidura suaveolens*. Used with permission from Mabeline72, Shutterstock.com

maximal contrast discrimination when viewing against skylight that is rich in shortwave components, termed the "skylight hypothesis" (Peichl et al. 2000). The ellipsoid of the cone inner segment in *Sorex araneus* contains a unique change in its mitochondria. The mitochondria are unusually large with an electron-dense matrix and a complex cristae pattern, termed megamitochondria (Lluch et al. 2002). Based on their structure, these megamitochondria collect divergent rays of light and refract them directly to the cone outer segment, acting as microlenses to enhance outer segment photon capture (Lluch et al. 2002). Other than *S. araneus*, megamitochondria have only been identified in zebrafish (Kim et al. 2005), tree shrews *Tupaia glis* and *Tupaia belangeri* (Knabe and Kuhn 1996), and New world flycatchers of *Empidonax spp* (Tyrrell et al. 2019). Retinal ganglion cells have not been evaluated in Soricidae but the optic nerve is small with approximate 1500 nerve fibers (Leitch et al. 2014).

Soricidae vision is poor, despite having a well-developed retina. The eye is likely hyperopic due to its small size preventing sharp image formation on the retina. However, the increased refractive power of the cornea due to the thick, keratin layer on the corneal epithelium, the reduction of spherical aberration by the lens, and the presence of megamitochondria may improve vision at short distances. Behavioral studies indicate that the main function of vision is to differentiate light from dark and to aid in photoentrainment of circadian rhythms (Churchfield 1990; Branis 1979). There is no response to flash photography or to high intensity beams of light (Branis and Burda 1994). This suggests that olfaction, tactile stimulation from the vibrissae, and auditory cues are likely more important than vision in prey identification, navigation, and social interactions.

Without functional vision, Soricidae may utilize echolocation to create an acoustic image for habitat assessment and foraging. Shrews are extremely vocal, producing approximately 12 different types of sounds including clicks, shrieks, chirps, and twitters ranging from the audible to ultrasonic frequency range (Gould et al. 1964; Churchfield 1990; Sanchez et al. 2019). The masked shrew (*Sorex cinereus*), wandering shrew (*Sorex vagrans*), American water shrew (*Sorex palustris*), and American short-tailed shrew (*Blarina brevicauda*) emit high frequency pulses around 30–60 Hz for 5–30 ms when exposed to novel environments. Behavioral studies revealed that *B. brevicauda* was able to determine the difference between an open and closed tube, simulating burrow openings, from a distance of 61 cm (Tomasi 1979). *S. vagrans* detected a target with a 4 × 4 cm hole from a distance of 30 cm (Buchler 1976). However, compared to echolocation in bats, the abilities in shrews are likely much more primitive and should be termed echo-based orientation (Sanchez et al. 2019).

Congenital or acquired ophthalmic disease has not been reported in the literature for any members of the Soricidae family.

Erinaceidae

Erinaceidae are the oldest living placental mammals based on fossil records extending back to the early Paleocene (66–-55 million years ago) of North America (Novacek 1986). The two subfamilies include Galericinae and Erinaceinae. The Galericinae subfamily is referred to as Hylomyinae by some researchers due to debate about whether the genera *Neohylomys* and *Neotetracus* are monophyletic based on mitochondrial DNA evaluation (He et al. 2012). Galericinae consist of 5 genera and 8 species and commonly called gymnures, hairy hedgehogs, or moonrats. While related to hedgehogs, their appearance is similar to a large shrew with a long snout and numerous vibrissae used for tactile sensation. In contrast to hedgehogs, they lack spines. They are carnivorous and have an acute sense of smell. Some are crepuscular while others strictly nocturnal. They inhabit moist jungle terrain in Southeast Asia. There is no available literature describing normal ocular anatomy, physiology, or visual capabilities of gymnures.

The subfamily Erinaceinae is composed of 5 genera and 17 species. The European hedgehog (*Erinaceus europaeus*) and the four-toed hedgehog (*Atelerix albiventris*) are the two most common species. In the United States, *A. albiventris*, also called the African pygmy hedgehog, is a common pet. There are significant state by state regulations on the legality of owning one due to historical subclinical foot-and-mouth disease infection. In the wild, *Erinaceus spp.* inhabit western and central Europe, northwestern Russia, and parts of Asia while *Atelerix spp* are native to Africa. Hedgehogs are nocturnal and omnivorous. Overall, Erinaceidae have the largest eyes of all Eulipotyphla with *E. europaeus* having a globe diameter of 7.2 mm (Williams et al. 2017).

Hedgehogs have a shallow orbit with a complete zygomatic arch in contrast to gymnures who lack this structure but instead have zygomatic process extending from the parietal, maxilla, and frontal bones (Nowak 1999). The hedgehog eye clinically appears exophthalmic with 360-degree scleral show (Fig. 41.7). The eye can be retropulsed with structures posterior to the globe including a retrobulbar fat pad, third eyelid, and Harderian gland (Kuonen et al. 2002). A lacrimal gland ventral to the Harderian gland and an orbital venous sinus are present (Turner et al. 2017; Hamlen 1997). The palpebral fissure is wide and eyelids lack cilia. Hedgehogs are one of three mammalian species that contain cartilage in the tarsal plate, with bats and leopards being the others (Duke-Elder 1958). Schirmer tear test I was less than 1 mm/min in *E. europaeus* (Williams et al. 2017) and 1.7 ± 1.2 mm/min in *Hemiechinus auritus* (Ghaffari et al. 2012) (Appendix 3). The iris is dark brown and the pupil circular. Intraocular pressure via rebound tonometry was 12.6 ± 1.8 mmHg in *E. europaeus* (Williams et al. 2017) and 20.1 ± 4 mmHg via applanation tonometry in *Hemiechinus auritus* (Ghaffari et al. 2012) (Appendix 3). The retina is holangiotic with 4 straight vessels extending to the ora serrata from a bright red optic disk (Johnson 1900). Based on their nocturnal lifestyle, hedgehogs are suspected to have a rod-dominant retina, and possibly a pure rod retina (Duke-Elder 1958). However, according to Menner in 1929, the retina of *E. europaeus* is composed of 3.75% cones and 96.25% rods (Stephan et al. 1991). Williams et al. (2017) reported hedgehogs have a rod rich retina with 2% cones citing Peichl et al. (2000). However, the animal referred to was *Echinops telfairi* (lesser hedgehog tenrec) and although they have the appearance of a hedgehog, they are members of the family Tenrecidae and not Erinaceidae. The optic nerve of hedgehogs is approximately 5.6 times the size of the shrew and has numerous central projections. Contralateral projections to the superior colliculus, pretectal complex, pars dorsalis and ventralis of the lateral geniculate nucleus, and the accessory optic nuclei are present. Ipsilateral projections to these areas also exist but are sparse (Dinopoulos et al. 1987). Using evoked potentials, Kaas et al. (1970) determined that hedgehogs have two visual fields (V I and V II). These fields receive input from the lateral geniculate nucleus and half of this cortical area is devoted to representing the central 35° of the contralateral visual field (Kaas et al. 1970). In contrast, shrews have a small primary visual cortex (Catania et al. 1999). Based on these findings, hedgehogs likely have the best vision of all Eulipotyphla.

Ophthalmic diseases in hedgehogs are not uncommon and account for approximately 5% of all reported pathologies with dermatologic (66% of cases), gastrointestinal (33%), neoplastic (21%), and musculoskeletal (15%) conditions most common (Gardhouse and Eshar 2015). In African pygmy hedgehogs (*A. albiventris*), cataracts (Fig. 41.8a), corneal ulceration with perforation (Fig. 41.8b), and proptosis were the most commonly diagnosed abnormalities (Gardhouse and Eshar 2015; Wheler et al. 2001). Williams et al. (2017) diagnosed 29% of European hedgehogs (*E. europaeus*) with at least one ocular abnormality including cataracts (19%), adnexal injury (2.3%), anophthalmia with granulation tissue filling the orbit (2%), orbital abscess (1.3%), corneal edema with ulceration (1.3%), uveitis (1.3%), conjunctivitis (1.3%), blepharitis secondary to *Trichophyton mentagrophytes* (1.3%), and nonulcerative keratitis (1%). Trichiasis was a common finding in hedgehogs that appeared clinically normal otherwise. Occasionally, globe penetration can occur from their own spines. Cataracts were mostly nuclear and there was no significant association

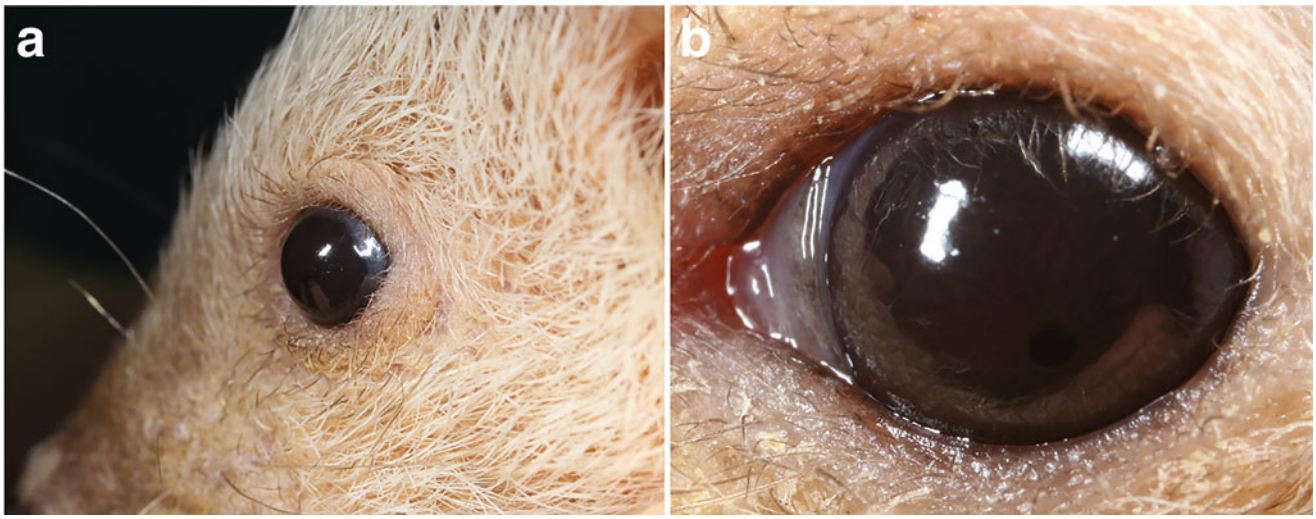

Fig. 41.7 Side (**a**) and close-up frontal view (**b**) of an African pygmy hedgehog (*A. albiventris*). Note the prominent eye, wide-open palpebral fissure, absence of eyelid cilia, and 360-degree scleral show. (Courtesy of Bret A. Moore)

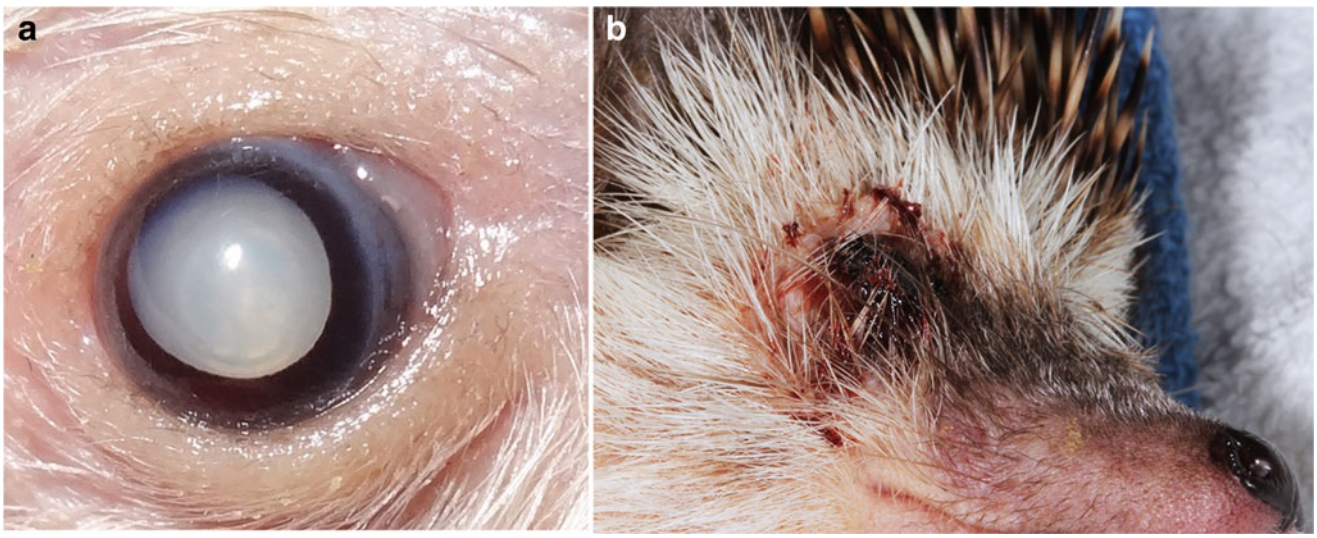

Fig. 41.8 (**a**) Complete cataract in the right eye of a hedgehog. (**b**) Corneal perforation of the right eye of an African pygmy hedgehog secondary to corneal desiccation following proptosis. (**a**—Courtesy Dr. Fabiano Montiani-Ferreira and Ana Carolina Rodarte. **b**—Courtesy Dr. Eric Ledbetter)

with age suggesting a genetic, nutritional, or other underlying etiology. Other reported ocular lesions include hyphema, vitreous hemorrhage, panophthalmitis, and meibomian cysts (Turner et al. 2017; Wheler et al. 2001).

Orbital disease is one of the most common reported conditions of captive hedgehogs. Proptosis is common due to the presence of a shallow orbit and macropalpebral fissure (Wheler et al. 2001). Captive hedgehogs tend to be obese and increased fat accumulation within the retrobulbar fat pad may predispose to proptosis. Orbital cellulitis (Wheler et al. 2001) and neoplasia are also predisposing factors for exophthalmos and proptosis. Neoplasia is quite common in hedgehogs with a reported prevalence of 32% (Hoefer 1994). While oral squamous cell carcinoma is most common (Gardhouse and Eshar 2015), orbital neoplasia has been reported including acinic cell carcinoma in an *A. albiventris* (Fukuzawa et al. 2004) and lacrimal ductal carcinoma in *E. europaeus* (Kuonen et al. 2002). Prognosis for vision or salvage of the globe following proptosis is poor, while overall prognosis with orbital neoplasia is likely grave.

References

Bowdich T (1821) An analysis of the natural classifications of Mammalia for the use of students and Travellers. J. Smith, Paris

Branis M (1979) Morphology of the eye of shrews (Soricidae, Insectivora). Acta Univ Carolinae-Biol:409–445

Branis M, Burda H (1994) Visual and hearing biology of shrews. Carnegie Mus Nat Hist 18:189–200
Brown R, Robinson P (2004) Melanopsin—shedding light on the elusive circadian photopigment. Chronobiol Int 21:189–204
Buchler E (1976) The use of echolocation by the wandering shrew (*Sorex vagrans*). Anim Behav 24:858–873
Carmona F, Jimenez R, Collinson J (2008) The molecular basis of defective lens development in the Iberian mole. BMC Biol 6:44
Carmona F, Glösmann M, Ou J et al (2010a) Retinal development and function in a 'blind' mole. Proc Biol Sci 277:1513–1522
Carmona F, Ou J, Jiménez R et al (2010b) Development of the cornea of true moles (Talpidae): morphogenesis and expression of *PAX6* and cytokeratins. J Anat 217:488–500
Carvalho L, Cowing J, Wilkie S et al (2007) The molecular evolution of avian ultraviolet and violet-sensitive visual pigments. Mol Biol Evol 24:1843–1852
Catania K, Lyon D, Mock O et al (1999) Cortical organization in shrews: evidence from five species. J Comp Neurol 410:55–72
Churchfield S (1990) The natural history of shrews. Comstock Publishing Associates, Ithaca, NY, p 1–21, 81–86111
Cvekl A, Piatigorsky J (1996) Lens development and crystallin gene expression: many roles for Pax-6. BioEssays 18:621–630
Derbridge J, Posthumus E, Chen H, et al (2015) *Solenodon paradoxus* (Soricomorpha: Solenodontidae). Mamm Species 47:100–106
Dinopoulos A, Karamanlidis A, Michaloudi H et al (1987) Retinal projections in the hedgehog (Erinaceus europaeus). An autoradiographic and horseradish peroxidase study. Anat Embryol 176:65–70
Duke-Elder S (1958) The eye in evolution, vol 1. Henry Kimpton, London, p 481,491
Eisnberg J, Gould E (1966) Behavior of *Solenodon paradoxus* in captivity with comments on behavior of other insectivore. Zoologica 51: 49–57
Fukuzawa R, Fukuzawa K, Abe H et al (2004) Acinic cell carcinoma in an African pygmy hedgehog (*Atelerix albiventrix*). Vet Clin Pathol 33:39–42
Gardhouse S, Eshar D (2015) Retrospective study of disease occurrence in captive African pygmy hedgehogs (*Atelerix albiventris*). Israel J Vet Med 70:32–36
Ghaffari M, Hajikhani R, Sahebjam F et al (2012) Intraocular pressure and Schirmer tear test results in clinically normal long-eared hedgehogs (*Hemiechinus auritus*): reference values. Vet Ophthalmol 15:206–209
Glösmann M, Steiner M, Peichl L et al (2008) Cone photoreceptors and potential UV vision in a subterranean insectivore, the European mole. J Vis 8:1–12
Gould E, Negus N, Novick. (1964) Evidence for echolocation in shrews. J Exp Zool 156:19–37
Gregory W (1910) The orders of mammalia. Bull Am Mus Nat Hist 27: 1–524
Grindley J, Davidson D, Hill R (1995) The role of Pax-6 in eye and nasal development. Development 121:1433–1442
Gruppe B (2010) Talpidae: Euroscaptor, Scapanus, Scalopus Aquaticus, Mogera, Neurotrichus Gibbsii, Talpa Europaea, Talpini, Urotrichini. Books LLC, Prasca
Haeckel E (1866) Generelle Morphologie der Organismen. Allgemeine Grundzüge der organischen Formen-Wissenschaft, mechanisch begründet durch die von Charles Darwin reformirte Descendenz-Theorie, vol 2. Georg Reimer, Berlin
Hamlen H (1997) Retro-orbital blood collection in the African hedgehog (*Atelerix albiventris*). Lab Anim 26:34–35
Harper J, Samuelson D, Reep R (2005) Corneal vascularization in the Florida manatee (*Trichechus manatus latirostris*) and three-dimensional reconstruction of vessels. Vet Ophthalmol 8:89–99
Hattar S, Liao H, Takao M et al (2002) Melanopsin-containing retinal ganglion cells: architecture, projections, and intrinsic photosensitivity. Science 295:1065–1070
He J, Bazan N, Bazan H (2010) Mapping the entire human corneal nerve architecture. Exp Eye Res 91:513–523
He K, Chen J, Gould G et al (2012) An estimation of erinaceidae phylogeny: a combined analysis approach. PLoS One 7:39304
Hoefer HL (1994) Hedgehogs. Vet Clin North Am Small Anim Pract 24(1):113–120
Jiménez R, Burgos M, Sánchez A et al (1990) The reproductive cycle of *Talpa occidentalis* in the southeastern Iberian Peninsula. Acta Theriol 35:165–169
Johannesson-Gross K (1988) Brightness discrimination of the mole (Talpa europaea) in learning experiments applying a modified tube-maze method. Zeitschrift für Säugetierkunde 53:193–201
Johnson G (1900) Contributions to the comparative anatomy of the mammalian eye, chiefly based on ophthalmoscopic examination. Philos Trans R Soc B 194:1–82
Kaas J, Hall W, Diamond I (1970) Cortical visual area I and II in the hedgehog: the relation between evoked potential maps and architectonic subdivisions. J Neurophysiol 33:273–306
Kennerley R, Nicoll M, Butler S et al (2019) Home range and habitat data for Hispaniolan mammals challenge assumptions for conservation management. Glob Ecol Conser 18:1–10
Kim J, Lee E, Chang B et al (2005) The presence of megamitochondria in the ellipsoid of photoreceptor inner segment of the zebrafish retina. Anat Histol Embryol 34:339–342
Kita M, Nakamura Y, Okumura Y et al (2004) Blarina toxin, a mammalian lethal venom from the short-tailed shrew *Blarina brevicauda*: isolation and characterization. Proc Natl Acad Sci U S A 10:7542–7547
Knabe W, Kuhn H (1996) Morphogenesis of megamitochondria in the retinal cone inner segments of *Typaia belangeri* (Scandentia). Cell Tissue Res 285:1–9
Kuonen V, Wilkie D, Morreale R et al (2002) Unilateral exophthalmia in a European hedgehog (*Erinaceus europaeus*) caused by a lacrimal ductal carcinoma. Vet Ophthalmol 5:161–165
Leitch D, Sarko D, Catania K (2014) Brain mass and cranial nerve size in shrews and moles. Sci Rep 4:6241
Lluch S, López-Fuster M, Ventura J (2002) Giant mitochondria in the retina cone inner segments of shrews of genus Sorex (Insectivora, Soricidae). Anat Rec 272:484–490
Lluch S, López-Fuster M, Ventura J (2009) Cornea, retina, and lens morphology in five Soricidae species (Soricomorpha: Mammalia). Anat Sci Int 84:312–322
Lund R, Lund J (1965) The visual system of the mole, *Talpa europaea*. Exp Neurol 13:302–316
Marfurt C, Murphy C, Florczak J (2001) Morphology and neurochemistry of canine corneal innervation. Invest Ophthalmol Vis Sci 42: 2242–2251
Novacek M (1986) The skull of leptictid insectivorans and the higher-level classification of eutherian mammals. Bull Am Mus Nat Hist 183:1–111
Nowak R (1999) Insectivores, in Walker's mammals of the world, vol 1, 6th edn. The Johns Hopkins University Press, Baltimore, pp 169–229
Ottenwalder J (2001) Systematics and biogeography of the west Indian genus Solenodon. In: Woods CA, Sergile FE (eds) Biogeography of the West Indies: patterns and perspectives. CRC Press, Boca Raton, FL, pp 253–329
Peichl L (2005) Diversity of mammalian photoreceptor properties: adaptations to habitat and lifestyle? Anat Rec A Discov Mol Cell Evol Biol 287:1001–1012
Peichl L, Künzle H, Vogel P (2000) Photoreceptor types and distributions in the retinae of insectivores. Vis Neurosci 17:937–948
Quilliam T (1966) The problem of vision in the ecology of *Talpa europaea*. Exp Eye Res 5:63–78

Sanchez L, Ohdachi S, Kawahara A et al (2019) Acoustic emissions of Sorex unguiculatus (Mammalia: Soricidae): assessing the echo-based orientation hypothesis. Ecol Evol 9:2629–2639

Stephan H, Baron G, Frahm H (1991) Insectivora. With a stereotaxic atlas of the hedgehog brain. In: Comparative brain research in mammals, vol 1. Springer, New York, pp 219–224

Tomasi T (1979) Echolocation by the short-tailed shrew *Blarina brevicauda*. J Mammal 60:751–759

Turner P, Brash M, Smith D (2017) Hedgehogs. In: Pathology of small mammal pets, 1st edn. Wiley Blackwell, pp 387–403

Turvey S, Meredith H, Scofield R (2008) Continued survival of Hispaniolan solenodon *paradoxus* in Haiti. Oryx 42:611–614

Tusques J (1954) Effect of thyroxin on the palpebral opening and on development of the ocular globe in Talpa europaea. C R Hebd Seances Acad Sci 238:2562–2564

Tyrrell L, Teixeira L, Dubielzig R et al (2019) A novel cellular structure in the retina of insectivorous birds. Sci Rep 9:15230

Waddell PJ, Okada N, Hasegawa M (1999) Towards resolving the interordinal relationships of placental mammals. Syst Biol 48:1–5

Wheler C, Grahn B, Pocknell A (2001) Unilateral proptosis and orbital cellulitis in eight African hedgehogs (*Atelerix albiventris*). J Zoo Wildl Med 32:236–241

Wible J (2008) On the cranial osteology of the Hispaniolan solenodon, *Solenodon paradoxus* Brandt, 1833 (Mammalia, Lipotyphla, Solenodontidae). Ann Carnegie Museum 77:321–402

Williams D, Adeyeye N, Visser E (2017) Ophthalmological abnormalities in wild European hedgehogs (*Erinaceus europaeus*): a survey of 300 animals. Open Vet J 7:261–267

Woodman N (2018) American recent Eulipotyphla: Nesophontids, Solenodons, moles, and shrews in the New World. In: Smithsonian contributions to zoology. Number 650. Smithsonian Institution Scholarly Press, Washington, DC, pp 1–5

Ophthalmology of Lagomorpha: Rabbits, Hares, and Pikas

42

Joshua Seth Eaton

© Chrisoula Skouritakis

Members of the order Lagomorpha comprise two families, the Leporidae (domestic and wild rabbits and hares) and the Ochotonidae (pikas). There are over 60 extant species of rabbits and hares. In the wild, rabbits and hares are herbivorous, non-hibernatory, and invariably terrestrial but are found in a diversity of natural habitats on multiple continents, ranging from the subtropics to open desert to boreal forests and arctic tundra (Nowak and Walker 1999) (Table 42.1). It is noteworthy, however, that many populations of Leporidae are not native, instead introduced to their respective regions or continents by humans (Nowak and Walker 1999). The European rabbit (*Oryctolagus cuniculus*), for example, is not native to Australia but was introduced to the continent in the nineteenth century and has become an invasive species, reported to have a negative impact on native ecosystems (Barrio et al. 2010; Fenner 2010). The Leporidae are preyed upon by many terrestrial and avian carnivorous species, and follow predominantly crepuscular and/or nocturnal activity patterns (Delaney et al. 2018). Despite similarities in habitat and activity, social structure differs between rabbits and hares, with rabbits tending to form colonies and hares being predominantly solitary animals (Flux and Angermann 1990). At birth, rabbit kits are blind and lack fur whereas leverets (baby hares) are born with a full fur-coat and are precocial (Delaney et al. 2018).

The Ochotonidae (pikas) comprise approximately 30 extant species. Pikas are predominantly diurnal and don't hibernate, instead creating "hay piles" of food in preparation for winter (Smith 2008). Unlike rabbits and hares, pikas predominantly inhabit mountainous climates with stepped or talus slope features, though some burrowing species also inhabit grasslands or meadows (Smith 2008). Today, pikas predominantly localize to mainland China and the western mountain ranges of North America. However, pikas comprise at least 1/3rd of the overall biodiversity of order Lagomorpha, globally (Smith 2008).

The general ecology and biology of the Lagomorpha have putatively influenced their ocular morphology and visual systems. Ocular morphology and diseases of the eye and orbit are particularly well-characterized in the domestic rabbit (*Oryctolagus cuniculi*) due to its worldwide popularity both as a pet and as a laboratory species. The chapter herein discusses pertinent ocular and orbital morphology and naturally-occurring diseases of the domestic rabbit eye with comparative perspectives relating to wild rabbits and hares and the pikas.

J. S. Eaton (✉)
Department of Surgical Sciences, School of Veterinary Medicine, University of Wisconsin, Madison, WI, USA
e-mail: jseaton2@wisc.edu

F. Montiani-Ferreira et al. (eds.), *Wild and Exotic Animal Ophthalmology*, https://doi.org/10.1007/978-3-030-81273-7_17

The Leporidae (Rabbits & Hares)

Like many species, the functional morphology of the eyes and orbits of rabbits and hares is intrinsically tied to their terrestrial habitats and largely to their susceptibility to predation by carnivores. Overall visual acuities reported for Leporidae are variable but generally considered low in comparison with other species (Van Hof 1967; Vaney 1980a). However, adaptations such as lateral eye position, a large cornea, and a merangiotic fundus and eccentric optic disk, among others, collectively enhance the Lagomorph's capacity to scan its environment to identify and respond to a threat. Furthermore, physiological variations such as a lower blink rate (~1 blink every 6 minutes (Toshida et al. 2007)), greater tear film stability (Leonard et al. 2016; Toshida et al. 2009), and greater potential for corneal endothelial regeneration in comparison with other species (Van Horn et al. 1977a) likely play important roles in how Leporidae protect themselves from predation and respond to ocular injury.

Numerous biometric and volumetric studies have been published to model the geometry of the rabbit eye, most commonly in laboratory strains like the New Zealand white (NZW) and Dutch belted. The most prominent biometric features of the rabbit eye include a relatively shallow anterior chamber and comparatively large axial lens diameter. Based on data collected from *in vivo* studies in adult rabbits, mean measurements for axial globe length, central corneal thickness, anterior chamber depth, axial lens diameter, and vitreous chamber depth are 16.83 mm, 0.40 mm, 2.08 mm, 6.77 mm, and 8.18 mm, respectively (Adel 2011; Bozkir et al. 1997; Langner et al. 2010; Reichard et al. 2010; Riau et al. 2012; Toni et al. 2010; Yüksel et al. 2015). The anterior chamber volume of the rabbit is approximately 0.2 ml, and the vitreous chamber volume ranges from 1.2–1.5 ml (Freddo et al. 1990; Yablonski et al. 1987; Gao et al. 2006). In European hares, similar *in vivo* biometric data from 20 adult animals from a single breeding farm demonstrated similar or slightly larger biometric dimensions with a mean axial globe length of 18.45 mm, central corneal thickness of 0.61 mm, anterior chamber depth of 2.66 mm, lens thickness of 7.18 mm, and vitreous chamber depth of 7.99 mm (Meomartino et al. 2018).

Leporid Anatomy & Physiology

The Skull and Orbit

The Leporid skull has a characteristically high arching profile (Fig. 42.1). The orbits are situated laterally on the skull, oriented approximately 85° from midline (Davis 1929) with about 150–175° between the two visual axes (Ringler and Newcomer 2014). While this conformation sacrifices binocular visual capacity to some degree (yielding <30° of horizontal binocular overlap), the lateral orientation of the globes provides rabbits and hares with very wide monocular fields and correspondingly, a nearly 360° binocular field (Hughes 1971a). The only true "blind spots" in the rabbit visual field lie just beneath and behind the head and are also associated with the optic disc (Hughes 1971a). However, changes in head, eye, and eyelid position can change not only the functional dimensions of the binocular field, but can also mitigate the obscuring of vision in these small blind zones (Hughes 1971a).

Despite having laterally situated eyes and a presumably reduced capacity for stereoscopic vision, studies have demonstrated that rabbits can solve discriminatory tasks that require binocular input (Choudhury 1980). Furthermore, despite previous convention claiming that changes in the Leporid visual field are restricted by minimal ocular movement and primarily dependent on changes in head position, study demonstrating saccadic eye movements and the presence of coordinated eye- and head-movements suggests that rabbits, in fact, may possess and utilize similar ocular movements to those of primates (Collewijn 1977).

The Leporid orbit is open and circular, and its situation within the skull places the globe in close proximity to the nasal passages and maxillary tooth roots medially and ventrally (Fig. 42.1). The frontal bone forms the dorsal limit of the orbit via a supraorbital process that extends over the superior aspect of the globe. The supraorbital process possesses two projections, one anterior and one posterior (the postorbital process), that contribute to the creation of foramina for the conduction of nerves and vessels (Davis 1929). In comparison with the rabbit, the postorbital process of the hare is broader and more triangular in shape (Nowak and Walker 1999). Inferior to the globe, the bony zygomatic arch is formed by the fusion of the zygomatic process of the maxillary bone anteriorly, the jugal bone centrally, and the zygomatic process of the squamosal bone caudally (Ringler and Newcomer 2014). A postorbital ligament spans the gap between the postorbital process and a frontal process that projects dorsally from the squamosal bone (Jašarević et al. 2010). The large (4 mm diameter) optic foramen is situated caudally and superiorly within the medial bony wall alisphenoid bone, just rostral to the squamosal bone (Fig. 42.1). Collectively, these osteological variations enhance the rabbit's nearly circumferential monocular visual fields but also leave the globe more susceptible to trauma; bony protection is only provided medially and rostrally, leaving the globe to extend ~5 mm anterior the zygomatic arch inferiorly, and ~12 mm anterior to the supraorbital process superiorly (Ringler and Newcomer 2014).

Table 42.1 Common Leporidae found in North, Central, and South America

Species	Common name	Geographic distribution	Habitat	Activity	Lifestyle
Sylvilagus aquaticus	Swamp rabbit	South central and Southeastern USA and Gulf Coast, Ohio River Valley	Lowland swamps and freshwater marshes	Crepuscular/ nocturnal	Herbivorous
Sylvilagus audubonii	Desert cottontail rabbit	Southwestern North America and Pacific coast	Arid regions, woodlands, grasslands, altitudes <6000 ft	Crepuscular/ nocturnal	Herbivorous
Sylvilagus bachmani	Brush rabbit	Western USA	Areas with dense brushy cover	Crepuscular/ nocturnal	Herbivorous
Sylvilagus brasiliensis	Forest cottontail	Central and South America	Moist forests and grasslands	Crepuscular/ nocturnal	Herbivorous
Sylvilagus floridanus	Eastern cottontail	Canada, Eastern and Central USA, Central American, Northwestern South America	Transitional habitats between woody vegetation and open land	Crepuscular/ nocturnal	Herbivorous, solitary
Sylvilagus palustris	Marsh rabbit	Southeastern USA	Lowland areas near freshwater marshes	Nocturnal	Herbivorous, solitary, semi-aquatic
Lepus americanus	Snowshoe hare	Canada and Northern USA	Open fields and coniferous lowlands, thickets, and cedar bogs	Crepuscular/ nocturnal	Herbivorous, solitary
Lepus arcticus	Arctic hare	Northern Greenland, Arctic islands, Canada	Mountainous tundras, rocky plateaus, and Arctic coasts	Mostly Nocturnal	Herbivorous, less carnivorous, mostly solitary
Lepus californicus	Black-tailed jackrabbit	Central and Southwestern USA, Mexico	Arid regions of desert, short-grass prairie, farmland, dunes	Nocturnal	Herbivorous
Lepus capensis	Cape hare	Non-forested Africa, Western and Central Asia	Open meadows, pastures, fields, marshes, arid desert	Nocturnal	Herbivorous
Lepus europaeus	Brown hare, European hare	Great Britain, Western Europe, Middle East, Central Asia, Canada, Northeastern USA	Open fields and pastures	Crepuscular/ nocturnal	Herbivorous, mostly solitary
Lepus townsendii	White-tailed jackrabbit	Western and Central Canada, USA	Open grasslands, pastures, less high Alpine tundra	Nocturnal	Herbivorous, solitary
Lepus alleni	Antelope jackrabbit	Western Coast of Mexico, Southern Arizona	Grasslands, desert	Crepuscular/ nocturnal	Herbivorous, solitary
Lepus othus	Alaskan hare	Northern and Western Alaska, Eastern Siberia	Rocky slopes or tundra	Crepuscular	Herbivorous, solitary
Brachylagus idahoensis	Pygmy rabbits	Western USA, North American Great Basin	Grasslands and prairies	Crepuscular/ nocturnal	Herbivorous, solitary

In comparison with other domestic mammals, Leporids have a similar complement of extraocular muscles including inferior, superior, lateral, and medial rectus muscles, superior and inferior oblique muscles, and the retractor bulbi muscle. Rabbits also possess a depressor palpebrae muscle, originating from the zygomatic arch, that inserts onto and retracts the inferior eyelid. (Ringler and Newcomer 2014).

Five distinct glands reside in the Leporid orbit: the zygomatic salivary gland, the lacrimal and infraorbital glands, and two glands associated with the third eyelid (nictitating membrane)—the Harderian (deep gland of the third eyelid), and superficial gland of the third eyelid (see section "The Adnexa"—sub section "Third Eyelid" for more details regarding the third eyelid glands). The large tubuloacinar lacrimal gland lies inferior to the globe and comprises two anatomically distinct portions, one upper and one lower; the aqueous secretions from each portion are delivered to the superior and inferior conjunctival fornix, respectively (Davis 1929; Ringler and Newcomer 2014). Other secondary lacrimal lobes have been described (Ringler and Newcomer 2014). Histologically, the lacrimal gland comprises ovoid-to-round acinar lumina, similar to those of the human lacrimal gland (Ringler and Newcomer 2014; Schechter et al. 2010). Its secretions are predominantly serous, but may also be mucinous (Ding et al. 2011). The infraorbital gland is smaller, resting just adjacent to the lower portion of the lacrimal gland. Its function is not as well understood. The zygomatic salivary gland occupies the anterior and inferior

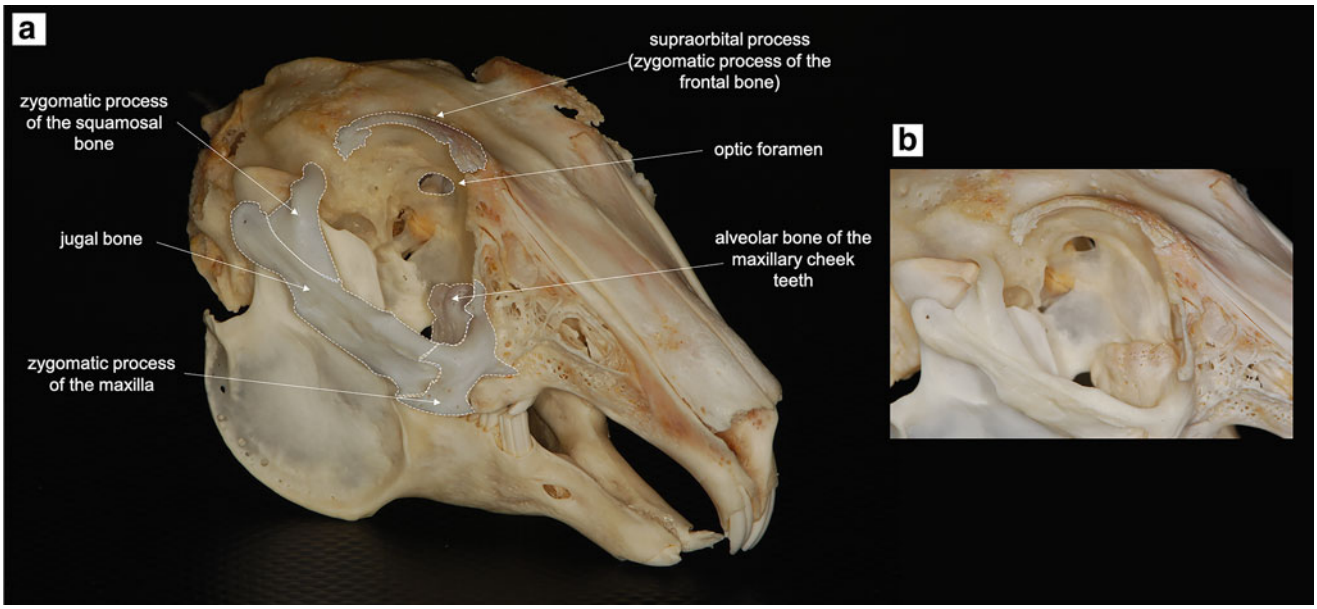

Fig. 42.1 Skull of the domestic rabbit (*Oryctolagus cuniculus*) (**a**) with magnified view showing detailed structures of the orbit (**b**)

aspect of the orbit, lying ventral to the lacrimal gland (Ringler and Newcomer 2014).

The globe and orbital tissues are principally supplied by the internal maxillary artery which enters the orbit via the anterior sphenoidal foramen. The external ophthalmic artery branches from the internal maxillary artery and anastomoses with the internal ophthalmic artery, a branch of the external carotid that enters the orbit via the optic foramen, supplying large orbital structures including the extraocular muscles and Harderian gland. This anastomosis also gives rise to the anterior and long and short ciliary arteries that supply the majority of the globe (Ringler and Newcomer 2014). One arterial circle is present in the iris, formed by 4 branches of the ciliary arteries (2 temporal and 2 nasal). Venous drainage is achieved via the vortex veins into an extensive posterior orbital venous sinus (Ringler and Newcomer 2014).

Of particular importance clinically and surgically (see section "Other Clinical Considerations in the Care and Treatment of Leporidae"), a robust vascular sinus lies in the ventral and medial aspect of the orbit near the base of the third eyelid. Due to its location, it is in close proximity to other soft tissue structures like the extraocular muscles and the Harderian gland. This sinus receives a large portion of the venous drainage from the eye and orbital soft tissues and can be easily damaged during surgeries to replace prolapsed orbital glands or to enucleate the globe. Hemorrhage associated with damage to this structure can be life-threatening, necessitating careful dissection and gentle tissue manipulation during any orbital surgery in any Leporid.

The Adnexa

Eyelids

In general, the features of the rabbit eyelid are grossly and histologically similar to other species. In rabbits, the palpebral fissure is approximately 10–16 mm in length and cilia are present on both the superior and inferior eyelids (Ringler and Newcomer 2014) (Fig. 42.2). Forty to fifty meibomian gland openings are present along the margins of each eyelid (Ringler and Newcomer 2014). Unlike most other species, however, rabbits only have a single nasolacrimal punctum, located inferiorly within the palpebral conjunctiva, approximately 3–4 mm from the eyelid margin (Davis 1929).

Third Eyelid

As in other mammalian species, the Leporid third eyelid is an anatomical reflection of the conjunctiva, contiguous with the palpebral and bulbar portions, and supported internally by a cartilaginous saucer-shaped "strut" (Davis 1929). Protrusion of the third eyelid is predominantly passive, enabled by globe withdrawal upon voluntary contraction of the retractor bulbi muscle. Movements of the third eyelid in the rabbit, however, are also aided by an extension or "slip" of muscle called the retractor palpebrae tertia. This accessory muscle is derived from the levator palpebrae superioris, inserting on the superior aspect of the third eyelid, and is innervated by the oculomotor nerve (cranial nerve III) (Davis 1929).

The thin, flat superficial gland of the third eyelid is associated with the cartilage, producing serous secretions that empty via small ducts onto the membrane's adjacent bulbar surface (Davis 1929). The larger Harderian gland is

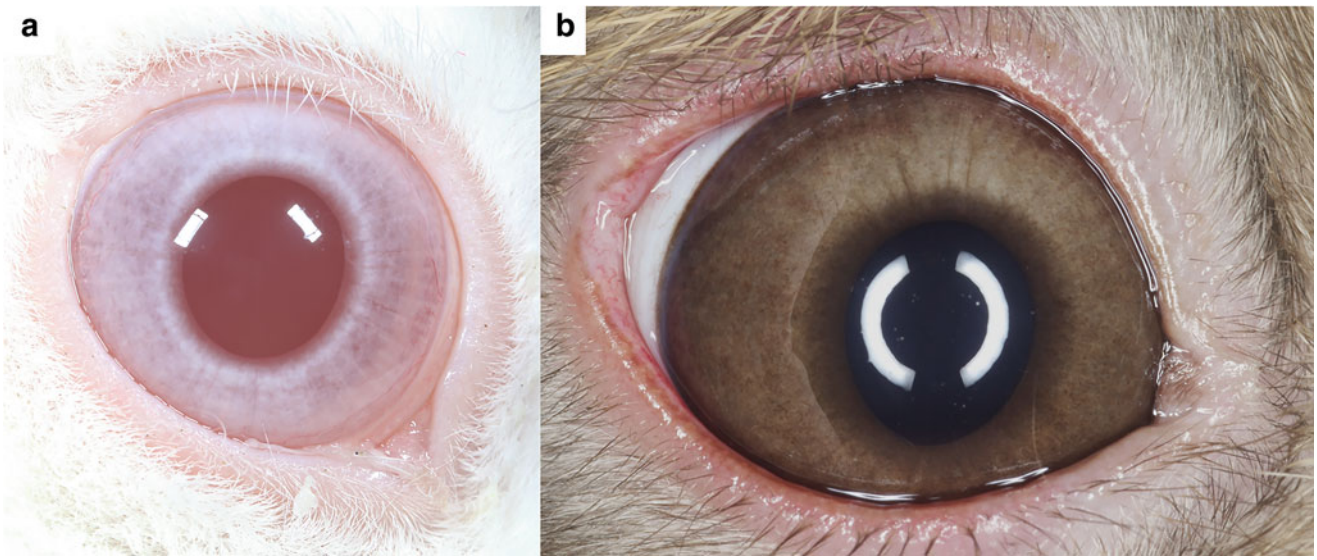

Fig. 42.2 External photographs showing the normal adnexa and anterior segment of the non-pigmented (**a**) and pigmented (**b**) domestic rabbit (*Oryctolagus cuniculus*)

also associated with the third eyelid but lies deeper within the ventral medial aspect of the orbit at the third eyelid's base (Sakai 1981). Due to its orbital location, the Harderian gland is also partially enveloped by the aforementioned orbital venous sinus. The Harderian gland is critical in the production of tear film lipids and is divided into two anatomically and histologically distinct upper and lower lobes (Ham et al. 2006; Seyama et al. 1992). The upper or "white" lobe comprises a predominantly columnar secretory epithelium with small intracellular lipid vacuoles, and the inferior or "pink" lobe bears a distinctly cuboidal epithelium and notably larger vacuoles (Björkman et al. 1960). It is also believed that this lower lobe produces a comparatively greater proportional of the tear film lipids (Payne 1994). There is some evidence in the rabbit that the Harderian gland produces porphyrins, though in comparatively lower amounts than in rodent species (Davidheiser and Figge 1958). Furthermore, both lobes appear to play a role in secretory immunoregulation (Ringler and Newcomer 2014). Clinically, the Harderian gland in rabbits can be distinguished on B-mode ultrasound as an ovoid to elongated structure with a coarse echotexture in the ventral retrobulbar space. In one study of 27 domestic rabbits, mean ultrasonographic dimensions of the gland measured 6.9 mm in diameter horizontally and 1.33 mm vertically (Hittmair et al. 2014a).

Nasolacrimal Duct System

The nasolacrimal duct system serves as a conduit between the ocular surface and the nasal cavity, preventing tear overflow by draining tears into the nasal passages. The morphology of the nasolacrimal drainage system in rabbits, however, is anatomically distinct from other mammals. The proximal opening to the system is a single, small lanceolate punctum within the palpebral conjunctiva of the medial inferior eyelid, approximately 3–4 mm internal to the eyelid margin (Davis 1929). In most other mammalian species, there are two puncta, one adjacent to the medial aspect of each eyelid margin. The duct courses through the lacrimal bone and into the maxilla via the lacrimal canal. Thereafter, the duct follows a remarkably tortuous anatomical route, characterized by abrupt changes in course, particularly adjacent to the roots of the maxillary cheek teeth and far rostrally near the incisors. The duct also abruptly narrows at numerous locations along its course, including at the foramen into the lacrimal bone and adjacent to the maxillary incisors (Burling et al. 1991; Marini et al. 1996). Collectively, these morphological features and the proximity of the duct to dental roots predispose the rabbit to obstructive disease and infections of the nasolacrimal duct system (see section "Diseases of the Nasolacrimal Drainage System").

The duct's epithelial lining is anatomically contiguous with the conjunctiva and ocular surface, and therefore microflora normally reside within the nasolacrimal drainage system. In one study of purpose-bred laboratory rabbits, the most common organisms isolated from the duct on irrigation were *Moraxella* spp., *Streptococcus viridans*, and *Neisseria* spp. In that same study, the nasolacrimal duct was a more consistent source for isolation of bacterial organisms than the conjunctiva (Marini et al. 1996).

The Ocular Surface and Anterior Segment

Tear Film

The tear film of the domestic rabbit is of unique interest in comparative ophthalmology and vision science. This is at

least partially due to the species' historical use as an animal model in the development of topical ocular therapeutics, including those that treat ocular surface diseases like dry eye (Schrader et al. 2008). A growing body of literature characterizing and investigating the rabbit ocular surface has demonstrated considerable differences that distinguish the rabbit tear film from that of other species. For example, the lipid layer is thicker in rabbits in comparison with humans and dogs, which may be at least partially attributed to the lack of a Harderian gland in the latter species (Korb et al. 1994; Korb et al. 1998). Furthermore, mucin expression patterns of corneal epithelial cells in rabbits are remarkably different from humans, non-human primates, and dogs, with rabbits expressing three mucins (MUC1, MUC4, and MUC16) at similar levels and the former species expressing primarily MUC16 (Leonard et al. 2016). Functionally, the abundance of these constituents yields a tear film that is more resistant to evaporation and likely represents an evolutionary advantage in this prey species. Correspondingly, rabbits are known to have a very infrequent blink rate, averaging 10–12 times per hour, and frequently lack a consistent menace response despite having intact vision, particularly in the clinical environment (Maini and Hartley 2019). This enhanced tear film stability can be observed when performing tear film break-up time (TBUT) evaluations to quantify tear film stability (Table 42.2). Values for TBUT using fluorescein-aided and non-fluorescein-aided methods in rabbits are reported as high as 50 seconds, nearly 3 times that of dogs, or even as long as 30 minutes in one study (Toshida et al. 2007; Wei et al. 2013), though systematic review has shown the latter to be an outlier in comparison with other published values (Doughty 2018).

Clinically, the aqueous tear film in rabbits can be measured objectively using methods similar to those used in other species including the Schirmer tear test (STT), phenol red thread test (PRTT), and endodontic paper point tear test (EPPTT). Normative values for these tests have been published and are summarized in Table 42.2 (also see Appendix).

Cornea, Sclera, and Conjunctiva

Rabbits have large corneas, occupying approximately 30% of the surface area of the external globe, with a diameter of 15 mm horizontally and 14 mm vertically (Andrew 2002). The central corneal thickness measures approximately 380–-400 microns with a non-keratinized epithelium measuring 30–40 microns, and a 7–8 micron thick Descemet's membrane subtending the single-layered corneal endothelium (Andrew 2001). Approximately 12–16 sensory nerve bundles enter the peripheral superficial corneal stroma at numerous sites around its circumference, branching centripetally within the anterior stroma and corneal epithelium (Rozsa and Beuerman 1982).

Endothelial cell density in juvenile rabbits is 4100 cells/mm (Barrio et al. 2010), decreasing with maturity. Reported endothelial cell densities in adult rabbits range from approximately 2000–3000 cells/mm (Barrio et al. 2010) (Doughty 1994; Sailstad and Peiffer Jr 1981). In most mammalian species, corneal endothelial cells possess limited capacity for regeneration, instead responding to physical damage by enlarging and/or migrating to re-establish cellular confluence. The rabbit corneal endothelium appears be an exception, with several studies demonstrating a comparatively robust capacity for endothelial cell mitosis. This capacity, however, is likely reduced in older rabbits (Van Horn et al. 1977a; Staatz and Van Horn 1980).

The sclera in domestic rabbits varies in thickness from anterior to posterior, measuring ~500 microns at the limbus, to 250 and 200 microns at the superior and inferior equator, respectively, to 180 microns at the posterior pole (Ringler and Newcomer 2014).

The conjunctiva comprises two anatomically contiguous portions, the palpebral and bulbar conjunctiva. The palpebral conjunctiva inserts on the eyelid margins and is 40 microns thick; the bulbar conjunctiva lines the external surface of the globe and is 10–30 microns thick (Ringler and Newcomer 2014). Numerous studies have described normal microbial flora of the conjunctival surface in domestic rabbits with varying results (Marini et al. 1996; Cooper et al. 2001; Okuda and Campbell 1974; Oriá et al. 2014; Pugliese et al. 2016; Bourguet et al. 2019). Across these studies, the most commonly isolated bacteria from normal rabbits were *Staphylococcus* spp., *Streptococcus* spp., and *Bacillus* spp. Other commonly isolated include *Pasteurella multocida*, *Corynebacterium* spp., and *Moraxella* spp. Fungal organisms such as *Aspergillus* spp., *Scopulariopsis* spp., and *Penicillium* spp. have also been cultured from the ocular surfaces of normal domestic rabbits (Bourguet et al. 2019).

Aqueous Humor, Anterior Uvea, and Iridocorneal Angle

The rabbit pupil forms a slight vertical oval at rest, and is circular when dilated. The rabbit iris is thin, measuring ~250 microns in thickness at its base and 90 microns at the pupil margin (Ringler and Newcomer 2014; Sheppard 1962). The ciliary musculature is diminutive, consistent with the rabbit's putatively poor accommodative capacity (~1.5 D) (Ringler and Newcomer 2014; Sheppard 1962). However, the ciliary processes are well-developed, arising from the anterior portion of the ciliary body, merging into the posterior surface of the iris, and extending to within 1 mm of the pupillary margin. Like other species with poor accommodative capacity, the processes are conjoined proximally by a ciliary web that conducts vascular connections between the processes while also providing structural support (Ringler and Newcomer 2014). Due to the putatively small contribution of the ciliary muscle to accommodation in rabbits, it has been proposed that accommodation can instead be achieved by changes in relative blood volume within the iris and ciliary processes to alter pupil diameter and lens

Table 42.2 Normative values for common clinical ocular diagnostic tests in the domestic rabbit

IOP—Applanation (mmHg)	IOP—Rebound (mmHg)	STT I (mm/min)	PRTT (mm/15 s)	Endodontic paper point tear test (mm/min)	Tear Break Up Time (s)	Reference
15.44	9.51					Pereira et al. (2011)
17.5–18.1						Sarchahi and Bozorgi (2012)
	18.37–19.69					Zhang et al. (2014)
		5.30				Abrams et al. (1990)
		4.85	20.88			Gürkan and Hayat (2005)
		7.58				Whittaker et al. (2015)
		8.00				Zhu et al. (2003)
		20.57 mm/3 min				Burgalassi et al. (1999)
12.89		7.27		12.43		Oriá et al. (2014)
				15.24		Oriá et al. (2014)
		5.2		13.8		Lima et al. (2015)
		5.4[a]	25[a]	18.8[a]		Rajaei et al. (2016)
		4.6[b]	23.6[b]	16.9[b]		Rajaei et al. (2016)
					1788	Wei et al. (2013)
					50	Toshida et al. (2007)
					21.8[c]	Doughty (2018)
					32.7[d]	Doughty (2018)

[a]Angora rabbits
[b]Dutch rabbits
[c]Systematic review of fluorescein-based methods
[d]Systematic review of non-fluorescein-based methods
IOP intraocular pressure, *STT* Schirmer tear test, *PRTT* phenol red thread test

position (Ringler and Newcomer 2014). The ciliary body and iris receive blood supply via the long ciliary artery, short posterior ciliary artery, and to some degree the ciliary artery (Ringler and Newcomer 2014).

The iridocorneal angle and aqueous outflow pathways bear similar functional morphology to other mammalian species with a circumferential network of trabecular meshwork at the anterior chamber periphery, deep to the limbus (Ruskell 1961). However, there is no distinct analog to the human Schlemm's canal within the distal aqueous outflow pathway. Instead, an intrascleral venous plexus is present that conducts aqueous humor into the ciliary venous system and orbital venous sinus (Fig. 42.3) (Ruskell 1961). This represents the conventional aqueous outflow pathway and comprises the major route of aqueous humor egress in the rabbit eye. Comparatively, unconventional outflow via the iris base contributes to only 3–8% of outflow (Johnson et al. 2017; Vézina 2012). Mean normal intraocular pressure (IOP) in the domestic rabbit ranges between 15–20 mmHg (Table 42.2, Appendix) (Ringler and Newcomer 2014), with diurnal fluctuations that yield lowest IOP at night and peak IOP levels during the day (Bar-Ilan 1984). Normal aqueous humor flow rate in domestic rabbits is 2.7 microliters/minute (Vézina 2012).

Lens

The rabbit lens comprises an external capsule, internal cortex, and nucleus as described in other mammalian species. The axial anterior-posterior lens diameter ranges from 6–8 mm (Adel 2011; Langner et al. 2010). Rabbits have a vertical lens suture anteriorly, and a horizontal suture posteriorly and the nucleus is often poorly-defined and indistinguishable from the cortex (Ringler and Newcomer 2014). Scientifically and clinically, a prominent physiological feature of the rabbit lens is the intrinsic capacity for lens epithelial cells to propagate and regenerate lens cortex following surgical removal. This has been evident not only in experimental models, but also reported clinically in pet rabbits undergoing routine cataract surgery (Gwon 2006; Gwon et al. 1993; Gwon et al. 1990; Gwon et al. 1992). (see section "Diseases of the Lens").

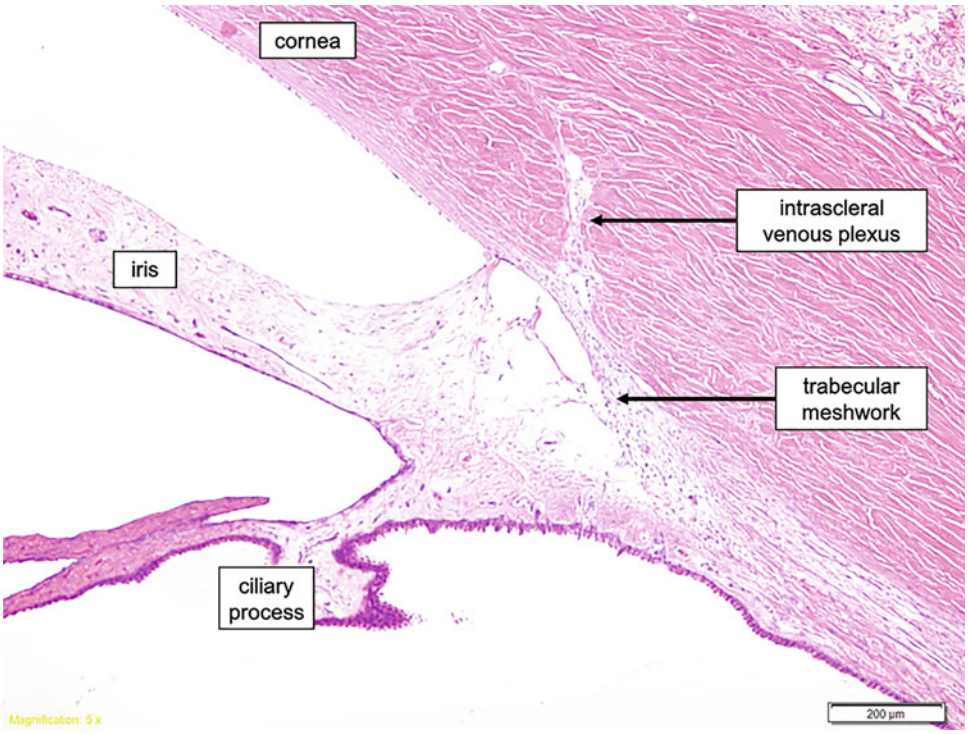

Fig. 42.3 Photomicrograph of the normal iridocorneal angle in a domestic rabbit. Image courtesy of the Comparative Ocular Pathology Laboratory of Wisconsin

The Posterior Segment

Vitreous

The rabbit vitreous comprises the majority of the globe volume. It consists of a rheologically gelatinous body consisting mostly of water, as well as hyaluronic acid and sparse cells (hyalocytes), both of which are concentrated primarily within 30 microns of the external vitreous surface (Ringler and Newcomer 2014; Vézina 2012). Structurally, the rabbit vitreous can be divided into distinct regions that include an external cortex, a well-defined and less gelatinous (more liquid) center, and an intermediate zone in between (Davis 1929; Ringler and Newcomer 2014). The rabbit also has a distinct canal of Cloquet, the central vitreous channel conducting the hyaloid vessel system during pre- and postnatal ocular development. In some juvenile and adult rabbit eyes, remnants of this vascular system may be observed (Los et al. 2000). In addition, a novel lamellar vitreous structure called the alae canalis Cloqueti has been described in domestic rabbits, radiating from the posterior lens to the medullary rays (Los and Nieuwenhuis 1999). The vitreous is not a static structure, as approximately 50% of its water content is replaced every 10–15 minutes in domestic rabbits (Ringler and Newcomer 2014).

Posterior Uvea (Choroid)

The Leporid choroid lacks a tapetum lucidum in all species. The choroid is thickest posteriorly and adjacent to the optic disk, and thinnest at the ora ciliaris retinae anteriorly (Ringler and Newcomer 2014). The choroid is also thicker inferiorly, and thicker and more heavily pigmented in the area of the visual streak just above the posterior pole and on either side of and below the optic disk (Davis 1929; Ringler and Newcomer 2014).

Retina and Optic Nerve

In the domestic rabbit, the retina is not completely differentiated until approximately 6 weeks after birth (Ringler and Newcomer 2014). The Leporid retina is grossly and histologically distinguished from other species by a unique merangiotic vascular arrangement in which the retinal arterioles and venules are confined to linear cascades that radiate in narrow projections immediately medial and lateral to the optic disk in parallel with myelinated nerve fibers (Stone and Dreher 1987) (Figs. 42.4 and 42.5). The remainder of the retina is avascular. Leporids also have a large, horizontally-ovoid optic disk (~1.5 mm diameter), normally visible as a deeply cupped white to white-pink structure within the superior and central fundus (Fig. 42.4). Clinically, the disk's morphology can complicate differentiation between normal appearance and pathology such as optic disk cupping associated with glaucoma (Fig. 42.6). The orbital portion of the optic nerve departs the globe at a very acute angle, bending ventrally before passing through the optic foramen (Ringler and Newcomer 2014).

A macula or area centralis is not present. However, rabbits do have a visual streak where ganglion cell density is highest, measuring about 3–4 mm in width, oriented parallel to and ~3 mm inferior to the optic disk and medullary rays (Stone and Dreher 1987). In the rabbit, overall retinal thickness is

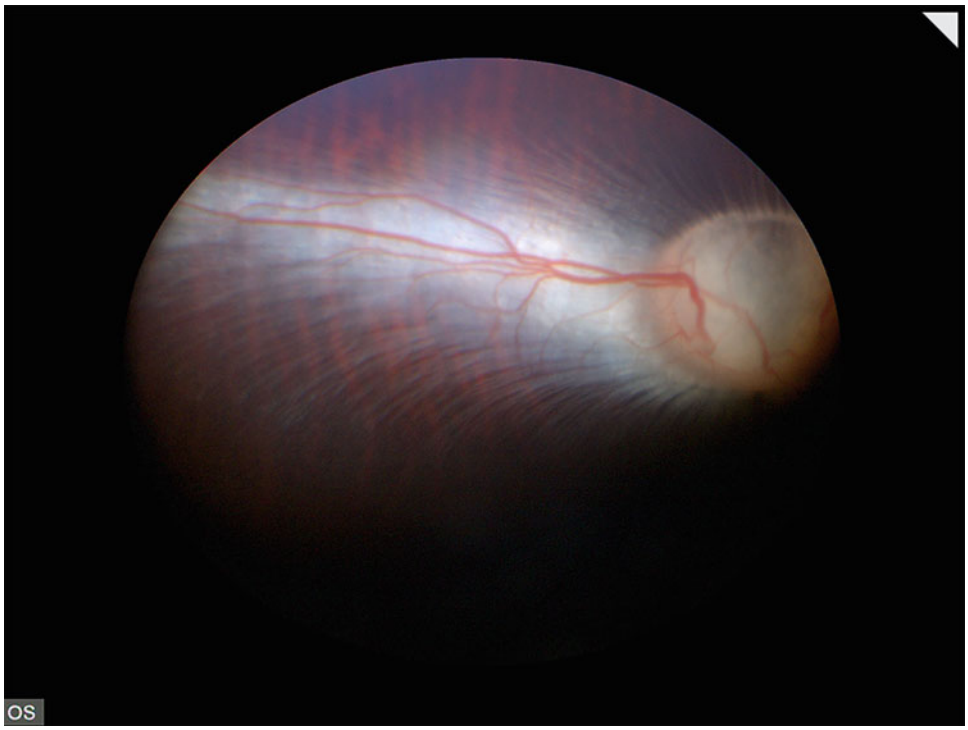

Fig. 42.4 The normal merangiotic fundus of a pigmented domestic rabbit (*Oryctolagus cuniculus*), focused on the optic disk and one medullary ray. Note the white myelinated fibers and minimally-branching blood vessels radiating from the optic disk. Image courtesy of Ellison Bentley, DVM, DACVO

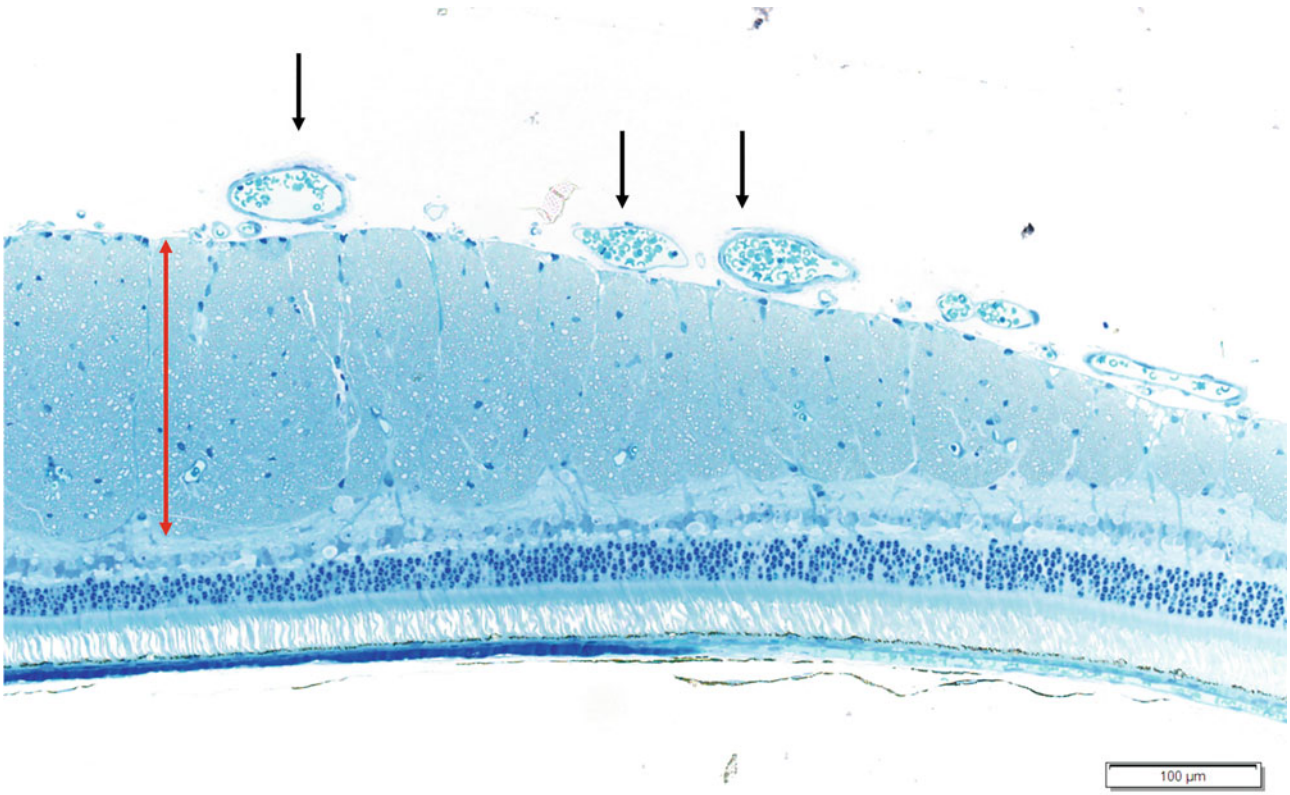

Fig. 42.5 Photomicrograph of the medullary ray in a normal rabbit, stained with toluidine blue. Note the abundant layer of myelin in the inner retina (red double-arrow) and large retinal blood vessels on the inner retinal surface (black arrows). Image courtesy of the Comparative Ocular Pathology Laboratory of Wisconsin

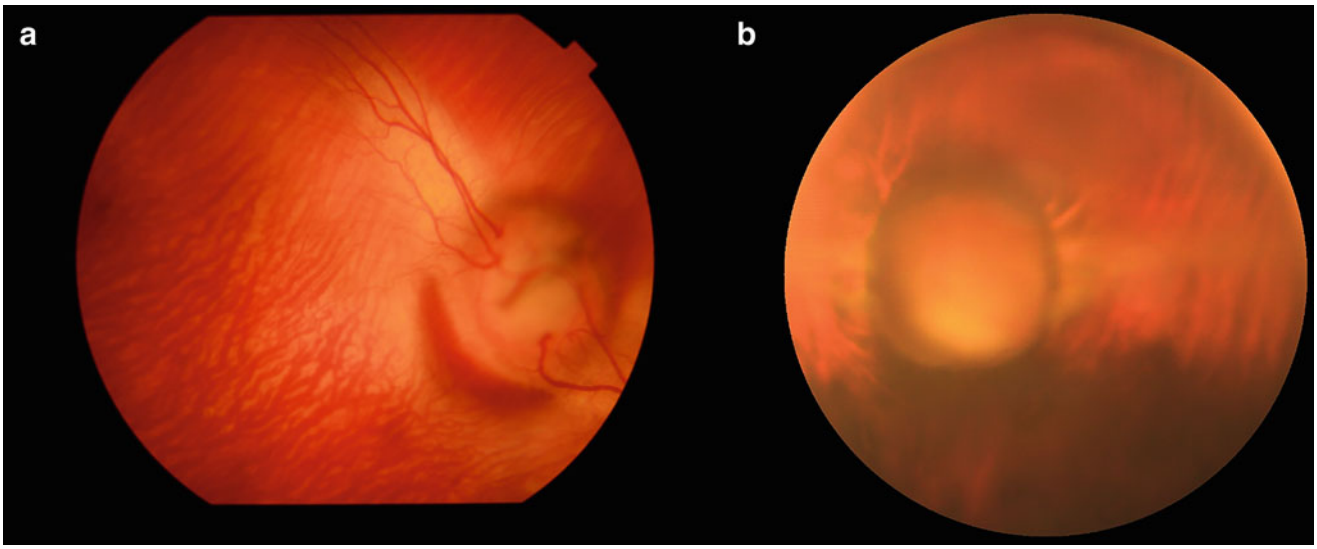

Fig. 42.6 The normally cupped optic disk in a normal, non-pigmented rabbit (*Oryctolagus cuniculus*) fundus (**a**) in comparison with pathologic optic disk cupping and retinal degeneration associated with glaucoma and buphthalmos (**b**). Images courtesy of Bret A. Moore, DVM, PhD, DACVO

comparatively thinner than in other species, ranging from 160 microns at the visual streak to 90 microns at the far periphery (ora serrata), to <40 microns beneath the vascular radiations and retinal vessels (Davis 1929). The retinal vasculature is supplied by the retinal artery which divides into nasal and temporal branches prior to entering the globe adjacent to the optic disk, creating the nasal and temporal branches which expand into the medullary rays (Ringler and Newcomer 2014). Most of the large vessels within the rays lie on the inner retinal surface (Fig. 42.5).

The microscopic arrangement of the retinal cellular and plexiform layers resembles the inverted pattern of most other vertebrates (Fig. 42.7). Of note, Müller cells and structural elements like the internal and external limiting membranes are particularly prominent in the rabbit retina, and rabbits also possess distinctly multinucleated cells within the retinal ganglion cell layer (Ringler and Newcomer 2014). There are a total of approximately 380,000 retinal ganglion cells in the rabbit retina (Vaney 1980b), and the rabbit visual acuity has been estimated at 3.4 cycles per degree (cpd) (Akaishi et al. 1995). Based on the presence of two photoreceptor pigments, domestic rabbit vision is dichromatic (Jacobs 1993). The rabbit photoreceptor profile is dominated by rods with only 5% of the photoreceptor layer comprising cones, primarily M- and S-cones (medium- and short-wavelength cones, respectively). Cones are most densely concentrated in the visual streak with 13,000 cells/mm (Barrio et al. 2010) compared to 7000 cells/mm (Barrio et al. 2010) in peripheral regions (Hughes 1971b).

There are distinct regional differences in the subtypes of cones within the rabbit retina outside the visual streak. Specifically, cones within the most inferior 5–6% of the retina are almost exclusively those with highest sensitivity to light in the blue wavelength spectrum (S-cones). Morphologically, this produces a crescent-shaped region (the "blue streak") in the far inferior periphery completely void of M-cones. One explanation for this arrangement proposes that a higher density of blue cones in the inferior retina produces heightened contrast against the corresponding visual field, namely the background of the sky. In theory, this would create greater sensitivity to detecting predators, particularly birds of prey (Juliusson et al. 1994). The rabbit also has a similar superior crescent and narrow region between the visual streak and the inferior crescent that are less specialized in terms of function but carry the "horizontal band" arrangement of other retinal anatomical features (Juliusson et al. 1994).

Ocular Diseases of Leporids

Diseases of the orbit and eye are common in domestic rabbits and have also been reported in wild rabbits and hares. In a recent retrospective study of 202 pet rabbits, 9.26% of animals were presented to veterinarians with an ocular complaint, most commonly for acquired diseases of the adnexa, cornea, or nasolacrimal drainage system (Tokashiki et al. 2019). Purely heritable diseases of Leporids are less commonly reported in clinical or epidemiological literature. However, certain conditions with proven heritable pathophysiology have been reported in domestic rabbits.

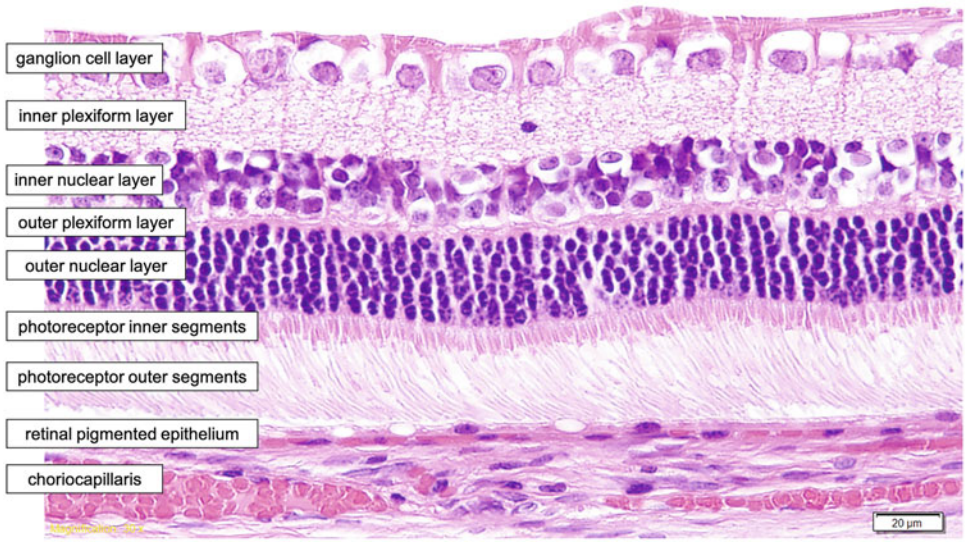

Fig. 42.7 Photomicrograph of the retinal layers in a normal domestic rabbit. Image courtesy of the Comparative Ocular Pathology Laboratory of Wisconsin

Congenital Ocular Malformations

Heritable ocular malformations present at birth are uncommon but have been reported in domestic rabbits (Kern 1997). It is noteworthy, however, that some congenital ocular malformations may be at least partially attributable to extrinsic factors such as nutritional deficiency or intrauterine toxin exposure (see below), so non-heritable causes must also be considered.

Microphthalmia

A congenitally small and malformed globe has been sporadically reported in the domestic rabbit. Proposed inheritance pattern varies with both autosomal recessive and dominant mechanisms described (Botha et al. 2014). There is also description of colobomatous microphthalmia in a domestic rabbit associated with suspected Vitamin E deficiency (Nielsen and Carlton 1995).

Anophthalmia

Complete lack of a globe, grossly and histologically, is rare but has been described in the domestic rabbit; however, a definitive inheritance pattern has not been identified. It is noteworthy that extrinsic factors such a ionizing radiation, toxin exposure, or in utero infection may also predispose to anophthalmia, and concomitant non-ocular birth defects may be observed (Botha et al. 2014).

Diseases of the Orbit

Orbital (Retrobulbar) Abscess

Space-occupying disease of the orbit (retrobulbar space) is common in domestic rabbits, particularly bacterial orbital abscesses. The rabbit's predisposition to orbital abscess is largely attributable to the anatomical proximity of the ventral orbit to the dome-like periapical roots of the cheek teeth (Fig. 42.1) (Capello 2016a; Reusch 2008). Infection of these roots can extend through the alveolar bone into the adjacent orbit. If severe and diffuse enough within the orbital bony and soft tissues, tooth root abscesses can cause clinically severe exophthalmia with corneal exposure and can cause severe ocular and intraocular inflammation (panophthalmitis) (Ward 2006). While there are no known published reports describing similar orbital abscesses in wild Leporids, dental disease has been documented in wild hares, suggesting a similar predisposition (Kelly 2020). Non-dental sources of orbital abscess are also described and may include local extension of severe rhinitis or sinusitis associated with *Pasteurella* spp. infections, migration of penetrating foreign bodies, penetrating trauma, or hematogenous spread of systemic infections (Graham 2014). Other bacterial isolates reported from orbital abscesses include *Pseudomonas aeruginosa* and *Actinomyces* spp., the latter often characterized by granulomatous inflammation with reactive bony lysis and proliferation (Gardhouse et al. 2017). Primary abscess of the Harderian gland has also been reported as a cause for orbital disease in rabbits (Bazior-Langhan 2012).

A presumptive diagnosis can often be based on clinical signs which commonly include exophthalmia (Fig. 42.8) (or enophthalmia if disease is primarily anterior to the globe), conjunctival hyperemia, chemosis, serous to mucoid/mucopurulent ocular discharge, poor blink and exposure keratitis (non-ulcerative or ulcerative), and variable systemic signs (fever, malaise, inappetence). Imaging can support the diagnosis and guide collection of fine-needle aspirates or biopsies if indicated. Skull radiographs frequently provide only limited information about structural

Fig. 42.8 Unilateral exophthalmia associated with an orbital abscess in a domestic rabbit (*Oryctolagus cuniculi*). Image courtesy of Bret A. Moore, DVM, PhD, DACVO

disease of the orbit and adjacent structures. Superimposition of bony tissues on orthogonal and oblique radiographic views may decrease the sensitivity and specificity of this modality for determining the cause and extent of an orbital abscess. Orbital ultrasound may be similarly insensitive for identifying cause and determining severity. Cross-sectional imaging with computed tomography (CT) is often considered diagnostically superior, capable of identifying more subtle dental disease and associated bony changes. Demonstration of purulent fluid within the orbital tissues, however, may be limited with CT. Identification of fluid for possible aspiration, or characterization of soft-tissue detail may be more easily achieved using magnetic resonance imaging (MRI), if available.

Several approaches have been described for treating orbital abscesses in rabbits. Medical therapy solely with broad-spectrum antibiotics and anti-inflammatories is often insufficient since penetration of therapeutic drug concentrations may be limited in abscessed tissues. Furthermore, conservative medical therapy often fails to address the underlying cause, particularly when active dental disease is involved. Even with specific treatment of underlying cause, additional and more aggressive therapy may be required to drain purulent material from the orbit and to debride diseased soft and bony orbital tissues. This may include surgical debridement of the affected tissue via the oral cavity with or without endoscopic assistance (Martínez-Jiménez et al. 2007) or via lateral facial approach (Ward 2006), in tandem with wound packing using antibiotic-soaked gauze sponges or antibiotic-impregnated beads or other devices (Ward 2006; Müller 2010; Taylor et al. 2010). In severe cases where significant and vision-threatening secondary ocular disease is present, exenteration with wide resection of affected orbital tissue may be the best option. Regardless of the chosen approach, culture and sensitivity of exudates as well as associated tissues is indicated, as co-infections may be encountered (Chen and Quesenberry 2006).

Prolapsed Harderian Gland

The tubuloalveolar Harderian gland with its two well-circumscribed lobes normally resides deep within the ventromedial orbit at the base of the third eyelid. Anterior prolapse of the Harderian gland has been described in domestic rabbits (Donzel et al. 2010; Janssens et al. 1999), but the cause for protrusion is not always immediately apparent. As with prolapsed third eyelid gland in dogs ("cherry eye"), an inherent weakness in the gland's supportive connective tissue may predispose to this condition (Janssens et al. 1999), but other causes such as trauma or concurrent space-occupying orbital disease (Fig. 42.9) must be considered. Lymphoma of the Harderian gland has been reported (Hittmair et al. 2014b); therefore, any neoplastic disease that enlarges the gland may predispose to prolapse.

The clinical appearance of prolapsed Harderian gland is typically diagnostic, presenting as third eyelid protrusion associated with a large, dark swelling at the ventromedial aspect of the globe (Fig. 42.9). Ultrasound of the gland may provide clinical information about the underlying cause for prolapse. Both lobes of the normal rabbit Harderian gland tend to be homogeneously hypoechoic, whereas pathologically enlarged glands may have a more heterogeneous echogenicity, and infiltrated glands (i.e., those with lymphoma) may bear hyperechoic nodular infiltrates (Hittmair et al. 2014b). If necessary, incisional biopsy of the gland can

Fig. 42.9 Retrobulbar (orbital) abscess in the right eye of a rabbit. Note the widened palpebral fissure, conjunctival hyperemia, prolapsed third eyelid and associated glands, and desiccation of the corneal surface. Image courtesy of Bret A. Moore, DVM, PhD, DACVO

be performed to confirm the presence of active inflammatory, neoplastic, or infectious infiltrative disease (Van Zeeland 2017). If neoplasia is confirmed within a prolapsed gland, excision is indicated. Otherwise, surgical repositioning of the gland using a modification of the Morgan pocket technique that is frequently used to reposition prolapsed third eyelid glands in dogs (Morgan et al. 1993) can also be performed successfully in rabbits (Donzel et al. 2010; Janssens et al. 1999) and also in combination with an orbital rim anchoring technique (Capello 2016b).

Paraneoplastic Exophthalmia

A unique form of paraneoplastic exophthalmia has been well characterized in domestic rabbits. The disease frequently presents bilaterally and is often associated with mediastinal neoplasms like thymomas. However, any space-occupying mediastinal mass, particularly one that is cranial to the heart base, may produce similar clinical signs (Maini and Hartley 2019). The putative pathophysiology of this condition begins with the compressive effects of a tumor or mass on the great veins within the mediastinum, leading to secondary congestion of the veins of the head and neck, including those providing venous return from the eye and orbit. The pathophysiology is likely enhanced by the presence of the aforementioned venous sinus in rabbit orbit which may expand when congested, contributing to anterior globe displacement. In one study, bilateral exophthalmia was observed in 6/13 rabbits with a mediastinal thymoma (Künzel et al. 2012).

Clinical signs may not be obvious to the rabbit owner and exophthalmia may be intermittent. Diagnostic clinical features include non-painful exophthalmia, typically bilateral, with protrusion of the third eyelids (Kostolich and Panciera 1992; Vernau et al. 1995; Wagner et al. 2005). It's noteworthy that these clinical signs may be most obvious upon ventroflexion of the neck. Treatment of the exophthalmia may require palliative lubrication of the corneal and conjunctival surface to prevent exposure, but definitive treatment must target the underlying cause in the mediastinum via surgical resection, chemotherapy, and/or radiation therapy (Morrisey and McEntee 2005).

Other Orbital Diseases

Primary retrobulbar neoplasia is not common in rabbits but lymphosarcoma of the Harderian gland has been reported (Volopich et al. 2005). Parasitic cysts (coenuri) have been

reported in rabbits in association with *Taenia serialis*, a species of tapeworm whose definitive hosts are dogs or other canids but whose life cycle may include intermediate host species like rabbits and hares (O'Reilly et al. 2002; Wills 2001). Caution should be used in treating these coenurid infections with praziquantel or other anthelmintics as rapid killing of the parasite can result in a significant immunologic inflammatory response which can worsen disease and endanger the adjacent globe (White Jr 2000). Despite limited supportive literature, surgical excision has proven to be curative (O'Reilly et al. 2002). Other reported causes of exophthalmia in domestic rabbits include salivary mucocele, and excessive retrobulbar fat accumulation associated with obesity (Wagner and Fehr 2007).

Diseases of the Adnexa and Ocular Surface

Infectious Causes of Blepharitis and Conjunctivitis

The majority of ocular diseases described in domestic and wild Leporids involve the adnexa and ocular surface. Infectious diseases of the eyelids and conjunctiva are exceptionally common, and bacterial, viral, fungal, and parasitic causes are described. Anatomically, the eyelids are contiguous at the eyelid margin with the palpebral conjunctiva, and the palpebral conjunctiva is contiguous with the third eyelid and bulbar conjunctiva on the globe surface. Therefore, many of the diseases that primarily involve the eyelids may extend to involve the conjunctiva/third eyelid and vice versa. Given the numerous causes for disease of the Leporid adnexa and ocular surface, rabbits and hares presenting with blepharitis and/or conjunctivitis should be diagnostically investigated with cytology and culture and biopsy or infectious serology/molecular diagnostics, when indicated.

Bacterial Blepharitis/Conjunctivitis

Treponema paraluiscuniculi: *Treponema paraluiscuniculi* (formerly *Treponema cuniculi*), the causative agent for "rabbit syphilis," is a microaerophilic, gram-negative spirochete. Pathogenic and non-pathogenic strains have been characterized, though it is difficult to distinguish them solely by morphology. Any rabbit can acquire *T. paraluiscuniculi* via direct horizontal transmission, but peri- and post-natal transmission from an infected dam to neonates can also occur (Digiacomo et al. 1985). In domestic rabbit colonies, subclinical disease frequently complicates identification of carriers. One study estimates a carrier incidence of up to 10% in enzootically-infected colonies and another demonstrated serologic positivity for *T. paraluiscuniculi* antibodies in 15–25% of rabbits (Ringler and Newcomer 2014). Stress, overcrowding, and poor sanitation may increase the incidence of clinical disease, particularly in purpose-bred colonies.

Lesions associated with *T. paraluiscuniculi* infection often involve the genitals, anus, lips, and eyelids. Eyelid lesions may begin as focal or multifocal erythematous swellings, progressing to development of papules and vesicles which can rupture and ulcerate, becoming more exudative and "crusted" in appearance (Fig. 42.10); secondary conjunctival hyperemia and ocular discharge are also common (Saito and Hasegawa 2004a). It has been suggested that infections acquired via maternal transmission are more likely to produce facial and eyelid lesions (Lennox and Kelleher 2009). Depending on the stage of disease, the associated signs may be non-specific. Therefore, diagnosis should be based upon clinical suspicion and cytologic or histologic demonstration of spirochete organisms. Serologic tests are available, but false negatives are possible (Graham 2014). It's also noteworthy that a long incubation period is often required for *T. paraluiscuniculi* to cause clinical disease (up to 3–6 weeks following initial exposure), and seropositivity can also be delayed by up to 5–6 weeks following initial exposure (Digiacomo et al. 1985; Digiacomo et al. 1984).

Treatment for *T. paraluiscuniculi* requires an appropriate antibiotic, typically subcutaneous penicillin, for an extended course (at least 3 weeks) (Varga 2014). However, there are concerns about the safety of penicillins in rabbits (see section "Other Clinical Considerations in the Care and Treatment of Leporidae"). Alternative treatment regimens have been published including chloramphenicol at 55 mg/kg per os (PO) twice daily (BID) for 4 weeks (Saito and Hasegawa 2004b), or azithromycin at 30 mg/kg/day PO once or twice daily for 15 days (Lukehart et al. 1990).

***Staphylococcus* spp.**: Various species of Staphylococcus are known to cause blepharitis and conjunctivitis in Leporids. *Staphylococcus aureus*, an unencapsulated gram-negative bacteria, is normally found in the nasopharyngeal, cutaneous, and conjunctival flora of rabbits and has also been cultured from rabbits with conjunctivitis (Hermans et al. 2003; Viana et al. 2007). Diagnosis is most easily achieved by cytology and culture of conjunctival swabs, and treatment guided by results of antibiotic sensitivity testing. It's noteworthy that methicillin-resistant strains of *S. aureus* (MRSA) have been documented in rabbits, primarily those from rabbitries with large populations of domestic rabbits in close contact (Agnoletti et al. 2014; Moreno-Grúa et al. 2018), though no specific cases of MRSA-associated blepharitis or conjunctivitis have been published to date. Some reports have described successful treatment of Staphylococcal conjunctivitis using an autogenous vaccine (Hinton 1977; Meulemans et al. 2011).

***Pasteurella* spp.**: Pasteurella species, primarily *Pasteurella multocida*, have been implicated as a primary cause for blepharitis and conjunctivitis in rabbits. However, the more common clinical manifestation is primary

Fig. 42.10 Blepharoconjunctivitis associated with *Treponema paraluiscuniculi* in a domestic rabbit (*Oryctolagus cuniculus*). Image courtesy of the University of California Davis Comparative Ophthalmology Service

conjunctivitis, often in tandem with rhinitis. *Pasteurella* spp. are gram-negative rods that are commonly harbored asymptomatically within the nasal cavities of rabbits. *Pasteurella* spp. may be transmitted horizontally via direct contact with oral, respiratory, or urogenital secretions, but aerosolized transmission has also been proposed (DiGiacomo et al. 1987). Vertical transmission during parturition or lactation is also reported. In one study, 75% of newborn rabbits nursing Pasteurella multocida-infected dams were seropositive for the bacteria on pharyngeal culture (Ringler and Newcomer 2014). Conjunctival inoculation may also develop due to retrograde extension of a nasal infection via the nasolacrimal ducts (Petersen Jones and Carrington 1988).

Clinically, the signs of conjunctivitis associated with Pasteurella infection are non-specific, characterized by conjunctival hyperemia and swelling (chemosis), and serous to mucoid or mucopurulent ocular discharge. Therefore, other ocular diseases that cause similar signs (i.e., dacryocystitis, entropion, corneal ulceration) must be excluded by examination. Microscopic diagnosis of Pasteurellosis can be a challenge since *Pasteurella* spp. are so ubiquitously isolated from healthy animals. Furthermore, culture and serology both lack sensitivity, with false negatives in up to 30% of animals via nasal swab, and seroconversion requiring up to 4 weeks following infection (Ringler and Newcomer 2014).

Pasteurella conjunctivitis is often susceptible to penicillins, but achieving therapeutic serum levels at the level of the ocular surface may be difficult; and penicillins may carry risk for severe dysbiosis and enterotoxemia in rabbits. Topical ophthalmic antibiotics that may be effective and carry less risk include tetracyclines, chloramphenicol, gentamicin, or enrofloxacin (Kern 1997). Note, however, that re-infection and recurrence of disease is not uncommon as this bacterial species is rarely eliminated from an individual animal, regardless of choice or duration of treatment.

Fusobacterium necrophorum: *F. necrophorum* is an anaerobic, gram-negative bacteria reported to cause dermatologic lesions of the head and neck, which may also involve the eyelids (Ringler and Newcomer 2014). These bacteria may be either coccobacillary or filamentous on cytology which can complicate diagnosis.

Viral Blepharitis/Conjunctivitis

Cottontail Rabbit Papillomavirus: Cottontail rabbit papillomavirus (Shope papillomavirus) is an epitheliotropic papovavirus that causes cutaneous wart-like growths most

commonly on the face and ears, often involving the eyelids (Hagen 1966; Weiner et al. 2010). As indicated by the name, this virus most commonly infects the natural host species cottontail rabbit (*Sylvilagus floridanus*) but can also infect brush rabbits (*Sylvilagus bachmani*), snowshoe hares (*Lepus americanus*), black-tailed jackrabbits (*Lepus californicus*), and domestic rabbits (*Oryctolagus cuniculus*) (Brabb and Di Giacomo 2012). Transmission is typically through direct contact, but the virus can also be transmitted by vectors like the rabbit tick (*Haemaphysalis leporis-palustris*) and biting mosquitos, the latter being the predominant route of transmission between wild and domestic rabbit species (Brabb and Di Giacomo 2012).

Diagnosis is based on clinical appearance of the skin lesions and can be confirmed by histologic examination. Lesions may be observed up to 3 times less frequently in infected cottontail rabbits than in domestic rabbits (Brabb and Di Giacomo 2012). Surgical resection can be used to manage the papillomatous lesions, though in one study these lesions spontaneously resolved in 35% of naturally-infected rabbits within 6 months (Brabb and Di Giacomo 2012). Though not common, papillomas can undergo malignant transformation into squamous cell carcinoma-like neoplasms in some rabbits (Danos et al. 1985).

Rabbit Oral Papillomavirus: Rabbit oral papillomavirus is a kappapapillomavirus that predominantly affects domestic rabbits. While primarily causing oral and lingual lesions, there is report of a highly homologous virus, believed to be oral papillomavirus, being isolated from lesions on the third eyelid and eyelid in a domestic rabbit (Munday et al. 2007).

Myxoma Virus: Myxoma virus is a leporipoxvirus that affects wild and domestic rabbits and hares, with a trophism for undifferentiated mesenchymal cells, leading to development of proliferative fibromatous masses within a mucinous matrix, often involving the eyelids and periocular skin (Brabb and Di Giacomo 2012). Numerous species are naturally susceptible on multiple continents including the domestic rabbit (*Oryctolagus cuniculi*), brush rabbit (*Sylvilagus bachmani*), forest rabbit (*Sylvilagus brasiliensis*), eastern cottontail rabbit (*Sylvilagus floridanus*), European hare (*Lepus europaeus*), and mountain hare (*Lepus timidus*) (Brabb and Di Giacomo 2012). Myxoma virus originated in the forest rabbit but in North America where myxoma virus is endemic in the Western continental United States, the natural reservoir is the brush rabbit (Regnery and Miller 1972). Transmission is vector-driven via biting flies or mosquitoes (Brabb and Di Giacomo 2012). Wild Leporids like the forest rabbit and European hare are relatively resistant to clinical disease, typically only developing small, localized fibromatous masses where vectors bite and transmit the virus (Fenner and Ratcliffe 1965).

In domestic rabbits or following infection with more virulent myxoma virus strains, disease may be more severe and life-threatening (myxomatosis) (Bertagnoli and Marchandeau 2015). In severely affected animals, peracute myxomatosis leads to death within 1 week, often without overt ocular signs other than eyelid edema. In acute disease, edematous, "droopy" eyelids develop early in the course of disease, with progression to death often occurring within 1–2 weeks (Brabb and Di Giacomo 2012). The subacute and chronic forms typically begin by causing blepharoconjunctivitis which often begins as hyperemia and progresses to chemosis with copious mucopurulent exudate (Brabb and Di Giacomo 2012). Certain strains such as the California and Lausanne strains are more commonly associated with peracute to acute disease with a high mortality rate (Ringler and Newcomer 2014). Co-infections with bacterial organisms like *Pasteurella* spp., *Pseudomonas aeruginosa*, and *Staphylococcus* spp. are also common in rabbits with myxomatosis (Brabb and Di Giacomo 2012).

Shope Fibroma Virus: Shope fibroma virus is a leporopoxvirus with antigenic similarity to myxoma virus. Disease is endemic in wild Leporid species like the eastern cottontail rabbit, but outbreaks of clinical disease can occur in domestic rabbits. Like myxoma virus, Shope fibroma virus is transmitted via biting arthropod vectors (Brabb and Di Giacomo 2012). Clinical disease is typically similar in wild and domestic rabbits, with small, roughly spherical masses developing at the sites of vector bites around the neck and head (Brabb and Di Giacomo 2012). In one study of client-owned pet rabbits, 19 tumors from 179 rabbits were associated with the Shope fibroma virus (Von Bomhard et al. 2007). The lesions may spontaneously regress, particularly in domestic rabbit species, and some references cite expedited regression following trauma or biopsy (Keller et al. 2007a). Experimentally, mutant malignant fibroma virus strains (recombinant forms of the myxoma and fibroma viruses) have been characterized and cause life-threatening infections with severe immunosuppression, characterized by widespread systemic malignant proliferative disease and opportunistic infections (Brabb and Di Giacomo 2012; Block et al. 1985).

Hare Fibroma Virus: Similar to Shope fibroma virus, hare fibroma virus (also a leporipoxvirus) has been reported to affect European hares in Western continental Europe. Clinical disease is not as well described, but is reported to involve development nodules on the eyelids and other cutaneous sites (Brabb and Di Giacomo 2012). The mode of transmission has not been confirmed.

Rabbit Poxvirus: Rabbit poxvirus is an orthopoxvirus, associated with outbreaks of conjunctivitis and systemic disease, most commonly in domestic rabbitries or laboratory colonies. Transmission is typically via direct contact with nasal discharge. Mortality rates are higher in young rabbits or lactating does. Acute disease often presents as facial and eyelid edema followed by purulent blepharoconjunctivitis

and even keratitis with corneal ulceration. Progression to death can be fast, occurring within 5–10 days of infection (Brabb and Di Giacomo 2012).

Leporid Herpesvirus 4: Leporid herpesvirus 4 is an alphaherpesvirus that can lead to facial swelling, eyelid edema and blepharitis, and conjunctivitis in domestic rabbits. The original description of this virus and its clinical features was from a rabbitry in Alaska (Jin et al. 2008a). The exact mode of transmission is not confirmed, but since the outbreak was originally reported in the warm summer months, biting arthropod vectors are the suspected mechanism, likely transmitting the virus from snowshoe hares to domestic rabbits (Jin et al. 2008a; Jin et al. 2008b). Diagnosis can be made using a polymerase chain reaction (PCR) assay.

Human Herpesvirus 1: There is a single report of transmission of human herpesvirus 1 to pet domestic rabbits causing conjunctivitis (Grest et al. 2002).

Rabbit Hemorrhagic Disease: Rabbit hemorrhagic disease is a reportable disease, typically causing acute, highly infectious systemic illness with high morbidity and mortality (Brabb and Di Giacomo 2012). It is caused by a calicivirus that infects wild rabbits and hares and occasionally domestic rabbits. Some carrier species like European brown and snowshoe hares, cottontail rabbits, black-tailed jackrabbits, and volcano rabbits (*Romerolagus diazi*) are resistant to clinical disease. Ocular signs are not commonly observed given the often rapid progression of peracute disease; but in one outbreak in Michigan, conjunctival hyperemia was a common clinical sign (Bergin et al. 2009).

Parasitic Blepharitis/Conjunctivitis

External parasites of the face such as *Notoedres cati* var. *cuniculi* ("rabbit mange") and *Sarcoptes* spp. can affect the eyelids, leading to alopecia and crusted lesions (Aulakh et al. 2003; Darzi et al. 2007) and are reportedly susceptible to routine acaricides (Sanku et al. 2018). The brown hare (*Lepus europaeus*) is considered a definitive host for *Thelazia callipaeda* and has been reported in wild rabbits in Europe (Gama et al. 2016; Otranto et al. 2009). *Toxoplasma gondii* can be transmitted in rabbits transplacentally or horizontally via direct contact with feces from infected cats (Splendore and Splendore 1908; Almeɾa et al. 2004; Machacova et al. 2015). Though not common, active toxoplasmosis may be associated with nasal discharge, as well as serous or seropurulent ocular discharge in rabbits.

Fungal Blepharitis

Though not common, generalized cutaneous fungal disease may extend to the eyelids. Causes of fungal skin disease in rabbits include *Trichophyton mentagrophytes*, *Microsporum canis* or *M. gypseum*, or *Dermatophilus congolensis* (White et al. 2002).

Non-Infectious Causes of Blepharitis and Conjunctivitis

Non-infectious blepharitis and conjunctivitis are most commonly husbandry-related. Trauma to the eyelids and ocular surface is more common in rabbits that are group-housed or those with access to substrates such as hay or straw. Blepharitis and conjunctivitis can also be associated with dusty bedding or cage substrates that lead to ocular surface irritation, pruritis, and in some cases, self-trauma (Buckley and Lowman 1979). Self-trauma can compromise the eyelid and conjunctival epithelium, predisposing to secondary bacterial infection. Treatment involves making corresponding husbandry changes. It's also noteworthy that collateral extension of inflammation from the tooth roots can cause secondary conjunctival and third eyelid hyperemia resembling primary conjunctivitis.

Other Diseases of the Eyelids

Entropion and Trichiasis

Primary (heritable) and secondary entropion (resulting from chronic blepharoconjunctivitis or trauma) have been reported in domestic rabbits. Primary entropion may present in juvenile rabbits (Fox et al. 1979; Yanoff 1983) and is more commonly reported in larger breeds like the New Zealand white and the French lop (Maini and Hartley 2019). As in other species, chronic entropion may lead to keratoconjunctivitis and corneal ulceration, and surgical correction is recommended. A routine Hotz-Celsus procedure has been used to correct primary entropion, while tension-releasing blepharoplasties like the V-Y blepharoplasty have been used to address secondary cicatricial entropion (Maini and Hartley 2019).

Distichiasis is not common but has been reported in rabbits (Maini and Hartley 2019), and heritable trichiasis is also described. One noteworthy form develops in French rex rabbits carrying a homozygous *r1/r1* mutation. Affected animals have deformed cilia, leading to chronic trichiasis and ocular irritation (Castle and Nachtsheim 1933; Kern 1989).

Neoplasia

Primary neoplasia of the eyelids (non-myxomatous/fibromatous) is not commonly reported in Leporids but case reports describing squamous cell carcinoma and melanoma have been published. The biological behavior of these neoplasms is difficult to determine due to the low number of published reports, but according to one report, eyelid melanoma may carry risk for recurrence and even distant metastasis (Von Bomhard et al. 2007). Furthermore, extensions of an orbital fibrosarcoma into the adjacent eyelid tissue has been described. Other uncommon tumors that may

involve the eyelids include trichoblastoma and papilloma (Maini and Hartley 2019; Van Zeeland 2017; Von Bomhard et al. 2007). Ultimately, any neoplasm that can affect the skin in rabbits may affect the eyelids (Fig. 42.11). Treatment of any eyelid or periocular neoplasm will depend on its size, location, invasiveness, and histological diagnosis.

Other Non-Infectious Ocular Surface Diseases

Keratoconjunctivitis Sicca (KCS)

Spontaneous KCS in domestic or wild rabbits is not as well characterized as in other domestic species like the dog. Like the dog, however, oral administration of sulfonamide antibiotics has been reported to reduce tear production, in one study by ~50% after 2 weeks of treatment (Shirani et al. 2010).

Conjunctival Overgrowth

Conjunctival overgrowth (ankyloblepharon, pseudopterygium, conjunctival stricture, circumferential epicorneal membranous occlusion, or conjunctival centripetalization) is not frequently diagnosed but is well characterized in the domestic rabbit. Young male dwarf rabbits are over-represented. The use of the term pseudopterygium, however, is misleading as human pterygium is associated with UV light and involves corneal adherence which are not features of conjunctival overgrowth (Roze et al. 2001). Instead, conjunctival overgrowth presents as an annular, elastic fold of bulbar conjunctiva growing from the limbus toward the axial cornea. However, in rabbits, there is no infiltration or disruption of the corneal epithelium and the tear film and corneal surface are clinically and histologically normal (Roze et al. 2001) (Fig. 42.12). This disease is putatively attributed to a dysplasia which leads to excessive production of normal conjunctival collagen.

While non-painful, conjunctival overgrowth can progress to impair vision. Medical therapy has proven ineffective so surgical treatments are advocated. One published approach involves making radial incisions in the abnormal nonadherent conjunctiva and fixating the sectors circumferentially into the conjunctival fornix using transpalpebral sutures. In this clinical report, there was no recurrence for up to 72 months using this technique (Allgoewer et al. 2008). Another report described resection of the overgrown conjunctiva and inversion of the cut edges behind the limbus followed by treatment with topical corticosteroids and cyclosporine A with low rate of recurrence after 11 months (Kim et al. 2013). Mitomycin C has also been reported as an adjunctive therapy (Yata et al. 1995).

Diseases of the Nasolacrimal Drainage System

Dacryocystitis

Owing to the complex anatomy of the nasolacrimal drainage system in the rabbit and the duct's proximity to other structures like the roots of the cheek teeth, obstructive inflammatory/infectious disease (dacryocystitis) is exceptionally common in rabbits. In one survey of 344 pet rabbits, 73% of presentations for ocular disease had signs of dacryocystitis (Burling et al. 1991). In a very large survey of 1000 pet rabbits in the United Kingdom, 3.5% of rabbits with ocular lesions or clinical signs were subsequently diagnosed with dacryocystitis (Williams 2012). The primary factor contributing to the development of dacryocystitis is local infection and/or inflammation within the duct system, predominantly at certain locations where the path of the duct is intrinsically convoluted or where the lumen becomes naturally narrowed. One proximal site is where the duct passes from the facial soft tissues into the bony lacrimal foramen to enter the nasal passage. The second more distal site is where the duct twists around the maxillary incisor tooth root (Burling et al. 1991; Marini et al. 1996). Dental disease may also be a predisposing factor. In one study of 28 rabbits with dacryocystitis, 50% had underlying dental disease, though a cause and effect relationship couldn't be confirmed in all of those cases (Florin et al. 2009).

The most common clinical sign of dacryocystitis is ocular discharge, often copious and mucoid to mucopurulent. In some cases, the origin of the discharge can be localized to the inferior nasolacrimal punctum. Other common clinical signs include conjunctival hyperemia and swelling. Localized or diffuse keratitis may also be observed which may be secondary to tear film alterations which, according to some references, yield a viscous and even a "gritty" character to the precorneal tear film (Bedard 2018).

Bacterial infection is the most commonly implicated etiologic cause for dacryocystitis in rabbits. Historically, the most common causative isolates reported have been *Pasteurella* spp. (Petersen Jones and Carrington 1988), though other isolates cultured from discharge in affected rabbits include *Staphylococcus* spp., *Moraxella* spp., *Oligella urethras*, *Pseudomonas* spp., and *Streptococcus viridans*. It's noteworthy that these isolates are also found on the surface in healthy rabbits (Brown 2006). According to one study of 103 rabbits (83 with clinical signs of ocular and/or nasal disease and 20 rabbits without), culture and sensitivity demonstrated no significant difference in isolation of bacteria on culture following irrigation of the nasolacrimal system, nor did the types of bacteria cultured from each differ significantly. However, in that study, *Pasteurella* spp. were the most commonly isolated species from animals with active clinical signs (Quinton et al. 2014).

Fig. 42.11 Plasmacytoma involving the right inferior eyelid in a domestic rabbit (*Oryctolagus cuniculus*). Image courtesy of Bret A. Moore, DVM, PhD, DACVO

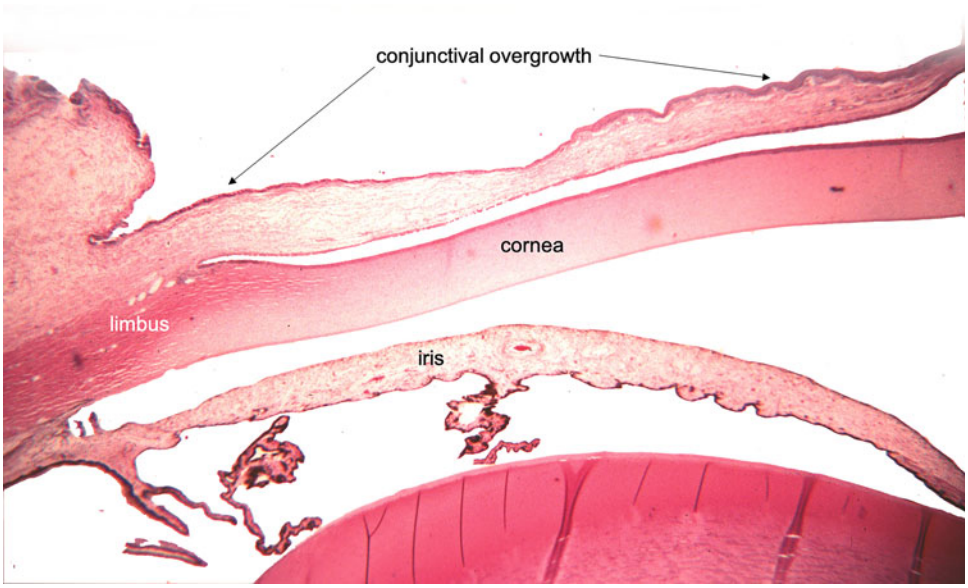

Fig. 42.12 Photomicrograph of conjunctival overgrowth in a rabbit. Image courtesy of the Comparative Ocular Pathology Laboratory of Wisconsin

Diagnosis is typically based on clinical signs, but additional tests to support the clinical diagnosis may include the Jones fluorescein dye passage test and cannulation of the punctum with a 27 gauge soft Teflon™ IV catheter or sterile metal cannula with irrigation (Brown 2006). In many rabbits, this is easiest to perform under sedation. A full physical examination and detailed oral examination must be performed to assess the health of the teeth. Diagnostic workup to identify and characterize the infectious etiology should include cytology and culture of ocular discharge. Advanced imaging can be performed with skull radiographs, or more ideally cross-sectional imaging with CT or MRI as well as contrast-aided study to delineate the NLD from proximal to distal (dacryocystorhinogram).

If tooth root disease is present and suspected to be the cause for dacryocystitis in a rabbit, the primary goal of treatment should be to address the dental issue. Systemic and topical antibiotic treatment of dacryocystitis should be guided by culture and sensitivity. According to one reference, the most appropriate initial choices are fluoroquinolones or sulfonamides (Florin et al. 2009). The duration of treatment may need to be quite protracted in some animals with one study citing a mean of 5.8 weeks as the necessary treatment duration with topical and/or systemic antibiotics. Furthermore, those cases requiring a longer course of therapy or those necessitating systemic antibiotic therapy may be at higher risk for a poorer outcome (Florin et al. 2009). Oral NSAIDs (i.e., meloxicam) can also be beneficial provided that there is no systemic contraindication. In some cases, serial irrigations as frequently as daily or weekly may be necessary. Balloon dilation has been reported as a viable means of treating in an experimental rabbit study (Goldstein et al. 2006).

Diseases of the Cornea

Ulcerative Keratitis

The cornea of the rabbit is large and conformationally exposed in comparison with other species. Therefore, corneal trauma is common, whether relating to bedding, organic material, or encounters with other animals (Andrew 2002). Focal keratitis may also be associated with persistent blepharitis, conjunctivitis, and dacryocystitis. Adnexal diseases like entropion, distichiasis, and trichiasis may also cause keratitis, and exposure secondary to facial nerve paralysis or exophthalmia associated with retrobulbar disease can lead to corneal ulceration. Corneal stromal abscesses have also reported in rabbits but are uncommon (Andrew 2002). If an underlying predisposing factor for any ulceration can be identified, treatment to resolve that factor is indicated to address keratitis.

In cases of ulcerative keratitis where the corneal epithelium is compromised and the stroma exposed and at risk for infection, a topical prophylactic antibiotic is indicated as well as a topical cycloplegic like atropine to relieve painful iridocyclospasm, if present. However, it's noteworthy that many rabbits possess endogenous atropinases in ocular tissues that may inactivate atropine and render it therapeutically ineffective (Verstraete and Osofsky 2005). If there is evidence of stromal loss, corneal malacia, and/or stromal infiltrate (Fig. 42.13), cytology and culture are indicated to investigate for underlying infection. Bacterial infections of the cornea are common and reports of keratomycosis with organisms like *Aspergillus fumigatus* have also been described (Bourguet et al. 2016). Fungal infection has been successfully treated with topical agents like terbinafine and miconazole, as they will pharmacologically penetrate the rabbit corneal epithelium and will reach therapeutic concentrations in the aqueous humor (Sun et al. 2007). Successful treatment with topical 0.1% povidone iodine solution has also been reported (Ford 2004; White et al. 1972). Voriconazole was studied as a 1% ophthalmic and achieved therapeutic concentrations in both the anterior chamber and the vitreous chamber, but the medication must be given frequently which may be a limiting factor (Hawkins 2014).

Non-healing or "indolent" corneal ulcerations without an overt or obvious underlying cause are occasionally encountered in rabbits (Fig. 42.14). Published treatment approaches include routine epithelial debridement following topical anesthetic instillation, as well as grid keratotomy or anterior stromal puncture as described for dogs with spontaneous chronic corneal epithelial defects (SCCEDs) (Andrew 2002). In one case series that included one rabbit with chronic indolent corneal ulceration, debridement was performed followed by topical administration of topical isobutylcyanoacrylate, reporting 2 weeks to healing after treatment (Bromberg 2002). Bandage collagen shields may also be used to encourage healing (Eshar et al. 2011).

Primary Viral Keratitis

Keratitis may be associated with viral infections involving poxviruses such as myxoma virus, Shope fibroma virus, and squirrel fibroma virus (McLeod Jr and Langlinais 1981) and may affect wild or domestic Leporids. Corneal lesions associated with the poxviruses are described as well-demarcated, tan-pink, mass-like swellings, frequently spanning the limbus and involving the conjunctiva (Keller et al. 2007a; McLeod Jr and Langlinais 1981). Corneal edema and vascularization may accompany the mass. Biopsy of corneal lesions can be used to confirm the diagnosis and electron microscopy used to directly identify viral particles, though differentiation between poxvirus types may be difficult as they are morphologically similar in appearance (McLeod Jr and Langlinais 1981; Keller et al. 2007b). Clinical presentation with concurrent and severe systemic illness is most consistent with myxoma virus-associated disease.

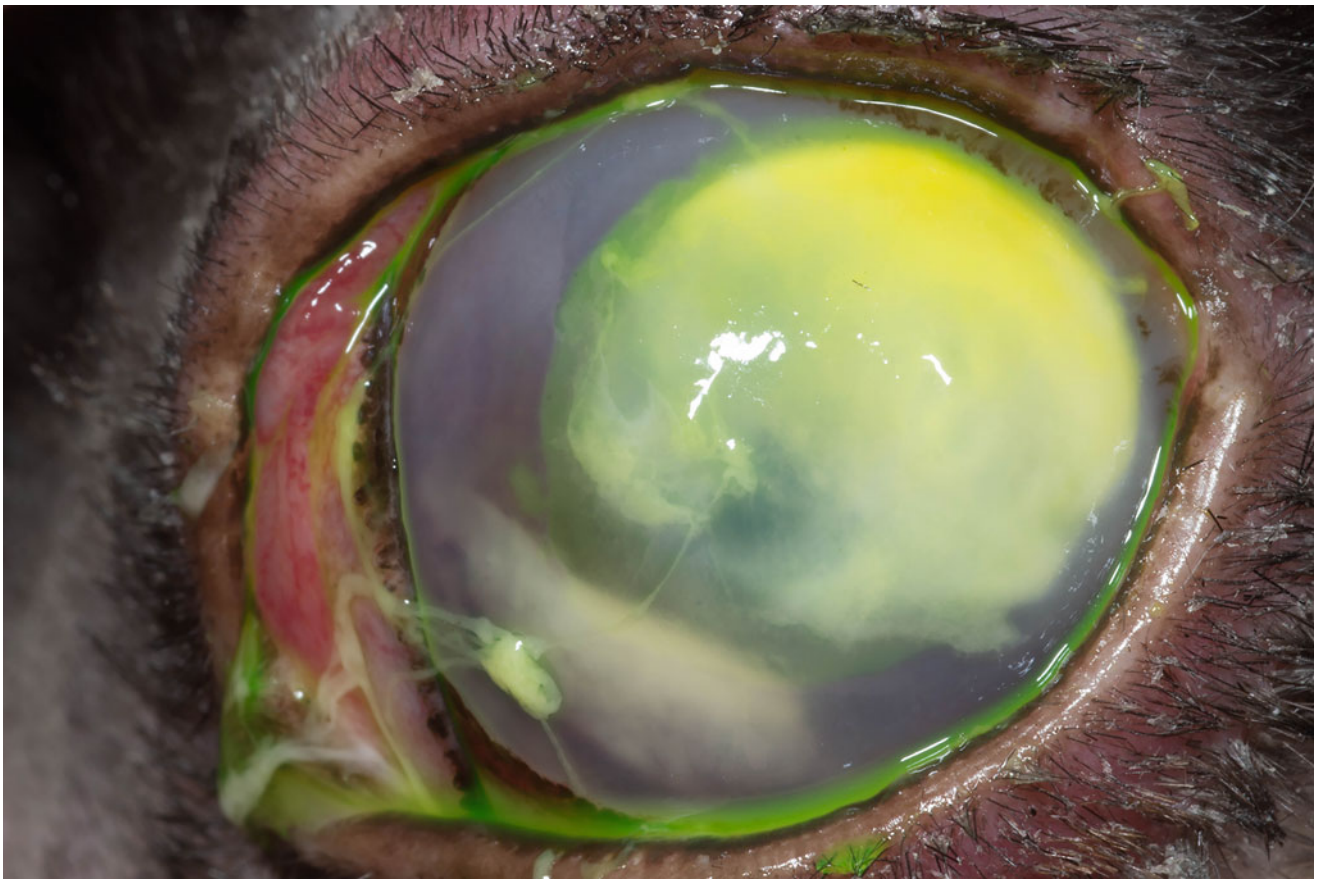

Fig. 42.13 Malacic stromal ulcerative keratitis in the left eye of a domestic rabbit. Image courtesy of Bret A. Moore, DVM, PhD, DACVO

Histologically, corneal lesions or masses associated with poxviruses comprise predominantly proliferative and pleomorphic mesenchymal cells and eosinophilic viral inclusions on electron microscopy (Keller et al. 2007a). In one case report of a Shope fibroma virus-associated corneal mass, subtotal surgical resection via keratectomy led to clinical resolution of the primary lesion (Keller et al. 2007a).

Leporid herpesvirus 2, also known as herpesvirus cuniculi, is a gammaherpesvirus often isolated from rabbits without any detectable clinical disease. There is, however, report of associated punctate keratitis and corneal scarification in a rabbit (Nesburn 1969).

Lipid Keratopathy

Lipid keratopathy (LK) is a non-ulcerative keratopathy characterized by focal-to-multifocal or coalescing pearly-white refractile opacities within the corneal stroma. These lesions are particularly common in rabbits receiving cholesterol-rich diets, such as those high in milk fat or fishmeal (Gwin and Gelatt 1977; Kouchi et al. 2006; Sebesteny et al. 1985). Corneal lipids are also putatively pro-inflammatory and therefore LK lesions maybe associated with corneal vascularization and local inflammation and infiltration, predominantly by macrophages containing foamy cytoplasm. These lesions may also be observed in Watanabe rabbits with heritable hyperlipidemia (Garibaldi and Goad 1988).

Corneal Dystrophy

Corneal dystrophy (CD) is common in domestic rabbits, particularly in purpose-bred laboratory strains. Dystrophy lesions are often observed in juvenile to young adult rabbits, are unassociated with underlying systemic disease, and are most often observed bilaterally in the central and paracentral cornea. Lesions may be focal or multifocal and may involve any corneal layer, though the epithelium and subepithelial stroma are most commonly affected.

Several distinct forms of CD have been described in domestic rabbits though inheritance patterns are not understood for most. One form in the Dutch belted rabbit is characterized by focal linear or curvilinear opacities present within the anterior subepithelial stroma (Moore et al. 1987). In one form in New Zealand white rabbits, raised corneal opacities within the peripheral/perilimbal and paracentral

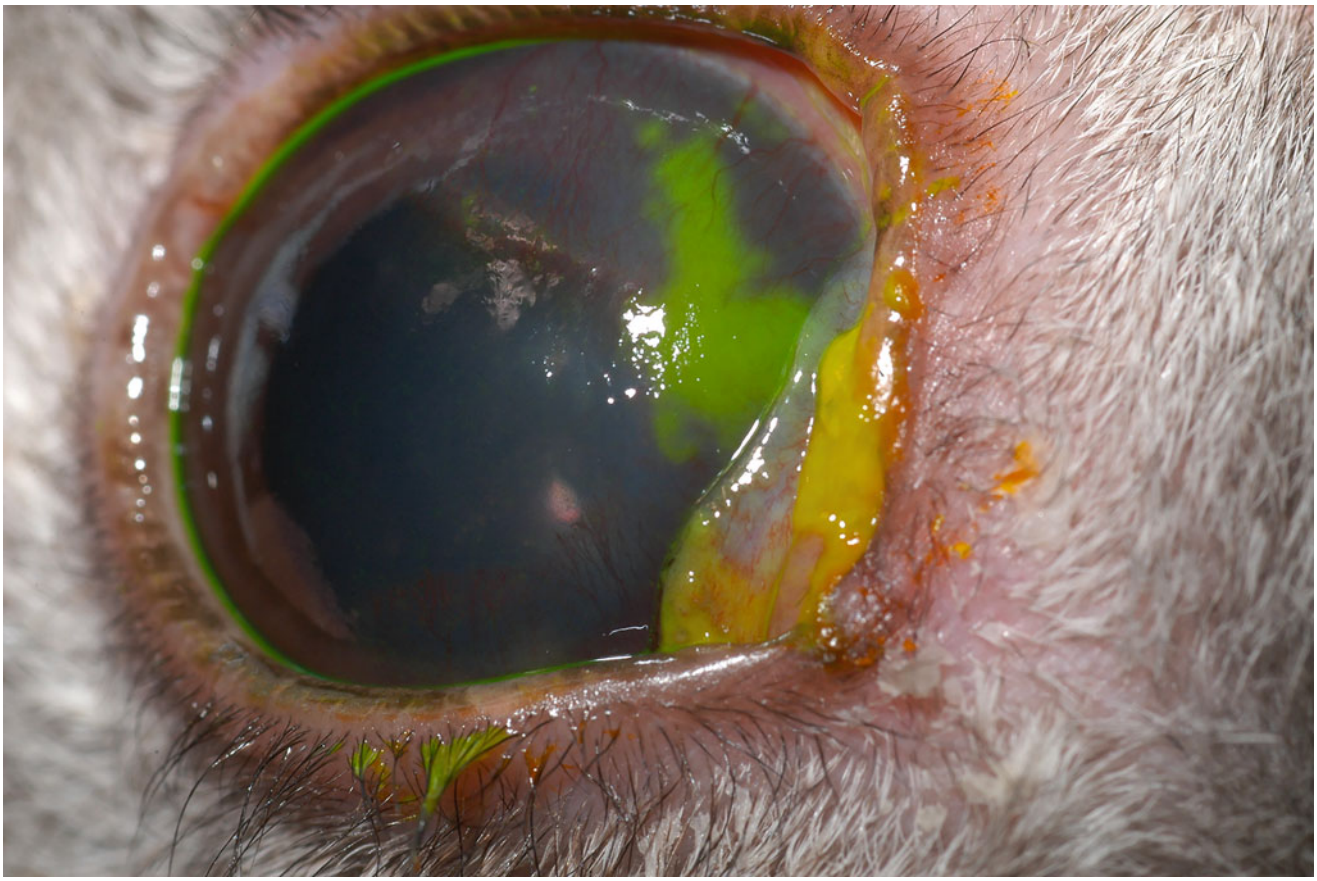

Fig. 42.14 Chronic, non-healing (indolent) corneal ulceration in a domestic rabbit. Note the fluorescein uptake in the dorsal cornea and associated superficial vascularization. Image courtesy of Bret A. Moore, DVM, PhD, DACVO

cornea have been described, characterized histologically by epithelial thickening and irregularity (Port and Dodd 1983). Corneal dystrophy lesions within the deep stroma have also been described in New Zealand white rabbits, characterized by well-circumscribed, focal to multifocal opacities distributed centrally or peripherally, immediately anterior to the Descemet's membrane. While a heritable cause or predisposition is suspected for this latter dystrophy, it's noteworthy that the affected population of these rabbits were all fed a commercial diet, with an incidence of 29% in the study population (Durand-Cavagna et al. 1998).

Eosinophilic Keratoconjunctivitis

Eosinophilic keratoconjunctivitis is not commonly diagnosed in domestic rabbits but bears similarities to similar disease entities in horses and cats. The lesions may involve the cornea or bulbar conjunctiva, presenting as yellow-white superficial corneal infiltrates that may be raised or plaque-like (Grinninger et al. 2012). Cytologically or histologically, granulation tissue and neutrophils are often present with obvious intracytoplasmic eosinophilic granules. Diagnosis is primarily based on clinical appearance and cytologic findings. Treatment to induce remission can be achieved with topical ophthalmic corticosteroids like dexamethasone TID-QID. Ophthalmic cyclosporine may also be used but is reported to be less effective (Grinninger et al. 2012). The prognosis in affected rabbits is good but as with other species, recurrence is possible.

Corneal Dermoid

Case reports have been published describing corneal dermoids in domestic rabbits which can be excised routinely via keratectomy/conjunctivectomy with a good postoperative prognosis for ocular comfort and maintenance of vision (Wagner et al. 2000).

Glaucoma

Glaucoma in rabbits can be primary (heritable) or secondary (a consequence of pre-existing ocular disease). Primary glaucoma in New Zealand white rabbits has been well characterized and is linked with the recessive *bu* gene (Hanna et al. 1962; Van Horn et al. 1977b). Homozygotes for *bu* are historically predisposed to glaucoma, though incomplete penetrance for the phenotype has been documented (Hanna et al. 1962). Furthermore, experimental recapitulation of disease has been challenging which supports

a possibly more complex pattern of heritability and/or phenotypic expression than originally believed. Carriers for the *bu* gene may also produce smaller litter sizes with poorer neonatal survival rates.

In *bu/bu* affected eyes, aqueous outflow is reduced by 3 months of age and increased intraocular pressure (IOP >21 mmHg) with buphthalmos (globe enlargement) typically develops by 5 months of age. However, clinically-evident glaucoma may develop in some rabbits as young as 1–3 months of age (Hanna et al. 1962; Van Horn et al. 1977b; Kolker et al. 1963). The end result of chronically increased IOP is optic nerve and retinal degeneration and blindness. Disease is often bilateral, but may be unilateral in some homozygotes. Primary glaucoma not definitively associated with the *bu* gene has also been described in domestic rabbits breeds like the French lop and the Flemish giant (Maini and Hartley 2019).

The precise pathophysiology underlying primary glaucoma in rabbits is not completely understood. Early histologic investigations of affected eyes with *bu*-associated glaucoma have identified structural abnormalities in the iridocorneal angle, putatively decreasing aqueous outflow and increasing IOP (Hanna et al. 1962; Kolker et al. 1963). Comparison of normal and abnormal globes identified structural abnormalities in the aqueous outflow tissue of affected eyes that suggested incomplete embryologic cleavage of the iridocorneal angle during development. Specifically, the trabecular meshwork (TM) in affected eyes is abnormal with notable tissue thickening and an unusually large amount of extracellular matrix between the pillars of TM (Tesluk et al. 1982; Ueno et al. 1999). It is noteworthy, though, that the specific features of pathophysiology may differ between affected strains and Leporid species.

Diagnosis of primary glaucoma is based on signalment, documentation of increased IOP (often associated with clinically-evident buphthalmos (Fig. 42.15), and lack of obvious underlying cause on ophthalmic examination. Treatment may be attempted with ophthalmic hypotensive medications like dorzolamide, a carbonic anhydrase inhibitor, three times daily and/or timolol (a beta blocker) twice daily. However, timolol should be used with caution in small rabbits due to systemic absorption and possible cardiopulmonary side effects. Ophthalmic pilocarpine, a direct-acting parasympathomimetic, reduced IOP by a maximum of 9.4 mmHg in one study of *bu/bu* eyes; in the same study, timolol reduced IOP by a maximum of 8.0 mmHg (Vareilles et al. 1980). It is noteworthy that buphthalmos can also result in exposure of the corneal surface and corneal ulceration due to impaired blink; therefore, topical antibiotic ointment or bland lubricant may be indicated to protect the corneal epithelium.

Secondary glaucoma in any Leporid may develop due to antecedent ocular disease such as uveitis, chronic cataract, intraocular hemorrhage, lens instability, or intraocular neoplasia. Treatment is aimed at the underlying cause, but ocular hypotensive medications (see above) can also be prescribed. In eyes with primary or secondary glaucoma in which medications cannot reduce IOP, enucleation (surgical removal of the eye) is indicated to ensure the animal's long-term comfort.

Fig. 42.15 Chronic bilateral buphthalmos associated with glaucoma in a domestic rabbit. Note the dilation of both pupils. Image courtesy of Bret A. Moore, DVM, PhD, DACVO

Diseases of the Uvea

Uveitis

Naturally-occurring uveal inflammation is relatively common in domestic rabbits and can be a secondary consequence of hematogenous or local spread of infectious diseases associated with *Pasteurella* spp. or *Staphylococcus* spp., or may be associated with non-specific systemic inflammatory disease or disseminated or metastatic neoplasia. There are also rare reports of uveitis in association with rabbit tuberculosis (Flatt 1974) and pleural effusion disease, a coronaviral infection (Fledelius et al. 1978). The most prominent and most frequent cause of uveitis in rabbits is infection with the microsporidial protozoan organism, *Encephalitozoon cuniculi*. *E. cuniculi* can be horizontally transmitted between adult animals via ingestion or inhalation of infective spores, typically from infected urine, or vertically via transplacental transmission.

The most common non-ocular clinical manifestations of *E. cuniculi* infection in Leporids include neurologic and renal disease which may be severe and fatal, though many domestic and wild rabbits or hares are seropositive and may carry the organism asymptomatically. The factor(s) that predispose to development of clinical disease are not understood. Furthermore, there is no known correlation between serum antibody titers and viral shedding, nor between antibodies and

severity of lesions observed postmortem (Harcourt-Brown 2004). Numerous studies have been conducted to determine the seroprevalence of *E. cuniculi* among clinically healthy Leporid populations, with results that may vary by region or by population (Table 42.3). Some studies involving pet rabbit populations did confirm a generally higher prevalence of seropositivity in subpopulations of rabbits with active clinical signs consistent with Encephalitozoonosis, including those with uveitis or ocular signs (Dipineto et al. 2008; Jeklová et al. 2019; Künzel and Joachim 2010; Lavazza et al. 2016). Polymerase chain reaction (PCR) assays looking for the organism in the urine or feces of animals with suspected Encephalitozoonosis may be of value, but false negatives may be encountered due to the unpredictable and intermittent shedding of infectious spores (Hedley 2016). It's also noteworthy that other Encephalitozoon species like *E. hellem* and *E. intestinalis* have been identified and linked to pathology and disease in wild Leporids like the European brown hare (Lepus europaeus) (De Bosschere et al. 2007).

Encephalitozoon cuniculi has been shown to localize to numerous ocular tissues including the periocular connective tissue, sclera, cornea, uvea, and retina (Jeklová et al. 2019). However, unlike other organisms, it has a unique predilection for the lens which may be a more common site of primary infection in rabbits that acquire *E. cuniculi* vertically (Künzel and Joachim 2010; Ozkan et al. 2019). Following infection of the lens, parasitophorous vacuoles may rupture, causing acute lens capsule disruption and a severe granulomatous phacoclastic uveitis, primarily of the anterior uvea (iris and ciliary body) (Künzel and Fisher 2018). In addition to the cardinal clinical indicators of uveitis such as aqueous flare, miosis, and congestion of iris vessels (rubeosis iridis), *E. cuniculi*-induced uveitis often produces white-to-pale-pink nodular granulomas (Fig. 42.16).

Regardless of cause, anterior uveitis may be empirically controlled with ophthalmic corticosteroids in combination with systemic NSAIDs (i.e., meloxicam) (Künzel et al. 2008), but the mainstay of therapy is specific treatment of the underlying cause for uveitis if it can be identified. In rabbits with Encephalitozoonosis, protozoal infection with a benzimidazole (i.e., albendazole, fenbendazole, oxibendazole) is indicated. However, many rabbits with *E. cuniculi*-associated uveitis do not respond favorably to medical treatment (Wolfer et al. 1993) and blinding and/or painful consequences can include secondary glaucoma and progressive cataract. Blinded, painful globes enucleated for presumptive Encephalitozoonosis should be carefully evaluated histologically, and one study has reported the successful and reliable use of immunohistochemistry of ocular tissues to confirm the diagnosis (Giordano et al. 2005). Furthermore, conventional PCR assays have demonstrated high sensitivity for detection of *E. cuniculi* DNA in the lenses of eyes with granulomatous uveitis (Csokai et al. 2009). Surgical removal of *E. cuniculi*-associated cataracts has been reported with varying success (See section "Diseases of the Lens").

Other Uveal Diseases

Uveal neoplasms are uncommon but have been described in rabbits and must be differentiated from the mass-like granulomas observed in eyes infected by *E. cuniculi*. Neoplasms that have been reported include malignant melanoma of the choroid, iris, and ciliary body (Brown and Pearce 1926) as well as lymphosarcoma (Van Zeeland 2017). There is also a report of non-neoplastic intraocular osseous metaplasia of the anterior in an adult female Holland lop, preceded by chronic uveitis and retinal detachment, but the exact pathophysiology in that case is unknown (Enders et al. 2018).

Diseases of the Lens

Cataract

Cataracts (lens opacities) are the most common lens disease in domestic rabbits (Fig. 42.17). Small cataracts of no known visual consequence are occasionally observed in purpose-bred laboratory strains, with studies reporting an overall incidence of 1.9–5.1% among both albino and pigmented strains (Holve et al. 2011; Jeong et al. 2005; Munger et al. 2002). Spontaneous cataracts have been frequently reported in the New Zealand white rabbit (Munger et al. 2002), particularly in inbred colonies (Peng et al. 2015) but are also reported in cross-bred strains. Incidence of age-associated cataracts differs between studies with some citing a higher prevalence in younger animals (<4 months) (Jeong et al. 2005), whereas others cited a higher prevalence in older animals (Munger et al. 2002). Other references surveying client-owned pet rabbits have cited an incidence of lens opacities as high as 17% (Williams 2012). Cataracts that progress to be mature (complete) or hypermature (resorbing) may be at risk for luxation into the anterior chamber or vitreous chamber (Figs. 42.18 and 42.19)

Heritability is likely at least a partial contributor to cataract development in rabbit populations, but extrinsic and environmental factors cannot be ruled out. Exclusively heritable cataract has been described in some purpose-bred domestic rabbits. The Cat-1 and Cat-2 cataract phenotypes described in New Zealand white rabbits demonstrate progressive opacification, but with differing underlying heritability and progression. Cat-1 opacities are inherited recessively and are bilateral, producing faint generalized dullness within the posterior lens at birth, thereafter progressing to complete lens opacification by approximately 2 months of age (Brock et al. 2012). Cat-2 opacities are inherited via an incomplete dominant mechanism with 40–60% penetrance and are often unilateral (Brock et al. 2012).

Table 42.3 Comparative seroprevalences of *Encephalitozoon cuniculi* in healthy Leporids from different geographical regions

Species	Country	Assay	Population	Prevalence	Reference
Oryctolagus cuniculus	United Kingdom	ELISA (Ab)	97 pets	52.00%	Keeble and Shaw (2006)
O. cuniculus	Germany	Unknown	–	45.10%	Ewringmann and Göbel (1999)
O. cuniculus	Italy	ELISA and CIA confirmation	1600 from commercial farms	31.60%	Santaniello et al. (2009)
O. cuniculus	Austria	ELISA (Ab)	40 pets	35.00%	Künzel et al. (2008)
O. cuniculus	Slovakia	IFAT and ELISA (Ab)	75 lab/colony rabbits	21.33%	Balent et al. (2004)
O. cuniculus	Slovakia	IFAT and ELISA (Ab)	47 wild rabbits	44.70%	Balent et al. (2004)
O. cuniculus	Southern Italy	ELISA and CIA confirmation	47 wild rabbits	68.10%	Dipineto et al. (2008)
O. cuniculus	Czech Republic	ELISA (Ab)	62 pets	24.2% (IgM), 51.6% (IgG)	Jeklova et al. (2010)
O. cuniculus	Central Italy	ELISA (Ab)	118 industrial rabbits 10 family farm rabbits 16 zoo rabbits 30 laboratory rabbits 9 pet rabbits	Industrial: 73.70% Family farms: 50.00% Zoo: 100.00% Laboratory: 57.00% Pet: 44.00%	Maestrini et al. (2017)
O. cuniculus	Australia	Indirect IFA	81 wild rabbits, 29 lab rabbits	24.70% wild rabbits, 75.90% lab	Thomas et al. (1997)
O. cuniculus	Taiwan	ELISA and CIA confirmation	155 pets	65.20% ELISA, 60.00% CIA	Tee et al. (2011)
O. cuniculus	Italy	CAI	516 pets	52.91%	Lavazza et al. (2016)
Lepus europaeus	Czech Republic, Austria, Slovakia	indirect IFA	701 wild hares	1.42%	Bártová et al. (2015)

ELISA enzyme-linked Immunosorbent assay, *Ab* antibody, *CIA* carbon immunoassay, *IFAT* indirect immunofluorescent antibody test

As mentioned above (see section "Uveitis"), cataract is also frequently associated with lenticular *E. cuniculi* infection and secondary uveitis (Ashton et al. 1976). *E. cuniculi*-associated uveitis is often difficult to control with medications alone and secondary formation of cataract cannot be reversed medically. Therefore, surgical removal of rabbit cataracts via phacoemulsification has been advocated as the most secure means of preserving vision in an affected eye while mitigating the local ocular infection. This approach is supported by published case reports or small case series describing successful phacoemulsification in domestic rabbits (Wolfer et al. 1993; Wolfer et al. 1995; Felchle and Sigler 2002; Gomes et al. 2018; Stiles et al. 1997). In some cases undergoing phacoemulsification, the irrigation fluids collected from the instrumentation tubing were submitted for PCR and were able to confirm diagnosis of E. cuniculi (Felchle and Sigler 2002).

A recent prospective study of 13 pet rabbits (22 eyes) undergoing phacoemulsification for unilateral or bilateral cataract removal reported more detailed information about surgical approach and outcomes for 12/13 cases (Sanchez et al. 2018). Intraoperative complications were uncommon but included a posterior capsular lens tear in one eye, intraoperative lens luxation in 2 eyes with mature cataracts, and expulsive choroidal hemorrhage in one eye. Three eyes had iris masses (suspected to be granulomas associated with *E. cuniculi*) at the time of surgery, and irrigation fluids in all 3 were PCR positive (whereas fluids from 6 rabbits without iris granulomas were PCR negative). The presence of a granulomatous iridal mass was associated with anterior capsular tears intraoperatively, but these did not ultimately complicate surgery or outcome. Iris hooks were required to facilitate pupil dilation in 2/3 eyes with granulomas that did not respond to topical dilation protocols. Following cataract removal, 17/22 eyes received intraocular lenses (IOL), and 18/22 received a capsular tension ring to inform a related study investigating the optimization of IOL design for rabbits.

In that investigational study, capsular tension ring diameter and streak retinoscopy were used to mathematically model and optimize the necessary dioptric strength and diameter for domestic rabbits (Sanchez et al. 2016). The conclusion was that an IOL should have a diameter of 0.5 mm less than the diameter of an implanted CTR, typically around 13 mm. The ideal dioptric strength to produce postoperative emmetropia was determined to be +58 D.

A common clinical belief among veterinary ophthalmologists and vision scientists is that rabbits

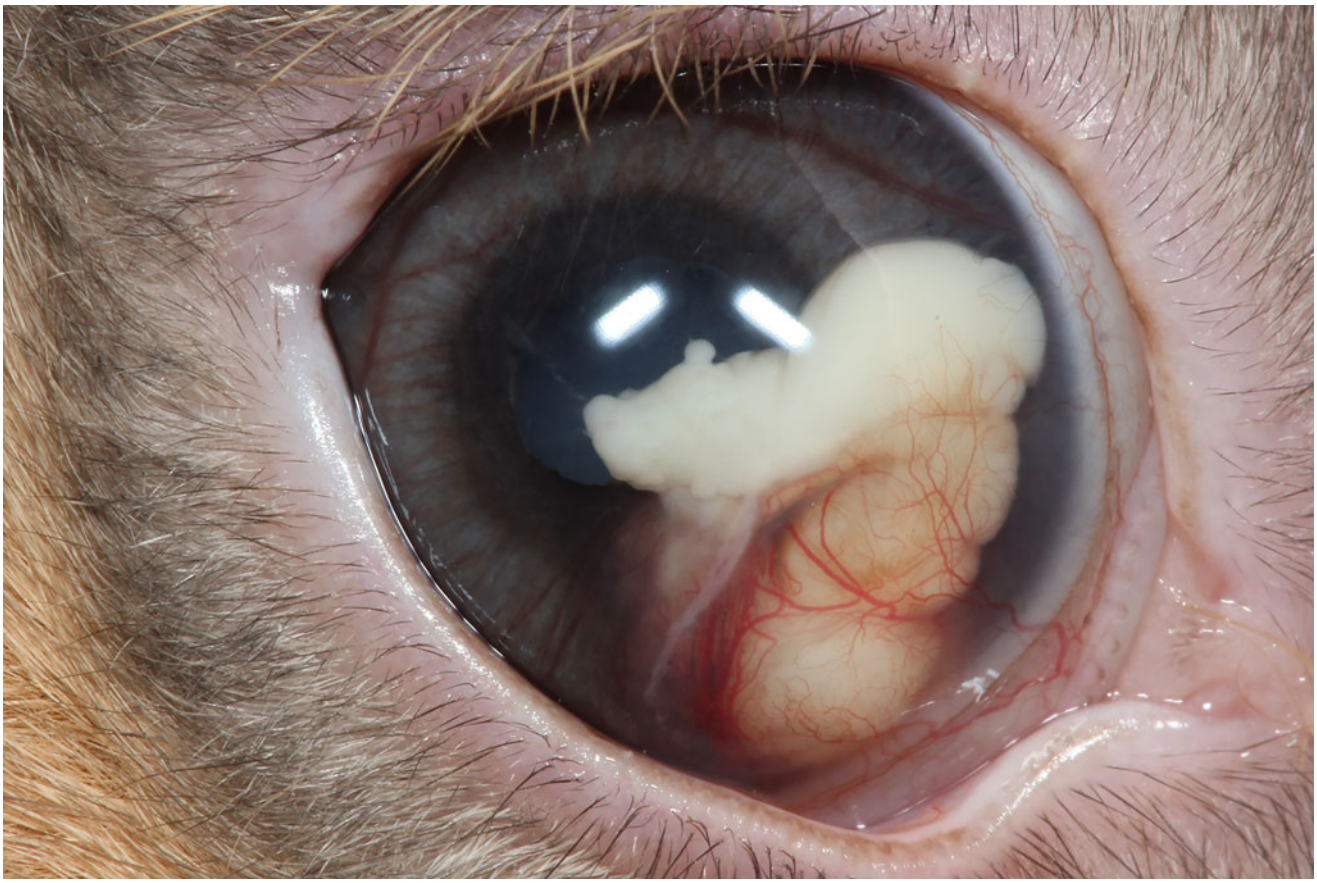

Fig. 42.16 Iridal granuloma and reactive keratitis associated with ocular *Encephalitozoon cuniculi* infection in a domestic rabbit. Image courtesy of Bret A. Moore, DVM, PhD, DACVO

undergoing even routine cataract removal via phacoemulsification are more likely to regenerate lens cortex postoperatively than other species. Investigational studies have demonstrated regeneration of lens cortex following phacoemulsification in young and adult rabbits, with "refilling" of 3/4 of the lens capsule by 2 and 3 months, respectively (Gwon et al. 1992). Similar regrowth was documented in another study evaluating an experimental model of inflammatory cataracts. However, the overall regenerative capacity was lower in these rabbits, which may suggest an effect of underlying cause for cataract on regeneration (Gwon et al. 1993). According to some clinical references, this regrowth may be so robust that it can herniate and displace an IOL postoperatively, leading to vision-threatening complications (Williams 2012). However, in the aforementioned prospective study in 12 rabbits undergoing phacoemulsification, only one eye developed cortical regrowth, qualitatively graded as mild (Sanchez et al. 2018).

Lens-Associated Intraocular Neoplasia

Unique intraocular malignancies have been described in domestic rabbits whose histologic features suggest lens-related trauma as the underlying pathophysiology. In a small case series of two eyes with chronic intraocular inflammation (one with concurrent cataract and secondary glaucoma), a pleomorphic, poorly differentiated, and biologically aggressive mesenchymal neoplasm was identified, originating from the lens (McPherson et al. 2009). In both eyes, chronic inflammation and/or prior trauma were both presumed to be predisposing factors, as reported in the feline literature (Zeiss et al. 2003). In another case report of a rabbit with a 6-year history of unilateral ocular inflammation and phthisis bulbi, enucleation and histopathology revealed an intraocular sarcoma, also originating from the lens (Dickinson et al. 2013). Most recently, a descriptive series of four globes from three rabbits negative for *E. cuniculi* and with known ocular trauma (accidental or iatrogenic secondary to intraocular surgery) were eventually enucleated, revealing a pleomorphic B-cell lymphosarcoma effacing the intraocular structures (Keller et al. 2019). Though there was no known association with systemic neoplasia in any of these cases and while a definitive prognosis is not yet clear, post-traumatic neoplasms should be included for rabbits with anterior segment inflammatory disease and

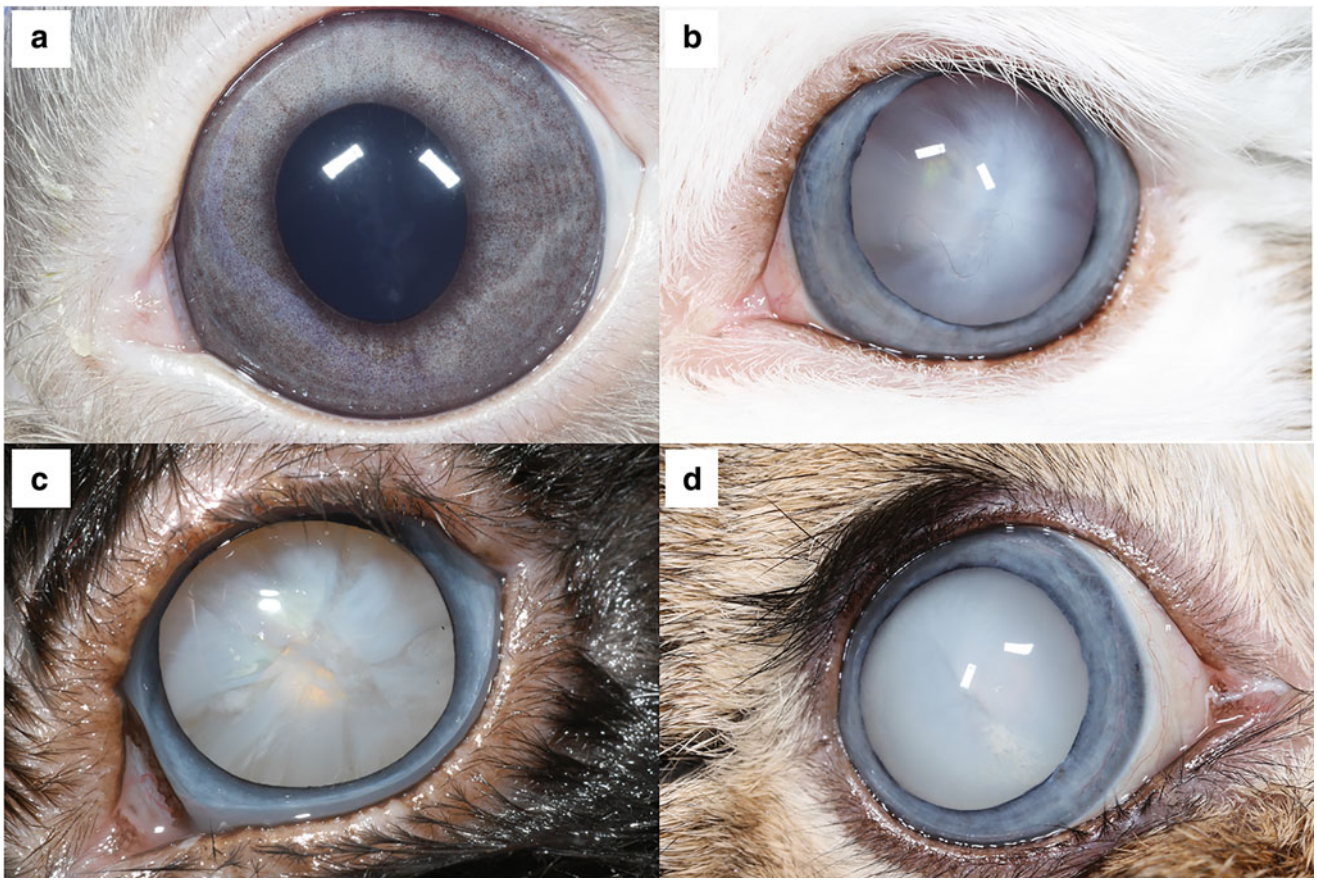

Fig. 42.17 Cataracts of varying stages (incipient (**a**), immature (**b**), and mature (**c**, **d**). Images courtesy of Bret A. Moore, DVM, PhD, DACVO

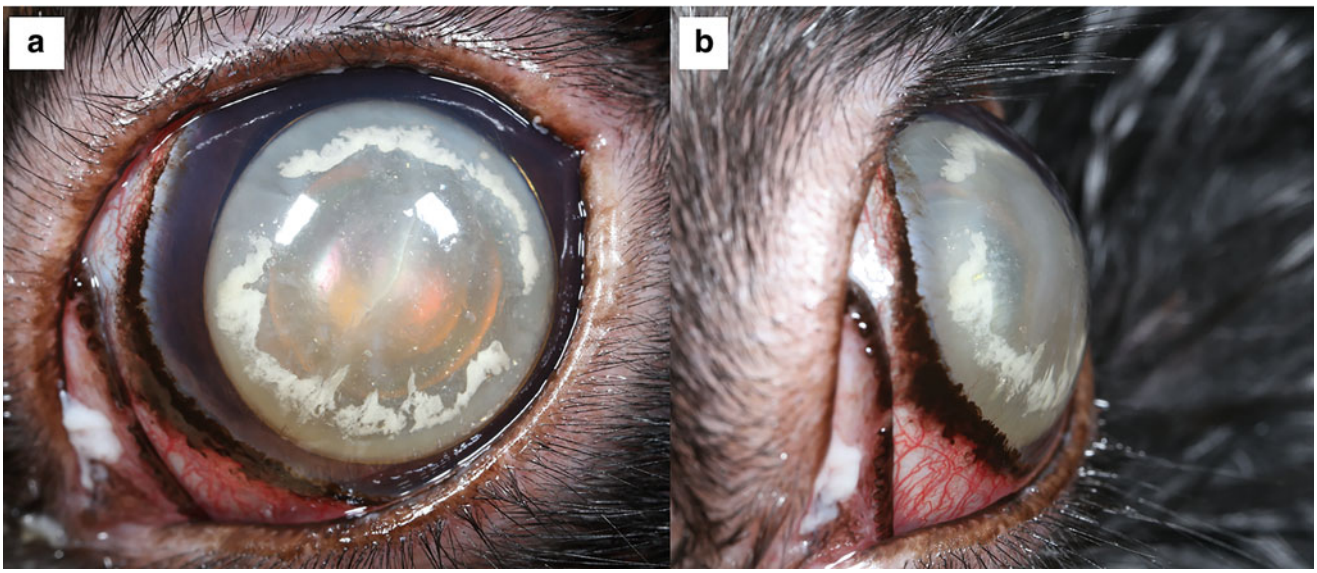

Fig. 42.18 Advanced cataract and anterior luxation of the lens in a domestic rabbit. Image courtesy of Bret A. Moore, DVM, PhD, DACVO

Fig. 42.19 Posterior luxation of the lens with mature cataract in a domestic rabbit. Image courtesy of the University of California Davis Comparative Ophthalmology Service

must be differentiated from *E. cuniculi*-associated disease or other neoplasms.

Diseases of the Posterior Segment

Primary, naturally-occurring diseases of the retina are not commonly reported or described in domestic rabbits or other Leporids. This may be attributed to lack of ability to perform funduscopic examination due to anterior segment pathology, or the relative avascularity of the Leporid retina which may mask subtle retinal disease on funduscopic examination. In this author's experience, multifocal retinal folds may be occasionally observed in the eyes of young purpose-bred New Zealand white and Dutch belted rabbits with no known functional consequence for vision. Functional electroretinographic testing, however, would more definitively identify any associated visual deficits. Furthermore, these folds may spontaneously resolve as affected rabbits grow, suggesting that the folds represent only a transient incongruency in growth rates of the globe and retina, as described in dogs (Barnett 1988). A form of presumed heritable retinal degeneration mimicking some features of human retinitis pigmentosa has also been described in a strain of domestic rabbits (Reichenbach and Baar 1985).

Any form of uveitis that affects that anterior uvea may extend posteriorly into the choroid, causing retinitis and even exudative retinal detachment. Retinitis was observed in one study of immunosuppressed rabbits experimentally infected with *E. cuniculi*, but this may not mimic the conditions and factors associated with natural infection (Leng et al. 1999).

Other Clinical Considerations in the Care and Treatment of Leporidae

Domestic rabbits are increasingly more popular as companion animals in North America and Europe, as well as Asia

and Australia (DeMello 2016). In turn, focused and specialty care of the domestic rabbit is becoming a more critical component of companion animal practice. In the context of medical and surgical treatment of ophthalmic disease, there are special considerations that practitioners must be mindful of in the care of rabbits. Due to lack of published data, it is not clear whether or not these considerations would universally apply to non-domestic Leporidae, but knowledge of these points could be useful in a wildlife medicine context as well.

Antibiotic, Corticosteroid, and Analgesic Use In Rabbits

In general, administration of a topical ophthalmic antibiotic has low risk as systemic absorption and distribution to other tissues is generally minimal. However, in some animals, even low serum concentrations of these antibiotics, particularly if administered for long periods of time (i.e., weeks to months) can lead to dysbiosis of the gastrointestinal tract flora, risking life-threatening enterotoxemia or enterocolitis (Deeb and DiGiacomo 2000). In general, the same precautions taken with systemic antibiotics should be practiced when prescribing ophthalmic antibiotics. Antibiotics that putatively carry higher risk of dysbiosis in Leporids include narrow-spectrum agents targeting gram positive bacteria such as penicillins (including amoxicillin and amoxicillin-clavulanate), clindamycin, lincosamides (lincomycin, clindamycin), cephalosporins (cefazolin, cefpodoxime), and macrolides (erythromycin). Safer choices include fluoroquinolones (except for pradofloxacin), tetracyclines, sulfonamides, gentamicin, fusidic acid, and chloramphenicol (Hedley 2018).

Topical and systemic corticosteroids may be indicated for the treatment of uveitis but should be used very cautiously due to the risks of immunosuppression, particularly in the gastrointestinal tract and in the inadvertent activation/reactivation of subclinical Pasteurellosis or Encephalitozoonosis (Hillyer 1994). In general, topical and systemic NSAIDs like diclofenac, ketorolac, and meloxicam can be used safely at recommended frequencies and doses. Additional analgesia can be safely achieved using systemic butorphanol, buprenorphine, and tramadol (Johnson 2012).

Anesthetic and Surgical Considerations for Ophthalmic Procedures

Most sedatives are not known to have considerable adverse effects on the rabbit eye. However, in one study of 16 adult New Zealand white rabbits, significant increases in IOP were observed for up to 20 minutes following administration of combinations of ketamine-acepromazine and ketamine-diazepam IM (Ghaffari and Moghaddassi 2010).

In cases where general anesthesia is required for a surgical procedure involving a rabbit eye, there are important species-related factors that both the anesthetist and surgeon should be aware of. Perhaps the most noteworthy pharmacologic consideration involves the use of a neuromuscular blocking agent (i.e., atracurium), required for ocular positioning for corneal and intraocular surgery. In a recent retrospective study of 14 rabbits undergoing general anesthesia for ocular surgery, noteworthy decreases in arterial blood pressure and body temperature (developing into severe intraoperative hypothermia in two animals) were observed, typically within 5 minutes following administration of intravenous atracurium at 0.44 mg/kg (Adami et al. 2019). While this effect was transient in many animals, it was temporarily markedly severe in some and refractory to fluid supplementation and vasopressors. Furthermore, it did not appear to be dose-dependent. Reversal of the atracurium with intramuscular neostigmine at 0.01 mg/kg was required in 12/14 rabbits and some required a second dose to facilitate recovery.

Surgical considerations when operating on the rabbit eye must also be kept in mind, particularly when performing orbital procedures like enucleation or exenteration. As in other species, an oculocardiac reflex exists in rabbits wherein manipulation of the globe and/or orbital tissues can induce bradycardia and hypotension. A study evaluating the effect of globe compression in conscious rabbits confirmed this effect on the heart rate when performing retropulsion of the globes (Turner Giannico et al. 2014). However, this study confirmed that this change in heart rate was more common with bilateral globe compression, a scenario that is not commonly encountered intraoperatively. Furthermore, the response of a conscious animal does not completely recapitulate that of an anesthetized animal so this should also be kept in mind when interpreting these results.

One of the most important considerations any surgeon should be mindful of in rabbits involves the risk of intraoperative hemorrhage when performing enucleation or exenteration. As described earlier in this chapter, rabbits possess a robust orbital venous sinus ventrally and medially behind the base of the third eyelid and Harderian gland, extending posteriorly. Due to its location, intraoperative disruption of this structure is commonly encountered with transection and removal of the third eyelid. If inadvertently lacerated intraoperatively, this plexus can bleed profusely and, if uncontrolled, hemorrhage can be life-threatening. Ligation or cauterization of this plexus may be ineffective unless the site of hemorrhage can be easily identified and clamped. If plexus compromise is encountered, the surgeon should immediately apply digital pressure to the area of hemorrhage using gauze sponges or cotton-tipped applicators. If topical bovine thrombin is available, it can be applied directly to the area under the gauze, or into a gelatin sponge at the area of digital compression. Firm pressure should be maintained for at least 10–15 minutes. Placement of absorbable gelatin sponges can be placed following release of digital pressure and removal of gauze sponges, and left in the orbital closure to facilitate clot formation. Recently, a

novel technique for enucleation in rabbits was described, advocating the use of an electrosurgical bipolar sealing device with a dolphin tip to pre-emptively ligate the orbital venous plexus (Moore et al. n.d.). Following modified transpalpebral dissection, the vessel-sealing device was used to transect the extraocular muscles and the optic nerve and retractor bulbi muscle. Finally, the base of the third eyelid was identified and transected using the sealer, carefully avoiding the venous plexus.

Enucleation sites should be closed in three layers (fascial, subcutaneous, and intradermal/subcuticular). Skin sutures should be avoided as rabbits will scratch at them and risk self-trauma and compromise of the surgical site, and because placement of Elizabethan collars is not practical in rabbits (Hillyer 1994; Diehl and McKinnon 2016).

Notes on the Ochotonidae

Compared to rabbits and hares, there is a paucity of literature specifically addressing the ocular morphology and naturally-occurring ocular diseases of the pikas. As stated above, this is likely a function of their relatively restricted global distribution. However, the pikas are of particular interest in an ecological context, as they are believed to represent important indicator species for climate change in North America and Asia. Throughout the Western United States, the American pika (*Ochotona princeps*), lives in a relatively restricted habitat range, concentrated mostly in the lower elevations of the Rocky and Sierra Nevada mountain ranges (Ray et al. 2012). In Asia, nearly half of the native pika species live in a similar habitat. There is a rapidly-growing body of scientific literature looking at the impacts that climate change have on the contraction of the pikas' natural habitats, with warming temperatures forcing these species into higher elevations (Ray et al. 2012). The net result has been a reduction in population numbers, particularly in the American Great Basin (Yandow et al. 2015).

Compared to the Leporid skull, those of pikas are not as arched, with well-developed pterygoid and masseter muscles, though muscular volumes may vary with species, particularly with respect to altitude (Matsunami et al. 2008; Liao et al. 2006). The orbits and eyes are also oriented laterally, though the globes are comparatively smaller than in rabbits and hares (Chapman and Flux 1990). The axial globe length is between 8–9 mm and the corneal diameter is 16 mm (Akaishi et al. 1995). A Harderian gland and orbital venous sinus are also present (Sakai 1981).

In one description of funduscopic examination findings in the Afghan pika (*Ochotona rufescens*), the investigators recognized remarkably little pharmacologic dilation in the pikas they examined following use of topical atropine. Furthermore, topical pilocarpine, a direct-acting parasympathomimetic, also had no subjective effect on pupil size (Yokota et al. 1983). In that description, a retinal vasculature was not distinguishable on ophthalmoscopy and choroidal vessels were only vaguely visible (Yokota et al. 1983). The retinal pigmented epithelium was pigmented and created a reddish-brown background to the fundus which may have complicated identification of vessels. However, another morphological study of two Afghan pikas failed to distinguish a retinal vascular network on light or electron microscopy (Luo et al. 1999). Electroretinographic function has been measured, demonstrating a diminutive a-wave, but a b-wave with a similar amplitude to that of albino rats and rabbits. The optic disk has is located approximately 30° superior to the posterior pole (Akaishi et al. 1995).

Subsequent detailed investigations examining the morphology of the Afghan pika retina have been published. In one survey of adult animals, the pika retina contained approximately 170,000 retinal ganglion cells and the optic nerve comprised between 160,000 and 190,000 fibers, markedly fewer than in the rabbit; and optic nerve fibers were also smaller in diameter than in the rabbit. However, based on the presence of a horizontal region of ganglion cell density (a visual streak) within the central retina and inferior to the optic disk, the acuity of pikas in this study was estimated to be higher than in rabbits at 7.3 cpd, which approaches the acuity of domestic cats. Morphologically, the pika visual streak has a peak retinal ganglion cell density just slightly dorsonasal to the retinal center.

Naturally-occurring ocular disease is scarcely discussed in the scientific literature. Cases of blepharitis are not published, but it's noteworthy that pikas are susceptible to ectoparasites such as *Demodex cuniculi* and *Otodectes* spp., which could cause cutaneous disease that affects the eyelids (Delaney et al. 2018). Ocular discharge and sinking of the eyes have also been observed in pikas with Vitamin A and/or D deficiency (Haga 1960).

Bibliography

Abrams K, Brooks D, Funk R, Theran P (1990) Evaluation of the Schirmer tear test in clinically normal rabbits. Am J Vet Res 51: 1912–1913

Adami C, Sanchez RF, Monticelli P (2019) Use of atracurium and its reversal with neostigmine in 14 pet rabbits undergoing ophthalmic surgery: a retrospective study. Vet Rec 184

Adel A (2011) Two dimensional sonography biometry evaluation of rabbits. Glob Vet 6:220–222

Agnoletti F et al (2014) First reporting of methicillin-resistant Staphylococcus aureus (MRSA) ST398 in an industrial rabbit holding and in farm-related people. Vet Microbiol 170:172–177

Akaishi Y, Uchiyama H, Ito H, Shimizu Y (1995) A morphological study of the retinal ganglion cells of the Afghan pika (Ochotona rufescens). Neurosci Res 22:1–12. https://doi.org/10.1016/0168-0102(94)00873-e

Allgoewer I, Malho P, Schulze H, Schäffer E (2008) Aberrant conjunctival stricture and overgrowth in the rabbit. Vet Ophthalmol 11:18–22

Almería S, Calvete C, Pagés A, Gauss C, Dubey J (2004) Factors affecting the seroprevalence of Toxoplasma gondii infection in wild rabbits (Oryctolagus cuniculus) from Spain. Vet Parasitol 123:265–270

Andrew SE (2001) Ocular manifestations of feline herpesvirus. J Feline Med Surg 3:9–16. https://doi.org/10.1053/jfms.2001.0110

Andrew SE (2002) Corneal diseases of rabbits. Vet Clin North Am Exot Anim Pract 5:341–356

Ashton N, Cook C, Clegg F (1976) Encephalitozoonosis (nosematosis) causing bilateral cataract in a rabbit. Br J Ophthalmol 60:618–631

Aulakh G, Singh S, Singla L, Singla N (2003) Pathology and therapy of natural notoedric acariosis in rabbits. J Vet Parasitol 17:127–129

Balent P, Halanova M, Sedlakova T, Valencakova A, CislakovÁ L (2004) Encephalitozoon cuniculi infection in rabbits and laboratory mice in eastern Slovakia. Bull Vet Inst 48:113–116

Bar-Ilan A (1984) Diurnal and seasonal variations in intraocular pressure in the rabbit. Exp Eye Res 39:175–181

Barnett K (1988) Inherited eye disease in the dog and cat. J Small Anim Pract 29:462–475

Barrio IC, Bueno CG, Banks PB, Tortosa FS (2010) Prey naiveté in an introduced prey species: the wild rabbit in Australia. Behav Ecol 21:986–991

Bártová E, Marková J, Sedlak K (2015) Prevalence of antibodies to Encephalitozoon cuniculi in European hares (Lepus europaeus). Ann Agric Environ Med 22

Bazior-Langhan J (2012) Disorders of the orbit and eyelids in rabbits. Point Vétérinaire 43:66–70

Bedard KM (2018) Ocular surface disease of rabbits. Medical and Surgical Management of Ocular Surface Disease in Exotic Animals, An Issue of Veterinary Clinics of North America: Exotic Animal Practice 22:1

Bergin IL et al (2009) Novel calicivirus identified in rabbits, Michigan, USA. Emerg Infect Dis 15:1955

Bertagnoli S, Marchandeau S (2015) Myxomatosis. Revue scientifique et technique (International Office of Epizootics) 34:539–547

Björkman N, Nicander L, Schantz B (1960) On the histology and ultrastructure of the Harderian gland in rabbits. Z Zellforsch Mikrosk Anat 52:93–104

Block W, Upton C, McFadden G (1985) Tumorigenic poxviruses: genomic organization of malignant rabbit virus, a recombinant between Shope fibroma virus and myxoma virus. Virology 140:113–124

Botha M, Petrescu-Mag IV, Hettig A (2014) Genetic disorders in domestic rabbits (Oryctolagus cuniculus). Rabbit Genetics 4:7–47

Bourguet A et al (2016) Keratomycosis in a pet rabbit (Oryctolagus cuniculus) treated with topical 1% terbinafine ointment. Vet Ophthalmol 19:504–509

Bourguet A et al (2019) Conjunctival bacterial and fungal flora and cutaneous fungal flora in healthy domestic rabbits (Oryctolagus cuniculus). J Small Anim Pract. https://doi.org/10.1111/jsap.12989

Bozkir G, Bozkir M, Dogan H, Aycan K, Güler B (1997) Measurements of axial length and radius of corneal curvature in the rabbit eye. Acta Med Okayama 51:9–11

Brabb T, Di Giacomo RF (2012) The laboratory rabbit, guinea pig, hamster, and other rodents. Elsevier, pp 365–413

Brock K, Gallaugher L, Bergdall VK, Dysko RC (2012) The laboratory rabbit, guinea pig, hamster, and other rodents. Elsevier, pp 503–528

Bromberg NM (2002) Cyanoacrylate tissue adhesive for treatment of refractory corneal ulceration. Vet Ophthalmol 5:55–60

Brown C (2006) Nasolacrimal duct lavage in rabbits. Lab Anim 35:22–24

Brown WH, Pearce L (1926) Melanoma (sarcoma) of the eye in a syphilitic rabbit. J Exp Med 43:807–813

Buckley P, Lowman DM (1979) Chronic non-infective conjunctivitis in rabbits. Lab Anim 13:69–73

Burgalassi S, Panichi L, Chetoni P, Saettone MF, Boldrini E (1999) Development of a simple dry eye model in the albino rabbit and evaluation of some tear substitutes. Ophthalmic Res 31:229–235

Burling K, Murphy C, Curiel J, Koblik P, Bellhorn R (1991) Anatomy of the rabbit nasolacrimal duct and its clinical implications. Prog Vet Comp Ophthalmol 1:33–40

Capello V (2016a) Surgical treatment of facial abscesses and facial surgery in pet rabbits. Vet Clin Exot Anim Pract 19:799–823

Capello V (2016b) Surgical treatment of prolapse of the deep lacrimal gland in a pet rabbit. J Exot Pet Med 25:44–51

Castle W, Nachtsheim H (1933) Linkage interrelations of three genes for rex (short) coat in the rabbit. Proc Natl Acad Sci U S A 19:1006

Chapman JA, Flux JE (1990) Rabbits, hares and pikas: status survey and conservation action plan. IUCN

Chen S, Quesenberry KE (2006) Rabbits. Saunders Manual Small Anim Pract 1858

Choudhury BP (1980) Binocular depth vision in the rabbit. Exp Neurol 68:453–464. https://doi.org/10.1016/0014-4886(80)90100-4

Collewijn H (1977) Eye- and head movements in freely moving rabbits. J Physiol 266:471–498. https://doi.org/10.1113/jphysiol.1977.sp011778

Cooper SC, McLellan GJ, Rycroft AN (2001) Conjunctival flora observed in 70 healthy domestic rabbits (Oryctolagus cuniculus). Vet Rec 149:232–235. https://doi.org/10.1136/vr.149.8.232

Csokai J et al (2009) Diagnostic markers for encephalitozoonosis in pet rabbits. Vet Parasitol 163:18–26

Danos O, Georges E, Orth G, Yaniv M (1985) Fine structure of the cottontail rabbit papillomavirus mRNAs expressed in the transplantable VX2 carcinoma. J Virol 53:735–741

Darzi MM, Mir MS, Shahardar RA, Pandit BA (2007) Clinico-pathological, histochemical and therapeutic studies on concurrent sarcoptic and notoedric acariosis in rabbits (Oryctolagus cuniculus). Veterinarski arhiv 77:167–175

Davidheiser RH, Figge FH (1958) Comparison of porphyrin producing enzyme activities in harderian glands of mice and other rodents. Proc Soc Exp Biol Med 97:775–778

Davis FA (1929) The anatomy and histology of the eye and orbit of the rabbit. Trans Am Ophthalmol Soc 27:400–402

De Bosschere H, Wang Z, Orlandi PA (2007) First diagnosis of Encephalitozoon intestinalis and E. Hellem in a European brown hare (Lepus europaeus) with kidney lesions. Zoonoses Public Health 54:131–134. https://doi.org/10.1111/j.1863-2378.2007.01034.x

Deeb BJ, DiGiacomo RE (2000) Respiratory diseases of rabbits. Vet Clin North Am Exot Anim Pract 3:465–480

Delaney MA, Treuting PM, Rothenburger JL (2018) Pathology of wildlife and zoo animals. Elsevier, pp 481–498

DeMello M (2016) Companion animals in everyday life. Springer, pp 91–107

Dickinson R, Bauer B, Gardhouse S, Grahn B (2013) Intraocular sarcoma associated with a rupture lens in a rabbit (Oryctolagus cuniculus). Vet Ophthalmol 16:168–172. https://doi.org/10.1111/vop.12049

Diehl KA, McKinnon J-A (2016) Eye removal surgeries in exotic pets. Vet Clin North Am Exot Anim Pract 19:245–267. https://doi.org/10.1016/j.cvex.2015.08.003

Digiacomo RF et al (1984) Clinical course and treatment of venereal spirochaetosis in New Zealand white rabbits. Br J Vener Dis 60:214–218. https://doi.org/10.1136/sti.60.4.214

Digiacomo RF et al (1985) Chronicity of infection with Treponema paraluis-cuniculi in New Zealand white rabbits. Genitourin Med 61:156–164. https://doi.org/10.1136/sti.61.3.156

DiGiacomo R, Jones C, Wathes C (1987) Transmission of Pasteurella multocida in rabbits. Lab Anim Sci 37:621–623

Ding C, Huang J, MacVeigh-Aloni M, Lu M (2011) Not all lacrimal epithelial cells are created equal—heterogeneity of the rabbit lacrimal gland and differential secretion. Curr Eye Res 36:971–978
Dipineto L et al (2008) Serological survey for antibodies to Encephalitozoon cuniculi in pet rabbits in Italy. Zoonoses Public Health 55:173–175
Donzel E et al (2010) Luxation de la glande de Harder chez un lapin bélier 45:155–160. https://doi.org/10.1016/j.anicom.2010.08.001
Doughty MJ (1994) The cornea and corneal endothelium in the aged rabbit. Optom Vis Sci 71:809–818
Doughty MJ (2018) Tear film stability and Tear Break Up Time (TBUT) in laboratory rabbits—a systematic review. Curr Eye Res 43:961–964
Durand-Cavagna G, Hubert M-F, Gerin G, Molon-Noblot S (1998) Spontaneous pre-Descemet's membrane corneal opacities in rabbits. Comp Med 48:310–313
Enders AM, Donovan TA, van der Woerdt A (2018) Pathology in practice. J Am Vet Med Assoc 253:991–994
Eshar D, Wyre N, Schoster J (2011) Use of collagen shields for treatment of chronic bilateral corneal ulcers in a pet rabbit. J Small Anim Pract 52:380–383
Ewringmann A, Göbel T (1999) Untersuchungen zur klinik und therapie der encephalitozoonose beim heimtierkaninchen. Kleintierpraxis 44:357–372
Felchle LM, Sigler RL (2002) Phacoemulsification for the management of Encephalitozoon cuniculi-induced phacoclastic uveitis in a rabbit. Vet Ophthalmol 5:211–215. https://doi.org/10.1046/j.1463-5224.2002.00240.x
Fenner F (2010) Deliberate introduction of the European rabbit, Oryctolagus cuniculus, into Australia. Rev Sci Tech 29:103
Fenner F, Ratcliffe FN (1965) Myxomatosis. Myxomatosis
Flatt RE (1974) The biology of the laboratory rabbit. Elsevier, pp 193–236
Fledelius H, Bruun L, Fennestad K, Andersen SR (1978) Uveitis in rabbits with pleural effusion disease: clinical and histopathological observations. Acta Ophthalmol 56:599–606
Florin M, Rusanen E, Haessig M, Richter M, Spiess BM (2009) Clinical presentation, treatment, and outcome of dacryocystitis in rabbits: a retrospective study of 28 cases (2003–2007). Vet Ophthalmol 12:350–356
Flux JE, Angermann R (1990) The hares and jackrabbits. In: Rabbits, hares and pikas. Status survey and conservation action plan. IUCN, pp 61–94
Ford MM (2004) Antifungals and their use in veterinary ophthalmology. Vet Clin Small Anim Pract 34:669–691
Fox J, Shalev M, Beaucage C, Smith M (1979) Congenital entropion in a litter of rabbits. Lab Anim Sci 29:509–511
Freddo TF, Bartels S, Barsotti M, Kamm RD (1990) The source of proteins in the aqueous humor of the normal rabbit. Invest Ophthalmol Vis Sci 31:125–137
Gama A et al (2016) First report of Thelazia callipaeda infection in wild European rabbits (Oryctolagus cuniculus) in Portugal. Parasit Vectors 9. https://doi.org/10.1186/s13071-016-1526-1
Gao H et al (2006) Intravitreal moxifloxacin: retinal safety study with electroretinography and histopathology in animal models. Invest Ophthalmol Vis Sci 47:1606–1611
Gardhouse S et al (2017) Pharmacokinetics and safety of ceftiofur crystalline free acid in New Zealand White rabbits (Oryctolagus cuniculus). Am J Vet Res 78:796–803
Garibaldi B, Goad MP (1988) Lipid keratopathy in the Watanabe (WHHL) rabbit. Vet Pathol 25:173–174
Ghaffari MS, Moghaddassi AP (2010) Effects of ketamine-diazepam and ketamine-acepromazine combinations on intraocular pressure in rabbits. Vet Anaesth Analg 37:269–272. https://doi.org/10.1111/j.1467-2995.2010.00531.x
Giordano C et al (2005) Immunohistochemical identification of Encephalitozoon cuniculi in phacoclastic uveitis in four rabbits. Vet Ophthalmol 8:271–275. https://doi.org/10.1111/j.1463-5224.2005.00394.x
Goldstein SM, Katowitz JA, Syed NA (2006) The histopathologic effects of balloon dacryoplasty on the rabbit nasolacrimal duct. J Pediatr Ophthalmol Strabismus 10:333–335. https://doi.org/10.1016/j.jaapos.2006.03.004
Gomes FE, De Matos R, Ledbetter E (2018) Phacoemulsification of bilateral cataracts in two pet rabbits. Open Vet J 8:125. https://doi.org/10.4314/ovj.v8i2.2
Graham JE (2014) Lagomorpha (pikas, rabbits, and hares). Fowler's Zoo Wildl Anim Med 8:375–384
Grest P, Albicker P, Hoelzle L, Wild P, Pospischil A (2002) Herpes simplex encephalitis in a domestic rabbit (Oryctolagus cuniculus). J Comp Pathol 126:308–311
Grinninger P et al (2012) Eosinophilic keratoconjunctivitis in two rabbits. Vet Ophthalmol 15:59–65. https://doi.org/10.1111/j.1463-5224.2011.00920.x
Gürkan T, Hayat A (2005) Evaluation of the Schirmer and phenol red thread tests for measuring tear secretion in rabbits. Vet Rec 156:485–487
Gwin R, Gelatt K (1977) Bilateral ocular lipidosis in a cottontail rabbit fed an all-milk diet. J Am Vet Med Assoc 171:887
Gwon A (2006) Lens regeneration in mammals: a review. Surv Ophthalmol 51:51–62. https://doi.org/10.1016/j.survophthal.2005.11.005
Gwon A, Gruber L, Mundwiler K (1990) A histologic study of lens regeneration in aphakic rabbits. Invest Ophthalmol Vis Sci 31:540–547
Gwon A, Jones R, Gruber L, Mantras C (1992) Lens regeneration in juvenile and adult rabbits measured by image analysis. Invest Ophthalmol Vis Sci 33:2279–2283
Gwon A, Gruber L, Mantras C, Cunanan C (1993) Lens regeneration in New Zealand albino rabbits after endocapsular cataract extraction. Invest Ophthalmol Vis Sci 34:2124–2129
Haga R (1960) Observations on the ecology of the Japanese pika. J Mammal 41:200–212
Hagen KW (1966) Spontaneous papillomatosis in domestic rabbits. Bulletin Wildl Dis Assoc 2:108–110
Ham BM, Cole RB, Jacob JT (2006) Identification and comparison of the polar phospholipids in normal and dry eye rabbit tears by MALDI-TOF mass spectrometry. Invest Ophthalmol Vis Sci 47:3330–3338
Hanna BL, Sawin PB, Sheppard LB (1962) Recessive buphthalmos in the rabbit. Genetics 47:519
Harcourt-Brown FM (2004) Encephalitozoon cuniculi infection in rabbits. Seminars Avian Exot Pet Med 13:86–93. https://doi.org/10.1053/j.saep.2004.01.004
Hawkins MG (2014) Advances in exotic mammal clinical therapeutics. J Exot Pet Med 23:39–49
Hedley J (2016) BSAVA Congress Proceedings 2016. BSAVA Library, pp 50–51
Hedley J (2018) Antibiotic usage in rabbits and rodents. In Pract 40:230–237
Hermans K, Devriese L, Haesebrouck F (2003) Rabbit staphylococcosis: difficult solutions for serious problems. Vet Microbiol 91:57–64
Hillyer EV (1994) Pet rabbits. Vet Clin North Am Small Anim Pract 24:25–65. https://doi.org/10.1016/s0195-5616(94)50002-0
Hinton M (1977) Treatment of purulent staphylococcal conjunctivitis in rabbits with autogenous vaccine. Lab Anim 11:163–164
Hittmair KM, Tichy A, Nell B (2014a) Ultrasonography of the Harderian gland in the rabbit, guinea pig, and chinchilla. Vet Ophthalmol 17:175–183. https://doi.org/10.1111/vop.12063

Hittmair KM, Tichy A, Nell B (2014b) Ultrasonography of the Harderian gland in the rabbit, guinea pig, and chinchilla. Vet Ophthalmol 17:175–183
Holve DL, Mundwiler KE, Pritt SL (2011) Incidence of spontaneous ocular lesions in laboratory rabbits. Comp Med 61:436–440
Hughes A (1971a) Topographical relationships between the anatomy and physiology of the rabbit visual system. Doc Ophthalmol 30:33–159. https://doi.org/10.1007/bf00142518
Hughes A (1971b) Topographical relationships between the anatomy and physiology of the rabbit visual system. Doc Ophthalmol 30:33–159
Jacobs GH (1993) The distribution and nature of colour vision among the mammals. Biol Rev 68:413–471. https://doi.org/10.1111/j.1469-185x.1993.tb00738.x
Janssens G, Simoens P, Muylle S, Lauwers H (1999) Bilateral prolapse of the deep gland of the third eyelid in a rabbit: diagnosis and treatment. Comp Med 49:105–109
Jašarević E et al (2010) Masticatory loading, function, and plasticity: a microanatomical analysis of mammalian circumorbital soft-tissue structures. Anat Rec 293:642–650
Jeklova E et al (2010) Usefulness of detection of specific IgM and IgG antibodies for diagnosis of clinical encephalitozoonosis in pet rabbits. Vet Parasitol 170:143–148
Jeklová E, Levá L, Kummer V, Jekl V, Faldyna M (2019) Immunohistochemical detection of encephalitozoon cuniculi in ocular structures of immunocompetent rabbits. Animals 9:988. https://doi.org/10.3390/ani9110988
Jeong MB et al (2005) Spontaneous ophthalmic diseases in 586 New Zealand white rabbits. Exp Anim 54:395–403
Jin L et al (2008a) An outbreak of fatal herpesvirus infection in domestic rabbits in Alaska. Vet Pathol 45:369–374
Jin L et al (2008b) Characterization of a novel alphaherpesvirus associated with fatal infections of domestic rabbits. Virology 378:13–20
Johnson DH (2012) Emergency presentations of the exotic small mammalian herbivore trauma patient. J Exot Ped Med 21:300–315. https://doi.org/10.1053/j.jepm.2012.09.006
Johnson M, McLaren JW, Overby DR (2017) Unconventional aqueous humor outflow: a review. Exp Eye Res 158:94–111
Juliusson B et al (1994) Complementary cone fields of the rabbit retina. Invest Ophthalmol Vis Sci 35:811–818
Keeble E, Shaw D (2006) Seroprevalence of antibodies to Encephalitozoon cuniculi in domestic rabbits in the United Kingdom. Vet Rec 158:539–544
Keller RL, Hendrix DVH, Greenacre C (2007a) Shope fibroma virus keratitis and spontaneous cataracts in a domestic rabbit. Vet Ophthalmol 10:190–195. https://doi.org/10.1111/j.1463-5224.2007.00531.x
Keller RL, Hendrix DV, Greenacre C (2007b) Shope fibroma virus keratitis and spontaneous cataracts in a domestic rabbit. Vet Ophthalmol 10:190–195
Keller KA et al (2019) Post-traumatic ocular lymphoma in three rabbits (Oryctolagus cuniculus). J Exot Pet Med 28:154–161. https://doi.org/10.1053/j.jepm.2018.02.041
Kelly A (2020) Welfare implications for hares, Lepus timidus hibernicus, taken from the wild for licensed hare coursing in Ireland. Animals 10:163
Kern TJ (1989) Ocular disorders of rabbits, rodents, and ferrets. In: Current veterinary therapy. WB Saunders, Philadelphia, pp 681–685
Kern TJ (1997) Rabbit and rodent ophthalmology. Seminars Avian Exot Pet Med 6:138–145. https://doi.org/10.1016/s1055-937x(97)80021-7
Kim J et al (2013) Surgical correction of aberrant conjunctival overgrowth in a rabbit: a case report. Irish Vet J 66:18. https://doi.org/10.1186/2046-0481-66-18
Kolker AE, Moses RA, Constant MA, Becker B (1963) The development of glaucoma in rabbits. Invest Ophthalmol Vis Sci 2:316–321
Korb DR et al (1994) Tear film lipid layer thickness as a function of blinking. Cornea 13:354–359
Korb DR et al (1998) Lacrimal gland, tear film, and dry eye syndromes, vol 2. Springer, pp 305–308
Kostolich M, Panciera RJ (1992) Thymoma in a domestic rabbit. Cornell Vet 82:125–129
Kouchi M, Ueda Y, Horie H, Tanaka K (2006) Ocular lesions in Watanabe heritable hyperlipidemic rabbits. Vet Ophthalmol 9:145–148
Künzel F, Fisher PG (2018) Clinical signs, diagnosis, and treatment of Encephalitozoon cuniculi infection in rabbits. Vet Clin North Am Exot Anim Pract 21:69–82. https://doi.org/10.1016/j.cvex.2017.08.002
Künzel F, Joachim A (2010) Encephalitozoonosis in rabbits. Parasitol Res 106:299–309. https://doi.org/10.1007/s00436-009-1679-3
Künzel F et al (2008) Clinical symptoms and diagnosis of encephalitozoonosis in pet rabbits. Vet Parasitol 151:115–124. https://doi.org/10.1016/j.vetpar.2007.11.005
Künzel F et al (2012) Thymomas in rabbits: clinical evaluation, diagnosis, and treatment. J Am Anim Hosp Assoc 48:97–104
Langner S et al (2010) 7.1 T MRI to assess the anterior segment of the eye. Invest Ophthalmol Vis Sci 51:6575–6581
Lavazza A et al (2016) Serological investigation on encephalitozoon cuniculi in pet rabbits in North-Central Italy. J Exot Pet Med 25:52–59. https://doi.org/10.1053/j.jepm.2015.12.004
Leng L, Štefkovič M, Révajová V, Halanová M, Horváth M (1999) Lethal encephalitozoonosis in cyclophosphamide-treated rabbits. Acta Vet Hung 47:85–93
Lennox AM, Kelleher S (2009) Bacterial and parasitic diseases of rabbits. Vet Clin North Am Exot Anim Pract 12:519–530
Leonard BC, Yañez-Soto B, Raghunathan VK, Abbott NL, Murphy CJ (2016) Species variation and spatial differences in mucin expression from corneal epithelial cells. Exp Eye Res 152:43–48
Liao J, Zhang Z, Liu N (2006) Altitudinal variation of skull size in Daurian pika (Ochotona daurica Pallas, 1868). Acta Zool Acad Sci Hung 52:319–329
Lima L, Lange RR, Turner-Giannico A, Montiani-Ferreira F (2015) Evaluation of standardized endodontic paper point tear test in New Zealand white rabbits and comparison between corneal sensitivity followed tear tests. Vet Ophthalmol 18:119–124. https://doi.org/10.1111/vop.12178
Los LI, Nieuwenhuis P (1999) Organization of the rabbit vitreous body: lamellae, Cloquet's channel and a novel structure, the 'alae canalis Cloqueti'. Exp Eye Res 69:343–350
Los LI, van Luyn MJ, Nieuwenhuis P (2000) Vascular remnants in the rabbit vitreous body. I. Morphological characteristics and relationship to vitreous embryonic development. Exp Eye Res 71:143–151
Lukehart SA, Fohn MJ, Baker-Zander SA (1990) Efficacy of azithromycin for therapy of active syphilis in the rabbit model. J Antimicrob Chemother 25:91–99
Luo Z-W et al (1999) Anatomical and neurochemical peculiarities of the pika retina: basis for lack of circadian rhythm of core temperature. Neurosci Lett 259:13–16. https://doi.org/10.1016/s0304-3940(98)00896-9
Machacova T, Bártová E, Sedlak K, Budikova M, Piccirillo A (2015) Risk factors involved in transmission of Toxoplasma gondii and Neospora caninum infection in rabbit farms in Northern Italy. Ann Agric Environ Med 22
Maestrini G et al (2017) Encephalitozoon cuniculi in rabbits: Serological screening and histopathological findings. Comp Immunol Microbiol Infect Dis 50:54–57. https://doi.org/10.1016/j.cimid.2016.11.012
Maini S, Hartley C (2019) Guide to ophthalmology in rabbits. In Pract 41:310–320

Marini RP et al (1996) Microbiologic, radiographic, and anatomic study of the nasolacrimal duct apparatus in the rabbit (Oryctolagus cuniculus). Lab Anim Sci 46:656–662
Martínez-Jiménez D et al (2007) Endosurgical treatment of a retrobulbar abscess in a rabbit. J Am Vet Med Assoc 230:868–872
Matsunami S, Oshida T, Ichikawa H (2008) Comparative skull morphology of two pika species (Ochotona princeps and O. hyperborea): implications for differences in feeding habits. Russ J Theriol 7:99–106
McLeod C Jr, Langlinais P (1981) Pox virus keratitis in a rabbit. Vet Pathol 18:834–836
McPherson L et al (2009) Intraocular sarcomas in two rabbits. J Vet Diagn Invest 21:547–551. https://doi.org/10.1177/104063870902100422
Meomartino L et al (2018) Ocular ultrasonographic and biometric features of European brown hares (Lepus europaeus). Anat Histol Embryol 47:250–253
Meulemans G, Haesebrouck F, Lipinska U, Duchateau L, Hermans K (2011) Efficacy of an autogenous vaccine against highly virulent *Staphylococcus aureus* infection in rabbits. World Rabbit Sci 19. https://doi.org/10.4995/wrs.2011.812
Moore C, Dubielzig R, Glaza S (1987) Anterior corneal dystrophy of American Dutch belted rabbits: biomicroscopic and histopathologic findings. Vet Pathol 24:28–33
Moore BA, Robertson J, Tarbert DK, Good KL, Paul-Murphy JR A novel surgical technique for enucleation in rabbits to reduce the risk of intra-and post-operative orbital hemorrhage. Vet Ophthalmol
Moreno-Grúa E et al (2018) Characterization of livestock-associated methicillin-resistant Staphylococcus aureus isolates obtained from commercial rabbitries located in the Iberian Peninsula. Front Microbiol 9:1812
Morgan R, Duddy J, McClurg K (1993) Prolapse of the gland of the third eyelid in dogs: a retrospective study of 89 cases (1980 to 1990). J Am Anim Hosp Assoc
Morrisey J, McEntee M (2005) Therapeutic options for thymoma in the rabbit. Seminars Avian Exot Pet Med 14:175–181. https://doi.org/10.1053/j.saep.2005.06.003
Müller N (2010) Retrobulbar abscesses in rabbits-treatment avoiding enucleation. Praktische Tierarzt 91:14–22
Munday JS, Aberdein D, Squires RA, Alfaras A, Wilson AM (2007) Persistent conjunctival papilloma due to oral papillomavirus infection in a rabbit in New Zealand. J Am Assoc Lab Anim Sci 46:69–71
Munger RJ, Langevin N, Podval J (2002) Spontaneous cataracts in laboratory rabbits. Vet Ophthalmol 5:177–181
Nesburn AB (1969) Isolation and characterization of a herpes-like virus from New Zealand albino rabbit kidney cell cultures: a probable reisolation of virus III of Rivers. J Virol 3:59–69
Nielsen JN, Carlton WW (1995) Colobomatous microphthalmos in a New Zealand white rabbit, arising from a colony with suspected vitamin E deficiency. Lab Anim Sci 45:320
Nowak RM, Walker EP (1999) Walker's mammals of the world, vol 1. JHU press
O'Reilly A, McCowan C, Hardman C, Stanley R (2002) Taenia serialis causing exophthalmos in a pet rabbit. Vet Ophthalmol 5:227–230
Okuda H, Campbell L (1974) Conjunctival bacterial flora of the clinically normal New Zealand white rabbit. Lab Anim Sci
Oriá AP et al (2014) Tear production, intraocular pressure and conjunctival microbiota, cytology and histology of New Zealand rabbits (Oryctolagus cuniculus). Pesquisa Veterinária Brasileira 34:1024–1028. https://doi.org/10.1590/s0100-736x2014001000016
Otranto D et al (2009) Thelazia callipaeda (Spirurida, Thelaziidae) in wild animals: report of new host species and ecological implications. Vet Parasitol 166:262–267. https://doi.org/10.1016/j.vetpar.2009.08.027
Ozkan O, Karagoz A, Kocak N (2019) First molecular evidence of ocular transmission of Encephalitozoonosis during the intrauterine period in rabbits. Parasitol Int 71:1–4. https://doi.org/10.1016/j.parint.2019.03.006
Payne A (1994) The harderian gland: a tercentennial review. J Anat 185:1
Peng X, Roshwalb S, Cooper TK, Zimmerman H, Christensen ND (2015) High incidence of spontaneous cataracts in aging laboratory rabbits of an inbred strain. Vet Ophthalmol 18:186–190
Pereira FQ, Bercht BS, Soares MG, da Mota MGB, Pigatto JAT (2011) Comparison of a rebound and an applanation tonometer for measuring intraocular pressure in normal rabbits. Vet Ophthalmol 14:321–326
Petersen Jones, S. & Carrington, S. Pasteurella dacryocystitis in rabbits. Vet Rec (1988).
Port C, Dodd D (1983) Two cases of corneal epithelial dystrophy in rabbits. Lab Anim Sci 33:587–588
Pugliese M et al (2016) Evaluation of the conjunctival bacterial flora in 140 rabbits (Oryctolagus cuniculus) farmed in Sicily Island. Slov Vet Res 53
Quinton J-F et al (2014) Results of bacterial culture and sensitivity testing from nasolacrimal duct flushes in one hundred and three both healthy and clinically ill pet rabbits (Oryctolagus cuniculus). Int J Appl Res Vet Med 12
Rajaei SM, Rafiee SM, Ghaffari MS, Masouleh MN, Jamshidian M (2016) Measurement of tear production in English Angora and Dutch rabbits. J Am Assoc Lab Anim Sci 55:221–223
Ray C, Beever E, Loarie S (2012) Retreat of the American pika: up the mountain or into the void. In: *Wildlife conservation in a changing climate*. University of Chicago Press, Chicago, IL, pp 245–270
Regnery DC, Miller JH (1972) A myxoma virus epizootic in a brush rabbit population. J Wildl Dis 8:327–331
Reichard M et al (2010) Comparative in vivo confocal microscopical study of the cornea anatomy of different laboratory animals. Curr Eye Res 35:1072–1080
Reichenbach A, Baar U (1985) Retinitis-pigmentosa-like tapetoretinal degeneration in a rabbit breed. Doc Ophthalmol 60:71–78
Reusch, B. Odontogenic abscesses in rabbits: guide to problem. (2008).
Riau AK et al (2012) Reproducibility and age-related changes of ocular parametric measurements in rabbits. BMC Vet Res 8:138
Ringler DH, Newcomer CE (2014) *The biology of the laboratory rabbit*. Academic press
Roze M, Ridings B, Lagadic M (2001) Comparative morphology of epicorneal conjunctival membranes in rabbits and human pterygium. Vet Ophthalmol 4:171–174. https://doi.org/10.1046/j.1463-5216.2001.00145.x
Rozsa AJ, Beuerman RW (1982) Density and organization of free nerve endings in the corneal epithelium of the rabbit. Pain 14:105–120
Ruskell GL (1961) Aqueous drainage paths in the rabbit: a neoprene latex cast study. Arch Ophthalmol 66:861–870
Sailstad DM, Peiffer R Jr (1981) Specular microscopic observations of the corneal endothelium in the normal rabbit. Lab Anim 15:393–395
Saito K, Hasegawa A (2004a) Clinical features of skin lesions in rabbit syphilis: a retrospective study of 63 cases (1999–2003). J Vet Med Sci 66:1247–1249
Saito K, Hasegawa A (2004b) Chloramphenicol treatment for rabbit syphilis. J Vet Med Sci 66:1301–1304
Sakai T (1981) The mammalian Harderian gland: morphology, biochemistry, function and phylogeny. Arch Histol Jpn 44:299–333
Sanchez RF, Becker R, Dawson C, Escanilla N, Lam R (2016) Calculation of posterior chamber intraocular lens (IOL) size and dioptric power for use in pet rabbits undergoing phacoemulsification. Vet Ophthalmol
Sanchez RF et al (2018) Rabbits with naturally occurring cataracts referred for phacoemulsification and intraocular lens implantation: a preliminary study of 12 cases. Vet Ophthalmol 21:399–412

Sanku B, Saidul I, Pankaj G (2018) Efficacy of ivermectin against Notoedres cati var cuniculi in New Zealand White rabbits. Vet Pract 19:29–30
Santaniello A et al (2009) Serological survey of Encephalitozoon cuniculi in farm rabbits in Italy. Res Vet Sci 87:67–69
Sarchahi AA, Bozorgi H (2012) Effect of tetracaine on intraocular pressure in normal and hypertensive rabbit eyes. J Ophthalmic Vis Res 7:29
Schechter JE, Warren DW, Mircheff AK (2010) A lacrimal gland is a lacrimal gland, but rodent's and rabbit's are not human. Ocul Surf 8: 111–134
Schrader S, Mircheff A, Geerling G (2008) *Surgery for the dry eye*, vol 41. Karger Publishers, pp 298–312
Sebesteny A, Sheraidah G, Trevan D, Alexander R, Ahmed A (1985) Lipid keratopathy and atheromatosis in an SPF laboratory rabbit colony attributable to diet. Lab Anim 19:180–188
Seyama Y, Kasama T, Yasugi E, Park S-H, Kano K (1992) Harderian glands. Springer, pp 195–217
Sheppard LB (1962) The anatomy and histology of the normal rabbit eye with special reference to the ciliary zone. Arch Ophthalmol 67: 87–100. https://doi.org/10.1001/archopht.1962.00960020089010
Shirani D, Ghaffari MS, Akbarein H, Asgari AHA (2010) Effects of short-term oral administration of trimethoprim-sulfamethoxazole on Schirmer II tear test results in clinically normal rabbits. Vet Rec 166: 623–625
Smith AT (2008) Lagomorph biology. Springer, pp 89–102
Splendore A, Splendore A (1908) Un nuovo protozoa parassita deconigli incontrato nelle lesioni anatomiche d'une malattia che ricorda in molti punti il Kalaazar dell'uoma, Nota preliminare pel
Staatz WD, Van Horn D (1980) The effects of aging and inflammation on corneal endothelial wound healing in rabbits. Invest Ophthalmol Vis Sci 19:983–986
Stiles J et al (1997) Encephalitozoon cuniculi in the lens of a rabbit with phacoclastic uveitis: confirmation and treatment. Vet Comp Ophthalmol 7:233–238
Stone J, Dreher Z (1987) Relationship between astrocytes, ganglion cells and vasculature of the retina. J Comp Neurol 255:35–49. https://doi.org/10.1002/cne.902550104
Sun X et al (2007) Pharmacokinetics of terbinafine in the rabbit ocular tissues after topical administration. Ophthalmic Res 39:81–83
Taylor WM, Beaufrère H, Mans C, Smith DA (2010) Long-term outcome of treatment of dental abscesses with a wound-packing technique in pet rabbits: 13 cases (1998–2007). J Am Vet Med Assoc 237:1444–1449
Tee K-Y et al (2011) Serological survey for antibodies to Encephalitozoon cuniculi in rabbits in Taiwan. Vet Parasitol 183: 68–71
Tesluk GC, Peiffer RL, Brown D (1982) A clinical and pathological study of inherited glaucoma in New Zealand white rabbits. Lab Anim 16:234–239
Thomas C, Finn M, Twigg L, Deplazes P, Thompson R (1997) Microsporidia (Encephalitozoon cuniculi) in wild rabbits in Australia. Aust Vet J 75:808–810. https://doi.org/10.1111/j.1751-0813.1997.tb15658.x
Tokashiki EY et al (2019) Retrospective study of conditions grouped by body systems in pet rabbits. J Exot Pet Med 29:207–211. https://doi.org/10.1053/j.jepm.2018.11.009
Toni MC et al (2010) Rabbits' eye globe sonographic biometry. Vet Ophthalmol 13:384–386
Toshida H, Nguyen DH, Beuerman RW, Murakami A (2007) Evaluation of novel dry eye model: preganglionic parasympathetic denervation in rabbit. Invest Ophthalmol Vis Sci 48:4468–4475
Toshida H, Nguyen DH, Beuerman RW, Murakami A (2009) Neurologic evaluation of acute lacrimomimetic effect of cyclosporine in an experimental rabbit dry eye model. Invest Ophthalmol Vis Sci 50: 2736–2741
Turner Giannico A et al (2014) Characterization of the oculocardiac reflex during compression of the globe in Beagle dogs and rabbits. Vet Ophthalmol 17:321–327. https://doi.org/10.1111/vop.12077
Ueno A et al (1999) Histopathological changes in iridocorneal angle of inherited glaucoma in rabbits. Graefes Arch Clin Exp Ophthalmol 237:654–660
Van Hof M (1967) Visual acuity in the rabbit. Vision Res 7:749–751
Van Horn DL, Sendele DD, Seideman S, Buco PJ (1977a) Regenerative capacity of the corneal endothelium in rabbit and cat. Invest Ophthalmol Vis Sci 16:597–613
Van Horn DL, Hyndiuk RA, Edelhauser HF, McDonald TO, De Santis LM (1977b) Ultrastructural alterations associated with loss of transparency in the cornea of buphthalmic rabbits. Exp Eye Res 25:171–182
Van Zeeland Y (2017) Rabbit oncology. Vet Clin North Am Exot Anim Pract 20:135–182. https://doi.org/10.1016/j.cvex.2016.07.005
Vaney DI (1980a) The grating acuity of the wild European rabbit. Vision Res
Vaney DI (1980b) A quantitative comparison between the ganglion cell populations and axonal outflows of the visual streak and periphery of the rabbit retina. J Comp Neurol 189:215–233
Vareilles P, Conquet P, Lotti V (1980) Intraocular pressure responses to antiglaucoma agents in spontaneous buphthalmic rabbits. Ophthalmic Res 12:296–302
Varga M (2014) Ophthalmic diseases. In: Textbook of rabbit medicine, 2nd edn. Butterworth-Heinemann, Edinburgh, pp 350–366
Vernau K, Grahn B, Clarke-Scott H, Sullivan N (1995) Thymoma in a geriatric rabbit with hypercalcemia and periodic exophthalmos. J Am Vet Med Assoc 206:820–822
Verstraete FJ, Osofsky A (2005) Dentistry in pet rabbits. Compendium 27:671–684
Vézina M (2012) Assessing ocular toxicology in laboratory animals. Springer, pp 1–21
Viana D, Selva L, Segura P, Penadés JR, Corpa JM (2007) Genotypic characterization of Staphylococcus aureus strains isolated from rabbit lesions. Vet Microbiol 121:288–298. https://doi.org/10.1016/j.vetmic.2006.12.003
Volopich S et al (2005) Malignant B-cell lymphoma of the Harder's gland in a rabbit. Vet Ophthalmol 8:259–263
Von Bomhard W et al (2007) Cutaneous neoplasms in pet rabbits: a retrospective study. Vet Pathol 44:579–588
Wagner F, Fehr M (2007) Common ophthalmic problems in pet rabbits. J Exot Pet Med 16:158–167
Wagner F, Brügmann M, Drommer W, Fehr M (2000) Corneal dermoid in a dwarf rabbit (Oryctolagus cuniculi). J Am Assoc Lab Anim Sci 39:39–40
Wagner F et al (2005) Recurrent bilateral exophthalmos associated with metastatic thymic carcinoma in a pet rabbit. J Small Anim Pract 46: 393–397
Ward ML (2006) Diagnosis and management of a retrobulbar abscess of periapical origin in a domestic rabbit. Vet Clin Exot Anim Pract 9: 657–665
Wei XE, Markoulli M, Zhao Z, Willcox MD (2013) Tear film break-up time in rabbits. Clin Exp Optom 96:70–75
Weiner CM et al (2010) Cottontail rabbit papillomavirus in langerhans cells in Sylvilagus spp. J Vet Diagn Invest 22:451–454. https://doi.org/10.1177/104063871002200321
White AC Jr (2000) Neurocysticercosis: updates on epidemiology, pathogenesis, diagnosis, and management. Annu Rev Med 51:187–206
White J, Stephens GM, Cinotti AA (1972) The use of povidone-iodine for treatment of fungi in rabbit eyes. Ann Ophthalmol 4:855–856
White SD, Bourdeau PJ, Meredith A (2002) Dermatologic problems of rabbits. Seminars Avian Exot Pet Med 11:141–150
Whittaker AL, Williams DL (2015) Evaluation of lacrimation characteristics in clinically normal New Zealand white rabbits by

using the Schirmer tear test I. J Am Assoc Lab Anim Sci 54(6): 783–787
Williams DL (2012) Ophthalmology of exotic pets. John Wiley & Sons
Wills J (2001) Coenurosis in a pet rabbit. Vet Rec 148:188
Wolfer J, Grahn B, Wilcock B, Percy D (1993) Phacoclastic uveitis in the rabbit. Prog Vet Comp Ophthalmol 3:92–97
Wolfer J, Grahn B, Taylor M, Laperriere E (1995) Treatment of phacoclastic uveitis in the rabbit by phacoemulsification. Am Coll Vet Ophthalmol
Yablonski M, Hayashi M, Cook D, Chubak G, Sirota M (1987) Fluorophotometric study of intravenous carbonic anhydrase inhibitors in rabbits. Invest Ophthalmol Vis Sci 28:2076–2082
Yandow LH, Chalfoun AD, Doak DF (2015) Climate tolerances and habitat requirements jointly shape the elevational distribution of the American pika (Ochotona princeps), with implications for climate change effects. PLoS One 10
Yanoff S (1983) Surgical correction for entropion in a baby rabbit. Vet Med Small Anim Clin
Yata S, Hara H, Kitano H (1995) Treatment of a rabbit with pseudosymblepharon. J Japan Vet Med Assoc 48:335–337
Yokota M, Suzuki H, Hata T, Sakamoto K, Takeda U (1983) Morphological studies on ocular and auditory character of Ochotoua rufescens. Exp Anim 32:159–165
Yüksel H et al (2015) Anterior segment parameters of rabbits with rotating Scheimpflug camera. Vet Ophthalmol 18:210–213
Zeiss C, Johnson E, Dubielzig R (2003) Feline intraocular tumors may arise from transformation of lens epithelium. Vet Pathol 40:355–362
Zhang H et al (2014) Validation of rebound tonometry for intraocular pressure measurement in the rabbit. Exp Eye Res 121:86–93
Zhu Z et al (2003) Lacrimal histopathology and ocular surface disease in a rabbit model of autoimmune dacryoadenitis. Cornea 22:25–32

Ophthalmology of Hystricomorpha: Porcupines, Guinea Pigs, Degus, Chinchillas, and Relatives

43

Bradford J. Holmberg

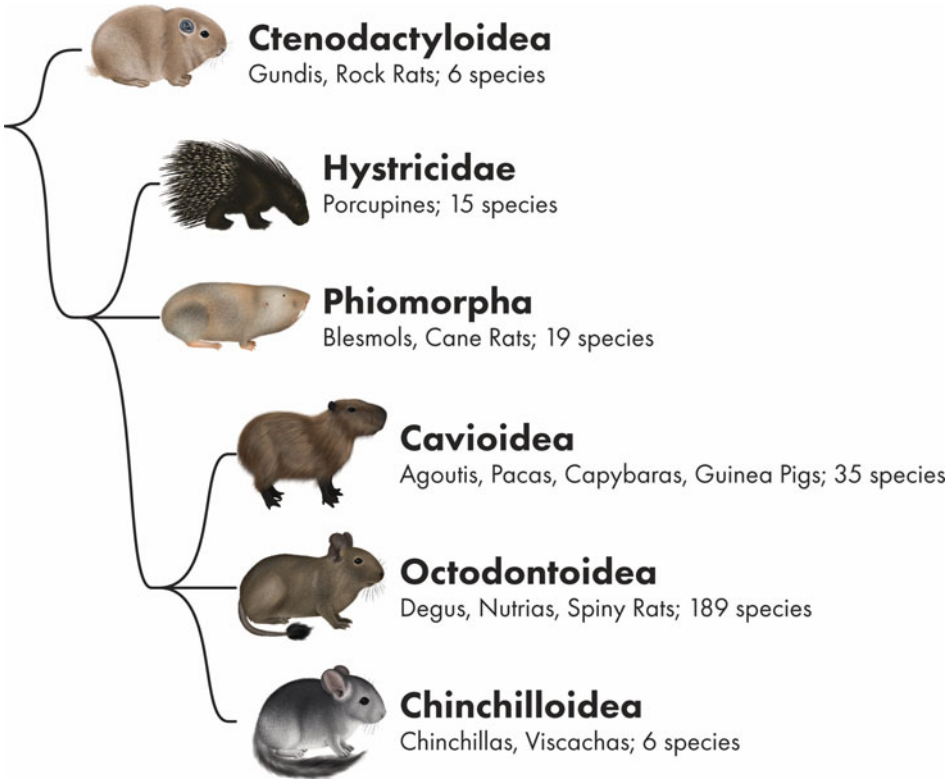

Introduction

Hystricomorpha is an extremely diverse suborder of Rodentia containing the infraorders Ctenodactyloidea and Hystricognathi. Ctenodactyloidea consists of gundis and Laotian rock rats. Hystricognathi consists of the parvorders Phiomorpha and Caviomorpha. Interestingly, porcupines fall into both groups with Old World porcupines (Hystricidae) members of Phiomorpha, and New World porcupines (Erethizontidae) members of Caviomorpha. Phiomorpha tends to inhabit Africa, Asia, and Europe, while Caviomorpha predominately resides in South America with some species in North America and the Caribbean. Prior to molecular phylogenetic studies, the Hystricognathi were classified based on the bone structure of their skulls. They are unique in that the medial masseter muscle passes through a greatly enlarged infraorbital foramen and connects to the

B. J. Holmberg (✉)
Animal Eye Center of New Jersey, Little Falls, NJ, USA

F. Montiani-Ferreira et al. (eds.), *Wild and Exotic Animal Ophthalmology*, https://doi.org/10.1007/978-3-030-81273-7_18

mandible; termed hystricomorphy. All Hystricomorphs have this conformation with the exception of Bathyergidae, who are protrogomorphous. However, examination of mitochondrial DNA (Montgelard et al. 2008) has confirmed their rightful inclusion within Histricognathi and hence Hystricomorpha.

Hystricomorphs range in size from the smallest mole rats at 3.5 in. (9 cm) in length and 1.2 oz. (30 g) in weight up to the largest rodent in the world, the capybara, at 48 in. (122 cm) in length and upwards of 150 pounds (68 kg) in weight. Similar to their size, there is great variability in their eyes. The globe of the naked mole rat, *Heterocephalus glaber*, measures 1.3 mm in diameter while the capybara, *Hydrochoerus hydrochaeris*, measures an astounding 22 mm. Ocular morphology is conserved within the suborder, but vision varies greatly.

Ctenodactyloidea (Gundis)

The family Ctenodactyloidea comprises four genera and five species including the common or North African gundi (*Ctenodactylus gundi*), Val's gundi (*Ctenodactylus vali*), Felou gundi (*Felovia vae*), Mzab gundi (*Massoutiera mzabi*), and Speke's pectinator (*Pectinator spekei*). Gundis are terrestrial mammals inhabiting rocky, sparsely vegetated desert terrains in northern Africa. They are strictly herbivores and are social with colonies containing up to 100 individuals depending on the availability of resources (Stuart and Stuart 2016). Their name loosely translates to "comb rat" due to the presence of comb-like bristles on the two inner appendages of the rear foot which are used for grooming. *Toxoplasma gondii* was first identified in the gundi in 1908 by Nicolle and Manceaux who named the organism based on its shape (from Greek: toxo—bow; plasma—creature) and animal of origin (gundi, suspected to be misspelled as gondii).

Gundis have large, laterally placed eyes with a substantial monocular visual field to aid in predator detection. They have a protected orbit with a prominent zygomatic arch, similar to Hystricidae. An orbital venous sinus is present as is a Harderian gland containing solid, intraluminal porphyrin deposits (Djeridane 1992). The gundi lens weighs approximately 85–150 mg and this measurement has been used for estimation of age (Ghawar et al. 2017). There is no additional literature describing ocular anatomy, physiology, visual capabilities, or ophthalmic disease in the gundi.

Hystricidae (Porcupines)

Porcupines are separated into two families including the Old World porcupines of Hystricidae and the New World porcupines of Erethizontidae. Both families belong to the infraorder Hystricognathi. Old World porcupines are nocturnal, terrestrial, and primarily inhabit southern Europe, western and southern Asia, and most of Africa. There are 3 genera (*Hystrix, Atherurus,* and *Trichys*) and 11 species. New World porcupines are generally nocturnal, predominately arboreal, and inhabit North and South America. There are 3 genera (*Coendou, Chaetomys,* and *Erethizon*) and 17 species. All species are herbivores and boast thousands of quills either clustered (Old World porcupines) or attached individually (New World porcupines) along their coat, especially on the back, sides, and tail. The quills are an important part of their defense strategy, based on aposematism. When not sufficient, they will emit a strong odor, bare teeth, and bristle the quills. Due to the potential danger from these barbs to the handler and to facilitate a more thorough and less stressful examination, immobilization is recommended. A combination of tiletamine and zolazepam (Telazol®) at a dose of 10 mg/kg is effective at immobilizing porcupines for approximately 44 minutes (Hale et al. 1994). Alternatively, an anesthesia induction chamber with an isoflurane vaporizer can be utilized. This technique may be inferior to injectable immobilization due to potential examiner exposure to inhalant anesthetic gas.

The porcupine eye is well protected by a deep orbit framed by a prominent zygomatic arch (Fig. 43.1). There is a 45-degree angle between the optic axis and midline, allowing a binocular overlap of approximately 50–60 degrees. The retractor bulbi muscles are present and well-developed aiding in protection of the globe (Duke-Elder 1958). The palpebral fissure is small. Eyelids lack cilia but there are numerous soft periocular hairs (Fig. 43.2a, b). A prominent third eyelid is present, which completely covers the globe, requiring manual retraction in order to visualize the globe in an anesthetized

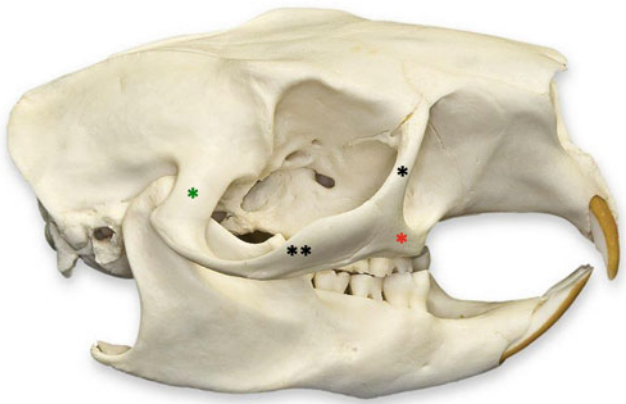

Fig. 43.1 Lateral view of the skull of a North American porcupine (*Erethizon dorsatum*). Note the deep, well-protected orbit that is framed by a prominent zygomatic arch. Double asterisk—zygomatic arch, single asterisk—frontal process of zygomatic bone, asterisk in red—temporal process of zygomatic bone, asterisk in green—zygomatic process of temporal bone

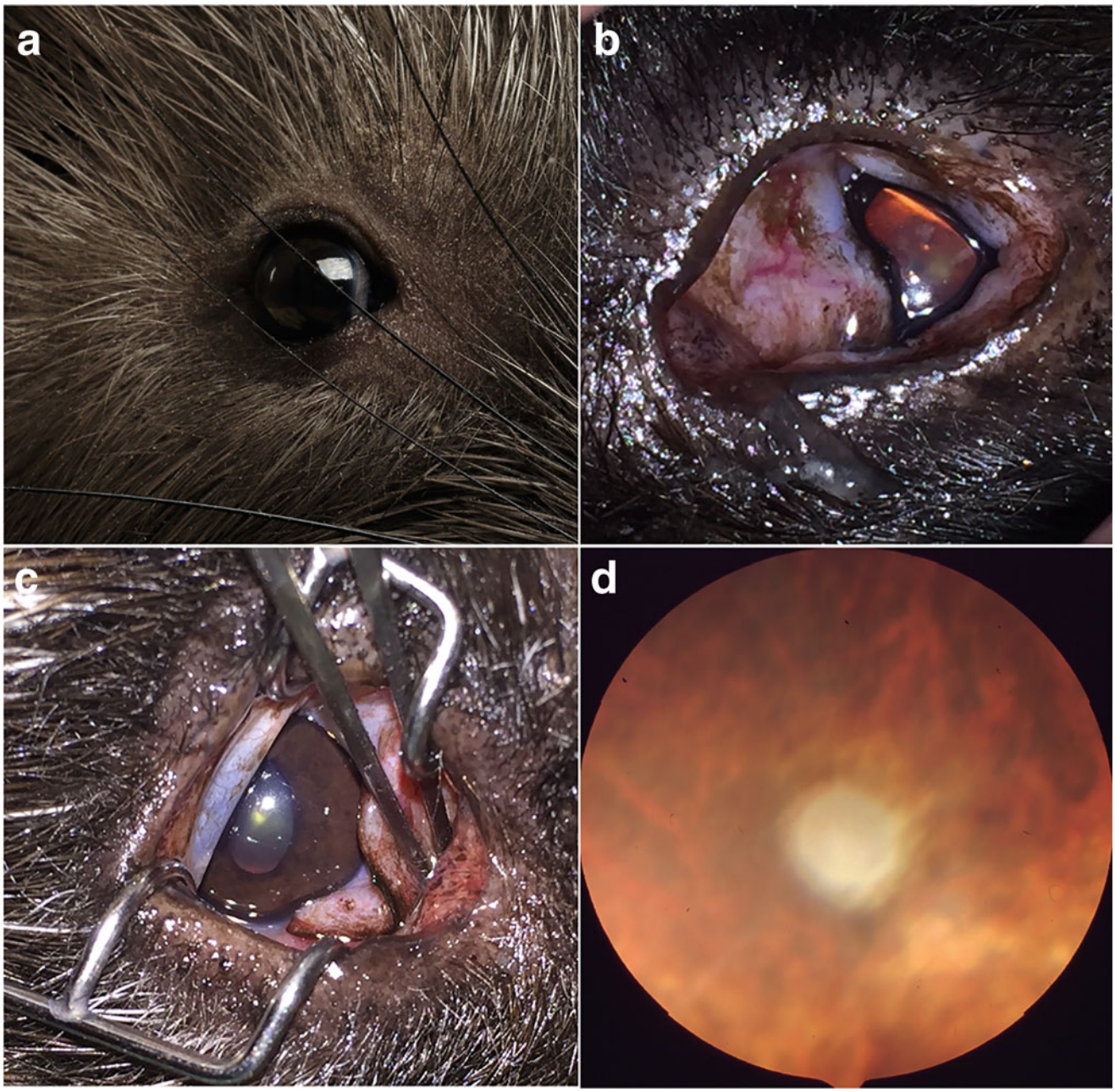

Fig. 43.2 (**a**, **b**) External photographs of the North American porcupine (*Erethizon dorsatum*). The eyelids lack cilia but there are numerous soft periocular hairs. With anesthesia (**b**), the eye is recessed in the deep orbit resulting in prominence of the third eyelid covering the majority of the globe. (**c**) External photo of the North American porcupine (*Erethizon dorsatum*). The third eyelid is retracted with forceps allowing visualization of the globe. The iris is dark brown and the pupil is vertically ovoid. (**d**) The fundus of the North American porcupine (*Erethizon dorsatum*) is anangiotic and atapetal with prominent choroidal vessels and a round optic disk. (**a**—Used with permission from Seregraff, Shutterstock.com. **d**—Courtesy: University of California, Davis Comparative Ophthalmology Service)

specimen. A bulbous gland of the third eyelid is apparent on exam, but whether this is a lacrimal, Harderian, or other is unknown. Inferior and superior lacrimal puncta are visible although the course of the nasolacrimal duct has not been described. The cornea resembles that of other mammals with an approximate thickness of 0.46 mm (Fernandez and Dubielzig 2013). The iris is dark brown and the pupil is vertically ovoid (Fig. 43.2c). Pharmacological dilation with 1% tropicamide results in a circular pupil. Examination of a small prickle of aged (14–16-year-old) porcupines revealed nuclear sclerosis, but no cataracts, suggesting that age-related cataracts are not prevalent (personal observation). Ciliary body musculature was absent histologically (Fernandez and Dubielzig 2013); therefore, significant accommodation is

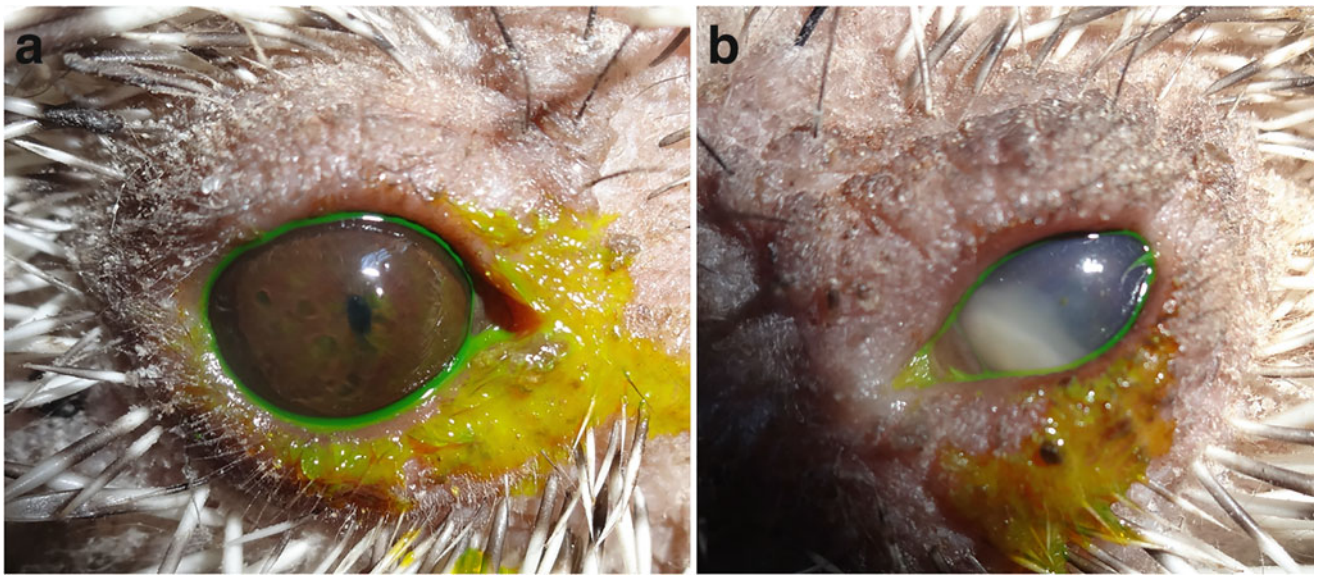

Fig. 43.3 Normal right eye (**a**) of the Brazilian porcupine (*Coendou prehensilis*). Anterior uveitis with hypopyon is present in the left eye (**b**) with an unknown etiology. (Courtesy: Dr. Ana Carolina Rodarte Almeida)

likely absent. On indirect ophthalmoscopy the retina has an identical appearance to that of guinea pigs with no visible retinal vessels, prominent choroidal vessels, lack of a tapeteum lucidum, and a round optic disk (Fig. 43.2d). However, in contrast to guinea pigs, porcupines have a true anangiotic fundus with no retinal vessels evident histologically (Fernandez and Dubielzig 2013). As expected for a mostly nocturnal mammal, the retina is rod-dominant (Duke-Elder 1958). Ophthalmic diagnostic testing in aged porcupines revealed a mean intraocular pressure via applanation tonometry of 13.5 ± 2 mmHg and a mean Schirmer tear test of 8 ± 2 mm/min (personal observation) (Appendix C).

Ophthalmic disease in porcupines has not been reported in the literature. Anterior uveitis with hypopyon has been observed in a Brazilian porcupine (*Coendou prehensilis*) by one of the authors (Fig. 43.3; F. Montiani-Ferreira). The underlying cause was unknown. Ocular and orbital trauma secondary to porcupine quill penetration or migration is not uncommon in dogs (Grahn et al. 1995; Fig. 43.4).

Phiomorpha (Blesmols, Cane Rats, and the Naked Mole Rat)

Phiomorpha are native to central and southwestern Africa, consisting of three families of rodents including Bathyergidae, Petromuridae, and Thryonomyidae. Bathyergidae or blesmols are the largest family with 5 genera and at least 21 species (Van Daele et al. 2007). The naked mole rat, *Heterocephalus glaber*, was originally part of Bathyergidae but has more recently been placed in its own family Heterocephalidae within Phiomorpha (Patterson and Upham 2014). Petromuridae includes one genus and species, *Petromus typicus*, the Dassie rat. Thryonomyidae includes one genus and two species, *Thryonomys gregorianus* and *Thryonomys swinderianus*, the cane rats. Other than genetic mapping to corroborate monophyly (Huchon and Douzery 2001), there is no literature describing anatomy or physiology in Petromuridae or Thryonomyidae.

Blesmols, commonly called mole rats, are not to be confused with true moles of the family Talpidae. Similar to true moles, blesmols are fossorial with cylindrical bodies with loose skin and short limbs. Unlike moles, they use their

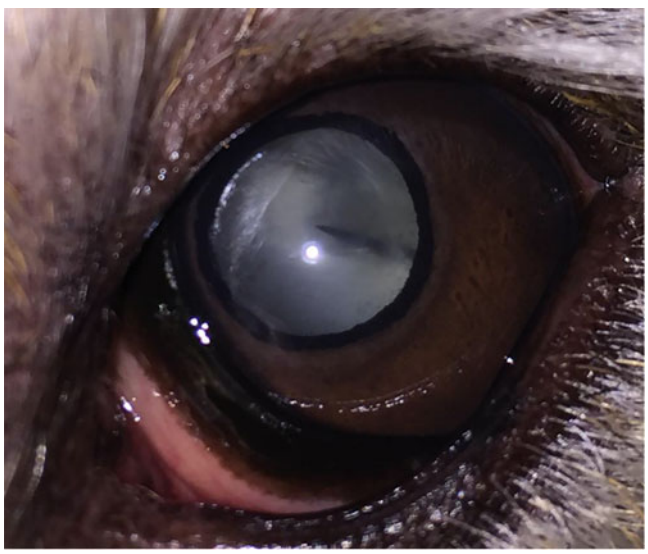

Fig. 43.4 Intralenticular migration of a porcupine quill in a 5-year-old Fox Wire Terrier dog

incisors more so than their forelimbs to dig burrows. Classification of Hystricognathi as hystricomorphs has been based on the possession of an enlarged infraorbital foramen through which a substantial portion of the zygomaticomandibularis muscle (medial masseter) extends. In contrast, Bathyergidae have a small infraorbital foramen, simply transmitting the infraorbital artery and the infraorbital branch of the maxillary nerve (Maier and Schrenk 1987). This anatomic arrangement, termed protrogomorphous, allows for increased lateral masseter muscle power facilitating high bite force and a wide gape (Cox et al. 2020). It is likely adaptive for digging, with blesmols the only Hystricomorph having this anatomic adaption.

Mole rats live almost a completely subterranean life within elaborate burrow systems that can extend over 3 kilometers and cover 100,000 square meters. They are herbivorous and range in social behavior with some species such as *Heterocephalus glaber* living in large colonies. One would expect fossorial animals that reside in a dark ecotope with restricted cues for spatial orientation to have regressed eyes and visual capabilities. However, compared to the blind mole rat (*Spalax ehrenbergi*) and true moles (*Talpa spp.*) that show evolutionary regression of certain aspects of the globe (see Chap. 41), blesmols have a morphologically normal eye (Fig. 43.5). The superficially placed eye is microphthalmic, relatively spherical, and ranges from 1.3 mm in diameter in

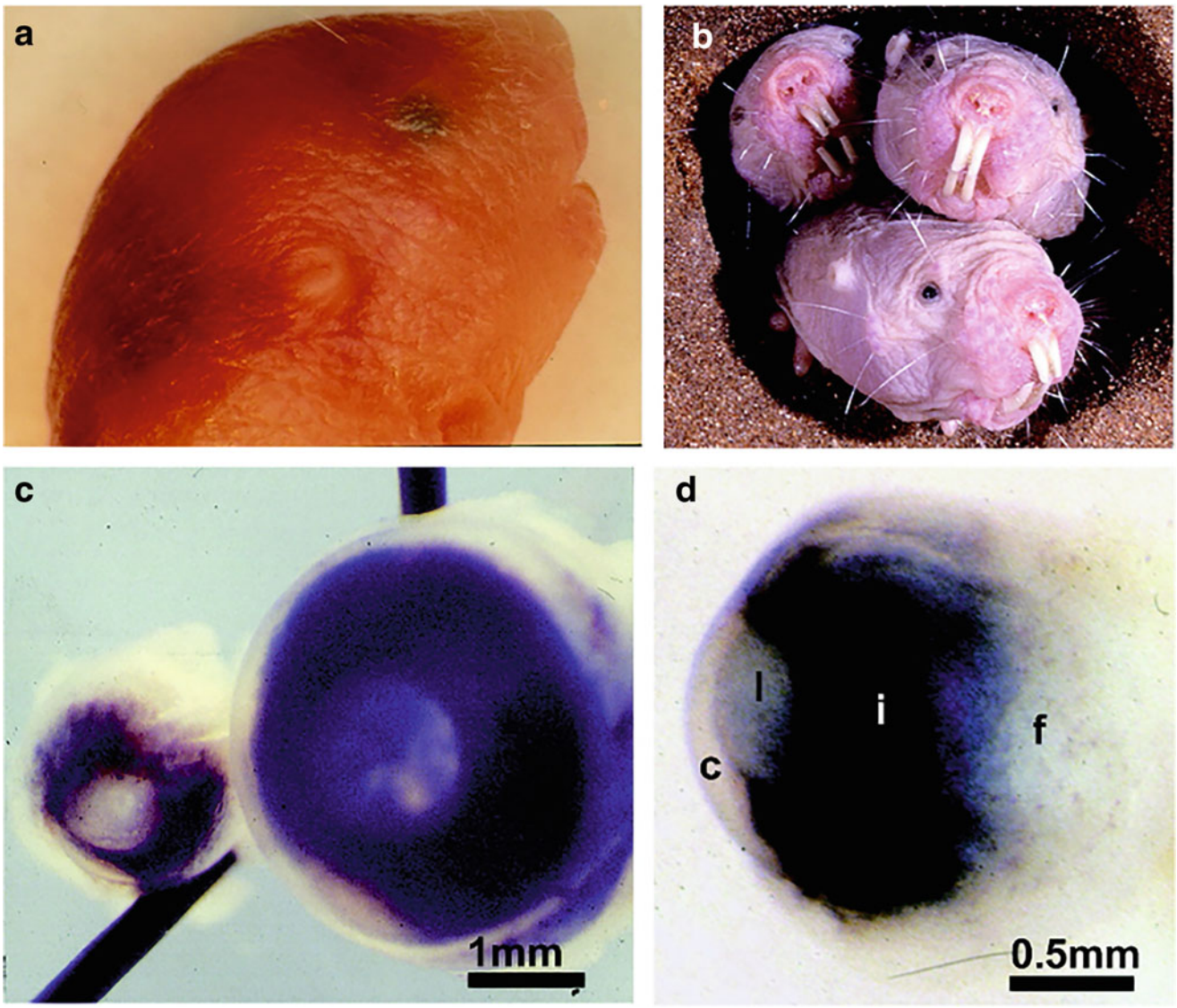

Fig. 43.5 Size of the globe and gross morphology in the mole rat. (**a**) The head of a neonatal mole rat. Eyelids are still fused. (**b**) Adult mole rats. Eyes are open because of being alarmed. (**c**) Comparison of the size of an eye from the adult mouse (right) to that from the adult mole rat (left). (**d**) The eye of an adult mole rat. Cornea (c), lens (l), highly pigmented irregularly shaped iris (i), and the layer of fat (f) covering the posterior hemisphere of the eye (Modified with permission: Nikitina et al. (2004) Post-natal development of the eye in the naked mole rat (*Heterocephalus glaber*). Anat Rec 277A:317–337)

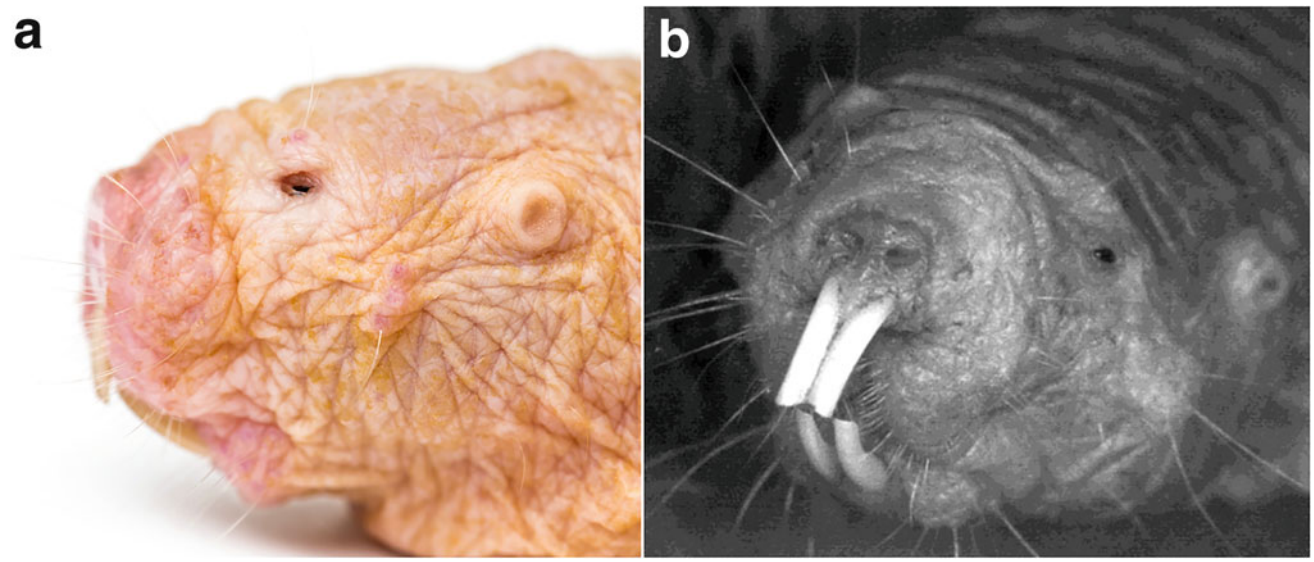

Fig. 43.6 Captive naked mole rats (*Heterocephalus glaber*). Although its visual system is greatly reduced, the naked mole rat retains an eyelid allowing the small eye to be directly exposed to light. Note the vibrissae on the snout and head as well as the large incisors used for digging. (**a**—Used with permission from Eric Isselee, Shutterstock.com. **b**—Used with permission from Mills S, Catania K (2004) Identification of retinal neurons in a regressive rodent eye (the naked mole rat). Vis Neurosci 21: 107–117)

H. glaber to 3.5 mm in diameter in *Bathyergus suillus* (Němec et al. 2008). Even with normal morphology, mole rats significantly rely on tactile information gained from numerous vibrissae on the head and snout as well as from the large front incisors (Fig. 43.6) as evidenced by a hypertrophied somatosensory cortex (Catania and Remple 2002). The eyelids appear normal and function appropriately. Extraocular muscles including superior, lateral, medial, and inferior rectus muscles, superior and inferior oblique muscles, and retractor bulbi muscles (McMullen et al. 2010) are present allowing ocular mobility (Cernuda-Cernuda et al. 2003). Myofiber density is reduced and sarcomere organization is less defined in mole rats compared to mice, consistent with reduced activity of these muscles. *Fukomys anselli* are an exception, having well-developed retractor bulbi muscles with an associated prominent oculomotor nucleus, with these muscles used to retract and protect the globe during digging (Němec et al. 2008). Retrobulbar fat is present, adhered to the posterior hemisphere (Fig. 43.5), as is a small Harderian gland ventral to the globe.

The cornea of mole rats is relatively conserved with a thickness of approximately 52 μm. An epithelial layer and thin stroma are present. The corneal endothelium is present but cells are irregular and rounded in shape containing numerous secretory vacuoles (Nikitina et al. 2004), suggesting typical tight junctional complexes are not present. Interestingly, the cornea of *Fukomys anselli* has ferrous inclusions in the corneal epithelium (Wegner et al. 2006a), suspected to be magnetite (Fe_3O_4). The ophthalmic branch of the trigeminal nerve may carry magnetic field information to the brain (Beason and Semm 1996) and serve in magnetic compass orientation. Application of topical anesthetic in *F. anselli* abolished preferred nesting direction and resulted in a random orientation pattern (Wegner et al. 2006a). Magnetoreception using corneal epithelial magnetite as a signal mediator between the eye and brain may be an additional adaptation aiding spatial orientation in mole rats living in an environment devoid of abundant light.

The uvea of blesmols is deeply pigmented, thick, and much larger than expected. The anterior uvea (iris and ciliary body) has a combined length of 0.69 mm, approximately 57% of the entire length of the mole rat eye (Nikitina et al. 2004). The pupil is irregular and a rudimentary muscle is present suggesting the ability to regulate retinal light exposure. With age, the iris atrophies evidenced by stromal thinning with pigment dispersion into the anterior chamber. The base of the iris is adhered to the cornea and the anterior chamber is shallow similar to other fossorial animals (Cei 1946). While the trabecular meshwork is well-developed at an early age, it degenerates and narrows with age (Nikitina et al. 2004). The ciliary body is flat and elongated, lacking ciliary processes, similar to other subterranean animals (Quilliam 1966). The large ciliary body may help protect the retina from sudden exposure to bright light upon emerging from the burrow during the day. The naked mole rat (*H. glaber*) has a large crystalline lens that appears to float freely within the optical media, as lens zonules are absent. The lens is round yet irregular with a prominent capsule and a thin layer of nucleated cells surrounding it entirely (Nikitina et al. 2004). These cells are flattened and squamous-like in adults, in contrast to the cuboidal shape found in other mammals. Central lens fibers retain nuclei, and fibers along

the posterior aspect of the lens are misshapen and lack regular arrangement. Gamma crystallins are essential for lens fiber differentiation. Unlike other species that continuously synthesize γ-crystallin until adulthood, naked mole rat lens fibers stop expression shortly after birth and residual γ-crystallins degrade with age (Nikitina et al. 2004). The absence of γ-crystallin expression in the mature lens may explain why adult fibers do not form concentric circles around the embryonic nucleus but instead elongate posteriorly. This posterior elongation leads to irregular fiber arrangement and anterior positioning of the lens nucleus. In contrast, the lens of the Cape dune mole rat (*Bathyergus suillus*) is small, develops normally, and retains normal expression of α- and γ-crystallins (Nikitina and Kidson 2014). Likewise the lens of the African mole rat (*F. anselli*) is small, clear, and biconvex with a stronger curvature along the posterior surface compared to the anterior surface (Peichl et al. 2004). There is significant variation in lens development among species and likely significant variation in vision.

Phiomorpha have an anangiotic retinal vascular pattern with conserved retinal structure (Cernuda-Cernuda et al. 2003). Traditional retinal neurons are present including multiple types of cone bipolar cells, rod bipolar cells, at least 1 horizontal cell type, several types of common amacrine cells, and multiple ganglion cell types (Mills and Catania 2004). However, the structural organization is less regular than that of more sighted animals. There are approximately 1000–3000 total retinal ganglion cells in *F. anselli* (Cernuda-Cernuda et al. 2003), and 6000 total retinal ganglion cells in *B. suillus* (Němec et al. 2008). In *H. glaber* there is a progressive loss of retinal ganglion cells with age such that the nerve fiber layer is no longer identifiable in adults (Nikitina et al. 2004). Interestingly, this reduction coincides with closure of the iridocorneal angle and whether or not these are related is unknown. The optic nerve is macroscopic with approximately 2000–6000 fibers and a thickness of 40–110 μm. The optic nerve is predominately myelinated in Bathyergidae, with the exception of *H. glaber* where less than 0.5% of the nerve is myelinated (Němec et al. 2008). Both rod and cone photoreceptors are present, with the retina being rod-dominant as expected. Rod densities range from 100,000 to 150,000/mm^2 and cone densities from 8000 to 15,000/mm^2 in *Fukomys spp*. (Peichl et al. 2004). Cones account for approximately 10% of all photoreceptors, which is much higher than surface-dwelling nocturnal mammals (<1–3% cones) and similar to that of diurnal and crepuscular mammals (8–95% cones; Peichl 2005). Evaluation of cone photoreceptors in *F. anselli* and *F. mechowi* revealed the presence of two opsins, a short wavelength sensitive cone (S-cone) and a long wavelength sensitive cone (L-cone). The majority of cone photoreceptors were dual pigment cones, expressing both S- and L-opsin. For example, 90% of cones of *F. anselli* expressed S-opsin with 70% being dual pigment cones and 20% conventional S-cones (exclusive S-opsin expression). Only 10% of cones were conventional L-cones (Peichl et al. 2004). Unlike *Fukomys spp*., cones of *H. glaber* only express S-opsin, with no detectable L-opsin. The presence of two photopigments in mole rats suggests that some color discrimination may be present.

Retinal projections have been explored in several Bathyergidae species. All subcortical visual centers are present, but poorly developed and reduced in size. The lateral geniculate nucleus and pretectal nucleus are moderately reduced and primarily receive contralateral retinal input. The superficial visual layers of the superior colliculus and accessory optic system are extremely reduced and can be considered vestigial. The suprachiasmatic nucleus is large, cytoarchitecturally well developed, and receives bilateral retinal input (Němec et al. 2008). A visual cortex is present in *Fukomys spp*. but small and displaced laterally. Light stimulation after a period of dark adaptation elicits c-Fos expression in the occipital cortex (Oelschläger et al. 2000) confirming an intact pathway. The presence of relatively clear optical media, an iris with a movable pupillary aperture, and a morphologically normal retina suggest the presence of an image forming retina, potentially with color discrimination. Based on estimates from peak retinal ganglion cell density and eye size, the upper limits of visual acuity are assessed as 0.3–0.5 cycles/degree in the African mole rat (Němec et al. 2008), much lower than humans who can resolve at 60–72 cycles/degree (Reymond and Cook 1984) and cats at 3–20 cycles/degree (Clark and Clark 2013). This suggests the brain would receive a very pixelated image. However, based on the diminished subcortical visual system and small visual cortex, this pixelated image is likely never interpreted. Vision guided navigation, foraging, mate selection, and predator avoidance are not present. Mole rats do not respond to simple visual stimuli but have light perception based on behavioral studies (Wegner et al. 2006b). The presence of robust retino-hypothalamic projections and a substantial suprachiasmatic nucleus suggest vision is utilized for entrainment of photoperiod as well as form and brightness discrimination. This may enable mole rats to localize breaches in burrows to prevent entrance of predators.

Acquired ophthalmic disease has not been reported in the literature for any members of Phiomorpha.

Cavioidea (Paca, Capybara, and Guinea Pigs)

Cavioidea is a superfamily of the Caviomorpha parvorder consisting of three living families including Cuniculidae, Dasyproctidae, and Caviidae. Three extinct families include Guiomys, Scotamys, and Eocardiidae. Dinomyidae was originally classified within this superfamily, but phylogenetic analysis has reclassified them into the superfamily

Chinchilloidea (Rasia and Candela 2019). Cavioidea boasts the largest living rodent in the world, *Hydrochoerus hydrochaeris* (capybara) at 4 feet long, 22 inches tall, and weighing upwards of 150 pounds (Herrera 1992).

There is one genus and three living species of the family Cuniculidae including the lowland paca (*Cuniculus paca*), mountain paca (*Cuniculus taczanowskii*), and a new species *Cuniculus hernandezi* (Castro et al. 2010). However, *C. hernandezi* is a *nomen nudum*; the proposed name does not conform to the requirements of the current International Code of Zoological Nomenclature (Ramírez-Chaves and Solari 2014). There is debate whether this is a novel species or the presence of isolated *C. taczanowskii* in a specific area of the central Andes in Colombia. *C. paca* is present in Central and South America from southern Mexico to northern Argentina where it inhabits forested areas near freshwater streams and rivers. *C. taczanowskii* lives in the northern Andes and the Páramo grasslands in northern South America. They favor areas with plentiful water as they are good swimmers and use water when threatened by predators, remaining submerged for up to 10 minutes (Wood 1861). They live in shallow burrows, are predominately nocturnal, and herbivorous.

Pacas have a closed orbit with massively enlarged zygomatic arches. Resonating chambers are formed by the broadened zygomatic arch together with concavities within the maxillary bone (Vaughan et al. 2015). Air is forced through these bony pouches amplifying sound made by grinding of the cheek teeth resulting in a loud, rumbling noise. Eyelids contain cilia only along the upper aspect (Fig. 43.7b) and openings of the superior and inferior lacrimal puncta are located nasally. A vestigial third eyelid is present (Fig. 43.7d). The bulbar conjunctiva has a blue/brown pigmentation (Fig. 43.7a). The pupil is circular accompanied by

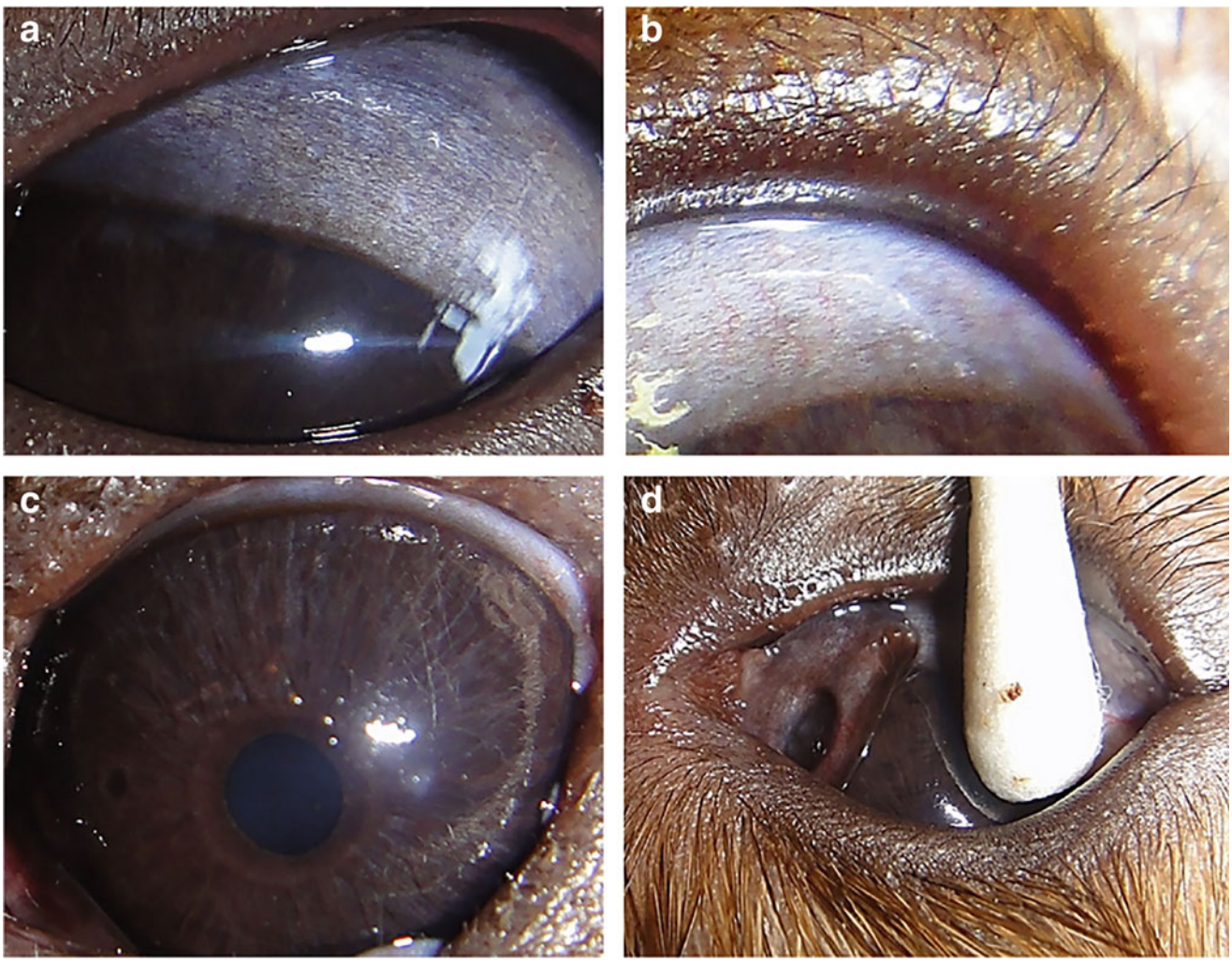

Fig. 43.7 Biomicroscopy findings in adult pacas (*C. paca*). (**a**) Blue/brown pigmented bulbar conjunctiva. (**b**) Eyelashes only on the superior eyelid. (**c**) Brown iris and round pupil. (**d**) Vestigial nictitating membrane. (Used with permission from: Balthazar da Silveira et al. (2018) Ophthalmic parameters in adult lowland paca (*Cuniculus paca*) raised in captivity. Vet Ophthalmol 21:42–47)

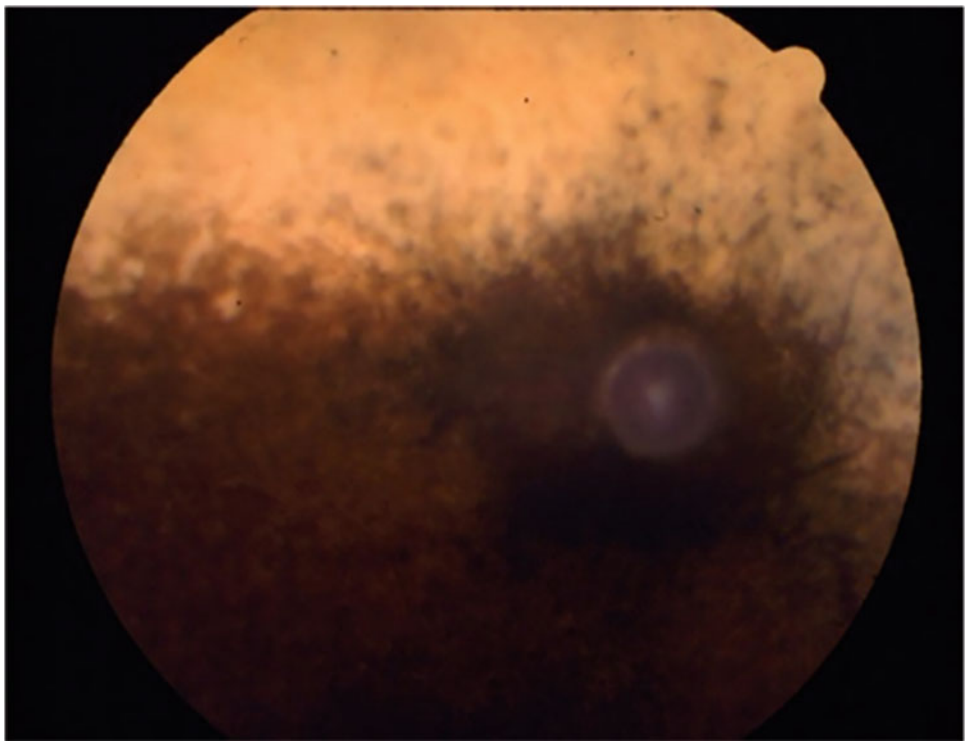

Fig. 43.8 Fundus image of an adult paca (*C. paca*). There is an anangiotic retinal vascular pattern, a round optic disk, and a superior tapetum. (Used with permission from: Balthazar da Silveira et al. (2018) Ophthalmic parameters in adult lowland paca (*Cuniculus paca*) raised in captivity. Vet Ophthalmol 21:42–47)

a dark brown iris (Fig. 43.7c). The central cornea is 0.35 mm thick and corneal endothelial density measured by a specular microscopy was 2083 cells/mm^2 (Balthazar da Silveira et al. 2018). Tear production was recorded at 4.1 ± 0.4 mm/min, and intraocular pressure via applanation tonometry was 6.3 ± 0.4 mmHg (Balthazar da Silveira et al. 2018) (Appendix C). The retina has an anangiotic vascular pattern with a round, small (1 mm), centrally located gray optic disk (Fig. 43.8). Interestingly, *C. paca* has an orange fibrous tapetum located in the superior fundus (Silveira et al. 1989; Braekevelt 1993; Balthazar da Silveira et al. 2018). The tapetum aids in low light vision, but is not common in rodents with the exception of the springhare (*Pedetes capensis*) and Old World flying squirrel (*Pteromys spp*; Fernandez and Dubielzig 2013; Duke-Elder 1958). The inferior fundus is deeply pigmented without visualization of choroidal vessels. Vision has not been assessed in pacas. However, a visual streak is present with the greatest density of ganglion cells located 8.5 mm temporal to the optic disk. The visual streak is poorly differentiated and the peak cell concentration of retinal ganglion cells (approximately 925 cells/mm^2) is much less than other Cavioidea (Silveira et al. 1989). This suggests that pacas may have the poorest vision of all Cavioidea, but further study is necessary before making any definitive conclusions.

There is no literature citing ophthalmic abnormalities in pacas.

Dasyproctidae is a family of large South American rodents including the genera *Myoprocta* (acouchis) and *Dasyprocta* (agoutis). There are two species of *Myoprocta*, *M. pratti* and *M. acouchy*. Acouchis are diurnal herbivores that inhabit the Amazon basin in Brazil. They are smaller than agoutis and are sometimes referred to as "tailed-agoutis" due to the presence of this appendage. There is no available literature on the anatomy, physiology, or visual capabilities of this genus. *Dasyprocta* includes 11 species native to Central America, northern and central South America, and the southern Lesser Antilles. Similar to acouchis they are diurnal and herbivorous living in rainforests, grassy plains, and cultivated fields, preferably near water.

The Azara's agouti or common agouti (*Dasyprocta azarae*) is the only species whose ocular anatomy has been described (Tavares-Somma et al. 2017). Agoutis have laterally placed eyes that are protected by a curved bony protuberance along the caudal frontal bone. The eyes are large and nearly spherical, measuring approximately 14 mm in diameter. Eyelid margins are deeply pigmented with numerous fine, long hairs extending ventrally from the upper eyelids (Fig. 43.9a; Tavares-Somma et al. 2017). Similar to other Cavioidea, a vestigial third eyelid is present in the medial canthus that is unable to cover or protect the globe. Palpebral fissure length is slightly larger than chinchillas (Müller et al. 2010) averaging 1.7 cm (Tavares-Somma et al. 2017). The cornea is much thicker than most rodents at 0.8 mm. Secretions from the Harderian and lacrimal glands promote corneal health. Tear production, as evaluated by the Schirmer tear test I, is much higher in agoutis (9.7 mm/min) compared to chinchillas (1 mm/min; Lima et al. 2010), pacas

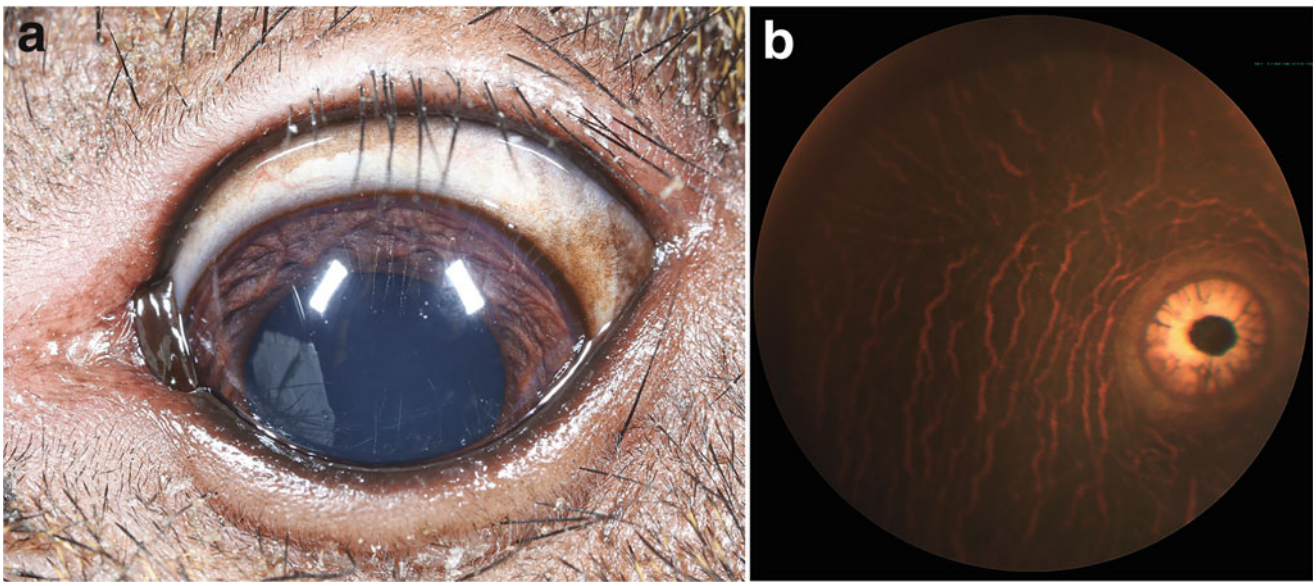

Fig. 43.9 Eye of the normal adult agouti (*Dasyprocta azarae*). (**a**) External photo showing deeply pigmented eyelid margins with numerous fine, long hairs extending ventrally from the upper eyelids. The iris is dark brown in this adult and the pupil is round. (**b**) Fundus image showing a deeply pigmented fundus still permitting visualization of large choroidal vessels. A paurangiotic retinal vascular pattern is present and a tapetum is absent. The optic nerve is circular with a dark, pigmented area centrally. (**a**—Courtesy of Bret A. Moore. **b**—Courtesy of Drs. Andre Tavares Somma and Fabiano Montiani-Ferreira)

(4.1 mm/min; Balthazar da Silveira et al. 2018), and guinea pigs (0.36 mm/min; Trost et al. 2007). However, the capybara has significantly higher tear production (15 mm/min; Montiani-Ferreira et al. 2008). The variability between these species within Caviomorpha may be due to eye size, conjunctival fornix depth, use of sedatives/anesthetics for testing, test technique, or differences in species specific ecological niches (Appendix C). Reflex tearing may also contribute to the higher tear production in agoutis, as they have greater corneal sensitivity (corneal touch threshold 4.5 cm; Tavares-Somma et al. 2017) compared to guinea pigs (corneal touch threshold 2 cm; Trost et al. 2007) and chinchillas (corneal touch threshold 0.3–1.2 cm; Müller et al. 2010; Lima et al. 2010). Corneal sensitivity in capybaras is unknown and speculation on its correlation to tear production cannot be assumed.

The iris of *D. azarae* is variably pigmented, having a gray hue in young animals along the ciliary zone and then becoming more progressively pigmented toward the pupil. Adults have a dark brown pupil (Fig. 43.9a). Pupils are circular, which is a common shape for diurnal animals. Intraocular pressure via applanation tonometry was 11.61 ± 0.44 mmHg (Tavares-Somma et al. 2017) (Appendix C). Applanation tonometry is likely accurate in this size eye, but validation of tonometer accuracy relative to manometric IOP has not been completed. Rebound tonometry has also not been evaluated.

The fundus of the common agouti is unique. The choroid is deeply pigmented and contains a radiating network of large vessels (Fig. 43.9b). Unlike the paca, a tapetum is absent. Retinal ganglion cells are numerous, with a total concentration of approximately 500,000 cells (Silveira et al. 1989). A well-organized visual streak is present superior to the optic disk with a peak density of 6250 cells/mm^2, which is much higher than capybaras and pacas (Silveira et al. 1989). The retina is rod-dominated with 47,000 cells/mm^2 in the periphery and 64,000 cells/mm^2 centrally (Rocha et al. 2009). Agoutis are dichromats with short wavelength sensitive cone photoreceptors (S-cones) and long wavelength sensitive cone photoreceptors (L-cones); L-cones account for 90% of all cones (Rocha et al. 2009). L-cone densities are highest in the visual streak, superior to the optic disk with a dorsoventral gradient. S-cones do not appear to be present in an identifiable visual streak. Cones coexpressing L and S-opsin (dual pigment cones) are not present. Cones account for 11–25% of all photoreceptors, which is common in diurnal animals (Peichl 2005). Located in the inferior temporal aspect of the fundus, the optic nerve is round with a dark circular pigmented area centrally (Fig. 43.9b). This pigmented area was suspected to be a conical projection consisting of remnants of a hyaloid vessel (Silveira et al. 1989). However, histopathology revealed melanocytic pigment granules interspersed between nerve fiber bundles and no evidence of hyaloid remnants (Tavares-Somma et al. 2017). Additionally, optical coherence tomography revealed a physiologic depression of almost the entire optic nerve head (Fig. 43.10). There are a variable number (14–30) of small blood vessels emanating from the optic disk and extending only into the

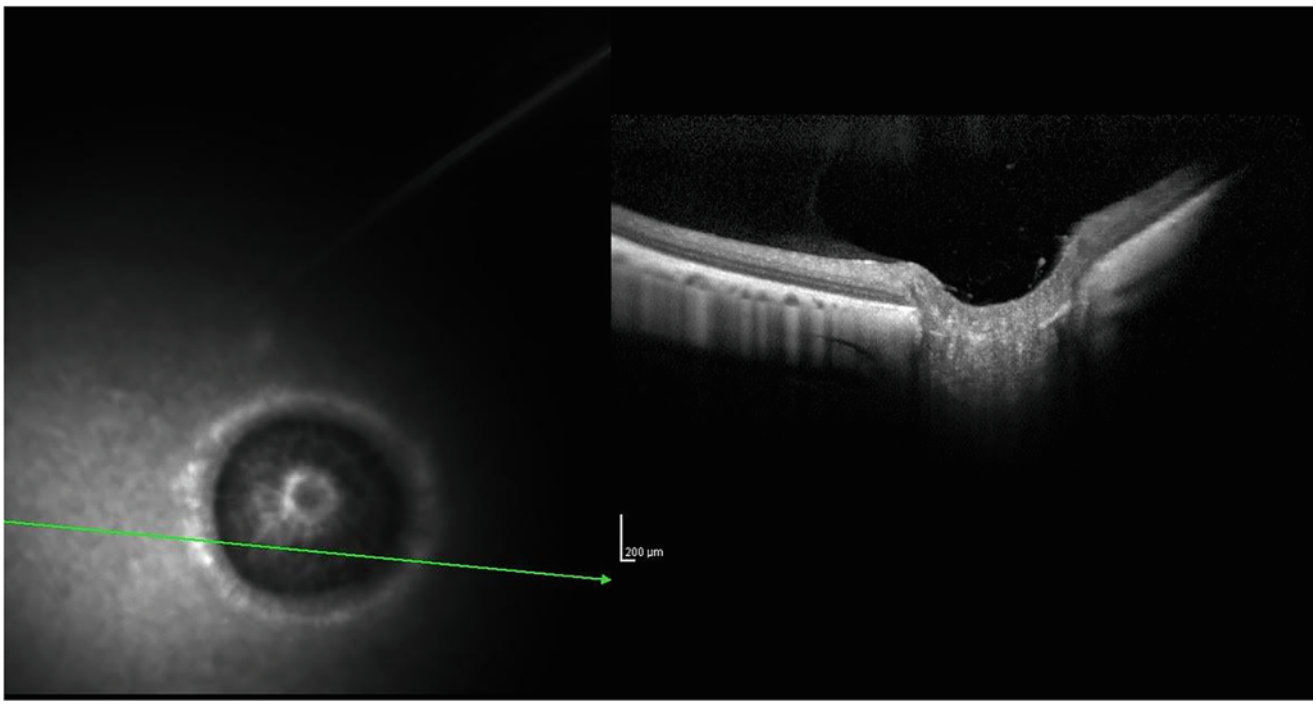

Fig. 43.10 Optical coherence tomography of the posterior pole of the eye of an adult agouti (*Dasyprocta azarae*). There is a large physiologic depression of almost the entire optic nerve head. (Courtesy: Drs. Andre Tavares Somma and Fabiano Montiani-Ferreira)

immediate peripapillary retina (Silveira et al. 1989; Tavares-Somma et al. 2017). This confirms that the agouti has a paurangiotic retinal vascular pattern similar to guinea pigs (Fernandez and Dubielzig 2013) and horses (DeSchaepdrijver et al. 1989).

Ophthalmic disease has not been reported in agoutis in the literature. The normal conjunctiva harbors numerous bacterial species, including both Gram-positive and Gram-negative species. Non-hemolytic *Streptococcus sp* is the most prevalent, followed by *Enterobacter harfinia*, *Escherichia coli*, and *Staphylococcus epidermidis* (Tavares-Somma et al. 2017). These isolates are present in healthy eyes, with no reports of infectious conjunctivitis. An Azarae's agouti with diabetes mellitus has been observed with a cataract (Fig. 43.11), with the assumption that the cataract is secondary to the diabetes.

Dolichotinae, Hydrochoerinae, and Caviinae are the three subfamilies of Caviidae. Dolichotinae include one genus, *Dolichotis*, commonly called maras. Maras primarily inhabit the Patagonian steppes of Argentina and are the fourth largest rodent in the world. There is no available literature describing ophthalmic anatomy, physiology, or vision. Hydrochoerinae include two living genera, *Kerodon* and *Hydrochoerus*, each with two species. *Kerodon* or rock cavies inhabit semi-arid regions of northeast Brazil known as the Caatinga. As their name implies they live in crevices and hollows of large granite boulders. While little is known about overall ocular anatomy, the retina and its central projections have been examined in rock cavies. A visual streak is present along the horizontal meridian in the superior retina and based on peak retinal ganglion cell density visual acuity is estimated to be 4.13 cycles/degree (Oliveira et al. 2018). This is similar to that reported for cats (Clark and Clark 2013) and far superior to that of the African mole rat (Němec et al. 2008). The

Fig. 43.11 Complete cataract in an agouti (*Dasyprocta azarae*), secondary to diabetes mellitus. (Courtesy of Dr. Fabiano Montiani-Ferreira)

Fig. 43.12 The normal eye of a capybara (*Hydrochoerus hydrochaeris*). (**a**) External photograph showing the presence of cilia along the superior eyelid only and brown pigmentation of the bulbar conjunctiva. (**b**) External photograph showing a vertically ovoid pupil. (**c**) Fundus photo showing dark pigmentation with prominent, radiating choroidal vessels. A paurangiotic retinal vascular pattern is present and a tapetum is absent. The optic nerve is round, dark, and contains a small central pit. (**a**, **b** Used with permission from Montiani-Ferreira et al. (2008) The capybara eye: clinical tests, anatomic and biometric features. Vet Ophthalmol 11:386–394. **c**—Courtesy: Ana Carolina Rodarte Almeida)

topographic distribution of retinal ganglion cells in *Kerodon rupestris* suggests the inferior visual field is used for object resolution, adjustment to ambient light intensity, and movement detection (Oliveira et al. 2018). Contralateral retinal projections to the suprachiasmatic nucleus are present and likely involved in photoperiod entrainment (Nascimento et al. 2010a). Direct retinal projections to the medial dorsal nucleus of the thalamus are present and these projections may be involved in modulation of visual recognition and object-reward association memory (Nascimento et al. 2010b).

Hydrochoerus hydrochaeris or capybara is the largest living rodent in the world. They are semi-aquatic, crepuscular, selectively herbivorous, and inhabit densely forested areas near bodies of water throughout South America, except Chile. Similar to pacas, they are superb swimmers and can avoid predators by remaining submerged for several minutes (Redford and Eisenberg 1992). The skull of capybaras is massive and rectangular, with an expanded zygomatic arch, circular orbit, and well-developed infraorbital foramen (Pereira et al. 2020). The eye is enormous compared to other rodents, with an axial globe length of approximately 22 mm (Montiani-Ferreira et al. 2008) similar to that of a large breed dog such as a Labrador Retreiver or Boxer (Chiwitt et al. 2017). The palpebral fissure is wide, as expected with such a large eye. The eyelids contain cilia on the upper eyelid only, superior and inferior lacrimal puncta are located nasally, and a vestigial third eyelid is present, similar to the paca (*C. paca*). A significant amount of melanin granules are present in the deep layers of the bulbar conjunctiva, giving the conjunctiva a brown appearance (Fig. 43.12a). This pigmentation may be an evolutionary adaptation to aid in protection of the eye from chronic ultraviolet light exposure from the environment. Conjunctival bacterial flora has been identified, with all isolates being Gram-positive. *Corynebacterium spp* were most prevalent, followed by *Micrococcus spp*, *Bacillus spp*, and *Staphylococcus spp* (Montiani-Ferreira et al. 2008). The cornea is broad with a horizontal diameter of approximately 17 mm. Morphologically, the cornea is similar to other mammals. The presence of Bowman's layer between the corneal epithelium and anterior stroma is similar to primates (except Lemur, *Lepilemur mustelinus*), guinea pigs, deer, giraffe, ox, zebu, and eland (Merindano et al. 2002; Cafaro et al. 2009). Corneal thickness is similar to other mammals, at 0.483 mm (Montiani-Ferreira et al. 2008) and secretions from the lacrimal gland, goblet cells, and Harderian gland maintain surface health. Tear production as measured by Schirmer tear test was 14.97 ± 4.6 mm/min, much higher than other Cavioidea (Appendix C). The larger capybara eye, a deeper conjunctival fornix (more significant lacrimal lake), or increased corneal sensitivity improving reflex tearing may explain the higher Schirmer tear test results in this species. Corneal sensitivity has not been evaluated in capybaras. The iris is variably pigmented, but usually dark brown. The pupil is vertically ovoid (Fig. 43.12b) and becomes circular with dilation, similar to porcupines. Intraocular pressure by applanation tonometry was 16.47 ± 4.28 mmHg (Montiani-Ferreira et al. 2008) (Appendix C). Fundic exam of the capybara is similar to the agouti. The choroid is pigmented with prominent, radiating choroidal vessels, absence of a tapetum, and a circular optic nerve with a small central pit (Fig. 43.12c). Capybaras have a paurangiotic retinal vascular pattern, as evidenced by 2–3-minute vessels extending off the edge of the optic nerve (Montiani-Ferreira et al. 2008). Total retinal ganglion cell population was 368,840 cells with these cells organized into a visual streak superior to the disk having a peak cell density of 2250 cells/mm^2 (Silveira et al. 1989), intermediate between pacas and agoutis. The location of the well-developed visual streak is regarded as a retinal specialization allowing them to view the whole horizon without specialized eye movements required for scanning with an area centralis (Stone 1983).

Fig. 43.13 External photograph of a capybara (*Hydrochoerus hydrochaeris*) with chronic, idiopathic keratoconjunctivitis. Note the arborizing superficial corneal blood vessels. (Courtesy: Dr. Ana Carolina Rodarte Almeida)

Ophthalmic abnormalities have not been reported in the literature. One case of keratoconjunctivitis in *H. hydrochaeris* was observed by one of the authors (F. Montiani-Ferreira) although the cause was unknown (Fig. 43.13).

Caviinae is best known for the domestic guinea pig, *Cavia porcellus*, but consists of three genera and at least 13 species including *Galea* (yellow-toothed cavies), *Microcavia* (mountain cavies) and *Cavia* (guinea pigs). All Caviinae are native to South America, crepuscular, and herbivorous. The domesticated guinea pig, *C. porcellus*, is not found in the wild. It likely represents a domesticated species of *C. tschudii*, but possibly *C. aperea or C. fulgida*. *C. porcellus* was domesticated as a livestock species for human food consumption and is still used in this capacity in South America today. Newer species of *Cavia* including *C. guianae* and *C. anolaimae* are suspected to be feral *C. porcellus* that were reintroduced into the wild (Zúñiga et al. 2002). In the United States, the domestic guinea pig is a popular pocket pet. The American Cavy Breeders Association currently recognizes 13 breeds of guinea pigs, each with their own specific characteristics. These include long-haired breeds (Peruvians, Silkies, and Coronets), short-haired breeds (American, Teddy, and White Crested), curly coat breeds (Texel), and those with rosettes (Abyssinian). An additional breed, the skinny pig, which is practically hairless other than the muzzle, feet, and legs, is suspected to be a cross between haired and hairless strains (Wu et al. 2020). The hairless strain is related to a spontaneous genetic mutant identified in the Hartley guinea pig colony (Sueki and Kligman 2003).

Guinea pigs have been extensively used in research, so much so that the epithet "guinea pig" came into use to describe human test subjects. Due to similarities between human and hairless guinea pig skin (Sueki et al. 2000), they have been used in dermatologic studies. Likewise, similarity in symptoms and immune response between humans and guinea pigs has led them to be models for infectious diseases including pulmonary, sexually transmitted, ocular, aural, and gastrointestinal. They are the animal model of choice for tuberculosis (*Mycobacterium tuberculosis*), Legionnaire's disease (*Legionella pneumophila* Philadelphia 1), chlamydia (*Chlamydia trachomatis*), syphilis (*Treponema pallidum* ssp. *palladium*), and *Staphylococcus aureus* infections (Padilla-Carlin et al. 2008). In ophthalmology, guinea pigs have been used as a model for ocular siderosis (Mumcuoglu et al. 2015), allergic and infectious conjunctivitis (Nakazawa et al. 2017; Rank et al. 2012), and myopia (Xiao et al. 2014).

The guinea pig eye sits in a bony orbit formed dorsally by a dense frontal bone and rostrally by a prominent lacrimal bone (Fig. 43.14a). This allows a large monocular visual field of 103–135 degrees, a binocular visual field of 20–63 degrees, and a combined visual field of 325–340 degrees (Duke-Elder 1958, Zhou et al. 2011). Their orbit is in close association with their tooth roots, and expectedly orbital disease is not uncommon (Fig. 43.14b). Guinea pigs have a unique extraocular muscle arrangement. They have the typical superior and inferior oblique muscles as well as superior and inferior recti. The retractor bulbi muscle surrounds the optic nerve longitudinally and inserts circumferentially into the posterior pole of the eye. The guinea pig has two medial recti muscles, a superior and inferior. More intriguing is the lack of a lateral rectus muscle (Fig. 43.15; Zhou et al. 2011). The laterally placed globe and near 360-degree visual field may render the lateral rectus redundant or unnecessary. However other species with similar visual fields such as the rabbit have lateral rectus muscles (Murphy et al. 1986). The superior oblique arises along the medial orbit, but unlike other mammals, it has been reported to not pass through a trochlea to exert a pulley-like effect (Cooper and Schiller 1975). The superior medial rectus muscle may work in conjunction with the superior oblique to aid in intorsion (internal rotation) of the globe to aid in binocular vision.

The guinea pig eyelid lack cilia, and the globe is moderately exposed (Fig. 43.16a). The cornea is large, occupying 80–90% of the interpalpebral fissure. It measures approximately 0.21–0.23 mm, thinner than most mammals (Fernandez and Dubielzig 2013; Cafaro et al. 2009). Corneal architecture mimics their family member, *H. hydrochaeris* (capybara) with the presence of Bowman's layer. Endothelial cell density has been reported at 2352 ± 49 cell/mm2. An early study revealed 90% of guinea pigs had fine superficial stromal vessels extending from the limbus and 6% with perilimbal corneal edema (Dwyer et al. 1983). A more recent

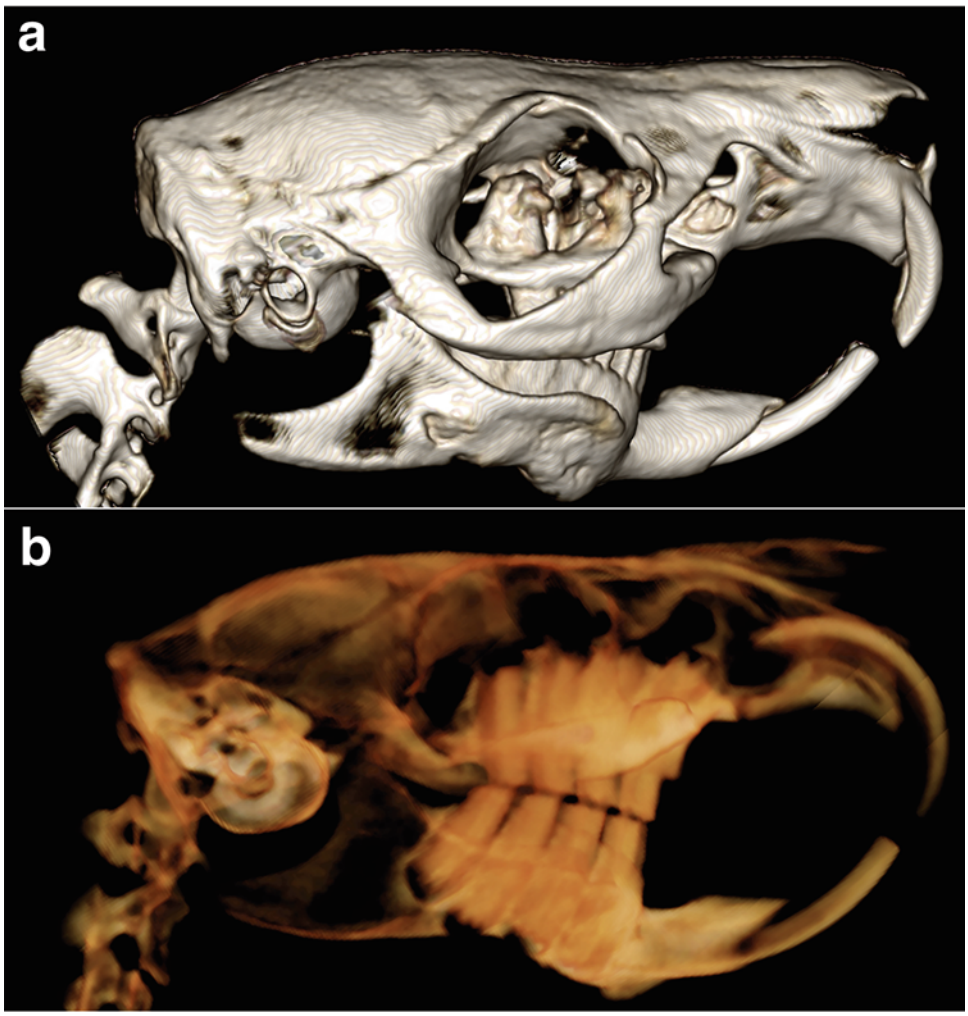

Fig. 43.14 CT scan of a guinea pig showing (**a**) a bony orbit formed dorsally by a dense frontal bone and rostrally by a prominent lacrimal bone, and (**b**) large tooth roots approaching the ventral orbit. (Courtesy of Bret A. Moore)

study did not confirm the presence of these vessels or edema (Cafaro et al. 2009), suggesting that corneal vascularization is not a normal finding in guinea pigs. The palpebral fissure is wide increasing corneal exposure. A vestigial third eyelid is present that is unable to cover or protect the corneal surface.

Corneal health in guinea pigs is suspected to be maintained by an extremely stable tear film. Guinea pigs blink infrequently, approximately 2–5 times per 20 minutes (Trost et al. 2007) similar to rabbits (Korb et al. 1998). However, aqueous tear production is low, with Schirmer tear test and phenol red thread test measurements at 0–3 mm/min and 16–21 mm/15 seconds, respectively (Trost et al. 2007; Coster et al. 2008) (Appendix C). Use of a modified 2.5 mm Schirmer tear test strip revealed tear levels at 8 mm/30 seconds and 10 mm/60 seconds (Nogradi et al. 2020). Corneal sensitivity is also low in guinea pigs, with a corneal touch threshold of 2 cm (Trost et al. 2007; Coster et al. 2008) suggesting guinea pigs lack reflex tearing. A recent study revealed a slight correlation between corneal sensitivity and reflex tearing in numerous species, including guinea pigs (Wieser et al. 2013). However, there was high variability in measurements preventing verification of a true correlation. Guinea pigs were the only studied species that had a negative correlation, with lower tearing measured by a Schirmer tear test I versus II. This supports the suspicion that guinea pigs do not possess reflex tearing. The relative lack of aqueous tear production, low blink frequency, reduced corneal sensitivity, and absence of reflex tearing in guinea pigs implies that another part of the tear film must be responsible for corneal health. Tear film break up time can be measured through an invasive (fluorescein stain) or noninvasive (interferometry, Keeler Tearscope-plus^{TM}) technique. In veterinary ophthalmology, fluorescein stain application is the most commonly used. With this technique, the tear film break up time in guinea pigs was significantly decreased at 5 seconds (Cafaro et al. 2009) compared to rabbits at 25 seconds (Zhu et al. 2003). Noninvasive measurement of tear film break up time has not been completed in guinea pigs, but in rabbits it is an astonishing 29.8 ± 3.4 minutes (Wei et al. 2013). As both species have similar blink frequencies, one would expect similar tear film break up times. These data suggest that the guinea pig tear film is not stable. It is possible

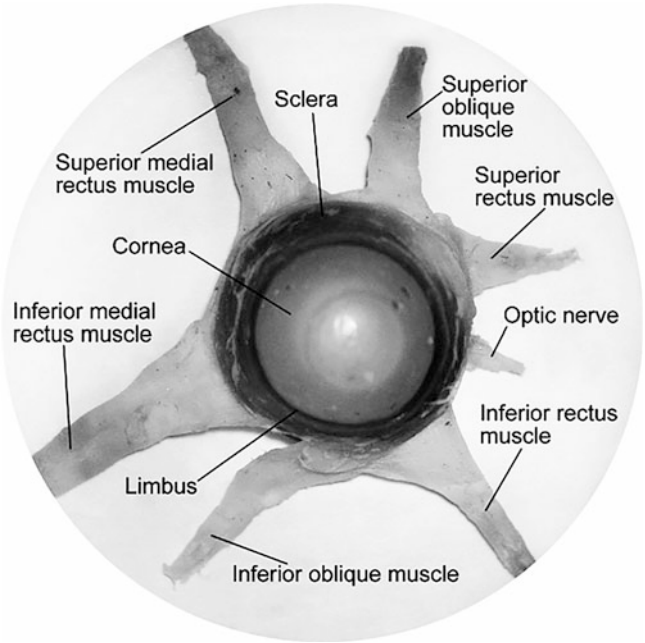

Fig. 43.15 Front view of the left eye of the guinea pig (*Cavia porcellus*). There are two medial rectus muscles (the superior medial muscle and the inferior medial muscle), two oblique muscles (the superior oblique muscle and the inferior oblique muscle), a superior rectus muscle, and an inferior rectus muscle. The lateral rectus muscle is absent. (With permission: Zhou et al. (2011) Microdissection of guinea pig extraocular muscles. Exp Ther Med 2:1183–1185)

that the tear film maintains stability through a different mechanism and classic testing does not account for this species difference. Other than the lacrimal gland (also called the infraorbital gland), guinea pigs have an additional four glands that contribute to the tear film as well as conjunctival goblet cells. These include the Harderian gland, two subconjunctival sebaceous glands, and the numerous Meibomian glands. An extraorbital gland was reported by Ballard (1937) and by Cooper and Schiller (1975), but recent literature does not confirm the presence of this gland. Ballard may have observed the zygomatic salivary gland, while Cooper and Schiller likely described the lacrimal gland (Gasser et al. 2011). The Harderian gland is enormous at approximately 1/2 to 2/3 the entire volume of the globe filling the posterior aspect of the orbit. It is attached to the periorbita and posterior globe with muscle and nerve fibers embedded in glandular nodules (Gasser et al. 2011). The subconjunctival sebaceous glands appear as a pair of triangular, 2.5 × 2 × 1 mm glands visible through the bulbar conjunctiva along the lateral canthus. These glands secrete a thick lipid substance through an excretory duct opening along the lateral canthus (Walde and Nell 2008). Meibomian glands are numerous (20–30 per eyelid) and are present along the entire superior and inferior eyelids housed in loose connective tissue (Gasser et al. 2011). Excretory ducts open along the eyelid margin, just anterior to the mucocutaneous junction. Conjunctival goblet cells secrete mucin and are of highest density in the nasal bulbar and palpebral conjunctival region. The lacrimal gland is large, triangular, and is located behind the orbital ligament along the lateral aspect of the bony orbit. It is visible with dissection within the ventrolateral orbit and is attached to the periosteum of the zygomatic bone. These five glands along with the conjunctival goblet cells influence surface ocular health and possibly tear film stability. Tears exit the ocular surface through the superior and inferior lacrimal puncta and follow a tortuous nasolacrimal duct containing 30–60 degree bends.

The guinea pig fundus is atapetal and clinically appears anangiotic (Fig. 43.16b, c). However, on histological examination, there are vessels on the optic nerve head that may extend just past the optic disk margin consistent with a

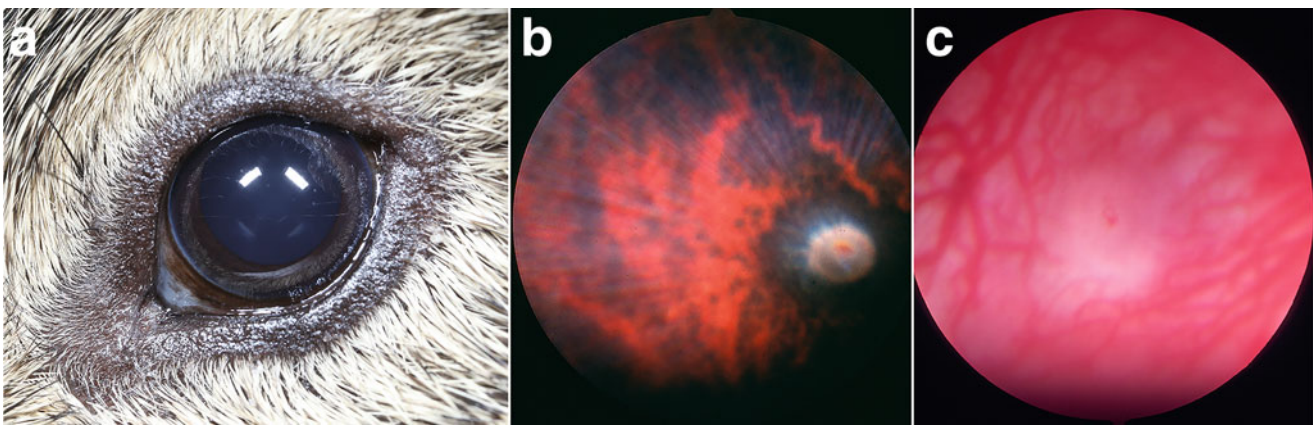

Fig. 43.16 Normal eyes of adult guinea pigs (*Cavia porcellus*). (**a**) An external photograph showing pigmented eyelid margins that lack cilia, and visualization of the limbus only at the medial and temporal aspects. A paurangiotic retinal vascular pattern is evident in both a (**b**) pigmented and (**c**) albino guinea pig. Note the glistening nerve fiber layer and the tuft of blood vessels on the surface of the optic disk. (**a**—Courtesy of Bret A. Moore. **b**, **c**—Courtesy of the University of California Davis, Comparative Ophthalmology Service)

paurangiotic retinal vascular pattern (Fernandez and Dubielzig 2013). The retina is rod-dominant with rods possessing a photopigment with a wavelength of maximal absorption at 494–500 nm. Guinea pigs are dichromats possessing a medium wavelength sensitive photopigment (M cone) with maximal absorbance at 529–530 nm and a short wavelength sensitive photopigment (S-cone) at 400–429 nm (Jacobs and Deegan 1994; Parry and Bowmaker 2002). M cones are the predominant photoreceptor in the dorsal retina, while the majority in the ventral retina are S-cones. A transition zone exists between these populations of cells with 10–20% of photoreceptors expressing both M- and S-opsin. The visual streak is located temporally and inferior to the optic disk, improving superior visual field clarity that may aid in predator detection. The optic disk is circular and nonmyelinated. A well-defined, collagenous lamina cribrosa is present that spans the scleral opening and resembles that of humans and tree shrews. This similarity may promote a guinea pig model for primary open angle glaucoma (POAG) in humans, although primary glaucoma has not been reported in guinea pigs. There is one report of secondary glaucoma, based on histopathologic evaluation (Schäffer and Pfleghaar 1995). Intraocular pressures in guinea pigs range from 4–10 mmHg via rebound tonometry and 13–21 with applanation tonometry (Coster et al. 2008; Ansari-Mood et al. 2016; Di et al. 2017) (Appendix C). Daily variations of up to 4 mmHg (rebound tonometry) or 7 mmHg (applanation tonometry) occur with the lowest reading during the light period (7AM–5PM) and highest reading during the dark period (8PM–6AM; Ansari-Mood et al. 2016). The effects of pressure lowering medications have not been thoroughly evaluated in guinea pigs. One study reported a reduction of 0–3 mmHg in intraocular pressure depending on medication used. Carteolol had no effect, while brinzolamide had the longest duration at 7 hours, and both brimonidine and latanoprost had the shortest duration at 1 hour (Di et al. 2017).

The guinea pig retina is thin, as expected due to its avascular nature. It measures approximately 147 μm (Jnawali et al. 2018) right at the limit of the theoretical oxygen diffusion maximum of 143 μm. The retinal ganglion cell layer along with the nerve fiber layer is approximately 60 μm in diameter. The retinal ganglion cell axons are organized into fascicles within the optic nerve head and become myelinated as they emerge from the caudal aspect of the lamina cribrosa (Ostrin and Wildsoet 2016). These optic nerve fibers are predominately medium sized, unlike those in humans and cats that are large. Nerve conduction is quite fast, with the guinea pig optic nerve having a myelin g-ratio (ratio of inner to outer radius of the myelin sheath for a circular axon cross section) of 0.81 (Guy et al. 1989). An optimal g-ratio is 0.6–0.7 (Rushton 1934; Chomiak and Hu 2009) with humans having a g-ratio of 0.7 (Cercignani et al. 2017). Retinal fibers terminate in the suprachiasmatic nucleus, lateral geniculate nucleus, pretectal nuclei, and superior colliculi (Lázár 1983). Over 90% of the geniculocortical axons arising from the dorsal lateral geniculate nucleus innervate layer 4 of the primary visual cortex (Sáez and Friedlander 2009).

Functional vision is present in guinea pigs, although ability to discriminate fine detail is poor. A menace response was present in 10% of animals and a dazzle reflex in 13% (Coster et al. 2008). Visual acuity estimated by retinal ganglion cell peak density assesses as 2.7 cycles per degree or a Snellen equivalent of 6/70 (Buttery et al. 1991). Although guinea pigs are used as a model to study myopia, they are born hypermetropic (+5.22 ± 0.23D) which rapidly reduces toward emmetropia within the first 3 weeks of age due to an increase in vitreous chamber depth (Zhou et al. 2006). However, streak retinoscopy in adult guinea pigs reveals persistence of hypermetropia with a refractive error of +3.27 to +3.50 D (Zhou et al. 2006; Jnawali et al. 2018). The presence of color vision in guinea pigs has been debated. In one study (Miles et al. 1956), guinea pigs could detect different light intensities but could not discriminate red from green or green from blue wavelength light. Behavioral studies performed by Jacobs and Deegan (1994) verified color discrimination with a spectral neutral point (where light appears achromatic) at approximately 480 nm.

Ophthalmic disorders are common in the domestic guinea pig (*C. porcellus*). Forty-five percent of animals surveyed were affected (Williams and Sullivan 2010), including both congenital and acquired diseases. Roan x roan Abyssinian guinea pigs may have congenital anophthalmos (Wagner and Manning 1976) or may be microphthalmic with cataract formation. Sows treated with tylosin tartrate (Tylan®) while pregnant may have pups with congenital cataracts (Williams and Gum 2013). A 3.6°C increase in basal temperature in pregnant sows resulted in exophthalmos in 7% and cataract in 3% of newborn pups (Edwards 1969). Corneal and conjunctival dermoids have been reported (Fig. 43.17; Brunschwig 1928; Wappler et al. 2002). Concurrent conjunctivitis, keratitis, and corneal ulceration may be present and therefore surgical resection is indicated. Surgery should be completed with significant magnification and with great care due to the excessively thin guinea pig cornea.

Adnexal disease is infrequently encountered in guinea pigs. Blepharitis secondary to dermatophytosis is most common. Juvenile, aged, or immune challenged guinea pigs may be infected by *Trichophyton mentagrophytes* and less commonly *Microsporum canis*. While eyelids can be affected, most cases involve the tip of the nose, inguinal area, and abdomen. Clinical signs include periocular pruritus, erythema, crusts, and alopecia. Skin scrapings and fungal culture can provide a definitive diagnosis. Topical therapy with 2% miconazole or 1% clotrimazole or oral therapy with itraconazole is usually curative. Conformational

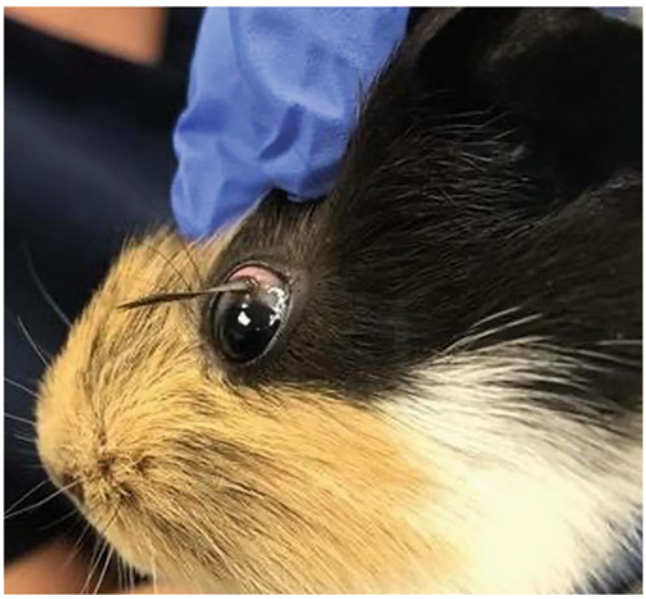

Fig. 43.17 Limbal dermoid in the left eye of an American guinea pig (*Cavia porcellus*)

abnormalities include entropion and trichiasis. Entropion has been suggested to be a heritable trait in the Texel, Rex, and Teddy breeds although a mode of inheritance has not been identified (Holmberg 2018). Surgical treatment utilizing a modified Hotz–Celsus is usually curative. Trichiasis arising from the medial canthus has been noted in the Texel breed (0.8% prevalence) and skinny pigs (30% prevalence; Wu et al. 2020). While usually clinically insignificant, treatment with a topical lubricating ointment may be used to decrease frictional irritation and potential keratitis or corneal fibrosis.

Fig. 43.18 Corneal laceration with iris prolapse in the right eye of a guinea pig (*Cavia porcellus*) following trauma due to a cat claw. (Courtesy of the University of California Davis, Comparative Ophthalmology Service)

Corneal disease is common due to trauma (Fig. 43.18), corneal exposure from orbital disease or facial nerve paralysis (Figs. 43.19 and 43.20), or ocular surface irritation due to a low blink frequency, low corneal sensitivity, lack of a protective third eyelid, and reduced tear production (Fig. 43.21). With prolonged exposure, placement of a temporary tarsorrhaphy is recommended to provide adequate protection to the cornea and enabling it to heal (Fig. 43.20). A single horizontal mattress suture with 5-0/6-0 nylon encompassing skin stents is usually sufficient (Fig. 43.20b). Corneal foreign bodies are common due to habitat with hay or straw becoming embedded in the conjunctiva or cornea leading to secondary ulcerative keratoconjunctivitis. Foreign bodies may result in infected stromal ulceration (Fig. 43.22) or even corneal perforation. Up to 70% of skinny pigs had some form of foreign body present on exam (Wu et al. 2020). Examination is facilitated with topical anesthesia and magnification. Foreign bodies can usually be easily removed with fine forceps and/or copious lavage with sterile balanced salt solution. After removal of the offending material, symptomatic treatment of corneal ulceration should be completed. Infectious keratoconjunctivitis may be caused by fecal contamination of the eye with *Salmonella weltevreden*, as noted in a guinea pig colony (Albert et al. 1991). Although bacterial isolates were susceptible to numerous antibiotics including ampicillin, tetracycline, chloramphenicol, gentamicin, and trimethoprim-sulfamethoxazole, animals were sacrificed to try and prevent further colony infection.

Conjunctivitis is common in guinea pigs, affecting 5% of a pet population (Williams and Sullivan 2010) and 70% of skinny pigs (Wu et al. 2020). Conjunctival microflora were present in 77–97% of animals and included *Corynebacteriu spp*, α-hemolytic *Streptococcus spp*, and *Staphylococcus epidermis* (Coster et al. 2008; Faghihi et al. 2019). These isolates likely represent nonpathogenic commensal flora of the conjunctiva. Skinny pig conjunctival flora is similar with α-hemolytic *Streptococcus spp* and coagulase-negative *Staphylococcus spp*. However, *Pasteurellaceae spp* (mostly *P. multocida*) were the most frequently isolated bacteria with 95% of animals having this organism; these may be pathogenic (Wu et al. 2020). Primary infectious conjunctivitis in guinea pigs has classically been associated with chlamydial organisms (Murray 1964). Animals present with minor conjunctival hyperemia to severe conjunctivitis with mucopurulent discharge. Diagnosis in young animals may be made through visualization of intracytoplasmic inclusion bodies in conjunctival epithelial cells or through PCR. *Chlamydophila psittaci*, also known as *Chlamydophila caviae*, is the causative agent. In one study (Lutz-Wohlgroth et al. 2006), 64% of symptomatic guinea pigs were PCR-positive for *C. caviae* while 23% of asymptomatic animals were positive. Guinea pig pet owners should be educated about the zoonotic potential of this organism.

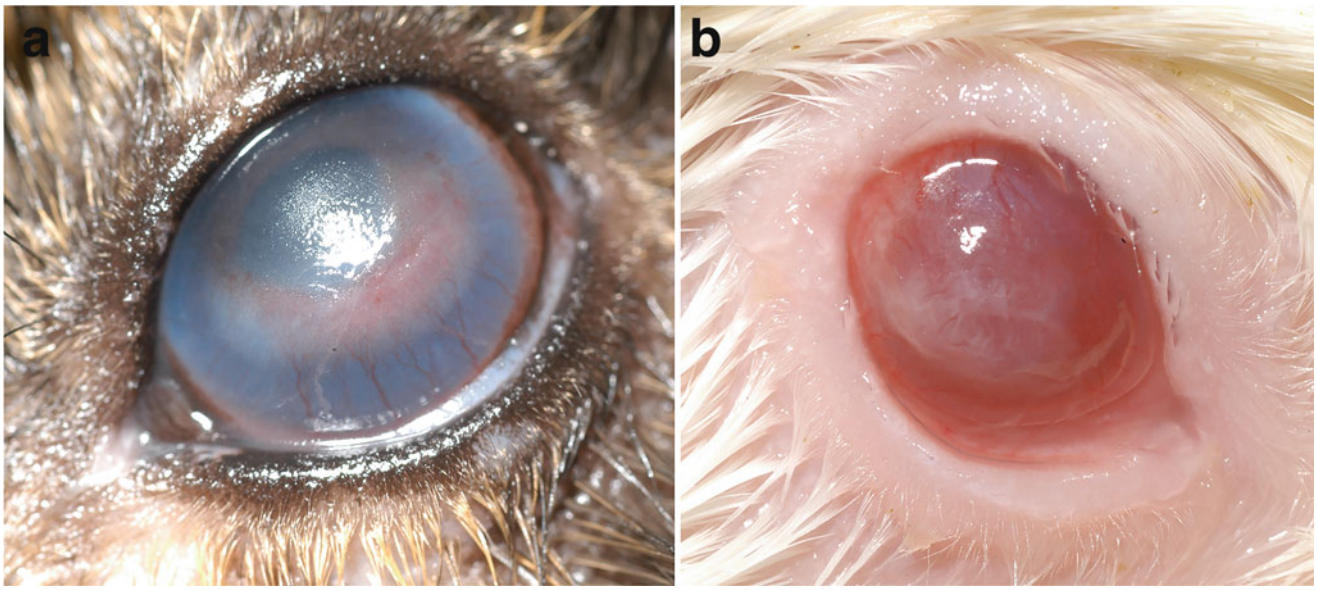

Fig. 43.19 Exposure keratitis in guinea pigs (*Cavia porcellus*) due to (**a**) retrobulbar abscess causing exophthalmos, and (**b**) facial nerve paralysis. Note the marked vascularization and fibrosis of both corneas. (Courtesy of Bret A. Moore)

Other infectious causes of conjunctivitis in guinea pigs include *Listeria monocytogenes*, *Salmonella spp*, *Pasteurella spp*, and *Staphylococcous aureus* (Faghihi et al. 2019). Thick, mucoid ocular discharge is common in guinea pigs with 22–30% of normal animals affected (Dwyer et al. 1983) and up to 80% of skinny pigs (Wu et al. 2020). This higher incidence in skinny pigs may be due to their conjunctival flora, higher incidence of trichiasis, or increased elasticity of the eyelids allowing more particulate debris accumulation. Observation of discharge with concurrent conjunctivitis and/or keratitis should prompt the clinician to evaluate the ocular surface for foreign material and consider bacterial culture of the discharge (Fig. 43.23). Non-infectious conjunctivitis may be present in vitamin C deficient guinea pigs. Usually concurrent systemic signs of malocclusion, respiratory disease, or renal disease are present. Treatment is aimed at restoring normal vitamin C levels through parenteral and oral supplementation.

Conjunctival masses may be observed within the inferior fornix. Overfed guinea pigs may have lipid accumulation in the ventral subconjunctiva, commonly called "fatty eye" or "pea eye" with a reported incidence of 2.3% (Fig. 43.24a, b; Williams and Sullivan 2010). This mass may be unilateral or bilateral and can cause focal ectropion depending on its size and location. Up to 10% of guinea pigs with subconjunctival lipid may also have corneal involvement, with stromal lipid deposition in the axial cornea. A discrete pink-red mass may appear at the medial canthus. This mass contains glandular tissue and is commonly called "flesh eye" (Fig. 43.24c). It has an incidence of 0.5% and may be analogous to a

Fig. 43.20 Exposure keratitis in a guinea pig (*Cavia porcellus*) due to facial nerve paralysis, resulting in (**a**) marked granulation tissue in the axial cornea. (**b**) A temporary tarsorrhaphy was placed with 6-0 nylon in a single horizontal mattress pattern, using medical tubing as stents. (**c**) Approximately 10 days after placement of the tarsorrhaphy, it was removed and revealed marked improvement to the corneal surface. (Courtesy of Bret A. Moore)

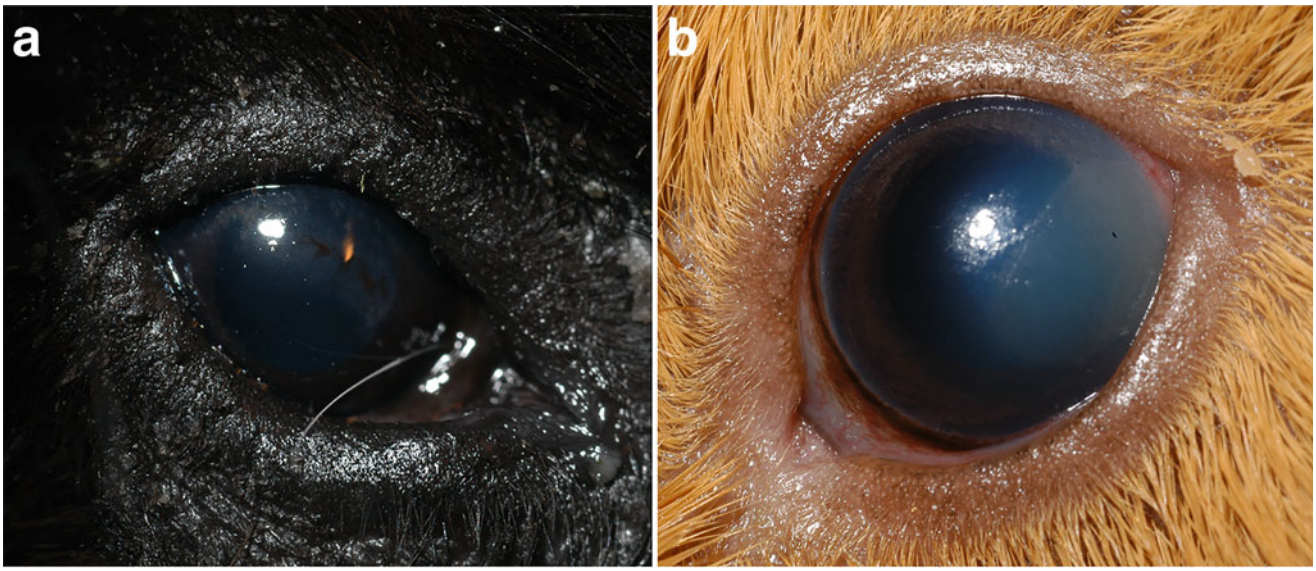

Fig. 43.21 Ulcerative keratitis in guinea pigs (*Cavia porcellus*) secondary to keratoconjunctivitis sicca caused by (**a**) facial nerve paralysis and (**b**) suspected immune-mediated inflammation of the lacrimal gland

prolapsed nictitans gland (Williams and Sullivan 2010). Differential diagnoses for conjunctival masses should also include conjunctival lymphosarcoma (Allgoewer et al. 1999) and liposarcoma (Quinton et al. 2013).

Cataracts were the most commonly reported abnormality in pet guinea pigs, with 17% affected with some degree of opacity (Williams and Sullivan 2010). Incipient cataracts (5.3%; Fig. 43.25) were most common, followed by immature (5%) and mature (3.4%) cataracts. Immature cataracts (Fig. 43.25) were suspected to be age-related, and younger guinea pigs were assumed to have inherited cataracts. Similar to viscachas (Gull et al. 2009), degus (Brown and Donnelly 2001), dogs (Basher and Roberts 1995), desert gerbils (Shafrir et al. 2006), and chinchillas (Ewringmann and Göbel 1998), guinea pigs develop diabetic cataracts. Eight percent of mature cataracts observed by Williams and Sullivan (2010) were present in diabetic animals. Cataracts in guinea pigs have been induced by galactose administration (Kosegarten and Maher 1978), L-tryptophan deficiency (vonSallmann et al. 1959), and possibly hypovitaminosis C (Williams and Sullivan 2010). Congenital, genetic cataracts have been identified in a laboratory strain (13/N) of guinea pigs secondary to a single splice-site mutation in the zeta-crystallin gene (Bettelheim et al. 1997). This defect is inherited in an autosomal dominant fashion (Stone and Amsbaugh 1984). Surgical removal of cataracts has not been reported in guinea pigs. Treatment with topical anti-inflammatory therapy is recommended if phacolytic uveitis is evident to prevent secondary complications such as corneal degeneration (Fig. 43.25d) and glaucoma.

Fig. 43.22 Infected stromal corneal ulcer in the left eye of a guinea pig (*Cavia porcellus*). (**a**) Note the significant cellular infiltrate, corneal edema, and circumferential stromal vascularization at initial presentation. (**b**) After 1 week of aggressive topical therapy, the cornea improved substantially, and (**c**) by 2 weeks was nearly normal. (Courtesy of the University of California Davis, Comparative Ophthalmology Service)

Fig. 43.23 Chronic nonulcerative keratitis and conjunctivitis in a guinea pig (*Cavia porcellus*). Note the discharge at the medial canthus and the periocular alopecia especially at the medial canthus. (Courtesy of the University of California Davis, Comparative Ophthalmology Service)

Osseous metaplasia, commonly referred to as heterotopic bone, has been identified in approximately 0.8% of guinea pigs (Griffith et al. 1988; Sandmeyer et al. 2011; Williams and Sullivan 2010). Bony metaplasia arises from the ciliary body stroma and expands within the anterior chamber giving the clinical appearance of a white, variably vascularized mass along the anterior aspect of the anterior chamber (Fig. 43.26). Histologically, bony spicules are surrounded by a fibrous envelope. Hematopoietically active bone marrow and vascular channels may be evident in some specimens (Griffith et al. 1988). The cause is unknown, but older animals are more likely to be affected and 15% have dystrophic mineralization elsewhere in the body. The role of the ciliary body in concentrating ascorbic acid may promote bone formation. Treatment is not necessary as concurrent ophthalmic disease is usually not present. However, sequelae include corneal edema if heterotopic bone contacts the corneal endothelium (Fig. 43.27a) and hyphema (Fig. 43.27b). Secondary glaucoma may also be a sequela to heterotopic bone formation, and has been suspected clinically (Fig. 43.27c). Additionally, glaucoma was diagnosed in several histologic samples of guinea pigs with heterotopic bone (Schäffer and Pfleghaar 1995).

Retinal disease in guinea pigs is rare. In a large survey study, none of the 1000 animals examined had any retinal disease (Williams and Sullivan 2010). A spontaneous rod-cone degenerative disease has been reported (Racine et al. 2003) with an autosomal recessive inheritance. Scotopic electroretinogram waveforms were severely diminished and light microscopy revealed an absence of the outer segment layer and a reduction in the outer nuclear layer thickness (Racine et al. 2011).

When blind and painful, enucleation is a feasible and relatively safe option for guinea pigs (Fig. 43.28). Blind guinea pigs tend to do well in their enclosure, and enucleation affords them rapid relief from chronically painful conditions if the eye has become blind. Massive orbital hemorrhage often noted in other pocket pets is not as typical, rather pronounced orbital fat is evident (Fig. 43.28d). Elizabethan collars can be fashioned from various materials and are generally well tolerated (Fig. 43.29).

Octodontoidea (Degus)

The superfamily Octodontoidea is a subset of the New World hystricognaths including 11 families that reside in southwestern South America. The common degu (*Octodon degus*) is the most recognized and studied species of Octodontoidea.

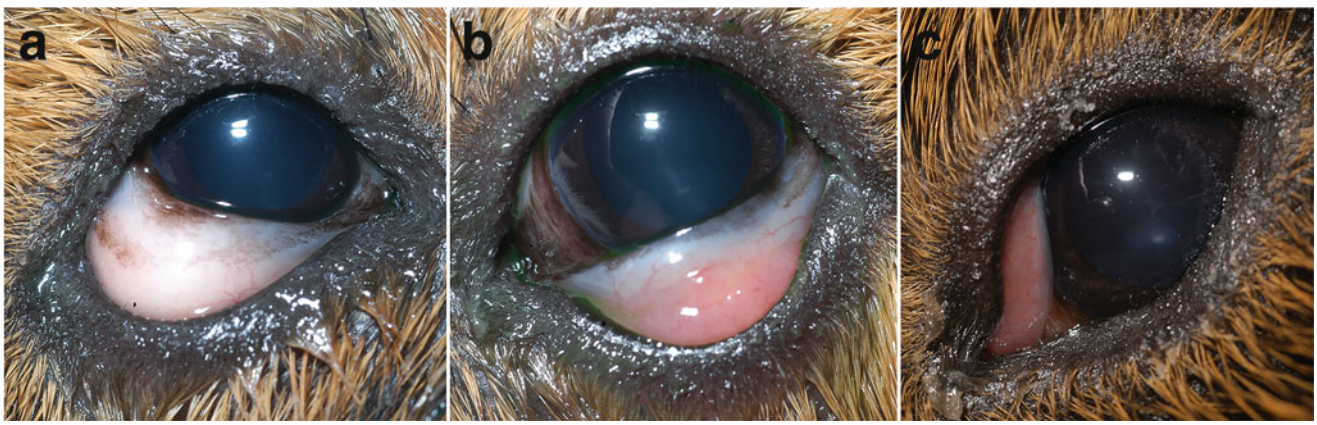

Fig. 43.24 (**a**) and (**b**) Lipid accumulation in the ventral subconjunctiva of a guinea pig, commonly called "fatty eye" or "pea eye". (**c**) "Flesh eye" in a guinea pig. Note the discrete pink-red mass at the medial canthus. This mass contains glandular tissue and may be analogous to a prolapsed nictitans gland. (Courtesy of the University of California Davis, Comparative Ophthalmology Service)

Fig. 43.25 Cataracts in guinea pigs (*Cavia porcellus*). (**a**) Nuclear fibrillar cataracts, (**b**) incipient nuclear cataract (also note the presence of heterotopic bone along the temporal anterior chamber), (**c**) a diffuse, late immature cataract, and (**d**) a hypermature cataract and chronic phacolytic uveitis, resulting in secondary corneal degeneration. (**a**, **c**, **d**—Courtesy of Bret A. Moore)

They have been extensively used as a laboratory model to study neurobiological development, tool-use training behavior (Okanoya et al. 2008), diabetic cataract formation (Brown and Donnelly 2001), Alzheimer-like pathology (Steffen et al. 2016), as well as other aging diseases (Hurley et al. 2018). Degus are endemic to the Chilean matorral ecoregion of central Chile. They are semi-fossorial, strictly herbivorous, and quite social, living in complex burrows that persist for years (Ebensperger et al. 2011). Of the four species of Octodon, two are diurnal (*O. degus*, *O.* pacificus) and two are nocturnal (*O. lunatus*, *O. bridgesi*). This difference allows for comparison of nocturnal vision versus diurnal vision within the same genus (Vega-Zuniga et al. 2013).

Octodons are precocious rodents born with a full coat of fur and open eyelids unlike mice and rats. Globe diameter in the common degu (*O. degus*) is 7.74 mm compared to 8.37 mm in its nocturnal cousin the moon-toothed degu (*O. lunatus*). Corneal diameter is also smaller in *O. degus* (6.24 mm) compared to *O. lunatus* (7.41 mm; Vega-Zuniga et al. 2013). Both species lack eyelid cilia, contain a robust Harderian gland (Tolivia et al. 1992), have a vertically ovoid pupil (Fig. 43.30) that becomes circular with pharmacological dilation, and have a basket-like protuberance in the center of the optic nerve. There is almost complete decussation of the optic nerve at the chiasm with few ipsilateral projections (Szabadfi et al. 2015).

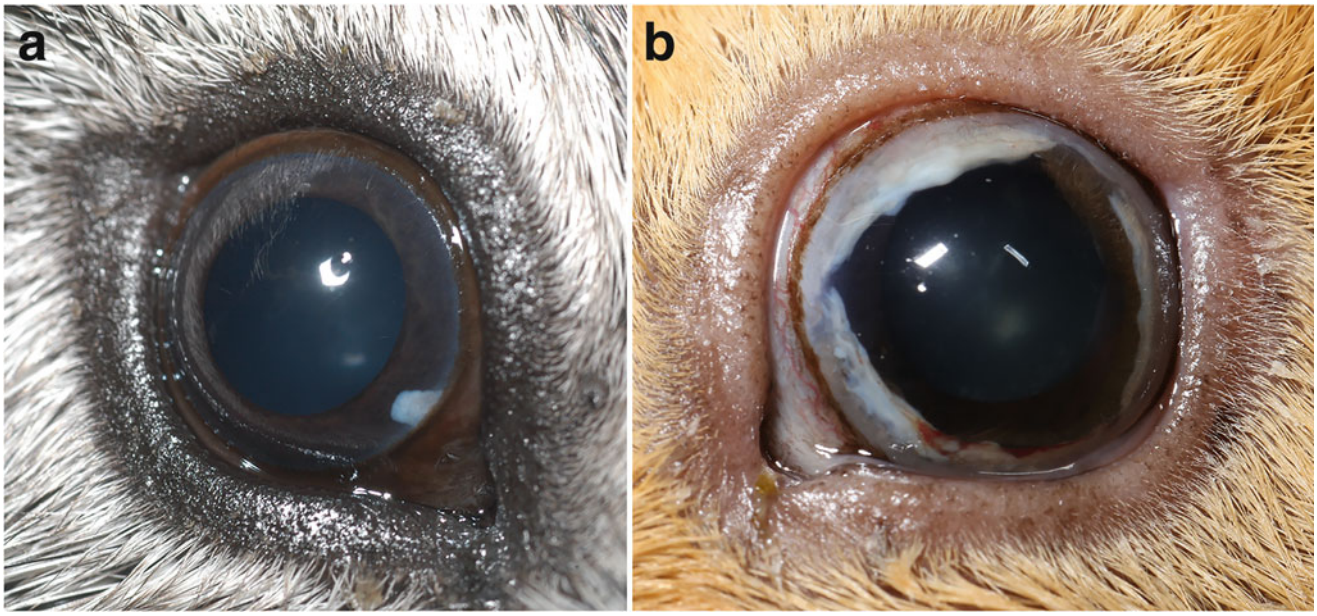

Fig. 43.26 Osseous choristoma or heterotopic bone formation in guinea pigs (*Cavia porcellus*). Note the white bone (**a**) isolated at the medial peripheral anterior chamber or (**b**) along nearly the entire anterior aspect of the anterior chamber. Upon close inspection, vascular channels are visible within the bone. (Courtesy of Bret A. Moore)

As expected for a prey species, the eyes are laterally placed in a protected orbit with a prominent zygomatic arch. This allows for a large monocular visual field. In *O. degus*, the monocular field is approximately 170 degrees, extending from −25 degrees of the contralateral hemisphere frontally to 145 degrees caudally of the ipsilateral hemisphere. *O. lunatus* has a larger monocular field of approximately 190 degrees, extending −50 degrees of the contralateral hemisphere frontally to 140 degrees caudally of the ipsilateral hemisphere (Vega-Zuniga et al. 2013). At 30 to 60 degrees above the snout, the binocular visual field is approximately 50 degrees in *O. degus* and 100 degrees in *O. lunatus* (Vega-Zuniga et al. 2013). The presence of binocular overlap allows the possibility of stereopsis, but does not ensure it. The lens absorbs short wavelength light, almost completely between 310 and 320 nm and only modestly absorbs middle to long wavelength light (Jacobs et al. 2003). With age, the lens demonstrates a progressive increase in optical density with further reduced transmission of short wavelength light, similar to that described in humans (Weale 1988).

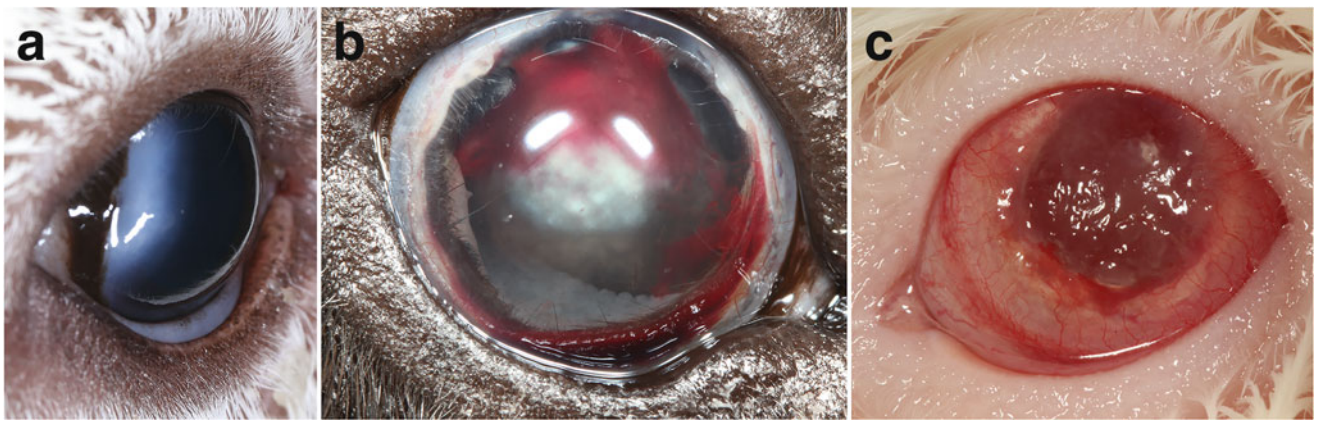

Fig. 43.27 Sequelae or suspected sequelae to heterotopic bone formation in guinea pigs (*Cavia porcellus*). (**a**) Corneal edema from bone contacting the corneal endothelium, (**b**) hyphema from leakage of vascular bone channels or fracture following trauma (note the hypermature cataract also present), and (**c**) a buphthalmic globe with chronic glaucoma (low intraocular pressure was evident at the time of this examination) and keratoconjunctivitis. (Courtesy of Bret A. Moore)

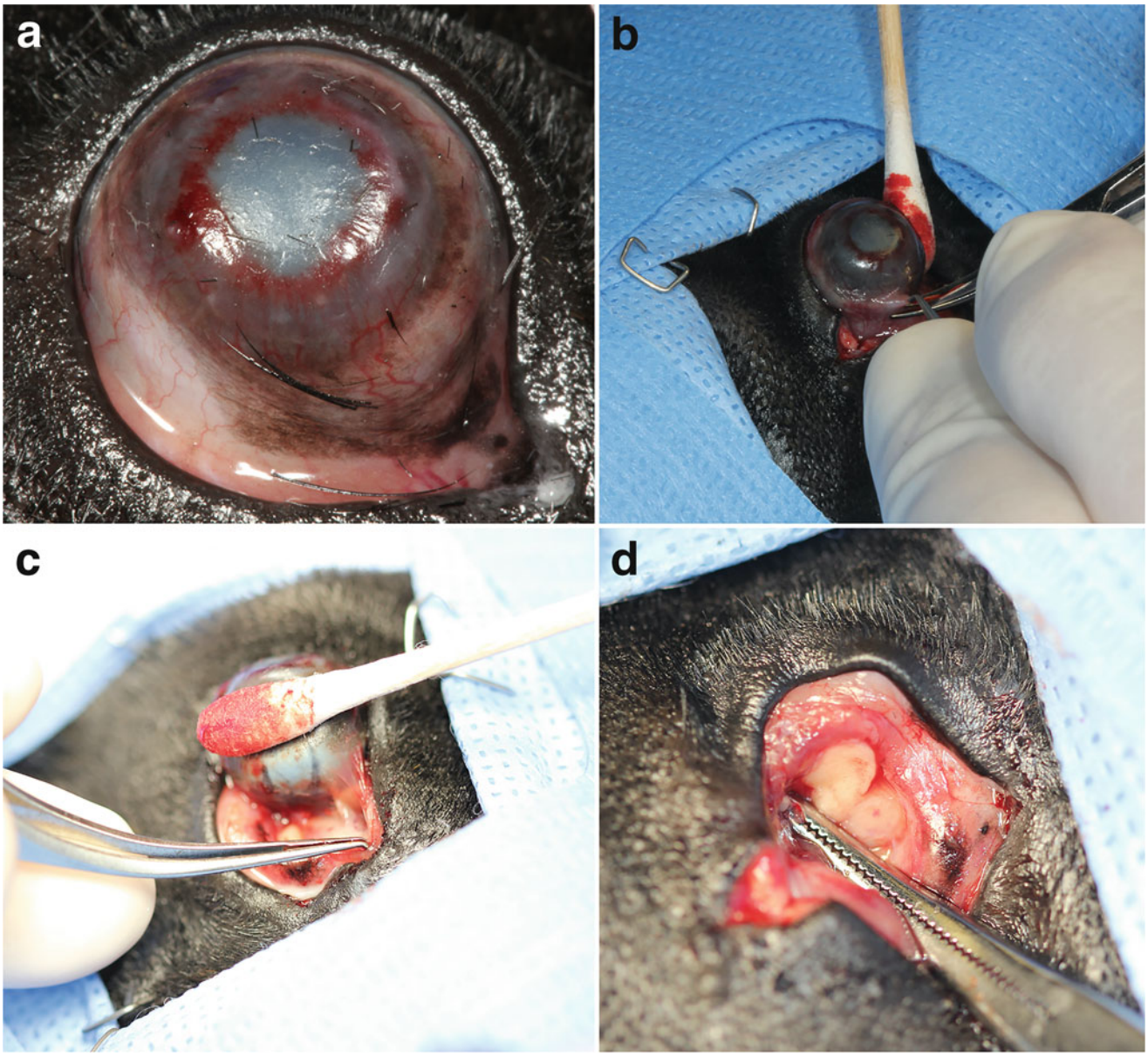

Fig. 43.28 Enucleation in a guinea pig (*Cavia porcellus*) for chronic ulcerative keratitis and exposure keratitis due to unresolving facial nerve paralysis. (**a**) Note the severely dry, scarred, and chronically irritated ocular surface. (**b**) A subconjunctival approach is rapid, and minimal bleeding occurs with proper tissue handling and dissection. (**c**) Extraocular muscles are transected near their scleral insertion to minimize hemorrhage and post-operative discomfort. (**d**) Note the presence of a marked amount of orbital fat following eye removal. (Courtesy of the University of California Davis, Comparative Ophthalmology Service)

The composition of the retina varies significantly between the nocturnal and diurnal Octodon species. While both species maintain the regular retinal architecture, nocturnal *O. lunatus* has approximately 180,000 retinal ganglion cells, significantly less than the 300,000 cells in the diurnal *O. degus*. Additionally, *O. lunatus* has a poorly developed visual streak but a well-developed area centralis near the optic disk containing 4352 cells/mm^2. The visual streak and area centralis are highly developed in *O. degus*, located temporal to the disk with a peak cell count of 6384 cells/mm^2 (Vega-Zuniga et al. 2013). Ipsilateral projections to the dorsal lateral geniculate nucleus and superior colliculus in nocturnal Octodons were 500% thicker than diurnal species, while contralateral projections to the dorsal lateral geniculate nucleus and superior colliculus were 15% thicker in diurnal species. Intrinsically photosensitive ganglion cells containing melanopsin are present and likely responsible for non-image forming responses including the pupillary light reflex and regulation of circadian rhythms (Palanca-Castan et al. 2020). These differences between the nocturnal and diurnal

Fig. 43.29 Guinea pigs (*Cavia porcellus*) generally tolerate Elizabetian collars well, which can be fashioned from various materials. (Courtesy of the University of California Davis, Comparative Ophthalmology Service)

species suggest enhancement of the visual system based on period of activity.

The common degu has a rod-dominate, but cone-rich retina with upwards of 9 million photoreceptors. Rods, accounting for approximately 6 million of these photoreceptors, contain the typical mammalian rod photopigment that has a peak sensitivity of 500 nm (Chavez et al. 2003). Three million photoreceptors are cones, having a peak density of 50,000 cells/mm^2 in an area superior to the optic disk (Jacobs et al. 2003). Electrophysiologic and immunohistochemical studies identified two cone photoreceptors in the degu, including a medium wavelength cone (M cone) with maximal sensitivity near 500 nm and a short wavelength cone (UV sensitive S-cone) with a maximal sensitivity near 360 nm (Chavez et al. 2003; Jacobs et al. 2003). The ratio of M:UV/S-cones is approximately 13:1, similar to that recorded in other mammals. Dichromatic vision is suspected to be present. Behavioral studies demonstrated the ability of degus to discriminate between spectrally distinct stimuli; consistently distinguishing UV (370 nm) from green (500 nm) light in the absence of any brightness variation (Jacobs et al. 2003). However, the utility of this color vision is unknown. Chavez et al. (2003) suggested that UV cones are involved in the detection of territorial urine marks and pheromone cues due to the UV reflectance of these substrates.

Fig. 43.30 Complete cataract in a diabetic degu (*Octodon degus*). Note the vertically ovoid pupil. (Courtesy: Vladimír Motyčka Source: www.biolib.cz/en/image/id139073/)

Cataracts are the most frequently diagnosed ophthalmic abnormality in laboratory and pet degus (Fig. 43.30). They represent approximately 80% of all ocular pathology reported with corneal ulceration, keratoconjunctivitis, and uveitis accounting for the rest (Jekl et al. 2011). Age-related cataracts are common in the wild, but diabetic cataracts are most common in captivity. Reduced insulin activity and alterations in insulin structure dramatically reduce the ability of degus to digest sugar (Opazo et al. 2004, 2005). Approximately 46% of degus in one study (Murphy et al. 1980) had hyperplastic changes in the islets of Langerhans, some containing amyloid deposits. Degus have high aldose reductase activity in the lens, approximately 5 fold higher than rats (Datiles and Fukui 1989). Together these promote the development of type 2 diabetes in degus fed a high sugar diet. Cataracts develop initially as irregular spherical aggregates in the cortex and then quickly become diffuse, within 4 weeks of becoming diabetic (Datiles and Fukui 1989). Feeding a low sugar diet dramatically reduces cataract formation, and the incidence of diabetes and diabetic cataracts is likely very low in the wild. Interestingly, the oral use of Pfizer's sorbinil, a potent aldose reductase inhibitor, completely prevented the formation of diabetic cataracts (Datiles and Fukui 1989). Similarly, topical administration of an aldose reductase inhibitor significantly delayed the onset of diabetic cataracts in dogs (Kador et al. 2010).

Chinchilloidea (Chinchillas)

Until recently, the superfamily Chinchilloidea was considered to contain the families Chinchillidae (chinchillas and viscachas) and Abrocomidae (chinchilla rats). Molecular phylogenetics revealed that Abrocomidae are true Octodontoidea and not members of Chinchilloidea. Similar research discovered Dinomyidae are a sister clade of Chinchillidae within Chinchilloidea (Huchon and Douzery 2001). The Dinomyidae originally included 24 species containing giant rodents such as *Josephoartigasia monesi* that was the size of a bison. All but one (*Dinomys branickii*) of these species has been extinct for up to 4 million years.

D. branickii, commonly called the pacarana, is a rare, nocturnal mammal with the appearance of a small paca. There is no published information on the anatomy, physiology, or any ophthalmic disease of this animal.

The Chinchillidae family consists of chinchillas and viscachas including two chinchilla species and five viscacha species. A new viscacha species (*Lagidium ahuacaense*) was recently observed in Ecuador in 2005 and formally described in 2009 (Ledesma et al. 2009). Viscachas are native to South America and live in rocky cliffs of the Andes mountains, with the exception of *Lagostomus maximus* (plains viscacha) that resides in the pampas of Argentina, Paraguay, and Bolivia (Gariboldi et al. 2019). While they appear similar to rabbits, they are not related. There are no reports of ocular anatomy, physiology, or disease in wild viscachas. However, in captivity 10% of viscachas (*L. maximus*) had cataracts with 90% being bilateral (Gull et al. 2009). Fifty-five percent of viscachas with bilateral cataracts also had fatty liver disease. The cataracts were independent of age and appeared to be associated with diet induced diabetes mellitus. The prevalence of bilateral cataracts in viscachas fed a diet high in fruits and grains was 29% but only 1.65% in those fed a high roughage diet (Gull et al. 2009). Viscachas are another mammal that appears to be sensitive to diabetic-induced cataracts similar to dogs (Basher and Roberts 1995), degus (Brown and Donnelly 2001), desert gerbils (Shafrir et al. 2006), chinchillas (Ewringmann and Göbel 1998), and streptozotocin-induced diabetic rats (White and Cinotti 1972).

Chinchillas are crepuscular rodents living in burrows or rock crevices within the Andes mountains, almost exclusively in Chile. Domesticated chinchillas are derived from *Chinchilla lanigera* and are captive bred as pets, for fur, and for research. Chinchillas have the densest fur of any land mammal with an average of 60 hairs sprouting from a single hair follicle. This favorable trait has led to over hunting and near extinction of *C. chinchilla*, while *C. lanigera* is endangered. In research, they are frequently used as a model for studying the auditory system due to their anatomical and physiological similarities to humans, especially of the inner ear and Eustachian tube structure (Shimoyama et al. 2016).

Similar to other hystricomorphs, chinchillas have a protected orbit with a laterally placed eye. A zygomatic arch is present with a robust lacrimal bone. The zygomasseteric system is hystricomorphous like other hystricomorphs where the enlarged medial masseter muscle passes through a greatly expanded infraorbital hiatus. An orbital venous sinus is present that has been used for blood collection in a laboratory setting (Brookhyser et al. 1977). The lateral placement of the eye promotes a very large monocular visual field that is useful in predator detection and avoidance. In return, the binocular visual field is less than 30 degrees limiting stereopsis (Duke-Elder 1958). The palpebral fissure is approximately 1.5 cm in length and appears almost circular exposing the large cornea. A third eyelid is present, but vestigial and unable to protect or cover the globe. A medial caruncle is present, with 30% of healthy chinchillas having associated trichiasis (Müller et al. 2010). This may be a variation of normal as no accompanying ocular signs were present. Fine cilia are present along the superior and inferior eyelids. Glands of Zeis and Moll accompany these hair follicles. Meibomian glands line the superior and inferior eyelids with a macroscopically widening of this glandular complex temporally. The lacrimal gland is crescent shaped and lies adjacent to the temporal aspect of the Meibomian gland complex (Voigt et al. 2012). Openings of the Meibomian glands along the eyelid margins are present, but microscopic. Additional structures supporting the precorneal tear film include a large Harderian gland and conjunctival, mucin-secreting goblet cells. The Harderian gland is the largest, most prominent ocular gland in chinchillas measuring approximately 0.5 cm (Hittmair et al. 2014), being firmly attached to the posterior hemisphere and extending nasally from the optic nerve to the equator (Voigt et al. 2012). Conjunctival goblet cells are most dense in the palpebral conjunctiva along the temporal and nasal quadrant. These glands likely significantly contribute to the stability of the tear film. Chinchillas infrequently blink, approximately only 2–4 times every 10 minutes (Lima et al. 2010). This is more frequent than the 2–5 times per 20 minutes in guinea pigs (Trost et al. 2007), but much less frequent than other mammals such as dogs at 3–5 times per minute (Carrington et al. 1987), and humans at 12 times per minute (Doughty 2016). With a low blink rate, one would expect higher tear production. However, tear production is low in chinchillas with a Schirmer tear test barely able to be recorded at 1 mm wetting per minute (Lima et al. 2010) and a phenol red thread test at 14 mm/15 seconds (Müller et al. 2010) (Appendix C). Tears drain through a superior and inferior lacrimal puncta connecting to the nasolacrimal duct that runs dorsal to the premolar and first molar apical tooth roots.

The chinchilla cornea is prominent and one of the largest of all mammals, occupying 40% of the total globe surface area (Lima et al. 2010) and measuring approximately 12.6 mm in diameter (Bercht et al. 2015). It has a high radius of curvature, expected due to its size. The classical layers of the cornea are present, with corneal thickness varying in measurement from 0.17 mm (Fernandez and Dubielzig 2013) to 0.25 mm (Bercht et al. 2015) to 0.34 mm (Lima et al. 2010). The variation in measurements is likely due to different methodologies including digital imaging from histopathologic samples (Fernandez and Dubielzig 2013), digital pachymetry (Bercht et al. 2015), and ultrasonic pachymetry (Lima et al. 2010). All of these reading confirm that the chinchilla cornea is significantly thinner than most

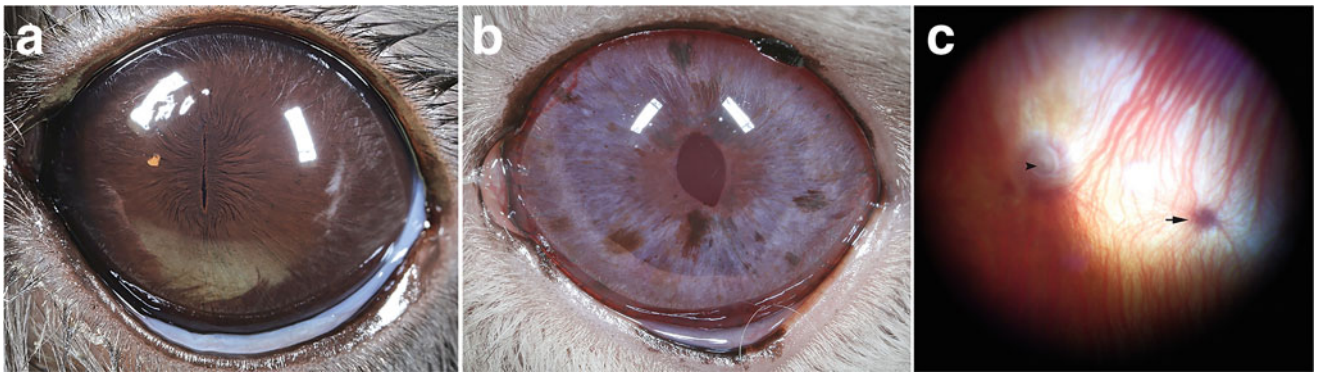

Fig. 43.31 The normal eye of chinchillas (*Chinchilla lanigera*). (**a**) External photograph of a normal pigmented chinchilla. Note the vertically ovoid pupil with almost complete constriction, only leaving stenopaic apertures for vision. (**b**) A normal color dilute (light gray) chinchilla has a lack of dark pigmentation of the iris as well as the vertically ovoid pupil. (**c**) Fundus photograph showing poor pigmentation in a color dilute chinchilla. An anangiotic retinal vascular pattern is present. Note the choroidal vasculature, the round optic disk with a central depression at the center (arrowhead), and one of the vortex ampullae in the ventral and temporal fundus (arrow). (**a**, **b**—Courtesy of Bret A. Moore. **c**—Used with permission from: Lima L, Montiani-Ferreira F, Tramontin M et al. (2010) The chinchilla eye: morphologic observations, echobiometric findings and reference values for selected ophthalmic diagnostic tests. Vet Ophthalmol 13 Suppl:14–25)

mammals, but similar to that of ferrets (Montiani-Ferreira et al. 2006). Specular microscopy revealed approximately 2800 corneal endothelial cells/mm^2 across all age groups of chinchillas (Bercht et al. 2015). Cells had normal polygonal appearance and decreased in number and increased in size with age, similar to other mammals.

The iris tends to be heavily pigmented in brown and gray chinchillas (Fig. 43.31a), but may be lighter in more color dilute animals (Fig. 43.31b). A major arterial circle and a stout iris constrictor muscle are present. The pupil is vertically ovoid and can almost completely constrict, leaving stenopaic apertures for vision (Fig. 43.31a). This degree of miosis may aid in protecting the retina from excessive light exposure, especially at high elevations, and may aid in visual acuity. The ability to fully dilate the pupil allows maximal light gathering to aid in nocturnal vision. The ciliary body is present but lacks musculature, suggesting accommodation is limited. The lens is very large, strongly biconvex, almost spherical, and occupies 50% of the axial diameter of the globe; 5.5 mm of the 11.5 mm globe (Lima et al. 2010). Aqueous exits through Schlemm's canal and intraocular pressures have been reported. Applanation tonometry revealed intraocular pressures of 18.5 ± 5.8 mmHg (Peiffer and Johnson 1980) and 17.7 ± 4.2 mmHg (Lima et al. 2010). In contrast, rebound tonometry revealed significantly lower pressures of 2.9 ± 1.8 mmHg (Müller et al. 2010) and 9.7 ± 2.5 mmHg (Snyder et al. 2017) (Appendix C).

Historically, the chinchilla was believed to be one of the few mammals with a pure rod retina (Detwiler 1949; Duke-Elder 1958). However, photopic electroretinography and immunohistochemistry have revealed that Chinchillas are dichromats with a medium-long wavelength (M/L) cone photoreceptor and a short wavelength (S) cone photoreceptor (Sandalon et al. 2019). The retina remains rod-dominant, with the highest concentration of cones in the central retina. Similar to other mammals, such as the degu, the ratio of M/L: S cone photoreceptors was 13:1 (Jacobs et al. 2003; Sandalon et al. 2019). The retina has an anangiotic vascular pattern and lacks a tapetum (Fig. 43.31c). Visualization of the retina with indirect or direct ophthalmoscopy can be difficult as the pupil responds poorly to pharmacological dilation. The choroid has a dense array of collecting vessels that converge into the vortex veins, similar to rats and hamsters (Ninomiya and Kuno 2001; Ninomiya and Inomata 2005). The optic disk is round, small (1 ± 0.08 mm), and contains a network of blood vessels on the surface (Lima et al. 2010; Fernandez and Dubielzig 2013). The optic nerve has variable myelination with 62% of examined animals having a physiologic cup (Müller et al. 2010).

Ophthalmic disease in the chinchilla has seldom been reported in the literature. Cataracts are the most common ocular abnormality in chinchillas, observed in 14–27% of examined animals (Fig. 43.32; Peiffer and Johnson 1980; Müller et al. 2010; Müller and Eule 2014). The majority of these animals were mature, suggesting the cataracts may be age-related. Diabetes mellitus is rare in chinchillas and is suspected to be type 2, possibly associated with diet as affected animals are obese. Similar to dogs, chinchillas can develop diabetic cataracts (Ewringmann and Göbel 1998; Müller and Eule 2014). Anterior lens luxation has been reported, but is not common.

Corneal disease is the second most commonly diagnosed ophthalmic abnormality in chinchillas. Corneal sensitivity is inversely proportional to corneal touch threshold. As measured with a Cochet–Bonnet esthesiometer, the corneal touch threshold in chinchillas ranges from 0.3 to 1.2 cm

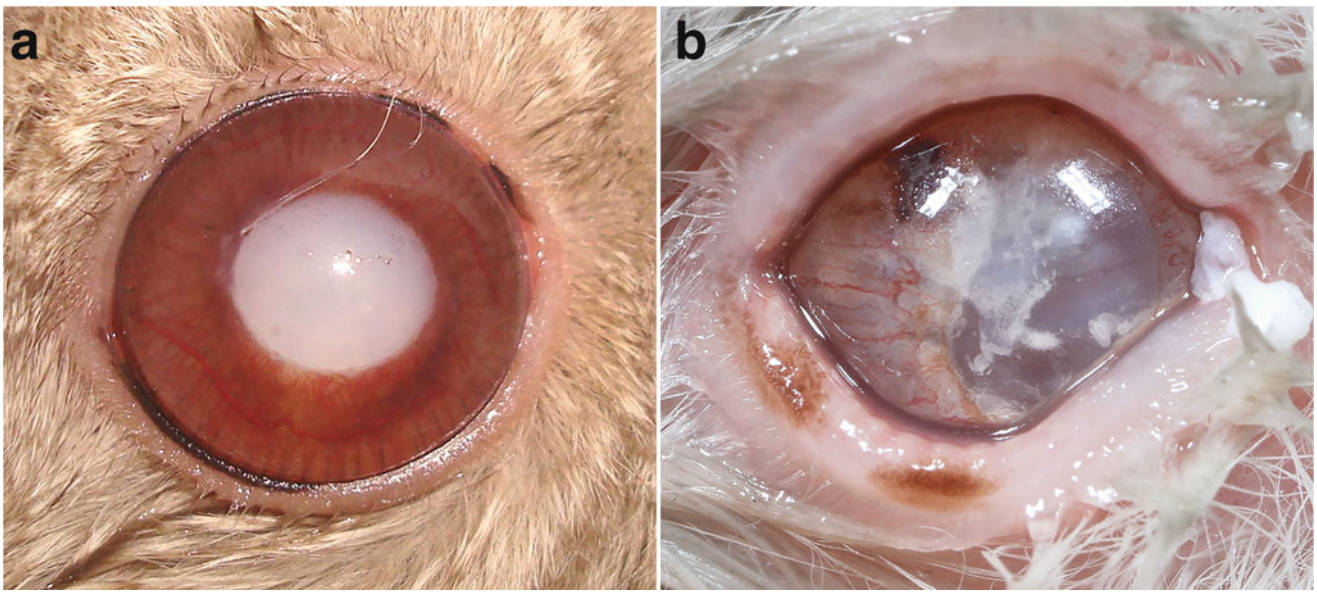

Fig. 43.32 Cataracts in chinchillas (*Chinchilla lanigera*). (**a**) A complete cataract, with altered pupil shaped secondary to posterior synechia from active phacolytic uveitis. (**b**) A resorbing cataract with severe posterior synechia secondary to chronic phacolytic uveitis. (**a**—Courtesy: Drs. Ana Carolina Rodarte Almeida and Fabiano Montiani-Ferreira. **b**—Courtesy of Bret A. Moore)

(Müller et al. 2010; Lima et al. 2010). Corneal sensitivity is low compared to dogs (1.2–1.4 cm; Robin et al. 2020; Cantarella et al. 2017) and humans (4.2–5.7 cm; Rao et al. 2010; Ahuja et al. 2012). Reduced corneal sensitivity along with the chinchilla's large, prominent cornea may predispose them to trauma and secondary corneal ulceration (Figs. 43.33 and 43.34). A superficial erosion was diagnosed in a chinchilla with chronic blepharospasm that was suspected to be related to a herpesvirus infection (Fig. 43.35).

Fig. 43.33 A superficial corneal ulcer in the left eye of a chinchilla (*Chinchilla lanigera*). (Courtesy of Dr. Fabiano Montiani-Ferreira)

Conjunctivitis is the third most commonly reported ophthalmic abnormality in chinchillas. Culture of the ocular surface results in bacterial growth in 92% of chinchillas (Lima et al. 2010), with 44% harboring one species, 35% with two species, and 12% with three species. These bacteria are considered normal flora and were almost exclusively Gram-positive. *Streptococcus spp.* and *Staphylococcus aureus* accounted for over 60% of all isolates. However, when clinical signs of conjunctivitis were present, 61.5% of isolated bacteria were Gram-negative with 50% being *Pseudomonas aeruginosa* (Ozawa et al. 2017). Many affected animals had concurrent respiratory signs. In the absence of respiratory disease, conjunctivitis in chinchillas is usually unilateral and is suspected to be secondary to excessive dust bathing, use of inappropriate dust, or insufficient cage ventilation (Müller et al. 2010). Treatment for bacterial conjunctivitis should be completed based on culture and sensitivity testing. Clinical resolution of conjunctivitis with appropriate treatment occurs in 88% of cases usually within 17 days (Ozawa et al. 2017). The presence and persistence of bacteria on the ocular surface may be complicated by low tearing levels and reduced corneal cleansing.

Orbital disease in chinchillas can be primary or it can be secondary to dental disease. A parasitic cyst (*Taenia coenurus*) in the ventral orbit has been described with surgical excision being curative (Holmberg et al. 2007). With continued growth of the maxillary premolar and first molar teeth, the apices can impinge upon the nasolacrimal duct leading to stenosis or occlusion of the duct. Epiphora is a common sequela to dental disease and was observed in

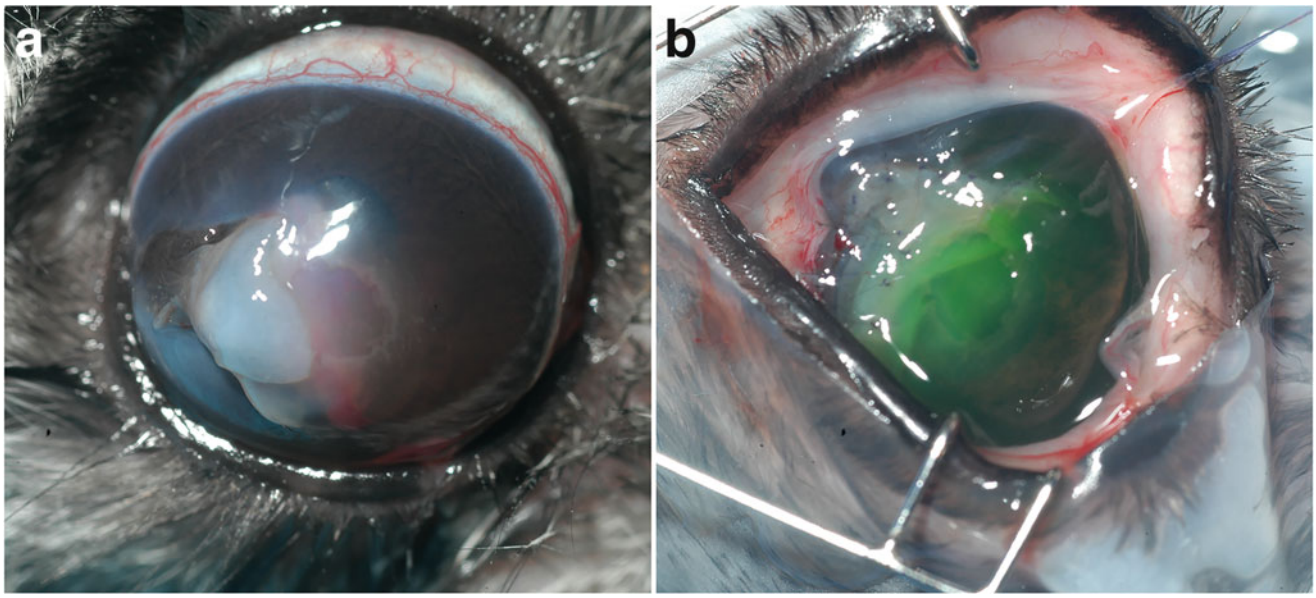

Fig. 43.34 A full-thickness corneal laceration in a chinchilla (*Chinchilla lanigera*), before (**a**) and after (**b**) surgical repair. (Courtesy of the University of California Davis, Comparative Ophthalmology Service)

6 percent of chinchillas (Müller and Eule 2014). Retrobulbar (Fig. 43.36) and periorbital abscess (Fig. 43.37) formation has also been reported. Any evidence of ocular discharge should encourage the clinician to complete a thorough dental exam. Radiography and computed tomography are helpful aids (Crossly et al. 1998). Ocular neoplasia appears to be rare in chinchillas, with just one case report of an intraocular pleomorphic iridociliary adenocarcinoma in the literature (Ueda et al. 2019). In this case, the neoplasm was aggressive, extended outside the globe and resulted in significant necrosis of orbital tissue. Metastasis to a cervical lymph node was present and the chinchilla perished shortly after diagnosis.

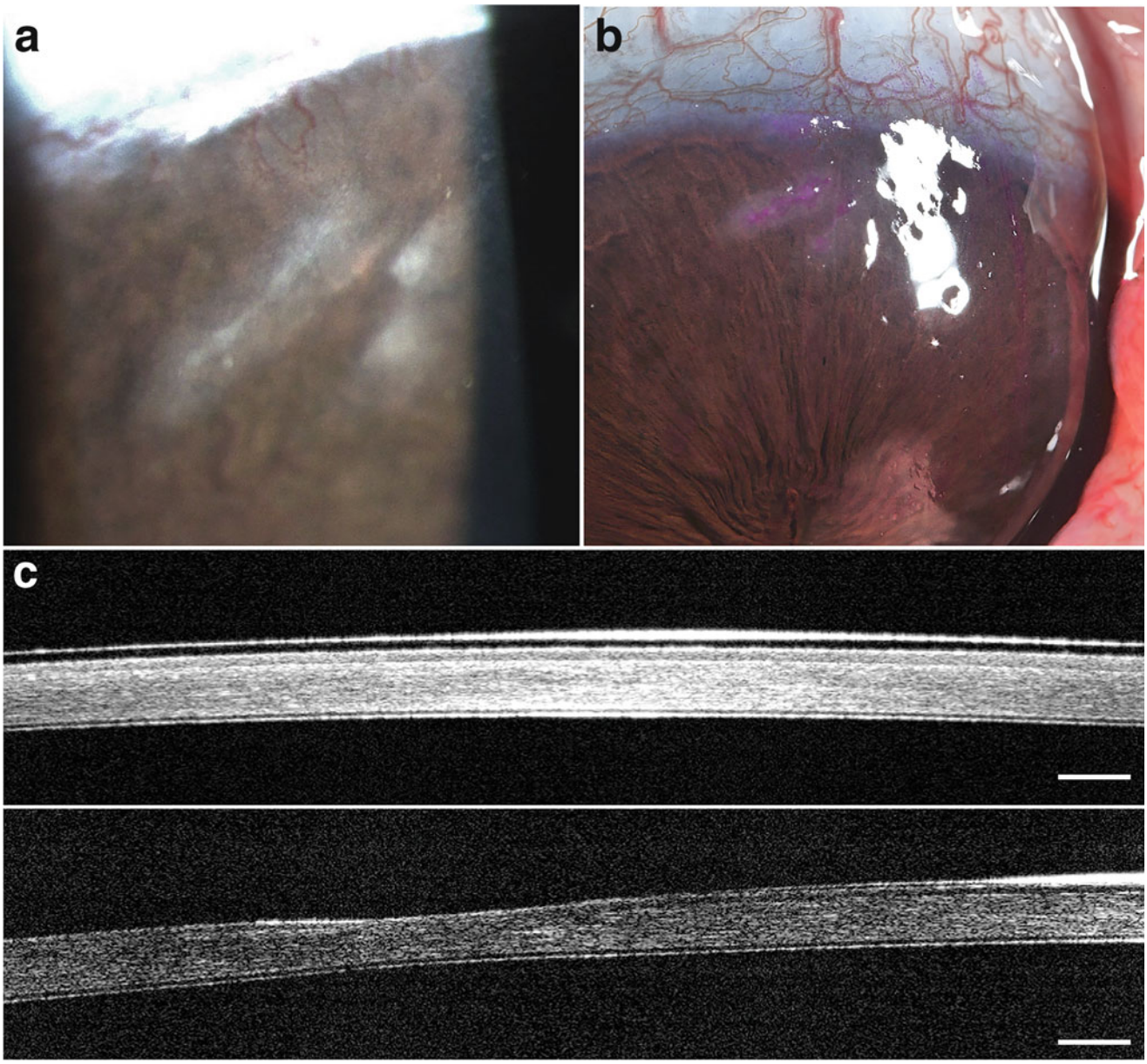

Fig. 43.35 A corneal erosion in a chinchilla (*Chinchilla lanigera*) that presented with chronic blepharospasm and serous ocular discharge from the left eye. (**a**) Note the corneal fibrosis and vascularization at slit-lamp examination. The area was fluorescein negative. (**b**) Staining with Rose Bengal was positive, indicating a corneal erosion. Confirmation was provided by optical coherence tomography, which showed that compared to a normal corneal region (**c**), the affected area was missing all but the corneal basal epithelium. (Courtesy of Bret A. Moore)

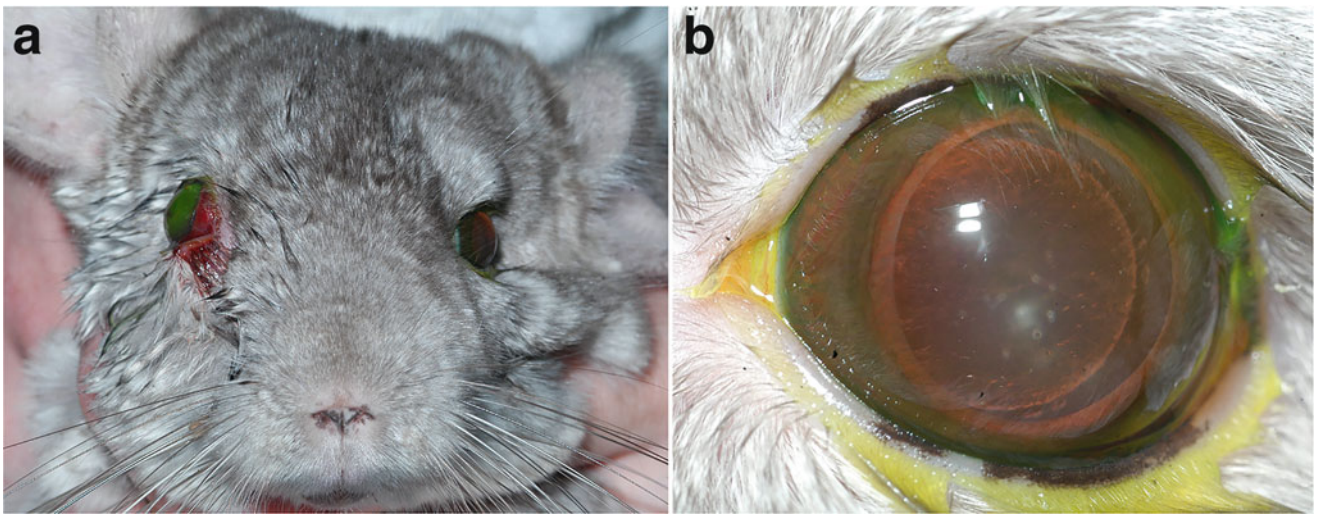

Fig. 43.36 Retrobulbar abscess in a chinchilla (*Chinchilla lanigera*). There is marked exophthalmos of the right eye (**a**), causing secondary exposure keratitis (**b**). Note the nuclear sclerosis in (**b**). (Courtesy of the University of California Davis, Comparative Ophthalmology Service)

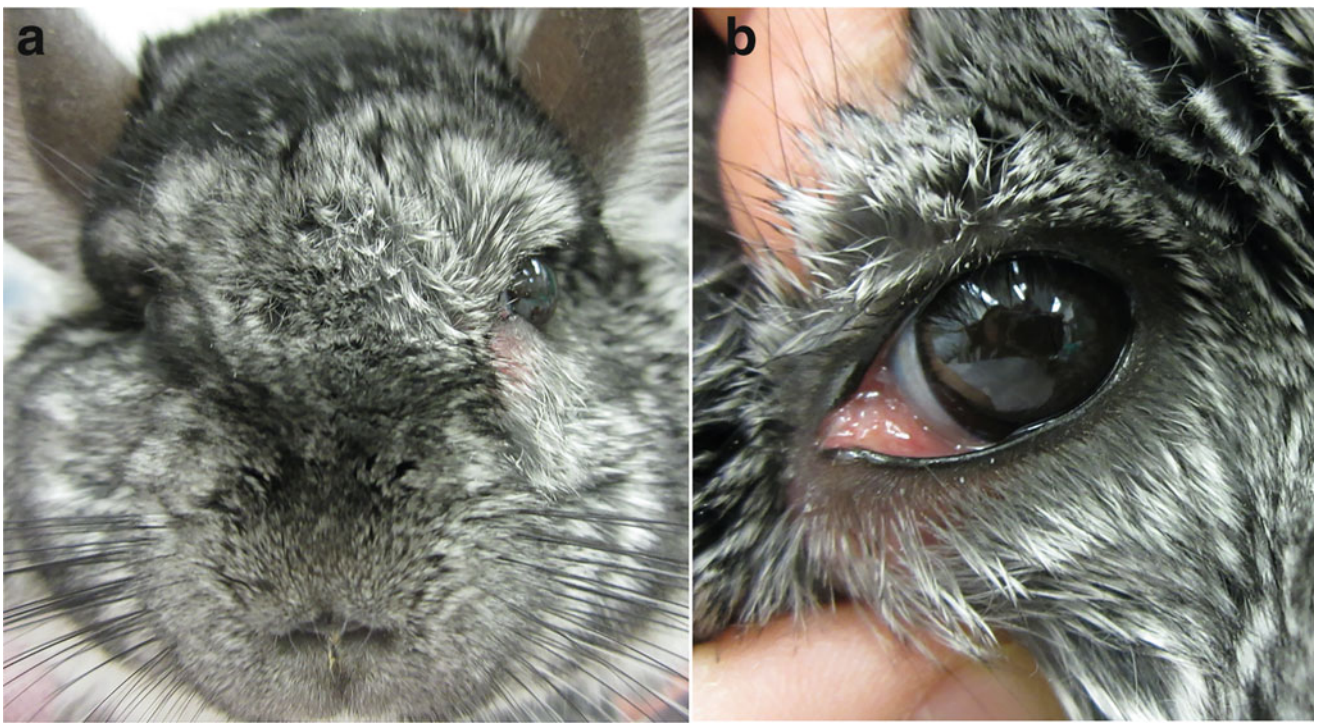

Fig. 43.37 Periorbital abscess in a chinchilla. There is substantial periocular swelling with mild exophthalmos of the left eye (**a**). The palpebral fissure is elongated secondary to significant inflammation at the medial canthus resulting in periocular erythema and severe chemosis (**b**). (Courtesy of the University of California Davis, Comparative Ophthalmology Service)

References

Ahuja Y, Baratz K, McLaren J et al (2012) Decreased corneal sensitivity and abnormal corneal nerves in Fuchs endothelial dystrophy. Cornea 31:1257–1263

Albert M, Ansaruzzaman M, Faruque S et al (1991) Outbreak of keratoconjunctivitis due to Salmonella weltevreden in a guinea pig colony. J Clin Microbiol 29:2002–2006

Allgoewer I, Ewringmann A, Pfleghaar S (1999) Lymphosarcoma with conjunctival manifestation in a guinea pig. Vet Ophthalmol 2:117–119

Ansari-Mood M, Mehdi-Rajaei S, Sadjadi R et al (2016) Twenty-four-hour measurement of intraocular pressure in guinea pigs (*Cavia porcellus*). J Am Assoc Lab Anim Sci 55:95–97

Ballard O (1937) The gross anatomy of Cavia cobaya with a comparative study of another hystricomorph rodent, Erethizon dorsatus. University of Kansas, Kansas

Balthazar da Silveira C, Lima T, Crivelaro R et al (2018) Ophthalmic parameters in adult lowland paca (*Cuniculus paca*) raised in captivity. Vet Ophthalmol 21:42–47

Basher T, Roberts S (1995) Ocular manifestations of diabetes mellitus: diabetic cataracts in dogs. Vet Clin North Am Small Anim Pract 25: 661–676

Beason R, Semm P (1996) Does the avian ophthalmic nerve carry magnetic navigational information? J Exp Biol 199:1241–1244

Bercht B, Albuquerque L, Araujo A et al (2015) Specular microscopy to determine corneal endothelial cell morphology and morphometry in chinchillas (*Chinchilla lanigera*) in vivo. Vet Ophthalmol 18(1): 137–142

Bettelheim F, Churchill A, Zigler J (1997) On the nature of hereditary cataract in strain 13/N guinea pigs. Curr Eye Res 16:917–924

Braekevelt C (1993) Fine structure of the tapetum lucidum of the paca (*Cuniculus paca*). Acta Anat 246:244–250

Brookhyser K, Aulerich R, Vomachka A (1977) Adaptation of the orbital venous sinus technique to the chinchilla (*Chinchilla lanigera*). Lab Anim Sci 27:251–254

Brown C, Donnelly T (2001) Cataracts and reduced fertility in Degus (*Octodon degus*). Lab Anim 30:25–26

Brunschwig A (1928) A dermoid of the cornea in a guinea pig. Am J Pathol 4:371–374

Buttery R, Hinrichsen C, Weller W et al (1991) How thick should a retina be? A comparative study of mammalian species with and without intraretinal vasculature. Vis Res 31:169–187

Cafaro T, Ortiz S, Maldonado C et al (2009) The cornea of guinea pigs: structural and functional studies. Vet Ophthalmol 12:234–241

Cantarella R, de Oliveira J, Dorbandt D et al (2017) Effects of topical flurbiprofen sodium, diclofenac sodium, ketorolac tromethamine and benzalkonium chloride on corneal sensitivity in normal dogs. Open Vet J 7:254–260

Carrington S, Bedford P, Guillon J et al (1987) Polarized light biomicroscopic observation on the pre-corneal film, and the normal tear film of the dog. J Small Anim Pract 28:605–622

Castro J, López J, Becerra F (2010) Una nueva especie de Cu- niculus (Rodentia: Cuniculidae) de la cordillera Central de Colombia. Revista de la Asociación Colombiana de Ciencias Biológicas 22: 122–131

Catania K, Remple M (2002) Somatosensory cortex dominated by the representation of teeth in the naked mole-rat brain. Proc Natl Acad Sci USA **99**:5692–5697

Cei G (1946) Ortogenesi parallela e degradazione degli organi della vista negli spalacidi. Monit Zool Ital Firenze 55:69–84

Cercignani M, Giulietti G, Dowell N et al (2017) Characterizing axonal myelination within the healthy population: a tract-by-tract mapping of effects of age and gender on the fiber g-ratio. Neurobiol Aging 49: 109–118

Cernuda-Cernuda R, Garcia-Fernández J, Gordign M et al (2003) The eye of the African mole-rat Cryptomys anselli: to see or not to see? Eur J Neurosci 17:709–720

Chavez A, Bozinovic F, Peichl L et al (2003) Retinal spectral sensitivity, fur coloration, and urine reflectance in the genus *Octodon* (Rodentia): implications for visual ecology. Invest Ophthalmol Vis Sci 44:2290–2296

Chiwitt C, Baines S, Mahoney P et al (2017) Ocular biometry by computed tomography in different dog breeds. Vet Ophthalmol 20: 411–419

Chomiak T, Hu B (2009) What is the optimal value of the g-ratio for myelinated fibers in the rat CNS? A theoretical approach. PLoS One 4:e7754

Clark D, Clark R (2013) The effects of time, luminance, and high contrast targets: revisiting grating acuity in the domestic cat. Exp Eye Res 116:75–78

Cooper G, Schiller AL (1975) Anatomy of the guinea pig. Harvard University Press, Cambridge, pp 369–389

Coster M, Stiles J, Krohne S et al (2008) Results of diagnostic ophthalmic testing in healthy guinea pigs. J Am Vet Med Assoc 15:1825–1833

Cox P, Faulkes C, Bennett N (2020) Masticatory musculature of the African mole-rats (Rodentia:Bathyergidae). PeerJ 8:e8847

Crossly D, Jackson A, Yates J et al (1998) Use of computed tomography to investigate cheek tooth abnormalities in chinchillas (*Chinchilla lanigera*). J Small Anim Pract 38:385–389

Datiles M, Fukui H (1989) Cataract prevention in diabetic Octodon degus with Pfizer's sorbinil. Curr Eye Res 8:233–237

DeSchaepdrijver L, Simoens P, Lauwers H et al (1989) Retinal vascular patterns in domestic animals. Res Vet Sci 47:34–42

Detwiler S (1949) The eye of the chinchilla (*C. lanigera*). J Morphol 84: 123–144

Di Y, Luo X, Qiao T et al (2017) Intraocular pressure with rebound tonometry and effects of topical intraocular pressure reducing medications in guinea pigs. Int J Ophthalmol 10:186–190

Djeridane Y (1992) The Harderian gland of desert rodents: a histological and ultrastructural study. J Anat 180:465–480

Doughty M (2016) Assessment of short-term variability in human spontaneous blink rate during video observation with or without head/chin support. Clin Exp Optom 99:135–141

Duke-Elder S (1958) The eye in evolution, vol 1. Henry Kimpton, London, p 610, 672, 688

Dwyer R, Darougar S, Monnickendam M (1983) Unusual features in the conjunctiva and cornea of the normal guinea-pig: clinical and histological studies. Br J Ophthalmol 67:737–741

Ebensperger L, Chesh A, Castro R et al (2011) Burrow limitations and group living in the communally rearing rodent *Octodon degus*. J Mammal 92:21–30

Edwards M (1969) Congenital defects in guinea pigs: fetal resorptions, abortions, and malformations following induced hyperthermia during early gestation. Teratology 2:313–328

Ewringmann A, Göbel T (1998) Diabetes mellitus bei Kaninchen, Meerschweinchen und Chinchilla. Kleintierpraxis 43:337–348

Faghihi J, Rajaei S, Ansarimood M et al (2019) Conjunctival microflora in guinea pigs with and without conjunctivitis. J Exot Pet Med 30: 65–68

Fernandez J, Dubielzig R (2013) Ocular comparative anatomy of the family Rodentia. Vet Ophthalmol 16(1):94–99

Gariboldi M, Inserra P, Lucero S et al (2019) Unexpected low genetic variation in the South American hystricognath rodent Lagostomus Maximus (Rodentia: Chinchillidae). PLoS One 14:e0221559

Gasser K, Fuchs-Baumgartinger A, Tichy A et al (2011) Investigations on the conjunctival goblet cells and on the characteristics of glands associated with the eye in the guinea pig. Vet Ophthalmol 14:26–40

Ghawar W, Snoussi M, Salem S et al (2017) Morphometric variation and its relation to the eyes lens weight among three species of wild rodents in Tunisia. Int J Fauna Biol Stud 4:30–38

Grahn B, Szentimrey D, Pharr J et al (1995) Ocular and orbital porcupine quills in the dog: a review and case series. Can Vet J 36:488–493

Griffith J, Sassani J, Bowman T et al (1988) Osseous choristoma of the ciliary body in guinea pigs. Vet Pathol 25:100–102

Gull J, Steinmetz H, Clauss M et al (2009) Occurrence of cataracts and fatty liver in captive plain viscachas (*Lagostomus maximus*) in relation to diet. J Zoo Wild Med 40:652–658

Guy J, Ellis E, Kelley K et al (1989) Spectra of G ratio, myelin sheath thickness, and axon and fiber diameter in the guinea pig optic nerve. J Comp Neurol 287:446–454

Hale M, Griesemer S, Fuller T (1994) Immobilization of porcupines with tiletamine hydrochloride and zolazepam hydrochloride (Telazol). J Wildl Dis 30:429–431

Herrera E (1992) Growth and dispersal of capybaras (*Hydrochaeris hydrochaeris*) in the Llanos of Venezuela. J Zool 228:307–316

Hittmair K, Tichy A, Nell B (2014) Ultrasonography of the harderian gland in the rabbit, guinea pig, and chinchilla. Vet Ophthalmol 17:175–183

Holmberg B (2018) Exotic pet and avian ophthalmology. In: Maggs D, Miller P, Ofri R (eds) Slatter's fundamentals of veterinary ophthalmology, 6th edn. Elsevier, St. Louis, pp 503–505

Holmberg B, Hollingsworth S, Osofsky A et al (2007) Taenia coenurus in the orbit of a chinchilla. Vet Ophthalmol 10:53–59

Huchon D, Douzery E (2001) From the old world to the new world: a molecular chronicle of the phylogeny and biogeography of hystricognath rodents. Mol Phylogenet Evol 20:238–251

Hurley M, Deacon R, Beyer K et al (2018) The long-lived Octodon degus as a rodent drug discovery model for Alzheimer's and other age-related diseases. Pharmacol Ther 188:36–44. https://doi.org/10.1016/j.pharmthera.2018.03.001

Jacobs G, Deegan J (1994) Spectral sensitivity, photopigments, and color vision in the guinea pig (Cavia porcellus). Behav Neurosci 108:993–1004

Jacobs G, Calderone J, Fenwick J et al (2003) Visual adaptations in a diurnal rodent, *Octodon degus*. J Comp Physiol A 189:347–361

Jekl V, Kauptman K, Knotek Z (2011) Diseases in pet degus: a retrospective study in 300 animals. J Sm Anim Pract 52:107–112

Jnawali A, Beach K, Ostrin L (2018) In vivo imaging of the retina, choroid, and optic nerve head in guinea pigs. Curr Eye Res 43:1006–1018

Kador P, Webb T, Bras D et al (2010) Topical kinostat™ ameliorates the clinical development and progression of cataracts in dogs with diabetes mellitus. Vet Ophthalmol 13:363–368

Korb D, Greiner J, Glonek J et al (1998) Human and rabbit lipid layer and interference pattern observations. Adv Exp Med Biol 438:305–308

Kosegarten D, Maher T (1978) Use of guinea pigs as model to study galactose-induced cataract formation. J Pharm Sci 67:1478–1479

Lázár G (1983) Retinal projections of the pigmented guinea pig. Acta Biol Hung 34:207–213

Ledesma K, Werner F, Spotorno A et al (2009) A new species of mountain viscacha (Chinchillidae: *Lagidium meyen*) from the Ecuadorean Andes. Zootaxa 2126:41–57

Lima L, Montiani-Ferreira F, Tramontin M et al (2010) The chinchilla eye: morphologic observations, echobiometric findings and reference values for selected ophthalmic diagnostic tests. Vet Ophthalmol 13(Suppl 1):14–25

Lutz-Wohlgroth L, Becker A, Brugnera E et al (2006) Chlamydiales in guinea-pigs and their zoonotic potential. J Vet Med A Physiol Clin Med 53:185–193

Maier W, Schrenk F (1987) The hystricomorphy of the Bathyergidae, as determined from ontogenetic evidence. Zeitschrift für Säugetierkunde 52:156–164

McMullen C, Anrade F, Crish S (2010) Underdeveloped extraocular muscles in the naked mole-rat (*Heterocephalus glaber*). Anat Rec (Hoboken) 293:918–923

Merindano M, Costa J, Canals M et al (2002) A comparative study of Bowman's layer in some mammals: relationships with other constituent corneal structures. Eur J Anat 6:133–139

Miles R, Ratoosh P, Meyer D (1956) Absence of color vision in guinea pig. J Neurophysiol 19:254–258

Mills S, Catania K (2004) Identification of retinal neurons in a regressive rodent eye (the naked mole rat). Vis Neurosci 21:107–117

Montgelard C, Forty E, Arnal V et al (2008) Suprafamilial relationships among Rodentia and the phylogenetic effect of removing fast-evolving nucleotides in mitochondrial, exon and intron fragments. BMC Evol Biol 8:321

Montiani-Ferreira F, Mattos B, Russ H (2006) Reference values for selected ophthalmic diagnostic tests of the ferret (*Mustela putorius furo*). Vet Ophthalmol 9:209–213

Montiani-Ferreira F et al (2008) The capybara eye: clinical tests, anatomic and biometric features. Vet Ophthalmol 11:386–394

Müller K, Eule J (2014) Ophthalmic disorders observed in pet chinchillas (*Chinchilla lanigera*). J Exotic Pet Med 23:201–205

Müller K, Mauler D, Eule J (2010) Reference values for selected ophthalmic diagnostic tests and clinical characteristics of chinchilla eyes (*Chinchilla lanigera*). Vet Ophthalmol 13:29–34

Mumcuoglu T, Ozge G, Soykut B et al (2015) An animal model (guinea pig) of ocular siderosis: histopathology, pharmacology, and electrophysiology. Curr Eye Res 40:314–320

Murphy JC et al (1980) Spontaneous lesions in the degu. In: Montali R, Migaki G (eds) The comparative pathology of zoo animals. Smithsonian Institution Press, Washington DC, pp 437–444

Murphy E, Garone M, Tashayyod D et al (1986) Innervation of extraocular muscles in the rabbit. J Comp Neurol 254:78–90

Murray E (1964) Guinea pig inclusion conjunctivitis virus: I. Isolation and identification as a member of the psittacosis-lymphogranuloma-trachoma group. J Infect Dis 114:1–12

Nakazawa Y, Oka M, Takehana M (2017) Model for studying anti-allergic drugs for allergic conjunctivitis in animals. Open Med (Wars) 12:231–238

Nascimento E, Cavalcante J, Cavalcante J et al (2010a) Retinal afferents to the thalamic mediodorsal nucleus in the rock cavy (*Kerodon rupestris*). Neurosci Lett 7:38–43

Nascimento E, Souza A, Duarte R et al (2010b) The suprachiasmatic nucleus and the intergeniculate leaflet in the rock cavy (*Kerodon rupestris*): retinal projections and immunohistochemical characterization. Brain Res 1320:34–46

Němec P, Cveková P, Benada O et al (2008) The visual system in subterranean African mole-rats (Rodentia, Bathyergidae): retina, subcortical visual nuclei and primary visual cortex. Brain Res Bull 75:356–364

Nicolle C, Manceaux L (1908) Sur une infection a corps de Leishman (ou organismes voisons) du gondi. C R Acad Sci 147:736

Nikitina N, Kidson S (2014) Eye development in the Cape dune mole rat. Dev Genes Evol 224:107–117

Nikitina N, Maughan-Brown B, O'Riain M et al (2004) Post-natal development of the eye in the naked mole rat (*Heterocephalus glaber*). Anat Rec 277A:317–337

Ninomiya H, Inomata T (2005) Microvasculature of the hamster eye: scanning electron microscopy of vascular corrosion casts. Vet Ophthalmol 8:7–12

Ninomiya H, Kuno H (2001) Microvasculature of the rat eye: scanning electron microscopy of vascular corrosion casts. Vet Ophthalmol 4:55–59

Nogradi A, Szentgáli Z, Battay M et al (2020) Measurement of tear production and establishment of reference values in guinea pigs (*Cavia porcellus*) using a modified Schirmer tear test. Vet Rec 186:321

Oelschläger H, Nakamura M, Herzog M et al (2000) Visual system labeled by c-Fos immunohistochemistry after light exposure in the 'blind' subterranean Zambian mole-rat (*Cryptomys anselli*). Brain Behav Evol 55:209–220

Okanoya K, Tokimoto N, Kumazawa N et al (2008) Tool-use training in a species of rodent: the emergency of an optimal motor strategy and functional understanding. PLoS One 3:e1860. https://doi.org/10.1371/journal.pone.0001860

Oliveira F, Nascimento-Júnior E, Cavalcante J et al (2018) Topographic specializations of catecholaminergic cells and ganglion cells and distribution of calcium binding proteins in the crepuscular rock cavy (*Kerodon Rupestris*) retina. J Chem Neuroanat 90:57–69

Opazo J, Soto-Gamboa M, Bozinovic F (2004) Blood glucose concentration in caviomorph rodents. Comp Biochem Physiol A Mol Integr Physiol 137:57–64

Opazo J, Palma R, Melo F et al (2005) Adaptive evolution of the insulin gene in caviomorph rodents. Mol Biol Evol 22:1290–1298

Ostrin L, Wildsoet C (2016) Optic nerve head and intraocular pressure in the guinea pig eye. Exp Eye Res 146:7–16

Ozawa S, Mans C, Szabo Z et al (2017) Epidemiology of bacterial conjunctivitis in chinchillas (*Chinchilla lanigera*): 49 cases (2005–2015). J Small Anim Pract 58:238–245

Padilla-Carlin D, McMurray D, Hickey A (2008) The guinea pig as a model of infectious disease. Comp Med 58:324–340

Palanca-Castan N, Harcha P, Neira D et al (2020) Chromatic pupillometry for the characterization of the pupillary light reflex in *Octodon degus*. Exp Eye Res 190:107866

Parry J, Bowmaker J (2002) Visual pigment coexpression in guinea pig cones: a microspectrophotometric study. Invest Ophthalmol Vis Sci 43:1662–1665

Patterson B, Upham N (2014) A newly recognized family from the Horn of Africa, the Heterocephalidae (Rodentia: Ctenohystrica). Zool J Linnean Soc 172:942–963

Peichl L (2005) Diversity of mammalian photoreceptor properties: adaptations to habitat and lifestyle? Anat Rec A Discov Mol Cell Evol Biol 287:1001–1012

Peichl L, Němec P, Burda H (2004) Unusual cone and rod properties in subterranean African mole-rats (Rodentia, Bathyergidae). E J Neurosci 19:1545–1558

Peiffer R, Johnson R (1980) Clinical ocular findings in a colony of chinchillas (*Chinchilla lanigera*). Lab Anim 14:331–335

Pereira F, Bete S, Inamassu L et al (2020) Anatomy of the skull in the capybara (Hydrochoerus hydrochaeris) using radiography and 3D computed tomography. Anat Histol Embryol 49:317–324

Quilliam T (1966) The problem of vision in the ecology of *Talpa europaea*. Exp Eye Res 5:63–78

Quinton J, Ollivier F, Dally C (2013) A case of well-differentiated palpebral liposarcoma in a guinea pig (Cavia porcellus). Vet Ophthalmol 16:155–159

Racine J, Behn D, Simard E et al (2003) Spontaneous occurrence of a potentially night blinding disorder in guinea pigs. Doc Ophthalmol 107:59–69

Racine J, Joly S, Lachapelle P (2011) Longitudinal assessment of retinal structure and function reveals a rod-cone degeneration in a guinea pig model initially presented as night blind. Doc Ophthalmol 123:1–19

Ramírez-Chaves H, Solari S (2014) On the availability of the name Cuniculus hernandezi Castro, López, and Becerra, 2010 (Rodentia: Cuniculidae). Actual Biol 36:59–62

Rank R, Bowlin A, Tormanen K et al (2012) Effect of inflammatory response on in vivo competition between two chlamydial variants in the guinea pig model of inclusion conjunctivitis. Infect Immun 80:612–619

Rao K, Leveque C, Pflugfelder S (2010) Corneal nerve regeneration in neurotrophic keratopathy following autologous plasma therapy. Br J Ophthalmol 94:584–591

Rasia L, Candela A (2019) Upper molar morphology, homologies and evolutionary patterns of chinchilloid rodents (Mammalia, Caviomorpha). J Anat 234:50–65

Redford KH, Eisenberg JF (1992) Mammals of the neotropics. The southern cone. The University of Chicago Press, Chicago, p 435

Reymond L, Cook M (1984) Relation between simultaneous spatial-discrimination thresholds and luminance in man. Behav Brain Res 14:51–59

Robin M, Papin A, Regnier A et al (2020) Corneal anesthesia associated with topical application of 2% lidocaine nonophthalmic gel to healthy canine eyes. Vet Ophthalmol 23:560–566

Rocha F, Ahnelt P, Peichl L et al (2009) The topography of cone photoreceptors in the retina of a diurnal rodent, the agouti (*Dasyprocta Aguti*). Vis Neurosci 26:167–175

Rushton W (1934) A physical analysis of the relation between threshold and interpolar length in the electric excitation of the medullated nerve. J Physiol 82:332–352

Sáez I, Friedlander M (2009) Synaptic output of individual layer 4 neurons in guinea pig visual cortex. J Neurosci 29:4930–4944

Sandalon S, Boykova A, Ross M et al (2019) Contrary to popular belief, chinchillas do not have a pure rod retina. Vet Ophthalmol 22:93–97

Sandmeyer L, Parker D, Grahn B (2011) Diagnostic ophthalmology. Can Vet J 52:801–802

Schäffer E, Pfleghaar S (1995) Secondary open angle glaucoma from osseous choristoma of the ciliary body in guinea pigs. Tierarztl Prax 23:410–414

Shafrir E, Ziv E, Kalman R (2006) Nutritionally induced diabetes in desert rodents as models of type 2 diabetes: Acomys cahirinus (spiny mice) and Psammomys obesus (desert gerbil). ILAR J 47:212–224

Shimoyama M, Smith J, De Pons J et al (2016) The chinchilla research resource database: resource for an otolaryngeal disease model. Database 2016:baw073

Silveira L, Picanço-Dinz C, Oswaldo-Cruz. (1989) Distribution and size of ganglion cells in the retinae of large Amazon rodents. Vis Neurosci 2:221–2335

Snyder K, Lewin A, Mans C et al (2017) Tonometer validation and intraocular pressure reference values in the normal chinchilla (*Chinchilla lanigera*). Vet Ophthalmol 21:4–9

Steffen J, Krohn M, Paarmann K et al (2016) Revisiting rodent models: *Octodon degus* as Alzheimer's disease model? Acta Neuropathol Commun 4:91

Stone J (1983) Parallel processing in the visual system: the classification of retinal ganglion cells and its impact on the neurobiology of vision. Plenum Press, New York

Stone S, Amsbaugh D (1984) Congential cataracts in strain 13 guinea pigs: an autosomal dominant human model. Invest Ophthalmol Vis Sci 25:606–607

Stuart C, Stuart C (2016) Mammals of North Africa and the Middle East. Bloomsbury Publishing Plc, London, p 105

Sueki H, Kligman A (2003) Cutaneous toxicity of chemical irritants on hairless guinea pigs. J Dermatol 30:859–870

Sueki H, Gammal C, Kudoh K et al (2000) Hairless guinea pig skin: anatomical basis for studies of cutaneous biology. Eur J Dermatol 10:357–364

Szabadfi K, Estrada C, Fernandez-Villalba E et al (2015) Retinal aging in the diurnal Chilean rodent (Octodon degus): histological, ultrastructural and neurochemical alterations of the vertical information processing pathway. Front Cell Neurosci 9:126

Tavares-Somma A, Seabra N, Moore B et al (2017) The eye of the Azara's agouti (*Dasyprocta azarae*): morphological observations

and selected ophthalmic diagnostic tests. J Zoo Wildl Med 48:1108–1119

Tolivia D, Antolin I, Menendez-Pelaez A et al (1992) Lymphoid cells in the harderian gland of the rodent *Octodon degus*. Anat Rec 234:438–442

Trost K, Skalichy M, Nell B (2007) Schirmer tear test, phenol red thread tear test, eye blink frequency and corneal sensitivity in the guinea pig. Vet Ophthalmol 10:143–146

Ueda K, Ueda A, Ozaki K (2019) Pleomorphic iridociliary adenocarcinoma with metastasis to the cervical lymph node in a chinchilla (*Chinchilla lanigera*). J Vet Med Sci 81:193–196

Van Daele PAAG, Verheyen E, Brunain M et al (2007) Cytochrome b sequence analysis reveals differential molecular evolution in African mole-rats of the chromosomally hyperdiverse genus *Fukomys* (Bathyergidae, Rodentia) from the Zambezian region. Mol Phylogenet Evol 45(1):142–157

Vaughan T, Ryan J, Czaplewski N (2015) Mammalogy, 6th edn. Jones & Bartlett Learning, Burlington, p 221

Vega-Zuniga T, Medina F, Fredes F et al (2013) Does nocturnality drive binocular vision? Octodontine rodents as a case study. PLoS One 8: e84199

Voigt S, Fuchs-Baumgartinger A, Egerbacher M et al (2012) Investigations on the conjunctival goblet cells and the characteristics of the glands associated with the eye in chinchillas (*Chinchilla lanigera*). Vet Ophthalmol 15:333–344

vonSallmann L, Reid M, Grimers P et al (1959) Tryptophan-deficiency cataract in guinea pigs. AMA Arch Ophthalmol 62:662–672

Wagner J, Manning P (1976) The biology of the guinea pig. Academic Press, New York, p 113

Walde I, Nell B (2008) Meerschweinchen. In: Walde I, Nell B, Schäffer EH, Köstlin R (eds) Augenheilkunde-Lehrbuch und Atlas Hund, Latze, Kaninchen und Meerschweinchen, Chapter 22, 3rd edn. Schattauer GmbH, Stuttgart, pp 761–764

Wappler O, Allgoewer I, Schaeffer E (2002) Conjunctival dermoid in two guinea pigs: a case report. Vet Ophthalmol 5:245–248

Weale R (1988) Age and the transmittance of the human crystalline lens. J Physiol 395:577–587

Wegner R, Begall S, Burda H (2006a) Magnetic compass in the cornea: local anesthesia impairs orientation in a mammal. J Exp Biol 209: 4747–4750

Wegner R, Begall S, Burda H (2006b) Light perception in 'blind' subterranean Zambian mole-rats. Anim Behav 72:1021–1024

Wei X, Markoulli M, Zhao Z et al (2013) Tear film break-up time in rabbits. Clin Exp Optom 96:70–75

White J, Cinotti A (1972) Streptozotocin-produced cataracts in rats. Investig Ophthalmol 11:56–57

Wieser B, Tichy A, Nell B (2013) Correlation between corneal sensitivity and quantity of reflex tearing in cows, horses, goats, sheep, dogs, cats, rabbits, and guinea pigs. Vet Ophthalmol 16:251–262

Williams D, Gum G (2013) Laboratory animal ophthalmology. In: Gelatt K, Gilger B, Kern T (eds) Veterinary ophthalmology, 5th edn. John Wiley and Sons, Ames, pp 1705–1709

Williams D, Sullivan A (2010) Ocular disease in the guinea pig (*Cavia porcellus*): a survey of 1000 animals. Vet Ophthalmol 13(Suppl 1): 52–62

Wood J (1861) The illustrated natural history: class mammalia. Routledge, Warne, and Routledge, London, p 579

Wu D, Henriksen M, Grant K et al (2020) Ocular findings and selected ophthalmic diagnostic tests in a group of young commercially available Guinea and Skinny pigs (Cavia porcellus). Vet Ophthalmol 23: 234–244

Xiao H, Fan Z, Tian X et al (2014) Comparison of form-deprived myopia and lens-induced myopia in guinea pigs. Int J Ophthalmol 7:245–250

Zhou X, Qu J, Xie R et al (2006) Normal development of refractive state and ocular dimensions in guinea pigs. Vis Res 46:2815–2823

Zhou J, Ge S, Gu P et al (2011) Microdissection of guinea pig extraocular muscles. Exp Ther Med 2:1183–1185

Zhu Z, Stevenson D, Schechter J et al (2003) Lacrimal histopathology and ocular surface disease in a rabbit model of autoimmune dacryoadenitis. Cornea 22:25–32

Zúñiga H, Pinto-Nolla M, Hernandez-Camacho J et al (2002) Revisión taxonómia de lase species del género Cavia (Rodentia: Caviidae) en Colombia. Acta Zool Mex 87:111–123

Ophthalmology of Sciuromorpha: Squirrels, Prairie Dogs, and Relatives

44

Jessica M. Meekins

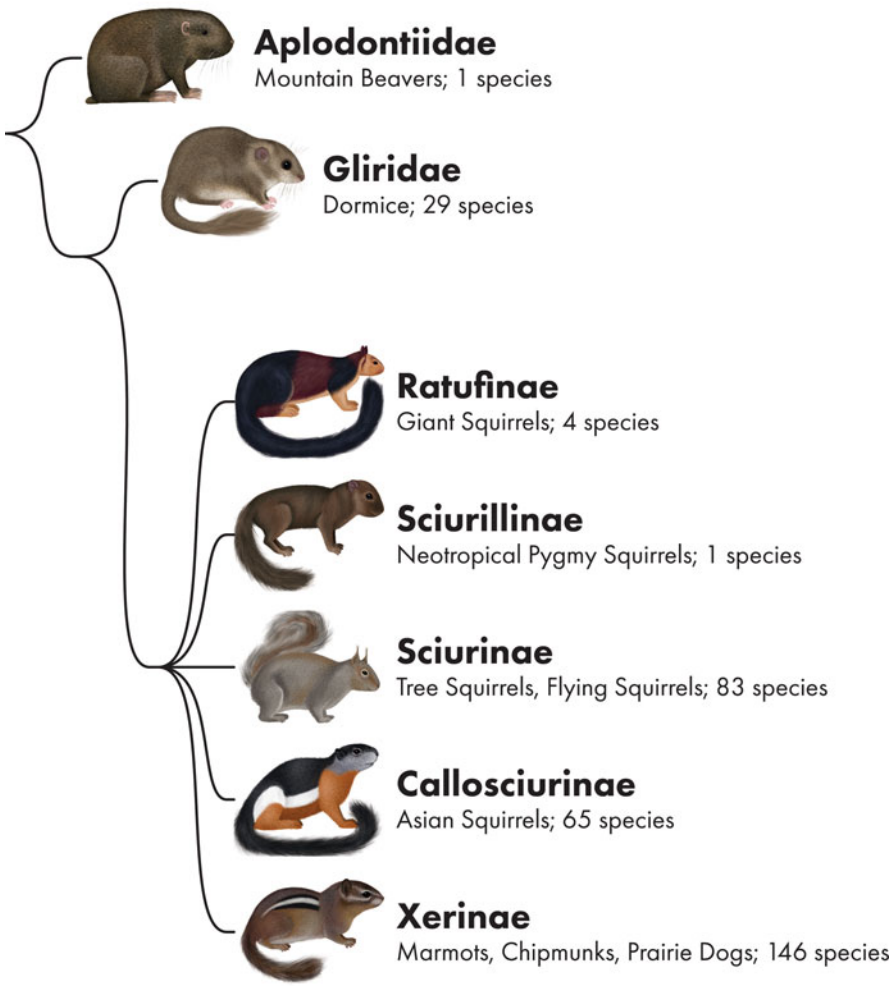

© Chrisoula Skouritakis

J. M. Meekins (✉)
College of Veterinary Medicine, Kansas State University, Manhattan, KS, USA
e-mail: jslack@vet.k-state.edu

The *Sciuromorpha* clade includes three families: *Sciuridae*, *Aplodontiidae*, and *Gliridae*. Of these families, the *Sciuridae*, or "squirrel-like," family contains the most noteworthy members, including squirrels, marmots, chipmunks, and

F. Montiani-Ferreira et al. (eds.), *Wild and Exotic Animal Ophthalmology*, https://doi.org/10.1007/978-3-030-81273-7_19

prairie dogs, while the *Aplodontiidae* family contains a single member, the mountain beaver, and the *Gliridae* family consists of the dormouse. Relatively little has been published regarding clinical ophthalmology in other members of this suborder, however, certain rodent species in this group have been used extensively in vision research; that information is beyond the scope if this clinically oriented reference text. The purpose of this chapter is to provide information on clinically relevant aspects of the eye for members of the *Sciuromorpha* clade.

Sciuridae: Squirrels (Ground, Tree, True Flying, Giant)

The genus *Sciurus* includes many of the common ground and tree squirrels that inhabit much of the world. Other members of the squirrel group, outside of the *Sciurus* genus, include true flying squirrels and giant squirrels. Very few studies relevant to the practice of clinical ophthalmology have been published for this group, though various species of ground squirrels have been used as an animal model for research on topics ranging from experimental myopia to the refractive state of the eye (Gur and Sivak 1979; Mcbrien et al. 1993; Mccourt and Jacobs 1984). The anatomy of the retinal photoreceptors and ganglion cells and retinal physiology topics have also been described (Blakeslee et al. 1988; Jacobs 1974; Leeper and Charlton 1985; Long and Fisher 1983). In the gray squirrel, a yellow pigment distributed evenly throughout the lens was determined to be protective of the retinal photoreceptors against near-UV radiation damage (Zigman and Paxhia 1988).

A recent study described the comparative histologic ocular anatomy in various rodent species, including several types of squirrels (Fernandez and Dubielzig 2013). Histologic corneal and retinal tissue thickness measurements and ocular fundus features from that study are summarized in Table 44.1. Intraocular musculature, including iris sphincter and dilator muscles and a ciliary muscle, were identified, in addition to Schlemm's canal, a circular canal within the sclera at the level of the iridocorneal angle that drains aqueous humor. All types of squirrels examined lacked a tapetum and demonstrated a holangiotic retinal vessel pattern (Fernandez and Dubielzig 2013). Ground squirrels had an optic disc that was linear in the horizontal plane (Fig. 44.1) and an asymmetrical retinal thickness, with the ventral retina thicker than the dorsal retina (Fig. 44.2) (Fernandez and Dubielzig 2013). Tree-dwelling squirrels, on the other hand, had a rounded but elongated optic disc and flying squirrels had the round optic disc typical of all other rodents (Fig. 44.1) (Fernandez and Dubielzig 2013).

Normal conjunctival microbiota has been reported in the Persian squirrel (*Sciurus anomalus*). Of 80 normal eyes, *Staphylococcus* spp. were the most frequently isolated organisms from 83% of samples, followed by *Corynebacterium* spp. from 56% of samples (Faghih et al. 2018). In another study, conjunctival lymphoid follicles were found in the palpebral conjunctiva from 4 of 6 examined fox squirrel (*Sciurus niger*) eyes (Astley et al. 2007).

A single case report exists that describes a clinical ocular abnormality in a member of the *Sciurus* genus. A six-year-old red squirrel (*Sciurus vulgaris orientis*) was diagnosed with malignant melanoma of the eyelids, with bilateral involvement of the upper-lower eyelids. Lung metastasis was identified on necropsy in that case (Fukui et al. 2002). Squirrel poxvirus (Leporipoxviridae) has also been reported to cause multifocal ulcerative blepharitis and is nearly 100% fatal in red squirrels. The disease is endemic in gray squirrels of North America, although clinical signs are typically mild if they develop at all (MacLachlan and Dubovi 2017). Eyelid skin is characterized by dermatitis, epithelial hypertrophy and hyperkeratosis, and ballooning degeneration and intracytoplasmatic inclusion bodies. Keratoconjunctivitis can develop as well (lymphoplasmacytic) with similar conjunctival epithelial ballooning degeneration and intracytoplasmatic inclusion bodies variably present (personal communication, Bret A. Moore). When captured and restrained or following trauma, squirrels may exude milky white ocular discharge (Fig. 44.3). The cause and origin are unknown. There are no other reports of naturally occurring diseases affecting the eye or adnexa of these squirrel species.

Marmots

The marmot is a large squirrel in the genus *Marmota*, of which there are 15 species, including the woodchuck (*Marmota monax*), also known as the groundhog. There are very few studies on clinically relevant ophthalmology topics in this group of animals. One study described comparative histologic anatomy in a variety of rodent species, including two woodchucks (Fernandez and Dubielzig 2013). Histologic corneal and retinal tissue thickness measurements and other ocular fundus features were reported (Table 44.1), in addition to other findings such as the presence of Schlemm's canal (Fernandez and Dubielzig 2013). Intraocular musculature, specifically the iris sphincter and dilator muscles and a ciliary muscle were also identified in the woodchuck eyes examined in this study (Fernandez and Dubielzig 2013). An atapetal choroid, an optic disc that is linear in the horizontal plane, and an asymmetrical retinal thickness, with the ventral retina thicker than the dorsal retina, were described as anatomic features of the ocular fundus (Fernandez and Dubielzig 2013). In another study, the eyes of two woodchucks were histologically evaluated for the presence of conjunctival lymphoid follicles, and none were found (Astley et al. 2007).

Table 44.1 Histologic corneal and retinal tissue measurements and ocular fundus features of select rodent species. Adapted from Fernandez and Dubielzig 2013. Measurements are expressed in mm. NR: not reported.

Species (common name)	Corneal thickness (total)	Retinal thickness (total)	Retinal blood vessels
Ground squirrel	0.31	0.16	Yes
Flying squirrel	0.21	0.23	Yes
Thirteen-lined ground squirrel	0.42	NR	Yes
Western gray squirrel	0.75	0.3	Yes
Woodchuck	0.35	0.25	Yes
Prairie dog	0.42	NR	NR

There are two case reports in the literature that describe ocular abnormalities in the woodchuck. Unilateral phthisis bulbi was identified in an 11-year-old captive-raised woodchuck diagnosed with a meningioma and was speculated to be related to a recurrent inflammatory process or secondary to trauma (Podell et al. 1988). Another case report described cerebral cysticercosis in a juvenile wild woodchuck, in which a large, multiloculated, fluctuant mass containing tapeworm cysticerci extended under the zygomatic arch and adjacent to the eye (Brojer et al. 2002). Despite the close proximity to the eye, no cysticerci were found in the globe or orbit in that case. Beyond the description of the histologic anatomy and absence of conjunctival follicles in the woodchuck eye, no reports of clinical anatomy or results of basic ophthalmic diagnostic tests have been published in this genus.

Chipmunks

The chipmunk (genus *Tamias*) is a small, striped rodent primarily found in North America. A study evaluating bacterial isolates from "infected eyes" of captive species at the London Zoo provides the only report of spontaneous ocular disease in the chipmunk (Williams et al. 2000). In that study, two chipmunks exhibiting bilateral ocular discharge were evaluated. The culture of conjunctival swab samples yielded

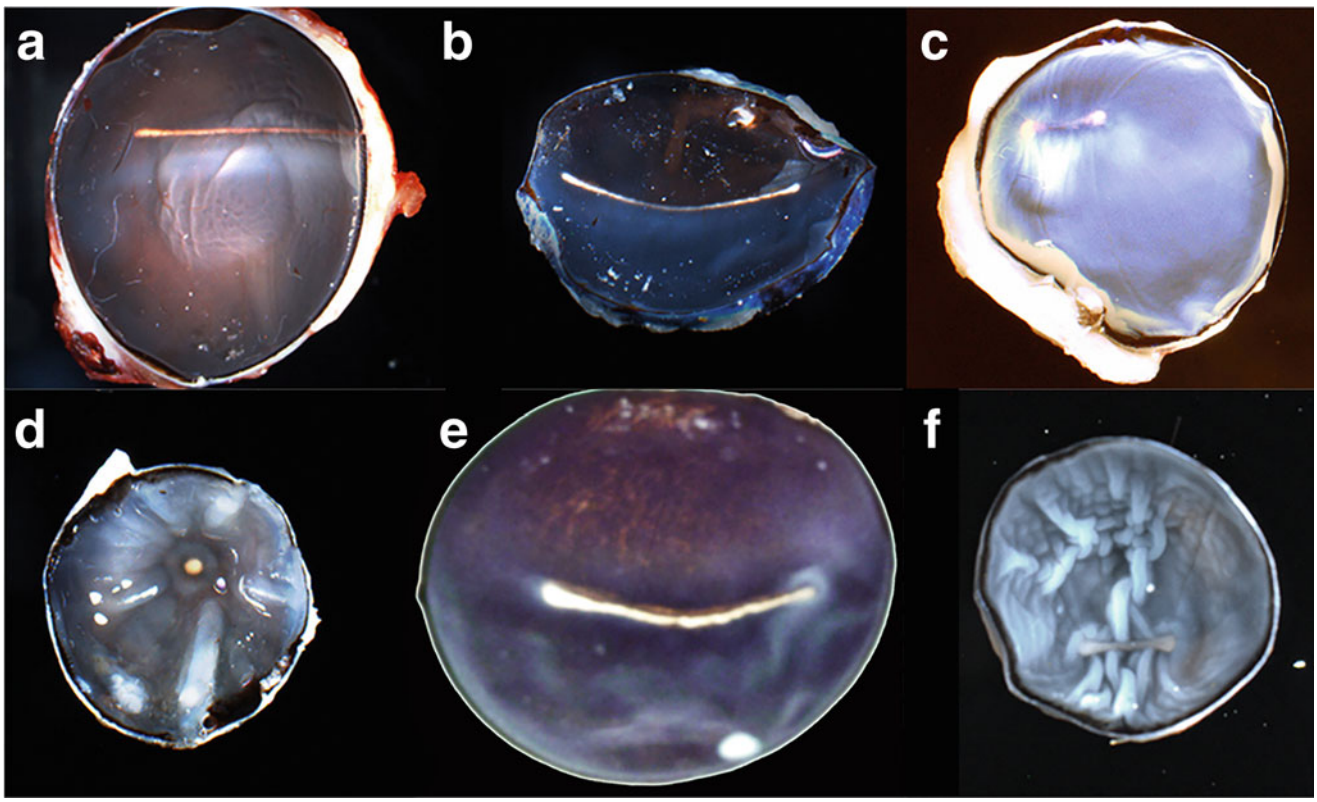

Fig. 44.1 Gross morphology of the optic disc in several rodent species. Note the linear optic disc in (**a**) the prairie dog (*Cynomys ludovicianus*), (**b**) the thirteen-lined ground squirrel (*Ictidomys tridecemlineatus*), and (**e**) the groundhog (*Marmota monax*), the elongated optic disc in (**c**) Western gray squirrel (*Sciurus griseus*) and the (**f**) Eastern gray squirrel (*Sciurus carolinensis*). Note the round optic disc in (**d**) the flying squirrel (*Pteromyini tribe*). Used with permission from John Wiley & Sons, Fig. 5: Fernandez JRR, Dubielzig RR. Ocular comparative anatomy of the family Rodentia. *Vet Ophthalmol*. 2013;16:94–99.

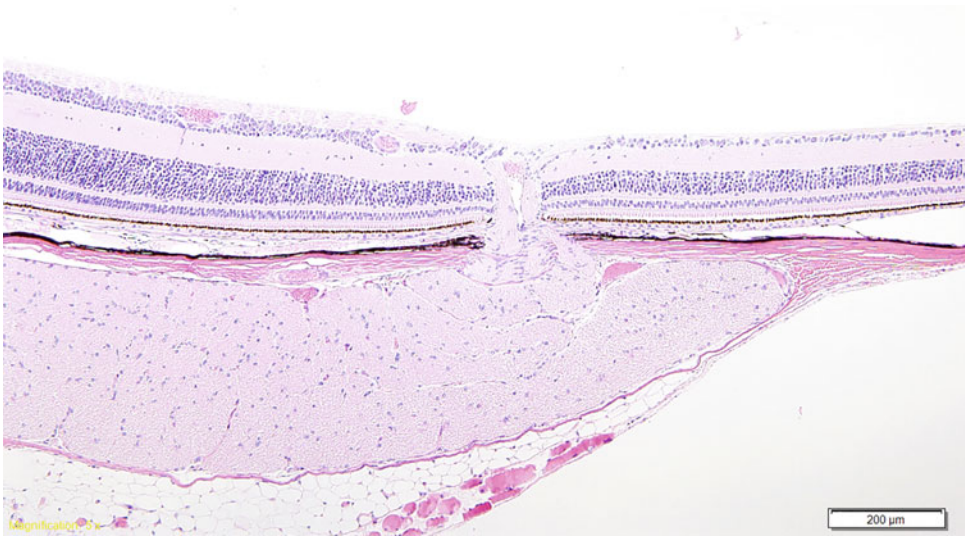

Fig. 44.2 Photomicrograph of the asymmetric retinal thickness in a ground squirrel. Note that the total retinal thickness is increased ventral to the optic disc (to the left in the photomicrograph). Courtesy of the Comparative Ocular Pathology Laboratory of Wisconsin

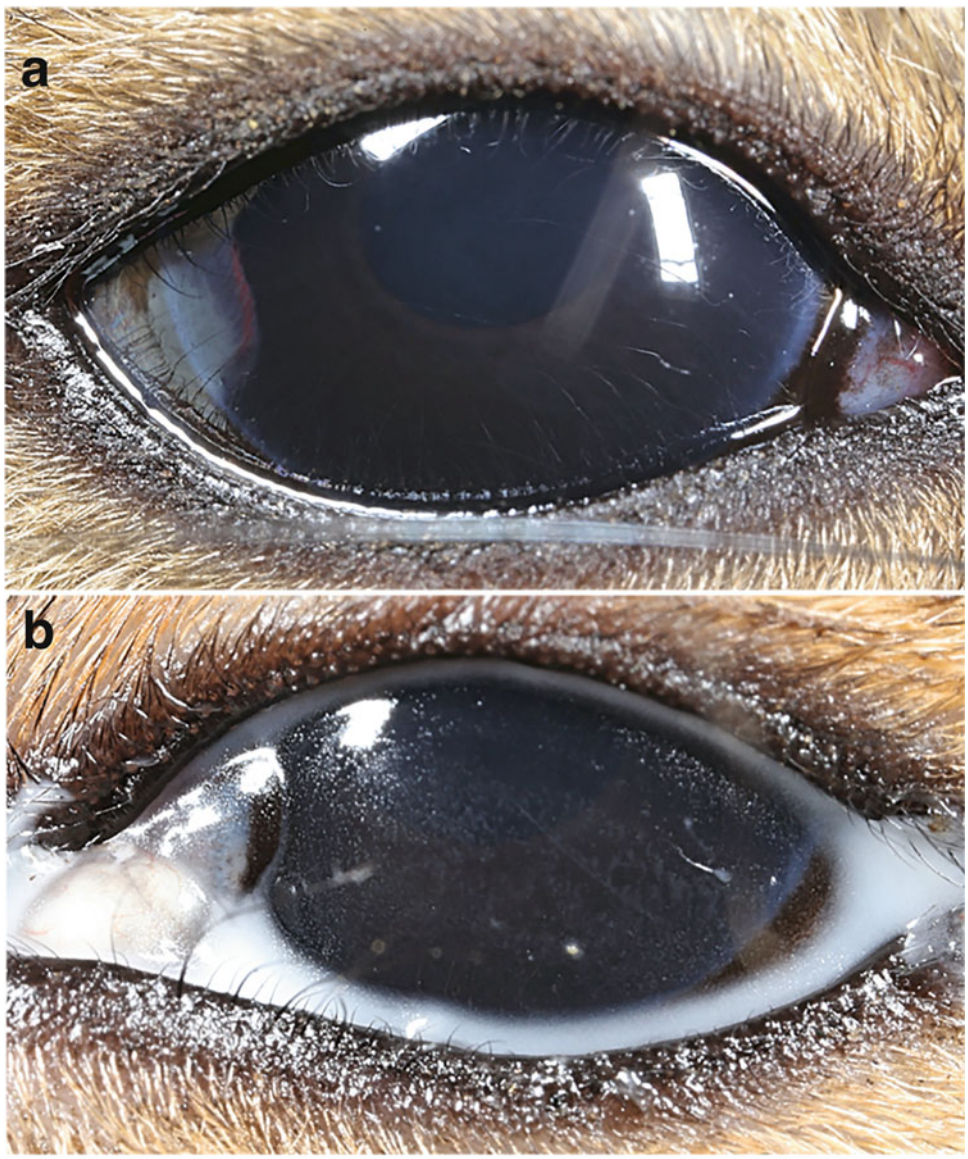

Fig. 44.3 Photographs of the eyes of Eastern fox squirrel (*Sciurus niger*). (**a**) Normal eye showing a small third eyelid and a darkly pigmented iris with a round pupil. (**b**) White, milky discharge following blunt trauma. Note the discharge distributed within the tear film affording a spectacled appearance. No other ocular abnormalities were noted. Courtesy of Bret A. Moore

a *Pseudomonas* sp. from one animal and a non-hemolytic *Staphylococcus* sp. from another animal (Williams et al. 2000). Both animals were treated with topical fusidic acid with minimal or no improvement. The *Pseudomonas* sp. organism was resistant to fusidic acid as reported by disc sensitivity, but the *Staphylococcus* sp. was susceptible to fusidic acid. Both isolates were susceptible to all other tested antibiotics, including cephalexin, amoxicillin, enrofloxacin, and chloramphenicol (Williams et al. 2000).

Researchers have investigated the retina and optic nerve of the chipmunk and have described the distribution and soma size of retinal ganglion cells (Wakakuwa et al. 1985a), ipsilaterally projecting retinal ganglion cells (Wakakuwa et al. 1985b), retinal inputs of the dorsal lateral geniculate nucleus relay cells (Morigiwa et al. 1988), and the composition and total fiber count of the optic nerve (Wakakuwa et al. 1987). A high density of retinal ganglion cells identified in a horizontally elongated area of the central retina made up the visual streak in chipmunk retinal whole-mounts, and the total cell count was estimated at 410,000 (Wakakuwa et al. 1985a). The temporal retina contained contralateral and ipsilateral projecting cells to the lateral geniculate nucleus, and the soma size was significantly larger for the ipsilateral than for the contralateral projecting cells (Wakakuwa et al. 1985b). The optic nerve, as evaluated by electron microscopy, was composed of approximately 5.65×10^5 axons, and almost all fibers were myelinated (Wakakuwa et al. 1987). Large diameter axons were concentrated in the temporal and ventral portion of the optic nerve, which corresponds with the location of large ganglion cells in the temporal retina (Wakakuwa et al. 1987). These interesting neuro-anatomical descriptions of the chipmunk retina and optic nerve represent the only ophthalmic anatomy description of the species, and there are no results of basic ophthalmic diagnostic tests beyond the conjunctival culture reported in two chipmunks.

Prairie Dogs

The prairie dog (genus *Cynomys*) is an herbivorous burrowing rodent native to North American grasslands. There are five species within the group, including black-tailed, white-tailed, Gunnison's, Utah, and Mexican. Eyes open at approximately 5 weeks of age. Studies have been published on the clinical and histologic anatomy and results of basic ocular diagnostic testing in the black-tailed prairie dog.

An initial study described comparative histologic anatomy in a variety of rodent species, including two black-tailed prairie dogs (Fernandez and Dubielzig 2013). Findings from that report established some of the unique features that were later described clinically in another study, in addition to reporting corneal thickness measurements (Table 44.1). The

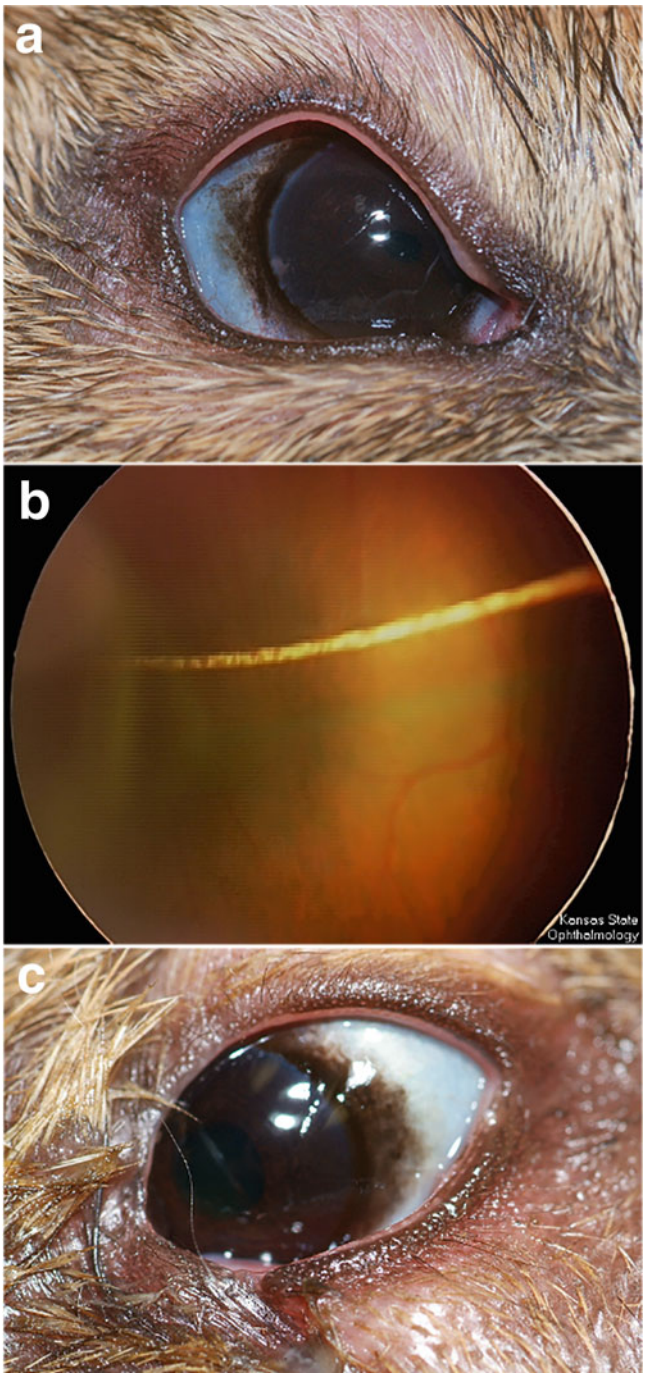

Fig. 44.4 Selected photographs of the eyes of the black-tailed prairie dog (*Cynomys ludovicianus*). **a**) The normal right eye with a thick, mucinous pre-corneal tear film, vestigial nictitating membrane, dark brown iris, and round pupil. **b**) Funduscopic image showing a holangiotic retina, lack of a tapetum, and horizontally elongated optic disc. **c**) An acquired eyelid margin defect (inferior nasal eyelid), the most commonly documented ocular abnormality in the black-tailed prairie dog. Periocular and eyelid margin defects attributed to trauma have been reported to be present in up to 30% of animals housed with other individuals. Used with permission from John Wiley & Sons, Figures 1,2, 4: Meekins JM, Eshar D, Rankin AJ, et al. Clinical and histologic description of ocular anatomy in captive black-tailed prairie dogs (Cynomys ludovicianus). *Vet Ophthalmol*. 2016;19:110-116

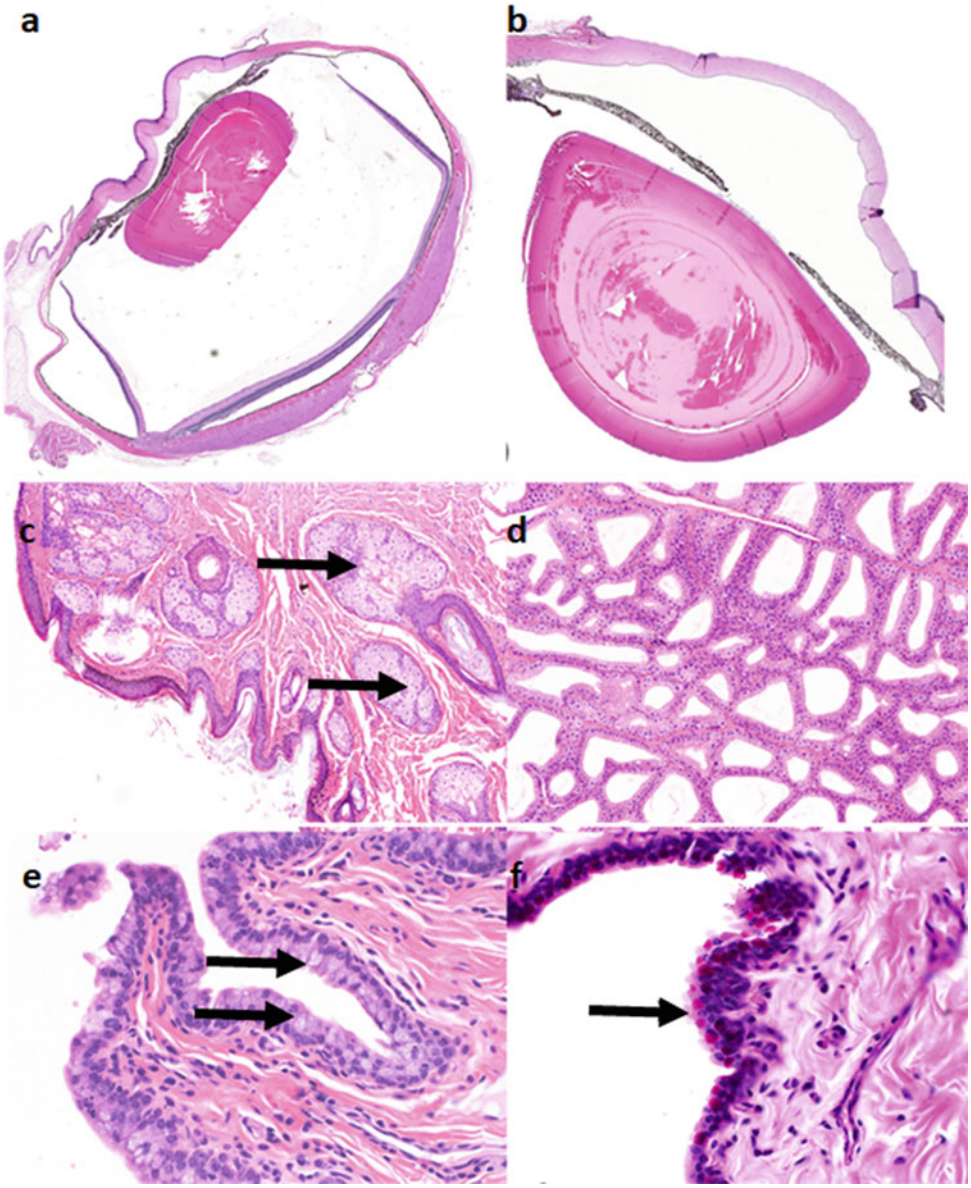

Fig. 44.5 Representative histologic images of the black-tailed prairie dog (*Cynomys ludovicianus*) globe and adnexa. (**a**) Subgross photomicrograph of the globe (hematoxylin-eosin [H&E] stain, x10). (**b**) Photomicrograph of the anterior segment, illustrating the cornea, iris, and lens (H&E stain, x30). (**c**) Prominent and numerous Meibomian glands in the eyelid (arrows, H&E stain, x200). (**d**) Large orbital gland, identified as the Harderian gland (H&E stain, x200). (**e**) Conjunctival epithelium with numerous goblet cells (arrows, H&E stain, x400). (**f**) Conjunctival epithelium with numerous goblet cells stained brightly pink (arrow; periodic acid-Schiff stain, x400). Used with permission from John Wiley & Sons, Fig. 5: Clinical and histologic description of ocular anatomy in captive black-tailed prairie dogs (*Cynomys ludovicianus*). *Vet Ophthalmol*. 2016;19:110–116

later study, which described and compared clinical and histologic ocular anatomy in the species, reported the presence of a Harderian gland, a thick, mucinous pre-corneal tear film, and a vestigial nictitating membrane (Fig. 44.4a) (Meekins et al. 2016). The limbus was heavily pigmented, the iris was a dark, homogenous brown, and the pupil was round (Meekins et al. 2016). The prairie dog ocular fundus was holangiotic, atapetal, and exhibited a horizontally elongated optic disc (Fig. 44.4b) (Meekins et al. 2016). Acquired lesions of the periocular and eyelid area were the most common ocular abnormalities, reported in 35.3% of examined eyes (Fig. 44.4c) (Meekins et al. 2016). Interestingly, some of these unique clinical features were supported by histology findings in normal prairie dog globes. There were numerous eyelid Meibomian glands (Fig. 44.5c) and conjunctival goblet cells (Fig. 44.5e, f) to explain the thick pre-corneal tear film, and the large orbital gland was confirmed to be a Harderian gland (Fig. 44.5d) (Meekins et al. 2016). Similar to some other rodent species, the retina was identified as asymmetrical, being thicker below the optic disc (Fig. 44.6a) (Meekins et al. 2016). Additionally, optic nerve fibers were found to penetrate through the lamina cribrosa to form the horizontally elongated optic disc (Fig. 44.6b, c).

Clinical diagnostic parameters have also been established in the black-tailed prairie dog (Appendix 3). A study reported tear measurement by various methods and characterized normal conjunctival bacterial flora by aerobic culture (Meekins et al. 2015). Intraocular pressure measurement was performed using rebound tonometry; initial attempts at applanation tonometry were unsuccessful due to limitations associated with the instrument tip and the small prairie dog eye (Meekins et al. 2015). Mean tear production was 13.6 ±

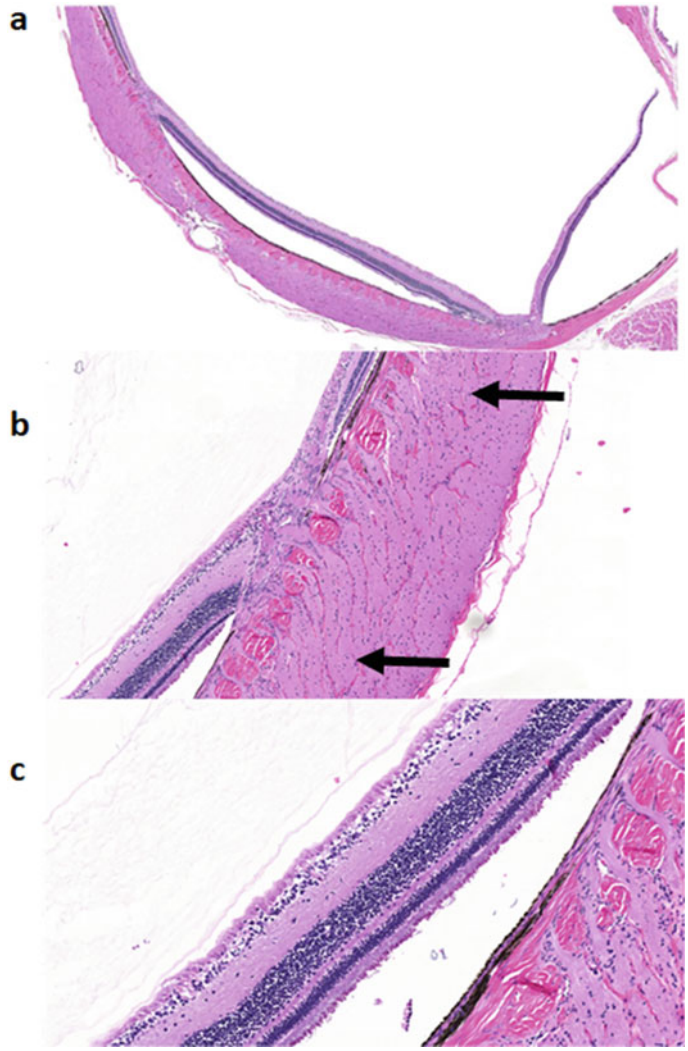

Fig. 44.6 Representative histologic images of the black-tailed prairie dog (*Cynomys ludovicianus*) ocular fundus. (**a**) Photomicrograph of the asymmetric retina, thicker ventral to the horizontally elongated optic disc (hematoxylin-eosin [H&E] stain, x30). (**b**) Extensions of the horizontally elongated optic disc (arrows) extending into the retina (H&E stain, x100). (**c**) Higher magnification of (**b**) illustrating the extensions from the optic nerve (H&E stain, x200). Used with permission from John Wiley & Sons, Fig. 6: Clinical and histologic description of ocular anatomy in captive black-tailed prairie dogs (*Cynomys ludovicianus*). *Vet Ophthalmol*. 2016;19:110–116

7.8 mm/15 sec for the phenol red thread test and 1.2 ± 0.9 mm/min for the modified Schirmer Tear Test. Mean intraocular pressure was 7.7 ± 2.2 mmHg using the rebound tonometer with the D setting (internal calibration for use in dogs). A total of 16 types of bacteria were isolated by aerobic conjunctival culture, and only one prairie dog in this study had no growth of bacteria from the conjunctival swab. The majority of animals (75%) had two to four different bacterial isolated, and the most commonly isolated bacterial genus was Staphylococcus (Meekins et al. 2015). *Staphylococcus xylosus* was the most common bacterium, isolated from the conjunctiva of 41.2% of normal prairie dogs (Meekins et al. 2015).

No other reports of ophthalmic disease in prairie dogs exist, although anecdotally, septicemia due to plague can cause ocular lesions (e.g., uveitis) (Delaney et al. 2018). Further work is needed to determine the frequency and types of ophthalmic abnormalities common to prairie dogs and other members of the Sciuromorphae.

Gliridae (Dormouse)

The common dormouse (*Muscardinus avellanarius*) is a woodland rodent with population numbers noted to be in decline in Britain over the last 100 years (Hurrell and Mcintosh 1984). During routine surveillance efforts in the early 1990s, one dormouse was diagnosed with bilateral purulent ocular discharge, blepharitis, and conjunctivitis, as well as left eye exophthalmos (Sainsbury et al. 1996). After initial treatment with topical and systemic antimicrobials and anti-inflammatories, clinical signs improved, and mobile nematodes were observed on the left cornea (Sainsbury et al. 1996). The parasites were identified as *Rhabditis orbitalis*, a microbiotrophic nematode that inhabits rodent nests and has not previously been reported to cause ocular disease (Schulte and Poinar 1991). Third stage juvenile nematodes enter the conjunctival sac of rodents and persist there for several days without causing disease (Schulte 1989).

Ocular clinical signs, including unilateral exophthalmos, ultimately resolved in the animal of this case report after treatment with the antiparasitic drug ivermectin (Sainsbury et al. 1996). This is the only report of ocular disease attributable to *R. orbitalis* in a rodent species.

This single case report represents the only report of naturally occurring ophthalmic disease in the species. There is no published information on ophthalmic anatomy or results of basic ocular diagnostic tests for the dormouse. As with many exotic animal species, additional research is needed to develop a complete understanding of normal ophthalmic anatomy and the diseases that may impact the eye in the *Sciuromorpha* clade.

References

Astley RA, Chodosh J, Caire W et al (2007) Conjunctival lymphoid follicles in new world rodents. *Anat Rec - Adv Integ Anat Evol Biol* 290:1190–1194

Blakeslee B, Jacobs GH, Neitz J (1988) Spectral mechanisms in the tree squirrel retina. *J Comp Physiol A - Sensory Neural Behav Physiol* 162:773–780

Brojer CM, Peregrine AS, Barker IK et al (2002) Cerebral cysticercosis in a woodchuck (*Marmota monax*). *J Wildl Dis* 38:621–624

Delaney MA, Treuting PM, Rothenburger JL (2018) Rodentia. In: Terio KA, McAlosse D, St Leger J (eds) Pathology of Wildlife and Zoo Animals. Elsevier Inc., London, UK, p 508

Faghih H, Aftab G, Rajaei SM et al (2018) Evaluation of conjunctival microbiota in clinically normal Persian squirrels (*Sciurus Anomalus*). *J Zoo Wildl Med* 49:794–797

Fernandez JRR, Dubielzig RR (2013) Ocular comparative anatomy of the family Rodentia. *Vet Ophthalmol* 16:94–99

Fukui D, Bando G, Kosuge M et al (2002) Malignant melanoma of the eyelid in a red squirrel (*Sciurus vulgaris orientis*). *J Vet Med Sci* 64: 261–264

Gur M, Sivak JG (1979) Refractive state of the eye of a small diurnal mammal – ground squirrel. *Am J Opto Physiol Optics* 56:689–695

Hurrell E, Mcintosh G (*1984*) Mammal-Society Dormouse Survey, January 1975 - April 1979. *Mamm Rev* 14:1–18

Jacobs GH (1974) Scotopic and photopic visual capacities of an arboreal squirrel (*Sciurus niger*). *Brain Behav Evol* 10:307–321

Leeper HF, Charlton JS (1985) Response properties of horizontal cells and photoreceptor cells in the retina of the tree squirrel. *Sciurus carolinensis J Neurophysiol* 54:1157–1166

Long KO, Fisher SK (1983) The distributions of photoreceptors and ganglion-cells in the California ground squirrel. *Spermophilus beecheyi J Comp Neurol* 221:329–340

Maclachlan NJ, Dubovi EJ (2017) Poxviridae. In: Fenner's Veterinary Virology. Elsevier Inc, London, UK, pp 173–174

Mcbrien NA, Moghaddam HO, New R et al (1993) Experimental myopia in a diurnal mammal (*Sciurus carolinensis*) with no accommodative ability. *J Physiol (Lond)* 469:427–441

Mccourt ME, Jacobs GH (1984) Refractive state, depth of focus and accommodation of the eye of the California ground squirrel (*Spermophilus beecheyi*). *Vision Res* 24:1261–1266

Meekins JM, Eshar D, Rankin AJ (2015) Tear production, intraocular pressure, and conjunctival bacterial flora in a group of captive black-tailed prairie dogs (*Cynomys ludovicianus*). *Vet Ophthalmol* 18 (Suppl 1):132–136

Meekins JM, Eshar D, Rankin AJ et al (2016) Clinical and histologic description of ocular anatomy in captive black-tailed prairie dogs (*Cynomys ludovicianus*). *Vet Ophthalmol* 19:110–116

Morigiwa K, Sawai H, Wakakuwa K et al (1988) Retinal inputs and laminar distributions of the dorsal lateral geniculate nucleus relay cells in the eastern chipmunk (*Tamias sibiricus asiaticus*). *Exp Brain Res* 71:527–540

Podell M, Pokras M, Gerlach P et al (1988) Meningioma in a woodchuck exhibiting central vestibular deficits. *J Wildl Dis* 24:695–699

Sainsbury AW, Bright PW, Morris PA et al (1996) Ocular disease associated with Rhabditis orbitalis nematodes in a common dormouse (*Muscardinus avellanarius*). *Vet Rec* 139:192–193

Schulte F (1989) Life-History of *Rhabditis (Pelodera) orbitalis* - a larval parasite in the eye orbits of Arvicolid and Murid rodents. *Proc Helminthol Soc Wash* 56:1–7

Schulte F, Poinar GO (1991) On the geographical-distribution and parasitism of *Rhabditis (Pelodera) orbitalis* (Nematoda, Rhabditidae). *J Helminthol Soc Washington* 58:82–84

Wakakuwa K, Washida A, Fukuda Y (1985a) Distribution and soma size of ganglion cells in the retina of the eastern chipmunk (*Tamias sibiricus asiaticus*). *Vision Res* 25:877–885

Wakakuwa K, Washida A, Fukuda Y (1985b) Ipsilaterally projecting retinal ganglion cells in the eastern chipmunk (*Tamias sibiricus asiaticus*). *Neurosci Lett* 55:219–224

Wakakuwa K, Watanabe M, Sugimoto T et al (1987) An electron microscopic analysis of the optic nerve of the eastern chipmunk (*Tamias sibiricus asiaticus*): total fiber count and retinotopic organisation. *Vision Res* 27:1891–1901

Williams DL, MacGregor S, Sainsbury AW (2000) Evaluation of bacteria isolated from infected eyes of captive, non-domestic animals. *Vet Rec* 146:515–518

Zigman S, Paxhia T (1988) The Nature and Properties of Squirrel Lens Yellow Pigment. *Exp Eye Res* 47:819–824

Ophthalmology of Castorimorpha: Beavers, Gophers, and Relatives

45

Jessica M. Meekins

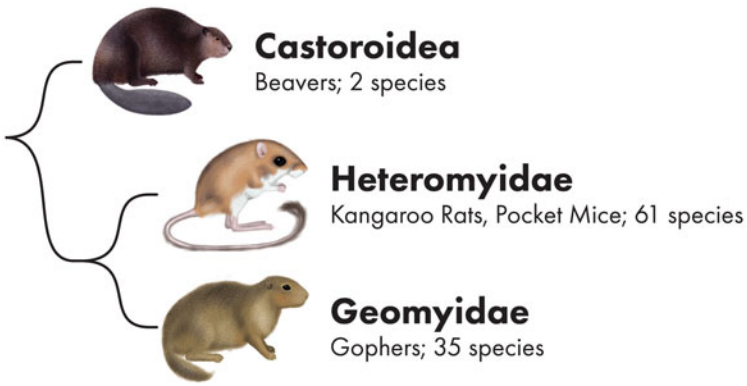

Introduction

Castorimorpha is the suborder of rodents that includes beavers, pocket gophers, pocket mice, kangaroo rats, and kangaroo mice. Information on clinical and histologic ophthalmic anatomy or naturally occurring ophthalmic diseases in this group of animals is limited and specifically restricted to published studies on the North American (Canadian) beaver and the pocket gopher. One study has characterized commensal conjunctival flora, intraocular pressure via applanation tonometry, and clinical anatomical features of the Canadian beaver eye. Other studies provide details of basic histologic anatomy in the species. The retinal anatomy of the pocket gopher has been described in detail, in an effort to identify unique features that have evolved in this primarily subterranean species. Though no naturally occurring diseases that affect the eye have been published for this group, a low documented prevalence of acquired ocular lesions attributable to trauma was reported in one study on the Canadian beaver. The purpose of this chapter is to provide information on clinically relevant aspects of the *Castorimorpha* eye.

J. M. Meekins (✉)
College of Veterinary Medicine, Kansas State University, Manhattan, KS, USA
e-mail: jslack@vet.k-state.edu

Castoroidea (Beavers)

The beaver is a semiaquatic and largely nocturnal rodent with two extant species: The North American (Canadian) beaver (*Castor canadensis*) and the Eurasian beaver (*Castor fiber*). Vision in the European beaver seems to be most adapted for a terrestrial rather than aquatic environment. The peak retinal ganglion cell density was shown to average 1700 cells/mm^2, enabling a maximum emmetropic visual acuity of about 3.3 cycles/degree in air, compared to a hyperopic visual acuity of only 1.4 cycles/degree underwater (Mass and Supin 2017). Another group described the gross and microscopic anatomy of the Canadian beaver eye in an effort to determine their accommodative capability (Ballard et al. 1989). Histologically, a well-developed iris sphincter muscle was identified close to the pupil margin, and a poorly developed dilator muscle was located near the posterior pigmented

F. Montiani-Ferreira et al. (eds.), *Wild and Exotic Animal Ophthalmology*, https://doi.org/10.1007/978-3-030-81273-7_20

Table 45.1 Histologic corneal and retinal tissue measurements and other ocular fundus features of the North American (Canadian) beaver eye (*Castor canadensis*)

Corneal thickness (mm)	Total	Epithelium	Stroma	Descemet's membrane
	0.43	0.05	0.36	0.01
Retinal thickness (mm)	Total	Retinal blood vessels	Optic nerve blood vessels	
	0.14	No	Yes	

Adapted from Fernandez and Dubielzig 2013

epithelium (Ballard et al. 1989). The ciliary muscle was longitudinally oriented and composed of small muscle bundles, and there was an average of 135 ciliary processes (Ballard et al. 1989). From the described morphology of the rudimentary ciliary muscle in this study, it was speculated that the accommodation ability of the beaver eye is poor (Ballard et al. 1989).

A more recent study investigated the comparative histologic ocular anatomy from various members of the family Rodentia, including two Canadian beavers (Fernandez and Dubielzig 2013). Information on histologic tissue thickness measurements and descriptive information on other ocular fundus features are presented in Table 45.1. This study confirmed some of the previous descriptions of ocular anatomy in the beaver, including the presence of iris sphincter and dilator muscles and a poorly developed ciliary muscle (Fernandez and Dubielzig 2013). Newly reported findings included the presence of Schlemm's canal, a circular canal within the sclera at the level of the iridocorneal angle that drains aqueous humor, in addition to an atapetal choroid and blood vessels within the optic nerve head (Fernandez and Dubielzig 2013).

Investigators have described clinical ophthalmic examination features, including anterior segment and ophthalmoscopy findings, in the Canadian beaver (Cullen 2003). Animals were sedated with intramuscular ketamine and subjected to conjunctival culture (aerobic, anaerobic, fungal) and intraocular pressure measurement via applanation tonometry. Normal external ocular structures included upper and lower lacrimal puncta and a vestigial nictitating membrane (Cullen 2003). The average palpebral fissure length was 9.36 ± 1.00 mm, while the horizontal and vertical corneal diameters were 9.05 ± 0.64 and 8.45 ± 0.69 mm, respectively (Cullen 2003). In contrast to previous anatomic studies, limbal pigment extended 1–2 mm into the peripheral cornea, resulting in a 120-degree dorsal corneal pigment arc (Cullen 2003). However, definitive conclusions regarding perilimbal corneal pigmentation in the beaver eye cannot be made on the basis of the currently available information due to the difference in evaluation technique (clinical vs. histologic examination) and the low total number of examined animals. The iris was heavily pigmented, and the pupil was round. The ocular fundus displayed an anangiotic retina, lacked a tapetum, and the optic disc was round (Fig. 45.1) (Cullen 2003). Mean intraocular pressure was 17.11 ± 6.39 mmHg for the right eye and 18.79 ± 5.63 mmHg for the left eye (Cullen 2003) (Appendix 3). The most commonly isolated bacterial genus from aerobic conjunctival culture was Micrococcus. Anaerobic bacteria were rarely isolated, with *Clostridium sordellii* and *Peptostreptococcus* spp. each identified from a single beaver. All samples were negative for fungal growth (Cullen 2003).

There was a low prevalence of ocular abnormalities, present only in 5–15% of the examined group of beavers (Cullen

Fig. 45.1 Ocular fundus of the North American (Canadian) beaver (*Castor canadensis*). Fundus photograph (**a**) and artist conception (**b**) showing an anangiotic vascular pattern with variable choroidal vessel visualization, the absence of a tapetum, and a round optic disc with subtle evidence of small capillaries. (**c**) Cross-section of the mid-peripheral retina. **a**—Used with permission by John Wiley & Sons, Fig. 3: Cullen, C. L. (2003). Normal ocular features, conjunctival microflora and intraocular pressure in the Canadian beaver (Castor canadensis). *Veterinary Ophthalmology, 6*(4), 279–284. doi: https://doi.org/10.1111/j.1463-5224.2003.00307.x **b**—Used with permission from Johnson GL. Contributions to the comparative anatomy of the mammalian eye chiefly based on ophthalmoscopic examination. Philosophical Transactions 1901;194:103 (Plate 20). Publisher: Royal Society Publishing. **c**—Courtesy of the Comparative Ocular Pathology Laboratory of Wisconsin

2003). The most common finding was incidental iris-to-iris persistent pupillary membranes that were present in 10% of animals. Additionally, evidence of previous ocular trauma consisting of periocular or eyelid scars was noted in two beavers. Phthisis bulbi was the most clinically significant finding, identified unilaterally in one beaver (Cullen 2003).

Pocket Gophers

The pocket gopher, commonly referred to as the gopher, is a small burrowing rodent that displays extensive tunneling activities. There are six genera and approximately 35 species of gophers. As animals that spend most of life in subterranean burrows, pocket gophers have been investigated to determine specific visual adaptations to an environment of extreme darkness. Retinal anatomy and responses to photic stimulation using electroretinography were reported in one study (Williams et al. 2005). The globe dimensions were also reported, with an axial length of 4.62 ± 0.165 mm and an equatorial diameter of 4.67 ± 0.226 mm (Williams et al. 2005). The total retinal thickness was 143.48 ± 6.49 μm and cones comprised approximately 25% of the total photoreceptor count (Williams et al. 2005). There was a relatively small variation in cone density across different areas of the retina, but generally, the cone population was densest in the ventral retina just below the optic nerve head (Williams et al. 2005).

Two cone opsin classes were identified in the pocket gopher retina, the M and the UV cones (Williams et al. 2005). Rodent retinas generally have a rod photopigment and two types of cone photopigment, the M cone pigment and either S or UV cone pigment. It is thought that the UV pigment was characteristic of the most recent common ancestor shared by all mammals, and many placental mammal cones have since shifted to longer wavelength sensitivities (typically associated with S cones) (Hunt et al. 2001; Shi and Yokoyama 2003). This includes rodents in the family *Sciuridae*, discussed in another chapter. Remaining members of the rodent family, including pocket gophers and others that are nocturnal or dwell in environments with minimal light exposure, have retained the shorter wavelength UV cone pigment sensitivity.

No reports on ophthalmic anatomy, or results of clinical ophthalmic examination or diagnostic testing, exist in other members of this rodent suborder. As with many exotic animal species, additional research is needed to develop a complete understanding of normal ophthalmic anatomy and the diseases that may impact the eye in the larger *Castorimorpha* group.

References

Ballard KA, Sivak JG, Howland HC (1989) Intraocular muscles of the Canadian River otter and Canadian beaver and their optical function. Can J Zool 67:469–474

Cullen CL (2003) Normal ocular features, conjunctival microflora and intraocular pressure in the Canadian beaver (*Castor canadensis*). Vet Ophthalmol 6:279–284

Fernandez JRR, Dubielzig RR (2013) Ocular comparative anatomy of the family Rodentia. Vet Ophthalmol 16:94–99

Hunt DM, Wilkie SE, Bowmaker JK et al (2001) Vision in the ultraviolet. Cell Mol Life Sci 58:1583–1598

Mass AM, Supin AY (2017) Estimates of underwater and aerial visual acuity in the European beaver *Castor fiber L.* based on morphological data. Doklady Biol Sci 473:35–38

Shi YS, Yokoyama S (2003) Molecular analysis of the evolutionary significance of ultraviolet vision in vertebrates. Proc Natl Acad Sci U S A 100:8308–8313

Williams GA, Calderone JB, Jacobs GH (2005) Photoreceptors and photopigments in a subterranean rodent, the pocket gopher (*Thomomys bottae*). J Comp Physiol A Neuroethol Sens Neural Behav Physiol 191:125–134

Ophthalmology of Myodonta: Mice, Rats, Hamsters, Gerbils, and Relatives

46

Joshua Seth Eaton

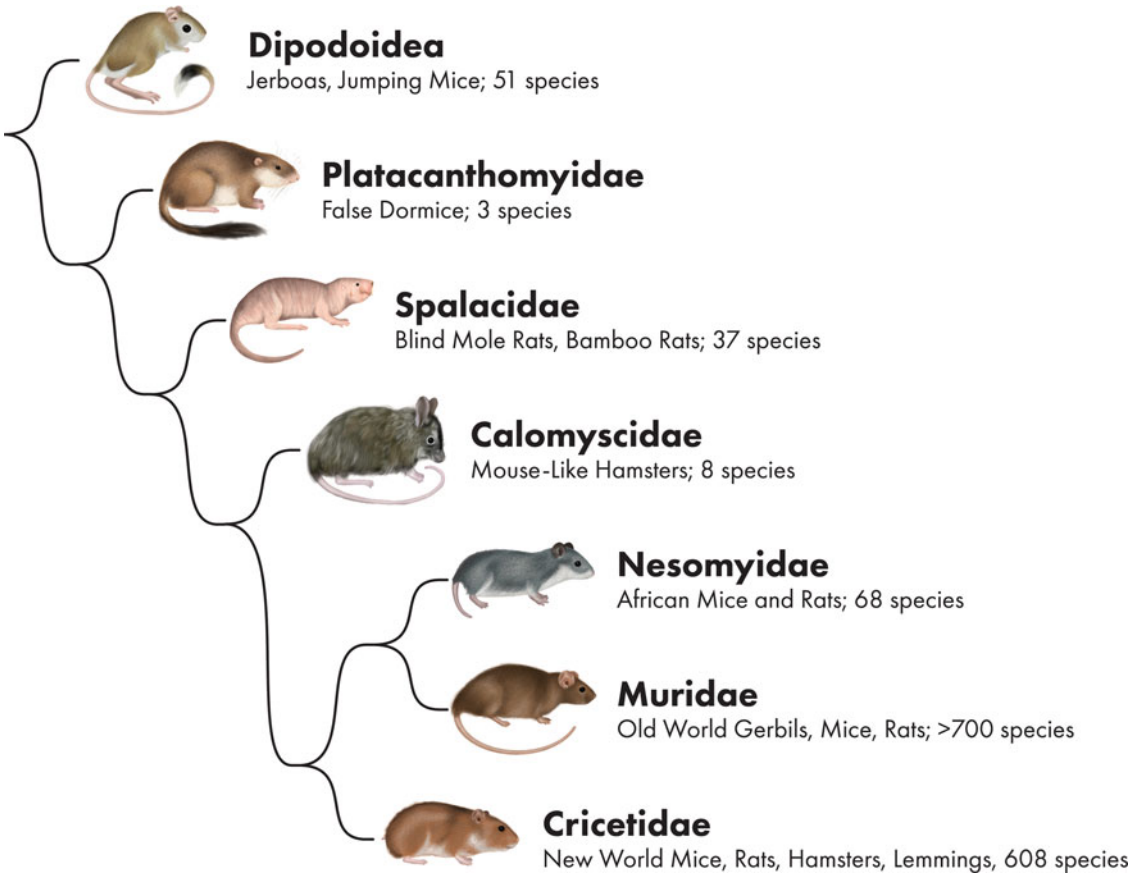

With over 2200 extant species, rodents (order Rodentia) represent the largest mammalian order and comprise 42% of global mammalian biodiversity (Donnelly et al. 2015). Rodents represent a diversity of morphological adaptations associated with their varied terrestrial and aquatic habitats, distributed throughout all continents except Antarctica. One common feature to all Rodentia is a powerful anatomical apparatus for chewing and gnawing, characterized by prominent rostral dentition and a large and often complex masseter muscle. The differing morphological characteristics and adaptations of the zygomasseteric apparatus are used to divide the Rodentia into five suborders including the

J. S. Eaton (✉)
Department of Surgical Sciences, School of Veterinary Medicine, University of Wisconsin–Madison, Madison, WI, USA
e-mail: jseaton2@wisc.edu

F. Montiani-Ferreira et al. (eds.), *Wild and Exotic Animal Ophthalmology*, https://doi.org/10.1007/978-3-030-81273-7_21

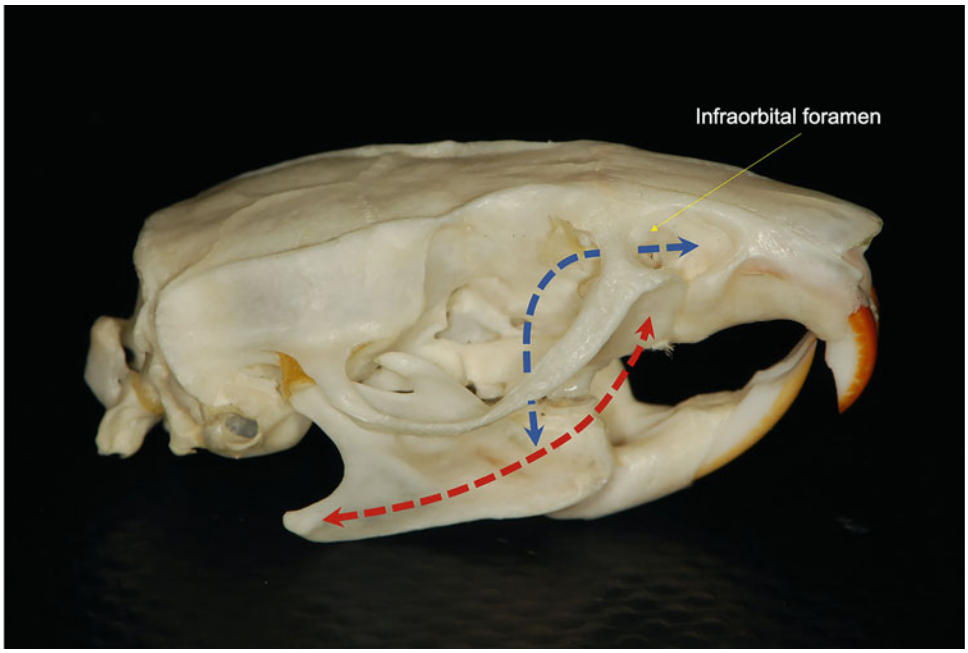

Fig. 46.1 Skull of the rat (*Rattus norvegicus*), depicting the masseter muscle configuration (blue and red dashed arrows) characteristic of the Myomorpha

Anomaluromorpha, Castorimorpha, Hystricomorpha, Sciuromorpha, and Myomorpha (Wilson and Reeder 2005).

Suborder Myomorpha (also referred to as the Myodonta) comprises seven families including the Muridae (Old World mice and rats, gerbils), Nesomyidae (African and Malagasy mice and rats), Cricetidae (New World rats and mice, voles, hamsters), Spalacidae (blind mole-rats, African mole-rats, zokors, and bamboo rats), Platacanthomyidae (spiny and pygmy dormice), Calomyscidae (mouse-like hamsters), and Dipodidae (birch mice, jerboas, and jumping mice). Like the other Rodent families, the Myomorph masseter muscle origin is more rostral to enable power and efficiency in chewing. Additional variation includes a relatively expanded infraorbital foramen through which a slip of the medial masseter muscle passes (Fig. 46.1). Interestingly, the zygomasseteric features of Dipodidae are more characteristic of the Hystricomorpha, with a very large infraorbital foramen and markedly enlarged medial masseter muscle. However, the lower portion of the Dipodid jaw is more characteristic of the Sciuromorpha, suggesting a closer phylogenetic relationship to the Myomorpha (Samuel et al. 2019).

As with skull morphology, the diverse habitats of the Myomorpha and their ubiquitous positions as prey species create a range of extrinsic influences and ecological stressors that have likely contributed to variations in ocular functional morphology. Collectively these variations can have significant impacts on optics, vision, and behavior. These features must be considered in the evaluation and treatment of any Myomorph with naturally-occurring ocular disease.

Furthermore, Myomorpha are also integral in the laboratory environment where domesticated or purpose-bred mice, rats, and other non-traditional rodent species are used as models of ocular disease and in vision science. In a functional genetic screening study of single gene knockout mouse mutants, 347/4364 genes were found to influence ocular phenotypes, 75% of which were previously unknown to result in ocular pathology (Moore et al. 2018a). Similarly, functional screens have also found systemic associations to ocular disease, such as with the integumentary system (Moore et al. 2019). Such contributions will likely prove invaluable to the discovery and treatment of developmental ocular disease in humans.

Despite the occurrence of numerous ocular abnormalities that have arisen as a result of purpose breeding in a laboratory setting, the eye of the laboratory mouse (and surely other species of the Myomorpha) has remained adapted for natural conditions (Shupe et al. 2006). The chapter herein is not intended as a review of the ophthalmic literature as it pertains to ophthalmic research and vision science, as numerous other comprehensive and informative texts and articles are available (Smith and Sundberg 2002; Mattapallil et al. 2012; Change et al. 2013; Moore et al. 2018a, b). Rather, this chapter will provide a review of comparative ocular anatomy and physiology, normative diagnostic values, as well as spontaneous ocular diseases of domestic and wild Myomorpha, with brief commentary on ophthalmic lesions prevalent within laboratory populations.

Anatomy and Physiology

There is a remarkable spectrum of ocular variation among the Myomorpha, ranging from the relatively large and prominent eyes of the Muridae and Cricetidae (Fig. 46.2), to the small,

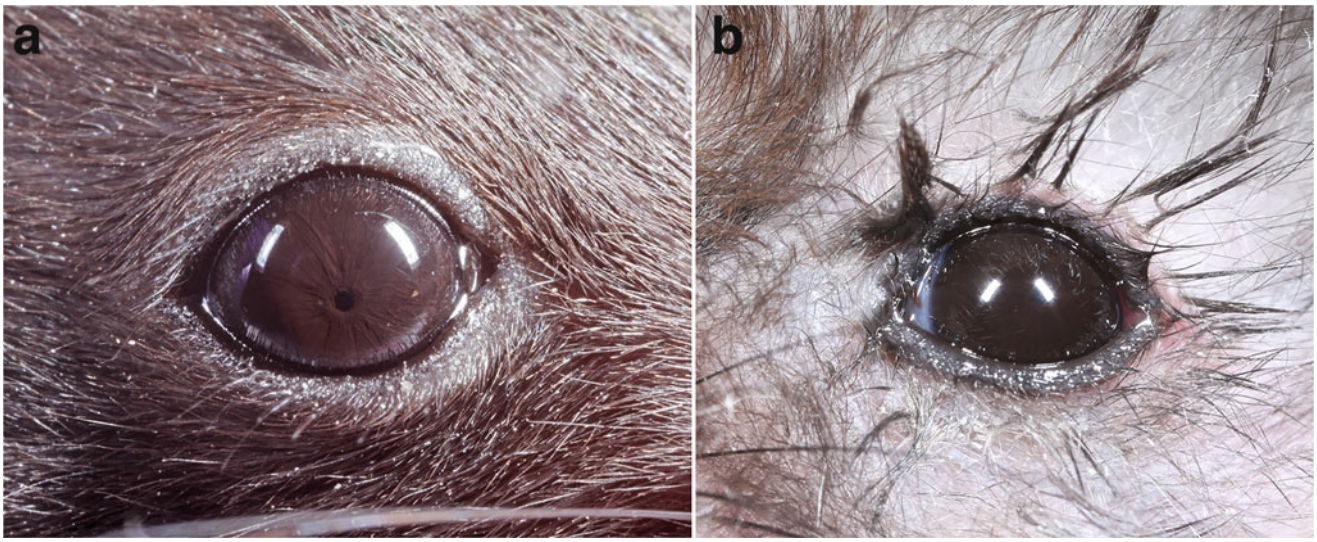

Fig. 46.2 External image of the eye of a normal laboratory mouse (*Mus musculus*) and hamster (*Mesocricetus auratus*). (**a**—Courtesy of Lionel Sebbag DVM, Ph.D., DACVO. **b**—Courtesy of Bret A. Moore, DVM, Ph.D., DACVO)

reduced eyes of the Platacanthomyidae, to the completely subcutaneous and regressed eyes of some Spalacidae. The majority of this chapter's discussion of ocular anatomy and physiology will focus on the functional morphology of the common Muridae and Cricetidae (mice, rats, gerbils, and hamsters) and other families with non-regressed eyes. A more detailed discussion of the reduced and regressed eyes of the Platacanthomydiae and Spalacidae can be found later in the chapter (see section "Ocular Reduction and Regression within the Myomorpha").

The overall visual systems of the non-regressed Myomorpha share many characteristics that putatively enhance their ability to scan their environment efficiently and evade predators. These features include lateral globe placement and a wide visual field as well as a relatively low blink rate in comparison to other species. Also as a strategy for avoiding predation, most members of the family are crepuscular or nocturnal and have visual systems that are largely adapted for dim-vision with consequently low visual acuity. Within this general "blueprint" for the Myomorph eye and orbit, however, there are interesting variations that likely relate to habitat. Members of this order may live in low grasslands, steppes, or high-altitude mountain ranges, may be solely terrestrial or semi-aquatic, or may dwell primarily in arboreal or subterranean (fossorial) habitats.

Generally speaking, functional morphology of the orbit, globe, and visual system is very similar in mice and rats, with differences in anatomical dimensions. A summary of published in vivo biometric dimensions of common Muridae can be found in Table 46.1. Myomorpha tend to have very low visual acuity in comparison to other species, attributed to retinal photoreceptor profiles dominated by rods which represent 95–98% of all photoreceptors in mice and rats (Smith et al. 2001; Wang et al. 2011; Jacobs et al. 2001; Sherwin 2010). Visual acuity in mice and rats is reportedly 0.5 and 0.94 cycles per degree (cpd), respectively (Wang et al. 2011). Acuity is putatively even lower in albino strains of mice and rats who possess up to 30% fewer total photoreceptors than

Table 46.1 Ocular dimensions (adult) for three common Myomorph rodents

	Axial globe length (mm)	Anterior chamber depth (mm)	Axial lens diameter (mm)	Vitreous chamber depth (mm)	Reference
Mouse (*Mus musculus*)	3.4	0.45	2.15		Puk et al. (2006)
	3.289	0.385	2.037	0.854	Tkatchenko et al. (2010)
	3.256	0.416	1.917	0.583	Chou et al. (2011)
	3.302	0.278	2.004	0.609	Barathi et al. (2008)
	3.16	0.56	1.73		Brown et al. (2005)
Rat (*Rattus norvegicus*)	6.91	1.03	4.57	1.32	Lozano and Twa (2013)
	5.6		3.3	1.5	Guggenheim et al. (2004)
Mongolian gerbil (*Meriones unguiculatus*)	6.11				Wilkinson (1986)

pigmented strains (Ilia and Jeffery 2000). However, other Murid species like the Mongolian gerbil possess higher acuities of up to 2 cpd, which may be associated with their comparatively diurnal activity and higher percentage of cone photoreceptors (Mankin et al. 2019). More details about comparative Myomorph retinal physiology can be found below under **Anatomy and Physiology, The Posterior Segment—Retina**.

The Skull and Orbit

In the Myomorpha (and in most rodent species), the orbits and globes are situated laterally (Fig. 46.1). In the mouse and rat, this orientation yields only ~40% and 40–60% binocular overlap, respectively (Heesy 2004; Drager 1978; Montero 1973). Even between pigmented and albino rat strains, there may be some degree of variability in binocular field, at least partially due to slight differences in eyelid position (Lund et al. 1974). The orbits of mice and rats provide very little bony protection, particularly dorsally (Smith et al. 2001; Hwang et al. 2012). This relative exposure is a factor that may contribute to higher risks for ocular injury associated with bedding, or following anesthesia in common Myomorphs like the mouse and rat (Kohn and Clifford 2002) (more details under **Ocular Diseases of the Myomorpha, The Anterior Segment—Cornea** and **Lens**). Much of the orbital support for the globe is provided by soft tissues, principally the orbital glands.

In the mouse and rat, the Harderian gland is the larger of two intraorbital glands, lying immediately adjacent to the base of the third eyelid and posterior globe and occupying a large portion of the ventromedial and posterior orbit (Djeridane 1996; Payne 1994; Seely 1987). Grossly, the Harderian gland comprises two distinct lobes, superior and inferior, with the latter approximately twice the size of the former in the mouse (Cohn 1955). The gland is encased in connective tissue which is loosely attached to the adjacent orbital fascia (Cohn 1955). Histologically, the gland is tubuloalveolar and secretions from both lobes are carried to the ocular surface via a common duct that opens onto the conjunctival surface adjacent to the third eyelid.

There does not appear to be consensus on the primary role of the Harderian gland, as a large body of research in mice, rats, and other Myomorpha has identified multiple possible functions. The high concentrations of lipids delivered to the ocular surface in Harderian secretions support a likely role in ocular surface health. Lipids (phospholipids, triglycerides, and cholesterols/cholesterol esters) are known to stabilize the precorneal tear film and delay its evaporation (Cohn 1955; Bron et al. 2004). These lipids may also have thermoregulatory functions in some Myomorpha (Miedel and Hankenson 2015). The Harderian gland has also be shown to produce porphyrins, nitrogenous pigments that are most characteristically observed in rodents affected by chromodacryorrhea (see **Ocular Diseases of the Myomorpha, The Anterior Segment—Chromodacryorrhea**) (Kohn and Clifford 2002). The precise function of Harderian porphyrins is not well understood. It is noteworthy that Harderian porphyrins produced in mice and rats are photodynamic and could lead to gland swelling, necrosis, or other pathology after prolonged or intense exposure to light (Johnson et al. 1979; Kurisu et al. 1996). Other Harderian substances include melatonin and pheromones which, in tandem with other hormonal substances, have been proposed to contribute to numerous glandular functions including immuno- and thermoregulation, function of the retinal–pineal axis, and sexual behavior (Miedel and Hankenson 2015; Beaumont et al. 2003). It is noteworthy though that there is still controversy as to whether Harderian melatonin is produced de novo in the gland or us taken up from circulation (Hoffman et al. 1985).

The Harderian gland has also been extensively studied in other Muridae such as gerbils. In the Mongolian gerbil (*Meriones unguiculatus*), the gland is divided into several lobes rather than distinct superior and inferior lobes as in mice and rats. The gerbil Harderian gland bears similar histological features to that of the mouse and rat, but microscopic study has also demonstrated the presence of myoepithelial cells adjacent to the gland alveoli (Sakai and Yohro 1981). In gerbils, the gland is covered by the endothelium of an orbital venous sinus (Sakai and Yohro 1981). In the Syrian hamster (*Mesocricetus auratus*), a Cricetid rodent, functions of the Harderian gland uniquely demonstrate sexual dimorphism. The microscopic morphology of Harderian lipid droplets differs between males and females; and female *M. auratus* produce up to 1000 times more porphyrin than males (Miedel and Hankenson 2015; Bucana and Nadakavukaren 1972). Furthermore, production of both substances is under androgenic control and may vary seasonally (Buzzell 1996). Sex-related differences in Harderian melatonin concentrations have also been shown in *M. auratus* and appear to be heavily influenced by androgenic hormones. Whereas Harderian melatonin in males tends to be constitutively low regardless of time of day, concentrations in females vary with light phase. In castrated males, the Harderian melatonin profile more closely resembled that of females (Hoffman et al. 1985).

The lacrimal glands of the mouse and rat orbit include the infraorbital and extraorbital lacrimal glands. The extraorbital gland is the principal lacrimal gland and does not reside within the orbit itself, lying subcutaneously temporal to the eye, just anterior to the pinna of the ear. The small intraorbital lacrimal gland is located beneath the bulbar conjunctiva adjacent to the lateral canthus. The lacrimal secretions of both glands are carried to the ocular surface via a common duct (Shinomiya et al. 2018).

The microvasculature of the richly-supplied mouse eye has been studied in detail. The mouse eye receives its primary blood supply from the external ophthalmic artery. This gives rise to the central retinal artery which supplies the holangiotic retinal vasculature (8–9 radiating retinal arterioles) and medial and lateral long posterior ciliary arteries which, in turn, supply the choriocapillaris and more anterior structures of the globe (Ninomiya and Inomata 2006). The configuration in the rat is relatively similar, though the primary arterial blood supply to the eye is from the posterior ciliary artery, derived from the inferior branch of the ophthalmic artery (Ninomiya and Kuno 2001; Bhutto and Amemiya 2001).

In the rat eye, there are two primary routes of venous drainage, via the posterior ciliary vein (which drains the choroid), and the vortex veins which drain anterior segment structures like the iris, ciliary body, and bulbar conjunctiva (Bhutto and Amemiya 1995). In contrast, the hamster eye has one venous drainage route, wherein the entire choroid and the anterior segments are drained by the vortex veins (Ninomiya and Inomata 2005). Most Myomorpha possess a large orbital venous structure, intimately associated with the Harderian gland and globe. These venous structures receive blood from the majority of the ocular and orbital structures (Smith et al. 2001; Sakai and Yohro 1981; Timm 1979). In the mouse and gerbil, this structure is called the orbital venous sinus (Smith et al. 2001; Ninomiya and Inomata 2006). In mice, the sinus represents a larger volume relative to the orbit than the analogous orbital venous plexus of the rat (Smith et al. 2001).

The Adnexa and Anterior Segment

Mice and rats have well-developed eyelids with a tarsal plate and Meibomian glands (Kohn and Clifford 2002) and conjunctival membranes bearing similar conjunctival anatomy to other species (Ramos et al. 2018) (Fig. 46.3a). The published descriptions of conjunctival lymphoid follicles in some New World Cricetidae like the deer mouse (*Peromyscus maniculatus*) and meadow vole (*Microtus pennsylvanicus*) support an immunologic function for the conjunctiva in Myomorpha as in other mammals (Astley et al. 2007). However, conjunctival follicles were notably absent in the common mouse (*Mus musculus*) in this study and there was considerable variation in the number and size of the follicles among other Cricetidae evaluated. The conjunctiva in Myomorpha like the mouse and rat is continuous with the conjunctiva of a third eyelid that is more rudimentary and less clinically obvious in comparison to species like the rabbit. However, it bears similar structural analogs with a fibrous stroma and hyaline cartilage as observed in many other mammalia (Ramos et al. 2018).

The corneas of mice and rats are relatively large, with diameters in the mouse and rat of 2.5 mm and 6.8 mm, respectively (Suckow et al. 2005; Henriksson et al. 2009). The central cornea is thicker than the peripheral cornea (Henriksson et al. 2009; Zhang et al. 2013). Among Myomorpha of relatively similar size, variations in corneal thickness have been described and may relate to differences in habitat and ecology. For example, semi-aquatic Cricetids like the European water vole (*Arvicola terrestris*) have a proportionally thicker cornea and sclera that may represent adaptations for their subterranean lifestyle, as well as life around, within, and sometimes under water (Lluch et al. 2007). As in other species, the cornea is avascular and receives nutrients and oxygen from the precorneal tear film, aqueous humor, and a circumferential system of episcleral arteries arising from superficial branches of the anterior ciliary artery (Ramos et al. 2018).

The cornea in most of the Myomorpha comprises a non-keratinized stratified epithelium and basement membrane, stroma, Descemet's membrane, and single-layered endothelium. It is thin, ranging from 0.9 mm in the dwarf hamster (*Phodopus roborovskii*), 0.11 mm in deer mouse (*Peromyscus maniculatus*), 0.16 mm in the laboratory mouse (*Mus musculus*), up to 0.32 mm in the Norway rat (*Rattus norvegicus*) (Fernandez and Dubielzig 2013). There is controversy among anatomists and investigators regarding

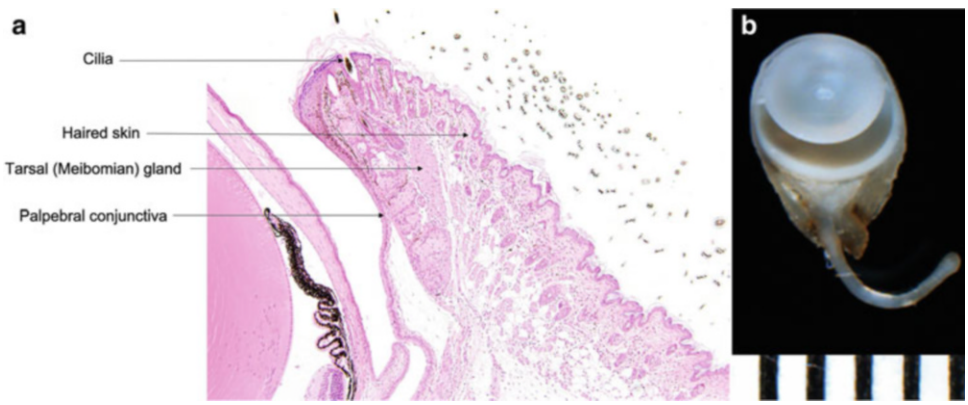

Fig. 46.3 (**a**) Histologic section of a normal eyelid in a mouse (*Mus musculus*). (**b**) Formalin-fixed section of the globe of a mouse (*Mus musculus*). (Courtesy of the Comparative Ocular Pathology Laboratory of Wisconsin)

the presence of a true Bowman's layer within the anterior corneal stroma. Historically, references have claimed absence of this structure in mice and rodents (Jakus 1954; Walls 1944) #3421, but more recent investigations have identified a distinct condensation of collagen immediately subtending the epithelium resembling the Bowman's layer observed in the human cornea (Lluch et al. 2007; Hayashi et al. 2002). Like rabbits, rats may also have the capacity to regenerate damaged or degenerate corneal endothelium due to a "reserve" of corneal endothelial cells within the corneal periphery and limbal region (Bredow et al. 2014; Choi et al. 2015).

A prominent morphologic feature in the mouse and rat s and Cricetidae like the voles is a large, nearly spherical lens that comprise the majority of the intraocular volume (Saadi-Brenkia et al. 2018). The strong convex curvatures formed by both the anterior and posterior lens capsule create markedly narrow anterior and vitreous chambers (Fig. 46.3b). Comparatively, the lenses of other Muridae like the fat sand rat (*Psammomys obesus*) and Cricetidae s like the golden hamster (*Mesocricetus auratus*) are described as less spheroid (Saadi-Brenkia et al. 2018; Beyerlein 1953).

Compared to a relatively large lens, the ciliary body in mice, rats, and hamsters is diminutive with a poorly-developed ciliary muscle. However, a pars plicata is present with well-defined ciliary processes, many of which arise anteriorly from the posterior iris (Smith et al. 2001; Beyerlein 1953; McMenamin and Al-Shakarchi 1989; Rodriguez-Ramos Fernandez and Dubielzig 2013). There is not a well-defined pars plana in mice and rats (Smith et al. 2001). Collectively, the anatomical discrepancy between a large lens and small ciliary muscle supports the putative conclusion that accommodation in most (if not all) Myomorpha is not mediated by ciliary contraction and relaxation as in many other mammals. However, there are structural adaptations of the iris (see below) that suggest other mechanisms that species may use to achieve focus.

In general, the iris of mice and rats is thin with a defined sphincter muscle and comparatively poorly-developed dilator muscle (Lluch et al. 2007). In some Cricetid species like voles, however, the pupillary sphincter is remarkably large in cross-sectional volume and more conspicuous than in Muridae (Lluch et al. 2007). The reason for this variation is not well understood, but it could provide a protective purpose, limiting light entry into the eyes of more diurnal voles. It is also possible, however, that changes in profile of this muscle when contracted or relaxed and/or other changes in iris conformation could serve an accommodative purpose. In golden hamsters, for example, the iris is heavily vascularized, with at least 1/3rd of its volume uniquely comprising blood sinuses instead of discrete vascular networks. Volumetric expansion of these sinuses could theoretically influence lens position or lens curvature (Beyerlein 1953). Similarly in the fat sand rat the ciliary processes are comparatively large, and the iris has been described as being "fastened" to the anterior lens surface, and possible capable of influencing its curvature (Saadi-Brenkia et al. 2018).

The aqueous outflow pathways in mice and rats have been well-characterized and structures like the trabecular meshwork bear many similarities to the conventional outflow pathways of humans and other mammals. Most notably, mice and rats possess a distinct analog to the human Schlemm's canal to collect aqueous humor that egresses via the trabecular meshwork (Van Der Merwe and Kidson 2014). Similarly, a distinct Schlemm's canal was also demonstrated in a study of 18 rodent species that included Cricetidae like the deer mice (*Peromyscus* spp.), hamsters (*Phodopus* spp., *Cricetulus* spp.), and meadow voles (*Microtus pennsylvanicus*) (Rodriguez-Ramos Fernandez and Dubielzig 2013).

The Posterior Segment

The retinas of mice, rats, gerbils, hamsters, and many other Myomorpha have a holangiotic vascular pattern originating from a central retinal artery (Smith et al. 2001). Retinal arterioles and venules extend from the optic disk in a spoke-like pattern branching minimally as they course toward the retinal periphery (Kern n.d.; McLenachan et al. 2015; Sayers and Smith 2010). The retinas of mice and rats are thick with respect to the small axial globe lengths in both species. Central retinal thickness is 189–230 microns in mice and 200 microns in rats (Buttery et al. 1991; Ferguson et al. 2013; Mohan et al. 2012; Zhou et al. 2008). There has been suggestion that the retina of the golden hamster may be tilted or "ramped" as previously proposed in species like the horse wherein the posterior curvature of the globe and retina is non-spherical, requiring changes in head position to achieve focus of an image on the retina (Beyerlein 1953). To date, however, there is no objective data supporting this theory and it remains controversial.

In general, the activity of Myomorpha tends to correlate with photoreceptor profile. Rod photoreceptors represent 95–98% of all photoreceptors in mice and rats which are largely crepuscular or nocturnal (Smith et al. 2001; Wang et al. 2011; Jacobs et al. 2001; Sherwin 2010). Other predominantly nocturnal species like voles have retinas with 90% rods, and evidence has historically suggested that the golden hamster retina does not possess cones at all (Lluch et al. 2007; Beyerlein 1953; Jacobs 1993). More recent investigations, however, have demonstrated the presence of at least one photopigment in hamsters and other Cricetidae (Calderone and Jacobs 1999; Lukáts et al. 2002). In contrast, the photoreceptor profile of diurnal gerbils comprises ~87% rods (Waiblinger 2010; Bytyqi and Layer 2005), and

electroretinographic cone responses have been documented in these species (Jacobs 1993).

Color perception may vary within the Myomorpha. Most references designate the Myomorpha as color-perceiving dichromats, possessing at least two cone photopigments (Jacobs 1993). For example, mice and rats both possess cones with green- and blue-spectral sensitivity (M-cones and S-cones, respectively) (Szel et al. 1992). In the mouse, cone photoreceptors are differentially distributed with the highest density of S-cones being found in the far ventral periphery (Szel et al. 1992). Numerous theories for this distribution have been proposed, many suggesting a function in enhancing contrast in the field above the head, permitting prey species like the mouse to more readily identify predators or other threats (Baden et al. 2013; Gouras and Ekesten 2004; Szél et al. 1994). Diurnal rodents may have cones with expanded sensitivities due to the presence of blue/green or green/red "hybrid" cones (Ramos et al. 2018). Some investigations have also demonstrated findings that suggest the presence of photopigments sensitive to light wavelengths near or within the UV spectrum in mice, rats, and voles (Jacobs 1993).

None of the Myomorpha have a macula or area centralis, but investigations have demonstrated a region of increased ganglion cell density in the dorsal retinas of mice and rats that may represent a visual streak (Smith et al. 2001; Buttery et al. 1991; Danias et al. 2002; Salinas-Navarro et al. 2009). A distinct visual streak has also been described in the Mongolian gerbil (*Meriones unguiculatus*) and Syrian hamster (*Mesocricetus auratus*) (Wikler et al. 1989). Across the retina, rats have a total of approximately 98,000–113,000 retinal ganglion cells (Danias et al. 2002; Potts et al. 1982) whereas the Syrian hamster and Mongolian gerbil have 75,000 and 150,000, respectively (Wikler et al. 1989).

The morphology of the cuboidal retinal pigmented epithelium (RPE) in mice and rats is largely influenced by the general degree of pigmentation in the overall animal, with albino or color-dilute strains possessing little to no melanin within the RPE cells. In some Myomorph species, however, there are intrinsic variations in RPE morphology. In voles, for example, the RPE is comparatively thicker than in other Muridae, with tall, nearly columnar cells containing an unusually high density of melanin granules (Lluch et al. 2007). The underlying choroid in the vole is also comparatively thick (Lluch et al. 2007).

Mice and rats lack a tapetum lucidum and this structure is not reported in members of other Myomorpha families (Kern n.d.; McLenachan et al. 2015; Sayers and Smith 2010). In mice, rats, and other common Myomorpha, the optic disk is unmyelinated and the optic nerve exits the globe via a fenestrated region of the posterior sclera called the lamina cribrosa (Ramos et al. 2018; Morrison et al. 1995). The ultrastructure of the tissue differs between species, with gerbils having a more robust lamina cribrosa that at least three layers of connective tissue whereas rats have only one layer, and hamsters fall in between with a more intermediate amount of tissue (Johansson 1987). The functional significance of these variations, however, is not well understood.

Ocular Diseases of the Myomorpha

Purpose-bred mice and rats and their visual systems are used in ocular research and vision science as models for studying ophthalmic disease and in the development of ocular therapeutics. Furthermore, the popularity of pet Myomorpha, including the mice, rats, hamsters, and gerbils grows each year. At last survey where rodent ownership data was collected in the United States by the AVMA (2012 AVMA. US pet ownership & demographics sourcebook: 2012 edition. Schaumburg (IL): AVMA; 2012.), nearly 2.5 million pet rodents were being kept in US households (Jekl et al. 2017); and the 2018 survey showed continued growth in popularity of pets hamsters and gerbils. In tandem with continued surveys and investigations of wild species, there is a growing body of literature shedding light on naturally occurring, spontaneous ocular disease in the Myomorpha.

Congenital Globe Malformations

Microphthalmia is a congenital condition wherein the globe and its structures are morphologically small and abnormal. Though rare, microphthalmia has been reported in mice and rats such as the common purpose-bred C57BL/6 J mouse and may affect females up to 6.2 times more frequently than males (Smith et al. 1994; Tyan 1992) (Fig. 46.4a). Other congenital ophthalmic abnormalities may be seen concordantly or separate from microphthalmia (anterior segment dysgenesis, corectopia, colobomatous malformations, etc.; Fig. 46.4b–d). Females of purpose-bred rat strains like the Fischer 344 also appear to be predisposed (Lee 1989).

The embryogenetic mechanisms underlying microphthalmia likely vary and may relate to truncated development of the hyaloid arterial system, deficiencies in embryologic tissue interactions (i.e., induction between the lens vesicle and surface ectoderm), or colobomatous mechanisms such as incomplete closure of the optic fissure (Browman and Ramsey 1943; Cook and Sulik 1986; Kobayashi and Otani 1981; Robinson et al. 1993). Furthermore, the inheritance pattern in these strains for microphthalmia is not well understood as there are apparent variations in expressivity (Kinney et al. 1982; Rao and Sesikeran 1992). In utero toxin exposure, hypoxia, nutritional deficiencies, and ionizing radiation are also predisposing factors (Tyan 1992; Chamberlain and Nelson 1963; Dickman

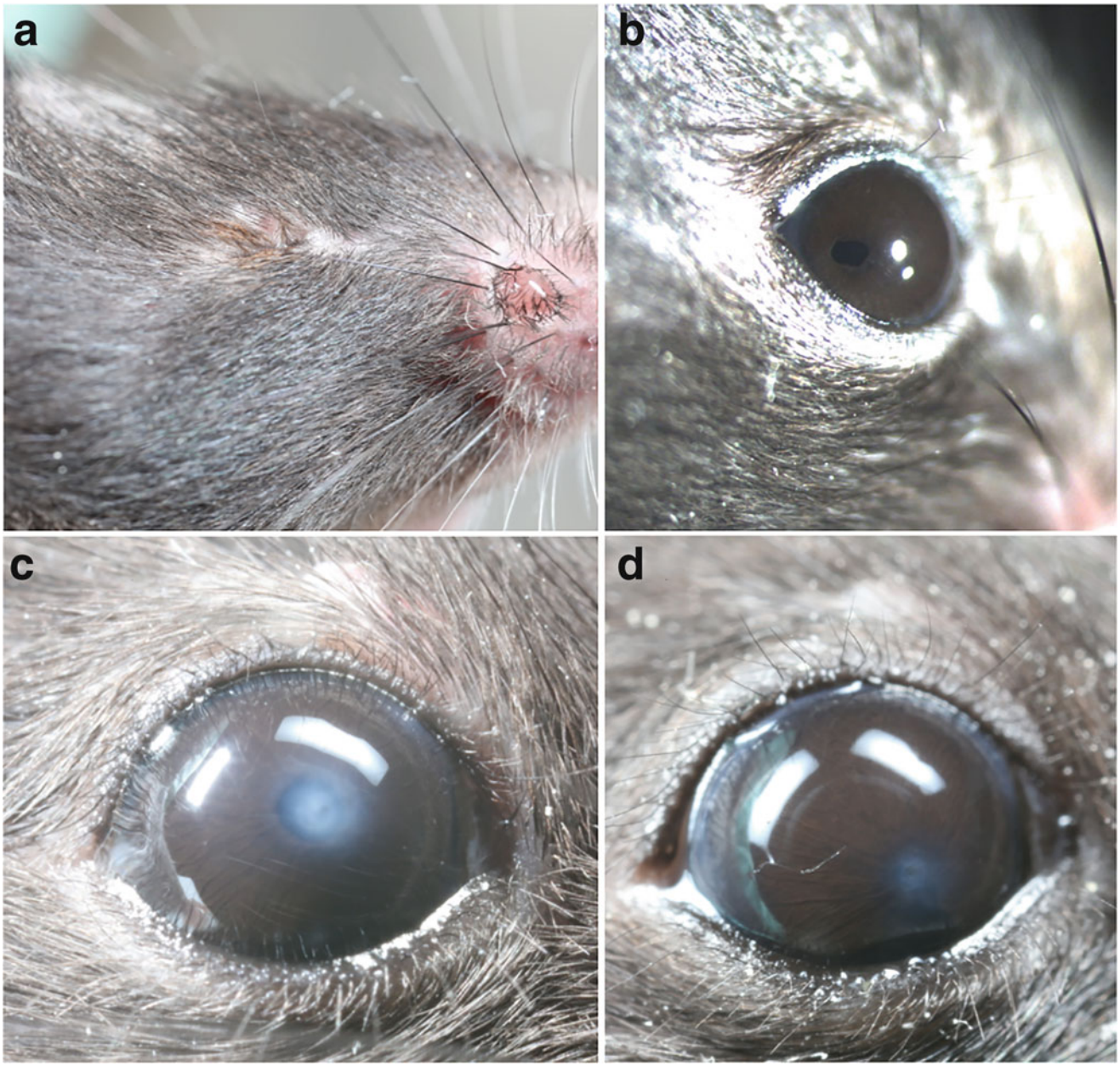

Fig. 46.4 External images of laboratory mice (*Mus musculus*) with congenital ocular abnormalities. (**a**) Microphthalmia, (**b**) corectopia, (**c**) anterior segment dysgenesis, and (**d**) corectopia and anterior segment dysgenesis. (Courtesy of Lionel Sebbag, DVM, Ph.D., DACVO)

et al. 1997; Germain et al. 1985; Hurley et al. 1971; Padmanabhan et al. 1981; Pierro and Spiggle 1969; Shirai 1978; Strömland et al. 1991). Microphthalmia has also been described as a heritable abnormality in the hamster, and in some forms, is associated with a lethal mutation (Jackson 1981; Hughes and Geeraets n.d.; Wada and Tsudzuki 1998; Robinson 1964). It may also be associated with toxin exposure in hamsters (Gale and Layton 1980; Willhite et al. 1986).

Diagnosis is based on clinical observation of an abnormally small eye and palpebral fissure, typically with other anomalous features including corneal opacities, abnormal anterior chamber conformation, cataract or lens malformation, retinal dysplasia, and anterior and posterior colobomas (Cook 1991; Williams 2012; Wyse and Hollenberg 1977). The primary differential diagnosis for microphthalmia is a phthisical globe, one that has become involuted and atrophied secondary to chronic inflammation or prior trauma. Therefore, the examiner must be careful to ask about and look for clinical evidence of trauma to make the differentiation.

Anophthalmia or lack of a clinically or histologically detectable globe is very rare in mice and rats. It has been

Fig. 46.5 Proptosis in a hamster (*Mesocricetus auratus*). (Photo courtesy of Christopher J. Murphy, DVM, PhD, DACVO)

reported in certain laboratory rat strains like the mutant CFY and others related to the Fischer 344 (Rao and Sesikeran 1992; Shibuya et al. 2000). Heritable and toxin-induced anophthalmia have also been described in the Syrian hamster (Yoon 1975; Sunderma Jr et al. 1981). Syrian hamsters homozygous for the White Bellied gene (*Wh*) are born without eyes, are deaf, and have a shorter life expectancy (Richardson 2008; Gilger et al. 2018). Affected animals are sometimes referred to as "anophthalmic whites" (Gilger et al. 2018).

When considering conditions like anophthalmia or microphthalmia in the Myomorpha, it is important for an examiner to remember that several families within the Order comprise species with reduced eyes or subcutaneous eyes (see section "Ocular Reduction and Regression within the Myomorpha"). These normal variations should not be mistaken for pathologic abnormalities.

Diseases of the Orbit

Spontaneous diseases of the orbit are not commonly reported in mice, rats, or other Myomorpha. Proptosis following blunt ocular or head trauma is reported (Fig. 46.5) (Richardson 2008), and may necessitate enucleation if the trauma to the eye is severe.

Disease of the orbital soft tissue can lead to space-occupying swelling and subsequent exophthalmia and ocular exposure (Fig. 46.6). Numerous causes have been described in common Myomorpha, most frequently associated with infection or neoplasia. Infectious disease of the orbit may be associated with viral diseases like sialoadenitis virus in rats due to swelling and inflammation of the Harderian gland (more details under **Diseases of the Adnexa and Ocular**

Fig. 46.6 Domestic rat (*Rattus norvegicus domestica*) with a retrobulbar abscess causing exophthalmos of the left eye. (Photo courtesy of Bret A. Moore, DVM, PhD, DACVO)

Surface—Sialoadenitis Virus). Bacterial infection with abscess formation in orbital soft tissues is also described. Periocular and orbital infections associated with *Pasteurella pneumotropica* are reported in mice and rats, who are primary carriers of this Gram-negative opportunistic bacteria. Hamsters and gerbils, however, may also be affected (Towne et al. 2014). Immunocompromised animals are at higher risk for clinical infection (Dickie et al. 1996). Spontaneous and contemporaneous bilateral abscess of the Harderian glands has also been reported in a Syrian hamster (Zaffarano et al. 2015). Dental disease may also be a nidus for bacterial orbital infection (van der Woerdt 2012).

Several Myomorphs serve as hosts for the parasite, *Rhabditis orbitalis*, a parasite whose third stage infective larvae may invade the ocular and orbital tissues. Affected species include the Muridae (mice, rats, and *Apodemus* spp.), and Cricetidae (*Arvicola terrestris*, *Clethrionomys* spp., *Microtus* spp., and *Lemmus trimucronatus*). Infective larvae may be retrieved from the conjunctival surface where they obtain nutrition from lacrimal secretions, but may also live quiescently in orbital tissues (Kocianová-Adamcová et al. 2006). Most infected animals are not clinical for this disease (Schulte 1989), though it may cause clinical ophthalmic disease in non-Myomorph rodents that are not typical hosts (Sainsbury et al. 1996). Larvae of a similar nematode, *Rhabditis strongyloides*, may also be found in the conjunctival sacs of Murid rodents and in Cricetidae like lemmings (*Dicrostonyx groenlandicus* and *Lemmus trimucronatus*) (Cliff et al. 1978). Similarly, affected lemmings often do not show clinical signs (Cliff et al. 1978).

Primary orbital neoplasms are rare in the Myomorpha but optic nerve meningiomas and Schwannomas have been reported in Fischer 344 rats. Dissimilar from meningiomas in other species like the human and dog, primary optic nerve meningiomas in rats may demonstrate a higher degree of malignancy and local invasiveness (Yoshitomi et al. 1991). Primary orbital Schwannomas are also biologically malignant (Yoshitomi and Boorman 1991a). Both neoplasms have shown tendency to propagate along the optic nerve and invade the contralateral orbit. It is noteworthy, however, that these descriptions were reported in surveys of control and test article-treated purpose-bred rats from large toxicology colonies, and therefore may not be reflective of true incidence of spontaneous disease in other Myomorpha. Other tumors of orbital tissues reported in mice and rats include adenomas and adenocarcinomas of the Harderian and lacrimal glands, gliomas of the optic nerve, fibrous histiocytomas, and unspecified sarcomas (Ramos et al. 2018; Greaves and Faccini 1981; Rothwell and Everitt 1986). In one study of mice, spontaneous Harderian gland neoplasms affected 18% of mice older than 18 months (Holland and Fry 1982). A spontaneous and primary amelanotic and malignant melanoma has also been described in the orbit of a rat (Kurotaki et al. 2008).

Diagnosis of an orbital abscess or neoplasm is based on clinical appearance of exophthalmia, often presenting with impaired blink and exposure keratitis and variable ocular discharge. Diagnostic imaging such as ultrasound, computed tomography (CT), or magnetic resonance imaging (MRI), where available, may provide support for the diagnosis. Differential considerations for an orbital abscess are similar to those in other species and include neoplasia, cysts, vascular anomalies, and facial vein thrombosis (Gilger et al. 2018). Buphthalmia related to chronically increased intraocular pressure should also be ruled out (Zaffarano et al. 2015). If severe enough, exposure keratitis and progressive corneal ulceration may result in globe perforation and endophthalmitis. Furthermore, inflammation associated with orbital infection may extend to involve the globe causing panophthalmitis. In the aforementioned case of a hamster with bilateral Harderian gland abscesses, some clinical improvement in ocular signs was observed after treatment with empirical oral antibiotics, but the animal still died, presumably as a result of spread of infection to the brain via the meninges (Zaffarano et al. 2015). Therefore, more aggressive treatment with parenteral antibiotics with or without exenteration may be necessary.

Diseases of the Adnexa and Ocular Surface

Primary diseases of the eyelids are not common in mice, rats, or other Myomorpha. Heritable conditions like primary entropion are rarely observed, most frequently reported in Syrian and dwarf hamsters (Richardson 2008; Gilger et al. 2018), and affected animals should be removed from breeding stock (Richardson 2008). Trichiasis, however is not uncommon, particularly in wire-haired breeds whose periocular hairs can contact the ocular surface and lead to secondary irritation and keratitis (Fig. 46.7). Amelanotic melanomas of the eyelid are rare but have been reported in a large survey of laboratory rats (Yoshitomi and Boorman 1993). In one survey of wild lemmings (*Dicrostonyx* spp.) suppurative cutaneous lesions of the eyelids were sporadically observed, caused by infection with *Escherichia coli*, *Alicaligenes faecalis*, *Proteus rettgeri*, *Acinetobacter calcoaceticus*, *Streptococcus bovis*, *S. epidermidis*, and *Klebsiella pneumoniae* (Cutlip and Dennis 1993). Blepharitis is not uncommon, and can be anterior as a reflection of dermatitis (e.g., Demodex sp., Fig. 46.8) or posterior and involve the Meibomian glands and conjunctiva (bacterial blepharitis, Fig. 46.9).

Conjunctivitis, which may be associated with blepharitis due to anatomical proximity of the conjunctiva and eyelids, is reported relatively commonly in mice and rats and other

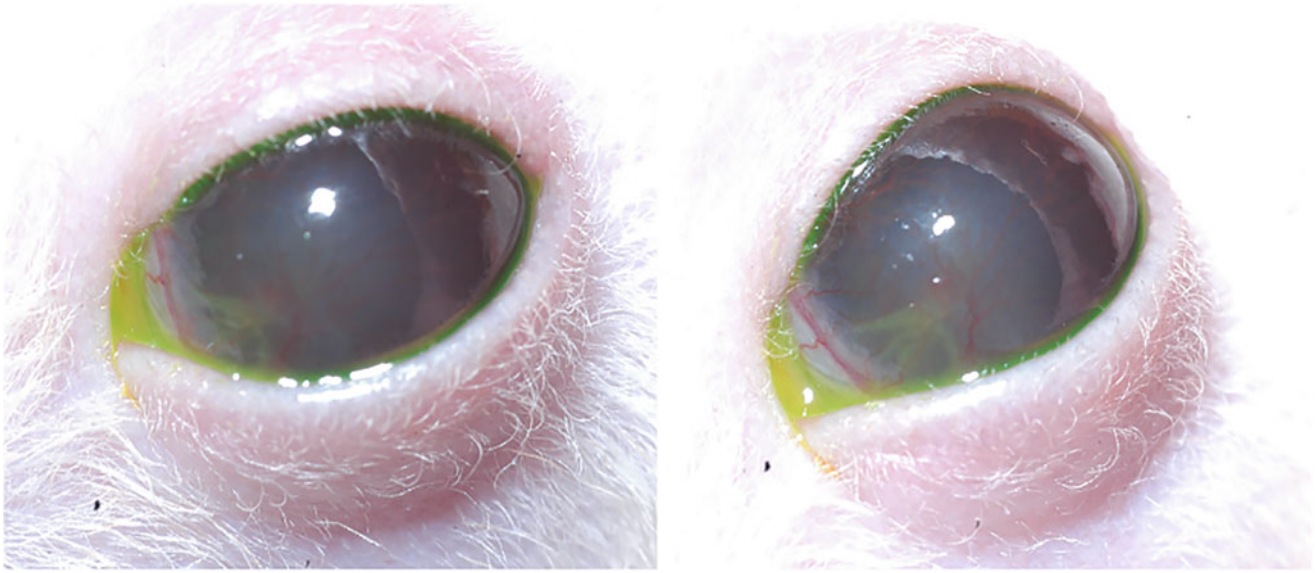

Fig. 46.7 Domestic rat (*Rattus norvegicus domestica*) with a chronic keratitis secondary to trichiasis. (Photo courtesy of the University of California Davis Comparative Ophthalmology Service)

common Myomorpha (Miedel and Hankenson 2015; Schoeb 2000). Conjunctivitis is most commonly associated with primary ocular infections but may also be associated with respiratory disease, extension of more generalized cutaneous disease, or as a secondary consequence of husbandry practices (Ellis and Mori 2001; Frisk 2012).

Numerous infectious organisms may cause blepharitis or conjunctivitis in otherwise healthy mice and rats, with younger animals potentially at higher risk for clinical disease (Williams 2007). Bacterial organisms include *Mycoplasma* spp., *Pseudomonas aeruginosa, Salmonella* spp., *Pasteurella* spp. (particularly *P. Pneumotropica* (Schoeb 2000)), *Streptobacillus moniliformis, Staphylococcus aureus, Staphylococcus xylosus, and Corynebacterium kutscheri* (Kern n.d.; van der Woerdt 2012; Frisk 2012; Beaumont 2002; Glastonbury et al. 1996; Hill 1974; Needham and Cooper 1975; Roberts and Gregory 1980). It is noteworthy that a number of these bacteria may also cause primary respiratory disease in mice and rats, and conjunctivitis may be seen in tandem with clinical signs of rhinitis or lower airway disease (Frisk 2012). In lemmings with Listeriosis, non-specific clinical signs of conjunctivitis with purulent ocular discharge and

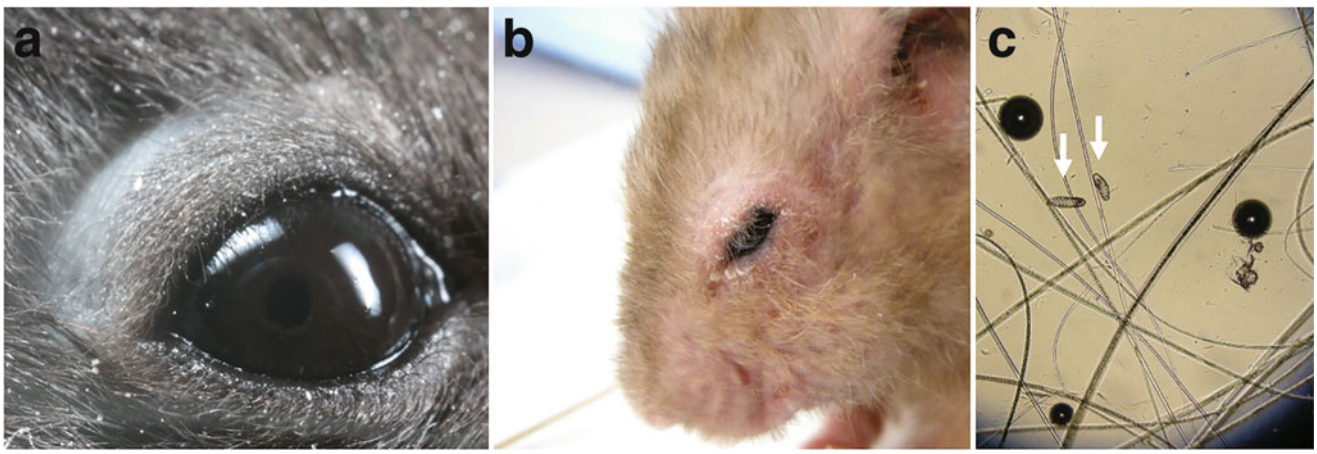

Fig. 46.8 Chronic anterior blepharitis in Myodonta. (**a**) A laboratory mouse (*Mus musculus*) demonstrating blepharitis of only the skin. (**b**,**c**) A hamster (*Mesocricetus auratus*) with chronic anterior blepharitis due to *Demodex creceti*. (**b**) Note the crusts and excoriations exhibited in the dermatitis. (**c**) Organisms are evident on a skin scrape cytologic prep (white arrows). (**a**—Courtesy of Lionel Sebbag, DVM, Ph.D., DACVO. **b**, **c**—Courtesy of the University of California Davis Comparative Ophthalmology Service)

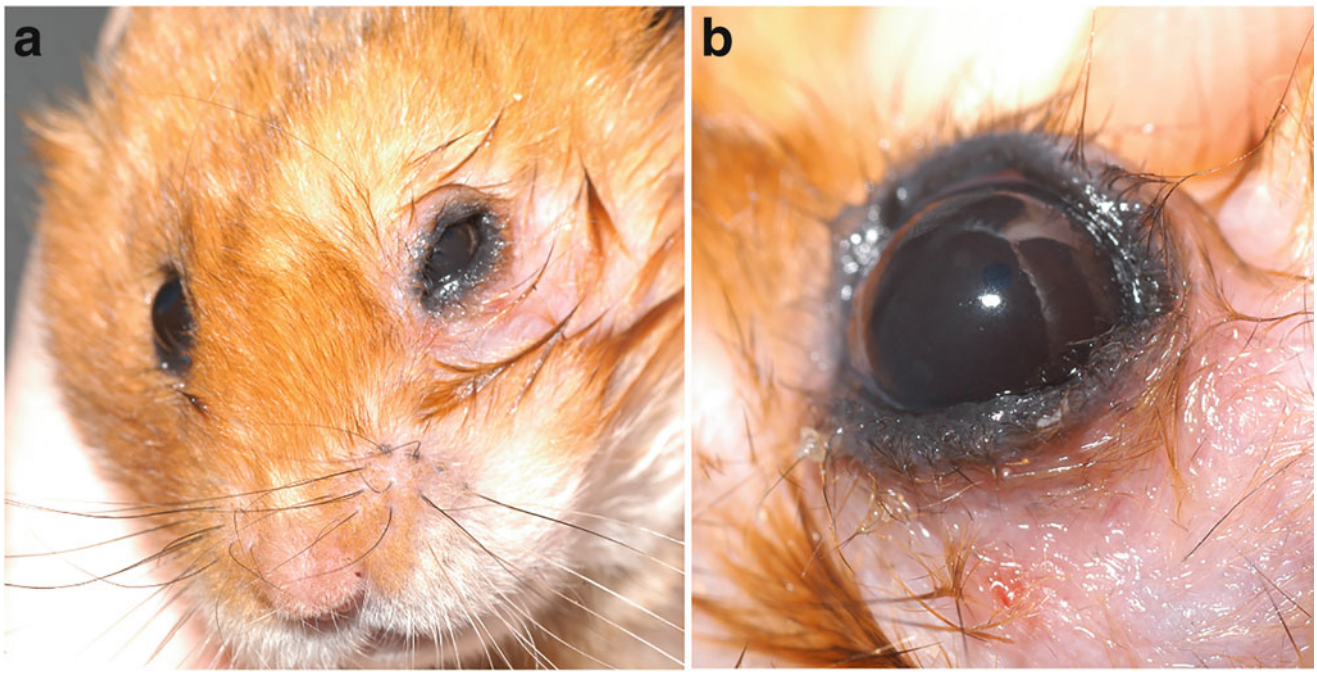

Fig. 46.9 A hamster (*Mesocricetus auratus*) with chronic posterior blepharitis (suspected bacterial), and secondary conjunctivitis. Note the hyperemic and swollen eyelids along with excessive seromucoid discharge from the left eye (**a**), closeup view of the same eye in (**b**). (Courtesy of the University of California Davis Comparative Ophthalmology Service)

blepharospasm may precede development of neurologic signs (Barrales 1953).

Viral organisms may also be associated with conjunctivitis in common Myomorpha. Lymphocytic choriomeningitis virus (LCV) can infect mice, rats, gerbils, and hamsters, though the latter two are often only carriers without clinical disease (Beaumont 2002; Batchelder et al. 2012; Field and Sibold 1998). Others include ectromelia virus and Sendai virus which may be associated with conjunctivitis in mice (Beaumont 2002).

Non-infectious conjunctivitis may be associated with trauma, particularly in animals that are housed in pairs or groups, or may be related to other husbandry-related practices. Certain beddings, particularly those that are coarse or dusty, may result in ocular irritation and conjunctival inflammation. Insufficient ventilation may also lead to conjunctival irritation due to buildup of ammonia within bedding and increase risk for conjunctivitis or secondary bacterial infections of the ocular surface (Richardson 2008; van der Woerdt 2012; Griffin et al. 1995; Young and Hill 1974). Conjunctivitis and keratitis have also been described in mice and rats receiving a diet deficient in Vitamin A (Kern n.d.). Non-infectious conjunctivitis in hamsters has been reported in association with spontaneous diabetes mellitus, particularly early in the course of disease (Miedel and Hankenson 2015).

As in other species, clinical signs of conjunctivitis in Myomorpha are non-specific, typically including conjunctival hyperemia, chemosis, and blepharospasm. Some animals may also develop chromodacryorrhea as a non-specific result of Harderian gland porphyrin secretion. As these signs may also be indicative of other ophthalmic diseases, the clinical approach should be focused on a complete history and husbandry analysis, and a thorough ophthalmic examination to rule out conditions such as corneal ulceration or uveitis. When indicated, cytology, culture, and sensitivity of conjunctival swabs and/or ocular discharge may identify causative infectious isolates.

Chromodacryorrhea is a unique finding in mice and rats, but may also be observed in gerbils. Chromodacryorrhea is characterized by red or red-orange fur staining and discoloration around the eye or eyes developing due to excess secretion of Harderian gland porphyrins onto the ocular surface (Williams 2012; Sakai 1981) (Fig. 46.10). Porphyrins are autofluorescent and can be differentiated from periocular hemorrhage using a Wood's lamp (Ellis and Mori 2001). There are numerous causes for chromodacryorrhea including nutritional deficiency, environmental stressors (excessive handling, re-housing, transport), or even generalized disease and poor health (Djeridane 1994; Williams 2002). It may also be associated with dental disease and secondary obstruction of the nasolacrimal duct system (Kern n.d.; Wagner and Farrar 1987). Chromodacryorrhea can be indicative of any infectious disease affecting the eye or periocular tissues, and is strongly associated with sialoadenitis virus (SDAV) infection in rats.

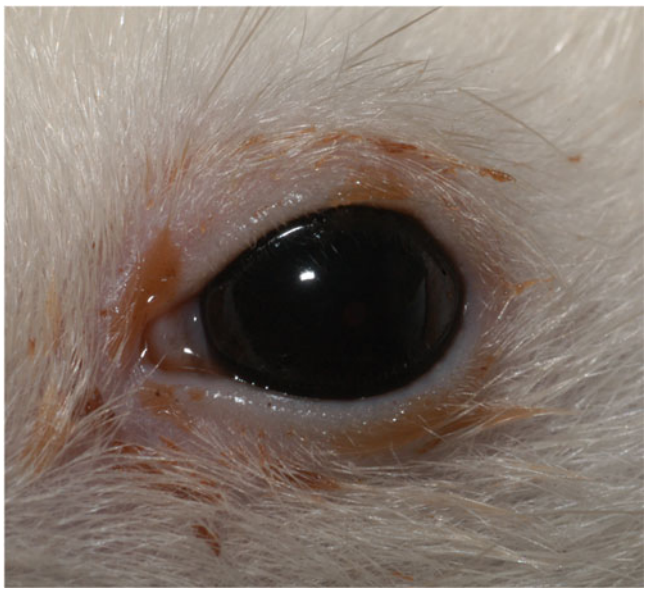

Fig. 46.10 Domestic rat (*Rattus norvegicus domestica*) with chromodacryorrhea. (Photo courtesy of Bret A. Moore, DVM, PhD, DACVO)

Sialoadenitis virus (SDAV) and Parker's rat coronavirus (PRC) are coronaviruses that primarily infect rats, often causing respiratory disease and inflammation of the lacrimal and salivary glands (Schoeb 2000; Hanna et al. 1984). Infection is transmitted via direct contact, aerosolization, or fomites like bedding or behavioral enrichment devices (Innes and Stanton 1961). Ocular signs may be the primary clinical manifestation of infection or may precede subsequent disease of the salivary glands or respiratory tract. In addition to chromodacryorrhea, acute disease associated with SDAV is often associated with keratoconjunctivitis with clinical signs such as blepharospasm and self-trauma, as well as periorbital swelling and even exophthalmos, presumptively due to Harderian and lacrimal gland swelling (Williams 2002; Innes and Stanton 1961; Carthew and Slinger 1981; Lai et al. 1976; Percy et al. 1989). If severe enough, periocular inflammation associated with SDAV can also cause intraocular disease such as uveitis, glaucoma, cataract, or retinal degeneration (Schoeb 2000; Kern 1989). In animals with more chronic disease, chronic conjunctivitis and/or keratitis may be the only manifestation of active SDAV-associated disease (Weisbroth and Peress 1977).

In most infected rats, acute disease associated with SDAV is self-limiting and not likely to be life-threatening. However, the clinical course of disease can persist for up to one month. Identification of infected animals can be a challenge as subclinical or chronic carrier states exist, increasing the risk for introducing infection to naive animals (Bhatt and Jacoby 1985; Eisenbrandt et al. 1982). While seropositivity for SDAV in domestic rats tends to be low, introduction of new animals should be preceded by screening and observation as well as serologic testing (Gannon and Carthew 1980; Pritchett-Corning et al. 2009). It is noteworthy that primary infection and seropositivity for SDAV do not necessarily protect an animal from re-infection which may be a higher risk in animals that are in poor health, immunocompromised, or affected by other stressors (Williams 2002; Kling 2011).

Primary tear film disorders are not well-described clinically in small Myomorpha. However, hamsters, mice, and rats are commonly used as models for investigations and studies of human dry eye and other ocular surface diseases; and baseline values for lacrimal production have been established under normal and abnormal conditions (Rajaei et al. 2013, 2015, 2016b; Lange et al. 2014; Kojima et al. 2014; Dursun et al. 2002; Hoffman et al. 1984). Reference values for some tests of the tear film and ocular surface in common Myomorpha are presented in Table 46.2 and Appendix C.

Diseases of the Cornea

As with other species, ulcerative and non-ulcerative keratitis in mice, rats, gerbils, and hamsters may be related to a multitude of causes, characterized by vascularization, edema, pigmentation, and fibrosis (Fig. 46.11a). Trauma to the cornea from an encounter with another animal when paired or group-housed, contact with coarse bedding, or collision with a behavioral enrichment device may cause corneal damage ranging from a superficial ulceration to corneal perforation (Fig. 46.11b–d) (Richardson 2008; Taradach et al. 1984). Exophthalmia or buphthalmia associated with orbital disease and high intraocular pressure, respectively, may also predispose to corneal ulceration. Similarly, facial nerve paralysis may result in prolonged corneal exposure and desiccation, leading to ulceration and scarring (Fig. 46.12) In rats, corneal opacities and keratitis may be associated with SDAV infection (Taradach et al. 1984).

Iatrogenic causes of keratitis and corneal opacity are also common, and are often associated with sedation or anesthesia in mice and rats. Following even brief anesthesia, mice and rats may develop irreversible corneal ulceration, corneal opacities, keratitis, or subepithelial calcific band keratopathy, sometimes within hours of recovery (Koehn et al. 2015; Turner and Albassam 2005). This phenomenon appears to have a greater association with certain anesthetic drugs like the alpha-2 agonist xylazine (Turner and Albassam 2005). The cause for post-anesthetic corneal disease in mice and rats is often attributed to the prominence of the globe in these species and exposure, but other hypotheses indicate that anesthetic effects such as local hypothermia or local hypoxia of the ocular tissues may be related. Rarely, opacities may be associated with congenital lesions like corneal dermoid, or

Table 46.2 Published normative values for selected ophthalmic diagnostic tests in three common Myomorph rodents (see Appendix C)

	IOP-applanation (mmHg)	IOP-rebound (mmHg)	STT I (mm/min)	PRTT (mm/15 s)	Endodontic paper point tear test (mm/min)	Tear break up time (s)	Reference
Mouse (*Mus musculus*)	13.7						Cohan and Bohr (2001a, b)
		10.6–19.3					Wang et al. (2005)
		11.7–13.2					Johnson et al. (2008)
			2.8–3.3 mm/2 min[a]				Hoffman et al. (1984)
				2.98 mm/1 min			Dursun et al. (2002)
					3.59–4.39		Lange et al. (2014)
						2.5–3.0	Kojima et al. (2014)
Rat (Rattus norvegicus)	15.5						Cohan and Bohr (2001a, b)
		18.4					Wang et al. (2005)
					6.18–6.45		Lange et al. (2014)
Syrian hamster (Mesocricetus auratus)		4.55	2.07 mm/min[b]	5.57/15 s	4.52		Rajaei et al. (2016a, b)
				6.8 mm/15s[c]			Rajaei et al. (2013, 2016b)
African giant pouched rat (Cricetomys gambianus)		7.7[d]					Heller et al. (2018)

IOP = intraocular pressure, STT = Schirmer tear test, PRTT = phenol red thread test
[a]Methods cite use of 0.5 × 3.0 mm strip of Whatman #1 filter paper, placed under the lower lid near the medial canthus
[b]Modified STT with standard 5 mm width strip cut into 2.5 mm width strip
[c]Value was statistically higher in females (8.5 mm/15 s) compared to males (5.1 mm/15 s)
[d]Animals were anesthetized and TonoVet was operated on "dog" calibration setting

acquired lesions such as epithelial inclusion cysts and ocular surface neoplasms (Williams 2002).

Acquired corneal lesions like scars and infiltrates in mice and rats should be differentiated, when possible, from corneal dystrophy. Corneal dystrophy is a heritable condition causing bilateral corneal opacification, and is particularly common in purpose-bred strains of mice and rats (Gillet et al. 1995) (also Pierro and Spiggle 1967) (Fig. 46.13). In some rat strains, like the Fischer 344 and Wistar albino rat, lesions may be present in 65–100% of animals (Eiben 2001; Hashimoto et al. 2013; Wilkie 2014; Wojcinski et al. 1999). While corneal dystrophy is heritable, it is not typically congenital, developing instead in older animals with a positive correlation between incidence and age (Taradach et al. 1984).

Lesions are most commonly distributed within the central or paracentral cornea. Corneal dystrophy may take multiple forms, characterized in some animals as fine, crystalline, translucent opacities and in others as more granular and opaque lesions, often localized to the subepithelial corneal stroma (Wilkie 2014; Bellhorn et al. 1988). Histologically, dystrophic lesions represent extracellular accumulations of calcium and phosphorus (Wilkie 2014). While uncommon, corneal dystrophy lesions may also be observed in hamsters (Taradach et al. 1984).

Glaucoma

Spontaneous glaucoma is uncommon but primary and secondary forms have been described in mice and rats and other common Myomorpha. Congenital glaucoma is rare, but has been reported in Fischer 344 and Wistar rats (Heywood 1975; Shibuya et al. 2001), whereas forms that present later in life, typically by 18 months of age, have been described in the Royal College of Surgeons rat (Naskar and Thanos 2006; Thanos and Naskar 2004). Other sporadic forms include a pigment dispersion glaucoma in the DBA/2 J mouse strain that closely mimics many features of a similar form of human glaucoma (McKinnon et al. 2009). Spontaneous buphthalmos has been reported in a small case series of Djungarian hamsters (*Phodopus sungorus campbelli*) (Ekesten and Dubielzig 1999) (Fig. 46.14a). The affected animals presented with bilaterally enlarged globes, observed at approximately 10–12 months of age, and behavioral changes attributed to vision loss. Other clinical features

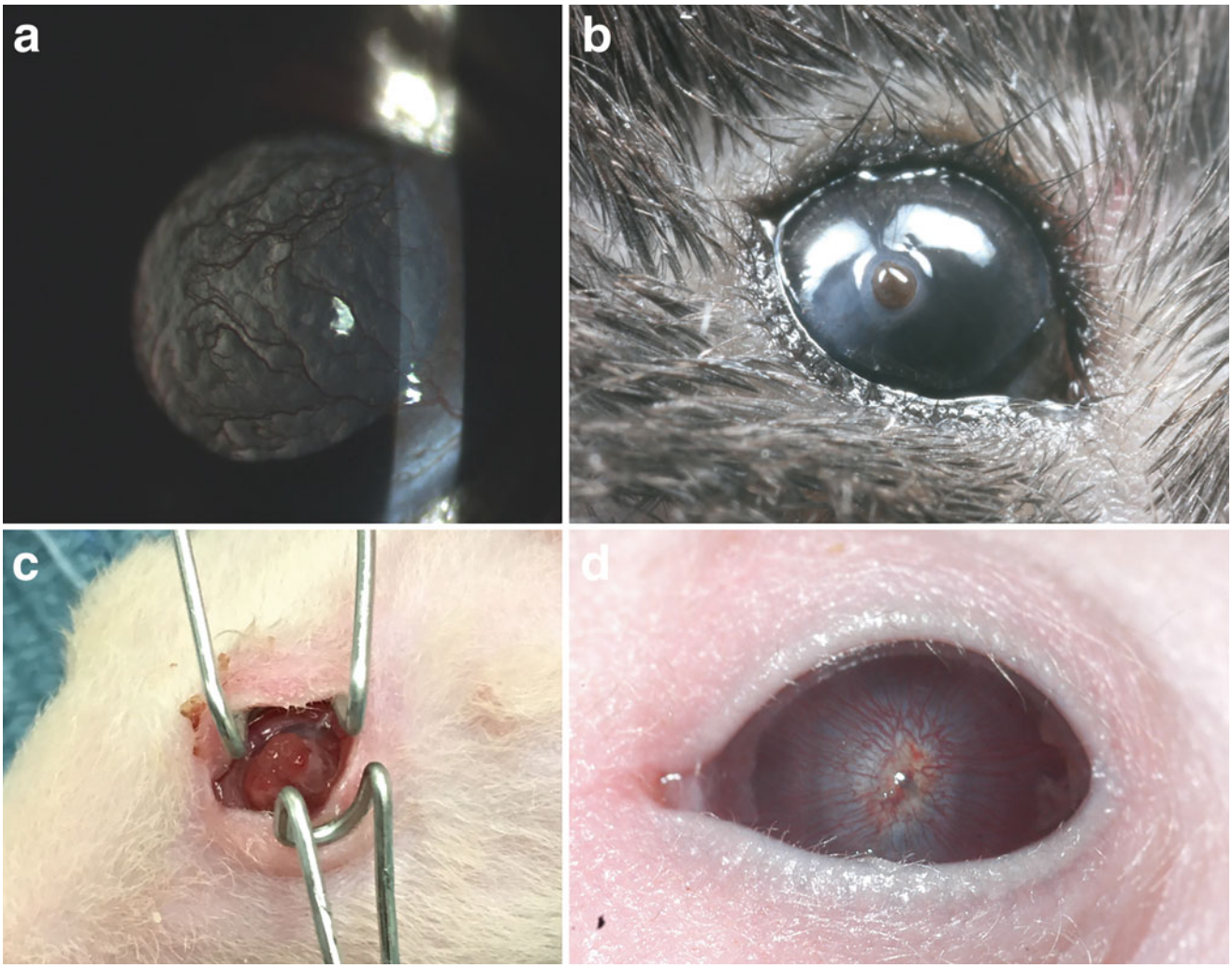

Fig. 46.11 Non-ulcerative (**a**) and ulcerative (**b**, **c**) keratitis in Myomorpha. (**a**) A laboratory mouse (*Mus musculus*) on slight-lamp retroillumination demonstrating corneal fibrosis and vascularization. (**b**) A laboratory mouse with a corneal perforation and iris prolapse, likely secondary to trauma with a cage-mate. (**c**, **d**) A domestic rat (*Rattus norvegicus domestica*) with a corneal perforation at initial examination (**c**) and after 3 weeks of healing (**d**). (**a**, **b**—Courtesy of Lionel Sebbag, DVM, Ph.D., DACVO. **b**, **c**—Courtesy of Bret A. Moore DVM, Ph.D., DACVO)

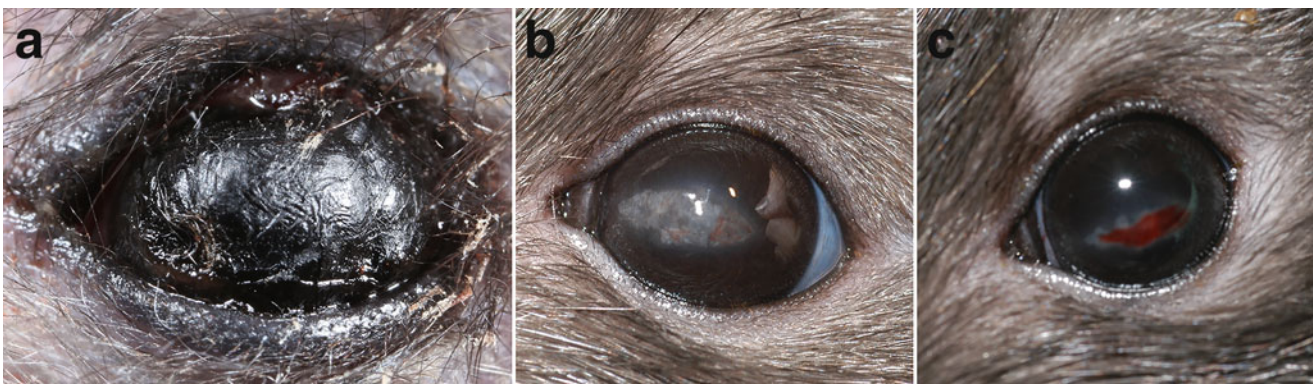

Fig. 46.12 Exposure keratopathy due to facial nerve paralysis in Myomorpha. (**a**) A hamster (*Mesocricetus auratus*) with extreme corneal dessication secondary to complete facial nerve paralysis following trauma. (**b**, **c**) A hooded rat (*Rattus norvegicus domestica*) with partial facial nerve paralysis, resulting in secondary corneal degeneration and vascularization only within the palpebral fissure (**b**), and intrastromal hemorrhage (**c**). (**a**—Courtesy of Lionel Sebbag, DVM, Ph.D., DACVO. **b**, **c**—Courtesy of the University of California Davis Comparative Ophthalmology Service)

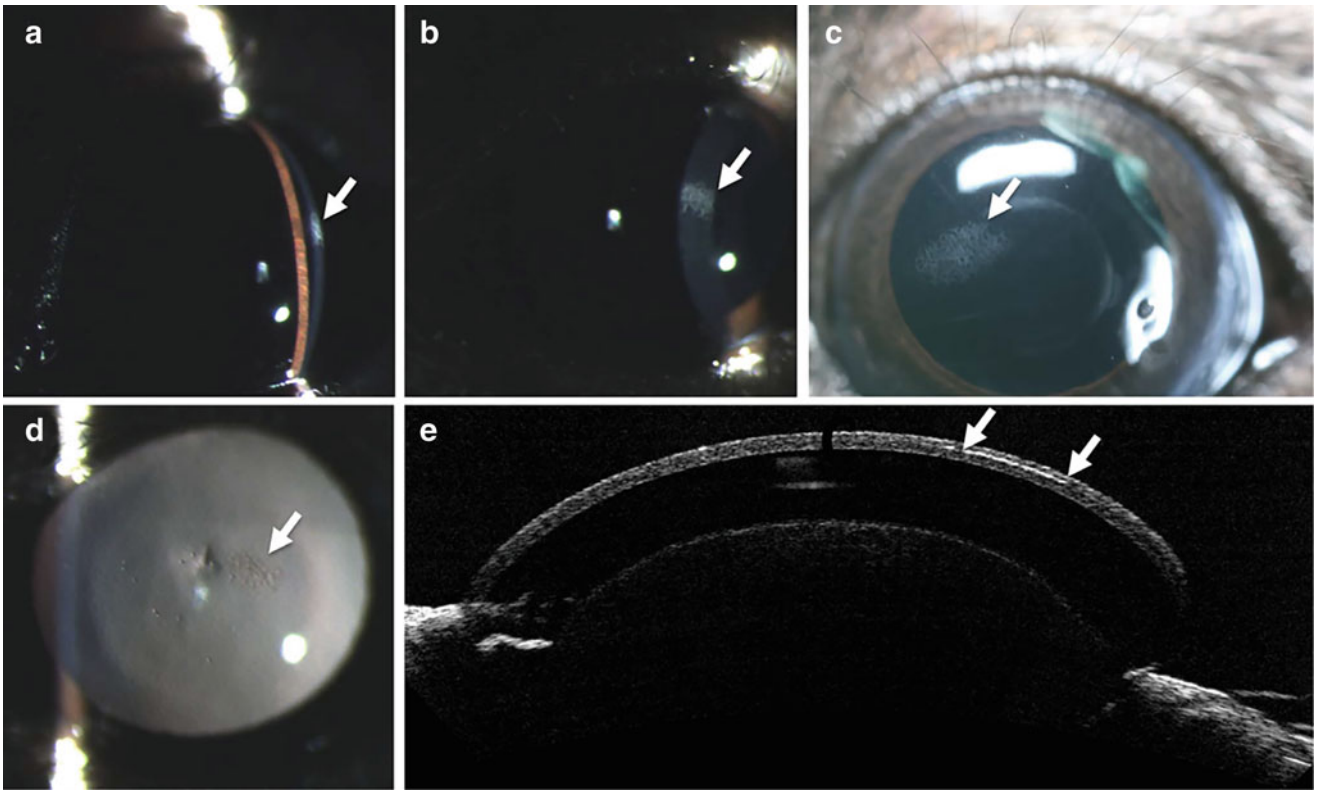

Fig. 46.13 Corneal abnormalities commonly seen in C57BL/6 N mice. Corneal deposits seen on slit lamp exam ranged from punctate in size to affecting nearly 60% of the corneal surface. Moderately sized corneal opacities are shown here with a 0.1-mm slit beam (**a**), a 0.8-mm slit beam (**b**), by direct inspection (**c**), and on retroillumination (**d**). Arrows point to the area of interest in (**a**–**d**). When examined by optical coherence tomography (**e**), the deposits appear to form a curvilinear hyperreflective opacity in the corneal stroma, seen between the two arrows. (Used with permission without modification from Fig. 1 of: "Moore BA, Roux MJ, Sebbag L, et al. A population study of common ocular abnormalities in C57BL/6 N rd8 mice. Investigative Ophthalmology and Visual Science 2018b;6:2252–2261")

included pupil dilation and total or subtotal loss of pupillary light reflex. Histology confirmed retinal degeneration secondary to high intraocular pressure; while a primary/heritable predisposition was suspected, secondary glaucoma could not be ruled out (van der Woerdt 2012; Ekesten and Dubielzig 1999). Affected animals should be removed from breeding stock (Richardson 2008).

One of the reasons that glaucoma is so infrequently diagnosed in small rodents is the often ambiguous nature of clinical signs of abnormally increased intraocular pressure. Clinical features like episcleral congestion and corneal edema may not be as prominent as in other species. In other cases, particularly animals with chronic disease, signs will be more obvious (Fig. 46.14b–c). In any Myomorph species with globe enlargement, pupil dilation, and/or signs of vision loss, a full ophthalmic examination should be performed in tandem with applanation or rebound tonometry. Tonometry can be a challenge in small rodents, particularly using commercial applanation tonometers whose contact footplates are large (>3 mm diameter) compared to the corneal diameter of mice and rats (Henriksson et al. 2009). Furthermore, applanation tonometers may under- or overestimate manometric IOP (Cohan and Bohr 2001a, b). Rebound tonometers which typically utilize a contact probe with a smaller tip diameter have become more popular in the laboratory and veterinary setting, and have proven to be accurate and precise, even in conscious mice (Kim et al. 2007; Pease et al. 2006; Saeki et al. 2008; Wang et al. 2005; Johnson et al. 2008). Normal intraocular pressure values for common Myomorpha have widely been reported (Rajaei et al. 2016b, 2017; Heller et al. 2018; Cohan and Bohr 2001a, b; Wang et al. 2005; Johnson et al. 2008) and are presented in Table 46.2 and Appendix C.

Diseases of the Uvea

Uveal disease in common Myomorpha can be generally categorized into heritable anomalies, inflammatory disease (uveitis), and neoplasia. Heritable anomalies are not common but colobomas of the anterior uvea (iris and ciliary body) have been reported in rats. Colobomas of the anterior uvea are typically incidental findings, presenting as corectopia (eccentricity of the pupil) (Fig. 46.4b) or dyscoria (abnormal

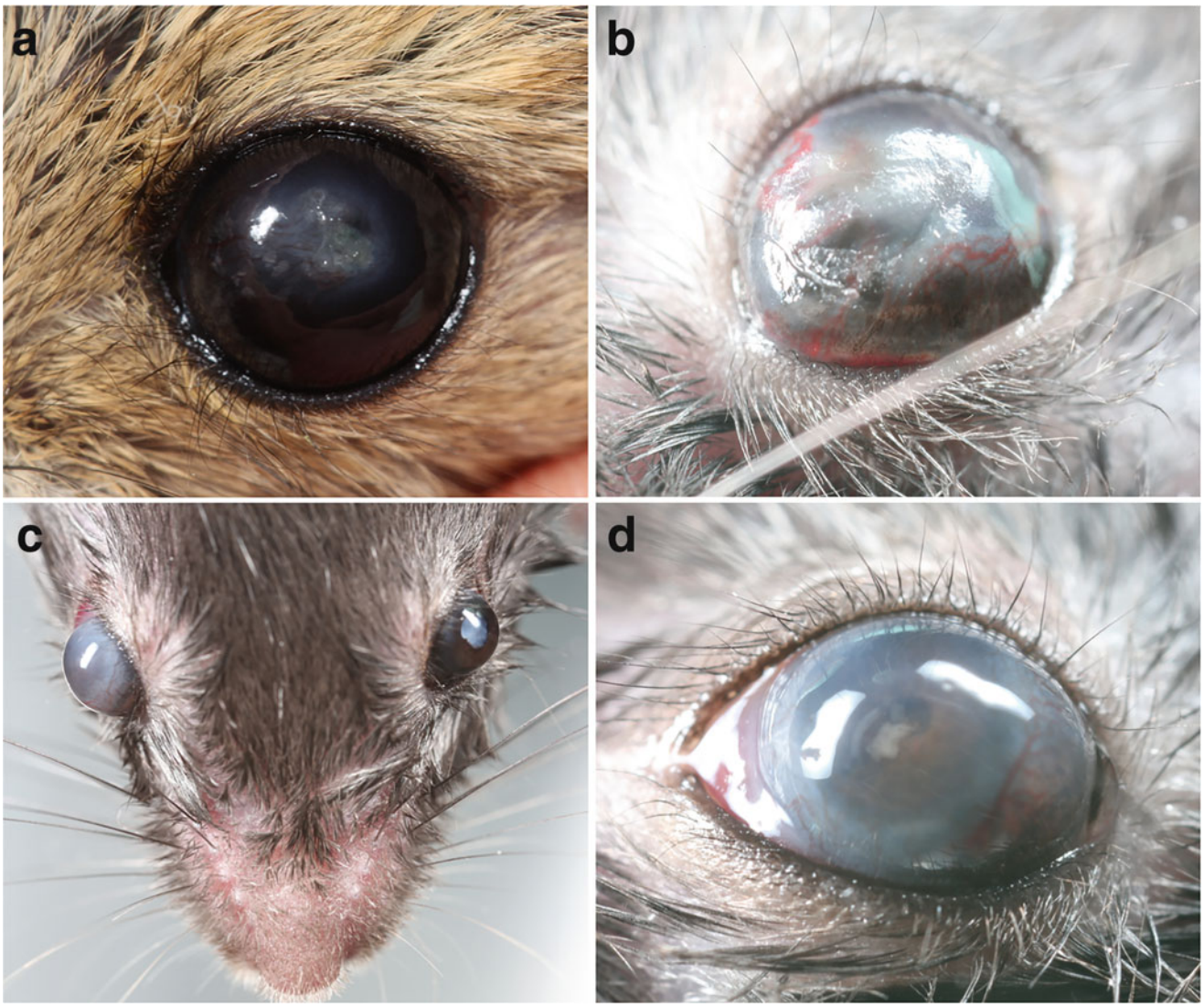

Fig. 46.14 Glaucoma in Myomorpha. (**a**) A hamster (*Mesocricetus auratus*) with unilateral buphthalmos resulting in secondary exposure keratopathy characterized by diffuse pigmentation and axial degeneration. (**b**–**d**) Chronic glaucoma in laboratory mice (*Mus musculus*). (**b**) Phthisis bulbi with marked chronic keratitis and a small globe following chronic glaucoma. (**c**, **d**) Chronic glaucoma in the right eye, likely secondary to cataracts and phacolytic uveitis. Note in (**c**) the buphthalmos and corneal edema in the right eye and the mature cataract in the left eye, and in a close up of the right eye (**d**), note the dyscoria due to posterior synechia, hypermature cataract, and keratitis. (**a**—Courtesy of Crystal Boles DVM. **b**–**d**—Courtesy of Lionel Sebbag, DVM, Ph.D., DACVO)

pupil shape) (Fig. 46.14d) (Rubin and Daly 1982) (also Matsuura et al. 2013). In some rats, colobomas may be associated with other structural ocular anomalies like colobomas of the optic nerve and even microphthalmia (Fig. 46.4a) (Taradach et al. 1984). Persistent pupillary membranes (PPMs), also presumed to be heritable, are described in mice and rats (Beaumont 2002; Taradach et al. 1984; Chacaltana et al. 2017; Heywood 1973; Saari 1975; Young et al. 1974) and in wild species like the Nesomyid African giant pouched rat (*Cricetomys gambianus*) (Heller et al. 2018).

Heritable anterior uveal anomalies may rarely be associated with glaucoma or hyphema (Saari 1975; Young et al. 1974) but are typically not likely to have an obvious effect on vision in affected eyes and do not require any specific treatment. However, it is noteworthy that adhesions of the iris to the cornea or lens (anterior or posterior synechia, respectively) indicative of active or chronic uveitis may bear a similar appearance to iris colobomas (Taradach et al. 1984) and should be differentiated.

Compared to other species, uveitis is not commonly diagnosed in mice and rats. Uveitis can be associated with exogenous causes like blunt or penetrating trauma, or can develop as a result of hematogenous spread of endogenous inflammation and/or infection. In theory, any systemic infection in a small rodent can gain access to the eye via

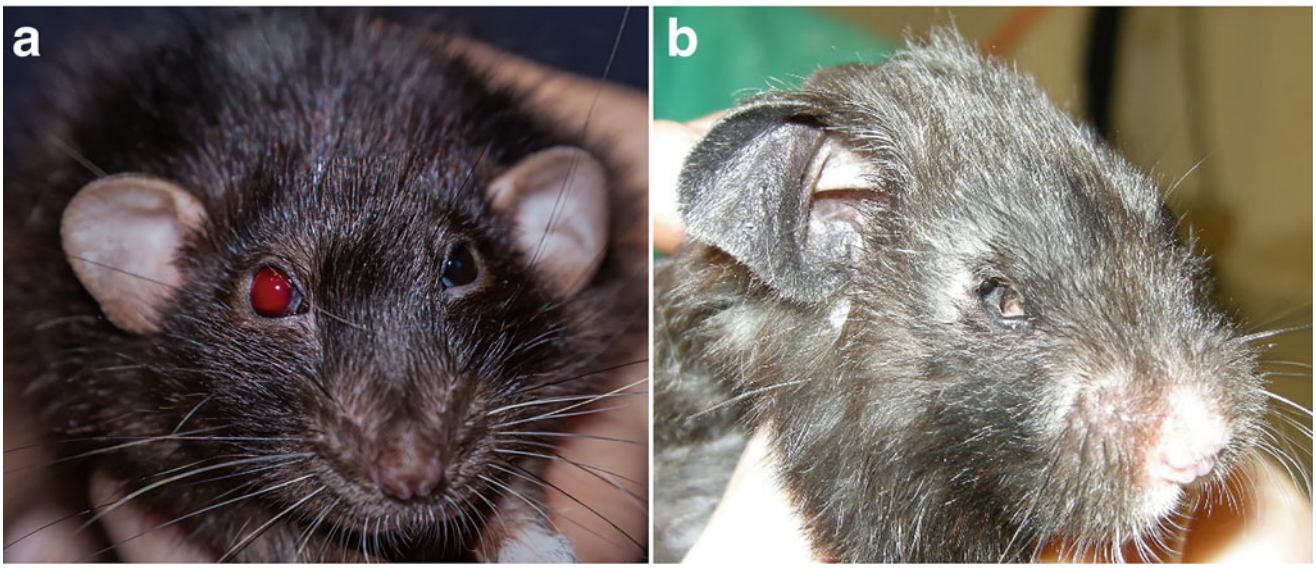

Fig. 46.15 (**a**) Hyphema in a black rat (*Rattus rattus*), the cause of which is unable to be determined. (**b**) Severe phthisis bulbi in a hamster (*Mesocricetus auratus*) following globe rupture and uveitis secondary to retrobulbar disease and exophthalmos. (**a**—Used with permission from Kai Beercrafter, Shutterstock.com. **b**—Courtesy of the University of California Davis Comparative Ophthalmology Service)

circulation, but the low incidence of uveitis in these Myomorph species complicates determination of a list of "common causes." In experimental studies of hamsters and surveys of wild Cricetids (white-footed mice (*Peromyscus leucopus*), deer mice (*P. maniculatus*), and meadow voles (*Microtus pennsylvanicus*)) in the Western United States, *Borrelia burgdorferi* bacteria were isolated from eyes (Ubico et al. 1996; Duray and Johnson 1986). The significance of this finding is unknown, but it suggests that these species may develop uveitis or other inflammatory ocular disease as in humans and other mammalian species.

There are also some mouse strains like the R161H and AIRE −/− mice, reported to develop a spontaneous, progressive immune-mediated forms of uveitis (Chen et al. 2015). Clinical manifestations are similar to those in other species, including blepharospasm, photophobia, aqueous flare and cells, corneal edema, miosis (pupil constriction), hyphema (intraocular bleeding), and hypopyon (cellular infiltration of the aqueous humor). One noteworthy challenge in rodents, however, is the clinical differentiation of hyphema associated with uveitis, from non-inflammatory hemorrhage associated with vascular leakage from persistent hyaloid vasculature or patent remnants of the tunica vasculosa lentis (see section "Diseases of the Posterior Segment" (Fig. 46.15a). Chronically, secondary glaucoma, cataract formation, and phthisis bulbi may occur (Fig. 46.15b).

Encephalitozoon cuniculi is a microsporidial pathogen well-known for causing clinical disease in domestic and wild rabbits (Bártová et al. 2015; Hedley n.d.; Wilson 1979). The most common clinical manifestations in infected rabbits include neurologic signs (central or peripheral), renal insufficiency, myocarditis, and phacoclastic uveitis due to infection and rupture of the lens (Hedley n.d.). Not all infected rabbits develop clinical signs, however, with many carrying the organism subclinically.

Among the Myomorpha, serologic prevalence of antibodies to *E. cuniculi* has been established in numerous studies but the range and extent of clinical disease, if any, in these species is not well understood. In one study of purpose-bred laboratory mice (C57BL/6 and ICR strains), 20/132 were seropositive for *E. cuniculi* by indirect fluorescent antibody technique (IFAT) and ELISA (Balent et al. 2004); and in one study of laboratory colonies of Syrian hamsters, 14–80% of animals were seropositive by IFAT (Chalupský et al. 1979). Non-domestic Muridae and Cricetidae may also be seropositive for *E. cuniculi* with up to 34% of house mice (*Mus musculus*) and 19% of voles (*Microtus* spp., and *Arvicola* spp.) being seropositive (Fuehrer et al. 2010; Hinney et al. 2016).

Of the Myomorpha, perhaps the species with the most overt clinical manifestations of *E. cuniculi* infection are lemmings within the genus *Dicrostonyx*. Infected animals may develop severe and life-threatening disease associated with disseminated granulomatous inflammation, particularly of the central nervous system (Cutlip and Beall 1989). The incidence of ocular manifestations of Encephalitozoonosis in any of these, species, however, is not reported.

Spontaneous neoplasms of the anterior uvea are rare but have described in common Myomorpha. Intraocular melanomas have been reported in mice, rats, and hamsters (Ramos et al. 2018; Yoshitomi and Boorman 1991b; Magnusson et al. 1978; Manning et al. 2004). Metastasis to

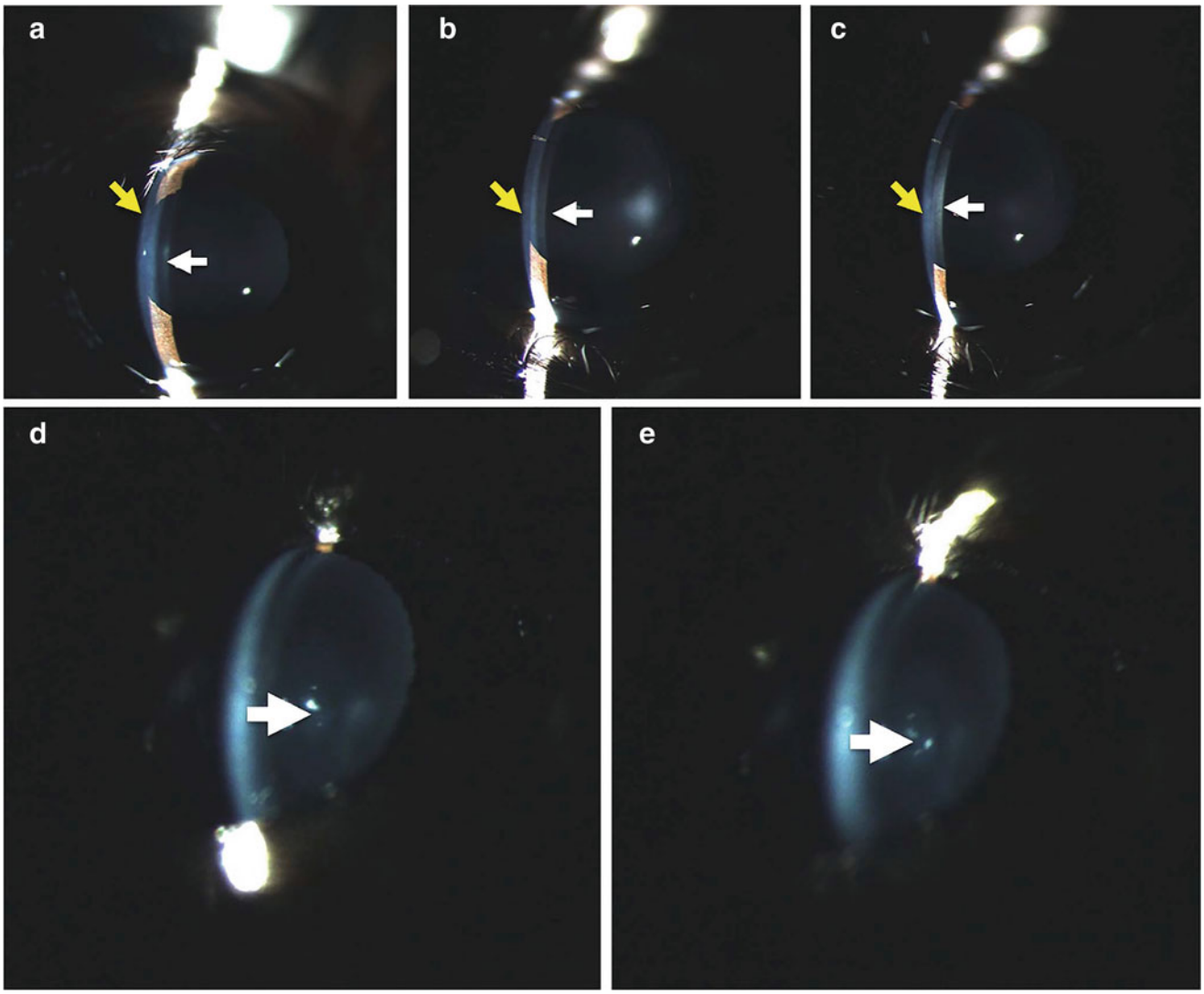

Fig. 46.16 Lenticular abnormalities commonly seen in C57BL/6 N mice. Increased optical density of the anterior lens capsule is common in adult mice of this strain. The normal translucence of the cornea and anterior lens capsule is shown in (**a**), where the anterior lens capsule (white arrow) is more lucent (less optically dense) than the cornea (yellow arrow), based on slit beam biomicroscopy. Abnormally increased anterior lens capsule translucencies are shown as being equally optically dense to the corneal slit beam (**b**) or more optically dense than the corneal slit beam (**c**). Furthermore, punctate nuclear opacities (**d**,**e**) are seen in nearly every mouse of the C57BL/6 N strain (white arrows point to three or four small nuclear cataracts). (Used with permission without modification from Fig. 2 of: "Moore BA, Roux MJ, Sebbag L, et al. A population study of common ocular abnormalities in C57BL/6 N rd8 mice. Investigative Ophthalmology and Visual Science 2018b;6:2252–2261")

the lung from a primary intraocular melanoma has been reported in a hamster (Mangkoewidjojo and Kim 1977). In a case report in a Chinese hamster (*Cricetulus griseus*), an intraocular melanoma with an unusual signet-ring morphology was described (Lima et al. 2012). In humans, this neoplastic morphology is more frequently associated with metastatic lesions. However, the overall rare incidence of intraocular melanomas in small Myomorpha complicates general conclusions about their typical biological behavior. Other ocular neoplasms described in mice and rats include squamous cell carcinoma, anterior uveal leiomyoma, and malignant Schwannoma (Ramos et al. 2018; Yoshitomi and Boorman 1991a; Haseman et al. 1998; Chandra and Frith 1993; Owen and Duprat 1987).

Diseases of the Lens

Spontaneous cataracts (lens opacities) are common in mice and rats, often affecting the anterior subcapsular, anterior cortical, or nuclear layers of the lens (Fig. 46.16). In large studies evaluating pigmented and albino purpose-bred laboratory mice, lens opacities were described in up to 13% of animals, even young animals (Taradach et al. 1984; Hubert

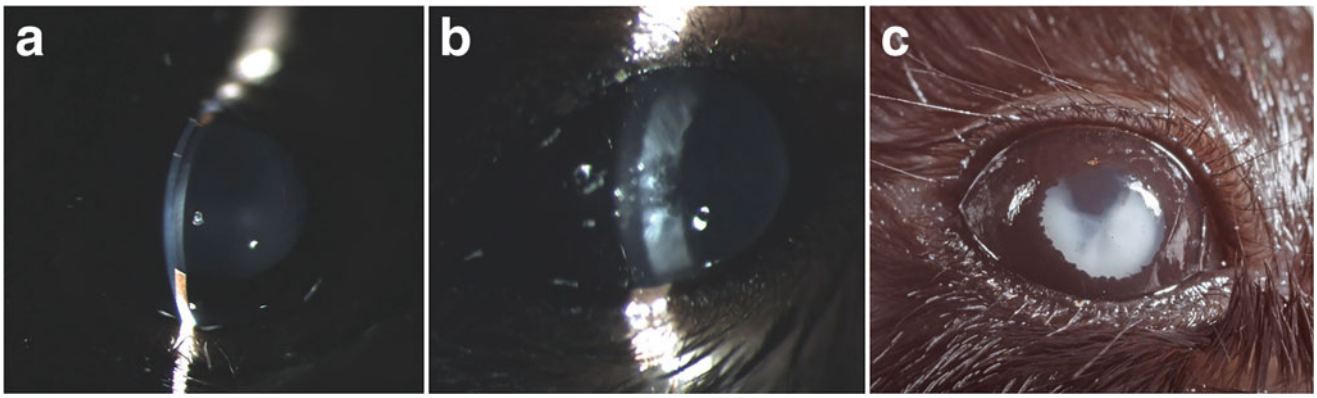

Fig. 46.17 Cataract formation following the administration of xylazine in a laboratory mouse (*Mus musculus*). (**a**,**b**) Altered translucency of the anterior lens capsule as cataract formation develops. (**c**) Nearly complete cataract formation, limiting the view of the posterior segment and prohibiting posterior imaging. (Courtesy of Lionel Sebbag, DVM, Ph. D., DACVO)

et al. 1999). Cataracts may be associated with a range of genetic mutations (Balazs and Rubin 1971; Durand et al. 2001; Graw 1999; Hartman 1968; Tripathi et al. 1991; Wolf et al. 2005; Zhang et al. 2017; Zigler 1990) (also Smith et al. 1997; Beasley 1963; Runge et al. 1992), including the lens rupture gene (Fraser and Herer 1948, 1950) or may be a function of increasing age, with studies citing incidences of 20–40% in mice ranging from 18–30 months of age (Taradach et al. 1984; Tucker and Baker 1967). Cataracts may also develop secondary to other diseases. Cataracts are also a consequence of retinal degeneration, as observed and characterized in the Royal College of Surgeons (RCS) rat, and may also be associated with spontaneous hypertension in Sprague-Dawley rats (Bourne et al. 1938). Iatrogenic cataracts may be transiently observed in mice, rats, hamsters, and gerbils that undergo surgeries requiring prolonged anesthesia with eyelid separation, or in association with administration of xylazine (Kern n.d.; Calderone et al. 1986; Heatley and Harris 2009) (also Ridder et al. 2002). Following administration of xylazine, cataract formation can occur quickly, progressing from slightly altered translucency to the lens capsule to complete cataracts in minutes, making ocular imaging and posterior segment evaluation challenging (Fig. 46.17).

Hamsters may also develop cataracts; and compared to mice and rats, are more likely to present with solitary posterior cortical opacities or complete (mature) cataracts (Richardson 2008; Taradach et al. 1984). Cataracts in hamsters may also be more common in older animals and in association with diabetes mellitus (Gilger et al. 2018). Cataracts have also been described in other less common Myomorpha. The fat sand rat (*Psammomys obesus*) may develop cataracts within two weeks of onset of diabetes mellitus, a disease typically elicited in this species when fed a high-energy, low-fiber diet (DiCarlo 2001). The mechanism of cataract formation is not completely understood, but it is noteworthy that rats have even higher lens aldose reductase activity than dogs. This suggests that an osmotic mechanism, similar to that described in dogs with diabetes mellitus, is involved (DiCarlo 2001).

Cataracts were also the most common incidental finding in a survey of Nesomyid African giant pouched rats. Of 64 eyes, 23 had some degree of lens opacity, most commonly characterized as small incipient anterior cortical, nuclear, or suture tip, or as punctate anterior lens capsule pigment. Immature cataracts were observed in 6 eyes, and hypermature cataract in one eye (Heller et al. 2018).

The presence of cataract(s) does not necessarily cause or equate to clinically-evident vision loss in any animal, as many cataracts are small (incipient) and only seen on close, magnified examination. Furthermore, cataracts are often solitary lesions, and may only affect one eye. However, some cataracts may progress to maturity and may be associated with other ocular lesions, both of which may impact vision. For example, posterior capsular cataracts may be associated with persistent hyaloid remnants spanning the central vitreous, particularly in younger mice and rats (Hubert et al. 1999). Some cataracts are also associated with other ocular anomalies like anterior segment cleavage dysgenesis, microphthalmia, and colobomas (Kern n.d.). Therefore, thorough dilated examination of the anterior and posterior segments is recommended in any small rodent eye presenting with cataract.

Diseases of the Posterior Segment

Lesions of the vitreous, including crystalline and pigment deposits (Fig. 46.18) are relatively common in mice and rats. Also common is persistence of the embryonic hyaloid vasculature (Fig. 46.19). This lesion may be observed as a small filamentous structure extending partially through the

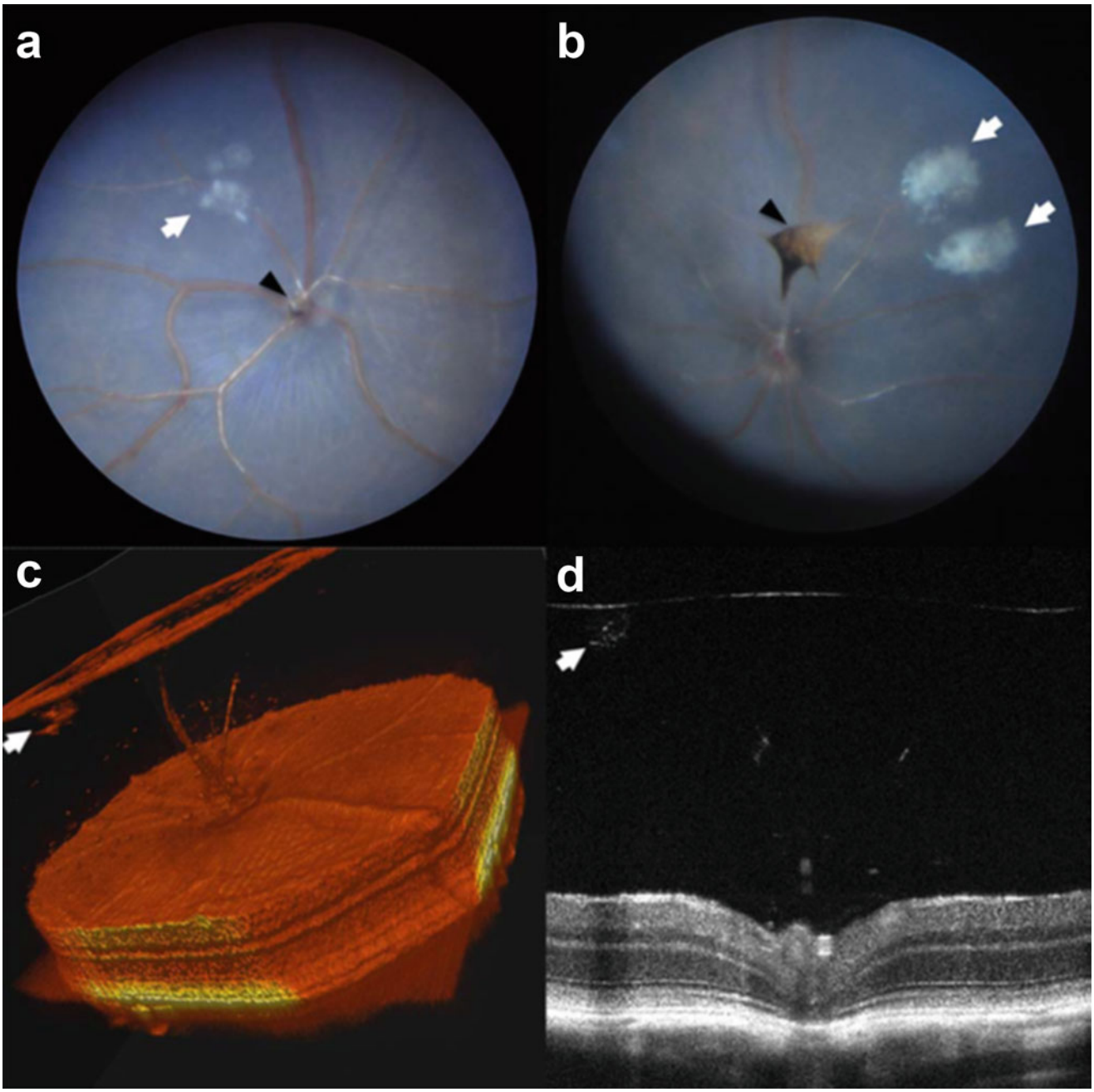

Fig. 46.18 Vitreous crystalline deposits seen in C57BL/6 N mice. Vitreous crystalline opacities of various sizes appearing in a celestial pattern (white arrows) in fundus photographs (**a**, **b**). 3D-rendered OCT (**c**) and standard cross-sectional OCT imaging (**d**). Incidental vitreous pigment (black arrowheads) can be seen (**a**, **b**). (Used with permission without modification from Fig. 3 of: "Moore BA, Roux MJ, Sebbag L, et al. A population study of common ocular abnormalities in C57BL/6 N rd8 mice. Investigative Ophthalmology and Visual Science 2018b;6: 2252–2261")

vitreous from the optic disk (Bergmeister's papilla) or extending from the posterior lens capsule. In some eyes, the hyaloid remnant may span the entire vitreous from the optic disk to the posterior lens. In the aforementioned study of African giant pouched rats, Bergmeister's papilla was commonly observed on funduscopic examination (Heller et al. 2018).

It is not uncommon to observe hyaloid remnants in weanling mice and rats, and for them to regress as animals reach maturity (Kern 1989; Wilkie 2014). In one study using angiography, 15% of adult mice up to 25 weeks of age had hyaloid remnants, some of which would have been unseen on ophthalmoscopic examination (McLenachan et al. 2015). In larger surveys of rats, these lesions were observed in up to

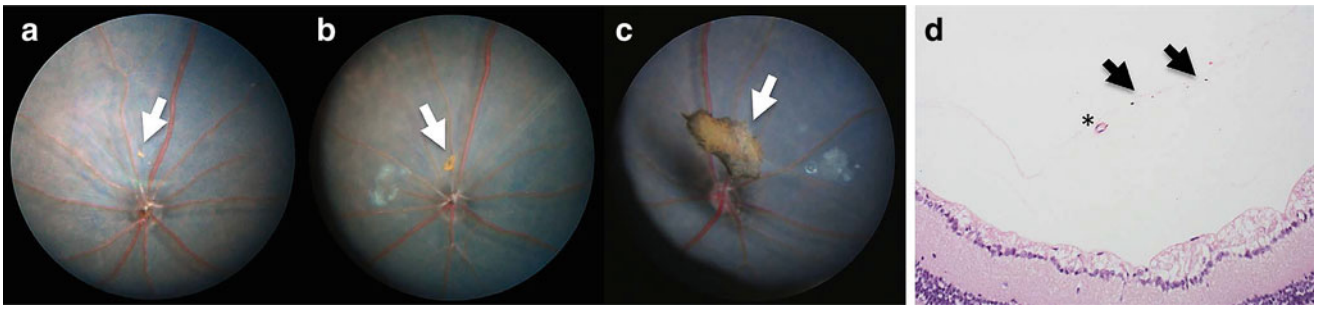

Fig. 46.19 Vitreous pigment is commonly seen in C57BL/6 N mice. Vitreous pigmentation located axially and often in association with the pole of the posterior lens capsule or optic nerve head (**a**–**c**; white arrows) is characteristic of persistent hyaloid vasculature or persistent hyperplastic primary vitreous. Also commonly found are punctate dispersed pigment flecks located throughout the vitreous chamber (**d**; black arrows). Additionally, (**d**) shows an example of an isolated blood vessel, representative of persistent hyaloid vasculature (asterisk). (Used with permission without modification from Fig. 4 of: "Moore BA, Roux MJ, Sebbag L, et al. A population study of common ocular abnormalities in C57BL/6 N rd8 mice. Investigative Ophthalmology and Visual Science 2018b;6:2252–2261")

60% of Sprague-Dawleys at 6 weeks of age (Taradach et al. 1984; Poulsom and Marshall 1985). In both species, these lesions typically have no structural or functional adverse consequence for the eye. Infrequently these hyaloid remnants are patent, however, and may be associated with spontaneous vitreous hemorrhage (Taradach et al. 1984).

Primary retinal disease or retinal lesions are sporadically described in common Myomorpha, ranging from benign incidental findings to more significant degenerative or inflammatory retinal disease with implications for vision. Small incidental lesions involving the retinal vessels have been described in mice and rats. Preretinal loops may be present in up to 12% of Sprague-Dawley rats (Hubert et al. 1994; Matsui and Kuno 1987), and retinal saccular aneurysms may also be observed sporadically, particularly in older mice and rats (Heywood 1973; Bellhorn 1973). These vascular lesions are not known to progress or have any impact on ocular function or vision.

Transient peripheral retinal folds have been described in young mice, putatively related to incongruous growth between the retina and the other ocular tunics (Hubert et al. 1999), without any known impact on visual function. However, true retinal dyplasias have also been described in numerous rat strains, characterized by focal-to-multifocal folding of the retina and photoreceptor separation from the underlying retinal pigmented epithelium (RPE) (Kuno et al. 1991; Lai and Rana 1985; Poulsom and Hayes 1988) (also Moore et al. 2018b; Chu et al. 2013; Pellissier et al. 2014; Sahu et al. 2015; Luhmann et al. 2015; van de Pavert et al. 2004; Aleman et al. 2011) (Fig. 46.20). There is also an apparent histological spectrum of lesion severity, with milder lesions involving only minimal folding and retinal detachment and occasional rosette formation, and more severe lesions involving comparatively greater disruption of the associated photoreceptors with subretinal and vitreal hemorrhage (Poulsom and Hayes 1988). The significance of lesion severity and its impact on vision is unknown, but have been well categorized by advanced posterior segment imaging (Paques et al. 2007; Antony et al. 2014; Berger et al. 2014; Li et al. 2016; Pennesi et al. 2012; Puk et al. 2013; Fischer et al. 2009). Retinal dysplasia has also been described in the Syrian hamster (*Mesocricetus auratus*). In a large survey of 1200 Syrian hamsters aged 6 weeks to 9 months, ophthalmoscopic examination of the retina revealed streak-like lesions and/or circular regions of depigmentation in 24 animals, though no behavioral evidence of vision impairment was present in any animals (Schiavo 1980). Histologically, these lesions present similar folds and rosettes with outer retinal disruption as in mice and rats (Schiavo 1980).

A unique linear retinopathy (also referred to as retinochoroidal degeneration, retinochoroidal atrophy, or retinal dystrophy) has been described in young purpose-bred rats, characterized by pale streak-like lesions within the ocular fundus (Hubert et al. 1994; Roman et al. 2016). Histologically, these lesions represent primary thinning of the outer retina and the underlying choroidal blood vessels (Schafer and Render 2012). There is no consensus on the heritability of this retinopathy, nor its pathogenesis or clinical significance with respect to visual function.

Diffuse retinal degeneration is described in mice and rats associated with a range of etiologies. Retinal degeneration may be associated with advancing age in any mouse or rat, but has been particularly well-described in Wistar and Sprague-Dawley rats (Tucker and Baker 1967; DiLoreto et al. 1994, 1995; Lai et al. 1978; Lin and Essner 1987, 1988; Schardein et al. 1975; Tucker 1997). Age-related cystoid degeneration may also be observed in some rats.

Early-onset heritable retinal degeneration has been characterized in mice in association with a fundamental mutation in *rd* which is associated with dysfunction of cGMP-phosphodiesterase (PDE) in rod photoreceptors. This leads to toxic accumulation of cGMP and photoreceptor degeneration (Keeler 1970) and functional blindness at an early age, though there are "fast" and "slow" forms which

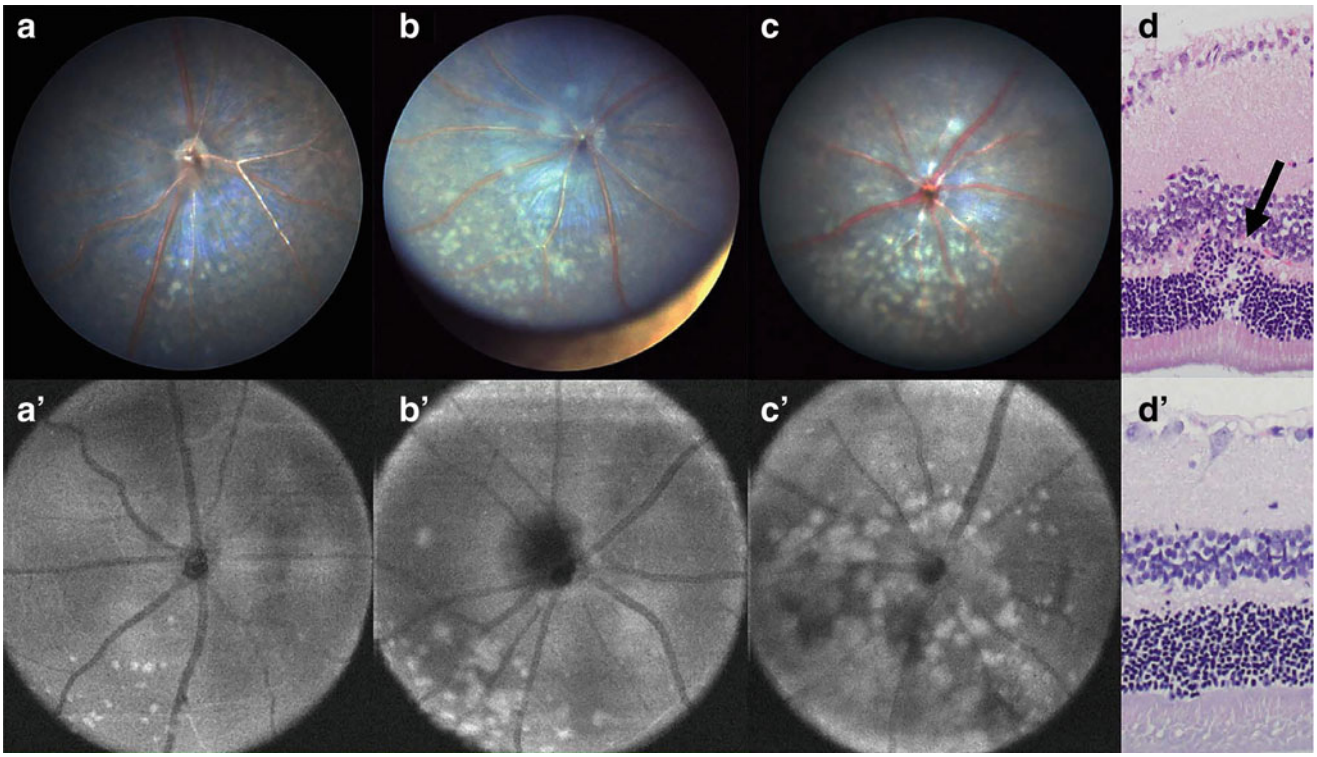

Fig. 46.20 Different grades of retinal dysplasia found in C57BL/6 N mice with the rd8 mutation. The degree of retinal dysplasia can be graded from mild (**a**, **a′**), moderate (**b**, **b′**), to severe (**c**, **c′**) dysplasia. Histologically, retinal folds and/or rosettes are noted in areas of lesions (**d**), but are not seen in unaffected areas (**d′**). Images in (**a**–**c**) are TEFI images, while (**a′**–**c′**) are en face OCT images. (Used with permission without modification from Fig. 5 of: "Moore BA, Roux MJ, Sebbag L, et al. A population study of common ocular abnormalities in C57BL/6 N rd8 mice. Investigative Ophthalmology and Visual Science 2018b;6: 2252–2261)

may influence the rapidity of onset and progression. On examination, animals are bilaterally affected with diffuse pallor of the retina and attenuation of the retinal vessels (Taradach et al. 1984; Hawes et al. 1999). In pigmented mice, there may also be generalized "mottling" or other pigmentary changes.

In rats, the Royal College of Surgeons (RCS) rat develops a heritable and generalized retinal degeneration related to a primary deficiency in RPE function, rendering it unable to properly phagocytose shed rod outer segments. This leads to accumulation of these photoreceptor waste products and retinal toxicity. As observed with *rd* mutations in mice, this form is early-onset and progressive. It is also associated with eventual development of secondary cataract (see **Diseases of the Lens—Cataracts**) as well as atrophy of the ciliary processes (Bourne et al. 1938; Yamaguchi et al. 1991; Zigler and Hess 1985). Funduscopic findings are also similar to *rd* mice, with generalized pallor of the fundus and retinal vascular attenuation (Taradach et al. 1984). Progression of the disease may also be expedited by excessive light exposure (LaVail and Battelle 1975).

Mice and rats are also particularly predisposed to light-induced (phototoxic) retinal degeneration. Even under standard vivarium lighting conditions, over 10% of rats older than 2 years have retinal lesions consistent with phototoxicity (Williams 2002) (also Bell et al. 2015). The exact mechanism of toxicity is not known, but three models centered around activation of retinal rhodopsin have been proposed (Noell et al. 1966; Gordon et al. 2002; Organisciak and Vaughan 2010). Excessive rhodopsin activation by light may lead to production of retinotoxic oxidative compounds, generation of a toxic product from the retinaldehyde component of rhodopsin, or creation of a metabolic abnormality that impacts retinal health.

Early descriptions of this retinopathy were in pigmented and albino rats in laboratory environments, exposed to short periods (<48 h) of high intensity light (with damage to the photoreceptors and RPE) or more prolonged exposure to continuous but low intensity light (with damage to only the photoreceptors) (Malik et al. 1986; Penn et al. 1985). Older animals are demonstrably more susceptible to phototoxic retinal degeneration (Malik et al. 1986; Joly et al. 2006). Other factors such as higher body temperature may impact the effect (Organisciak et al. 1995) and pigmentation may impart some degree of protection from phototoxicity (Rapp and Williams 1980; Rapp et al. 1990). Photic retinal

degeneration has also been reported in albino hamsters (Richardson 2008).

Ultimately, the consequence of retinal phototoxicity is blindness, with electroretinographic attenuation observed even after one day of continuous light exposure. Ophthalmoscopic lesions of fundus pallor and retinal vascular attenuation may not be visible until at least one week following exposure. Husbandry practices can effectively prevent phototoxicity, most notably by limiting light levels in an enclosure or habitat, providing areas for animal shelter or retreat within an enclosure and, most importantly, providing cycled illumination (12 h on, 12 h off) (Kern n.d.; Bellhorn et al. 1980; De Vera Mudry et al. 2013).

Incidental chorioretinal scarring may be observed in mice and rats without obvious cause or impact on visual function (Wilkie 2014; Van Herck et al. 1992). It has also been observed as an incidental finding in wild Myomorph species like the African giant pouched rat (Heller et al. 2018). Retinal degeneration may also be observed following inflammatory insult to the posterior segment. In mice, retinal degeneration may develop due to infection with lymphocytic choriomeningitis virus (LCM). While many mice are asymptomatic carriers for this virus, others may develop an associated immunopathologic retinitis, putatively related to retinal necrosis and an autoimmune reaction to retinal autoantigens (del Cerro et al. 1982; Monjan et al. 1972). In rats, SDAV infection may be associated with degenerative lesions of the choroid, RPE, and photoreceptors, though they may be incidental and not associated with detectable vision impairment (Tanaka et al. 1993).

A retinopathy has also been described in association with diabetes mellitus in Chinese hamsters (*Cricetulus griseus*) and may contribute to the spontaneous acute blindness that has been anecdotally reported in affected hamsters (Miedel and Hankenson 2015). Hamsters are also known to be susceptible to *Toxoplasma gondii*, and studies have demonstrated white, cystic lesions within the inner retina and subsequent retinal atrophy in experimentally infected animals (Valentine et al. 2012).

Primary neoplastic disease of the posterior segment is not commonly reported in the Myomorpha, but lymphosarcoma may disseminate to the choroid in mice, resulting in retinal infiltration and retinal detachment (Ramos et al. 2018).

Diseases of the optic nerve are rarely reported in the Myomorpha. Heritable abnormalities such as optic nerve dysplasia and aplasia are described, with the latter possibly being associated with retinal dysplasia (Shibuya et al. 1989, 1992, 1998). In many cases, however, there are not concurrent ocular abnormalities which can make clinical diagnosis of both conditions difficult (Shibuya et al. 1998). Optic disk colobomas are also reported in rats but ophthalmoscopic diagnosis may be complicated by the optic disks of small dimensions and lack of myelin (Hubert et al. 1994; Matsui and Kuno 1987; Taradach et al. 1981).

Ocular Reduction and Regression within the Myomorpha

While references have generally commented on the relatively large size of the eye in many Myomorpha species, (Lluch et al. 2008; Heard-Booth and Kirk 2012), there is remarkable diversity in globe dimensions, morphology, and the overall visual system within the Order. Some species within several Myomorph families like the Cricetidae, Platacanthomyidae, and Spalacidae demonstrate a tendency toward overall reduction in globe size and in some species, remarkable regression of ocular tissues. These variations are largely attributed to habitat and lifestyle. For example, predominantly subterranean (fossorial) Cricetid rodents like the voles (*Microtus* and *Arvicolinae* spp.) and Brazilian shrew mouse (*Blarinomys breviceps*) have notably reduced eye size in comparison to other members of their family like the hamsters (Donnelly et al. 2015; Lluch et al. 2007; Missagia and Perini 2018).

While most families within the Myomorpha possess general similarities in ocular functional anatomy, those of the Platacanthomyidae and Spalacidae families are characterized by a remarkable reduction in ocular size and presumably reduced visual function. Interesting anatomical variations in the Platacanthomyid Genus *Typhlomys* (the "blind mice") include reductions in lens size and vitreous chamber depth (with a total ocular axial length of only 1.4 mm), and the presence of an unusually folded retina that contains no more than 2500 retinal ganglion cells (Panyutina et al. 2017). Furthermore, *Typhlomys* species possess a mutation of the gene for interphotoreceptor retinoid binding protein (IRBP), a critical protein in the normal phototransduction cycle (Cheng et al. 2017). Collectively, these morphologic anomalies strongly suggest an inability for *Typhlomys* species to perceive and transmit an image to the brain as in other Myomorpha.

As the *Typhlomys* are a presumptively nocturnal species that lives in a semi-arboreal habitat, these variations are unexpected. Historically, activity in dim light or dark conditions has appeared to favor the evolutionary development and maintenance of larger, sighted eyes (Hall et al. 2012). Recent research, however, has presented evidence that *Typhlomys* species may instead rely on echolocation, as in Microchiropteran bats, for long-range navigation, even between tree branches.

The Spalacidae present nearly full ocular anatomical and functional regression of the overall visual system, creating an intrinsic microphthalmia which differentiates them morphologically from other families within the Order. There are over 35 extant species within the family Spalacidae,

predominantly found in Asia, Africa, and Eastern Europe, and predominantly across grasslands and forested habitats. They are non-hibernatory, predominantly solitary, and almost exclusively live underground in burrows, surfacing typically only to forage.

Putatively, ocular regression in the Spalacidae is an evolutionary adaptation to a predominantly fossorial or subterranean lifestyle. Physiologically, maintenance of a visual system is "energetically expensive" (Sumner-Rooney 2018). Thus, in environments where visual acuity is not of specific benefit to a species, evolution diverts its attention to the development of other systems and structures. In nocturnal species, like many of the Myomorpha, for example, morphologic and physiologic adaptation to low light may involve maximization of retinal sensitivity by sacrificing visual acuity or other visual specializations such as loss of color vision, spatial resolution, and neural summation (Sumner-Rooney 2018).

The blind mole-rat (*Spalax ehrenbergi*) has perhaps one of the most widely studied visual systems of the Spalacidae. Its common name, however, is a distinct misnomer as the species not only has eyes, but is not truly blind. Embryologically, the eyes of the blind mole-rat begin their differentiation identically to those of species with non-regressed eyes, with primordial tissue differentiation into tissues that would become surface epithelia, the lens, and the retina (Sanyal et al. 1990). However, early in the process of differentiation, the embryologic predecessor tissues of the anterior uvea (iris and ciliary body), proliferate within the anterior segment, preventing the formation of a normal anterior chamber, corneal stroma, Descemet's membrane, and endothelium. Thus the remaining anterior segment in the mature globe comprises predominantly pigmented and hypertrophied uvea (Herbin et al. 1995). The lens fibers differentiate abnormally, resulting in a vacuolated and disorganized nucleus at maturity. The optic fissure also fails to completely close, leaving the eyes structurally colobomatous and microphthalmic (Herbin et al. 1995).

At maturity, the globes of blind mole-rats are small (~0.6 mm in diameter) and situated subcutaneously, lacking an open palpebral fissure or other typical adnexal features (Burda 2006). There is a distinct and hypertrophied Harderian gland in which the reduced globe is embedded; but unlike similar glands in other non-Spalacidae, is bears only a rudimentary ductal system that opens into a conjunctival sac that is closed externally (Shanas et al. 1996). Secretions from the Harderian gland drain into the nasal cavity via a patent nasolacrimal drainage system, or through an anteromedial excretory duct that empties onto the surface of the adjacent skin. The Harderian gland of the blind mole-rat is also believed to produce pheromones that may fundamentally underlie the species' notoriety as an "aggressive" rodent. The globe also lacks distinct extraocular muscles or the cranial nerves expected in other mammalian species (Shanas et al. 1996).

Despite these developmental and morphological anomalies, the retina of the blind mole-rat interestingly undergoes relatively normal retinal embryogenesis developing distinct strata that, while reduced in thickness, include photoreceptor and retinal ganglion cell layers (Esquiva et al. 2016). Surprisingly, photoreceptors of Spalacidae like the blind mole-rat possess at least 3 photopigments (Burda 2006). Rod photopigments are at least 90% homologous with those of other mammals and structurally retain all features of a functional photoreceptor pigment (Janssen 2000). Short-wave cones, however, are absent (Burda 2006). The presence of 11-cis-retinaldehyde-based opsin in the photoreceptors and normal synapses of these cells in the outer plexiform layer support the belief that these eyes retain the ability to perceive light (Herbin et al. 1995). This is also supported by the identification of neurochemical activity in the suprachiasmatic nucleus (SCN) of the hypothalamus following exposure of the globe to light (Herbin et al. 1995). In mammals, this nucleus is known to play important roles in the synchronization of hormonal, physiological, and behavioral aspects of the photoperiodic life cycle (Cooper et al. 1993a).

The retina of the blind mole-rat has only ~900 retinal ganglion cells (RGCs) (Esquiva et al. 2016). Collectively, this relative paucity of RGCs yields a reduced optic nerve with fewer fibers in comparison to other species. Despite this reduction, the gross size of the optic nerve in the blind mole-rat and others like the lesser mole-rat (*Spalax leucodon*) may not be considerably reduced due to the persistence of glial cells and connective tissue (Herbin et al. 1995). The optic nerve fibers of these species are exclusively unmyelinated which differ distinctly from other mammals in which myelinated optic nerve fibers are more abundant.

The neuronal projections produced by the blind mole-rat retina course bilaterally to central centers that would typically receive afferent retinal signals in non-fossorial rodents (Cooper et al. 1993b). However, the morphology and distribution of these projections are reduced and comparatively disorganized and not likely to contribute to form perception and visual interpretation. Selective hypertrophy of structures and pathways that appear to mediate photoperiodic functions, including an expanded network of retinal projections to the SCN of the hypothalamus (Cooper et al. 1993a), remain and are comparatively well-developed. Collectively, these neuroanatomic and physiologic features suggest that the subcutaneous eyes of blind mole rats and similar species are critical to the normal mechanisms that dictate aspects of their activity, behavior, and ecology.

It is noteworthy that not all members of the family Spalacidae have subcutaneous eyes like those of the blind and lesser mole-rat. In the lesser bamboo rat (*Cannomys*

badius), reduced eyes are present but morphologically more similar to those of other Myomorpha and Rodents (Finlay and Sengelaub 1981). Furthermore, the common name "mole rat" is shared by other non-Myomorph species like the naked mole-rat (*Heterocephalus glaber*) and Ansell's mole rat (*Fukomys anselli*) whose eyes, though reduced, are not subcutaneous and do not possess the same morphologic anomalies as those of the blind mole rat. Conversely, the naked mole rat globe has a distinct cornea and lens (Hetling et al. 2005); and *F. Anselli*, despite having a reduced globe size and relatively small optic nerve, possesses a retina with a comparatively high percentage of cone cells (10%), predominantly short-wavelength blue cones (Burda 2006). Therefore, one must pay close attention to phylogeny as common nomenclature can create confusion.

Other Clinical Considerations in the Care and Treatment of Myomorpha

Examination

Clinical examination in small Myomorph rodents can pose challenges to the clinician or examiner, principally due to the small size of the globe in mice, rats, gerbils, and hamsters and others in the Order. Thorough assessment of the anterior segment requires high magnification, typically provided by a slit lamp biomicroscope. Detailed examination of the fundus requires dilation of the pupil with 0.5–1.0% tropicamide with or without topical phenylephrine. Pharmacologic dilation typically lasts for 1 h in non-pigmented rodents and up to 3–5 h in pigmented rodents (Wilkie 2014). It is noteworthy that anecdotal reports have indicated that achieving pupillary dilation in the hamster may be difficult with tropicamide alone, and hamsters may still constrict their pupils with light stimulation, even after full dilation (Taradach et al. 1984). Ophthalmoscopic examination requires indirect lenses with high dioptric strength (40D ideally for rats and hamsters, and 60D for mice and gerbils).

Examiners of small Myomorpha must also be aware of the intrinsic magnification factor in small eyes like those of the mouse and rat (Murphy and Rowland 1987). An often confusing optical effect of this magnification during ophthalmoscopic examination of the fundus is the artifactual "floating" appearance of the retinal vasculature. This artifact is so prominent in these species, that it may be misinterpreted as retinal separation.

Amaurosis in Rats

Amaurosis is blindness without identifiable structural cause on ophthalmic examination. Aged rats particularly those of higher body weight are at risk for development of pituitary adenomas (Jekl et al. 2017; Haseman et al. 1998). In one study of laboratory strains like the Fischer 344 and Sprague-Dawley rats, incidences were 45% and 39%, respectively; and female rats may be at higher risk (Dinse et al. 2010). These tumors may grow large enough to compress the optic chasm and cause amaurotic blindness (Mayer et al. 2011). Treatment of a blinding pituitary adenoma in a rat has been described using the dopamine receptor agonist cabergoline, resulting in subjective return to visual function within 3 days and clinical reduction in tumor size on MRI at 8 weeks of therapy (Mayer et al. 2011). However, recurrence of the tumor occurred at 8.5 months after beginning treatment in that report.

Antibiotic Use in Rodents

As in other species like the rabbit, practitioners should be cautious when prescribing medications, including topical ophthalmic medications as they could induce severe disease associated with dysbiosis and gastrointestinal disruption. In any Myomorph species, the practitioner should be very cautious about administering penicillins, lincosamides, aminoglycosides, cephalosporins, and erythromycin (Hedley 2018). In hamsters, the above antibiotics may be associated with severe necrotizing cecocolitis that can be life-threatening. Antibiotics that are safer include metronidazole, sulfonamides, chloramphenicol, fluoroquinolone, and tetracyclines, the two latter being commercially available in the US (Hedley 2018).

Anesthetic and Surgical Considerations

Unlike other species, small rodents may have low-grade and subclinical respiratory disease, including respiratory infections, which risk complicating anesthesia. Other important factors that must be considered are that the majority of rodents are obligate nose-breathers, so care should be taken to ensure that the nares are unobstructed. Due to their large body surface area to volume ratio, small rodents are also at higher risk for hypothermia, fluid losses, and dehydration while under general anesthesia. Due to their high metabolic rate, any small rodent should not be fasted for prolonged periods prior to being anesthetized. Mice should be fasted for no longer than 60 min and rats, gerbils, and hamsters for no longer than 90 min prior to anesthesia (Girling 2009). However, with proper preparation and attention, anesthesia can safely be maintained for very long periods of time, as needed in some electrophysiologic studies (Barriga-Rivera et al. 2018).

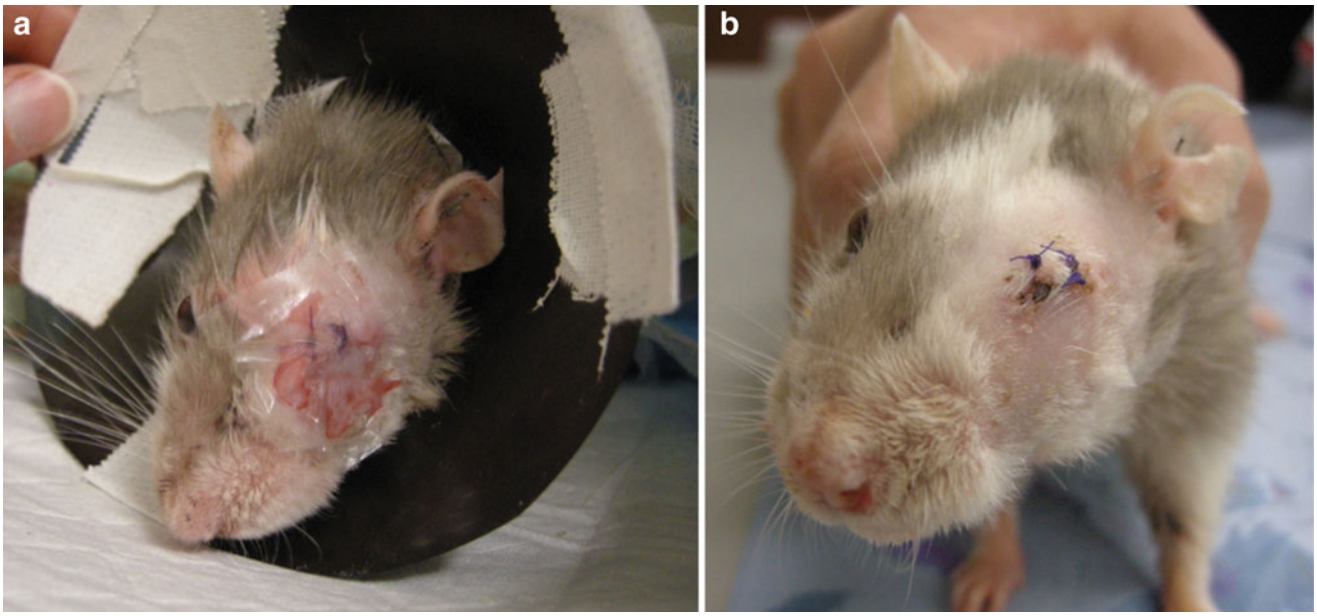

Fig. 46.21 Post-op enucleation in a domestic rat (*Rattus norvegicus domestica*). (**a**) The immediate post-operative period, demonstrating the creation of an E-collar out of an old X-ray film. (**b**) Post-operative 2-weeks showing a healing incision. (Courtesy of the University of California Davis Comparative Ophthalmology Service)

Anesthetic drugs that are most commonly used in rodents include ketamine, xylazine, and medetomidine. Ketamine and xylazine can be administered intramuscularly (IM) or intraperitoneally (IP), generally yielding 30 min of anesthesia at 100–150 mg/kg and 5 mg/kg, respectively, in mice and hamsters, and 90 mg/kg and 5 mg/kg in rats (Girling 2009). In mice and hamsters, ketamine/xylaxine can be administered at 100–150 mg/kg and 5 mg/kg, respectively. It is noteworthy, however, that gerbils appear to be more sensitive to hypotension with alpha-2 agonists like xylazine, requiring reduction of the dose to 2–3 mg/kg. Other options in rodents include medetomidine at 0.5 mg/kg. Analgesics that are routinely used in rodents include butorphanol, buprenorphine, carprofen, flunixin, and meloxicam (Girling 2009). Gas anesthesia can be challenging due to the small size, especially when needing access to the eyes for ophthalmic procedures. However, special facemasks can be made and fitted to the face as needed (Bacellar et al. 2013).

In rodents with intractable ophthalmic disease-causing pain and blindness, enucleation may be indicated (Fig 46.21). This procedure is relatively commonly performed under general anesthesia in referral hospitals that routinely receive and treat pet rodents. Enucleation techniques published for larger animals (i.e., transpalpebral and subconjunctival approaches) are difficult to perform in small rodents; and as in rabbits, care to avoid the large orbital venous sinus or plexus should be taken. In one study of 2 rats and 13 mice undergoing routine enucleation, the surgical approach involved a routine preoperative ophthalmic preparation, proptosis of the globe and orbital glands using iris forceps, and direct transection of the globe's attachments. Sterile swabs were used to provide hemostasis and absorbable gelatin foam sponges packed into the orbit prior to closure. The eyelid margins were resected and the site closed with interrupted sutures and skin glue. Though almost all the animals resumed normal facial grooming behavior near or at the site immediately postoperatively, the only complication that was observed was dehiscence in one animal (Wilding et al. 2015).

References

Aleman TS, Cideciyan AV, Aguirre GK et al (2011) Human CRB1-associated retinal degeneration: comparison with the rd8 Crb1-mutant mouse model. Invest Ophthalmol Vis Sci 52:6898–6910

Antony BJ, Jeong W, Abràmoff MD, Vance J, Sohn EH, Garvin MK (2014) Automated 3D segmentation of intraretinal surfaces in SD-OCT volumes in normal and diabetic mice. Transl Vis Sci Technol 3(5):8

Astley RA, Chodosh J, Caire W, Wilson GM (2007) Conjunctival lymphoid follicles in new world rodents. 290:1190–1194. https://doi.org/10.1002/ar.20579

Bacellar M, Querubin J, Peterson-Jones SM (2013) A facemask for gaseous anesthesia in laboratory rodents and chicks that allows easy access to the eyes for ophthalmic procedures. Vet Ophthalmol 16:316–317

Baden T et al (2013) A tale of two retinal domains: near-optimal sampling of achromatic contrasts in natural scenes through asymmetric photoreceptor distribution. Neuron 80:1206–1217

Balazs T, Rubin L (1971) A note on the lens in aging Sprague-Dawley rats. Lab Anim Sci 21:267–268

Balent P, Halanova M, Sedlakova T, Valencakova A, Cislaková L (2004) Encephalitozoon cuniculi infection in rabbits and laboratory mice in eastern Slovakia. Bull Vet Inst Pulawy 48:113–116
Barathi V, Boopathi V, Yap EP, Beuerman RW (2008) Two models of experimental myopia in the mouse. Vis Res 48:904–916
Barrales D (1953) Listeriosis in lemmings. Can J Public Health 44:180–184
Barriga-Rivera A, Tatarinoff V, Lovell NH et al (2018) Long-term anesthetic protocol in rats: feasibility in electrophysiology studies in visual prosthesis. Vet Ophthalmol 21:290–297
Bártová E, Marková J, Sedlak K (2015) Prevalence of antibodies to Encephalitozoon cuniculi in European hares (Lepus europaeus). Ann Agric Environ Med 22:674–676
Batchelder M, Keller LS, Sauer MB, West WL (2012) The laboratory rabbit, Guinea pig, hamster, and other rodents. Elsevier, pp 1131–1155
Beasley AB (1963) Inheritance and development of a lens abnormality in the mouse. J Morphol 112:1–11
Beaumont SL (2002) Ocular disorders of pet mice and rats. Vet Clin North Am Exot Anim Pract 5:311–324
Beaumont SL, Maggs DJ, Clarke HE (2003) Effects of bovine lactoferrin on in vitro replication of feline herpesvirus. Vet Ophthalmol 6:245–250
Bell BA, Kaul C, Bonilha VL, Rayborn ME, Shadrach K, Hollyfield JG (2015) The BALB/c mouse: effect of standard vivarium lighting on retinal pathology during aging. Exp Eye Res 135:192–205
Bellhorn RW (1973) Ophthalmologic disorders of exotic and laboratory animals. Vet Clin North Am 3:345–356
Bellhorn RW, Burns MS, Benjamin JV (1980) Retinal vessel abnormalities of phototoxic retinopathy in rats. Invest Ophthalmol Vis Sci 19:584–595
Bellhorn R, Korte G, Abrutyn D (1988) Spontaneous corneal degeneration in the rat. Lab Anim Sci 38:46–50
Berger A, Cavallero S, Dominguez E et al (2014) Spectral-domain optical coherence tomography of the rodent eye: highlighting layers of the outer retina using signal averaging and comparison with histology. PLoS One 9:e96494
Beyerlein L (1953) The gross and microscopic structure of the hamster eye with special reference to accommodation
Bhatt P, Jacoby R (1985) Epizootiological observations of natural and experimental infection with sialodacryoadenitis virus in rats. Lab Anim Sci 35:129–134
Bhutto I, Amemiya T (1995) Corrosion cast demonstration of retinal vasculature of normal Wistar-Kyoto rats. Cells Tissues Organs 153:290–300
Bhutto IA, Amemiya T (2001) Microvascular architecture of the rat choroid: corrosion cast study. Anat Rec 264:63–71
Bourne MC, Campbell DA, Tansley K (1938) Hereditary degeneration of the rat retina. Br J Ophthalmol 22:613
Bredow L, Schwartzkopff J, Reinhard T (2014) Regeneration of corneal endothelial cells following keratoplasty in rats with bullous keratopathy. Mol Vis 20:683
Bron A, Tiffany J, Gouveia S, Yokoi N, Voon L (2004) Functional aspects of the tear film lipid layer. Exp Eye Res 78:347–360
Browman LG, Ramsey F (1943) Embryology of microphthalmos in Rattus norvegicus. Arch Ophthalmol 30:338–351
Brown AS, Zhang M, Cucevic V, Pavlin CJ, Foster FS (2005) In vivo assessment of postnatal murine ocular development by ultrasound biomicroscopy. Curr Eye Res 30:45–51
Bucana CD, Nadakavukaren MJ (1972) Fine structure of the hamster harderian gland. 129:178–187. https://doi.org/10.1007/bf00306934
Burda H (2006) Ear and eye in subterranean mole-rats, Fukomys anselli (Bathyergidae) and Spalax ehrenbergi (Spalacidae): progressive specialisation or regressive degeneration? 56:475–486. https://doi.org/10.1163/157075606778967847
Buttery RG, Hinrichsen CF, Weller WL, Haight JR (1991) How thick should a retina be? A comparative study of mammalian species with and without intraretinal vasculature. Vis Res 31:169–187
Buzzell GR (1996) Sexual dimorphism in the Harderian gland of the Syrian hamster is controlled and maintained by hormones, despite seasonal fluctuations in hormone levels: functional implications. Microsc Res Tech 34:133–138
Bytyqi AH, Layer PG (2005) Lamina formation in the Mongolian gerbil retina (Meriones unguiculatus). 209:217–225. https://doi.org/10.1007/s00429-004-0443-9
Calderone JB, Jacobs GH (1999) Cone receptor variations and their functional consequences in two species of hamster. Vis Neurosci 16:53–63
Calderone L, Grimes P, Shalev M (1986) Acute reversible cataract induced by xylazine and by ketamine-xylazine anesthesia in rats and mice. Exp Eye Res 42:331–337
Carthew P, Slinger R (1981) Diagnosis of sialodacryoadenitis virus infection of rats in a virulent enzootic outbreak. Lab Anim 15:339–342
Chacaltana FDYC et al (2017) Persistent papillary membrane in Wistar laboratory rats (Rattus Norvegicus, Albinus variation, Wistar). Ciência Rural 47
Chalupský J, Vávra J, Bedrník P (1979) Encephalitozoonosis in laboratory animals—a serological survey. Folia Parasitol 26:1–8
Chamberlain JG, Nelson MM (1963) Multiple congenital abnormalities in the rat resulting from acute maternal niacin deficiency during pregnancy. Exp Biol Med 112:836–840
Chandra M, Frith C (1993) Histopathologic and immunohistochemical features of two spontaneously generated ocular schwannomas in Sprague Dawley rats. Lab Anim Sci 43:500–502
Change B, Hurd R, Wang J et al (2013) Survey of common eye diseases in laboratory mouse strains. Investig Ophthalmol Vis Sci 7:4974–4981
Chen J, Qian H, Horai R, Chan C-C, Caspi R (2015) Mouse models of experimental autoimmune uveitis: comparative analysis of adjuvant-induced vs spontaneous models of uveitis. Curr Mol Med 15:550–557
Cheng F et al (2017) Phylogeny and systematic revision of the genus Typhlomys (Rodentia, Platacanthomyidae), with description of a new species. J Mammal 98:731–743. https://doi.org/10.1093/jmammal/gyx016
Choi SO et al (2015) Recovery of corneal endothelial cells from periphery after injury. PLoS One 10:e0138076
Chou T-H et al (2011) Postnatal elongation of eye size in DBA/2J mice compared with C57BL/6J mice: in vivo analysis with whole-eye OCT. Invest Ophthalmol Vis Sci 52:3604–3612
Chu XK, Wang Y, Ardeljan D, Tuo J, Chan CC (2013) Controversial view of a genetically altered mouse model of focal retinal degeneration. Bioengineered 4:130–135
Cliff GM, Anderson RC, Mallory FF (1978) Dauerlarvae of Pelodera strongyloides (Schneider, 1860) (Nematoda: Rhabditidae) in the conjunctival sacs of lemmings. 56:2117–2121. https://doi.org/10.1139/z78-287
Cohan BE, Bohr DF (2001a) Goldmann applanation tonometry in the conscious rat. Invest Ophthalmol Vis Sci 42(2):340–342
Cohan BE, Bohr DF (2001b) Measurement of intraocular pressure in awake mice. Invest Ophthalmol Vis Sci 42(11):2560–2562
Cohn SA (1955) Histochemical observations on the Harderian gland of the albino mouse. J Histochem Cytochem 3:342–353
Cook CS (1991) Eye and ear. Springer, pp 125–132
Cook CS, Sulik KK (1986) Sequential scanning electron microscopic analyses of normal and spontaneously occurring abnormal ocular development in C57B1/6J mice. Scan Electron Microsc:1215–1227
Cooper HM, Herbin M, Nevo E (1993a) Ocular regression conceals adaptive progression of the visual system in a blind subterranean mammal. Nature 361:156–159

Cooper HM, Herbin M, Nevo E (1993b) Visual system of a naturally microphthalmic mammal: the blind mole rat, Spalax ehrenbergi. 328:313–350. https://doi.org/10.1002/cne.903280302
Cutlip R, Beall C (1989) Encephalitozoonosis in arctic lemmings. Lab Anim Sci 39:331–333
Cutlip RC, Dennis ED (1993) Retrospective study of diseases in a captive Lemming Colony. 29:620–622. https://doi.org/10.7589/0090-3558-29.4.620
Danias J et al (2002) Cytoarchitecture of the retinal ganglion cells in the rat. Invest Ophthalmol Vis Sci 43:587–594
De Vera Mudry MC, Kronenberg S, Komatsu S-i, Aguirre GD (2013) Blinded by the light: retinal phototoxicity in the context of safety studies. Toxicol Pathol 41:813–825
del Cerro M, Grover DA, Monjan AA, Pfau CJ, Dematte JE (1982) Chronic retinitis in rats infected as neonates with lymphocytic choriomeningitis virus: a clinical, histopathologic, and electroretinographic study. Invest Ophthalmol Vis Sci 23:697–714
DiCarlo C (2001) Cataracts in the fat sand rat: an ocular complication of diabetes. Uniformed Services Univ of the Health Sciences, Bethesda, MD
Dickie P et al (1996) Myopathy and spontaneous Pasteurella pneumotropica-induced abscess formation in an HIV-1 transgenic mouse model. J Acquir Immune Defic Syndr 13:101–116
Dickman ED, Thaller C, Smith SM (1997) Temporally-regulated retinoic acid depletion produces specific neural crest, ocular and nervous system defects. Development 124:3111–3121
DiLoreto D et al (1994) The influences of age, retinal topography, and gender on retinal degeneration in the Fischer 344 rat. Brain Res 647:181–191
DiLoreto D, Ison JR, Bowen GP, Cox C, Cerro M d (1995) A functional analysis of the age-related degeneration in the Fischer 344 rat. Curr Eye Res 14:303–310
Dinse GE, Peddada SD, Harris SF, Elmore SA (2010) Comparison of NTP historical control tumor incidence rates in female Harlan Sprague Dawley and Fischer 344/N rats. Toxicol Pathol 38:765–775
Djeridane Y (1994) The harderian gland and its excretory duct in the Wistar rat. A histological and ultrastructural study. J Anat 184:553
Djeridane Y (1996) Comparative histological and ultrastructural studies of the Harderian gland of rodents. Microsc Res Tech 34:28–38
Donnelly TM, Bergin I, Ihrig M (2015) Laboratory animal medicine. Elsevier, pp 285–349
Drager UC (1978) Observations on monocular deprivation in mice. J Neurophysiol 41:28–42
Durand G et al (2001) Spontaneous polar anterior subcapsular lenticular opacity in Sprague-Dawley rats. Comp Med 51:176–179
Duray PH, Johnson RC (1986) The histopathology of experimentally infected hamsters with the Lyme disease spirochete, Borrelia burgdorferi. Proc Soc Exp Biol Med 181:263–269
Dursun D et al (2002) A mouse model of keratoconjunctivitis sicca. Invest Ophthalmol Vis Sci 43:632–638
Eiben R (2001) Frequency of spontaneous opacities in the cornea and lens observed in chronic toxicity studies in Wistar rats: experience with a standardized terminology glossary (Hattersheimer Kreis). Res Commun Pharmacol Toxicol 6:238–251
Eisenbrandt D, Hubbard G, Schmidt R (1982) A subclinical epizootic of sialodacryoadenitis in rats. Lab Anim Sci 32:655–659
Ekesten B, Dubielzig RR (1999) Spontaneous buphthalmos in the Djungarian hamster (Phodopus sungorus campbelli). Vet Ophthalmol 2:251–254
Ellis C, Mori M (2001) Skin diseases of rodents and small exotic mammals. Vet Clin North Am Exot Anim Pract 4:493–542
Esquiva G, Avivi A, Hannibal J (2016) Cone opsin in the subterranean blind mole rat, Spalax Ehrenbergi: immunohistochemical characterization, distribution, and connectivity. Front Neuroanat 10:61. https://doi.org/10.3389/fnana
Ferguson LR, Dominguez JM II, Balaiya S, Grover S, Chalam KV (2013) Retinal thickness normative data in wild-type mice using customized miniature SD-OCT. PLoS One 8:e67265
Fernandez JR-R, Dubielzig RR (2013) Ocular comparative anatomy of the family Rodentia. Vet Ophthalmol 16(Suppl 1):94–99
Field KJ, Sibold AL (1998) The laboratory hamster and gerbil. CRC Press
Finlay BL, Sengelaub DR (1981) Toward a neuroethology of mammalian vision. 3:133–149. https://doi.org/10.1016/0166-4328(81)90044-9
Fischer MD, Huber G, Beck SC et al (2009) Noninvasive, in vivo assessment of mouse retinal structure using optical coherence tomography. PLoS One 4:e7507
Fraser FC, Herer ML (1948) Lens rupture, a new recessive gene in the house mouse. J Hered 39:149
Fraser FC, Herer ML (1950) The inheritance and expression of the lens rupture' gene in the house mouse. J Hered 41:3
Frisk CS (2012) The laboratory rabbit, Guinea pig, hamster, and other rodents. Elsevier, pp 797–820
Fuehrer H-P, Blöschl I, Siehs C, Hassl A (2010) Detection of toxoplasma gondii, Neospora caninum, and Encephalitozoon cuniculi in the brains of common voles (Microtus arvalis) and water voles (Arvicola terrestris) by gene amplification techniques in western Austria (Vorarlberg). Parasitol Res 107:469–473
Gale TF, Layton WM (1980) The susceptibility of inbred strains of hamsters to cadmium-induced embryotoxicity. Teratology 21:181–186
Gannon J, Carthew P (1980) Prevalence of indigenous viruses in laboratory animal colonies in the United Kingdom 1978–1979. Lab Anim 14:309–311
Germain MA, Webster WS, Edwards MJ (1985) Hyperthermia as a teratogen: parameters determining hyperthermia-induced head defects in the rat. Teratology 31:265–272
Gilger BC et al (2018) Standards for ocular toxicology and inflammation. Springer, pp 141–168
Gillet J et al (1995) Ocular toxicology. Springer, pp 335–342
Girling S (2009) Rabbits, ferrets and rodent Anaesthesia. Anaesthesia for veterinary nurses, pp 317–335
Glastonbury JRW, Morton JG, Matthews LM (1996) Streptobacillus moniliformis infection in Swiss white mice. J Vet Diagn Invest 8:202–209
Gordon WC, Casey DM, Lukiw WJ, Bazan NG (2002) DNA damage and repair in light-induced photoreceptor degeneration. Invest Ophthalmol Vis Sci 43:3511–3521
Gouras P, Ekesten B (2004) Why do mice have ultra-violet vision? Exp Eye Res 79:887–892
Graw J (1999) Mouse models of congenital cataract. Eye 13:438
Greaves P, Faccini J (1981) Spontaneous fibrous histiocytic neoplasms in rats. Br J Cancer 43:402–411
Griffin HE, Boyce JT, Bontempo JM (1995) Diagnostic exercise: ophthalmitis in nude mice housed in ventilated micro-isolator cages. Lab Anim Sci 45:595
Guggenheim J, Creer R, Qin X-J (2004) Postnatal refractive development in the Brown Norway rat: limitations of standard refractive and ocular component dimension measurement techniques. Curr Eye Res 29:369–376
Hall MI, Kamilar JM, Kirk EC (2012) Eye shape and the nocturnal bottleneck of mammals. Proc R Soc B Biol Sci 279:4962–4968
Hanna PE, Percy DH, Paturzo F, Bhatt PN (1984) Sialodacryoadenitis in the rat: effects of immunosuppression on the course of the disease. Am J Vet Res 45:2077–2083
Hartman H (1968) Naturally occurring cataracts in the term fetal rat. J Am Vet Med Assoc 153:832–840
Haseman JK, Hailey JR, Morris RW (1998) Spontaneous neoplasm incidences in Fischer 344 rats and B6C3F1 mice in two-year

carcinogenicity studies: a National Toxicology Program update. Toxicol Pathol 26:428–441. https://doi.org/10.1177/019262339802600318
Hashimoto S et al (2013) Corneal mineralization in Wistar Hannover rats. J Toxicol Pathol 26:275–281
Hawes NL et al (1999) Mouse fundus photography and angiography: a catalogue of normal and mutant phenotypes. Mol Vis 5:22
Hayashi S, Osawa T, Tohyama K (2002) Comparative observations on corneas, with special reference to Bowman's layer and Descemet's membrane in mammals and amphibians. J Morphol 254:247–258
Heard-Booth AN, Kirk EC (2012) The influence of maximum running speed on eye size: a test of Leuckart's law in mammals. Anat Rec Adv Integr Anat Evol Biol 295:1053–1062. https://doi.org/10.1002/ar.22480
Heatley JJ, Harris MC (2009) Manual of exotic pet practice. Elsevier, pp 406–432
Hedley J (2018) Antibiotic usage in rabbits and rodents. In Pract 40:230–237
Hedley J (n.d.) BSAVA Congress proceedings 2016. BSAVA Library, pp 50–51
Heesy CP (2004) On the relationship between orbit orientation and binocular visual field overlap in mammals. Anat Rec 281:1104–1110
Heller AR, Ledbetter EC, Singh B, Lee DN, Ophir AG (2018) Ophthalmic examination findings and intraocular pressures in wild-caught African giant pouched rats (Cricetomys spp.). Vet Ophthalmol. https://doi.org/10.1111/vop.12534
Henriksson JT, McDermott AM, Bergmanson JP (2009) Dimensions and morphology of the cornea in three strains of mice. Invest Ophthalmol Vis Sci 50:3648–3654
Herbin M et al (1995) Ultrastructural study of the optic nerve in blind mole-rats (Spalacidae, Spalax). 12:253. https://doi.org/10.1017/s0952523800007938
Hetling JR et al (2005) Features of visual function in the naked mole-rat Heterocephalus glaber. J Comp Physiol A 191:317–330. https://doi.org/10.1007/s00359-004-0584-6
Heywood R (1973) Some clinical observations on the eyes of Sprague-Dawley rats. Lab Anim 7:19–27
Heywood R (1975) Glaucoma in the rat. Br Vet J 131:213–221
Hill A (1974) Experimental and natural infection of the conjunctiva of rats. Lab Anim 8:305–310
Hinney B, Sak B, Joachim A, Kváč M (2016) More than a rabbit's tale—Encephalitozoon spp. in wild mammals and birds. https://doi.org/10.1016/j.ijppaw.2016.01.001
Hoffman RW, Alspaugh MA, Waggie KS, Durham JB, Walker SE (1984) Sjögren's syndrome in MRL/l and MRL/n mice. Arthritis Rheum 27:157–165
Hoffman RA, Johnson LB, Reiter RJ (1985) Harderian glands of golden hamsters: temporal and sexual differences in immunoreactive melatonin. 2:161–168. https://doi.org/10.1111/j.1600-079x.1985.tb00636.x
Holland J, Fry R (1982) Neoplasms of the integumentary system and Harderian gland. The mouse in biomedical research. 4:513–528
Hubert M-F, Gillet J-P, Durand-Cavagna G (1994) Spontaneous retinal changes in Sprague Dawley rats. Lab Anim Sci 44:561–567
Hubert M-F, Gerin G, Durand-Cavagna G (1999) Spontaneous ophthalmic lesions in young Swiss mice. Comp Med 49:232–240
Hughes R, Geeraets W (n.d.) Genetics. 962- & . 428 East Preston St, Baltimore, MD 21202.
Hurley LS, Gowan J, Swenerton H (1971) Teratogenic effects of short-term and transitory zinc deficiency in rats. Teratology 4:199–204
Hwang K, Park S, Kim DJ (2012) Lateral orbital rim; open or closed in mammals. J Craniofac Surg 23:1870–1872
Ilia M, Jeffery G (2000) Retinal cell addition and rod production depend on early stages of ocular melanin synthesis. J Comp Neurol 420:437–444
Innes JM, Stanton MF (1961) Acute disease of the submaxillary and Harderian glands (sialo-dacryoadenitis) of rats with Cytomegaly and no inclusion bodies: with comments on Normal gross and microscopic structure of the exocrine glands in the head and neck of rats. Am J Pathol 38:455
Jackson CG (1981) Prenatal development of the microphthalmic eye in the golden hamster. J Morphol 167:65–90
Jacobs GH (1993) The distribution and nature of colour vision among the mammals. Biol Rev 68:413–471. https://doi.org/10.1111/j.1469-185x.1993.tb00738.x
Jacobs GH, Fenwick JA, Williams GA (2001) Cone-based vision of rats for ultraviolet and visible lights. J Exp Biol 204:2439–2446
Jakus MA (1954) Studies on the cornea*: I. The fine structure of the rat cornea. Am J Ophthalmol 38:40–53
Janssen JWH (2000) A fully functional rod visual pigment in a blind mammal. A case for adaptive functional reorganization? 275:38674–38679. https://doi.org/10.1074/jbc.m008254200
Jekl V, Hauptman K, Knotek Z (2017) Evidence-based advances in rodent medicine. Vet Clin Exot Anim Pract 20:805–816
Johansson J-O (1987) The lamina cribrosa in the eyes of rats, hamsters, gerbils and Guinea pigs. 128:55–62. https://doi.org/10.1159/000146315
Johnson D, Rudeen P, O'steen W (1979) Photically induced experimental exophthalmos: role of Harderian and pituitary glands. Invest Ophthalmol Vis Sci 18:1280–1285
Johnson TV, Fan S, Toris CB (2008) Rebound tonometry in conscious, conditioned mice avoids the acute and profound effects of anesthesia on intraocular pressure. J Ocul Pharmacol Ther 24:175–185
Joly S, Pernet V, Dorfman AL, Chemtob S, Lachapelle P (2006) Light-induced retinopathy: comparing adult and juvenile rats. Invest Ophthalmol Vis Sci 47:3202–3212
Keeler CE (1970) Reoccurrence of four-row rodless mice. Arch Ophthalmol 84:499–504
Kern TJ (1989) Ocular disorders of rabbits, rodents, and ferrets. In: Current veterinary therapy. WB Saunders, Philadelphia, pp 681–685
Kern TJ (n.d.) Seminars in avian and exotic pet medicine. Elsevier, pp 138–145
Kim CY, Kuehn MH, Anderson MG, Kwon YH (2007) Intraocular pressure measurement in mice: a comparison between Goldmann and rebound tonometry. Eye (Lond) 21:1202–1209
Kinney HC, Klintworth GK, Lesiewicz J, Goldsmith LA, Wilkening B (1982) Congenital cystic microphthalmia and consequent anophthalmia in the rat: a study in abnormal ocular morphogenesis. Teratology 26:203–212
Kling MA (2011) A review of respiratory system anatomy, physiology, and disease in the mouse, rat, hamster, and gerbil. Vet Clin North Am Exot Anim Pract 14:287
Kobayashi K, Otani K (1981) Morphogenesis of the hereditary microphthalmia in a new strain of rat. J Morphol 167:265–276
Kocianová-Adamcová M, Špakulová M, Kocianová E (2006) Long-term variation in an occurrence of Rhabditis orbitalis parasitic larvae (Nematoda, Rhabditidae) in the eyes of montane rodents. Helminthologia 43:232–236
Koehn D, Meyer KJ, Syed NA, Anderson MG (2015) Ketamine/Xylazine-induced corneal damage in mice. PLoS One 10:e0132804
Kohn DF, Clifford CB (2002) Biology and diseases of rats. Laboratory Animal Medicine 2:121–167
Kojima T et al (2014) The effects of 3% diquafosol sodium application on the tear functions and ocular surface of the cu, Zn-superoxide dismutase-1 (Sod1)–knockout mice. Mol Vis 20:929
Kuno H, Usui T, Eydelloth SR, Wolf ED (1991) Spontaneous ophthalmic lesions in young Sprague-Dawley rats. J Vet Med Sci 53:607–614
Kurisu K, Sawamoto O, Watanabe H, Ito A (1996) Sequential changes in the harderian gland of rats exposed to high intensity light. Lab Anim Sci 46:71–76

Kurotaki T, Tomonari Y, Kanno T, Wako Y, Tsuchitani M (2008) Malignant amelanotic melanoma behind the left eye in a female Crj: CD (SD) IGS rat: a case report. Vet Pathol 45:681–684
Lai V, Rana M (1985) Folding of photoreceptor cell layer: a new form of retinal lesion in rat. Invest Ophthalmol Vis Sci 26:771–774
Lai Y, Jacoby R, Bhatt P, Jonas A (1976) Keratoconjunctivitis associated with sialodacryoadenitis in rats. Invest Ophthalmol Vis Sci 15:538–541
Lai Y-L, Jacoby RO, Jonas AM (1978) Age-related and light-associated retinal changes in Fischer rats. Invest Ophthalmol Vis Sci 17:634–638
Lange RR, Lima L, Przydzimirski AC, Montiani-Ferreira F (2014) Reference values for the production of the aqueous fraction of the tear film measured by the standardized endodontic absorbent paper point test in different exotic and laboratory animal species. Vet Ophthalmol 17:41–45
LaVail MM, Battelle B-A (1975) Influence of eye pigmentation and light deprivation on inherited retinal dystrophy in the rat. Exp Eye Res 21:167–192
Lee P (1989) Ophthalmic findings in laboratory animals. Anim Eye Res 8:1–12
Li Y, Fariss RN, Qian JW, Cohen ED, Qian H (2016) Light-induced thickening of photoreceptor outer segment layer detected by ultra-high resolution OCT imaging. Invest Ophthalmol Vis Sci 57: OCT105–OCT111
Lima L, Montiani-Ferreira F, Sousa R, Langohr I (2012) Intraocular signet-ring cell melanoma in a hamster (Cricetulus griseus). 15:53–58. https://doi.org/10.1111/j.1463-5224.2010.00871.x
Lin W, Essner E (1987) An electron microscopic study of retinal degeneration in Sprague-Dawley rats. Lab Anim Sci 37:180–186
Lin W-L, Essner E (1988) Retinal dystrophy in Wistar-Furth rats. Exp Eye Res 46:1–12
Lluch S, Ventura J, López-Fuster MJ (2007) Eye morphology in some wild rodents. 0:070817155721003. https://doi.org/10.1111/j.1439-0264.2007.00796.x
Lluch S, Ventura J, López-Fuster M (2008) Eye morphology in some wild rodents. Anat Histol Embryol 37:41–51
Lozano DC, Twa MD (2013) Development of a rat schematic eye from in vivo biometry and the correction of lateral magnification in SD-OCT ImagingLateral magnification correction in SD-OCT imaging. Invest Ophthalmol Vis Sci 54(9):6446–6455
Luhmann UF, Carvalho LS, Holthaus SM et al (2015) The severity of retinal pathology in homozygous Crb1rd8/rd8 mice is dependent on additional genetic factors. Hum Mol Genet 24:128–141
Lukáts Á et al (2002) Visual pigment coexpression in all cones of two rodents, the Siberian hamster, and the pouched mouse. Invest Ophthalmol Vis Sci 43:2468–2473
Lund R, Lund JS, Wise RP (1974) The organization of the retinal projection to the dorsal lateral geniculate nucleus in pigmented and albino rats. J Comp Neurol 158:383–403
Magnusson G, Majeed S, Offer J (1978) Intraocular melanoma in the rat. Lab Anim 12:249–252
Malik S, Cohen D, Meyer E, Perlman I (1986) Light damage in the developing retina of the albino rat: an electroretinographic study. Invest Ophthalmol Vis Sci 27:164–167
Mangkoewidjojo S, Kim J (1977) Malignant melanoma metastatic to the lung in a pet hamster. Lab Anim 11:125–127
Mankin EA et al (2019) The hippocampal code for space in Mongolian gerbils. Hippocampus. https://doi.org/10.1002/hipo.23075
Manning WS, Greenlee PG, Norton JN (2004) Ocular melanoma in a long Evans rat. J Am Assoc Lab Anim Sci 43:44–46
Matsui K, Kuno H (1987) Spontaneous ocular fundus abnormalities in the rat. Anim Eye Res 6:25–41
Matsuura T, Tsuji N, Kodama Y et al (2013) Iridal coloboma induces dyscoria during miosis in FLS mice. Vet Ophthalmol 16:186–191
Mattapallil MJ, Wawrousek EF, Chan CC et al (2012) The Rd8 mutation of the Crb1 gene is present in vendor lines of C57BL/6N mice and embryonic stem cells, and confounds ocular induced mutant phenotypes. Invest Ophthalmol Vis Sci 53:2921–2927
Mayer J, Sato A, Kiupel M, DeCubellis J, Donnelly T (2011) Extralabel use of cabergoline in the treatment of a pituitary adenoma in a rat. J Am Vet Med Assoc 239:656–660
McKinnon SJ et al (2009) Mouse models of retinal ganglion cell death and glaucoma. Exp Eye Res 88(4):816–824
McLenachan S et al (2015) Angiography reveals novel features of the retinal vasculature in healthy and diabetic mice. Exp Eye Res 138:6–21
McMenamin P, Al-Shakarchi M (1989) The effect of various levels of intraocular pressure on the rat aqueous outflow system. J Anat 162: 67
Miedel EL, Hankenson FC (2015) Laboratory animal medicine. Elsevier, pp 209–245
Missagia RV, Perini FA (2018) Skull morphology of the Brazilian shrew mouse Blarinomys breviceps (Akodontini; Sigmodontinae), with comparative notes on Akodontini rodents. Zool Anz 277:148–161. https://doi.org/10.1016/j.jcz.2018.09.005
Mohan K et al (2012) Characterization of structure and function of the mouse retina using pattern electroretinography, pupil light reflex, and optical coherence tomography. Vet Ophthalmol 15:94–104
Monjan AA, Silverstein AM, Cole GA (1972) Lymphocytic choriomeningitis virus-induced retinopathy in newborn rats. Investig Ophthalmol 11:850–856
Montero V (1973) Evoked responses in the rat's cortex to contralateral, ipsilateral and restricted photic stimulation. Brain Res 53:192–196
Moore BA, Leonard BC, Sebbag L et al (2018a) Identification of genes required for eye development by high-throughput screening of mouse knockouts. Commun Biol 1:236. https://doi.org/10.1038/s42003-018-0226
Moore BA, Roux MJ, Sebbag L et al (2018b) A population study of common ocular abnormalities in C57BL/6N rd8 mice. Investig Ophthalmol Vis Sci 6:2252–2261
Moore BA, Flenniken AM, Clary D et al (2019) Genome-wide screening of mouse knockouts reveals novel genes required for normal integumentary and oculocutaneous structure and function. Sci Rep 9: 11211. https://doi.org/10.1038/s41598-019-47286-2
Morrison J et al (1995) Structure and composition of the rodent lamina cribrosa. Exp Eye Res 60:127–135
Murphy CJ, Rowland HC (1987) The optics of comparative ophthalmoscopy. Vis Res 27:599–607
Naskar R, Thanos S (2006) Retinal gene profiling in a hereditary rodent model of elevated intraocular pressure. Mol Vis 12:1199–1210
Needham J, Cooper J (1975) An eye infection in laboratory mice associated with Pasteurella pneumotropica. Lab Anim 9:197–200
Ninomiya H, Inomata T (2005) Microvasculature of the hamster eye: scanning electron microscopy of vascular corrosion casts. Vet Ophthalmol 8:7–12
Ninomiya H, Inomata T (2006) Microvasculature of the mouse eye: scanning electron microscopy of vascular corrosion casts. 43:149–159. https://doi.org/10.1016/j.jeas.2006.05.002
Ninomiya H, Kuno H (2001) Microvasculature of the rat eye: scanning electron microscopy of vascular corrosion casts. Vet Ophthalmol 4: 55–59
Noell WK, Walker VS, Kang BS, Berman S (1966) Retinal damage by light in rats. Invest Ophthalmol Vis Sci 5:450–473
Organisciak DT, Vaughan DK (2010) Retinal light damage: mechanisms and protection. Prog Retin Eye Res 29:113–134
Organisciak DT, Darrow RM, Noell WK, Blanks JC (1995) Hyperthermia accelerates retinal light damage in rats. Invest Ophthalmol Vis Sci 36:997–1008
Owen R, Duprat P (1987) Leiomyoma of the iris in a Sprague-Dawley rat. J Comp Pathol 97:227–229

Padmanabhan R, Singh G, Singh S (1981) Malformations of the eye resulting from maternal hypervitaminosis a during gestation in the rat. Cells Tissues Organs 110:291–298
Panyutina AA, Kuznetsov AN, Volodin IA, Abramov AV, Soldatova IB (2017) A blind climber: the first evidence of ultrasonic echolocation in arboreal mammals. Integr Zool 12:172–184. https://doi.org/10.1111/1749-4877.12249
Paques M, Guyomard JL, Simonutti M et al (2007) Panretinal, high-resolution color photography of the mouse fundus. Invest Ophthalmol Vis Sci 48:2769–2774
Payne A (1994) The Harderian gland: a tercentennial review. J Anat 185:1
Pease ME, Hammond JC, Quigley HA (2006) Manometric calibration and comparison of TonoLab and TonoPen tonometers in rats with experimental glaucoma and in normal mice. J Glaucoma 15:512–519
Pellissier LP, Lundvig DM, Tanimoto N et al (2014) CRB2 acts as a modifying factor of CRB1-related retinal dystrophies in mice. Hum Mol Genet 23:3759–3771
Penn JS, Baker BN, Howard AG, Williams TP (1985) Retinal light-damage in albino rats: lysosomal enzymes, rhodopsin, and age. Exp Eye Res 41:275–284
Pennesi ME, Michaels KV, Magee SS et al (2012) Long-term characterization of retinal degeneration in rd1 and rd10 mice using spectral domain optical coherence tomography. Invest Ophthalmol Vis Sci 53:4644–4656
Percy D, Wojcinski Z, Schunk M (1989) Sequential changes in the Harderian and exorbital lacrimal glands in Wistar rats infected with sialodacryoadenitis virus. Vet Pathol 26:238–245
Pierro LJ, Spiggle J (1967) Congenital eye defects in the mouse I: corneal opacity in C57black mice. J Exp Zool 166:25–38
Pierro LJ, Spiggle J (1969) Congenital eye defects in the mouse. II. The influence of litter size, litter spacing, and suckling of offspring on risk of eye defects in C57BL mice. Teratology 2:337–343
Potts R, Dreher B, Bennett M (1982) The loss of ganglion cells in the developing retina of the rat. Dev Brain Res 3:481–486
Poulsom R, Hayes B (1988) Congenital retinal folds in Sheffield-Wistar rats. Graefes Arch Clin Exp Ophthalmol 226:31–33
Poulsom R, Marshall J (1985) Persistent hyaloid vasculature and vitreal haemorrhage in albino rats: a morphological and histological study. Exp Eye Res 40:155–160
Pritchett-Corning KR, Cosentino J, Clifford CB (2009) Contemporary prevalence of infectious agents in laboratory mice and rats. Lab Anim 43:165–173
Puk O, Dalke C, Favor J, de Angelis MH, Graw J (2006) Variations of eye size parameters among different strains of mice. Mamm Genome 17:851–857
Puk O, de Angelis MH, Graw J (2013) Longitudinal fundus and retinal studies with SD-OCT: a comparison of five mouse inbred strains. Mamm Genome 24:198–205
Rajaei SM, Sadjadi R, Sabzevari A, Ghaffari MS (2013) Results of phenol red thread test in clinically normal Syrian hamsters (Mesocricetus auratus). Vet Ophthalmol 16:436–439
Rajaei SM, Mood MA, Ghaffari MS et al (2015) Effects of short-term oral administration of trimethoprim-sulfamethoxazole on tear production in clinically normal Syrian hamsters. Vet Ophthalmol 18:83–85
Rajaei SM et al (2016) Results of selected ophthalmic diagnostic tests for clinically normal Syrian hamsters (Mesocricetus auratus). Am J Vet Res 77(1):72–76
Rajaei SM, Mood MA, Sadjadi R, Azizi F (2016a) Intraocular pressure, tear production, and ocular Echobiometry in Guinea pigs (Cavia porcellus). J Am Assoc Lab Anim Sci 55:475–479
Rajaei SM, Mood MA, Sadjadi R et al (2016b) Results of selected ophthalmic diagnostic tests for clinically normal Syrian hamsters (*Mesocricetus auratus*). Am J Vet Res 77:72–76
Rajaei SM, Mood MA, Paryani MR et al (2017) Effects of diurnal variation and anesthetic agents on intraocular pressure in Syrian hamsters (*Mesocricetus auratus*). Am J Vet Res 78:85–89
Ramos MF et al (2018) Nonproliferative and proliferative lesions of the Ratand mouse special sense organs (ocular [eye and glands], olfactory and Otic). J Toxicol Pathol 31:97S
Rao S, Sesikeran B (1992) Congenital anophthalmia in CFY rats: a newly identified autosomal recessive mutation. Laboratory animal science (USA)
Rapp L, Williams T (1980) The role of ocular pigmentation in protecting against retinal light damage. Vis Res 20:1127–1131
Rapp LM, Tolman BL, Koutz CA, Thum LA (1990) Predisposing factors to light-induced photoreceptor cell damage: retinal changes in maturing rats. Exp Eye Res 51:177–184
Richardson VC (2008) Diseases of small domestic rodents. John Wiley & Sons
Ridder W III, Nusinowitz S, Heckenlively RJ (2002) Causes of cataract development in anesthetized mice. Exp Eye Res 75:365–370
Roberts S, Gregory B (1980) Facultative Pasteurella ophthalmitis in hooded Lister rats. Lab Anim 14:323–324
Robinson R (1964) Genetic studies of the Syrian hamster. Genetica 35:241–250
Robinson ML, Holmgren A, Dewey MJ (1993) Genetic control of ocular morphogenesis: defective lens development associated with ocular anomalies in C57BL/6 mice. Exp Eye Res 56:7–16
Rodriguez-Ramos Fernandez J, Dubielzig RR (2013) Ocular comparative anatomy of the family Rodentia. 16:94–99. https://doi.org/10.1111/vop.12070
Roman D et al (2016) Ocular toxicity of AUY922 in pigmented and albino rats. Toxicol Appl Pharmacol 309:55–62
Rothwell T, Everitt A (1986) Exophthalmos in ageing rats with Harderian gland disease. Lab Anim 20:97–100
Rubin LF, Daly IW (1982) Ectopic pupil in mice. Lab Anim Sci 32:64
Runge PE, Hawes HL, Heckenlively JR, Langley SH, Roderick TH (1992) Autosomal dominant mouse cataract (Lop-10): consistent differences of expression in heterozygotes. Invest Ophthalmol Vis Sci 33:3202–3208
Saadi-Brenkia O, Hanniche N, Lounis S (2018) Microscopic anatomy of ocular globe in diurnal desert rodent Psammomys obesus (Cretzschmar, 1828). J Basic Appl Zool 79:43
Saari M (1975) Vascular remnants of pupillary membrane in the albino rat eye. Cells Tissues Organs 91:376–379
Saeki T, Aihara M, Ohashi M, Araie M (2008) The efficacy of TonoLab in detecting physiological and pharmacological changes of mouse intraocular pressure—comparison with TonoPen and microneedle manometery. Curr Eye Res 33:247–252
Sahu B, Chavali VR, Alapati A et al (2015) Presence of rd8 mutation does not alter the ocular phenotype of late-onset retinal degeneration mouse model. Mol Vis 21:273–284
Sainsbury A, Bright P, Morris P, Harris E (1996) British Medical Journal Publishing Group
Sakai T (1981) The mammalian Harderian gland: morphology, biochemistry, function and phylogeny. Arch Histol Jpn 44:299–333
Sakai T, Yohro T (1981) A histological study of the Harderian gland of Mongolian gerbils, Meriones meridianus. Anat Rec 200:259–270. https://doi.org/10.1002/ar.1092000304
Salinas-Navarro M et al (2009) A computerized analysis of the entire retinal ganglion cell population and its spatial distribution in adult rats. Vis Res 49:115–126
Samuel MO, Wanmi N, Oopade J (2019) Comparative topographic analyses on the foramen magnums of two hystricomorphs—the crested porcupine (Hystrix cristata) and greater cane rat (Thryonomys swinderianus). Implications for typology, phylogeny and evolution in rodents. Folia Morphol (Warsz). https://doi.org/10.5603/FM.a2019.0083

Sanyal S, Jansen H, De Grip W, Nevo E, De Jong W (1990) The eye of the blind mole rat, Spalax ehrenbergi. Rudiment with hidden function? Invest Ophthalmol Vis Sci 31:1398–1404
Sayers I, Smith S (2010) BSAVA manual of exotic pets. BSAVA Library, pp 1–27
Schafer KA, Render JA (2012) Assessing ocular toxicology in laboratory animals. Springer, pp 159–217
Schardein J, Lucas J, Fitzgerald J (1975) Retinal dystrophy in Sprague-Dawley rats. Lab Anim Sci 25:323–326
Schiavo D (1980) Multifocal retinal dysplasia in the Syrian hamster LAK: LVG (SYR). J Environ Pathol Toxicol 3:569–576
Schoeb TR (2000) Respiratory diseases of rodents. Vet Clin North Am Exot Anim Pract 3:481–496
Schulte F (1989) Life history of Rhabditis (Pelodera) orbitalis—a larval parasite in the eye orbits of arvicolid and murid rodents. Proc Helminthol Soc Wash 56:1–7
Seely J (1987) The Harderian gland. Lab Anim 16:33–39
Shanas U, Arensburg B, Hammel I, Hod I, Terkel J (1996) Quantitative histomorphology of the blind mole rat harderian gland. J Anat 188: 341
Sherwin C (2010) The husbandry and welfare of non-traditional laboratory rodents. In: Hubrecht R, Kirkwood J (eds) UFAW handbook on the care and management of laboratory animals. Wiley-Blackwell, pp 359–369
Shibuya K, Tajima M, Yamate J, Kudow S (1989) SAGE Publications Sage CA, Los Angeles, CA
Shibuya K, Tajima M, Yamate J (1992) Unilateral optic nerve aplasia in an F344 rat with special reference to pathomorphological changes of the optic nerve pathways. J Vet Med Sci 54:571–574
Shibuya K, Tajima N, Nunoya T (1998) Optic nerve dysplasia associated with meningeal defect in Sprague-Dawley rats. Vet Pathol 35:323–329
Shibuya K, Tajima M, Nunoya T (2000) Anophthalmia and retinal degeneration associated with stenosis of the optic foramen in Fischer 344 rats. Vet Pathol 37:264–267
Shibuya K, Nunoya T, Tajima M, Sakurai Y (2001) A case of primary congenital glaucoma in Fischer344 rat. J Toxicol Pathol 13:119–121
Shinomiya K, Ueta M, Kinoshita S (2018) A new dry eye mouse model produced by exorbital and intraorbital lacrimal gland excision. Sci Rep 8. https://doi.org/10.1038/s41598-018-19578-6
Shirai S (1978) Eye abnormalities in mouse fetuses caused by simultaneous irradiation of x-rays and ultrasound, 2. Senten Ijo 18:269–279
Shupe JM, Kristan DM, Austad SN et al (2006) The eye of the laboratory mouse remains anatomically adapted for natural conditions. Brain Behav Evol 67:39–52
Smith RS, Sundberg JP (2002) Strain background disease characteristics. In: John SWM, Nishina PM, Smith RS, Sundberg J (eds) Systemic evaluation of the mouse eye: anatomy, physiology, and biomethods. CRC Press, Boca Raton, FL, pp 67–75
Smith RS, Roderick TH, Sundberg JP (1994) Microphthalmia and associated abnormalities in inbred black mice. Lab Anim Sci 44: 551–560
Smith RS, Sundberg JP, Linder CC (1997) Mouse mutations as models for studying cataracts. Pathobiology 65:146–154
Smith RS, John SW, Nishina PM, Sundberg JP (2001) Systematic evaluation of the mouse eye: anatomy, pathology, and biomethods. CRC Press
Strömland K, Miller M, Cook C (1991) Ocular teratology. Surv Ophthalmol 35:429–446
Suckow MA, Weisbroth SH, Franklin CL (2005) The laboratory rat. Academic Press
Sumner-Rooney L (2018) The kingdom of the blind: disentangling fundamental drivers in the evolution of eye loss. Integr Comp Biol. https://doi.org/10.1093/icb/icy047
Sunderma FW Jr, Shen SK, Reid MC, Allpass PR (1981) Teratogenicity and embryotoxicity of nickel carbonyl in Syrian hamsters. Teratog Carcinog Mutagen 1:223–233
Szel A et al (1992) Unique topographic separation of two spectral classes of cones in the mouse retina. J Comp Neurol 325:327–342
Szél A et al (1994) Different patterns of retinal cone topography in two genera of rodents, Mus and Apodemus. Cell Tissue Res 276:143–150
Tanaka K et al (1993) Focal chorioretinal atrophy in rats. J Toxicol Pathol 6:205–211
Taradach C, Regnier B, Perraud J (1981) Eye lesions in Sprague-Dawley rats: type and incidence in relation to age. Lab Anim 15: 285–287
Taradach C, Greaves P, Rubin LF (1984) Spontaneous eye lesions in laboratory animals: incidence in relation to age. CRC Crit Rev Toxicol 12:121–147
Thanos S, Naskar R (2004) Correlation between retinal ganglion cell death and chronically developing inherited glaucoma in a new rat mutant. Exp Eye Res 79:119–129
Timm KI (1979) Orbital venous anatomy of the rat. Lab Anim Sci 29: 636–638
Tkatchenko TV, Shen Y, Tkatchenko AV (2010) Analysis of postnatal eye development in the mouse with high-resolution small animal magnetic resonance imaging. Invest Ophthalmol Vis Sci 51:21–27
Towne JW et al (2014) Elimination of Pasteurella pneumotropica from a mouse barrier facility by using a modified enrofloxacin treatment regimen. J Am Assoc Lab Anim Sci 53:517–522
Tripathi B, Tripathi R, Borisuth N, Dhaliwal R, Dhaliwal D (1991) Rodent models of congenital and hereditary cataract in man. Lens Eye Toxic Res 8:373–413
Tucker M (1997) Special sense organs and associated tissues. In: Diseases of the Wistar rat. Taylor and Francis, London, pp 237–245
Tucker MJ, Baker D (1967) Diseases of specific pathogen-free mice. In: Pathology of laboratory rats and mice. Blackwell Scientific, Oxford, pp 787–823
Turner PV, Albassam MA (2005) Susceptibility of rats to corneal lesions after injectable anesthesia. Comp Med 55:175–182
Tyan ML (1992) Effects of H-2 and vitamin a on eye defects in congenic mice. Proc Soc Exp Biol Med 199:123–127
Ubico SR, McLean RG, Cooksey LM (1996) Susceptibility of selected rodent species from Colorado to Borrelia burgdorferi. 32:293–299. https://doi.org/10.7589/0090-3558-32.2.293
Valentine H, Daugherity EK, Singh B, Maurer KJ (2012) The laboratory rabbit, Guinea pig, hamster, and other rodents. Elsevier, pp 875–906
van de Pavert SA, Kantardzhieva A, Malysheva A et al (2004) Crumbs homologue 1 is required for maintenance of photoreceptor cell polarization and adhesion during light exposure. J Cell Sci 117: 4169–4177
Van Der Merwe EL, Kidson SH (2014) The three-dimensional organisation of the post-trabecular aqueous outflow pathway and limbal vasculature in the mouse. 125:226–235. https://doi.org/10.1016/j.exer.2014.06.011
van der Woerdt A (2012) Ophthalmologic diseases in small pet mammals. Ferrets, Rabbits, and Rodents:523
Van Herck H et al (1992) Histological changes in the orbital region of rats after orbital puncture. Lab Anim 26:53–58
Wada A, Tsudzuki M (1998) Brief communication. Microphthalmia: a morphogenetic lethal mutation of the campbelli hamster (Phodopus campbelli). J Hered 89:93–96
Wagner JE, Farrar PL (1987) Husbandry and medicine of small rodents. Vet Clin N Am Small Anim Pract 17:1061–1087
Waiblinger E (2010) The laboratory gerbil. In: UFAW handbook on the care and management of laboratory animals, 8th edn. Wiley-Blackwell, Oxford, UK, pp 327–347
Walls GL (1944) LWW

Wang W-H, Millar JC, Pang I-H, Wax MB, Clark AF (2005) Noninvasive measurement of rodent intraocular pressure with a rebound tonometer. Invest Ophthalmol Vis Sci 46:4617–4621

Wang YV, Weick M, Demb JB (2011) Spectral and temporal sensitivity of cone-mediated responses in mouse retinal ganglion cells. J Neurosci 31:7670–7681

Weisbroth S, Peress N (1977) Ophthalmic lesions and dacryoadenitis: a naturally occurring aspect of sialodacryoadenitis virus infection of the laboratory rat. Lab Anim Sci 27:466

Wikler KC, Perez G, Finlay BL (1989) Duration of retinogenesis: its relationship to retinal organization in two cricetine rodents. 285: 157–176. https://doi.org/10.1002/cne.902850202

Wilding LA, Uchihashi M, Bergin IL, Nowland MH (2015) Enucleation for treating rodent ocular disease. J Am Assoc Lab Anim Sci 54: 328–332

Wilkie DA (2014) The ophthalmic examination as it pertains to general ocular toxicology: basic and advanced techniques and species-associated findings. Ocular Pharmacology and Toxicology:143–203

Wilkinson F (1986) Eye and brain growth in the Mongolian gerbil (Meriones unguiculatus). Behav Brain Res 19:59–69

Willhite C, Hill R, Irving D (1986) Isotretinoin-induced craniofacial malformations in humans and hamsters. J Craniofac Genet Dev Biol Suppl 2:193–209

Williams DL (2002) Ocular disease in rats: a review. Vet Ophthalmol 5: 183–191

Williams D (2007) Rabbit and rodent ophthalmology. Eur J Companion Anim Pract 17:242–252

Williams DL (2012) Ophthalmology of exotic pets. John Wiley & Sons

Wilson JM (1979) Encephalitozoon cuniculi in wild European rabbits and a fox. Res Vet Sci 26:114–114

Wilson DE, Reeder DM (2005) Mammal species of the world: a taxonomic and geographic reference, vol 1. JHU Press

Wojcinski Z et al (1999) A spontaneous corneal change in juvenile Wistar rats. J Comp Pathol 120:281–294

Wolf N et al (2005) Age-related cataract progression in five mouse models for anti-oxidant protection or hormonal influence. Exp Eye Res 81:276–285

Wyse J, Hollenberg M (1977) Complicated colobomatous microphthalmos in the BW rat: a new form of inherited retinal degeneration. Dev Dyn 149:377–411

Yamaguchi K, Yamaguchi K, Sheedlo HJ, Turner JE (1991) Ciliary body degeneration in the Royal College of surgeons dystrophic rat. Exp Eye Res 52:539–548

Yoon CH (1975) Total retinal degeneration in apparent anophthalmos of the Syrian hamster. Invest Ophthalmol Vis Sci 14:321–325

Yoshitomi K, Boorman G (1991a) Intraocular and orbital malignant schwannomas in F344 rats. Vet Pathol 28:457–466

Yoshitomi K, Boorman G (1991b) Spontaneous amelanotic melanomas of the uveal tract in F344 rats. Vet Pathol 28:403–409

Yoshitomi K, Boorman G (1993) Palpebral amelanotic melanomas in F344 rats. Vet Pathol 30:280–286

Yoshitomi K, Everitt J, Boorman G (1991) Primary optic nerve meningiomas in F344 rats. Vet Pathol 28:79–81

Young C, Hill A (1974) Conjunctivitis in a colony of rats. Lab Anim 8: 301–304

Young C, Festlng M, Barnett K (1974) Buphthalmos (congenital glaucoma) in the rat. Lab Anim 8:21–31

Zaffarano BA, Allbaugh RA, Whitley EM (2015) Bilateral Harderian gland abscesses in a Syrian dwarf hamster (Mesocricetus auratus). J Exot Pet Med 24:209–214

Zhang H et al (2013) The measurement of corneal thickness from center to limbus in vivo in C57BL/6 and BALB/c mice using two-photon imaging. 115:255–262. https://doi.org/10.1016/j.exer.2013.07.025

Zhang J, Yan H, Lou MF (2017) Does oxidative stress play any role in diabetic cataract formation?—re-evaluation using a thioltransferase gene knockout mouse model. Exp Eye Res:161, 36–142

Zhou X et al (2008) Biometric measurement of the mouse eye using optical coherence tomography with focal plane advancement. Vis Res 48:1137–1143

Zigler JS (1990) Animal models for the study of maturity-onset and hereditary cataract. Exp Eye Res 50:651–657

Zigler J, Hess H (1985) Cataracts in the Royal College of surgeons rat: evidence for initiation by lipid peroxidation products. Exp Eye Res 41:67–76

Ophthalmology of Primatomorpha: Lemurs, Tarsiers, Monkeys, Apes, and Relatives

47

Sara M. Thomasy

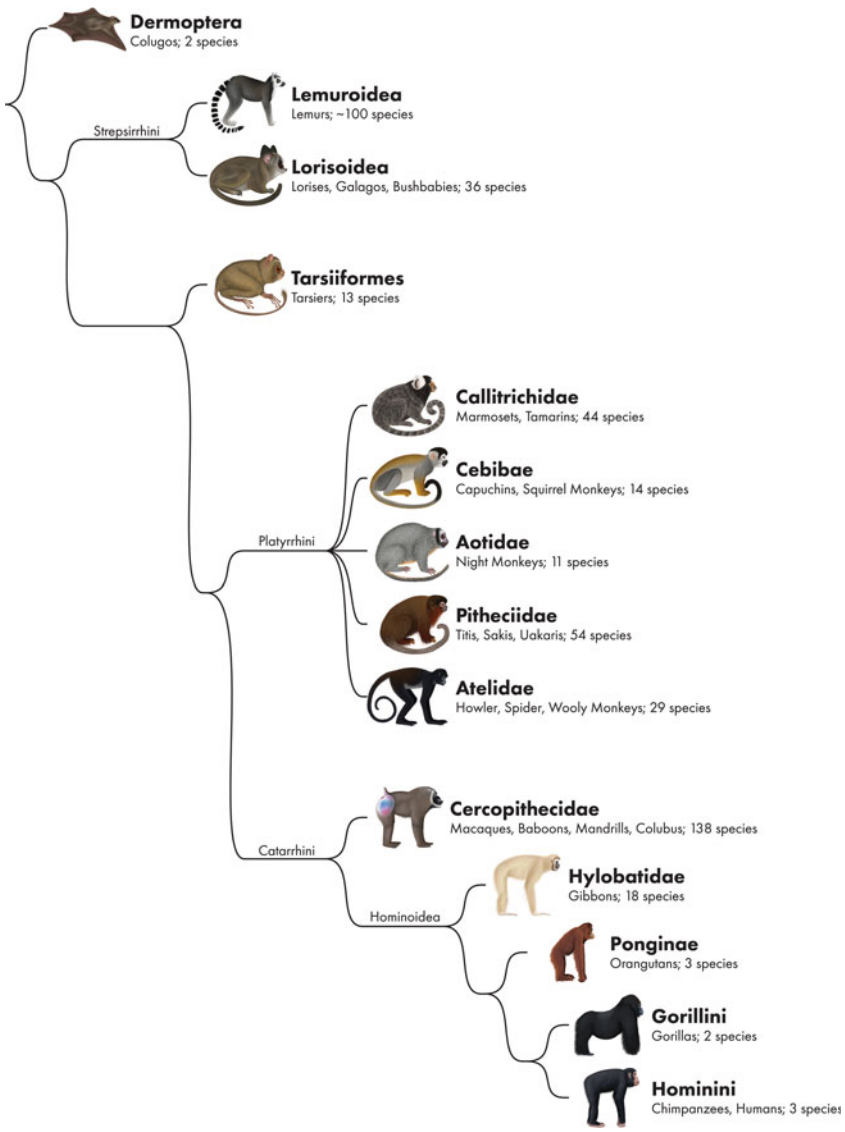

S. M. Thomasy (✉)
Department of Surgical and Radiological Sciences, School of Veterinary Medicine, University of California-Davis, Davis, CA, USA

Department of Ophthalmology and Vision Science, School of Medicine, University of California-Davis, Davis, CA, USA

California National Primate Research Center, University of California-Davis, Davis, CA, USA
e-mail: smthomasy@ucdavis.edu

F. Montiani-Ferreira et al. (eds.), *Wild and Exotic Animal Ophthalmology*, https://doi.org/10.1007/978-3-030-81273-7_22

Nonhuman primates (NHP) exhibit incredible diversity in their vision with eyes uniquely adapted to their ecological niche (Plate 47.1). Eye size varies widely from the massive globes of the nocturnal tarsier to the small eyes of the diurnal gorilla which account for 4.5% and ~ 0.01% of their body weight, respectively (Schultz 1969). Color vision also differs among NHPs as all galagos and loris are nocturnal and monochromatic while all catarrhines are diurnal and trichromatic. Furthermore, retinal specializations vary with a fovea absent and present in strepsirrhines and haplorhines, respectively. Nonhuman primates exhibit high visual acuity relative to other mammals with frontally positioned eyes to improve binocular and stereoscopic vision (Plate 47.1).

The Primate order is comprised of two suborders—Strepsirhini and Haplorhini. The suborder Strepsirhini includes two infraorders—Lemuriformes and Lorisiformes, while the suborder Haplorhini includes two infraorders—Tarsiiformes and Simiiformes. The Simiiformes are comprised of two parvorders—Catarrhini and Platyrrhini. The Platyrrhini parvorder is divided into two superfamilies—Cercopithecoidea and Hominoidea. The visual adaptations, ocular morphology, and common diseases for each of these groups will be described herein.

Lemurs, Lorises, Pottos, and Bushbabies (Strepsirrhini)

The suborder Strepsirrhini is comprised of 2 infraorders—Lemuriformes and Lorisiformes—with >125 extant species worldwide (Mittermeier 2013). The Lemuriformes include 5 families of lemurs all endemic to Madagascar: Cheirogaleidae (e.g., mouse lemurs), Daubaentoniidae (e.g., aye-aye), Indriidae (e.g., wooly lemurs), Lemuridae (e.g., ring-tailed lemur), and Lepilemuridae (e.g., sportive lemurs). The Lorisiformes include 2 families: Lorisidae (e.g., lorises)

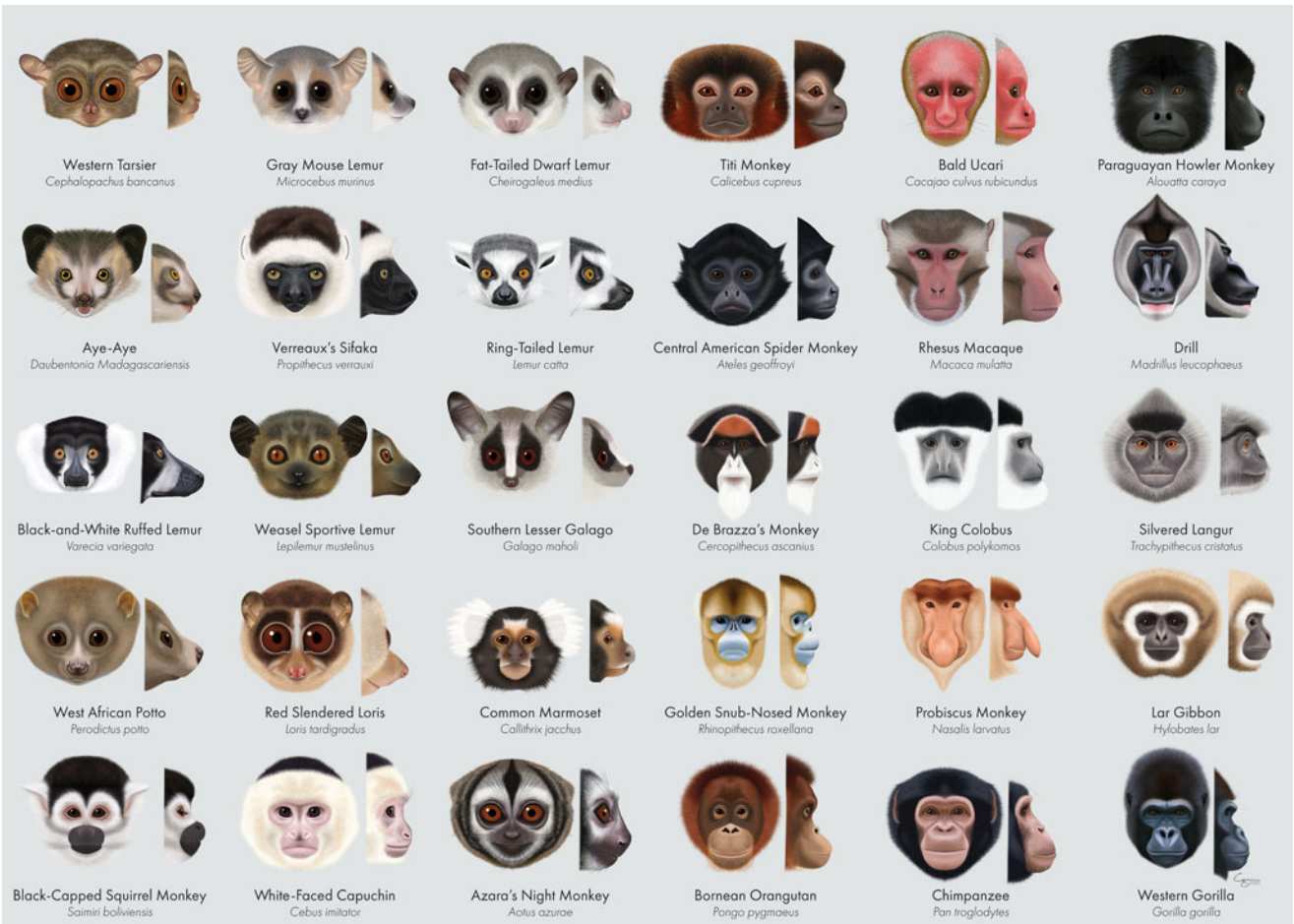

Plate 47.1 Frontal and right lateral view of selected nonhuman primate faces from representative groups. Note the incredible diversity exhibited. Figure copyright Chrisoula Toupadakis Skouritakis

from south and southeast Asia and central Africa and Galadonidae (e.g., galagos) from Africa. Strepsirrhines are small to medium-bodied primates with smaller brains compared to similarly sized simians. This suborder is defined by a wet nose or rhinarium, similar to that of dogs or cats.

Consistent with all primates, strepsirrhines have forward-facing eyes for improved binocular and stereoptic vision with higher visual acuity than most other mammals (Kirk 2006). While the gray mouse lemur (*Microcebus murinus*) has a relatively low visual acuity (4.2 cycles/degree) and smallest axial globe length (9.2 mm) for a primate, its acuity is still greater than some taxa (e.g., *Loxodonta*, African elephant) with much larger eyes (Dkhissi-Benyahya et al. 2001; Ross and Kirk 2007; Kirk and Kay 2004). Visual acuity in strepsirrhines is influenced by activity pattern, diet, and phylogenetic history with a diurnal lifestyle and visual predation important selective factors favoring high visual acuity in this suborder. Numerous members of Strepsirrhini are nocturnal including those in Cheirogaleidae, Daubaentoniidae, Lepilemuridae, and Lorisiforme groups as well as some members of the Indriidae family (Valenta et al. 2016). Thus, these species have ocular adaptations for a nocturnal lifestyle including large to enormous eyes with large pupils, a cellular, choroidal tapetum lucidum, rod-dominant retinas, and monochromatic or dichromatic color vision (Fig. 47.1). By contrast, diurnal strepsirrhines have anatomical adaptations for high-acuity vision including small corneas relative to eye diameter, cone-dominated retinas, and dichromatic or polymorphic trichromatic color vision (Kirk 2004, 2006; Jacobs and Deegan 1993). Some species within Strepsirrhini exhibit a cathemeral lifestyle whereby animals are irregularly active during day or night depending on the prevailing circumstances. Accordingly, cathemeral species exhibit visual system traits such as intermediate eye size, variable presence of tapetum lucidum, and dichromatic or polymorphic trichromatic color vision that suggest evolutionary compromise (Kirk 2006).

Diets vary markedly among strepsirrhines with smaller angwantibos and galagos primarily consuming insects while bamboo lemurs, indriids, and sportive lemurs are folivores; pottos and Asian lorises are faunivore-frugivores. Some species including mouse and ring-tailed lemurs are generalists that exploit a large variety of food sources depending on their seasonal availability. Lemuriformes face a variety of aerial and terrestrial predators in Madagascar such that vision is critical to avoiding predation (Jolly 1966; Sauther 1989; Macedonia 1990, 1993; Gould and Sauther 2006). Similarly, the Lorisiformes must be similarly vigilant in monitoring for a number of predators including reptiles, diurnal raptors, owls, small mammalian carnivores (e.g., linsang), as well as larger primates (Svensson et al. 2018).

Ocular Anatomy, Examination, and Diagnostic Testing

Some species of strepsirrhines such as the gray mouse lemurs (*Microcebus murinus*) can be examined awake with manual restraint (Beltran et al. 2007). However, larger species such as *Lemur catta* require sedation for a thorough ophthalmic examination and various anesthetic protocols have been described in strepsirrhines (Chinnadurai and Williams 2016; Gaudio et al. 2018; Larsen et al. 2011; Williams et al. 2003; Langan et al. 2000; Springer et al. 2015). Atracurium was used for neuromuscular blockade with general anesthesia to remove a corneal foreign body from a ring-tailed lemur (Merlin and Veres-Nyeki 2017). Specifically, the lemur was pre-medicated with 0.03 mg/kg medetomidine, 0.02 mg/kg buprenorphine, and 0.3 mg/kg midazolam administered intramuscularly which resulted in excellent sedation 15 minutes later. General anesthesia was induced with 7 mg of intravenous propofol and maintained with sevoflurane with an end-tidal concentration of 2.2–3.7% following endotracheal intubation.

Strepsirrhines all have postorbital bars created by a connection between the frontal and zygomatic bones framing the orbit consistent with other primates (Rose 2006). However, they lack a thin wall of bone posterior to the globe, termed the postorbital closure, which is only observed in haplorhine primates (Rose 2006; Tattersall 2007). The Aye-aye (*Daubentonia madagascariensis*) skull is short and high with frontal orbits that are deviated superiorly with a facial conformation resembling that of a squirrel (Schwitzwer et al. 2013). Eye size varies considerably among the strepsirrhines with *Loris* species exhibiting the largest eyes of any living primate other than tarsiers while *Lemur* species have relatively average sized eyes by comparison (Rosenberger et al. 2016). In a red-fronted brown lemur *(Eulemur rufifrons*), anterior chamber (AC) depth, lens thickness, and axial globe length were reported as 2, 0.7–0.8, and 16 mm, respectively (Hartley 2014). Eye set is similarly variable with *Lemur catta* demonstrating deeply recessed eyes that protrude only 12% while the eyes of loris and galagos are more prominent and protrude 34%–47% (Rosenberger et al. 2016). Both diet and activity pattern influence eye size with the largest-eyed nocturnal prosimians (*Tarsius, Loris*, and *Galago*) consuming a primarily carnivorous diet while nocturnal strepsirrhines (*Cheirogaleus, Perodicticus, Nycticebus*, and *Otelemur*) with an eye size similar to that of diurnal primates are primarily herbivores (Kirk 2006).

Visual acuity has been assessed by anatomical or behavioral methods in six strepsirrhine species and ranked from greatest to least is the nocturnal Senegal bushbaby (*Galago senegalensis*; 6.7 cycles/degree), diurnal ring-tailed lemur

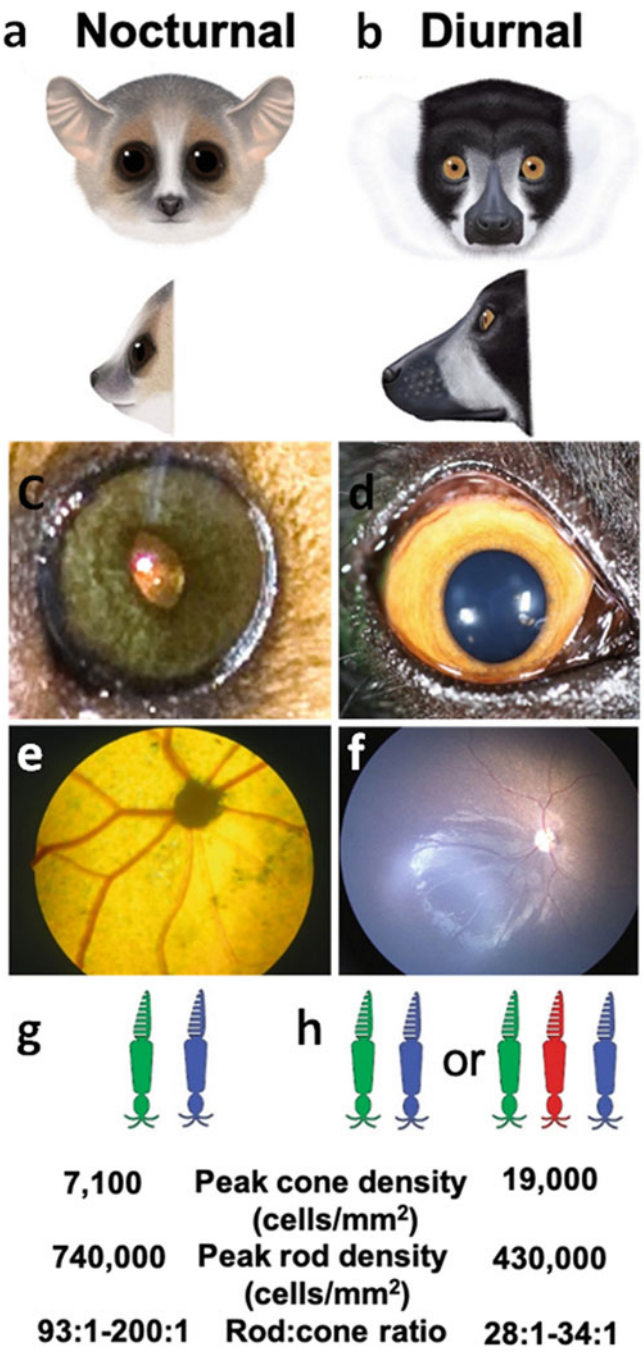

Fig. 47.1 Nocturnal and diurnal strepsirrhines vary with regard to eye size and prominence, pupil size, presence of a tapetum, number of cone opsins, and density of rods and cones. The gray mouse lemur (*Microcebus murinus*, **a**) and the black and white ruffed lemur (*Varecia variegata*, **b**) are used as exemplars of nocturnal and diurnal species. Note the large, prominent eyes and pear-shaped pupils with a tapetal reflection visible of the gray mouse lemur (**a and c**) in comparison with the moderately sized, recessed eyes and round pupils of the black and white ruffed lemur (**b and d**). All nocturnal strepsirrhines have a reflective cellular tapetum (**e**) while diurnal species from *Varecia* and *Eulemur* lack one (**f**). Gray mouse lemurs are dichromats (**g**) while black and white ruffed lemurs exhibit polymorphic trichromatic vision (**h**) such that males are dichromats while most females are trichromats. Unsurprisingly, nocturnal species exhibit a greater rod density and rod:cone ratio while diurnal species have a higher cone density (Peichl et al. 2019). Photo of the anterior segment of a gray mouse lemur (**c**) is from Ranomafana National Park, Ranomafana, Madagascar courtesy of David Thyberg, Shutterstock.com. Fundus photo of a young, male black and white ruffed lemur from the Tulsa Zoo in (**f**) is courtesy of Dr. Jonathan Pucket

(*Lemur catta*; 6.4 cycles/degree), nocturnal thick-tailed greater galago (*Otolemur crassicaudatus*; 4.9 cycles/degree), cathemeral blue-eyed black lemur (*Eulemur macaco flavifrons*; 4.5 cycles/degree), nocturnal gray mouse lemur (*Microcebus murinus*; 4.2 cycles/degree), and nocturnal fat-tailed dwarf lemur (*Cheirogaleus medius*; 2.8 cycles/degree) (Veilleux and Kirk 2009; Neuringer et al. 1981; Dkhissi-Benyahya et al. 2001; Treff 1967). Both diet and activity pattern are important determinants of visual acuity with carnivores requiring higher visual acuity than herbivores.

Iris color is variable among the strepsirrhines due to melanin deposition in the iris stroma (Fig. 47.2). Blue irides are a fixed trait in blue-eyed black lemurs (*Eulemur macaco flavifrons*) who likely evolved from black lemurs (*Eulemur macaco macaco*) with brown eyes; this trait is present in 3 other primates—macaques (*Macaca* sp.), spider monkeys (*Ateles* sp.), and humans (*Homo sapiens*) (Eiberg et al. 2008; Yamigawa 1979; Hernandez-Camacho and Cooper 1976). While the human causal mutation is primarily due to a regulatory variant of the *OCA2* gene encoding for melasomal transmembrane protein within an intron of *HERC2* (Eiberg et al. 2008; Sturm et al. 2008), this mutation is not responsible for blue irides in lemurs suggesting that this trait evolved convergently by a distinct molecular path (Meyer et al. 2013). The blue-eyed black lemur genome was sequenced at 21x coverage to provide the most complete reference lemur genome assembled to date (Meyer et al. 2015). Although polymorphisms were identified in *MITF* (encoding melanocyte inducing transcription factor) as well as several other genes involved in melanin biosynthesis, none completely segregated between *Eulemur macaco flavifrons* and *Eulemur macaco macaco* (Meyer et al. 2015). Thus, the causal mutation for blue irides remains elusive in all primate species except *Homo sapiens*.

The lenses of strepsirrhines are relatively large and round in comparison with the flatter, more discoid shape of haplorhine primates (Fig. 47.3). Activity of several enzymes in the glutathione pathway varied with age in the lenses of 6 nonhuman primates; similar responses to aging were observed in the Old World simians—Bornean orangutan (*Pongo pygmaeus*), pigtail monkey (*Macaca nemestrina*), and olive baboon (*Papio anubis*)—versus the prosimians—Northern lesser galago (*Galago senegalensis*), thick-tailed

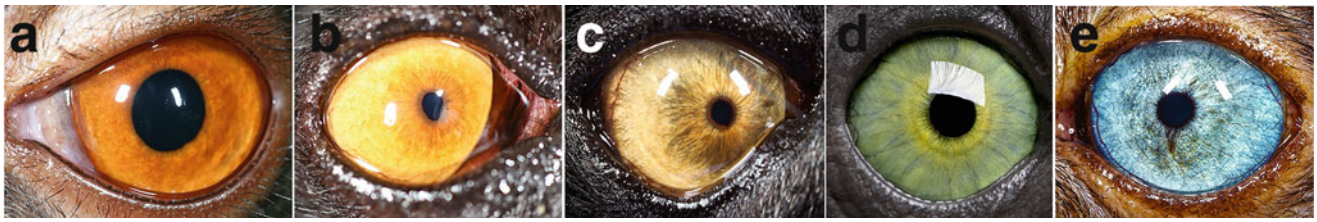

Fig. 47.2 A rainbow of lemur irises. Orange irides were identified in a 3-year-old male Mongoose lemur *(Eulemur mongoz)* (**a**). Yellow-orange (**b**) and yellow (**c**) irides were observed in 5- and 26-year-old female black and white ruffed lemurs (*Varecia variegata*), respectively. Brilliant green irides (**d**) were found in a 3-month-old crested sifaka (*Propithecus coronatus*). Bright blue irides (**e**) were documented in a 22-year-old male blue-eyed black lemur (*Eulemur macaco flavifrons*). Photo credit Eric Isselee, Shutterstock.com (**d**). (**e**) Courtesy of Bret A. Moore

greater galago (*Otolemur crassicaudatus*) and gray mouse lemur (*Microcebus murinus*) (Holleschau and Rathbun 1994; Rathbun and Holleschau 1992). Aqueous ascorbate concentrations vary among different species with nocturnal thick-tailed greater galagos (*Otolemur crassicaudatus*) demonstrating much lower concentrations in comparison with diurnal rhesus macaques (*Macaca mulatta*) and green monkeys (*Chlorocebus aethiops*) (Ringvold 1980; Kinsey and Jackson 1949; Davson and Luck 1959).

Intraocular pressure (IOP) has been measured in normal gray mouse lemurs (*Microcebus murinus*, n = 516) with a mean ± SD calibrated IOP of 20.3 ± 2.8 mm Hg; IOP measurements were not affected by age, eye side, colony, or sex (Dubicanac et al. 2018) (Appendix 3). For this species, the TonoVet® was superior to the TonoPen™ in terms of practicality particularly the small probe tip for contacting the cornea, lack of need for topical anesthesia, less time spent acquiring the measurements, and more accurate measured values (Dubicanac et al. 2018).

Most strepsirrhines, particularly the nocturnal species, have a reflective cellular tapetum lucidum including all members of the Cheirogaleidae, Daubaentoniidae, Indriidae, Lepilemuridae, Lorisidae, and Galagidae families (Figs. 47.1 and 47.4). The diurnal ruffed lemurs (Varecia sp.) and cathemeral brown lemurs (*Eulemur* sp.) are the only genera of Lemuridae without a tapetum (Peichl et al. 2019). Interestingly, sifakas (*Propithecus* sp.) retain a tapetum despite being diurnal with medium/long wavelength cone opsin

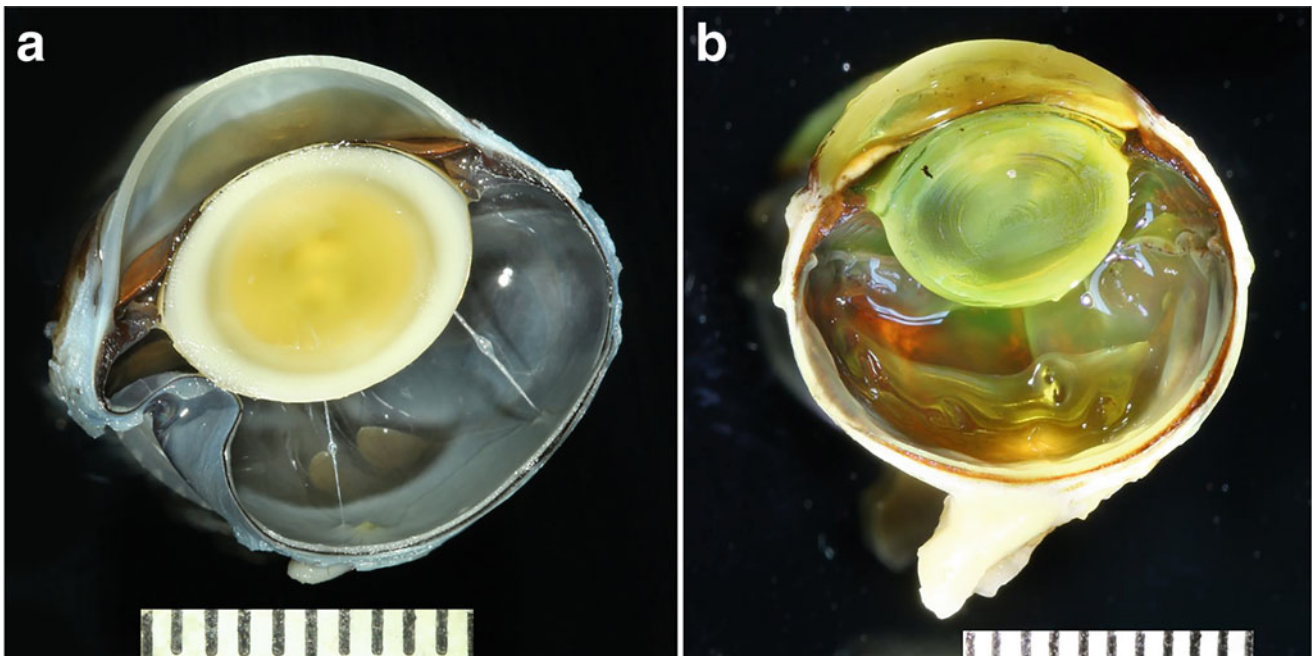

Fig. 47.3 Strepsirrhines have large, round lenses irrespective of lifestyle. Gross images of hemi-sectioned globes from a 15-year-old female nocturnal *Galago* of unknown species (**a**) and a 24-year-old male diurnal ring-tailed lemur (*Lemur catta*, **b**) with normal eyes. Contrast the large, relatively round lenses present in these individuals with the flat, discoid lenses of haplorhine primates (Figs. 47.16 and 47.34). Images courtesy of the Comparative Ocular Pathology Laboratory of Wisconsin (COPLOW)

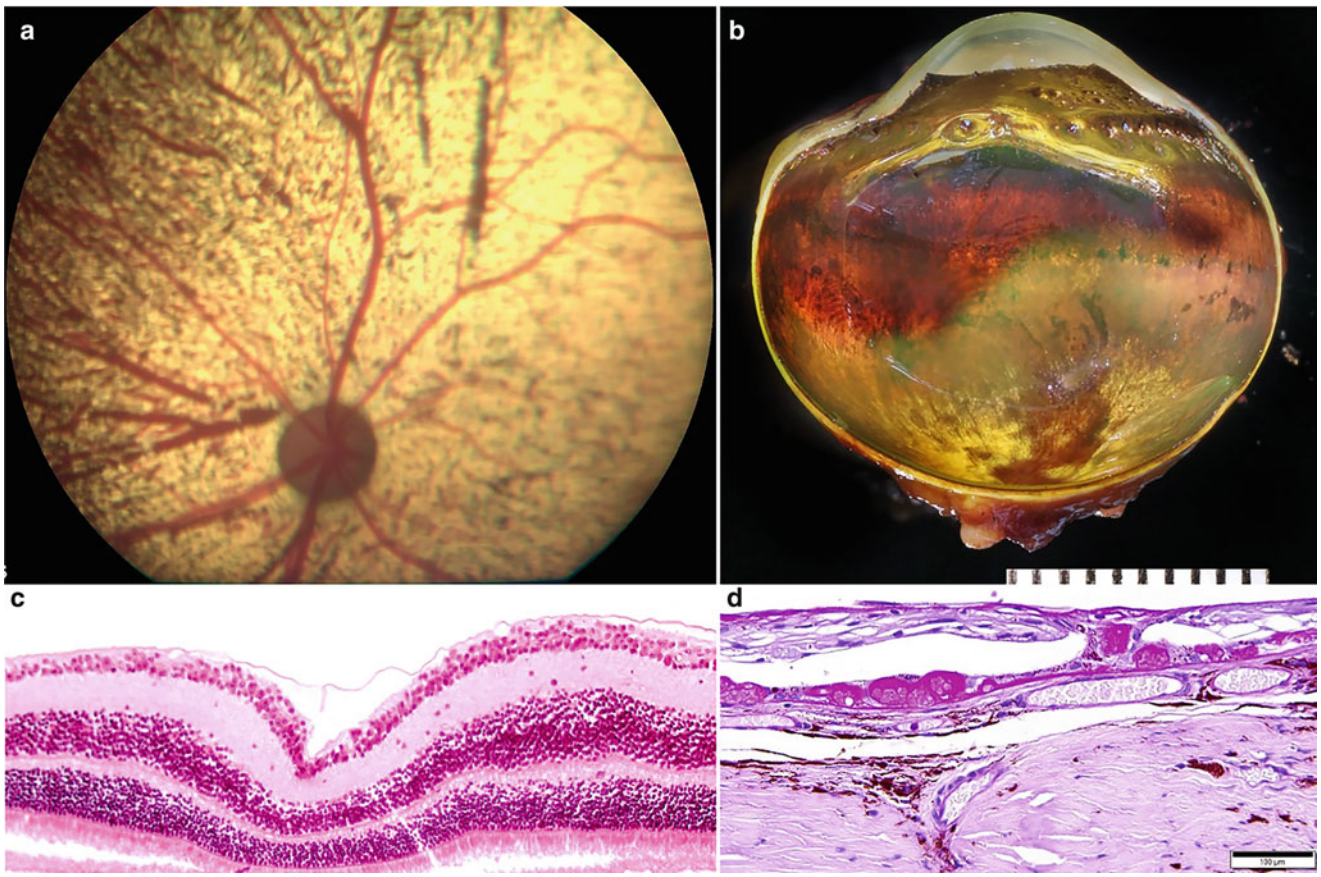

Fig. 47.4 Normal fundus and retinal architecture (**a** and **c**) as well as hypermature cataract with lens capsule rupture, secondary glaucoma and drusen-like lesions (**b** and **d**) in ring-tailed lemurs (*Lemur catta*). A normal fundus of a 6-year-old castrated male ring-tailed lemur with a holangiotic retina vascular pattern, round optic disc and yellow cellular tapetum (**a**); normal retinal histology of a ring-tailed lemur (**c**). The left eye of a 16.5-year-old captive female ring-tailed lemur was enucleated for buphthalmos; severe corneal edema made it impossible to examine intraocular structures. Gross and histologic examination of this left globe identified a hypermature cataract with lens capsule rupture and secondary glaucoma; a yellow tapetum was visible (**b**). The retina is markedly degenerated due to chronic glaucoma; drusen-like lesions were identified incidentally under the retinal pigmented epithelium (**d**). Photo courtesy of Drs. Aleksandra Rawicka and Nunzio D'Anna, Clinica Veterinaria Roma Sud (**a**). Images (**b–d**) courtesy of the Comparative Ophthalmic Pathology Laboratory of Wisconsin (COPLOW)

(*OPN1LW*) polymorphism such that females are predominantly trichromats while males are dichromats (Peichl et al. 2019). The tapetal cells of strepsirrhines contain abundant riboflavin similar to cats (Pirie 1959; Elliott and Futterman 1963). Riboflavin fluoresces at 520 nm which approaches the maximum absorbance of rhodopsin (500 nm) thus allowing the lemur and feline tapeta to amplify light with fluorescence as well as reflect it (Ollivier et al. 2004b).

In contrast to most other primates, the strepsirrhines lack a fovea with an area centralis present instead (Dkhissi-Benyahya et al. 2001). Nocturnal strepsirrhines including the Lorisidae, Galagidae families as well as some members of Cheirogaleidae are monochromats. These species contain a single functional medium/long-wavelength (M/LWS)-sensitive cone opsin while the short-wavelength sensitive cones are nonfunctional due to accumulation of deleterious mutations in the *OPN1SW* gene (Veilleux et al. 2013). Interestingly, habitat type may influence retention of a functional *OPN1SW* gene in nocturnal lemurs with species living in open canopy more likely to be dichromats versus those living in a closed canopy (Veilleux et al. 2013). Nocturnal lemurs with dichromacy include the Daubentoniidae family as well as some members of Cheirogaleidae and Indriidae. Diurnal strepsirrhines are either dichromats or exhibit polymorphic trichromacy whereby a single locus of the X-chromosome encodes an M/LWS opsin. In the polymorphic trichromats, heterozygous females are trichromats while homozygous females and males are dichromats. Some diurnal members of the Indriidae and Lemuridae families exhibit this polymorphism which has been proposed to be evolutionarily advantageous in the detection of red fruit particularly during the dry season when food is more sparse (Veilleux et al. 2016; Valenta et al. 2016). Specifically, social groups of Verreaux's sifaka (*Propithecus verreauxi*) with trichromats

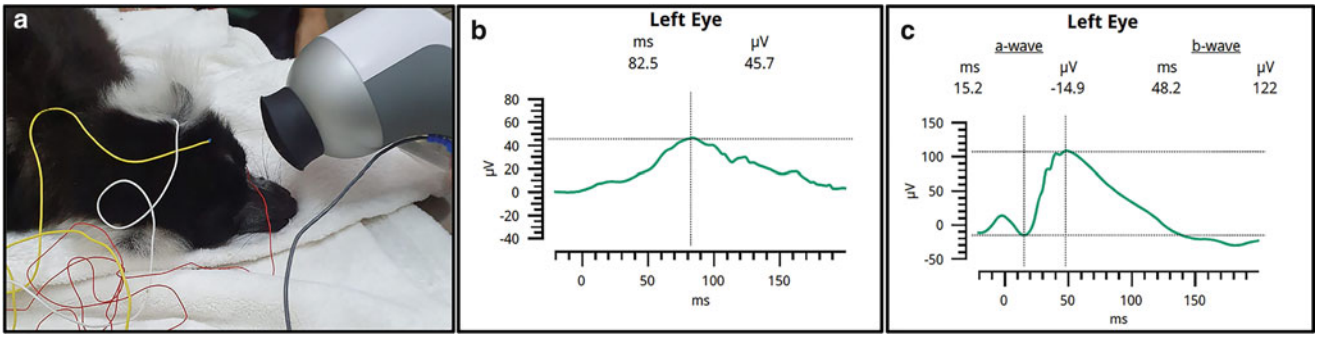

Fig. 47.5 Electroretinography in a 20-year-old female black-and-white ruffed lemur (*Varecia variegate*). Electroretinography was performed under sedation using a RETevet, LKC Technologies (**a**). Mixed rod-cone response (3 cdxsec/m2, **b**) and rod response (0.01 cdxsec/m2, **c**) after 20 min of dark adaptation for the left eye. Images courtesy of Dr. Ron Ofri from Koret School of Veterinary Medicine, Hebrew University of Jerusalem

have higher body masses and spend more time consuming fruit than those with only dichromats (Veilleux et al. 2016). Unsurprisingly, cone densities are greater in diurnal versus nocturnal strepsirrhines in the area centralis; rod densities are higher than cones in all strepsirrhines studied with an increased density observed in nocturnal versus diurnal species (Moritz et al. 2014; Peichl et al. 2019). Relative to the fovea of haplorhines, the area centralis of strepsirrhines tends to have less cones and more rods provided diurnal activity pattern is controlled (Moritz et al. 2014). Electroretinography has been used sporadically in strepsirrhines to determine their color vision (Jacobs and Deegan 2003b, c; Graveline et al. 1966; Jacobs et al. 2002); unpublished reports do exist on its use for diagnostic purposes (Fig. 47.5).

Ophthalmic Disease

Similar to canines and felines infected with systemic blastomycosis, a case report in a 5-year-old male red ruffed lemur (*Varecia rubra*) identified aggregates of neutrophils and macrophages with inter- and intracellular *Blastomycosis dermatitidis* organisms in the choroid on necropsy (Rosser et al. 2016). Disseminated toxoplasmosis has been reported in captive ring-tailed lemurs and can cause chorioretinitis (Fig. 47.6) (Dubey et al. 1985; Juan-Sallés et al. 2011; Spencer et al. 2004). Although rare, other systemic mycoses and protozoal infections have been reported in lemurs suggesting that a complete ophthalmic examination, particularly of the fundus, may be beneficial in increasing the index of suspicion for disseminated fungal or protozoal disease (Burton et al. 1986; Williams 2014; Hoffmann and Rossmann 1972; Ragazzo et al. 2018).

In a review of the known literature concerning ocular disease in 318 captive-bred gray mouse lemurs (*Microcebus murinus*), prevalence was high at >35% with cataracts (n = 100, 31%), pupil seclusion (n = 11, 4%), synechiae (n = 10, 3%) and corneal degeneration (n = 9, 3%) most commonly observed (Beltran et al. 2007; Dubicanac et al. 2017) (Fig. 47.7). In a 4.5-year-old male gray mouse lemur with corneal degeneration, xanthomatous sclerokeratitis was found (Alleaume et al. 2017). Clinically, multifocal, dense white corneal opacities arising from the limbus were found in both eyes. On histology, severe diffuse granulomatous scleritis and focal keratitis with intralesional cholesterol were found. The underlying cause remains unidentified but systemic lipid metabolic disorders and/or focal pathology (e.g., inflammation or hemorrhage) were speculated. A corneal foreign body was successfully removed from a ring-tailed lemur (*Lemur catta*) under general anesthesia with atracurium for neuromuscular blockade (Merlin and Veres-Nyeki 2017).

Cataracts were particularly common in aged mouse lemurs with >50% prevalence in those greater than 7 years of age (Fig. 47.7) (Beltran et al. 2007). Nuclear sclerosis (Fig. 47.6) and cataracts (Figs. 47.4 and 47.7) also appear to be relatively common in other species of captive lemurs. Similar to other captive NHPs with vision-impairing cataracts (de Faber et al. 2004; Leiva et al. 2012), phacoemulsification successfully performed to restore vision. Herein, a routine cataract surgery in a 5-year-old red-fronted brown lemur (*Eulemur rufifrons*) will be described (Hartley 2014). Atropine 2% ophthalmic solution combined with phenylephrine 2.5% was effective at achieving rapid, complete dilation in lemurs. A clear, stepped, 3.2 mm corneal incision was made with a Beaver blade then slit knife without iris prolapse; 1.2% hyaluronate was effective at maintaining the anterior chamber. The lens capsule of this lemur was thin and elastic with a soft cataract such that lens proteins extruded after the initial capsulorrhexis incision. The majority of lens material was removed with 1 second of phacoemulsification with irrigation-aspiration used to remove the remaining cortical material. The cornea was then sutured with two simple interrupted sutures with 9–0 Vicryl. Intracameral cefuroxime

Fig. 47.6 Strepsirrhines display a variety of ocular lesions. Chorioretinal scars secondary to disseminated toxoplasmosis in an older adult, female black and white ruffed lemur (*Lemur catta*) from the Tulsa Zoo (**a**); photo credit to Dr. Jonathan Pucket, Oklahoma Veterinary Specialists. Nuclear sclerosis in a 22-year-old male blue-eyed black lemur (*Eulemur macaco flavifrons*) (**b**). Ocular trauma with secondary glaucoma with buphthalmos and extensive corneal fibrosis and melanosis observed in a Milne-Edward's sifaka (*Propithecus edwardsi*) from Ranomafana National Park, Ranomafana, Madagascar; photo courtesy of Martin Lindsay, Alamy Stock Photo (**c**). **b**—Courtesy of Bret A. Moore

(1.25 mg) followed by subconjunctival injections of cefuroxime (50 mg) and methylprednisolone (1 mg) were performed OU. Ofloxacin 0.3% ophthalmic solution then neomycin-polymyxin-dexamethasone ophthalmic ointment (Maxitrol) 5 minutes later were administered post-operatively. Midazolam (0.2 mg/kg) and buprenorphine (0.02 mg/kg) were useful to reduce the activity of the lemur following cataract surgery (Gaudio et al. 2018; Merlin and Veres-Nyeki 2017). To prevent lemurs from rubbing their eyes following surgery or with globe fragility, an Elizabethan collar can be placed with the larger opening placed over the shoulders. Hand feeding or a different type of food bowl may be necessary while the Elizabethan collar is in place.

A retrospective review of histopathology reports from captive lorises and pottos found that ocular lesions were ~ 9% among the 367 individuals included in the study. Ocular lesions were most common in mountain red slender loris (*Loris tardigradus nycticeboides*) at 25% with cataract, synechiae, blindness, and neural degeneration reported. Ocular trauma with secondary glaucoma can also occur in wild strepsirrhines with buphthalmos and extensive corneal fibrosis and melanosis observed in a wild Milne-Edward's sifaka

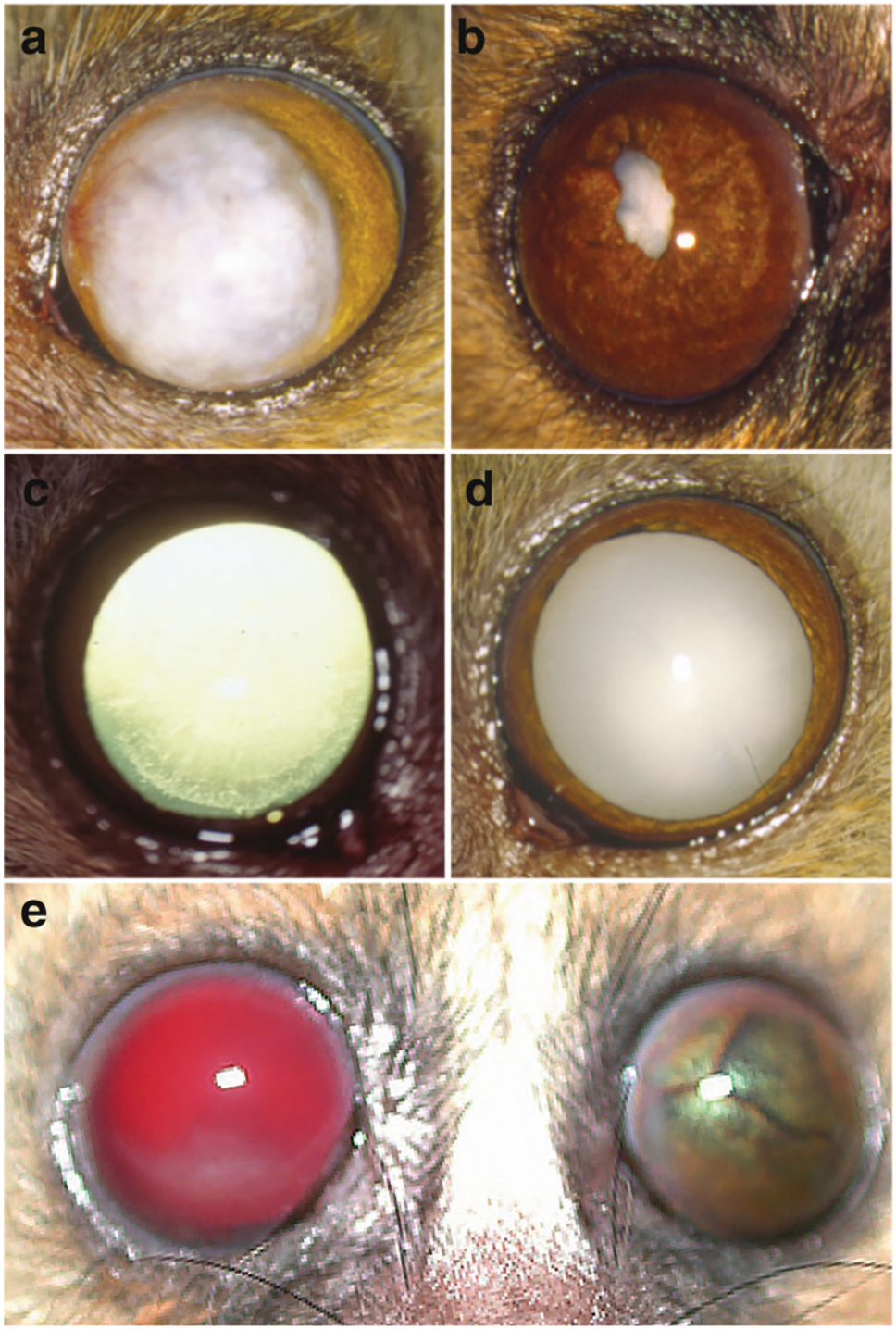

Fig. 47.7 Captive gray mouse lemurs demonstrate a variety of ophthalmic lesions. (**a**) Extensive, dense, coalescing dull white stromal deposits consistent with corneal degeneration in the left eye of an 8.9-year-old gray mouse lemur; superficial corneal vessels extend from the medial limbus into the affected stroma. (**b**) An adult mouse lemur with dyscoria and miosis due to extensive posterior synechiae as well as a hypermature cataract; the iris changes were presumably from phacolytic uveitis. (**c**) An adult mouse lemur with an early immature posterior cortical cataract in the right eye. (**d**) An adult mouse lemur with a mature cataract in the left eye. (**e**) Complete hyphema of the right eye and pupil seclusion and dyscoria in the left eye of an adult mouse lemur. Photos courtesy of Dr. William Beltran, University of Pennsylvania

(*Propithecus edwardsi*) (Fig. 47.6). Ocular neoplasia was rare with an iridal melanoma identified in a single lowland red slender loris (*Loris tardigradus tardigradus*). Ocular disease was rarely the primary cause of death or euthanasia with a single report in one mountain red slender loris (*Loris tardigradus nycticeboides*) and one Sunda slow loris (*Nycticebus coucang*).

Tarsiers (Tarsiidae)

The infraorder Tarsiiformes contains only one extant family Tarsiidae with 11 species all located in Southeast Asia. Tarsiers are small prosimians with long hind limbs due to elongated tarsal bones for which they are named. Intriguingly, tarsiers have enormous eyes up to 18 mm in diameter

that are proportionally larger than any mammal. For comparison, the eyes of the Western tarsier (*Cephalopachus bancanus*) are largest of all in this family (Fig. 47.8) and would be equivalent to the size of large grapefruits in a human (Rozenbaum et al. 2008; Shekelle et al. 2013).

Tarsiers are most active at night but lack a reflective tapetum lucidum intrinsic to most nocturnal species and thus utilize their massive eyes to increase sensitivity under dim light conditions. It has been suggested that the ancestors of tarsiers may have been diurnal and that orbital hypertrophy occurred in response to their readaptation to nocturnality. If this theory is correct, fossil evidence implies that this return to a nocturnal life occurred ~40 million years ago (Shekelle et al. 2013).

As the only completely carnivorous primate, tarsiers have a visual system adapted to that of a predatory and prey species. They rely heavily on insects for food and catch ~35% of these directly from the air (Roberts and Kohn 1993). This insectivorous diet is complemented by consumption of bats, freshwater crabs, frogs, small birds, and snakes when available (Jablonski and Crompton 1994; Niemitz 1973). Simultaneously, tarsiers must be watchful for predators that include arboreal snakes, civets, monitor lizards, and raptors (Gursky 1997, 2000; Jachowski and Pizzaras 2005). As such, it is expected that any degradation of vision would markedly decrease survival of individuals in the wild. Therefore, assessment of visual status and ocular care by veterinarians is critical during rehabilitation of tarsiers with the intent to release back into the wild.

Ocular Anatomy and Examination

Tarsiers are easily stressed and sedation protocols that include telazol (5–11 mg/kg) supplemented with dexmedetomidine (25 μg/kg) have been described for blood collection and measurement of auditory brainstem response (Moritz et al. 2017; Ramsier et al. 2012). Thus, ophthalmic examinations may be facilitated by administration of sedatives.

The massive eyes of tarsiers dominate its head such that each eye exceeds the size of its brain (Rozenbaum et al. 2008). For comparison, the eyes of tarsiers, other nocturnal primates, diurnal primates, and humans comprise 4.5, 0.3, 0.15, and 0.03% of their total body weight, respectively (Schultz 1969). To accommodate such large eyes, the orbits enlarged (Fig. 47.9) and the extraocular muscles shrank such that their globes move little. Consequently, the tarsier has modified cervical vertebrae that allow the head to swivel nearly 180° in either direction to extend its visual field (Fig. 47.8) (Ankel-Simons and Simons 2003). Tarsiers also exhibit a postorbital septum that is found in all primates but few other mammals (Fig. 47.9). In primates, this adaptation facilitated enlargement of the brain case while simultaneously allowing jaw and muscle development for mastication and stabilizing vision during chewing. However, tarsiers evolved a novel postorbital morphology in response to their markedly enlarged eyes with the postorbital septum developing after birth (Smith et al. 2013).

The frontal eye position observed in tarsier species results in a large binocular field (127°) with a total visual field of 186° (Ross 2000). This is a consistent feature of all primates resulting in enhanced depth perception and stereopsis. The globe protrudes well beyond the brow for maximal light capture (Plate 47.1, Fig. 47.8) with only half residing within the orbit (Ankel-Simons 2007). The corneas of tarsiers are enlarged and prominent with a larger radius of curvature in comparison with humans and a relatively deep anterior chamber. Their iris is orange or brown in color with a pupil that can widely dilate to facilitate light entry in darkness then constrict to ~0.5 mm during the day (Fig. 47.8). The pupil is horizontal ovoid in shape which contrasts with the slit-shaped pupil of many nocturnal animals (Fig. 47.8) (Land 2006). In order to collect maximal light and focus on the retina, the crystalline lens is large and relatively round (10 mm diameter, 6.5 mm thick) in comparison with most other primates where it is thin and disc-shaped (Collins et al. 2005). A major structural protein in the lenses of all vertebrates, αA-crystallin, has been used to deduce phylogenetic relationships among primates and between them and other mammalian species (Jaworski 1995). Specifically, the DNA sequence of αA-crystallin demonstrated that tarsiers are more closely related to strepsirrhines than haplorhines, an area of controversy in the past (Jaworski 1995).

In addition to lacking a tapetum, tarsiers also retain other characteristics consistent with a diurnal ancestor including a fovea for high-acuity vision and two cone opsins—a short (S) as well as a medium/long (M/L) wavelength (Moritz et al. 2017). Tarsiers may use their fovea to facilitate insect capture during crepuscular hours (with dichromacy), to calibrate an auditory localization pathway (Moritz et al. 2014) or for a yet undiscovered mechanism (Schwab 2012). The avascular, deep fovea is located 2.7–3 mm temporal to the optic disc (Fig. 47.10) (Polyak 1957; Castenholz 1984; Hendrickson et al. 2000; Ross 2004; Wolin and Massopust 1967). The M/L cones dominate the tarsier retina particularly in the center and adjacent to the fovea; foveal cone density has not been established (Hendrickson et al. 2000). The smaller population of S-cones are rarely found in the central retina but increase in density in a wide ring surrounding the peripheral retina (Fig. 47.10), presumably to assist the peripheral rods in prey detection in dim light (Hendrickson et al. 2000). While S-cone distribution varies among primates, this

Fig. 47.8 Tarsiers demonstrate enormous, immobile eyes with ~180° of cervical rotation in either direction to increase its visual field (**a**). All tarsiers have a large, highly curved cornea and horizontally oval pupils (**a–c**) that constrict markedly under bright light conditions (**b and c**). Western tarsiers (*Cephalopachus bancanus*) have the largest eyes of all the tarsier species; photo courtesy of Ryan M. Bolton, Shutterstock.com (**a**). Photos of Philippine tarsiers (*Tarsier syrichta*) from Bohol, Philippines courtesy of Lano Lan, Shutterstock.com (**b**) and Khoroshunova Olga, Shutterstock.com (**c**)

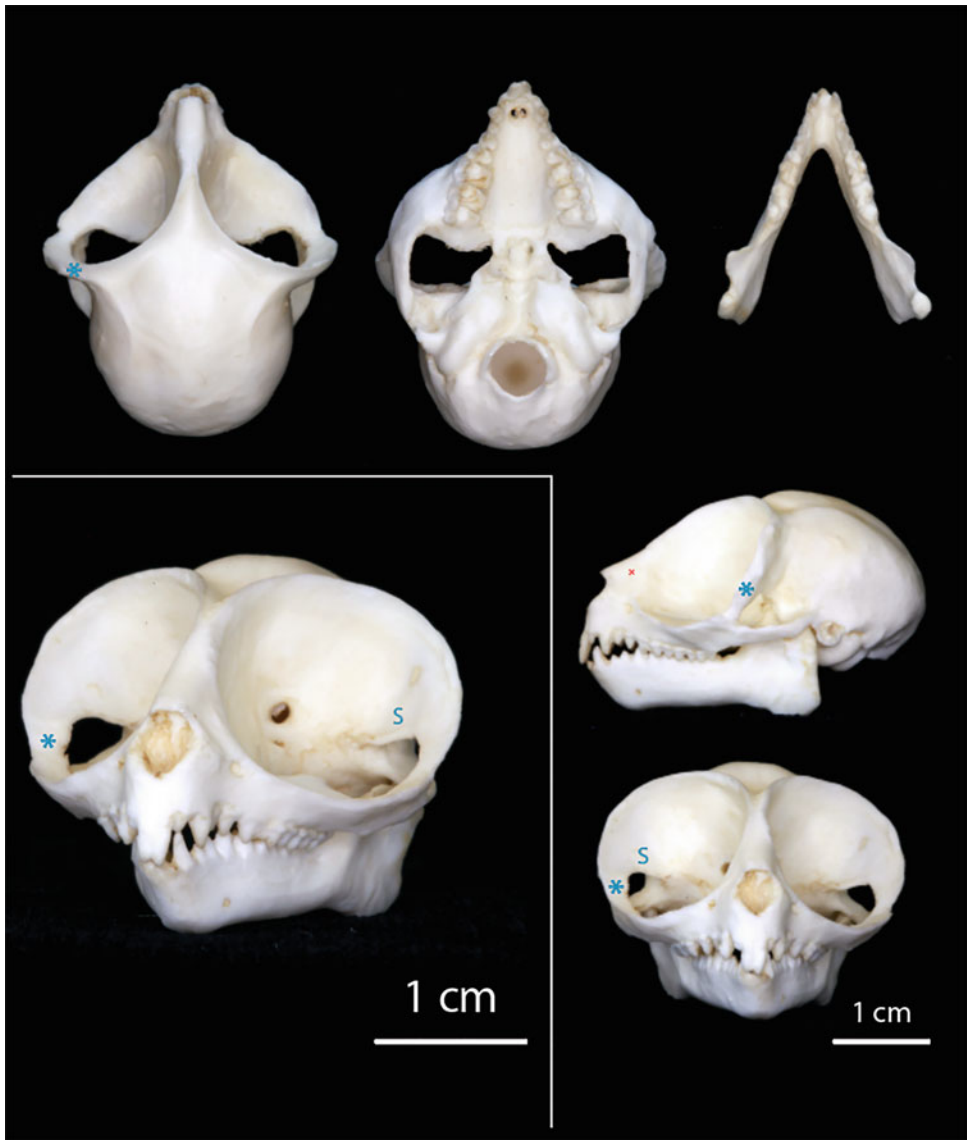

Fig. 47.9 A replica of a tarsier skull demonstrates the massive orbits required to house its large eyes. The postorbital septum (s) and postorbital bar (*) are visible representing an intermediate phenotype between haplorhines and strepsirrhines

encircling peripheral distribution is unique. Interestingly, tarsier cones lack calcium-binding protein more consistent with nocturnal New World monkeys than diurnal Old World monkeys (Hendrickson et al. 2000). Retinal ganglion cell density in tarsiers is more consistent with diurnal macaques than nocturnal lemurs (Tetreault et al. 2004). The sequence of interphotoreceptor retinoid binding protein has been used to construct phylogenetic trees suggested that Tarsiiformes is more closely related to Haplorhini than Strepsirrhini (Poux and Douzery 2004). In aggregate, these data suggest that the retina and choroid of tarsiers exhibit characteristics of both related Old World primates and distant New World monkeys. For those interested in viewing the world through the eyes of a tarsier, researchers at Dartmouth have created virtual reality "tarsier goggles" that traverse dense forests in Borneo from the perspective of a *Cephalopachus bancanus* (Gochman et al. 2019).

Ophthalmic Disease

To the best of our knowledge, there are no tarsiers in any zoo collection in North America and previous attempts to house them in captivity suggest that they do not survive or breed well. As such, there has been limited opportunity for veterinarians to examine tarsiers for ocular lesions. However, it would be unsurprising if they suffered from ocular trauma due to their large, prominent globes as well lesions that occur commonly in other prosimians such as cataracts.

New World Monkeys (Platyrrhines)

The parvorder Platyrrhini is part of the suborder Haplorhini with 156 extant species worldwide (Mittermeier 2013). Primates in the suborder Haplorhini are distinguished by

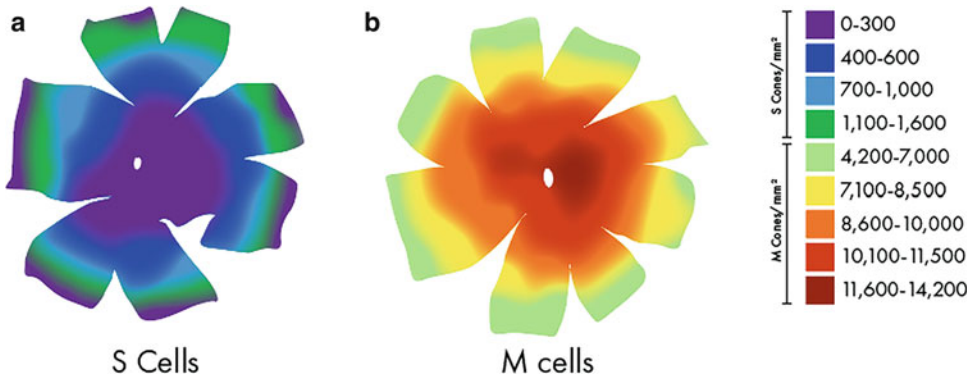

Fig. 47.10 Density of M/L (**a**) or S (**b**) cones in the tarsier retina. Note the highest density of S cones forms a ring in the peripheral retina (**b**). Adapted with permission from Hendrickson and colleagues (Hendrickson et al. 2000)

their dry nose or rhinum while those in Strepsirrhini have a wet nose. Platyrrhines are further distinguished by broad, flat nostrils while catarrhines have narrow nostrils that face downwards. The parvorder Platyrrhini is divided into five families—Aotidae (night monkeys), Callitrichidae (marmosets and tamarins), Cebidae (squirrel monkeys and capuchins), Pitheciidae (titis, sakis, and uacaris), and Atelidae (howlers, spider and woolly monkeys and muriquis). Approximately 40 million years ago, ancestors of this parvorder traveled to South America such that all members currently reside in the tropical regions of Central and South America and Mexico, hence the name New World monkey.

Color vision in platyrrhines is highly pleomorphic due to variation of opsins on the X chromosomes (Fig. 47.11) (Jacobs and Deegan 2003a). In catarrhines, the middle- (M) and long- (L) wavelength sensitive cone pigments are on the X-chromosome while an autosomal gene encodes the short- (S)-wavelength sensitive pigment (Nathans et al. 1986). By contrast, platyrrhines typically only have one X-chromosome opsin with multiple alleles permitting different types of dichromatic color vision while some females are trichromats if they are heterozygous at this locus (Jacobs et al. 1996b; Talebi et al. 2006; Boissinot et al. 1998; Travis et al. 1988; Jacobs and Deegan 2003a). An exception to this are the *Aotus* species which are dichromats due to their nocturnal lifestyle (Wikler and Rakic 1990). By contrast, male and female howler monkeys (*Alouatta* sp.) are obligatory trichromats with the spectral tuning of their L and M opsins optimized to distinguish fruit among leaves (Regan et al. 1998). Furthermore, members of *Alouatta* have a fovea with a greater peak cone density in the foveal pit than every other diurnal platyrrhine or catarrhine primate, including humans (Franco et al. 2000; Curcio et al. 1990). However, the retinal ganglion cell and amacrine cell density and distribution of *Alouatta* sp. were consistent with diurnal platyrrhine or catarrhine primates suggesting that there is a marked gradient in foveal cone density to support high chromatic acuity in a focal central area (Muniz et al. 2014). Despite these interspecies differences, retinal pathways for color transmission and processing remain largely conserved in dichromats and trichromats. Interestingly, Opn5 is expressed in the ganglion cell and inner nuclear layers of the common marmoset retina as well as the preoptic hypothalamus and appears to function as an ultraviolet sensor in the brain (Yamashita et al. 2014). The diversity of opsins in a variety of platyrrhines have been investigated by behavioral, electroretinographic, immunohistochemical, and genetic means, and we direct the readers to these studies for their interest (de Lima et al. 2015; Corso et al. 2016; Bunce 2015; Goulart et al. 2017; Jacobs and Neitz 1987; Jacobs and Deegan 2005; Martin and Grunert 1999; Travis et al. 1988; Tovée et al. 1992; Williams et al. 1992; Kawamura 2016; Jacobs and Deegan 2003a; Jacobs and Williams 2006).

Platyrrhines demonstrate marked diversity in their behavior, diet, morphology, and distribution. All are arboreal. Most are diurnal with the exception of the nocturnal night monkeys (*Aotus* sp.). The diet of platyrrhines can consist of fruit, insects, gums, and/or leaves. Their small to medium size can leave them vulnerable to predation by a diverse range of aerial predators including raptors, felids, and snakes. Thus, visual scanning for both aerial and terrestrial predators is critical in addition to other predator-avoidance behaviors such as careful selection of sleeping sights, huddled group sleeping, predator-specific vocalizations, sentinels, retirement prior to sunset, and arousal after sunrise among others (Barros et al. 2004). It was postulated that arboreal primates, particularly those living in small groups, may rely more on auditory versus visual communication due to the low visibility among the trees (Santana et al. 2012). However recent work suggests that visual displays are critical in communicating aggression, fear, play, and affiliation in common marmosets (*Callithrix jacchus*) and their dramatic facial coloration (Plate 47.1) promotes the visibility of these displays to their conspecifics (de Boer et al. 2013).

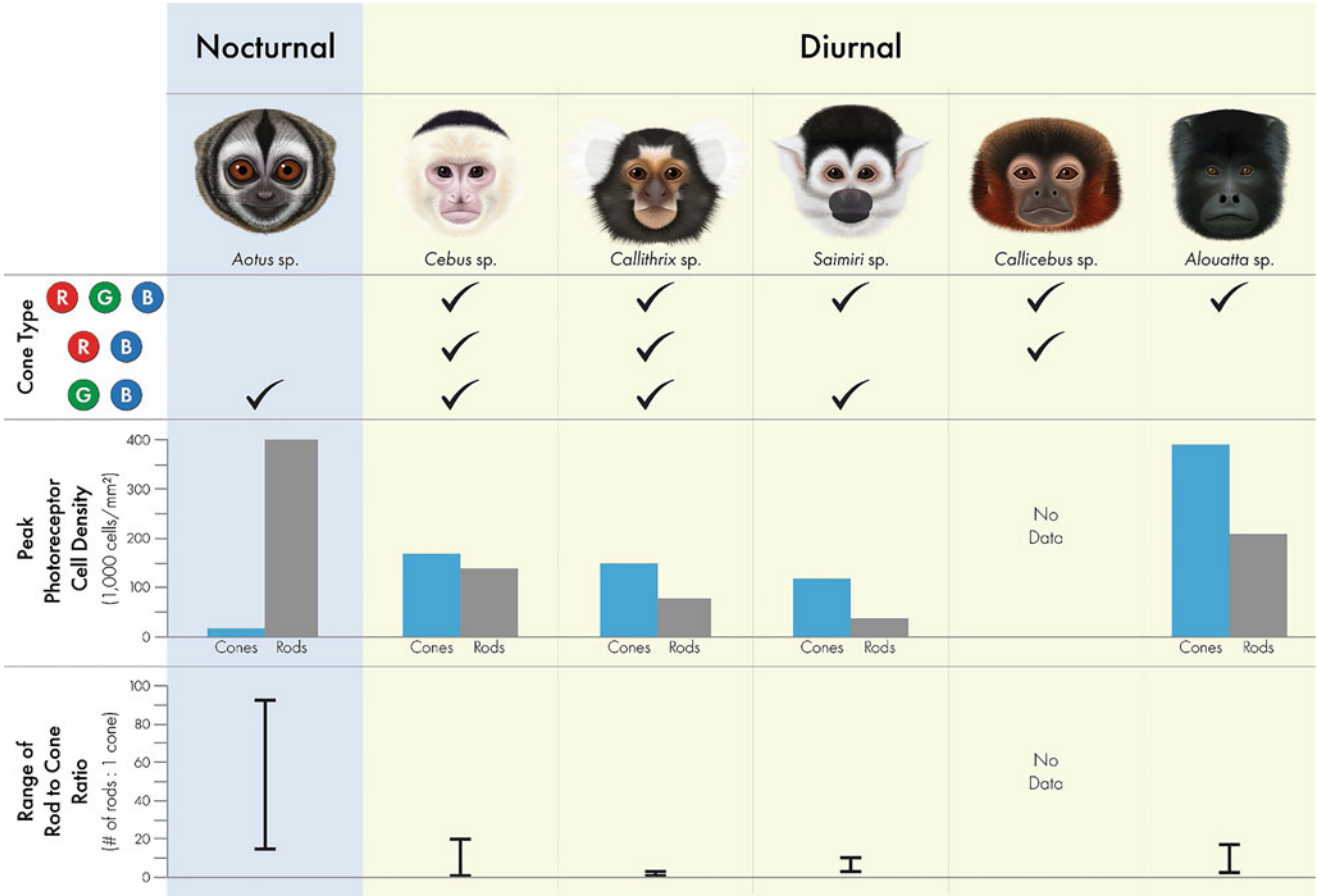

Fig. 47.11 Platyrrhines demonstrate pleomorphism in color vision ranging from dichromacy in night monkeys (*Aotus* sp.) to obligatory trichromacy in howler monkeys (*Alouatta* sp.). Other platyrrhines including capuchins (*Cebus* sp.), marmosets (*Callithrix* sp.), squirrel monkeys (*Saimiri* sp.), and titi monkeys (*Callicebus* sp). have one X-chromosome opsin with multiple alleles permitting different types of dichromatic color vision while some females are trichromats if they are heterozygous at the locus. As the only nocturnal species, the night monkeys have a markedly greater density of rods than cones while the diurnal species exhibit more cones than rods; the ratio of rods to cones also varies between these platyrrhines (Andrade da Costa and Hokoc 2000; Jacobs, Neitz et al. 1996b; Kawamura 2016; Finlay, Franco et al. 2008; Wikler and Rakic 1990)

New World primates particularly *Saimiri, Callithrix, Saguinus, Cebus, Aotus, and Alouatta* sp. are commonly used for biomedical research (Torres et al. 2010). Thus, much of what we know about their vision, normative ocular measurements, ocular lesions, and susceptibility to disease have been obtained in captive versus wild animals often under experimental conditions.

Ocular Anatomy, Examination, and Diagnostic Testing

Chemical restraint using a variety of agents has been described for platyrrhines including midazolam (0.5 mg/kg) and butorphanol (0.3 mg/kg) with dexmedetomidine (10 μg/kg) or ketamine (10 mg/kg) in brown howler monkeys (*Alouatta guariba clamitans*) (Fagundes et al. 2020), dexmedetomidine (10 μg/kg) and ketamine (15 mg/kg) in golden-headed lion tamarins (*Leontopithecus chrysomelas*) (Ferraro et al. 2019), and dexmedetomidine (30 or 50 μg/kg) and ketamine (7.5 mg/kg) in black capuchin monkeys (*Sapajus nigritus*) (Chagas et al. 2018). In common marmosets (*Callithrix jacchus*), alphaxalone (12 mg/kg) provided superior quality and reliability of immobilization in comparison with ketamine (50 mg/kg), ketamine (25 mg/kg) and medetomidine (0.5 mg/kg), as well as ketamine (23 and ketamine (10 mg/kg) or dexmedetomidine (10 μg/kg), with midazolam (0.5 mg/kg) and butorphanol (0.3 mg/kg), IM (Bakker et al. 2013). In particular, an unacceptably long recovery period was noted for ketamine/medetomidine protocols suggesting that α2 agonists should not be used initially for sedation in this species. Most ophthalmic examinations will require sedation in platyrrhines so species-specific protocols should be used if available given the variety in response to certain agents. Normative Schirmer tear test, intraocular pressure, refractive error, ocular

biometry, and endothelial cell density values for platyrrhines were typically measured with sedation (Table 47.1, Appendix 3) although Cochet-bonnet aesthesiometry, ultrasonic pachymetry, and rebound tonometry could be performed with manual restraint in some species (Fig. 47.12). Measurement of tear production can vary by species (Figs. 47.13 and 47.14) and phenol red thread test or use of standardized endodontic absorbent paper points may be preferable in species with small palpebral fissures such as black-tufted marmosets (*Callithrix pencillata*) (Lange et al. 2012) (Appendix 3).

Conjunctival swabs obtained from 15 bearded capuchins (*Sapajus libidinosus*) demonstrated the gram-positive genera—*Staphylococcus* spp., *Streptococcus* sp., and *Bacillus* sp. as well as the gram-negative bacteria—*Escherichia coli* and *Enterococcus* sp. (Bezerra et al. 2019). The *Staphylococcus* species are primary residents of the normal ocular microbiota in neotropical primates (Oria, Pinna, Almeida, et al. 2013a) and thus their isolation in most eyes of the bearded capuchins was unsurprising. Interestingly, *Staphylococcus* species were not identified in 5 Guianan brown capuchins (*Sapajus apella*) with *Micrococcus* sp., *Streptococcus* sp., and *Corynebacterium* sp. comprising the primary isolates (Montiani-Ferreira et al. 2008). The two species of enterobacteria isolated in the bearded capuchins was consistent with other investigations of platyrrhines including Guianan brown capuchins, black-and-gold howler monkeys (*Alouatta caraya*), golden-bellied capuchins (*Sapajus xanthosternos*), common marmosets (*Callithrix jacchus*), and black-tufted marmosets (*Callithrix penicillata*) (Oria, Pinna, Almeida, et al. 2013a; Galera et al. 2002). The enterobacteria identified in the bearded capuchins are natural inhabitants of the intestine of mammals and are excreted in feces, suggesting possible contamination of the conjunctiva with fecal matter. Given that large numbers of bearded capuchins were living in the same place (Bezerra et al. 2019), there was ample opportunity for contact with objects and water contaminated with feces. Thus, whether these gram-negative bacteria are commensal or temporary residents in the conjunctiva requires further study.

All platyrrhines have a short rostrum, with the orbit completely encompassed by bone and possessing a circular aspect around of the eye. Their orbits and globe face rostrally and there is a complete bony plate behind the orbit separating them from the temporal fossa (Fig. 47.15). The rostral position of their orbits provides superb binocular vision, a critical morphologic feature of all primates. Computed tomography (CT) of the eye, adnexa, and orbit of living and formalin-fixed samples of capuchins (*Sapajus* sp.) was performed to describe relevant anatomy for this species; histology was also done (Silva et al. 2017). The CT scans demonstrated no anatomical differences between live and formalin-fixed tissues. The capuchins studied demonstrated little scleral exposure with mild pigment present, marked limbal pigmentation, a rounded orbit, and absence of the frontal notch and supraorbital foramen. Masson's trichrome stain was used to identify the meibomian glands, corneal epithelium, and Bowman's layer, while melanocytes and Bruch's membrane were observed in the choroid, and photoreceptors in the retina and nerve fiber bundles in the lamina cribrosa were seen. Toluidine blue highlighted Bowman's layer, Descemet's membrane and the endothelium, melanocytes in the choroid, and the retinal nuclear layers and retinal pigmented epithelium. Thus, the close similarity in anatomy and histology of capuchins and humans suggests that this genus is an important experimental model for ophthalmic research.

The anatomy of the lacrimal gland has been described in the Guianan brown capuchin (*Sapajus apella*) and consists of an intraorbital and extraorbital portion connected by a band of glandular tissue (Veiga Neto et al. 1992). The intraorbital lacrimal gland is thin and flat and overlies the superotemporal aspect of the globe and the lateral rectus. By contrast, the extraorbital lacrimal gland is half-moon shaped and compact and is located in the temporal fossa between the temporalis muscle and the temporal aspect of the zygomatic bone. Ultrastructurally, both portions are similar in appearance and consistent with other mammalian species (Ruskell 1968; Scott and Pease 1959; Kühnel 1968).

In primates including common marmosets (*Callithrix jacchus*) and humans, a Schlemm's canal and a large, powerful ciliary muscle are part of the iridocorneal angle (Costa-Vila et al. 1987). Fibers are fixed in the sclera behind Schlemm's canal to form the scleral spur. Others are anchored in the membrane in front of Schlemm's canal, with thin fibers connecting Descemet's membrane and anterior face of the iris. Thus, these portions of the uveal trabecula in primates can be considered a vestige of the pectinate ligament that is so robust in domestic species such as the dog, cat, and horse.

The collagen fibril organization of the common marmoset (*Callithrix jacchus*) cornea was investigated with wide-angle X-ray diffraction and demonstrated a circumferential annulus of highly aligned collagen at the limbus (Boote et al. 2004). Similar to humans, this annulus varied in width, fibril angular spread, and collagen density around its circumference. By contrast, the more central cornea exhibits a lamellar orientation with proportionally more fibrils oriented along the superior–inferior corneal meridian contrasting with that of the human cornea, where there is an orthogonal arrangement of preferentially aligned fibrils. These differences could impact both the mechanical and optical properties of the cornea particularly the utility of this species as a model for human refractive surgery. Primates, including common marmosets (*Callithrix jacchus*), contain a well-developed

Table 47.1 Schirmer tear test, intraocular pressure, refractive error, and ocular biometry measurements for platyrrhines

Species (# of animals, unless otherwise specified)	Measurement conditions	STT-1 (mm/min)	IOP (mm Hg)	Refractive error (D)	CCT (μm)	Axial globe length (mm)	Lens thickness (mm)	AC depth (mm)	VC depth (mm)	Keratometry (D)	Endothelial cell density (cells/mm^2)	Reference
Humboldt's night monkey (*Aotus trivirgatus*, n = 18)	Ketamine (5 mg/kg), acepromazine (0.5 mg/kg)		13 ± 1		450 ± 40 (n = 6), 470 ± 20 (n = 6)					50.1 ± 1.8	2304 ± 280	Jester et al. (1981); Steel et al. (1981)
Bearded capuchin (*Sapajus libidinosus*, n = 15)	Detomidine (40 μg/kg), ketamine (5 mg/kg)	3 ± 3	13 ± 3			16.32 ± 1.24	2.86 ± 0.96	2.47 ± 0.41	10.97 ± 0.48			Bezerra et al. (2019)
Golden-bellied capuchin (*Sapajus xanthosternos*, n = 12)	Tiletamine and zolazepam (2 mg/kg)	15 ± 6	19 ± 4									Oria et al. (2013a)
Guianan brown capuchin (*Sapajus apella*, n = 15)	No sedation	15 ± 5	18 ± 4		460 ± 30							Montiani-Ferreira et al. (2008)
Common marmoset (*Callithrix jacchus*,)	Variable			+0.36	300 ± 40	10.9	2.07 ± 0.1	1.34 ± 0.10	5.84 ± 0.07; 7.19 ± 0.44		3671	Benavente-Perez et al. (2012); Morita and Shimomura (1996); Troilo et al. (1993)
Black-tufted marmoset (*Callithrix penicillata*)	No sedation	−0.46 ± 3.4*										Lange et al. (2012)
Black-tufted marmoset (*Callithrix penicillata*)	No sedation		12.7 ± 2.3		330 ± 30	10.63 ± 0.43	2.05 ± 0.22	1.58 ± 0.18				Lange (2012)
South American squirrel monkey (*Saimiri sciureus*)	No sedation	4.7 ± 2.7	9.2 ± 2.2		430 ± 60	14,23 ± 0,33	2.45 ± 0.22	2.54 ± 0.19	9.14 ± 0.35			Lange (2012)
Feline night monkey (*Aotus azarae infulatus*)	No sedation	2.1 ± 2.3	13.7 ± 5.6		440 ± 40	18.85 ± 0.58	4.75 ± 0.28	4.19 ± 0.27	9.89 ± 0.48			Lange (2012)

STT-1, Schirmer tear test-1; IOP, intraocular pressure; CCT, central corneal thickness, AC, anterior chamber; VC, vitreous chamber

Fig. 47.12 Ocular diagnostic tests can be performed in manually restrained platyrrhines. Cochet-Bonnet aesthesiometry (**a**) and rebound tonometry (**b**) are performed in an Azara's night monkey (*Aotus azarae*) and corneal thickness is measured with ultrasonic pachymetry in a squirrel monkey (*Saimiri sciureus*) (**c**). Images courtesy of Dr. Fabiano Montiani-Ferreira and Rogério Ribas Lange

lamina cribrosa with a marked concentration of astrocytic filaments distal to it as well as lack intraretinal myelination (Morcos and Chan-Ling 2000).

Platyrrhines have a brown iris with a round pupil and discoid lens (Fig. 47.16). Lens mass scales similarly with molar wear in Paraguayan howler monkeys (*Alouatta caraya*) suggesting that lens weight can be used as a surrogate for aging wild nonhuman primates (Malinow and Corcoran 1966). The vitreous is a solid gel in nearly all adult primate species with two known exceptions—Humboldt's night monkey (*Aotus trivirgatus*) and thick-tailed greater galago (*Otelemur crassicaudatus*). The normal vitreous of the adult Humboldt's night monkey is a viscous, collagen-free liquid with a highly structured hyaluronic acid and a small amount of noncollagenous proteins (Chakrabarti and Hultsch 1976). By contrast, infants of this species have a vitreous comprised of a highly elastic gel with a collagen-like network (Hultsch 1981). It then liquefies completely by 2 years of age (human age equivalent of 8–10 years). Common marmosets (*Callithrix jacchus*) received repeat intravitreal (IVT) injections of 10 or 20 µl of a placebo (70 mM mannitol, 20 mM histidine pH 6.5, and 0.04% polysorbate) to determine their utility as an alternative to cynomolgus macaques (*Macaca fascicularis*) for intravitreal toxicological studies. No ophthalmic or electroretinographic changes were observed over time or between the two dose volumes. A transient increase in IOP was observed immediately after dosing, which was more marked after dosing of 20 versus 10 µL. No histologic changes were observed at termination of the study in either group.

Platyrrhines in general possess a heavily pigmented fundus with a holangiotic retina (Fig. 47.17). Fluorescein

Fig. 47.13 Most platyrrhine species have a palpebral fissure that permits performance of a Schirmer's tear test I to measure aqueous tear production, including the (**a**) Squirrel monkey (*Saimiri sciureus*) and (**b**) Azara's night monkey (*Aotus azarae*). Images courtesy of Dr. Fabiano Montiani-Ferreira and Rogério Ribas Lange

Fig. 47.14 Tests to measure the aqueous fraction of the tear film in species with smaller eyes and palpebral fissures, such as the black-tufted marmosets (Callithrix penicillata), demonstrate that alternatives to the Schirmer tear test I are preferable. (**a**) Modified Schirmer's test I. Note that the width of half of a Schirmer's test strip occupies almost the entire palpebral fissure. There is limited space to insert the strip and this makes the procedure difficult to perform in this species. (**b**) Phenol red thread test demonstrating the color change where the thread was moistened. (**c**) Standardized endodontic absorbent paper point securely inserted in the conjunctival fornix, which was performed by only one person and without the use of any instruments for eyelid manipulation. Reprinted with permission (Lange et al. 2012)

Fig. 47.15 All platyrrhines have nearly flat faces and forward-facing complete bony orbits. A short rostrum is visible in three platyrrhine species (**a**, **b**, and **c**). They also possess complete (enclosed) bony orbits that face rostrally with a complete bony plate behind the orbit separating it from the temporal fossa (**d**, **e** and **f**). The frontward position of their orbits provides acute binocular vision, which is a defining morphologic feature in this group. Their skulls, like those of other monkeys, have large and globular brain cases. These features can be seen in macerated skulls from: (**a**) Southern brown howler (*Alouatta guariba clamitans*); (**b**) Black capuchin (*Sapajus nigritus*); (**c**) Southern muriqui (*Brachyteles arachnoides*). Pictures taken with permission at the Capao da Imbuia Natural History Museum (Curitiba, PR, Brazil)

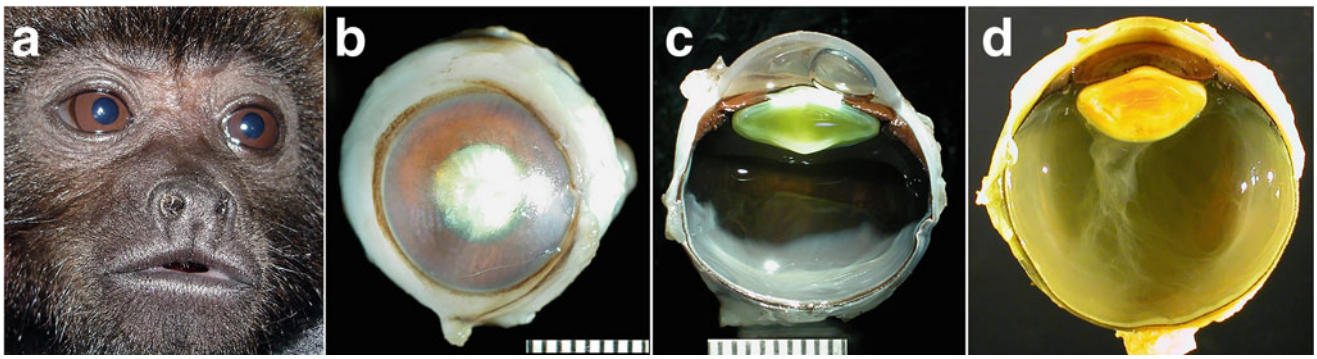

Fig. 47.16 Platyrrhines have a brown iris, round pupil, flat, discoid lens, and a heavily pigmented fundus with a holangiotic retina. External appearance of the eyes of a howler monkey (Alouatta guariba, **a**). Note the brown iris and round pupil. Gross images of the anterior segment of a 17-year-old female night monkey *(Aotus* sp., **b**) and hemi-sectioned globe from the aforementioned monkey (**c**), and a 14-year-old male Goeldi's marmoset (*Callimico goeldii*, **d**). Contrast these flat, discoid lenses with the relatively round lenses of strepsirrhine primates (Fig. 47.3) and note the similarities to that of the hominids (Fig. 47.34). A. Images courtesy of Dr. Fabiano Montiani-Ferreira (**a**) and Comparative Ophthalmic Pathology Laboratory of Wisconsin (COPLOW) (**b–d**)

angiography was performed in the common marmoset (*Callithrix jacchus*), Humboldt's night monkey (*Aotus trivirgatus*), and common squirrel monkey (*Saimiri sciureus*) using 0.3 ml (~85, ~38, and ~ 33 mg/kg for each, respectively) of 10% sodium fluorescein (Smith et al. 1964). The bald uakari (*Cacajao calvus*), common marmoset and the squirrel monkey demonstrated a virtually identical fundic appearance to that of a human (Fig. 47.17) while the Humboldt's night monkey had a smaller optic nerve head and more granular choroid. Furthermore, the perifoveal vessels were better defined in squirrel monkeys and marmosets versus the night monkey. The number of vessels ending around the macula was ~17–20 in the squirrel monkey, ~13–14 in the marmoset, and ~ 12–17 in the night monkey. Spreading of fluorescein around the macula was noted in later phases in the marmoset suggesting an excessive dose was administered and less can be used in this species. The procedure was well tolerated in all animals with no adverse events observed. Full-field electroretinography (ERG) and ERG flicker photometry to measure spectral sensitivity have been performed in several platyrrhine species (Bouskila et al. 2014; Jacobs and Deegan 2005; Jacobs and Williams 2006; Jacobs and Deegan 2003a) (Fig. 47.17). The full-field ERGs in Green monkeys (*Chlorocebus sabaeus*) were consistent those found in humans and macaques (Bouskila et al. 2014). These results suggest that platyrrhines also may serve as excellent NHP models to assess retinal structure and function during ocular drug development or visual deprivation research.

Normal retinal development has been described in marmosets and mimics that observed in macaques and humans (Hendrickson et al. 2006; Hendrickson et al. 2009; Springer et al. 2011; Böhm et al. 2016; Hendrickson et al. 2016). The retinal proteome of the rat without a macula and common marmoset (*Callithrix jacchus*) with a macula demonstrated similar aging changes (Böhm et al. 2013); the proteome of the retinal pigmented epithelium (RPE) has also been described in this monkey (König et al. 2019). Nonhuman primates have >17 types of retinal ganglion cells (RGC) that have been identified by their dendritic morphology and stratification but reliable molecular markers are rare; calretinin, a calcium-binding protein, was used to identify 3 types of thorny RGCs in common marmosets (Chandra et al. 2017; Percival et al. 2013). The midget (M)-RGC distribution in diurnal Guianan brown capuchin (*Sapajus apella*) and nocturnal Azara's night monkey (*Aotus azarae*) is similar to that reported for Old World primates, such as macaques, with peak density in the foveal slope and a decline in cells toward the periphery (Lima et al. 1993). In both species, a nasotemporal asymmetry exists with a greater density in the nasal versus temporal region. Interestingly, the nocturnal *Aotus azarae* exhibited a larger proportion of M-RGCs versus the diurnal Guianan brown capuchin or macaque species (Lima et al. 1993). Both M- and parasol (P)-RGCs are highly conserved among catarrhines and platyrrhines suggesting that they evolved prior to the divergence of these species (Silveira et al. 2004; Goodchild et al. 1996); differences in the proportion and dendritic coverage of these RGC classes exist between the central and peripheral retina in the common marmoset (Gomes et al. 2005). Furthermore, foveal input of RGCs to koniocellular pathways, a third visual afferent stream in addition to magnocellular and parvocellular pathways, is similar between common marmosets and cynomolgus macaques (Percival et al. 2013). The morphology of and synaptic input to small bistratified (Blue-ON) RGCs have been described in common marmosets and tufted capuchins (Ghosh and Grünert 1999; Ghosh et al. 1997; Silveira et al. 1999; Ghosh et al. 1996; Percival et al. 2009). The same morphologic bipolar cell types—6 types of diffuse bipolar cells, 2 types of midget

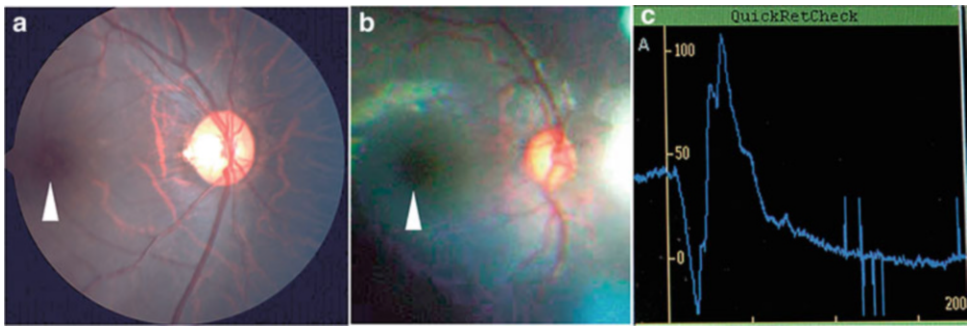

Fig. 47.17 Normal fundus and electroretinogram of platyrrhines. The fundus of a bald uakari (*Cacajao calvus*, **a**) and a black-tufted marmoset (*Callithrix penicillata*, **b**) exhibit holangiotic retinas with variable pigmentation such that some choroidal vessels are visible, a reflective nerve fiber layer, and a nearly round optic nerve head. Note the fovea (arrowheads) temporal to the optic disc. (**c**) Scotopic electroretinography was performed in a red-faced spider monkey (*Ateles paniscus*, **c**). Reproducible values of amplitude and latency were obtained for the a- and b-waves, under well-controlled adaptation and stimulus conditions using a portable mini Ganzfield ERG unit (HMsERG model 1000, RetVet Corp, Columbia, MO, USA). Images courtesy of Dr. Fabiano Montiani-Ferreira (**b** and **c**)

bipolar cells, a blue cone bipolar cell, and a rod bipolar cell—were observed in common marmosets and macaques suggesting that bipolar diversity is conserved feature in primates (Chan et al. 2001; Luo et al. 1999; Telkes et al. 2008; Lee and Grünert 2007; Jusuf et al. 2006b, 2006a; Masri et al. 2016); bipolar cells also provide input to melanopsin-containing ganglion cells in a similar manner in both species (Grünert et al. 2011; Jusuf et al. 2007). The expression of different types of glutamate receptors in OFF midget bipolar cells was described in the common marmoset (Puller et al. 2007). A quantitative analysis of inner retinal cells in the common marmoset demonstrated similar proportions of bipolar, amacrine, horizontal, and Müller cells in the central and peripheral retina; marmoset and macaque proportions were similar after accounting for differences in rod and cone populations between the two species (Weltzien et al. 2015). The calcium-binding protein, secretagogin, was used to map the location and neurotransmission of regular and displaced medium-field amacrine cells in the common marmoset retina (Weltzien et al. 2014). Horizontal cells in New and Old World monkeys are also similar, including their connectivity with short wavelength sensitive cones, suggesting this wiring is likely common among all primates (Chan and Grunert 1998; Chan et al. 1997). Nonhuman primates including common marmosets displayed similar pattern of expression of molecular markers for rods and cones; S-cones displayed an intermediate pattern of expression between rods and L- and M-cones in all species studied (Craft et al. 2014). In common marmosets, the topography and spatial density of cone photoreceptors and ganglion cells is similar to that of the macaque retina (Tovée et al. 1992). In aggregate, these observations suggest that primate retinal architecture, particularly in the fovea, is conserved across catarrhines and platyrrhines to maximize spatial resolution (Tovée et al. 1992; Kremers and Lee 1998; Franco et al. 2000; Hiraoka et al. 2012; Andrade da Costa and Hokoc 2000; Finlay et al. 2008).

Common marmosets (*Callithrix jacchus*) can be restrained in chairs and trained to complete simple oculomotor tasks (Johnston et al. 2018), have been used to study the oculovestibular reflex (Anzai and Nagao 2014) as well as the motion dependence of smooth eye pursuits (Mitchell et al. 2015). In addition, functional magnetic resonance imaging has been performed on awake common marmosets completing simple visual tasks (Hung et al. 2015). The visual pathways and striate cortex of platyrrhines including capuchins (*Cebus* and *Sapajus* sp.) (Kaas et al. 1978; Rosa et al. 1991; Rosa et al. 1992; Hendrickson et al. 1978; Acuna et al. 1983; Wilson et al. 2016), marmosets (Engelberth et al. 2008; Hendrickson et al. 2015; Roe et al. 2005; Sengpiel et al. 1996; Ribic et al. 2011; Fonta et al. 1997; Palmer and Rosa 2006; McLoughlin and Schiessl 2006; Bourne and Rosa 2003; Nowak and Barone 2009; Yu et al. 2018; Cusick et al. 1984; DeBruyn and Casagrande 1981; Weber and Giolli 1986; Spatz 1979; Fonta et al. 2000; Eiber et al. 2018a; Cavalcante et al. 2005; de Sousa et al. 2013; Martin et al. 1997; Weiss et al. 1998; Kremers 1998; Spatz 1978; White et al. 2001; White et al. 1998; Blessing et al. 2004; Webb et al. 2005; Szmajda et al. 2008; Federer et al. 2009; Tailby et al. 2010; Kozyrev et al. 2007; Percival et al. 2011; Buzás et al. 2008; Buzás et al. 2006; Victor et al. 2007; Martin et al. 2011; Roy et al. 2009; Hashemi-Nezhad et al. 2008; Eiber et al. 2018b; Yeh et al. 1995; Chaplin et al. 2013; Huo et al. 2019; Tailby et al. 2008; FitzGibbon et al. 2015; Wallace et al. 2016), saki monkeys (*Pithecia* sp.) (Kaas et al. 1978), spider monkeys (*Ateles* sp.) (Hubel and Wiesel 1968; Florence et al. 1986; Hendrickson et al. 1978), squirrel monkeys (*Saimiri* sp.) (Kaas et al. 1978), and titi monkeys (*Callicebus* sp.) (Baldwin and Krubitzer 2018) have been extensively studied and we refer the readers to these primary

sources should they be of interest. Specifically, S-cone signal distribution, S-cone recipient field properties in subcortical pathways, and S-cone visual and extrastriate visual cortical pathways have been extensively studied in marmosets and are reviewed here (Martin and Lee 2014; Jayakumar et al. 2013). Marmosets were used to investigate the phenomenon of blindsight or retention of some visually guided behavior following damage to the primary visual cortex and we direct the reader to this detailed review (Hagan et al. 2017). Finally, marmosets are a promising model for investigating active vision and its underlying neural circuits (Mitchell et al. 2014; Mitchell and Leopold 2015; Solomon and Rosa 2014), evaluating the differences in visual processing of central and peripheral stimuli (Yu et al. 2015), and broadening our understanding of circadian timing system (Lima et al. 2012).

Ophthalmic Disease

In a clinical survey of 526 captive tamarins and marmosets, 109 animals (21%) had at least one ocular lesion (Buyukmihci and Richter 1979). Nine species were evaluated including cotton-top tamarin (*Saguinus oedipus*, n = 218), Illiger's saddle-back tamarin (*Saguinus illigeri*, n = 134), common marmoset (*Callithrix jacchus*, n = 89), *Saguinus* hybrids (n = 42), Geoffroy's saddle-back tamarin (*Saguinus nigrifrons*, n = 23), black-mantled tamarin (*Saguinus nigricollis*, n = 9), Andean saddle-back tamarin (*Saguinus leucogenys*, n = 6), red-mantled saddle-back tamarin (*Saguinus lagonotus*, n = 3), Spix's saddle-back tamarin (*Saguinus fuscicollis*, n = 1), and pygmy marmoset (*Cebuella pygmaea*, n = 1). The most common lesions involved the eyelids (n = 50), and included obstructed meibomian ducts (n = 20), trauma (n = 15), tumors (n = 5), entropion (n = 2), ectropion (n = 2), distichiasis (n = 2), unequal palpebral fissures (n = 2), and lagophthalmos (n = 1) (Buyukmihci and Richter 1979). In addition to eyelid trauma, other traumatic/inflammatory lesions were relatively common including keratitis (n = 9), corneal pigmentation (n = 6), and collapsed anterior chamber due to previous globe rupture (n = 1). Cataracts were frequent (n = 32) and typically nuclear (n = 18); nuclear opacities did not progress over a period of 5–6 months. Cataracts in other locations were typically associated with trauma or uveitis with concurrent posterior synechiae (n = 5) or lens pigmentation (n = 4); bilaterally symmetrical, posterior cortical cataracts were rarely found (n = 3). Ocular developmental lesions included persistent pupillary membranes (n = 6), optic disc ectasia (n = 2), and a *Saguinus* hybrid with microphthalmia in the right eye and a cystic left eye. Iris cysts were rare (n = 2). Neuro-ophthalmic conditions identified were esotropia (n = 2), anisocoria (n = 2), and facial nerve paralysis (n = 1) due to squamous cell carcinoma (Richter and Buyukmihci 1979). Fundic lesions included focal depigmentation/chorioretinal scars (n = 18), optic disc irregularity (n = 3), progressive retinal and optic nerve atrophy (n = 1), drusen-like lesion (n = 1), and optic disc pigmentation (n = 1). Of all the lesions described, only 2 animals (0.04%) exhibited vision impairment from microphthalmia and cystic eye or progressive retinal and optic nerve atrophy. Congenital malformations including microphthalmia and ocular hypertelorism have been described in a newborn common marmoset (*Callithrix jacchus*) that appeared clinically and radiographically similar to human 13-trisomy syndrome (Pugsley 1985). Ocular trauma is common in other species as well with cicatricial entropion and symblepharon documented in a squirrel monkey (*Saimiri* sp., Fig. 47.18).

Herpes simplex virus-1 (HSV-1) is highly pathogenic to NHPs, typically resulting in acute, fatal encephalitis but species variability exists particularly in platyrrhines. A 20-year-old male intact white-faced saki monkey (*Pithecia pithecia*) was diagnosed with ulcerative keratitis and reflex uveitis OD; conjunctival swabs were positive for HSV-1 using PCR (Bauer et al. 2018). Initial clinical signs resolved with supportive treatment, and the animal was treated with acyclovir (5 mg/kg PO twice daily) during flare-ups. Enucleation OD was performed >2 years after initial presentation due to progression of clinical disease and chronic, erosive keratoconjunctivitis, mild to moderate chronic lymphohistiocytic iridocyclitis and chronic retinal detachment with degeneration were found on histopathology; no viral inclusions were identified. At 2 months following surgery, the monkey was euthanized following acute presentation of severe neurologic signs, including ataxia and blindness. Histopathology, PCR analysis, and sequencing confirmed viral encephalitis from HSV-1. This study and others suggest that some platyrrhines may only present with ocular HSV-1, (Felsburg et al. 1973; Gozalo et al. 2008; Varnell et al. 1987) and can thus be chronically managed with oral antivirals. For example, experimental inoculations of one cornea in Guianan brown capuchins (*Sapajus apella*) with HSV-1 and HSV-2 resulted in typical clinical signs including follicular conjunctivitis and superficial ulcerative keratitis (Felsburg et al. 1973). Although throat swabs were positive for the virus inoculated and contralateral ocular signs were observed, none of the monkeys developed neurological signs.

An odontogenic intraorbital abscess was diagnosed in an adult male Guianan brown capuchin (*Sapajus apella*) that was presented for weight loss, periorbital edema, exophthalmos OD and ipsilateral purulent nasal discharge (Oria et al. 2013b). Treatment was initiated with ketoprofen (5 mg/kg SC, SID) and enrofloxacin (5 mg/kg SC, SID) but his condition worsened and he was anesthetized for a physical examination. An absent menace response and pupillary light reflex,

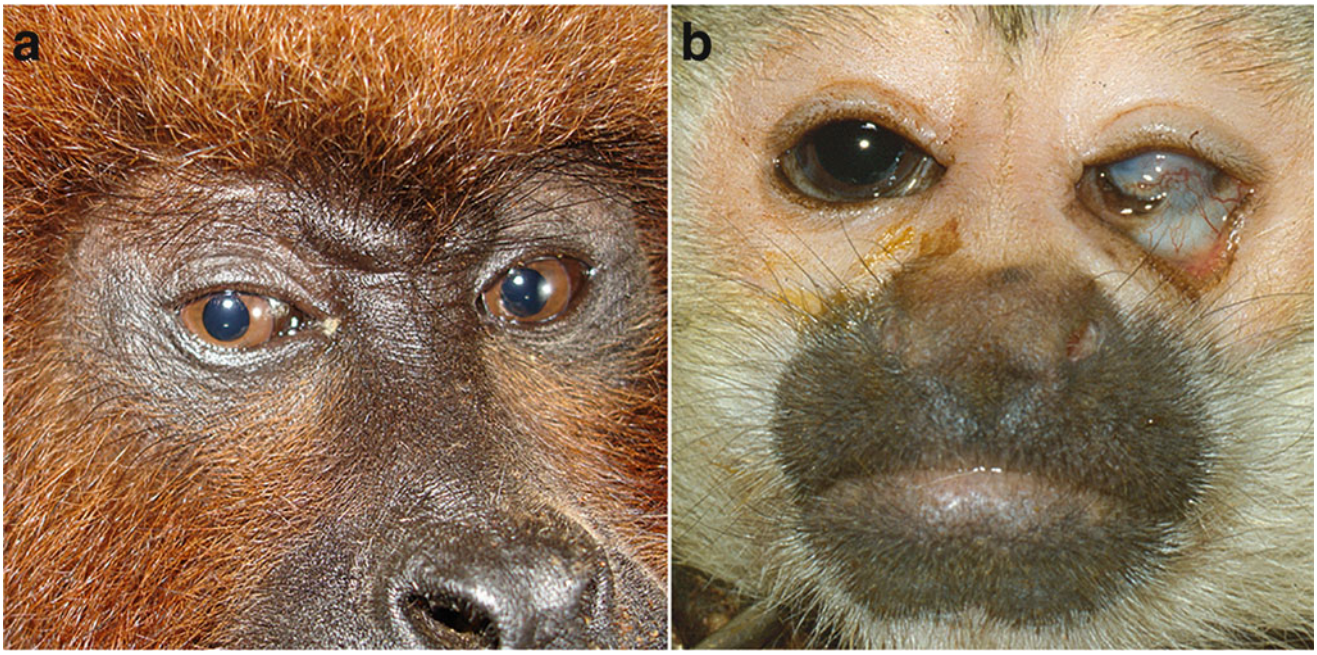

Fig. 47.18 Ocular surface lesions have been documented in platyrrhines. (**a**) Bacterial conjunctivitis in the right eye of a brown howler monkey (*Alouatta guariba*). Note the blepharospasm and ocular discharge; image courtesy of Fabiano Montiani-Ferreira. (**b**) Cicatricial ectropion and symblepharon in the left eye of a squirrel monkey (*Saimiri* sp.); image courtesy of Dr. Dennis Brooks

severe exophthalmos, lagophthalmia, pain on palpation, chemosis, conjunctival hyperemia, corneal desiccation, and ulceration were identified OD; all canine teeth were also fractured at the root with pulp exposure. A complete blood count demonstrated anemia and leukocytosis. Skill radiographs suggested a periodontal abscess of the right upper canine tooth and computed tomography demonstrated isodense material in the right maxillary sinus and orbit. Orbital exenteration was performed, the enrofloxacin was discontinued and treatment was initiated with azithromycin (40 mg/kg SC, BID). Culture and susceptibility testing of the orbital secretions identified *Proteus* sp., *Staphylococcus* sp., β-hemolytic *Streptococcus* sp., and *Escherichia coli* susceptible to amikacin, gentamicin, and tobramycin. The azithromycin was discontinued and a 21-day course of gentamicin (4 mg/kg SC, BID) was administered. At 30 days after exenteration, a purulent medial canthal discharge was still observed. The right upper canine was extracted under anesthesia and gentamicin was administered for an additional 21 days.

Ocular Surface Disease and Refractive Error

A pyogenic granuloma of the left superior eyelid was excised from a 3.5-year-old woolly monkey (*Lagothrix* sp.) (Karpinski 1975). Two months prior, purulent ocular discharge was observed from the left eye. Ophthalmic examination under injectable anesthesia with ketamine (2.3 mg/kg) revealed a discrete, ovoid, firm, red mass with a friable surface on the palpebral conjunctiva of the left superior eyelid. Differential considerations for this mass in a nonhuman primate included a foreign body, ruptured internal chalazion, fungal granuloma, protozoal granuloma, amyloidosis (Glass et al. 1971), tuberculosis, and lymphoma (Tabor 1973). An incisional biopsy was performed which demonstrated a mononuclear intra- and subepithelial infiltrate. Two weeks later, the mass had increased in size to encompass the entire superior eyelid margin and evert it. Following injectable anesthesia with ketamine and local infiltration of the eyelid with lidocaine, an excisional biopsy of the mass was performed 1 mm from the palpebral margin leaving only the skin of the superior eyelid. The remaining unaffected palpebral conjunctiva was sutured with 6–0 collagen in a simple interrupted pattern while burying the knots. Post-operatively, neomycin-polymyxin B-dexamethasone ophthalmic solution (Maxitrol®) was applied. One month later, the surgical site had healed and the eyelid had returned to a normal position. The biopsy identified granulation tissue with epithelial hyperplasia and a diffuse mononuclear and eosinophilic infiltrate; lipid clefts were also present. Thus, this lesion likely represented a lipogranuloma from a ruptured chalazion.

Conjunctivitis due to allergic and bacterial causes has been described. Allergic conjunctivitis was reported in a 6-month-old black-headed spider monkey (*Ateles fusciceps*) (Hoopes et al. 1977). Clinical signs were ocular rubbing, blepharoedema, and chemosis in both eyes. Topical chloramphenicol ophthalmic ointment OU TID and subcutaneous benzathine penicillin G (4,600 U/kg) every 3 days

administered for 2 weeks resolved the signs. However, the conjunctivitis recurred multiple times over a 9-month-period despite treatment with topical ophthalmic antibiotics and corticosteroids with subconjunctival and systemic antibiotics which only resulted in transient improvement; a topical antiviral was ineffective. Four conjunctival cultures performed during this 9-month period isolated *Staphylococcus aureus* and a *Streptococcus* sp. which were both susceptible to most antibiotics that were utilized. Multiple conjunctival biopsies demonstrated marked epithelial hyperplasia with mucosal papillary folds and expansion of the submucosa by edema and an infiltrate of neutrophils, mast cells, and plasma cells. Special stains for bacteria, fungi, and acid-fast organisms were negative. At 10 months, an allergic or autoimmune etiology was presumptively diagnosed and topical neomycin-dexamethasone ophthalmic ointment TID and intramuscular dexamethasone (~0.3 mg/kg) BID were instituted then tapered over 14 days with complete resolution of clinical signs. During the next 5 months, mild flare-ups occurred which were responsive to short courses of systemic methylprednisolone (~0.04 mg/kg). No recurrences of conjunctivitis were observed in the 18 months that followed. Bacterial conjunctivitis is occasionally reported in captive New World monkeys and is usually sudden in onset and unilateral. The conjunctiva usually is reddened, edematous and there are variable amounts of mucopurulent exudate in the conjunctival sac or canthus (Fig. 47.18). Topical treatment with broad-spectrum antibiotics usually is effective (Montiani-Ferreira, F., personal communication, 2021).

Dry eye was described in three male Ma's night monkeys (*Aotus nancymaae*) from prior ocular experimental procedures (Schuler et al. 2009). Schirmer's tear tests performed under sedation with intramuscular ketamine (~12.5 mg/kg) and xylazine (~1.25 mg/kg) were initially 0 in the 5 affected eyes. Treatment with a 0.5% cyclosporine ophthalmic emulsion (Restasis®, Allergan) twice daily decreased eye rubbing and conjunctivitis and increased mean and highest tear production to 4.4 ± 2.6 and 7.4 ± 3.9 mm/5 min, respectively. Positive reinforcement was used to train the monkeys to receive the treatment without sedation and it could eventually be performed without protective leather gloves. Experimental chronic vitamin A deficiency in 4 adult common marmosets resulted in xerophthalmia and keratomalacia with corneal rupture occurring in one individual (Hayes 1974).

Humboldt's night monkeys (*Aotus trivirgatus*) have been used as a trachoma disease model; monkeys experimentally infected with *Chlamydia trachomatis* in the eye displayed severe, acute conjunctivitis with mucopurulent discharge and marked intracytoplasmic inclusions on cytology (Fraser 1976). The condition was self-limiting with animals disease-free by 5 weeks and animals were resistant to re-infection for up to 6 months. This disease course contrasts with the mild clinical signs observed in other NHPs such as rhesus macaques, cynomolgus macaques, and Grivet monkeys (*Chlorocebus aethiops*); Taiwanese macaques (*Macaca cyclopis*) also displayed mild clinical signs with few intracytoplasmic inclusions. In aggregate, these data suggest that night monkeys may be more susceptible to trachoma than Old World NHPs and could develop disease if exposed to *Chlamydia trachomatis* in the wild or captivity. Ocular inserts compromised of N-vinylpyrrolidone impregnated with erythromycin completed suppressed clinical signs in this night monkey trachoma model (Hosaka et al. 1983).

Optical defocus with negative and positive lenses were used to induce myopia and hyperopia, respectively, in common marmosets to study differences in gene expression in the retina, choroid, and RPE gene expression; some genes identified have been linked with myopia in humans suggesting common disease pathways and identifying novel therapeutic targets (Tkatchenko et al. 2018; Shelton et al. 2008). Exposing common marmosets to simultaneous negative and positive defocus with multifocal lenses resulted in less myopia and may be an effective treatment protocol to prevent or treat this condition in human patients (Benavente-Perez et al. 2012). Myopia can also be induced in adult common marmosets with form deprivation via eyelid closure but varied with age (Troilo et al. 2000b; Troilo and Nickla 2005); changes in choroidal thickness and scleral proteoglycan synthesis were observed with this visual deprivation (Troilo et al. 2000a; Rada, Nickla, and Troilo 2000). Radial keratotomy for low to moderate myopia was evaluated in normal Humboldt's night monkeys (*Aotus trivirgatus*); corneal flattening was variable and unstable following the procedure similar to human studies (Jester et al. 1981; Steel et al. 1981). This species was also used to study corneal epithelial histology following contact lens wear (Bergmanson 1987; Bergmanson et al. 1985) as well as long-term corneal wound healing following phototherapeutic keratectomy (Marshall et al. 1988).

Intraocular Disease

Unilateral or bilateral cataracts of varying stages have been described in several species of New World monkeys, including a woolly monkey (Peiffer and Gelatt 1976), Geoffrey's spider monkey (*Ateles geoffroyi*) (Peiffer and Jacobson 1978), as well as marmosets and tamarins (Buyukmihci and Richter 1979; Leiva et al. 2012). Informal reports of cataracts in a brown howler monkey (*Alouatta guariba*), red-faced spider monkey (*Ateles paniscus*), and pygmy marmoset (*Cebuella pygmaea*) also exist (Montiani-Ferreira, F., personal communication, 2021) (Fig. 47.19). An adult brown howler monkey (*Alouatta guariba*) with hypermature cataracts and a focal posterior synechia was brought by the Brazilian wildlife services to seek veterinary care at the

Fig. 47.19 Multiple species of platyrrhines have been diagnosed with cataracts. A unilateral hypermature cataract was identified in a young adult, male capuchin monkey (*Cebus apella*, **a**). Bilateral hypermature cataracts in a young adult, male pygmy marmoset (*Cebuella* sp., **b**) rescued by the Brazilian Army in the Amazon Rainforest. Bilateral mature cataracts were found in a red-faced spider monkey (*Ateles paniscus*, **c** and **d**). Photo credits to Thiago Alegre Coelho Ferreira (**a**) and Dr. Fabiano Montiani-Ferreira (**b**–**d**)

Federal University of Paraná, Curitiba-PR, Brazil. The affected eye (left) was submitted to B-mode ultrasonography, which revealed a complete retinal detachment. Electroretinography showed no response to any stimulus in the left eye indicating absent outer retinal function (Montiani-Ferreira, F., personal communication 2021) (Fig. 47.20).

A condition similar to normotensive glaucoma has been reported whereby 11% of aged common marmosets (*Callithrix jacchus*) demonstrated loss of visual cortex volume with MRI and degeneration of the lateral geniculate nuclei and visual cortex with histology; IOP was normal in these individuals (Noro et al. 2019). Laser trabeculoplasty administered twice at 2-week intervals induced glaucoma in common marmosets resulted in persistent IOP elevation and optic disc cupping observed clinically and retinal ganglion cell loss and axonal atrophy observed histologically (Shimazawa et al. 2013). In aggregate, these studies suggest that both normotensive and hypertensive glaucoma can occur

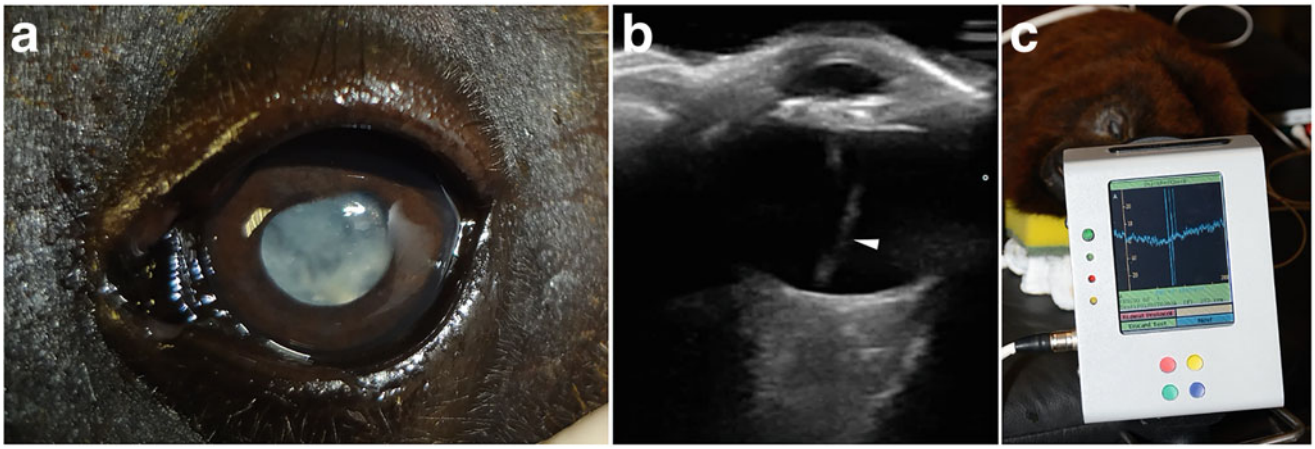

Fig. 47.20 Hypermature cataracts, posterior synechia, retinal detachment, and absent retinal function in a brown howler monkey (*Alouatta guariba*). Note the dyscoric pupil and hypermature cataract in the left eye (**a**). B-mode ultrasonography revealed the presence of a complete retinal detachment (arrowhead, **b**). Electroretinography using a portable mini Ganzfield ERG unit (HMsERG model 1000, RetVet Corp, Columbia, MO, USA) showed no response to any flashlight stimulus consistent with absent outer retinal function (**c**). Images courtesy of Dr. Fabiano Montiani-Ferreira

in platyrrhines. Indeed, secondary glaucoma has been identified in free-living New World monkeys as well (Fig. 47.21).

Diurnal rhythms were not only observed with IOP in common marmosets (*Callithrix jacchus*) but also with axial globe length and choroidal thickness; IOP was highest during the dark period suggesting that once daily glaucoma medications should be administered in the early evening for platyrrhines (Nickla et al. 2002). Normal Guianan brown capuchins (*Sapajus apella*) were used to demonstrate that the topical α2 agonists, xylazine and UK-14, 304–18, as well as the dopamine (DA_2) agonist, N,N-disubstituted 5-OHAminotetralin, decreased IOP and caused miosis (Burke and Potter 1986; Crosson et al. 1987), the serotonin receptor (5HT2) antagonist, ketanserin, lowered IOP (Chang et al. 1985), and the ergoline derivative, LY141865, decreased IOP and caused mydriasis (Potter and Burke 1982). Furthermore, tufted capuchins were instrumental in the preclinical development of brimonidine, an α2 agonist, that is commonly used to treat glaucoma in humans (Burke and Schwartz 1996). These studies suggest that drugs that are effective in the treatment of glaucoma in humans are likely to be efficacious in platyrrhines.

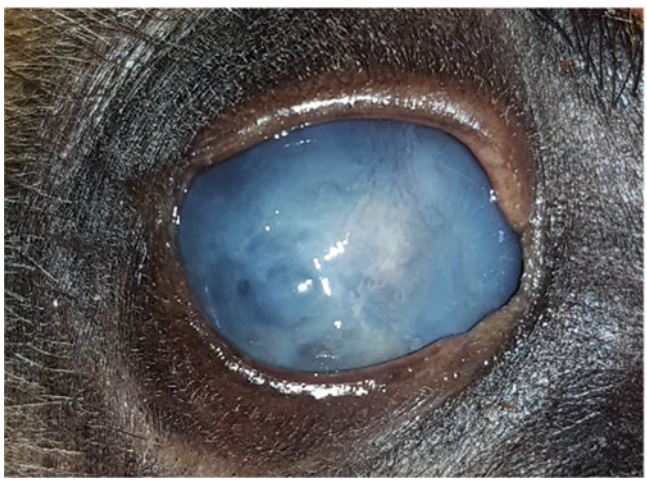

Fig. 47.21 Buphthalmos and severe corneal edema due to secondary glaucoma in the right eye of a free-living brown howler monkey (*Alouatta guariba*). Image courtesy of Dr. Thiago Alegre Coelho Ferreira

Healthy night monkeys (*Aotus* sp.) were used to demonstrate the ability of cyclocryosurgery (Quigley 1976) to lower intraocular pressure (IOP) suggesting that these methods would be effective at treating glaucoma in primates; severe anterior uveitis with hyphema was observed immediately after surgery but resolved after a week. An experimental model of filtering bleb surgery using posterior lip sclerectomies was developed in night monkeys (*Aotus* sp.) (Desjardins et al. 1986). This procedure combined with subconjunctival 5-fluorouracil (3 mg) in healthy night monkeys significantly decreased IOP in comparison with saline-injected eyes but complications were observed including corneal epithelial defects, hyphema, and collapsed anterior chambers (Gressel, Parrish, and Folberg 1984). Posterior lip sclerectomies combined with subconjunctival 5-fluorouridine 5′-monophosphate (6 mg) in the aforementioned species were associated with severe complications including corneal infection, hyphema, and bone marrow aplasia (Skuta et al. 1987) and thus are not recommended to manage glaucoma.

Night monkeys (*Aotus* sp.) were used to study retinopathy induced by intravitreal silicone oil (Mukai et al. 1975). In contrast to cats, white-fronted capuchin (*Cebus albifrons*) and cynomolgus macaque infants fed a diet deficient in

taurine exhibited growth depression but normal retinal development (Hayes et al. 1980). Choroidal neovascularization (CNV) has been induced with a laser in common marmosets (*Callithrix jacchus*) as a model for the wet form of age-related macular degeneration to demonstrate that a single intravenous dose of edaravone, a free radical scavenger, decreased CNV area versus controls (Masuda et al. 2016). Diabetic retinopathy has been induced in common marmosets fed a galactose enriched diet exhibited thickening of the foveal and perifoveal retina with optical coherence tomography and retinal microaneurysms with histology suggesting that diabetic NHPs are likely to develop a similar retinopathy to their human counterparts (Chronopoulos et al. 2015).

Retinal cells derived from common marmoset pluripotent stem cells provide potentially unlimited cell sources for testing tolerability and immunogenicity following autologous or allogeneic transplantation using NHPs in early translational research programs (Torrez et al. 2012). Common marmosets (*Callithrix jacchus*) were used to demonstrate robust transduction efficiency of a 200-bp mGluR6 enhancer in combination with a basal SV40 promoter for AAV-mediated gene delivery to ON-type bipolar cells around the fovea and far peripheral retina (Lu et al. 2016). A recombinant adeno-associated virus serotype 2 (rAAV2) fusion construct of channelopsin-2 (Chop2) and green fluorescent protein (GFP) (Chop2-GFP) was expressed in all major neurons of the inner retina and channelrhodopsin-2 mediated light responses were electrophysiologically recorded in the common marmoset suggesting that these now photosensitive cells could be used as a novel treatment for blindness from retinal degeneration (Ivanova et al. 2010).

Old World Monkeys (Superfamily Cercopithecoidea)

The suborder Haplorhini is divided into the parvorder Catarrhini with monkeys that have narrow, downward facing nostrils and the parvorder Platyrrhini with monkeys that display broad, flat nostrils. The parvorder Catarrhini is subdivided into two superfamilies—Cercopithecoidea and Hominoidea. The latter superfamily is discussed in section 51.5. The superfamily Cercopithecoidea includes the single family, Cercopithecidae, which includes the largest number of species at 159 worldwide (Mittermeier 2013). This family is divided into two subfamilies—Cercopithecinae and Colobinae—based on diet with cheek-pouched monkeys eating primarily fruit and leaf-eating monkeys consuming mainly foliage, respectively. The subfamily Cercopithecinae is subdivided into two tribes—Papionini with 45 species including macaques, mangabeys, and baboons and Cercopithecini with 36 species including talapoins, green monkeys, and guenons. The subfamily Colobinae is subdivided into two tribes—Colobini with 23 species including colobus and Presbytini with 55 species including langurs, doucs, and snub-nosed monkeys. Cercopithids reside in tropical and subtropical Africa, portions of the Arabian Peninsula, the Indian Subcontinent, as well as large parts of East and Southeast Asia, hence the name Old World monkey.

Cercopithids exhibit diverse behavior, diet, morphology, and distribution. All are diurnal and most are arboreal with all retaining the ability to climb trees but some are highly or semi-terrestrial. Their diet consists of fruit, leaves, seeds, buds, roots, as well as invertebrates and small vertebrates. The size of cercopithids ranges widely from talapoins (*Miopithecus*) weighing ~1 kg to the Mandrill (*Mandrillus sphinx*) weighing up to 50 kg. Catarrhine primates, including cercopithids, all have trichromatic color vision from an X-chromosome opsin duplication occurring ~35 million years ago that resulted in separate genes encoding for the middle- (M) and long- (L) wavelength sensitive cone pigments (Nathans et al. 1986). Trichromacy is particularly useful in catarrhines for the detection of fruit or young leaves against the background of mature leaves (Sumner and Mollon 2000; Dominy and Lucas 2001) as well as interpreting the multicolored face of the male mandrill which communicates dominance as a multicomponent signal (Renoult et al. 2011). Furthermore, visual social attention is an important aspect of cercopithid behavior and varies even among closely related species. For example, gaze types varied with more glancing versus looking behaviors exhibited in gray-cheeked mangabeys (*Lophocebus albigena*) and red-capped mangabeys (*Cercocebus torquatus*), respectively (Blois-Heulin 1999).

Old World primates particularly macaques (*Macaca* sp.) and baboons (*Papio* sp.) are commonly used for biomedical research with the colobus monkey (*Colobus* sp.), mandrill (*Mandrillus* sp.), mangabey (*Cercocebus* sp.), and Patas monkey (*Erythrocebus* sp.) more sporadically studied (Ward and Vallender 2012) (Fig. 47.22).

Ocular Anatomy, Examination, and Diagnostic Testing

Chemical restraint using a variety of protocols have been reported in cercopithids (Field et al. 1966; Pulley et al. 2004; Wada et al. 2020). To perform ophthalmic examinations and diagnostic testing in rhesus macaques at CNPRC, ketamine (10 mg/kg, IM) is administered as initial sedation and rebound tonometry is performed. Then, dexmedetomidine (0.075 mg/kg) and midazolam (0.10 mg/kg) are administered intramuscularly. If additional sedation is required, we administer additional doses of ketamine (5 mg/kg, IM) and/or dexmedetomidine (0.037 mg/kg, IM); the total doses do not exceed 30 mg/kg for ketamine and

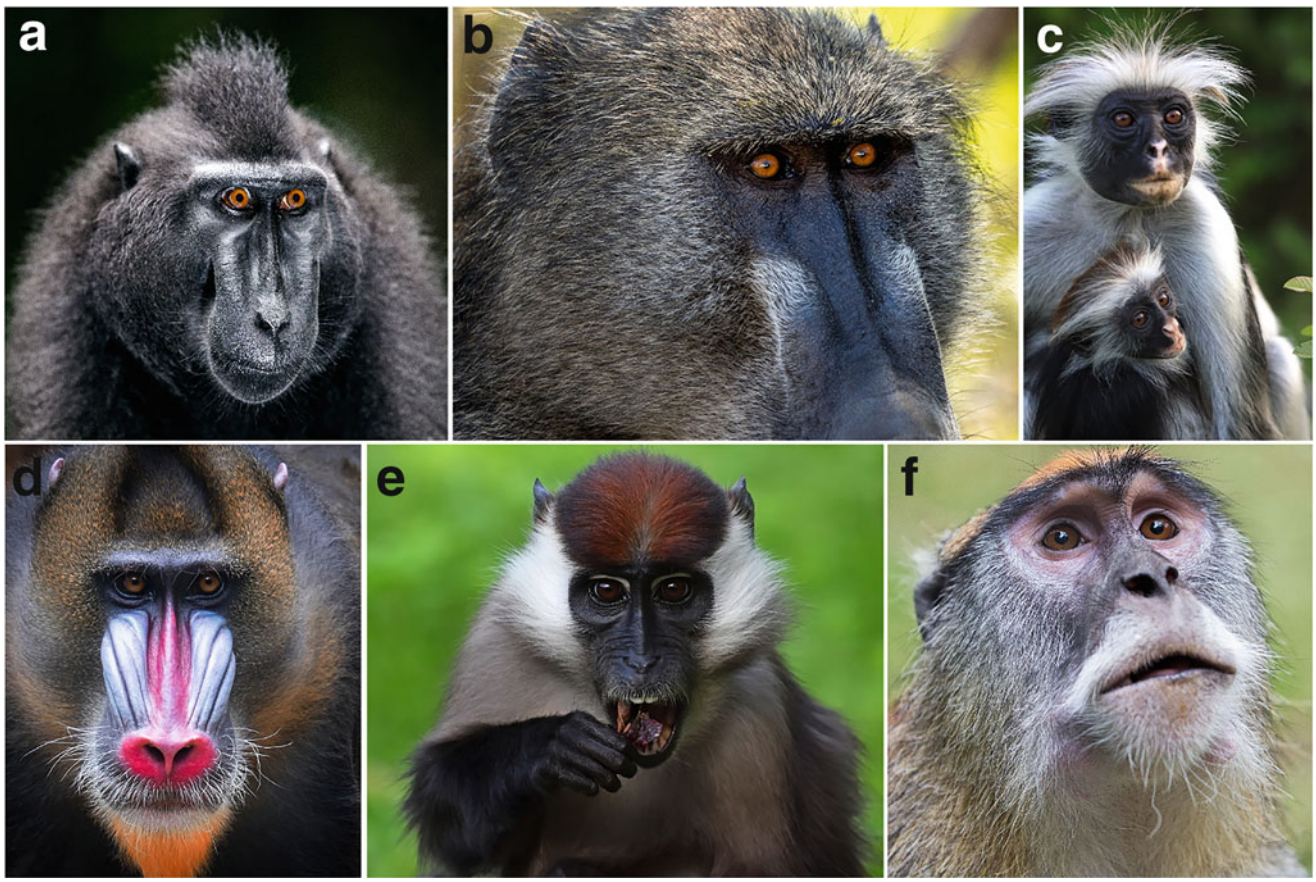

Fig. 47.22 Cercopithids especially the macaque (**a**) and baboon (**b**) are commonly used for ocular research while the colobus monkey (**c**), mandrill (**d**), mangabey (**e**), and Patas monkey (**f**) are more sporadically utilized. Note the forward-facing eyes of varying prominence that typify nonhuman primates. Photo credits for Crested macaque (*Macaca nigra*) by Edwin Butter, Shutterstock.com (**a**); olive baboon (*Papio anubis*) by Clayton Harrison, Shutterstock.com (**b**), Zanzibar red colobus (*Piliocolobus kirkii*) by Robin Batista, Shutterstock.com (**c**), mandrill (*Mandrillus sphinx*) by Hok Liang Irwan Gunadi, Shutterstock.com (**d**); red-capped mangabey (*Cercocebus torquatus*) by Breaking the Walls, Shutterstock.com (**e**); Patas monkey (*Erythrocebus patas*) by Bogdan Vija, Shutterstock.com (**f**)

0.015 mg/kg dexmedetomidine. In a two-hour time period with the aforementioned sedation, we are typically able to perform rebound tonometry, assessment of PLRs, specular microscopy, scotopic and photopic electroretinography, slit lamp examination of the anterior segment, indirect ophthalmoscopy, fundus photography, FD-OCT with cSLO to examine the retina, choroid and optic nerve, refraction, A-scan ocular biometry, ultrasound pachymetry of the central cornea, and fluorescein stain to give a comprehensive assessment of ocular health (Appendix 3). To facilitate this ophthalmic testing, the sedated macaques are placed in sternal recumbency on mobile carts padded with memory foam to approximate the height of the instruments.

Iridal color varies in rhesus macaques similar to that in humans with blue, green, hazel, and brown irises identified (Fig. 47.23). In addition to macaques, blue irides are found in blue-eyed black lemurs (*Eulemur macaco flavifrons*) (Fig. 47.2), spider monkeys (*Ateles* sp.), and humans (*Homo sapiens*) (Eiberg et al. 2008; Yamigawa 1979; Hernandez-Camacho and Cooper 1976). However, the precise causal mutation for blue irides is unknown in all species but humans.

Schirmer tear test-1 (STT-1) values have been evaluated in 62 normal rhesus macaques with a mean (95% confidence interval) of 15 (6–24) mm/min reported (Jaax et al. 1984) (Appendix 3). Importantly, this study did not identify a significant difference between physical restraint and chemical immobilization with ketamine (10 mg/kg) or between males and females. Thus, the STT-1 can provide meaningful results when tranquilization is required to safely restrain rhesus macaques and presumably other NHPs.

Intraocular pressure has been measured with a variety of techniques in multiple cercopithicid species under variable conditions. Consistent with other animals, applanation tonometry underestimates intraocular pressure in anesthetized cynomolgus macaques in comparison with manometry

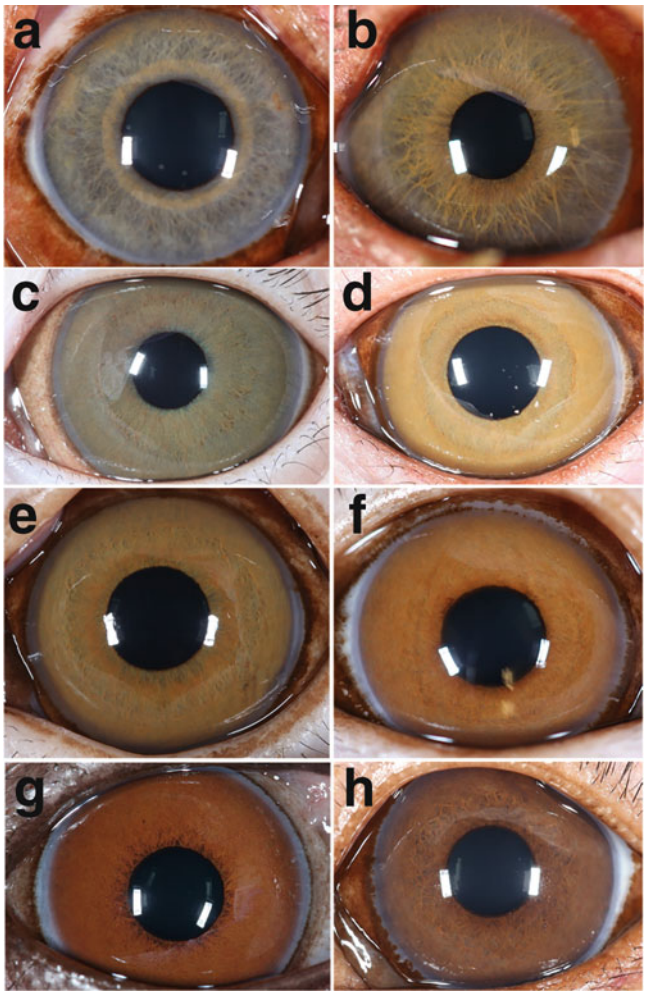

Fig. 47.23 Rhesus macaques exhibit iris color variation similar to that of humans. While uncommon, blue irides can be found in macaques (**a**) as well as hazel (**b and e**), and green (**c**) irises. Brown is the most common iridal color observed and varies in shade (**d, f–h**)

(Peterson et al. 1996; Miller and Bentley 2015) (Appendix 3). In a study of rhesus macaques utilizing a floating-tip pneumatonometer, no significant differences were identified between left and right eyes or males and females but juveniles had higher IOPs than adults (Bito et al. 1979). Chemical restraint is typically required to perform IOP measurements although animals can be trained to tolerate this procedure. In cynomolgus macaques, ketamine (10 mg/kg) appears to influence IOP less than other sedatives or anesthetics including methohexital (15 mg/kg) with pentobarbital (30 mg/kg), 1–2% halothane, and ketamine (10 mg/kg) with diazepam (1 mg/kg); all injectables were administered intramuscularly (Erickson-Lamy et al. 1984). In aggregate, these data demonstrate that normal IOP in catarrhines is similar to humans and it is thus unsurprising that these species are commonly used to test novel therapeutics that modulate IOP (Sugrue 1996; Rasmussen and Kaufman 2005).

At birth, the fundus of normal rhesus macaques lack pigment with a remnant of the hyaloid artery visible until 2–3 weeks postnatal (Johnson et al. 1977). By 3 months, the fundus is partially pigmented and macular and foveal reflexes are present (Fig. 47.24). By 6–12 months, there is a clear delineation of the fovea and macula (Fig. 47.24). The fundus from 1–10 years has a blue-green gray sheen which changes to blue-gray brown at 10–15 years although color variation exists (Fig. 47.24). At >15 years of age, the fundus is gray-brown and the delineation between the fovea and macula is less clear. Cynomolgus macaques exhibit similar fundus changes with a salmon pink fundus and macula, light orange ONH, and persistent hyaloid artery visible at birth (Suzuki, Narita, and Fukui 1985b; Suzuki et al. 1984). By 3 days, the macula had darkened and the persistent hyaloid artery disappeared by 21–45 days (Suzuki, Narita, and Fukui 1985b). At 3–4 weeks, the fundus changed to blue-green in color and between 6 weeks and 1 year the ONH became orange. By 7 years, the fundus was brown and the ONH remained orange in color. In rhesus macaques, a golden coat color is found in ~0.01% of macaques, from Cayo Santiago, a small island off the east coast of Puerto Rico, and is associated with nasal hypopigmentation in the fundus such that choroidal vessels were visible; temporal hypopigmentation occurred more rarely and only in association with nasal hypopigmentation (Dawson et al. 2004). The macula remained pigmented with little variation and no lesions associated with albinism were present. Pigmented uveal melanocytes also alter visualization of the choroid and sclera using enhanced depth-optical coherence tomography (ED-OCT) in rhesus macaques (Yiu et al. 2016). Specifically, a distinct hyporeflective choriocapillaris layer is present while the choroidal-scleral junction cannot be visualized thus impacting the ability to measure these layers.

When comparing macular anatomy and thickness of chorioretinal layers in normal rhesus macaques, high-resolution histological sections had better distinction between the ganglion cell layer (GCL) and inner plexiform layer than SD-OCT imaging; histology identified Henle nerve fibers in the outer plexiform layer (OPL) while SD-OCT did not (Yiu et al. 2018). In addition, the first hyperreflective band between the external limiting membrane (ELM) and retinal pigment epithelium (RPE) was wider on SD-OCT than the junction between photoreceptor inner and outer segments observed with histology. Finally, the GCL, inner nuclear layer, and OPL were significantly thicker on histology, particularly in the fovea; while the outer nuclear layer, choriocapillaris, and outer choroid were thicker on SD-OCT. These results show that both SD-OCT and high-resolution histological sections allow reliable measurements of chorioretinal layers in macaques, but offer distinct advantages for different sublayers.

The ONH morphology was described in normal rhesus macaques as horizontally ovoid with retinal arterioles significantly wider in inferotemporal and superotemporal regions versus the superonasal and inferoronasal regions (Jonas and Hayreh 2000). In most eyes, the foveola was temporal and inferior to the center of the optic disc. Parapapillary atrophy was distinguished as a peripheral alpha zone with irregular pigmentation and a central beta zone with visible large choroidal vessels and Bruch's membrane; the alpha zone occurring significantly more frequently than the beta zone. The neuroretinal rim or the intrapapillary equivalent of the RNFL is significantly broader in the inferior region followed by the superior, then nasal, and finally temporal regions. The RNFL was most visible in the inferotemporal region followed by superiotemporal, then superonasal and finally inferonasal regions; RNFL visibility significantly decreased with age. Aging also impacted retinal ganglion axons with a loss of ~4300 fibers/year but no significant effect was found on mean axonal diameter (Morrison et al. 1990). In another study, RGC axonal fibers decreased from 1.6 million to 40,000 between 4–10 and 27–33 years of age (Sandell and Peters 2001).

In the Patas monkey (*Erythrocebus patas*), neural circuitry of the lateral geniculate nucleus and visual cortex has been studied during development (Garey and de Courten 1983) and following recovery from monocular visual deprivation (Blakemore et al. 1981; Garey and Vital-Durand 1981; Swindale et al. 1981).

Ophthalmic Disease

Surveys of ocular lesions have been performed in large colonies of baboons and macaques. In a 2-year clinical survey and histologic survey of ophthalmic lesions in >300 baboons (*Papio* sp.) and macaques (*Macaca mulatta* and *arctoides*) in one colony, the most common abnormalities identified were conjunctivitis or corneal lesions (n = 11), myopia (n = 7), uveal colobomas (n = 3), cataract (n = 1), ocular trauma with anterior synechia and lens capsule rupture (n = 1), retinal detachment (n = 1), and peripheral cystoid retinal degeneration (n = 1) (Schmidt 1971b). Physiologic cupping of the optic disc was documented in 4 baboons but is likely a normal variation in these species. Ocular disease was surveyed in 2100 cynomolgus macaques with 185 lesions identified in 167 (8%) individuals most commonly involving the fundus (n = 140, 76%), cornea (n = 15, 8%), lens (n = 14, 8%), iris/anterior chamber (n = 7, 4%), lens (n = 7, 4%), and conjunctiva (n = 2, 1%) (Kuhlman et al. 1992). A post-mortem survey of 100 free-ranging Chacma baboons (*Papio ursinus*) identified 4 animals with macroscopic lesions including lens capsule rupture consistent with penetrating trauma (n = 3) and unilateral microphthalmia with a posterior polar cataract (n = 1); 30% demonstrated peripheral cystoid retinal degeneration on histology. Naturally-occurring ocular disease is uncommon in macaque breeding colonies representing only 0.8% of clinical cases at the Tulane National Primate Research Center (TNPRC) from 2002 to 2006 with 32% of ocular abnormalities due to trauma, 29% were blepharitis, 21% were conjunctivitis, and 2.9% were corneal ulcers (Ribka and Dubielzig 2008). A male infant rhesus macaque from TNPRC was presented for severe corneal edema and hyphema in the right eye. An enucleation was performed 3 days later and corneal hyperkeratosis, broad anterior synechiae, axial corneal stromal loss with outpouching, cataract and optic nerve atrophy was identified with histopathology.

Herpes simplex virus-1 (HSV-1) is highly pathogenic to NHPs, typically resulting in acute, fatal encephalitis but species variability exists particularly in platyrrhines. A 20-year-old male intact white-faced saki monkey (*Pithecia pithecia*) was diagnosed with ulcerative keratitis and reflex uveitis OD; conjunctival swabs were positive for HSV-1 using PCR (Bauer et al. 2018). Initial clinical signs resolved with supportive treatment, and the animal was treated with acyclovir (5 mg/kg PO twice daily) during flare-ups. Enucleation OD was performed >2 years after initial presentation due to progression of clinical disease and chronic, erosive keratoconjunctivitis, mild to moderate chronic lymphohistiocytic iridocyclitis and chronic retinal detachment with degeneration were found on histopathology; no viral inclusions were identified. At 2 months following surgery, the monkey was euthanized following acute presentation of severe neurologic signs, including ataxia and blindness. Histopathology, PCR analysis, and sequencing confirmed viral encephalitis from HSV-1. This study and others suggest that some platyrrhines may only present with ocular HSV-1, (Felsburg et al. 1973; Gozalo et al. 2008; Varnell et al. 1987) and can thus be chronically managed with oral antivirals. For example, experimental inoculations of one cornea in Guianan brown capuchins (*Sapajus apella*) with HSV-1 and HSV-2 resulted in typical clinical signs including follicular conjunctivitis and superficial ulcerative keratitis (Felsburg et al. 1973). Although throat swabs were positive for the virus inoculated and contralateral ocular signs were observed, none of the monkeys developed neurological signs.

Intramuscular challenge of a rhesus macaque with Ebola virus resulted in blepharoconjunctivitis and clinical decline ~3 weeks after apparent clinical recovery. Following euthanasia, necrotizing scleritis, conjunctivitis, optic neuritis, and choriomeningoencephalitis were histologically diagnosed; strong Ebola virus antigen staining was found in the lesions (Alves et al. 2016). Given the spectrum and frequency of ocular disorders following Ebola virus infection, NHP models will be critical to understanding the etiopathogenesis of this late-term complication.

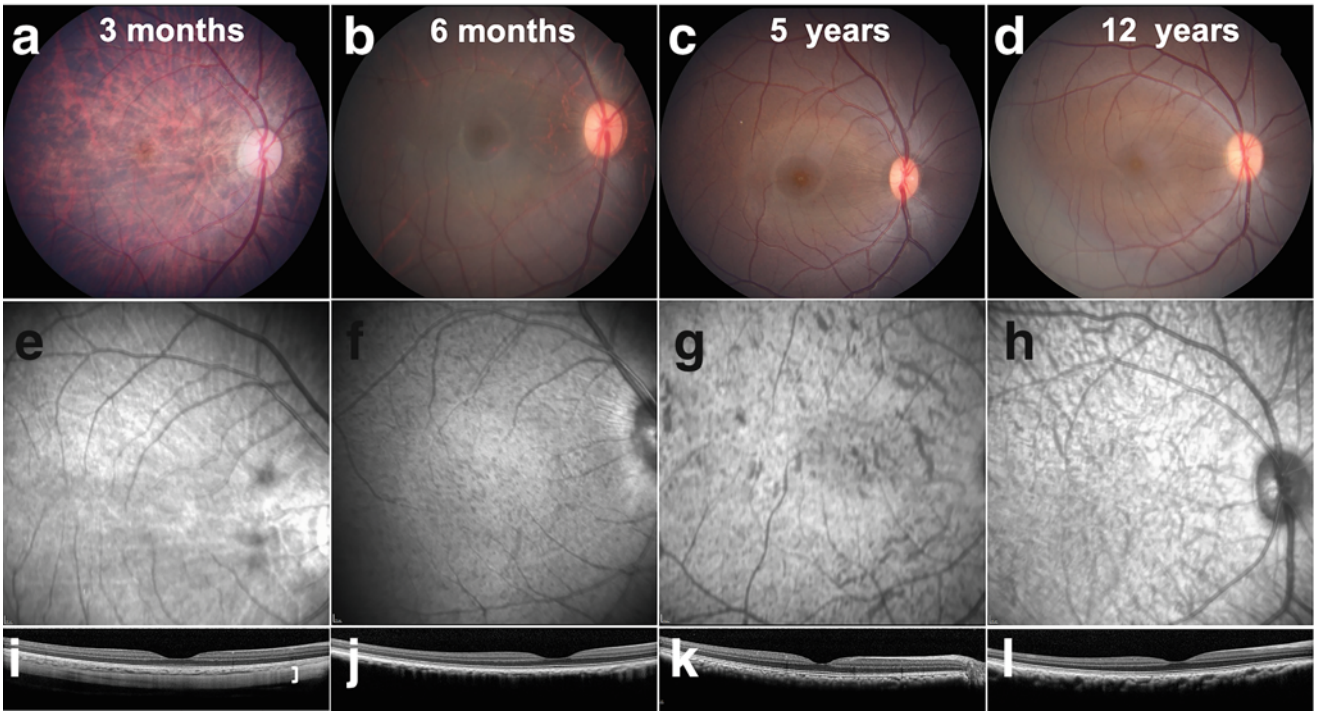

Fig. 47.24 Pigmentation changes with age and alters the appearance of the fundus in the rhesus macaque with color fundus photography (**a–d**), near infrared imaging (**e–h**), and FD-OCT (**i–l**). At 3 months, the fundus is partially pigmented but choroidal vessels are still visible with color (**a**) and near infrared photography (**e**); macular and foveal reflexes are present. With FD-OCT, the sclera (**white bracket**) is visible due to lack of RPE pigment (**i**). By 6 months, there is a clear delineation of the fovea and macula (**b**); increased pigmentation of the RPE prevents visualization of most choroidal vessels (**b** and **f**) such that the sclera is no longer visible with FD-OCT (**j**). At 5 and 12 years, the fundus appearance is quite similar with color photography with a blue-gray brown sheen (**c** and **d**), near infrared imaging (**g** and **h**) and FD-OCT (**k** and **l**)

Orbital and Ocular Surface Disease

Orbital cellulitis and retrobulbar abscesses due to bacteria or fungi have been reported in rhesus macaques (Martin et al. 1969; Rosenberg and Blouin 1979). A rhesus infant was presented with worsening unilateral exophthalmos, ventral strabismus and corneal ulceration; a retrobulbar aspirate and temporary tarsorrhaphy were performed and treatment was begun with chloramphenicol 33.3 mg/kg TID. Cytology of the purulent exudate demonstrated abundant neutrophils and aerobic bacterial culture identified a penicillinase-producing *Staphylococcus aureus*, susceptible to oxacillin. The chloramphenicol was discontinued and oxacillin was initiated at 16.7 mg/kg TID. An adult rhesus macaque with orbital cellulitis due to *Fusobacterium* and *Bacteroides* was successfully managed with systemic antibiotics, non-steroidal anti-inflammatory drugs and analgesics (Fig. 47.25). A wild-caught rhesus macaque of unknown age was found to have severe unilateral ulcerative blepharitis and a large, firm, mobile mass with a draining tract was inferior to the right mandible. No bacteria were isolated and local and systemic antibiotics for 10 days did not improve the clinical signs. A complete blood count demonstrated marked neutrophilia with a left shift and a serum biochemistry panel identified severe hyperglycemia suggesting the patient had diabetes mellitus. Humane euthanasia was performed and *Mucor spp*. was isolated from the orbit and submandibular granulomas and the frontal bone, frontal and paranasal sinuses, turbinates and periorbital connective tissue of the right eye were also infiltrated with granulomatous tissue. Rhino-orbital cerebral mucormycosis most commonly occurs in human patients with immunocompromise and is considered a medical and surgical emergency (Ak and Gupta 2020). Treatment involves reversing the immunosuppressive state, extensive surgical debridement, and administration of IV antifungals. Exenteration is sometimes necessary to address the orbital involvement.

An adult cynomolgus macaque was diagnosed with bilateral inferior entropion and secondary corneal fibrosis due to periocular folds (Peiffer, Johnson, and Wilkerson 1980). Clinical signs were chronic blepharospasm and epiphora OU. Following administration of ketamine (20 mg/kg), the folds were excised with straight scissors and a continuous suture pattern with 4–0 polyglactin used to close the wound. Eyelid and facial conformation was normal with no evidence of ocular irritation at two months post-operative.

Fig. 47.25 Severe bacterial orbital cellulitis occurs in rhesus macaques and typically responds to systemic antibiotics and non-steroidal anti-inflammatory drugs. A 5-year-old female rhesus macaque was presented to the California National Primate Research Center (CNPRC) veterinary staff with severe periocular swelling and erythema, exophthalmos, conjunctival hyperemia, and chemosis OS; mydriasis was secondary to topical atropine and tropicamide administration (**a and b**). A retrobulbar aspirate was performed and submitted for aerobic and anaerobic bacterial culture; *Fusobacterium* and *Bacteroides* were identified. The patient was administered ceftriaxone (50 mg/kg q 24 h, IV), buprenorphine (0.03 mg/kg q 12 h, IM), ketoprofen (5 mg/kg q 24 h, IM), and topical neomycin-polymyxin bacitracin ophthalmic ointment for 1 week. Metronidazole (50 mg/kg q 24 h, SC) was initiated 48 h after the initial medical regimen for 15 days. After the initial week of therapy, cefazolin (25 mg/kg q 12 h, IM) and meloxicam (0.2 mg/kg q 24, SC) were administered for 4 and 2 weeks, respectively. Marked improvement was observed at 3 weeks after initiating treatment with only mild periocular swelling observed (**c**), however the patient did not have a direct or consensual pupillary light reflex OS suggesting damage to the optic nerve. Another adult macaque demonstrates severe periocular and orbital swelling and mucopurulent discharge such that the globe could not be visualized consistent with orbital cellulitis (**d**). Photos courtesy of Dr. Laura Garzel, CNPRC (**a–c**) and Dr. Dennis Brooks, University of Florida (**d**)

Differential considerations for conjunctivitis in cercopithids include allergic, infectious, traumatic, and idiopathic causes. Allergic conjunctivitis and atopic dermatitis due to a latex sensitivity were reported in an adult rhesus macaque (Macy et al. 2001). A number of viruses cause conjunctivitis in cercopithids including simian adenoviruses (SAdV) with SAdV-15 reported in infant macaques (Landon and Bennett 1969) and SdAV-17 attributed to an outbreak in Patas monkeys (*Eyrthrocebus patas*) (Tyrrell et al. 1960); rhesus macaques experimentally infected with measles have more severe symptoms, including conjunctivitis, versus cynomolgus macaques (El Mubarak et al. 2007; Auwaerter

et al. 1999). In outbreak of *Streptococcus equi* subsp. *zooepidemicus* in 45 rhesus macaques, clinical signs included severe fibrinopurulent conjunctivitis, rhinitis, and respiratory distress; severely affected individuals were treated with enrofloxacin (2.5 mg/kg) and benzylpenicillin (40000–80,000 IE/kg) but 6 animals eventually died (Mätz-Rensing et al. 2009). In 6 immunodeficient rhesus macaques experimentally infected with simian immunodeficiency virus (SIV), *Cryptosporidium* was found on histopathology of the conjunctiva with some organisms accompanied by inflammation although the eyelids, conjunctiva, and globes were grossly normal at necropsy (Baskin 1996). This study suggests that disseminated cryptosporidiosis can occur in immunodeficient NHPs and should be considered as a differential for conjunctivitis in these animals. Ocular oxyspirusosis has been reported in several NHPs housed at zoos; the parasites residing in the conjunctival sac and nasolacrimal duct caused conjunctivitis (Ivanova et al. 2007). Wood shavings lodged in the conjunctival fornix were responsible for blepharoconjunctivitis and orbital cellulitis that were initially unresponsive to antibiotics and corticosteroids but eventually resolved over time (Williams 2013). Finally, an outbreak of idiopathic, unilateral conjunctivitis was observed in rhesus and stump-tailed macaques with a rapid onset of conjunctival hyperemia and chemosis with mucopurulent exudate, short course of 6–7 days and complete recovery; bacterial cultures of the exudate were negative (Schmidt 1971b). Idiopathic conjunctivitis was also rarely documented in 2 of 2100 wild-caught cynomolgus macaques; it was unilateral accompanied by excessive lacrimation and resolved without treatment (Kuhlman et al. 1992).

Keratoconjunctivitis sicca (KCS) or dry eye was reported in a rhesus macaque with STT-1 values of 0–3 (normal range 6–24) mm/min (Jaax et al. 1984). Treatment with topical pilocarpine and an antibiotic for 3 weeks increased the STT-1 to 18 mm/min. The rapid, severe onset and resolution with pilocarpine suggests that neurogenic KCS may have been the underlying cause. Severe dry eye can be induced in rhesus macaques by removing the primary lacrimal gland and vestigial nictitans then treating the conjunctiva with 50% trichloroacetic acid (Qin et al. 2014); labial salivary gland transplantation increased STT-1 values and decreased fluorescein and lissamine green staining scores in this disease model but did not improve ocular surface tissue morphology histologically (Qin et al. 2018). A lacrimal myoepithelioma was described in a geriatric rhesus macaque that developed ptosis of the left upper eyelid due to a mass that had been initially documented 10 years previously (Munday et al. 2004). The mass was surgically excised, and the ptosis rapidly resolved with no recurrence observed 6 months after surgery.

Corneal lesions were rare in a large survey of wild-caught cynomolgus macaques at 0.7% with opacities and melanosis most frequent; concurrent eyelid lacerations or scars suggest that trauma may have been an underlying cause in several individuals (Kuhlman et al. 1992). At the California National Primate Research Center (CNPRC), corneal lesions are also uncommon in rhesus macaques with arcus lipoides and corneal fibrosis most commonly observed (Fig. 47.26). Unilateral moderate to severe corneal edema was identified in 17 free-ranging rhesus macaques in the Western Himalayas and resolved in 7–10 days with daily topical prednisolone acetate and ciprofloxacin ophthalmic solution and ketoprofen (1 mg/kg, IM), a single dose of ivermectin (1 mg, IM), and vitamin A (600,000 IU, IM) every other day; lens-induced uveitis or ocular trauma was suspected (Kumar and Sankhyan 2015). Two sooty mangabeys (*Cercocebus atys*) infected with *Mycobacterium leprae* demonstrated lymphocytes in the ciliary body as well as the superficial conjunctival stroma; one individual also had limbal inflammatory infiltrate with acid-fast bacilli in the corneal stroma and nerves as well as blood vessel walls consistent with lepromatous leprosy (Malaty et al. 1988). Nonhuman primates can be naturally infected with *Mycobacterium leprae* and could thus exhibit ocular manifestations of this disease such as keratitis and uveitis (Honap et al. 2018; Bala Murugan et al. 2020). Macaques have been used extensively to study corneal wound healing following keratotomy with and without suturing (Melles et al. 1994; Melles et al. 1995a; Melles et al. 1995b), phototherapeutic keratectomy (Fantes et al. 1990; Hanna et al. 1990; Hanna et al. 1992; Qi et al. 1999; Wang et al. 1996), penetrating keratoplasty (Bourne 1978; Kelley et al. 1984; Lee et al. 2017; Li et al. 1992), and alkali burn (Chung 1988; Paterson and Pfister 1973) due to their similar corneal anatomy and physiology to humans.

Intraocular Disease

Congenital ocular defects including aniridia, persistent pupillary membranes, and colobomas have been identified in cercopithids (Figs. 47.27 and 47.28). Persistent pupillary membranes are rarely observed with a 0.2% and 0.03% prevalence reported in rhesus and cynomolgus macaques, respectively (Kirk 1972; Suzuki, Narita, and Fukui 1985b; Burek et al. 1974). Ocular colobomas may be more common with a 1.3% prevalence in a histologic survey of globes from euthanized baboons, rhesus macaques, and chimpanzees (Schmidt 1971a). Atypical iridal and lens colobomas of the right eye were histologically confirmed in an adult olive baboon (*Papio anubis*) with an elliptical pupil; rudimentary iridal stroma with folded, posterior pigmented epithelium and a flattened nasal lens were found. An adult rhesus macaque was clinical diagnosed with a right iridal defect and cataract; a discontinuity of the iridal epithelium at the iris base and

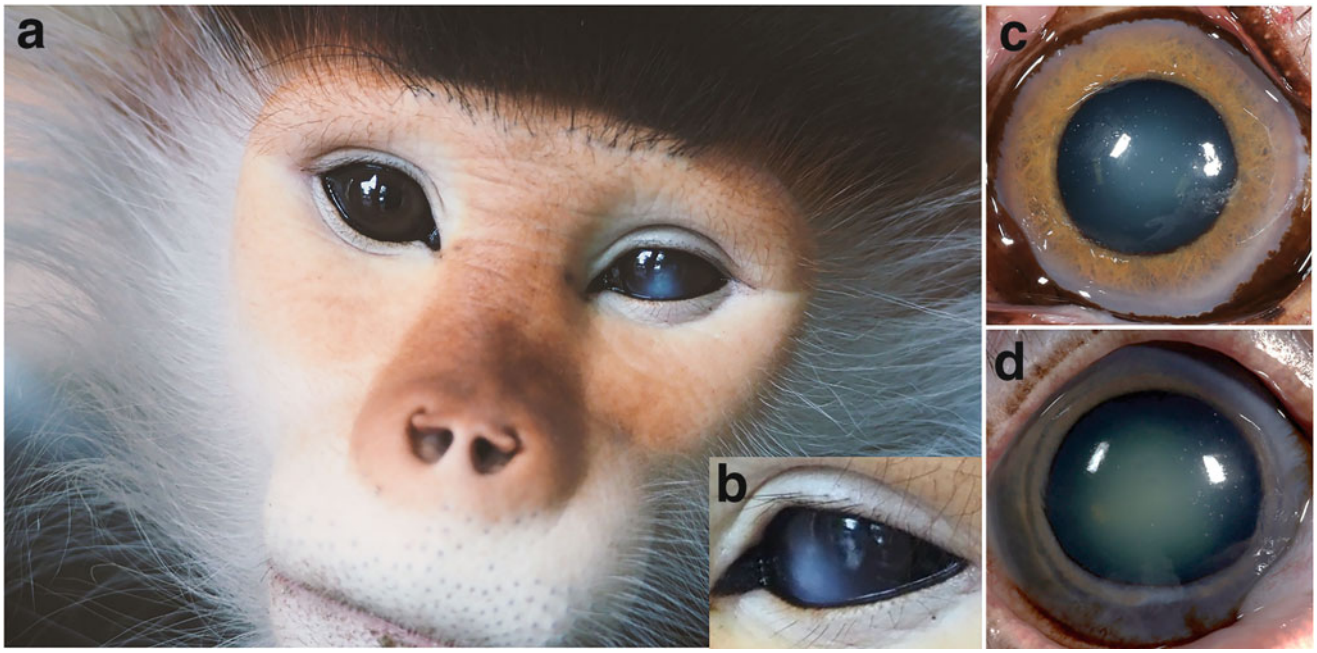

Fig. 47.26 Corneal and lens lesions of a red-shanked douc langur (*Pygathrix nemaeus*) and geriatric rhesus macaques. Focal corneal edema and a focal cataract visible in the pupil is observed in the left eye of a red-shanked douc langur (**a** and **b**). These lesions are most likely due to trauma although a development lesion cannot be ruled out. Photo credit to gnepppphoto, Shutterstock.com (**a** and **b**). The left eye of 29-year-old female rhesus macaque demonstrated white perilimbal opacity consistent with arcus lipoides and moderate nuclear sclerosis (**c**). The right eye of a 28-year-old female rhesus macaque demonstrated gray-blue perilimbal opacity consistent with arcus lipoides and dense brunescent nuclear sclerosis (**d**)

between the iris and ciliary body, subcapsular bladder cells, and a notch in the lateral lens were observed histologically confirming iridal and lens colobomas and a subcapsular cataract. Retinal and choroidal colobomas were grossly and histologically diagnosed in an olive baboon at necropsy. A choroidal coloboma with scleral ectasia and retinal dysplasia in the lateral fundus was identified in a 3.5-year-old female cynomolgus macaque (Kuhlman et al. 1992). We have identified bilateral chorioretinal colobomas in an infant born from a female rhesus macaque infected with Zika virus during late first trimester of pregnancy (Fig. 47.28), but these lesions did not impact axial elongation and retinal development (Yiu et al. 2020b). Thus, in utero Zika virus infection appears to impact fetal retinal development resulting in congenital ocular defects, but does not seem to alter postnatal growth.

Differential considerations for anterior uveitis in cercopithids include infectious, inflammatory, idiopathic, traumatic, and neoplastic causes (Fig. 47.27). A 2-year-old rhesus macaque initially developed enteritis then a fatal septicemia with ocular and brain involvement due to *Diplococcus pneumoniae*; ocular signs included hemorrhagic conjunctivitis, keratitis, hypopyon, and nystagmus (Herman and Fox 1971). Following confirmation of the organism with blood and cerebrospinal fluid cultures, systemic chloramphenicol, subconjunctival chloramphenicol, and topical neomycin-polymyxin-bacitracin ophthalmic ointment were initiated with supportive care but the patient died 10 days later. At necropsy, a severe, diffuse, suppurative panophthalmitis was diagnosed in both eyes as well as pneumonia, peritonitis, and meningoencephalitis. Experimental infection of rhesus macaques with *Borrelia burgdorferi* exhibit all critical manifestations of Lyme disease in contrast to other animal models, including uveitis, with clinical signs typically developing 3–4 months after inoculation (England et al. 1997). Cynomolgus macaques were immunized with a live strain of *Toxoplasma gondii* then repeatedly inoculated with organisms or antigens into the macula resulting in anterior uveitis, vitritis, retinal vasculitis, and focal retinal edema at the injection site (Webb, Tabbara, and O'Connor 1984) but necrotizing retinochoroiditis was not observed as previously (Culbertson et al. 1982). On histology, lymphoplasmacytic foci were observed in the ciliary body and choroid with normal retinal architecture; two individuals that were euthanized with active clinical vasculitis were confirmed to have arteritis histologically. This study suggests that hyperimmunization may have prevented necrotizing toxoplasmic retinochoroiditis. Posterior synechiae was identified with anterior capsular cataract were identified in two cynomolgus macaques indicative of chronic uveitis without an obvious underlying cause; concurrent diffuse chorioretinal lesions were identified in the same eye of one macaque (Kuhlman

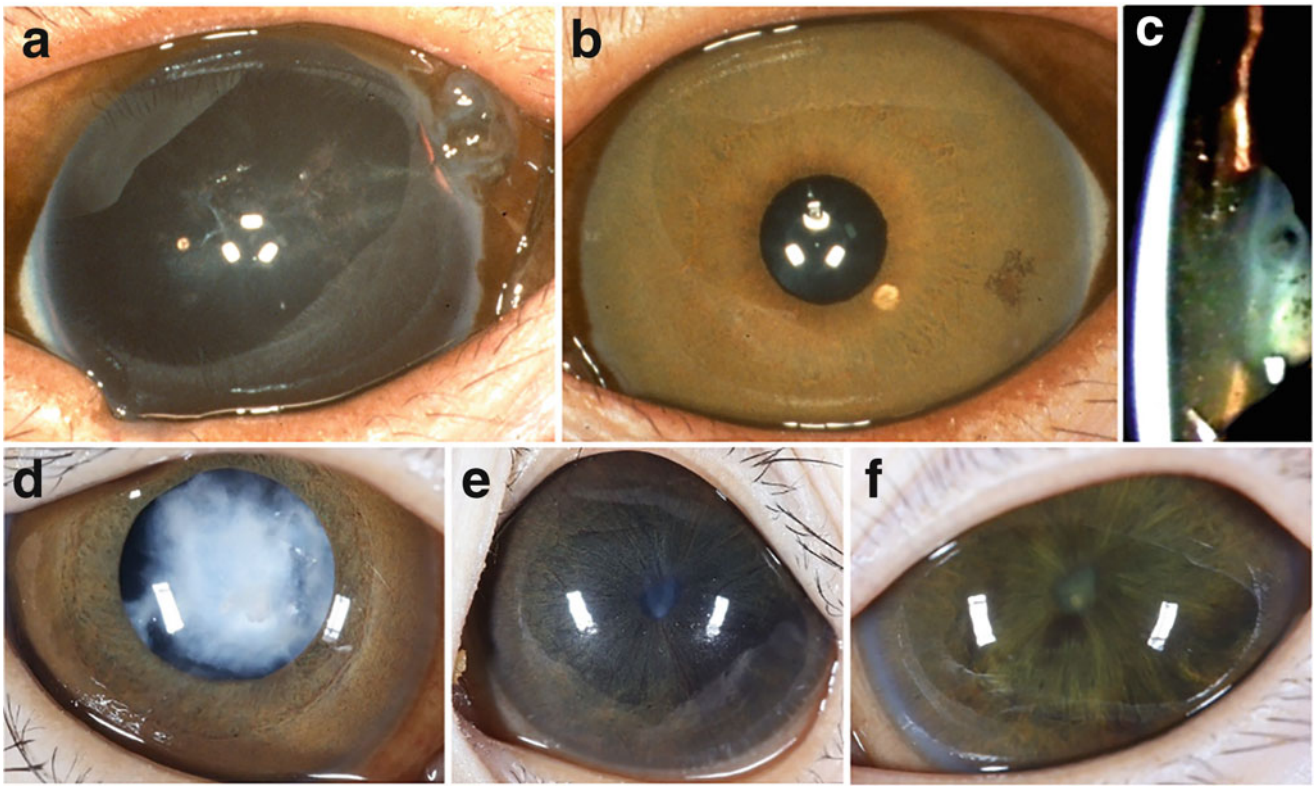

Fig. 47.27 Diversity of uveal and lens lesions in rhesus macaques. Aniridia in the right eye of a rhesus macaque with an inferior eyelid defect also present (**a**); the left eye was normal (**b**). A slit beam demonstrates aqueous flare, cells and fibrin in the anterior chamber of a macaque consistent with anterior uveitis (**c**). Hypermature cataracts were present in both eyes of a 1.3-year-old female rhesus macaque (**d, e**) (Casanova et al. 2021). The left eye also had buphthalmos, iris bombe, and rubeosis iridis (**e**); IOP was 56 mm Hg. Three weeks following an intravitreal injection of 15 mg of gentamicin (0.15 ml) and 1 mg of dexamethasone (0.25 ml), 2+ aqueous flare and 1+ aqueous cell was visible but IOP was markedly reduced at <2 mm Hg (**f**) as described in a case report by Casanova and colleagues (Casanova et al. 2021)

et al. 1992). Iridodialysis due to witnessed or suspected trauma has been reported in a cynomolgus macaque (Kuhlman et al. 1992) and rhesus macaques (Barlow et al. 2000; Bellhorn 1973). In a rhesus macaque receiving a routine physical exam, focal iridodialysis with no other abnormalities was observed (Barlow et al. 2000). Six months later, extensive iridodialysis with a concurrent anterior cortical cataract was identified; the unaffected iris and iridocorneal angle, fundus, and IOP were normal. No treatment was performed given that the macaque appeared visual and comfortable; ophthalmic exams and IOP monitoring every 6 months were instituted to assess for glaucoma.

Spontaneous primary open-angle glaucoma (POAG) and normotensive glaucoma have been described in Cayo Santiago rhesus macaques; congenital glaucoma was recently identified in an infant at the Caribbean Primate Research Center (Fig. 47.29). In studies of Cayo Santiago rhesus macaques, applanation tonometry with a Tonopen was used to measure IOP under ketamine sedation (Dawson et al. 1993; Dawson et al. 1998). Of nine matriarchal lineages assessed, two had a > 40% prevalence of ocular hypertension (IOP ≥22 mg Hg) suggestive of an underlying genetic component (Widdig et al. 2016; Dawson et al. 1993). In 6 hypertensive macaques that were examined over time, ONH pallor, reduced function in peripheral visual fields, and progressive loss of ON axons were observed (Dawson et al. 1993). Of 701 eyes examined from 345 Cayo Santiago rhesus macaques, 18% of eyes had an IOP greater than 2 standard deviations from the normal of 15 ± 2 mm Hg (Dawson et al. 1998). Higher cup/disc ratios (C/D) of the optic nerve head (ONH) tended to cluster with high IOPs although some eyes with C/D ratios >0.5 did have a normal IOP. Intraocular pressure and (C/D) ratio were used to assign macaques to three groups—healthy control, normotensive glaucoma, and hypertensive POAG—in a study of diurnal IOP variability (Komaromy et al. 1998). In all groups, IOP was greatest in the afternoon versus the morning; IOP was significantly greater in the hypertensive individuals versus the normotensive and control macaques. The ONH C/D ratio was significantly larger in the hypertensive and normotensive glaucomatous NHPs versus the normal controls. Finally, naturally-occurring POAG macaques had lower and less variable IOPs in comparison with those with laser-induced ocular hypertension (Dawson et al. 2005). In aggregate, these

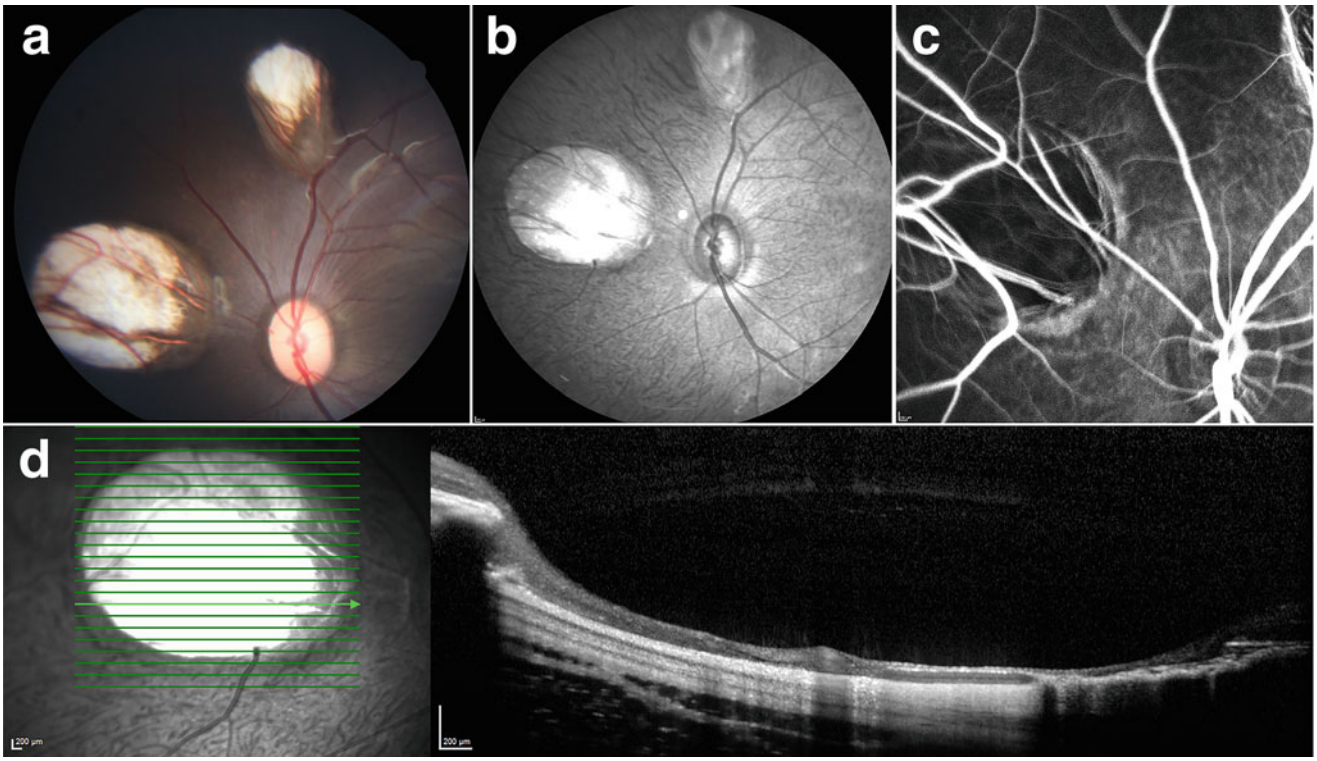

Fig. 47.28 Multimodal imaging of chorioretinal colobomas in the left eye of a rhesus macaque infant infected with Zika virus (Yiu et al. 2020b). Color (**a**), near infrared imaging (**b**), and fluorescein angiography (**c**) demonstrate a chorioretinal lesion ~5 ONHs in diameter in the nasal fundus and a similarly appearing lesion ~1.5 ONHs in diameter in the superior fundus; retinal vessels overly the lesions which are devoid of retina and choroid such that the sclera is visible. With FD-OCT (**d**), scleral outpouching is visible and is lined by a thin, dysplastic layer of tissue, consistent with a coloboma

studies suggest that these naturally-occurring POAG and normotensive models are compelling to study neuroprotective therapies as well as those that target the TM.

Laser-induced ocular hypertension is the most common method to induce glaucoma in NHPs whereby circumferential photocoagulation of the trabecular meshwork is performed with an argon or diode laser (Gaasterland and Kupfer 1974; Wang et al. 1998). Ketamine tranquilization (10 mg/kg) is preferred to inhalant anesthesia (e.g., 1% isoflurane) for measuring IOP in NHPs as isoflurane markedly depressed IOP as measured with applanation tonometry in hypertensive eyes of rhesus macaques with laser-induced ocular hypertension; no changes occurred in normotensive eyes (Kim et al. 2012). In a study of diurnal variability in rhesus macaques with laser-induced ocular hypertension, IOP and its variation over time were significantly greater in glaucomatous versus normotensive eyes; the glaucomatous eyes of some animals exhibit a decrease in IOP in the afternoon while others had an increase (Ollivier, Brooks, et al. 2004a). This study suggests that it is critical to measure IOP at the same time daily and adequately power studies to account for large fluctuations in IOP between individuals with laser-induced ocular hypertension. Another limitation of this model is the remaining normal TM softens and alters its protein composition in response to the increased IOP which contrasts with humans with POAG that exhibit a stiffer TM than normal controls (Eaton et al. 2017; Last et al. 2011). Thus, this model may be good for studying drugs that target aqueous humor production or neuroprotection, it is of limited use for drugs that effect the TM.

In a large survey of 2100 cynomolgus macaques, cataracts were identified in 13 (0.6%) with variable locations and stages reported including anterior capsule (n = 5), immature to mature (n = 4), posterior capsule, posterior subcapsule, anterior and posterior capsule, and nucleus (n = 1 each). Etiologic causes of cataract reported in catarrhines include congenital, heritable, inflammatory, metabolic, nutritional, senile, traumatic, and toxic causes. Specifically, bilateral cataracts were reported in juvenile cynomolgus and rhesus macaques with a prevalence of ~0.07%; lens resorption was commonly observed (Casanova et al. 2021; Sasaki et al. 2011; Kessler and Rawlins 1985; Suzuki et al. 1986; Schmidt 1971a) (Fig. 47.27). Lens-induced uveitis can result from cataracts, particularly with hypermaturity, and cause secondary glaucoma (Casanova et al. 2021). Heritable cataracts were described in a family of green monkey (*Chlorocebus sabaeus*); the cataracts were observed in all offspring at <1 year of age (Souri 1973). Diabetic cataracts have been

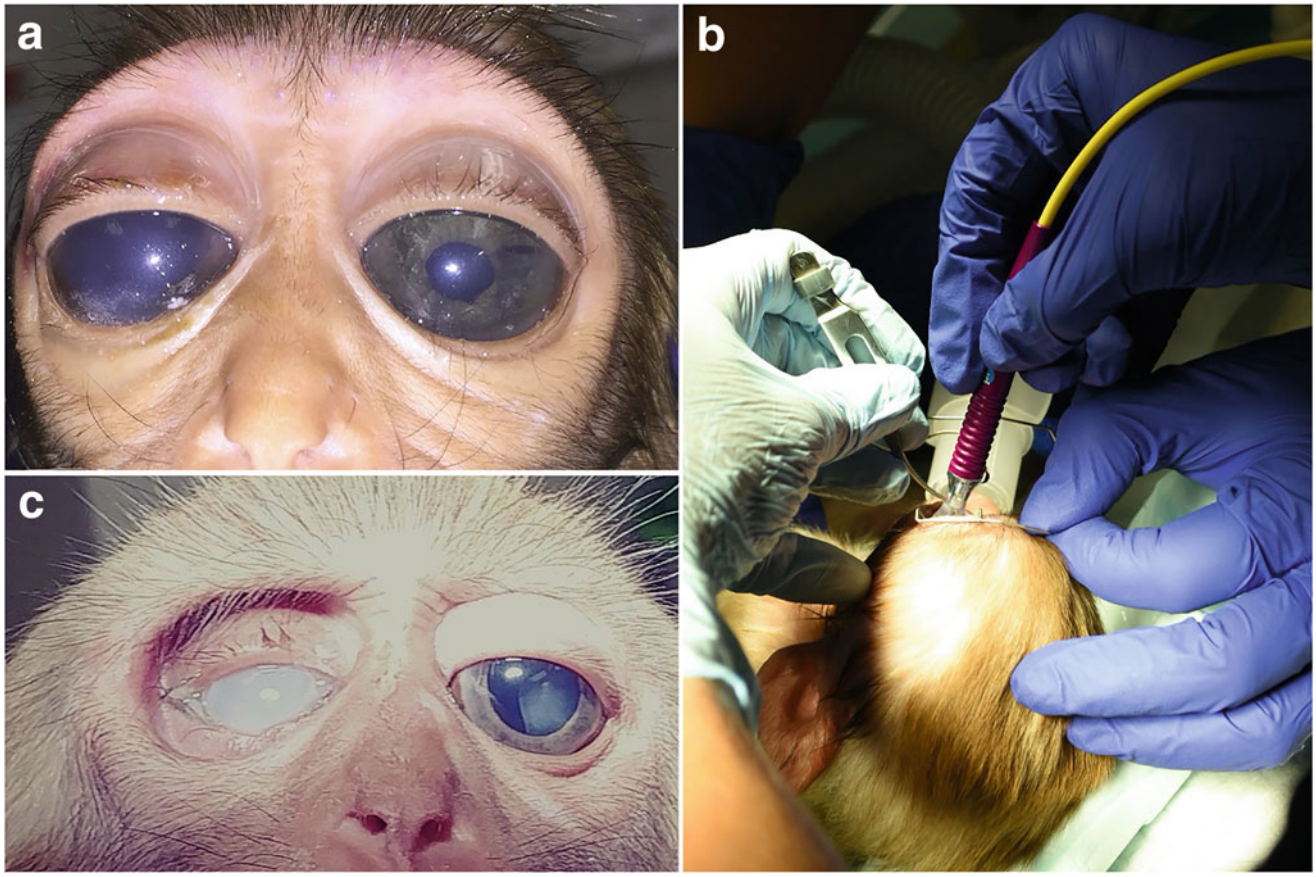

Fig. 47.29 Severe congenital glaucoma in a 4-month-old male rhesus macaque was managed with transscleral cyclophotocoagulation (TSCP) with a Micropulse® laser and topical latanoprost. At initial exam (**a**), this infant had marked buphthalmos and subluxated lenses OU with marked and mild corneal edema in the right and left eyes, respectively; IOPs were 56 and 54 mm Hg. Menace response was negative OD and positive OS. Micropulse® TSCP was performed immediately lowering IOP to 26 mm Hg OU with reduced corneal edema OS (**b**). In the first post-operative month, IOPs were between 4–16 mm Hg OU, then increased to 20–26 mm Hg OU at 2 months post-operative. Topical latanoprost ophthalmic solution was initiated OU once daily. At 2 years post-operative, he remained sighted OS until he developed infectious keratitis with malacia OD and a cataract OS (**c**)

identified in Celebes crested macaques (*Macaca nigra*) who have spontaneous diabetes mellitus at ~50% incidence as well as in a cynomolgus macaque with insular amyloidosis and diabetes mellitus (Howard 1974; Cromeens and Stephens 1985). Inducible diabetes mellitus with streptozotocin (20 mg/kg) injected into the pancreas or intravenous alloxan also causes cataracts and this model has been described in Southern pig-tailed macaques (*Macaca nemestrina*) and rhesus macaques (Howard and Peterson 1973; Farnsworth et al. 1980; Bansal et al. 1986). In the aforementioned spontaneous and inducible models of diabetes mellitus, the prevalence of bilateral cataracts ranged from 11 to 40%. Cataracts that were suspected to be due to hypocalcemia were reported in two neonatal Grivets (*Chlorocebus aethiops*) which had low calcium in serum and aqueous humor as well as in their dams' milk (Plesker et al. 2005). Penetrating trauma was suspected in a male infant rhesus macaque that was enucleated for severe corneal edema and hyphema in the right eye; anterior synechiae and cataract were found with histopathology (Ribka and Dubielzig 2008). Whole body radiation (9.5–9 Gy) of rhesus macaques resulted in a 17% and 100% incidence of cataracts at <3 years and > 10 years, respectively (Sonneveld et al. 1979). Extracapsular lens extraction without and with intraocular lens (IOL) implantation using Choyce Mark VIII, Binkhorst iridocapsular or shearing posterior chamber lenses was performed in rhesus macaques (Irvine 1981). The IOLs were well tolerated with little inflammation observed but posterior capsular opacification was found with all IOL types (Fox et al. 1979; Irvine 1981, 1980). Lens subluxation with iridodonesis and dyscoria was found in a cynomolgus macaque (Kuhlman et al. 1992).

Vitreous syneresis was described in 28 of 30 eyes from 15 rhesus macaques ages 2–7 years and ranged from fine, randomly-spaced strands to thick intertwining fibrous networks with clumping at the periphery (Stuck et al. 1977). The syneresis varied between eyes and tended to be more extensive in the older animals. In all eyes, the fundus

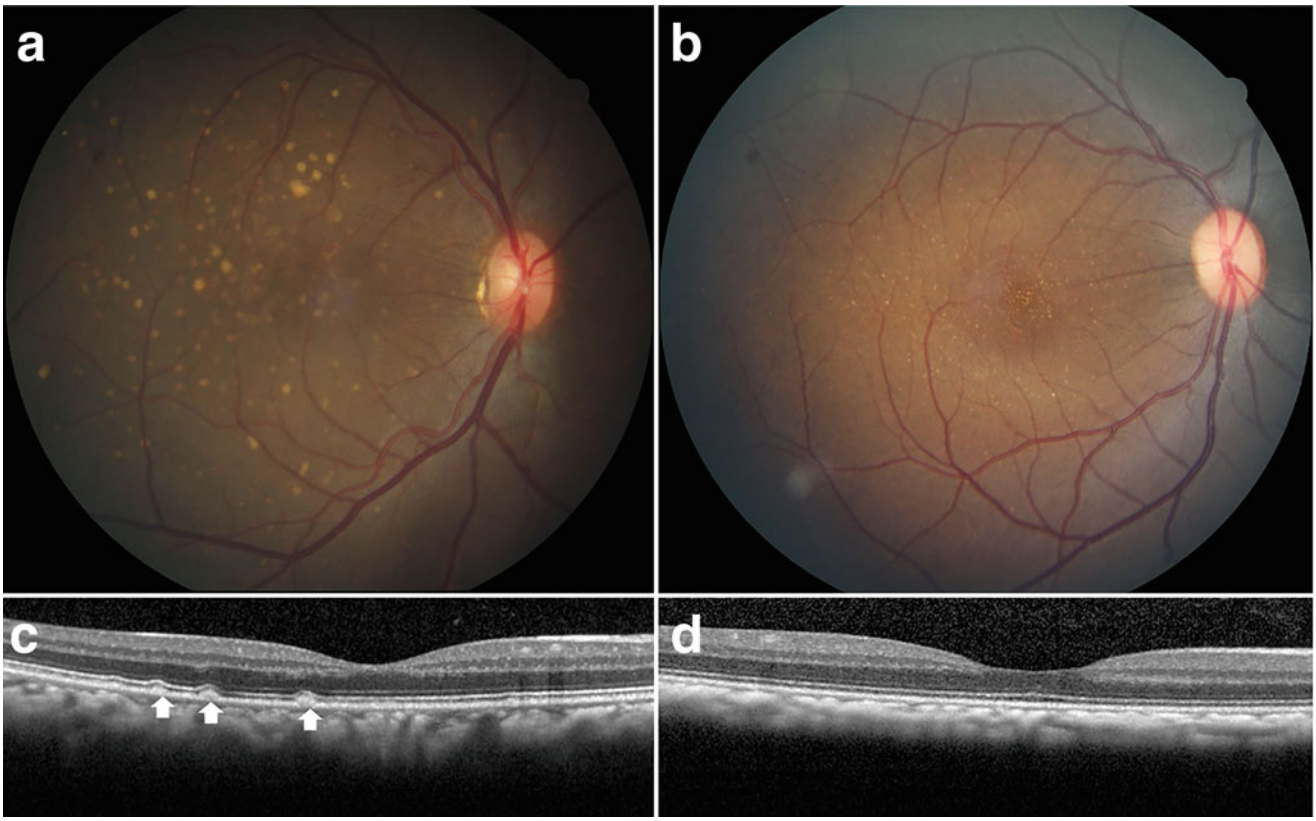

Fig. 47.30 Soft drusen and hard punctate lesions in rhesus macaques with color photography (**a** and **b**) and FD-OCT (**c** and **d**). Intraretinal hemorrhages are localized to the inner nuclear layer (INL) with SD-OCT in a 12-year-old male macaque. Soft drusen (**a**) are larger, more variable in size, and less dense than hard punctate lesions (**b**). With FD-OCT, soft drusen appears as dome-shaped hyperreflective deposits located between the RPE and Bruch's membrane (**c**) while hard punctate lesions were undetectable even on high density scans, with no visible disruptions of the RPE, outer retina, or choroid (**d**). Data from Yiu and co-authors (Yiu et al. 2017)

was easily visible with indirect ophthalmoscopy and fundus photography. Asteroid hyalosis was rare in a survey of cynomolgus macaques with a 0.3% prevalence, always unilateral, and more common in individuals >5 years of age (Kuhlman et al. 1992). A filamentous, cylindrical, mobile foreign body was identified in the vitreous of a cynomolgus macaque and observed over a 1-year period with no overt ocular signs (Kuhlman et al. 1992).

Drusenoid lesions in rhesus macaques have been documented in a number of studies with frequencies varying from 6–74% (El-Mofty et al. 1978; Yiu et al. 2017; Stafford et al. 1984; Olin et al. 1995; Gouras et al. 2008; Hope et al. 1992; Engel et al. 1988; Monaco and Wormington 1990); these lesions have also been described in an olive baboon (Barnett et al. 1972). The variable prevalence is presumably due to differences in ultraviolet light exposure, diet, age, genetics, and the methods used to detect and categorize lesions. Using multimodal imaging with fundus photography (spectral domain optical coherence tomography (SD-OCT), fundus autofluorescence (FAF), and infrared (IR), the drusenoid lesions can be separated into two groups—soft drusen and hard, punctate lesions (Yiu et al. 2017). While both are poorly visualized on IR and demonstrate variable FAF intensity, soft drusen is larger and appears as hyperreflective deposits between the retinal pigmented epithelium and Bruch's membrane with SD-OCT while hard, punctate lesions are smaller and unidentifiable using SD-OCT (Fig. 47.30). Over time, most soft drusen increases in size although a small number of lesions regress or completely collapse (Yiu, Chung, et al. 2020a). Ultrastructurally, soft drusen in rhesus is consistent with that seen in early to intermediate age-related macular degeneration (AMD) making them a compelling model to study novel preventative and therapeutic strategies.

Heritable retinal disease has been sporadically identified in macaques. Achromatopsia due to a missense mutation in the catalytic region of the alpha-prime subunit of cone phosphodiesterase 6C (*PDE6C*) was reported in four rhesus macaques at the California National Primate Research Center (CNPRC) (Moshiri et al. 2019). The macaques demonstrated abnormal behaviors consistent with visual impairment including decreased ability to navigate new environments, using their forelimbs to feel for walls and obstacles, eye covering to reduce light or visual stimuli, and being led by

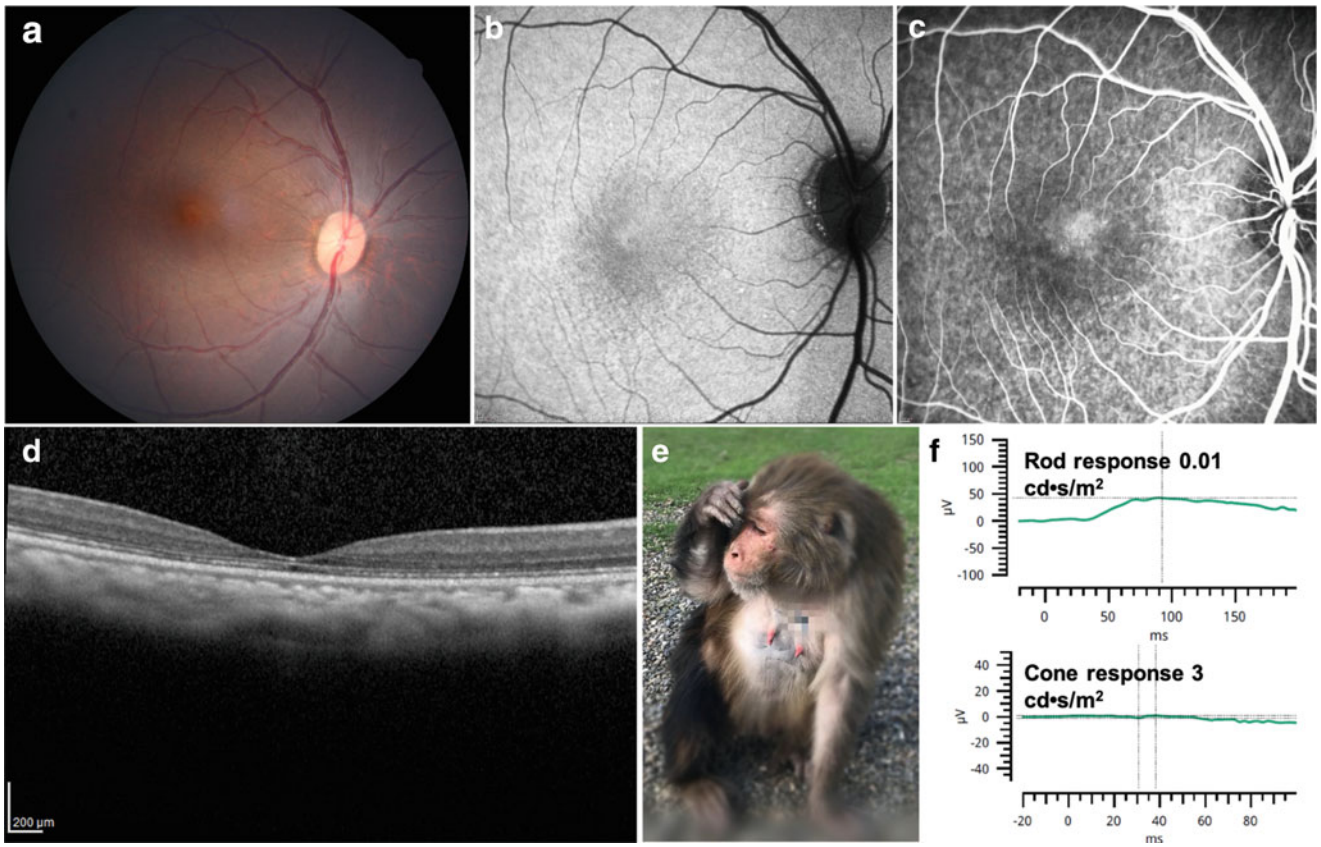

Fig. 47.31 Multimodal imaging and electroretinography of a rhesus macaque with achromatopsia due to a *PDE6C mutation*. Color fundus photography (**a**) of a 12-year-old female demonstrates prominent pigment within the fovea, while an annulus of foveal hypoautofluorescence is visible with blue autofluorescence imaging (**b**). Fluorescein angiography shows a bull's eye pattern of foveal staining surrounded by parafoveal hypofluorescence. With FD-OCT, total retinal thickness is reduced due to thinning in the outer nuclear layer and photoreceptor outer segments and the foveal center is markedly thin (**c**). This macaque exhibits photophobia by shading her eyes with her hand (**d**). With electroretinography, normal rod-mediated waveforms are present with a decreased amplitude (**e**) but cone-mediated responses were absent (**f**). Achromatopsia in this rhesus macaque was first reported by Moshiri and colleagues (Moshiri et al. 2019)

unaffected members holding their hand (Fig. 47.31). Clinical ophthalmic examination and multimodal retinal imaging of the affected macaques demonstrated increased foveal pigmentation, retinal thinning from thinning of the outer nuclear layer and photoreceptor outer segments, and a subtle bull's eye maculopathy (Fig. 47.31). Electroretinography demonstrated a relatively normal scotopic response but an absent photopic one in the affected macaques (Fig. 47.31). Bardet-Biedl syndrome (BBS) was identified in three related rhesus macaques due to a frameshift mutation in exon 3 of the *BBS7* gene, which is predicted to produce a nonfunctional protein (Peterson et al. 2019). The affected macaques displayed severe macular degeneration with absent photoreceptor layers, degeneration of the retinal pigment epithelium, and retinal vascular atrophy with retinal imaging. A loss of scotopic and photopic a-waves and markedly reduced and delayed b-waves was found with electroretinography. Histology revealed marked photoreceptor and inner retinal neuron loss, dramatic thinning and disorganization of all retinal cell layers, abundant microglia, absent of displaced RPE cells, and marked gliosis in the subretinal space; the far periphery was the only region that retained normal retinal structure and organization, including the presence of photoreceptors. In aggregate, these retinal findings were consistent with retinitis pigmentosa. Thus the ocular changes combined with abnormal kidney structure and function, low total brain volume, and hypogonadism were consistent with human BBS. Oculocutaneous albinism (OCA) was identified in rhesus macaques with a biallelic mutation in *TYR*, encoding tyrosinase, and a homozygous *OCA2* mutation, encoding the P protein; in vitro assays confirmed that these mutations both impact melanin synthesis (Wu et al. 2020). All OCA-affected macaques displayed horizontal nystagmus although visual acuity and retinal function were not assessed. On ophthalmic exam, extensive hypopigmentation of the fundus was identified such that choroidal vasculature was visible; the fovea centralis was absent. With SD-OCT, foveal hypoplasia was observed with thinning of the inner and outer photoreceptor segments, outer nuclear layer and retinal pigmented epithelium in the OCA-affected versus control rhesus

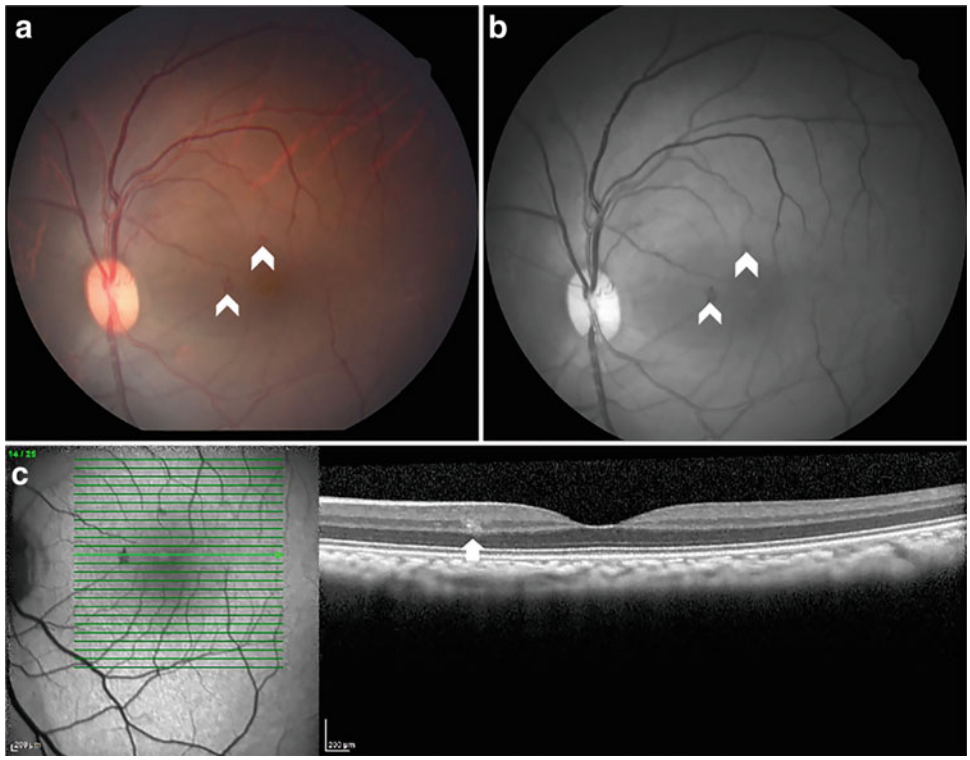

Fig. 47.32 Intraretinal hemorrhages are localized to the inner nuclear layer (INL) with SD-OCT in a 12-year-old male rhesus macaque. Color (**a**) and red-free fundus photography (**b**) demonstrate two small intraretinal hemorrhages in the macula (white carets). Blue autofluorescence with spectral-domain OCT (**c**) demonstrates that the hemorrhage resides within the INL (white arrow)

macaques. These preclinical NHP models will be critical for testing novel therapies with a high predictive value for translation to human patients.

In baboons, a heritable retinal disease has also been described although the underlying gene was not identified. Cone-rod dystrophy was found in 3 individuals—8, 10, and 13 years of age—from an inbred captive population of Guinea baboons (*Papio papio*). Behavioral observations consisted of decreased allogrooming, cleaning of the hair and skin with fingers which requires high visual acuity, in the youngest baboon and absent allogrooming and using hands to locate food in the older ones. Clinically, the initial fundoscopic lesion consisted of a hypopigmented lesion in the fovea and progressed to a mottled, atrophic fovea with retinal vascular attenuation and optic disc pallor. With fluorescein angiography, subtle foveal hyperfluorescence was first observed in early disease and progressed to marked foveal hyperfluorescence in late disease consistent with pigment loss in the RPE. Electroretinography demonstrated absent photopic and reduced scotopic and flicker responses in the youngest baboon and absent photopic and flicker with markedly reduced scotopic responses in late disease. Histology confirmed that cone outer segments were initially affected followed by all photoreceptors.

Retinal hemorrhages in cynomolgus macaques are uncommon with a prevalence of 0.5–1.2% (Suzuki et al. 1985a; Kuhlman et al. 1992). At birth, ~70% of naturally-born cynomolgus macaques had retinal hemorrhages which disappeared by 3–14 days postnatal (Suzuki and Cho 1984). These were more common in those delivered naturally (22/36, 67%) versus those born by cesarean section (10/30, 33%) (Suzuki et al. 1984). In neonatal rhesus macaques, retinal hemorrhages were also observed and postulated to be a result of cranial trauma or vitamin K deficiency (Johnson et al. 1977). In middle-aged, obese rhesus macaques, diabetes mellitus can develop spontaneously and is a naturally-occurring model of diabetic retinopathy (Johnson et al. 2005). In these animals, intraretinal hemorrhages were observed with large areas of no or poor choriocapillary perfusion using indocyanine green angiography. In these regions of choriocapillary loss, there was a marked decline in photoreceptor inner and outer segments with concurrent reductions in the multifocal ERG. Hard drusen and basal laminar deposits were present on Bruch's membrane adjacent to the nonperfused choriocapillaris. In a survey of 237 rhesus macaques, retinal hemorrhages were identified in ten individuals >8 years of age (unpublished data, Fig. 47.32).

Vascular anomalies were identified in 10% of captive cynomolgus macaques and included arterial and/or venous tortuosity, artery-vein crossing, copper-wire artery, inosculation of the artery, vascularization of vein, and persistent hyaloid artery (Suzuki et al. 1985). An arteriovenous shunt in the retina and a racemose hemangioma of the optic nerve head have been described in rhesus macaques (Horiuchi et al. 1976; Bellhorn et al. 1972).

Both spontaneous and inducible forms of chorioretinopathy have been described in macaques. In cynomolgus macaques, chorioretinopathy was identified in 4% with focal, multifocal, peripapillary, peripheral, and linear forms described (Kuhlman et al. 1992). With no histology or functional data available, it was difficult to interpret the impact of these findings. Central serous chorioretinopathy was induced in Japanese macaques (*Macaca fuscatus*) with repeated intravenous epinephrine injections and displayed disciform serious retinal detachment at the posterior pole and fluorescein dye leakage at the RPE with FA; histology and electron microscopy demonstrated RPE degeneration with adjacent endothelial damage of the choriocapillaris (Yoshioka and Katsume 1982a, 1982b; Yoshioka et al. 1982, 1984a; Yoshioka et al. 1984b).

There are several reports of infectious chorioretinitis occurring in macaques. Systemic cryptococcosis was reported in a rhesus and a Formosan rock macaque (*Macaca cyclopis*) with CNS lesions identified in both; the latter presented with apparent blindness and *Cryptococcus neoformans* organisms were identified within the retina with secondary intraretinal separations. Experimental infection of rhesus and stump-tailed macaques with intracarotid injection of *Histoplasma capsulatum* produced both acute and chronic choroidal inflammatory lesions (Anderson et al. 1992). Intraocular granulomas from tuberculosis were identified in a rhesus macaque and Geoffrey's spider monkey and the animals were euthanized; bacterial culture of lung tissue confirmed *Mycobacterium bovis* and *Mycobacterium tuberculosis*, respectively (West et al. 1981). The absence of overt clinical signs in both of these NHPs emphasizes the importance of regular testing for tuberculosis in NHP colonies given the public health significance of this disease. An experimental animal model of ocular onchocerciasis was created in cynomolgus macaques by intravitreal injections of live and dead *Onchocerca volvulus* microfilariae. On ophthalmic examination, live organisms caused multifocal regions of progressive RPE loss with pigment clumping while dead organisms resulted in mild vitritis with less overt chorioretinal abnormalities. Histopathology was consistent with the clinical findings with outer retinal thinning and pigment migration into the retina in both groups and more severe inflammation in the macaques treated with live versus dead organisms (Semba et al. 1991). In an experimental model of ocular toxoplasmosis in immunosuppressed cynomolgus macaques, live *Toxoplasma* organisms were injected onto the macula of one eye of each NHP resulting in chorioretinitis which resolved without treatment. Three months later, immunosuppression was induced with total lymphoid irradiation but no chorioretinal changes were observed suggesting that cellular immunodeficiency alone is responsible for recurrent chorioretinal toxoplasmosis. In summary, macaques are susceptible to many infectious diseases that cause chorioretinitis, some with zoonotic potential, so caution should be taken when handling animals suspected to have infectious chorioretinitis.

Retinal degeneration can occur in cercopithicids for a variety of causes. Nutritional retinal degeneration due to deficiency of vitamin A or E was described in cynomolgus and rhesus macaques (Rodger et al. 1961; Hayes 1974). With a vitamin A deficient diet, cone outer segment damage occurred initially in the mid-peripheral retina followed by rod and cone damage in the macula (Hayes 1974). Outer nuclear layer degeneration and lipid-laden lysosomes in the RPE due to photopigment depletion were the only other changes observed with electron microscopy. Rhesus macaques fed a vitamin A deficient diet initially developed nyctalopia then hemeralopia later in the disease course as demonstrated with behavioral testing (Rodger et al. 1961). With a vitamin E deficient diet, marked disruption of outer segments of both rods and cones with accumulation of lipofuscin in the RPE of the macula due to lipid peroxidation was observed but the b-wave and vision remained normal (Hayes 1974). Cynomolgus macaque and white-fronted capuchin (*Cebus albifrons*) infants fed a taurine deficient diet exhibited normal retinal development (Hayes et al. 1980). Phototoxic retinal degeneration was demonstrated in rhesus and cynomolgus macaques exposed to light from instrumentation used to perform ophthalmic examinations or surgery (Calkins, Hochheimer, and D'Anna 1980). Operating microscopes produced the most retinal light exposure followed by slit lamps and finally ophthalmoscopes. Severe chorioretinal lesions of ~3 ONH diameters in length were observed in macaques following 1 h of continuous exposure to an operating microscope. Thus, it is important to mitigate retinal light exposure during ocular surgery particularly in patients with dilated pupils and clear ocular media. Macular degeneration was rare in large surveys of cynomolgus macaques at 0.4–0.7% (Kuhlman et al. 1992; Suzuki et al. 1985) and has also been reported in baboons (Bellhorn 1973; Ishmael and Bradley 1974). In one report, cystoid macular degeneration with a retinal hole was identified histologically; differential considerations for this condition include senility, cardiovascular disease, hereditary macular dystrophy, and trauma (Ishmael and Bradley 1974). In wild-caught cynomolgus macaques, bilateral macular lesions were identified in 3 of 8 individuals; one of the macaques with bilateral macular degeneration was diabetic (Kuhlman et al. 1992). Given the importance of the macula in visual acuity, it is unsurprising that cynomolgus macaques with macular degeneration had lower visual acuity versus those with a normal retina and that the decrease in vision correlated with the lesion size (Suzuki et al. 1990). Unilateral extensive chorioretinal degeneration of unknown cause, involving at least one quadrant, was found in 5 wild-caught cynomolgus macaques that were < 5 years of age (Kuhlman

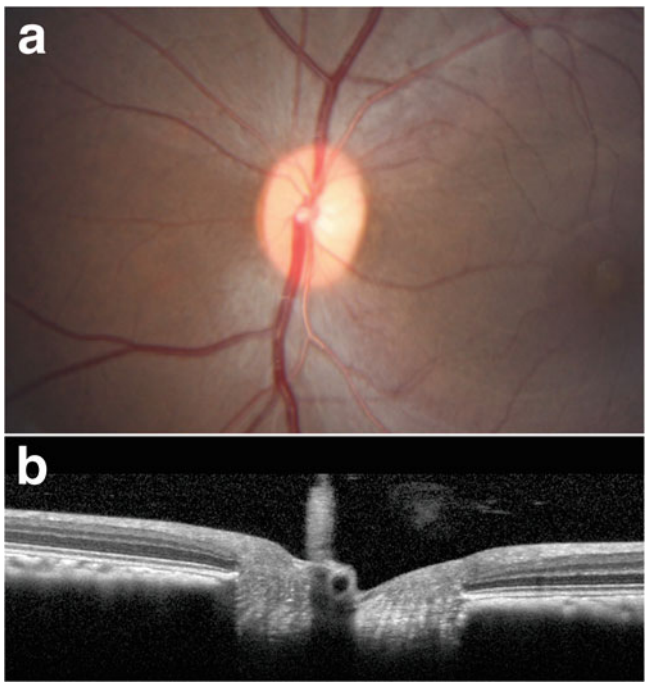

Fig. 47.33 Bergmeister's papilla is visible on color fundus photography (**a**) and FD-OCT (**b**) in a 9-year-old rhesus macaque

et al. 1992). Peripheral retinal degeneration was diagnosed in 7% of colony-born cynomolgus macaques (Suzuki et al. 1985), but these lesions did not appear to impact vision (Suzuki et al. 1990). Peripheral cystoid retinal degeneration was documented in baboons with the largest and greatest density of cysts adjacent to the ora serrata and in the temporal retina (Schmidt 1971b; McConnell et al. 1974).

Intraocular tumors have been rarely reported in cercopithids (Albert et al. 2009; Mukai et al. 1980). A primary choroidal melanoma was described in a 7-year-old female cynomolgus macaque (Albert et al. 2009). On fundic examination, an elevated choroidal mass with some intrinsic peripheral pigmentation was identified in the left eye; fluorescein angiography demonstrated intrinsic circulation within the mass with hyperfluorescent regions. With FD-OCT, a highly reflected choroidal mass was found surrounded by subretinal and intraretinal fluid. B-scan ultrasound demonstrated that the mass had medium internal reflectivity with acoustic hollowness and excavation of the underlying sclera. Two years after initial presentation, the macaques were euthanized and histopathology confirmed a choroidal melanoma. In a study of newborn baboons injected intravitreally with human adenovirus type 12, 3 of 21 infants developed an intravitreal mass 12–36 months later (Mukai et al. 1980). Following euthanasia in 2 infants, histopathology demonstrated dense, uniformly distributed neuroblastoma-like cells with Flexner-Wintersteiner rosettes in some areas consistent with a retinoblastoma.

Optic Nerve and Neuro-Ophthalmic Disease

Optic nerve abnormalities including aberrant myelination, micropapilla, coloboma, and atrophy have been reported in macaques. Aberrant myelination, micropapilla, and ONH colobomas were rare in cynomolgus macaques at 0.1%–1.4%, 0.3%, and 0.09–0.3%, respectively (Suzuki et al. 1985; Kuhlman et al. 1992). Rhesus and cynomolgus macaques with idiopathic optic nerve atrophy exhibit temporal peripapillary RNFL thinning, degeneration of RGC axons with gliosis, and decreases in the pattern electroretinogram (ERG) suggesting that they would be a good model for human optic atrophy (Piper et al. 2013; Fortune et al. 2005; Kuhlman et al. 1992). Bergmeister's papilla or remnants of the hyaloid artery were commonly found on the ONH of cynomolgus macaques examined with FD-OCT with cSLO occurring in at least one eye of 79% of animals (Denk et al. 2020), and we have observed them in rhesus macaques as well (Fig. 47.33).

Both spontaneous and inducible models of congenital strabismus are described in macaques. Naturally-occurring congenital strabismus was reported in a colony of Southern pig-tailed macaques with a 4% incidence (*Macaca nemestrina*); 12 esotropes and 1 exotrope were identified and amblyopia found in those tested for visual acuity (Kiorpes and Boothe 1981; Kiorpes et al. 1985). No differences in horizontal recti size or path were identified between normal macaques and those with naturally-occurring strabismus with MRI or histology; the accessory lateral rectus was present in all macaques and its features did not correlate with those with strabismus (Narasimhan et al. 2007). Strabismus can be induced in NHPs by contact lens occlusion, prism-goggle wear, or lid suturing (Tychsen and Scott 2003; Wong et al. 2003; Tusa et al. 2002). Animal models, particularly NHPs, have greatly advanced our understanding of the neural basis of amblyopia as detailed in this review (Tusa et al. 2002).

Congenital nystagmus with exotropia was induced by alternating tarsorrhaphies within 24 h of birth with one eye closed for 25 days then opened and the second eye immediately closed for the next 25 days (Repka and Tusa 1995). Models of congenital strabismus were used to study the impact of extraocular muscle tenotomy (Wong and Tychsen 2002), to determine the timing of surgical repair (Wong et al. 2003), to determine neural anatomy of the tendinoscleral (enthesial) portion of the extraocular muscle tendon (Hertle et al. 2002), and to ascertain the development of gaze-stabilizing systems (Tusa et al. 2001).

Intracranial meningiomas have been reported in a macaque and a baboon (Tanaka and Canfield 2012; Oliveira et al. 2011). A 21-year-old female rhesus macaque was presented for anisocoria due to mydriasis OS; the direct PLR OS was delayed and the consensual PLR was absent

from the right to left eye consistent with an efferent lesion (Tanaka and Canfield 2012). Two weeks later, ptosis, marked mydriasis, with absent direct and consensual PLRS were identified OS; 0.1% pilocarpine ophthalmic solution constricted the pupil OS ruling out iris sphincter damage. In aggregate, these signs were consistent with internal and external ophthalmoplegia. Following a week of oral prednisone (2 mg/kg PO BID), no improvement was identified and the primate was euthanized. At necropsy, an intracranial meningioma was found at the base of the brain, centered over the left lateral aspect of the sella turcica and compressing the midbrain superiorly and medially where CNs III and IV penetrate the dura mater to enter the cavernous sinus. A 7-year-old female baboon was euthanized following worsening clinical signs including head pressing, staggering, visual impairment, and vestibular disease (Oliveira et al. 2011). An intracranial meningioma was found arising from the floor of the cranium and compressing the left aspect of the cerebellum and brainstem.

Apes (Superfamily Hominoidea)

The superfamily Hominoidea is part of the suborder Haplorhini and parvorder Catarrhini with 25 extant species in the world (Mittermeier 2013). This superfamily is divided into two families—Hylobatidae (gibbons) and Hominidae (African apes and humans). Hominoidae members range in size—gibbons are considered lesser apes due to their smaller size while the larger chimpanzees, bonobos, orangutans, and humans are considered great apes. This superfamily is defined by the freedom in their shoulder joint to permit brachiation or arm swinging. Given the vast swath of knowledge regarding the eyes of *Homo sapiens*, the remainder of this chapter will focus on the other species within this superfamily.

All catarrhines, including apes, have trichromatic color vision due to an X-chromosome opsin duplication occurring ~35 million years ago which resulted in separate genes coding for the middle- (M) and long- (L) wavelength sensitive cone pigments (Nathans et al. 1986). In conjunction with an autosomal gene encoding the short- (S)-wavelength sensitive pigment, this provides the 3 cone photoreceptor classes responsible for trichromacy. While behavioral testing of color vision in lar gibbons (*Hylobates lar*) suggested that they had trouble distinguishing blue and gray (Tigges 1963), studies of their spectral sensitivity with electrophysiology demonstrated separate M and L photopigments that were indistinguishable from that of the common chimpanzee (*Pan troglodytes*), a confirmed trichromat (Jacobs, Deegan, and Moran 1996a; Deegan and Jacobs 2001). In contrast to humans with a relatively high L/M defects that cause dichromacy or anomalous trichromacy, a study of 152 gibbons in 3 different genera (*Hylobates*, *Nomascus*, and *Symphalangus*) found all L and M opsins present with no L/M hybrid genes identified (Hiwatashi et al. 2011). These results suggest that maintenance of trichromacy is critical to the visual ecology of nonhuman catarrhines such as gibbons. Indeed, gibbons are primarily frugivores with most species spending ~60% of their feeding time eating fruit pulp (Chivers 2013). The visual cortex of the black gibbon (*Hylobates concolor*) is similar to those of monkeys and presumably humans (Vital-Durand and Blakemore 1981).

Gibbons are frugivorous, arboreal, monogamous, territorial, and use brachiation as their primary means of locomotion. Great apes are fundamentally frugivorous but supplement their diet with other easily digestible plant components. Orangutans are primarily arboreal while the African apes are semi-terrestrial with bonobos and chimpanzees spending more time in trees than gorillas. Leopards, large snakes, and birds of prey are the primary predators for gibbons. The great apes have few natural predators with leopards being the primary predator for the orangutan, chimpanzee, and gorilla while bonobo occasionally succumb to crocodile.

Ocular Anatomy and Examination

Due to the large size of apes, chemical restraint is typically required to perform a complete ophthalmic examination with midazolam (0.6 mg/kg PO) and tiletamine-zolazepam (3 mg/kg IM) reported to be effective (Leiva et al. 2012). A variety of other anesthetic protocols have also been described (Johnson et al. 2010; Fahlman et al. 2006; Hendrix 2006; Strong et al. 2018; Adami et al. 2013; Hyeroba et al. 2013; Cerveny et al. 2012; Adami et al. 2012; Sleeman et al. 2000).

The shape of the orbital opening varies among hominoids with elliptical elongation more frequent in chimpanzees (*Pan troglodytes*) and humans while quadrangularity predominates in gorillas (*Gorilla gorilla*); no sexual dimorphism was identified in the 3 species studied (Schmittbuhl et al. 1999). Nonhuman apes also have a lateral orbital margin that is significantly more forward in comparison with the human orbit which results in these species relying more on head versus eye motion for visual exploration (Denion et al. 2015).

All apes are diurnal. Consistent with other diurnal haplorhines, apes exhibit horizontal cornea diameters that are much smaller relative to their transverse globe diameter in comparison with nocturnal haplorhines (Kirk 2004). This smaller cornea: globe ratio in combination with a small, flat, anterior lens (Fig. 47.34) results in anterior displacement of the posterior nodal point producing a larger retinal image and thus enhanced visual acuity (Prince 1956; Kirk 2004; Walls 1942; Duke-Elder 1958; Hughes 1977; Ross 2000). In a study of 13 primate species, corneal morphology and

Table 47.2 Intraocular pressure, refractive error, and ocular biometry measurements for chimpanzees and gorillas. Data collected from normal chimpanzees (Young and Farrer 1964; Dobbie 2020) and gorillas (Liang et al. 2005)

Species (# of animals, unless otherwise specified)	Measurement conditions	IOP (mm Hg)	Refractive error (D)	Central corneal thickness (microns)	Axial globe length (mm)	Lens thickness (mm)	Anterior chamber depth (mm)	Keratometry (D)	Corneal diameter (mm)
Chimpanzee (n = 43)	Penthol sodium anesthesia, cyclopentolate cycloplegia, supine position	15.6 ± 4.7 (n = 42)	−0.6 ± 1.4						
Chimpanzee (n = 22)	Awake	18.4 ± 4.7 (n = 16)							
Chimpanzee (n = 33)	Anesthesia	14.3 ± 4.0		450 ± 40	21.4 ± 0.7	3.8 ± 0.7	3.6 ± 0.5		
Gorilla (n = 5)	Isoflurane, mydriasis with tropicamide and phenylephrine	15.6 ± 4.7	+1.2 ± 0.6	489 ± 52	22.8 ± 0.7	4.23 ± 0.34	4.00 ± 0.26	44.4 ± 1.6	13.4 ± 0.8 (H) 12.7 ± 0.8 (V)

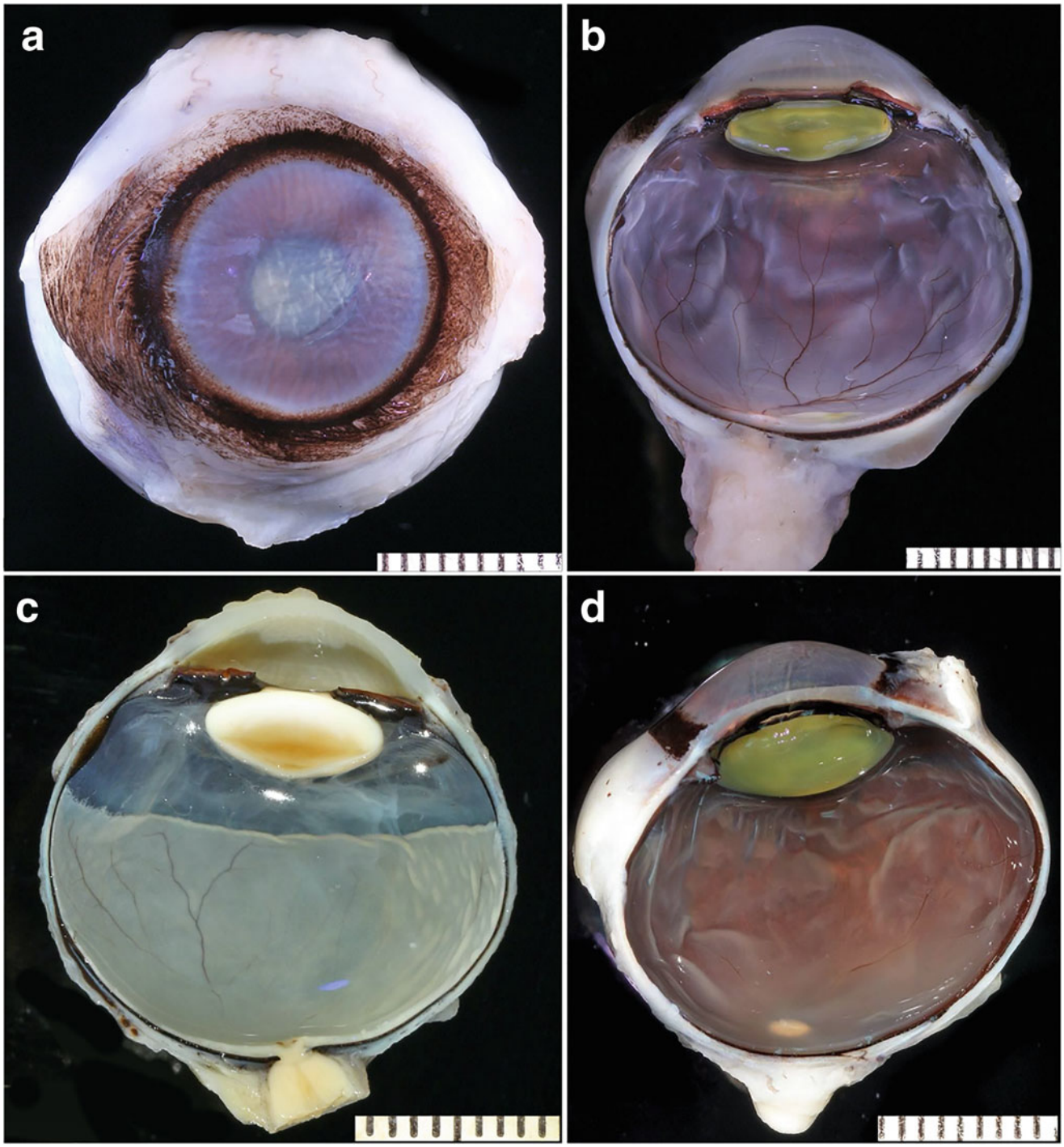

Fig. 47.34 Nonhuman hominids have a brown iris, flat, discoid lens and a heavily pigmented fundus with a holangiotic retina. Gross images of the anterior segment of a 31-year-old male Western lowland gorilla (*Gorilla gorilla gorilla*, **a**) and hemi-sectioned globes from the aforementioned gorilla (**b**), a 9-year-old Sumatran orangutan (*Pongo abelii*, **c**) and a 41-year-old female chimpanzee (*Pan troglodytes*, **d**) with normal eyes. Contrast these flat, discoid lenses with the relatively round lenses of strepsirrhine primates (Fig. 47.3). Images courtesy of the Comparative Ophthalmic Pathology Laboratory of Wisconsin (COPLOW)

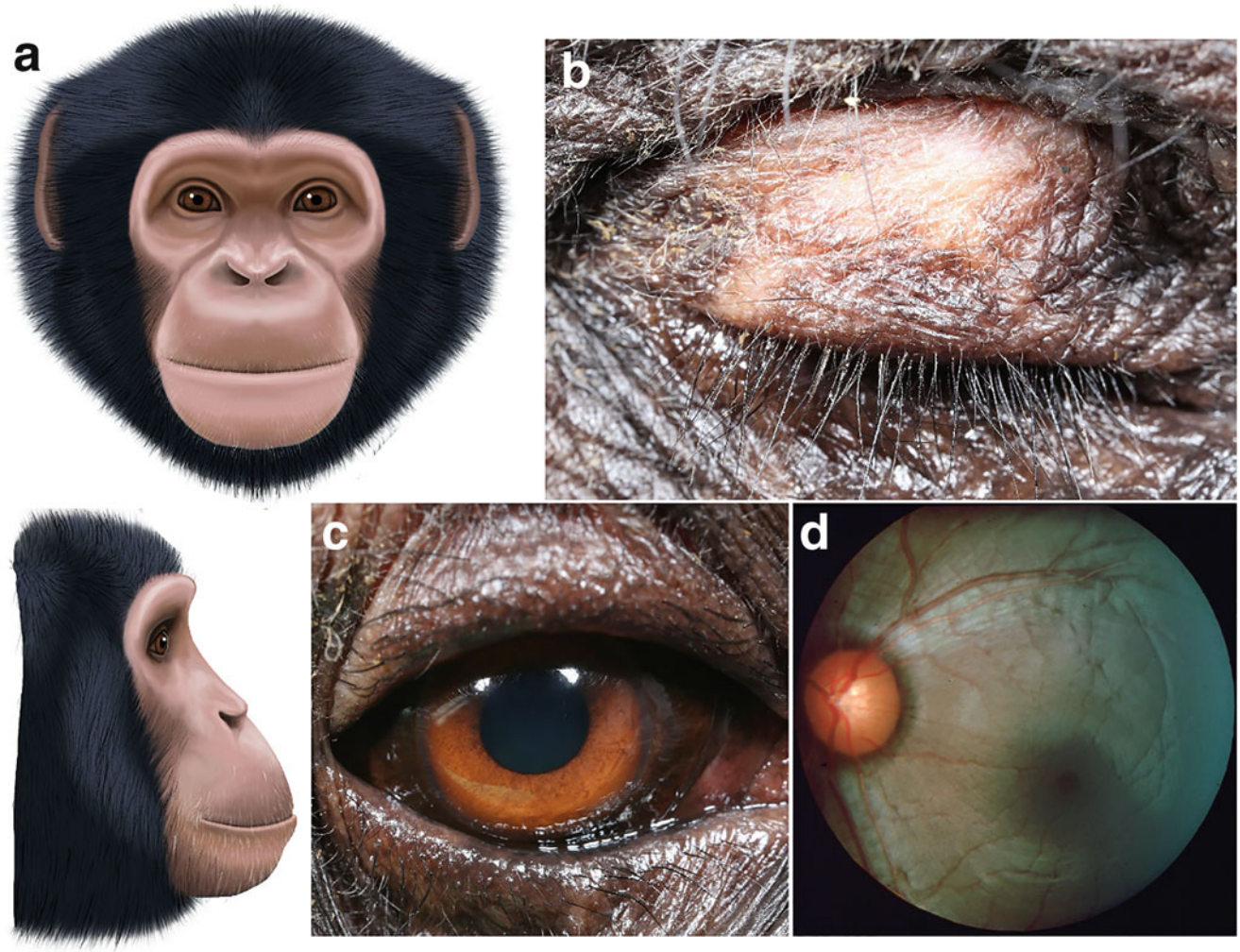

Fig. 47.35 Nonhuman hominids exhibit heavily pigmented skin, hair, iris, and fundus. Normal pigmentation of the face of a chimpanzee (**a**). A 28-year-old captive male chimpanzee demonstrates abundant pigment in the adnexa and eyelashes with a brown iris (**b** and **c**). The normal fundus of a 7-year-old male chimpanzee is heavily pigmented with a round macula, round optic nerve head and reflective nerve fiber layer (**d**). **b, c**—Courtesy of Bret A. Moore

morphometry of the chimpanzee (*Pan troglodytes*) and gorilla (*Gorilla gorilla*) was closest to that of a human. Specifically, the 3 aforementioned species had a relatively thick cornea, epithelium, Bowman's layer, and endothelium relative to other species. Ocular biometry, refraction, and intraocular pressure measurements have been reported in normal chimpanzees and gorillas (Table 47.2, Appendix 3) (Liang et al. 2005; Young and Farrer 1964). In the same population of captive gorillas, cultures of the eyelid margin and bulbar conjunctiva isolated *Candida* sp. (n = 5), *Micrococcus* sp. (n = 3), *Staphylococcus aureus* (n = 4), *Staphylococcus epidermidis* (n = 3), and *Staphylococcus saccharolyticus* (n = 3) (Liang et al. 2005).

Except in rare cases of oculocutaneous albinism (Prado-Martinez et al. 2013), the skin, iris, and fundus of apes are heavily pigmented in all species but *Homo sapiens* (Plate 47.1, Fig. 47.35). In humans, blue irides are primarily due to a regulatory variant of the *OCA2* gene encoding for melasomal transmembrane protein within an intron of *HERC2* (Eiberg et al. 2008; Sturm et al. 2008). Other genes that impact blue and green iridal coloration in humans include *SLC24A4* and *TYR* (Sulem et al. 2007).

Ophthalmic Disease

In a 2-year clinical survey and histologic survey of ophthalmic lesions in chimpanzees (*Pan troglodytes*) in one colony, the most common abnormalities identified were conjunctivitis or corneal lesions (n = 10), myopia (n = 7), uveal colobomas (n = 3), cataract (n = 1), and retinal detachment (n = 1) (Schmidt 1971b). Physiologic cupping of the optic disc was common (n = 35) suggesting that it is a normal variation in these species. One chimpanzee in this colony was

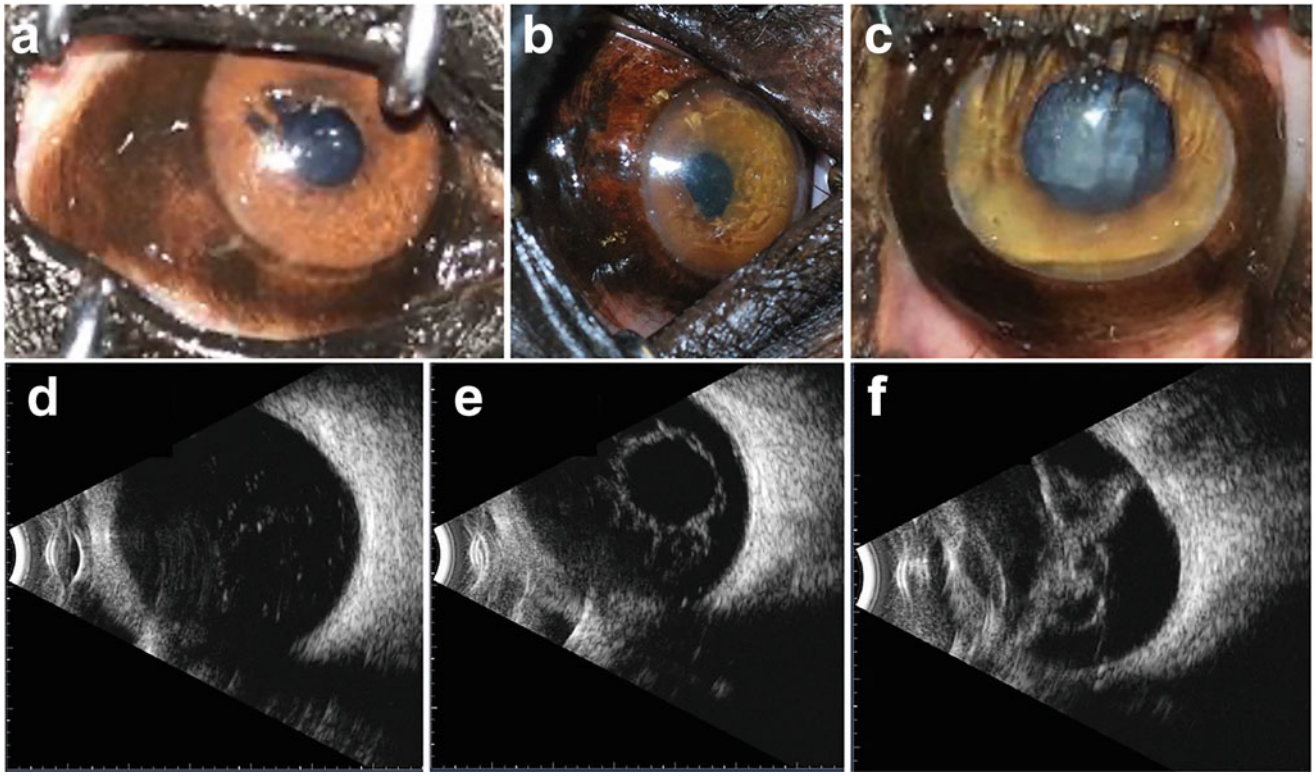

Fig. 47.36 Lesions observed in chimpanzees by ophthalmic examination and ocular B-scan ultrasound. (**a**) Iris nevi OD a 16-year-old female. (**b**) Dyscoric pupil and deep anterior chamber OD in a 12-year-old male pseudophake. (**c**) Late immature cataract OD in a 26-year-old male. B-mode ultrasound (Accutome with 15 mHz probe with a maximum depth of 50 mm and gain of 64 dB) was performed. (**d**) Vitreal degeneration was identified in the male from (**c**). (**e**) A dislocated IOL was identified in the pseudophake from (**b**). (**f**) A retinal detachment was identified in a 34-year-old male. Images courtesy of Dr. Kerri-Lee Dobbie from University of Pretoria

enucleated for unilateral vision loss and retinal and choroidal colobomas were histologically confirmed in the left eye (Schmidt 1971a). In a study of free-living chimpanzees, the most common ophthalmic findings were iridal melanosis (n = 11), dyscoria (n = 3), and mature cataracts (n = 2); ocular B-mode ultrasound identified other lesions including vitreous syneresis, retinal detachment, and IOL dislocation (Fig. 47.36) (Dobbie 2020).

A left retrobulbar coenurus cyst was reported in a captive lar gibbon (*Hylobates lar*). Clinical signs included exophthalmos, decreased retropulsion, conjunctival hyperemia and chemosis with papilledema; fundic examination identified retinal venous dilation and retinal striae at the posterior pole. Skull radiographs identified a retrobulbar mass in the inferonasal quadrant of the left orbit with secondary orbital enlargement and superior displacement of the supraorbital ridge with thinning. Following euthanasia, a necropsy revealed a left orbital cyst. Histopathologic examination of the cyst identified multiple scolices, but the species of tapeworm was not determined.

Multiple nodular lesions of the eyelids, ears, lip, and nares consisting of live *Anatrichostoma* nematodes and eggs have been reported in two lar gibbons (*Hylobates lar*) (Breznock and Pulley 1975). No treatment was provided and the lesions diminished in size and number over a year of observation but remained firm on palpation. In human cases of anatrichostomamiasis, treatment has been successfully reported with albendazole daily for 3 days or mebendazole twice daily for 20 days (Eberhard et al. 2014; Eberhard et al. 2010). Given that a few human cases of anatrichosomiasis have been reported, infected animals should be handled with care (Eberhard et al. 2014).

Corneal ulcers can occur from infectious and non-infectious causes in hominids. Ocular manifestations of alphaherpesviruses in captive chimpanzees have been reported and included severe photophobia and blepharospasm sometimes with concomitant corneal ulceration (Bezner 2019). While corneal scrapings for viral isolation were negative, dramatic improvement was observed with valacyclovir 1 g PO BID or acyclovir 400 mg PO QID. Specifically, antiviral medications decreased the clinical disease course from weeks to days. The alphaherpesvirus most likely responsible is chimpanzee herpesvirus (ChHV) which is more closely related to herpes simplex virus type 1 versus

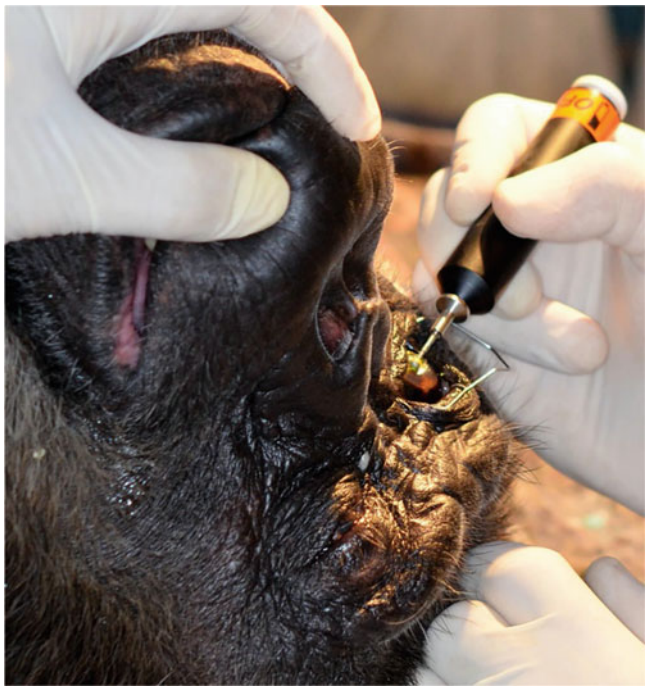

Fig. 47.37 A diamond burr debridement was performed in a 30-year-old adult male chimpanzee with chronic, recurrent corneal erosions. The chimpanzee had been treated for multiple months with topical tobramycin OD for a corneal ulcer. On ophthalmic examination, blepharospasm, epiphora, and an opaque cornea with multiple regions of erosion were identified. Fluorescein stain seeped underneath the epithelial margins consistent with a recurrent corneal erosion. The patient was induced and maintained under general anesthesia with propofol; topical anesthetic was applied. A diamond burr debridement was performed and the patient was treated with topical ciprofloxacin QID for 10 days. The epithelium healed ~14 days after the procedure but corneal scarring remained. Images courtesy of Dr. Fabiano Montiani-Ferreira

type 2 (Luebcke et al. 2006). A recurrent corneal erosion was identified in a geriatric chimpanzee and successfully managed with a diamond burr debridement (Fig. 47.37).

Ocular coccidioidomycosis was reported in a captive chimpanzee living in a sanctuary in Arizona, an endemic region for *Coccidioides immitis* (Hoffman et al. 2007). Severe, unilateral conjunctivitis was initially observed followed by granulomas involving the inferior conjunctiva and anterior uvea. Treatment with the experimental triazole, BayR3783, and subconjunctival triamcinolone reduced the ocular mass but damage from the chronic uveitis resulted in corneal fibrosis, anterior synechiae of the inferior iris, and lens subluxation. Coccidiomycosis has also been reported in other chimpanzees as well as gorillas (Koistinen et al. 2018; Herrin et al. 2005; Marzke et al. 1988; Reed et al. 1985; Hood and Galgiani 1985); ocular manifestations of systemic coccidiomycosis in human patients are rare and diagnosis can be challenging (Rodenbiker and Ganley 1980). A thorough ophthalmic examination should be performed for apes diagnosed with systemic mycoses to detect subclinical disease.

Oculocutaneous albinism with white hair, pink skin, blue irides, photophobia, and decreased visual acuity was diagnosed in a Western lowland gorilla (*Gorilla gorilla*) originally from Equatorial Guinea that was eventually captured and brought to a zoo (Prado-Martinez et al. 2013). The causal genetic variant was identified by whole-genome sequencing as a single nucleotide variant in the transmembrane region of *SLC45A2*. Genome-wide patterns of autozygosity also established that this gorilla's parents were related and is thus the first report of inbreeding in wild Western lowland gorilla. Albinism has also been reported in a Bornean orangutan (*Pongo pygmaeus wurmbii*) (Chappell 2018; Brady 2017) and a western chimpanzee (*Pan troglodytes verus*) (Farah 2001). A myriad of causal genes for oculocutaneous albinism have been identified in *Homo sapiens* that may be responsible for the albinism identified in the aforementioned species (Kamaraj and Purohit 2014).

Cataracts of varying stages have been reported in nonhuman apes (Figs. 47.36, 47.38, and 47.39) (Leiva et al. 2012; de Faber et al. 2004; Warwick et al. 2017; Schmidt 1971b; Montiani-Ferreira et al. 2010). Trisomy 22 was described in a captive chimpanzee with infantile cataract, nystagmus strabismus and keratoconus with concomitant stunted growth, congenital atrial septal defect, and hypodontia; these clinical signs are consistent with Down syndrome in humans (Hirata et al. 2017). Phacoemulsification for cataracts has been performed in captive chimpanzees (*Pan troglodytes*), western lowland gorilla (*Gorilla gorilla gorilla*), orangutan (*Pongo pygmaeus*), and lar gibbon (*Hylobates lar*) (Figs. 47.38 and 47.39); intraocular lenses with powers ranging from +16 to +25 D were implanted in all cases but one orangutan (Leiva et al. 2012; de Faber et al. 2004; Warwick et al. 2017; Montiani-Ferreira et al. 2010). One-handed (n = 7 eyes) or two-handed (n = 2) phacoemulsification was performed routinely with the following modifications: (1). A lateral 2.7–3.2 mm clear corneal incision was made to avoid the supraorbital crest; (2) hydrodissection was performed immediately after the capsulectomy with balanced salt solution through a 27-gauge cannula; (3) hypermature cataracts (n = 3) could be removed with irrigation/aspiration only; 4) suture knots were buried for the corneal incision closure (n = 7) (Leiva et al. 2012). Mild photophobia was reported immediately after surgery. Long term, all animals showed increased activity and socialization after surgery. In two animals that were euthanized for reasons unrelated to their eyes, ocular histopathology found mild to moderate lens fiber regrowth with dispersed lens epithelial cells (Leiva et al. 2012). Aged wild bonobos and chimpanzees exhibit increased distance while doing a visual task, grooming, suggesting that their accommodative ability decreases with age (Ryu et al. 2016; Fujisawa et al. 2010). This observation is presumably due to increased rigidity of their crystalline lens similar to humans with presbyopia.

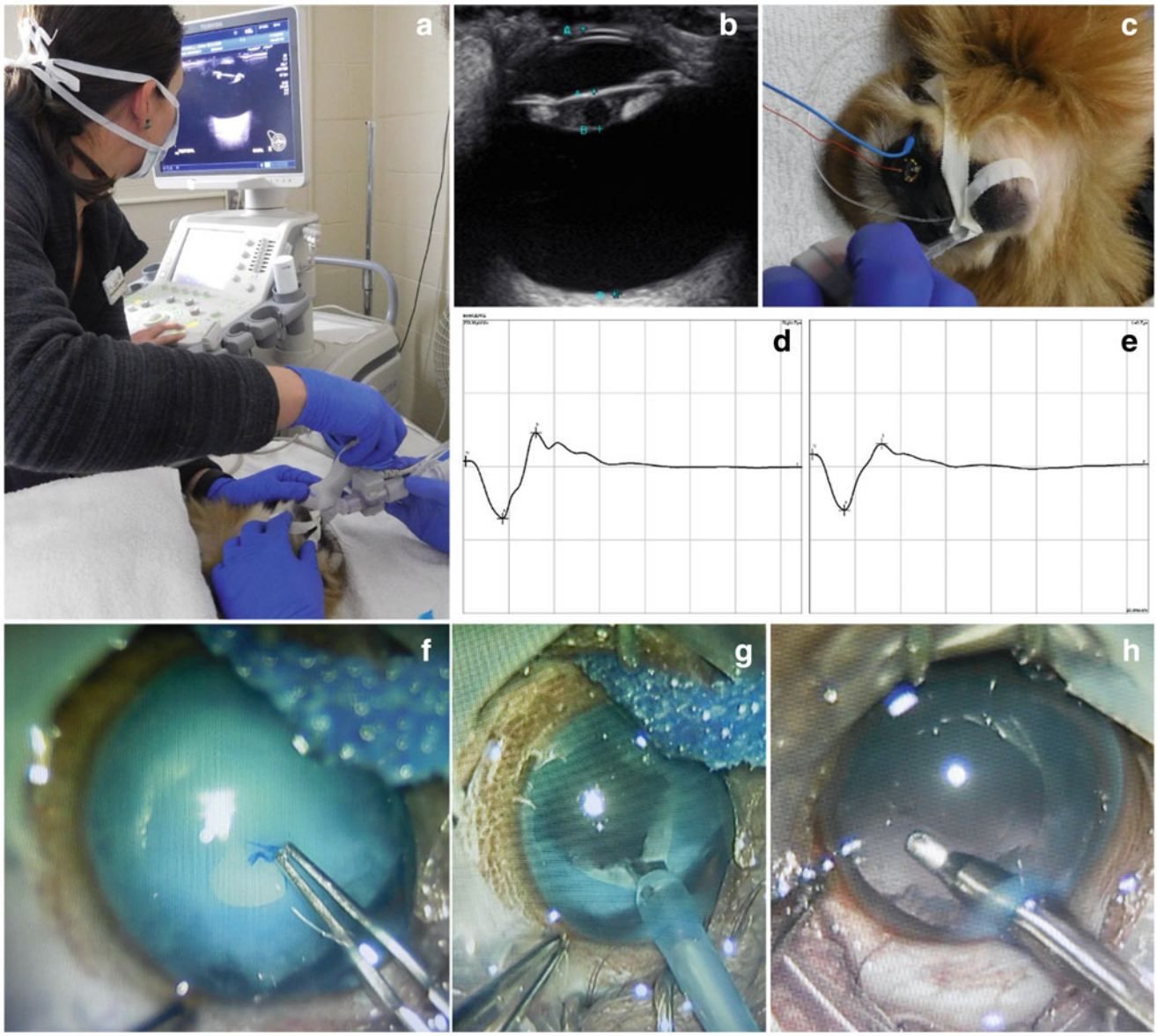

Fig. 47.38 Ocular ultrasound, electroretinography and phacoemulsification for bilateral, hypermature cataracts in a lar gibbon (*Hylobates lar*). On ophthalmic examination, hyperpigmentation of both irides, deep anterior chambers, and hypermature, resorbing cataracts were identified in both eyes (oculus uterque, OU). Intraocular pressure as measured by applanation tonometry were 16 mm Hg in the right eye (oculus dexter, OD) and 18 mm Hg in the left eye (oculus sinister, OS). Horizontal corneal diameters using Jameson calipers were 12 mm OU. Ocular ultrasound (**a**) of a 2-year-old female lar gibbon was performed under general anesthesia and revealed bilateral cataracts and deep anterior chambers; a superior-inferior scan of the left eye reveals an increased vitreous length and thinner lens (**b**) in comparison with the right eye. Anterior chamber depth, lens thickness, vitreous length, and axial globe length OD and OS as measured by B-scan ultrasound were 4.2 and 3.8, 2.6 and 1.8, 11.6 and 12.7, and 18.2 and 18.1 mm, respectively. Electroretinography was also performed under general anesthesia (**c**) and dark-adapted waveforms were generated for the right (**d**) and left eyes (**e**). A-wave amplitudes and implicit times were 196 and 190 μV and 17.6 and 15.6 ms for OD and OS, respectively; B-wave amplitudes and implicit times were 293 and 226 μV and 32.3 and 32.0 ms, respectively. One-handed phacoemulsification was performed under inhalant anesthesia with isoflurane with paralysis using intravenous atracurium. The lens capsule was stained with trypan blue to facilitate a continuous curvilinear capsulorhexis (**f**). Phacoemulsification was rapid at 0.5 s OD and 1.9 s OS (**g**). Irrigation-aspiration was performed to remove any remaining cortex (**h**). The gibbon was left aphakic. There were minimal focal capsular plaques noted at the dorsal equator at the conclusion of surgery OU. Three simple sutures of 9–0 Vicryl were placed to close the two-step limbal incisions. Post-operative treatment included topical neomycin-polymyxin-dexamethasone ophthalmic ointment OU twice daily and atropine ophthalmic ointment OU once daily as well as oral amoxicillin-clavulanate (x mg/kg) twice daily and meloxicam (x mg/kg) once daily. At two weeks post-operative, an ophthalmic examination under isoflurane anesthesia revealed that the corneal incisions were intact with sutures present, trace anterior chamber cell, aphakia and a normal fundic examination OU. The gibbon exhibited improved vision with no signs of ocular discomfort following surgery. Images courtesy of Dr. Jessica Meekins from Kansas State University

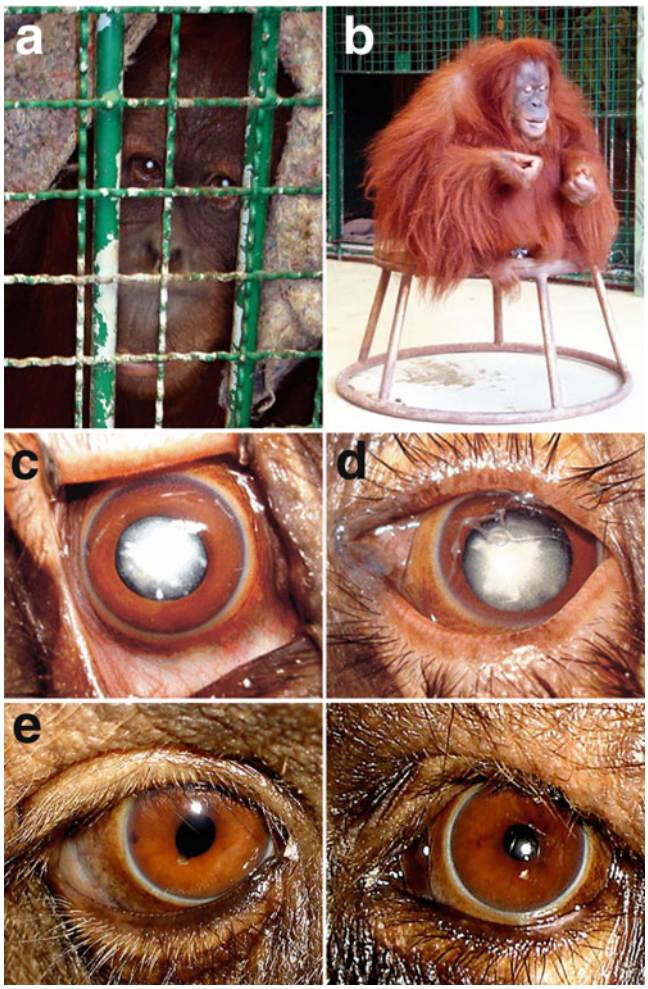

Fig. 47.39 Bilateral cataracts in an orangutan were corrected with phacoemulsification. (**a**) A 14-year-old, female, captive-born orangutan (*Pongo pygmaeus*) developed vision impairment from bilateral, mature cataracts (**a–d**). At 2 months post-phacoemulsification, dyscoria, a focal iridal scar adjacent to the pupillary margin at approximately 7 o'clock, were identified in the aphakic right eye (**e**). These lesions were produced by the phacoemulsification needle tip. A round pupil and clear, deep anterior chamber, and aphakia were identified OS. The surgery successfully restored vision and normal activity to this orangutan. Reprinted with permission (Montiani-Ferreira et al. 2010)

Single case reports of two common retinal diseases in humans—hypertensive retinopathy and age-related macular degeneration (AMD)—were described in captive geriatric western lowland gorillas (*Gorilla gorilla gorilla*). Hypertensive retinopathy was diagnosed in a 34-year-old female gorilla, which was euthanized due to acute blindness from bilateral, complete retinal detachments (Niemuth et al. 2014). In the three months prior to euthanasia, the gorilla was evaluated for ocular discomfort, somnolence, and headholding; uveitis, cataracts, and partial retinal detachments were diagnosed. During this time, the gorilla was anesthetized five times for procedures unrelated to the eyes and 6 of 9 systolic blood pressure measurements >160 mm Hg were recorded. Repeated complete blood counts, clinical chemistry panels, and urinalyses failed to identify an underlying cause; primary systemic hypertension was diagnosed. Oral enalapril maleate (0.03 mg/kg) every 24 h was instituted, then increased to twice daily a month later, but no response was observed prior to euthanasia. On gross examination at necropsy, bilateral, complete retinal detachments with subretinal hemorrhage were identified. With histology, small arteries and arterioles in the eye demonstrated mild to marked thickening with inflammation present within the walls and occasional intramural eosinophilic material consistent with necrotizing arteriolitis (Niemuth et al. 2014). Early age-related macular degeneration (AMD) was found in a 31-year-old female gorilla, which exhibited decreased vision for near objects but retained good distance vision (Steinmetz et al. 2012). Fundic examination demonstrated drusen-like lesion in the macula of both eyes, consistent with the dry form of AMD. Dietary supplementation was initiated with omega-3 fatty acids (30 mg/kg) and vitamin E (8 mg/kg) to delay disease progression.

References

Acuna C, Gonzalez F, Dominguez R (1983) Sensorimotor unit activity related to intention in the pulvinar of behaving Cebus Apella monkeys. Exp Brain Res 52:411–422

Adami C, Wenker C, Hoby S, Bergadano A (2012) Evaluation of effectiveness, safety and reliability of intramuscular medetomidine-ketamine for captive great apes. Vet Rec 171:196

Adami C, Wenker C, Hoby S, Morath U, Bergadano A (2013) Anaesthesia with medetomidine-ketamine-isoflurane with and without midazolam, in eight captive chimpanzees (Pan troglodytes) premedicated with oral zuclopenthixol. Schweiz Arch Tierheilkd 155:471–476

Ak AK, Gupta V (2020) Rhino-orbital Cerebral Mucormycosis. *StatPearls*. StatPearls Publishing. Copyright © 2020, StatPearls Publishing LLC.: Treasure Island (FL))

Albert DM, Dubielzig RR, Li Y, Lin T, Neekhra A, Orilla W, Ramos M, Salamat MS, Burke JA (2009) Choroidal melanoma occurring in a nonhuman primate. Arch Ophthalmol 127:1080–1082

Alleaume C, Mrini ME, Laloy E, Marchal J, Aujard F, Chahory S (2017) Scleral and corneal xanthomatous inflammation in a gray mouse lemur (Microcebus murinus). Vet Ophthalmol 20:177–180

Alves DA, Honko AN, Kortepeter MG, Sun M, Johnson JC, Lugo-Roman LA, Hensley LE (2016) Necrotizing Scleritis, conjunctivitis, and other pathologic findings in the left eye and brain of an Ebola virus-infected rhesus macaque (Macaca mulatta) with apparent recovery and a delayed time of death. J Infect Dis 213:57–60

Anderson A, Clifford W, Palvolgyi I, Rife L, Taylor C, Smith RE (1992) Immunopathology of chronic experimental histoplasmic choroiditis in the primate. Invest Ophthalmol Vis Sci 33:1637–1641

Andrade da Costa BL, Hokoc JN (2000) Photoreceptor topography of the retina in the New World monkey Cebus apella. Vis Res 40:2395–2409

Ankel-Simons F (2007) Primate anatomy: an introduction. London, Elsevier

Ankel-Simons FA, Simons C (2003) The axial skeleton of primates: how does genus Tarsius fit? In: Wright PC, Simons EL, Gursky S (eds) Tarsiers: past, present, and future. Rutgers University, New Brunswick, NJ

Anzai M, Nagao S (2014) Motor learning in common marmosets: vestibulo-ocular reflex adaptation and its sensitivity to inhibitors of Purkinje cell long-term depression. Neurosci Res 83:33–42

Auwaerter PG, Rota PA, Elkins WR, Adams RJ, DeLozier T, Shi Y, Bellini WJ, Murphy BR, Griffin DE (1999) Measles virus infection in rhesus macaques: altered immune responses and comparison of the virulence of six different virus strains. J Infect Dis 180:950–958

Bakker J, Uilenreef JJ, Pelt ER, Brok HP, Remarque EJ, Langermans JA (2013) Comparison of three different sedative-anaesthetic protocols (ketamine, ketamine-medetomidine and alphaxalone) in common marmosets (Callithrix jacchus). BMC Vet Res 9:113

Bala Murugan S, Mahendradas P, Dutta Majumder P, Kamath Y (2020) Ocular leprosy: from bench to bedside. Curr Opin Ophthalmol 31: 514–520

Baldwin MKL, Krubitzer L (2018) Architectonic characteristics of the visual thalamus and superior colliculus in titi monkeys. J Comp Neurol 526:1760–1776

Bansal N, Majumdar S, Chakravarti RN (1986) Frequency and size of atherosclerotic plaques in vasectomized diabetic monkeys. Int J Fertil 31:298–304

Barlow SC, Semes LP, Cartner SC (2000) Iridodialysis in a rhesus macaque: a case report. Comp Med 50:673–674

Barnett KC, Heywood R, Hague PH (1972) Colloid degeneration of the retina in a baboon. J Comp Pathol 82:117–118

Barros M, Alencar C, Tomaz C (2004) Differences in aerial and terrestrial visual scanning in captive black tufted-ear marmosets (Callithrix penicillata) exposed to a novel environment. Folia Primatol (Basel) 75:85–92

Baskin GB (1996) Cryptosporidiosis of the conjunctiva in SIV-infected rhesus monkeys. J Parasitol 82:630–632

Bauer KL, Steeil JC, Adkins EA, Childress AL, Wellehan JFX Jr, Kerns KL, Sarro SJ, Holder KA (2018) Management of Ocular Human herpesvirus 1 infection in a White-faced Saki monkey (Pithecia pithecia). Comp Med 68:319–323

Bellhorn RW (1973) Ophthalmologic disorders of exotic and laboratory animals. Vet Clin North Am 3:345–356

Bellhorn RW, Friedman AH, Henkind P (1972) Racemose (cirsoid) hemangioma in rhesus monkey retina. Am J Ophthalmol 74:517–522

Beltran WA, Vanore M, Ollivet F, Nemoz-Bertholet F, Aujard F, Clerc B, Chahory S (2007) Ocular findings in two colonies of gray mouse lemurs (Microcebus murinus). Vet Ophthalmol 10:43–49

Benavente-Perez A, Nour A, Troilo D (2012) The effect of simultaneous negative and positive defocus on eye growth and development of refractive state in marmosets. Invest Ophthalmol Vis Sci 53:6479–6487

Bergmanson JP (1987) Histopathological analysis of the corneal epithelium after contact lens wear. J Am Optom Assoc 58:812–818

Bergmanson JP, Ruben CM, Chu LW (1985) Epithelial morphological response to soft hydrogel contact lenses. Br J Ophthalmol 69:373–379

Bezerra KPG, de Lucena RB, Stipp DT, Costa FS, Reis VV, Borges PF, Bopp S, Campos DB, Talieri IC (2019) Determination of baseline values for routine ophthalmic tests in bearded capuchin (Sapajus libidinosus). J Med Primatol 48:3–9

Bezner J (2019) Medical aspects of chimpanzee rehabilitation and sanctuary medicine. In: Miller RE, Lamberski N, Calle P (eds) Fowler's zoo and wild animal medicine. Elsevier, St. Louis, MO

Bito LZ, Merritt SQ, DeRousseau CJ (1979) Intraocular pressure of rhesus monkey (Macaca mulatta). I. an initial survey of two free-breeding colonies. Invest Ophthalmol Vis Sci 18:785–793

Blakemore C, Vital-Durand F, Garey LJ (1981) Recovery from monocular deprivation in the monkey. I. Reversal of physiological effects in the visual cortex. Proc R Soc Lond B Biol Sci 213:399–423

Blessing EM, Solomon SG, Hashemi-Nezhad M, Morris BJ, Martin PR (2004) Chromatic and spatial properties of parvocellular cells in the lateral geniculate nucleus of the marmoset (Callithrix jacchus). J Physiol 557:229–245

Blois-Heulin C (1999) Variability in social visual attention in the red-capped mangabey (Cercocebus torquatus torquatus) and the grey-cheeked mangabey (Cercocebus albigena albigena). Folia Primatol (Basel) 70:264–268

de Boer RA, Overduin-de Vries AM, Louwerse AL, Sterck EH (2013) The behavioral context of visual displays in common marmosets (Callithrix jacchus). Am J Primatol 75:1084–1095

Böhm MR, Mertsch S, König S, Spieker T, Thanos S (2013) Macula-less rat and macula-bearing monkey retinas exhibit common lifelong proteomic changes. Neurobiol Aging 34:2659–2675

Böhm MR, Hodes F, Brockhaus K, Hummel S, Schlatt S, Melkonyan H, Thanos S (2016) Is Angiostatin involved in physiological foveal Avascularity? Invest Ophthalmol Vis Sci 57:4536–4552

Boissinot S, Tan Y, Shyue SK, Schneider H, Sampaio I, Neiswanger K, Hewett-Emmett D, Li WH (1998) Origins and antiquity of X-linked triallelic color vision systems in New World monkeys. Proc Natl Acad Sci U S A 95:13749–13754

Boote C, Dennis S, Meek K (2004) Spatial mapping of collagen fibril organisation in primate cornea-an X-ray diffraction investigation. J Struct Biol 146:359–367

Bourne WM (1978) Penetrating keratoplasty with fresh and cryopreserved corneas. Donor endothelial cell survival in primates. Arch Ophthalmol 96:1073–1074

Bourne JA, Rosa MG (2003) Preparation for the in vivo recording of neuronal responses in the visual cortex of anaesthetised marmosets (Callithrix jacchus). Brain Res Brain Res Protoc 11:168–177

Bouskila J, Javadi P, Palmour RM, Bouchard JF, Ptito M (2014) Standardized full-field electroretinography in the Green monkey (Chlorocebus sabaeus). PLoS One 9:e111569

Brady H (2017) Extremely Rare Albino Orangutan Found in Indonesia. In: National Geographic

Breznock AW, Pulley LT (1975) Anatrichosoma infection in two white-handed gibbons. J Am Vet Med Assoc 167:631–633

Bunce JA (2015) Incorporating ecology and social system into formal hypotheses to guide field studies of color vision in primates. Am J Primatol 77:516–526

Burek JD, McElyea U Jr, Fox JG, Stookey JL (1974) Persistent pupillary membranes in a rhesus monkey. J Am Vet Med Assoc 164:719–721

Burke JA, Potter DE (1986) Ocular effects of a relatively selective alpha 2 agonist (UK-14, 304–18) in cats, rabbits and monkeys. Curr Eye Res 5:665–676

Burke J, Schwartz M (1996) Preclinical evaluation of brimonidine. Surv Ophthalmol 41(Suppl 1):S9–S18

Burton M, Morton RJ, Ramsay E, Stair EL (1986) Coccidioidomycosis in a ring-tailed lemur. J Am Vet Med Assoc 189:1209–1211

Buyukmihci N, Richter CB (1979) Prevalence of ocular disease in a colony of tamarins and marmosets. Lab Anim Sci 29:800–804

Buzás P, Blessing EM, Szmajda BA, Martin PR (2006) Specificity of M and L cone inputs to receptive fields in the parvocellular pathway: random wiring with functional bias. J Neurosci 26:11148–11161

Buzás P, Szmajda BA, Hashemi-Nezhad M, Dreher B, Martin PR (2008) Color signals in the primary visual cortex of marmosets. J Vis 8:7.1-16

Calkins JL, Hochheimer BF, D'Anna SA (1980) Potential hazards from specific ophthalmic devices. Vis Res 20:1039–1053

Casanova MI, Chen R, Garzel LM, Olstad KJ, Kim S, Harris RA, Li Y, Raveendran M, Liang Q, Wang J, Yiu G, Stout JT, Roberts JA, Rogers J, Moshiri A, Thomasy SM (2021) Clinical presentation,

treatment, and genetic and histopathological analysis of juvenile cataracts and secondary glaucoma in a rhesus macaque (Macaca mulatta). J Med Primatol. https://doi.org/10.1111/jmp.12560
Castenholz A (1984) The eye of Tarsius. In: Niemitz C (ed) Biology of tarsiers. Stuttgart, Gustav Fischer Verlag
Cavalcante JS, Costa MS, Santee UR, Britto LR (2005) Retinal projections to the midline and intralaminar thalamic nuclei in the common marmoset (Callithrix jacchus). Brain Res 1043:42–47
Cerveny SN, D'Agostino JJ, Davis MR, Payton ME (2012) Comparison of laryngeal mask airway use with endotracheal intubation during anesthesia of western lowland gorillas (Gorilla gorilla gorilla). J Zoo Wildl Med 43:759–767
Chagas J, Santos L, Silva Filho JR, Bondan C (2018) Anaesthetic and cardiorespiratory effects of ketamine plus dexmedetomidine for chemical restraint in black capuchin monkeys (Sapajus nigritus). N Z Vet J 66:79–84
Chakrabarti B, Hultsch E (1976) Owl monkey vitreous: a novel for hyaluronic acid structural studies. Biochem Biophys Res Commun 71:1189–1193
Chan TL, Grunert U (1998) Horizontal cell connections with short wavelength-sensitive cones in the retina: a comparison between New World and Old World primates. J Comp Neurol 393:196–209
Chan TL, Goodchild AK, Martin PR (1997) The morphology and distribution of horizontal cells in the retina of a New World monkey, the marmoset Callithrix jacchus: a comparison with macaque monkey. Vis Neurosci 14:125–140
Chan TL, Martin PR, Clunas N, Grünert U (2001) Bipolar cell diversity in the primate retina: morphologic and immunocytochemical analysis of a new world monkey, the marmoset Callithrix jacchus. J Comp Neurol 437:219–239
Chandra AJ, Lee SCS, Grünert U (2017) Thorny ganglion cells in marmoset retina: morphological and neurochemical characterization with antibodies against calretinin. J Comp Neurol 525:3962–3974
Chang FW, Burke JA, Potter DE (1985) Mechanism of the ocular hypotensive action of ketanserin. J Ocul Pharmacol 1:137–147
Chaplin TA, Yu HH, Rosa MG (2013) Representation of the visual field in the primary visual area of the marmoset monkey: magnification factors, point-image size, and proportionality to retinal ganglion cell density. J Comp Neurol 521:1001–1019
Chappell B (2018) Alba The Albino Orangutan Is Now Free, Living In The Trees Again. In: National Public Radio
Chinnadurai SK, Williams C (2016) The minimum alveolar concentration of sevoflurane in ring-tailed lemurs (Lemur catta) and aye-ayes (Daubentonia madagascariensis). Vet Anaesth Analg 43:76–80
Chivers DJ (2013) Family Hyblobatidae (gibbons). In: Mittermeier RA, Rylands AB, Wilson DE (eds) Handbook of the mammals of the world. Lynx Edicions, Barcelona, Spain
Chronopoulos A, Roy S, Beglova E, Mansfield K, Wachtman L, Roy S (2015) Hyperhexosemia-induced retinal vascular pathology in a novel primate model of diabetic retinopathy. Diabetes 64:2603–2608
Chung JH (1988) Experimental corneal alkali wound healing. Acta Ophthalmol Suppl 187:1–35
Collins CE, Hendrickson A, Kaas JH (2005) Overview of the visual system of Tarsius. Anat Rec A Discov Mol Cell Evol Biol 287: 1013–1025
Corso J, Bowler M, Heymann EW, Roos C, Mundy NI (2016) Highly polymorphic colour vision in a New World monkey with red facial skin, the bald uakari (Cacajao calvus). Proc Biol Sci 283
Costa-Vila J, Barastegui C, Ruano-Gil D (1987) Morphological significance of the pectineal ligament of the eye. Acta Anat (Basel) 130: 247–250
Craft CM, Huang J, Possin DE, Hendrickson A (2014) Primate short-wavelength cones share molecular markers with rods. Adv Exp Med Biol 801:49–56
Cromeens DM, Stephens LC (1985) Insular amyloidosis and diabetes mellitus in a crab-eating macaque (Macaca fascicularis). Lab Anim Sci 35:642–645
Crosson CE, Burke JA, Chan MF, Potter DE (1987) Ocular effects of a N,N-disubstituted 5-OH aminotetralin (N-0437): evidence for a dual mechanism of action. Curr Eye Res 6:1319–1326
Culbertson WW, Tabbara KF, O'Connor R (1982) Experimental ocular toxoplasmosis in primates. Arch Ophthalmol 100:321–323
Curcio CA, Sloan KR, Kalina RE, Hendrickson AE (1990) Human photoreceptor topography. J Comp Neurol 292:497–523
Cusick CG, Gould HJ 3rd, Kaas JH (1984) Interhemispheric connections of visual cortex of owl monkeys (Aotus trivirgatus), marmosets (Callithrix jacchus), and galagos (Galago crassicaudatus). J Comp Neurol 230:311–336
Davson H, Luck CP (1959) Chemistry and rate of turnover of the ocular fluids of the bush baby (Galago crassicaudatus Agisymbanus). J Physiol 145:433–439
Dawson WW, Brooks DE, Hope GM, Samuelson DA, Sherwood MB, Engel HM, Kessler MJ (1993) Primary open angle glaucomas in the rhesus monkey. Br J Ophthalmol 77:302–310
Dawson WW, Brooks DE, Dawson JC, Sherwood MB, Kessler MJ, Garcia A (1998) Signs of glaucoma in rhesus monkeys from a restricted gene pool. J Glaucoma 7:343–348
Dawson WW, Jeffery G, Dawson JC, Kessler MJ, Rodriguez J, Westergaard GC (2004) Fundus pigment distribution in rhesus monkeys. Vet Ophthalmol 7:391–396
Dawson WW, Dawson JC, Hope GM, Brooks DE, Percicot CL (2005) Repeat sample intraocular pressure variance in induced and naturally ocular hypertensive monkeys. J Glaucoma 14:426–431
DeBruyn EJ, Casagrande VA (1981) Demonstration of ocular dominance columns in a New World primate by means of monocular deprivation. Brain Res 207:453–458
Deegan JF 2nd, Jacobs GH (2001) Spectral sensitivity of gibbons: implications for photopigments and color vision. Folia Primatol (Basel) 72:26–29
Denion E, Hitier M, Levieil E, Mouriaux F (2015) Human rather than ape-like orbital morphology allows much greater lateral visual field expansion with eye abduction. Sci Rep 5:12437
Denk N, Maloca PM, Steiner G, Booler H, Freichel C, Niklaus S, Schnitzer TK, Hasler PW (2020) Retinal features in Cynomolgus macaques (Macaca fascicularis) assessed by using scanning laser ophthalmoscopy and spectral domain optical coherence tomography. Comp Med 70:145–151
Desjardins DC, Parrish RK 2nd, Folberg R, Nevarez J, Heuer DK, Gressel MG (1986) Wound healing after filtering surgery in owl monkeys. Arch Ophthalmol 104:1835–1839
Dkhissi-Benyahya O, Szel A, Degrip WJ, Cooper HM (2001) Short and mid-wavelength cone distribution in a nocturnal Strepsirrhine primate (Microcebus murinus). J Comp Neurol 438:490–504
Dobbie KS (2020) Ocular findings and intraocular lens power in captive chimpanzees (Pan troglodytes). University of Pretoria
Dominy NJ, Lucas PW (2001) Ecological importance of trichromatic vision to primates. Nature 410:363–366
Dubey JP, Kramer LW, Weisbrode SE (1985) Acute death associated with toxoplasma gondii in ring-tailed lemurs. J Am Vet Med Assoc 187:1272–1273
Dubicanac M, Radespiel U, Zimmermann E (2017) A review on ocular findings in mouse lemurs: potential links to age and genetic background. Primate Biology 4:215–228
Dubicanac M, Joly M, Struve J, Nolte I, Mestre-Frances N, Verdier JM, Zimmermann E (2018) Intraocular pressure in the smallest primate aging model: the gray mouse lemur. Vet Ophthalmol 21:319–327
Duke-Elder S (1958) The eye in evolution. C.V. Mosby, St. Louis, MO
Eaton S, Raghunathan VK, Christian BJ, Morgan JT, Ver Hoeve JN, Yang CC, Gong H, Rasmussen CA, Miller P, Russell P, Nork TM, Murphy CJ (2017) Dynamic compensation occurs in the aqueous outflow pathway in non-human primates with experimental glaucoma. In *Association for Research in Vision and Ophthalmology Annual Meeting*, Baltimore, MD

Eberhard ML, Mathison B, Bishop H, Handoo NQ, Hellstein JW (2010) Zoonotic anatrichosomiasis in an Illinois resident. Am J Trop Med Hyg 83:342–344

Eberhard ML, Hellstein JW, Lanzel EA (2014) Zoonotic anatrichosomiasis in a mother and daughter. J Clin Microbiol 52:3127–3129

Eiber CD, Pietersen ANJ, Zeater N, Solomon SG, Martin PR (2018a) Chromatic summation and receptive field properties of blue-on and blue-off cells in marmoset lateral geniculate nucleus. Vis Res 151: 41–52

Eiber CD, Rahman AS, Pietersen ANJ, Zeater N, Dreher B, Solomon SG, Martin PR (2018b) Receptive Field properties of Koniocellular on/off neurons in the lateral geniculate nucleus of marmoset monkeys. J Neurosci 38:10384–10398

Eiberg H, Troelsen J, Nielsen M, Mikkelsen A, Mengel-From J, Kjaer KW, Hansen L (2008) Blue eye color in humans may be caused by a perfectly associated founder mutation in a regulatory element located within the HERC2 gene inhibiting OCA2 expression. Hum Genet 123:177–187

El Mubarak HS, Yuksel S, van Amerongen G, Mulder PG, Mukhtar MM, Osterhaus AD, de Swart RL (2007) Infection of cynomolgus macaques (Macaca fascicularis) and rhesus macaques (Macaca mulatta) with different wild-type measles viruses. J Gen Virol 88: 2028–2034

Elliott JH, Futterman S (1963) Fluorescence in the tapetum of the cat's eye. Identification, assay and localization of riboflavin in the tapetum and a proposed mechanism by which it may facilitate vision. Arch Ophthalmol 70:531–534

El-Mofty A, Gouras P, Eisner G, Balazs EA (1978) Macular degeneration in rhesus monkey (Macaca mulatta). Exp Eye Res 27:499–502

Engel HM, Dawson WW, Ulshafer RJ, Hines MW, Kessler MJ (1988) Degenerative changes in maculas of rhesus monkeys. Ophthalmologica 196:143–150

Engelberth RC, de Pontes AL, do Nascimento RB, de Lima RR, de Lima RR, de Toledo CA, de Oliveira Costa MS, Britto LR, de Souza Cavalcante J (2008) Discrete retinal input to the parabrachial complex of a new-world primate, the common marmoset (Callithrix jacchus). Neurosci Lett 443:99–103

England JD, Bohm RP Jr, Roberts ED, Philipp MT (1997) Lyme neuroborreliosis in the rhesus monkey. Semin Neurol 17:53–56

Erickson-Lamy KA, Kaufman PL, McDermott ML, France NK (1984) Comparative anesthetic effects on aqueous humor dynamics in the cynomolgus monkey. Arch Ophthalmol 102:1815–1820

de Faber JT, Pameijer JH, Schaftenaar W (2004) Cataract surgery with foldable intraocular lens implants in captive lowland gorillas (Gorilla gorilla gorilla). J Zoo Wildl Med 35:520–524

Fagundes N, Castro ML, Silva RA, De Lima MPA, Braga CS, Dos Santos EAR, Oliveira MA, Mattoso CRS, Pimenta ELM, Beier SL (2020) Comparison of midazolam and butorphanol combined with ketamine or dexmedetomidine for chemical restraint in howler monkeys (Alouatta Guariba clamitans) for vasectomy. J Med Primatol 49:179–187

Fahlman A, Bosi EJ, Nyman G (2006) Reversible anesthesia of southeast Asian primates with medetomidine, zolazepam, and tiletamine. J Zoo Wildl Med 37:558–561

Fantes FE, Hanna KD, Waring GO 3rd, Pouliquen Y, Thompson KP, Savoldelli M (1990) Wound healing after excimer laser keratomileusis (photorefractive keratectomy) in monkeys. Arch Ophthalmol 108:665–675

Farah D (2001) Warfare's forgotten casualties. In: The Washington Post

Farnsworth PN, Burke PA, Wagner BJ, Fu SC, Regan TJ (1980) Diabetic cataracts in the rhesus monkey lens. Metab Pediatr Ophthalmol 4:31–42

Federer F, Ichida JM, Jeffs J, Schiessl I, McLoughlin N, Angelucci A (2009) Four projection streams from primate V1 to the cytochrome oxidase stripes of V2. J Neurosci 29:15455–15471

Felsburg PJ, Heberling RL, Kalter SS (1973) Experimental corneal infection of the cebus monkey with herpesvirus hominis type 1 and type 2. Arch Gesamte Virusforsch 40:350–358

Ferraro MAR, Molina CV, Gris VN, Kierulff MCM, Bueno MG, Cortopassi SRG (2019) Early reversal of ketamine/dexmedetomidine chemical immobilization by atipamezole in golden-headed lion tamarins (Leontopithecus chrysomelas). J Med Primatol 48:351–356

Field WE, Yelnosky J, Mundy J, Mitchell J (1966) Use of droperidol and fentanyl for analgesia and sedation in primates. J Am Vet Med Assoc 149:896–901

Finlay BL, Franco EC, Yamada ES, Crowley JC, Parsons M, Muniz JA, Silveira LC (2008) Number and topography of cones, rods and optic nerve axons in new and Old World primates. Vis Neurosci 25:289–299

FitzGibbon T, Eriköz B, Grünert U, Martin PR (2015) Analysis of the lateral geniculate nucleus in dichromatic and trichromatic marmosets. J Comp Neurol 523:1948–1966

Florence SL, Conley M, Casagrande VA (1986) Ocular dominance columns and retinal projections in New World spider monkeys (Ateles ater). J Comp Neurol 243:234–248

Fonta C, Chappert C, Imbert M (1997) N-methyl-D-aspartate subunit R1 involvement in the postnatal organization of the primary visual cortex of Callithrix jacchus. J Comp Neurol 386:260–276

Fonta C, Chappert C, Imbert M (2000) Effect of monocular deprivation on NMDAR1 immunostaining in ocular dominance columns of the marmoset Callithrix jacchus. Vis Neurosci 17:345–352

Fortune B, Wang L, Bui BV, Burgoyne CF, Cioffi GA (2005) Idiopathic bilateral optic atrophy in the rhesus macaque. Invest Ophthalmol Vis Sci 46:3943–3956

Fox SA, Vainisi SJ, Gerstein MA (1979) Lens extraction with anterior chamber lens implantation in the macaque. Am J Vet Res 40:214–220

Franco EC, Finlay BL, Silveira LC, Yamada ES, Crowley JC (2000) Conservation of absolute foveal area in New World monkeys. A constraint on eye size and conformation. Brain Behav Evol 56:276–286

Fraser CE (1976) The owl monkey (Aotus trivirgatus) as an animal model in trachoma research. Lab Anim Sci 26:1138–1141

Fujisawa M, Matsubayashi K, Soumah AG, Kasahara Y, Nakatsuka M, Matsuzawa T (2010) Farsightedness (presbyopia) in a wild elderly chimpanzee: the first report. Geriatr Gerontol Int 10:113–114

Gaasterland D, Kupfer C (1974) Experimental glaucoma in the rhesus monkey. Investig Ophthalmol 13:455–457

Galera PD, Ávila MO, Ribeiro CR, Sandos FV (2002) Estudo da microbiota da conjuntiva ocular de macacos-prego (Cebus apella – Linnaeus, 1758) e macacos bugio (Alouatta caraya – Humboldt, 1812), pro-venientes do reservatório de Manso, MT, Brasil. Arq Inst Biol (Sao Paulo) 69:33–36

Garey LJ, de Courten C (1983) Structural development of the lateral geniculate nucleus and visual cortex in monkey and man. Behav Brain Res 10:3–13

Garey LJ, Vital-Durand F (1981) Recovery from monocular deprivation in the monkey. II. Reversal of morphological effects in the lateral geniculate nucleus. Proc R Soc Lond B Biol Sci 213:425–433

Gaudio E, Voltan L, De Benedictis GM (2018) Alfaxalone anaesthesia in Lemur catta following dexmedetomidine-butorphanol-midazolam sedation. Vet Anaesth Analg 45:351–356

Ghosh KK, Grünert U (1999) Synaptic input to small bistratified (blue-ON) ganglion cells in the retina of a new world monkey, the marmoset Callithrix jacchus. J Comp Neurol 413:417–428

Ghosh KK, Goodchild AK, Sefton AE, Martin PR (1996) Morphology of retinal ganglion cells in a new world monkey, the marmoset Callithrix jacchus. J Comp Neurol 366:76–92

Ghosh KK, Martin PR, Grünert U (1997) Morphological analysis of the blue cone pathway in the retina of a New World monkey, the marmoset Callithrix jacchus. J Comp Neurol 379:211–225
Glass R, Scheie HG, Yanoff M (1971) Conjunctival amyloidosis arising from a plasmacytoma. Ann Ophthalmol 3:823–825
Gochman SR, Lord MM, Goyal N, Chow K, Cooper BK, Gray LK, Guo SX, Hill KA, Liao SK, Peng S, Seong HJ, Wang A, Yoon EK, Zhang S, Lobel E, Tregubov T, Dominy NJ (2019) Tarsier goggles: a virtual reality tool for experiencing the optics of a darkadapted primate visual system. Evo Edu Outreach 12:1–8
Gomes FL, Silveira LC, Saito CA, Yamada ES (2005) Density, proportion, and dendritic coverage of retinal ganglion cells of the common marmoset (Callithrix jacchus jacchus). Braz J Med Biol Res 38: 915–924
Goodchild AK, Ghosh KK, Martin PR (1996) Comparison of photoreceptor spatial density and ganglion cell morphology in the retina of human, macaque monkey, cat, and the marmoset Callithrix jacchus. J Comp Neurol 366:55–75
Goulart V, Boubli JP, Young RJ (2017) Medium/Long wavelength sensitive opsin diversity in Pitheciidae. Sci Rep 7:7737
Gould L, Sauther M (2006) Anti-predator strategies in a diurnal prosimian, the ring-tailed lemur (Lemur catta), at the Beza Mahafaly special reserve, Madagascar. In: Gursky S, Nekaris K (eds) Primate Anti-Predator Strategies. Springer, New York, NY
Gouras P, Ivert L, Landauer N, Mattison JA, Ingram DK, Neuringer M (2008) Drusenoid maculopathy in rhesus monkeys (Macaca mulatta): effects of age and gender. Graefes Arch Clin Exp Ophthalmol 246:1395–1402
Gozalo AS, Montoya EJ, Weller RE (2008) Dyscoria associated with herpesvirus infection in owl monkeys (Aotus nancymae). J Am Assoc Lab Anim Sci 47:68–71
Graveline J, Bert J, Quere MA, Godet R, Collomb H (1966) Electroretinogram of a Lemurian: Galago senegalensis. C R Seances Soc Biol Fil 160:187–189
Gressel MG, Parrish RK 2nd, Folberg R (1984) 5-fluorouracil and glaucoma filtering surgery: I. an animal model. Ophthalmology 91: 378–383
Grünert U, Jusuf PR, Lee SC, Nguyen DT (2011) Bipolar input to melanopsin containing ganglion cells in primate retina. Vis Neurosci 28:39–50
Gursky S (1997) Modeling maternal time budgets: the impact of lactation and infant transport on the time budget of the spectral tarsier, Tarsius spectrum. State University of New York at Stony Brook
Gursky S (2000) Sociality in the spectral tarsier, Tarsius spectrum. Am J Primatol 51:89–101
Hagan MA, Rosa MG, Lui LL (2017) Neural plasticity following lesions of the primate occipital lobe: the marmoset as an animal model for studies of blindsight. Dev Neurobiol 77:314–327
Hanna KD, Pouliquen YM, Savoldelli M, Fantes F, Thompson KP, Waring GO 3rd, Samson J (1990) Corneal wound healing in monkeys 18 months after excimer laser photorefractive keratectomy. Refract Corneal Surg 6:340–345
Hanna KD, Pouliquen YM, Waring GO 3rd, Savoldelli M, Fantes F, Thompson KP (1992) Corneal wound healing in monkeys after repeated excimer laser photorefractive keratectomy. Arch Ophthalmol 110:1286–1291
Hartley C (2014) In: Hamor R (ed) lemur phaco surgery. The University of Georgia: VOPH-L
Hashemi-Nezhad M, Blessing EM, Dreher B, Martin PR (2008) Segregation of short-wavelength sensitive ("blue") cone signals among neurons in the lateral geniculate nucleus and striate cortex of marmosets. Vis Res 48:2604–2614
Hayes KC (1974) Retinal degeneration in monkeys induced by deficiencies of vitamin E or a. Investig Ophthalmol 13:499–510
Hayes KC, Stephan ZF, Sturman JA (1980) Growth depression in taurine-depleted infant monkeys. J Nutr 110:2058–2064
Hendrickson AE, Wilson JR, Ogren MP (1978) The neuroanatomical organization of pathways between the dorsal lateral geniculate nucleus and visual cortex in Old World and New World primates. J Comp Neurol 182:123–136
Hendrickson A, Djajadi HR, Nakamura L, Possin DE, Sajuthi D (2000) Nocturnal tarsier retina has both short and long/medium-wavelength cones in an unusual topography. J Comp Neurol 424:718–730
Hendrickson A, Troilo D, Possin D, Springer A (2006) Development of the neural retina and its vasculature in the marmoset Callithrix jacchus. J Comp Neurol 497:270–286
Hendrickson A, Troilo D, Djajadi H, Possin D, Springer A (2009) Expression of synaptic and phototransduction markers during photoreceptor development in the marmoset monkey Callithrix jacchus. J Comp Neurol 512:218–231
Hendrickson A, Warner CE, Possin D, Huang J, Kwan WC, Bourne JA (2015) Retrograde transneuronal degeneration in the retina and lateral geniculate nucleus of the V1-lesioned marmoset monkey. Brain Struct Funct 220:351–360
Hendrickson A, Possin D, Kwan WC, Huang J, Bourne JA (2016) The temporal profile of retinal cell genesis in the marmoset monkey. J Comp Neurol 524:1193–1207
Hendrix PK (2006) Anesthetic management of an orangutan (pongo abelii/pygmaeus) undergoing laparoscopic tubal ligation. J Zoo Wildl Med 37:531–534
Herman PH, Fox JG (1971) Panophthalmitis associated with diplococcic septicemia in a rhesus monkey. J Am Vet Med Assoc 159:560–562
Hernandez-Camacho J, Cooper RW (1976) The nonhuman primates of Colombia. In: eds, pp. 35–69. In: Thorington RW, Heltne PG (eds) Neotropical primates: Field studies and conservation. National Academy of Sciences, Washington, DC
Herrin KV, Miranda A, Loebenberg D (2005) Posaconazole therapy for systemic coccidioidomycosis in a chimpanzee (Pan troglodytes): a case report. Mycoses 48:447–452
Hertle RW, Chan CC, Galita DA, Maybodi M, Crawford MA (2002) Neuroanatomy of the extraocular muscle tendon enthesis in macaque, normal human, and patients with congenital nystagmus. J AAPOS 6:319–327
Hiraoka M, Inoue K, Kawano H, Takada M (2012) Localization of papillofoveal bundles in primates. Anat Rec (Hoboken) 295:347–354
Hirata S, Hirai H, Nogami E, Morimura N, Udono T (2017) Chimpanzee down syndrome: a case study of trisomy 22 in a captive chimpanzee. Primates 58:267–273
Hiwatashi T, Mikami A, Katsumura T, Suryobroto B, Perwitasari-Farajallah D, Malaivijitnond S, Siriaroonrat B, Oota H, Goto S, Kawamura S (2011) Gene conversion and purifying selection shape nucleotide variation in gibbon L/M opsin genes. BMC Evol Biol 11:312
Hoffman K, Videan EN, Fritz J, Murphy J (2007) Diagnosis and treatment of ocular coccidioidomycosis in a female captive chimpanzee (Pan troglodytes): a case study. Ann N Y Acad Sci 1111:404–410
Hoffmann DH, Rossmann H (1972) Ocular lesions caused by Entamoeba histolytica. Z Tropenmed Parasitol 23:241–244
Holleschau AM, Rathbun WB (1994) The effects of age on glutathione peroxidase and glutathione reductase activities in lenses of Old World simians and prosimians. Curr Eye Res 13:331–336
Honap TP, Pfister LA, Housman G, Mills S, Tarara RP, Suzuki K, Cuozzo FP, Sauther ML, Rosenberg MS, Stone AC (2018) Mycobacterium leprae genomes from naturally infected nonhuman primates. PLoS Negl Trop Dis 12:e0006190
Hood HB, Galgiani J (1985) Treatment of a male lowland gorilla for coccidioidomycosis with ketoconazole at the Phoenix zoo. In: Einstein HE, Cantanzaro A (eds) Fourth international conference on Coccidioidomycosis. National Foundation for Infectious Diseases, Washington, DC

Hoopes J, Montali RJ, Ensley PK, Bush M, Koch SA (1977) Allergic conjunctivitis in a juvenile black spider monkey. J Am Vet Med Assoc 171:870–871

Hope GM, Dawson WW, Engel HM, Ulshafer RJ, Kessler MJ, Sherwood MB (1992) A primate model for age related macular drusen. Br J Ophthalmol 76:11–16

Horiuchi T, Gass DM, David NJ (1976) Arteriovenous malformation in the retina of a monkey. Am J Ophthalmol 82:896–904

Hosaka S, Ozawa H, Tanzawa H, Kinitomo T, Nichols RL (1983) In vivo evaluation of ocular inserts of hydrogel impregnated with antibiotics for trachoma therapy. Biomaterials 4:243–248

Howard CF Jr (1974) Diabetes in Macaca nigra: metabolic and histologic changes. Diabetologia 10(Suppl):671–677

Howard CF Jr, Peterson LH (1973) Cataract development in streptozotocin-diabetic monkeys (Macaca nemestrina). Lab Anim Sci 23:366–369

Hubel DH, Wiesel TN (1968) Receptive fields and functional architecture of monkey striate cortex. J Physiol 195:215–243

Hughes A (1977) The topography of vision in mammals of contrasting life style: comparative optics and retinal organization. In: Criscitelli F (ed) Handbook of sensory physiology: the visual system in vertebrates. Springer Verlag, New York, NY

Hultsch E (1981) The vitreous of the baby owl monkey. A model for rapid and complete gel-liquefaction. Dev Ophthalmol 2:1–7

Hung CC, Yen CC, Ciuchta JL, Papoti D, Bock NA, Leopold DA, Silva AC (2015) Functional MRI of visual responses in the awake, behaving marmoset. NeuroImage 120:1–11

Huo BX, Zeater N, Lin MK, Takahashi YS, Hanada M, Nagashima J, Lee BC, Hata J, Zaheer A, Grünert U, Miller MI, Rosa MGP, Okano H, Martin PR, Mitra PP (2019) Relation of koniocellular layers of dorsal lateral geniculate to inferior pulvinar nuclei in common marmosets. Eur J Neurosci 50:4004–4017

Hyeroba D, Apell P, Goldberg T, Shafer LA, Kidega T, Asimwe C (2013) Ketamine-medetomidine regimen for chemical immobilisation of free-ranging chimpanzees (Pan troglodytes schweinfurthii) in Uganda. Vet Rec 172:475

Irvine AR (1980) Extracapsular cataract extraction and pseudophakos implantation in primates: a clinico-pathologic study. Trans Am Ophthalmol Soc 78:780–807

Irvine AR (1981) Extracapsular cataract extraction and pseudophakos implantation in primates: a clinico-pathologic study. Ophthalmic Surg 12:27–38

Ishmael J, Bradley WA (1974) Cystoid degeneration of the macula with hole formation in a baboon. J Comp Pathol 84:67–71

Ivanova E, Spiridonov S, Bain O (2007) Ocular oxyspirurosis of primates in zoos: intermediate host, worm morphology, and probable origin of the infection in the Moscow zoo. Parasite 14:287–298

Ivanova E, Hwang GS, Pan ZH, Troilo D (2010) Evaluation of AAV-mediated expression of Chop2-GFP in the marmoset retina. Invest Ophthalmol Vis Sci 51:5288–5296

Jaax GP, Graham RR, Rozmiarek H (1984) The Schirmer tear test in rhesus monkeys (Macaca mulatta). Lab Anim Sci 34:293–294

Jablonski NG, Crompton R, H. (1994) Feeding behavior, mastication, and tooth wear in the western tarsier (Tarsius bancanus). Intl J Primatol 15:29–59

Jachowski DS, Pizzaras C (2005) Introducing an innovative semi-captive environment for the Philippine tarsier (Tarsius syrichta). Zoo Biol 24:101–109

Jacobs GH, Deegan JF (1993) Photopigments underlying color vision in ringtail lemurs (lemur caffa) and Brown lemurs (Eulemur fulvus). Am J Primatol 30:243–256

Jacobs GH, Deegan JF 2nd (2003a) Cone pigment variations in four genera of new world monkeys. Vis Res 43:227–236

Jacobs GH, Deegan JF 2nd (2003b) Diurnality and cone photopigment polymorphism in strepsirrhines: examination of linkage in Lemur catta. Am J Phys Anthropol 122:66–72

Jacobs GH, Deegan JF II (2003c) Photopigment polymorphism in prosimians and the origins of primate trichromacy. In: Mollon JD, Pokorny J, Knoblauch K (eds) Normal and defective colour vision. Oxford University Press, Oxford, England

Jacobs GH, Deegan JF 2nd (2005) Polymorphic New World monkeys with more than three M/L cone types. J Opt Soc Am A Opt Image Sci Vis 22:2072–2080

Jacobs GH, Neitz J (1987) Polymorphism of the middle wavelength cone in two species of south American monkey: Cebus apella and Callicebus moloch. Vis Res 27:1263–1268

Jacobs GH, Williams GA (2006) L and M cone proportions in polymorphic New World monkeys. Vis Neurosci 23:365–370

Jacobs GH, Deegan JF 2nd, Moran JL (1996a) ERG measurements of the spectral sensitivity of common chimpanzee (Pan troglodytes). Vis Res 36:2587–2594

Jacobs GH, Neitz M, Deegan JF, Neitz J (1996b) Trichromatic colour vision in New World monkeys. Nature 382:156–158

Jacobs GH, Deegan JF 2nd, Tan Y, Li WH (2002) Opsin gene and photopigment polymorphism in a prosimian primate. Vis Res 42:11–18

Jaworski CJ (1995) A reassessment of mammalian alpha A-crystallin sequences using DNA sequencing: implications for anthropoid affinities of tarsier. J Mol Evol 41:901–908

Jayakumar J, Dreher B, Vidyasagar TR (2013) Tracking blue cone signals in the primate brain. Clin Exp Optom 96:259–266

Jester JV, Steel D, Salz J, Miyashiro J, Rife L, Schanzlin DJ, Smith RE (1981) Radial keratotomy in non-human primate eyes. Am J Ophthalmol 92:153–171

Johnson PT, Tucek P, McGowan MA (1977) Ocular fundus of the normal rhesus monkey. (typical appearance from birth through 15 years). Vet Med Small Anim Clin 72:645–648

Johnson MA, Lutty GA, McLeod DS, Otsuji T, Flower RW, Sandagar G, Alexander T, Steidl SM, Hansen BC (2005) Ocular structure and function in an aged monkey with spontaneous diabetes mellitus. Exp Eye Res 80:37–42

Johnson JA, Atkins AL, Heard DJ (2010) Application of the laryngeal mask airway for anesthesia in three chimpanzees and one gibbon. J Zoo Wildl Med 41:535–537

Johnston KD, Barker K, Schaeffer L, Schaeffer D, Everling S (2018) Methods for chair restraint and training of the common marmoset on oculomotor tasks. J Neurophysiol 119:1636–1646

Jolly A (1966) Lemur behavior: a Madagascar Field study. University of Chicago Press, Chicago, IL

Jonas JB, Hayreh SS (2000) Ophthalmoscopic appearance of the normal optic nerve head in rhesus monkeys. Invest Ophthalmol Vis Sci 41:2978–2983

Juan-Sallés C, Mainez M, Marco A, Sanchís AM (2011) Localized toxoplasmosis in a ring-tailed lemur (Lemur catta) causing placentitis, stillbirths, and disseminated fetal infection. J Vet Diagn Investig 23:1041–1045

Jusuf PR, Martin PR, Grünert U (2006a) Random wiring in the midget pathway of primate retina. J Neurosci 26:3908–3917

Jusuf PR, Martin PR, Grünert U (2006b) Synaptic connectivity in the midget-parvocellular pathway of primate central retina. J Comp Neurol 494:260–274

Jusuf PR, Lee SC, Hannibal J, Grünert U (2007) Characterization and synaptic connectivity of melanopsin-containing ganglion cells in the primate retina. Eur J Neurosci 26:2906–2921

Kaas JH, Huerta MF, Weber JT, Harting JK (1978) Patterns of retinal terminations and laminar organization of the lateral geniculate nucleus of primates. J Comp Neurol 182:517–553

Kamaraj B, Purohit R (2014) Mutational analysis of oculocutaneous albinism: a compact review. Biomed Res Int 2014:905472

Karpinski LG (1975) Chronic granuloma of the upper eyelid of a woolly monkey. Vet Med Small Anim Clin 70:950–952

Kawamura S (2016) Color vision diversity and significance in primates inferred from genetic and field studies. Genes Genomics 38:779–791
Kelley CG, Yamaguchi T, Santana E, Kaufman HE (1984) A primate model of human corneal transplantation. Invest Ophthalmol Vis Sci 25:1061–1064
Kessler MJ, Rawlins RG (1985) Congenital cataracts in a free-ranging rhesus monkey. J Med Primatol 14:225–228
Kim J, Sapp HL Jr, Plummer CE, Brooks DE, Kim D, Kim MS (2012) IOP change undergoing anesthesia in rhesus macaques (Macaca mulatta) with laser-induced ocular hypertension. J Vet Med Sci 74: 1359–1361
Kinsey VE, Jackson B (1949) Investigation of the blood-aqueous barrier in the newborn; to ascorbic acid. Am J Ophthalmol 32:374–378
Kiorpes L, Boothe RG (1981) Naturally occurring strabismus in monkeys (Macaca nemestrina). Invest Ophthalmol Vis Sci 20:257–263
Kiorpes L, Boothe RG, Carlson MR, Alfi D (1985) Frequency of naturally occurring strabismus in monkeys. J Pediatr Ophthalmol Strabismus 22:60–64
Kirk JH (1972) Persistent pupillary membrane: developmental review and an occurrence in Macaca mulatta. Lab Anim Sci 22:122–125
Kirk EC (2004) Comparative morphology of the eye in primates. Anat Rec A Discov Mol Cell Evol Biol 281:1095–1103
Kirk EC (2006) Eye morphology in cathemeral lemurids and other mammals. Folia Primatol (Basel) 77:27–49
Kirk EC, Kay RF (2004) The evolution of high visual acuity in Anthropoidea. In: Ross CF, Kay RF (eds) Anthropoid origins: new visions. Kluwer Academic/Plenum Publishers, New York
Koistinen K, Mullaney L, Bell T, Zaki S, Nalca A, Frick O, Livingston V, Robinson CG, Estep JS, Batey KL, Dick EJ Jr, Owston MA (2018) Coccidioidomycosis in nonhuman primates: pathologic and clinical findings. Vet Pathol 55:905–915
Komaromy AM, Brooks DE, Kubilis PS, Dawson WW, Sapp HL Jr, Nelson G, Collins BR, Sherwood MB (1998) Diurnal intraocular pressure curves in healthy rhesus macaques (Macaca mulatta) and rhesus macaques with normotensive and hypertensive primary open-angle glaucoma. J Glaucoma 7:128–131
König S, Hadrian K, Schlatt S, Wistuba J, Thanos S, Böhm MRR (2019) Topographic protein profiling of the age-related proteome in the retinal pigment epithelium of Callithrix jacchus with respect to macular degeneration. J Proteome 191:1–15
Kozyrev V, Silveira LC, Kremers J (2007) Linking lateral interactions in flicker perception to lateral geniculate nucleus cell responses. J Physiol 581:1083–1100
Kremers J (1998) Spatial and temporal response properties of the major retino-geniculate pathways of old and New World monkeys. Doc Ophthalmol 95:229–245
Kremers J, Lee BB (1998) Comparative retinal physiology in anthropoids. Vis Res 38:3339–3344
Kuhlman SM, Rubin LF, Ridgeway RL (1992) Prevalence of ophthalmic lesions in wild-caught cynomolgus monkeys. Prog Vet Comp Ophthalmol 2:20–28
Kühnel W (1968) Vergleichende histologische, histochemische und elektronenmikroskopische Untersuchungen an Tränendrüsen. Z Zellforsch Mikrosk Anat 89:550–572
Kumar V, Sankhyan V (2015) Medicinal management of corneal opacity in free ranging rhesus macaques (Macaca mulatta) of Shivalik hills in Western Himalayas, northern India. Open Vet J 5:56–57
Land MF (2006) Visual optics: the shapes of pupils. Curr Biol 16:R167–R168
Landon JC, Bennett DG (1969) Viral induced simian conjunctivitis. Nature 222
Langan GP, Harvey RC, O'Rourke D, Fontenot MB, Schumacher J (2000) Cardiopulmonary effects of sevoflurane in Garnett's greater bush baby (Otolemur garnettii). Comp Med 50:639–643
Lange RR (2012) Anatomy, morphology and eye physiology of some species of interest in wild animals and laboratory medicine with emphasis on neotropical primates. Federal University of Paraná
Lange RR, Lima L, Montiani-Ferreira F (2012) Measurement of tear production in black-tufted marmosets (Callithrix penicillata) using three different methods: modified Schirmer's I, phenol red thread and standardized endodontic absorbent paper points. Vet Ophthalmol 15: 376–382
Larsen RS, Moresco A, Sauther ML, Cuozzo FP (2011) Field anesthesia of wild ring-tailed lemurs (Lemur catta) using tiletamine-zolazepam, medetomidine, and butorphanol. J Zoo Wildl Med 42:75–87
Last JA, Pan T, Ding Y, Reilly CM, Keller K, Acott TS, Fautsch MP, Murphy CJ, Russell P (2011) Elastic modulus determination of normal and glaucomatous human trabecular meshwork. Invest Ophthalmol Vis Sci 52:2147–2152
Lee SC, Grünert U (2007) Connections of diffuse bipolar cells in primate retina are biased against S-cones. J Comp Neurol 502:126–140
Lee W, Mammen A, Dhaliwal DK, Long C, Miyagawa Y, Ayares D, Cooper DK, Hara H (2017) Development of retrocorneal membrane following pig-to-monkey penetrating keratoplasty. Xenotransplantation 24
Leiva M, Pena T, Bayon A, de Leon M, Morales I (2012) Phacoemulsification considerations in nonhuman primates. J Med Primatol 41: 317–324
Li C, Xu JT, Kong FS, Li JL (1992) Experimental studies on penetrating heterokeratoplasty with human corneal grafts in monkey eyes. Cornea 11:66–72
Liang D, Alvarado TP, Oral D, Vargas JM, Denena MM, McCulley JP (2005) Ophthalmic examination of the captive western lowland gorilla (Gorilla gorilla gorilla). J Zoo Wildl Med 36:430–433
Lima SM, Silveira LC, Perry VH (1993) The M-ganglion cell density gradient in New World monkeys. Braz J Med Biol Res 26:961–964
Lima RR, Pinato L, Nascimento RB, Engelberth RC, Nascimento ES, Cavalcante JC, Britto LR, Costa MS, Cavalcante JS (2012) Retinal projections and neurochemical characterization of the pregeniculate nucleus of the common marmoset (Callithrix jacchus). J Chem Neuroanat 44:34–44
de Lima EM, Pessoa DM, Sena L, de Melo AG, de Castro PH, Oliveira-Mendes AC, Schneider MP, Pessoa VF (2015) Polymorphic color vision in captive Uta Hick's cuxius, or bearded sakis (Chiropotes utahickae). Am J Primatol 77:66–75
Lu Q, Ganjawala TH, Ivanova E, Cheng JG, Troilo D, Pan ZH (2016) AAV-mediated transduction and targeting of retinal bipolar cells with improved mGluR6 promoters in rodents and primates. Gene Ther 23:680–689
Luebcke E, Dubovi E, Black D, Ohsawa K, Eberle R (2006) Isolation and characterization of a chimpanzee alphaherpesvirus. J Gen Virol 87:11–19
Luo X, Ghosh KK, Martin PR, Grünert U (1999) Analysis of two types of cone bipolar cells in the retina of a New World monkey, the marmoset, Callithrix jacchus. Vis Neurosci 16:707–719
Macedonia J (1990) What is communicated in the anti-predator calls of lemurs: evidence from playback experiments with ring-tailed and ruffed lemurs. Ethology 86:177–190
Macedonia J (1993) The vocal repertoire of the ringtailed lemur (Lemur catta). Folia Primatol 61:186–217
Macy JD Jr, Huether MJ, Beattie TA, Findlay HA, Zeiss C (2001) Latex sensitivity in a macaque (Macaca mulatta). Comp Med 51:467–472
Malaty R, Meyers WM, Walsh GP, Binford CH, Zimmerman LE, Baskin GB, Gormus BJ, Martin LN, Wolf RH (1988) Histopathological changes in the eyes of mangabey monkeys with lepromatous leprosy. Int J Lepr Other Mycobact Dis 56:443–448
Malinow MR, Corcoran A (1966) Growth of the lens in howler monkeys (Alouatta caraya). J Mammal 47:58–63

Marshall J, Trokel SL, Rothery S, Krueger RR (1988) Long-term healing of the central cornea after photorefractive keratectomy using an excimer laser. Ophthalmology 95:1411–1421

Martin PR, Grunert U (1999) Analysis of the short wavelength-sensitive ("blue") cone mosaic in the primate retina: comparison of New World and Old World monkeys. J Comp Neurol 406:1–14

Martin PR, Lee BB (2014) Distribution and specificity of S-cone ("blue cone") signals in subcortical visual pathways. Vis Neurosci 31:177–187

Martin JE, Kroe DJ, Bostrom RE, Johnson DJ, Whitney RA Jr (1969) Rhino-orbital phycomycosis in a rhesus monkey (Macaca mulatta). J Am Vet Med Assoc 155:1253–1257

Martin PR, White AJ, Goodchild AK, Wilder HD, Sefton AE (1997) Evidence that blue-on cells are part of the third geniculocortical pathway in primates. Eur J Neurosci 9:1536–1541

Martin PR, Blessing EM, Buzás P, Szmajda BA, Forte JD (2011) Transmission of colour and acuity signals by parvocellular cells in marmoset monkeys. J Physiol 589:2795–2812

Marzke M, Hawkey D, Fritz J (1988) Coccidioidomycosis in the chimpanzee. Am J Primatol 14:432

Masri RA, Percival KA, Koizumi A, Martin PR, Grünert U (2016) Connectivity between the OFF bipolar type DB3a and six types of ganglion cell in the marmoset retina. J Comp Neurol 524:1839–1858

Masuda T, Shimazawa M, Takata S, Nakamura S, Tsuruma K, Hara H (2016) Edaravone is a free radical scavenger that protects against laser-induced choroidal neovascularization in mice and common marmosets. Exp Eye Res 146:196–205

Mätz-Rensing K, Winkelmann J, Becker T, Burckhardt I, van der Linden M, Köndgen S, Leendertz F, Kaup FJ (2009) Outbreak of Streptococcus equi subsp. zooepidemicus infection in a group of rhesus monkeys (Macaca mulatta). J Med Primatol 38:328–334

McConnell EE, Basson PA, de Vos V, Myers BJ, Kuntz RE (1974) A survey of diseases among 100 free-ranging baboons (Papio ursinus) from the Kruger national park. Onderstepoort J Vet Res 41:97–167

McLoughlin N, Schiessl I (2006) Orientation selectivity in the common marmoset (Callithrix jacchus): the periodicity of orientation columns in V1 and V2. NeuroImage 31:76–85

Melles GR, Binder PS, Anderson JA (1994) Variation in healing throughout the depth of long-term, unsutured, corneal wounds in human autopsy specimens and monkeys. Arch Ophthalmol 112: 100–109

Melles GR, Binder PS, Beekhuis WH, Wijdh RH, Moore MN, Anderson JA, SundarRaj N (1995a) Scar tissue orientation in unsutured and sutured corneal wound healing. Br J Ophthalmol 79: 760–765

Melles GR, Binder PS, Beekhuis WH, Wijdh RH, Rietveld FJ (1995b) Healing of reopened-and-sutured radial keratotomy wounds. J Cataract Refract Surg 21:620–626

Merlin T, Veres-Nyeki K (2017) The use of atracurium in an anaesthetized ring-tailed lemur (Lemur catta). Vet Anaesth Analg 44:1403–1405

Meyer WK, Zhang S, Hayakawa S, Imai H, Przeworski M (2013) The convergent evolution of blue iris pigmentation in primates took distinct molecular paths. Am J Phys Anthropol 151:398–407

Meyer WK, Venkat A, Kermany AR, van de Geijn B, Zhang S, Przeworski M (2015) Evolutionary history inferred from the de novo assembly of a nonmodel organism, the blue-eyed black lemur. Mol Ecol 24:4392–4405

Miller PE, Bentley E (2015) Clinical signs and diagnosis of the canine primary Glaucomas. Vet Clin North Am Small Anim Pract 45:1183–1212, vi

Mitchell JF, Leopold DA (2015) The marmoset monkey as a model for visual neuroscience. Neurosci Res 93:20–46

Mitchell JF, Reynolds JH, Miller CT (2014) Active vision in marmosets: a model system for visual neuroscience. J Neurosci 34:1183–1194

Mitchell JF, Priebe NJ, Miller CT (2015) Motion dependence of smooth pursuit eye movements in the marmoset. J Neurophysiol 113:3954–3960

Mittermeier RA (2013) Introduction. In: Mittermeier RA, Rylands AB, Wilson DE (eds) Handbook of the mammals of the world. Lynx Edicions, Barcelona, Spain

Monaco WA, Wormington CM (1990) The rhesus monkey as an animal model for age-related maculopathy. Optom Vis Sci 67:532–537

Montiani-Ferreira F, Shaw G, Mattos BC, Russ HH, Vilani RG (2008) Reference values for selected ophthalmic diagnostic tests of the capuchin monkey (Cebus apella). Vet Ophthalmol 11:197–201

Montiani-Ferreira F, Lima L, Bacellar M, D'Otaviano Vilani RG, Fedullo JD, Lange RR (2010) Bilateral phacoemulsification in an orangutan (Pongo pygmaeus). Vet Ophthalmol 13(Suppl):91–99

Morcos Y, Chan-Ling T (2000) Concentration of astrocytic filaments at the retinal optic nerve junction is coincident with the absence of intra-retinal myelination: comparative and developmental evidence. J Neurocytol 29:665–678

Morita H, Shimomura K (1996) Specular microscopy of the corneal endothelial cells in common marmosets. J Vet Med Sci 58:277–279

Moritz GL, Melin AD, Yu FTY, Bernard H, Ong PS, Dominy NJ (2014) Niche convergence suggests functionality of the nocturnal fovea. Front Integr Neurosci 8:61

Moritz GL, Ong PS, Perry GH, Dominy NJ (2017) Functional preservation and variation in the cone opsin genes of nocturnal tarsiers. Philos Trans R Soc Lond Ser B Biol Sci 372:1–10

Morrison JC, Cork LC, Dunkelberger GR, Brown A, Quigley HA (1990) Aging changes of the rhesus monkey optic nerve. Invest Ophthalmol Vis Sci 31:1623–1627

Moshiri A, Chen R, Kim S, Harris RA, Li Y, Raveendran M, Davis S, Liang Q, Pomerantz O, Wang J, Garzel L, Cameron A, Yiu G, Stout JT, Huang Y, Murphy CJ, Roberts J, Gopalakrishna KN, Boyd K, Artemyev NO, Rogers J, Thomasy SM (2019) A nonhuman primate model of inherited retinal disease. J Clin Invest 129:863–874

Mukai N, Lee PF, Oguri M, Schepens CL (1975) A long-term evaluation of silicone retinopathy in monkeys. Can J Ophthalmol 10:391–402

Mukai N, Kalter SS, Cummins LB, Matthews VA, Nishida T, Nakajima T (1980) Retinal tumor induced in the baboon by human adenovirus 12. Science 210:1023–1025

Munday JS, Rodriguez NA, Thomas DA (2004) Lacrimal gland myoepithelioma in a rhesus macaque (Macaca mulatta). Comp Med 54:443–446

Muniz JA, de Athaide LM, Gomes BD, Finlay BL, Silveira LC (2014) Ganglion cell and displaced amacrine cell density distribution in the retina of the howler monkey (Alouatta caraya). PLoS One 9:e115291

Narasimhan A, Tychsen L, Poukens V, Demer JL (2007) Horizontal rectus muscle anatomy in naturally and artificially strabismic monkeys. Invest Ophthalmol Vis Sci 48:2576–2588

Nathans J, Thomas D, Hogness DS (1986) Molecular genetics of human color vision: the genes encoding blue, green, and red pigments. Science 232:193–202

Neuringer M, Kosobud A, Cochrane G (1981) Visual acuity of Lemur catta, a diurnal prosimian. Invest Ophthalmol Vis Sci 20:49

Nickla DL, Wildsoet CF, Troilo D (2002) Diurnal rhythms in intraocular pressure, axial length, and choroidal thickness in a primate model of eye growth, the common marmoset. Invest Ophthalmol Vis Sci 43: 2519–2528

Niemitz C (1973) Tarsius bancanus (Horsfields tarsier) preying on snakes. Lab Prim News 12:18–19

Niemuth JN, De Voe RS, Jennings SH, Loomis MR, Troan BV (2014) Malignant hypertension and retinopathy in a western lowland gorilla (Gorilla gorilla gorilla). J Med Primatol 43:276–279

Noro T, Namekata K, Kimura A, Azuchi Y, Hashimoto N, Moriya-Ito K, Komaki Y, Lee CY, Okahara N, Guo X, Harada C, Kim E, Nakano T, Tsuneoka H, Inoue T, Sasaki E, Tokuno H, Harada T

(2019) Normal tension glaucoma-like degeneration of the visual system in aged marmosets. Sci Rep 9:14852
Nowak LG, Barone P (2009) Contrast adaptation contributes to contrast-invariance of orientation tuning of primate V1 cells. PLoS One 4: e4781
Olin KL, Morse LS, Murphy C, Paul-Murphy J, Line S, Bellhorn RW, Hjelmeland LM, Keen CL (1995) Trace element status and free radical defense in elderly rhesus macaques (Macaca mulatta) with macular drusen. Proc Soc Exp Biol Med 208:370–377
Oliveira FN, Porter BF, Dick EJ Jr, Hubbard GB (2011) Intracranial meningioma in a baboon (Papio spp.). J Comp Pathol 145:414–418
Ollivier FJ, Brooks DE, Kallberg ME, Sapp HL, Komáromy AM, Stevens GR, Dawson WW, Sherwood MB, Lambrou GN (2004a) Time-specific intraocular pressure curves in rhesus macaques (Macaca mulatta) with laser-induced ocular hypertension. Vet Ophthalmol 7:23–27
Ollivier FJ, Samuelson DA, Brooks DE, Lewis PA, Kallberg ME, Komaromy AM (2004b) Comparative morphology of the tapetum lucidum (among selected species). Vet Ophthalmol 7:11–22
Oria AP, Pinna MH, Almeida DS, da Silva RM, Pinheiro AC, Santana FO, Costa TR, Meneses ID, Martins Filho EF, Oliveira AV (2013a) Conjunctival flora, Schirmer's tear test, intraocular pressure, and conjunctival cytology in neotropical primates from Salvador, Brazil. J Med Primatol 42:287–292
Oria AP, Pinna MH, Estrela-Lima A, Junior DG, Liborio FA, de Assis Dorea F, Neto AV, Oliveira MN, Requiao K (2013b) Exophthalmos due to odontogenic intraorbital abscess in Cebus apella. J Med Primatol 42:101–104
Palmer SM, Rosa MG (2006) A distinct anatomical network of cortical areas for analysis of motion in far peripheral vision. Eur J Neurosci 24:2389–2405
Paterson CA, Pfister RR (1973) Ocular hypertensive response to alkali burns in the monkey. Exp Eye Res 17:449–453
Peichl L, Kaiser A, Rakotondraparany F, Dubielzig RR, Goodman SM, Kappeler PM (2019) Diversity of photoreceptor arrangements in nocturnal, cathemeral and diurnal Malagasy lemurs. J Comp Neurol 527:13–37
Peiffer RL, Gelatt KN (1976) Cataract in a wooly monkey. Mod Vet Pract 57:609–610
Peiffer RL, Jacobson ER (1978) Cataract resorption in a spider monkey. J Am Vet Med Assoc 173:1234–1235
Peiffer RL Jr, Johnson PT, Wilkerson BJ (1980) Peripalpebral folds and entropion in a male crab-eating macaque (Macaca fascicularis). Lab Anim Sci 30:113–115
Percival KA, Jusuf PR, Martin PR, Grünert U (2009) Synaptic inputs onto small bistratified (blue-ON/yellow-OFF) ganglion cells in marmoset retina. J Comp Neurol 517:655–669
Percival KA, Martin PR, Grünert U (2011) Synaptic inputs to two types of koniocellular pathway ganglion cells in marmoset retina. J Comp Neurol 519:2135–2153
Percival KA, Martin PR, Grünert U (2013) Organisation of koniocellular-projecting ganglion cells and diffuse bipolar cells in the primate fovea. Eur J Neurosci 37:1072–1089
Peterson JA, Kiland JA, Croft MA, Kaufman PL (1996) Intraocular pressure measurement in cynomolgus monkeys. Tono-pen versus manometry. Invest Ophthalmol Vis Sci 37:1197–1199
Peterson SM, McGill TJ, Puthussery T, Stoddard J, Renner L, Lewis AD, Colgin LMA, Gayet J, Wang X, Prongay K, Cullin C, Dozier BL, Ferguson B, Neuringer M (2019) Bardet-Biedl syndrome in rhesus macaques: a nonhuman primate model of retinitis pigmentosa. Exp Eye Res 189:107825
Piper C, Fortune B, Cull G, Cioffi GA, Wang L (2013) Basal blood flow and autoregulation changes in the optic nerve of rhesus monkeys with idiopathic bilateral optic atrophy. Invest Ophthalmol Vis Sci 54:714–721
Pirie A (1959) Crystals of riboflavin making up the tapetum lucidum in the eye of a lemur. Nature 183:985–986
Plesker R, Hetzel U, Schmidt W (2005) Cataracts in a laboratory colony of African green monkeys (Chlorocebus aethiops). J Med Primatol 34:139–146
Polyak S (1957) The vertebrate visual system. University of Chicago Press, Chicago
Potter DE, Burke JA (1982) Effects of ergoline derivatives on intraocular pressure and iris function in rabbits and monkeys. Curr Eye Res 2:281–288
Poux C, Douzery EJ (2004) Primate phylogeny, evolutionary rate variations, and divergence times: a contribution from the nuclear gene IRBP. Am J Phys Anthropol 124:1–16
Prado-Martinez J, Hernando-Herraez I, Lorente-Galdos B, Dabad M, Ramirez O, Baeza-Delgado C, Morcillo-Suarez C, Alkan C, Hormozdiari F, Raineri E, Estelle J, Fernandez-Callejo M, Valles M, Ritscher L, Schoneberg T, de la Calle-Mustienes E, Casillas S, Rubio-Acero R, Mele M, Engelken J, Caceres M, Gomez-Skarmeta JL, Gut M, Bertranpetit J, Gut IG, Abello T, Eichler EE, Mingarro I, Lalueza-Fox C, Navarro A, Marques-Bonet T (2013) The genome sequencing of an albino Western lowland gorilla reveals inbreeding in the wild. BMC Genomics 14: 363
Prince JH (1956) Crystalline Lens. In: Prince JH (ed) Comparative anatomy of the eye. Thomas, Springfield, IL
Pugsley SL (1985) Congenital malformations in a common marmoset (Callithrix jacchus) similar to human 13-trisomy syndrome. Lab Anim 19:123–124
Puller C, Haverkamp S, Grünert U (2007) OFF midget bipolar cells in the retina of the marmoset, Callithrix jacchus, express AMPA receptors. J Comp Neurol 502:442–454
Pulley AC, Roberts JA, Lerche NW (2004) Four preanesthetic oral sedation protocols for rhesus macaques (Macaca mulatta). J Zoo Wildl Med 35:497–502
Qi Y, Lian J, Wang K, Wang Y (1999) The immunohistochemical changes of TGF-beta, type I and III collagen in corneal healing after photorefractive keratectomy. Zhonghua Yan Ke Za Zhi 35(274–6):15
Qin Y, Tan X, Zhang Y, Jie Y, Labbe A, Pan Z (2014) A new nonhuman primate model of severe dry eye. Cornea 33:510–517
Qin Y, Zhang Y, Liang Q, Xu X, Li Q, Pan Z, Labbé A (2018) Labial salivary gland transplantation for severe dry eye in a rhesus monkey model. Invest Ophthalmol Vis Sci 59:2478–2486
Quigley HA (1976) Histological and physiological studies of cyclocryotherapy in primate and human eyes. Am J Ophthalmol 82:722–732
Rada JA, Nickla DL, Troilo D (2000) Decreased proteoglycan synthesis associated with form deprivation myopia in mature primate eyes. Invest Ophthalmol Vis Sci 41:2050–2058
Ragazzo LJ, Zohdy S, Velonabison M, Herrera J, Wright PC, Gillespie TR (2018) Entamoeba histolytica infection in wild lemurs associated with proximity to humans. Vet Parasitol 249:98–101
Ramsier MA, Cunningham AJ, Moritz GL, Finneran JJ, Williams CV, Ong PS, Gursky-Doyen SL, Dominy NJ (2012) Primate communication in the pure ultrasound. Biol Lett 8:508–511
Rasmussen CA, Kaufman PL (2005) Primate glaucoma models. J Glaucoma 14:311–314
Rathbun WB, Holleschau AM (1992) The effects of age on glutathione synthesis enzymes in lenses of Old World simians and prosimians. Curr Eye Res 11:601–607
Reed RE, Bicknell EJ, Hood HB (1985) A thirty-year record of coccidioidomycosis in exotic pets and zoo animals in Arizona. In: Einstein HE, Cantanzaro A (eds) 4th international conference on Coccidioidomycosis. National Foundation for Infectious Diseases, Washington, DC

Regan BC, Julliot C, Simmen B, Vienot F, Charles-Dominique P, Mollon JD (1998) Frugivory and colour vision in Alouatta seniculus, a trichromatic platyrrhine monkey. Vis Res 38:3321–3327
Renoult JP, Schaefer HM, Sallé B, Charpentier MJ (2011) The evolution of the multicoloured face of mandrills: insights from the perceptual space of colour vision. PLoS One 6:e29117
Repka MX, Tusa RJ (1995) Refractive error and axial length in a primate model of strabismus and congenital nystagmus. Invest Ophthalmol Vis Sci 36:2672–2677
Ribic A, Flügge G, Schlumbohm C, Mätz-Rensing K, Walter L, Fuchs E (2011) Activity-dependent regulation of MHC class I expression in the developing primary visual cortex of the common marmoset monkey. Behav Brain Funct 7:1
Ribka EP, Dubielzig RR (2008) Multiple ophthalmic abnormalities in an infant rhesus macaque (Macaca mulatta). J Med Primatol 37(Suppl 1):16–19
Richter CB, Buyukmihci N (1979) Squamous cell carcinoma of the epidermis in an aged white-lipped tamarin (Saguinus fuscicollis leucogenys Gray). Vet Pathol 16:263–265
Ringvold A (1980) Aqueous humour and ultraviolet radiation. Acta Ophthalmol 58:69–82
Roberts M, Kohn F (1993) Habitat use, foraging behavior, and activity patterns in reproducing western tarsier, Tarsius bancanus, in captivity: a management synthesis. Zoo Biol 12:217–232
Rodenbiker HT, Ganley JP (1980) Ocular coccidioidomycosis. Surv Ophthalmol 24:263–290
Rodger FC, Grover AD, Fazal A (1961) Experimental Hemeralopia uncomplicated by Xerophthalmia in Macacus rhesus. Br J Ophthalmol 45:96–108
Roe AW, Fritsches K, Pettigrew JD (2005) Optical imaging of functional organization of V1 and V2 in marmoset visual cortex. Anat Rec A Discov Mol Cell Evol Biol 287:1213–1225
Rosa MG, Gattass R, Soares JG (1991) A quantitative analysis of cytochrome oxidase-rich patches in the primary visual cortex of Cebus monkeys: topographic distribution and effects of late monocular enucleation. Exp Brain Res 84:195–209
Rosa MG, Gattass R, Fiorani M Jr, Soares JG (1992) Laminar, columnar and topographic aspects of ocular dominance in the primary visual cortex of Cebus monkeys. Exp Brain Res 88:249–264
Rose KD (2006) The beginning of the age of mammals. Johns Hopkins University Press, Baltimore, MD
Rosenberg DP, Blouin P (1979) Retrobulbar abscess in an infant rhesus monkey. J Am Vet Med Assoc 175:994–996
Rosenberger AL, Smith TD, DeLeon VB, Burrows AM, Schenck R, Halenar LB (2016) Eye size and set in small-bodied fossil primates: a three-dimensional method. Anat Rec (Hoboken) 299:1671–1689
Ross CF (2000) Into the light: the origin of Anthropoidea. Annu Rev Anthropol 29:147–194
Ross CF (2004) The tarsier fovea: functionless vestige on nocturnal adaptation? In: Ross CF, Kay RF (eds) Anthropoid origins: new visions. Kluwer Academic, New York
Ross CF, Kirk EC (2007) Evolution of eye size and shape in primates. J Hum Evol 52:294–313
Rosser MF, Lindemann DM, Barger AM, Allender MC, Hsiao SH, Howes ME (2016) Systemic Blastomycosis in a captive red ruffed lemur (Varecia Rubra). J Zoo Wildl Med 47:912–916
Roy S, Jayakumar J, Martin PR, Dreher B, Saalmann YB, Hu D, Vidyasagar TR (2009) Segregation of short-wavelength-sensitive (S) cone signals in the macaque dorsal lateral geniculate nucleus. Eur J Neurosci 30:1517–1526
Rozenbaum I, Faschinger C, Ritch R (2008) Small primate, big eyes. Arch Ophthalmol 126:542
Ruskell GL (1968) The fine structure of nerve terminations in the lacrimal glands of monkeys. J Anat 103:65–76
Ryu H, Graham KE, Sakamaki T, Furuichi T (2016) Long-sightedness in old wild bonobos during grooming. Curr Biol 26:R1131–R1R32
Sandell JH, Peters A (2001) Effects of age on nerve fibers in the rhesus monkey optic nerve. J Comp Neurol 429:541–553
Santana SE, Lynch Alfaro J, Alfaro ME (2012) Adaptive evolution of facial colour patterns in Neotropical primates. Proc Biol Sci 279: 2204–2211
Sasaki Y, Kodama R, Iwashige S, Fujishima J, Yoshikawa T, Kamimura Y, Maeda H (2011) Bilateral cataract in a cynomolgus monkey. J Toxicol Pathol 24:69–73
Sauther M (1989) Antipredator behavior in troops of free-ranging Lemur catta at Beza Mahafaly special reserve, Madagascar. Intl J Primatol 10:595–606
Schmidt RE (1971a) Colobomas in non-human primates. Folia Primatol (Basel) 14:256–262
Schmidt RE (1971b) Ophthalmic lesions in non-human primates. Vet Pathol 8:28–36
Schmittbuhl M, Le Minor JM, Allenbach B, Schaaf A (1999) Shape of the orbital opening: individual characterization and analysis of variability in modern humans, Gorilla gorilla, and Pan troglodytes. Ann Anat 181:299–307
Schuler AM, Tustin GT, Abee CR, Scammell JG (2009) Restasis for the treatment of 'dry eye' in Aotus nancymaae. J Med Primatol 38:318–320
Schultz AH (1969) The life of primates. Weidenfels and Nicholson, London
Schwab IR (2012) The age of mammals. In: Schwab IR (ed) Evolution's witness: how eyes evolved. Oxford University Press, New York, NY
Schwitzwer C, Mittermeier RA, Louis EE, Richardson MC (2013) Family Daubentoniidae (Aye-Aye). In: Mittermeier RA, Rylands AB, Wilson DE (eds) Handbook of the mammals of the world. Lynx Edicions, Barcelona, Spain
Scott BL, Pease DC (1959) Electron microscopy of the salivary and lacrimal glands of the rat. Am J Anat 104:115–161
Semba RD, Donnelly JJ, Young E, Green WR, Scott AL, Taylor HR (1991) Experimental ocular onchocerciasis in cynomolgus monkeys. IV. Chorioretinitis elicited by Onchocerca volvulus microfilariae. Invest Ophthalmol Vis Sci 32:1499–1507
Sengpiel F, Troilo D, Kind PC, Graham B, Blakemore C (1996) Functional architecture of area 17 in normal and monocularly deprived marmosets (Callithrix jacchus). Vis Neurosci 13:145–160
Shekelle M, Gurskey-Doyen S, Richardson MC (2013) Family Tarsiidae (tarsiers). In: Mittermeier RA, Rylands AB, Wilson DE (eds) Handbook of the mammals of the world. Lynx Edicions, Barcelona, Spain
Shelton L, Troilo D, Lerner MR, Gusev Y, Brackett DJ, Rada JS (2008) Microarray analysis of choroid/RPE gene expression in marmoset eyes undergoing changes in ocular growth and refraction. Mol Vis 14:1465–1479
Shimazawa M, Nakamura S, Miwa M, Tsuruma K, Aihara M, Nakamura K, Hara H (2013) Establishment of the ocular hypertension model using the common marmoset. Exp Eye Res 111:1–8
Silva DN, Oria AP, Araujo NL, Martins-Filho E, Muramoto C, Liborio FA, Estrela-Lima A (2017) Morphological study of the eye and adnexa in capuchin monkeys (Sapajus sp.). PLoS One 12:e0186569
Silveira LC, Lee BB, Yamada ES, Kremers J, Hunt DM, Martin PR, Gomes FL (1999) Ganglion cells of a short-wavelength-sensitive cone pathway in New World monkeys: morphology and physiology. Vis Neurosci 16:333–343
Silveira LC, Saito CA, Lee BB, Kremers J, da Silva Filho M, Kilavik BE, Yamada ES, Perry VH (2004) Morphology and physiology of primate M- and P-cells. Prog Brain Res 144:21–46
Skuta GL, Assil K, Parrish RK 2nd, Folberg R, Weinreb RN (1987) Filtering surgery in owl monkeys treated with the antimetabolite 5-fluorouridine 5′-monophosphate entrapped in multivesicular liposomes. Am J Ophthalmol 103:714–716
Sleeman JM, Cameron K, Mudakikwa AB, Nizeyi JB, Anderson S, Cooper JE, Richardson HM, Macfie EJ, Hastings B, Foster JW

(2000) Field anesthesia of free-living mountain gorillas (Gorilla gorilla beringei) from the Virunga volcano region, Central Africa. J Zoo Wildl Med 31:9–14

Smith JL, Reynolds DH, Rane L, Justice J Jr (1964) The fundus oculi in the squirrel, owl, and marmoset monkey. Am J Ophthalmol 57:431–435

Smith TD, Deleon VB, Rosenberger AL (2013) At birth, tarsiers lack a postorbital bar or septum. Anat Rec (Hoboken) 296:365–377

Solomon SG, Rosa MG (2014) A simpler primate brain: the visual system of the marmoset monkey. Front Neural Circuits 8:96

Sonneveld P, Peperkamp E, van Bekkum DW (1979) Incidence of cataracts in rhesus monkeys treated with whole-body irradiation. Radiology 133:227–229

Souri E (1973) Eye diseases in two families of animals. Vet Med Small Anim Clin 68:1011–1014

de Sousa TB, de Santana MA, Silva Ade M, Guzen FP, Oliveira FG, Cavalcante JC, Cavalcante Jde S, Costa MS, Nascimento ES Jr (2013) Mediodorsal thalamic nucleus receives a direct retinal input in marmoset monkey (Callithrix jacchus): a subunit B cholera toxin study. Ann Anat 195:32–38

Spatz WB (1978) The retino-geniculo-cortical pathway in Callithrix. I. Intraspecific variations in the lamination pattern of the lateral geniculate nucleus. Exp Brain Res 33:551–563

Spatz WB (1979) The retino-geniculo-cortical pathway in Callithrix. II. The geniculo-cortical projection. Exp Brain Res 36:401–410

Spencer JA, Joiner KS, Hilton CD, Dubey JP, Toivio-Kinnucan M, Minc JK, Blagburn BL (2004) Disseminated toxoplasmosis in a captive ring-tailed lemur (Lemur catta). J Parasitol 90:904–906

Springer AD, Troilo D, Possin D, Hendrickson AE (2011) Foveal cone density shows a rapid postnatal maturation in the marmoset monkey. Vis Neurosci 28:473–484

Springer A, Razafimanantsoa L, Fichtel C, Kappeler PM (2015) Comparison of three short-term immobilization regimes in wild Verreaux's Sifakas (Propithecus Verreauxi): ketamine-Xylazine, ketamine-Xylazine-atropine, and Tiletamine-Zolazepam. J Zoo Wildl Med 46:482–490

Stafford TJ, Anness SH, Fine BS (1984) Spontaneous degenerative maculopathy in the monkey. Ophthalmology 91:513–521

Steel D, Jester JV, Salz J, Villasenor RA, Lee JS, Schanzlin DJ, Smith RE (1981) Modification of corneal curvature following radial keratotomy in primates. Ophthalmology 88:747–754

Steinmetz A, Bernhard A, Sahr S, Oechtering G (2012) Suspected macular degeneration in a captive Western lowland gorilla (Gorilla gorilla gorilla). Vet Ophthalmol 15(Suppl 2):139–141

Strong V, Moller T, Tillman AS, Traff S, Guevara L, Martin M, Redrobe S, White K (2018) A clinical study to evaluate the cardiopulmonary characteristics of two different anaesthetic protocols for immobilization of healthy chimpanzees (Pan troglodytes). Vet Anaesth Analg 45:794–801

Stuck BE, Talsma DM, Beatrice ES (1977) Vitreal syneresis in rhesus monkeys. Invest Ophthalmol Vis Sci 16:1068–1070

Sturm RA, Duffy DL, Zhao ZZ, Leite FP, Stark MS, Hayward NK, Martin NG, Montgomery GW (2008) A single SNP in an evolutionary conserved region within intron 86 of the HERC2 gene determines human blue-brown eye color. Am J Hum Genet 82:424–431

Sugrue MF (1996) The preclinical pharmacology of dorzolamide hydrochloride, a topical carbonic anhydrase inhibitor. J Ocul Pharmacol Ther 12:363–376

Sulem P, Gudbjartsson DF, Stacey SN, Helgason A, Rafnar T, Magnusson KP, Manolescu A, Karason A, Palsson A, Thorleifsson G, Jakobsdottir M, Steinberg S, Palsson S, Jonasson F, Sigurgeirsson B, Thorisdottir K, Ragnarsson R, Benediktsdottir KR, Aben KK, Kiemeney LA, Olafsson JH, Gulcher J, Kong A, Thorsteinsdottir U, Stefansson K (2007) Genetic determinants of hair, eye and skin pigmentation in Europeans. Nat Genet 39:1443–1452

Sumner P, Mollon JD (2000) Catarrhine photopigments are optimized for detecting targets against a foliage background. J Exp Biol 203:1963–1986

Suzuki MT, Cho F (1984) Characteristic findings of the ocular fundus in colony-born cynomolgus monkeys aged from 0 day to 19 years. Anim Eye Res 3:13–16

Suzuki MT, Narita H, Tanaka Y, Cho F, Fukui M (1984) Ophthalmoscopic observations of ocular fundus in colony-born cynomolgus monkeys aged from 0 day to 90 days. Jikken Dobutsu 33:173–180

Suzuki MT, Narita H, Cho F, Fukui M, Honjo S (1985a) Abnormal findings in the ocular fundi of colony-born cynomolgus monkeys. Jikken Dobutsu 34:131–140

Suzuki MT, Narita H, Fukui M (1985b) Persistent pupillary membranes in a cynomolgus monkey. Jikken Dobutsu 34:81–84

Suzuki MT, Narita H, Hanari K, Fukui M, Cho F, Honjo S (1986) Congenital cataract in a cynomolgus monkey. Jikken Dobutsu 35:193–197

Suzuki MT, Ogawa H, Cho F, Honjo S (1990) Visual function of cynomolgus monkeys with macula degeneration and peripheral retinal degeneration. Jikken Dobutsu 39:571–575

Svensson MS, Nekaris KAI, Bearder SK, Bettridge CM, Butynski TM, Cheyne SM, Das N, de Jong YA, Luhrs AM, Luncz LV, Maddock ST, Perkin A, Pimley E, Poindexter SA, Reinhardt KD, Spaan D, Stark DJ, Starr CR, Nijman V (2018) Sleep patterns, daytime predation, and the evolution of diurnal sleep site selection in lorisiforms. Am J Phys Anthropol 166:563–577

Swindale NV, Vital-Durand F, Blakemore C (1981) Recovery from monocular deprivation in the monkey. III. Reversal of anatomical effects in the visual cortex. Proc R Soc Lond B Biol Sci 213:435–450

Szmajda BA, Grünert U, Martin PR (2008) Retinal ganglion cell inputs to the koniocellular pathway. J Comp Neurol 510:251–268

Tabor GL (1973) Benign lymphocytic lymphoma of the upper eyelid and left plica semilunaris. Ann Ophthalmol 5:964–965

Tailby C, Szmajda BA, Buzás P, Lee BB, Martin PR (2008) Transmission of blue (S) cone signals through the primate lateral geniculate nucleus. J Physiol 586:5947–5967

Tailby C, Dobbie WJ, Solomon SG, Szmajda BA, Hashemi-Nezhad M, Forte JD, Martin PR (2010) Receptive field asymmetries produce color-dependent direction selectivity in primate lateral geniculate nucleus. J Vis 10:1

Talebi MG, Pope TR, Vogel ER, Neitz M, Dominy NJ (2006) Polymorphism of visual pigment genes in the muriqui (primates, Atelidae). Mol Ecol 15:551–558

Tanaka T, Canfield DR (2012) Intracranial meningioma with ophthalmoplegia in a rhesus macaque (Macaca mulatta). Comp Med 62:439–442

Tattersall I (2007) Origin of the Malagsy Strepsirhine primates. In: Gould L, Sauther ML (eds) Lemurs: ecology and adaptation. Springer, New York, NY

Telkes I, Lee SC, Jusuf PR, Grünert U (2008) The midget-parvocellular pathway of marmoset retina: a quantitative light microscopic study. J Comp Neurol 510:539–549

Tetreault N, Hakeem A, Allman JM (2004) The distribution and size of retinal ganglion cells in Microcebus murinus, Cheirogaleus medius, and Tarsius syrichta: implications for the evolution of sensory systems in primates systems in primates. In: Ross CF, Kay RF (eds) Anthropoid origins: new visions. Kluwer Academic/Plenum Publishers, New York

Tigges J (1963) On color vision in gibbon and orang-utan. Folia Primatol 1:188–198

Tkatchenko TV, Troilo D, Benavente-Perez A, Tkatchenko AV (2018) Gene expression in response to optical defocus of opposite signs

reveals bidirectional mechanism of visually guided eye growth. PLoS Biol 16:e2006021
Torres LB, Silva Araujo BH, Gomes de Castro PH, Romero Cabral F, Sarges Marruaz K, Silva Araujo M, Gomes da Silva S, Muniz JA, Cavalheiro EA (2010) The use of new world primates for biomedical research: an overview of the last four decades. Am J Primatol 72: 1055–1061
Torrez LB, Perez Y, Yang J, Zur Nieden NI, Klassen H, Liew CG (2012) Derivation of neural progenitors and retinal pigment epithelium from common marmoset and human pluripotent stem cells. Stem Cells Int 2012:417865
Tovée MJ, Bowmaker JK, Mollon JD (1992) The relationship between cone pigments and behavioural sensitivity in a New World monkey (Callithrix jacchus jacchus). Vis Res 32:867–878
Travis DS, Bowmaker JK, Mollon JD (1988) Polymorphism of visual pigments in a callitrichid monkey. Vis Res 28:481–490
Treff HA (1967) Tiefensehscharfe und Sehscharfe beim Galago (Galago senegalensis). Z Vgl Physiol 54:26–57
Troilo D, Nickla DL (2005) The response to visual form deprivation differs with age in marmosets. Invest Ophthalmol Vis Sci 46:1873–1881
Troilo D, Howland HC, Judge SJ (1993) Visual optics and retinal cone topography in the common marmoset (Callithrix jacchus). Vis Res 33:1301–1310
Troilo D, Nickla DL, Wildsoet CF (2000a) Choroidal thickness changes during altered eye growth and refractive state in a primate. Invest Ophthalmol Vis Sci 41:1249–1258
Troilo D, Nickla DL, Wildsoet CF (2000b) Form deprivation myopia in mature common marmosets (Callithrix jacchus). Invest Ophthalmol Vis Sci 41:2043–2049
Tusa RJ, Mustari MJ, Burrows AF, Fuchs AF (2001) Gaze-stabilizing deficits and latent nystagmus in monkeys with brief, early-onset visual deprivation: eye movement recordings. J Neurophysiol 86: 651–661
Tusa RJ, Mustari MJ, Das VE, Boothe RG (2002) Animal models for visual deprivation-induced strabismus and nystagmus. Ann N Y Acad Sci 956:346–360
Tychsen L, Scott C (2003) Maldevelopment of convergence eye movements in macaque monkeys with small- and large-angle infantile esotropia. Invest Ophthalmol Vis Sci 44:3358–3368
Tyrrell DA, Buckland FE, Lancaster MC, Valentine RC (1960) Some properties of a strain of SV 17 virus isolated from an epidemic of conjunctivitis and rhinorrhoea in monkeys (Erythrocebus patas). Br J Exp Pathol 41:610–616
Valenta K, Edwards M, Rafaliarison RR, Johnson SE, Holmes SM, Brown KA, Dominy NJ, Lehman SM, Parra EJ, Melin AD (2016) Visual ecology of true lemurs suggests a cathemeral origin for the primate cone opsin polymorphism. Funct Ecol 30:932–942
Varnell ED, Kaufman HE, Hill JM, Wolf RH (1987) A primate model for acute and recurrent herpetic keratitis. Curr Eye Res 6:277–279
Veiga Neto ER, Tamega OJ, Zorzetto NL, Dall Pai V (1992) Anatomical aspects of the lacrimal gland of the tufted capuchin (Cebus apella). J Anat 180(Pt 1):75–80
Veilleux CC, Kirk EC (2009) Visual acuity in the cathemeral strepsirrhine Eulemur macaco flavifrons. Am J Primatol 71:343–352
Veilleux CC, Louis EE Jr, Bolnick DA (2013) Nocturnal light environments influence color vision and signatures of selection on the OPN1SW opsin gene in nocturnal lemurs. Mol Biol Evol 30: 1420–1437
Veilleux CC, Scarry CJ, Di Fiore A, Kirk EC, Bolnick DA, Lewis RJ (2016) Group benefit associated with polymorphic trichromacy in a Malagasy primate (Propithecus verreauxi). Sci Rep 6:38418
Victor JD, Blessing EM, Forte JD, Buzás P, Martin PR (2007) Response variability of marmoset parvocellular neurons. J Physiol 579:29–51
Vital-Durand F, Blakemore C (1981) Visual cortex of an anthropoid ape. Nature 291:588–590
Wada S, Koyama H, Yamashita K (2020) Sedative and physiological effects of alfaxalone intramuscular administration in cynomolgus monkeys (Macaca fascicularis). J Vet Med Sci 82:1021–1029
Wallace DJ, Fitzpatrick D, Kerr JND (2016) Primate thalamus: more than meets an eye. Curr Biol 26:R60–r61
Walls GL (1942) The vertebrate eye and its adaptive radiation. Hafner, New York, NY
Wang Z, Li S, Chen J, Yang B, Zheng H (1996) The healing of excimer laser ablated cornea and the effects of corticosteroid. Zhonghua Yan Ke Za Zhi 32:245–251
Wang RF, Schumer RA, Serle JB, Podos SM (1998) A comparison of argon laser and diode laser photocoagulation of the trabecular meshwork to produce the glaucoma monkey model. J Glaucoma 7:45–49
Ward JM, Vallender EJ (2012) The resurgence and genetic implications of New World primates in biomedical research. Trends Genet 28: 586–591
Warwick A, Redrobe S, Lotery A, Watts J (2017) Bilateral cataract surgery with intraocular lens implant in a captive western lowland gorilla. J Med Primatol 46:252–255
Webb RM, Tabbara KF, O'Connor GR (1984) Retinal vasculitis in ocular toxoplasmosis in nonhuman primates. Retina 4:182–188
Webb BS, Tinsley CJ, Vincent CJ, Derrington AM (2005) Spatial distribution of suppressive signals outside the classical receptive field in lateral geniculate nucleus. J Neurophysiol 94:1789–1797
Weber JT, Giolli RA (1986) The medial terminal nucleus of the monkey: evidence for a 'complete' accessory optic system. Brain Res 365:164–168
Weiss S, Kremers J, Maurer J (1998) Interaction between rod and cone signals in responses of lateral geniculate neurons in dichromatic marmosets (Callithrix jacchus). Vis Neurosci 15:931–943
Weltzien F, Dimarco S, Protti DA, Daraio T, Martin PR, Grünert U (2014) Characterization of secretagogin-immunoreactive amacrine cells in marmoset retina. J Comp Neurol 522:435–455
Weltzien F, Percival KA, Martin PR, Grünert U (2015) Analysis of bipolar and amacrine populations in marmoset retina. J Comp Neurol 523:313–334
West CS, Vainisi SJ, Vygantas CM, Beluhan FZ (1981) Intraocular granulomas associated with tuberculosis in primates. J Am Vet Med Assoc 179:1240–1244
White AJ, Wilder HD, Goodchild AK, Sefton AJ, Martin PR (1998) Segregation of receptive field properties in the lateral geniculate nucleus of a new-world monkey, the marmoset Callithrix jacchus. J Neurophysiol 80:2063–2076
White AJ, Solomon SG, Martin PR (2001) Spatial properties of koniocellular cells in the lateral geniculate nucleus of the marmoset Callithrix jacchus. J Physiol 533:519–535
Widdig A, Kessler MJ, Bercovitch FB, Berard JD, Duggleby C, Nürnberg P, Rawlins RG, Sauermann U, Wang Q, Krawczak M, Schmidtke J (2016) Genetic studies on the Cayo Santiago rhesus macaques: a review of 40 years of research. Am J Primatol 78:44–62
Wikler KC, Rakic P (1990) Distribution of photoreceptor subtypes in the retina of diurnal and nocturnal primates. J Neurosci 10:3390–3401
Williams DL (2013) Laboratory animal ophthalmology. In: Gelatt KN, Gilber BC, Kern TJ (eds) Vet Ophthalmol. John Wiley and Sons, Aimes, IA
Williams C (2014) Fungal infections. In: Miller R, Fowler M (eds) Fowler's zoo and wild animal medicine. Elsevier Health Sciences, St. Louis
Williams AJ, Hunt DM, Bowmaker JK, Mollon JD (1992) The polymorphic photopigments of the marmoset: spectral tuning and genetic basis. EMBO J 11:2039–2045
Williams CV, Glenn KM, Levine JF, Horne WA (2003) Comparison of the efficacy and cardiorespiratory effects of medetomidine-based anesthetic protocols in ring-tailed lemurs (Lemur catta). J Zoo Wildl Med 34:163–170

Wilson DA, Tomonaga M, Vick SJ (2016) Eye preferences in capuchin monkeys (Sapajus apella). Primates 57:433–440

Wolin LR, Massopust LC Jr (1967) Characteristics of the ocular fundus in primates. J Anat 101:693–699

Wong AM, Tychsen L (2002) Effects of extraocular muscle tenotomy on congenital nystagmus in macaque monkeys. J AAPOS 6:100–107

Wong AM, Foeller P, Bradley D, Burkhalter A, Tychsen L (2003) Early versus delayed repair of infantile strabismus in macaque monkeys: I. ocular motor effects. J AAPOS 7:200–209

Wu KC, Lv JN, Yang H, Yang FM, Lin R, Lin Q, Shen RJ, Wang JB, Duan WH, Hu M, Zhang J, He ZL, Jin ZB (2020) Nonhuman primate model of Oculocutaneous albinism with TYR and OCA2 mutations. Research (Wash D C) 2020:1658678

Yamashita T, Ono K, Ohuchi H, Yumoto A, Gotoh H, Tomonari S, Sakai K, Fujita H, Imamoto Y, Noji S, Nakamura K, Shichida Y (2014) Evolution of mammalian Opn5 as a specialized UV-absorbing pigment by a single amino acid mutation. J Biol Chem 289:3991–4000

Yamigawa J (1979) Some external characters of the Japanese monkeys (Macaca fuscata). The Journal of Anthropological Society of Nippon 87:483–497

Yeh T, Lee BB, Kremers J, Cowing JA, Hunt DM, Martin PR, Troy JB (1995) Visual responses in the lateral geniculate nucleus of dichromatic and trichromatic marmosets (Callithrix jacchus). J Neurosci 15:7892–7904

Yiu G, Vuong VS, Oltjen S, Cunefare D, Farsiu S, Garzel L, Roberts J, Thomasy SM (2016) Effect of uveal melanocytes on choroidal morphology in rhesus macaques and humans on enhanced-depth imaging optical coherence tomography. Invest Ophthalmol Vis Sci 57:5764–5771

Yiu G, Tieu E, Munevar C, Wong B, Cunefare D, Farsiu S, Garzel L, Roberts J, Thomasy SM (2017) In vivo multimodal imaging of Drusenoid lesions in rhesus macaques. Sci Rep 7:15013

Yiu G, Wang Z, Munevar C, Tieu E, Shibata B, Wong B, Cunefare D, Farsiu S, Roberts J, Thomasy SM (2018) Comparison of chorioretinal layers in rhesus macaques using spectral-domain optical coherence tomography and high-resolution histological sections. Exp Eye Res 168:69–76

Yiu G, Chung SH, Mollhoff IN, Wang Y, Nguyen UT, Shibata B, Cunefare D, Farsiu S, Roberts J, Thomasy SM (2020a) Long-term evolution and Remodeling of soft Drusen in rhesus macaques. Invest Ophthalmol Vis Sci 61:32

Yiu G, Thomasy SM, Casanova MI, Rusakevich A, Keesler RI, Watanabe J, Usachenko J, Singapuri A, Ball EE, Bliss-Moreau E, Guo W, Webster H, Singh T, Permar S, Ardeshir A, Coffey LL, Van Rompay KK (2020b) Evolution of ocular defects in infant macaques following in utero Zika virus infection. JCI Insight 5:e143947

Yoshioka H, Katsume Y (1982a) Experimental central serous chorioretinopathy. III: ultrastructural findings. Jpn J Ophthalmol 26:397–409

Yoshioka H, Katsume Y (1982b) Studies on experimental central serous chorioretinopathy. A light and electron microscopy. Nippon Ganka Gakkai Zasshi 86:738–749

Yoshioka H, Katsume Y, Akune H (1982) Experimental central serous chorioretinopathy in monkey eyes: fluorescein angiographic findings. Ophthalmologica 185:168–178

Yoshioka H, Katsume Y, Akune H (1984a) Studies on experimental central serous chorioretinopathy. Fluorescein angiography and histopathology during the course of spontaneous remission. Nippon Ganka Gakkai Zasshi 88:819–828

Yoshioka H, Katsume Y, Akune H, Nagasaki H (1984b) Experimental central serous chorioretinopathy. IV: fluorescein angiography and electron microscopy during spontaneous healing process. Kurume Med J 31:89–99

Young FA, Farrer DN (1964) Refractive characteristics of chimpanzees. Am J Optom Arch Am Acad Optom 41:81–91

Yu HH, Chaplin TA, Rosa MG (2015) Representation of central and peripheral vision in the primate cerebral cortex: insights from studies of the marmoset brain. Neurosci Res 93:47–61

Yu HH, Atapour N, Chaplin TA, Worthy KH, Rosa MGP (2018) Robust visual responses and Normal Retinotopy in primate lateral geniculate nucleus following Long-term lesions of striate cortex. J Neurosci 38: 3955–3970

Appendix C: Normative Ocular Data (Clinical Tests and Morphological Parameters) for Different Wild and Exotic Mammals

Andre Tavares Somma and Fabiano Montiani-Ferreira

Normal ophthalmic examination clinical tests and parameters have been established and reported in many species of domestic and wild animals. Knowledge of these normal values is important in order to be able to correctly interpret data from ophthalmic examinations and determine when there is an ocular abnormality. As in other areas of veterinary science, without the appropriate parameters, the sensitivity and specificity of ocular clinical tests are substantially lowered, which often can cause erroneous diagnoses. A correct diagnosis consequently is essential to establish a suitable treatment protocol to treat ocular disease, hopefully at an early stage. Reference values that are specific for the species being examined and knowledge of the exact equipment used are essential information for an accurate interpretation of clinical data. The challenge that the wild and exotic animal ophthalmologist faces is daunting, since there are so many different species with so many different eye sizes, morphologic features, and physiologic variations.

The following expressions: "values," "range," "parameters," "findings" after one of these words: "normal," "normative," or "reference" have been used interchangeably in the ophthalmology literature. Statistical purists, however, argue that the term "range" is actually incorrect, because in statistical terminology, range actually is a single value (the difference between the highest and lowest value). The same applies to interquartile range (IQR), which also is a single value. IQR is a measure of statistical dispersion, being equal to the difference between 75th and 25th percentiles, or between upper and lower quartiles, IQR = Q3 − Q1. In statistics, the three most common measures of central tendency are the mean, median, and mode. Each of these measures calculates the location of the central point using a different method. The mean is the arithmetic average and it is the most commonly used measure of central tendency. The median is the middle value. The mean has one main disadvantage: it is particularly susceptible to the influence of outliers. Median is the value that splits the dataset in half. To find the median, order your data from smallest to largest, and then find the data point that has an equal amount of values above it and below it. When the data is skewed (i.e., the frequency distribution for our data is skewed) it is preferred to report the median over the mean. The mode is the value that occurs the most frequently in your data set. Generally, the mode is used for categorical data where we wish to know which the most common category is.

From what is known from domestic animals and some exotic species as well as humans, it is possible that factors such as age, time of the day, and geographic location will influence normal ocular parameters. Obviously, not all species of wild and exotic animals had their eyes investigated. When this happens, normal parameters can be immediately produced from other animals of the zoo collection or from the supposedly normal fellow eye, when the abnormality is unilateral. Thus, as one can imagine, this field of ophthalmic research still has a lot to grow, compared to what is known in human and domestic animal ophthalmology.

Besides the basic necessary knowledge of ocular anatomy to perform an ophthalmic examination, several newer clinical parameters are becoming available for domestic animals and human beings due to the advancement of technology being used for ophthalmology and visual sciences. Nevertheless, measurement of tear production and the determination of intraocular pressure (IOP) are somewhat considered as minimum information necessary for an acceptable ophthalmic examination. The Schirmer test is the standard method for quantitative assessment of tear production in human and domestic animal ophthalmology, more specifically Schirmer tear test 1 (STT1), which measures the reflex plus basal tear secretion. However, for many small species of wild and exotic animals, the 5-mm width might be too big to fit in the palpebral aperture. Additionally, the tear volume normally produced might be too small to be absorbed and measured by the 35-mm length strip. In these cases, there are some options available such as (1) The Modified Schirmer Tear Test (mSTT), which is the regular Schirmer tear test strip cut in half (turning it into two 2.5 mm wide

A. T. Somma · F. Montiani-Ferreira (✉)
Comparative Ophthalmology Laboratory, Clinical and Surgical Service, Federal University of Paraná (UFPR), Curitiba, PR, Brazil
e-mail: montiani@ufpr.br

F. Montiani-Ferreira et al. (eds.), *Wild and Exotic Animal Ophthalmology*, https://doi.org/10.1007/978-3-030-81273-7

strips); (2) The phenol red thread test (PRT), which is much narrower than STT1 and mSTT; (3) Paper point tear test (PPTT), which uses a standardized endodontic sterile absorbent paper point, inserted into the conjunctival fornix. The endodontic points are more rigid than mSTT and PRT, facilitating the insertion into the fornix.

Some of the problems with mSTT are: Once the sterile package is open and the examiner handles the strips, they are not going to be sterile anymore. In addition, even when care is taken to section the STT strips as accurately as possible human error can generate different widths of the mSTTs (not standardized), thereby affecting the test results. The production of industrialized mSTTs to make them commercially available would help prevent potential variability. Disadvantages and limitations of the PRT test include the lack of commercial availability in certain countries, price, difficulty to perform the test itself, and paucity of normal parameters. Problems with the PPTT include potential lack of standardization since absorbent capacities of different brands of endodontic paper points can vary. Originally, the PPTT test was developed at LABOCO-UFPR, Brazil and was first reported in marmosets by Lange (2012), to be used with a specific brand and size of paper point (Roeko Color–size30, Langenau, Germany). The production of industrialized and standardized versions of PPTT also would help to prevent variability. Other researchers started to use different brands and sizes of paper points and consequently, the results cannot be compared.

As mentioned above, IOP measurement is an important part of the ophthalmic examination. It is an extremely valuable test to help differentiating cases of red eye in general, but especially glaucoma from uveitis. Applanation tonometry using the Tonopen® might be difficult to use in small eyes (a corneal diameter less than 5 mm). The tip of the Tonovet® rebound tonometer is much smaller becoming invaluable for IOP measurements in many small species.

Ultrasonic corneal pachymetry is a reliable in vivo method to measure corneal thickness. The technique permits measurement of the cornea in a normal physiologic state. The instrument measures the time required for ultrasonic energy to traverse the cornea and, using a preset constant for velocity of sound, converts this to a measure of thickness. Central corneal thickness is commonly reported as a normal parameter in different wild and exotic animal species.

Baseline corneal touch threshold (CTT) may vary substantially among different species. Knowledge of normal data might be important for a better understanding of an animal's behavior and its visual ecology. In addition, familiarity with CTT variation among species facilitates the evaluation and interpretation of ocular reflexes during the ophthalmic examination and gives a better estimate of the duration of action of topical anesthetics. Corneal sensitivity can be determined by evaluating the corneal touch threshold (CTT) using a Cochet-Bonnet esthesiometer. CTT is another commonly reported parameter in wild and exotic animal ophthalmology literature.

Previous knowledge of normal ocular dimensions, such as axial globe length (AGL) or palpebral fissure length (PFL) in wild and exotic animals facilitates the evaluation of ophthalmic disease in these species, including ophthalmic examination, surgical planning, diagnostic imaging, gross examination, and histopathology.

Snakes, ablepharine geckos, and skinks possess a spectacle covering the cornea, developed from fused eyelids and separated from the corneal surface by an epithelial-lined sub-spectacular space. Thus, the cornea is not exposed to environment and not directly assessable to the veterinary ophthalmologist, rendering Schirmer tear test, tonometry, corneal pachymetry, and corneal sensitivity procedures impossible to be performed in these species.

Several wild and exotic species, some of them threatened to be extinct, heavily depend on vision for survival. Thus, better ophthalmic care will aid indirectly in the conservation of such species and which in turn benefits the whole environment and ecosystems.

Hopefully, the information gathered here in the form of an inclusive table will provide a resource to what has been already published for veterinary ophthalmologists and researchers working with wild and exotic animal ophthalmology (Table 1).

Table 1 Normative data for ophthalmic clinical tests and morphological parameters in selected wild and exotic animals

	IOP		Lacrimal production			CCT		CTT	PFL	Investigator
Animal species	Mean ± SD Median/eye side/age/sex/time/anesthesia (when indicated)	Tonometer type	Mean ± SD Median/eye side/anesthesia (when indicated)			Mean ± SD Median/age (when indicated)	Method	Mean ± SD	Mean ± SD	
	(mmHg)		STT (mm/min) STTII (when indicated)	PRT (mm/15s)	PPTT (mm/min)	(μm)		(cm)	(mm)	
Addax nasomaculatus Addax	11.3 ± 3.2	TonopenXL®	28.8 ± 8.3							Ofri et al. (2002)
Aepyceros melampus Impala	8.0 ± 1.2	TonopenXL®	18.8 ± 1.8							Ofri et al. (2002)
Ailuropoda melanoleuca Giant panda bear	16.43 ± 3.011		15.4 ± 4.1							Oliveira (2021)
Ammotragus lervia Barbary sheep	19.47 ± 3.9	Tonovet®	27.22 ± 3.6			630.07 ± 20.67	Ultrasound pachymetry			Fornazari et al. (2016)
Anoura caudifer Tailed tailless bat	7.28 ± 2.70	Tonovet® (upright position)			1.89 ± 0.62				3.92 ± 0.51	Somma et al. (2020)
Aotus azarae infulatu Azara's *night* monkey	13.7 ± 5.6	Tonovet®	2.1 ± 2.3			440 ± 40	Ultrasound pachymetry			Lange (2012)
Aotus trivirgatus Humboldt's night monkey Owl monkey	13 ± 1					450 ± 40				Jester et al. (1981)
						470 ± 20				Steel et al. (1981)
	25.95 ± 1.09	Pneumatic tonometer								Lamble and Lamble (1976)
Artibeus lituratus Great fruit-eating bat	11.0 ± 3.28	Tonovet® (upright position)			2.53 ± 1.65				5.04 ± 0.45	Somma et al. (2020)
Arctocephalus australis South	Juvenile OD 17.52 Juvenile OS 18.4	Tonovet®								Sheldon et al. (2017)

(continued)

Table 1 (continued)

	IOP		Lacrimal production			CCT		CTT	PFL	Investigator
Animal species	Mean ± SD Median/eye side/age/sex/time/anesthesia (when indicated)	Tonometer type	Mean ± SD Median/eye side/anesthesia (when indicated)			Mean ± SD Median/age (when indicated)	Method	Mean ± SD	Mean ± SD	
	(mmHg)		STT (mm/min) STTII (when indicated)	PRT (mm/15s)	PPTT (mm/min)	(μm)		(cm)	(mm)	
American Fur Seals	Adult OD 32.9 Adult OS 32.3									
Blastocerus dichotomus Marsh deer			5							Crivelaro (2014)
Callithrix penicillate Black-tufted marmoset			mSTT1: 0.46 ± 3.41	13.27 ± 5.41	9.32 ± 3.09				7.83 ± 0.72	Lange et al. (2012)
Capra ibex Alpine ibex	13.1 ± 2.43	TonopenXL®	11.7 ± 3.87							Kvapil et al. (2018)
Capra ibex nubiana Nubian ibex	17.95 + 4.78	Schiotz	13.2 + 5.1							Ofri et al. (1998a) Ofri et al. (1999)
Capra hicus Pygmy goats	7.88 11.85 10.8	TonoVet®-P TonoVet®-D TonoPen®	15.8							Broadwater et al. (2007)
Castor canadensis American beaver	17.11 ± 6.39 OD 18.79 ± 5.63 OS	TonopenXL®							9.36 ± 1.00	Cullen (2003)
Cavia porcellus Guinea pig	Young: 8.53 ± 1.28	TonoVet®								Cairó et al. (2018)
	Adult: 13.20 ± 1.28	TonopenVet®								
	Adult: 10.93 ± 3.61	TonopenVet®								
	17.3–22.7	TonoVet®								Ostrin and Wildsoet (2016)
	16.34	TonoPen®								Ansari-Mood et al. (2016)
	6.19	TonoVet®								
						230				Cafaro et al. (2009)

			0.36 ± 1.09 STTII: 0.43 ±1.29	16 ± 4.7				2.0		Trost et al. (2007)
	18.27 ± 4.55	TonopenVet®	Before topical anesthesia: 3 After topical anesthesia: 4	Before topical anesthesia: 21.26 ± 4.19 After topical anesthesia: 22.47 ± 3.31				2.0		Coster et al. (2008)
								13.50 ± 6.09	11.35 ± 0.88	Wieser et al. (2013)
			7.58 ± 3.19 at 30 s 10.42 ± 3.92 at 60 s							Nogradi et al. (2020)
	6.81 ± 1.41	TonoVet®		14.33 ± 1.35	8.54 ± 1.08					Rajaei et al. (2016c)
Cebus apella Tufted capuchin	18.4 ± 3.8	TonopenXL®	14.9 ± 5.1			460 ± 30	Ultrasound pachymetry			Montiani-Ferreira et al. (2008b)
Cebus xanthosternos Golden-bellied capuchin	19.62 ± 4.57	TonopenXL®	14.92 ± 5.46							Oriá et al. (2013)
Cerdocyon thous Crab-eating fox	10.70 ± 3.43	TonoVet® calibration D	4.33 ± 2.96						17.45 ± 1.55	Carvalho et al. (2020)
	5.66 ± 3.44	TonoVet® calibration P								
	11.70 ± 5.70	TonopenXL®								
	10.43 ± 3.84		13.37 ± 3.79			540 ± 60	Tissue morphometry			Renzo et al. (2020)
Ceratotherium simum White rhinoceros	32.1 ± 10.4	TonopenXL®	17.6 ± 3.1							Ofri et al. (2002)
Chinchilla lanigera	18·5 ± 5·75									Peiffer and Johnson (1980)

(continued)

Table 1 (continued)

	IOP		Lacrimal production			CCT		CTT	PFL	Investigator
Animal species	Mean ± SD Median/eye side/age/sex/time/ anesthesia (when indicated)	Tonometer type	Mean ± SD Median/eye side/anesthesia (when indicated)			Mean ± SD Median/ age (when indicated)	Method	Mean ± SD	Mean ± SD	
	(mmHg)		STT (mm/min) STTII (when indicated)	PRT (mm/15s)	PPTT (mm/min)	(μm)		(cm)	(mm)	
Long-tailed chinchilla	2.9 ± 1.8	TonoVet®	14.6 ± 3.5	14.6 ± 3.5				1.24 ± 0.46	14.4 ± 0.01	Müller et al. (2010)
	17.71 ± 4.17	TonopenXL®	1.07 ± 0.54							Lima et al. (2010)
	9.7 ± 2.5	TonoVet®								Snyder et al. (2018)
	2.49 ± 0.56	TonoVet®								Chacaltana et al. (2016)
	28.52 ± 12.48	Tonopen® Avia®Vet™			I: 7.98 ± 1.95 II: 9.71 ± 3.52					Richards and Trbolová (2016)
Connochaetes gnou Black wildebeest White-tailed wildebeests	15.5 ± 3.7	TonopenXL®	19.3 ± 4.6							Ofri et al. (2002)
Cricetomys spp. African giant pouched rat	7.7 ± 2.9	TonoVet®								Heller et al. (2018)
Chrysocyon brachyurus Maned wolf	20 ± 6		11 ± 5							Honsho et al. (2016)
	11.00 ± 2.77	TonoVet® calibration D	9.31 ± 7.40						22.79 ± 1.63	Carvalho et al. (2020)
	6.78 ± 2.58	TonoVet® calibration P								
	18.6 ± 4.2	TonopenXL®								Montiani-Ferreira (2001)

Cuniculus paca Lowland paca	6.34 ± 0.43	TonopenVet®	4.10 ± 0.44			350 ± 10	Ultrasound pachymetry			Balthazar da Silveira et al. (2018)
Cynomys ludovicianus Black-tailed prairie dog	7.7 ± 2.2	TonoVet®	1.2 ± 0.9	13.6 ± 7.8						Meekins et al. (2015)
Dama dama European fallow deer	16.1 ± 4.5	TonoVet® P setting	18.7 ± 5.1							Pacheco et al. (2018)
	21.5 ± 5.1	TonoVet® H setting								
	14.1 ± 2.48	TonopenXL®	17.8 ± 3.16							Kvapil et al. (2018)
Dama mesopotamica Persian fallow deer	11.9 ± 3.3	TonopenXL®	10.5 ± 6.5							Ofri et al. (2001)
Dasyprocta azarae Azara's agouti	11.61 ± 0.44	TonopenXL®	9.73 ± 0.47			800 ± 3.0	B-mode ultrasonography	4.50 ± 0.36	17.0 ± 0.025	Tavares-Somma et al. (2017)
Didelphis albiventris White-eared opossum			mSTT1: 0 ± 1.63	19.79 ± 2.61	16.25 ± 1.82					Oria et al. (2019)
Didelphis aurita Big-eared opossum	7 ± 2.16	TonoVet® H setting								
	7 ± 2.58	TonoVet® D Setting								Baumworcel (2021)
			mSTT1: 0 ± 1.63	5.22 ± 2.92	10.9 ± 3.04					Oria et al. (2019)
Camelus dromedarius Dromedary camel	Calf 14–18									Marzok et al. (2017)
	Immature > 32.5	TonopenXL®	22–26							Marzok and El-khodery (2015), Marzok et al. (2017)
	Mature > 28.5		30–34							
Erinaceus europaeus European hedgehog	12.6 ± 1.8	TonoVet®								Williams et al. (2017)
Elephas maximus Asian elephant			34.3 ± 1.7			1700 ± 200	B-mode ultrasonography			Tuntivanich et al. (2002) Bapodra et al. (2010)

(continued)

Table 1 (continued)

	IOP		Lacrimal production			CCT		CTT	PFL	Investigator
Animal species	Mean ± SD Median/eye side/age/sex/time/ anesthesia (when indicated)	Tonometer type	Mean ± SD Median/eye side/anesthesia (when indicated)			Mean ± SD Median/ age (when indicated)	Method	Mean ± SD	Mean ± SD	
	(mmHg)		STT (mm/min) STTII (when indicated)	PRT (mm/15s)	PPTT (mm/min)	(μm)		(cm)	(mm)	
Equus quagga burchelli Burchell's zebra			23.4 ± 3.4							Ofri et al. (1999)
Equus quagga boehmi Grant's Zebra	25.30 + 3.06	Schiotz								Ofri et al. (1998a)
	29.47 + 3.43	Tonopen								
Gazella thomsoni Thomson's gazelle	7.6 ± 1.6	TonopenXL®								Ofri et al. (2000)
Hemiechinus auratus Long-eared hedgehog	20.1 ± 4.0	TonopenVet®	1.7 ± 1.2							Ghaffari et al. (2012)
Hydrochaeris hydrochaeris Capybara	18.4 ± 3.8	TonopenXL®	14.9 ± 5.1			460 ± 30	Ultrasound pachymetry			Montiani-Ferreira et al. (2008a)
Lama glama Llama	13.10 ± 0.35	Tonopen®								Willis et al. (2000)
			20.30 ± 2.96							Pigatto et al. (2010)
	16.96 ± 3.51	Tonopen®								Nuhsbaum et al. (2000)
Leopardus tigrinus Oncilla or northern tiger cat	14.3	TonopenXL®	14.71			800 ± 60	B-mode ultrasonography			Gentil et al. (2016)
Macaca fascicularis Crab-eating macaque or	19.2	Goldmann applanating prism								Hahnenberger (1980)
	8.36 (anesthetized)									Kaufman and Davis (1980)

Cynomolgus Macaques			11.16 mm ± 2.02							Kossler et al. (2019)
Macaca mulatta Rhesus macaque	Infant 20.6 ± 4.5 Adult 15.5 ± 2.8	Floating-tip applanation pneumatonograph								De Rousseau and Bito (1981)
	Infant: 15.7 ± 2.0 Adult: 14.5 ± 2.0									Bito et al. (1979)
	General mean: 14.9 ± 2.1	Floating-tip applanation pneumatonograph	15.1							Jaax et al. (1984)
	17.95 (anesthetized)	TonoVet®								Yu et al. (2009)
Macaca thibetana Tibetan macaque	Conscious at 12:00: 29.3 ± 3.1 Conscious at 03:00: 19.7 ± 2.8	TonoVet®								Yi et al. (2012)
	Anesthesia at 12:00: 22.1 ± 2.4 Anesthesia at 03:00: 19.7 ± 1.4									
Macropus fuliginosus Western gray kangaroo	10.69 ± 3.59 17.38 ± 4.44	TonoVet® TonopenXL®								Labelle et al. (2010)
Macropus rufus Red kangaroo	17.45 ± 7.23	TonopenXL®	22.6 ± 6.07							Takle et al. (2010)
Mazama americana Red brocket	14 (median)	TonopenXL®	6.5 (median)							Crivelaro (2014)
Mazama bororo Small red brocket	10 (median)		5.5 (median)							
Mazama gouazoubira Brown Brocket	15.3 ± 3.1		8.9 ± 1.8							Martins et al. (2007)
	9 (median)		4.5 (median)							Crivelaro (2014)
Mazama nana Pygmy brocket	14 (median)		5.0 (median)							
Mazama nemorivaga Amazonian brown brocket	5 (median)		4.5 (median)							

(continued)

Table 1 (continued)

	IOP		Lacrimal production			CCT		CTT	PFL	Investigator
Animal species	Mean ± SD Median/eye side/age/sex/time/ anesthesia (when indicated)	Tonometer type	Mean ± SD Median/eye side/anesthesia (when indicated)			Mean ± SD Median/ age (when indicated)	Method	Mean ± SD	Mean ± SD	
	(mmHg)		STT (mm/min) STTII (when indicated)	PRT (mm/15s)	PPTT (mm/min)	(μm)		(cm)	(mm)	
Melursus ursinus Sloth bears	12.5 ± 5.2 (median 12)		11.6 6.0 (median 11)							Hartley et al. (2014)
Mesocricetus auratus Golden hamster	7 AM: 2.58 ± 0.87 3 PM: 4.46 ± 1.58 11 PM: 5.96 ± 1.23 4.55 ± 1.33	TonoVet®								Rajaei et al. (2017)
		TonoVet®	mSTT: 2.07 ± 0.97	5.57 ± 1.51	4.52 ± 1.55				5.84 ± 0.45	Rajaei et al. (2016b)
				6.8 ± 2.5						Rajaei et al. (2013)
Microcebus murinus Gray mouse lemur	9.2 ± 1.53 23.83 ± 5.89	TonoVet® TonopenVet®								Dubicanac et al. (2018)
Mustela putorius furo Ferret	14.50 ± 3.27	TonopenXL®	5.31 ± 1.32			337 ± 20	Ultrasound pachymetry			Montiani-Ferreira et al. (2006)
	14.07 ± 0.35	TonoVet®								Di Girolamo et al. (2013)
	15.44 ± 1.11	TonopenVet®								
Mus musculus House mouse	16.2 ± 0.4	Tonolab®								Miller et al. (2020)
				Young: 2.85 ± 0.4 Aged: 11.23 ± 2.0		Young: 83.7 ± 1.55 Aged: 92.4 ± 3.6	SD-OCT anterior segment scan	Young: 5.5 ± 0.1 Aged: 4.85 ± 0.3		De Silva et al. (2019)
	15 ± 5		3 ± 0.2 in 2 min		3 ± 1 mm/min					Holmberg (2008)
					4.39 ± 1.45					Lange et al. (2014)

									3.59 ± 0.27	
Nasua nasua Coati	9.50 ± 2.43	TonoVet® calibration P	2.50 ± 2.39						10.98 ± 1.67	Carvalho et al. (2021)
	14.60 ± 2.82	TonoVet® calibration D								
	18.66 ± 4.16	TonopenXL®								
Odocoileus virginianus White-tailed deer	Fawns: 16.21 ± 4.97 4.05 ± 5.03	Tonopen® TonoVet®	12.32 ± 4.46							Villar et al. (2020)
	Adults: 15.57 ± 2.88 12.87 ± 2.57	Tonopen® TonoVet®								
			3.5							Crivelaro (2014)
Oryctolagus cuniculus European rabbit	12.89 ± 2.80	TonopenXL®	7.27 ± 2.51		Dentsply (Color size 30): 12.43 ± 1.69 Roeko color (Color size 30): 15.24 ± 2.07					Oriá et al. (2014)
			3	20.88				14.75 ± 6.97	16.8 ± 1.64	Wieser et al. (2013)
			4.85							Gürkan and Hayat (2005)
			5.30 ± 2.96							Abrams et al. (1990)
	13 ± 6		5 ± 3.0	24 ± 4.0						Holmberg (2008)
English angora			5.4 ± 1.6	25.0 ± 2.7						Rajaei et al. (2016a)
Dutch rabbits			4.6 ± 1.2	23.6 ± 2.3						
White New Zealand			11.3 ± 1.0		18.8 ± 2.1 16.9 ± 1.7					Chen et al. (2021)
Oryx dammah Scimitar oryx	15.8 ± 1.5	TonopenXL®								Ofri et al. (2002)

(continued)

Table 1 (continued)

	IOP		Lacrimal production			CCT		CTT	PFL	Investigator
Animal species	Mean ± SD Median/eye side/age/sex/time/anesthesia (when indicated)	Tonometer type	Mean ± SD Median/eye side/anesthesia (when indicated)			Mean ± SD Median/age (when indicated)	Method	Mean ± SD	Mean ± SD	
	(mmHg)		STT (mm/min) STTII (when indicated)	PRT (mm/15s)	PPTT (mm/min)	(μm)		(cm)	(mm)	
Scimitar-horned oryx										
Oryx leucoryx Arabian oryx	22.68 ± 8.1	Schiotz								Ofri et al. (1998a)
	11.76 ± 3.4	Tonopen	12.7 ± 4.8							Ofri et al. (1999)
Otaria byronia South American sea lion	Males 31 ± 11 OD Males 31 ± 9 OS	TonoVet®								Sheldon et al. (2019)
	Females 27 ± 10 OD Females 24 ± 9 OS									
Ovis aries musimon Mouflon	14.9 ± 2.20	TonopenXL®	17.9 ± 3.87							Kvapil et al. (2018)
	18.05 ± 4.85	Applanation tonometry								Pietro et al. (2015)
Ovis orientalis Asiatic mouflon	17.93 ± 5.24	TonopenXL®	15.05 ± 1.79 15.50 ± 1.71							Puddu et al. (2002)
Ozotoceros bezoarticus Pampas deer			1.5							Crivelaro (2014)
Pteropus hypomelanus Small flying fox	Upright position: 12.1 ± 1.10 Hanging position: 17.45 ± 1.11			20.5 ± 2.23					14.75 ± 0.28 mm	Blackwood et al. (2010)
Pteropus pumilus Little golden-mantled flying fox	Upright position: 15.63 ± 1.01 Hanging position: 22.5 ± 1.27			19.3 ± 2.23					10.2 ± 0.22 mm	Blackwood et al. (2010)
Pteropus vampyrus	Upright position: 14.2 ± 0.89 Hanging position: 18.2 ± 1.37			20.9 ± 2.28					15.28 ±	Blackwood et al. (2010)

Large flying fox									0.21 mm	
Petaurus breviceps Sugar glider	2 ± 2.6	TonoVet®	2.2 ± 6.7	0 ± 0						Fraess et al. (2021)
Panthera leo Lion	Male: 24.9 ± 2.0 Female: 20.9 ± 2.4	Schiotz Schiotz								Ofri et al. (1998b)
			Anesthesia protocol I: 14.0 ± 4.9 OS 12.8 ± 8.0 OD Anesthesia protocol II: 24.1 ± 4.4 OD 24.6 ± 4.3 OS							Ofri et al. (1997)
	≤ 1 year: 12.8 ± 4.1	Tonopen®								
	≥ 1 year: 23.9 ± 4.1	Tonopen®								Ofri et al. (2008)
Pan troglodytes Chimpanzee	14 ± 4.2		13.4 ± 5.3							Sigmund et al. (2020)
Phascolarctos cinereus Koala	Conscious 15.3 ± 5.1 Anesthetized 13.8 ± 3.4	TonopenVet®	Conscious 10.3 ± 3.6 Anesthetized 3.8 ± 4.0							Grundon et al. (2011)
Rattus norvegicus Brown rat Common rat					6.18 ± 2.06				6.45 ± 0.09	Lange et al. (2014)
	13.0 ± 1.2									Cabrera et al. (1999)
	17.30 ± 5.35 +3.6	Tonopen®								Mermoud et al. (1994)
	15 ± 5		8 ± 3 in 5 min	14 ± 3 in 2 min						Holmberg (2008)
	8.2 ± 1.5 at 4-mm; 9.4 ± 1.8 at 6-mm; and 10.5 ± 1.5 at 8-mm probe-cornea distance (anesthetized Wistar rats)	TonoVet®								Rodrigues et al. (2021)
	11.75 ± 2.05	TonoLab®								Liu et al. (2014)

(continued)

Table 1 (continued)

	IOP		Lacrimal production			CCT		CTT	PFL	Investigator
Animal species	Mean ± SD Median/eye side/age/sex/time/ anesthesia (when indicated)	Tonometer type	Mean ± SD Median/eye side/anesthesia (when indicated)			Mean ± SD Median/ age (when indicated)	Method	Mean ± SD	Mean ± SD	
	(mmHg)		STT (mm/min) STTII (when indicated)	PRT (mm/15s)	PPTT (mm/min)	(μm)		(cm)	(mm)	
	8.75 ± 1.06 20min post-anesthesia									
Rhinoceros unicornis Indian rhinoceros	31.2 ± 6.62	Tonopen®	18.2 ± 3.49			130 ± 10	B-mode ultrasonography			Bapodra and Wolfe (2014)
Rupicapra rupicapra Chamois	10.2 ± 2.5	TonoPenXL®	14.5 ± 3.0							Kvapil et al. (2018)
Rusa unicolor Sambar deer	11.4 ± 2.8	TonoPenXL®	18.8 ± 4.7							Oriá et al. (2015)
Saimiri sciureus Common squirrel monkey	9.2 ± 2.2	TonoVet®	4.7 ± 2.7							Lange (2012)
Sapajus libidinosus Black-striped capuchin	13.3 ± 3.32	Tono-Pen AVIA®	2.50 ± 2.94							Bezerra et al. (2019)
Tamandua tetradactyla Southern tamandua			8.50 ± 4.13		14.13 ± 3.24				15.91 ± 2.51	de Araujo et al. (2017)
Taurotragus oryx Common eland	14.6 ± 4.0	TonoPenXL®	18.7 ± 5.9							Ofri et al. (2001)
Vicugña pacos *Lama guanicoe pacos* *Lama pacos* Alpaca	14.85 ± 0.45	Tonopen®								Willis et al. (2000)
	16.14 ± 3.74	Tonopen®								Nuhsbaum et al. (2000)
	17.2 ± 5.5	TonoVet®								Faulkner et al. (2020)
	16.4 ± 5.3	Tonopen®	20.0 ± 6							

										McDonald et al. (2018)
			20.88 ± 4.04							Rankin et al. (2012)
								Crias (all regions): 4 Adults (all regions): 2 Central: 3.45 ± 0.71 Ventral: 2.95 ± 0.72 Medial: 2.93 ± 0.73 Dorsal: 2.56 ± 0.63 Lateral: 2.18 ± 0.57		Welihozkiy et al. (2011)
Zalophus californianus California sea lion	32.8 ± 5.31 OD	Tonopen®								Mejia-Fava et al. (2009)

IOP intraocular pressure, *CCT* central corneal thickness, *CTT* corneal touch threshold, *PFL* palpebral fissure length, *mSTT* modified Schirmer tear test, *STT* Schirmer tear test, *PPTT* paper point tear test, *PRT* The phenol red thread test, *OS* oculus sinister or left eye, *OD* oculus dexter or right eye, *OU* oculus uterque or both eyes

References

Abrams KL, Brooks DE, Funk RS, Theran P (1990) Evaluation of the Schirmer tear test in clinically normal rabbits. Am J Vet Res 51(12): 1912–1913

Ansari-Mood M, Mehdi-Rajaei S, Sadjadi R, Selk-Ghaffari M, Williams DL (2016) Twenty-four-hour measurement of intraocular pressure in Guinea pigs (Cavia porcellus). J Am Assoc Lab Anim Sci 55(1): 95–97

Balthazar da Silveira CP, Lima TB, Crivelaro RM, de Lacerda LC, Pádua IR, Renzo R et al (2018) Ophthalmic parameters in adult lowland paca (Cuniculus paca) raised in captivity. Vet Ophthalmol 21(1):42–47

Bapodra P, Bouts T, Mahoney P, Turner S, Silva-Fletcher A, Waters M (2010) Ultrasonographic anatomy of the Asian elephant (*Elephas maximus*) eye. J Zoo Wildl Med 41(3):409–417

Bapodra P, Wolfe BA (2014) Baseline assessment of ophthalmic parameters in the greater one-horned rhinoceros (*Rhinoceros unicornis*). J Zoo Wildl Med 45(4):859–886

Baumworcel N. (2021) Personal communication

Bezerra KPG, de Lucena RB, Stipp DT, Costa FS, Reis VV, Borges PF et al (2019) Determination of baseline values for routine ophthalmic tests in bearded capuchin (*Sapajus libidinosus*). J Med Primatol 48(1):3–9

Bito LZ, Merritt SQ, DeRousseau CJ (1979) Intraocular pressure of rhesus monkey (Macaca mulatta). I. An initial survey of two free-breeding colonies. Invest Ophthalmol Vis Sci 18(8):785–793

Blackwood SE, Plummer CE, Crumley W, Mackay EO, Brooks DE, Barrie KP (2010) Ocular parameters in a captive colony of fruit bats. Vet Ophthalmol 13:72–79

Broadwater JJ, Schorling JJ, Herring IP, Pickett JP (2007) Ophthalmic examination findings in adult pygmy goats (Capra hicus). Vet Ophthalmol 10(5):269–273

Cabrera CL, Wagner LA, Schork MA, Bohr DF, Cohan BE (1999) Intraocular pressure measurement in the conscious rat. Acta Ophthalmol Scand 77(1):33–36

Cafaro TA, Oritz SG, Maldonado C et al (2009) The cornea of guinea pig: structural and functional studies. Vet Ophthalmol 12(4):231–241

Cairó M, Peña MT, Rios J, Melero A, Martorell J, Leiva M (2018) Assessment of intraocular pressure by applanation and rebound tonometry in guinea pigs of different ages. J Exotic Pet Med 27(1):25–31

Carvalho CM, Rodarte-Almeida AC, Beanes AS, Machado MT, Galera PD (2020) Ophthalmic contributions to assessing eyes of two neotropical canids: Cerdocyon thous and Chrysocyon brachyurus. Vet Ophthalmol 23(3):460–471

Carvalho CM, Rodarte-Almeida ACV, Moore BA, Borges BP, Machado MTS, Galera PD (2021) Ocular examination findings and measurements of tear production and tonometry of ring-tailed coatis (Nasua nasua). Vet Ophthalmol 24(3):210–217

Chacaltana FDYC, Pigatto JAT, Denardin IT (2016) Assessment of intraocular pressure in chinchillas of different age groups using rebound tonometry. Ciência Rural 46(8):1466–1471

Chen XM, Kuang JB, Yu HY, Wu ZN, Wang SY, Zhou SY (2021) A novel rabbit dry eye model induced by a controlled drying system. Transl Vis Sci Technol 10(4):32

Coster ME, Stiles J, Krohne SG, Raskin RE (2008) Results of diagnostic ophthalmic testing in healthy guinea pigs. J Am Vet Med Assoc 232(12):1825–1833

Crivelaro RM (2014) Parâmetros oftálmicos em diferentes espécies de cervídeos brasileiros mantidos em cativeiro. Master of Sciences Degree Dissertation. Jaboticabal, 84 p

Cullen CL (2003) Normal ocular features, conjunctival microflora and intraocular pressure in the Canadian beaver (Castor canadensis). Vet Ophthalmol 6(4):279–284

de Araujo NLLC, Raposo ACS, Pinho ACNL, Pinna MH, Galera PD, Júnior DCG, Oriá AP (2017) Conjunctival bacterial flora, antibiogram, and lacrimal production tests of collared anteater (Tamandua tetradactyla). J Zoo Wildl Med 48(1):7–12

De Rousseau CJ, Bito LZ (1981) Intraocular pressure of rhesus monkeys (Macaca mulatta). II. Juvenile ocular hypertension and its apparent relationship to ocular growth. Exp Eye Res 32(4):407–417

De Silva MEH, Hill LJ, Downie LE, Chinnery HR (2019) The effects of aging on corneal and ocular surface homeostasis in mice. Invest Ophthalmol Vis Sci 60(7):2705–2715

Di Girolamo N, Andreani V, Guandalini A, Selleri P (2013) Evaluation of intraocular pressure in conscious ferrets (Mustela putorius furo) by means of rebound tonometry and comparison with applanation tonometry. Vet Rec vetrec-2012

Dubicanac M, Joly M, Strüve J, Nolte I, Mestre-Francés N, Verdier JM, Zimmermann E (2018) Intraocular pressure in the smallest primate aging model: the gray mouse lemur. Vet Ophthalmol 21(3):319–327

Faulkner J, Williams DL, Mueller K (2020) Ophthalmology of clinically normal alpacas (*Vicugna pacos*) in the United Kingdom: a cross-sectional study. Vet Rec 186(16):e7

Fornazari GA, Montiani-Ferreira F, de Barros Filho IR, Somma AT, Somma B (2016) The eye of the Barbary sheep or aoudad (Ammotragus lervia): reference values for selected ophthalmic diagnostic tests, morphologic and biometric observations. Open Vet J 6(2):102–113

Fraess GA, Sadar MJ, Daniels JB, Sharkey LC, Henriksen ML (2021) Clinical ophthalmological diagnostic description of 10 healthy sugar gliders (Petaurus breviceps) and prevalence of ocular-related presentations in a larger hospital population. Vet Ophthalmol 24(1):80–92

Gentil FG, Fischborn JCJ, Agostini P, Champion T, Freitas GC, Dalmolin F (2016) Parâmetros oftálmicos e biométricos do bulbo ocular de gato do mato (*Leopardus tigrinus* – Schreber, 1775), Anais do SEPE - Seminário de Ensino. Pesquisa e Extensão da UFFS 6:1

Ghaffari MS, Hajikhani R, Sahebjam F, Akbarein H, Golezardy H (2012) Intraocular pressure and Schirmer tear test results in clinically normal Long-Eared Hedgehogs (Hemiechinus auritus): reference values. Vet Ophthalmol 15(3):206–209

F. Montiani-Ferreira et al. (eds.), *Wild and Exotic Animal Ophthalmology*, https://doi.org/10.1007/978-3-030-81273-7

Grundon RA, Anderson GA, Lynch M, Hardman C, O'Reilly A, Stanley RG (2011) Schirmer tear tests and intraocular pressures in conscious and anesthetized koalas (Phascolarctus cinereus). Vet Ophthalmol 14(5):292–295

Gürkan T, Hayat A (2005) Evaluation of the Schirmer and phenol red thread tests for measuring tear secretion in rabbits. Vet Rec 156:485–487

Hahnenberger R (1980) Influence of morphine and naltrexone on the intraocular pressure of conscious cynomolgus monkeys (Macaca fascicularis). Albrecht von Graefes Archiv für klinische und experimentelle Ophthalmologie 214:27–31

Hartley C, Busse C, Matas Reira M, Bacon HJ, Arun AS, Khadekar Y, Selvaraj I, Satyanarayan K, Seshamani G, Knight A (2014) Ocular findings in sloth bears (*Melursus ursinus*) rescued from the dancing bear trade in India. Abstracts: 45th Annual Meeting of the American College of Veterinary Ophthalmologists, Ft Worth, Texas. Vet Ophthalmol 17(6):E31–E49

Heller AR, Ledbetter EC, Singh B, Lee DN, Ophir AG (2018) Ophthalmic examination findings and intraocular pressures in wild-caught African giant pouched rats (Cricetomys spp.). Vet Ophthalmol 21(5):471–476

Holmberg BJ (2008) Ophthalmology of exotic pets. Slatter's Fundamentals Vet Ophthalmol:427–441

Honsho CS, Jorge AT, Oliveira LT, Paulino-Junior D, Mattos-Junior E, Nishimura LT, Dias WO (2016) Intraocular pressure and Schirmer tear test values in maned wolf (Chrysocyon brachyurus). Pesqui Vet Bras 36(9):919–923

Jaax GP, Graham RR, Rozmiarek H (1984) The Schirmer tear test in rhesus monkeys (Macaca mulatta). Lab Anim Sci 34(3):293–294

Jester JV, Steel D, Salz J, Miyashiro J, Rife L, Schanzlin DJ, Smith RE (1981) Radial keratotomy in non-human primate eyes. Am J Ophthalmol 92(2):153–171

Kaufman PL, Davis GE (1980) 'Minified' Goldmann applanating prism for tonometry in monkeys and humans. Arch Ophthalmol 98:542–546

Kossler AL, Brinton M, Patel ZM, Dalal R, Ta CN, Palanker D (2019) Chronic electrical stimulation for tear secretion: lacrimal vs. anterior ethmoid nerve. Ocular Surface 17(4):822–827

Kvapil P, Pirš T, Slavec B et al (2018) Tear production, intraocular pressure and conjunctival bacterial flora in selected captive wild ruminants. Vet Ophthalmol 21:52–57

Labelle AL, Low M, Hamor RE, Breaux CB, Langan JN, Zarfoss MK, Zachariah TT (2010) Ophthalmic examination findings in a captive colony of western gray kangaroos (Macropus fuliginosus). J Zoo Wildl Med 41(3):461–467

Lamble JW, Lamble AP (1976) The effect of miotics on the intraocular pressure of conscious owl monkeys. Invest Ophthalmol Vis Sci 15(10):848–851

Lange RR (2012) Anatomia, morfologia e fisiologia ocular de algumas espécies de interesse na medicina de animais selvagens e de laboratório com ênfase em primatas neotropicais". Anatomy, morphology and eye physiology of some species of interest in wild animals and laboratory medicine with emphasis on neotropical primates (Doctoral dissertation, "Universidade Federal do Paraná. Federal University of Paraná, 2012)

Lange RR, Lima L, Montiani-Ferreira F (2012) Measurement of tear production in black-tufted marmosets (Callithrix penicillata) using three different methods: modified Schirmer's I, phenol red thread and standardized endodontic absorbent paper points. Vet Ophthalmol 15(6):376–382

Lange RR, Lima L, Przydzimirski AC, Montiani-Ferreira F (2014) Reference values for the production of the aqueous fraction of the tear film measured by the standardized endodontic absorbent paper point test in different exotic and laboratory animal species. Vet Ophthalmol 17(1):41–45

Lima L, Montiani-Ferreira F, Tramontin M, Leigue dos Santos L, Machado M, Ribas Lange R, Helena Abil Russ H (2010) The chinchilla eye: morphologic observations, echobiometric findings and reference values for selected ophthalmic diagnostic tests. Vet Ophthalmol 13:14–25

Liu LF, Huang CK, Zhang MZ (2014) Reliability of Tonolab measurements in rats. Int J Ophthalmol 7(6):930–934

Martins BC, Oriá AP, Souza AL, Campos CF, Almeida DE, Duarte RA, Schocken-Iturrino RP (2007) Ophthalmic patterns of captive brown brocket deer (*Mazama gouazoubira*). J Zoo Wildl Med 38(4): 526–533

Marzok MA, Badawy AM, El-khodery SA (2017) Reference values and repeatability of the Schirmer tear tests I and II in domesticated, clinically normal dromedary camels (*Camelus dromedarius*). Vet Ophthalmol 20:259–265

Marzok MA, El-khodery SA (2015) Intraocular pressure in clinically normal dromedary camels (Camelus dromedarius). Am J Vet Res 76: 149–154

McDonald JE, Knollinger AM, Dees DD, MacLaren NE (2018) Determination of Schirmer tear test-1 values in clinically normal alpacas (Vicugña pacos) in North America. Vet Ophthalmol 21(1):101–103

Meekins JM, Eshar D, Rankin AJ (2015) Tear production, intraocular pressure, and conjunctival bacterial flora in a group of captive black-tailed prairie dogs (Cynomys ludovicianus). Vet Ophthalmol 18: 132–136

Mejia-Fava JC, Ballweber L, Colitz CMH et al (2009) Use of rebound tonometry as a diagnostic tool to diagnose glaucoma in the captive California sea lion. Vet Ophthalmol 12:405

Mermoud A, Baerveldt G, Minckler DS, Lee MB, Rao NA (1994) Intraocular pressure in Lewis rats. Invest Ophthalmol Vis Sci 35(5):2455–2460

Miller S, Daily L, Ploss M, Greig I, Ross R, Rayana NP, Dai J, Sugali CK, Mao W, Straiker A (2020) Evidence that cannabinoid CB1 receptors regulate intraocular pressure via two opposing mechanisms. Exp Eye Res 200:108241

Montiani-Ferreira F (2001) Ophthalmology. In: Fowler ME, Cubas Z (eds) Biology, medicine and surgery of South American wild animals. Iowa State Press, Ames, pp 437–456

Montiani-Ferreira F, Mattos BC, Russ HHA (2006) Reference values for selected ophthalmic diagnostic tests of the ferret (Mustela putorius furo). Vet Ophthalmol 9(4):209–213

Montiani-Ferreira F, Shaw G, Mattos BC, Russ HH, Vilani RG (2008b) Reference values for selected ophthalmic diagnostic tests of the capuchin monkey (Cebus apella). Vet Ophthalmol 11(3):197–201

Montiani-Ferreira F, Truppel J, Tramontin MH, D'Octaviano Vilani RG, Lange RR (2008a) The capybara eye: clinical tests, anatomic and biometric features. Vet Ophthalmol 11(6):386–394

Müller K, Mauler DA, Eule JC (2010) Reference values for selected ophthalmic diagnostic tests and clinical characteristics of chinchilla eyes (Chinchilla lanigera). Vet Ophthalmol 13:29–34

Nogradi AL, Szentgáli Z, Battay M, Cope I, Gál J, Németh T (2020) Measurement of tear production and establishment of reference values in guinea pigs (Cavia porcellus) using a modified Schirmer tear test. Vet Rec 186(10):321

Nuhsbaum MT, Gionfriddo JR, Powell CC, Aubin ML (2000) Intraocular pressure in normal llamas (Lama glama) and alpacas (Lama pacos). Vet Ophthalmol 3(1):31–34

Ofri R, Horowitz IH, Jacobson S, Kass PH (1997) Tear production in lions (*Panthera leo*): the effect of two anesthetic protocols. Vet Comp Ophthalmol 7:173–175

Ofri R, Horowitz I, Jacobson S, Kass PH (1998a) The effects of anesthesia and gender on intraocular pressure in lions (*Panthera leo*). J Zoo Wildl Med 29:307–310

Ofri R, Horowitz IH, Kass PH (1998b) Tonometry in three herbivorous wildlife species. Vet Ophthalmol 1(1):21–24

Ofri R, Horowitz I, Kass PH (1999) Tear production in three captive wild herbivores in Israel. J Wildl Dis 35(1):134–136
Ofri R, Horowitz IH, Kass PH (2000) How low can we get? Tonometry in the Thomson gazelle (Gazella thomsoni). J Glaucoma 9(2): 187–189
Ofri R, Horowitz IH, Levison M, Kass PH (2001) Intraocular pressure and tear production in captive eland and fallow deer. J Wildl Dis 37(2):387–390
Ofri R, Raz D, Shvartsman E, Horowitz IH, Kass PH (2002) Intraocular pressure and tear production in five herbivorous wildlife species. Vet Rec 151(9):265–268
Ofri R, Steinmetz A, Thielebein J, Horowitz IH, Oechtering G, Kass PH (2008) Factors affecting intraocular pressure in lions. Vet J 177(1): 124–129
Oliveira R (2021) Personal communication
Oriá AP, Gomes Junior DC, Arraes EA, Estrela-Lima A, Pinna MH, Meneses ÍD, Martins Filho EF (2014) Tear production, intraocular pressure and conjunctival microbiota, cytology and histology of New Zealand rabbits (Oryctolagus cuniculus). Pesqui Vet Bras 34(10):1024–1028
Oriá AP, Gomes Junior DC, Oliveira AV, Curvelo VP, Estrela-Lima A, Pinna MH, Meneses ÍD, Filho EF, Ofri R (2015) Selected ophthalmic diagnostic tests, bony orbit anatomy, and ocular histology in sambar deer (Rusa unicolor). Vet Ophthalmol 18(Suppl 1):125–131
Oriá AP, Pinna MH, Almeida DS, da Silva RMM, Pinheiro ACO, Santana FO, Oliveira AVD (2013) Conjunctival flora, Schirmer's tear test, intraocular pressure, and conjunctival cytology in neotropical primates from Salvador, Brazil. J Med Primatol 42(6): 287–292
Oria AP, Raposo AC, Araujo NLLC, Romano JV, Martins-Filho EF, Gomes Junior D, Galera PD (2019) Evaluation of tear production in juvenile opossum using three different methods. Pesqui Vet Bras 39(1):61–65
Ostrin LA, Wildsoet CF (2016) Optic nerve head and intraocular pressure in the guinea pig eye. Exp Eye Res 146:7–16. https://doi.org/10.1016/j.exer.2015.12.007
Pacheco RE, Bauer BS, Sadar MJ (2018) Measurement of tear production and intraocular pressure in conscious captive European fallow deer (Dama dama). Veterinary medicine and science 4(3):227–236
Peiffer RL, Johnson PT (1980) Clinical ocular findings in a colony of chinchillas (Chinchilla laniger). Lab Anim 14(4):331–335
Pietro SD, Pugliese A, Macciotta L, Pugliese M (2015) Reference values for intraocular pressure and Schirmer Tear Test in healthy wild European mouflons (Ovis orientalis musimon). Large Anim Rev 21(4):173–176
Pigatto JAT, et al (2010) Evaluation of Schirmer Tear Test in healthy lamas. ECVO proceedings. Berlin, Abstract no 43
Puddu G, Schirru F, Petruzzi V, Incardona A, Di Pietro S (2002) Intraocular pressure and Schirmer Tear Test in normal Sardinian wild muflons. University of Sassari, Italy 1–3. https://citeseerx.ist.psu.edu/viewdoc/download?doi=10.1.1.531.600&rep=rep1&type=pdf
Rajaei SM, Mood MA, Paryani MR, Williams DL (2017) Effects of diurnal variation and anesthetic agents on intraocular pressure in Syrian hamsters (Mesocricetus auratus). Am J Vet Res 78(1):85–89
Rajaei SM, Mood MA, Sadjadi R, Williams DL (2016b) Results of selected ophthalmic diagnostic tests for clinically normal Syrian hamsters (Mesocricetus auratus). Am J Vet Res 77(1):72–76
Rajaei SM, Mood MA, Sadjadi R et al (2016c) Intraocular pressure, tear production, and ocular echobiometry in guinea pigs (Cavia porcellus). J Am Assoc Lab Anim Sci 55:475–479
Rajaei SM, Rafiee SM, Ghaffari MS, Masouleh MN, Jamshidian M (2016a) Measurement of tear production in English angora and Dutch rabbits. J Am Assoc Lab Anim Sci 55(2):221–223
Rajaei SM, Sadjadi R, Sabzevari A, Ghaffari MS (2013) Results of phenol red thread test in clinically normal Syrian hamsters (Mesocricetus auratus). Vet Ophthalmol 16(6):436–439
Rankin AJ, Hosking KG, Roush JK (2012) Corneal sensitivity in healthy, immature, and adult alpacas. Vet Ophthalmol 15(1):31–35
Renzo R, Aldrovani M, Crivelaro RM, Thiesen R, de Barros Sobrinho AAF, Balthazar da Silveira CP, Garcia AP, Campos GCS, Werther K, Laus JL (2020) The eye of crab-eating fox (*Cerdocyon thous*): anatomical characteristics and normative values of selected diagnostic tests, morphometry of corneal tissue, and arrangements of corneal stromal collagen fibers. J Zoo Wildl Med 51(2):280–289
Richards M, Trbolová A (2016) Reference values for the ophthalmic Schirmer Tear Test and the intraocular pressure in healthy Chinchillas. Folia Veterinaria 60(3):29–33
Rodrigues BD, Montiani-Ferreira F, Bortolini M, Somma AT, Komáromy AM, Dornbusch PT (2021) Intraocular pressure measurements using the TONOVET® rebound tonometer: influence of the probe-cornea distance. Vet Ophthalmol 24(Suppl 1):175–185
Sheldon JD, Adkesson MJ, Allender M, Jankowski G, Cárdenas-Alayza S (2017) Measurement of intraocular pressures using rebound tonometry in South American fur seals (*Arctocephalus australis*) and South American Sea Lions (Otaria flavescens) from Punta San Juan, Peru. International Association for Aquatic Animal Medicine 48th Annual Meeting and Conference, Cancún, MX
Sheldon JD, Adkesson MJ, Allender MC, Jankowski G, Cárdenas-Alayza S (2019) Measurement of intraocular pressure using rebound tonometry in anesthetized free-ranging South American Sea Lions (*Otaria byronia*). J Wildl Dis 55(4):885–888
Sigmund AB, Cushing AC, Hendrix DVH (2020) Ophthalmic findings in 10 captive, anesthetized chimpanzees (Pan troglodytes). Vet Ophthalmol 23(4):760–763
Snyder KC, Lewin AC, Mans C, McLellan GJ (2018) Tonometer validation and intraocular pressure reference values in the normal chinchilla (Chinchilla lanigera). Vet Ophthalmol 21(1):4–9
Somma AT, Coimbra CM, Lange RR, Moore BA, Montiani-Ferreira F (2020) Reference values for selected ophthalmic diagnostic tests in two species of microchiroptera bats (Artibeus lituratus and Anoura caudifer). Vet Ophthalmol 23(4):61–66
Steel D, Jester JV, Salz J, Villasenor RA, Lee JS, Schanzlin DJ, Smith RE (1981) Modification of corneal curvature following radial keratotomy in primates. Ophthalmology 88:747–754
Takle GL, Suedmeyer WK, Hunkeler A (2010) Selected diagnostic ophthalmic tests in the red kangaroo (macropus rufus). J Zoo Wildl Med 41(2):224–233
Tavares-Somma A, Seabra N, Moore BA, Sato M, Lange RR, Montiani-Ferreira F (2017) The eye of the azara's agouti (Dasyprocta azarae): morphological observations and selected ophthalmic diagnostic tests. J Zoo Wildl Med 48(4):1108–1119
Trost K, Skalicky M, Nell B (2007) Schirmer tear test, phenol red thread tear test, eye blink frequency and corneal sensitivity in the guinea pig. Vet Ophthalmol 10(3):143–146
Tuntivanich P, Soontornvipart K, Tuntivanich N, Wongaumnuaykul S, Briksawan P (2002) Schirmer tear test in clinically normal Asian elephants. Vet Res Commun 26(4):297–299
Villar T, Pascoli AL, Klein A, Chacaltana FC, Capistrano E, Shipley CF, Martins BC (2020) Tear production, intraocular pressure, and central corneal thickness in white-tailed deer (Odocoileus virginianus). Vet Ophthalmol 23(1):123–128

Welihozkiy A, Bedenice D, Price LL, Pizzirani S, Pirie CG (2011) Measurement of corneal sensitivity in 20 ophthalmologically normal alpacas. Vet Ophthalmol 14(5):333–336

Wieser B, Tichy A, Nell B (2013) Correlation between corneal sensitivity and quantity of reflex tearing in cows, horses, goats, sheep, dogs, cats, rabbits, and guinea pigs. Vet Ophthalmol 16(4):251–262

Williams DL, Adeyeye N, Visser E (2017) Ophthalmological abnormalities in wild European hedgehogs (Erinaceus europaeus): a survey of 300 animals. Open Vet J 7:261–267

Willis AM, Anderson DE, Gemensky AJ, Wilkie DA, Silveira F (2000) Evaluation of intraocular pressure in eyes of clinically normal llamas and alpacas. Am J Vet Res 61(12):1542–1544

Yi Y, Zeng T, Zhou L, Cai SP, Yin Y, Wang Y, Liu XY (2012) Experimental Tibetan monkey domestication and its application for intraocular pressure measurement. Int J Ophthalmol 5(3):277

Yu W, Cao G, Qiu J, Liu X, Ma J, Li N, Yu M, Yan N, Chen L, Pang IH (2009) Evaluation of monkey intraocular pressure by rebound tonometer. Mol Vis 15:2196–2201

Index

F. Montiani-Ferreira et al. (eds.), *Wild and Exotic Animal Ophthalmology*, https://doi.org/10.1007/978-3-030-81273-7